

Assessment of the Cyclic Strain Approach for the Evaluation of Initial Liquefaction

by

Eduardo Rodriguez-Arriaga

Thesis submitted to the faculty of the Virginia Polytechnic Institute and State University in
partial fulfillment of the requirements for the degree of

Master of Science

In

Civil Engineering

Russell A. Green

Joseph E. Dove

Adrian Rodriguez-Marek

May 9, 2017

Blacksburg, VA

Keywords: Liquefaction; Cyclic Strain Approach; Threshold Strain; Pore Pressure Generation

Copyright© 2017, Eduardo Rodriguez-Arriaga

ALL RIGHTS RESERVED

Assessment of the Cyclic Strain Approach for the Evaluation of Initial Liquefaction

Eduardo Rodriguez-Arriaga

ABSTRACT

Field-based liquefaction evaluation procedures include the stress-based, strain-based, and energy-based based approaches. The existence of a volumetric threshold shear strain, γ_{tv} , under which there is no development of excess pore pressures, and the unique relationship between pore pressure ratio and cyclic shear strain, γ_c , make a compelling argument for using a strain-based approach. However, the cyclic strain approach has not yet been standardized for field evaluations. The primary objective of this thesis is to use published databases of 415 shear-wave velocity and 230 Standard Penetration Test liquefaction field case histories to investigate the performance of the cyclic strain approach for the evaluation of initial liquefaction relative to the cyclic stress approach. Additionally, the concept of the γ_{tv} is expressed in terms of the peak ground surface acceleration and defined as the threshold a_{max} . Computing $(a_{max})_t$ could provide a fast and simple evaluation for initial liquefaction, where no liquefaction is expected for a minimum computed $(a_{max})_t$ determined from the case histories. The variant of the strain-based procedure proposed herein avoids the direct need for laboratory cyclic testing by employing pore pressure generation models that are functions of cyclic shear strain, number of equivalent cycles, and relative density to predict initial liquefaction. The results from the proposed procedure are compared with those of the stress-based approach to determine which better matches the field observations of the case histories. It was found that the cyclic strain approach resulted in 70% to 77% correct predictions. In contrast, the cyclic stress approach yielded 87% to 90% correct predictions. The reasons why the predictions were not always correct with the cyclic strain approach are due to inherent limitations of the cyclic strain approach. Most significantly, an inherent and potentially fatal limitation of the strain-based procedure is it ignoring the softening of the soil stiffness due to excess pore pressure in representing the earthquake loading in terms of γ_c and n_{eq} .

Assessment of the Cyclic Strain Approach for the Evaluation of Initial Liquefaction

Eduardo Rodriguez-Arriaga

GENERAL AUDIENCE ABSTRACT

Earthquakes can cause heavy damage when they occur. One of the ways in which this happens is when the earthquake shaking causes the soil to behave like a liquid. This is the phenomenon known as liquefaction. An example of liquefaction is a person sinking in quicksand. Relating this to earthquakes, liquefaction can be thought of as a building sinking in quicksand that formed as a consequence of earthquake shaking. Destructive cases of liquefaction have been reported in almost all major earthquakes. When cases of liquefaction are properly documented, they can provide information that will help engineers and scientists assess the efficacy of existing liquefaction evaluation procedures and/or to develop new procedures. There are different methods to evaluate the occurrence of liquefaction, with the cyclic stress approach being the most widely used. This study assesses the efficacy of an alternative approach to see if it yields better predictions of liquefaction triggering than the cyclic stress approach. The approach under consideration is called the cyclic strain approach. To examine the effectiveness of the cyclic strain approach, sites that experienced liquefaction in the past were analyzed to see if the predictions made with the approach matched the past field observations. Due to potential shortcomings in implementing the strain based procedure, as well as inherent limitations of the procedure, the strain-based procedure yielded predictions that were inferior to the more widely used stress-based procedure.

Dedication

I dedicate this thesis to my family and friends. A special mention to my parents for all their love and support and putting me through the best education possible. I appreciate their sacrifices, and I wouldn't have been able to get this far without them.

I also dedicate this thesis to my brother for bringing a smile to my face and always being upfront with me without any reservations.

I dedicate this work to my first country, El Salvador, for teaching me the humbling experience of living through a major earthquake and instilling in me strong values through the example of its hard-working people and its warm culture.

愛

Acknowledgements

This study is based on work supported in part by the U.S. National Science Foundation (NSF) grants CMMI-1030564 and CMMI-1435494; this support is gratefully acknowledged. Also, the author gratefully acknowledges Professor Mladen Vucetic, UCLA, for providing the author with a copy of his Ph.D. dissertation. I am deeply grateful for the advice and guidance of my committee members: Dr. Russell A. Green, Dr. Joseph E. Dove, and Dr. Adrian Rodriguez-Marek, as well as other faculty members in the Geotechnical Engineering Program at Virginia Tech: Dr. George M. Filz and Dr. Thomas L. Brandon. I extend a special mention to my advisor Dr. Russell A. Green for his advice, guidance, support, and encouragement throughout the course of all my graduate studies. However, any opinions, findings, and conclusions or recommendations expressed in this thesis are those of the author and do not necessarily reflect the views of NSF or others.

Table of Contents

Chapter 1: Introduction	1
1.1 Problem Statement	1
1.2 Organization	1
1.3 Attribution	1
Chapter 2: Assessment of the Cyclic Strain Approach for the Evaluation of Initial Liquefaction..	3
2.1 Abstract	3
2.2 Introduction	3
2.3 Background Information	6
2.3.1 <i>Liquefaction Evaluation Procedures</i>	6
2.3.1.1 <i>Simplified Stress-Based Approach</i>	6
2.3.1.2 <i>Dobry et al. Strain-Based Approach</i>	8
2.4 Proposed Alternative Implementation of the Dobry et al. (1982) Strain-Based Procedure	9
2.4.1 <i>Determination of γ_c and n_{eq}</i>	9
2.4.1.1 <i>Ishibashi and Zhang (1993) Normalized Shear Modulus Reductions Curves</i>	11
2.4.1.2 <i>Number of Equivalent Cycles, n_{eq}</i>	12
2.4.2 <i>Threshold Shear Strain (γ_{tv}) and Threshold Peak Ground Acceleration, $(a_{max})_t$</i>	13
2.4.3 <i>Excess Pore Pressure Generation for $\gamma_c > \gamma_{tv}$</i>	15
2.4.3.1 <i>Byrne (1991) Model</i>	15
2.4.3.2 <i>Vucetic and Dobry (1986) Model</i>	17

2.4.3.3	<i>Comparison of the Byrne (1991) and Vucetic and Dobry (1986) Models</i>	19
2.4.4	<i>Assessing Whether Liquefaction is Triggered</i>	21
2.4.5	<i>Analyzing Field Case Histories</i>	21
2.4.5.1	<i>Kayen et al. (2013), V_s Database</i>	21
2.4.5.2	<i>Boulangier et al. (2012), SPT Database</i>	24
2.5	<i>Results</i>	25
2.5.1	<i>Determination of γ_c and n_{eq}</i>	26
2.5.2	<i>Threshold Shear Strain (γ_{tv}) and Threshold Peak Ground Acceleration, $(a_{max})_t$</i>	28
2.5.3	<i>Excess Pore Pressure Generation for $\gamma_c > \gamma_{tv}$</i>	30
2.5.4	<i>Assessing Whether Liquefaction is Triggered</i>	34
2.6	<i>Discussion</i>	35
2.6.1	<i>Cyclic Shear Strains and Number of Equivalent Cycles</i>	35
2.6.2	<i>Threshold Strains and Accelerations</i>	37
2.6.3	<i>Liquefaction Triggering Predictions</i>	38
2.6.4	<i>Future Work</i>	40
2.7	<i>Conclusions</i>	40
2.8	<i>References</i>	42
Chapter 3:	<i>Thesis Conclusions</i>	48
3.1	<i>Summary</i>	48
3.2	<i>Key Findings</i>	48

3.3 Recommendations for Future Work.....	49
Appendix A: Earthquake Liquefaction Databases	51
Appendix B: Normalized Shear Modulus Reduction Curves for the Liquefaction Case Histories from the Kayen et al. and Boulanger et al. Databases	55
Appendix C: Pore Pressure Ratio Versus Cyclic Shear Strain for the Kayen et al. Database using the Byrne (1991) and Vucetic and Dobry (1986) Models	381
Appendix D: Pore Pressure Ratio Versus Cyclic Shear Strain for the Boulanger et al. Database using the Byrne (1991) and Vucetic and Dobry (1986) Models.....	414

Chapter 1: Introduction

1.1 Problem Statement

The primary objective of this thesis is to use published databases of 415 small strain shear-wave velocity (V_s) and 230 Standard Penetration Test (SPT) liquefaction field case histories to investigate whether the cyclic strain approach can provide better predictions than the stress-based approach for evaluating liquefaction triggering. Liquefaction is a phenomenon triggered by the cyclic shear loading of loose to medium dense saturated cohesionless soil under undrained conditions. Almost all major earthquakes have reported destructive cases of liquefaction, and as such, this phenomenon is an important problem facing earthquake engineers. The usage of the cyclic strain approach has proven to successfully predict pore pressure generation and liquefaction triggering in laboratory tests, but with the V_s and SPT databases, this approach can be examined against liquefaction case histories. The results from the procedure are used to explain trends and discuss the limitations of the cyclic strain approach when compared to the results of the cyclic stress approach.

1.2 Organization

This thesis is organized into three chapters and four appendices (A-D). The second chapter is a manuscript that will be submitted as a technical paper to the Elsevier journal Soil Dynamics and Earthquake Engineering. Attribution of this manuscript is presented in the following section. The third chapter of this thesis provides a summary of the work performed, the key findings, and recommendations for future work. The end matter of this thesis contains four appendices which supply further detail about the: V_s and SPT databases used in the analysis of the cyclic strain approach, shear modulus degradation curves used in analyzing the liquefaction case histories, and figures and tables illustrating excess pore pressure ratio as a function of cyclic shear strain computed using two different pore pressure generation models.

1.3 Attribution

The manuscript contained in Chapter 2 titled: “Assessment of the Cyclic Strain Approach for the Evaluation of Initial Liquefaction,” authored by E. Rodriguez-Arriaga and R. A. Green will be submitted as a technical paper to the Elsevier journal Soil Dynamics and Earthquake Engineering.

The following provides information about the contributing co-author and his primary role pertaining to this paper:

Russell A. Green, Ph.D., P.E., Department of Civil and Environmental Engineering, Virginia Tech, Blacksburg, Virginia, U.S.A.

- Research Advisor to the lead author who provided significant guidance and support during the entirety of the research project. Dr. Green is also credited for contributing in the development of one of the adopted relationships used in this study for computing the number of equivalent cycles.

Chapter 2: Assessment of the Cyclic Strain Approach for the Evaluation of Initial Liquefaction

2.1 Abstract

The cyclic strain approach has been highly praised for providing consistent results for liquefaction evaluation in the laboratory. To learn about its applicability in the field, this paper assessed the cyclic strain approach by applying it to both small strain shear wave velocity (V_s) and Standard Penetration Test (SPT) case histories and comparing the results to those obtained with the stress-based approach. Toward this end, cyclic shear strains, γ_c , were computed using an alternative implementation of the Dobry et al. (1982) procedure. The concept of the threshold volumetric shear strain, γ_{tv} , was expressed in terms of the peak ground surface acceleration to define the threshold a_{max} , which provides a fast and simple way to evaluate whether a more detailed evaluation of liquefaction potential is warranted. From the analysis of field case histories, the threshold a_{max} was found to range from 0.08 to 0.12 g. For cases where $\gamma_c > \gamma_{tv}$, excess pore pressures will develop, and it is necessary to quantify them to evaluate liquefaction potential. This was accomplished by implementing the pore pressure generation models by Byrne (1991) and by Vucetic and Dobry (1986). The results showed that the Byrne (1991) model yielded more accurate and far fewer false negative predictions than the Vucetic and Dobry (1986) model. Considering only cases with fine contents $\leq 5\%$ resulted in slightly more accurate predictions, but not enough to indicate that the presence of fines is significantly biasing the prediction statistics of the strain-based procedure. Ultimately, the stress-based approach yielded more accurate predictions (87%–90%) compared to the cyclic strain approach (70%–77% with the Byrne, 1991, model). One likely reason for the lack of accuracy in the strain-based procedure's predictions is the inherent and potentially fatal limitation of the procedure is it ignoring the softening of the soil stiffness due to excess pore pressure when representing the earthquake loading in terms of γ_c and $n_{eq\gamma}$.

2.2 Introduction

The primary objective of the study presented herein is to evaluate the efficacy of the strain-based liquefaction triggering evaluation procedure implemented using a pragmatic variant of the procedure originally proposed by Dobry et al. (1982). Liquefaction is a phenomenon that results

from the contractive tendencies of loose to medium dense soils when sheared. For saturated cohesionless soils, this tendency results in the transfer of the overburden stress to the pore fluid, with the commensurate increase in pore water pressure and decrease in effective confining stress. Liquefaction has occurred in most major earthquakes and has caused significant damage to infrastructure (e.g., Cubrinovski and Green, 2010; Cubrinovski et al., 2011; Green et al., 2011; Olson et al., 2011; among many others).

The most widely used procedure for evaluating liquefaction triggering potential is the simplified stress-based procedure originally proposed by Whitman (1971) and Seed and Idriss (1971). This procedure is semi-empirical and has undergone periodic updates as a result of findings from new laboratory studies and/or the collection and analysis of additional field case history data (e.g., Youd et al., 2001; Cetin et al., 2004; Idriss and Boulanger, 2004). Inherent to this procedure is the quantification of the seismic demand imposed on the soil expressed in terms of cyclic shear stress.

Despite the popularity of the stress-based procedures, multiple studies have shown that excess pore water pressure better correlates to cyclic strain than to cyclic stress (e.g., Figure 2.1) (e.g., Martin et al., 1975; Dobry et al., 1982; Byrne, 1991). The reason for this is the relative movement of soil particles, which is requisite for excess pore water pressure generation, relates to the induced strain, regardless of amplitude of the stress applied to soil. As a result, Dobry et al. (1982) proposed a strain-based liquefaction triggering evaluation procedure. Although the Dobry et al. procedure generally received a positive reception by the liquefaction researchers, it has failed to be adopted into practice. One reason for this is likely the requirement to perform strain-controlled cyclic laboratory tests on undisturbed and/or reconstituted specimens. This is in contrast to the simplified stress-based procedures wherein in-situ test metrics are the primary parameters used to evaluate liquefaction potential, with laboratory index tests and grain size distribution analyses having supporting roles if their performance is deemed necessary.

Herein an alternative approach to implementing the Dobry et al. (1982) strain-based procedure is proposed which circumvents the need for performing strain-controlled cyclic laboratory tests. Per this procedure, strain-based numerical excess pore pressure generation models are used in lieu of developing analogous relationships from laboratory tests. The soil parameters required to implement the procedure include: relative density (D_r), secant shear modulus (G), and grain size distribution characteristics of the soil (i.e., fines content: FC; coefficient of uniformity: C_u). These

are not too different from the soil parameters required to implement the stress-based simplified procedures and can be estimated using simple relationships or conservative assumptions.

To assess the efficacy of the proposed variant of the Dobry et al. (1982) strain-based procedure, earthquake liquefaction case histories in the small strain shear wave velocity (V_s) database, which consists of 415 case histories compiled by Kayen et al. (2013), and in the Standard Penetration Test (SPT) database, which consists of 230 case histories compiled by Boulanger et al. (2012), are evaluated. By evaluating field case histories, the efficacy of the strain-based procedure can be assessed both in an absolute sense (i.e., with respect to field observations) and in a relative sense (i.e., relative to the efficacy of stress-based procedures). Additionally, using the two types of liquefaction case history databases in the assessment allows the significance on the computed results of using one type of in-situ test metric to estimate other needed parameters versus using the other type of in-situ test metric.

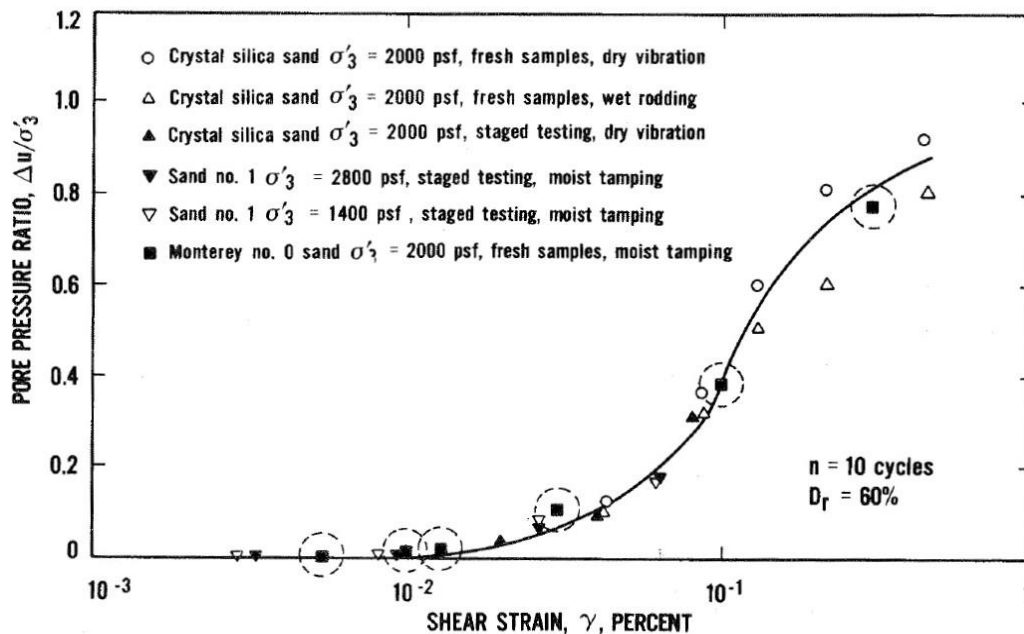


Figure 2.1 Porewater pressure buildup in cyclic triaxial strain-controlled tests, after ten loading cycles, as a function of cyclic shear strain, for various normally consolidated saturated sands at $D_r = 60$ percent and for various pressures (Dobry et al., 1982).

The following sections present the background information related with both the cyclic stress and cyclic strain approaches. Next, the steps used to implement the proposed variant of the strain-based

procedure are outlined, and the liquefaction case history databases used in the assessment are discussed. The results from the assessment are then presented and discussed.

2.3 Background Information

2.3.1 Liquefaction Evaluation Procedures

2.3.1.1 Simplified Stress-Based Approach

As stated in the Introduction, the simplified stress-based procedure is the most widely used approach for evaluating liquefaction triggering. Per this procedure the seismic demand is quantified in terms of Cyclic Stress Ratio (CSR), which is the cyclic shear stress (τ_c) induced at a given depth in the soil profile normalized by the initial vertical effective stress (σ'_{vo}) at that same depth. The word “simplified” in the procedure’s title originated from the proposed use of a form of Newton’s Second Law to compute τ_c at a given depth in the profile, in lieu of performing numerical site response analyses. The resulting “simplified” expression for CSR is given by Eq. 1:

$$CSR = \frac{\tau_c}{\sigma'_{vo}} = 0.65 \left(\frac{a_{max}}{g} \right) \left(\frac{\sigma_v}{\sigma'_{vo}} \right) r_d \quad (1)$$

where: a_{max} = maximum horizontal acceleration at the ground surface; g = acceleration due to gravity; σ_v and σ'_{vo} = total and initial effective vertical stresses, respectively; and r_d = stress reduction factor that accounts for the non-rigid response of the soil profile.

Additional factors are applied to Eq. 1, the need for which was largely based on results from laboratory studies, to account for durational effects of the shaking (MSF: Magnitude Scaling Factor, where the reference motion duration is for a $M_w 7.5$ earthquake), initial effective overburden stress (K_σ , where the reference initial effective overburden stress is 1 atm), and initial static shear stress (K_α , where the initial static shear stress is zero, e.g., level ground conditions). The resulting expression for the normalized CSR (i.e., CSR*: CSR normalized for motion duration

for a $M_w 7.5$ event, 1 atm initial effective overburden stress, and level ground conditions) is given by Eq. 2:

$$CSR^* = \frac{CSR}{MSF \cdot K_\sigma \cdot K_\alpha} = 0.65 \left(\frac{a_{max}}{g} \right) \left(\frac{\sigma_v}{\sigma'_{vo}} \right) r_d \frac{1}{MSF \cdot K_\sigma \cdot K_\alpha} \quad (2)$$

Case histories compiled from post-earthquake investigations were categorized as either “Liquefaction” or “No Liquefaction,” largely based on whether evidence of liquefaction was or was not observed at the sites. By plotting CSR^* for each of the case histories as a function of the corresponding in-situ test metric (e.g., SPT N-value or V_s), normalized for clean sand conditions and an initial effective overburden stress of 1 atm, it can be observed that the “Liquefaction” and “No Liquefaction” cases tended to lie in two different regions of the graph. The “boundary” separating these two sets of case histories is referred to as the Cyclic Resistance Ratio ($CRR_{M7.5}$) and represents the capacity of the soil to resist liquefaction. This boundary can be expressed as a function of the normalized in-situ test metrics.

Consistent with the conventional definition for factor of safety (FS), the FS against liquefaction (FS_{Liq}) is defined as the capacity of the soil to resist liquefaction divided by the seismic demand:

$$FS_{Liq} = \frac{CRR_{M7.5}}{CSR^*} \quad (3)$$

As discussed later in this paper, the efficacy of the deterministic variants of the Kayen et al. (2013) V_s -based and Idriss and Boulanger (2008) SPT-based simplified liquefaction evaluation procedures are used herein to compare with that of the proposed variant of the Dobry et al. (1982) strain-based procedure.

2.3.1.2 Dobry et al. Strain-Based Approach

Early studies showed that volumetric strain in a given soil subjected to cyclic loading under drained conditions almost uniquely correlates with the amplitude of the applied cyclic shear strain (γ_c), rather than the applied τ_c (e.g., Silver and Seed, 1971). The corollary of this finding is that the excess pore pressure ratio (r_u : $r_u = \Delta u / \sigma'_{vo}$, where Δu is the excess pore water pressure) in a given soil subjected to cyclic loading under undrained conditions almost uniquely correlates with the amplitude of the applied γ_c , rather than the applied τ_c (e.g., Martin et al., 1975). Building on these findings, Dobry et al. (1982) proposed a strain-based approach for evaluating liquefaction triggering potential, as an alternative to the stress-based approach.

Starting with the simplified equation to compute τ_c , Dobry et al. (1982) proposed a simplified equation to compute γ_c :

$$\gamma_c = \frac{\tau_c}{G} \quad (4)$$

$$\gamma_c = 0.65 \left(\frac{a_{max}}{g} \right) \frac{\sigma_v r_d}{G_{max} (G/G_{max})_{\gamma_c}} \quad (5)$$

where G is the secant shear modulus of the soil, G_{max} = small-strain ($\gamma_c \leq 10^{-4}\%$) secant shear modulus of the soil; and $(G/G_{max})_{\gamma_c}$ = normalized shear modulus reduction ratio of the soil corresponding to γ_c . Dobry et al. (1982) found that there is a limiting value of γ_c , below which no excess pore water pressure develop, regardless of the number of applied load cycles (n_{eq}); they refer to this limiting value of γ_c as the threshold volumetric shear strain (γ_{tv}). Dobry et al. found that for normally consolidated clean and silty sands $\gamma_{tv} \approx 0.01\%$.

The strain-based liquefaction triggering evaluation procedure proposed by Dobry et al. (1982) consists of four steps:

Step 1. Determination of γ_c and n_{eq} . γ_c is calculated using Eq. 5; the equivalent number of cycles, n_{eq} , can be obtained from established correlations with earthquake parameters.

Step 2. Comparison between γ_c and the threshold strain of the soil, γ_{tv} . If $\gamma_c < \gamma_{tv}$, neither pore pressure buildup nor liquefaction will occur and the evaluation ends here.

Step 3. If $\gamma_c > \gamma_{tv}$, the values of γ_c and n_{eq} should be used in conjunction with experimental curves developed from strain-controlled cyclic tests performed on undisturbed and/or reconstituted samples prepared to the same D_r as the soil in-situ (e.g., Figure 2.1) to estimate the value of the excess pore water pressure ratio, r_u , at the end of earthquake shaking.

Step 4. The value of r_u estimated in Step 3 is used to decide if the site will experience initial liquefaction ($r_u \approx 1.0$) or not ($r_u < 1.0$).

Laboratory studies performed around the same time Dobry et al. (1982) published their procedure showed that the cyclic resistance of reconstituted soil samples prepared to a given D_r was heavily dependent on the sample preparation method (e.g., Mitchell et al., 1976). However, these studies based their findings on stress-controlled cyclic test data, while the experimental curves required to be developed in Step 3 should be based on strain-controlled cyclic test data. Unlike stress-controlled tests, the cyclic resistance of a given soil prepared to a given D_r is relatively insensitive to method used to reconstitute the sample. The reason for this is that the sample preparation method inherently influences the sample stiffness. Accordingly, for a given applied shear stress, the amplitudes of the shear strains induced in samples prepared by different methods will differ, and excess pore pressure generation (and liquefaction) is a strain phenomenon.

2.4 Proposed Alternative Implementation of the Dobry et al. (1982) Strain-Based Procedure

2.4.1 Determination of γ_c and n_{eq}

Step 1 of the Dobry et al. (1982) strain-based is to determine γ_c and n_{eq} , which represents the amplitude and duration of the applied earthquake loading. As stated above, Dobry et al. (1982) built on the “simplified” expression for τ_c developed for the simplified stress-based procedure and proposed an analogous “simplified” expression for γ_c (Eq. 5). In this expression the stiffness of the soil is represented by $G_{max} \times (G/G_{max})_{\gamma_c}$, where G_{max} is the small-strain secant shear modulus of the soil which can be computed from V_s and $(G/G_{max})_{\gamma_c}$ is the normalized shear modulus reduction ratio of the soil corresponding to γ_c . Relationships for G/G_{max} as a function of γ_c have been

proposed by several investigators (Figure 2.2) and often include predictive variables such as mean effective confining stress (σ'_{mo}), plasticity index (PI), overconsolidation ratio (OCR), etc. (e.g., Ishibashi and Zhang, 1993; Darendeli, 2001; and Menq, 2003). However, because the G/G_{max} relationships are expressed as a function of γ_c , an iterative procedure is required to determine $(G/G_{max})_{\gamma_c}$ and hence γ_c using Eq. 5.

In this study the G/G_{max} relationship proposed by Ishibashi and Zhang (1993) is used to compute γ_c mainly because the Darendeli (2001) and Menq (2003) curves require more detailed information about the soil to implement. Since some of this information is not included with the liquefaction case history databases, the uncertainty inherent to estimating these variables only adds to the uncertainty in the computed γ_c values.

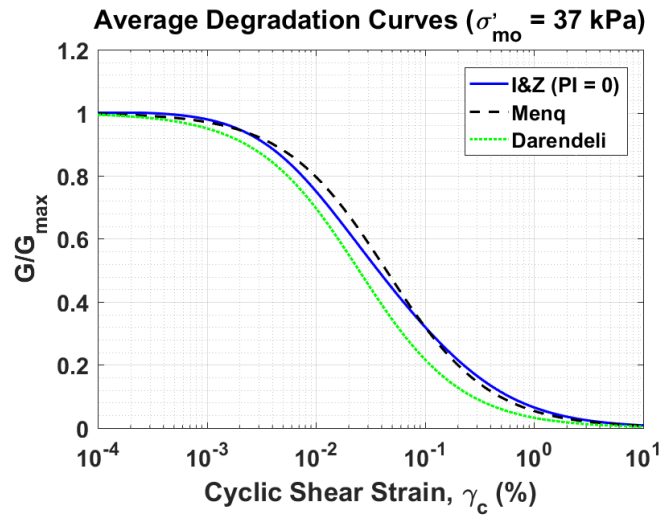


Figure 2.2 Comparison of normalized shear modulus degradation curves using the Ishibashi and Zhang (1993), Darendeli (2001), and Menq (2003) for clean sand.

In using Eq. 5 to compute γ_c in this study, the r_d relationship proposed by Lasley et al. (2016) for active, shallow crustal tectonic regimes (e.g., western United States: WUS) was employed. The expressions used with this relationship are the following:

$$r_d = (1 - \alpha) \exp\left(\frac{-Z}{\beta}\right) + \alpha \quad (6a)$$

$$\alpha = \exp(-4.373 + 0.4491 \cdot M_w) \quad (6b)$$

$$\beta = -20.11 + 6.247 \cdot M_w \quad (6c)$$

where: α = limiting value of r_d at large depths and can range from 0 to 1; β controls the curvature of the functions at shallow depths; z = depth in meters; and M_w is the moment magnitude.

2.4.1.1 *Ishibashi and Zhang (1993) Normalized Shear Modulus Reduction Curves*

The expressions required for the Ishibashi and Zhang (1993) modulus reduction curves are:

$$\frac{G}{G_{max}} = K(\gamma_c, PI) \sigma'_{mo}{}^{m(\gamma_c, PI) - m_o} \quad (7a)$$

$$m(\gamma_c, PI) - m_o = 0.272 \left[1 - \tanh \left\{ \ln \left(\frac{0.000556}{\gamma_c} \right)^{0.4} \right\} \right] e^{-0.0145PI^{1.3}} \quad (7b)$$

$$K(\gamma_c, PI) = 0.5 \left[1 + \tanh \left\{ \ln \left(\frac{0.000102 + n(PI)^{0.492}}{\gamma_c} \right) \right\} \right] \quad (7c)$$

$$n(PI) = \begin{cases} 0.0 & PI = 0 \\ 3.37 \cdot 10^{-6} PI^{1.404} & 0 < PI \leq 15 \\ 7.0 \cdot 10^{-7} PI^{1.976} & 15 < PI \leq 70 \\ 2.7 \cdot 10^{-5} PI^{1.115} & PI > 70 \end{cases} \quad (7d)$$

where: $K(\gamma_c, PI)$ is a decreasing function of γ_c and $m(\gamma_c, PI)$ is an increasing function of γ_c , both obtained from statistical regression of experimental data. The initial mean effective confining stress is computed as:

$$\sigma'_{mo} = \frac{\sigma'_{vo}(1 + 2K_o)}{3} \quad (8)$$

where: K_o is the at-rest lateral earth pressure coefficient, which for normally consolidated, loose sands can be assumed to be 0.5 or can be estimated using relationships such as that proposed by Jaky (1944).

In using Eq. 7 to compute $(G/G_{max})_{\gamma_c}$ and γ_c in this study, $PI = 0$ was assumed because the soils analyzed are non-plastic, and a convergence criterion of 0.05% between γ_c values computed in sequential iterations was used.

2.4.1.2 Number of Equivalent Cycles, n_{eq}

As required in Step 1 of the Dobry et al. (1982) strain-based procedure, the equivalent number of cycles (i.e., n_{eq}) for the earthquake loading is required, which Dobry et al. states is a function of earthquake magnitude. At the time of the writing of Dobry et al. (1982), a few relationships for equivalent number of stress cycles ($n_{eq\tau}$) had been developed (e.g., Seed et al., 1975), but the authors are not aware of any equivalent number of strain cycles ($n_{eq\gamma}$) relationships having had been developed. Accordingly, Dobry et al. (1982) likely assumed that $n_{eq\tau}$ and $n_{eq\gamma}$ were equivalent, which is not necessarily the case (e.g., Green and Terri, 2005). Even today, few relationships have been developed for $n_{eq\gamma}$ (e.g., Green and Lee, 2006; Chen et al., 2010; Lee and Green, 2017), but these relationships were developed for evaluating seismic compression in dry or partially saturated soils, not for evaluating liquefaction in saturated soils.

Despite its questionable applicability for use in a strain-based liquefaction evaluation procedure, the $n_{eq\tau}$ relationship proposed by Lasley et al. (2017) is used herein. The reason for selecting this relationship is because it was more rigorously developed than other existing $n_{eq\tau}$ and $n_{eq\gamma}$ relationships and none of the alternative relationships are anymore applicable for use in the strain-based liquefaction procedure than the Lasley et al. relationship. Lasley et al. (2017) built upon the work by Green and Terri (2005) and Lee (2009) and developed their relationship for earthquake magnitudes between 4.9 to 7.9 in shallow crustal active tectonic regions.

To account for multidirectional shaking, Green and Terri (2005) performed separate site response analyses for each horizontal component in a pair of motions, added the energy dissipated at the respective depths for each component of motion, and set the amplitude of the equivalent cycle as

the 0.65 times the geometric mean of the maximum shear stresses experienced at a given depth. The same process of accounting for multidirectional shaking was used by Lasley et al. (2017) and referred to as Approach 2. With this approach, $n_{eq\tau}$ represents the combined influence of both horizontal components of motion, with the resulting relationship given as:

$$\ln(n_{eq\tau}) = 0.4605 - 0.4082 \cdot \ln(a_{max}) + 0.2332 \cdot M_w \quad (9)$$

where a_{max} is in units of g. This correlation shows a negative correlation between $n_{eq\tau}$ and a_{max} , as shown in Figure 2.3.

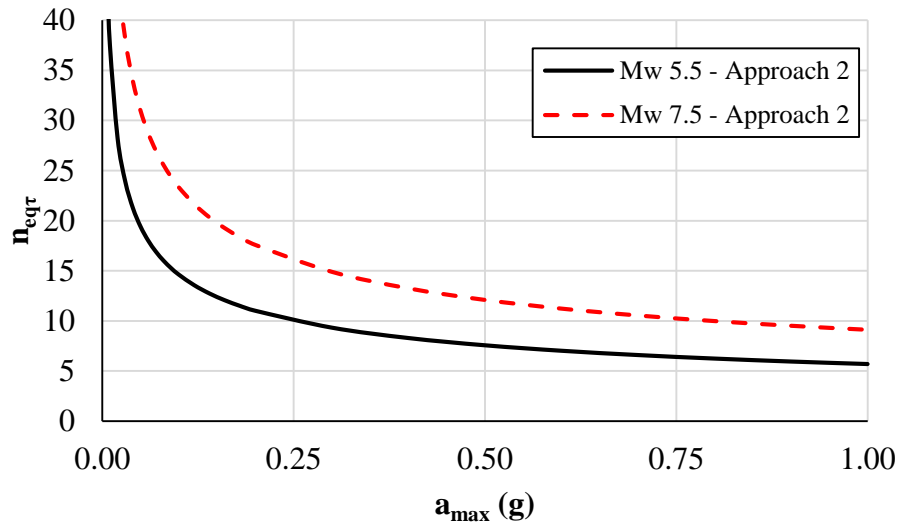


Figure 2.3 Values of $n_{eq\tau}$ predicted with the Lasley et al. (2017) correlation.

2.4.2 Threshold Shear Strain (γ_{tv}) and Threshold Peak Ground Acceleration, $(a_{max})_t$

Step 2 of the Dobry et al. (1982) strain-based procedure determines whether $\gamma_c < \gamma_{tv}$. As stated previously, for normally consolidated clean and silty sands $\gamma_{tv} \approx 0.01\%$ (e.g., Silver and Seed, 1971; Youd, 1972; Stoll and Kald, 1977; Dobry et al., 1982; Vucetic, 1994; Abdoun et al., 2013; among others). The strain value was determined experimentally where the results of cyclic testing showed that when $\gamma_c \leq 0.01\%$ no excess pore water pressures were generated, even when subjected to a large number of cycles. In addition, Dobry et al. (1982) presented analytical results, using a

simple cubic array of quartz spheres, where the calculations also showed $\gamma_{tv} \approx 0.01\%$. Consistent with published studies, γ_{tv} was taken to be 0.01% in this assessment. However, inherent to Eq. 5 is the 0.65 factor that is introduced via Eq. 1. This factor was included in Eq. 1 to yield a CSR value that is more representative of the seismic demand for the entire duration of shaking (e.g., Whitman, 1971). However, any exceedance of γ_{tv} throughout the duration of shaking would seemingly result in excess pore pressure generation, not just when the “average” induced shear strain over the entire duration of shaking exceeds γ_{tv} . As a result, it is questionable whether the 0.65 factor should be included in computation of γ_c for comparison with γ_{tv} ; excluding the 0.65 factor from Eq. 5 results in:

$$\gamma_c^* = \left(\frac{a_{max}}{g}\right) \frac{\sigma_v r_d}{G_{max}(G/G_{max})_{\gamma_c}} \quad (10)$$

where the “*” is added to γ_c to distinguish this value of cyclic shear strain from the value computed using Eq. 5.

To provide a simple and fast screening method to determine whether or not the cyclic shear strain exceeds the threshold strain, Eq. 5 was used to develop a relationship for the peak ground surface acceleration required to induce a γ_c at a given depth in the soil profile equal to γ_{tv} . This acceleration is referred to as the threshold peak ground surface acceleration, $(a_{max})_t$, and below this value no excess pore pressures develop; $(a_{max})_t$ is expressed as:

$$(a_{max})_t = 0.000154 \frac{G_{max}(G/G_{max})_{\gamma_{tv}}}{\sigma_v r_d} \quad (11)$$

where: $(a_{max})_t$ is in units of g; and $(G/G_{max})_{\gamma_{tv}}$ = normalized shear modulus reduction ratio of the soil corresponding to γ_{tv} . Similar to the discussion above regarding to whether the 0.65 factor should be included in Eq. 5, excluding this factor in deriving the expression for $(a_{max})_t$, results in:

$$(a_{max})_t^* = 0.0001 \frac{G_{max}(G/G_{max})_{\gamma_{tv}}}{\sigma_v r_d} \quad (12)$$

where the “*” is added to $(a_{max})_t$ to distinguish this value of threshold peak ground surface acceleration from the value computed using Eq. 11.

2.4.3 Excess Pore Pressure Generation for $\gamma_c > \gamma_{tv}$

Step 3 of the Dobry et al. (1982) strain-based procedure considers the scenario when $\gamma_c > \gamma_{tv}$. For this scenario, excess pore pressures will develop in the soil, and the magnitude of the generated excess pore pressures need to be estimated to determine whether liquefaction will be triggered. Per the Dobry et al. (1982) procedure, strain-controlled cyclic laboratory tests are required to be performed on undisturbed and/or specimens reconstituted to the same D_r as the soil in-situ. The result of the testing is a relationship such as that shown in Figure 2.1 for the specific soil, D_r , and n_{eq} of interest. As stated in the Introduction, the requirement to perform cyclic laboratory tests may be one reason why the strain-based approach has not been adopted into practice. In lieu of developing a relationship between r_u and γ_c from laboratory tests, herein it is proposed that strain-based numerical pore pressure generation models be used for this purpose. Specifically, the models proposed by Byrne (1991) and Vucetic and Dobry (1986) are used herein.

2.4.3.1 Byrne (1991) Excess Pore Water Pressure Model

Byrne (1991) simplified the Martin et al. (1975) strain-based pore pressure generation model, which relates the increment of volumetric strain that would occur under drained conditions in a soil having a given D_r subjected to a half cycle of loading of amplitude γ_c to the increment in excess pore water pressure that would have been generated in the soil under undrained conditions. Byrne (1991) proposed the following expression for computing the volumetric strain that would occur under drained conditions in a soil having a given D_r subjected to a half cycle of loading of amplitude γ_c :

$$(\Delta\varepsilon_v)_{1/2 \text{ cycle}} = 0.5 \cdot (\gamma_c - \gamma_{tv}) \cdot C_1 \cdot e^{\left\{-C_2 \frac{\varepsilon_v}{(\gamma_c - \gamma_{tv})}\right\}} \quad (13a)$$

where: $(\Delta\varepsilon_v)_{1/2 \text{ cycle}}$ is the increment in volumetric strain resulting from the i^{th} half cycle of loading; ε_v is the accumulated volumetric strain at the end of the $(i-1)$ half cycle of loading; γ_c is the amplitude of the induced shear strain in the soil subjected to the i^{th} half cycle of loading; and C_1 and C_2 are calibration coefficients. Although not consistent with the value of γ_{tv} proposed by Dobry et al. (1982), Byrne (1991) recommends that $\gamma_{tv} = 0.00005$ m/m, and thus, this value is used in implementing the model herein.

Byrne (1991) showed that C_1 and C_2 are correlated and are a function of D_r , or penetration resistance, and proposed the following expressions for the coefficients for clean sands:

$$C_1 = 8.7 \cdot (N_{1,60})^{-1.25} \quad (13b)$$

$$C_2 = 0.4/C_1 \quad (13c)$$

where $N_{1,60}$ normalized SPT penetration resistance. The volumetric strain that occurs in a given soil sample subjected to a half cycle of loading under drained conditions is related to the excess pore pressure that would be generated in the soil sample under undrained conditions, $(\Delta u)_{1/2 \text{ cycle}}$, via the constrained modulus (M):

$$(\Delta u)_{1/2 \text{ cycle}} = M \cdot (\Delta\varepsilon_v)_{1/2 \text{ cycle}} \quad (13d)$$

Byrne (1991) recommends the following relationship to estimate M :

$$M = K_m P_a \left(\frac{\sigma'_v}{P_a} \right)^m \quad (13e)$$

where σ'_v is the effective stress at the end of the (i-1) half cycle of loading; P_a is atmospheric pressure; and K_m and m are calibration coefficients. Byrne (1991) found that $K_m \approx 1600$ and $m \approx 0.5$ give moduli that are in good agreement with values reported by Martin et al. (1975) as well as results of liquefaction tests.

The excess pore water pressure, and corresponding r_u , that is generated in the soil sample after $n_{eq\gamma}$ cycles of loading (or $2 \times n_{eq\gamma}$ half cycles of loading) are given as:

$$\Delta u = \sum_1^{2 \cdot n_{eq\gamma}} (\Delta u)_{1/2 \text{ cycle}} \quad (13f)$$

$$r_u = \frac{\Delta u}{\sigma'_{vo}} \leq 1.0 \quad (13g)$$

2.4.3.2 Vucetic and Dobry (1986) Model

Vucetic and Dobry (1986) developed an empirical relationship among r_u , γ_c , and $n_{eq\gamma}$ from undrained, strain-controlled cyclic shear test data on clean sands. Their model is given as:

$$r_u = \frac{p \cdot f \cdot n_{eq\gamma} \cdot F \cdot (\gamma_c - \gamma_{tv})^s}{1 + f \cdot n_{eq\gamma} \cdot F \cdot (\gamma_c - \gamma_{tv})^s} \quad (14)$$

where: r_u = residual excess pore pressure ratio after $n_{eq\gamma}$ cycles of applied loading; $f = 1$ or 2 for one- or two-dimensional loading, respectively; and p , F , and s are curve-fitting constants. The variable f was taken to be unity in this study because the Lasley et al. (2017) correlation for $n_{eq\tau}$ combines the influence of both horizontal components of motion. Again, despite its questionable applicability for use in a strain-based liquefaction evaluation procedure, the $n_{eq\tau}$ relationship proposed by Lasley et al. (2017) is used herein because it was more rigorously developed than

other existing $n_{eq\tau}$ and $n_{eq\gamma}$ relationships and none of the alternative relationships are anymore applicable for use in the strain-based liquefaction procedure than the Lasley et al. relationship.

Mei et al. (2015) proposed empirical correlations for the three curve-fitting parameters (p , F , and s) to avoid the need of performing laboratory cyclic testing to calibrate the model. Mei et al. suggested setting $p = 1$ and $s = 1$ based on the analysis of data from laboratory cyclic tests that they performed and from others (Dobry et al., 1985; Vucetic and Dobry, 1986; and Matasovic, 1993). Additionally, Mei et al. (2015) developed a correlation among F , D_r , and C_u . They noted that F reflects the rate of Δu generation and should be inversely related to D_r and directly related to C_u . Figure 2.4 shows their proposed correlation for clean, subangular to subrounded silica sands.

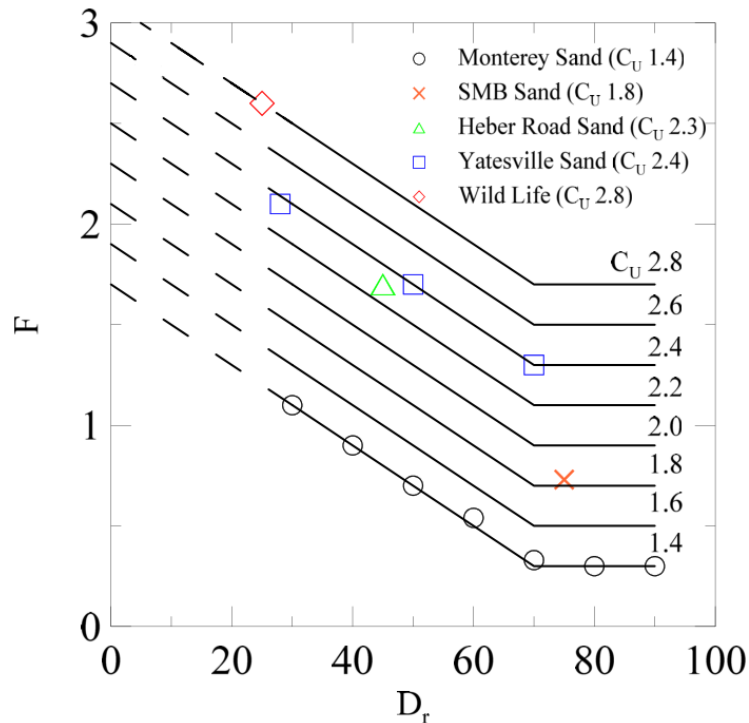


Figure 2.4 Proposed correlation to estimate curve-fitting parameter F for the Vucetic and Dobry (1986) model (Mei et al., 2015).

Alternatively, F can be estimated using the correlation proposed by Carlton (2014), which related F to V_s . This correlation is shown in Figure 2.5.

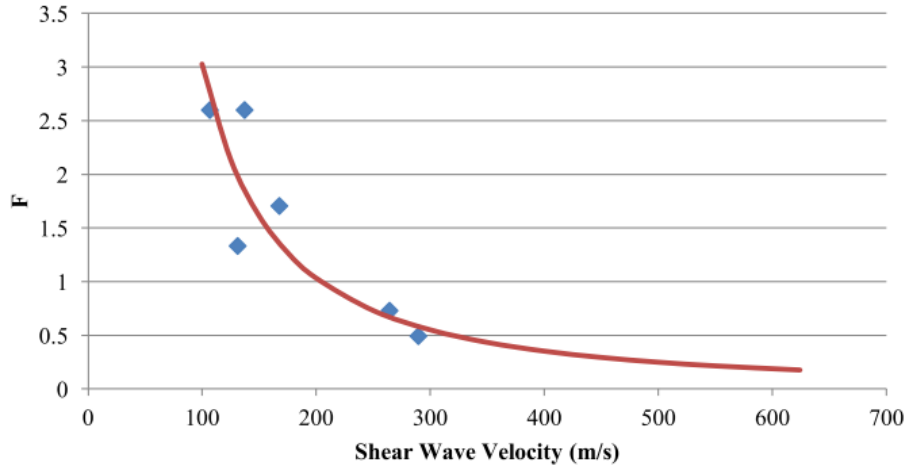


Figure 2.5 Correlation between F and V_s (Matasovic and Ordóñez, 2012; Carlton, 2014).

Mei et al. (2105) refer to Dobry et al. (1982), stating that γ_{lv} is usually between 0.01 and 0.02% for most sands. Herein, $\gamma_{lv} = 0.01\%$ is assumed in implementing the Vucetic and Dobry (1986) model.

2.4.3.3 Comparison of the Byrne (1991) and Vucetic and Dobry (1986) Models

A plot of the Byrne (1991) and Vucetic and Dobry (1986) cyclic strain models calibrated for a clean sand having a $D_r = 60\%$, $\sigma'_{vo} = 100$ kPa, and $n_{eq\gamma} = 10$ is shown in Figure 2.6. Also plotted in this figure is the curve previously plotted in Figure 2.1 (Dobry et al., 1982). As may be observed from Figure 2.6, the Byrne (1991) and Vucetic and Dobry (1986) models, respectively, represent approximate upper and lower bounds of the data. Figure 2.7 shows a further comparison of the two models for loose ($D_r = 30\%$) and medium dense ($D_r = 60\%$) soils having $\sigma'_{vo} = 100$ kPa for increasing values of $n_{eq\gamma}$. Similar to Figure 2.6, the curves in Figure 2.7 show that the Byrne (1991) model predicts a faster Δu generation rate than the Vucetic and Dobry (1986) model does. Additionally, as expected, for both models r_u increases more rapidly in looser soils than denser soils when subjected to the same loading. Also, for a given sample subject to a given amplitude γ_c , r_u increases as $n_{eq\gamma}$ increases.

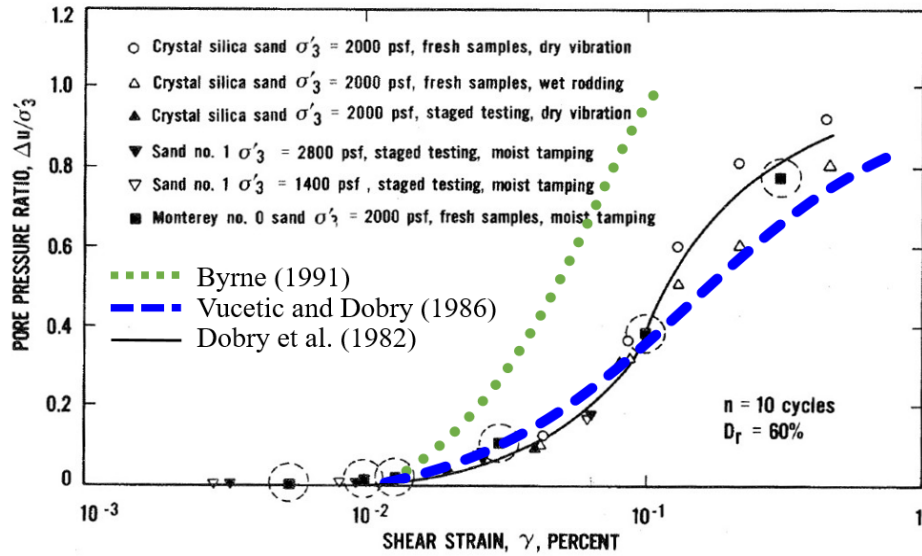


Figure 2.6 Comparison of pore pressure generation models, with $C_u = 2.1$ for the Vucetic and Dobry (1986) model, to experimental data from Dobry et al. (1982) for strain-controlled cyclic triaxial tests performed on samples having $D_r = 60\%$.

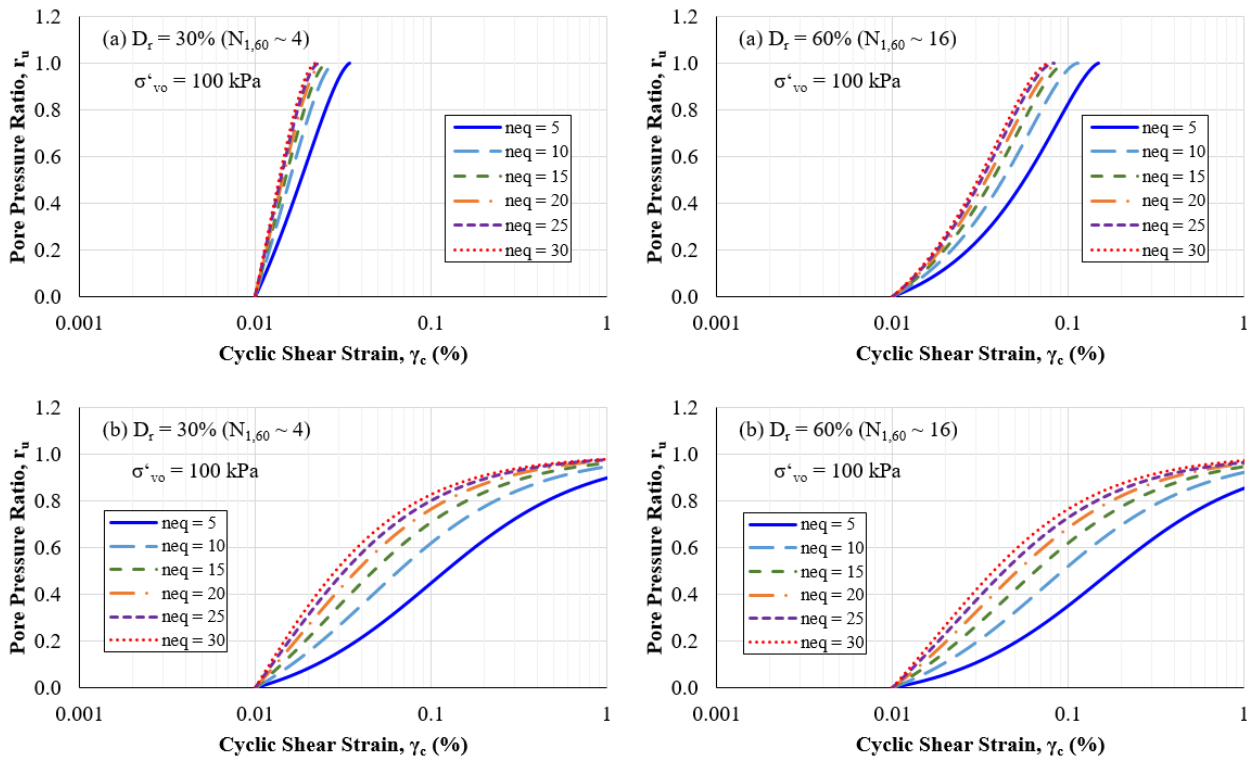


Figure 2.7 Curves of pore pressure ratio versus cyclic shear strain at different numbers of equivalent cycles for loose and medium dense soils using the: (a) Byrne (1991) model; and (b) Vucetic and Dobry (1986) model.

2.4.4 Assessing Whether Liquefaction is Triggered

The final step in the Dobry et al. (1982) strain-based procedure (i.e., Step 4) is to evaluate whether liquefaction is triggered. Dobry et al. (1982) defined liquefaction as $r_u = 1$; therefore, a value of r_u computed from Step 3 that is less than 1 implies that liquefaction is not triggered. However, depending on the density of the soil, $r_u < 1$ can still result in damage to nearby infrastructure. Accordingly, for looser soils, defining liquefaction by an $r_u \leq 1.0$ would be appropriate.

2.4.5 Analyzing Field Case Histories

The efficacy of the alternative implementation of the Dobry et al. (1982) strain-based procedure is assessed by analyzing field case histories compiled by Kayen et al. (2013) and Boulanger et al. (2012). By evaluating field case histories, the efficacy of the strain-based procedure can be assessed both in an absolute sense (i.e., with respect to field observations) and in a relative sense (i.e., relative to the efficacy of the stress-based procedures). Additionally, using the two types of liquefaction case history databases (V_s : Kayen et al., 2013; SPT: Boulanger et al., 2012) in the assessment process allows the significance on the computed results of using one type of in-situ test metric to estimate other needed parameters versus using the other type of in-situ test metric.

Both the Kayen et al. (2013) and the Boulanger et al. (2012) databases include information about a_{max} , σ'_{vo} , σ_v , and depth of the critical layer for each case histories. The approaches used to estimate the other required parameters are discussed in the following sections on the respective case history databases. Also, additional information about the liquefaction case history databases used in this study is provided in Appendix A.

2.4.5.1 Kayen et al. (2013), V_s Database

The Kayen et al. (2013) V_s liquefaction case history database is composed of 415 case histories, where V_s measurements were mainly made using the spectral analysis of surface waves method (SASW). Out of the 415 cases, 287 were catalogued as “Liquefaction” cases, 124 were catalogued as “No Liquefaction” cases, and four cases were considered to be on the margin between liquefaction and no liquefaction (i.e., “Marginal” cases). The case histories are from 34

earthquakes from sites in Japan (223 cases), the United States (105 in California, 24 in Idaho, and 9 in Alaska), China (30), Taiwan (20), Greece (2), and Turkey (2). Some of these sites are the same ones compiled in the SPT database by Cetin et al. (2000) and the Cone Penetration Test (CPT) database by Moss et al. (2003). Figure 2.8 shows a histogram for the database in terms of earthquake magnitude and liquefaction occurrence.

To implement the alternative form of the Dobry et al. (1982) strain-based procedure to evaluate the V_s case histories, the following parameters need to be estimated:

- Total unit weight (γ_t) of the critical layer to compute G_{max} from the listed value of V_s .
- Normalized SPT penetration resistance ($N_{1,60}$) to compute C_1 and C_2 for the Byrne (1991) excess pore water pressure generation model.

Small strain shear wave velocity and G_{max} are related by the following expression:

$$G_{max} = \left(\frac{\gamma_t}{g}\right) V_s^2 \quad (15)$$

However, the Kayen et al. (2013) database does not list values of γ_t for the critical layer. Assuming that most of the soils below the ground water table depth found at the case history sites were sands or silty sands, the values of γ_t were approximated in the range from 16 to 20.5 kN/m³ (100 to 130 lbs/ft³) to match the reported values of σ'_{v0} and σ_v listed in the database.

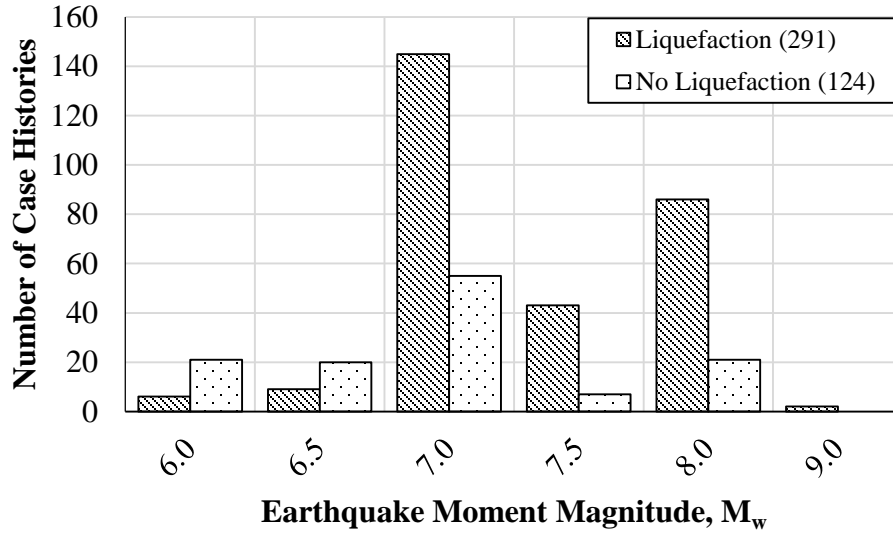


Figure 2.8 Histogram of the Kayen et al. (2013) Vs database.

To estimate SPT-N value converted to a uniform reference energy ratio of 60% of the theoretical SPT energy (i.e., N_{60}) from V_s , the relationship proposed by Wair et al. (2012) for all Holocene aged soils was used:

$$V_s = 26.0 \cdot N_{60}^{0.215} \cdot \sigma'_{vo}{}^{0.275} \quad (16)$$

where V_s is in m/sec; and σ'_{vo} is in kPa. Once N_{60} was determined, $N_{1,60}$ needed to determine C_1 and C_2 for the Byrne (1991) excess pore water pressure generation model, was computed using the following relationship:

$$N_{1,60} = C_N \cdot N_{60} \quad (17a)$$

where: C_N normalizes N_{60} to an effective overburden pressure of approximately 1 atm and is given by (Liao and Whitman, 1986):

$$C_N = \left(\frac{P_a}{\sigma'_{vo}}\right)^{0.5} \leq 1.7 \quad (17b)$$

where P_a has the same units as σ'_{vo} .

2.4.5.2 Boulanger et al. (2012), SPT Database

In addition to the Kayen et al. (2013) V_s database, the Boulanger et al. (2012) SPT database was also analyzed in this study. The Boulanger et al. (2012) database is composed of 230 case histories, where 115 were catalogued as “Liquefaction” cases, 112 were catalogued as “No Liquefaction” cases, and three cases were considered “Marginal.” The case histories are from 22 earthquakes from sites in Japan (150 cases), the United States (59 in California), China (11), Argentina (5), Guatemala (3), and Philippines (2). Figure 2.9 shows a histogram for the database in terms of earthquake magnitude and liquefaction occurrence.

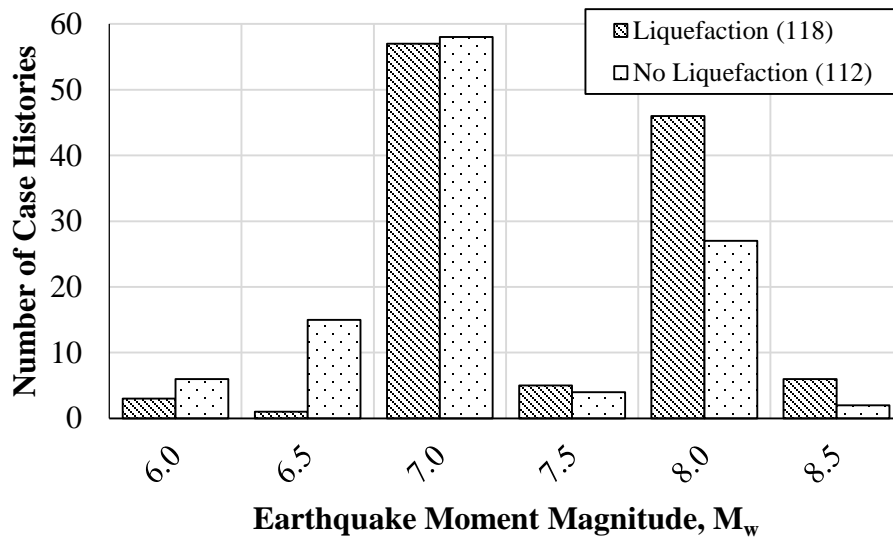


Figure 2.9 Histogram of the Boulanger et al. (2012) SPT database.

To implement the alternative form of the Dobry et al. (1982) strain-based procedure to evaluate the SPT case histories, the following parameters need to be estimated:

- G_{max} to compute γ_c .

- D_r and C_u to determine the F parameter for the Vucetic and Dobry (1986) excess pore pressure generation model using the correlation proposed by Mei et al. (2015).

Eq. 16 was used to estimate V_s for each of the SPT case histories (Wair et al., 2012). Eq. 15 was then used to compute G_{max} , where γ_t was estimated using the same approach outlined above for the V_s case histories. The following relationship presented by Idriss and Boulanger (2008) for sands was used to obtain D_r from $N_{1,60}$:

$$D_r = \sqrt{\frac{N_{1,60}}{46}} \quad (18)$$

where: σ'_{vo} is in kPa; and D_r is constrained between 30% and 90%. For all cases, an average value of $C_u = 2.1$ was assumed.

To account for fines in the soil, the “clean sands” correction was applied to $N_{1,60}$ (i.e., $N_{1,60cs}$) and used in all relationships to estimate the needed parameters. However, due to the uncertainty in the appropriateness of this approach, a subset of the SPT case histories that have a $FC \leq 5\%$ was analyzed separately from the entire SPT database. This subset consisted of 116 cases: 62 Liquefaction cases and 54 No Liquefaction cases.

2.5 Results

As outlined in the previous section, Step 1 of the alternative implementation of the Dobry et al. (1982) strain-based procedure entails computing γ_c and $n_{eq\gamma}$. Next, in Step 2 γ_c and γ_{tv} are compared, and if $\gamma_c < \gamma_{tv}$ then no excess pore pressures are predicted to develop and the procedure comes to an end. However, if $\gamma_c > \gamma_{tv}$, the procedure proceeds to Step 3 where γ_c and $n_{eq\gamma}$ from Step 1 are used in conjunction with the numerical pore water pressure generation models to estimate r_u . Finally, Step 4 entails determining if liquefaction is predicted to trigger based on the computed r_u values from Step 3. The results for this procedure applied to the Kayen et al. (2013) V_s database and the Boulanger et al. (2012) SPT database are presented in this section.

2.5.1 Determination of γ_c and $n_{eq\gamma}$

To compute γ_c and γ_c^* for each case history, it was necessary to use an iterative approach in conjunction with the shear modulus degradation curves. Example results are shown for two of the case histories in Figure 2.10 using the Ishibashi and Zhang (1993) relationship. In implementing the iteration algorithm to compute γ_c , a maximum cap of 3% was imposed. This was done because it is doubtful that strains larger than this were induced in-situ solely as a result of earthquake shaking and the validity of the shear modulus degradation curves become questionable at larger strains. Appendix B provides the shear modulus degradation curves for all the case histories in the Kayen et al. (2013) and Boulanger et al. (2012) databases showing their corresponding converged values of γ_c and γ_c^* . Plots of the γ_c and γ_c^* values for all the case histories as a function of V_s (for the case histories in Kayen et al., 2013) and $N_{1,60cs}$ (for the case histories in Boulanger et al., 2012) are shown in Figures 2.13 and 2.14.

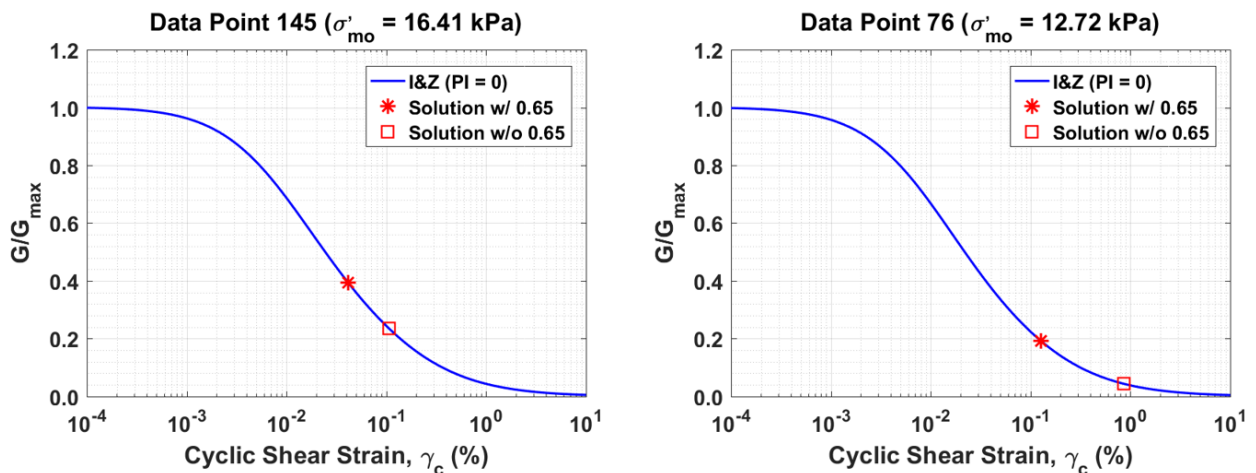


Figure 2.10 Example of the converged solutions of cyclic shear strain using the Ishibashi and Zhang (1993) shear modulus degradation curves with two case histories from the Kayen et al. (2013) database.

Eq. 9, proposed by Lasley et al. (2017), was used to compute $n_{eq\tau}$ for each case history, consistent with the inherent assumption made Dobry et al. (1982) wherein $n_{eq\gamma}$ and $n_{eq\tau}$ are equivalent. The results are presented as a function of a_{max} and M_w in Figures 2.11 and 2.12 for the Kayen et al. (2013) and Boulanger et al. (2012) databases, respectively.

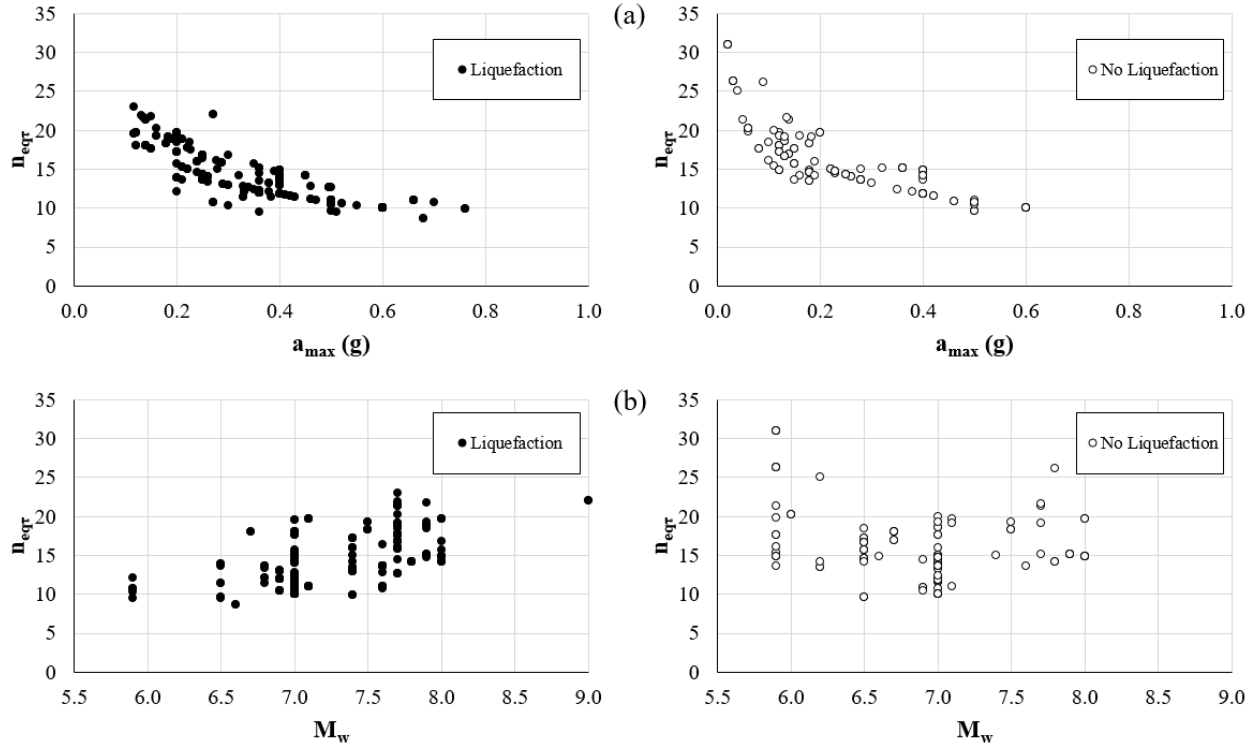


Figure 2.11 Results of n_{eqr} for the Kayen et al. (2013) database as a function of (a) a_{max} and (b) M_w .

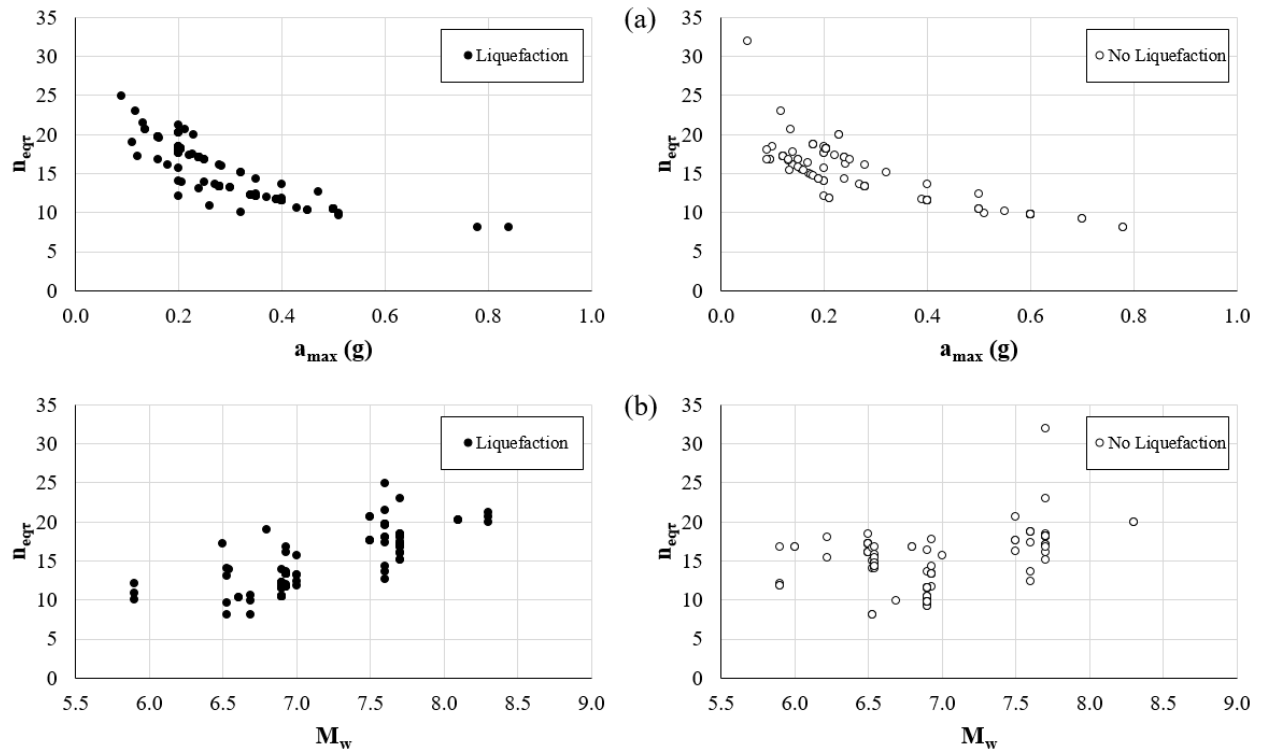


Figure 2.12 Results of n_{eqr} for Boulanger et al. (2012) database as a function of (a) a_{max} and (b) M_w .

2.5.2 Threshold Shear Strain (γ_{IV}) and Threshold Peak Ground Acceleration, (a_{max})_t

As stated in the previous section, the computed γ_c and γ_c^* for both Kayen et al. (2013) and Boulanger et al. (2012) databases are shown in Figures 2.13 and 2.14. As may be observed from Figure 2.13, the γ_c below which there are no “Liquefaction” cases are 0.03% and 0.05% for the Kayen et al. and Boulanger et al. databases, respectively (Table 2.1). On the other hand, Figure 2.14 shows that these limiting γ_c^* values are 0.075% and 0.115% for the Kayen et al. and Boulanger et al. databases, respectively (Table 2.1). Note, however, these values of γ_c and γ_c^* conceptually are not synonymous to γ_{IV} because it is unknown whether any pore pressures were generated in some of the “No Liquefaction” cases having γ_c and γ_c^* less than these values. Also, the relative magnitudes of the limiting γ_c values are more consistent with the laboratory determined value of γ_{IV} (i.e., $\gamma_c = 0.03\%$ to 0.05% versus $\gamma_{IV} \approx 0.01\%$) than the limiting values of γ_c^* .

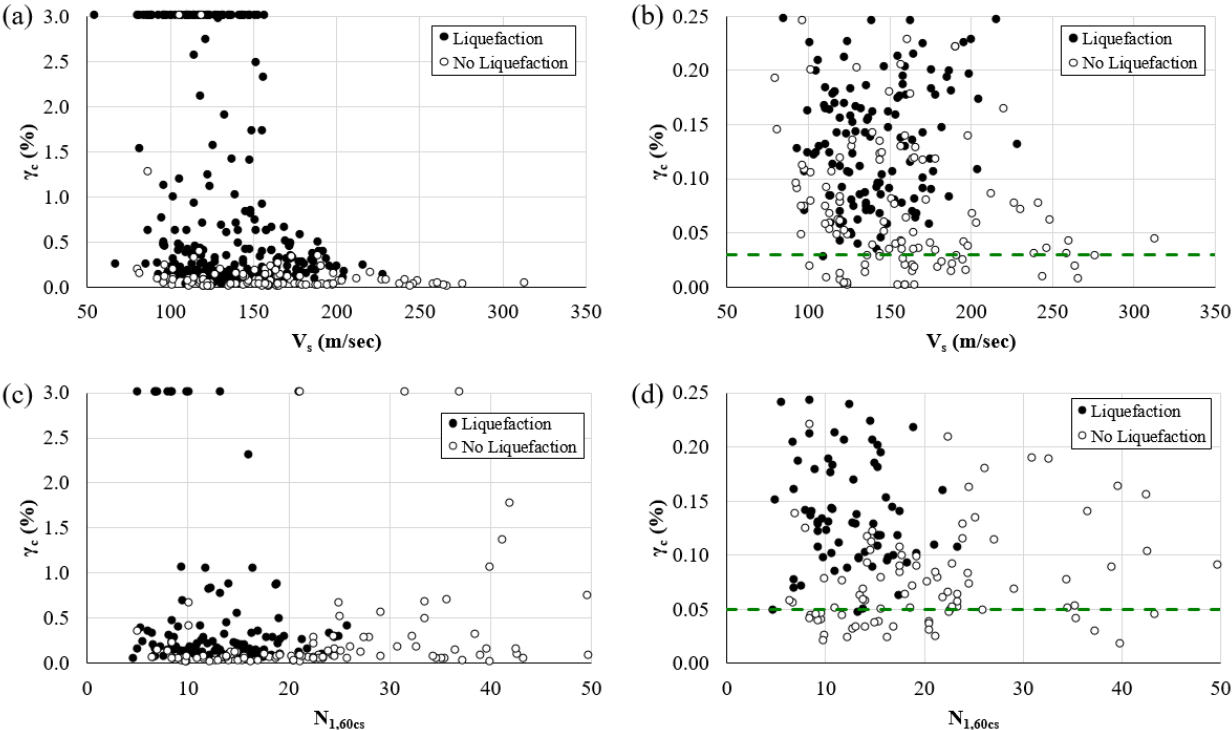


Figure 2.13 (a) & (b) γ_c versus V_s for the Kayen et al. (2013) database; and (c) & (d) γ_c versus $N_{1,60cs}$ for the Boulanger et al. (2012) database; (b) and (d) are zoomed-in plots of (a) and (c).

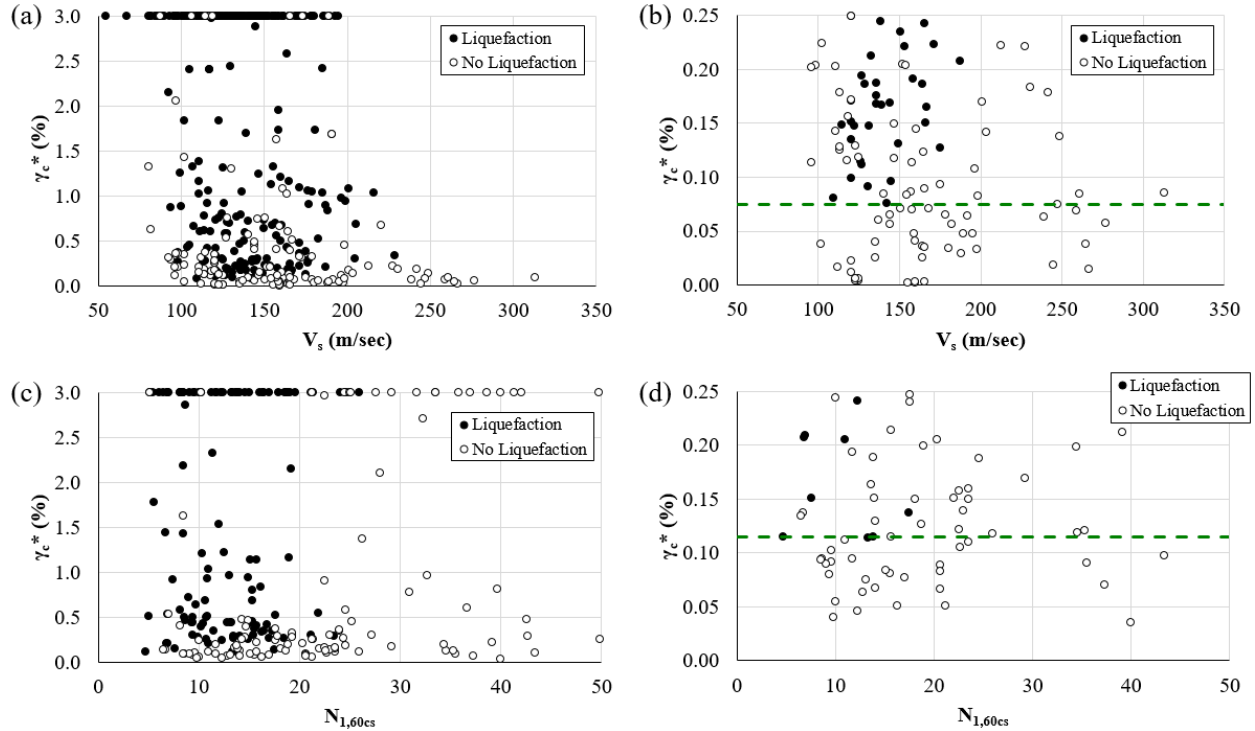


Figure 2.14 (a) & (b) γ_c^* versus V_s for the Kayen et al. (2013) database; and (c) & (d) γ_c^* versus $N_{1,60cs}$ for the Boulanger et al. (2012) database; (b) and (d) are zoomed-in plots of (a) and (c).

As stated previously, to provide a simple and fast screening method to determine whether or not the cyclic shear strain exceeds the threshold strain, the threshold peak ground surface acceleration can be compared with the a_{max} for the design earthquake motions. Figure 2.15 shows a plot of the a_{max} values as a function of M_w for the case histories in the Kayen et al. (2013) and Boulanger et al. (2012) databases. As may be observed from this figure, the lowest a_{max} values for Liquefaction cases are approximately 0.12 and 0.09 g in the V_s and SPT databases, respectively. In comparison, the limiting values of $(a_{max})_t$ and $(a_{max})_t^*$ computed using Eq. 11 and Eq. 12, respectively, for the Kayen et al. (2013) database are 0.12 and 0.08 g and for the Boulanger et al. (2012) database are 0.08 g and 0.055 g. The limiting a_{max} values are very consistent with the limiting $(a_{max})_t$ values for both databases.

A summary of the computed γ_c , γ_c^* , a_{max} , $(a_{max})_t$, and $(a_{max})_t^*$ values for both the Kayen et al. (2013) V_s database and the Boulanger et al. (2012) SPT database are listed in Table 2.1.

Table 2.1 Values for the upper limits of γ_{tv} and $(a_{max})_t$

Database	γ_c (%)	γ_c^* (%)	a_{max} (g)	$(a_{max})_t$ (g)	$(a_{max})_t^*$ (g)
Kayen et al. (2013)	0.03	0.075	0.12	0.12	0.08
Boulanger et al. (2012)	0.05	0.115	0.09	0.08	0.055

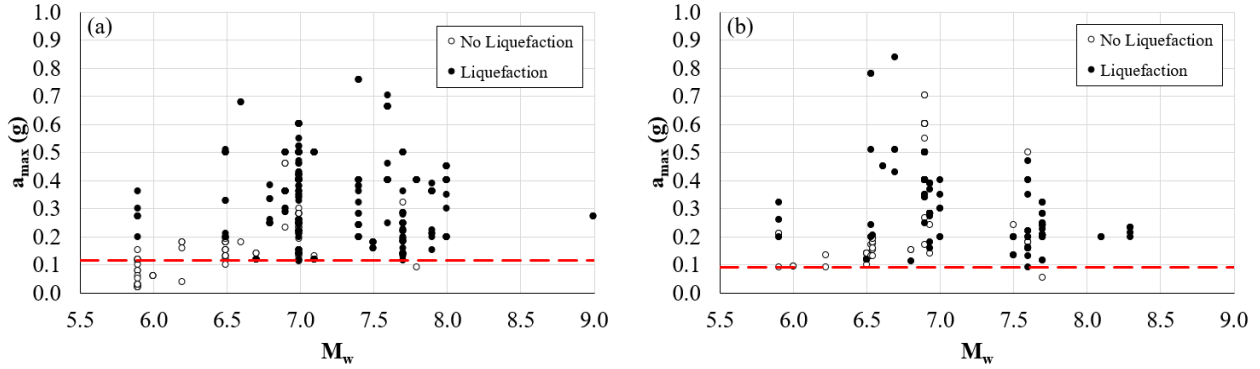


Figure 2.15 Plots of a_{max} versus M_w for: (a) the Kayen et al. (2013) V_s database; and (b) the Boulanger et al. (2012) SPT database.

2.5.3 Excess Pore Pressure Generation for $\gamma_c > \gamma_{tv}$

For the cases where $\gamma_c > \gamma_{tv}$, the Byrne (1991) and Vucetic and Dobry (1986) pore pressure generation models are used in conjunction with the Lasley et al. (2017) $n_{eq\tau}$ relationship to estimate r_u for the case histories compiled in the Kayen et al. (2013) and Boulanger et al. (2012) databases. In this study, the “Marginal” liquefaction case histories in the two databases (seven in total for the two databases) were treated as “Liquefaction” cases to simplify the reporting of results with a binary denomination of either “Liquefaction” or “No Liquefaction.” Also, note that the Lasley et al. (2017) $n_{eq\tau}$ relationship was developed for use in evaluating liquefaction in conjunction with Eq. 1, which has the 0.65 factor in it. Accordingly, when using this $n_{eq\tau}$ relationship in conjunction with the strain-based procedure, Eq. 5 should be used to compute the cyclic strain and not Eq. 10 (i.e., γ_c , not γ_c^*) for use with the numerical pore pressure generation models to estimate r_u .

For the case histories in the Kayen et al. (2013) V_s database, the Wair et al. (2012) relationship is used to estimate N_{60} , from which $N_{1,60}$ is computed. Then, $N_{1,60}$ is used to determine the calibration coefficients for the Byrne (1991) model, while the Carlton (2014) relationship is used to obtain F to calibrate the Vucetic and Dobry (1986) model. Sample results for case histories having low (100 – 120 m/sec) and high (200 – 314 m/sec) V_s values are plotted in Figures 2.16 and 2.17 for r_u

values computed using the Byrne (1991) and Vucetic and Dobry (1986) pore pressure generation models, respectively. A complete presentation of the r_u computed for all the case histories in the Kayen et al. (2013) database is given in Appendix C.

As may be observed from Figures 2.16 and 2.17, the case histories are grouped in bins based on n_{eqT} (i.e., duration of cyclic loading). However, the cases are not separated based on σ'_{vo} because laboratory test results presented in Dobry et al. (1982) showed that the vertical effective stress did not affect r_u generation for strain controlled loading. Also, the cases for $M_w > 7.9$ are identified with a distinct marker since the Lasley et al. (2017) n_{eqT} correlation was not developed for these large magnitude events. Consistent with the trends shown in Figures 2.6 and 2.7, the Byrne (1991) predicts higher r_u values for the case histories than does the Vucetic and Dobry (1986) model.

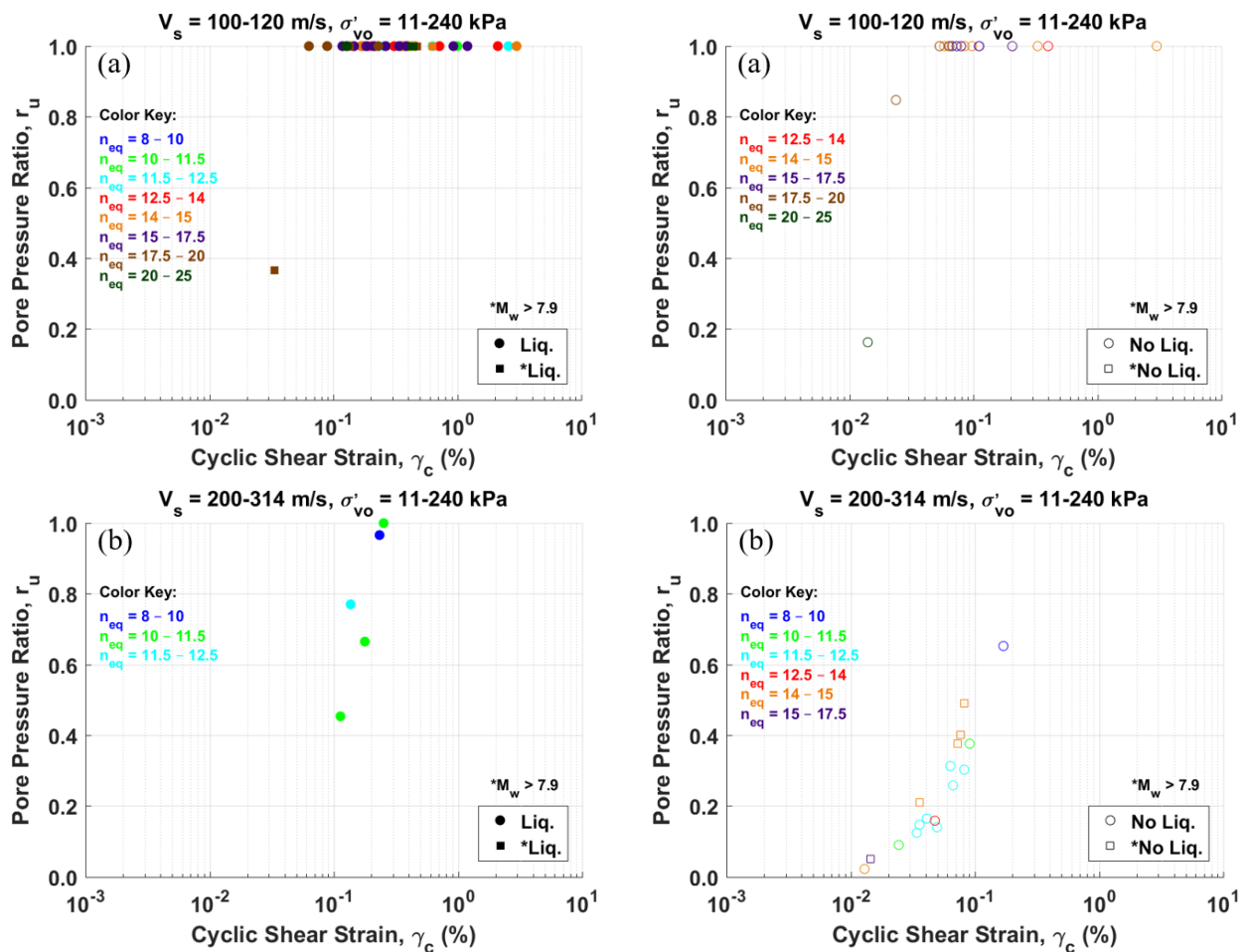


Figure 2.16 Estimated r_u computed using the Byrne (1991) model for sample case histories from the Kayen et al. (2013) V_s database: (a) $V_s = 100-120$ m/sec; and (b) $V_s = 200-314$ m/sec.

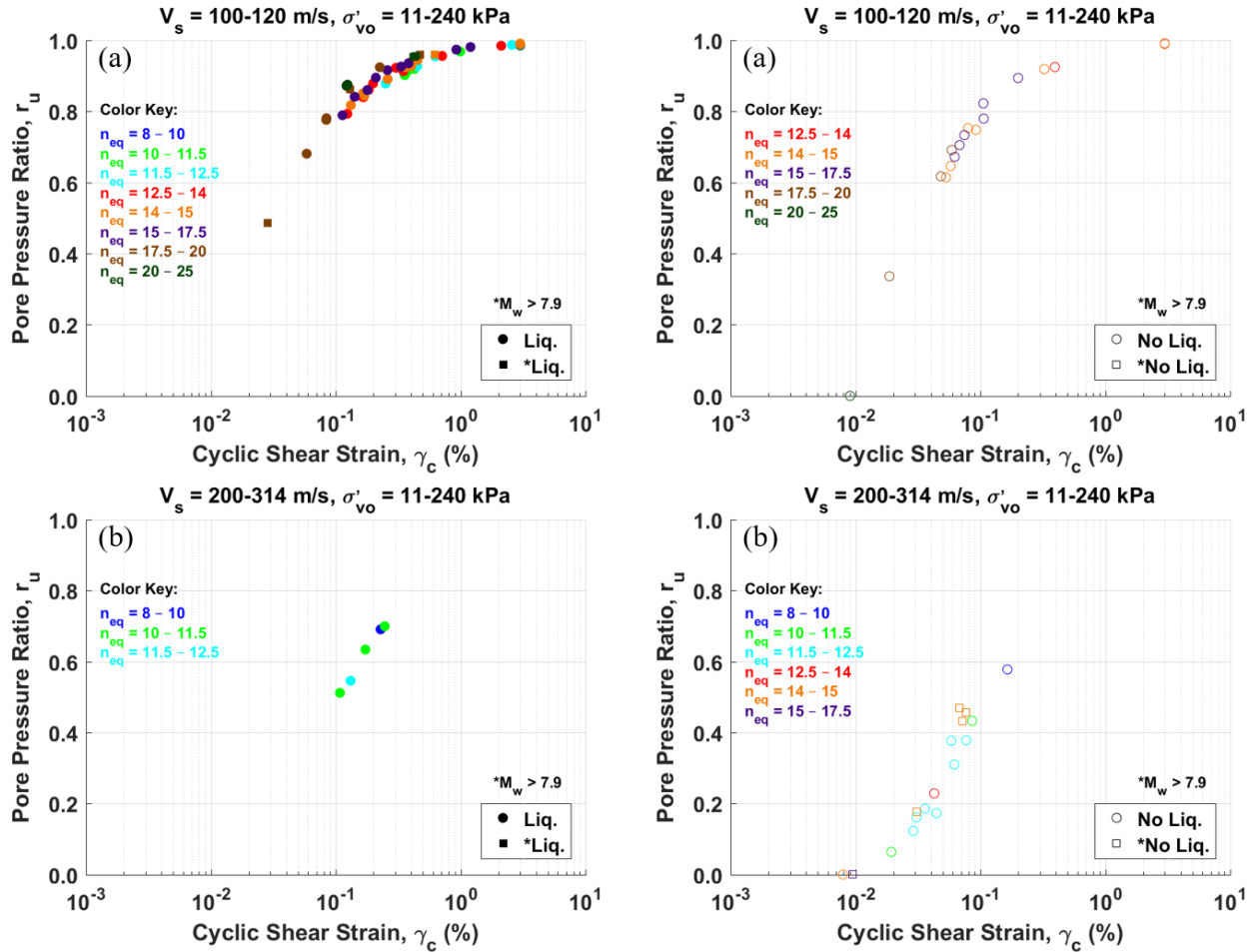


Figure 2.17 Estimated r_u computed using the Vucetic and Dobry (1986) model for sample case histories from the Kayen et al. (2013) V_s database: (a) $V_s = 100\text{-}120$ m/sec; and (b) $V_s = 200\text{-}314$ m/sec.

Analogous plots to those in Figures 2.16 and 2.17 for the Kayen et al. (2013) V_s database are shown in Figures 2.18 and 2.19 for the Boulanger et al. (2012) SPT database. A complete presentation of the r_u computed for all the case histories in the Boulanger et al. (2012) database is given in Appendix D. In analyzing the SPT case histories, the Wair et al. (2012) correlation is used to estimate V_s values, which in turn are used to compute G_{\max} values that are needed to compute γ_c per Eq. 5. The calibration coefficients for the Byrne (1991) excess pore pressure generation model can be determined directly from $N_{1,60cs}$ values, so no additional correlations are required. However, both D_r and C_u need to be estimated to determine the calibration coefficients for the Vucetic and Dobry (1986) excess pore pressure generation model. As stated previously, Eq. 18 (Idriss and Boulanger, 2008) is used to estimate D_r and an average value of C_u is assumed (i.e., C_u

= 2.1). Consistent with the trends shown in Figures 2.6, 2.7, 2.16, and 2.17, the Byrne (1991) model predicts higher r_u values for the case histories than does the Vucetic and Dobry (1986) model.

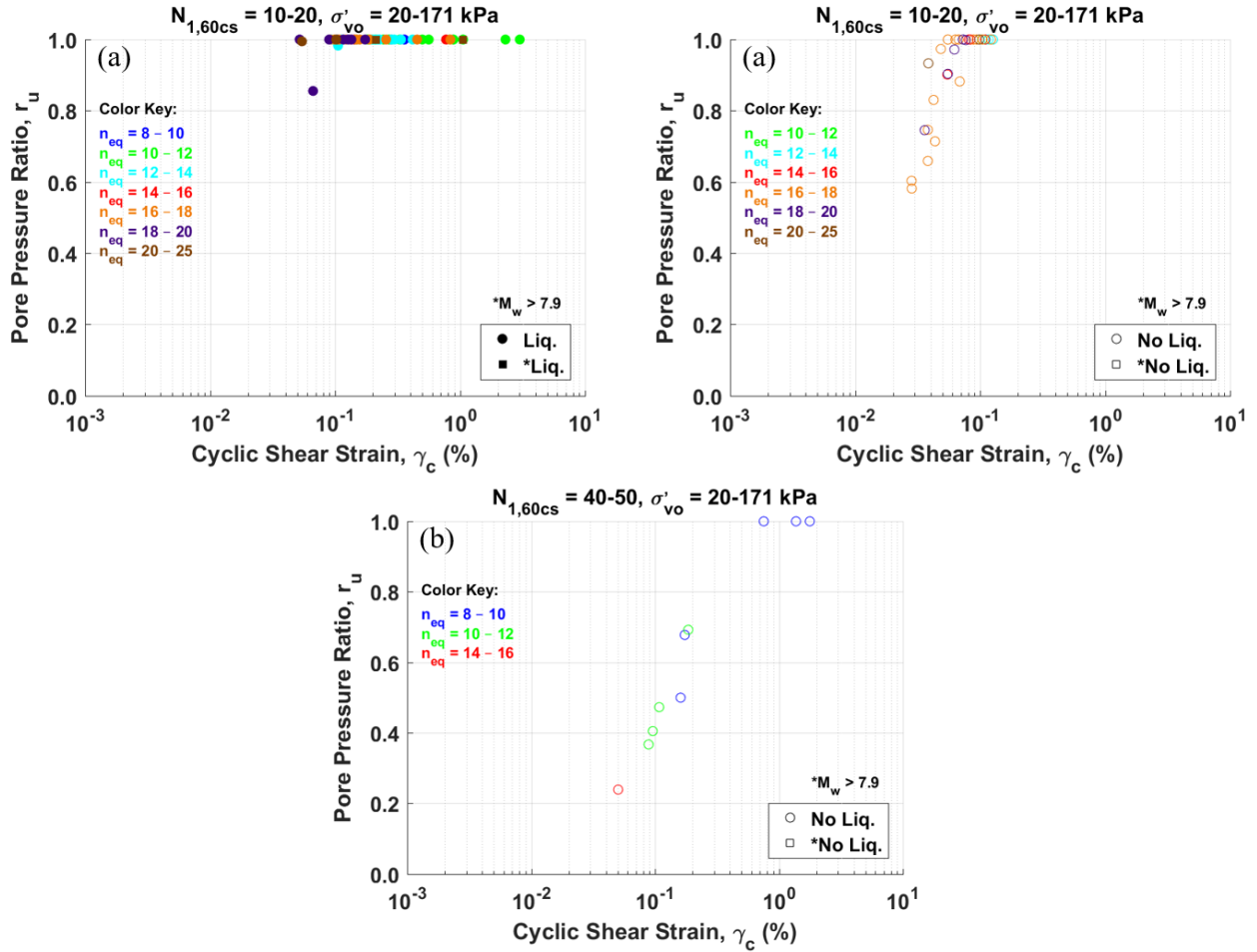


Figure 2.18 Estimated r_u computed using the Byrne (1991) model with the Boulanger et al. (2012) SPT database: (a) $N_{1,60cs} = 10-20$ blws/30 cm; and (b) $N_{1,60cs} = 40-50$ blws/30 cm.

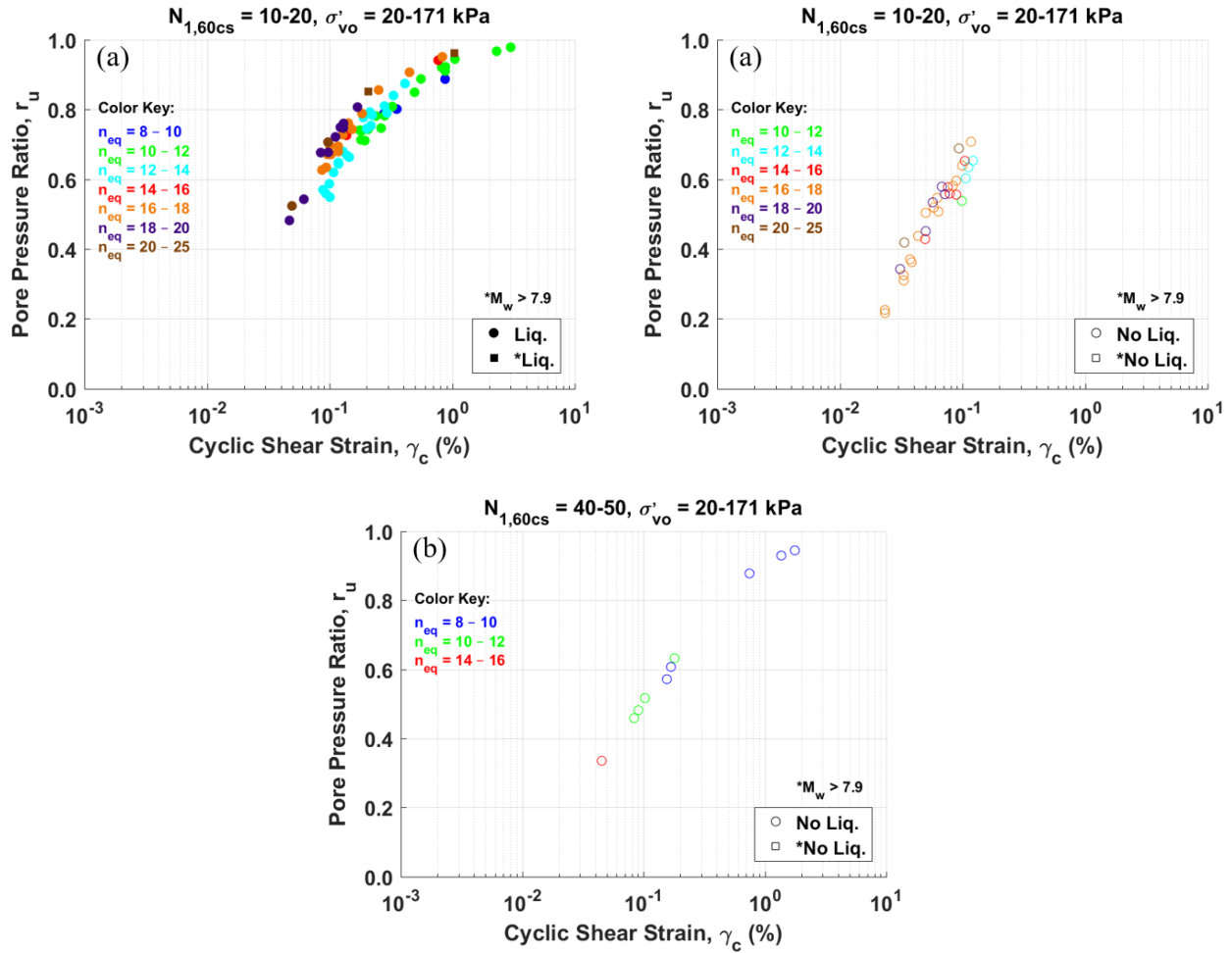


Figure 2.19 Estimated r_u computed using the Vucetic and Dobry (1986) model with the Boulanger et al. (2012) SPT database: (a) $N_{1,60cs} = 10-20$ blws/30 cm; and (b) $N_{1,60cs} = 40-50$ blws/30 cm.

2.5.4 Assessing Whether Liquefaction is Triggered

The final step in the alternative implementation of the Dobry et al. (1982) procedure is to assess the values of r_u computed in Step 3 to determine whether or not liquefaction is triggered. However, in interpreting the results from Step 3, the strict definition of liquefaction (i.e., $r_u = 1$) was relaxed some to a more pragmatic value of r_u that could potentially have damaging effects on nearby infrastructure. The criterion used to define liquefaction for the Byrne (1991) and Vucetic and Dobry (1986) models was $r_u = 0.95$. The results are listed in Table 2.2 in terms of True Positive, True Negative, False Positive, and False Negative, which are defined as:

- True Positive: liquefaction is predicted and was observed (i.e., it was a “Liquefaction” case).
- True Negative: liquefaction is not predicted and was not observed (i.e., it was a “No Liquefaction” case).
- False Positive: liquefaction is predicted but was not observed (i.e., it was a “No Liquefaction” case).
- False Negative: liquefaction is not predicted but was observed (i.e., it was a “Liquefaction” case).

Accordingly, True Positives and True Negatives are accurate predictions, False Positive is an inaccurate but conservative prediction, and False Negative is an inaccurate and unconservative prediction. Use of the Byrne (1991) model resulted in both more accurate, more conservative, and fewer unconservative predictions than those made using the Vucetic and Dobry (1986) model for both the V_s and SPT databases. When the Byrne (1991) model is used to analyze the SPT case histories, the results are less accurate but more conservative than when used to analyze the V_s case histories. Also of particular note is that most of the predictions made for the SPT case histories using the Byrne (1991) model were either accurate or conservative, in contrast to 11% of the predictions made for the V_s case histories that were inaccurate and unconservative.

Table 2.2 Predictions versus field observations using γ_c

Database	Kayen et al. (2013) (415 case histories)		Boulanger et al. (2012) (230 case histories)	
	Byrne (1991)	Vucetic and Dobry (1986)	Byrne (1991)	Vucetic and Dobry (1986)
True Positive	60%	24%	50%	6%
True Negative	16%	29%	20%	47%
False Positive	13%	1%	29%	1%
False Negative	11%	46%	1%	46%

2.6 Discussion

2.6.1 Cyclic Shear Strains and Number of Equivalent Cycles

As listed in Table 2.1, the limiting values of γ_c and γ_c^* (i.e., no Liquefaction case histories have γ_c and γ_c^* values below the limiting values) differ for the V_s and SPT databases, and differ from γ_{tv} . This could be due to the uncertainties in the various correlations used to estimate unknown

parameters needed to compute γ_c and γ_c^* . However, the ranges of the scenarios represented in the databases is limited (e.g., NRC, 2016), and as a result, the lack of robustness of both databases is likely the most contributing factor for having differing values of γ_c and γ_c^* for the two databases.

Specific to whether γ_c or γ_c^* should be compared to γ_{tv} , from a strict mechanics perspective, the author contends that γ_c^* should be used for this comparison. However, γ_c and γ_c^* are simply limiting values of the induced shear strain, where only No Liquefaction case histories have induced strains less than these limiting values. This is not to say that no excess pore water pressures developed in the No Liquefaction case histories that had induced strains less than the limiting values of γ_c and γ_c^* . Accordingly, using γ_c^* to compare with γ_{tv} to determine whether a more detailed liquefaction evaluation needs to be performed is conservative. From a pragmatic perspective using the limiting value of γ_c to compare with γ_{tv} may be more appropriate (i.e., less conservative than using the limiting value of γ_c^* , yet not unconservative from a liquefaction hazard perspective). Towards this end, from Figures 2.13 and 2.14 it can be observed that when $\gamma_c > 0.5\%$ liquefaction is very likely and when $\gamma_c < 0.03\%$ liquefaction is very unlikely, with this latter criterion being very consistent with the $\gamma_{tv} \approx 0.01\%$ proposed by Dobry et al. (1982).

Finally, the “simplified” procedure to compute γ_c proposed by Dobry et al. (1982) (i.e., Eq. 5) assumes that $G_{max} \times (G/G_{max})_{\gamma_c}$ is uninfluenced by the softening of the soil due to the generation of excess pore water pressures. However, this is known not to be the case when $\gamma_c > \gamma_{tv}$. Dobry et al. (1982) allude to this, stating that “...some additional research is needed to develop definite rules for computing γ_c .” The author actually views this as an inherent and fatal limitation of the strain-based procedure. The representation of chaotic earthquake ground motions in an “equivalently damaging” and simplified form requires the specification of the simplified motion’s amplitude (e.g., γ_c) and duration (e.g., $n_{eq\gamma}$). By assuming $G_{max} \times (G/G_{max})_{\gamma_c}$ is uninfluenced by the generation of excess pore water pressures in computing γ_c , then the softening of the soil due excess pore pressure generation needs to be accounted for in computing $n_{eq\gamma}$. However, assuming that $n_{eq\gamma}$ is equivalent to $n_{eq\tau}$, where the latter is computed using a “total stress” approach (e.g., Seed et al., 1975; Green and Terri, 2005), does not satisfy this need. Furthermore, to the author’s knowledge, no existing relationship $n_{eq\gamma}$ accounts for the softening effects of the soil due to excess pore water, nor has any framework been proposed in literature on how to compute $n_{eq\gamma}$ that accounts for the softening effects of the soil due to excess pore water.

As an alternative to requiring $n_{eq\gamma}$ to account for the softening effects due to excess pore water pressure, γ_c could be computed for each half cycle of loading using Eq. 5, wherein the effective confining stress used to compute $G_{max} \times (G/G_{max})_{\gamma_c}$, and hence γ_c , is updated to account for excess pore pressure generation each half cycle of loading. This would require that relationships such as that shown in Figure 2.1 be generated for $n_{eq\gamma} = 0.5$ cycles. This is certainly feasible, but in essence, this is what the Byrne (1991) strain-based pore pressure generation model does, with the Byrne (1991) model being more versatile than this potential form of the Dobry et al. (1982) strain procedure.

2.6.2 Threshold Strains and Accelerations

Dobry et al. (1982) performed a parametric study to compute $(a_{max})_t$ for loose and dense soils, assuming the same value of total unit weight of the soil above and below the water table of 18 kN/m^3 (115 pcf) and $(G/G_{max})_{ytv} = 0.75$. For the soil conditions that were most susceptible to liquefaction, the lowest value of $(a_{max})_t$ they computed was 0.05 g, compared to 0.08 – 0.12 g determined herein from the analysis of the Kayen et al. (2013) and Boulanger et al. (2012) databases. However, both of these sets of $(a_{max})_t$ values include the 0.65 factor, initially included in the simplified expression to estimate a CSR value that is representative of the peak seismic demand over the entire duration of shaking. Analyzing the case histories without the 0.65 factor applied, results in slightly lower range of threshold acceleration of 0.055 – 0.08 g. As with γ_c^* , from a strict mechanics perspective, the author contends that the 0.65 factor should not be applied in computing $(a_{max})_t$. However, from a pragmatic perspective in using $(a_{max})_t$ as a screening tool to determine whether a more detailed liquefaction evaluation needs to be performed, including the 0.65 factor could be justified because the likelihood is very low of triggering liquefaction that would be damaging to infrastructure for ground motions having a_{max} values as low as 0.08 – 0.12 g.

2.6.3 *Liquefaction Triggering Predictions*

Table 2.2 summarizes the statistics regarding the prediction accuracy of the alternative implementation of the Dobry et al. (1982) strain-based procedure using the Byrne (1991) and the Vucetic and Dobry (1986) numerical pore pressure generation models. The data in the table showed that the predictions made using the Byrne (1991) model were both more accurate, more conservative, and less unconservative than those made using the Vucetic and Dobry (1986) model. In comparing the efficacy of the strain-based procedure implemented for cases where V_s versus $N_{1,60cs}$ are known and other parameters are estimated, knowing $N_{1,60cs}$ yields less unconservative predictions. There are several possible reasons for this. First, $N_{1,60cs}$ better correlates to D_r than does V_s ; in contrast, V_s better correlates to void ratio (e.g., Richart et al., 1970) than $N_{1,60cs}$ does. As a result, two soils that have the same void ratio, but drastically different D_r , will likely have V_s values that are closer to each other than their $N_{1,60cs}$ values will be. Ultimately, D_r has more influence on a soil's liquefaction resistance than void ratio does, and hence, $N_{1,60cs}$ is likely a better in-situ test metric for correlating to liquefaction resistance than V_s is.

Second, in implementing the strain-based procedure for cases where V_s was known, N_{60} was estimated using the Eq. 16 (Wair et al., 2012). Because this expression is empirical, the details of how the regression was performed to develop the expression dictates whether it can be reliably used in a reverse implementation (i.e., used to estimate N_{60} for cases where V_s are known, as opposed to being used in forward implementation to estimate V_s for cases where N_{60} are known). As a result, the use of the Wair et al. (2012) relationship to estimate N_{60} for the V_s case histories is a shortcoming of how the author implemented the procedure and not a shortcoming of either the strain-based procedure or using V_s as an in-situ metric to characterize the soil.

Third, the Byrne (1991) and Vucetic and Dobry (1986) pore pressure generation models were developed for clean sands (i.e., sands with $FC \leq 5\%$). For the V_s case histories, FC were unknown and therefore ignored in implementing the strain-based procedure; this is clearly a shortcoming in implementing the procedure. However, for the SPT case histories, $N_{1,60cs}$ values (as opposed to $N_{1,60}$ values) were used to calibrate the pore pressure generation models. As mentioned previously, there is uncertainty about the appropriateness of doing this. To determine if this approach for accounting for FC impacted the accuracy of the strain-based procedure, a subset of the SPT case histories from Boulanger et al. (2012) that have $FC \leq 5\%$ was analyzed. This subset consisted of

116 cases (out of a total of 230 cases in the database): 62 “Liquefaction” cases and 54 “No Liquefaction” cases.

The prediction statistics for the clean sand SPT cases and the entire SPT database are presented in Table 2.3. A complete presentation of the r_u computed for all the case histories in the Boulanger et al. (2012) database, to include the subset having $FC \leq 5\%$ is given in Appendix D. As may be observed from Table 2.3, the overall accuracy of the procedure increases from 70% to 77% when only clean sand case histories are analyzed using the Byrne (1991) model, with the False Negative (i.e., unconservative predictions) percentage remaining essentially the same. This implies that developing calibration coefficients for the Byrne (1991) that are functions of FC will increase the prediction accuracy of the alternative implementation of the strain-based approach or that the “clean sands” correction applied to the $N_{1,60}$ need to be improved. Regardless, the accuracy of the strain-based procedure is not significantly influenced by the FC of the soil.

Table 2.3 Predictions versus field observations for both the strain- and stress-based procedures

Database	Kayen et al. (2013) (415 cases)			Boulanger et al. (2012) (230 cases)			Boulanger et al. (2012) FC \leq 5% (116 cases)		
	Byrne (1991)	Vucetic and Dobry (1986)	Stress	Byrne (1991)	Vucetic and Dobry (1986)	Stress	Byrne (1991)	Vucetic and Dobry (1986)	Stress
True Positive	60%	24%	68%	50%	6%	48%	52%	6%	52%
True Negative	16%	29%	19%	20%	47%	39%	25%	45%	38%
Accurate Predictions	76%	53%	87%	70%	53%	87%	77%	51%	90%
False Positive	13%	1%	11%	29%	1%	10%	21%	2%	8%
False Negative	11%	46%	2%	1%	46%	3%	2%	47%	2%
Incorrect Predictions	24%	47%	13%	30%	47%	13%	23%	49%	10%

Given that the strain-based procedure is being proposed as a potential alternative to the widely used stress-based procedures, the efficacy of the strain-based procedure needs to be compared with that of the stress-based procedures. Towards this end, the data from Table 2.2 is reproduced in Table 2.3, wherein the True Positive, True Negative, False Positive, and False Negative statistics

for both the Kayen et al. (2013) and the Idriss and Boulanger (2008) deterministic simplified stress-based procedures are also listed. From the values in Table 2.3, it can be observed that both of the stress-based procedures yield more accurate predictions (and hence less incorrect predictions) than the strain-based procedure, regardless of which numerical pore pressure generation model is used. However, it should be noted that the databases used to assess the efficacy of the stress-based procedure were essentially the same ones used to develop the CRR curves inherent to the procedures (i.e., the stress-based procedures were in essence “calibrated” using the databases), while this is not the case for the strain-base procedure. From this perspective the prediction statistics listed in Table 2.3 are inherently biased in favor of the stress-based procedures.

2.6.4 Future Work

Several shortcomings were identified in the alternative implementation of the Dobry et al. (1982) strain-based procedure that is proposed herein. These include using the Wair et al. (2012) relationship to estimate N_{60} from V_s values (i.e., reverse implementation) and accounting for FC solely by the “clean sand” correction applied to $N_{1,60}$ for the SPT case histories and ignoring the influence of FC for the V_s case histories. These shortcomings could be overcome if sites are characterized by both penetration and V_s in-situ test metrics and if calibration coefficients for the pore pressure generation models are developed as functions of FC. Also, the prediction statistics presented herein used to compare the efficacy of the strain- versus stress-based procedures were inherently biased in favor of the stress-based procedures. To truly test the relative efficacy of the two procedures it is necessary to examine independent case histories that were not used in the development of either the strain- or stress-based approaches. Finally, the strain-based procedure could be used to evaluate the CPT case histories. This will likely increase the absolute efficacy of the strain-based procedure, but its relative efficacy to stress-based procedures would likely be unaffected.

2.7 Conclusions

The existence of a volumetric threshold shear strain, below which there is no development of excess pore pressures, and the unique relationship between pore pressure ratio and cyclic shear

strain, make compelling arguments for adopting a strain-based approach to evaluate liquefaction potential. This paper assessed an alternative form of the Dobry et al. (1982) cyclic strain approach for the evaluation of initial liquefaction when applied to both V_s and SPT case histories and compared it to the stress-based approaches to determine which yielded better results. Toward this end, γ_c was computed using the Dobry et al. (1982) procedure in conjunction with shear modulus degradation curves by Ishibashi and Zhang (1993), and $n_{eq\gamma}$ were estimated using the correlation by Lasley et al. (2017). The concept of the γ_{tv} was expressed in terms of the peak ground surface acceleration and defined as the threshold a_{max} . It was shown that computing $(a_{max})_t$ could provide a fast and simple evaluation for initial liquefaction, where no liquefaction is expected for a minimum computed $(a_{max})_t$ ranging from 0.08 to 0.12 g. In addition, the upper limits of the γ_{tv} were determined to be 0.03–0.05% with the case histories.

If either $\gamma_c > \gamma_{tv}$ or $a_{max} > (a_{max})_t$, excess pore pressures are predicted to develop, and it becomes necessary to quantify these pore pressures to evaluate liquefaction triggering potential. This was accomplished by implementing the pore pressure generation models by Byrne (1991) and by Vucetic and Dobry (1986), with curve fitting parameters by Mei et al. (2015). The results of this effort indicate that the Vucetic and Dobry (1986) model yielded more inaccurate and unconservative predictions, and fewer conservative predictions, than the Byrne (1991) model for both the V_s and SPT databases. There is uncertainty about the appropriateness of using $N_{1,60cs}$ to estimate V_s and the coefficients for the Byrne (1991) model for soils with fines because both correlations were developed for clean sands. For this reason, the SPT cases with $FC \leq 5\%$ were analyzed as a subset, but the predictions for this subset of case histories were only slightly better predictions than those for the entire SPT database. In contrast, the cyclic stress approach yielded more accurate predictions (87%–90%) than the cyclic strain approach (70%–77% with the Byrne, 1991, model). One likely reason for the lack of accuracy in the strain-based procedure's predictions is the inherent and potentially fatal limitation of the procedure is it ignoring the softening of the soil stiffness due to excess pore pressure when representing the earthquake loading in terms of γ_c and $n_{eq\gamma}$.

Requiring measurements of both V_s and penetration resistance for sites being evaluated would undoubtedly improve the accuracy of the cyclic strain approach because there would be less reliance of correlations to estimate needed parameters. However, it is unknown whether this would

significantly improve the efficacy of the strain-based procedure to make it competitive with the stress-based procedure.

2.8 References

- Abdoun, T., Gonzalez, M.A., Thevanayagam, S., Dobry, R., Elgamal, A., Zeghal, M., Mercado, M. V., and El Shamy, U. (2013). “Centrifuge and Large-Scale Modeling of Seismic Pore Pressures in Sands: Cyclic Strain Interpretation.” *Journal of Geotechnical and Geoenvironmental Engineering*, ASCE, 139(8), 1215–1234.
- Boulanger, R.W., Wilson, D.W., and Idriss, I.M. (2012). “Examination and reevaluation of SPT-based liquefaction triggering case histories.” *Journal of Geotechnical and Geoenvironmental Engineering*, ASCE, 138(8), 898–909.
- Byrne, P.M. (1991). “A cyclic shear-volume coupling and pore pressure model for sand.” *Proc., 2nd International Conf. on Recent Advances in Geotechnical Earthquake Engineering and Soil Dynamics*, St. Louis, 47-55.
- Carlton, B. (2014). *An improved description of the seismic response of sites with high plasticity soils, organic clays, and deep soft soil deposits*. PhD Dissertation, Department of Civil and Environmental Engineering, University of California, Berkeley, CA.
- Cetin, K.O., Seed, R.B., Moss, R.E.S., Der Kiureghian, A., Tokimatsu, K., Harder, Jr., L.F., and Kayen, R.E. (2000). *Field case histories for SPT-based in situ liquefaction potential evaluation*. PEER Report No. UCB/GT-2000/09, Pacific Earthquake Engineering Research, Berkeley, CA.
- Cetin, K.O., Seed, R.B., Der Kiureghian, A., Tokimatsu, K., Harder, Jr., L.F., Kayen, R.E., and Moss, R.E.S. (2004). “SPT-based probabilistic and deterministic assessment of seismic soil liquefaction potential.” *Journal of Geotechnical and Geoenvironmental Engineering*, ASCE, 130(12), 1314–1340.

- Chen, Q., Gao, G., Green, R.A., and Zhang, L. (2010). “Computation of Equivalent Number of Uniform Strain Cycles for Seismic Compression of Sand Subjected to Multidirectional Earthquake Loading,” *World Earthquake Engineering*, 26, 6-12. (in Chinese)
- Cubrinovski, M. and Green, R.A. (eds.) (2010). “Geotechnical Reconnaissance of the 2010 Darfield (Canterbury) Earthquake,” (contributing authors in alphabetical order: J. Allen, S. Ashford, E. Bowman, B. Bradley, B. Cox, M. Cubrinovski, R. Green, T. Hutchinson, E. Kavazanjian, R. Orense, M. Pender, M. Quigley, and L. Wotherspoon), *Bulletin of the New Zealand Society for Earthquake Engineering*, 43(4), 243-320.
- Cubrinovski, M., Bradley, B., Wotherspoon, L., Green, R., Bray, J., Woods, C., Pender, M., Allen, J., Bradshaw, A., Rix, G., Taylor, M., Robinson, K., Henderson, D., Giorgini, S., Ma, K., Winkley, A., Zupan, J., O’Rourke, T., DePascale, G., and Wells, D. (2011). Geotechnical aspects of the 22 February 2011 Christchurch earthquake, *Bulletin of the New Zealand Society for Earthquake Engineering*, 43(4), 205-226.
- Darendeli, M.B. (2001). *Development of a new family of normalized modulus reduction and material damping curves*. Ph.D. Dissertation, Department of Civil, Architectural, and Environmental Engineering, University of Texas, Austin, TX.
- Dobry, R., Ladd, R., Yokel, F., Chung, R., and Powell, D. (1982). *Prediction of pore water pressure buildup and liquefaction of sands during earthquakes by the cyclic strain method*. NBS Building Science Series 138, National Bureau of Standards, Washington, DC.
- Dobry, R., Pierce, W.G., Dyvik, R., Thomas, G.E., and Ladd, R.S. (1985). *Pore pressure model for cyclic straining of sand*. Research Report 1985-06, Rensselaer Polytechnic Institute, Troy, NY.
- Green, R.A. and Terri, G.A. (2005). “Number of equivalent cycles concept for liquefaction evaluations—Revisited.” *Journal of Geotechnical and Geoenvironmental Engineering*, ASCE, 131(4), 477–488.

- Green, R.A., Olson, S.M., Cox, B.R., Rix, G.J., Rathje, E., Bachhuber, J., French, J., Lasley, S., and Martin, N. (2011). “Geotechnical Aspects of Failures at Port-au-Prince Seaport during the 12 January 2010 Haiti Earthquake.” *Earthquake Spectra*, 27(S1), S43-S65.
- Idriss, I.M. and Boulanger, R.W. (2004). “Semi-empirical procedures for evaluating liquefaction potential during earthquakes.” *Proc., 11th Int. Conf. on Soil Dyn. and Earthquake Eng., and 3rd Int. Conf. on Earthquake Geotech. Eng.* (D. Doolin, A. Kammerer, T. Nogami, R. B. Seed, and I. Towhata, eds.), Stallion Press, Singapore, Vol. 1, 32–56.
- Idriss, I.M. and Boulanger, R.W. (2008). *Soil Liquefaction During Earthquakes*. EERI MNO 12, Earthquake Engineering Research Institute, Oakland, CA.
- Jaky, J. (1944). “The coefficient of earth pressure at rest.” *Magyar Mérnök és Építész Egylet Közönyve (Journal of the Society of Hungarian Architects and Engineers)*, 78(22), 355-358 (in Hungarian).
- Kayen, R., Moss, R.E.S., Thompson, E.M., Seed, R.B., Cetin, K.O., Der Kiureghian, A., Tanaka, Y., and Tokimatsu, K. (2013). “Shear-wave velocity–based probabilistic and deterministic assessment of seismic soil liquefaction potential.” *Journal of Geotechnical and Geoenvironmental Engineering*, ASCE, 139(3), 407–419.
- Lasley, S.J., Green, R.A., and Rodriguez-Marek, A. (2017). “Number of equivalent stress cycles for liquefaction evaluations in active tectonic and stable continental regions.” *Journal of Geotechnical and Geoenvironmental Engineering*, ASCE, 143(4), 04016116-1.
- Lasley, S.J., Green, R.A., and Rodriguez-Marek, A. (2016). “New stress reduction coefficient relationship for liquefaction triggering analyses.” *Journal of Geotechnical and Geoenvironmental Engineering*, ASCE, 142(11), 06016013-1.
- Lee, J. (2009). *Engineering characterization of earthquake ground motions*. Ph.D. Dissertation, Department of Civil and Environmental Engineering, University of Michigan, Ann Arbor, MI.

- Lee, J. and Green, R.A. (2017). “Number of equivalent strain cycles for active tectonic and stable continental regions,” *Proc. 19th Intern. Conf. on Soil Mechanics and Geotechnical Engineering*, Seoul, Korea, 17-22 September. (*in press*)
- Liao, S. and Whitman, R.V. (1986). “Overburden correction factors for SPT in sand.” *Journal of Geotechnical Engineering*, ASCE, 112(3), 373–377.
- Martin, G.R., Finn, W.D.L., and Seed, H.B. (1975). “Fundamentals of liquefaction under cyclic loading.” *Journal of the Geotechnical Engineering Division*, ASCE, 101(GT5), 423–483.
- Matasovic, N. (1993). “Seismic response of composite horizontally-layered soil deposits”. University of California, Los Angeles: xxix, 452 leaves.
- Matasovic, N. and Ordóñez, G.A. (2012). *D-MOD2000 – a computer program for seismic site response analysis of horizontally layered soil deposits, earthfill dams, and solid waste landfills*. GeoMotions, LLC, Lacey, Washington, USA.
- Mei, X., Olson, S.M., and Hashash, Y.M.A. (2015). “Empirical curve-fitting parameters for a porewater pressure generation model for use in 1-D effective stress-based site response Analysis.” *6th International Conference on Earthquake Geotechnical Engineering*. Christchurch, New Zealand.
- Menq, F.Y. (2003). *Dynamic properties of sandy and gravelly soils*. Ph.D. Dissertation, Department of Civil, Architectural, and Environmental Engineering, University of Texas, Austin, TX.
- Mitchell, J.K., Chatoian, J.M., and Carpenter, G.C. (1976). *The influences of sand fabric on liquefaction behavior*. Report no. TE-76-1. Contract report no. S-76-5 to U.S. Army Engineer Waterways Experiment Station.
- Moss, R.E.S., Seed, R.B., Kayen, R.E., Stewart, J.P., Youd, T.L., and Tokimatsu, K. (2003). “Field case histories for CPT-based in situ liquefaction potential evaluation.” Geoengineering Research Report No. UCB/GE-2003/04., Univ. of California, Berkeley, CA.

- NRC (1985). *Liquefaction of soils during earthquakes*. National Research Council, The National Academy Press, Washington, DC.
- NRC (2016). *State of the Art and Practice in the Assessment of Earthquake-Induced Soil Liquefaction and Consequences*. National Research Council, The National Academies Press, Washington, DC.
- Olson, S.M., Green, R.A., Lasley, S., Martin, N., Cox, B.R., Rathje, E., Bachhuber, J., and French, J. (2011). “Documenting Liquefaction and Lateral Spreading Triggered by the 12 January 2010 Haiti Earthquake.” *Earthquake Spectra*, 27(S1), S93-S116.
- Richart, Jr., F.E., Hall, J.R., and Woods, R.D. (1970). *Vibrations of Soils and Foundations*, Prentice Hall, Englewood Cliffs, New Jersey, 401 pp.
- Silver, M.L. and Seed, H.B. (1971). “Volume changes in sands during cyclic loading.” *Journal of the Soil Mechanics and Foundations Division*, ASCE, 97(SM9), 1171–82.
- Seed, H.B. and Idriss, I.M. (1971). “Simplified procedure for evaluating soil liquefaction potential.” *Journal of the Soil Mechanics and Foundations Division*, ASCE, 97(9), 1249–1273.
- Seed, H.B., Idriss, I.M., Makdisi, F., and Banerjee, N. (1975). “Representation of irregular stress time histories by equivalent uniform stress series in liquefaction analyses, EERC 75-29.” *Earthquake Engineering Research Center*, University of California, Berkeley.
- Stoll, R.D. and Kald, L. (1977). “Threshold of dilation under cyclic loading.” *Journal of the Geotechnical Engineering Division*, ASCE, 103(GT10), 1174–1178.
- Vucetic, M. and Dobry, R. (1986). *Pore pressure build-up and liquefaction at level sandy sites during earthquakes*. Research Rep. CE-86-3, Dept. of Civil Engineering, Rensselaer Polytechnic Institute, Troy, NY.
- Vucetic, M. (1994). “Cyclic threshold shear strains in soils.” *Journal of Geotechnical Engineering*, ASCE, 120, 2208–2228.

- Wair, B.R., Dejong, J.T., and Shantz, T. (2012). *Guidelines for estimation of shear wave velocity profiles*. Pacific Earthquake Engineering Research Center Report 2012/08, Pacific Earthquake Engineering Center, Berkeley, CA.
- Whitman, R.V. (1971). "Resistance of soil to liquefaction and settlement." *Soils and Foundations*, 11(4), 59–68.
- Youd, T.L. (1972). "Compaction of sands by repeated shear straining." *Journal of the Soil Mechanics and Foundations Division*, ASCE, 98(SM7), 709-25.
- Youd, T.L., Idriss, I.M., Andrus, R.D., Arango, I., Castro, G., Christian, J.T., Dobry, R., Finn, W.D.L., Harder, Jr., L.F., Hynes, M.E., Ishihara, K., Koester, J.P., Liao, S.S.C., Marcuson III, W.F., Martin, G.R., Mitchell, J.K., Moriwaki, Y., Power, M.S., Robertson, P.K., Seed, R.B., and Stokoe, II, K.H. (2001). "Liquefaction resistance of soils: summary report from the 1996 NCEER and 1998 NCEER/NSF workshops on evaluation of liquefaction resistance of soils." *Journal of Geotechnical and Geoenvironmental Engineering*, ASCE, 127(10), 817–833.

Chapter 3. Thesis Conclusions

3.1 Summary

The objective of this thesis was to assess efficacy of the cyclic strain approach for evaluating initial liquefaction and to determine if it yielded better predictions than the stress-based approach. A modified version of the procedure outlined by Dobry et al. (1982) was adapted to apply the cyclic strain approach. The following steps were used to apply the cyclic strain approach: (1) calculate γ_c , with shear modulus degradation curves (Ishibashi and Zhang, 1993), and n_{eq} , with a published correlation (Lasley et al., 2017); (2) compare γ_c to γ_{tv} , and if $\gamma_c < \gamma_{tv}$, no excess pore pressures develop and the evaluations ends here; (3) if $\gamma_c > \gamma_{tv}$, compute r_u with the pore pressure generation models by Byrne (1991) and Vucetic and Dobry (1986), with curve-fitting parameters by Mei et al. (2015); (4) finally, the value of r_u is used to predict liquefaction, where $r_u \geq 0.95$ is defined as initial liquefaction. Additionally, the concept of the γ_{tv} was translated to define $(a_{max})_t$, which provides a fast and simple screening criterion to determine whether a more detailed evaluation of liquefaction potential is warranted.

The results of this procedure showed that the Byrne (1991) model provides more accurate predictions for both the V_s and SPT databases and fewer False Negatives. On the other hand, the Vucetic and Dobry (1986) model yielded lower results of r_u and less accurate and less conservative predictions. The Boulanger et al. (2012) database included cases with fine contents less than or equal to 5%. When these cases were analyzed the accuracy of the procedure increased slightly. The cyclic strain approach underperformed in comparison with the cyclic stress approach, which yielded more correct predictions.

3.2 Key Findings

Analysis of the results from applying the cyclic strain approach, with the Kayen et al. (2013) V_s and Boulanger et al. (2012) SPT databases, to define the threshold peak ground surface acceleration and implement pore pressure generation models produced the following key findings:

- The upper limits of the γ_{tv} were determined to be 0.03–0.05% from case histories.

- The computation of $(a_{\max})_t$ could provide a fast and simple screening criterion to determine whether a more detailed liquefaction evaluation is required, where no additional analyses are needed when $a_{\max} \leq (a_{\max})_t$ (0.08–0.12 g).
- Use of the Byrne (1991) model resulted in both more accurate, more conservative, and fewer unconservative predictions than those made using the Vucetic and Dobry (1986) model for both the V_s and SPT databases. When the Byrne (1991) model is used to analyze the SPT case histories, the results are less accurate but more conservative than when used to analyze the V_s case histories.
- Analysis of the cases with $FC \leq 5\%$ resulted in improved predictions relative to the entire case history database, but not significantly so.
- One likely reason for the lack of accuracy in the strain-based procedure's predictions is the inherent and potentially fatal limitation of the procedure is it ignoring the softening of the soil stiffness due to excess pore pressure when representing the earthquake loading in terms of γ_c and $n_{eq\gamma}$.
- The stress-based procedures yield more accurate predictions than the strain-based procedure, regardless of which numerical pore pressure generation model is used. However, it should be noted that the databases used to assess the efficacy of the stress-based procedure were essentially the same ones used to develop the CRR curves inherent to the procedures (i.e., the stress-based procedures were in essence “calibrated” using the databases), while this is not the case for the strain-base procedure.

3.3 Recommendations for Future Work

Based on the findings presented in this study, recommendations for extended research include:

- Assess the efficacy of the proposed variant of the strain-based procedures using case histories where both penetration resistance (e.g., SPT or CPT) and V_s measurements are known. This will minimize the uncertainty introduced by using correlations to estimate unknown parameters.

- Examine case histories not used in the derivation of either the strain- or stress-based approaches to truly test the relative efficacy of the two procedures. This will avoid comparing prediction statistics from the strain- and stress-based procedures, where the bias is in favor of the stress-based procedure.
- Calibrate the pore pressure generation models with cyclic testing for site specific soils to account for factors such as fines content, coefficient of uniformity, and plasticity.
- Evaluate the CPT case histories using the strain-based procedure.

Appendix A: Earthquake Liquefaction Databases

Appendix A provides tables showing information about the case histories included in the Kayen et al. (2013) and Boulanger et al. (2012) databases. Electronic supplements are provided with the full information included in the original publications along with parameters used in this study. The first table shown is for the Kayen et al. database and the second table is for the Boulanger et al. database.

Table A1. Liquefaction case histories (415) used with the adopted procedure for the cyclic strain approach (Data from Kayen et al. 2013)

Earthquake	M _w	σ'_{vo} (kPa)					Liquefied	
		11.0-35	35-60	60-85	85-110	110-240	YES	NO
1906 San Francisco Earthquake, California USA	7.7	–	1	–	–	1	1	1
1948 Fukui Earthquake, Japan	7.1	2	4	4	1	–	10	1
1964 Niigata Earthquake, Japan	7.5	–	3	5	1	–	6	3
1968 Tokachi Oki Earthquake, Japan	7.9	1	3	1	–	–	5	–
1973 Miyagi Ken Oki Earthquake, Japan	7.4	1	7	1	2	–	10	1
1975 Haicheng Earthquake, China	7.1	1	2	2	1	–	5	1
1976 Tangshan Earthquake, China	8	9	13	2	–	–	16	8
1978 Miyagi Ken Oki Earthquake, Japan	6.7	–	7	1	–	–	2	6
1979 Imperial Valley Earthquake, California, USA	6.5	1	10	–	–	–	4	7
1980 Mid Chiba Earthquake, Japan	5.9	–	–	1	–	1	–	2
1981 Westmorland Earthquake, California, USA	5.9	–	11	–	–	–	6	5
1983 Nihonkai-Chubu Earthquake, Japan	7.7	–	7	1	–	–	8	–
1983 Nihonkai-Chubu Aftershocks, Japan	7	–	2	–	–	–	2	–
1983 Bora Peak Earthquake, Idaho, USA	6.9	19	5	–	–	–	20	4
1986 Lotung LSST Earthquake Events, Taiwan	6	1	–	–	–	–	–	1
1986 Lotung LSST Earthquake Events, Taiwan	6.6	1	–	–	–	–	–	1
1986 Lotung LSST Earthquake Events, Taiwan	6.2	4	–	–	–	–	–	4
1986 Chiba-Ibaragi-Kenyo, Japan	6	–	–	1	–	1	–	2
1987 Chiba-Toho-Oki, Japan	6.5	–	–	–	–	1	–	1
1987 Superstition Hills Earthquake, California, USA	6.5	1	10	–	–	–	3	8
1987 Elmore Ranch Earthquake, California, USA	5.9	1	10	–	–	–	–	11
1989 Loma Prieta Earthquake, California, USA	7	5	26	17	10	1	42	17
1993 Kushiro Earthquake, Japan	7.6	2	3	2	1	–	8	–
1993 Hokkaido Nansei Oki Earthquake, Japan	7.7	7	12	8	–	–	24	3
1995 Hyogo Nambu Earthquake, Japan	7	3	21	37	17	7	67	18

1999 Chi Chi Earthquake, Japan	7.6	6	5	1	1	1	13	1
1999 Druce Earthquake, Turkey	7.4	–	–	2	–	–	2	–
2000 Tottori Seibu Earthquake, Japan	6.8	–	1	2	–	–	3	–
2001 Geiyo-Hiroshima Ken Earthquake, Japan	6.8	3	–	1	1	–	5	–
2002 Denali Fault Earthquake, Alaska, USA	7.9	9	–	–	–	–	4	5
2003 Sanriku-Minami Earthquake, Japan	7	1	7	1	2	–	2	9
2003 Tokachi Oki Earthquake, Japan	7.8	1	4	4	1	–	7	3
2003 Tokachi Oki Aftershock, Japan	7.1	–	–	1	–	–	–	1
2007 Niigata Chuetsu Oki, Japan	6.6	1	1	–	–	–	2	–
2008 Achaia-Elia Earthquake, Greece	6.5	–	2	–	–	–	2	–
2011 Tohoku Aftershock, April 11, 2011	7.4	1	6	2	1	–	10	–
2011 Tohoku Earthquake Mainshock, March 11, 2011	9	–	2	–	–	–	2	–
Total		81	185	97	39	13	291	124

Table A2. Liquefaction case histories (230) used with the adopted procedure for the cyclic strain approach (Data from Boulanger et al. 2012)

Earthquake	M _w	FC (%)			σ'vo (kPa)					Liquefied	
		≤ 5	6 – 34	> 34	20-35	35-60	60-85	85-110	110-171	YES	NO
1944 Tohankai earthquake, Japan	8.1	–	3	–	–	1	2	–	–	3	–
1948 Fukui earthquake, Japan	7.3	2	–	–	–	1	–	1	–	2	–
1964 Niigata earthquake, Japan	7.6	10	2	–	–	5	4	3	–	8	4
1968 earthquake	7.5	–	–	1	–	1	–	–	–	–	1
1968 Tokachi-Oki earthquake, Japan	8.3	4	1	–	–	4	1	–	–	3	2
1971 San Fernando earthquake, USA	6.6	–	–	2	–	–	–	2	–	2	–
1975 Haicheng earthquake, China	7.0	1	–	3	–	–	1	3	–	3	1
1976 Guatemala City earthquake, Guatemala	7.5	3	–	–	1	–	1	1	–	2	1
1976 Tangshan earthquake, China	7.6	2	5	–	1	4	3	–	–	5	2
1977 Caucete earthquake, Argentina	7.4	3	1	1	–	3	–	1	1	3	2
1978 Miyagiken-Oki earthquake, Japan	6.5	7	6	1	2	7	5	–	–	1	13
1978 Miyagiken-Oki earthquake, Japan	7.7	10	9	1	2	8	9	–	–	14	6
1979 Imperial Valley earthquake, USA	6.5	–	6	3	2	6	1	–	–	4	5
1980 Mid-Chiba earthquake, Japan	6.0	–	2	–	–	1	–	–	1	–	2
1981 WestMorland earthquake, England	5.9	–	4	3	2	5	–	–	–	3	4
1982 Urakawa-Oki earthquake, Japan	6.9	1	–	–	1	–	–	–	–	–	1
1983 Nihonkai-Chubu earthquake, Japan	6.8	3	–	–	–	2	1	–	–	1	2
1983 Nihonkai-Chubu earthquake, Japan	7.7	26	2	1	2	18	8	1	–	16	13
1984 Earhquake	7.5	–	–	1	–	1	–	–	–	–	1
1987 Superstition Hills earthquake, USA	6.2	–	1	1	–	2	–	–	–	–	2
1987 Superstition Hills earthquake, USA	6.5	–	7	3	2	7	1	–	–	1	9
1989 Loma Prieta earthquake, USA	6.9	14	9	2	3	6	7	9	–	16	9
1990 Luzon earthquake, Phillipines	7.7	–	2	–	–	–	1	1	–	1	1
1993 Kushiro-Oki earthquake, Japan	7.6	3	–	–	–	1	1	–	1	2	1
1994 Northridge earthquake, USA	6.7	–	2	2	–	–	–	3	1	3	1
1995 Hyogoken-Nambu (Kobe) earthquake, Japan	6.9	27	26	1	1	20	19	5	9	25	29
Total		116	88	26	19	103	65	30	13	118	112

**Appendix B: Normalized Shear Modulus Reduction Curves for the
Liquefaction Case Histories from the Kayen et al. and Boulanger et al.
Databases**

Shear modulus degradation curves for all the sites in the databases with their corresponding converged values of γ_c are presented in Appendix B. First, the curves for the Kayen et al. database are shown (415 curves) and followed by the curves for the Boulanger et al. database (230 curves).

Shear Modulus Degradation Curves for the Kayen et al.
database (415 curves)

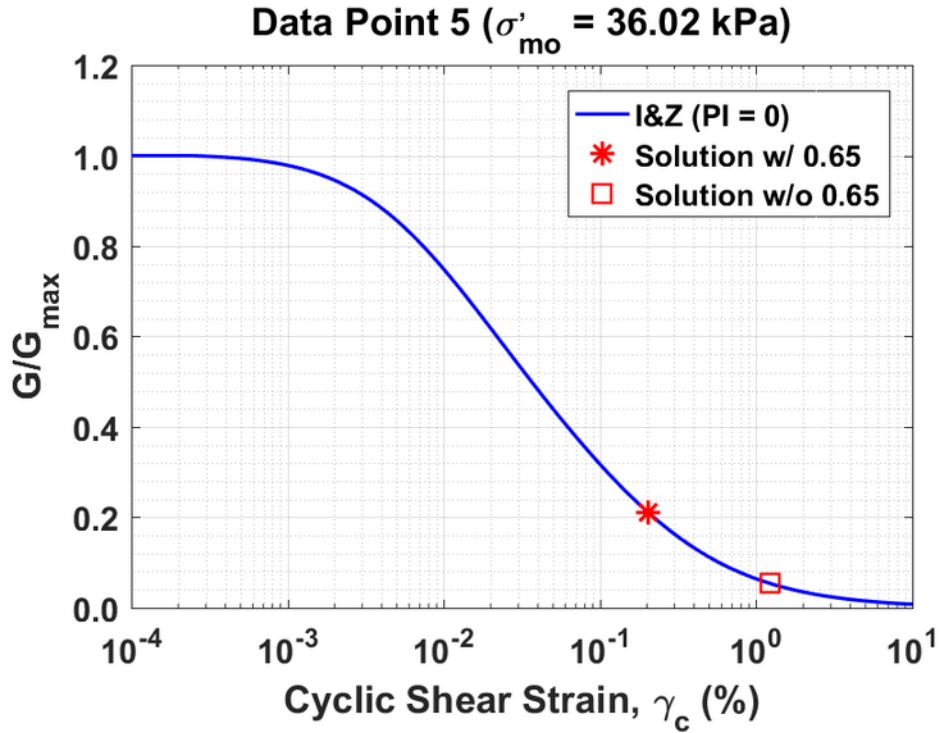


Figure B1. Normalized shear modulus reduction curves for Data Point 5 of the Kayen et al. database showing the solutions w/ and w/o the 0.65 factor

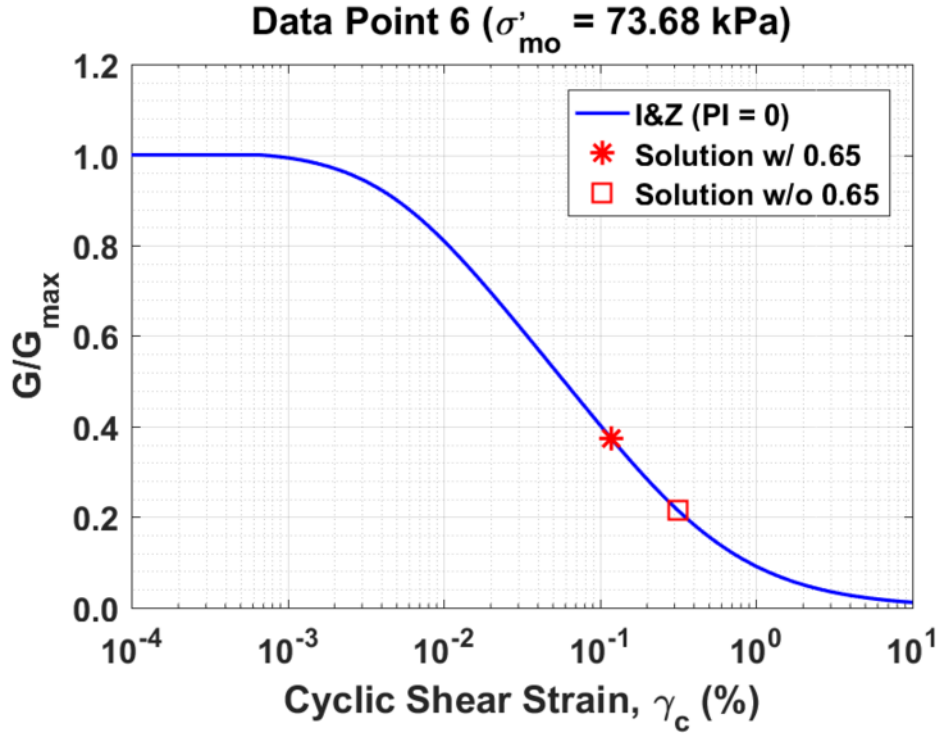


Figure B2. Normalized shear modulus reduction curves for Data Point 6 of the Kayen et al. database showing the solutions w/ and w/o the 0.65 factor

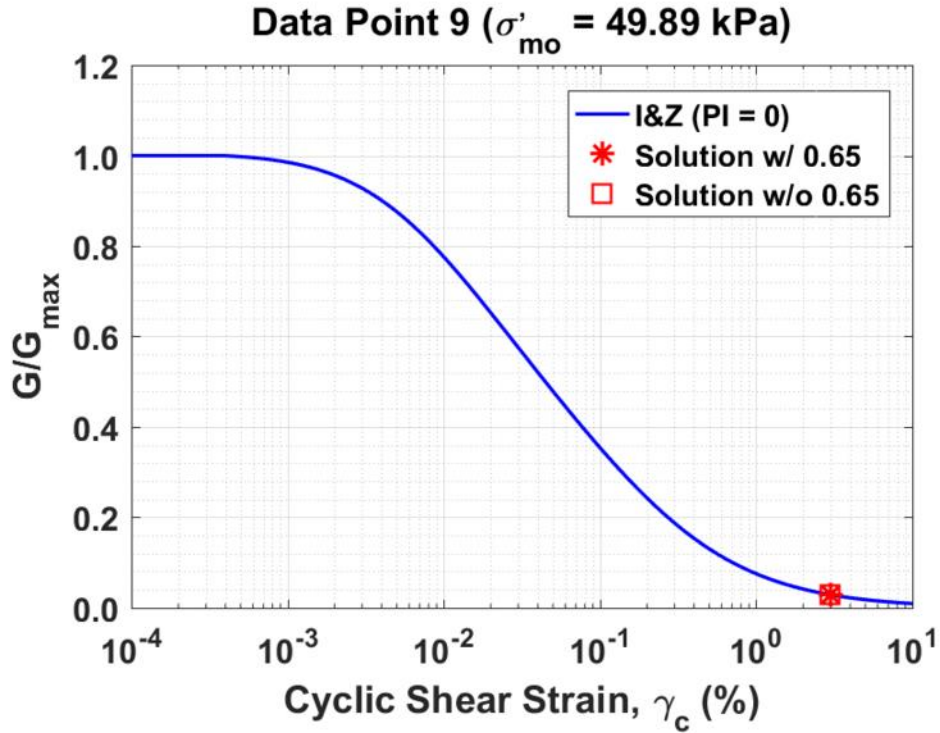


Figure B3. Normalized shear modulus reduction curves for Data Point 9 of the Kayen et al. database showing the solutions w/ and w/o the 0.65 factor

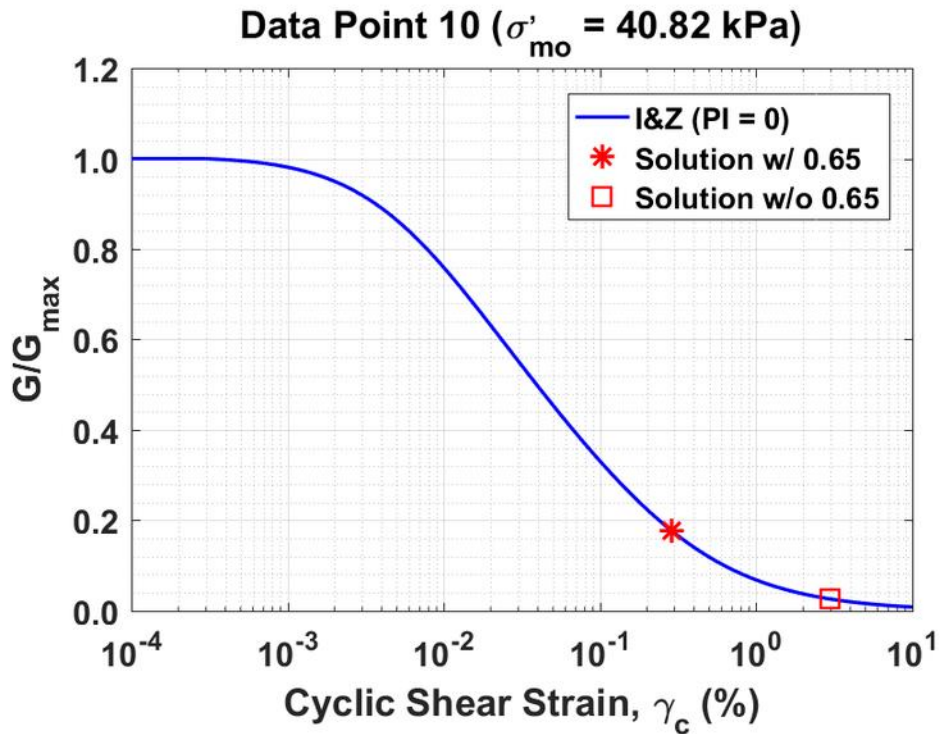


Figure B4. Normalized shear modulus reduction curves for Data Point 10 of the Kayen et al. database showing the solutions w/ and w/o the 0.65 factor

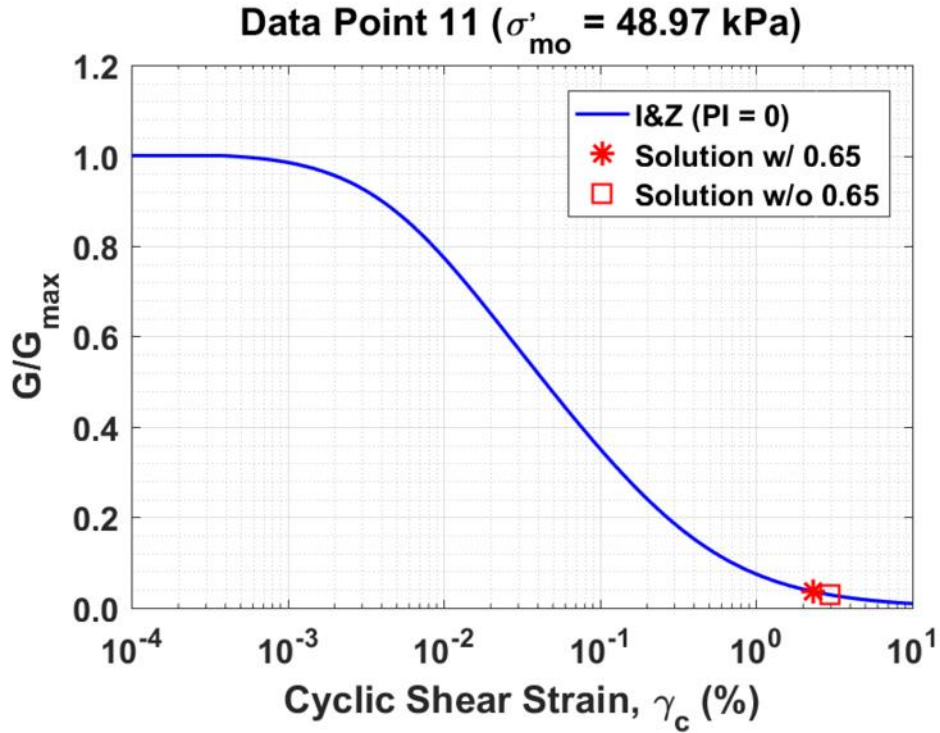


Figure B5. Normalized shear modulus reduction curves for Data Point 11 of the Kayen et al. database showing the solutions w/ and w/o the 0.65 factor

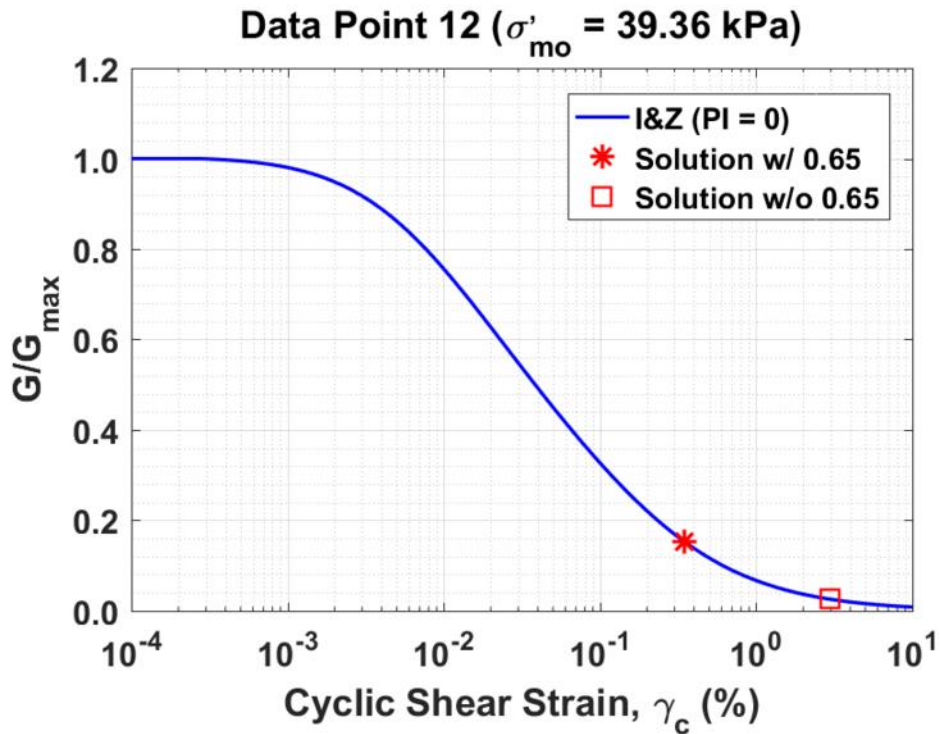


Figure B6. Normalized shear modulus reduction curves for Data Point 12 of the Kayen et al. database showing the solutions w/ and w/o the 0.65 factor

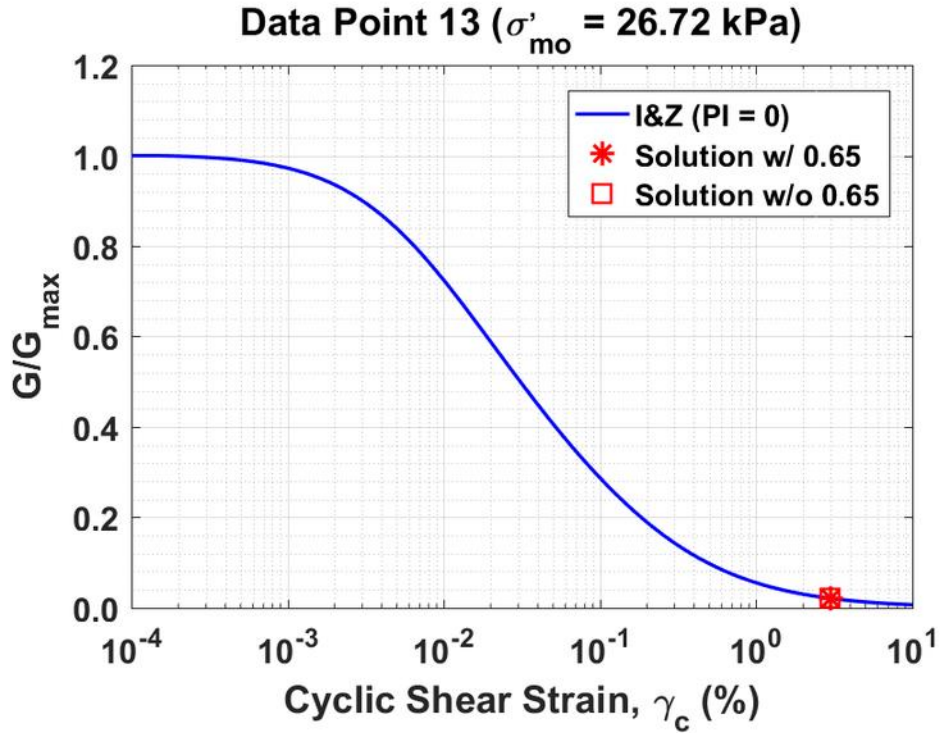


Figure B7. Normalized shear modulus reduction curves for Data Point 13 of the Kayen et al. database showing the solutions w/ and w/o the 0.65 factor

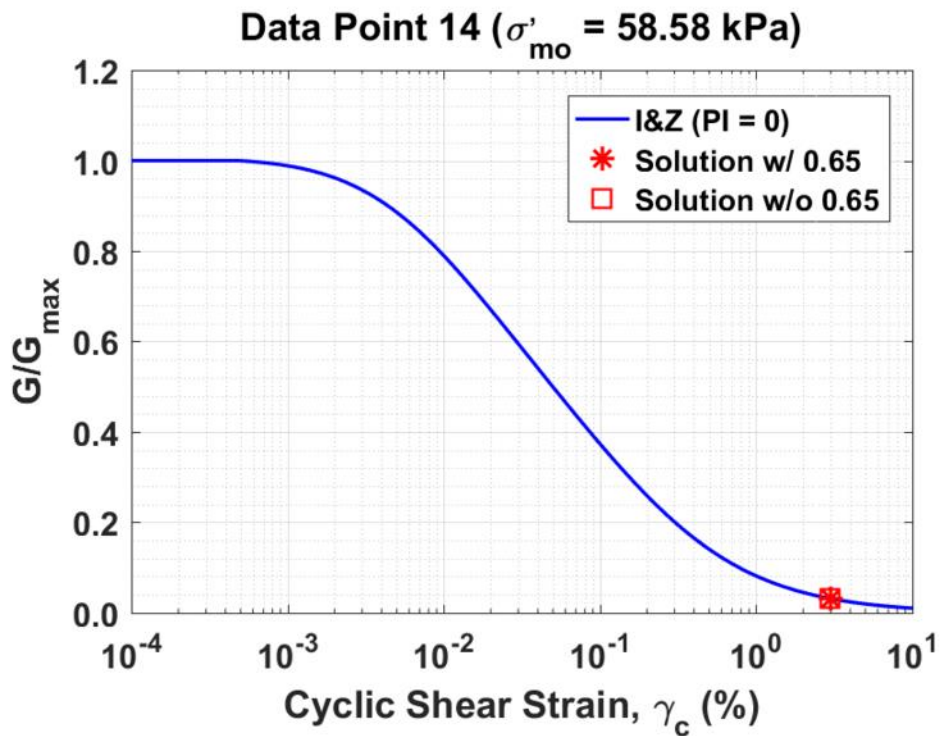


Figure B8. Normalized shear modulus reduction curves for Data Point 14 of the Kayen et al. database showing the solutions w/ and w/o the 0.65 factor

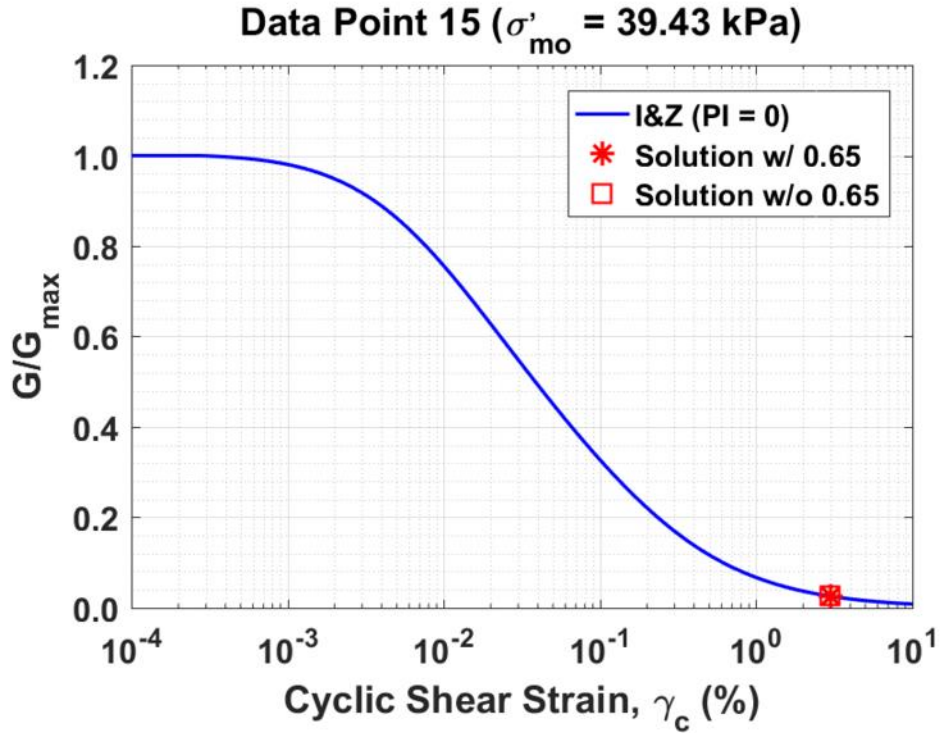


Figure B9. Normalized shear modulus reduction curves for Data Point 15 of the Kayen et al. database showing the solutions w/ and w/o the 0.65 factor

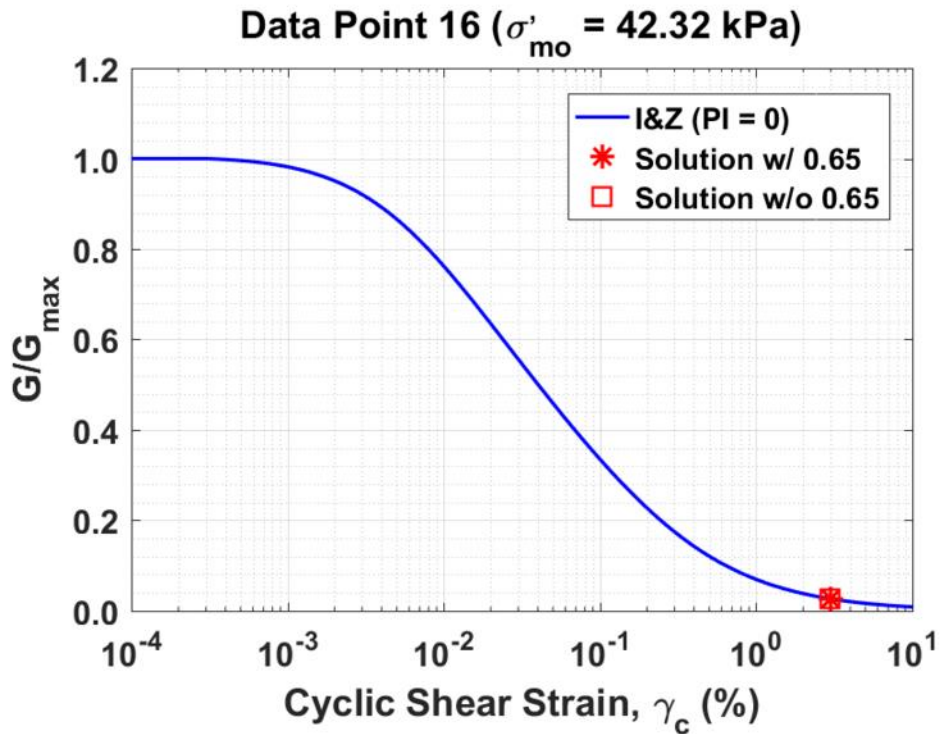


Figure B10. Normalized shear modulus reduction curves for Data Point 16 of the Kayen et al. database showing the solutions w/ and w/o the 0.65 factor

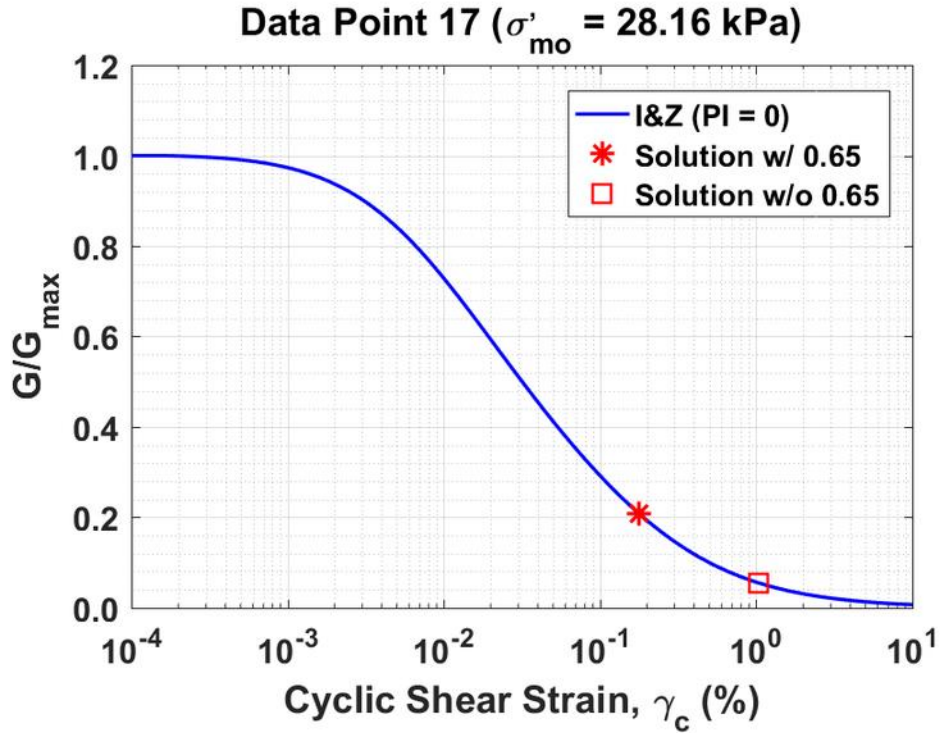


Figure B11. Normalized shear modulus reduction curves for Data Point 17 of the Kayen et al. database showing the solutions w/ and w/o the 0.65 factor

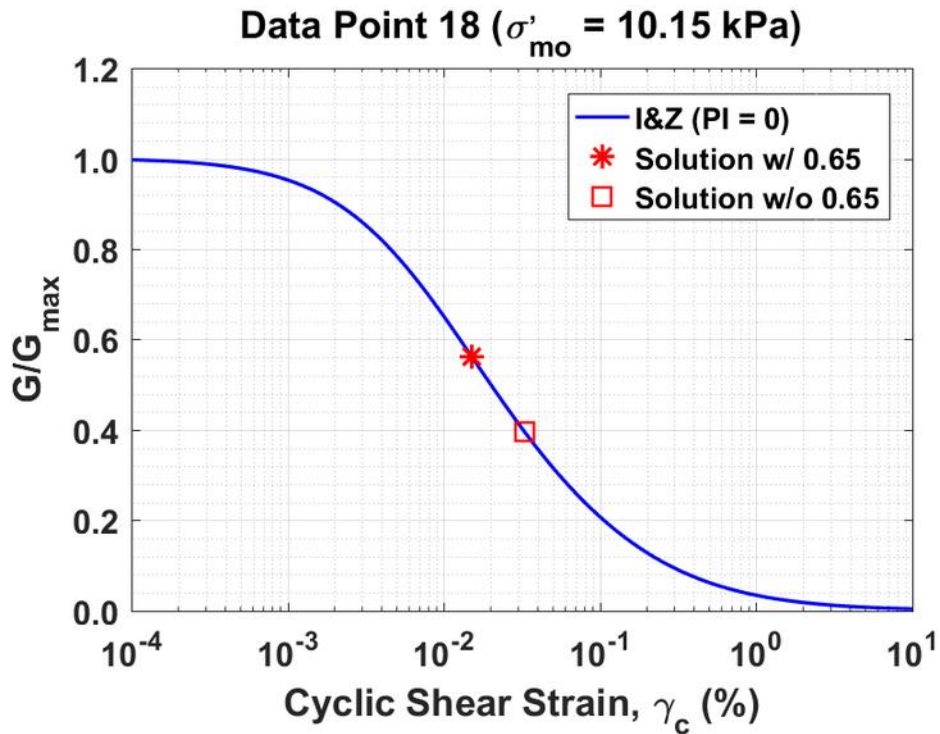


Figure B12. Normalized shear modulus reduction curves for Data Point 18 of the Kayen et al. database showing the solutions w/ and w/o the 0.65 factor

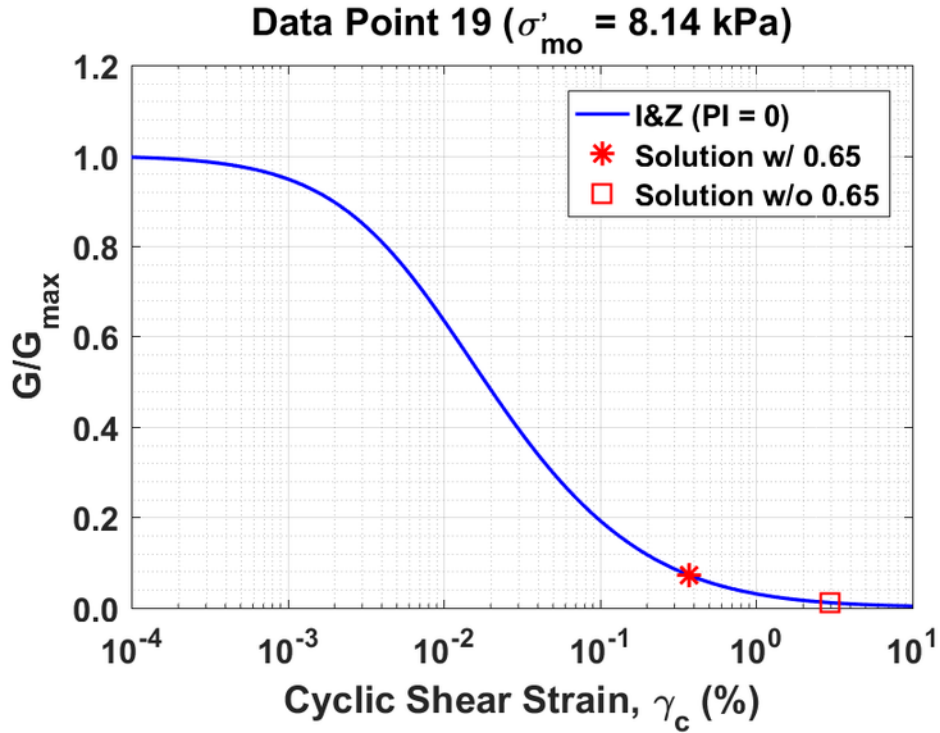


Figure B13. Normalized shear modulus reduction curves for Data Point 19 of the Kayen et al. database showing the solutions w/ and w/o the 0.65 factor

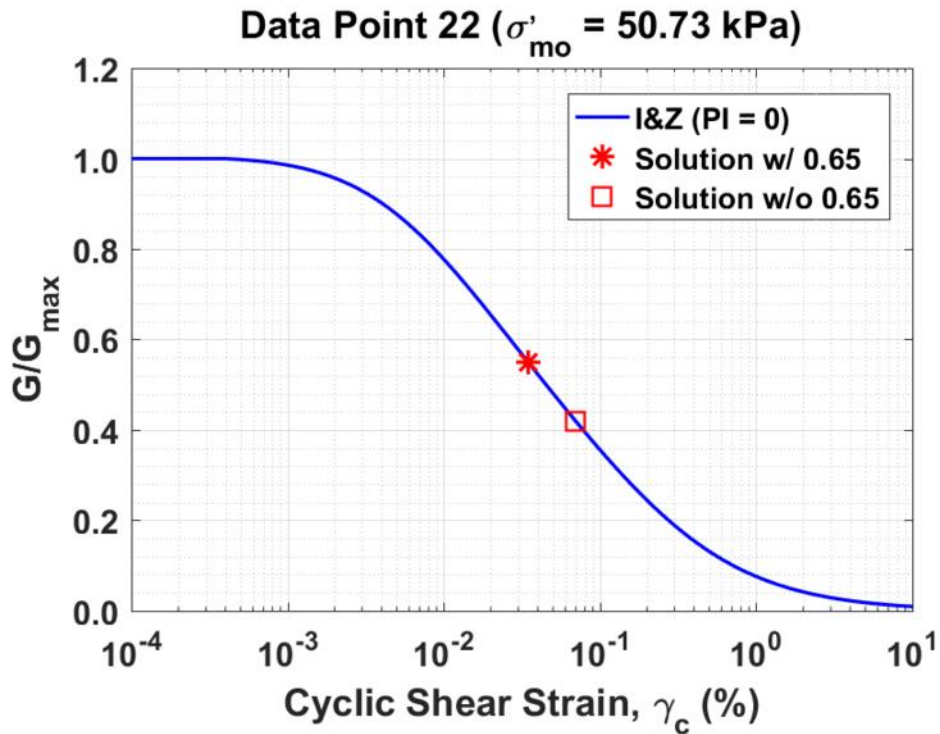


Figure B14. Normalized shear modulus reduction curves for Data Point 22 of the Kayen et al. database showing the solutions w/ and w/o the 0.65 factor

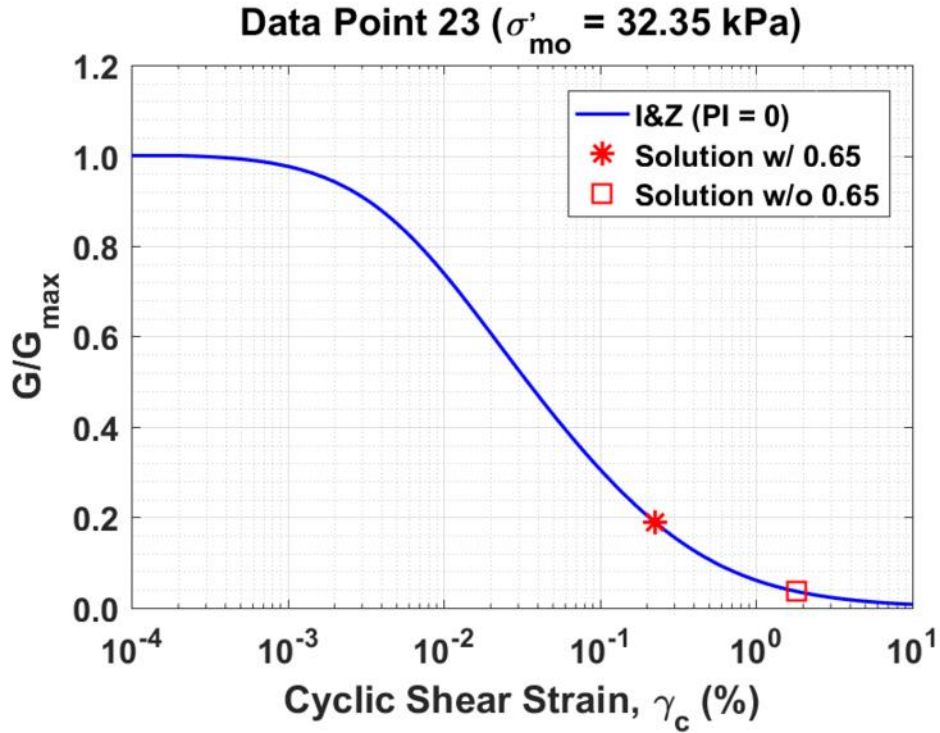


Figure B15. Normalized shear modulus reduction curves for Data Point 23 of the Kayen et al. database showing the solutions w/ and w/o the 0.65 factor

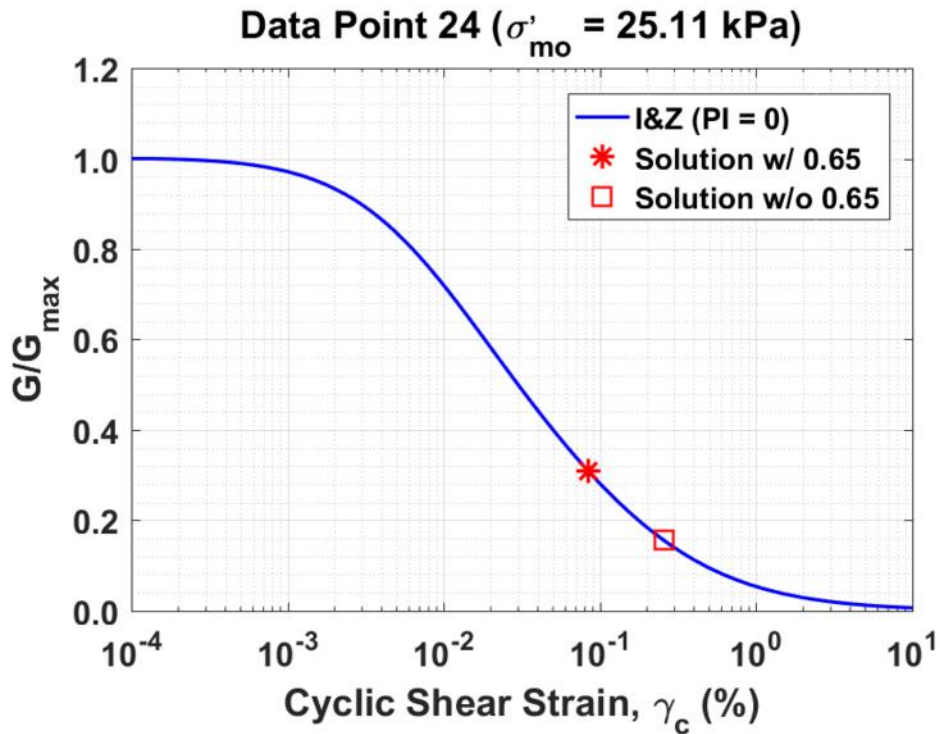


Figure B16. Normalized shear modulus reduction curves for Data Point 24 of the Kayen et al. database showing the solutions w/ and w/o the 0.65 factor

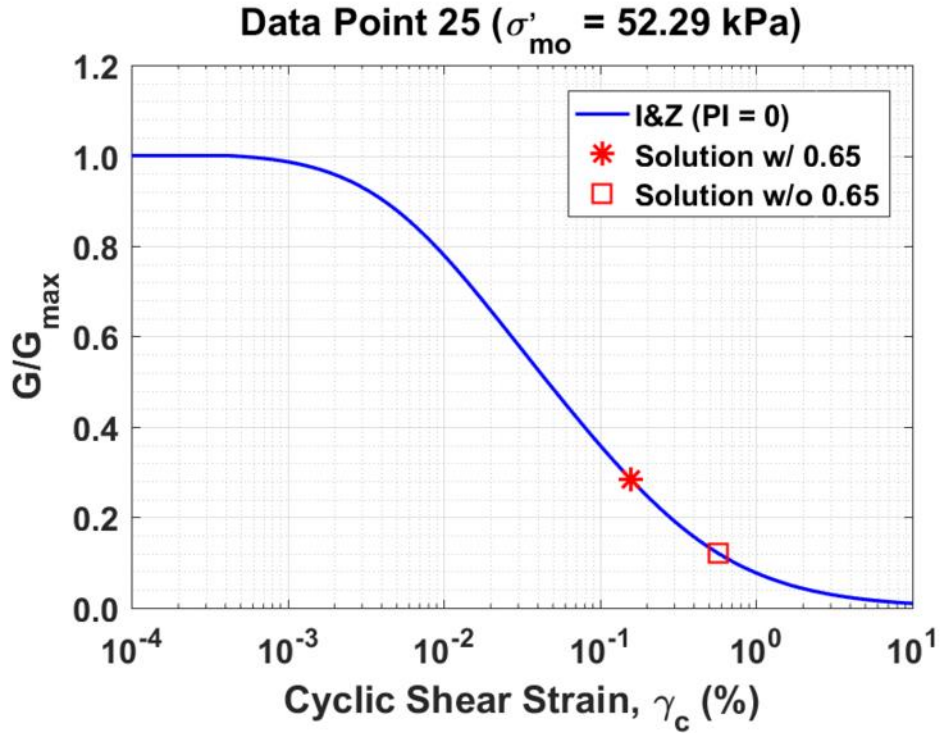


Figure B17. Normalized shear modulus reduction curves for Data Point 25 of the Kayen et al. database showing the solutions w/ and w/o the 0.65 factor

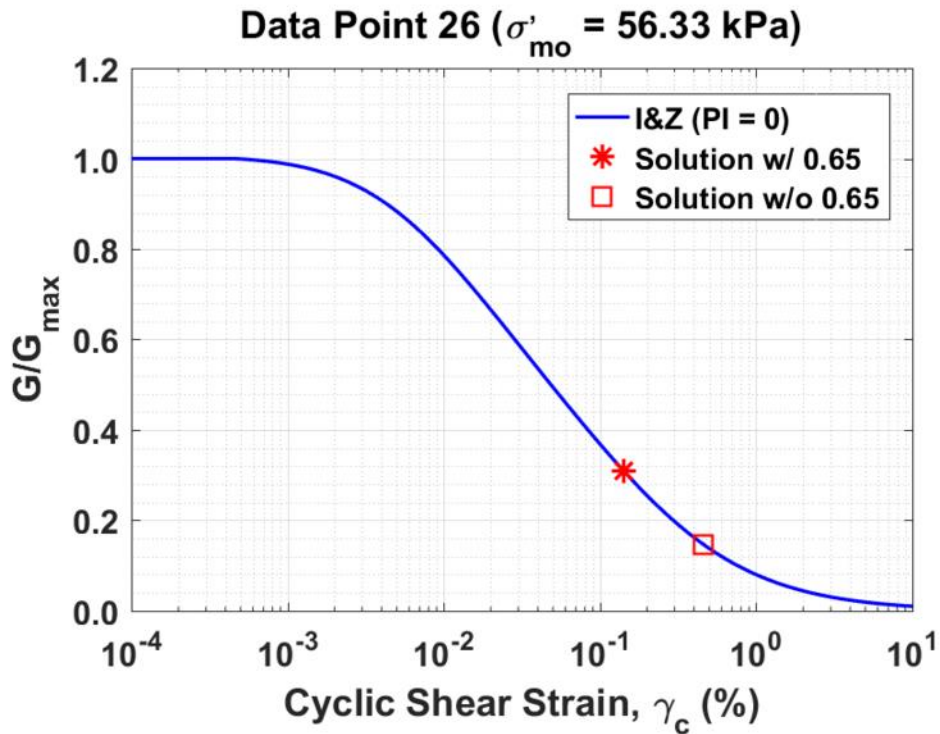


Figure B18. Normalized shear modulus reduction curves for Data Point 26 of the Kayen et al. database showing the solutions w/ and w/o the 0.65 factor

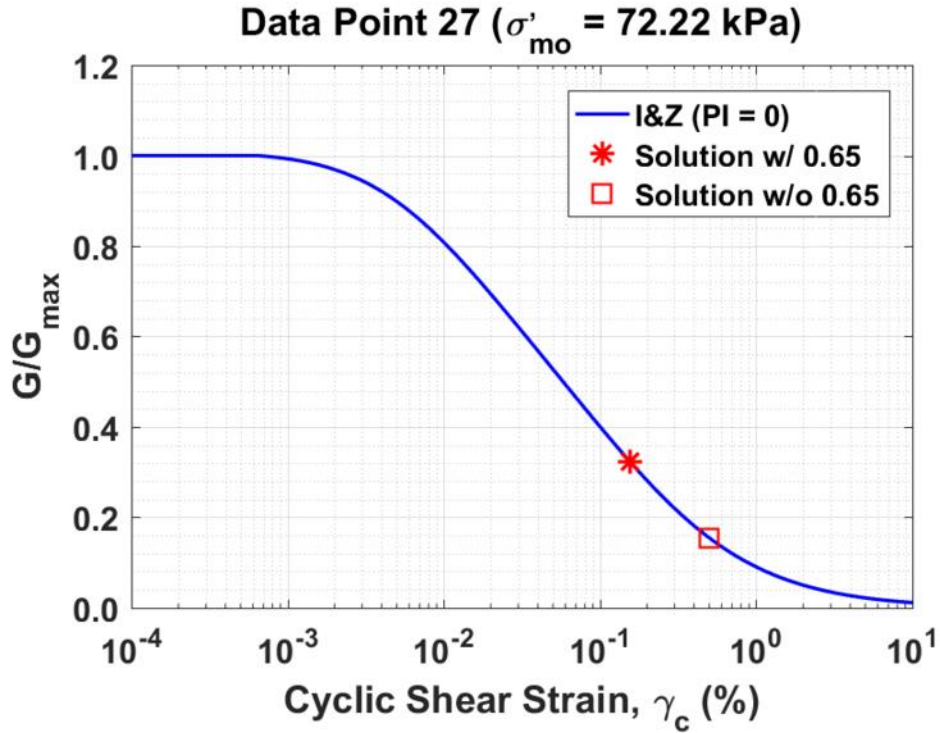


Figure B19. Normalized shear modulus reduction curves for Data Point 27 of the Kayen et al. database showing the solutions w/ and w/o the 0.65 factor

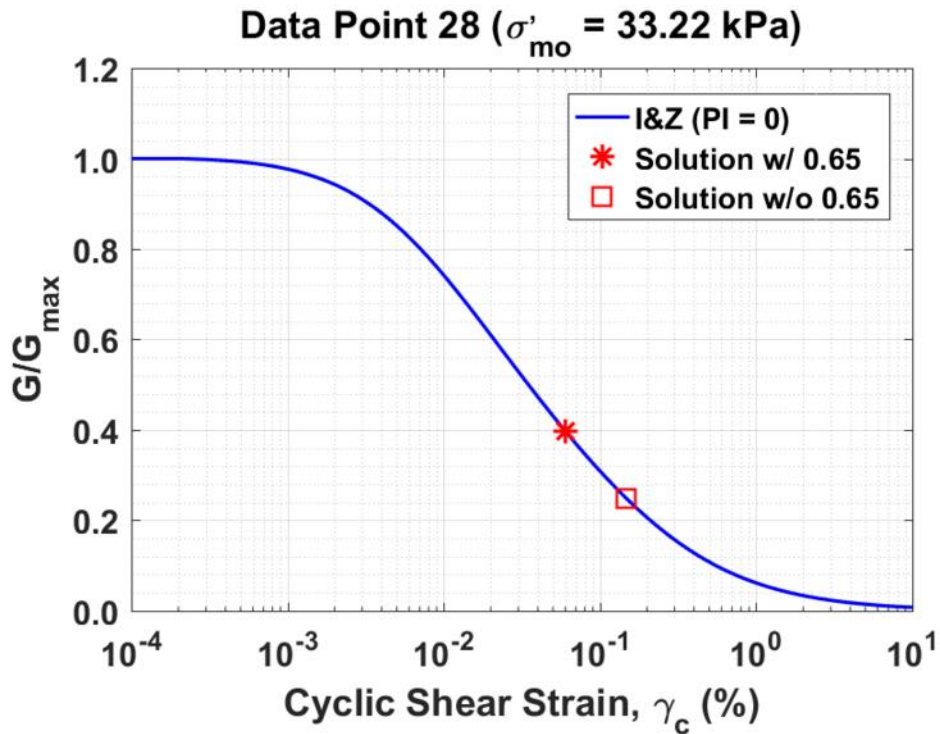


Figure B20. Normalized shear modulus reduction curves for Data Point 28 of the Kayen et al. database showing the solutions w/ and w/o the 0.65 factor

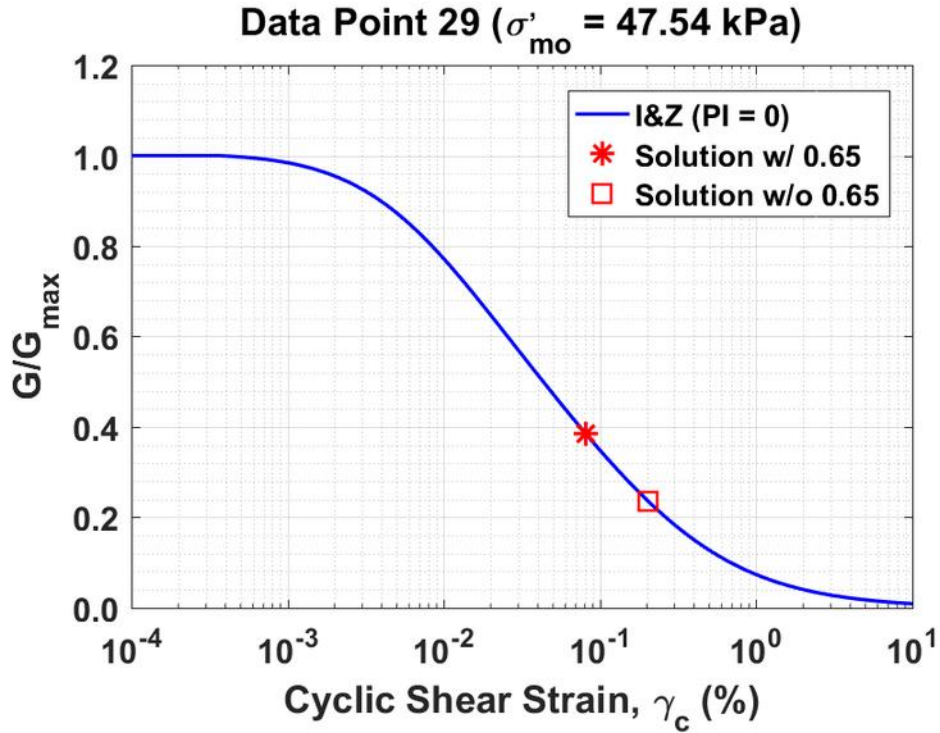


Figure B21. Normalized shear modulus reduction curves for Data Point 29 of the Kayen et al. database showing the solutions w/ and w/o the 0.65 factor

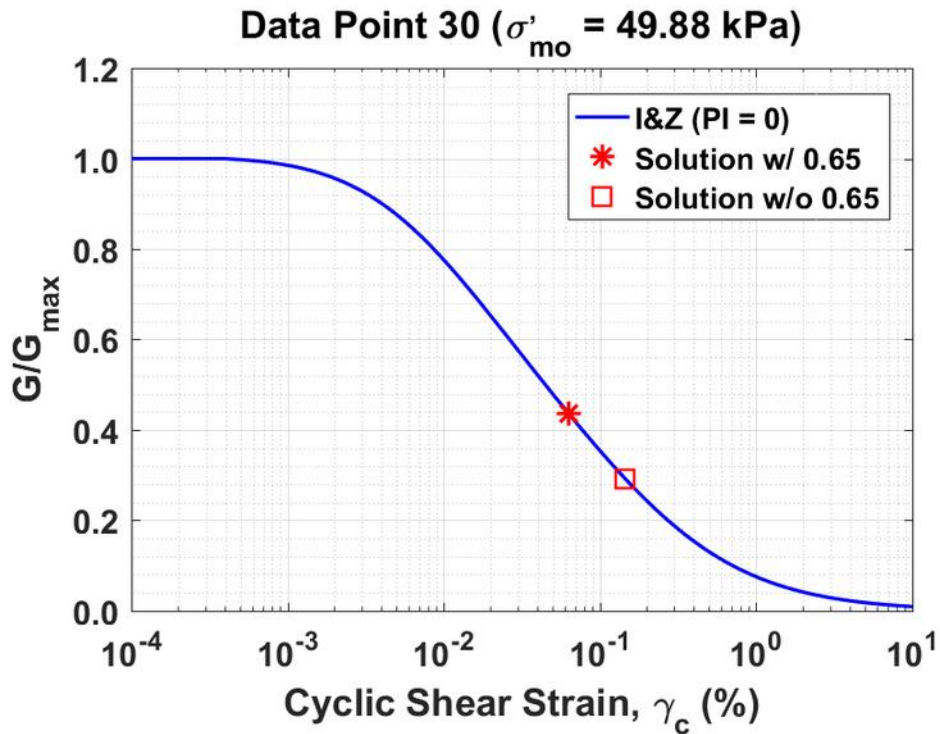


Figure B22. Normalized shear modulus reduction curves for Data Point 30 of the Kayen et al. database showing the solutions w/ and w/o the 0.65 factor

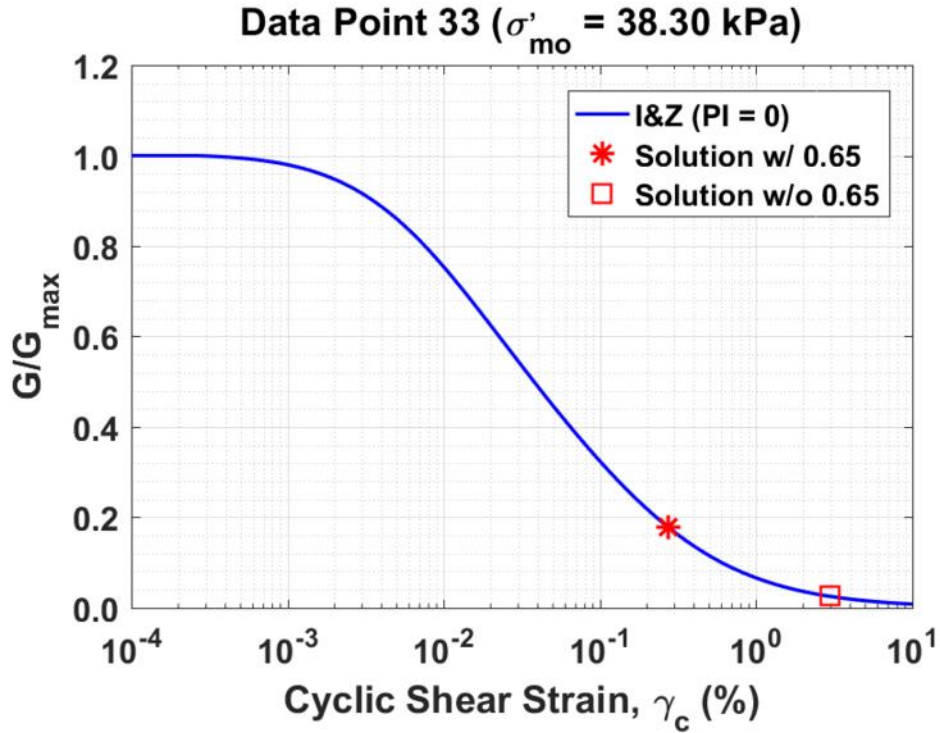


Figure B23. Normalized shear modulus reduction curves for Data Point 33 of the Kayen et al. database showing the solutions w/ and w/o the 0.65 factor

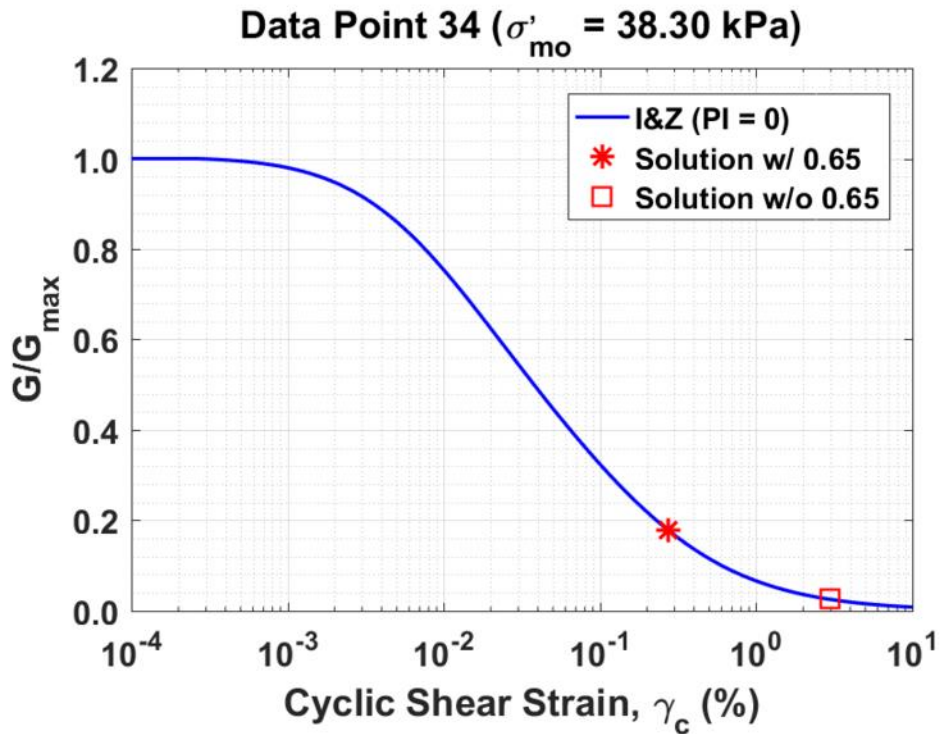


Figure B24. Normalized shear modulus reduction curves for Data Point 34 of the Kayen et al. database showing the solutions w/ and w/o the 0.65 factor

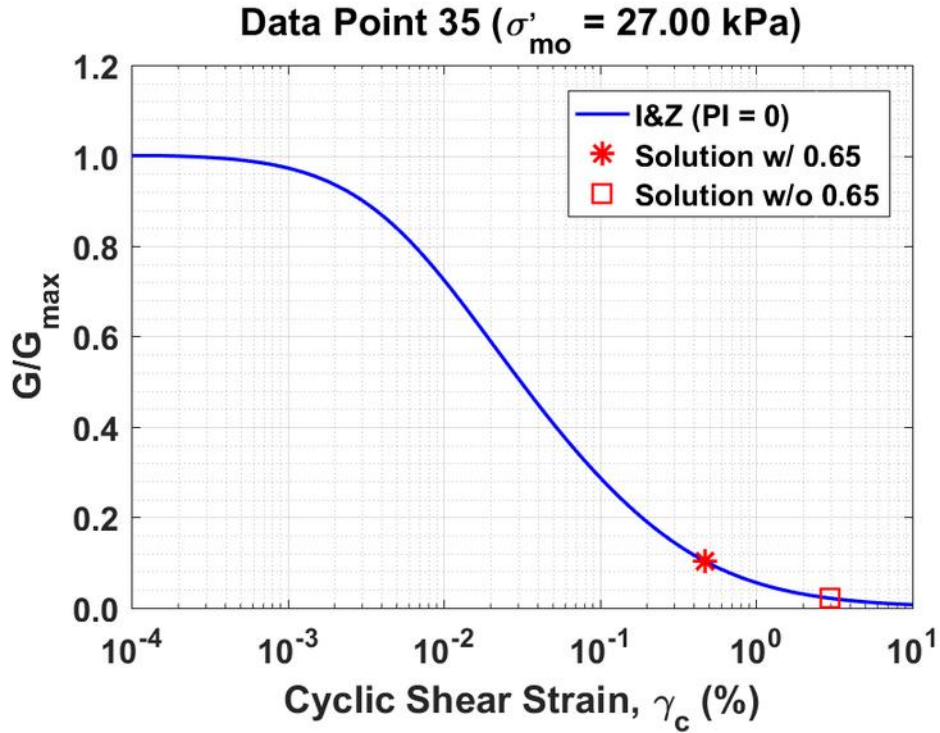


Figure B25. Normalized shear modulus reduction curves for Data Point 35 of the Kayen et al. database showing the solutions w/ and w/o the 0.65 factor

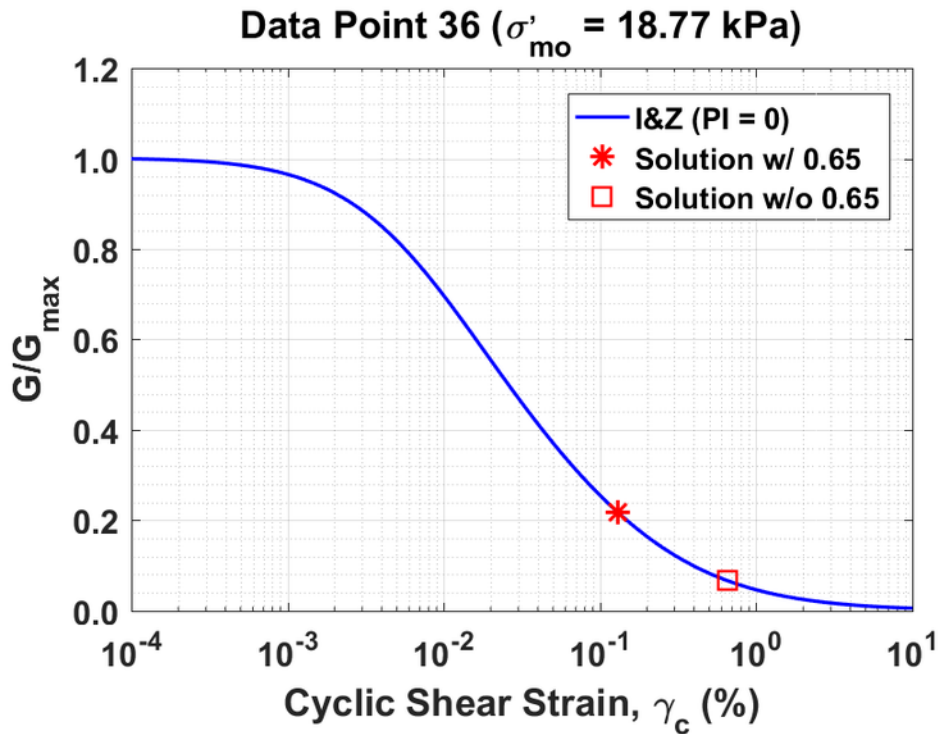


Figure B26. Normalized shear modulus reduction curves for Data Point 36 of the Kayen et al. database showing the solutions w/ and w/o the 0.65 factor

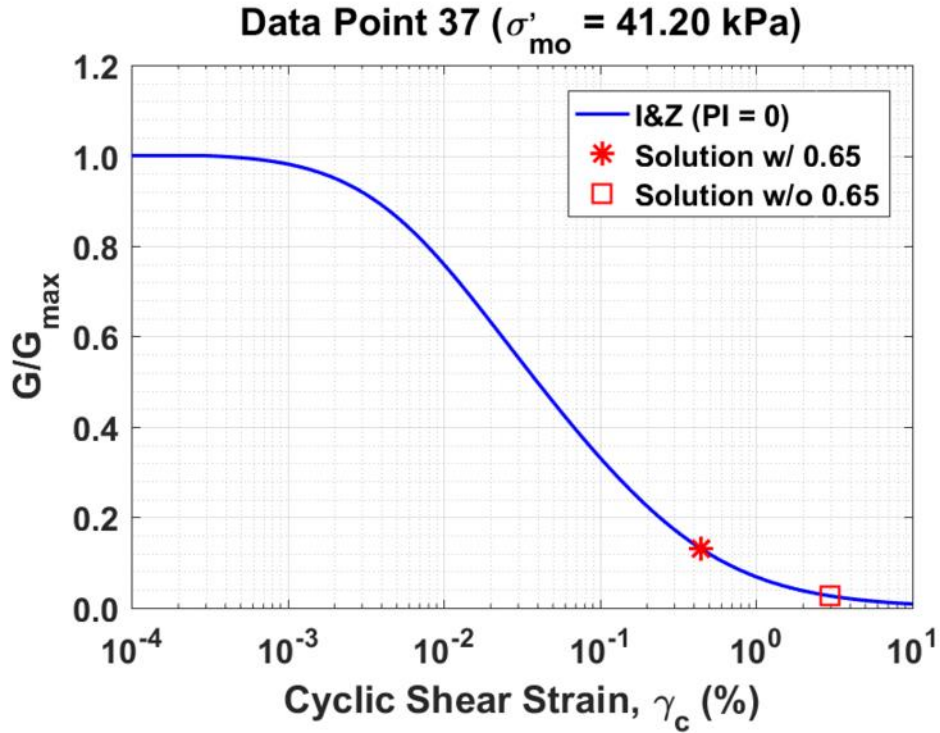


Figure B27. Normalized shear modulus reduction curves for Data Point 37 of the Kayen et al. database showing the solutions w/ and w/o the 0.65 factor

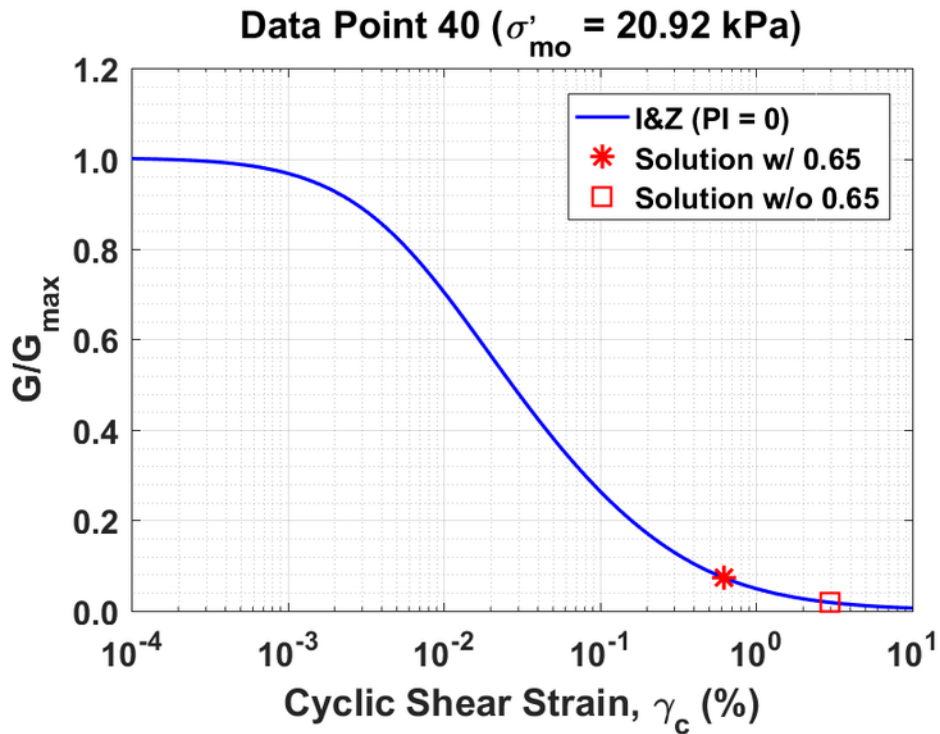


Figure B28. Normalized shear modulus reduction curves for Data Point 40 of the Kayen et al. database showing the solutions w/ and w/o the 0.65 factor

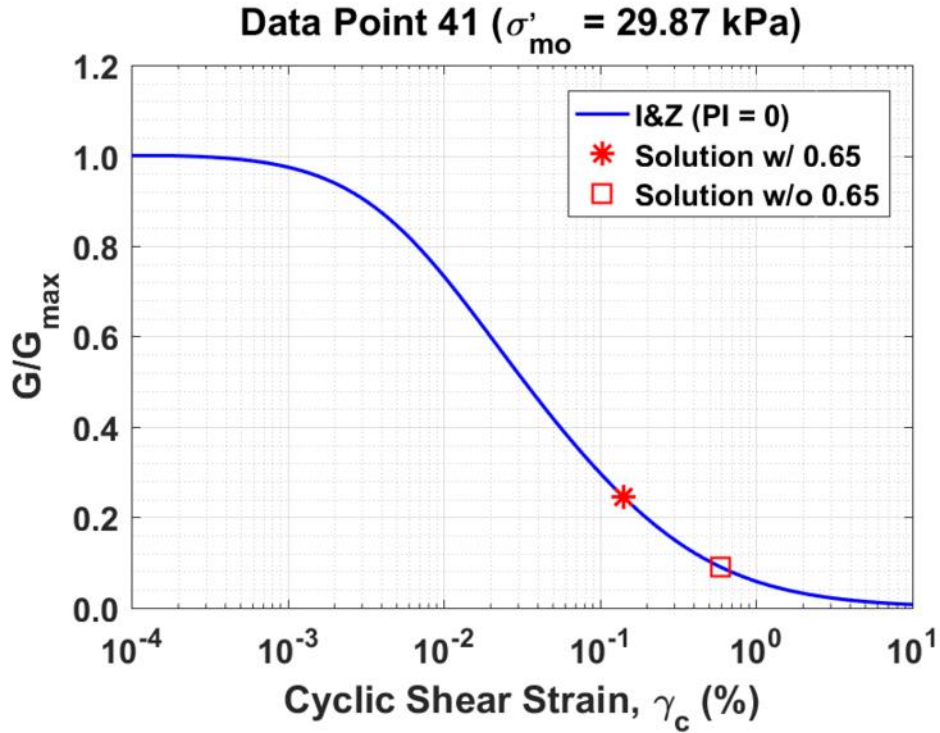


Figure B29. Normalized shear modulus reduction curves for Data Point 41 of the Kayen et al. database showing the solutions w/ and w/o the 0.65 factor

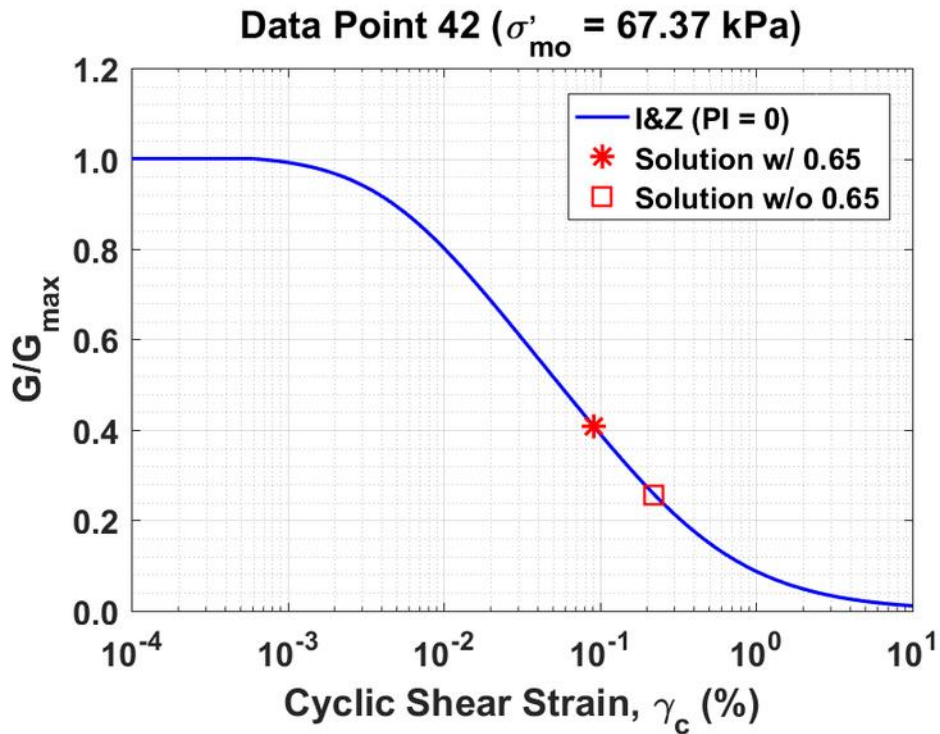


Figure B30. Normalized shear modulus reduction curves for Data Point 42 of the Kayen et al. database showing the solutions w/ and w/o the 0.65 factor

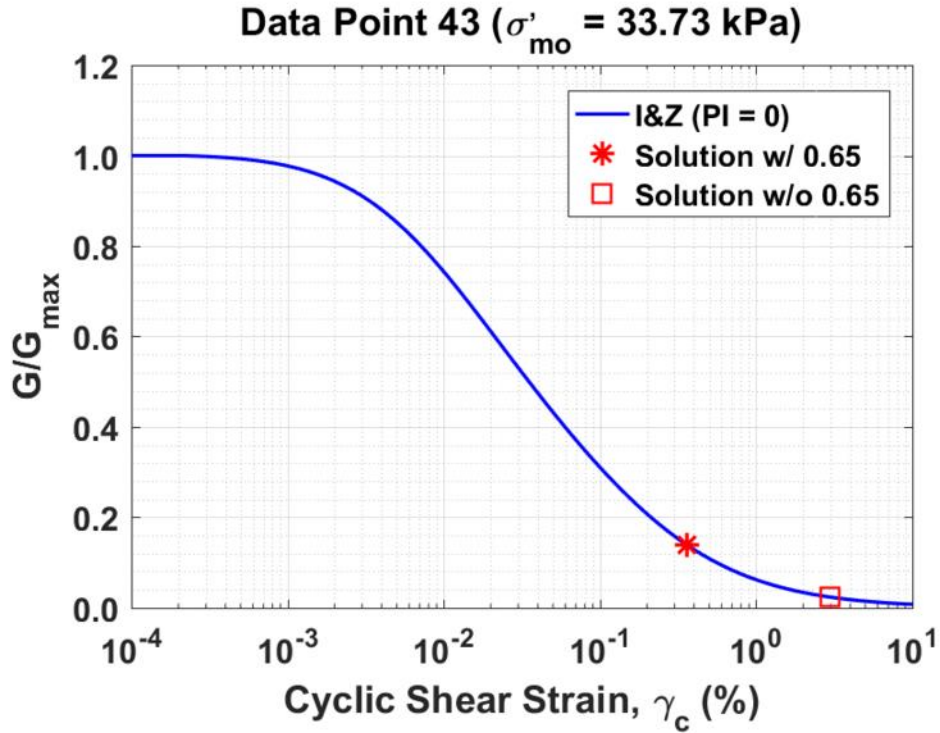


Figure B31. Normalized shear modulus reduction curves for Data Point 43 of the Kayen et al. database showing the solutions w/ and w/o the 0.65 factor

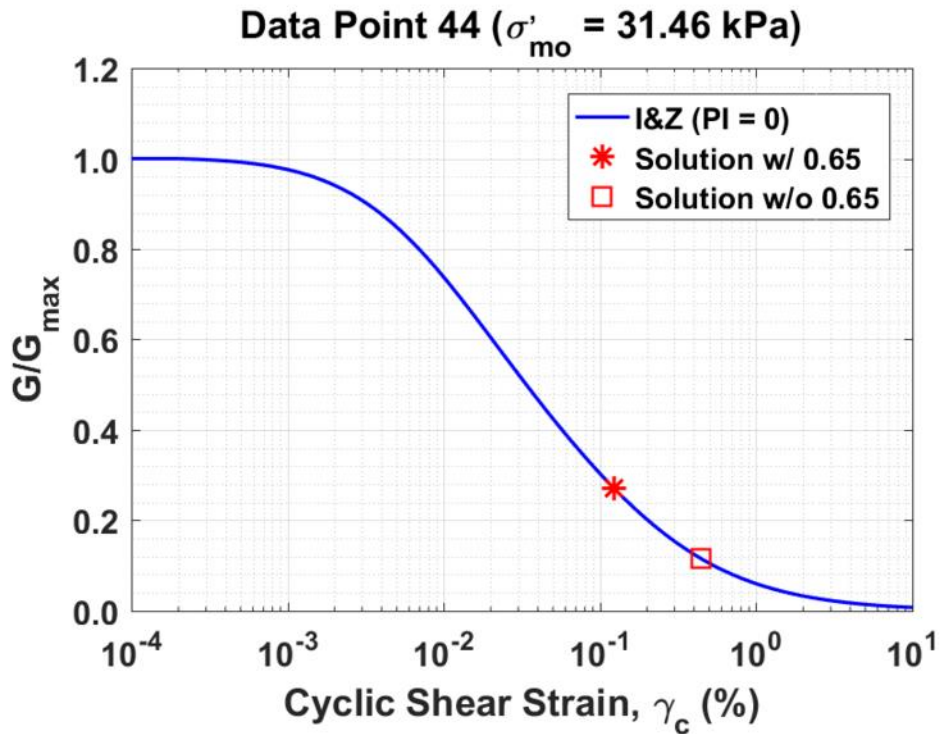


Figure B32. Normalized shear modulus reduction curves for Data Point 44 of the Kayen et al. database showing the solutions w/ and w/o the 0.65 factor

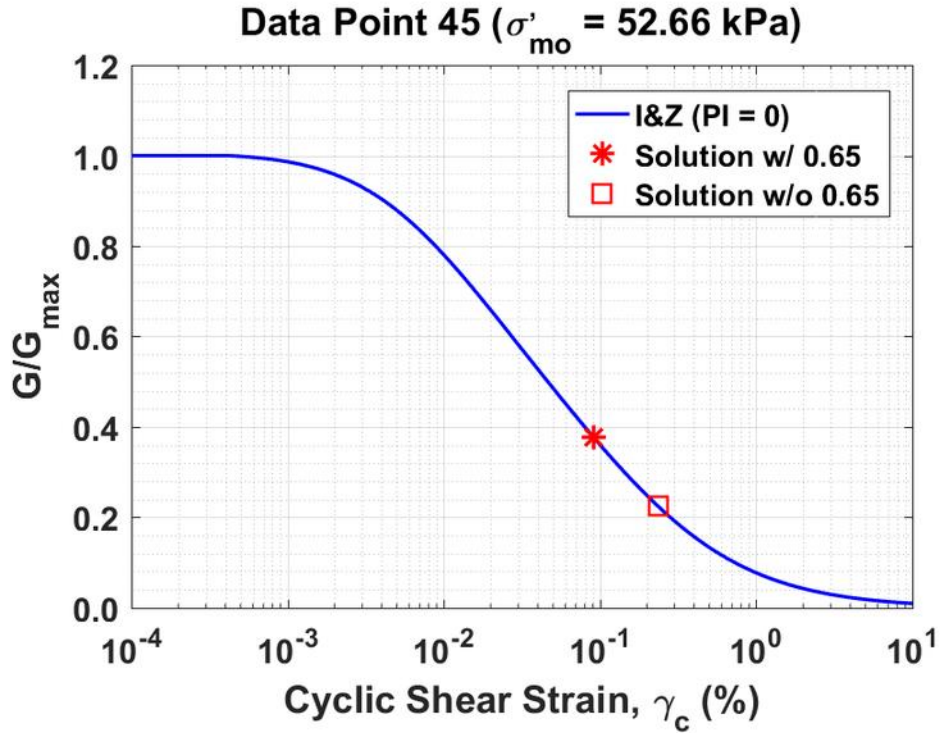


Figure B33. Normalized shear modulus reduction curves for Data Point 45 of the Kayen et al. database showing the solutions w/ and w/o the 0.65 factor

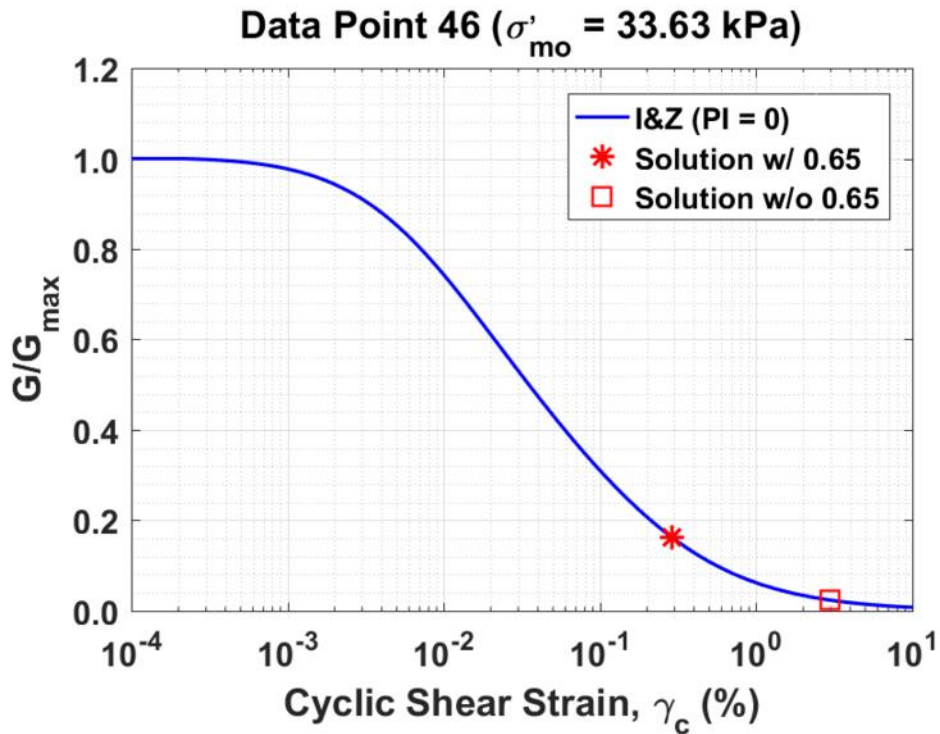


Figure B34. Normalized shear modulus reduction curves for Data Point 46 of the Kayen et al. database showing the solutions w/ and w/o the 0.65 factor

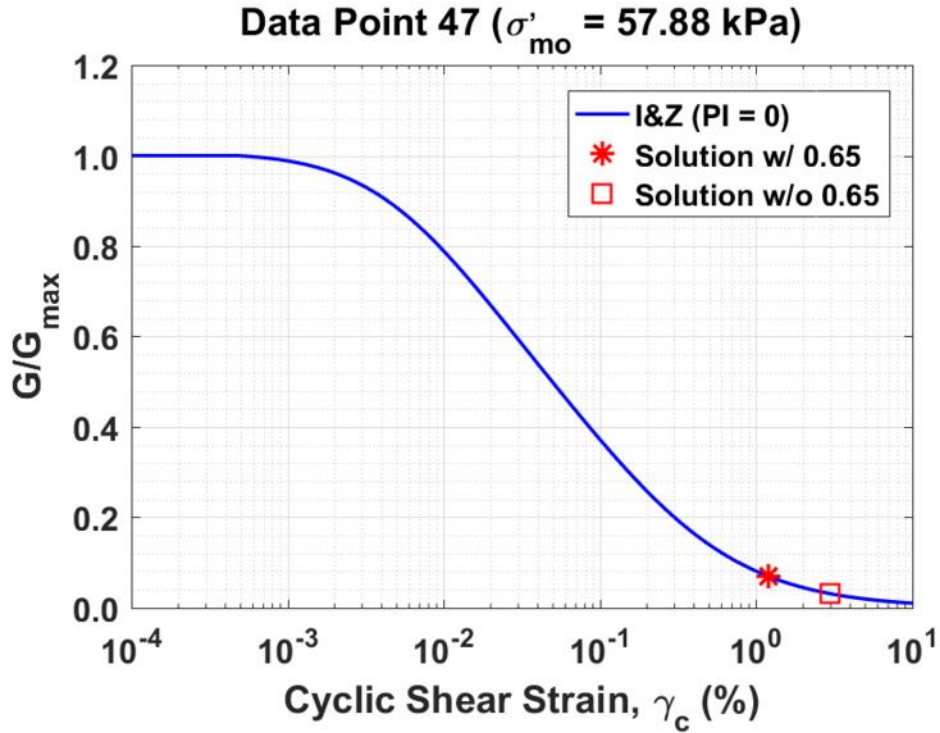


Figure B35. Normalized shear modulus reduction curves for Data Point 47 of the Kayen et al. database showing the solutions w/ and w/o the 0.65 factor

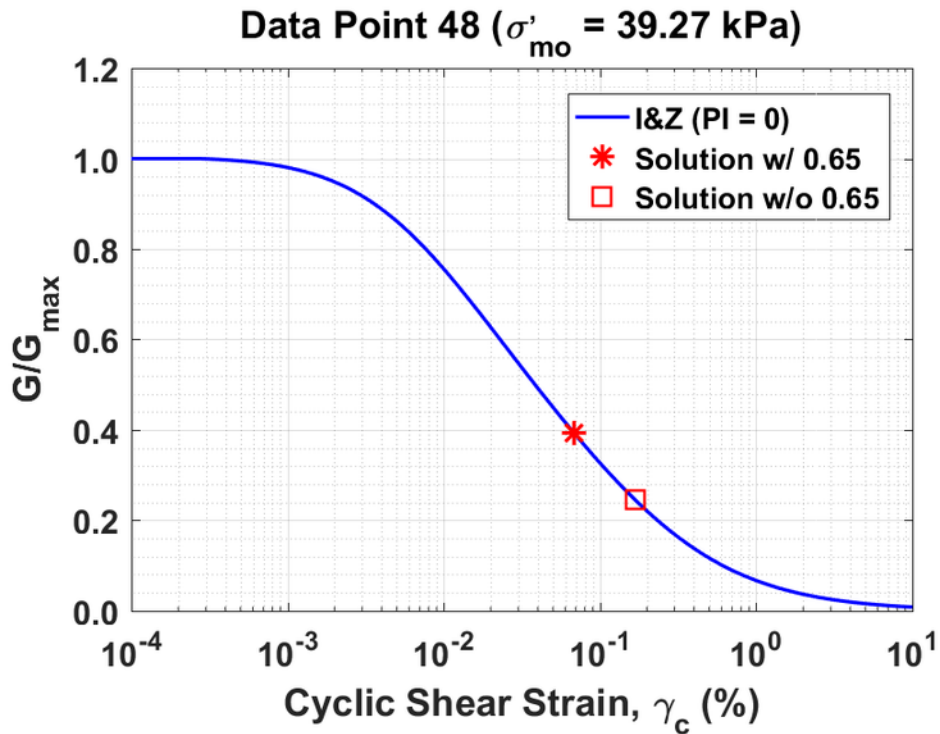


Figure B36. Normalized shear modulus reduction curves for Data Point 48 of the Kayen et al. database showing the solutions w/ and w/o the 0.65 factor

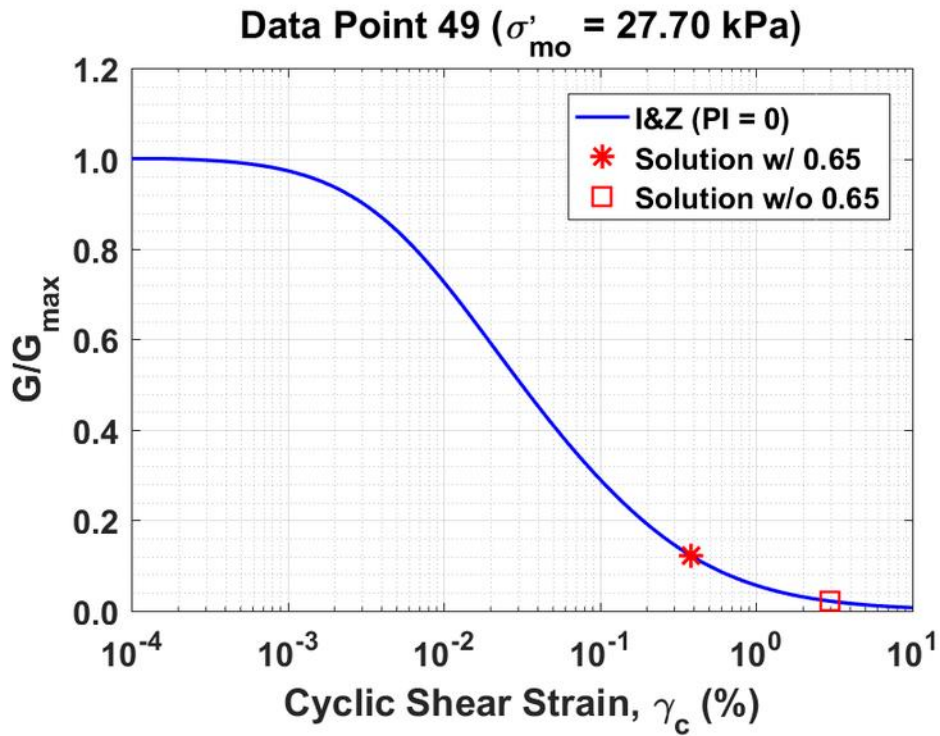


Figure B37. Normalized shear modulus reduction curves for Data Point 49 of the Kayen et al. database showing the solutions w/ and w/o the 0.65 factor

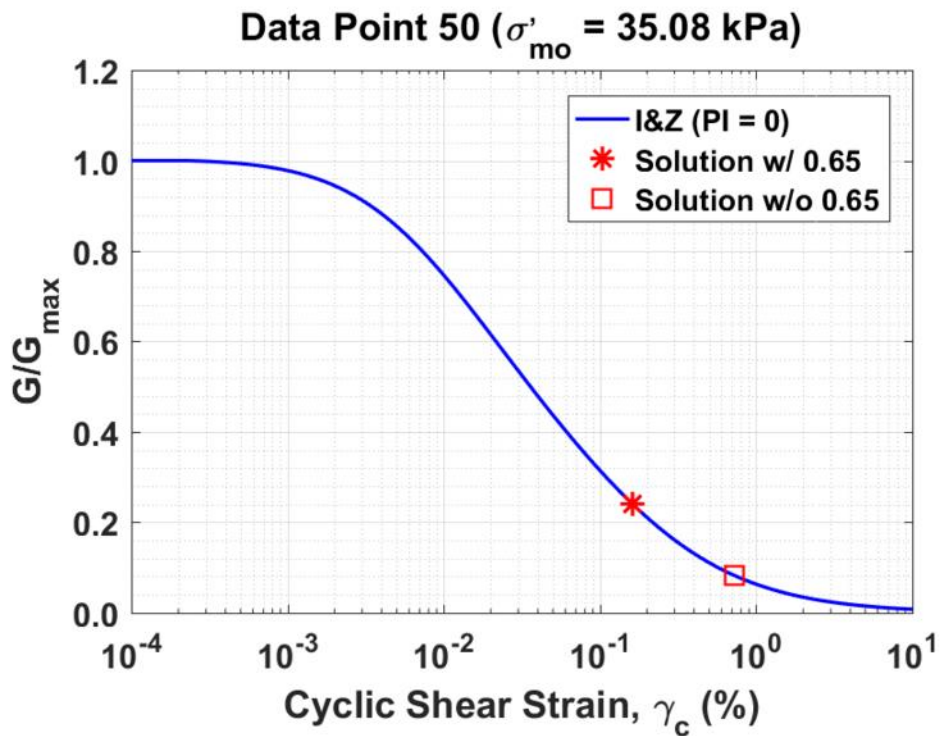


Figure B38. Normalized shear modulus reduction curves for Data Point 50 of the Kayen et al. database showing the solutions w/ and w/o the 0.65 factor

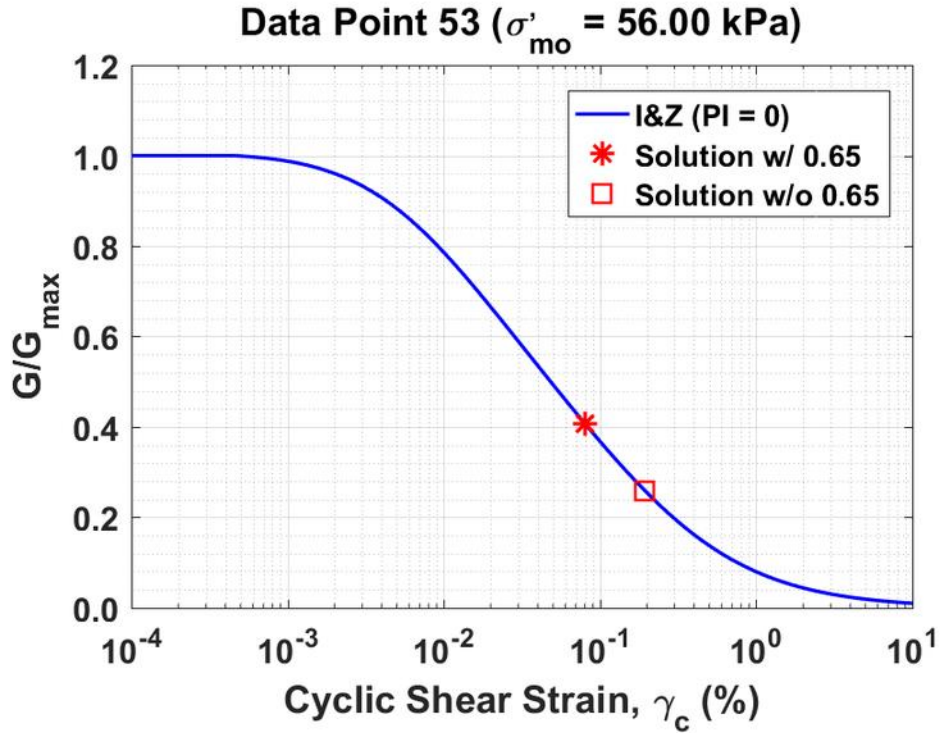


Figure B39. Normalized shear modulus reduction curves for Data Point 53 of the Kayen et al. database showing the solutions w/ and w/o the 0.65 factor

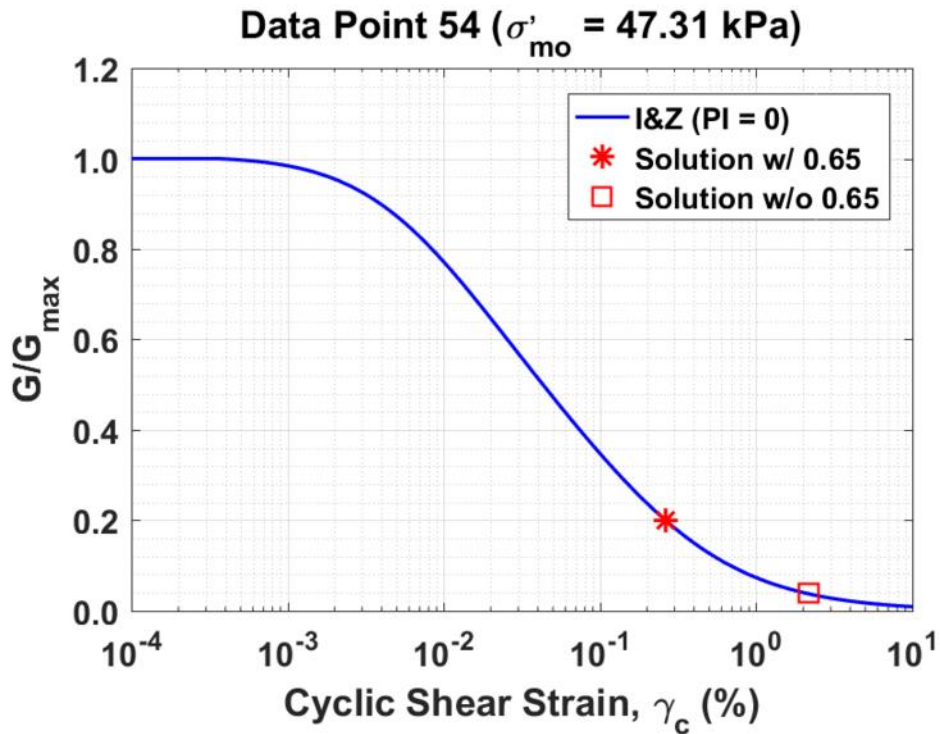


Figure B40. Normalized shear modulus reduction curves for Data Point 54 of the Kayen et al. database showing the solutions w/ and w/o the 0.65 factor

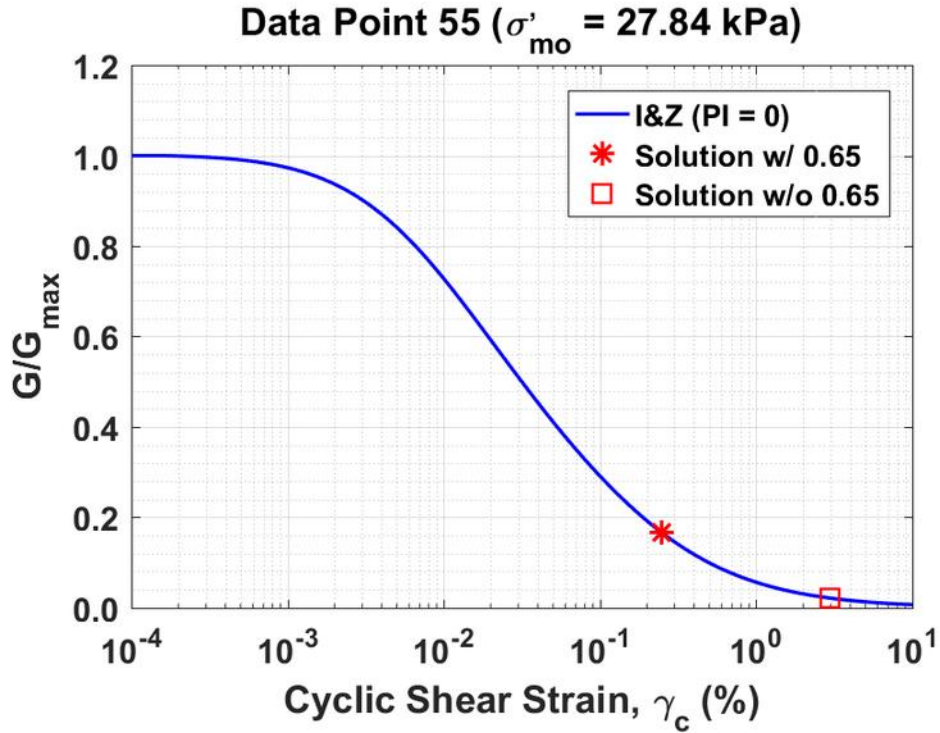


Figure B41. Normalized shear modulus reduction curves for Data Point 55 of the Kayen et al. database showing the solutions w/ and w/o the 0.65 factor

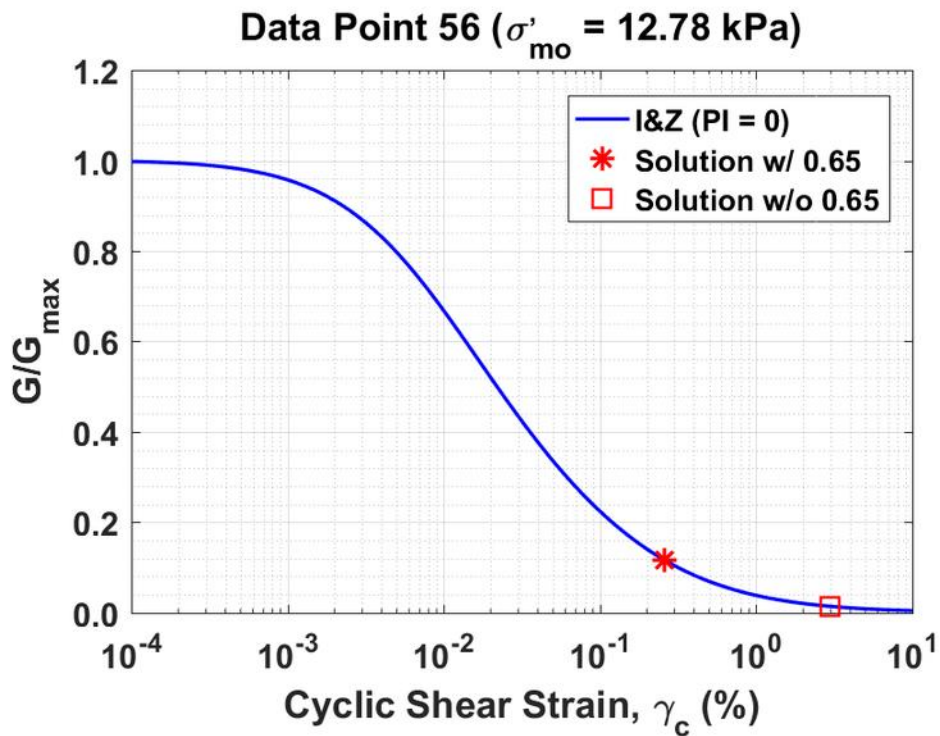


Figure B42. Normalized shear modulus reduction curves for Data Point 56 of the Kayen et al. database showing the solutions w/ and w/o the 0.65 factor

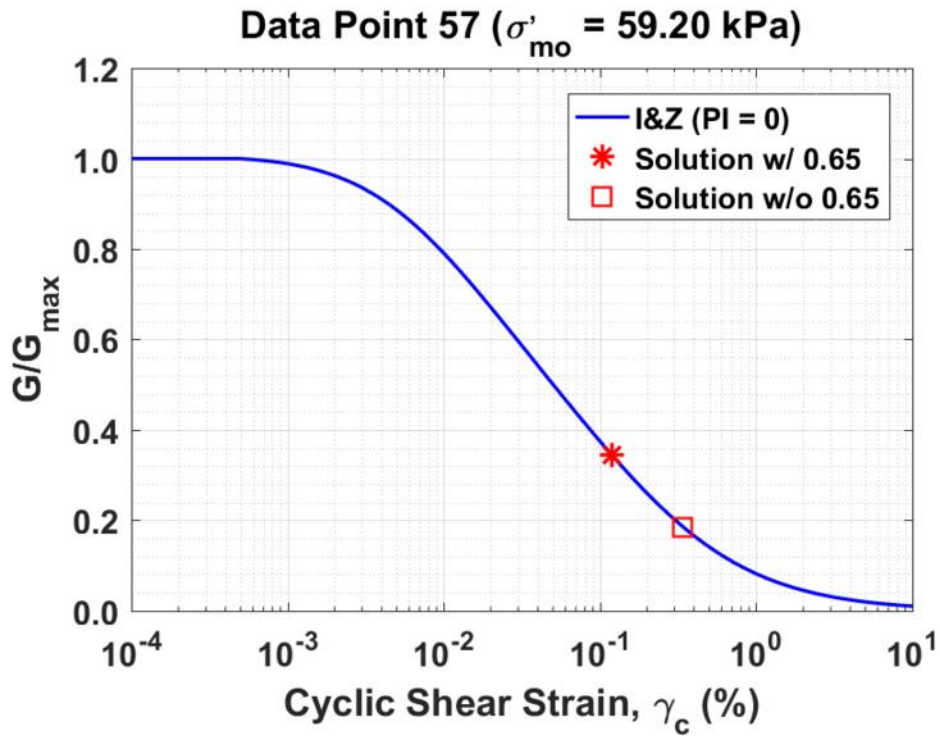


Figure B43. Normalized shear modulus reduction curves for Data Point 57 of the Kayen et al. database showing the solutions w/ and w/o the 0.65 factor

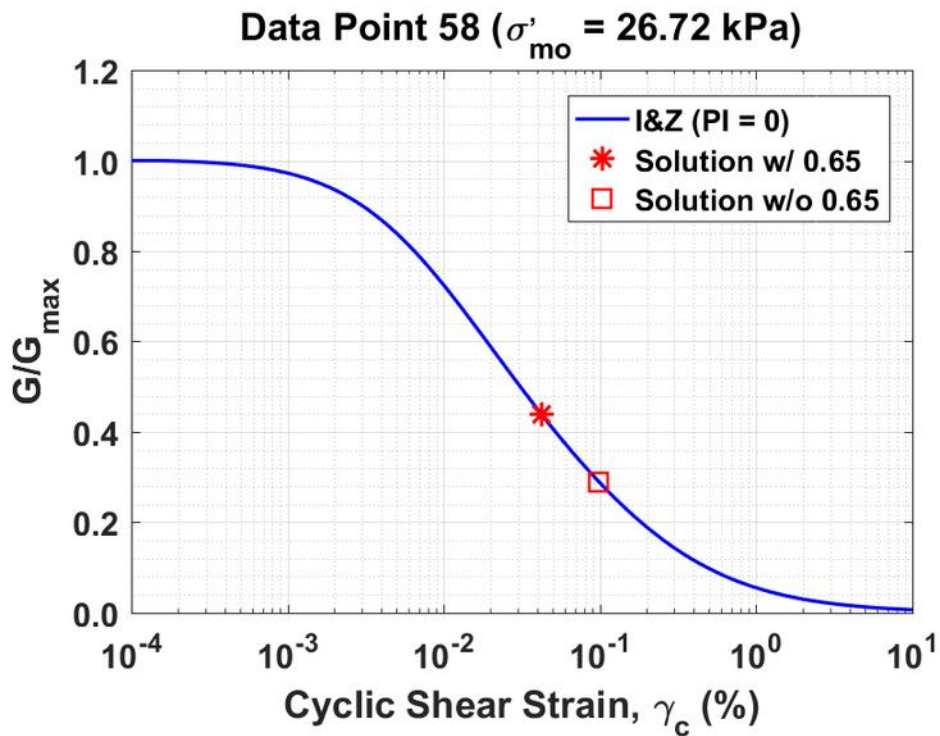


Figure B44. Normalized shear modulus reduction curves for Data Point 58 of the Kayen et al. database showing the solutions w/ and w/o the 0.65 factor

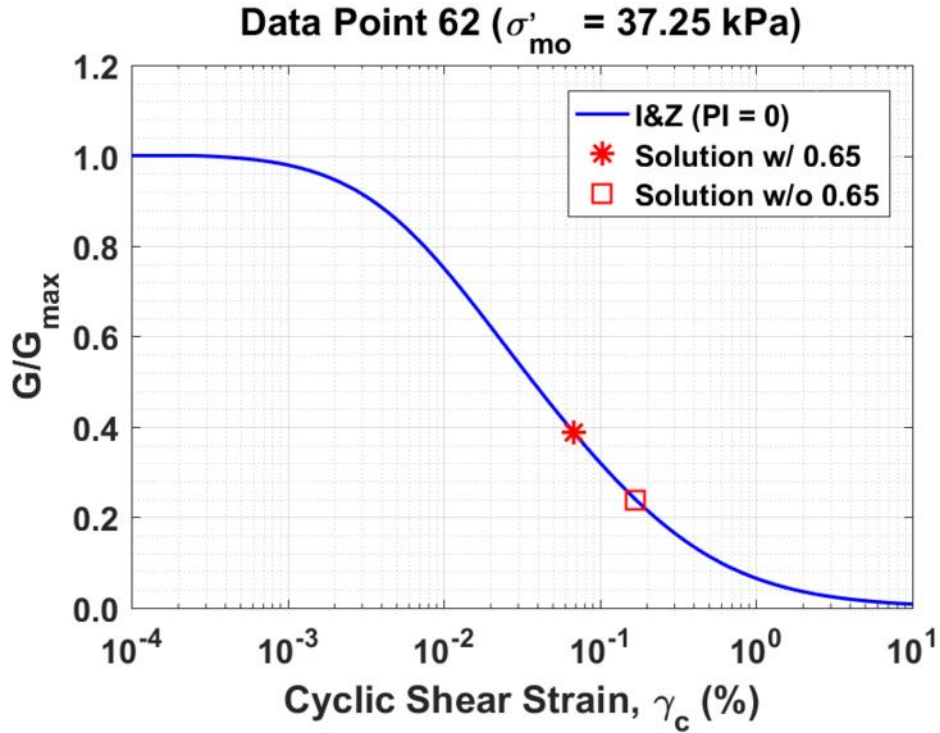


Figure B45. Normalized shear modulus reduction curves for Data Point 62 of the Kayen et al. database showing the solutions w/ and w/o the 0.65 factor

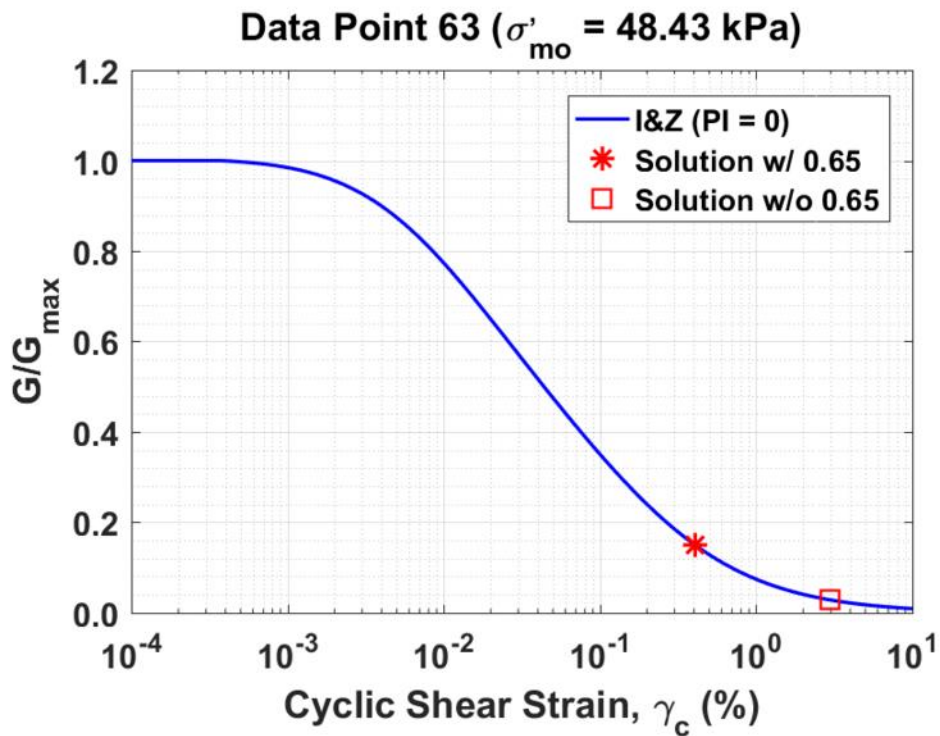


Figure B46. Normalized shear modulus reduction curves for Data Point 63 of the Kayen et al. database showing the solutions w/ and w/o the 0.65 factor

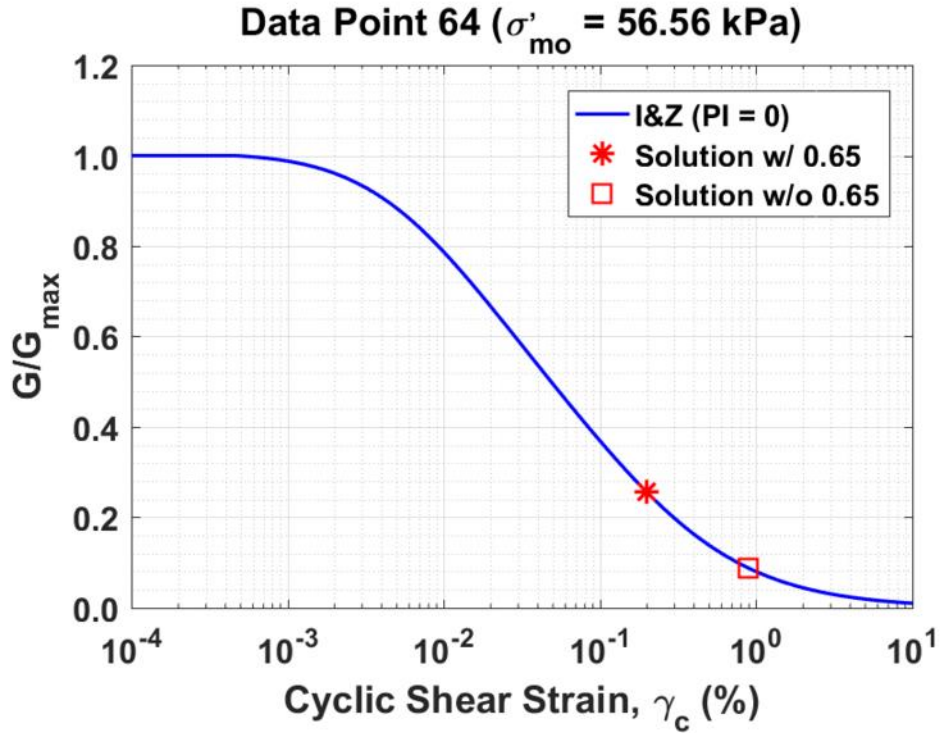


Figure B47. Normalized shear modulus reduction curves for Data Point 64 of the Kayen et al. database showing the solutions w/ and w/o the 0.65 factor

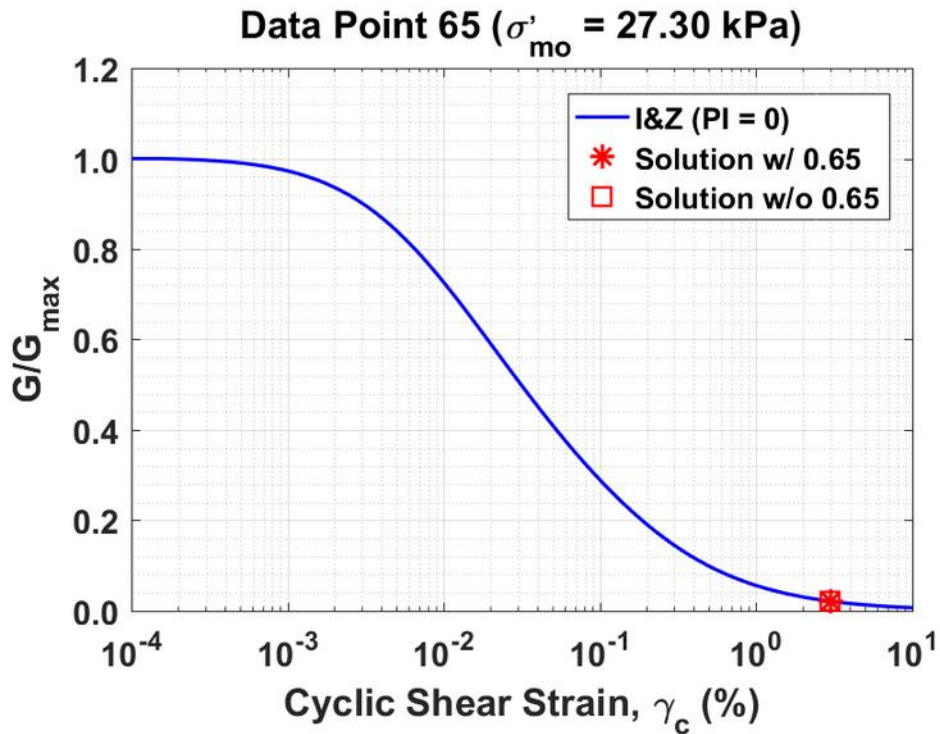


Figure B48. Normalized shear modulus reduction curves for Data Point 65 of the Kayen et al. database showing the solutions w/ and w/o the 0.65 factor

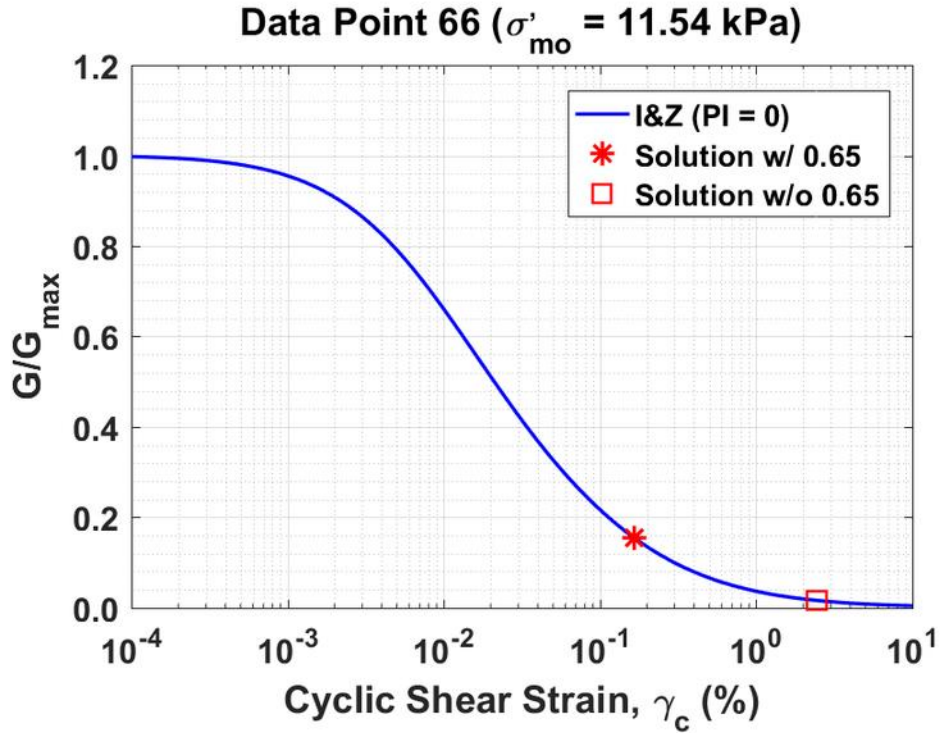


Figure B49. Normalized shear modulus reduction curves for Data Point 66 of the Kayen et al. database showing the solutions w/ and w/o the 0.65 factor

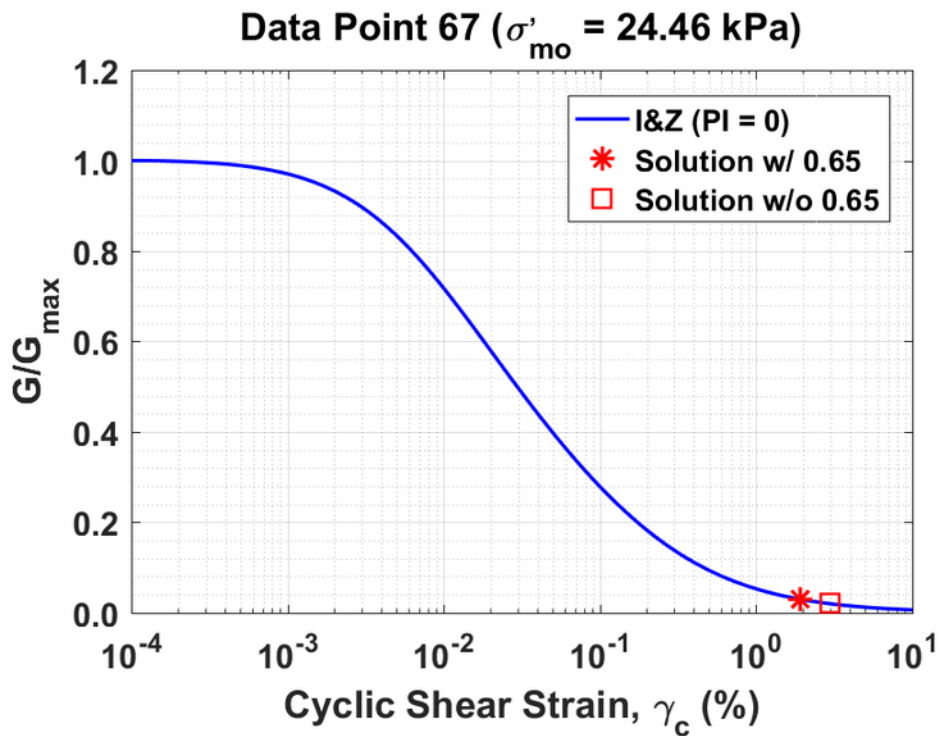


Figure B50. Normalized shear modulus reduction curves for Data Point 67 of the Kayen et al. database showing the solutions w/ and w/o the 0.65 factor

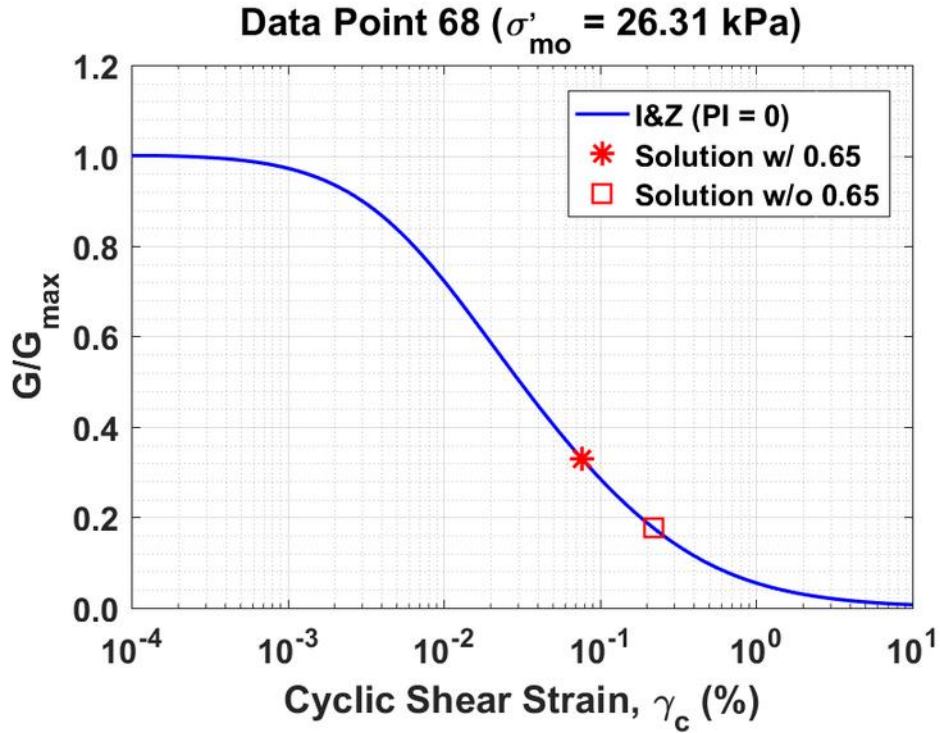


Figure B51. Normalized shear modulus reduction curves for Data Point 68 of the Kayen et al. database showing the solutions w/ and w/o the 0.65 factor

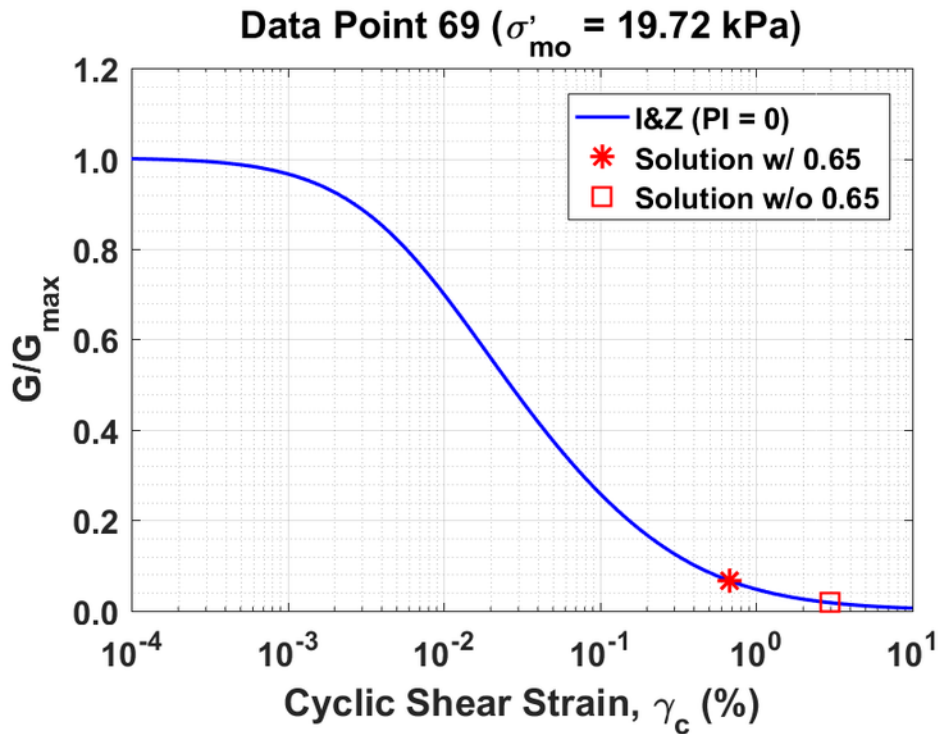


Figure B52. Normalized shear modulus reduction curves for Data Point 69 of the Kayen et al. database showing the solutions w/ and w/o the 0.65 factor

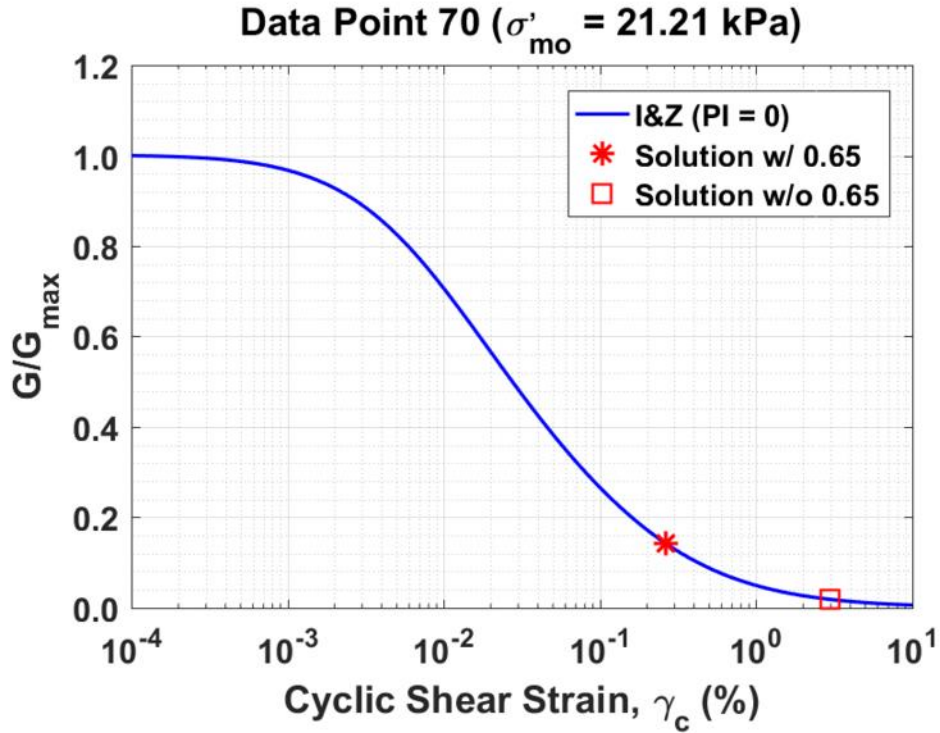


Figure B53. Normalized shear modulus reduction curves for Data Point 70 of the Kayen et al. database showing the solutions w/ and w/o the 0.65 factor

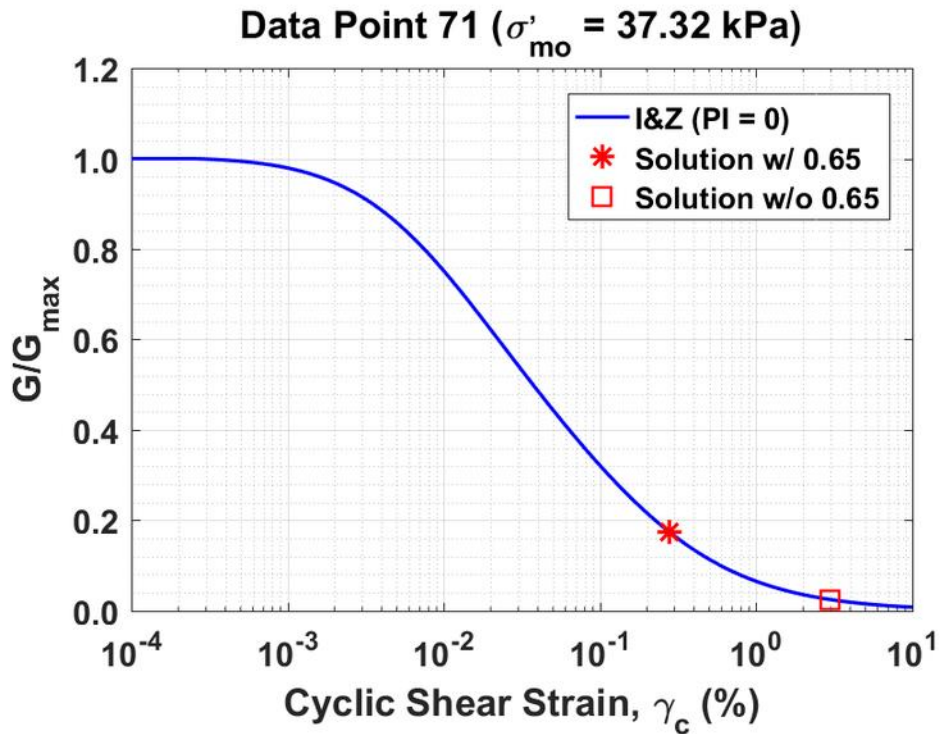


Figure B54. Normalized shear modulus reduction curves for Data Point 71 of the Kayen et al. database showing the solutions w/ and w/o the 0.65 factor

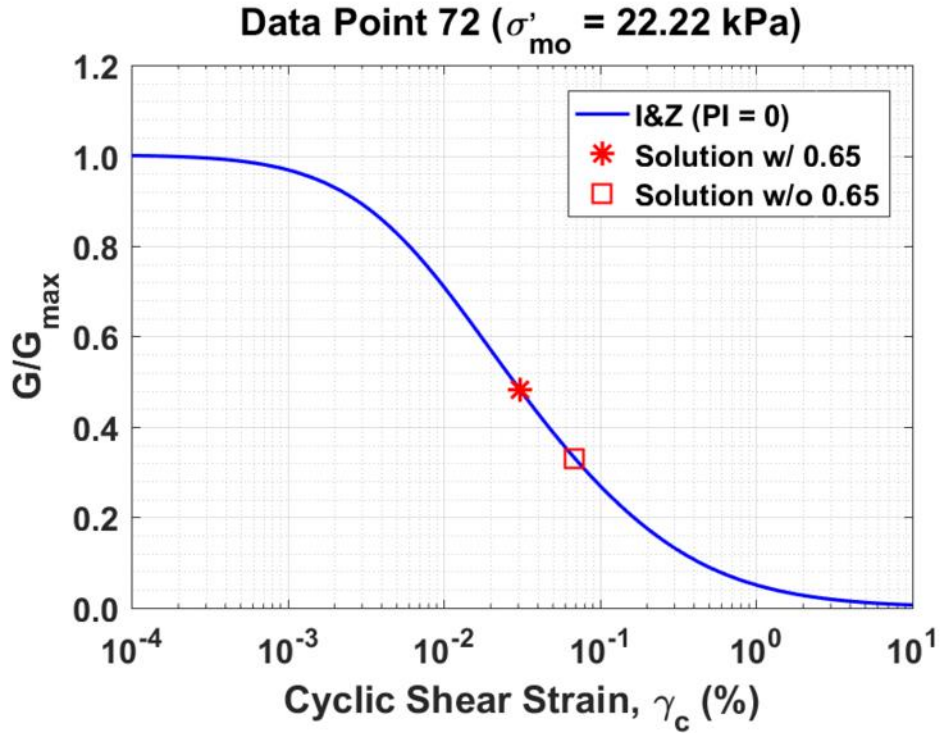


Figure B55. Normalized shear modulus reduction curves for Data Point 72 of the Kayen et al. database showing the solutions w/ and w/o the 0.65 factor

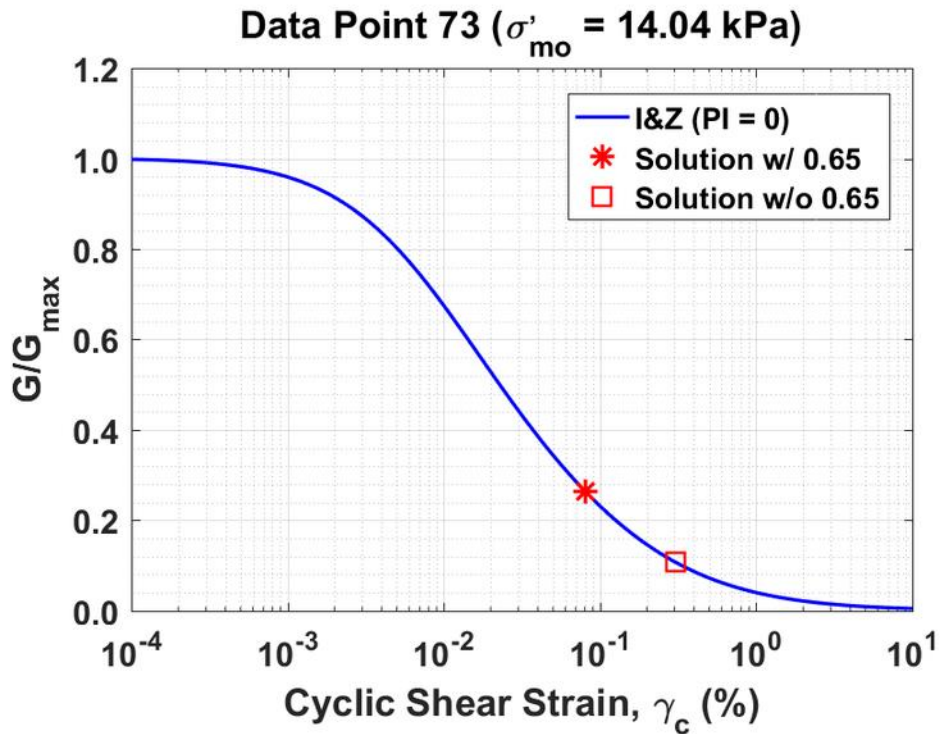


Figure B56. Normalized shear modulus reduction curves for Data Point 73 of the Kayen et al. database showing the solutions w/ and w/o the 0.65 factor

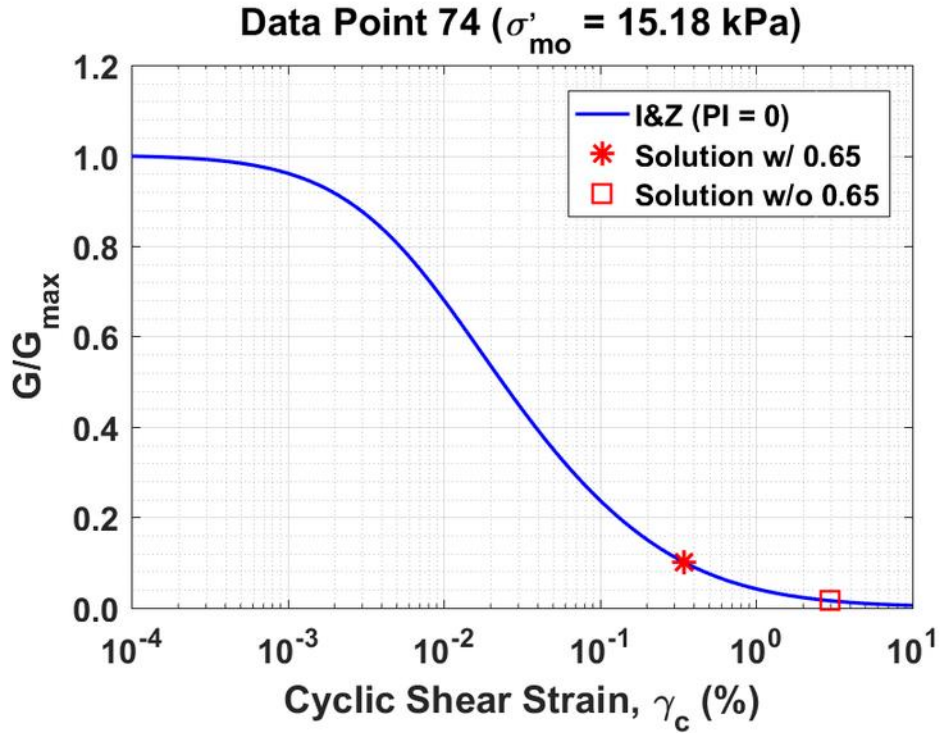


Figure B57. Normalized shear modulus reduction curves for Data Point 74 of the Kayen et al. database showing the solutions w/ and w/o the 0.65 factor

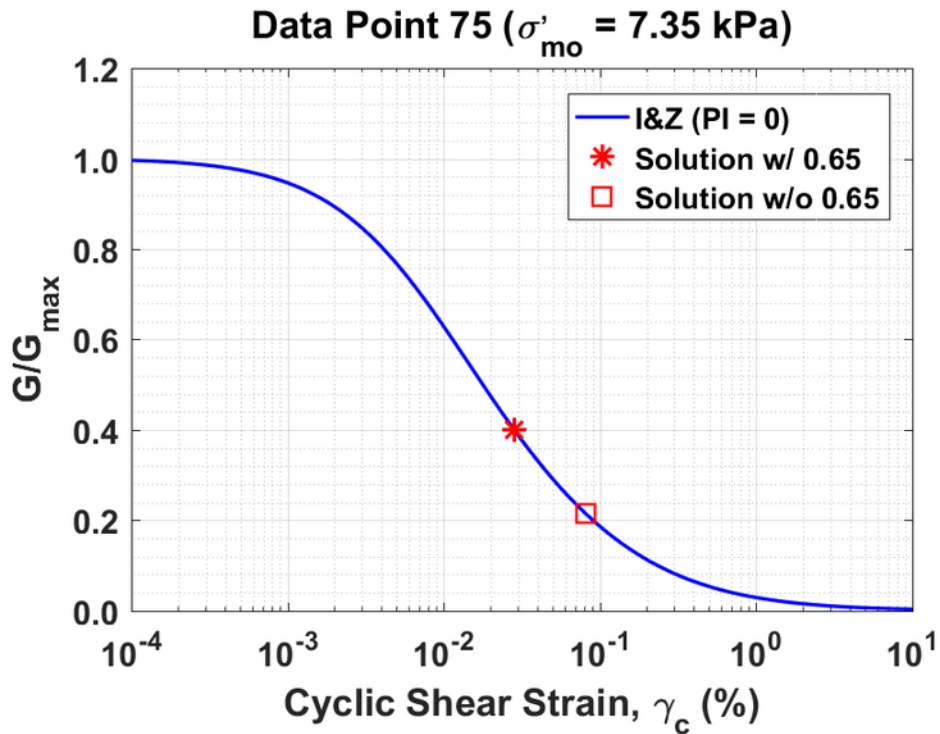


Figure B58. Normalized shear modulus reduction curves for Data Point 75 of the Kayen et al. database showing the solutions w/ and w/o the 0.65 factor

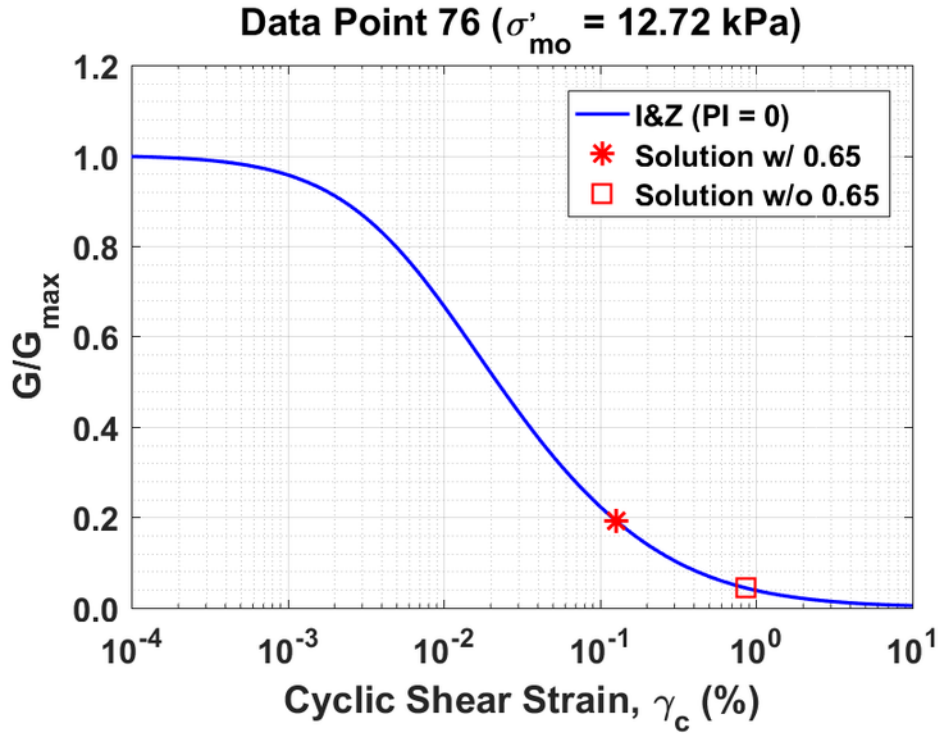


Figure B59. Normalized shear modulus reduction curves for Data Point 76 of the Kayen et al. database showing the solutions w/ and w/o the 0.65 factor

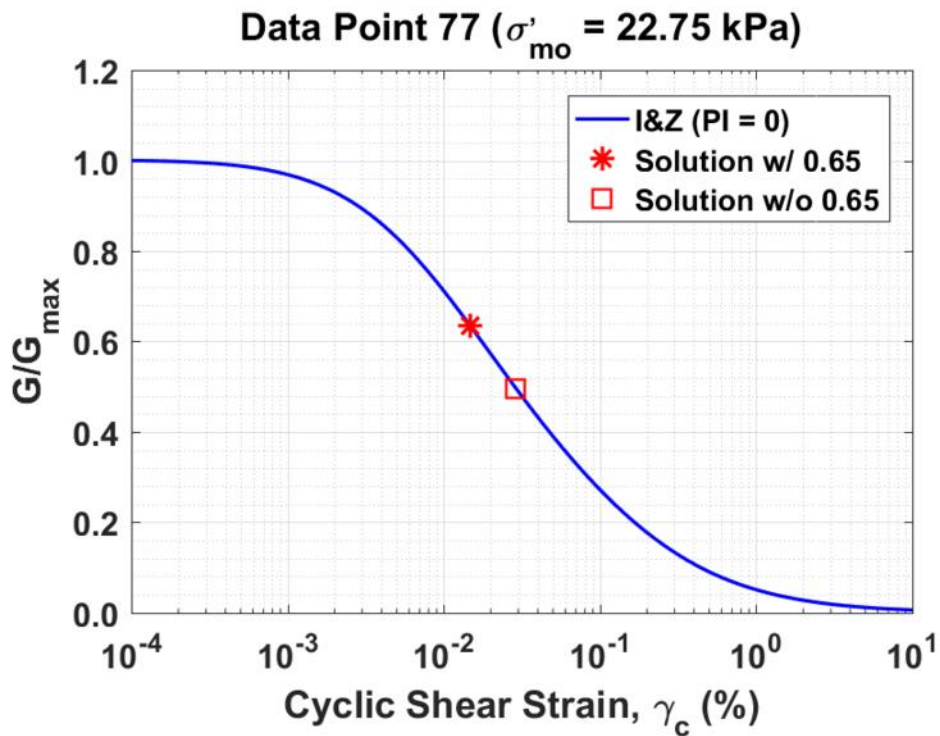


Figure B60. Normalized shear modulus reduction curves for Data Point 77 of the Kayen et al. database showing the solutions w/ and w/o the 0.65 factor

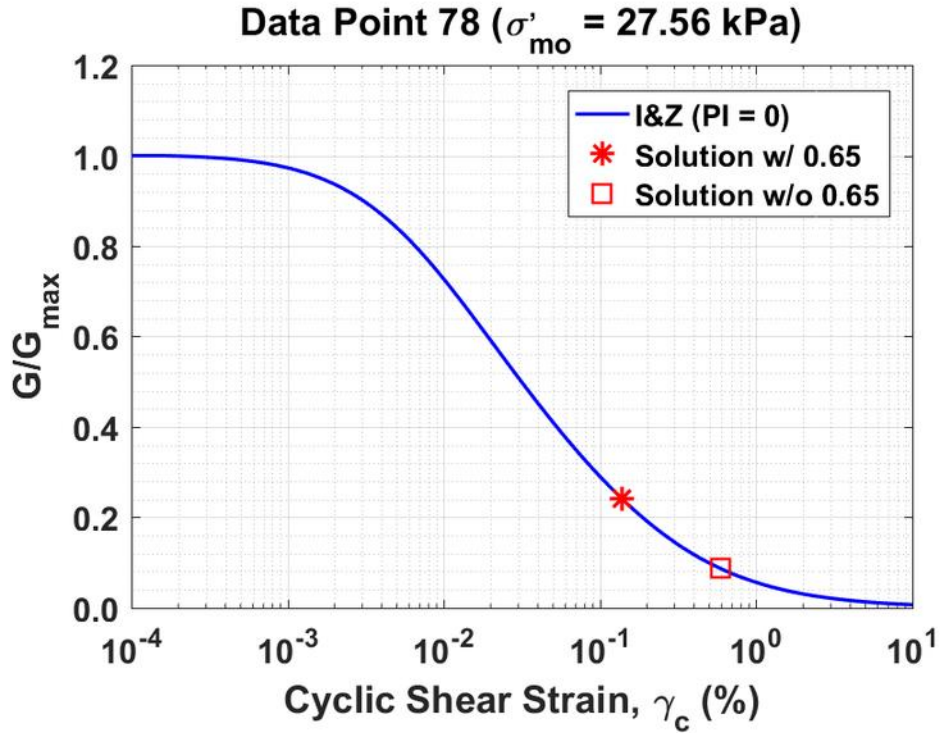


Figure B61. Normalized shear modulus reduction curves for Data Point 78 of the Kayen et al. database showing the solutions w/ and w/o the 0.65 factor

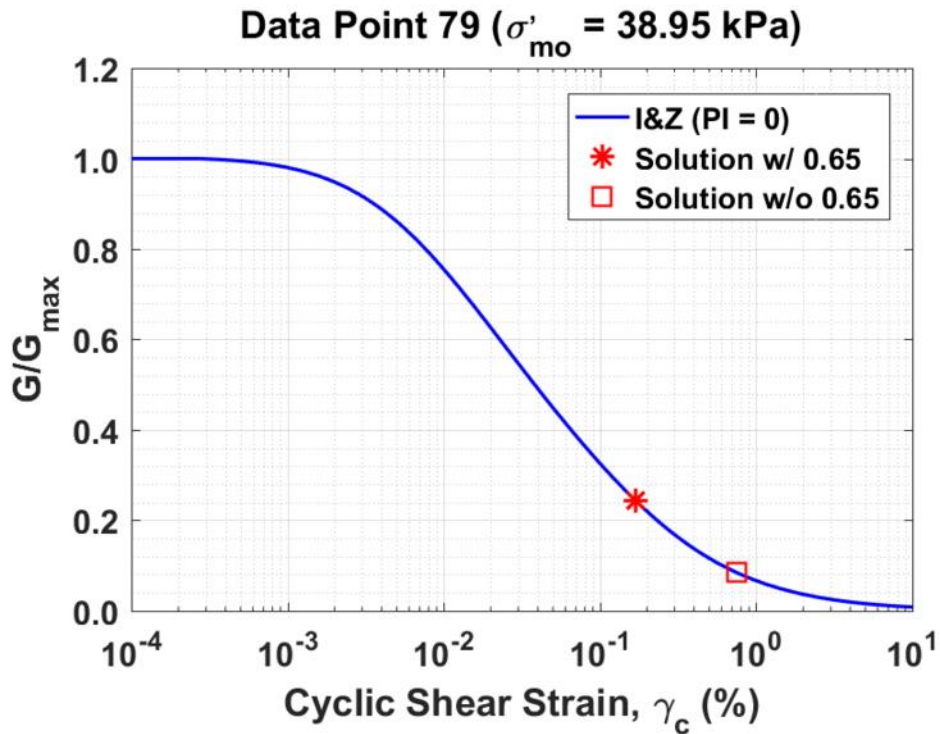


Figure B62. Normalized shear modulus reduction curves for Data Point 79 of the Kayen et al. database showing the solutions w/ and w/o the 0.65 factor

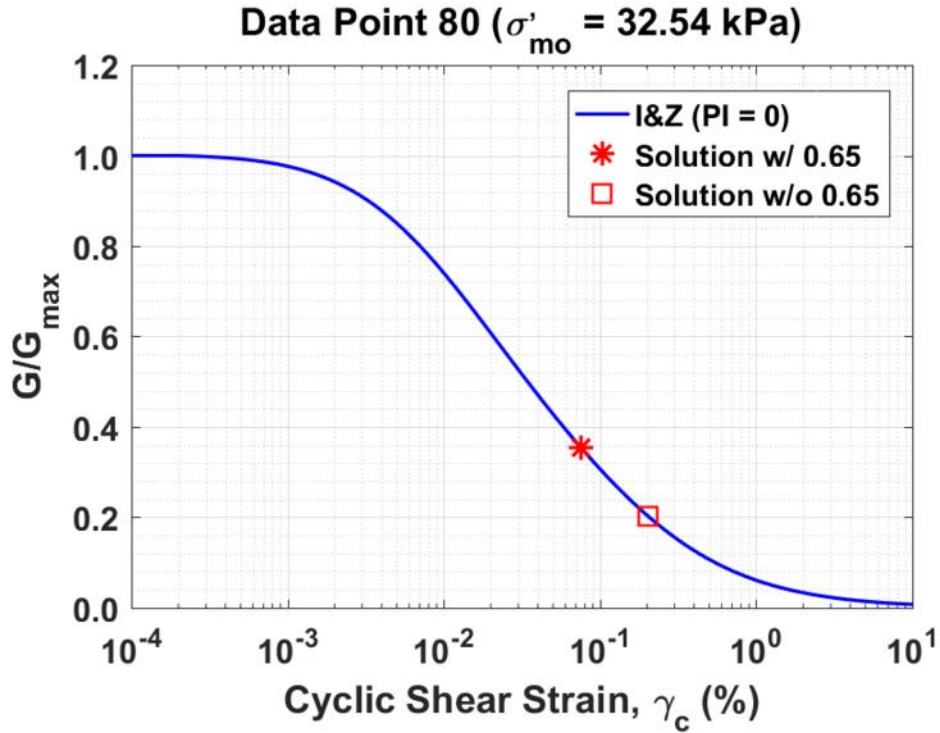


Figure 63. Normalized shear modulus reduction curves for Data Point 80 of the Kayen et al. database showing the solutions w/ and w/o the 0.65 factor

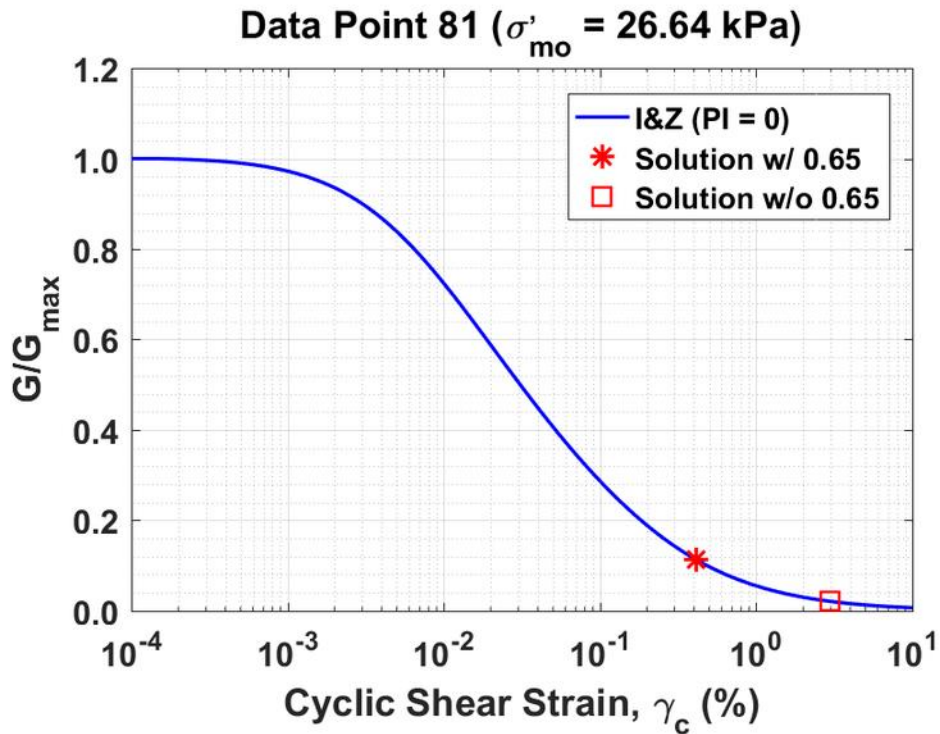


Figure B64. Normalized shear modulus reduction curves for Data Point 81 of the Kayen et al. database showing the solutions w/ and w/o the 0.65 factor

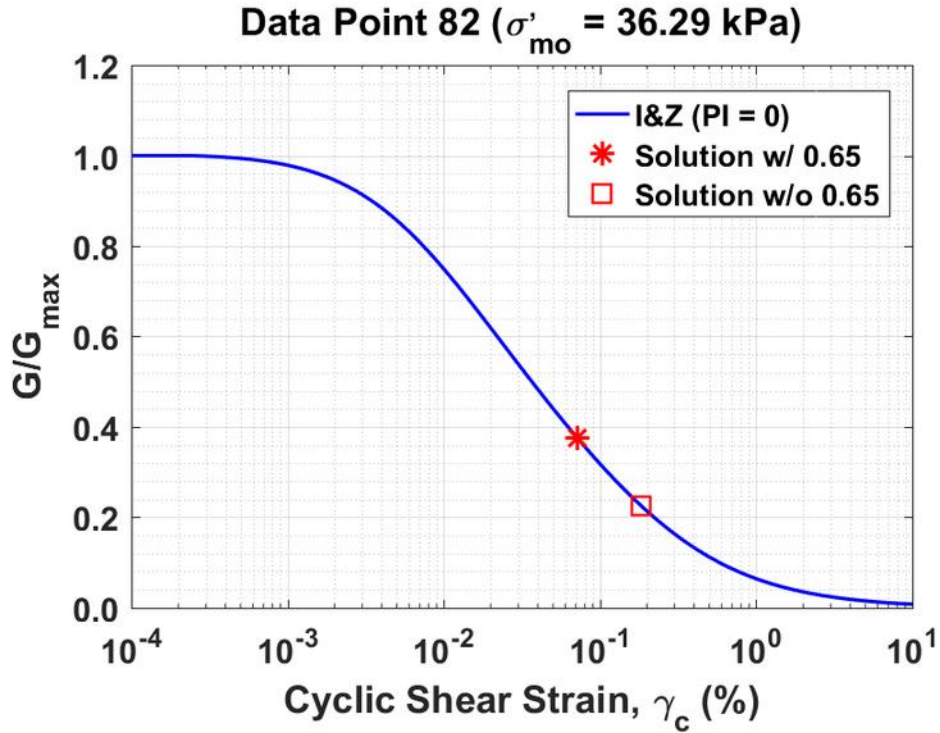


Figure B65. Normalized shear modulus reduction curves for Data Point 82 of the Kayen et al. database showing the solutions w/ and w/o the 0.65 factor

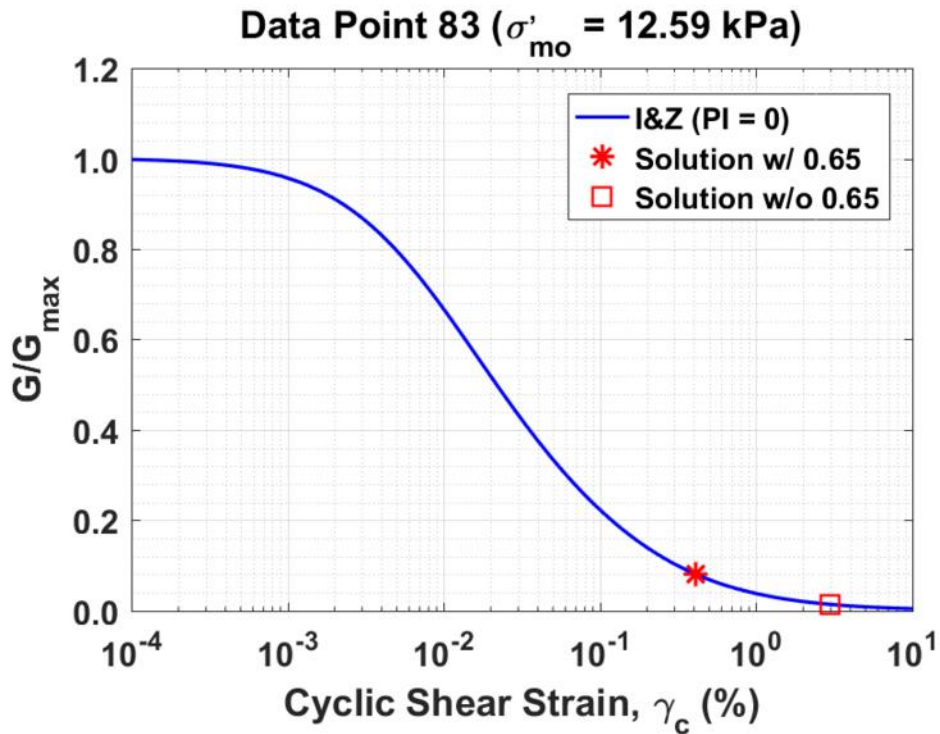


Figure B66. Normalized shear modulus reduction curves for Data Point 83 of the Kayen et al. database showing the solutions w/ and w/o the 0.65 factor

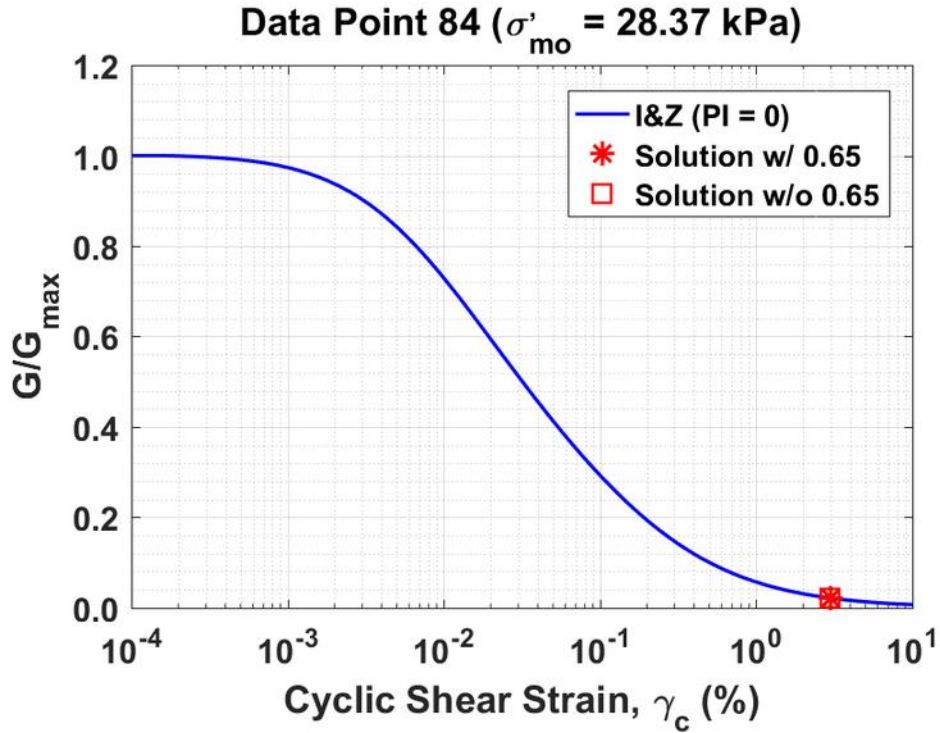


Figure B67. Normalized shear modulus reduction curves for Data Point 84 of the Kayen et al. database showing the solutions w/ and w/o the 0.65 factor

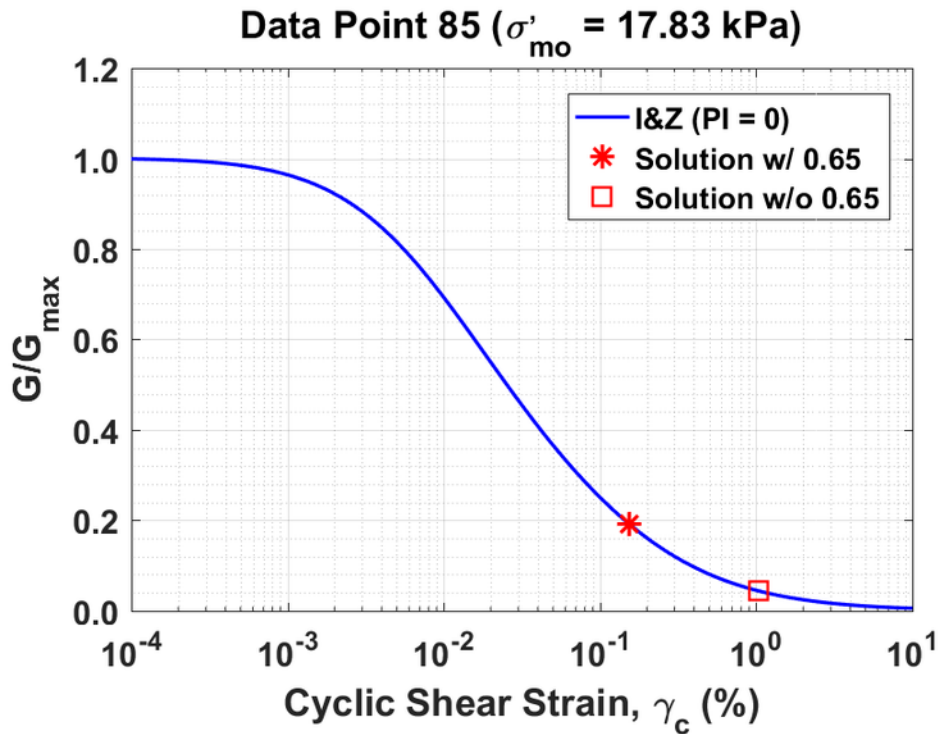


Figure B68. Normalized shear modulus reduction curves for Data Point 85 of the Kayen et al. database showing the solutions w/ and w/o the 0.65 factor

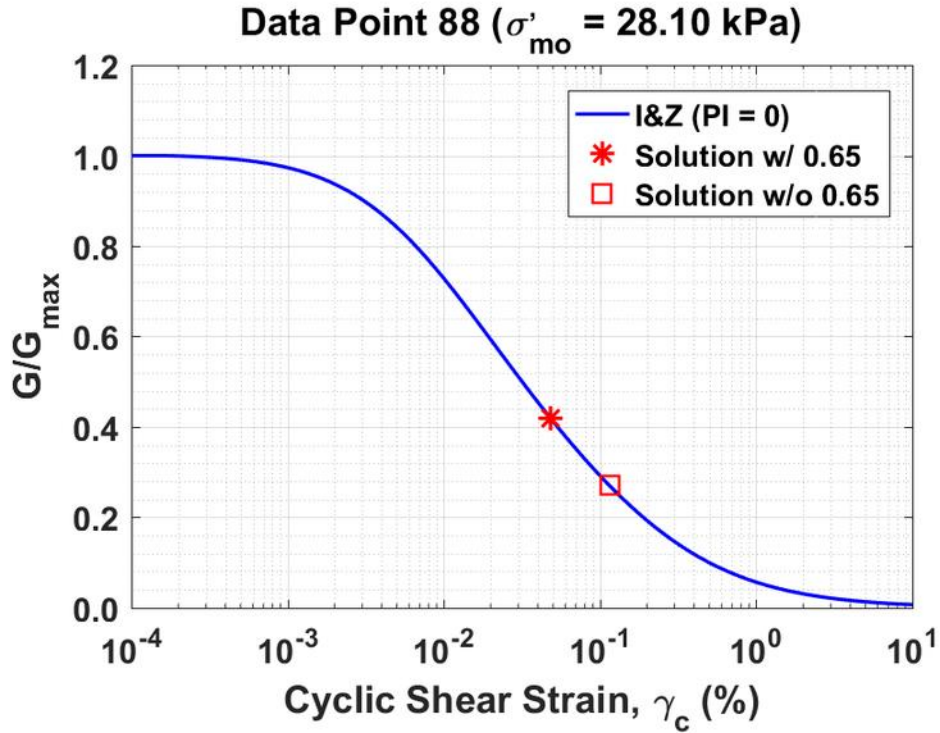


Figure B69. Normalized shear modulus reduction curves for Data Point 88 of the Kayen et al. database showing the solutions w/ and w/o the 0.65 factor

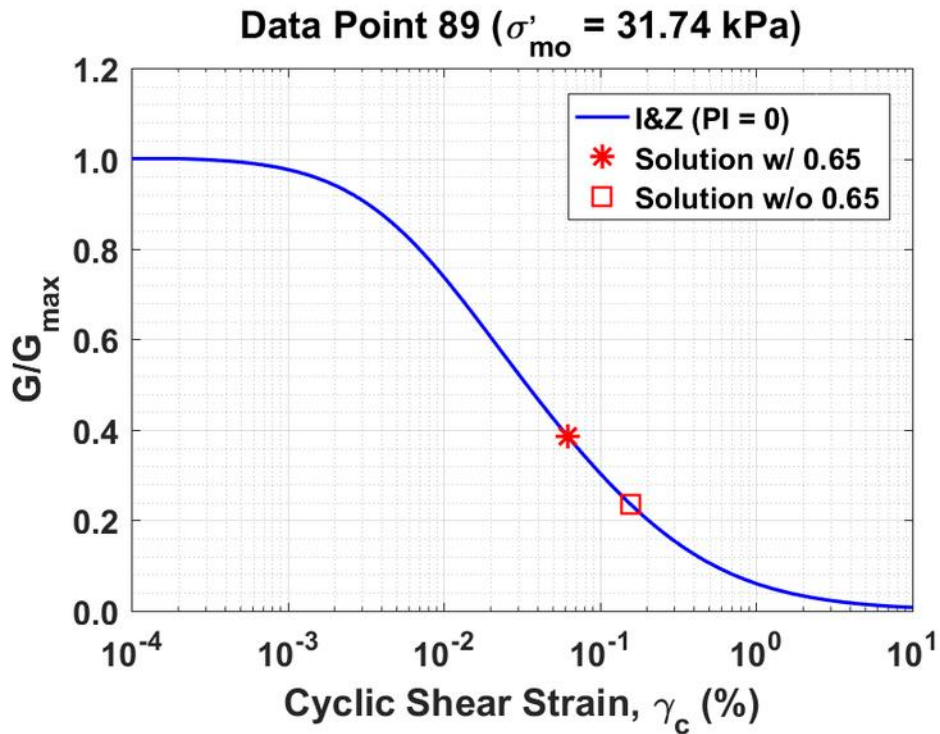


Figure B70. Normalized shear modulus reduction curves for Data Point 89 of the Kayen et al. database showing the solutions w/ and w/o the 0.65 factor

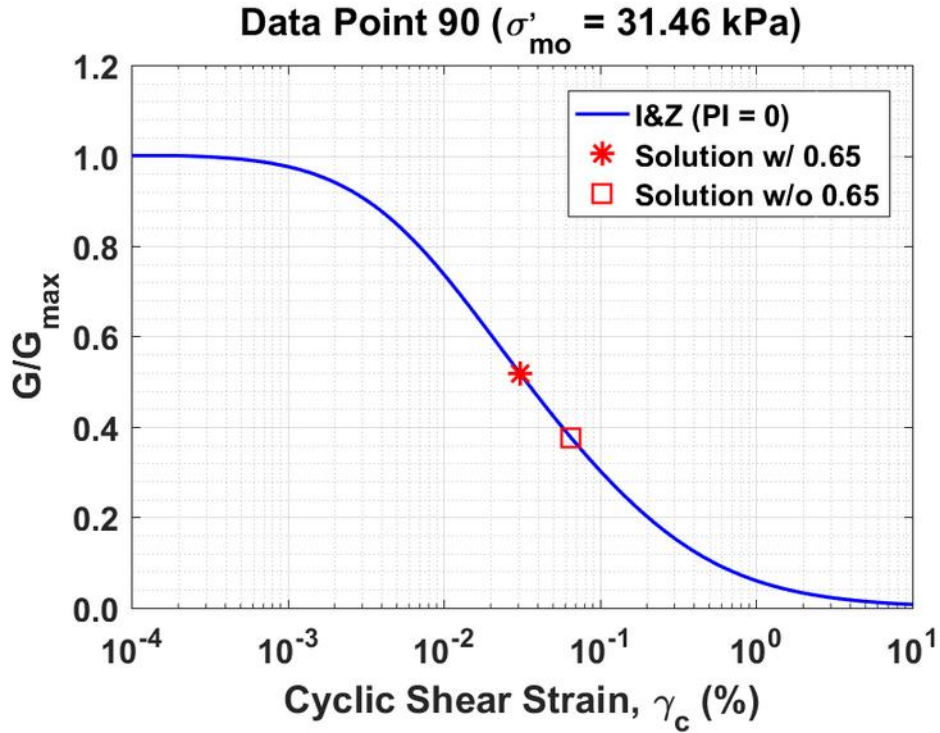


Figure B71. Normalized shear modulus reduction curves for Data Point 90 of the Kayen et al. database showing the solutions w/ and w/o the 0.65 factor

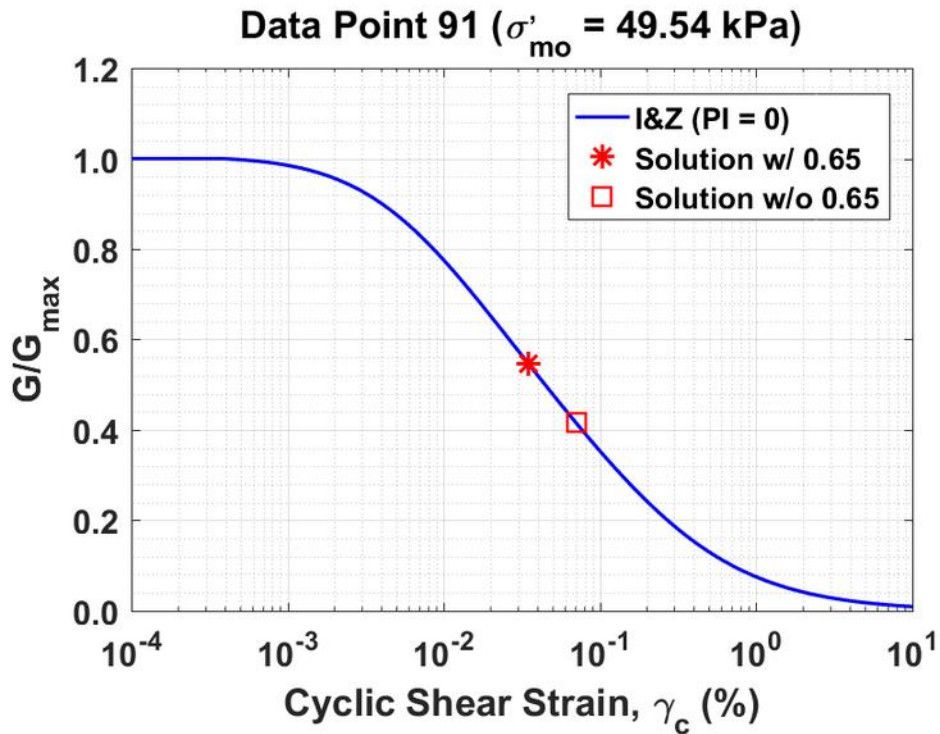


Figure B72. Normalized shear modulus reduction curves for Data Point 91 of the Kayen et al. database showing the solutions w/ and w/o the 0.65 factor

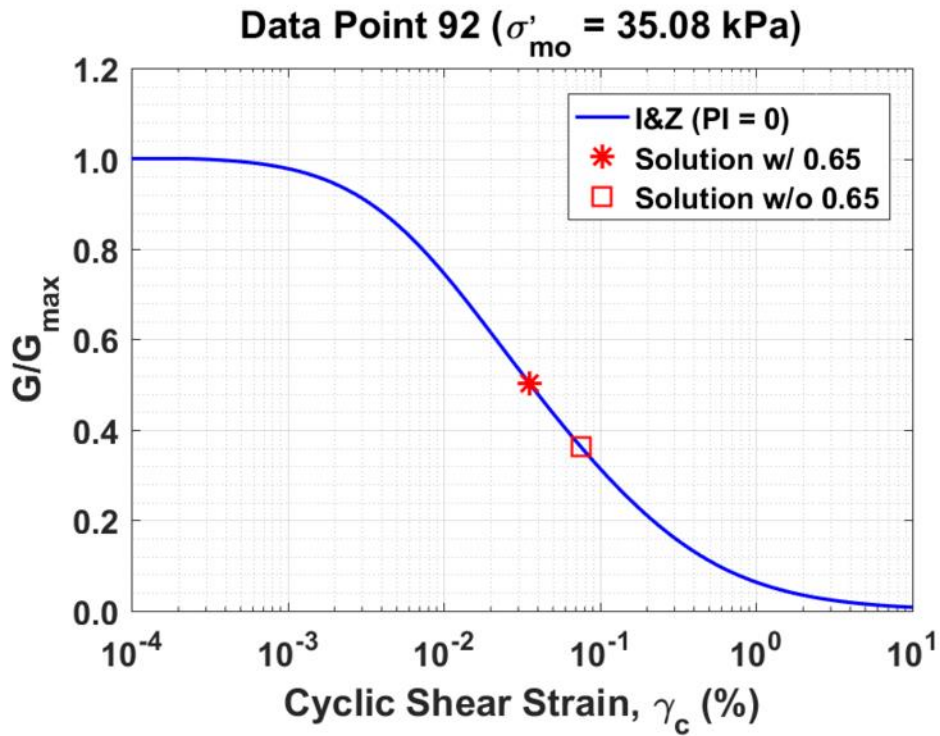


Figure B73. Normalized shear modulus reduction curves for Data Point 92 of the Kayen et al. database showing the solutions w/ and w/o the 0.65 factor

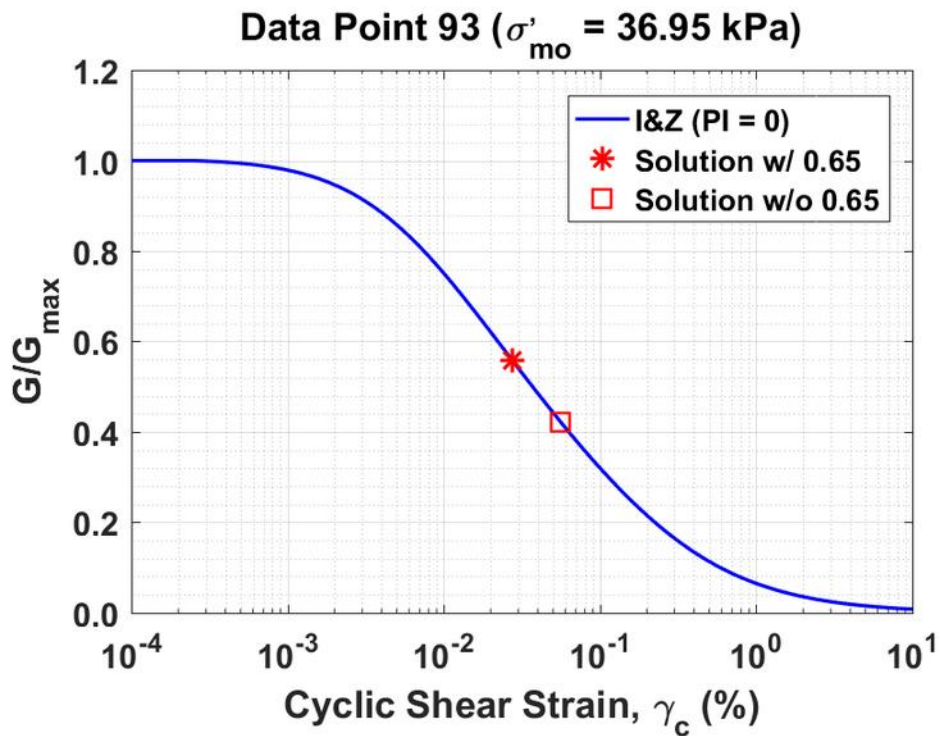


Figure B74. Normalized shear modulus reduction curves for Data Point 93 of the Kayen et al. database showing the solutions w/ and w/o the 0.65 factor

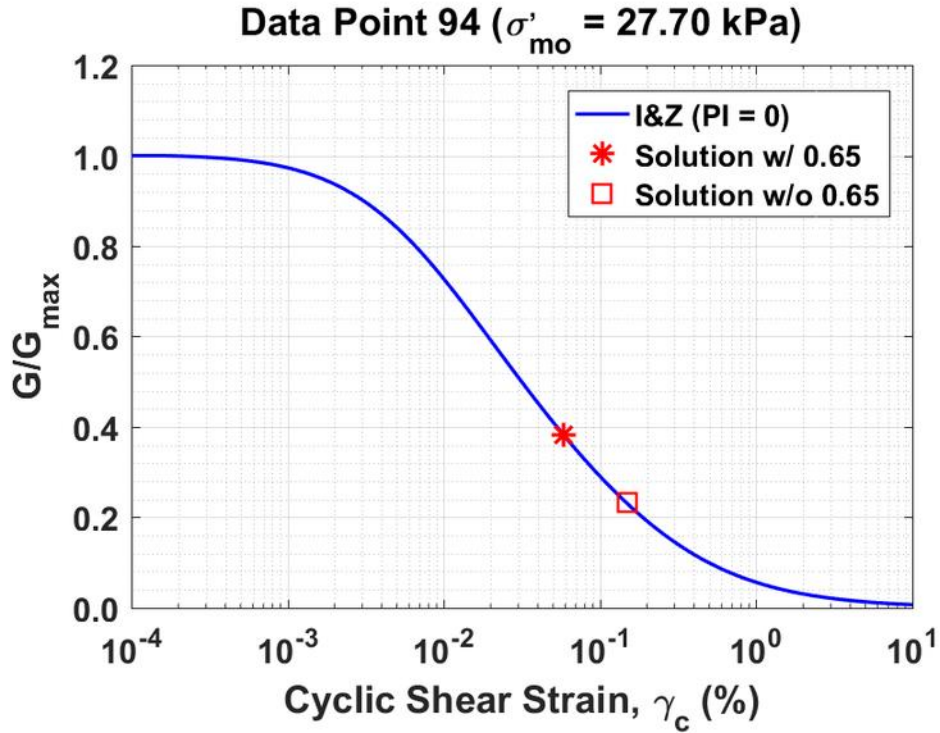


Figure B75. Normalized shear modulus reduction curves for Data Point 94 of the Kayen et al. database showing the solutions w/ and w/o the 0.65 factor

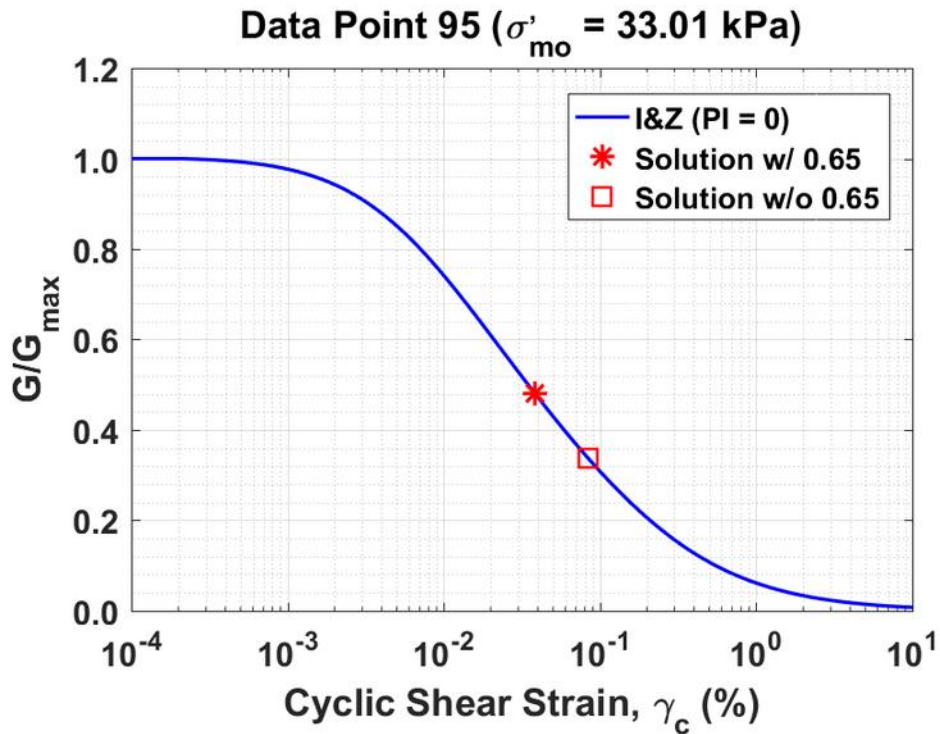


Figure B76. Normalized shear modulus reduction curves for Data Point 95 of the Kayen et al. database showing the solutions w/ and w/o the 0.65 factor

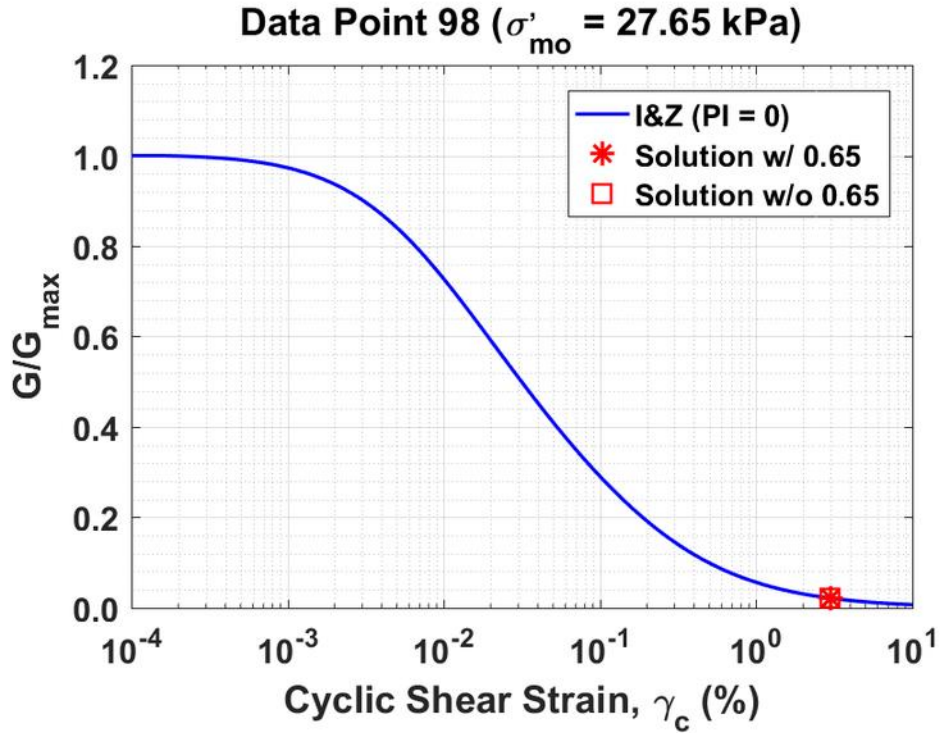


Figure B77. Normalized shear modulus reduction curves for Data Point 98 of the Kayen et al. database showing the solutions w/ and w/o the 0.65 factor

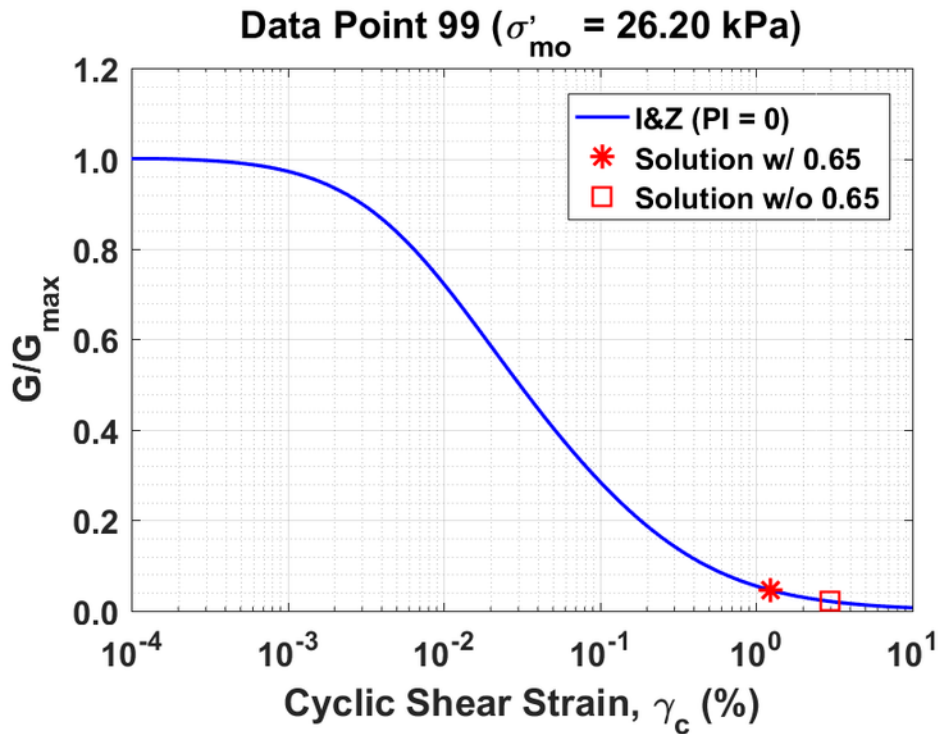


Figure B78. Normalized shear modulus reduction curves for Data Point 99 of the Kayen et al. database showing the solutions w/ and w/o the 0.65 factor

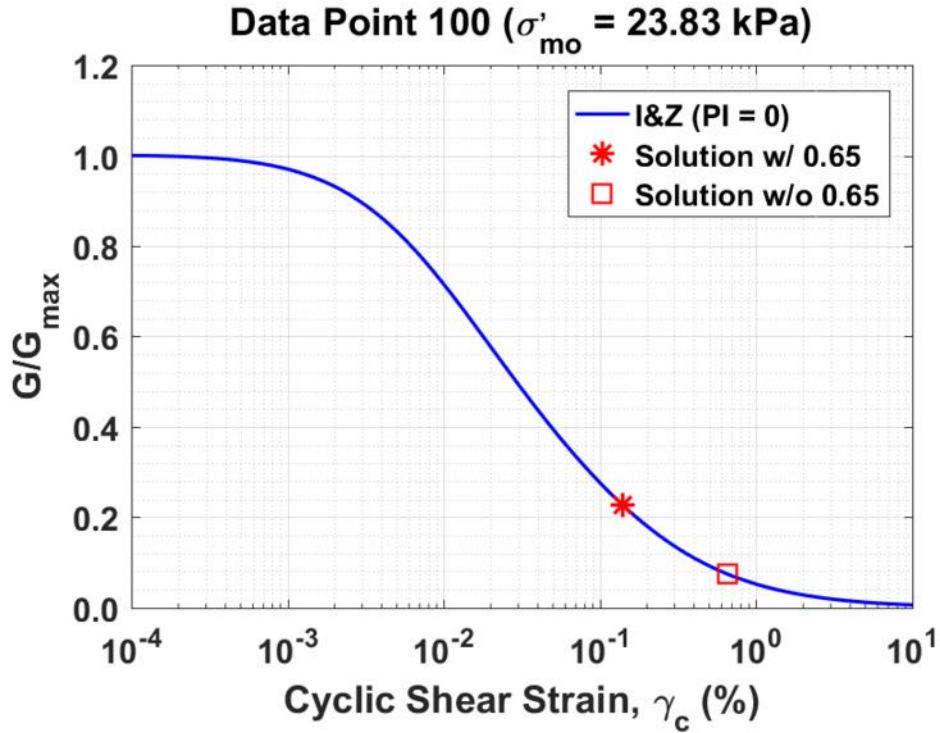


Figure B79. Normalized shear modulus reduction curves for Data Point 100 of the Kayen et al. database showing the solutions w/ and w/o the 0.65 factor

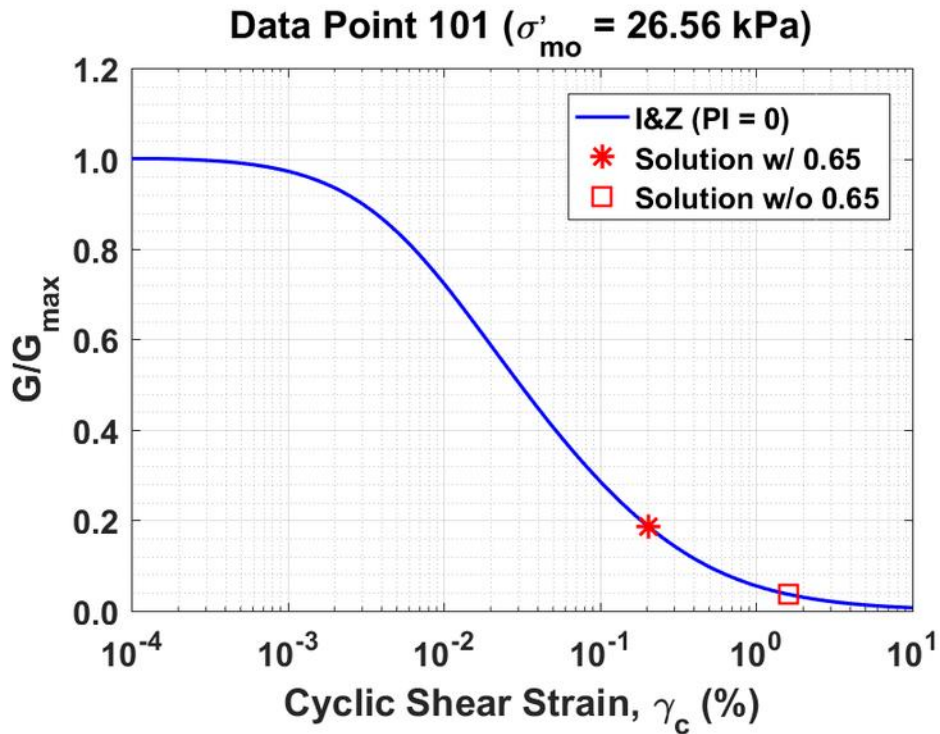


Figure B80. Normalized shear modulus reduction curves for Data Point 101 of the Kayen et al. database showing the solutions w/ and w/o the 0.65 factor

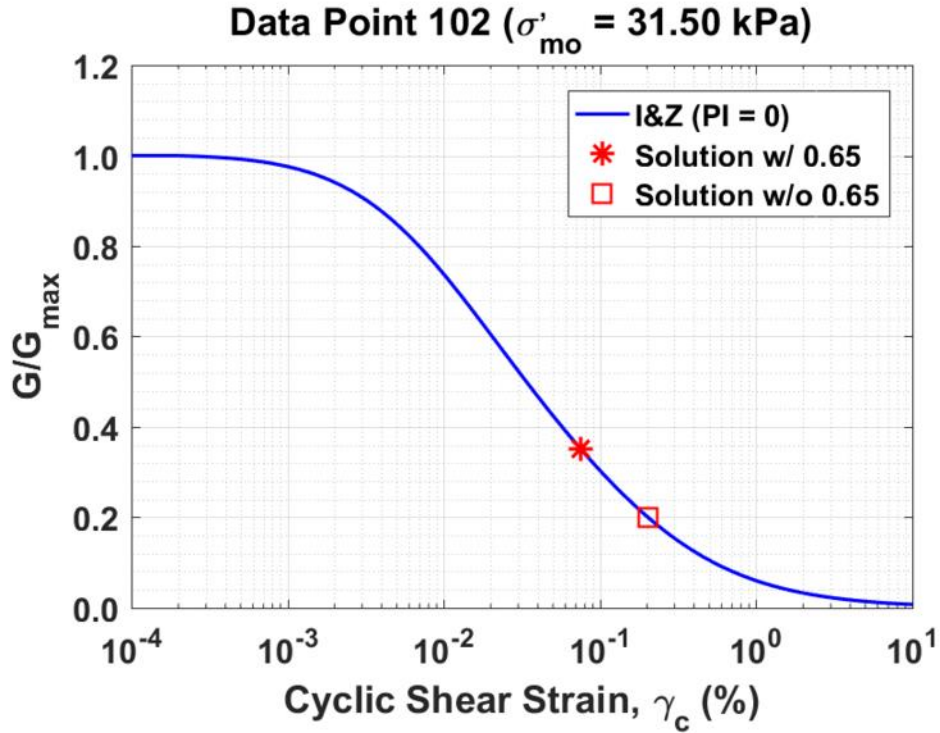


Figure B81. Normalized shear modulus reduction curves for Data Point 102 of the Kayen et al. database showing the solutions w/ and w/o the 0.65 factor

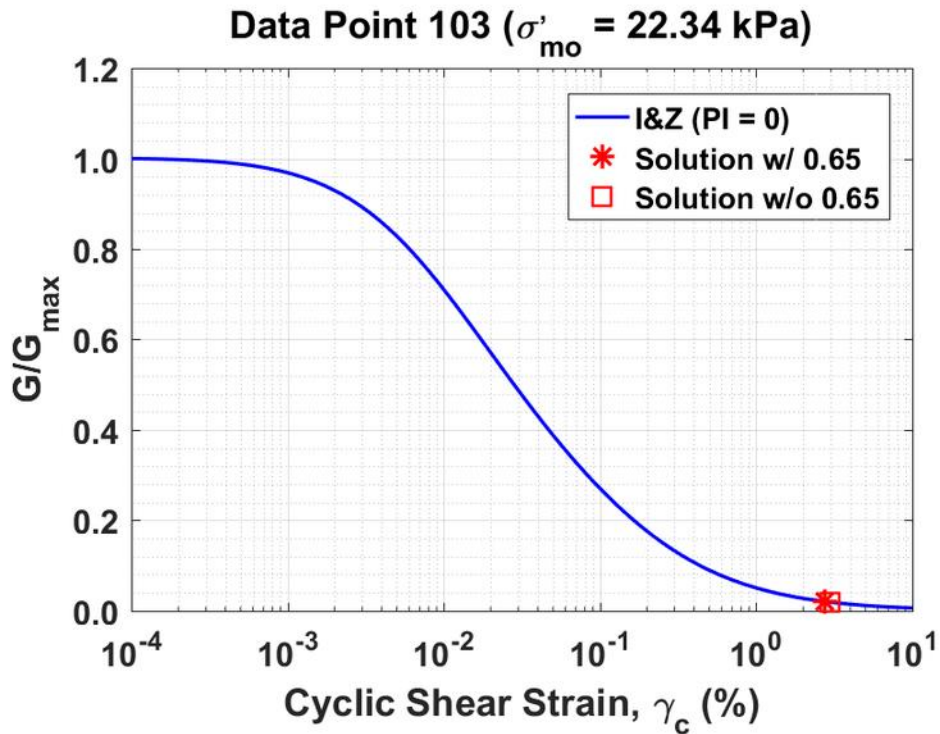


Figure B82. Normalized shear modulus reduction curves for Data Point 103 of the Kayen et al. database showing the solutions w/ and w/o the 0.65 factor

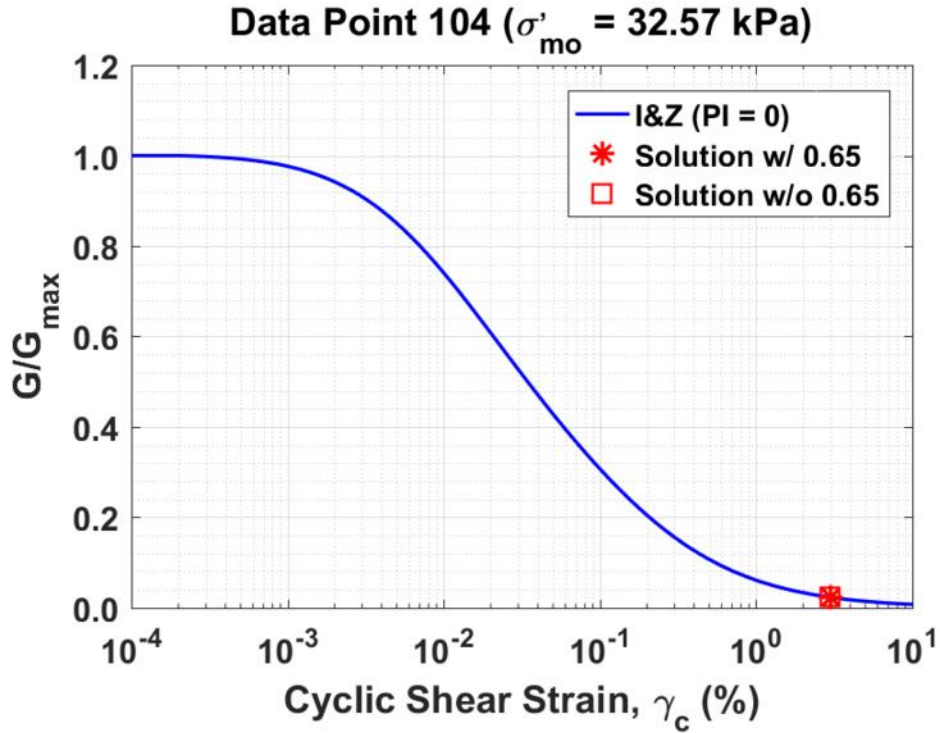


Figure B83. Normalized shear modulus reduction curves for Data Point 104 of the Kayen et al. database showing the solutions w/ and w/o the 0.65 factor

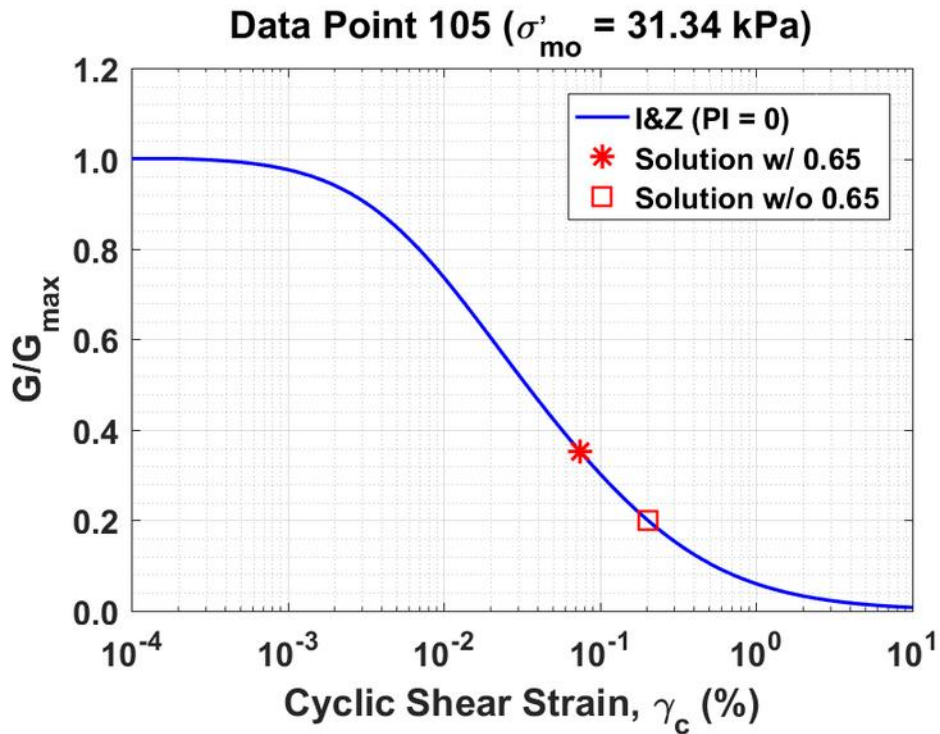


Figure B84. Normalized shear modulus reduction curves for Data Point 105 of the Kayen et al. database showing the solutions w/ and w/o the 0.65 factor

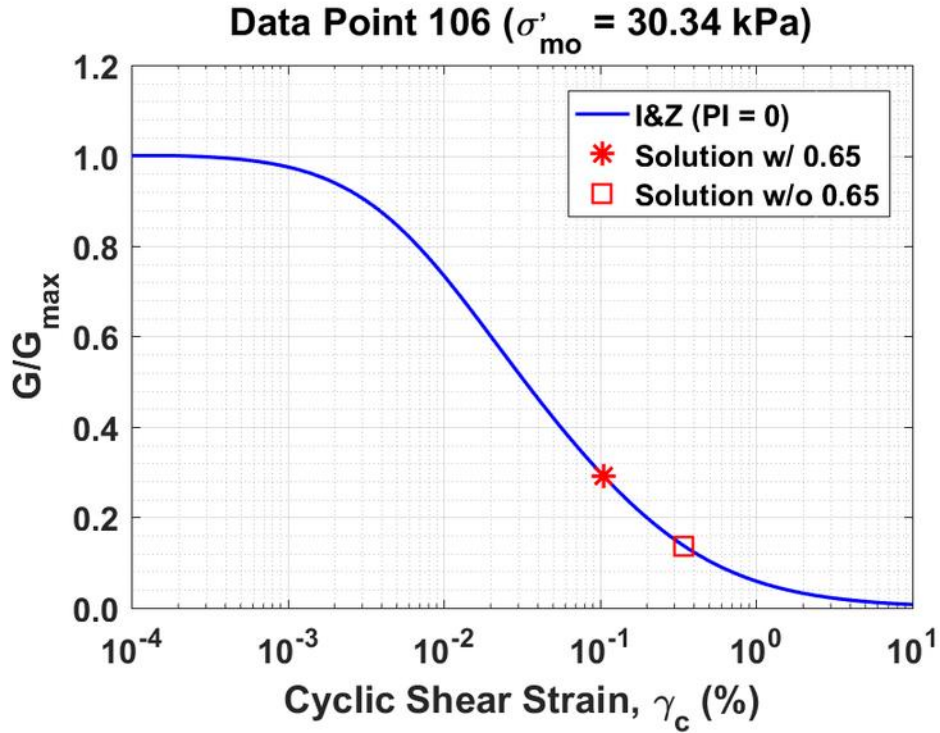


Figure B85. Normalized shear modulus reduction curves for Data Point 106 of the Kayen et al. database showing the solutions w/ and w/o the 0.65 factor

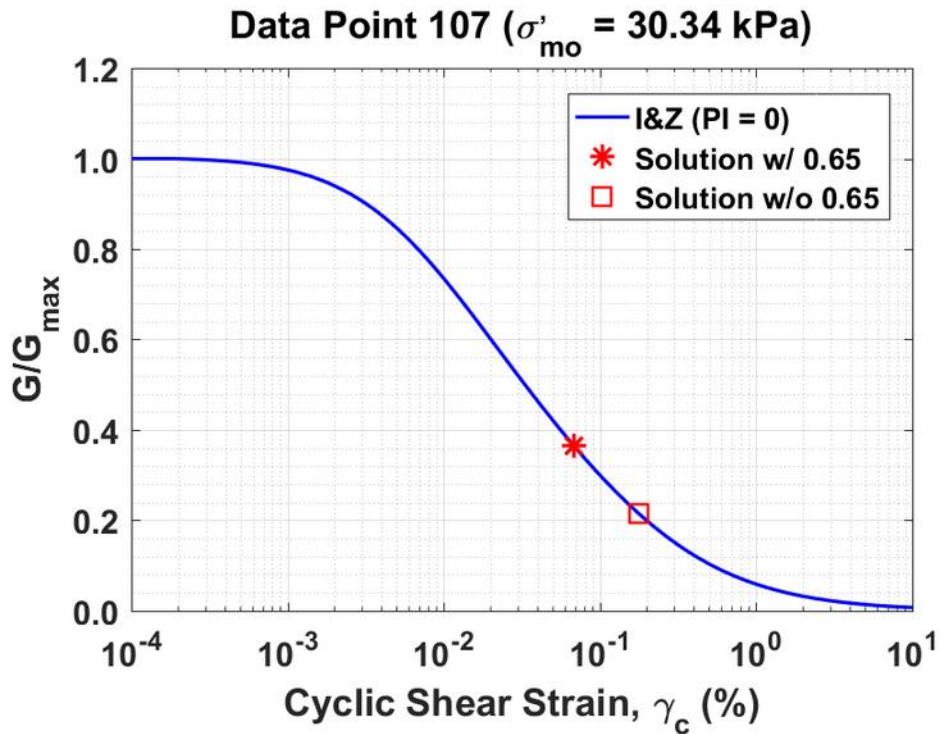


Figure B86. Normalized shear modulus reduction curves for Data Point 107 of the Kayen et al. database showing the solutions w/ and w/o the 0.65 factor

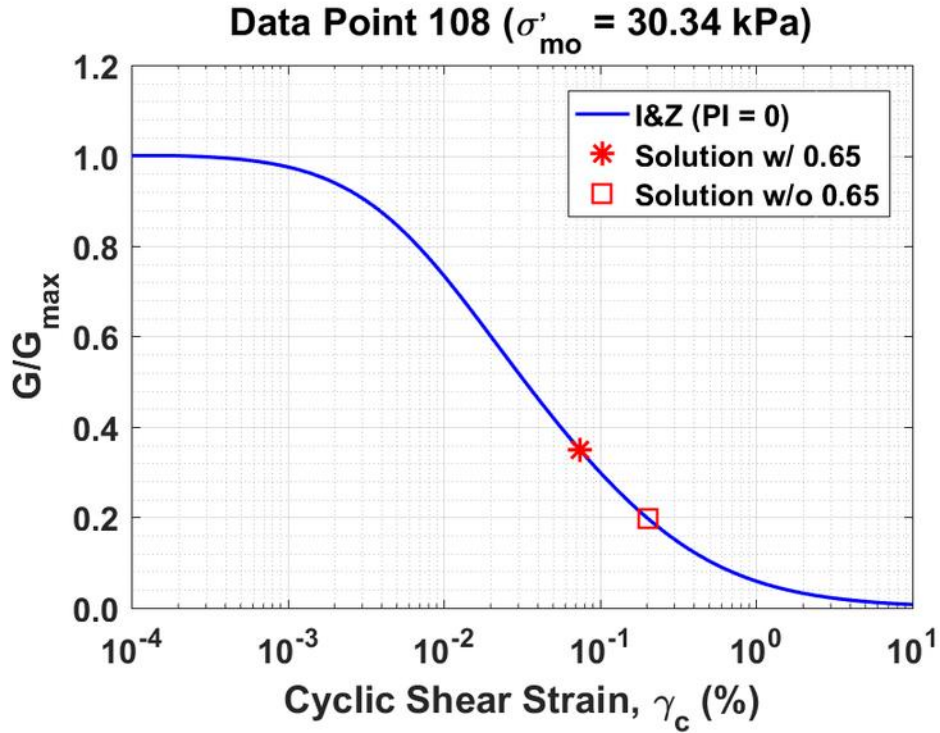


Figure B87. Normalized shear modulus reduction curves for Data Point 108 of the Kayen et al. database showing the solutions w/ and w/o the 0.65 factor

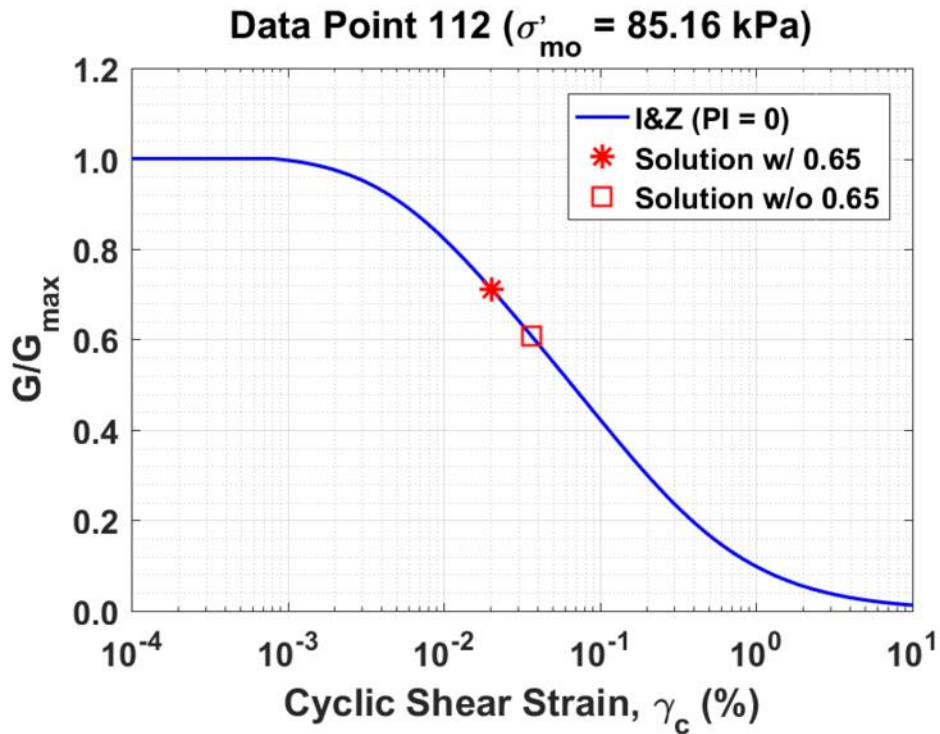


Figure B88. Normalized shear modulus reduction curves for Data Point 112 of the Kayen et al. database showing the solutions w/ and w/o the 0.65 factor

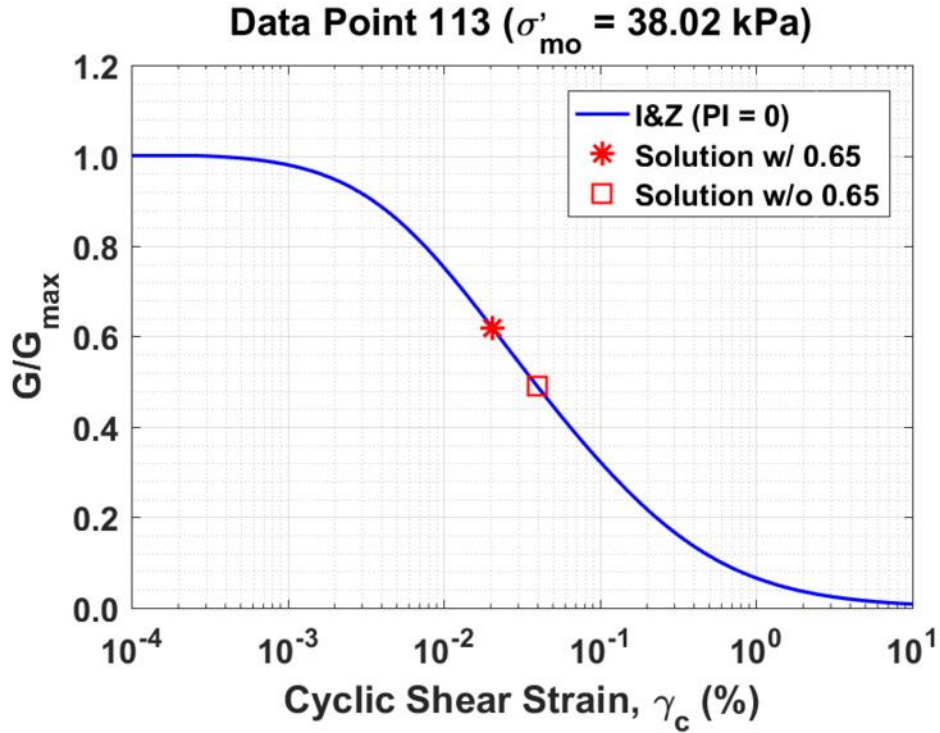


Figure B89. Normalized shear modulus reduction curves for Data Point 113 of the Kayen et al. database showing the solutions w/ and w/o the 0.65 factor

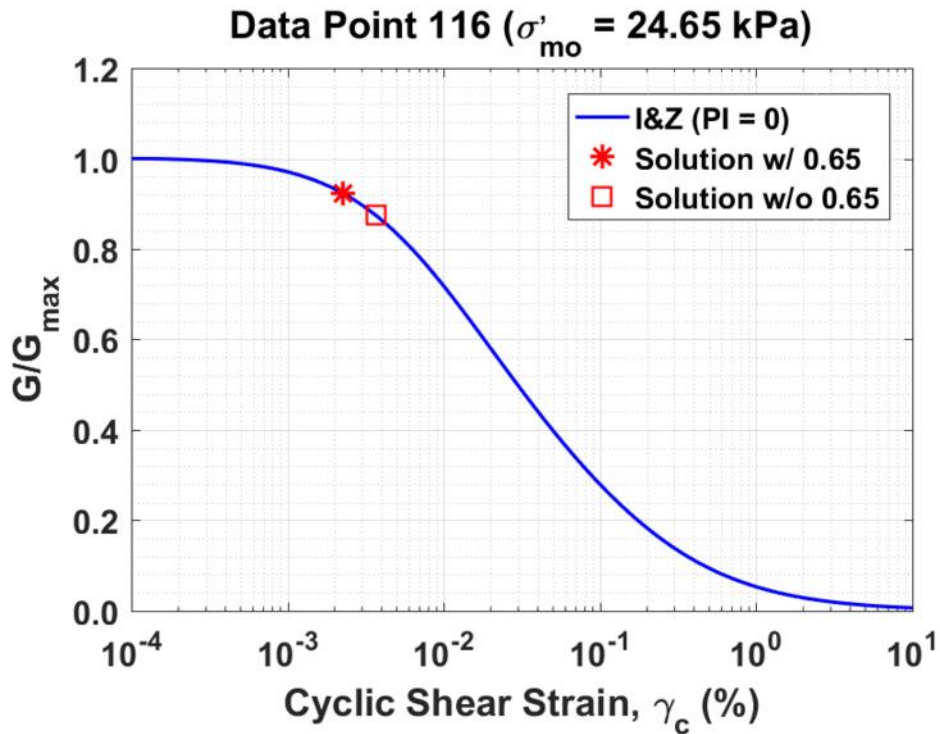


Figure B90. Normalized shear modulus reduction curves for Data Point 116 of the Kayen et al. database showing the solutions w/ and w/o the 0.65 factor

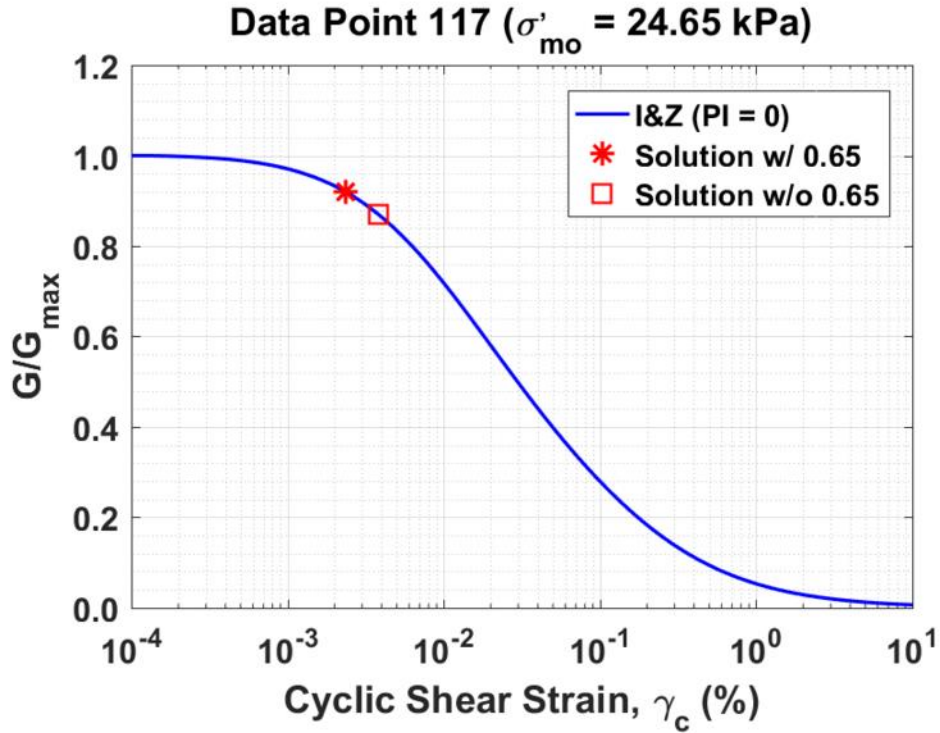


Figure B91. Normalized shear modulus reduction curves for Data Point 117 of the Kayen et al. database showing the solutions w/ and w/o the 0.65 factor

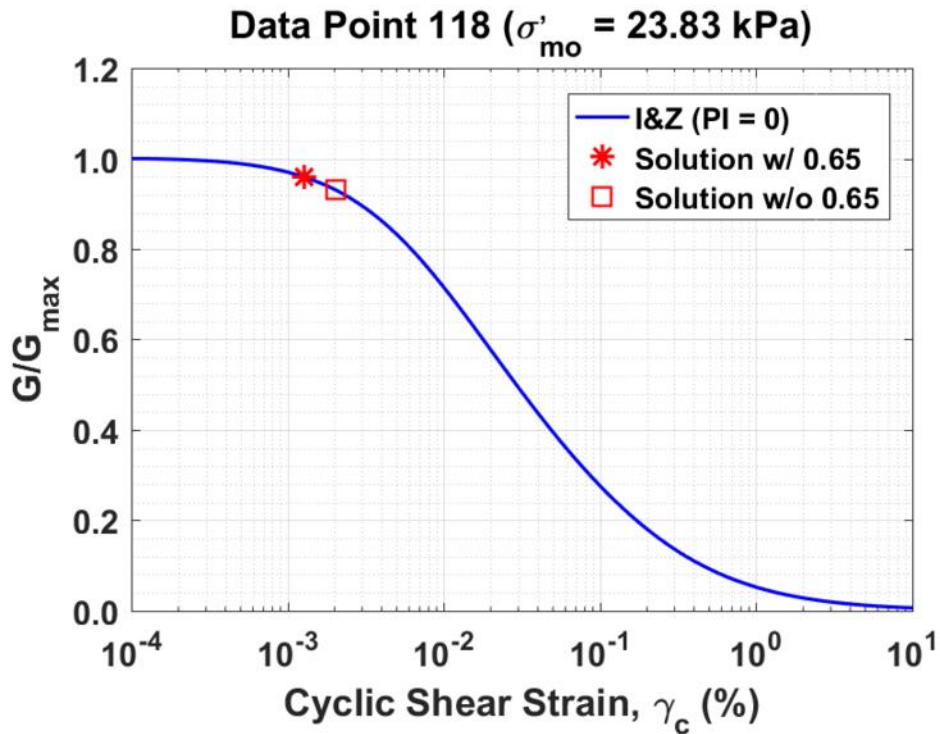


Figure B92. Normalized shear modulus reduction curves for Data Point 118 of the Kayen et al. database showing the solutions w/ and w/o the 0.65 factor

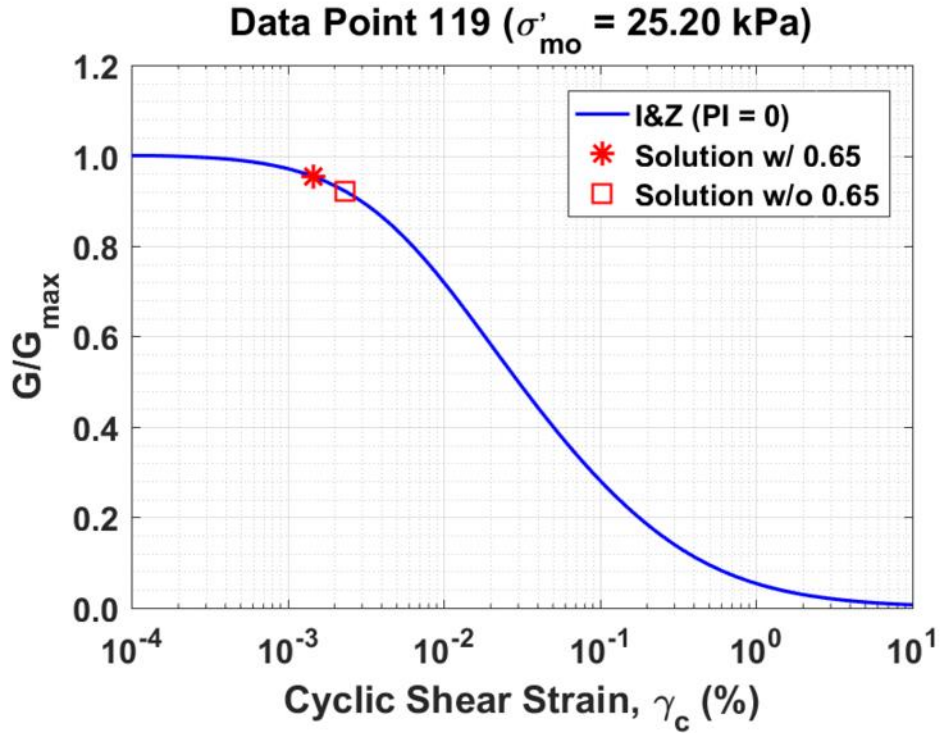


Figure B93. Normalized shear modulus reduction curves for Data Point 119 of the Kayen et al. database showing the solutions w/ and w/o the 0.65 factor

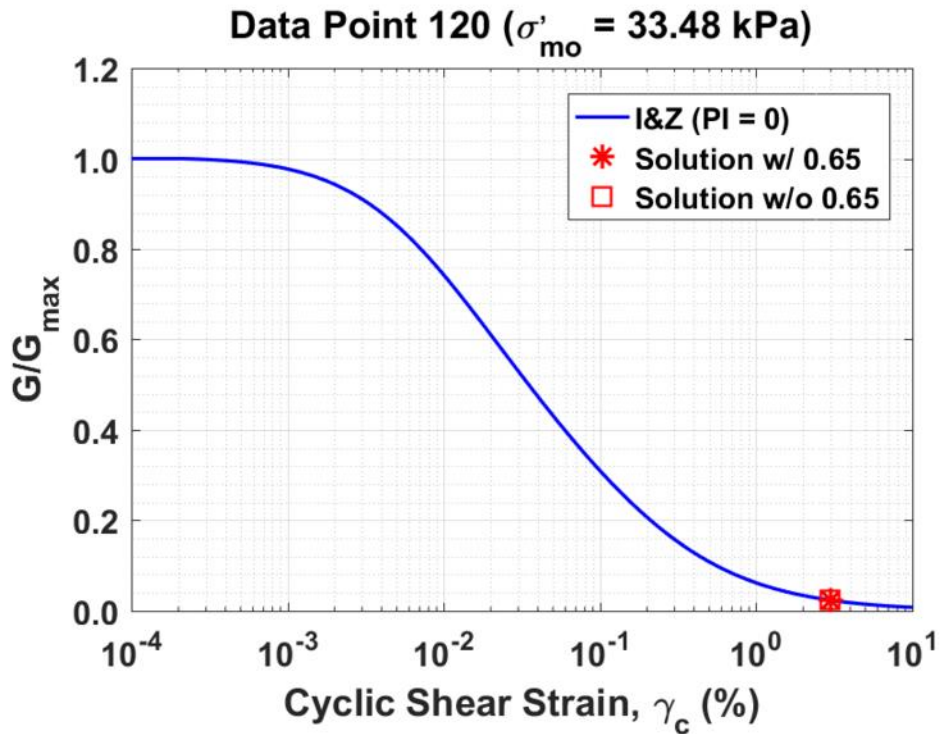


Figure B94. Normalized shear modulus reduction curves for Data Point 120 of the Kayen et al. database showing the solutions w/ and w/o the 0.65 factor

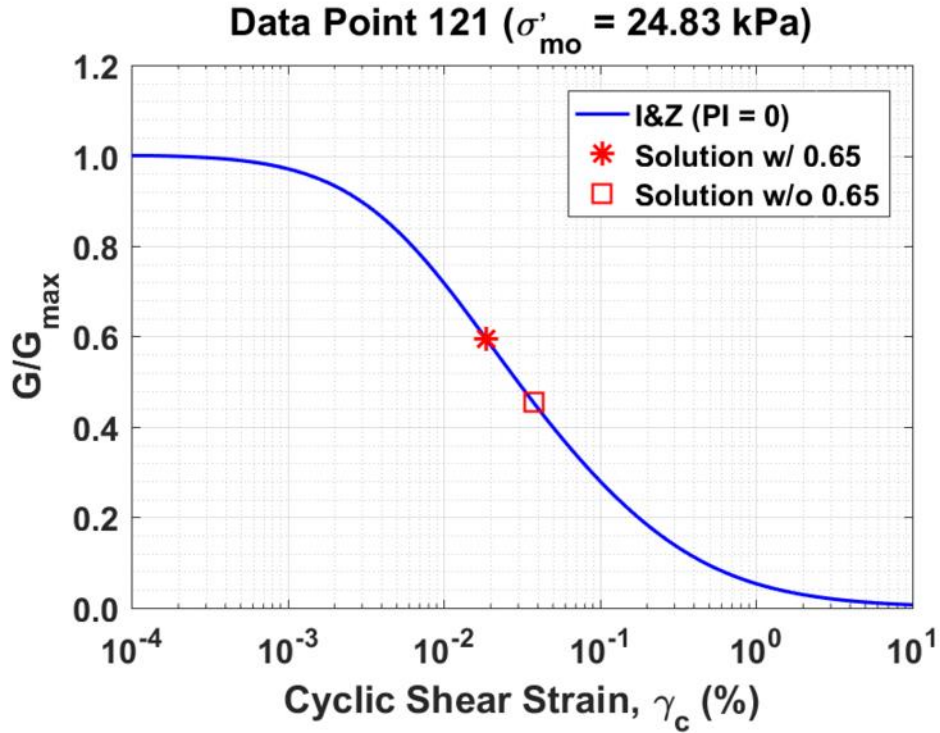


Figure B95. Normalized shear modulus reduction curves for Data Point 121 of the Kayen et al. database showing the solutions w/ and w/o the 0.65 factor

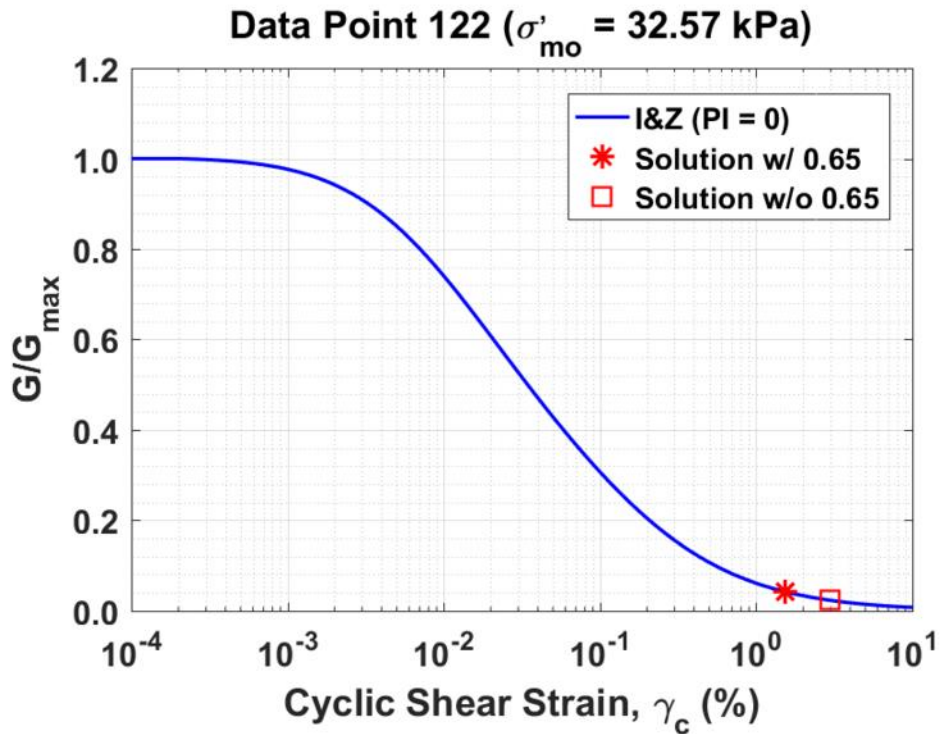


Figure B96. Normalized shear modulus reduction curves for Data Point 122 of the Kayen et al. database showing the solutions w/ and w/o the 0.65 factor

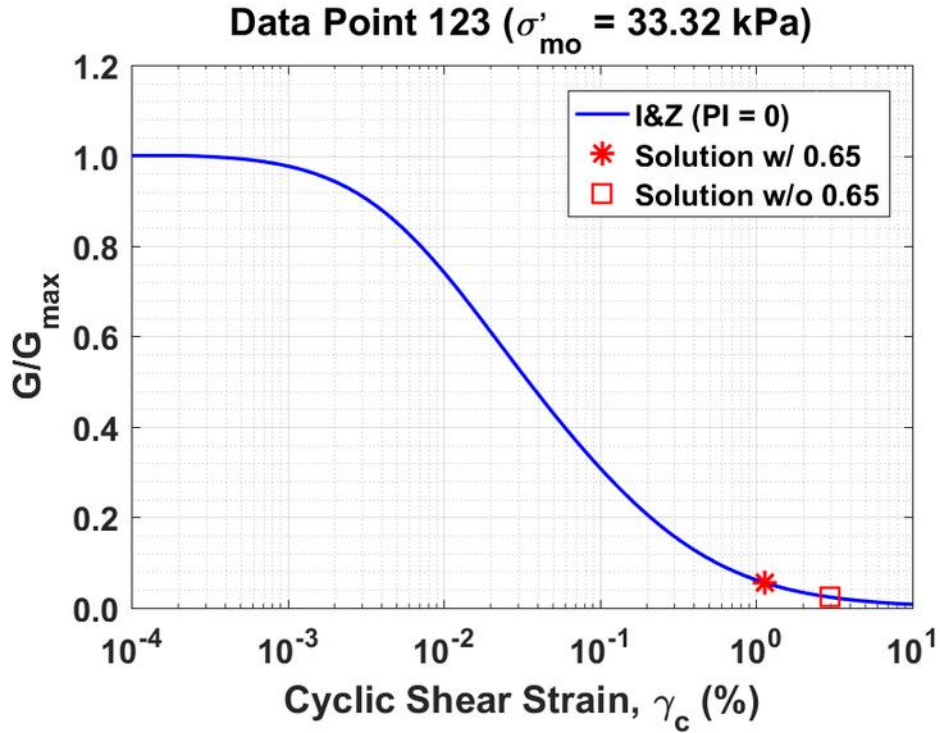


Figure B97. Normalized shear modulus reduction curves for Data Point 123 of the Kayen et al. database showing the solutions w/ and w/o the 0.65 factor

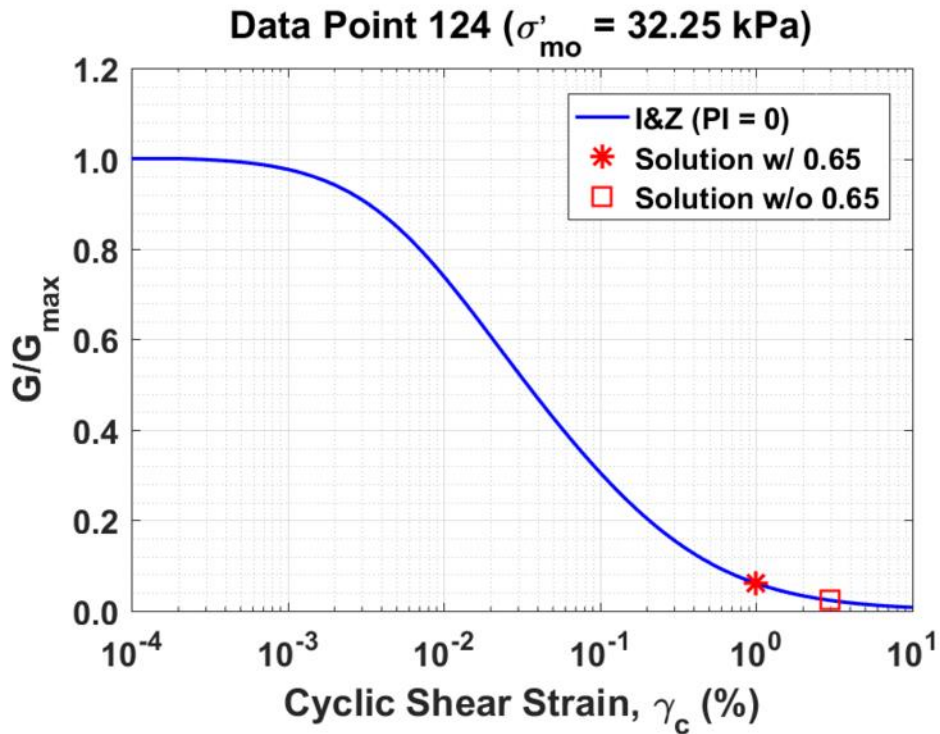


Figure B98. Normalized shear modulus reduction curves for Data Point 124 of the Kayen et al. database showing the solutions w/ and w/o the 0.65 factor

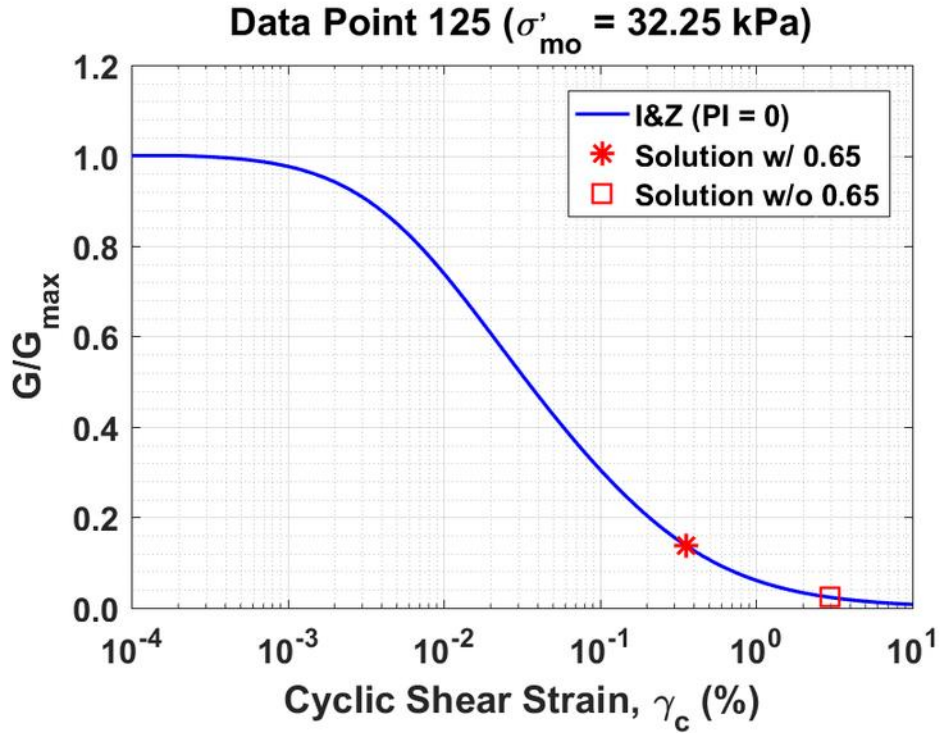


Figure B99. Normalized shear modulus reduction curves for Data Point 125 of the Kayen et al. database showing the solutions w/ and w/o the 0.65 factor

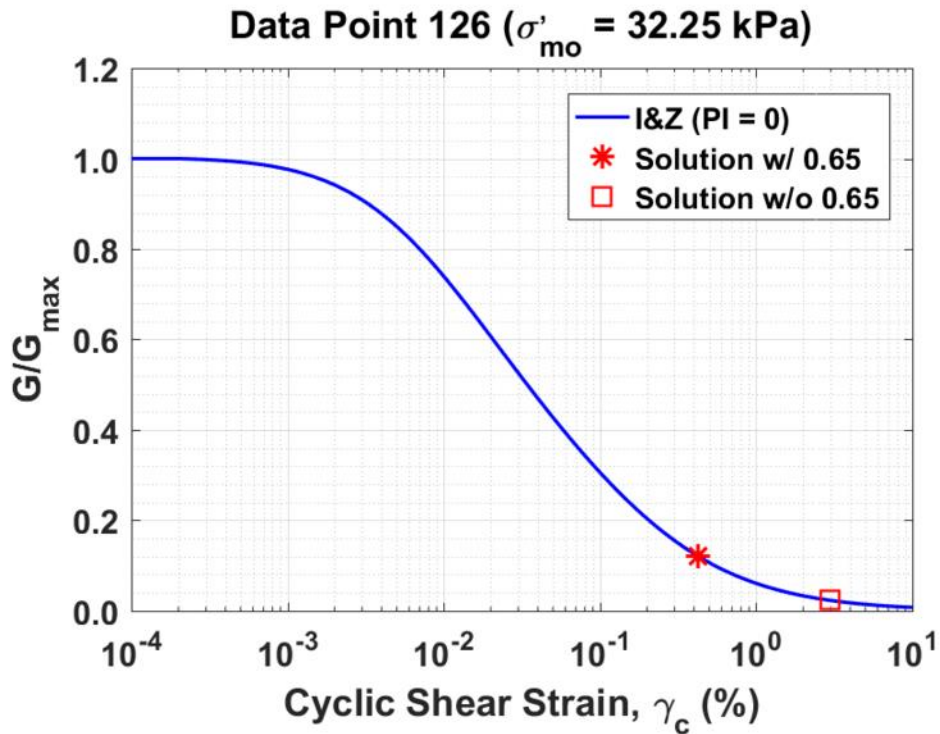


Figure B100. Normalized shear modulus reduction curves for Data Point 126 of the Kayen et al. database showing the solutions w/ and w/o the 0.65 factor

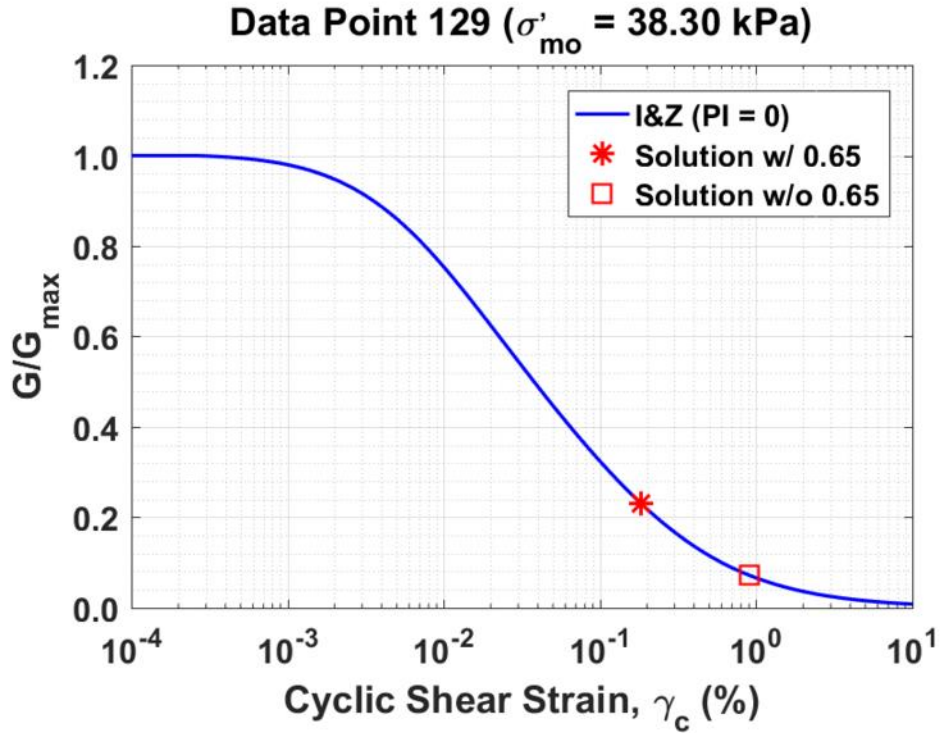


Figure B101. Normalized shear modulus reduction curves for Data Point 129 of the Kayen et al. database showing the solutions w/ and w/o the 0.65 factor

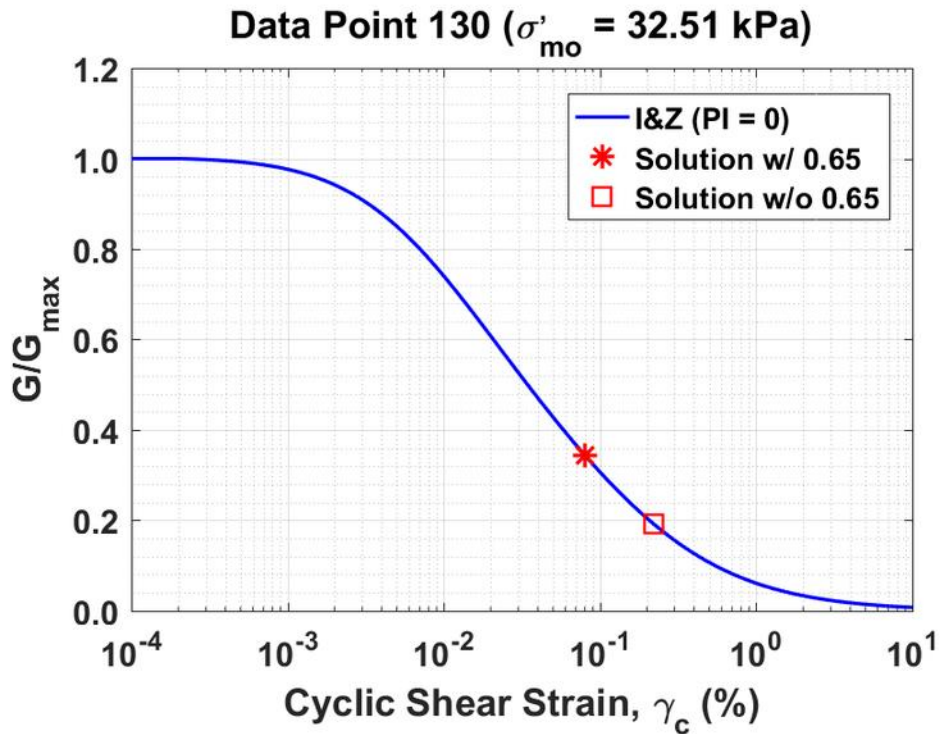


Figure B102. Normalized shear modulus reduction curves for Data Point 130 of the Kayen et al. database showing the solutions w/ and w/o the 0.65 factor

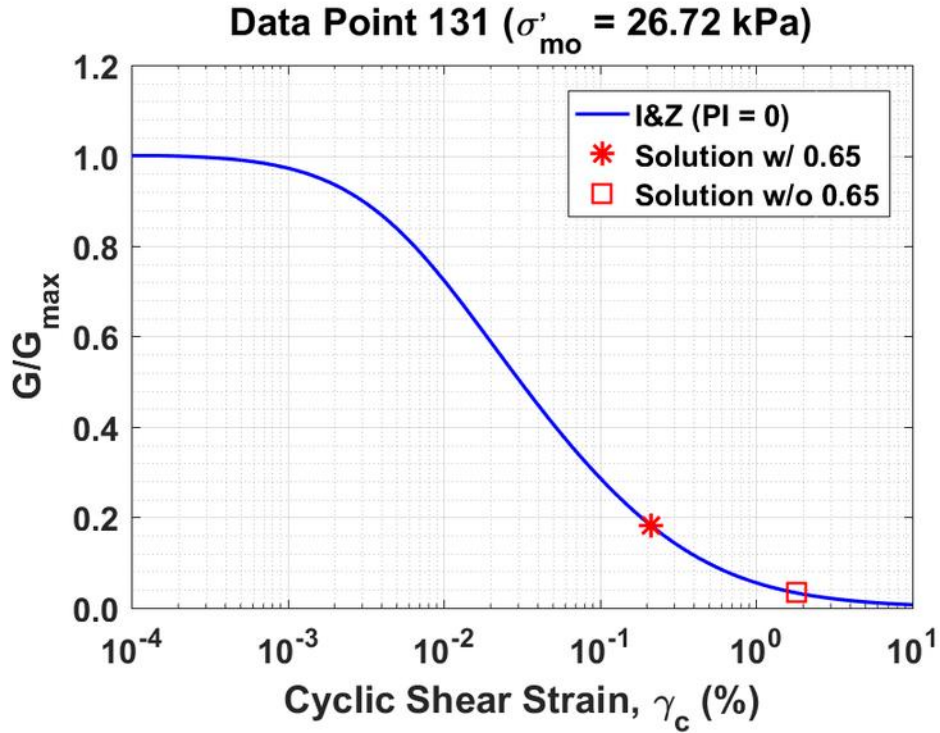


Figure B103. Normalized shear modulus reduction curves for Data Point 131 of the Kayen et al. database showing the solutions w/ and w/o the 0.65 factor

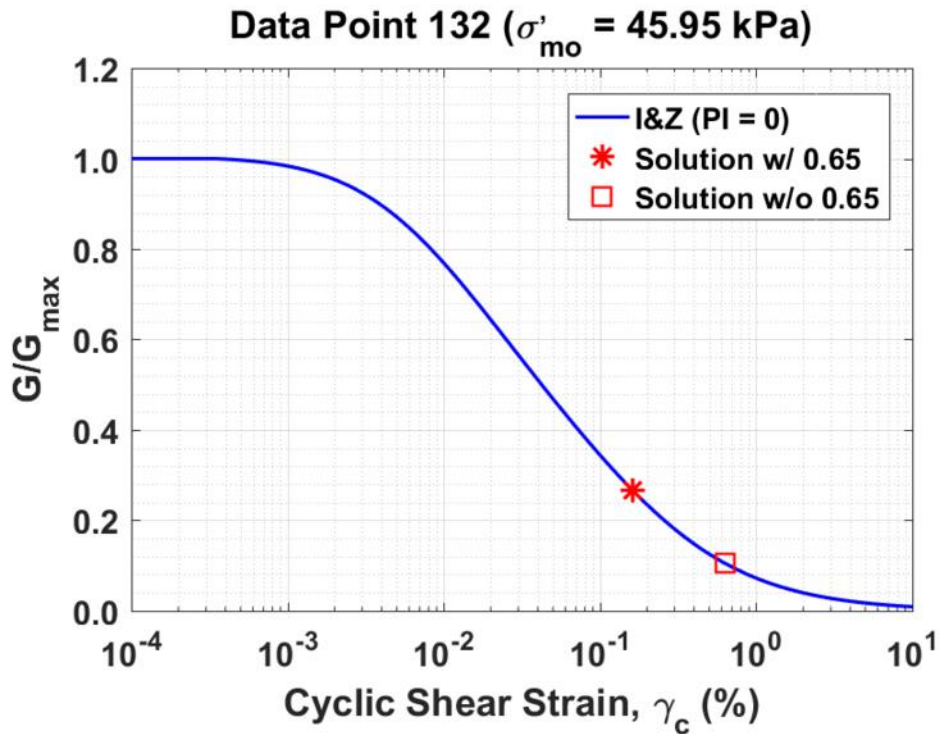


Figure B104. Normalized shear modulus reduction curves for Data Point 132 of the Kayen et al. database showing the solutions w/ and w/o the 0.65 factor

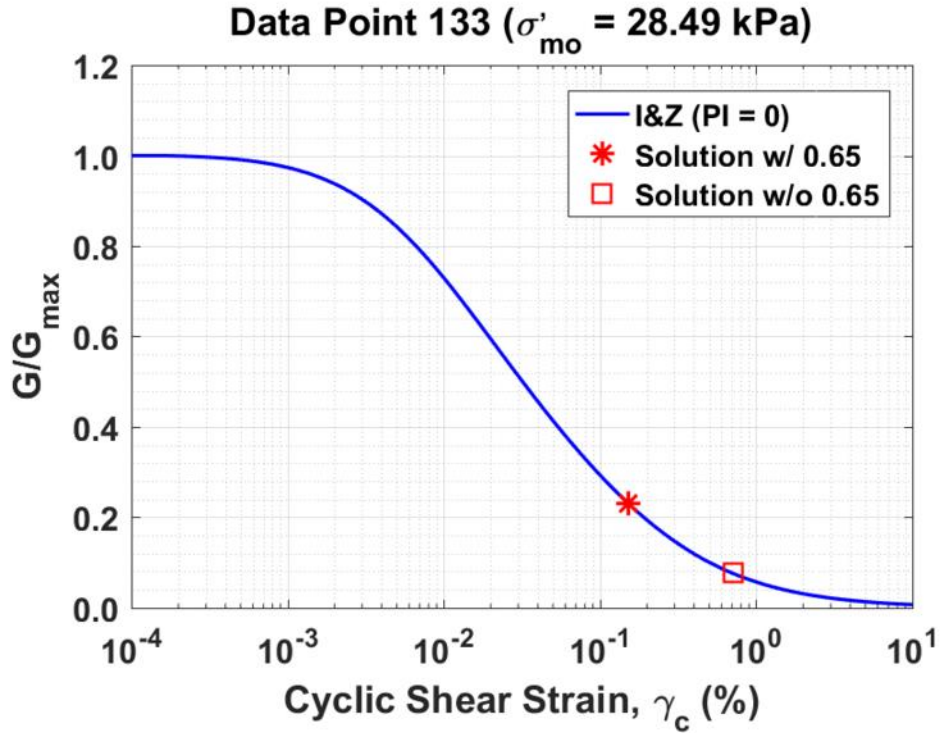


Figure B105. Normalized shear modulus reduction curves for Data Point 133 of the Kayen et al. database showing the solutions w/ and w/o the 0.65 factor

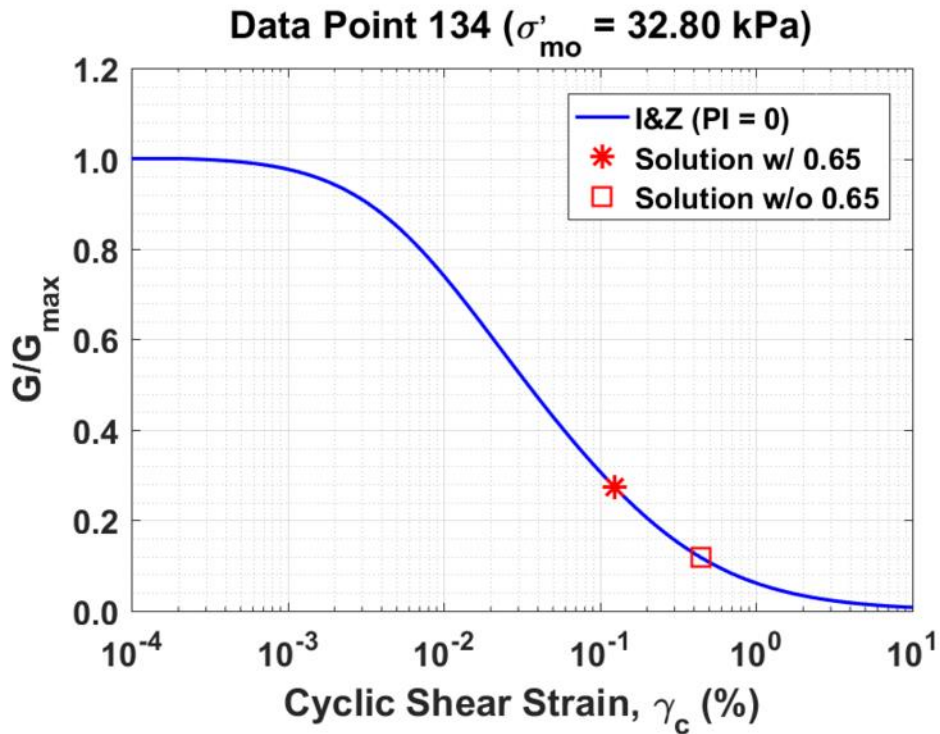


Figure B106. Normalized shear modulus reduction curves for Data Point 134 of the Kayen et al. database showing the solutions w/ and w/o the 0.65 factor

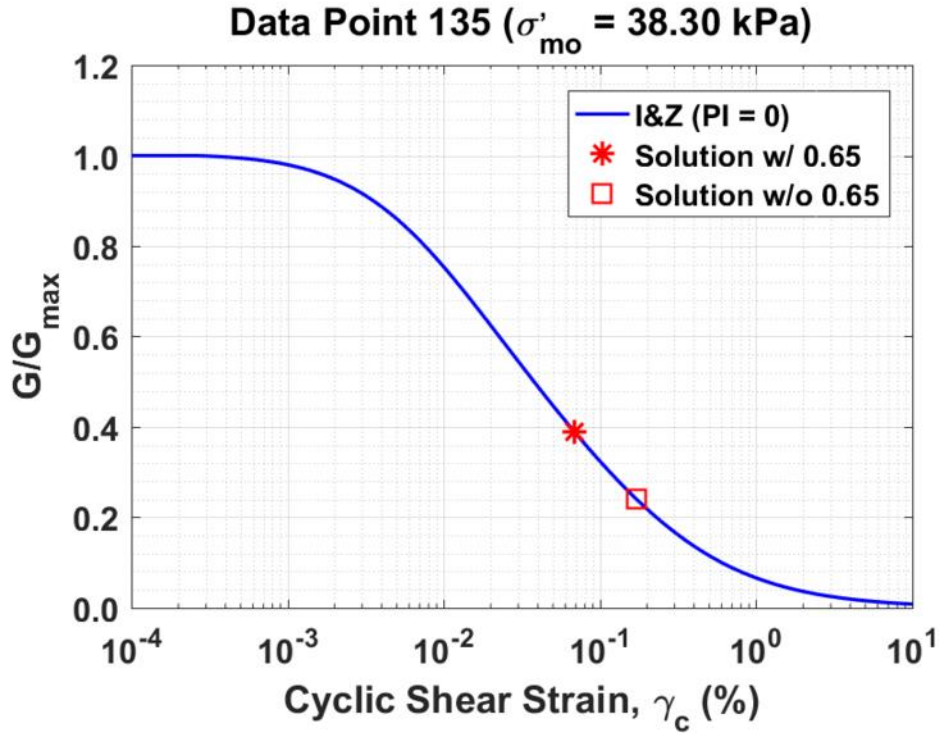


Figure B107. Normalized shear modulus reduction curves for Data Point 135 of the Kayen et al. database showing the solutions w/ and w/o the 0.65 factor

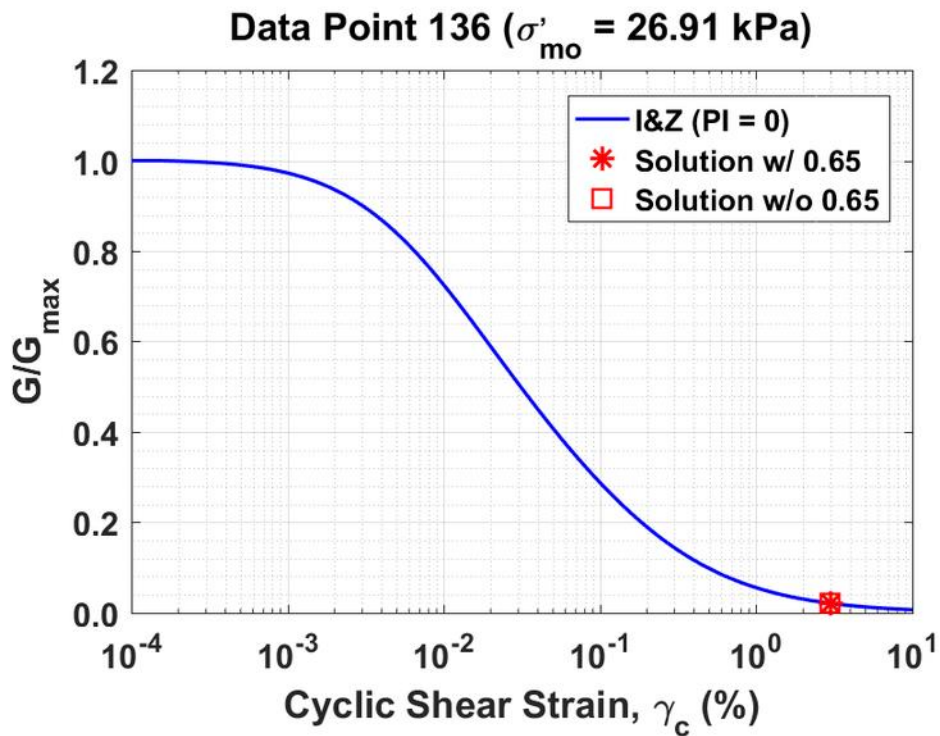


Figure B108. Normalized shear modulus reduction curves for Data Point 136 of the Kayen et al. database showing the solutions w/ and w/o the 0.65 factor

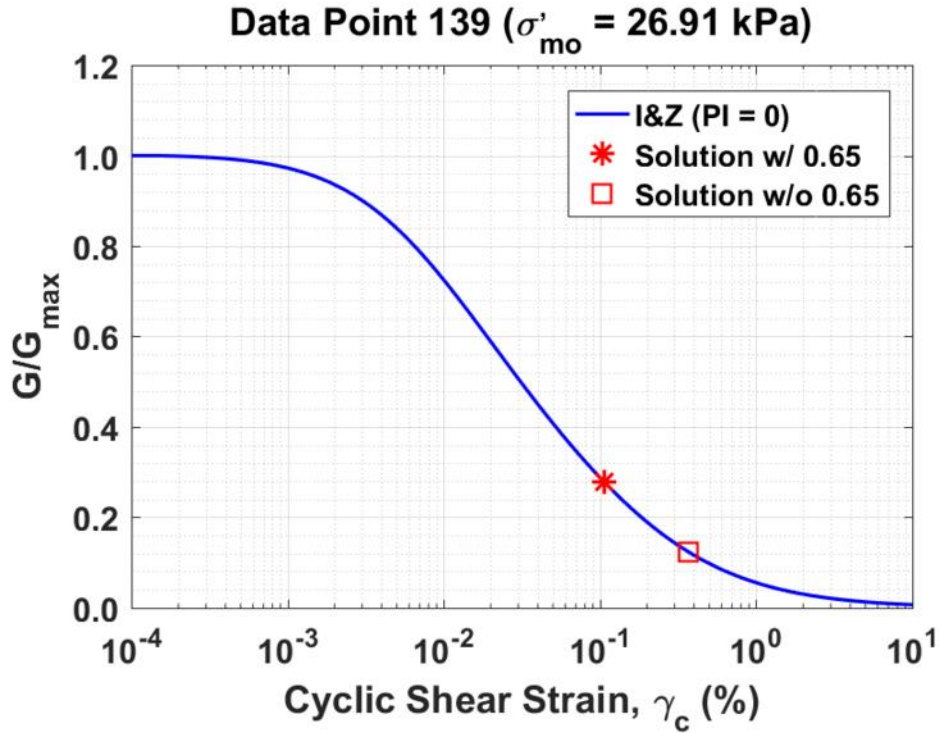


Figure B109. Normalized shear modulus reduction curves for Data Point 139 of the Kayen et al. database showing the solutions w/ and w/o the 0.65 factor

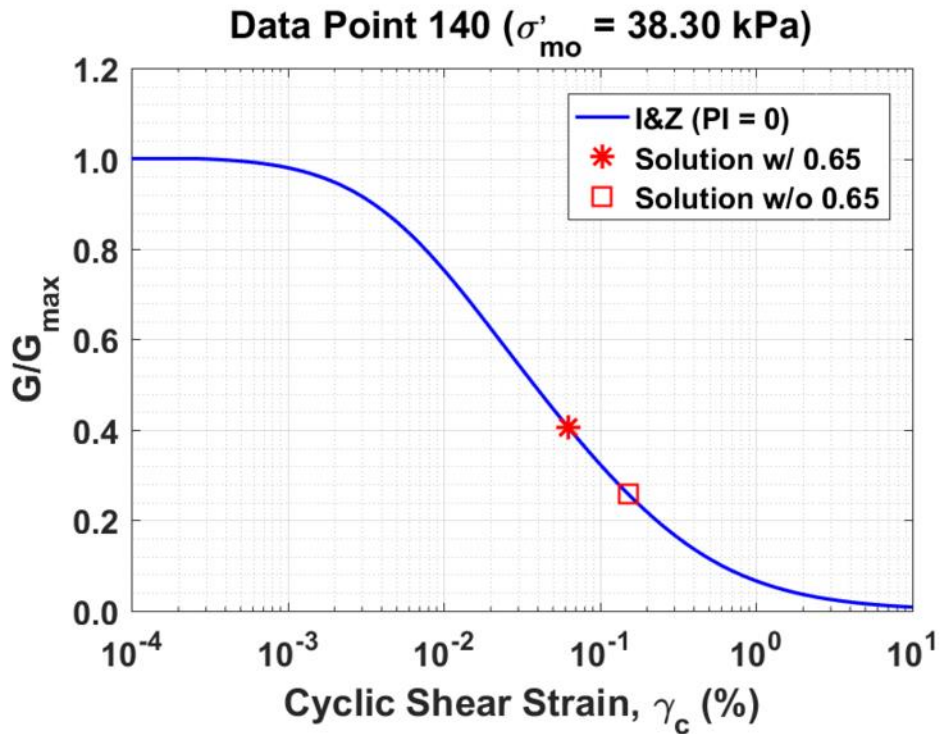


Figure B110. Normalized shear modulus reduction curves for Data Point 140 of the Kayen et al. database showing the solutions w/ and w/o the 0.65 factor

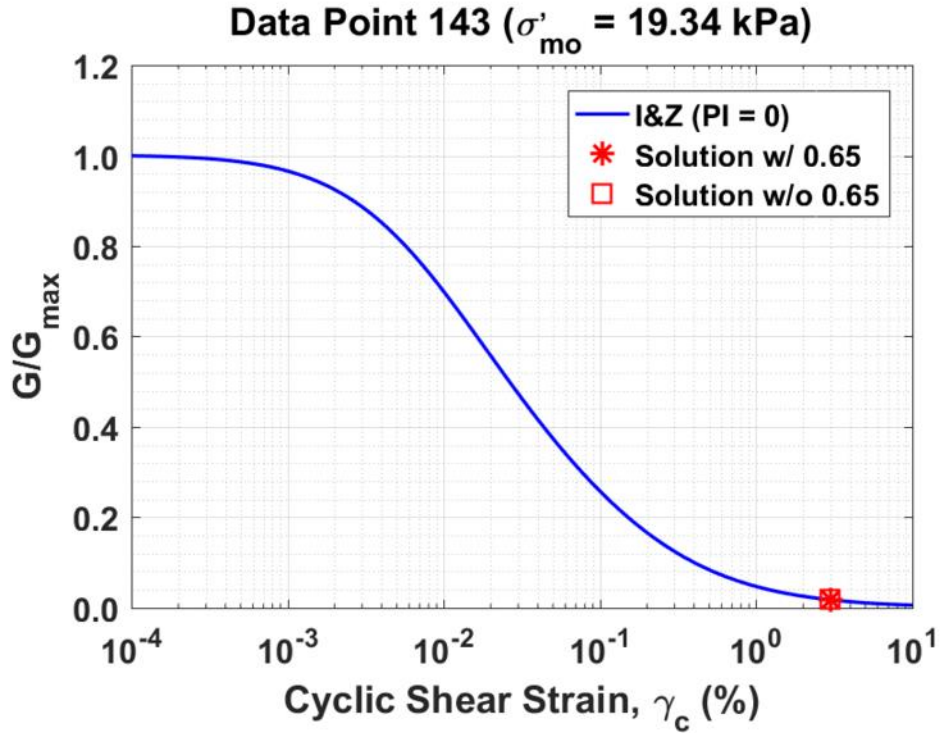


Figure B111. Normalized shear modulus reduction curves for Data Point 143 of the Kayen et al. database showing the solutions w/ and w/o the 0.65 factor

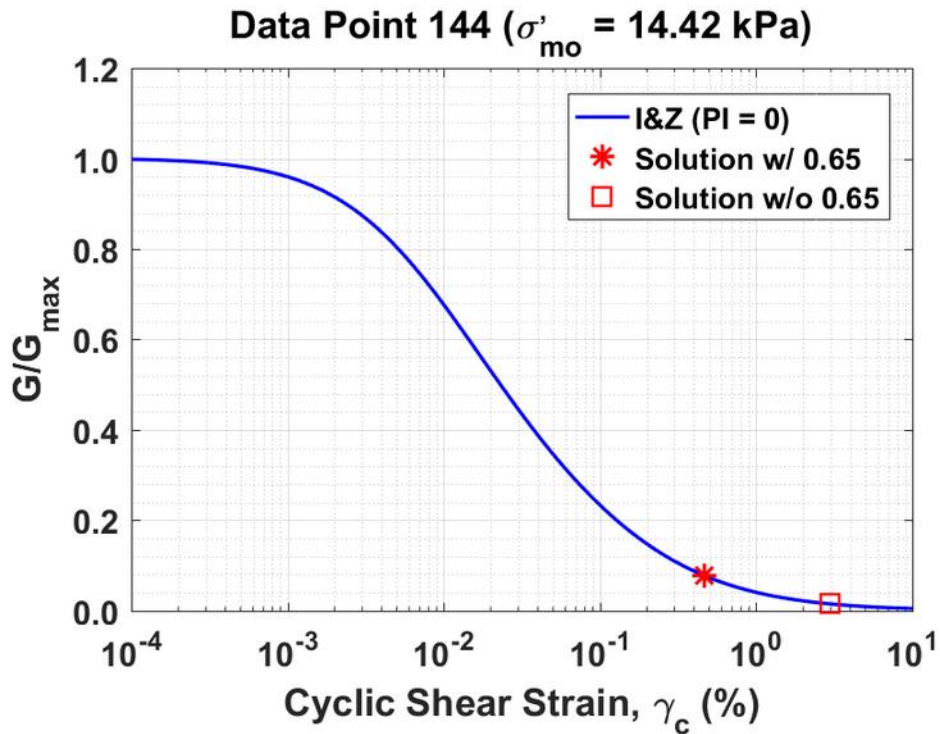


Figure B112. Normalized shear modulus reduction curves for Data Point 144 of the Kayen et al. database showing the solutions w/ and w/o the 0.65 factor

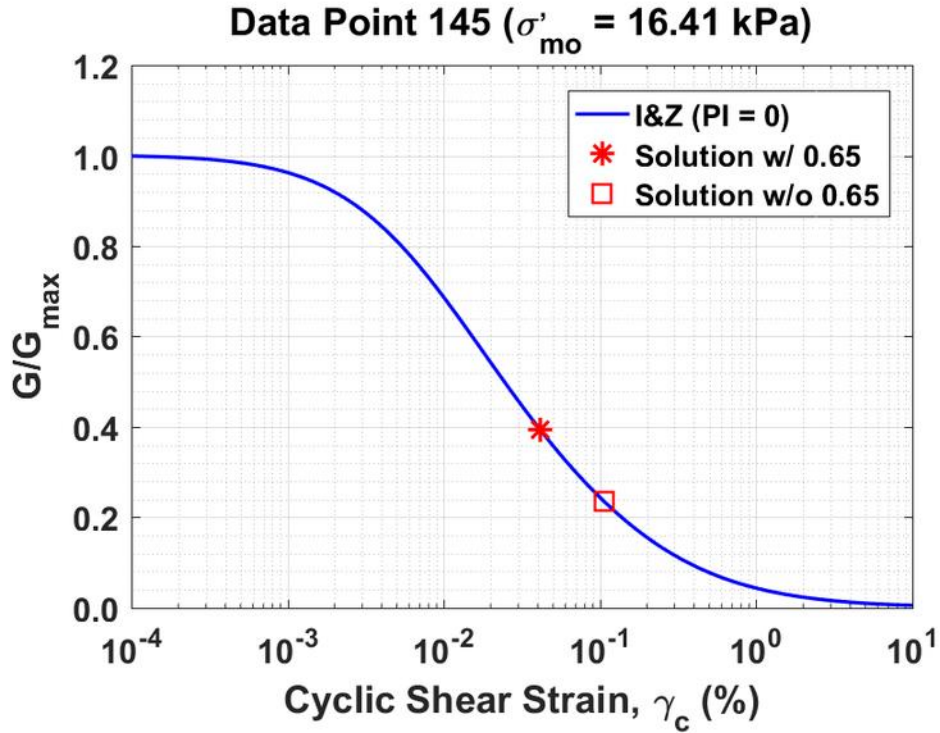


Figure B113. Normalized shear modulus reduction curves for Data Point 145 of the Kayen et al. database showing the solutions w/ and w/o the 0.65 factor

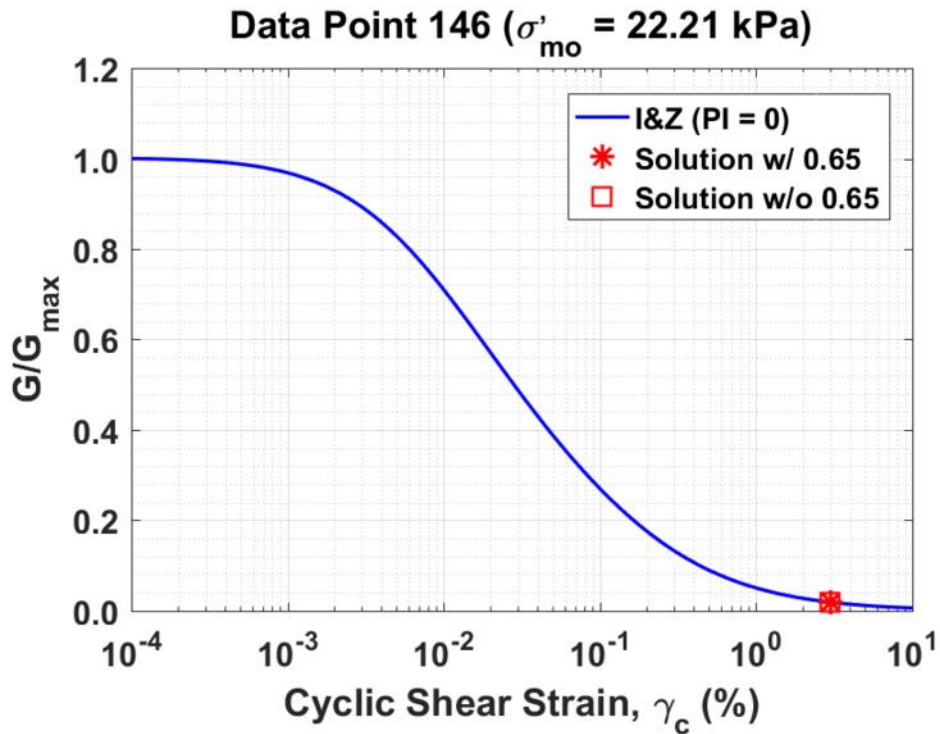


Figure B114. Normalized shear modulus reduction curves for Data Point 146 of the Kayen et al. database showing the solutions w/ and w/o the 0.65 factor

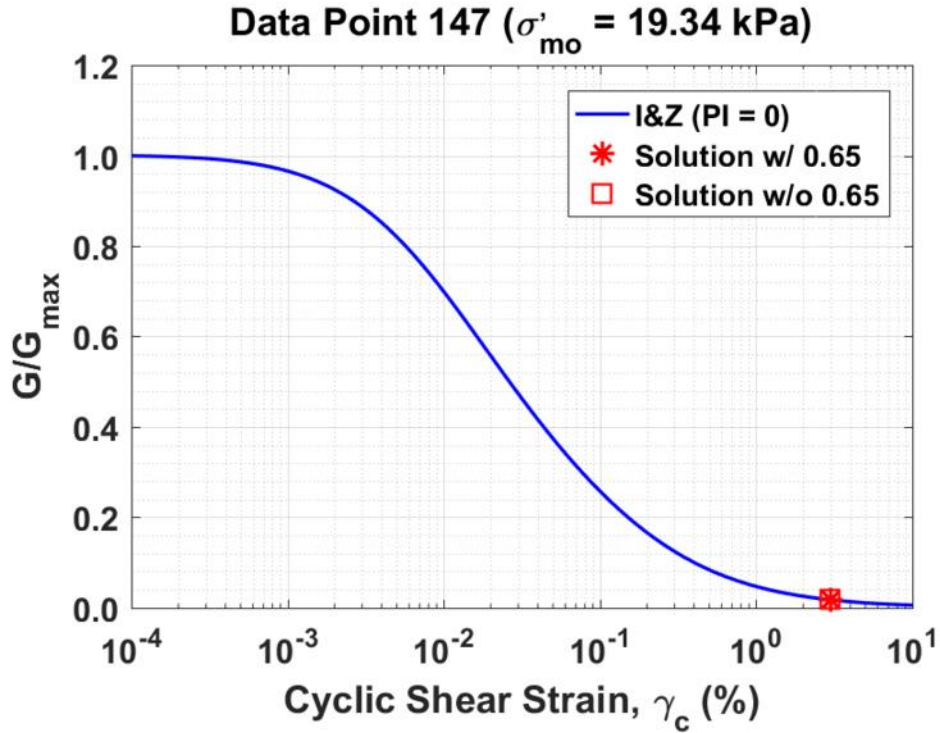


Figure B115. Normalized shear modulus reduction curves for Data Point 147 of the Kayen et al. database showing the solutions w/ and w/o the 0.65 factor

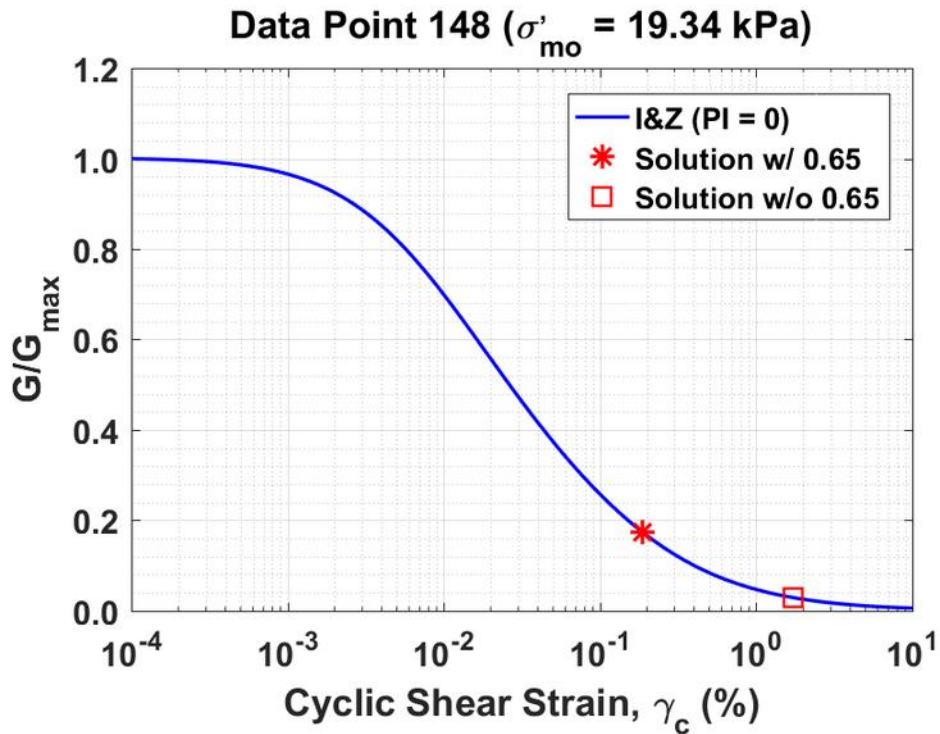


Figure B116. Normalized shear modulus reduction curves for Data Point 148 of the Kayen et al. database showing the solutions w/ and w/o the 0.65 factor

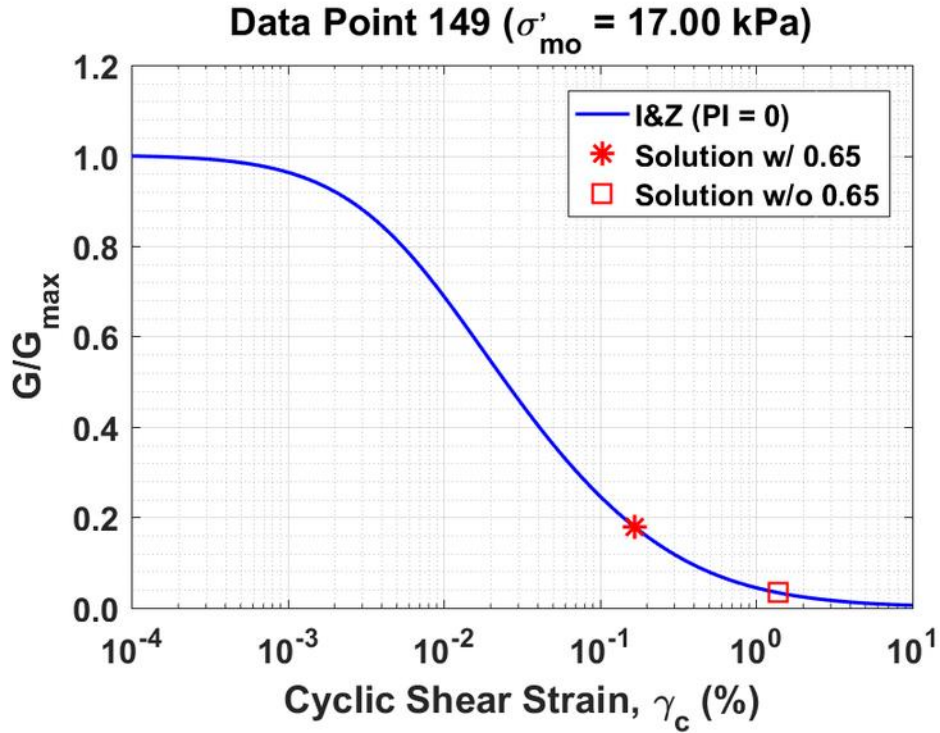


Figure B116. Normalized shear modulus reduction curves for Data Point 149 of the Kayen et al. database showing the solutions w/ and w/o the 0.65 factor

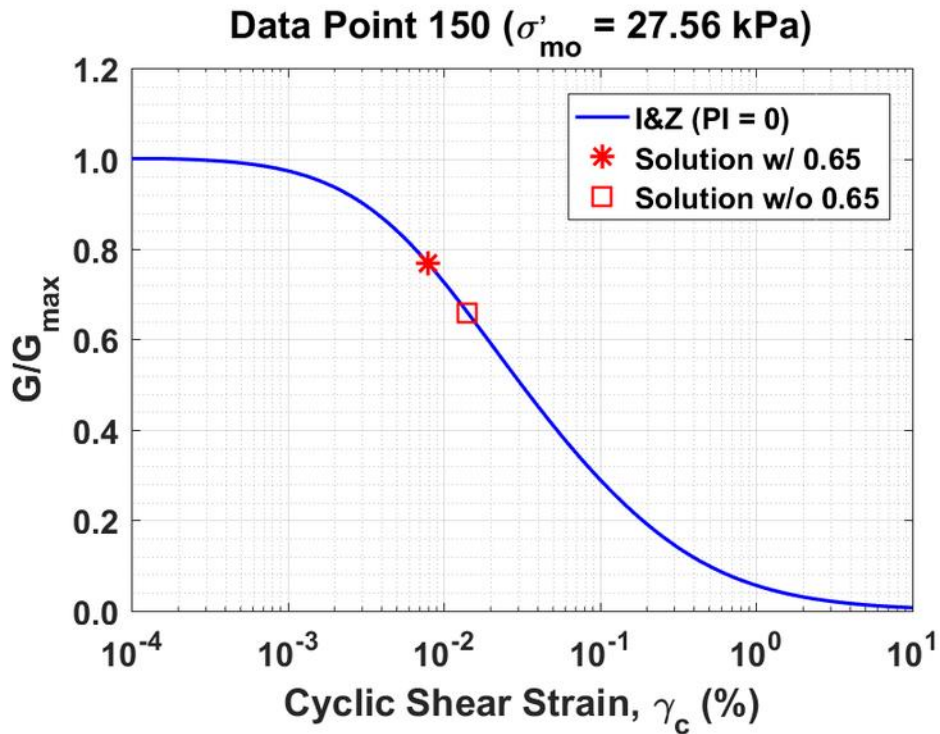


Figure B117. Normalized shear modulus reduction curves for Data Point 150 of the Kayen et al. database showing the solutions w/ and w/o the 0.65 factor

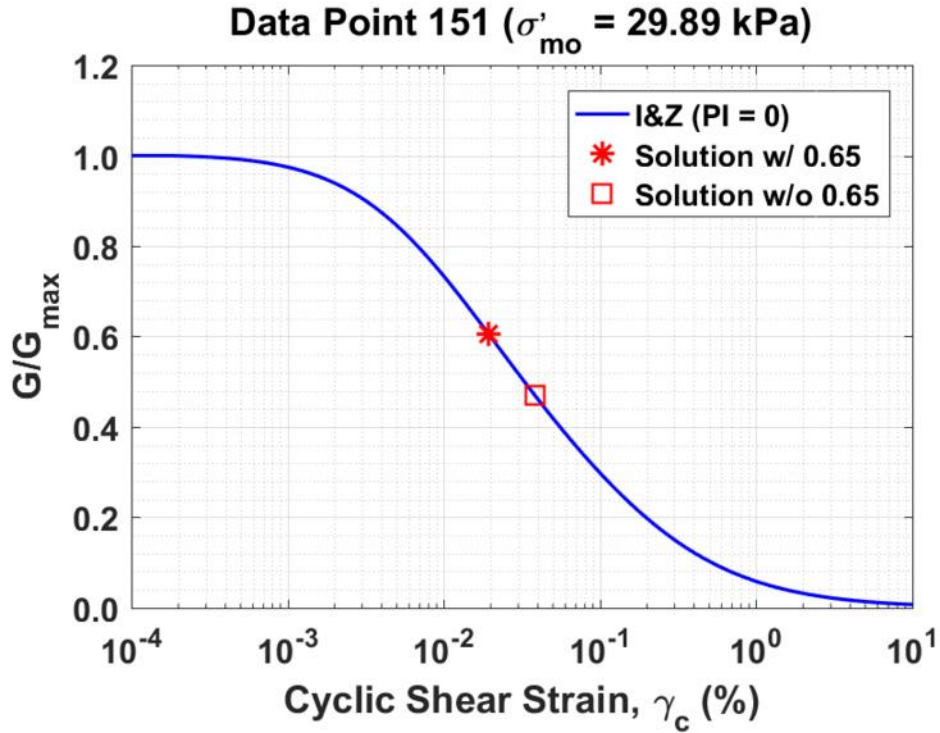


Figure B118. Normalized shear modulus reduction curves for Data Point 151 of the Kayen et al. database showing the solutions w/ and w/o the 0.65 factor

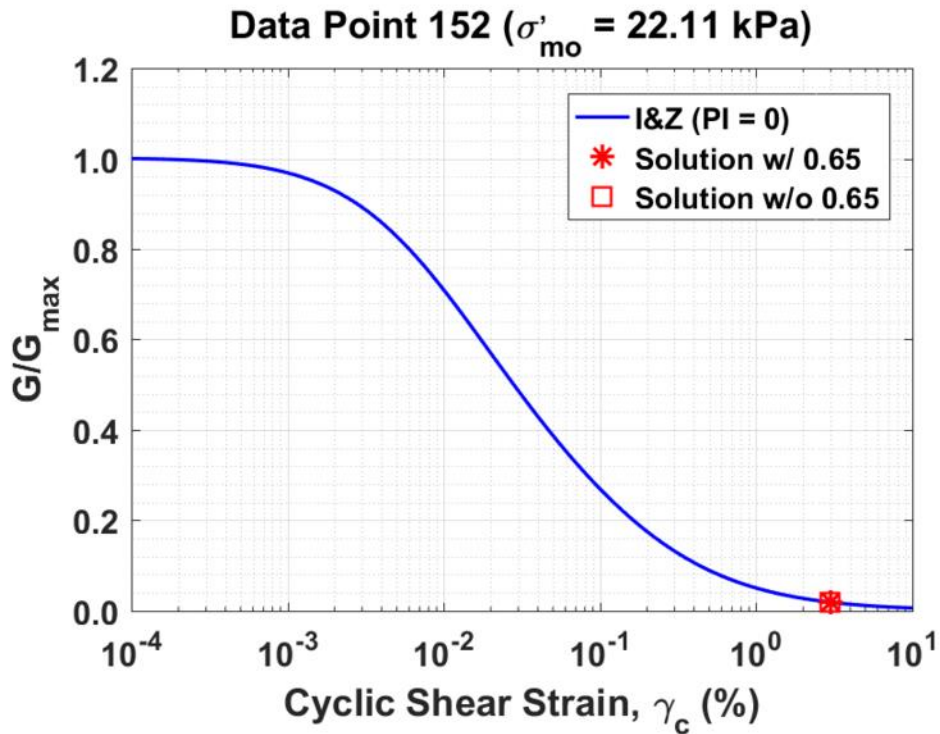


Figure B119. Normalized shear modulus reduction curves for Data Point 152 of the Kayen et al. database showing the solutions w/ and w/o the 0.65 factor

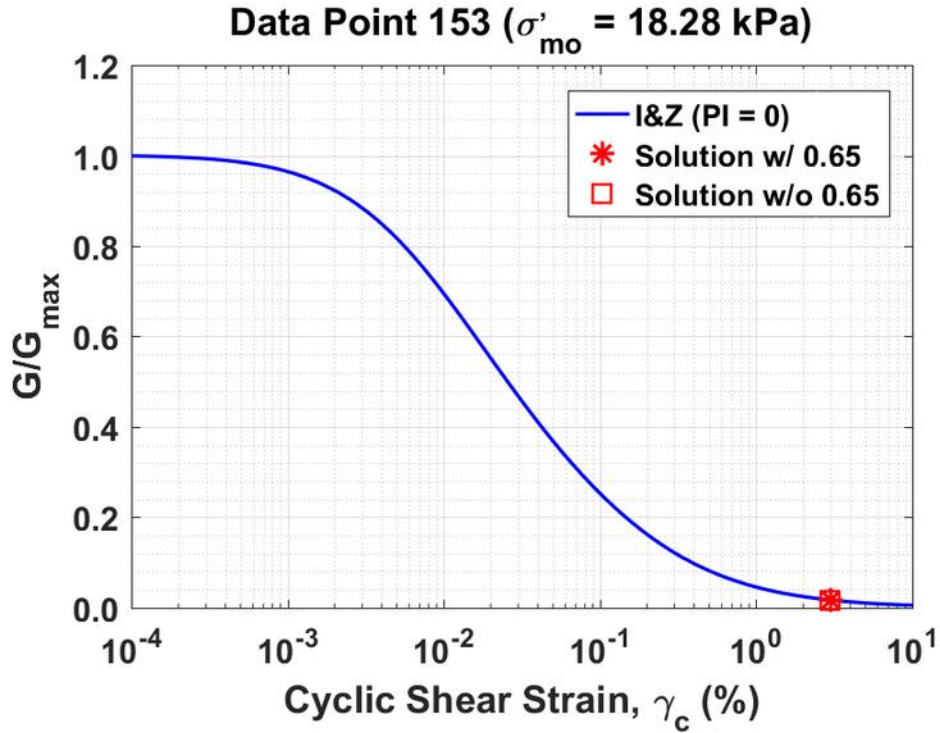


Figure B120. Normalized shear modulus reduction curves for Data Point 153 of the Kayen et al. database showing the solutions w/ and w/o the 0.65 factor

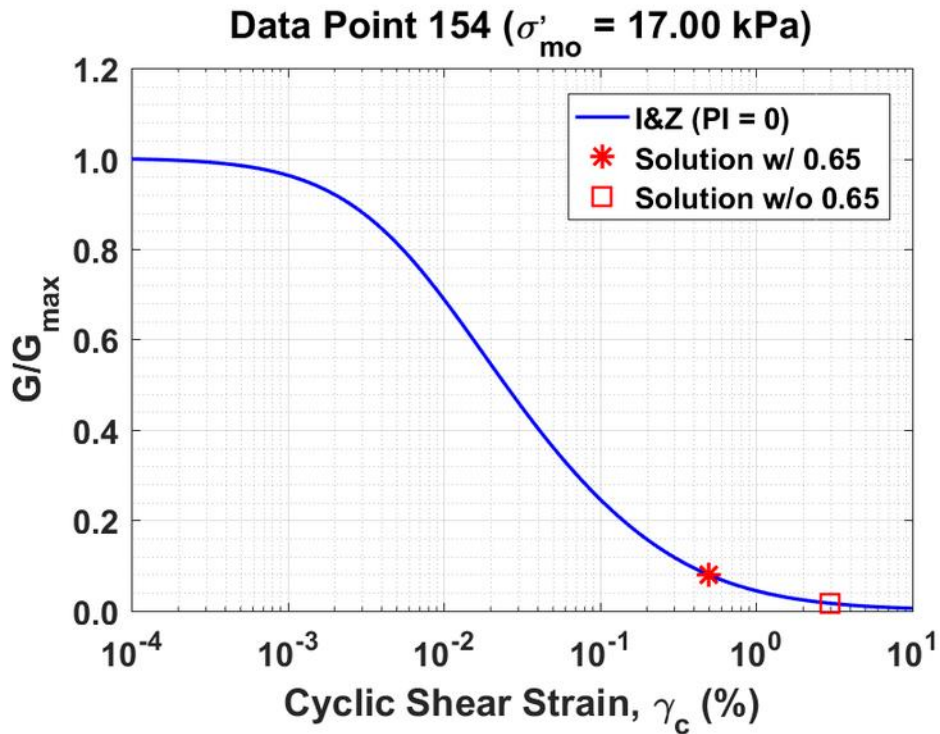


Figure B121. Normalized shear modulus reduction curves for Data Point 154 of the Kayen et al. database showing the solutions w/ and w/o the 0.65 factor

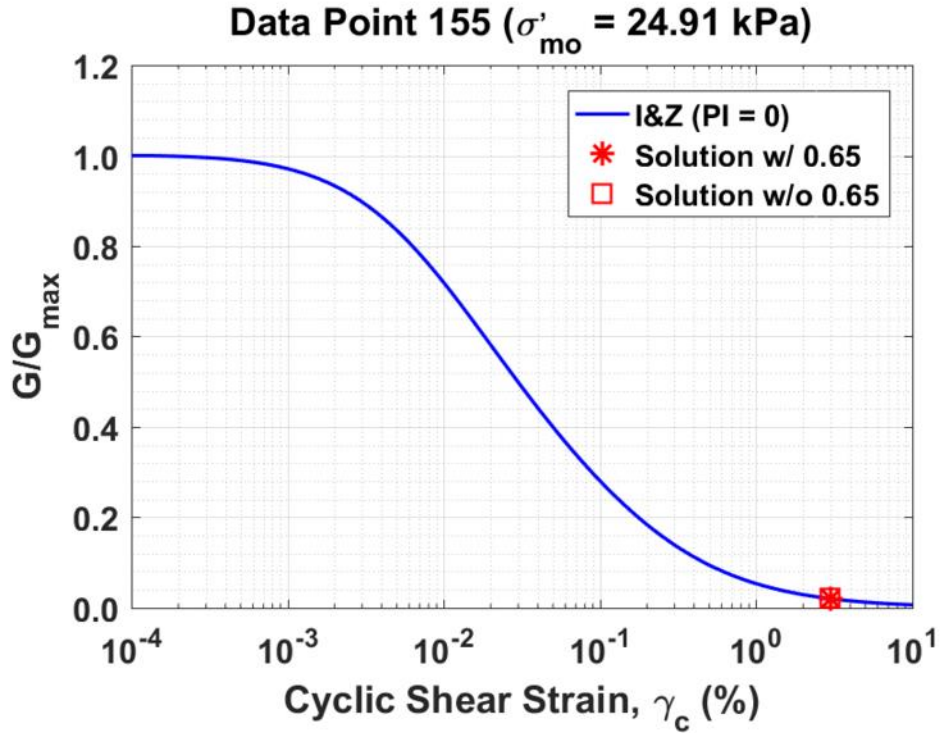


Figure B122. Normalized shear modulus reduction curves for Data Point 155 of the Kayen et al. database showing the solutions w/ and w/o the 0.65 factor

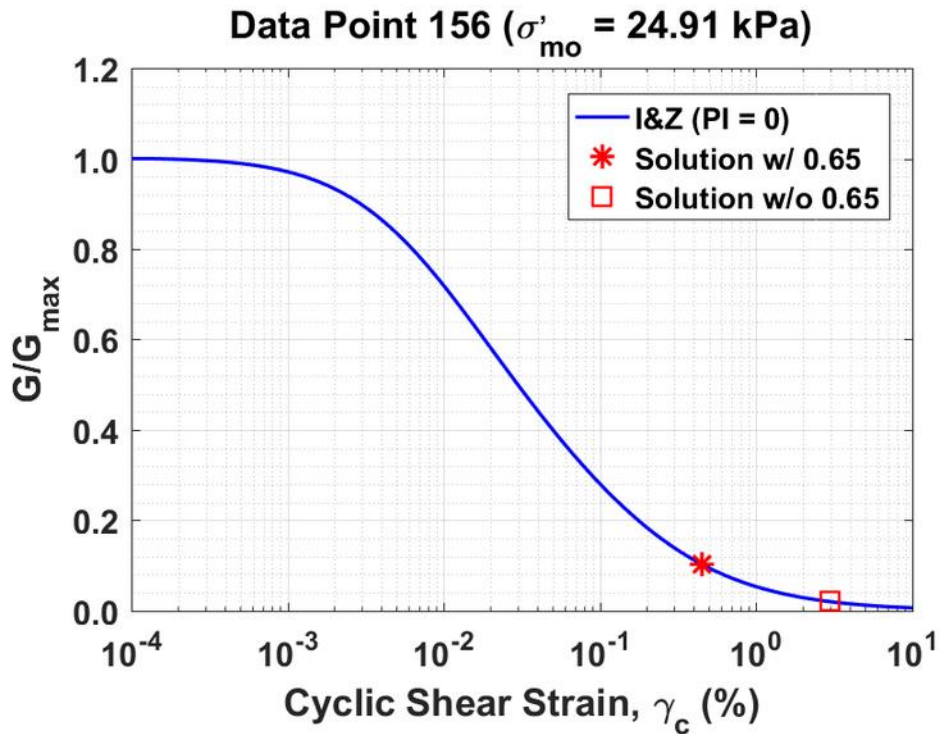


Figure B123. Normalized shear modulus reduction curves for Data Point 156 of the Kayen et al. database showing the solutions w/ and w/o the 0.65 factor

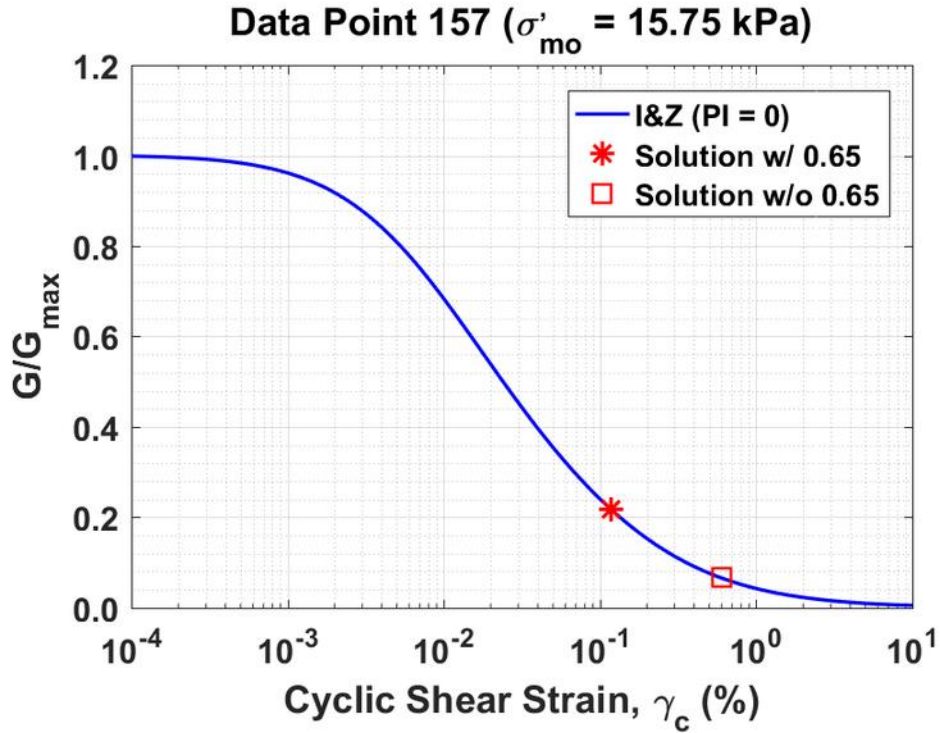


Figure B124. Normalized shear modulus reduction curves for Data Point 157 of the Kayen et al. database showing the solutions w/ and w/o the 0.65 factor

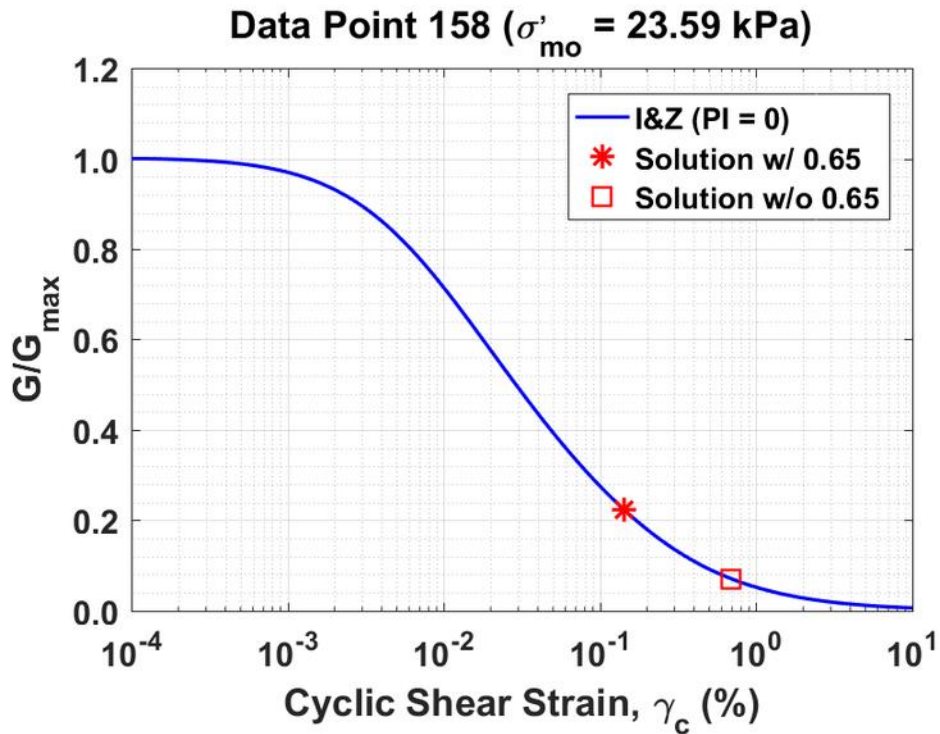


Figure B125. Normalized shear modulus reduction curves for Data Point 158 of the Kayen et al. database showing the solutions w/ and w/o the 0.65 factor

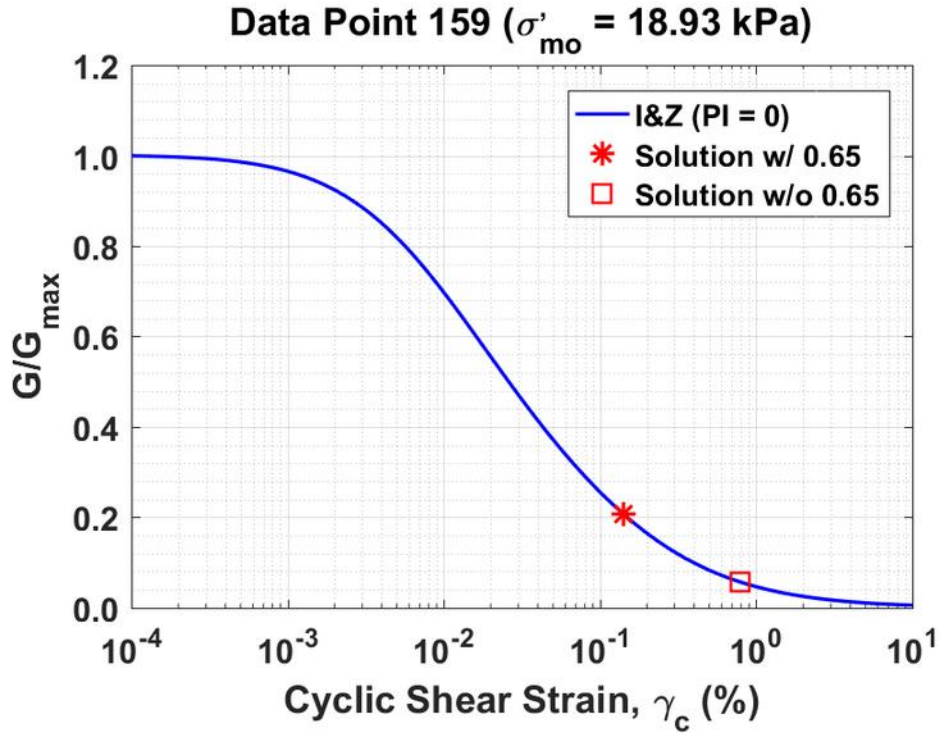


Figure B126. Normalized shear modulus reduction curves for Data Point 159 of the Kayen et al. database showing the solutions w/ and w/o the 0.65 factor

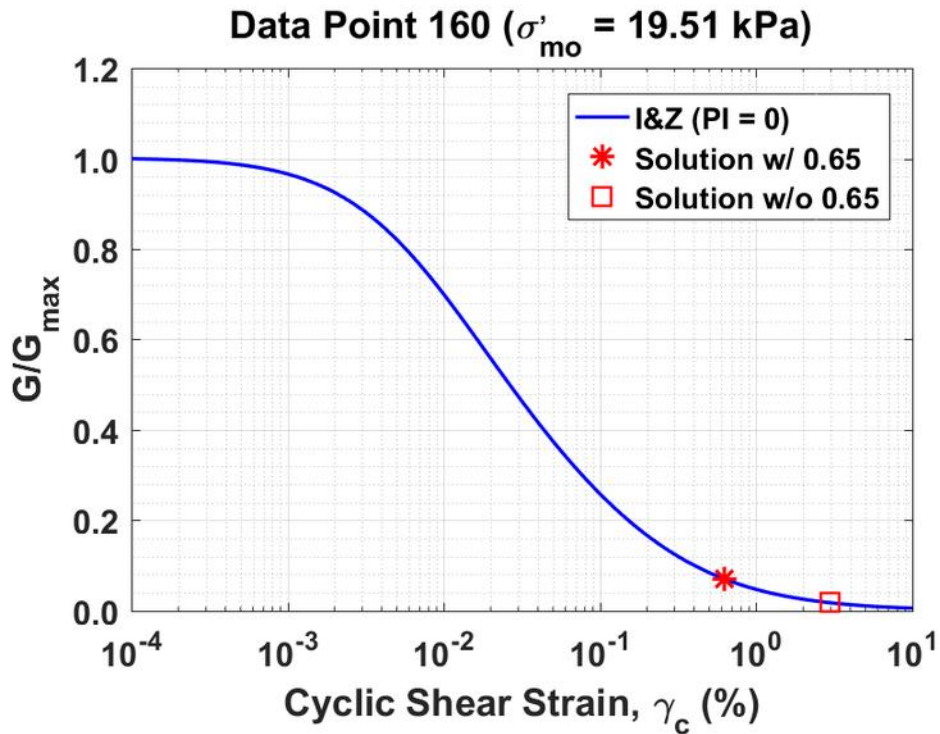


Figure B127. Normalized shear modulus reduction curves for Data Point 160 of the Kayen et al. database showing the solutions w/ and w/o the 0.65 factor

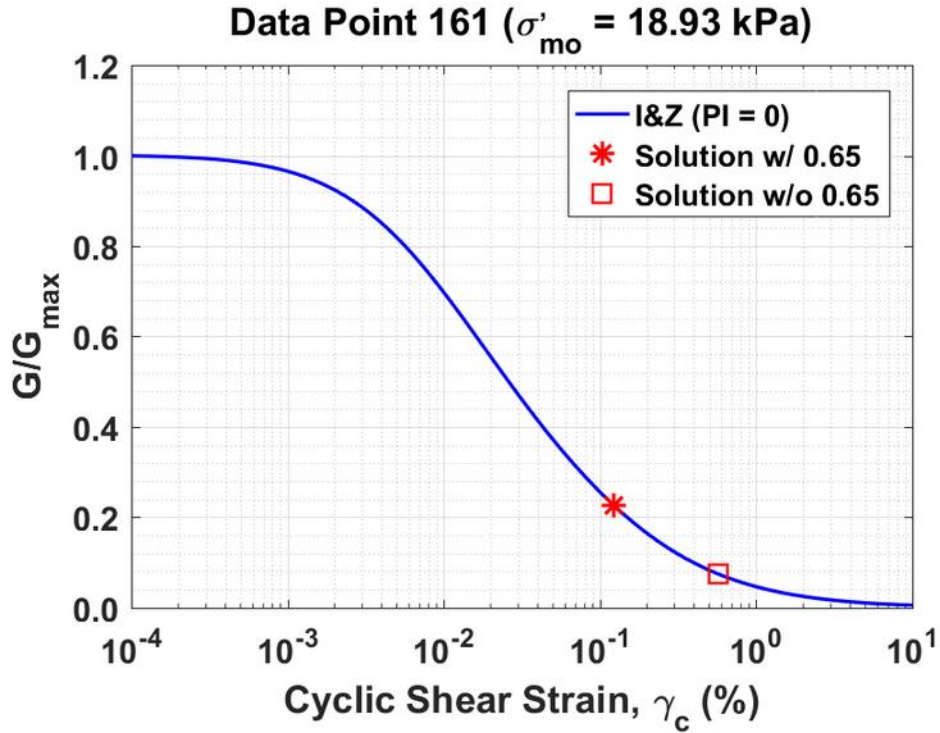


Figure B128. Normalized shear modulus reduction curves for Data Point 161 of the Kayen et al. database showing the solutions w/ and w/o the 0.65 factor

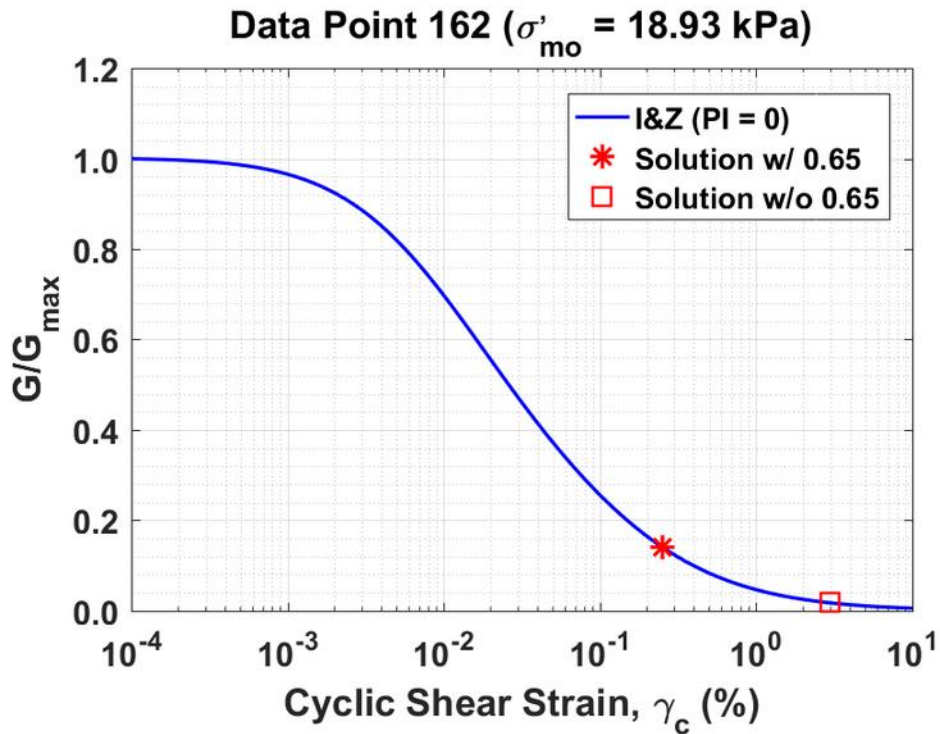


Figure B129. Normalized shear modulus reduction curves for Data Point 162 of the Kayen et al. database showing the solutions w/ and w/o the 0.65 factor

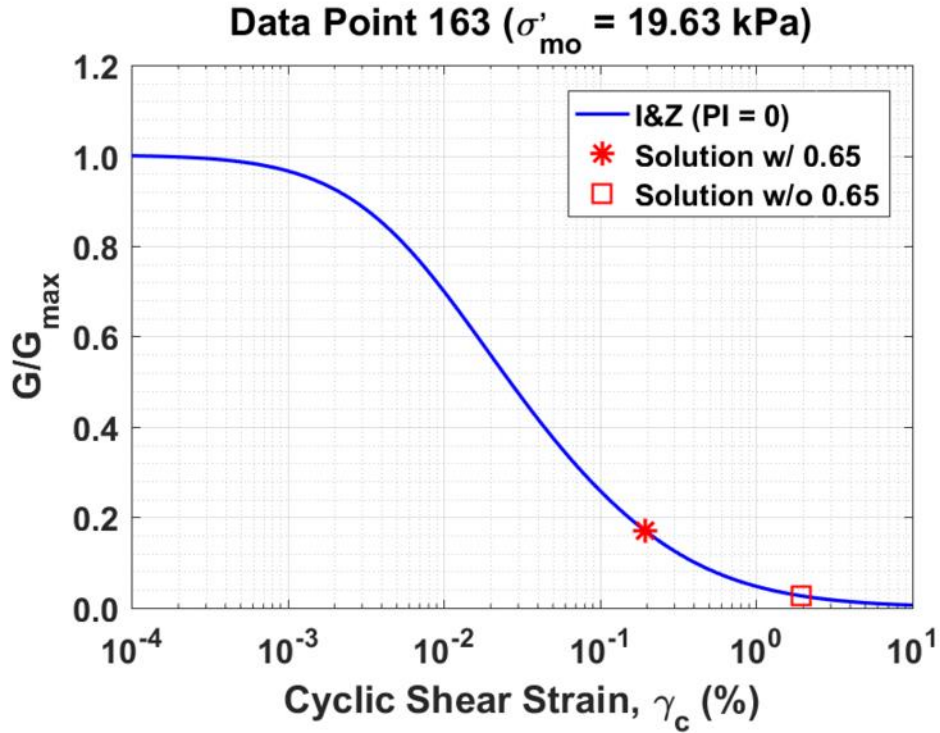


Figure B130. Normalized shear modulus reduction curves for Data Point 163 of the Kayen et al. database showing the solutions w/ and w/o the 0.65 factor

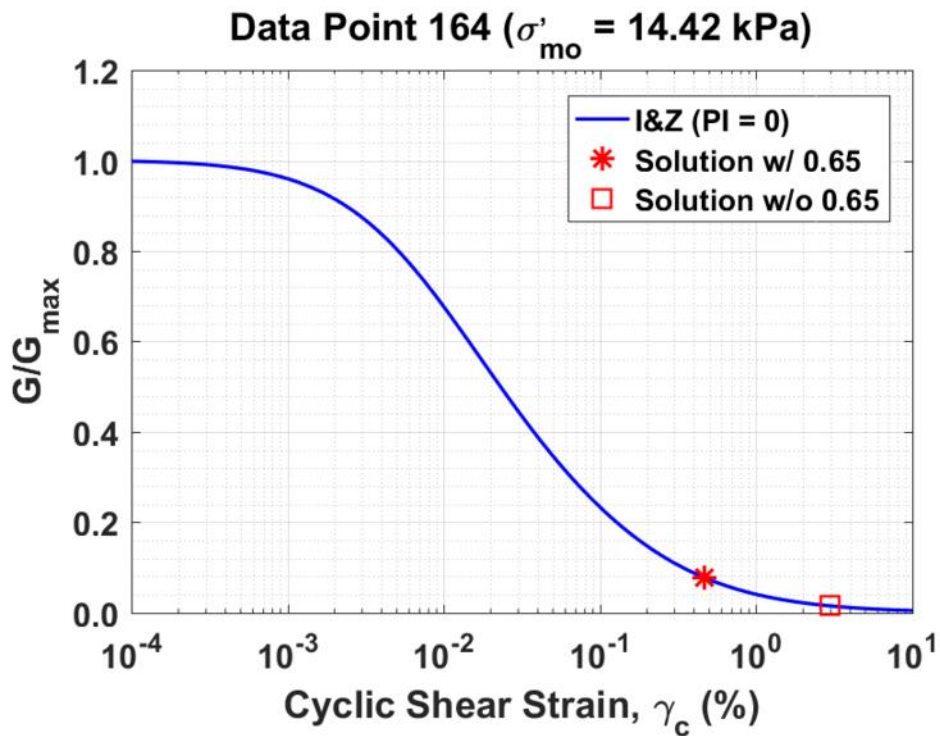


Figure B131. Normalized shear modulus reduction curves for Data Point 164 of the Kayen et al. database showing the solutions w/ and w/o the 0.65 factor

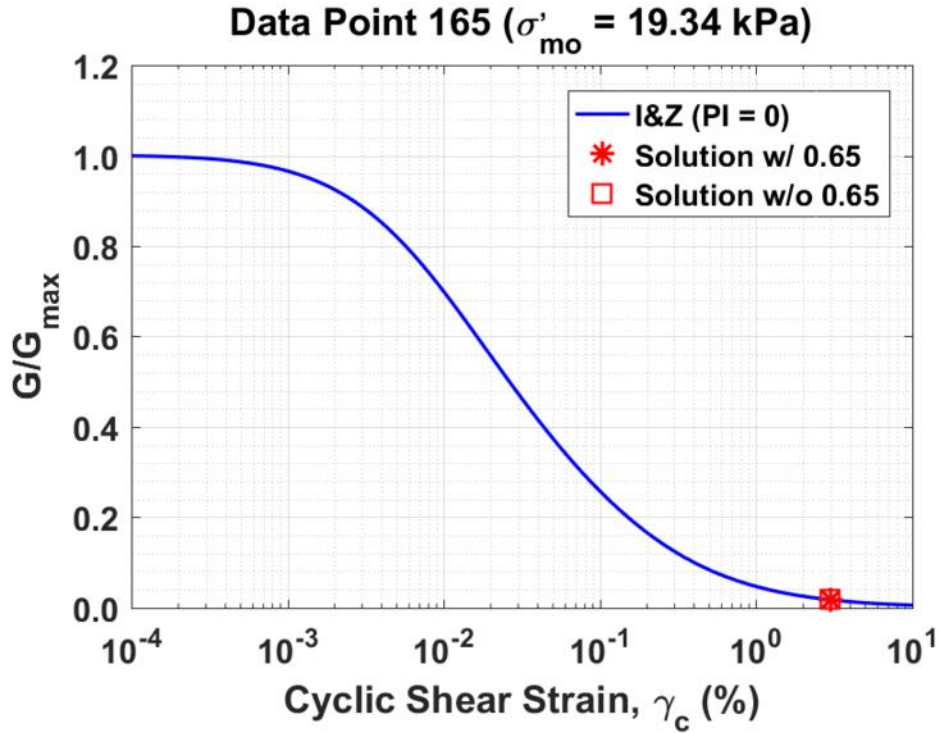


Figure B132. Normalized shear modulus reduction curves for Data Point 165 of the Kayen et al. database showing the solutions w/ and w/o the 0.65 factor

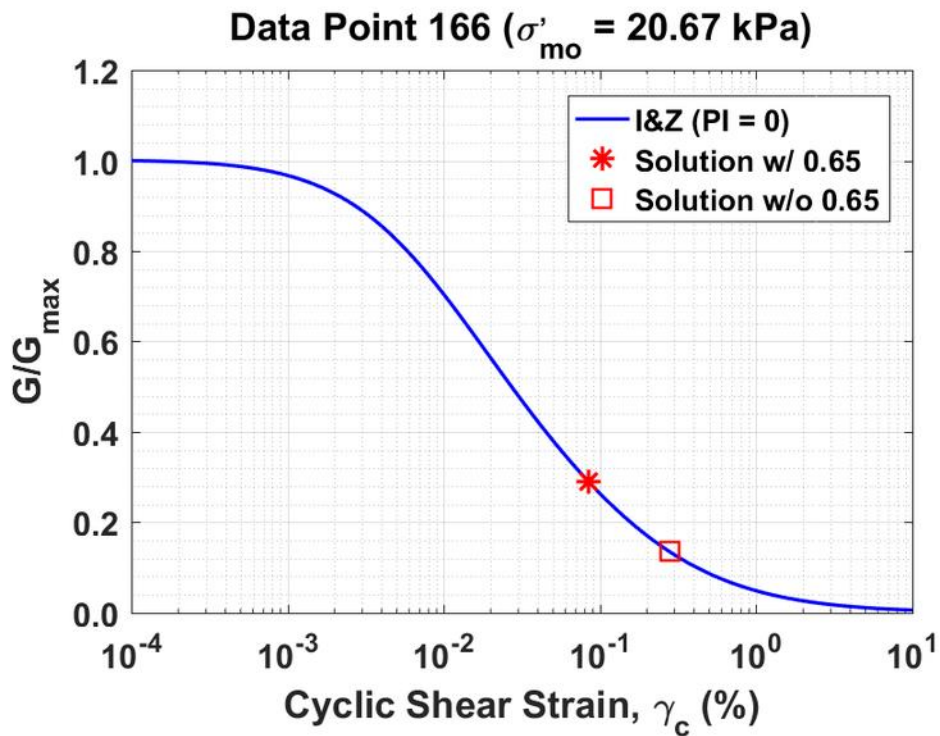


Figure B133. Normalized shear modulus reduction curves for Data Point 166 of the Kayen et al. database showing the solutions w/ and w/o the 0.65 factor

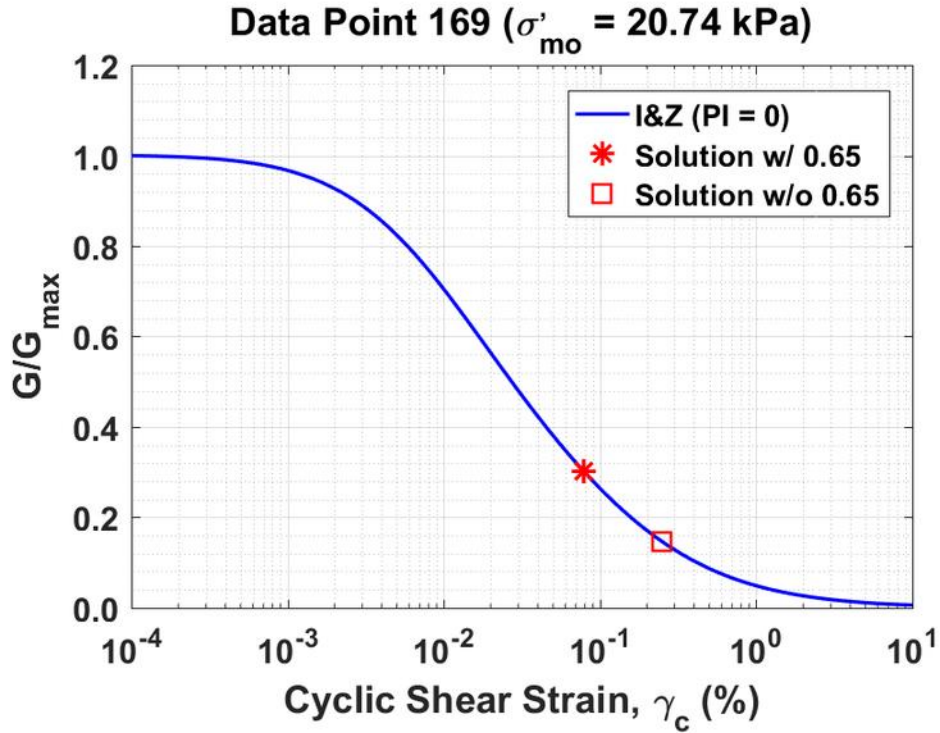


Figure B134. Normalized shear modulus reduction curves for Data Point 169 of the Kayen et al. database showing the solutions w/ and w/o the 0.65 factor

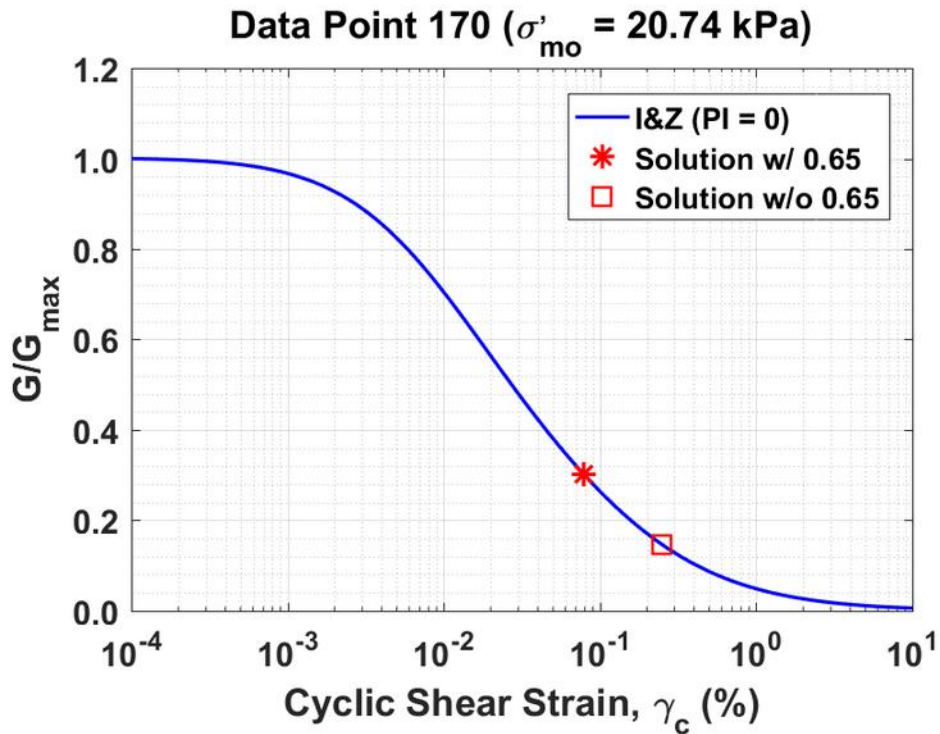


Figure B135. Normalized shear modulus reduction curves for Data Point 170 of the Kayen et al. database showing the solutions w/ and w/o the 0.65 factor

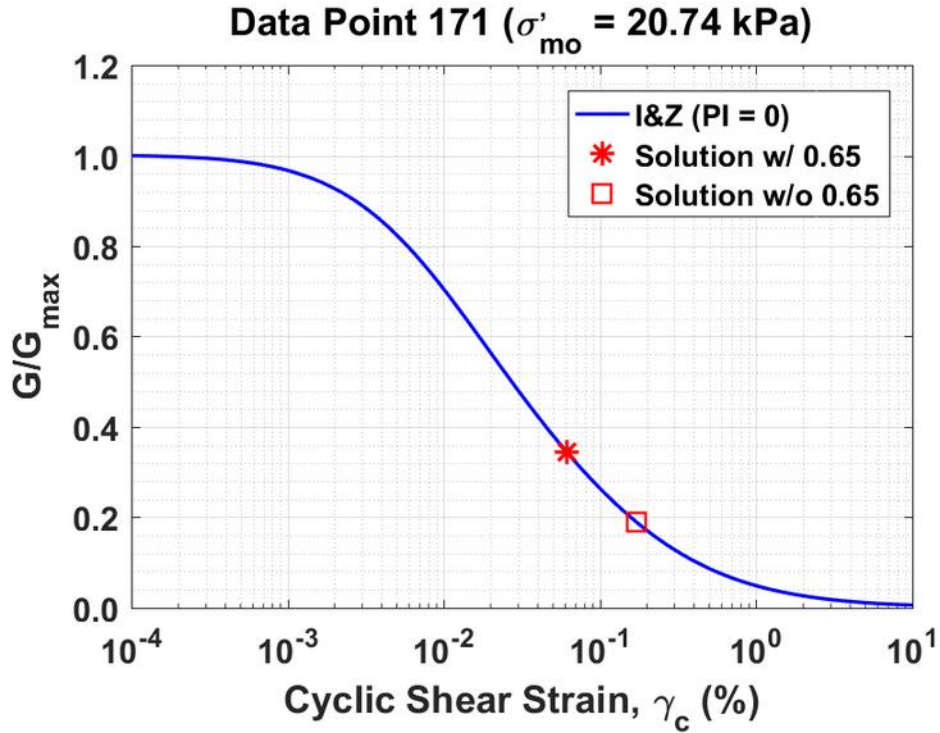


Figure B136. Normalized shear modulus reduction curves for Data Point 171 of the Kayen et al. database showing the solutions w/ and w/o the 0.65 factor

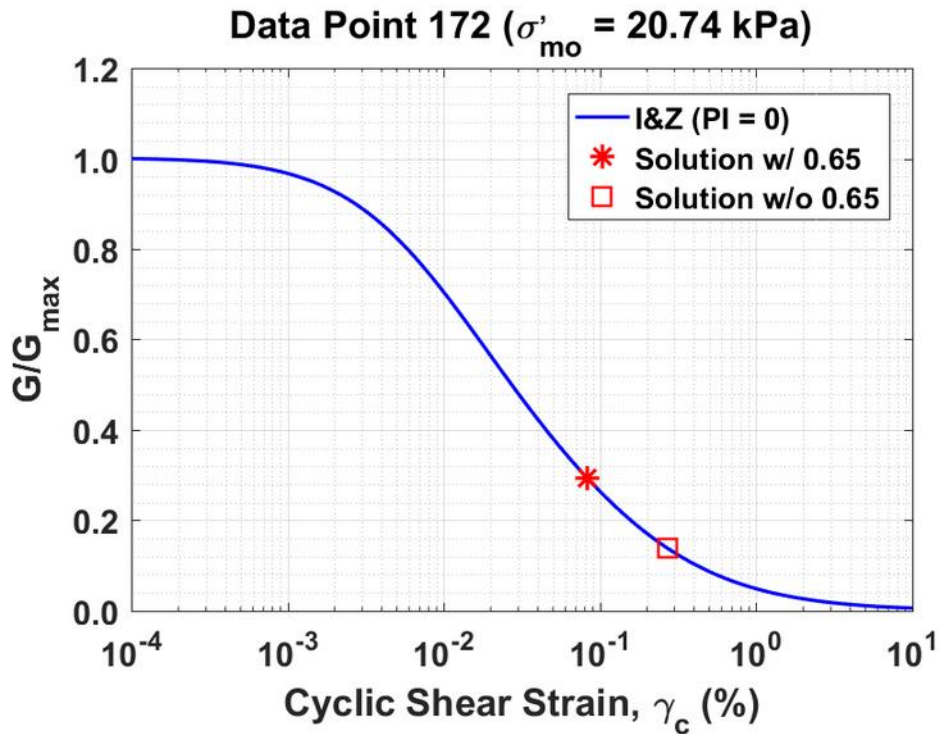


Figure B137. Normalized shear modulus reduction curves for Data Point 172 of the Kayen et al. database showing the solutions w/ and w/o the 0.65 factor

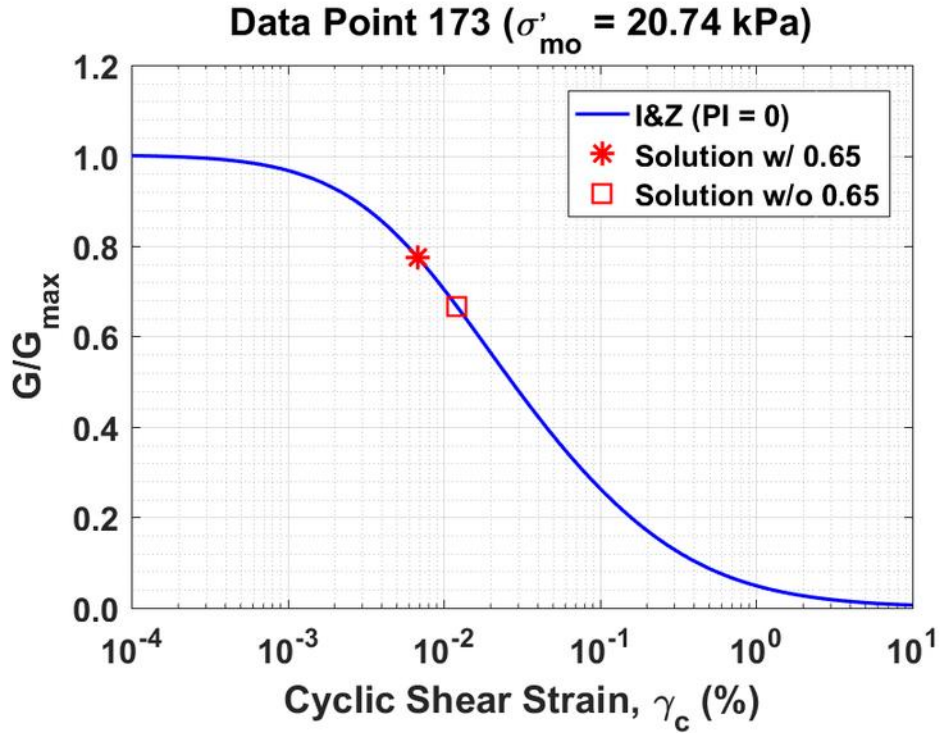


Figure B138. Normalized shear modulus reduction curves for Data Point 173 of the Kayen et al. database showing the solutions w/ and w/o the 0.65 factor

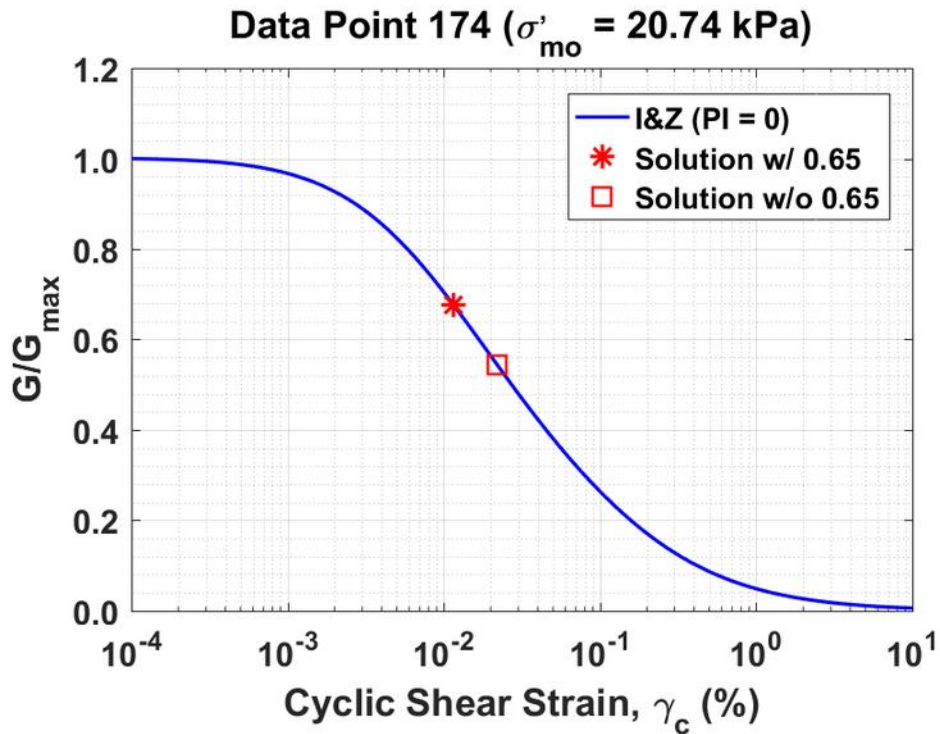


Figure B139. Normalized shear modulus reduction curves for Data Point 174 of the Kayen et al. database showing the solutions w/ and w/o the 0.65 factor

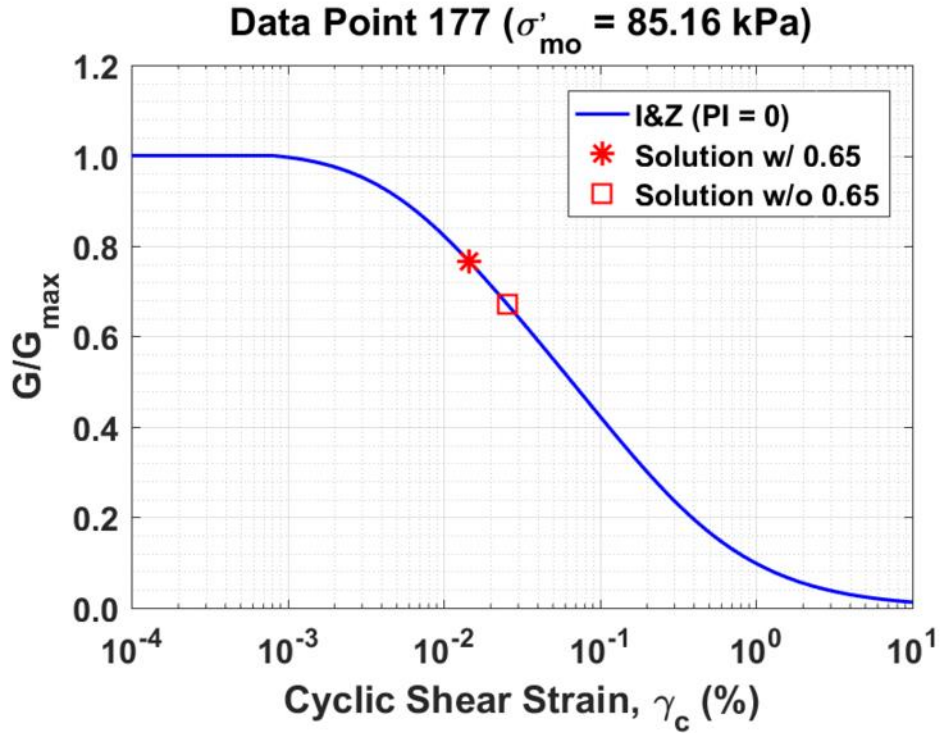


Figure B140. Normalized shear modulus reduction curves for Data Point 177 of the Kayen et al. database showing the solutions w/ and w/o the 0.65 factor

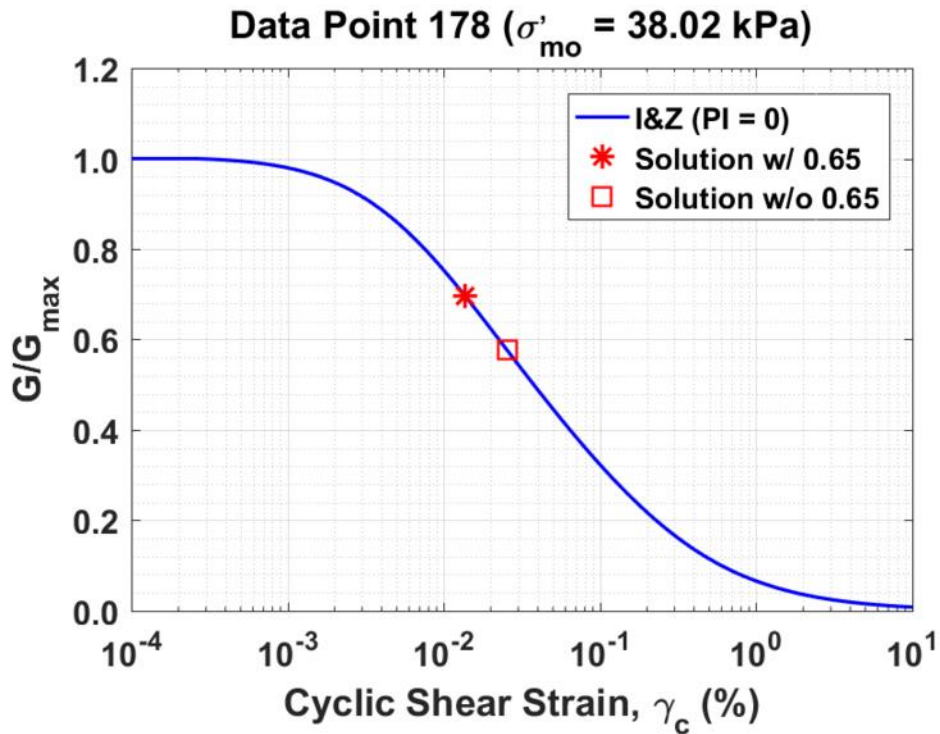


Figure B141. Normalized shear modulus reduction curves for Data Point 178 of the Kayen et al. database showing the solutions w/ and w/o the 0.65 factor

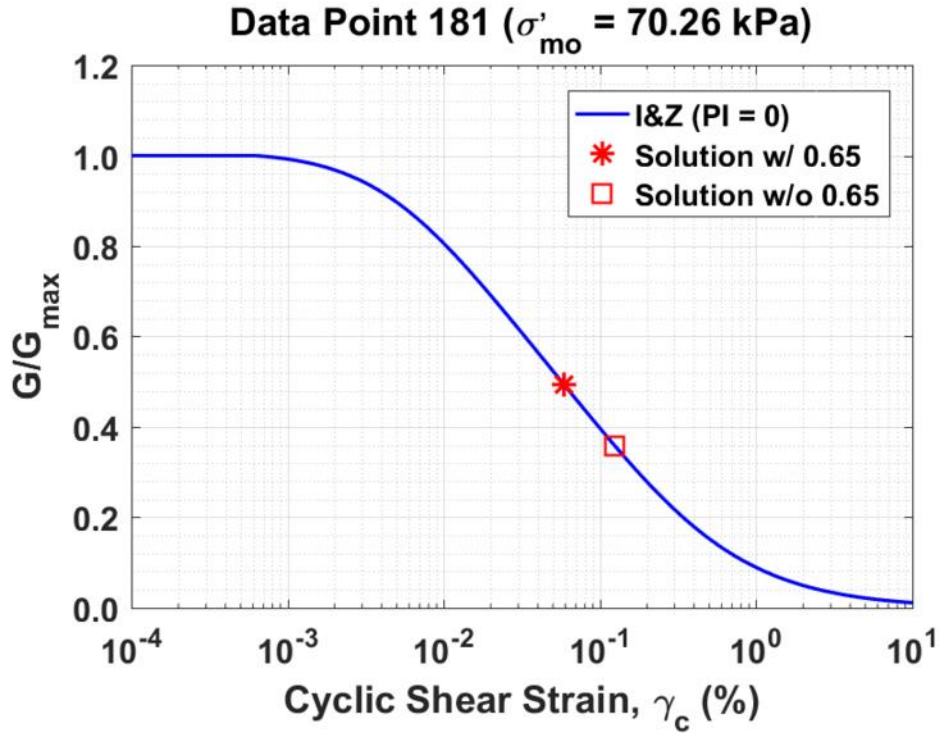


Figure B142. Normalized shear modulus reduction curves for Data Point 181 of the Kayen et al. database showing the solutions w/ and w/o the 0.65 factor

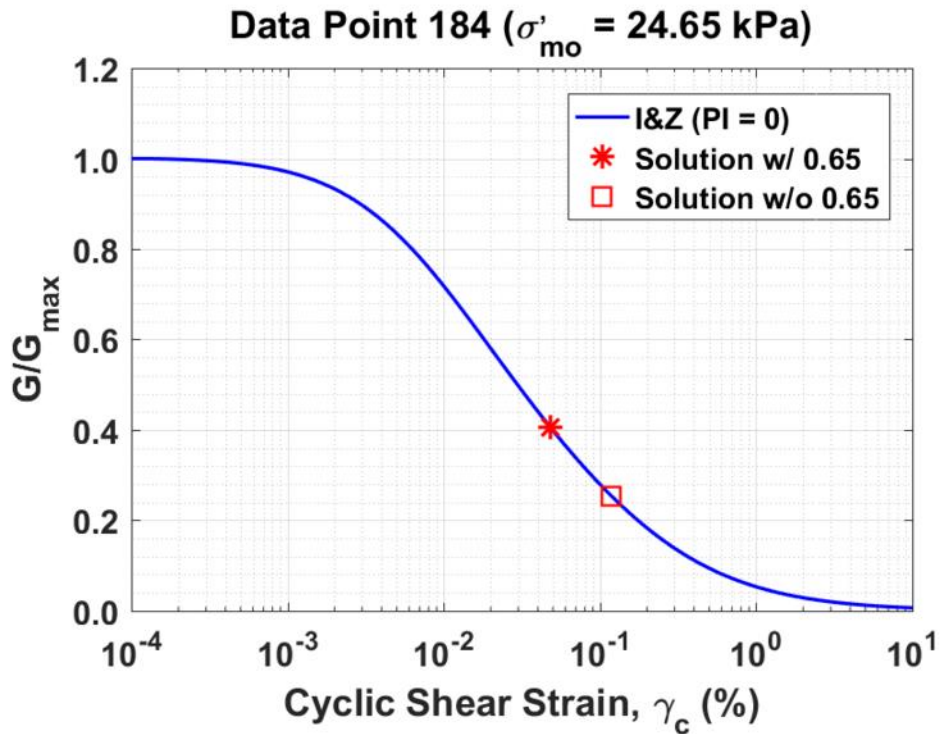


Figure B143. Normalized shear modulus reduction curves for Data Point 184 of the Kayen et al. database showing the solutions w/ and w/o the 0.65 factor

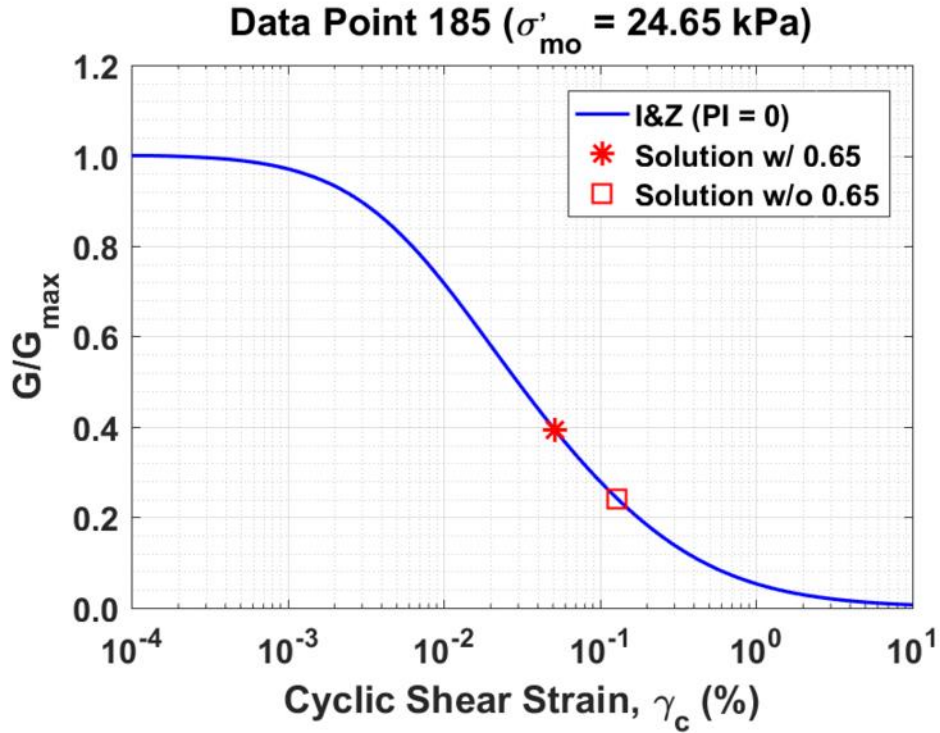


Figure B145. Normalized shear modulus reduction curves for Data Point 185 of the Kayen et al. database showing the solutions w/ and w/o the 0.65 factor

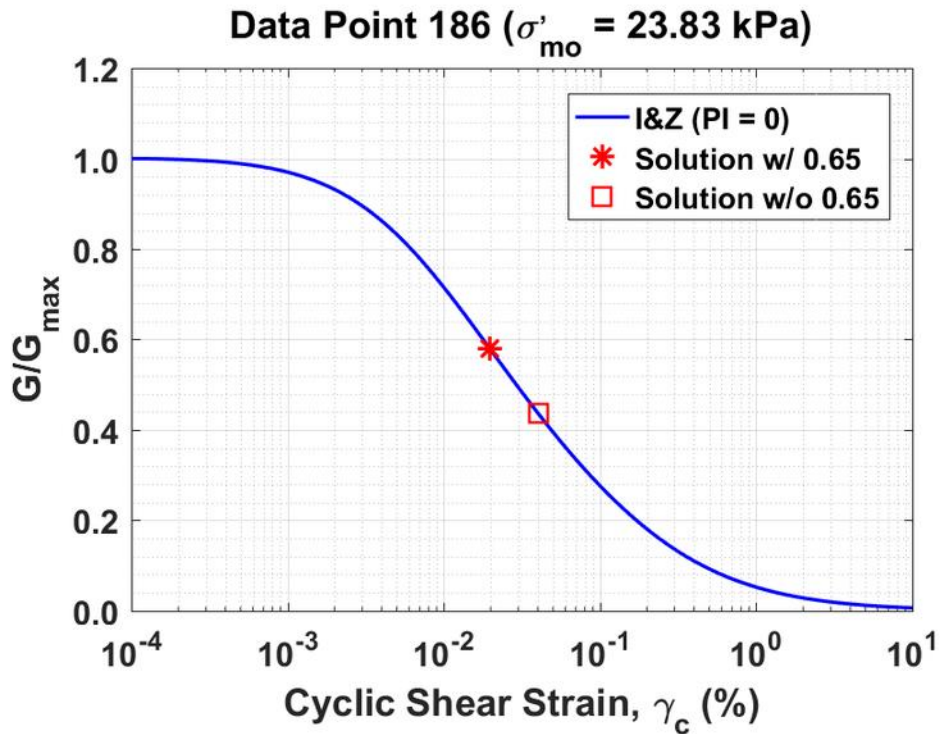


Figure B146. Normalized shear modulus reduction curves for Data Point 186 of the Kayen et al. database showing the solutions w/ and w/o the 0.65 factor

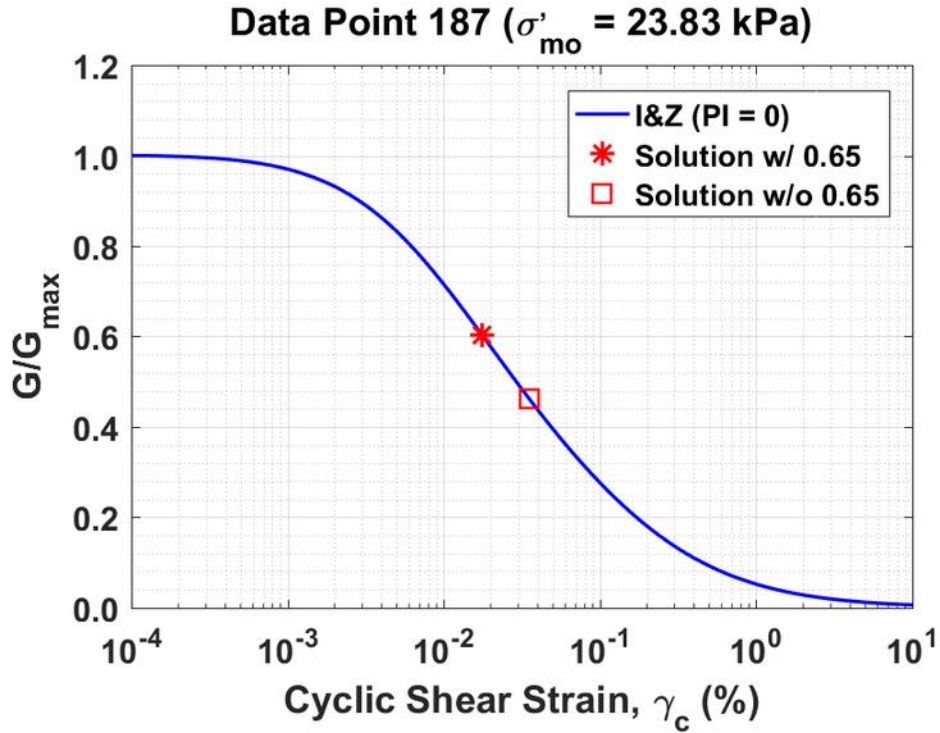


Figure B147. Normalized shear modulus reduction curves for Data Point 187 of the Kayen et al. database showing the solutions w/ and w/o the 0.65 factor

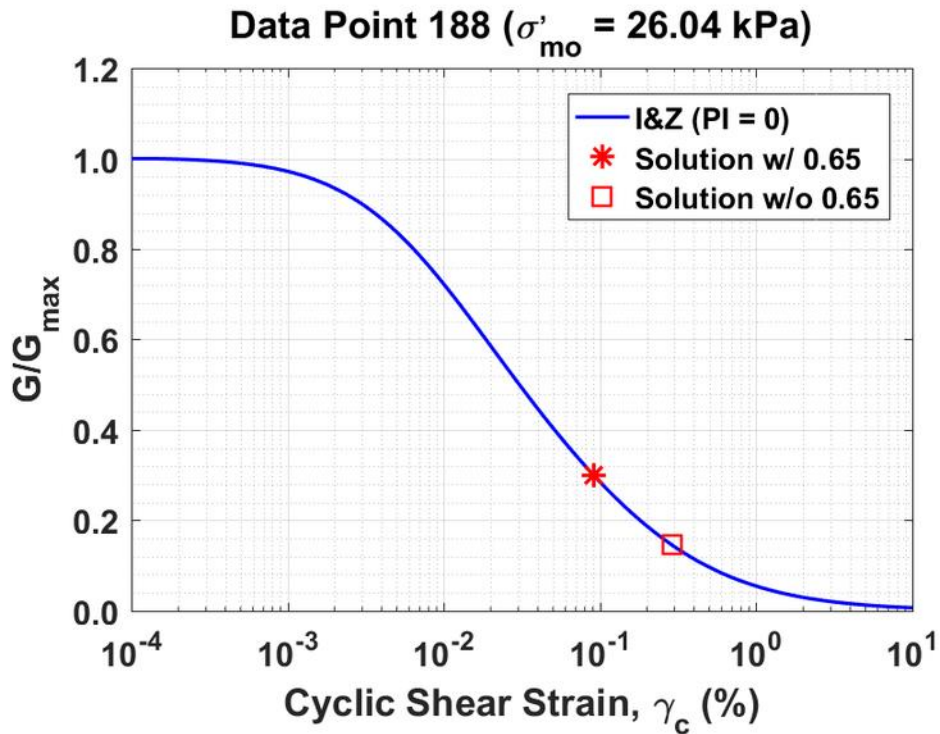


Figure B148. Normalized shear modulus reduction curves for Data Point 188 of the Kayen et al. database showing the solutions w/ and w/o the 0.65 factor

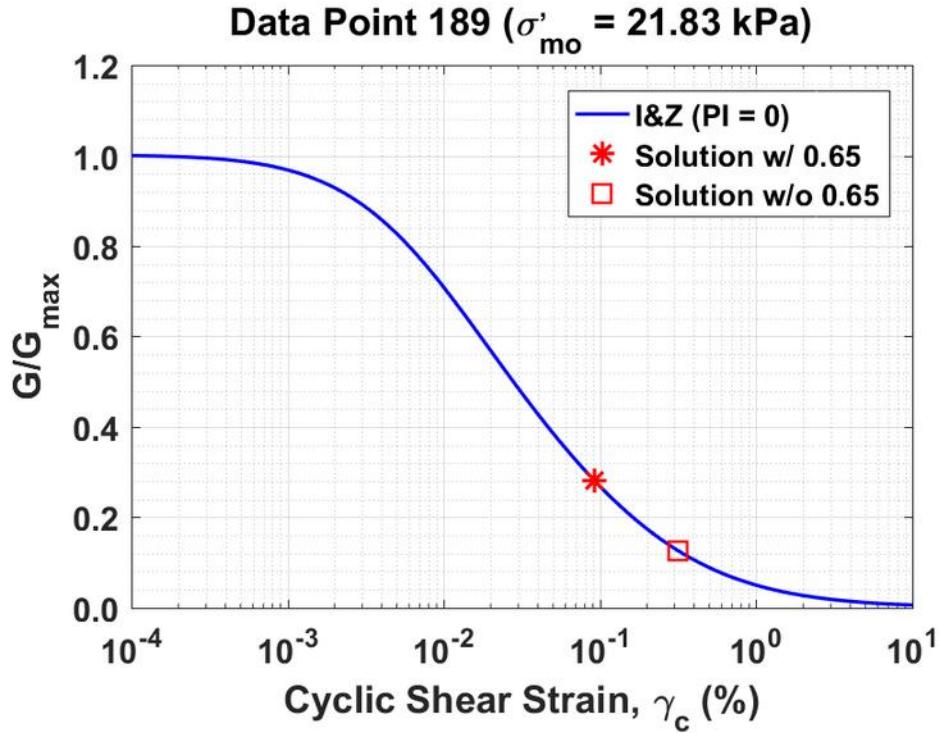


Figure B149. Normalized shear modulus reduction curves for Data Point 189 of the Kayen et al. database showing the solutions w/ and w/o the 0.65 factor

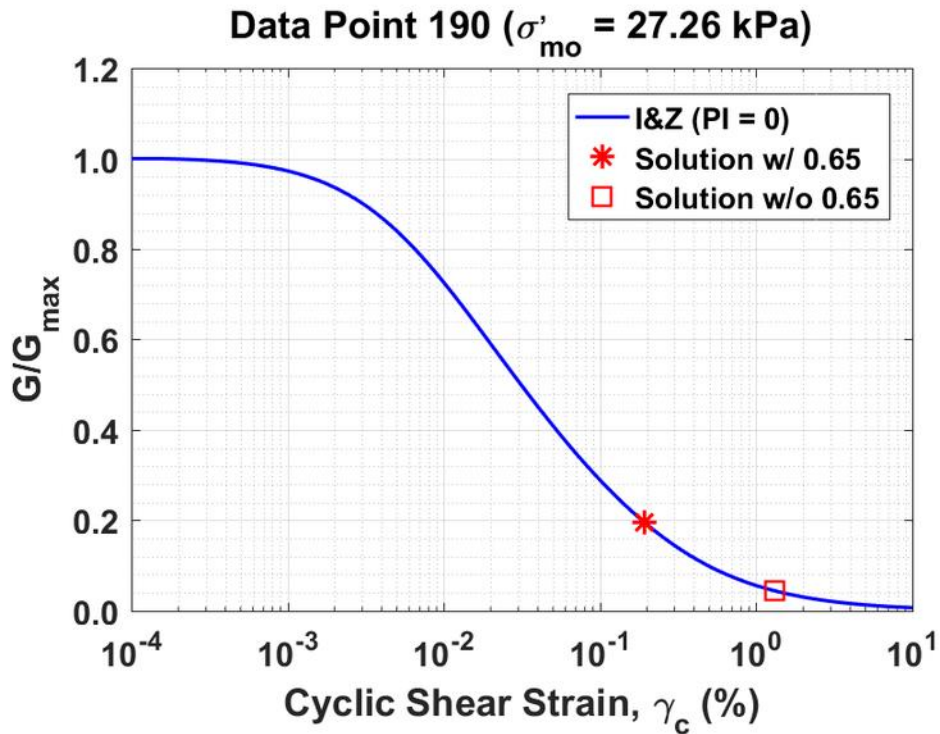


Figure B150. Normalized shear modulus reduction curves for Data Point 190 of the Kayen et al. database showing the solutions w/ and w/o the 0.65 factor

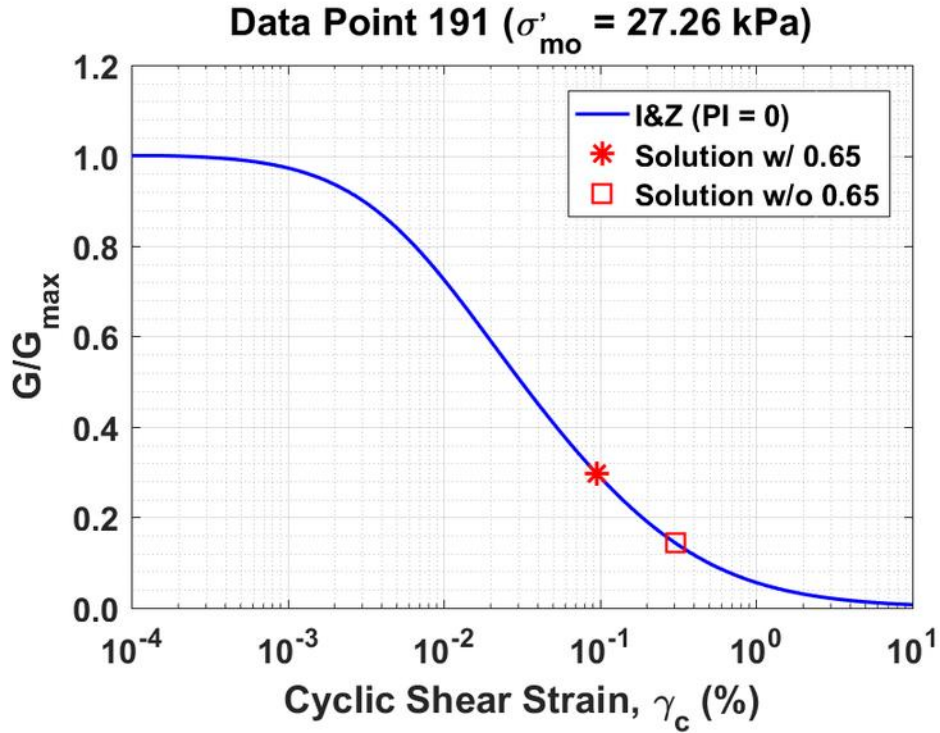


Figure B151. Normalized shear modulus reduction curves for Data Point 191 of the Kayen et al. database showing the solutions w/ and w/o the 0.65 factor

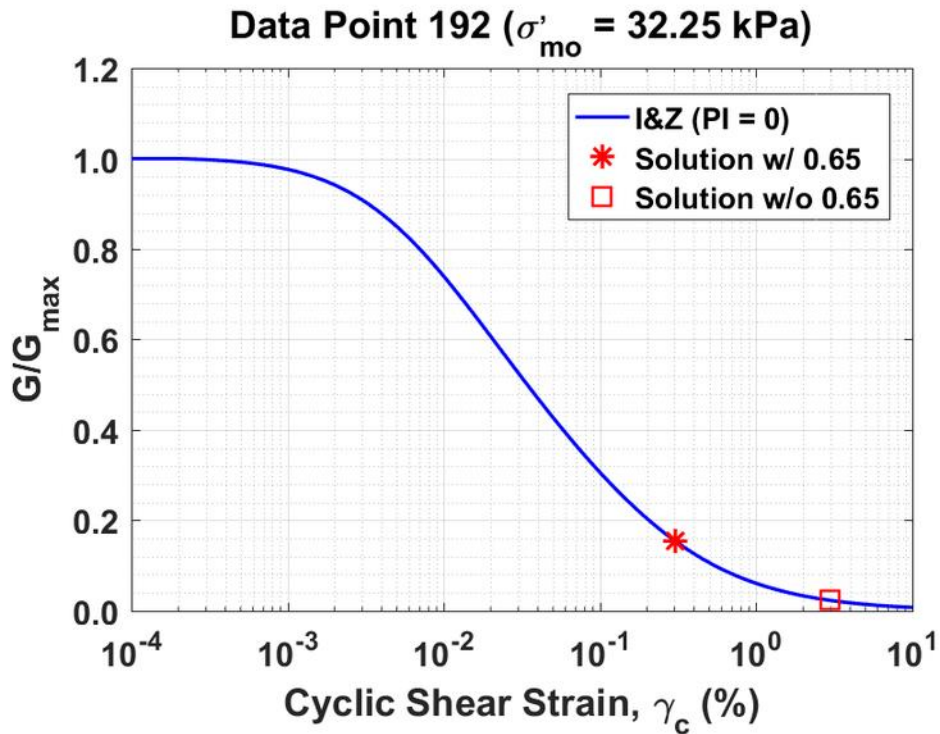


Figure B152. Normalized shear modulus reduction curves for Data Point 192 of the Kayen et al. database showing the solutions w/ and w/o the 0.65 factor

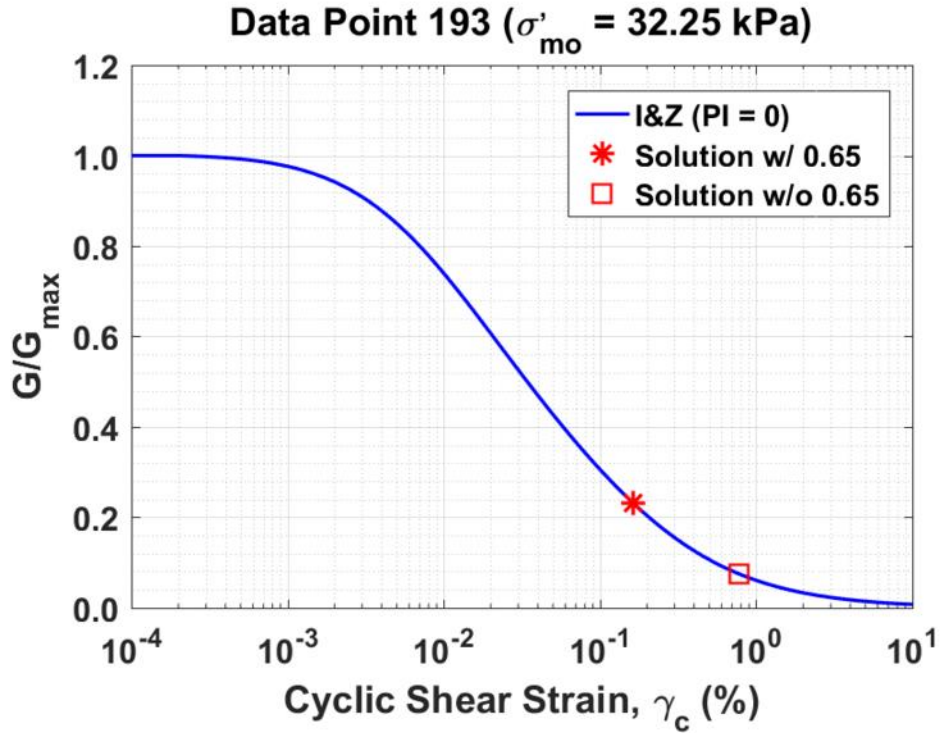


Figure B153. Normalized shear modulus reduction curves for Data Point 193 of the Kayen et al. database showing the solutions w/ and w/o the 0.65 factor

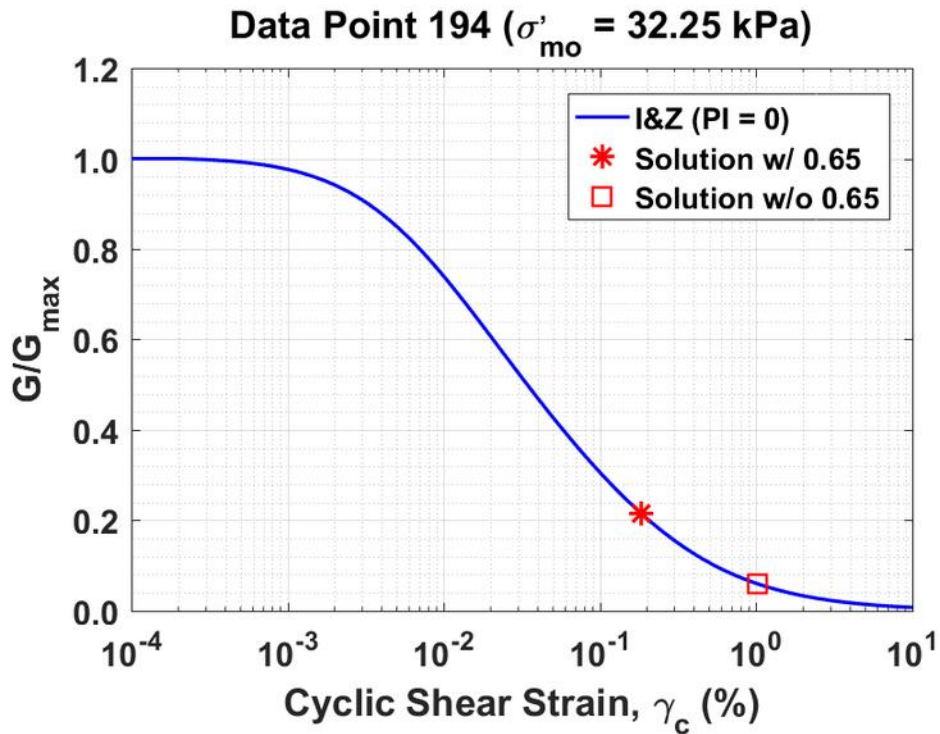


Figure B154. Normalized shear modulus reduction curves for Data Point 194 of the Kayen et al. database showing the solutions w/ and w/o the 0.65 factor

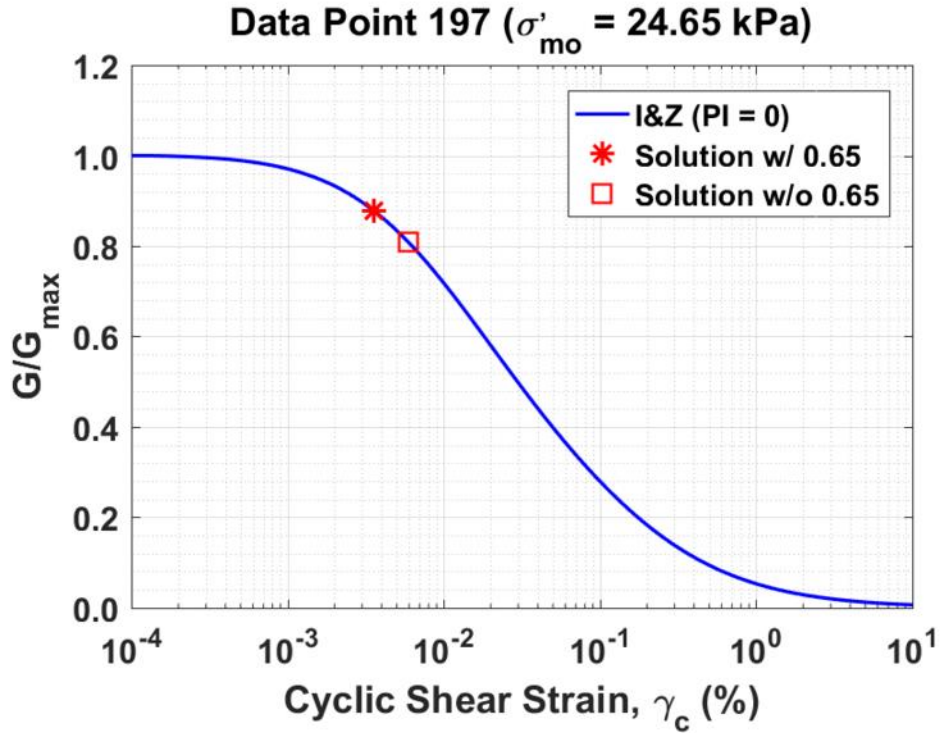


Figure B155. Normalized shear modulus reduction curves for Data Point 197 of the Kayen et al. database showing the solutions w/ and w/o the 0.65 factor

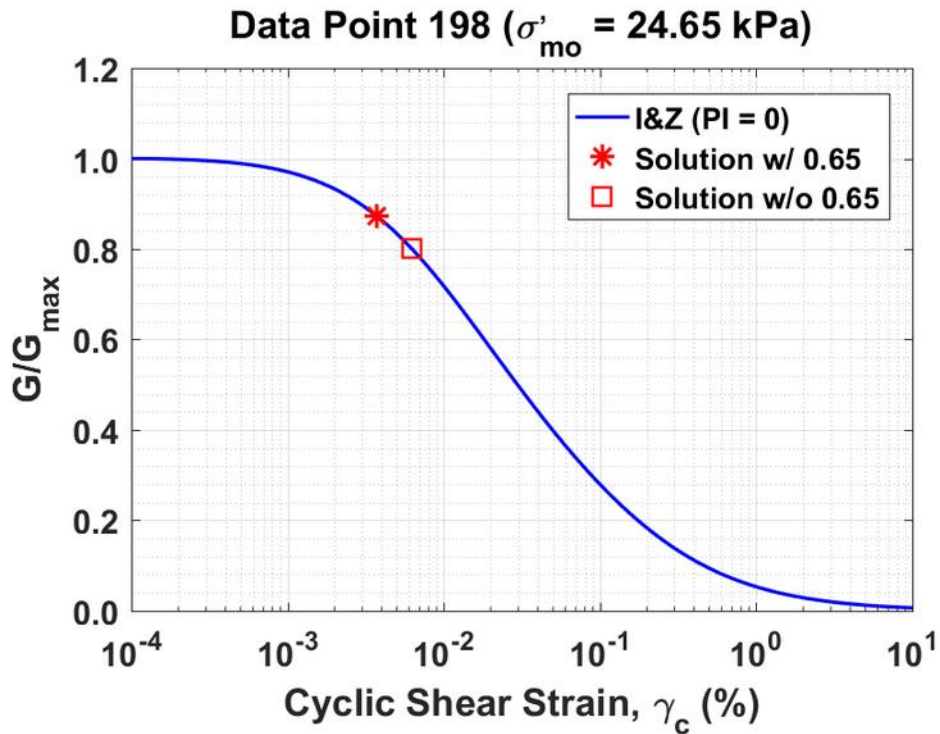


Figure B156. Normalized shear modulus reduction curves for Data Point 198 of the Kayen et al. database showing the solutions w/ and w/o the 0.65 factor

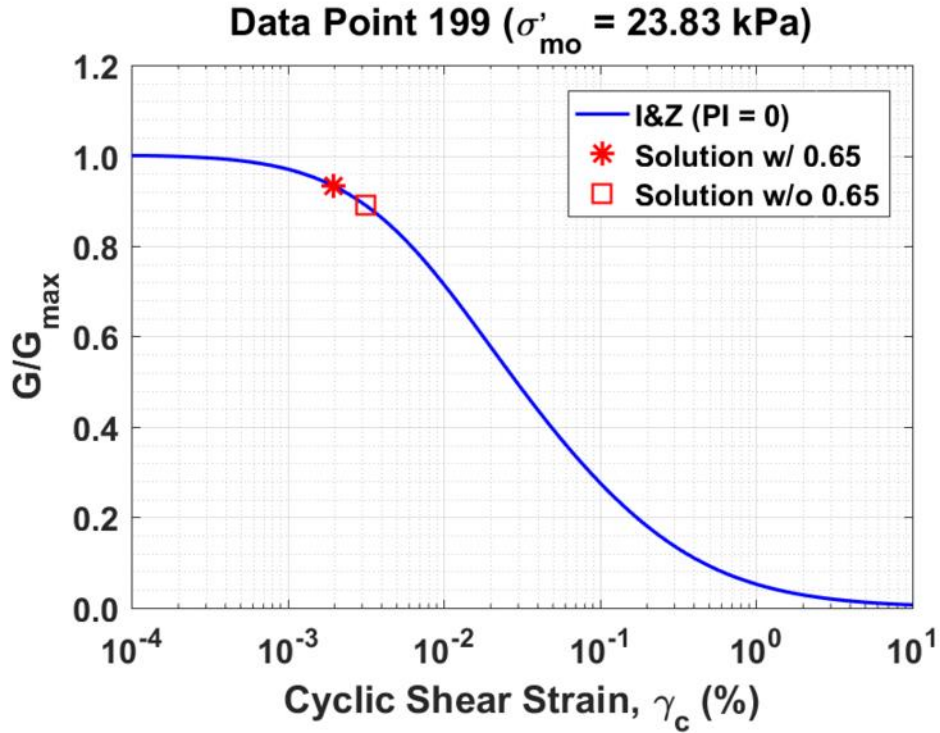


Figure B157. Normalized shear modulus reduction curves for Data Point 199 of the Kayen et al. database showing the solutions w/ and w/o the 0.65 factor

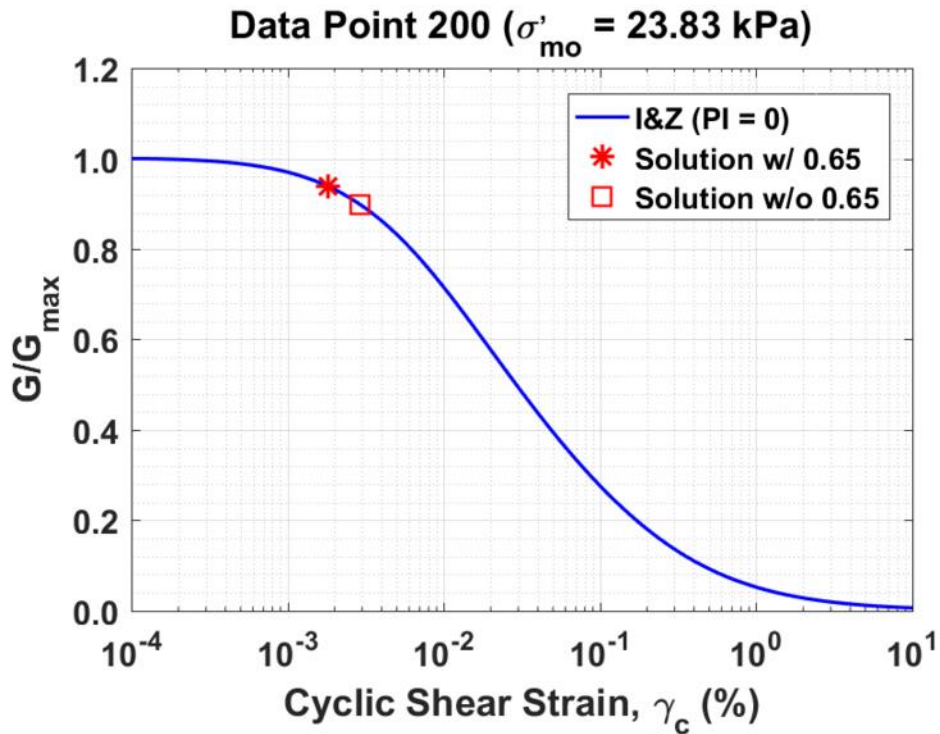


Figure B158. Normalized shear modulus reduction curves for Data Point 200 of the Kayen et al. database showing the solutions w/ and w/o the 0.65 factor

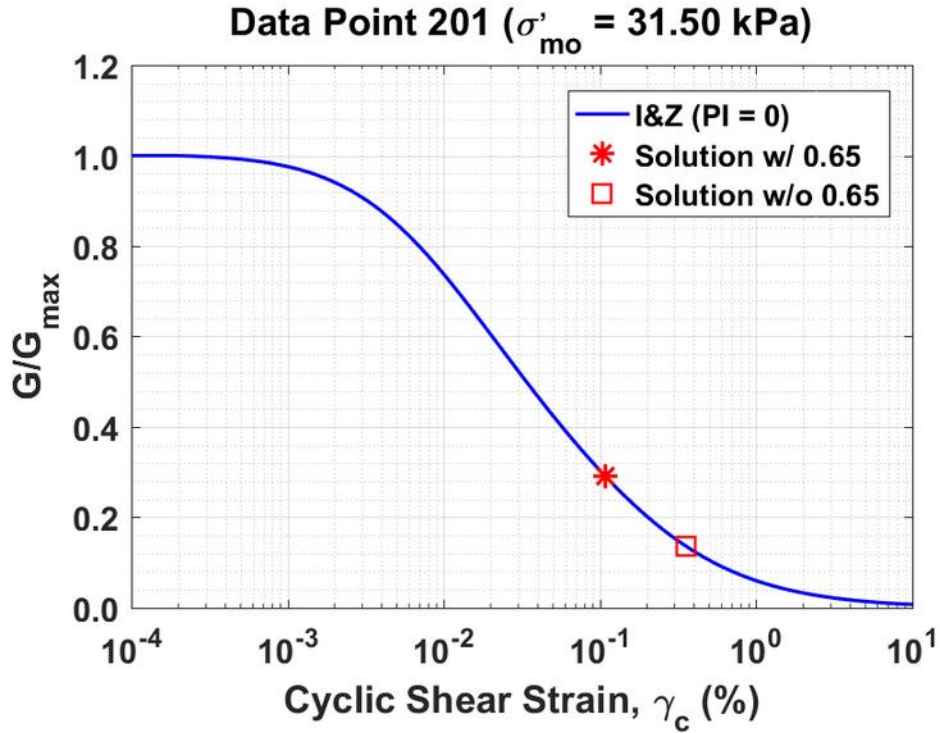


Figure B159. Normalized shear modulus reduction curves for Data Point 201 of the Kayen et al. database showing the solutions w/ and w/o the 0.65 factor

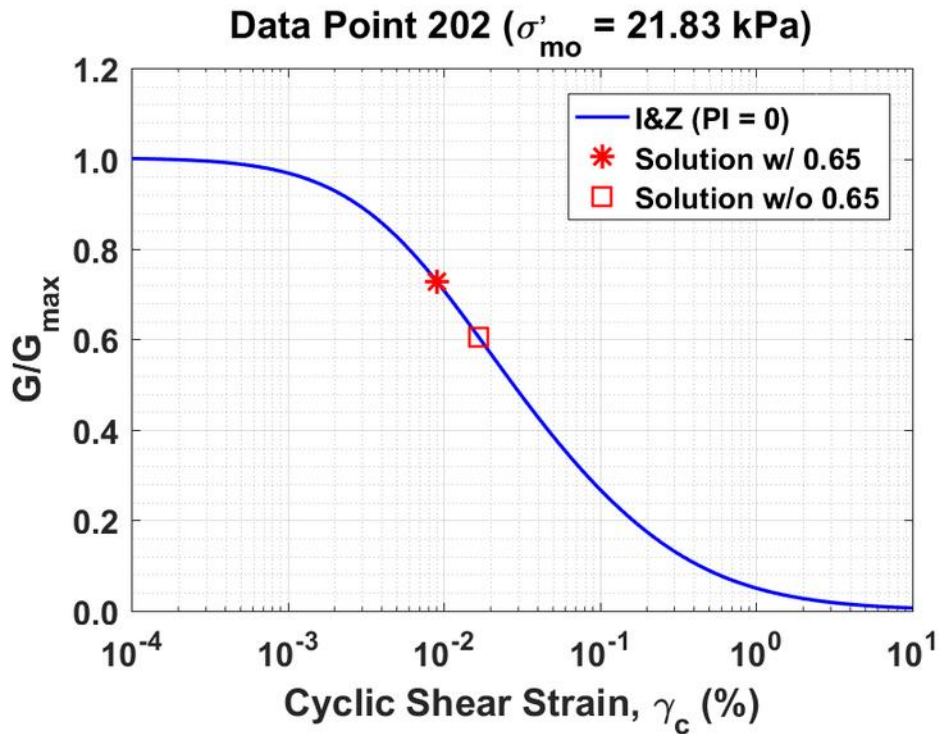


Figure B160. Normalized shear modulus reduction curves for Data Point 201 of the Kayen et al. database showing the solutions w/ and w/o the 0.65 factor

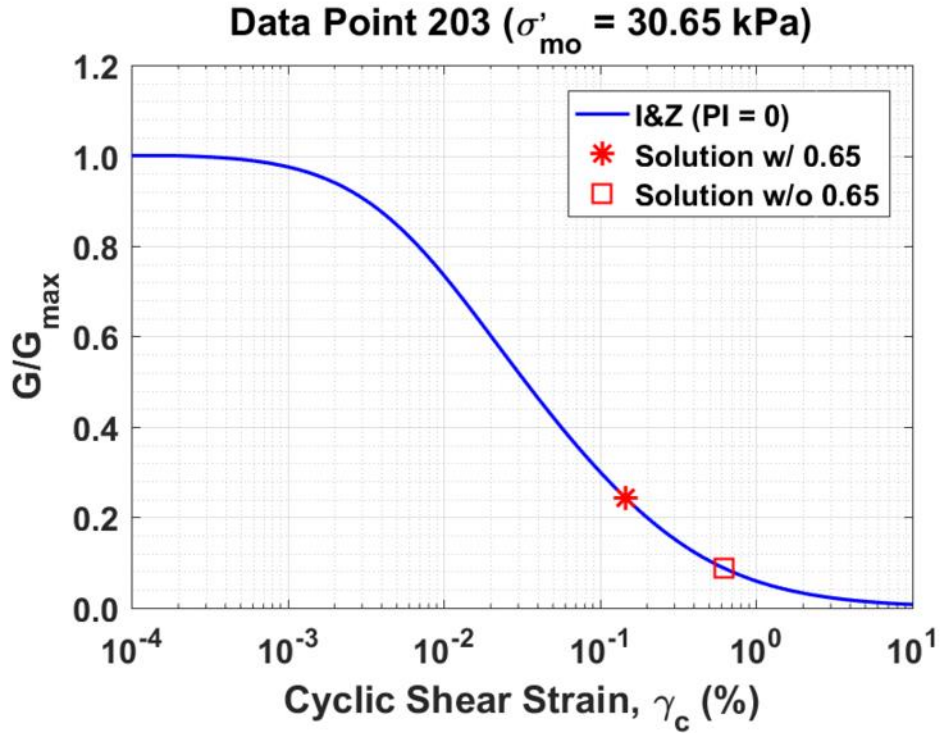


Figure B161. Normalized shear modulus reduction curves for Data Point 203 of the Kayen et al. database showing the solutions w/ and w/o the 0.65 factor

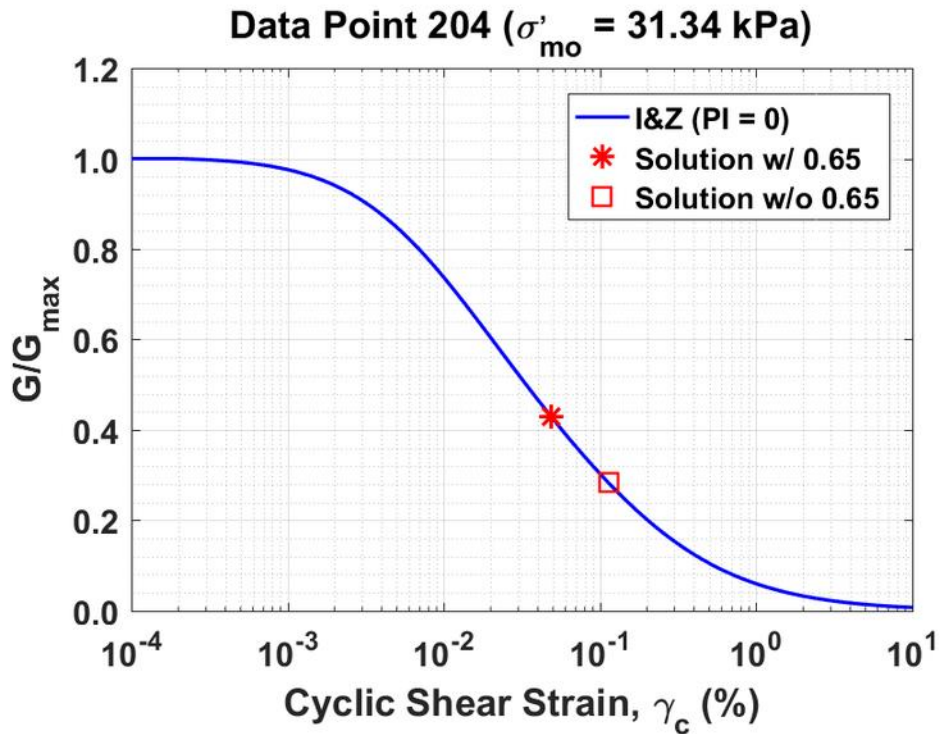


Figure B162. Normalized shear modulus reduction curves for Data Point 204 of the Kayen et al. database showing the solutions w/ and w/o the 0.65 factor

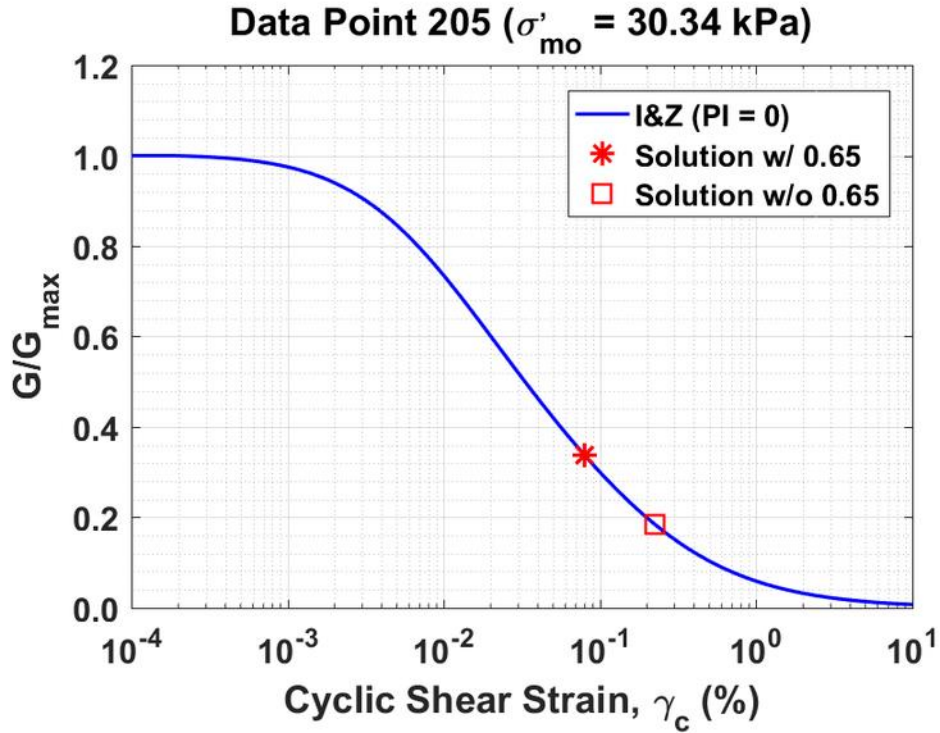


Figure B163. Normalized shear modulus reduction curves for Data Point 205 of the Kayen et al. database showing the solutions w/ and w/o the 0.65 factor

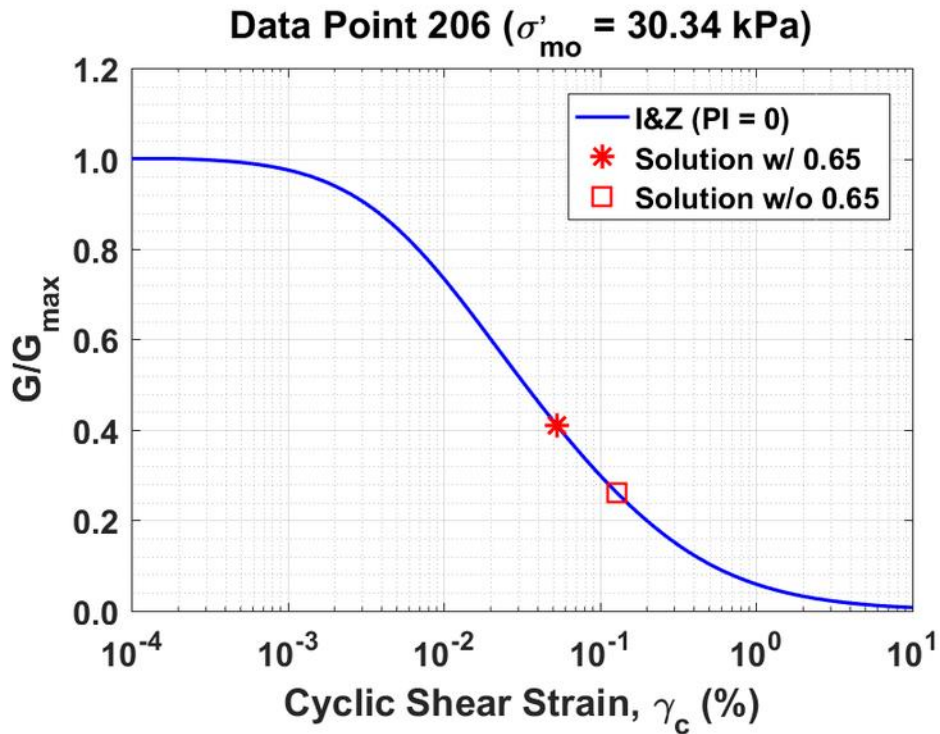


Figure B164. Normalized shear modulus reduction curves for Data Point 206 of the Kayen et al. database showing the solutions w/ and w/o the 0.65 factor

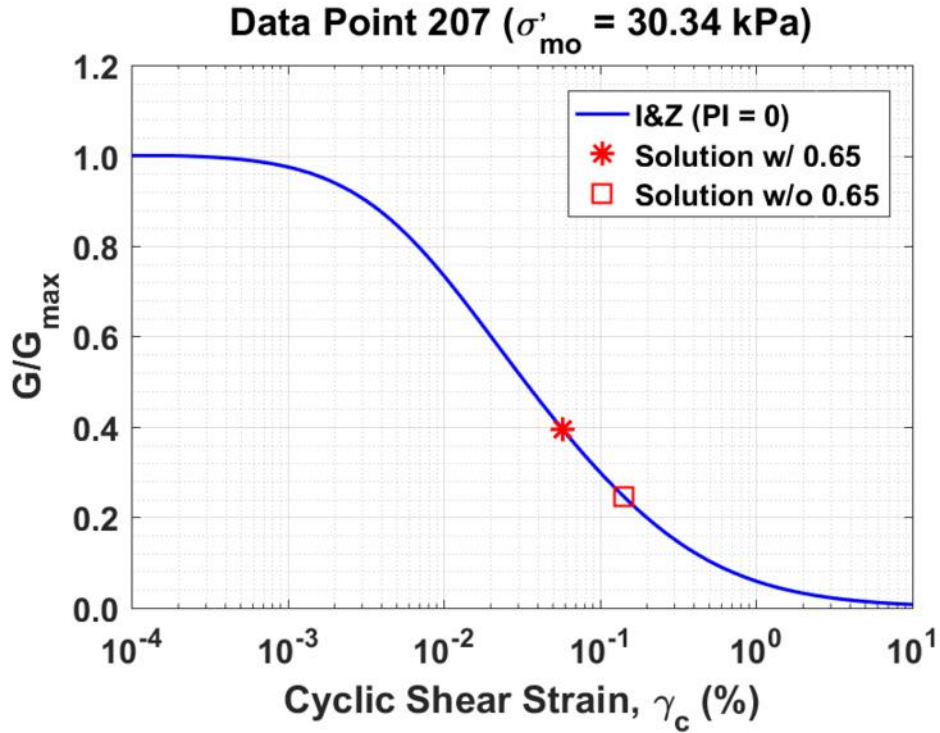


Figure B165. Normalized shear modulus reduction curves for Data Point 207 of the Kayen et al. database showing the solutions w/ and w/o the 0.65 factor

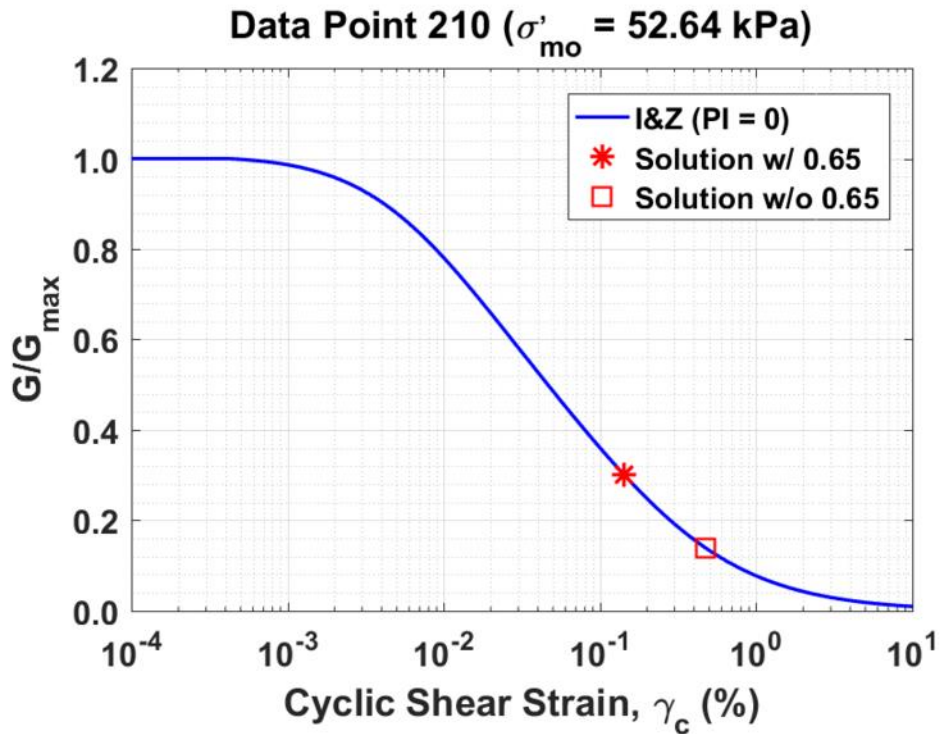


Figure B166. Normalized shear modulus reduction curves for Data Point 210 of the Kayen et al. database showing the solutions w/ and w/o the 0.65 factor

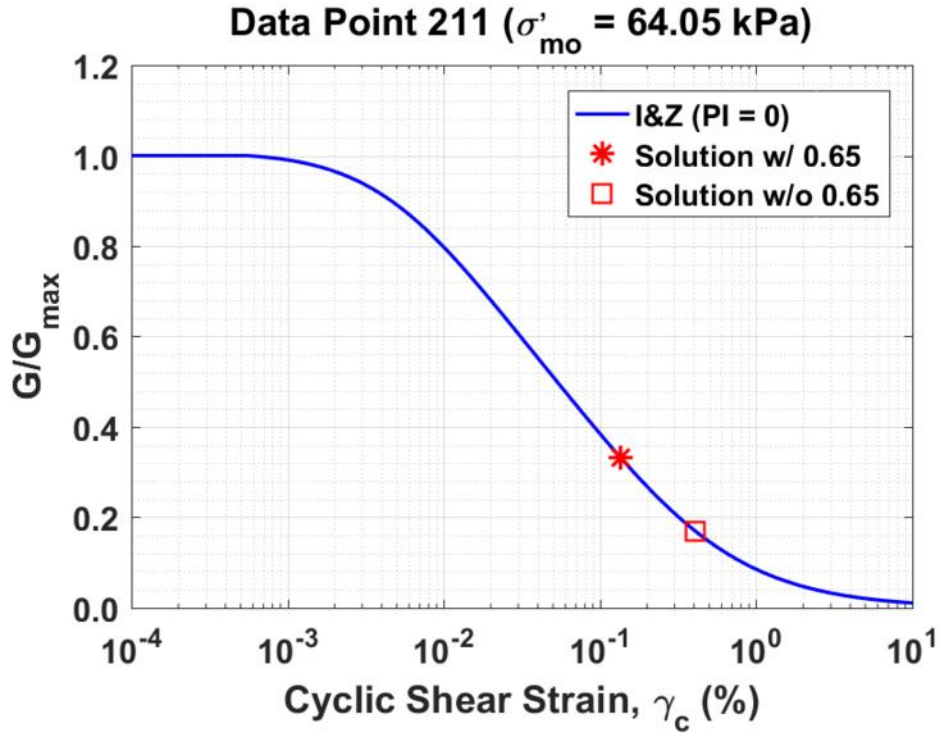


Figure B167. Normalized shear modulus reduction curves for Data Point 211 of the Kayen et al. database showing the solutions w/ and w/o the 0.65 factor

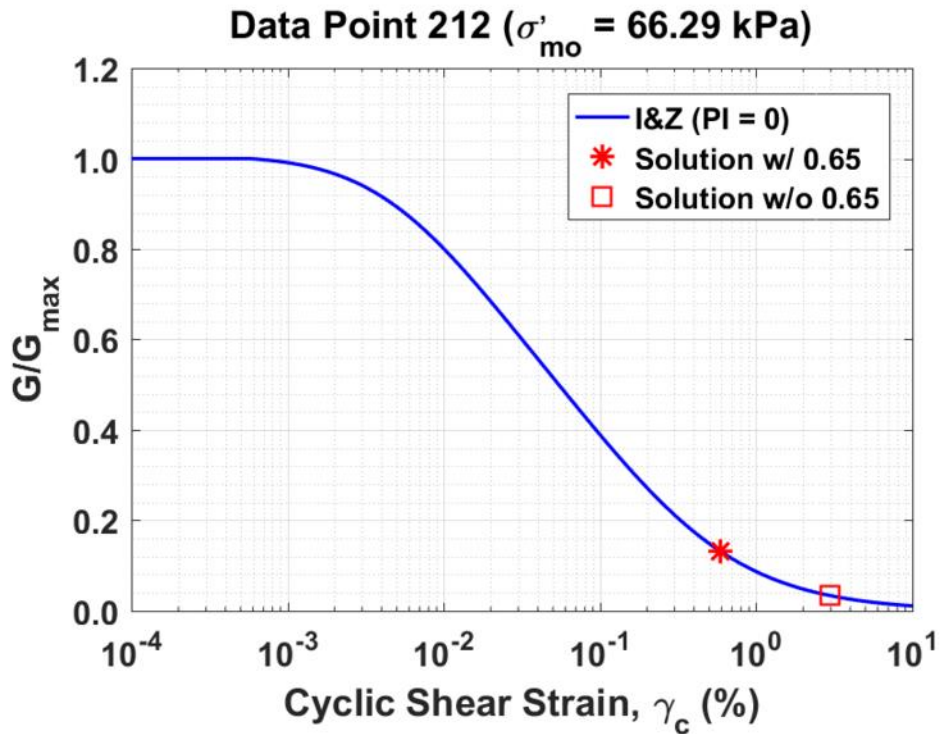


Figure B168. Normalized shear modulus reduction curves for Data Point 212 of the Kayen et al. database showing the solutions w/ and w/o the 0.65 factor

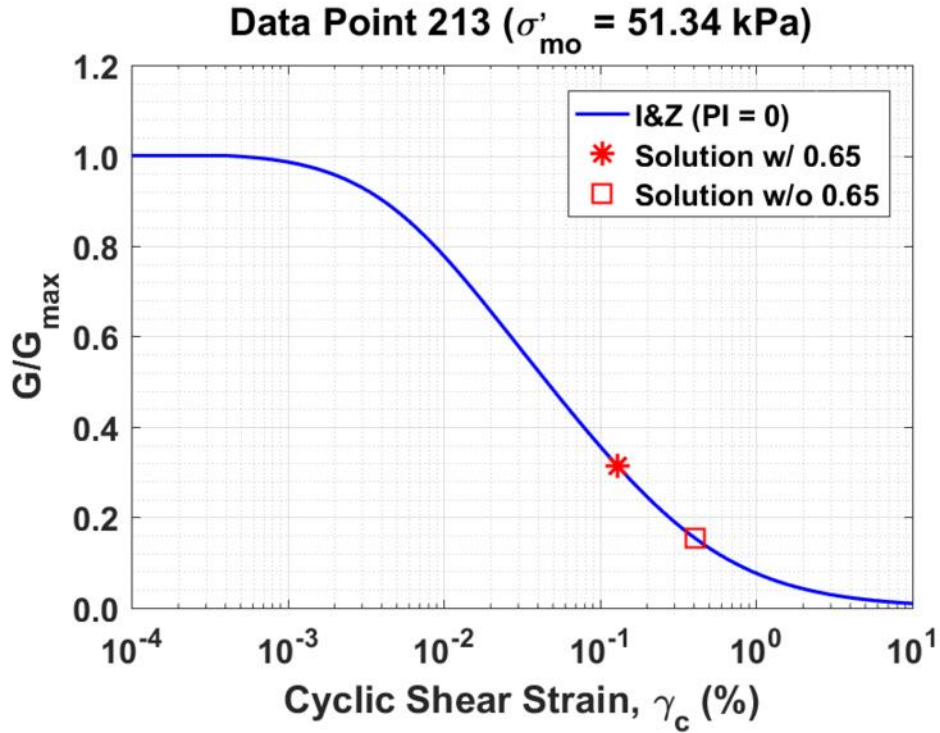


Figure B169. Normalized shear modulus reduction curves for Data Point 213 of the Kayen et al. database showing the solutions w/ and w/o the 0.65 factor

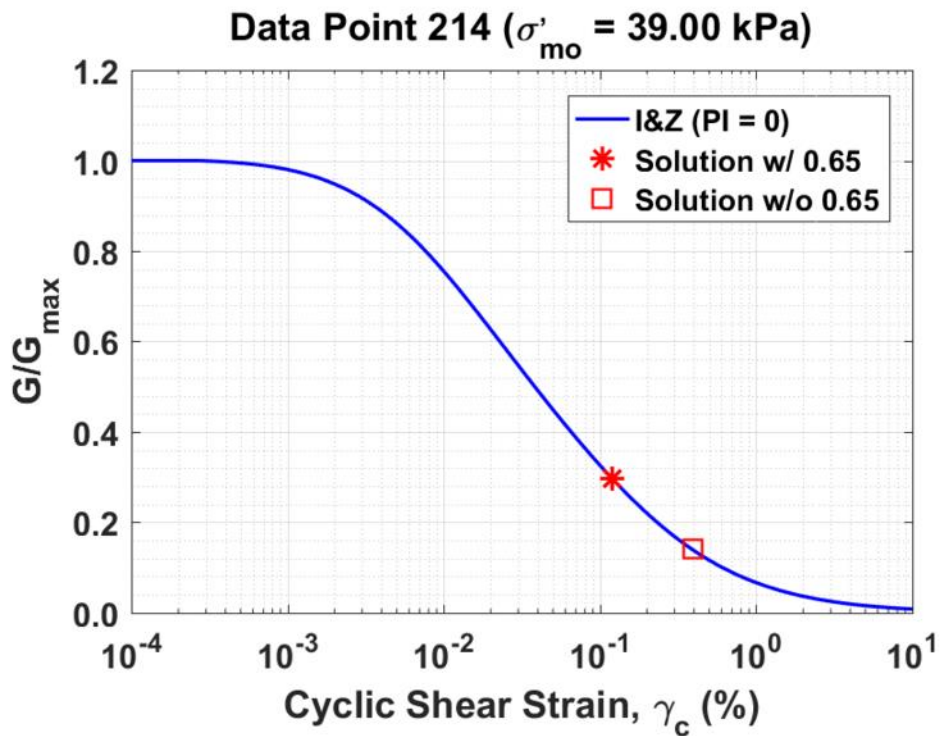


Figure B170. Normalized shear modulus reduction curves for Data Point 214 of the Kayen et al. database showing the solutions w/ and w/o the 0.65 factor

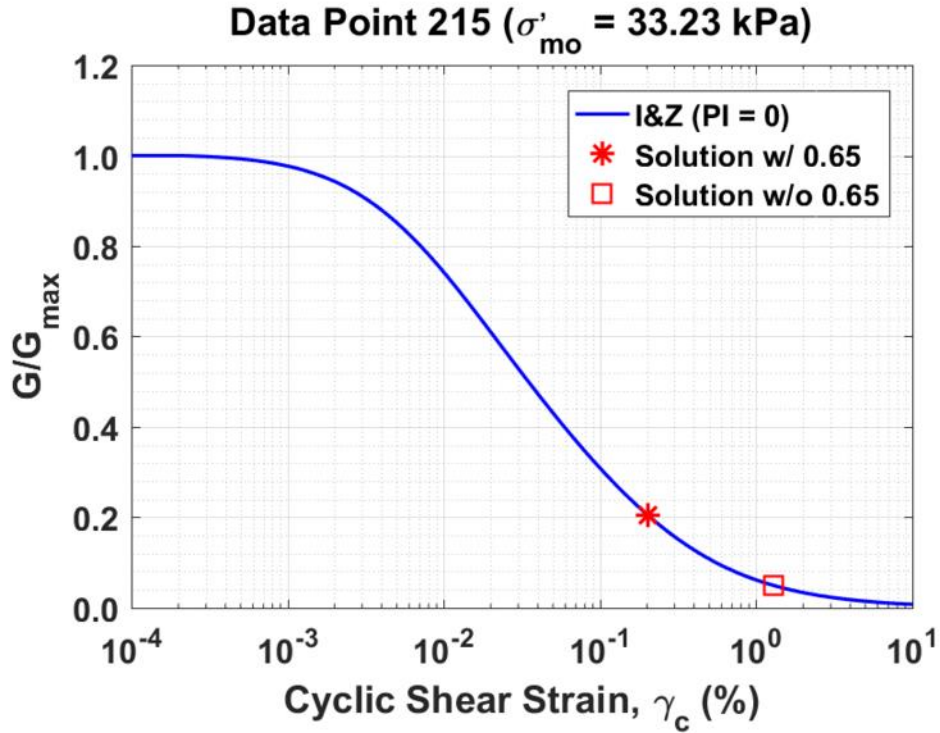


Figure B171. Normalized shear modulus reduction curves for Data Point 215 of the Kayen et al. database showing the solutions w/ and w/o the 0.65 factor

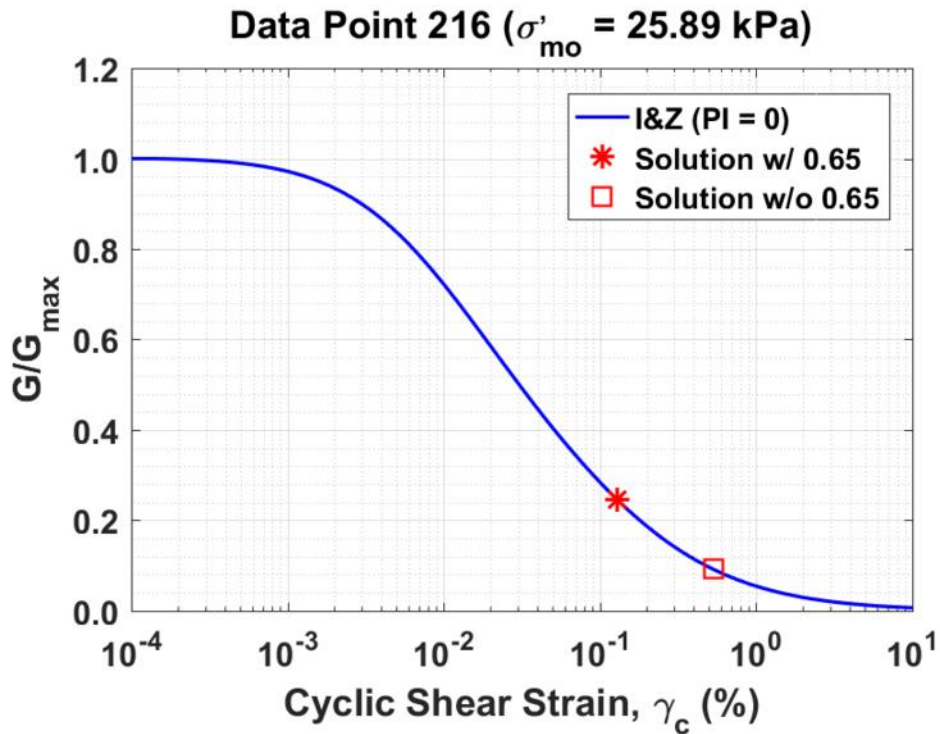


Figure B172. Normalized shear modulus reduction curves for Data Point 216 of the Kayen et al. database showing the solutions w/ and w/o the 0.65 factor

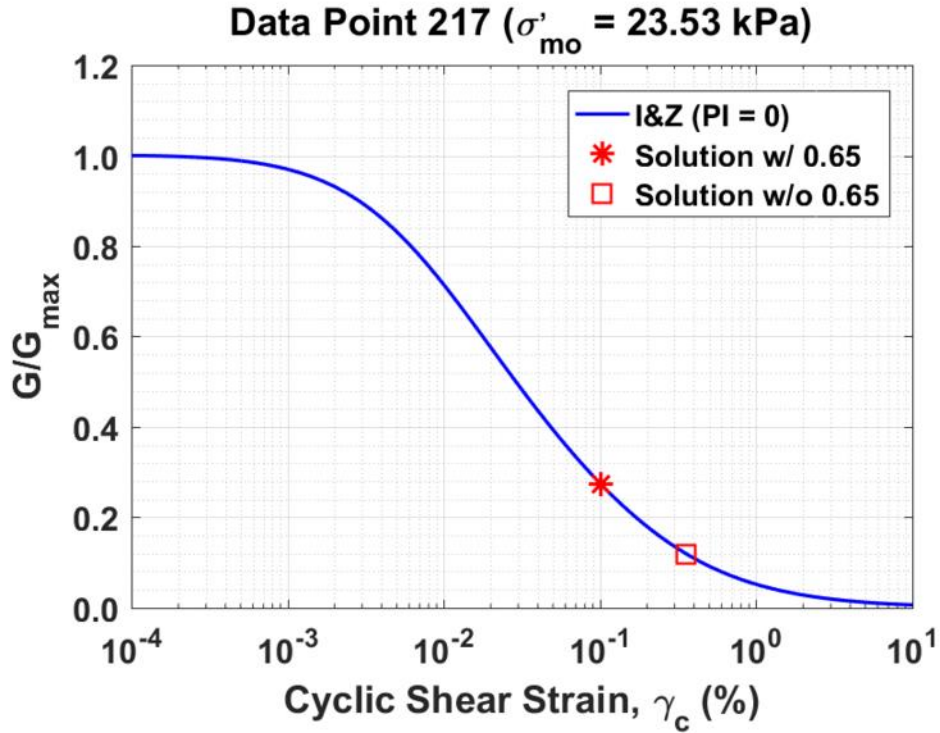


Figure B173. Normalized shear modulus reduction curves for Data Point 217 of the Kayen et al. database showing the solutions w/ and w/o the 0.65 factor

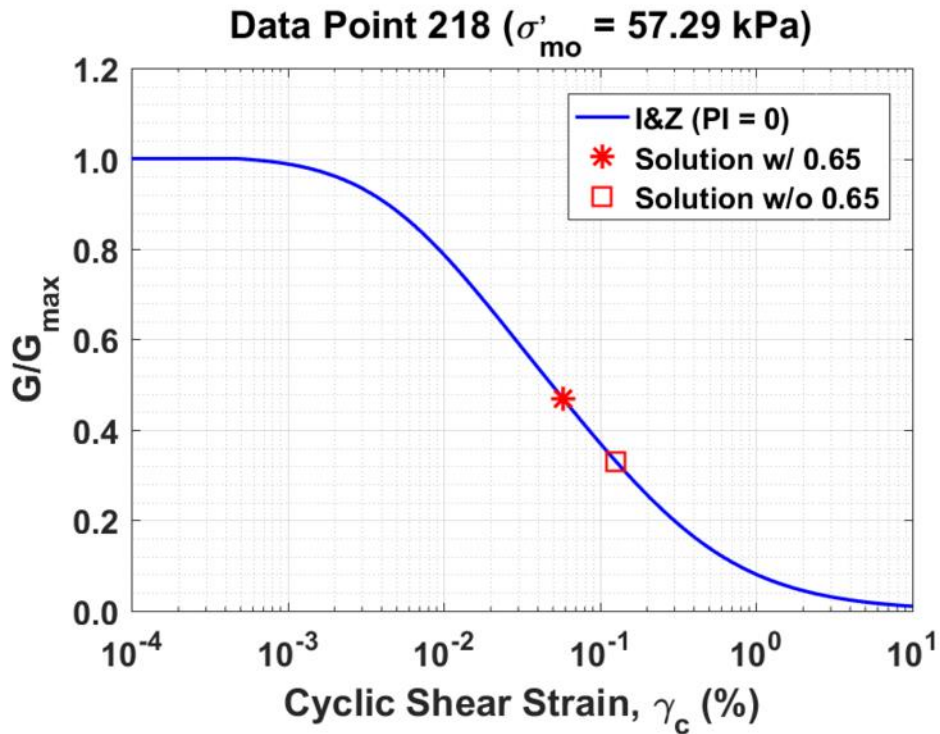


Figure B174. Normalized shear modulus reduction curves for Data Point 218 of the Kayen et al. database showing the solutions w/ and w/o the 0.65 factor

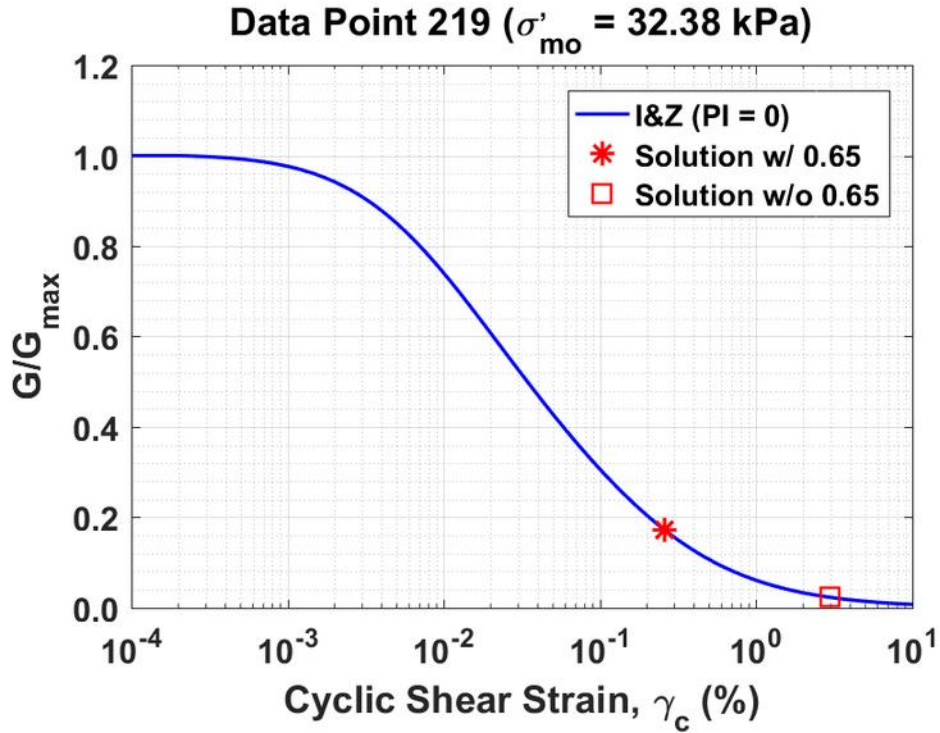


Figure B175. Normalized shear modulus reduction curves for Data Point 219 of the Kayen et al. database showing the solutions w/ and w/o the 0.65 factor

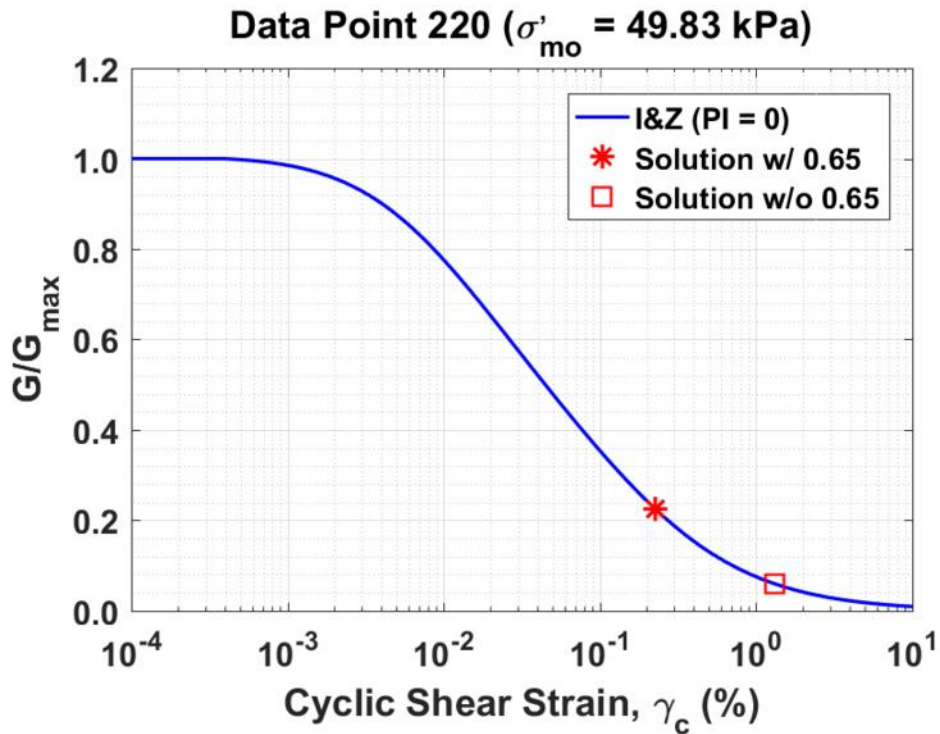


Figure B176. Normalized shear modulus reduction curves for Data Point 220 of the Kayen et al. database showing the solutions w/ and w/o the 0.65 factor

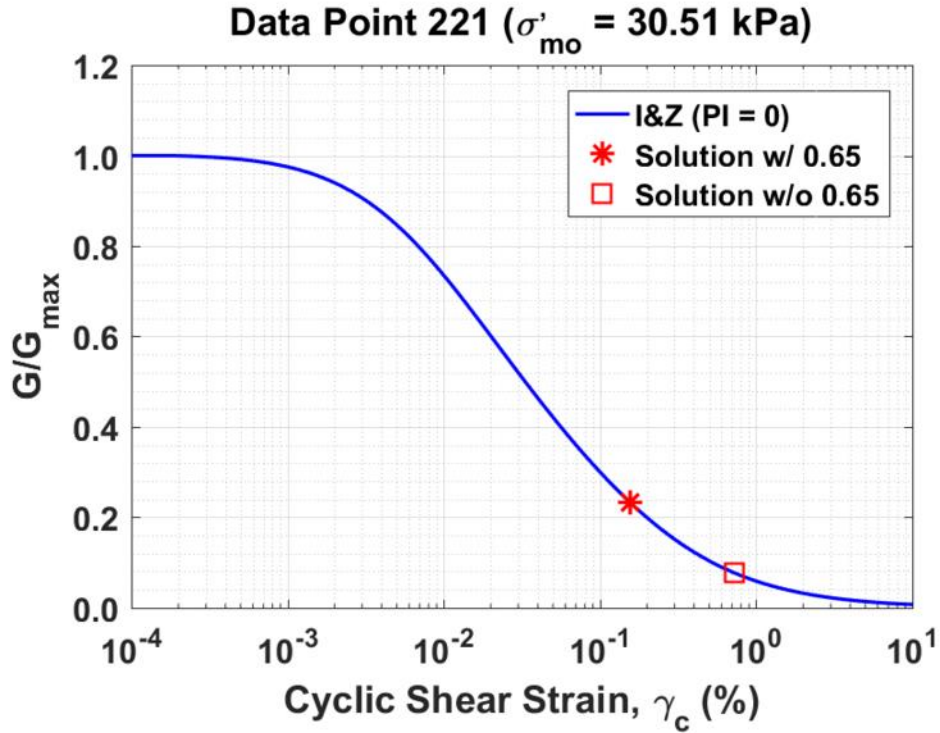


Figure B177. Normalized shear modulus reduction curves for Data Point 221 of the Kayen et al. database showing the solutions w/ and w/o the 0.65 factor

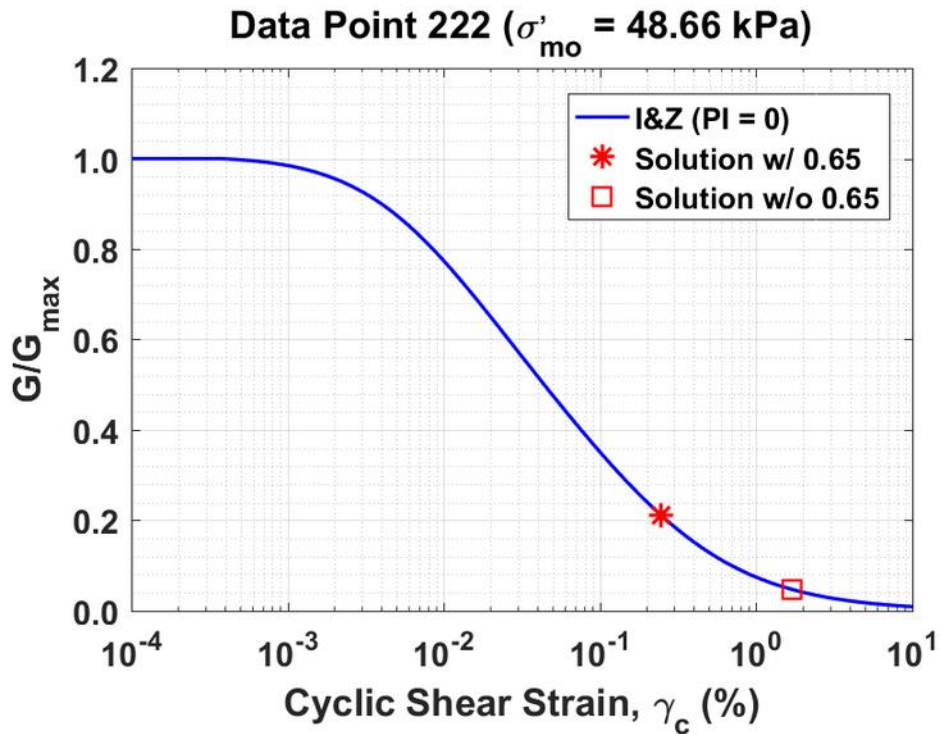


Figure B178. Normalized shear modulus reduction curves for Data Point 222 of the Kayen et al. database showing the solutions w/ and w/o the 0.65 factor

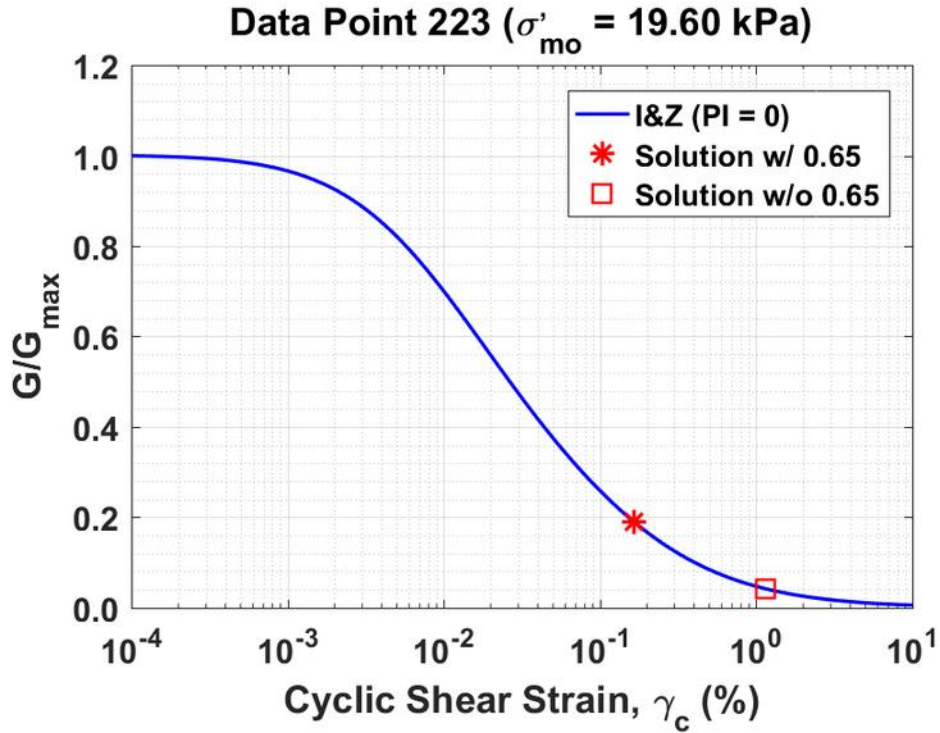


Figure B179. Normalized shear modulus reduction curves for Data Point 223 of the Kayen et al. database showing the solutions w/ and w/o the 0.65 factor

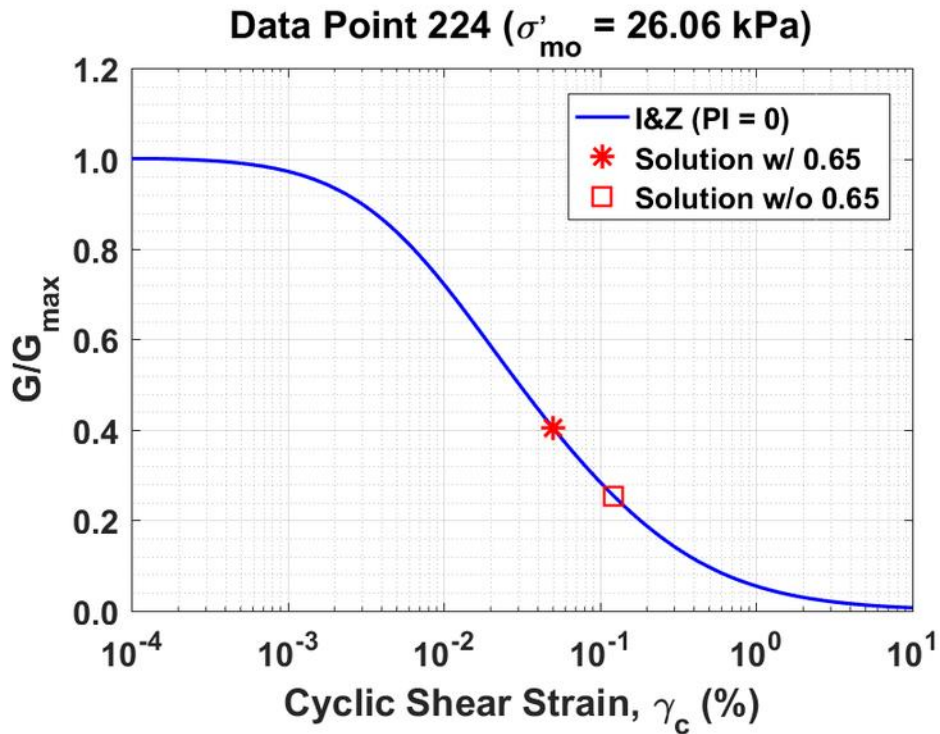


Figure B180. Normalized shear modulus reduction curves for Data Point 224 of the Kayen et al. database showing the solutions w/ and w/o the 0.65 factor

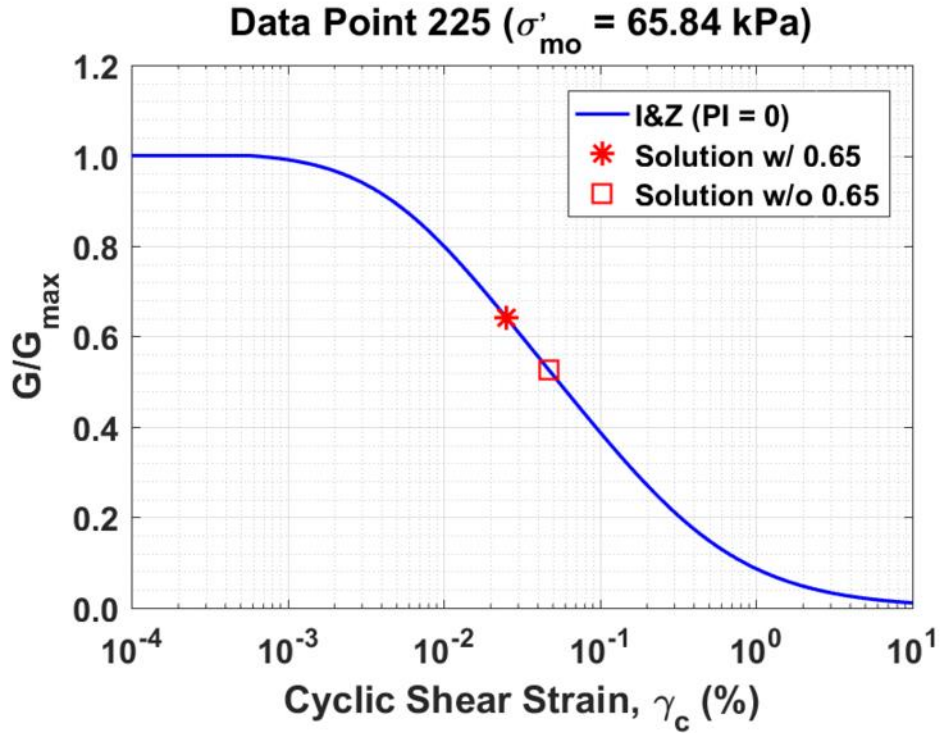


Figure B181. Normalized shear modulus reduction curves for Data Point 225 of the Kayen et al. database showing the solutions w/ and w/o the 0.65 factor

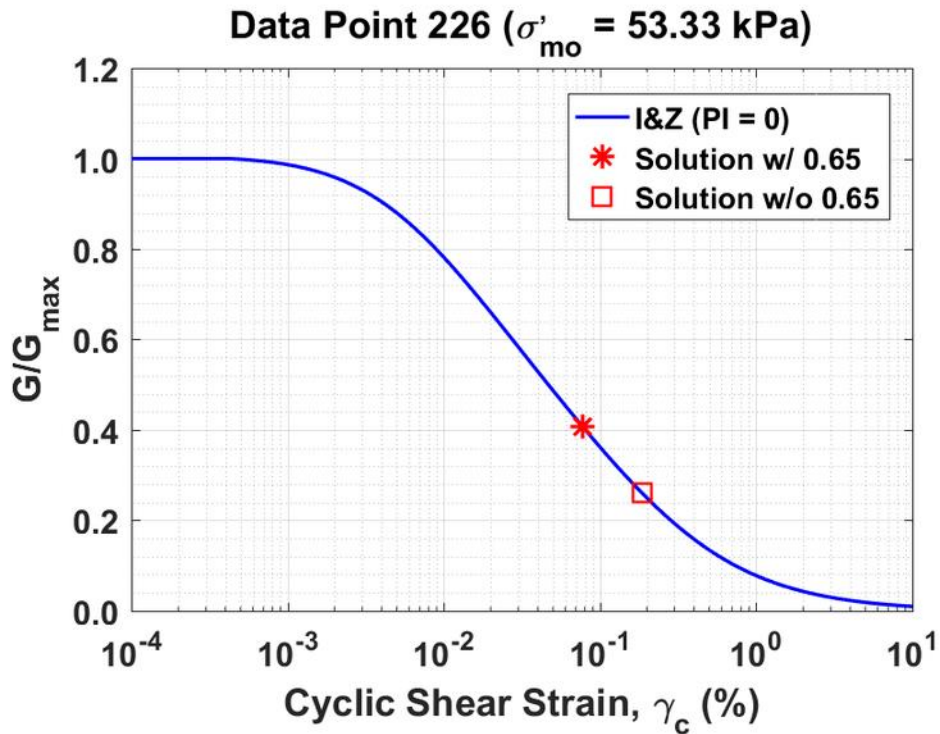


Figure B182. Normalized shear modulus reduction curves for Data Point 226 of the Kayen et al. database showing the solutions w/ and w/o the 0.65 factor

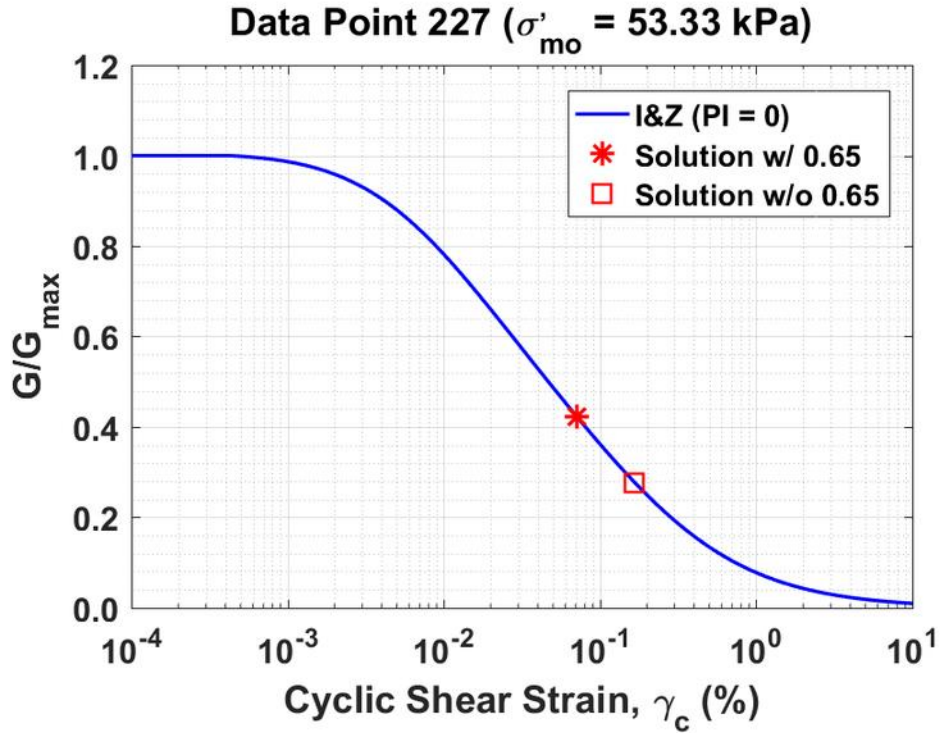


Figure B183. Normalized shear modulus reduction curves for Data Point 227 of the Kayen et al. database showing the solutions w/ and w/o the 0.65 factor

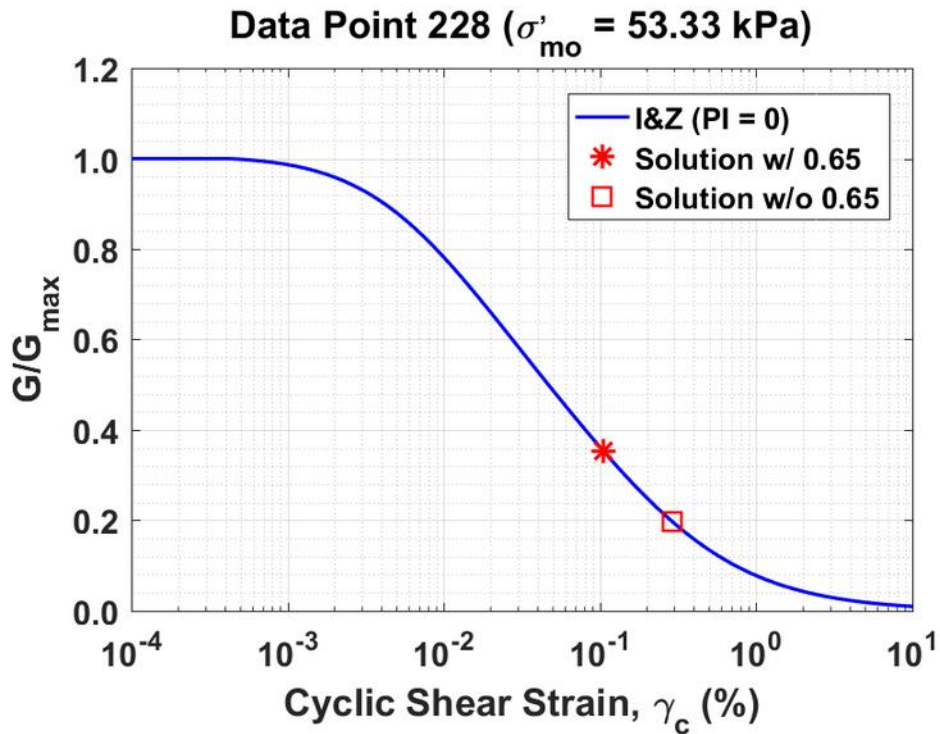


Figure B184. Normalized shear modulus reduction curves for Data Point 228 of the Kayen et al. database showing the solutions w/ and w/o the 0.65 factor

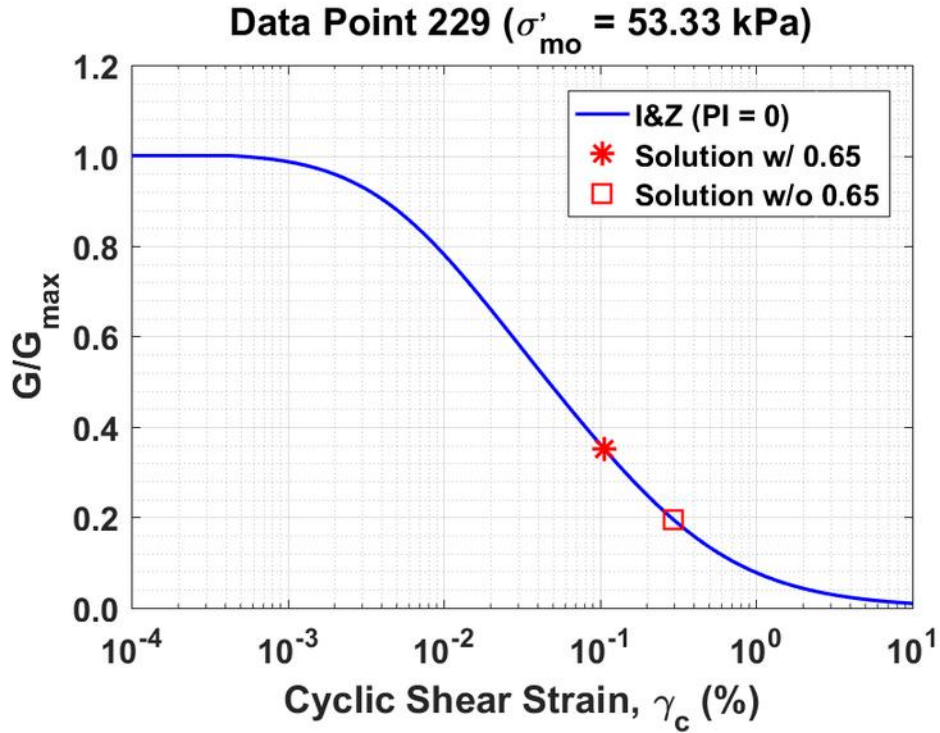


Figure B185. Normalized shear modulus reduction curves for Data Point 229 of the Kayen et al. database showing the solutions w/ and w/o the 0.65 factor

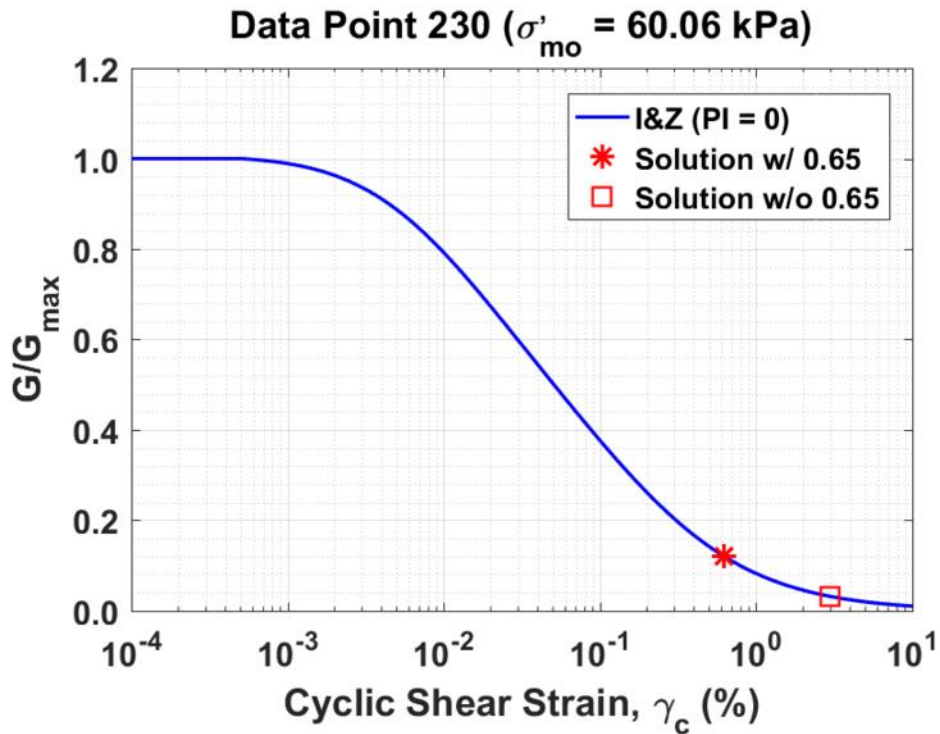


Figure B186. Normalized shear modulus reduction curves for Data Point 230 of the Kayen et al. database showing the solutions w/ and w/o the 0.65 factor

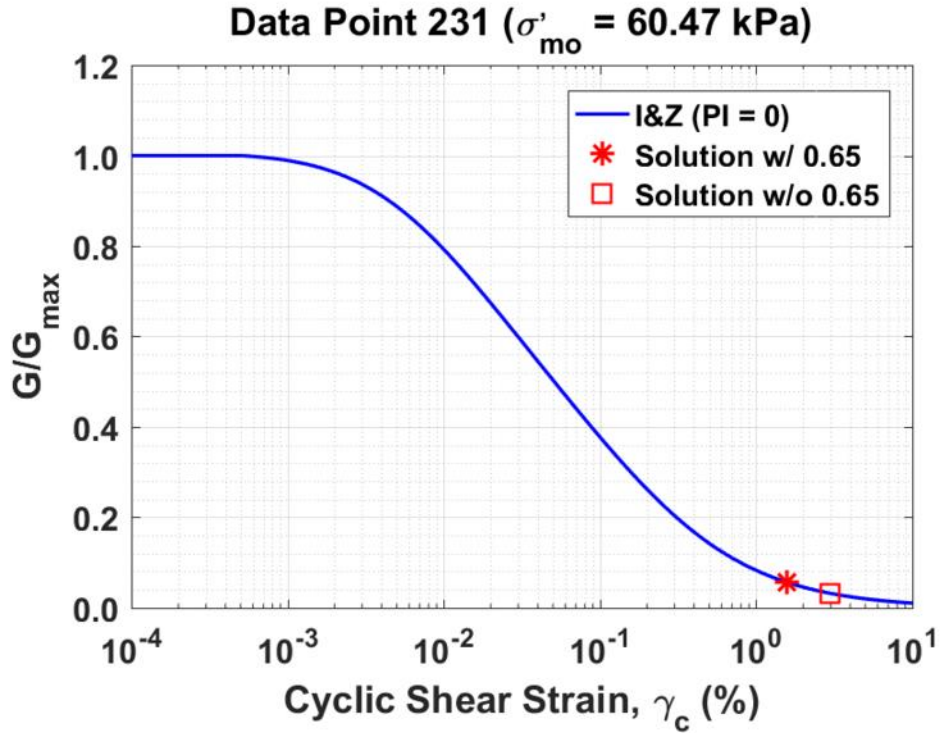


Figure B187. Normalized shear modulus reduction curves for Data Point 231 of the Kayen et al. database showing the solutions w/ and w/o the 0.65 factor

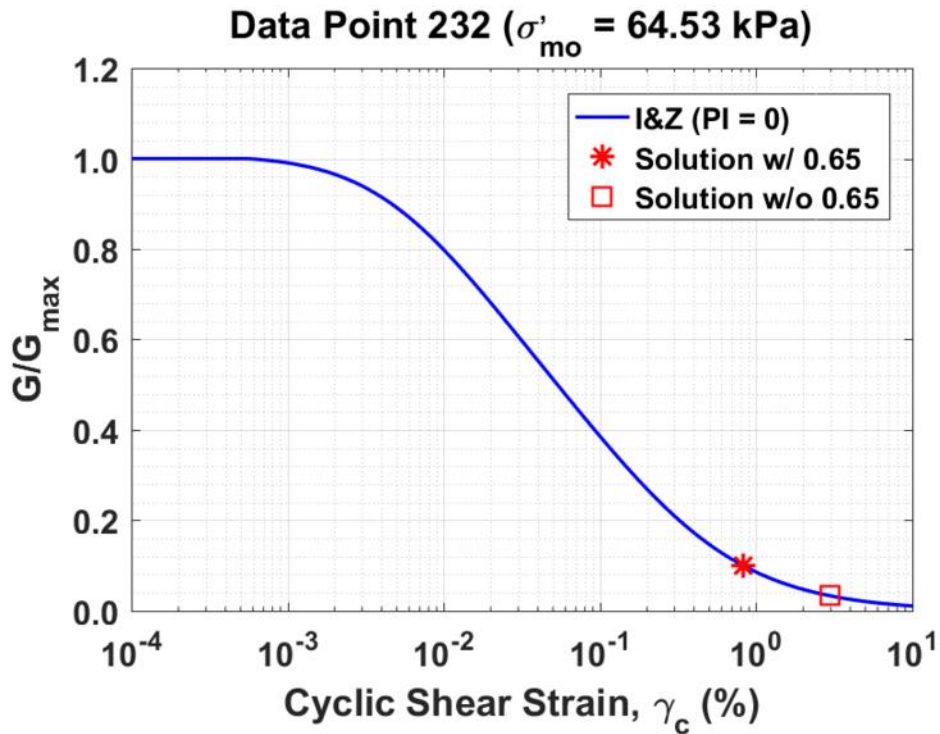


Figure B188. Normalized shear modulus reduction curves for Data Point 232 of the Kayen et al. database showing the solutions w/ and w/o the 0.65 factor

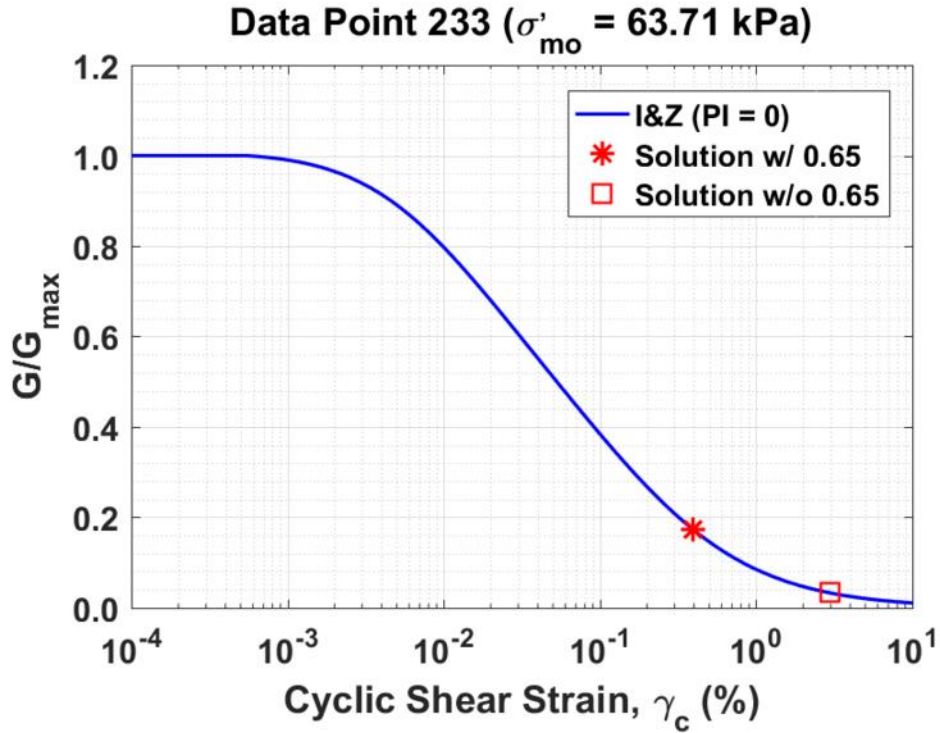


Figure B189. Normalized shear modulus reduction curves for Data Point 233 of the Kayen et al. database showing the solutions w/ and w/o the 0.65 factor

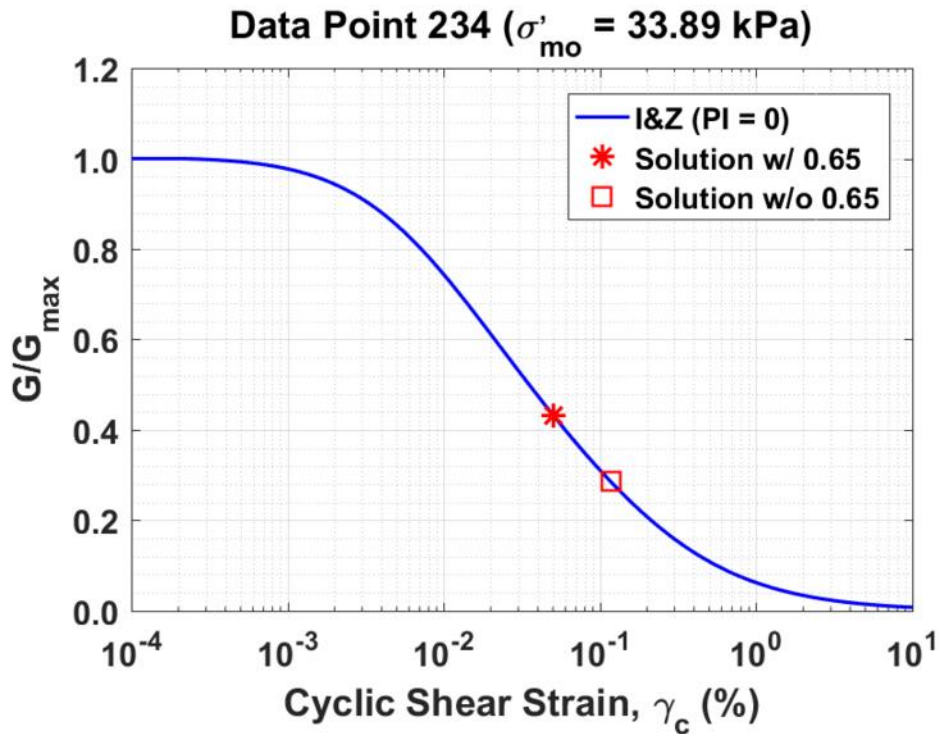


Figure B190. Normalized shear modulus reduction curves for Data Point 234 of the Kayen et al. database showing the solutions w/ and w/o the 0.65 factor

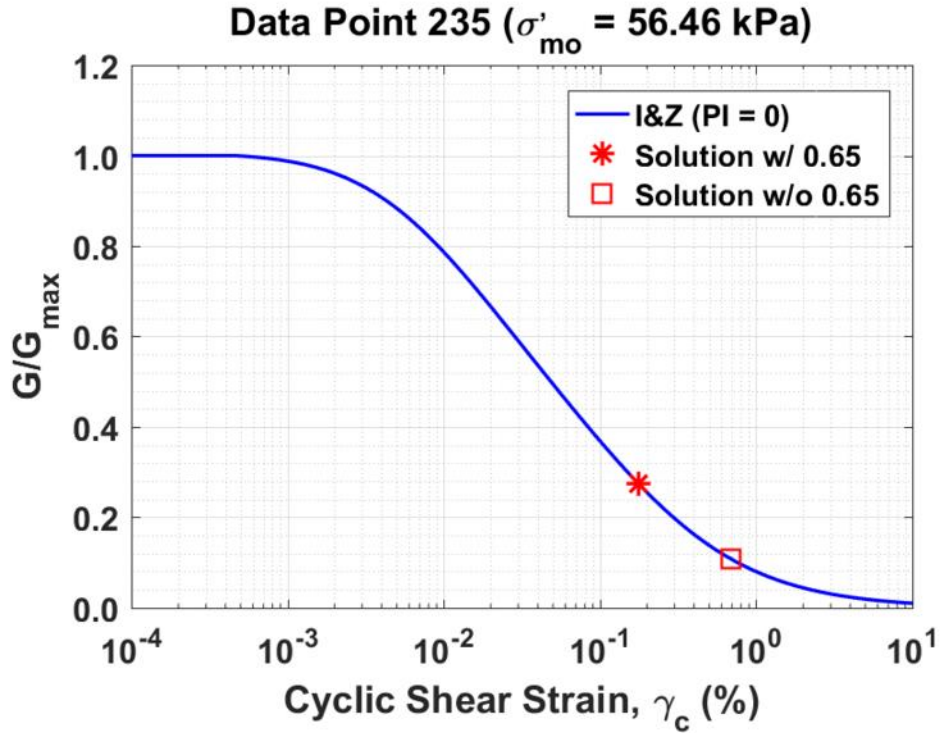


Figure B191. Normalized shear modulus reduction curves for Data Point 235 of the Kayen et al. database showing the solutions w/ and w/o the 0.65 factor

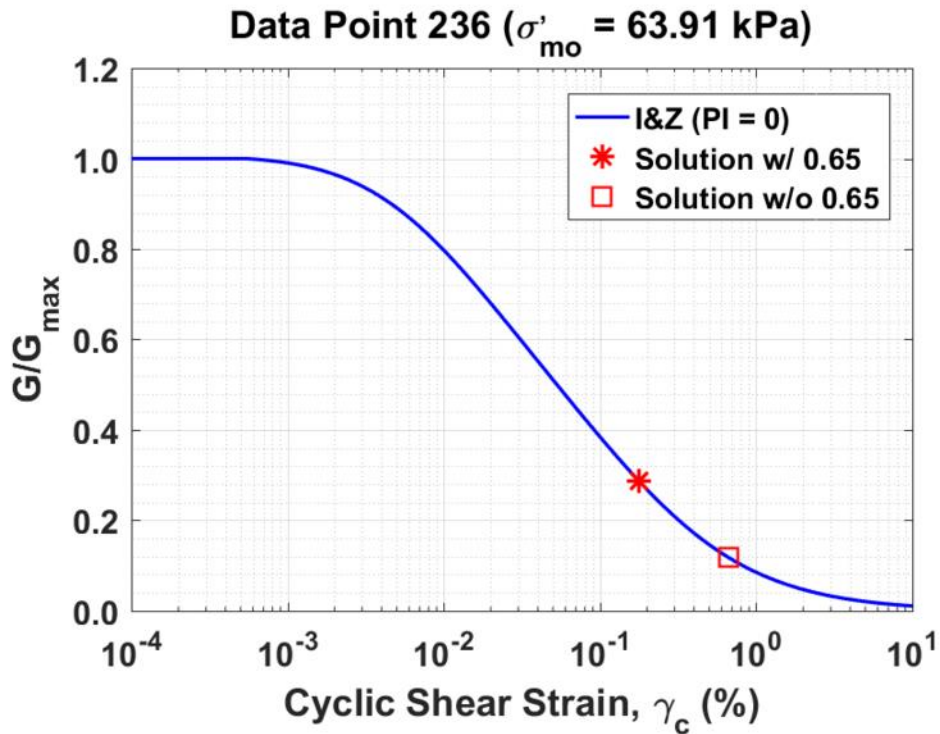


Figure B192. Normalized shear modulus reduction curves for Data Point 236 of the Kayen et al. database showing the solutions w/ and w/o the 0.65 factor

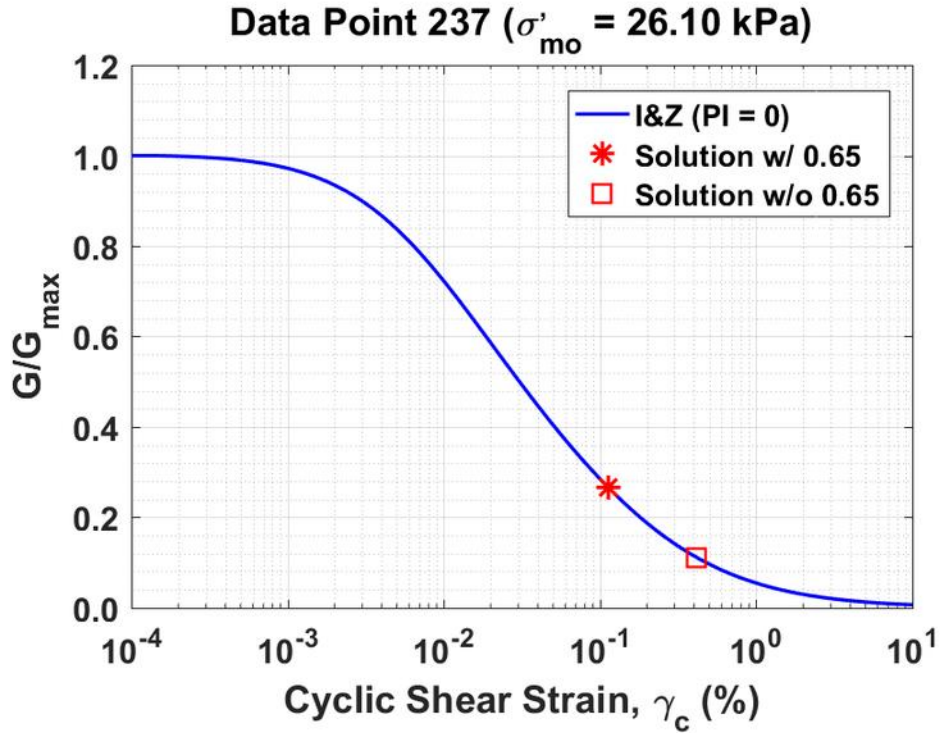


Figure B193. Normalized shear modulus reduction curves for Data Point 237 of the Kayen et al. database showing the solutions w/ and w/o the 0.65 factor

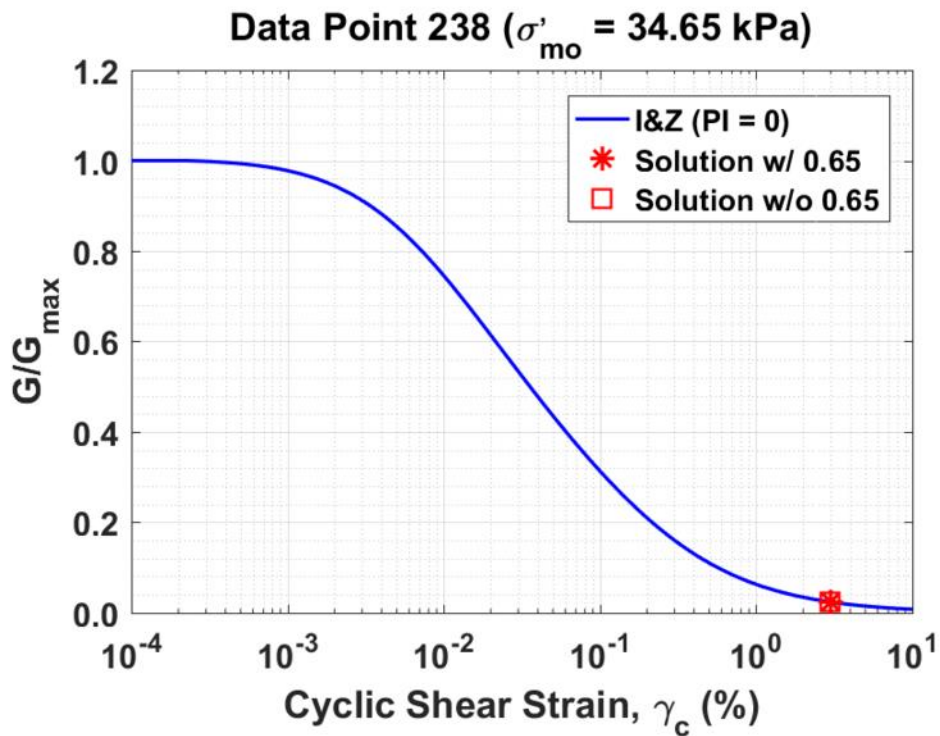


Figure B194. Normalized shear modulus reduction curves for Data Point 238 of the Kayen et al. database showing the solutions w/ and w/o the 0.65 factor

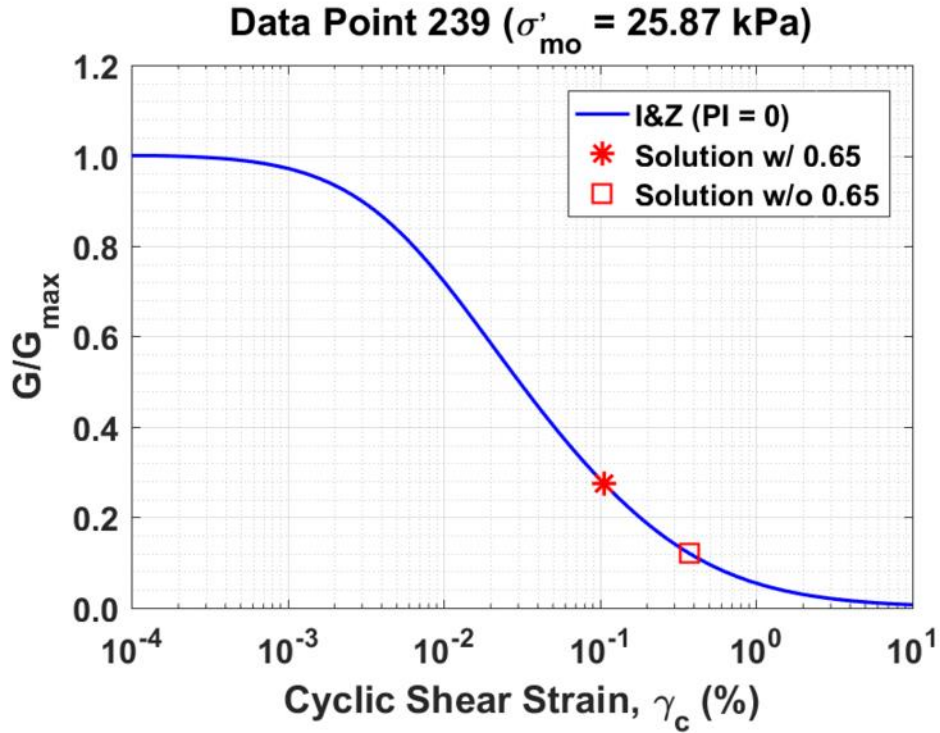


Figure B195. Normalized shear modulus reduction curves for Data Point 239 of the Kayen et al. database showing the solutions w/ and w/o the 0.65 factor

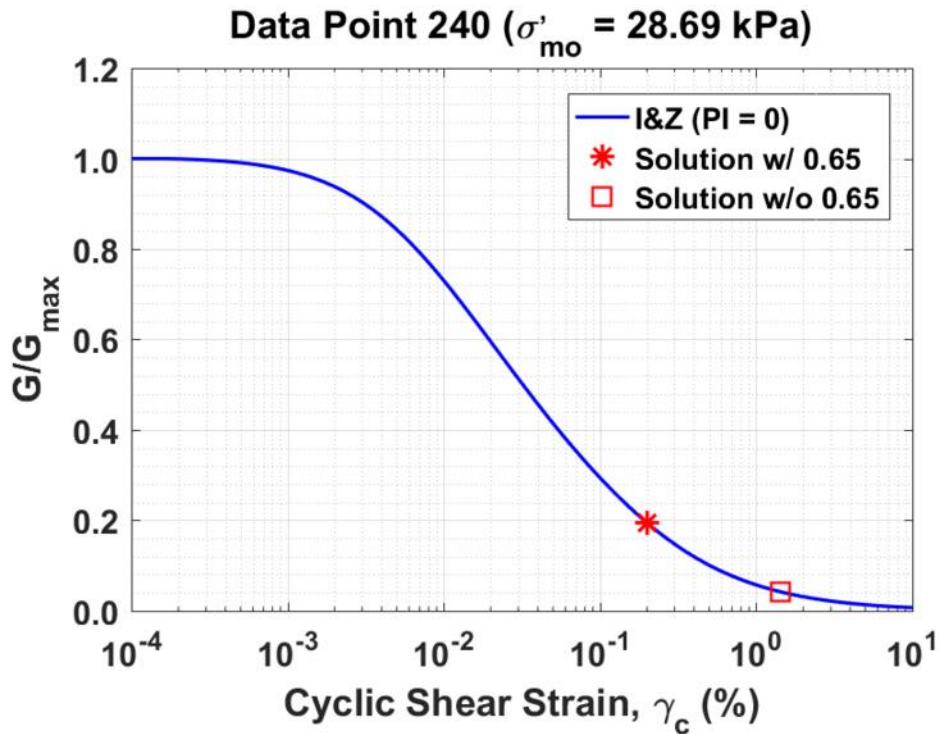


Figure B196. Normalized shear modulus reduction curves for Data Point 240 of the Kayen et al. database showing the solutions w/ and w/o the 0.65 factor

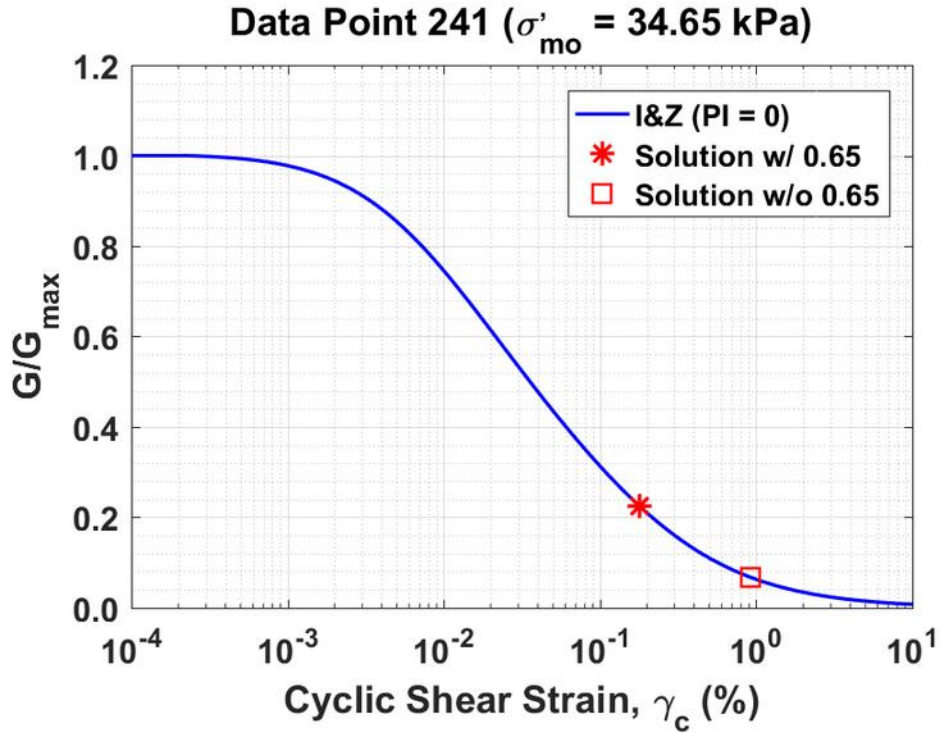


Figure B197. Normalized shear modulus reduction curves for Data Point 241 of the Kayen et al. database showing the solutions w/ and w/o the 0.65 factor

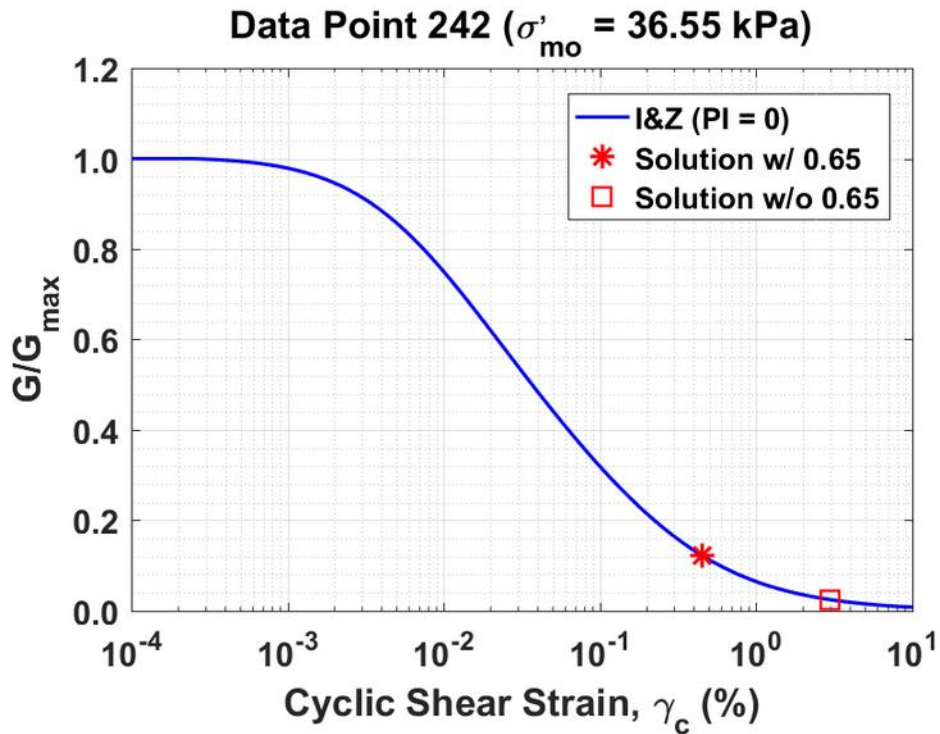


Figure B198. Normalized shear modulus reduction curves for Data Point 242 of the Kayen et al. database showing the solutions w/ and w/o the 0.65 factor

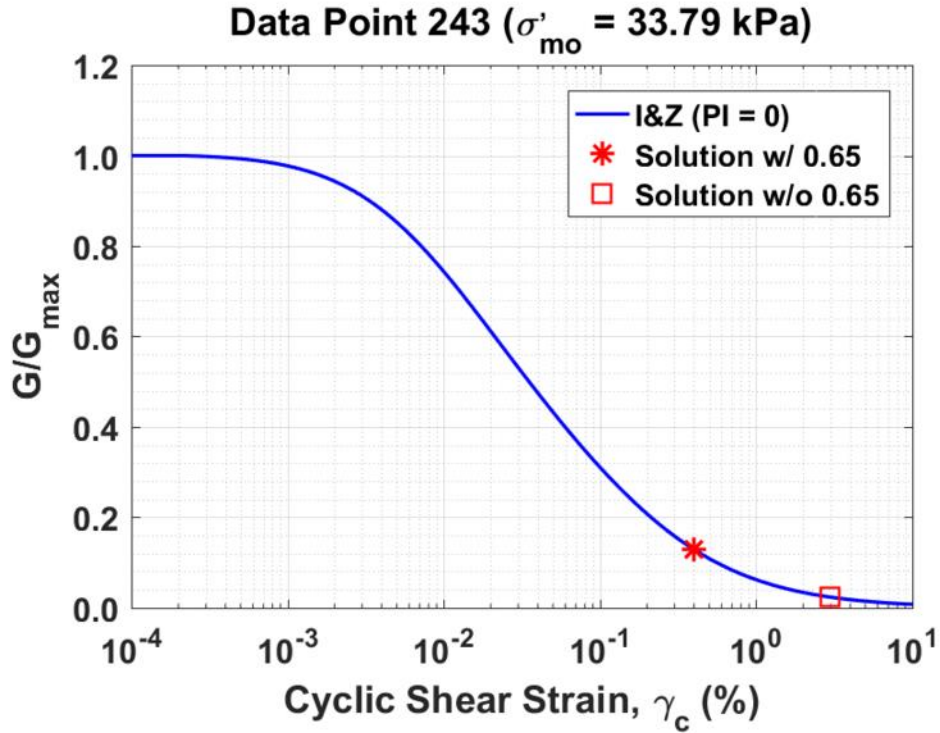


Figure B199. Normalized shear modulus reduction curves for Data Point 243 of the Kayen et al. database showing the solutions w/ and w/o the 0.65 factor

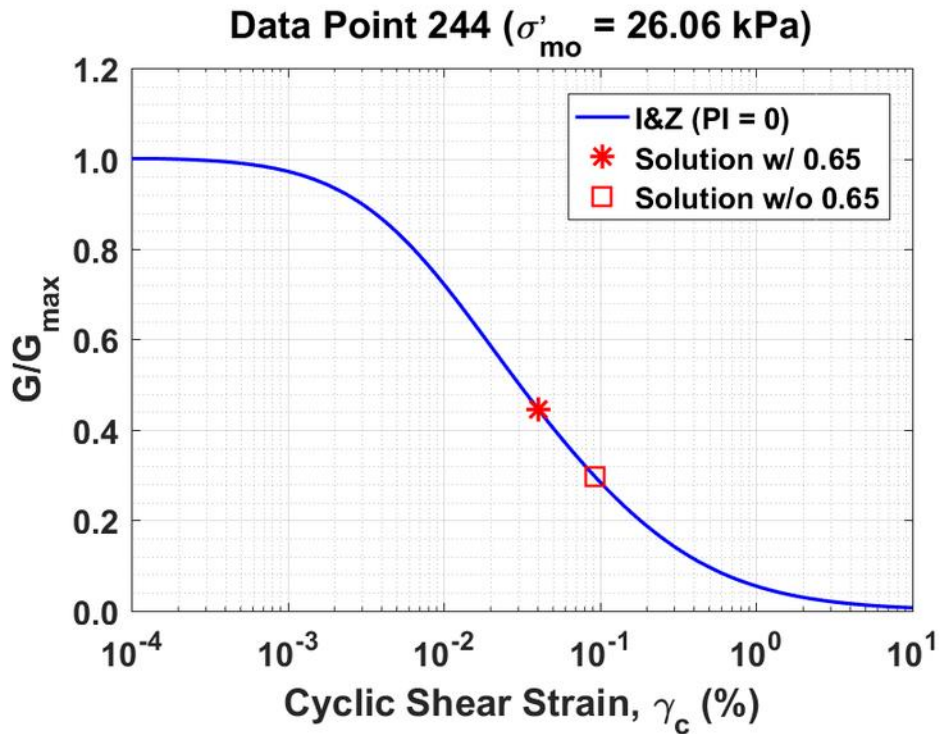


Figure B200. Normalized shear modulus reduction curves for Data Point 244 of the Kayen et al. database showing the solutions w/ and w/o the 0.65 factor

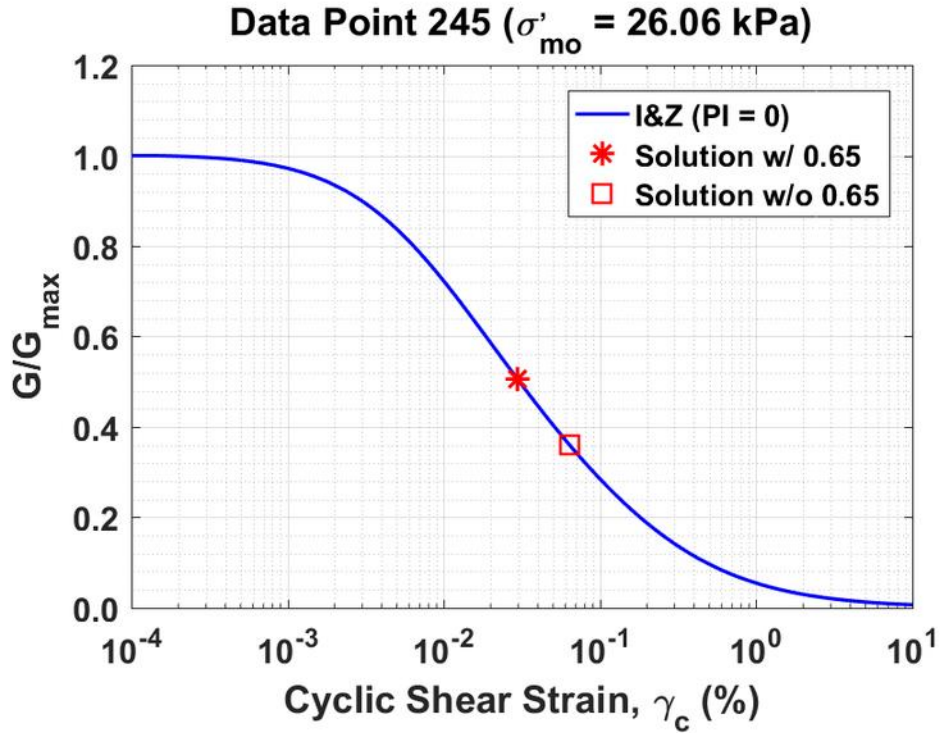


Figure B201. Normalized shear modulus reduction curves for Data Point 245 of the Kayen et al. database showing the solutions w/ and w/o the 0.65 factor

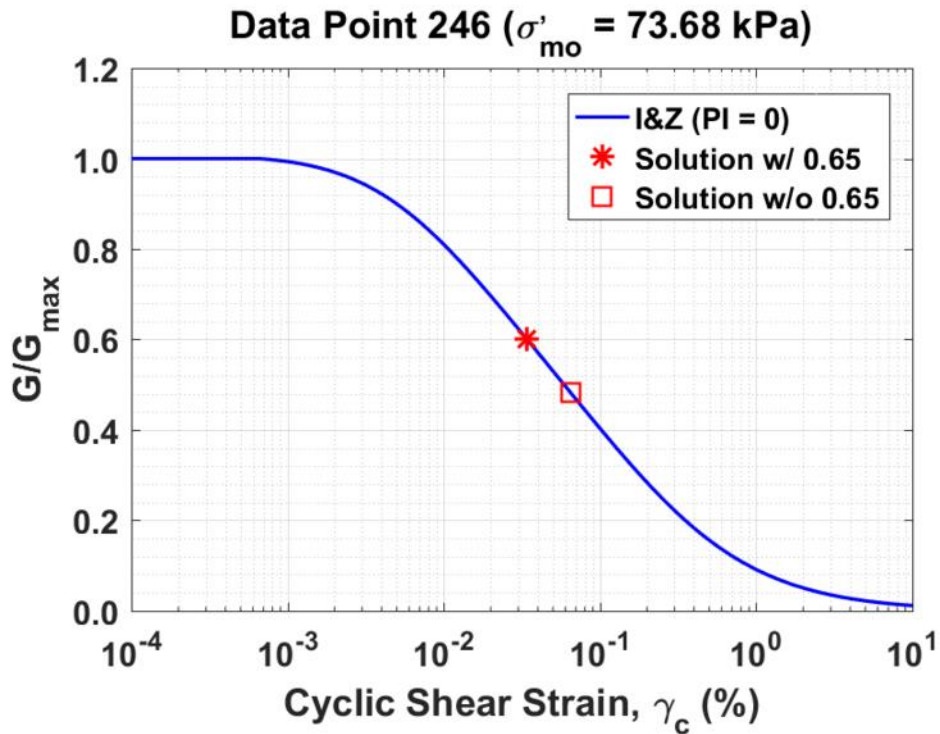


Figure B202. Normalized shear modulus reduction curves for Data Point 246 of the Kayen et al. database showing the solutions w/ and w/o the 0.65 factor

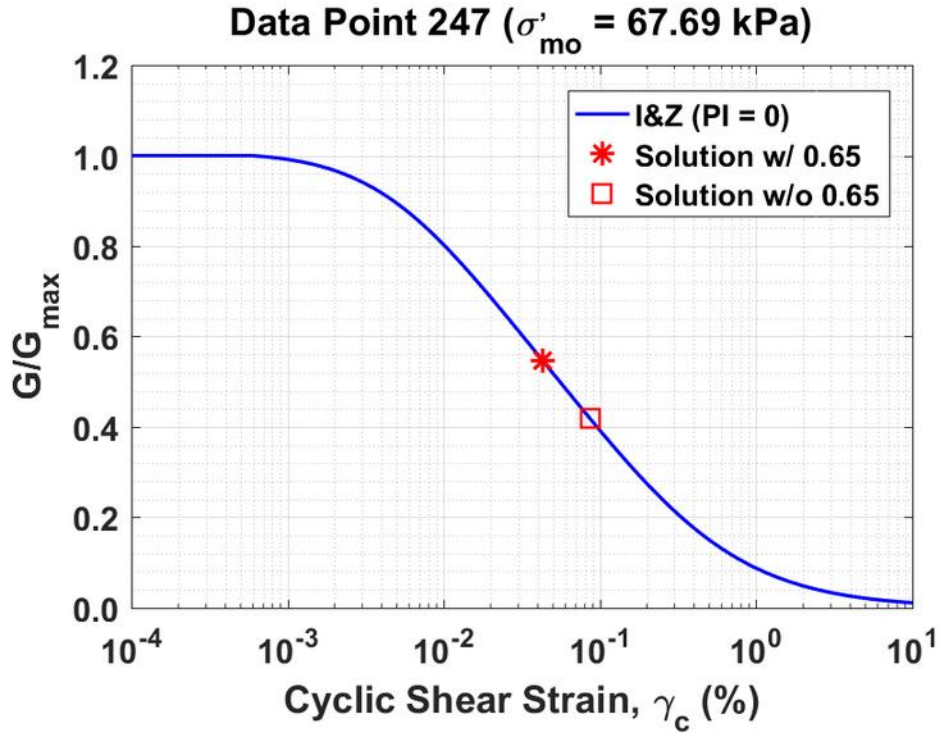


Figure B203. Normalized shear modulus reduction curves for Data Point 247 of the Kayen et al. database showing the solutions w/ and w/o the 0.65 factor

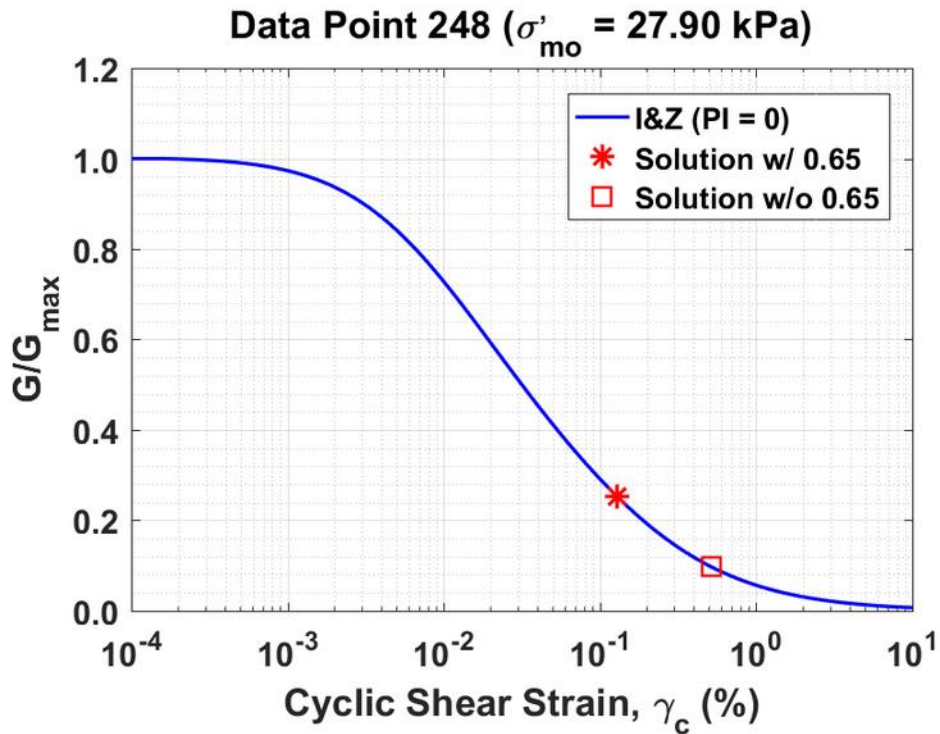


Figure B204. Normalized shear modulus reduction curves for Data Point 248 of the Kayen et al. database showing the solutions w/ and w/o the 0.65 factor

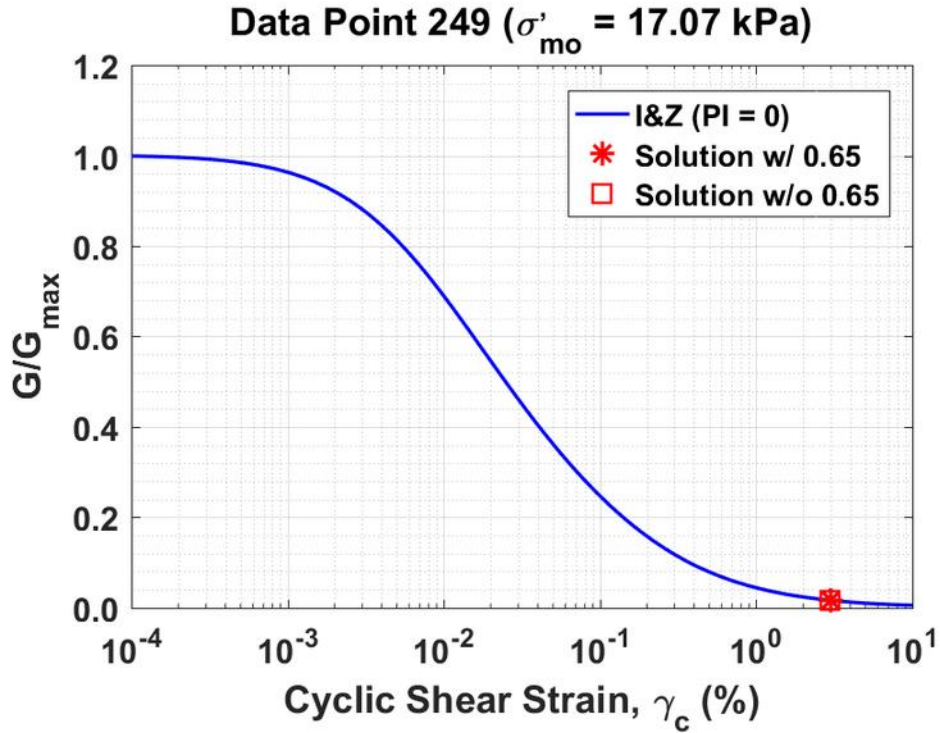


Figure B205. Normalized shear modulus reduction curves for Data Point 249 of the Kayen et al. database showing the solutions w/ and w/o the 0.65 factor

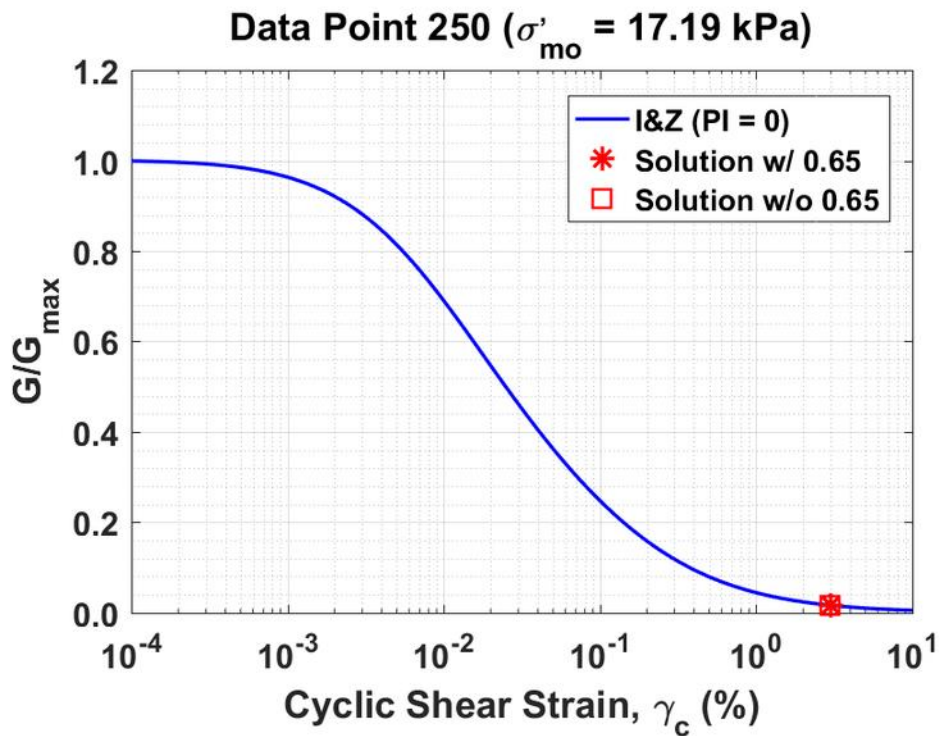


Figure B206. Normalized shear modulus reduction curves for Data Point 250 of the Kayen et al. database showing the solutions w/ and w/o the 0.65 factor

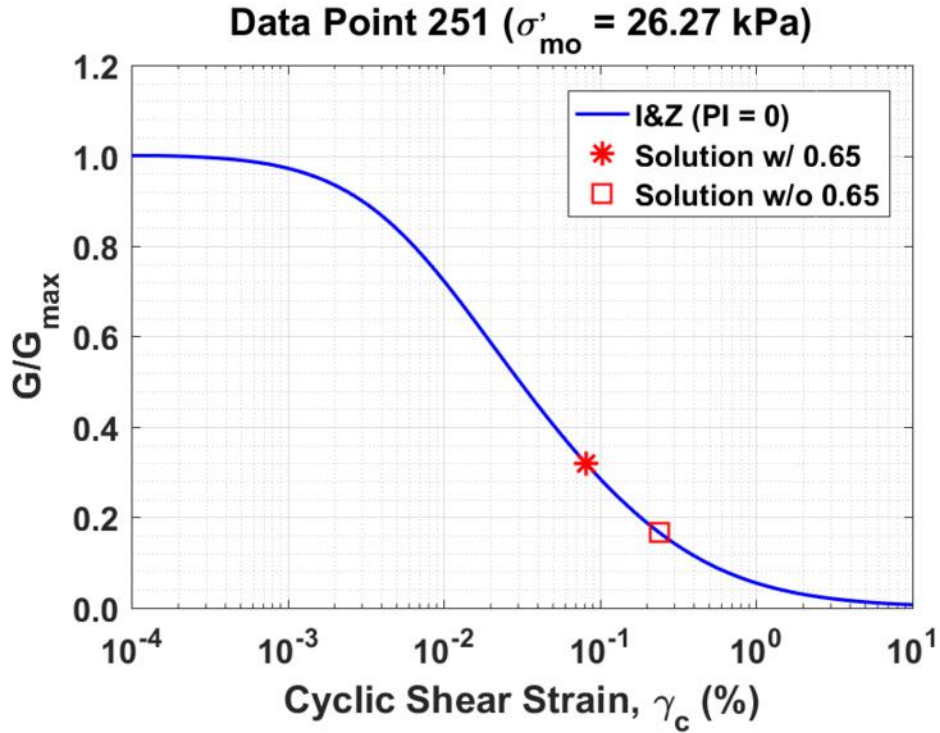


Figure B207. Normalized shear modulus reduction curves for Data Point 251 of the Kayen et al. database showing the solutions w/ and w/o the 0.65 factor

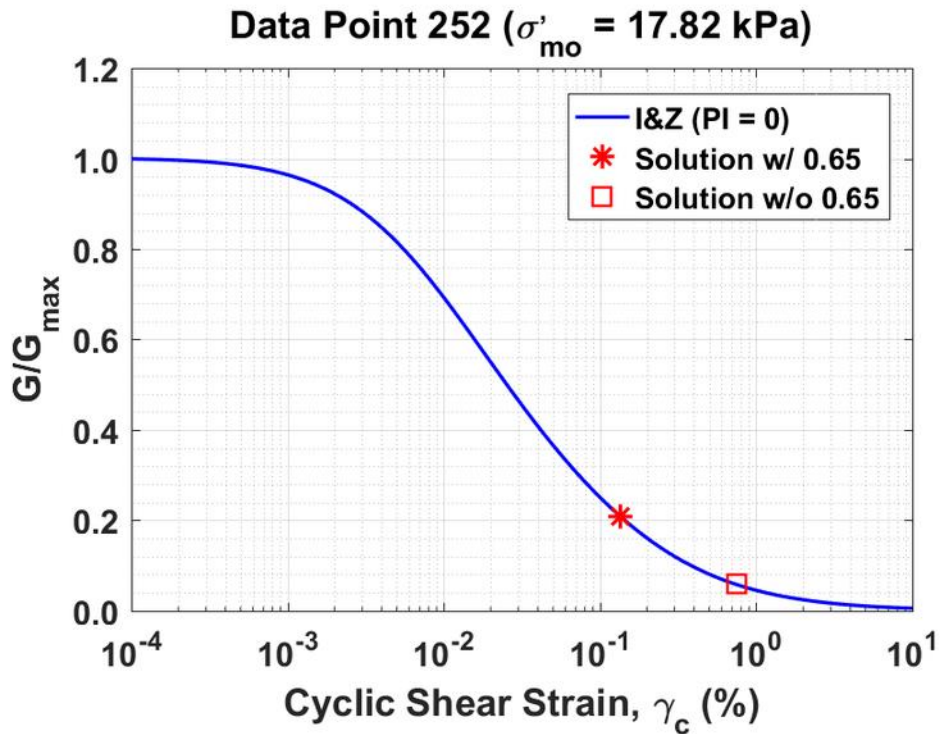


Figure B208. Normalized shear modulus reduction curves for Data Point 252 of the Kayen et al. database showing the solutions w/ and w/o the 0.65 factor

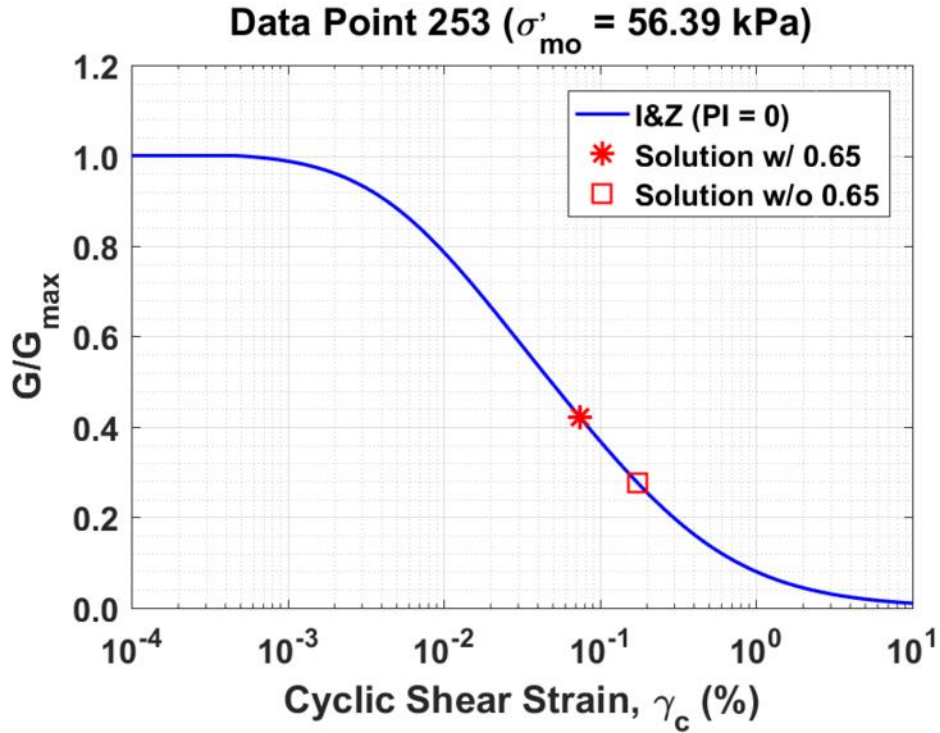


Figure B209. Normalized shear modulus reduction curves for Data Point 253 of the Kayen et al. database showing the solutions w/ and w/o the 0.65 factor

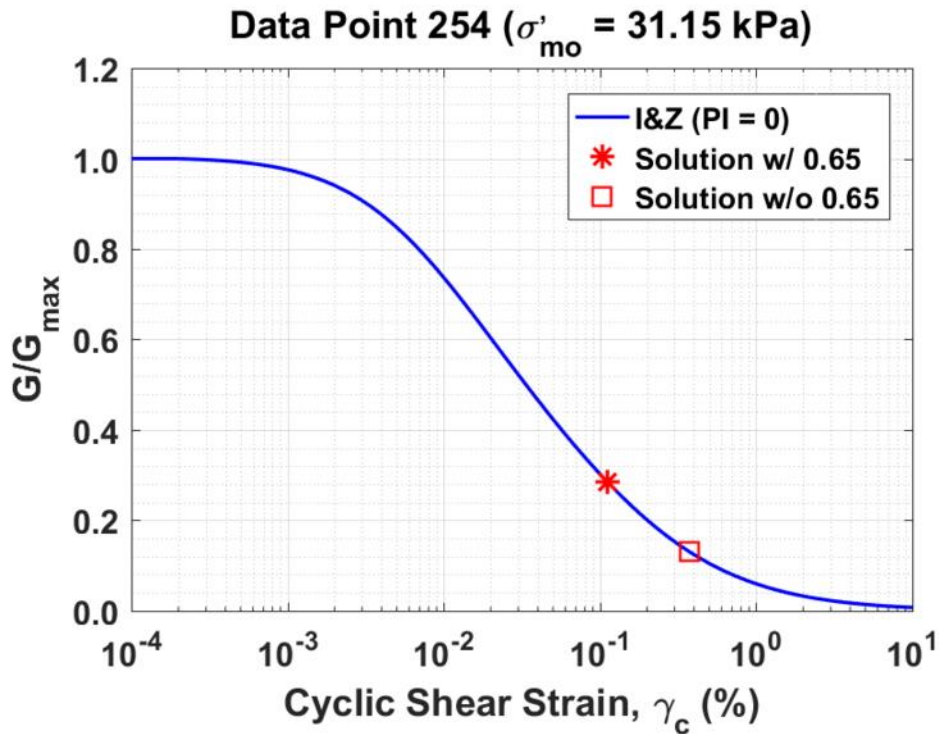


Figure B210. Normalized shear modulus reduction curves for Data Point 254 of the Kayen et al. database showing the solutions w/ and w/o the 0.65 factor

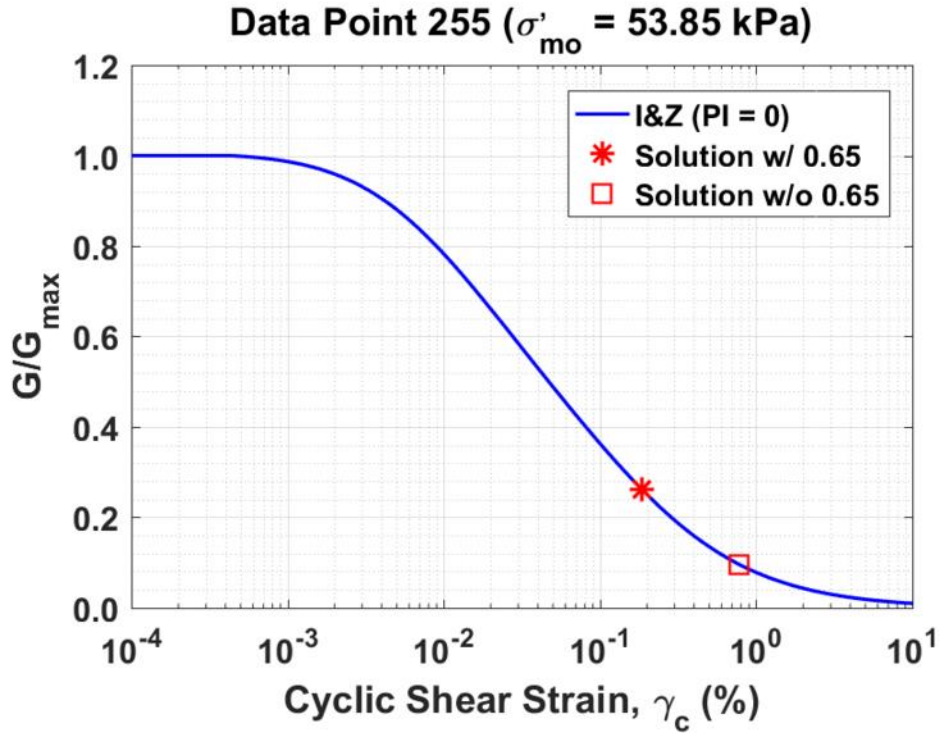


Figure B211. Normalized shear modulus reduction curves for Data Point 255 of the Kayen et al. database showing the solutions w/ and w/o the 0.65 factor

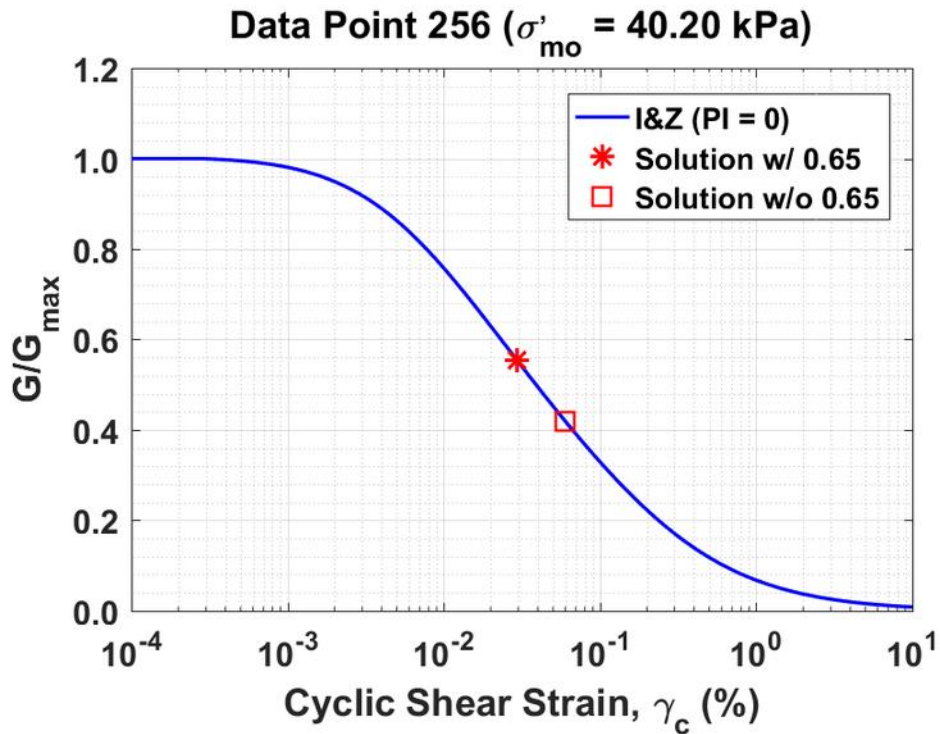


Figure B212. Normalized shear modulus reduction curves for Data Point 256 of the Kayen et al. database showing the solutions w/ and w/o the 0.65 factor

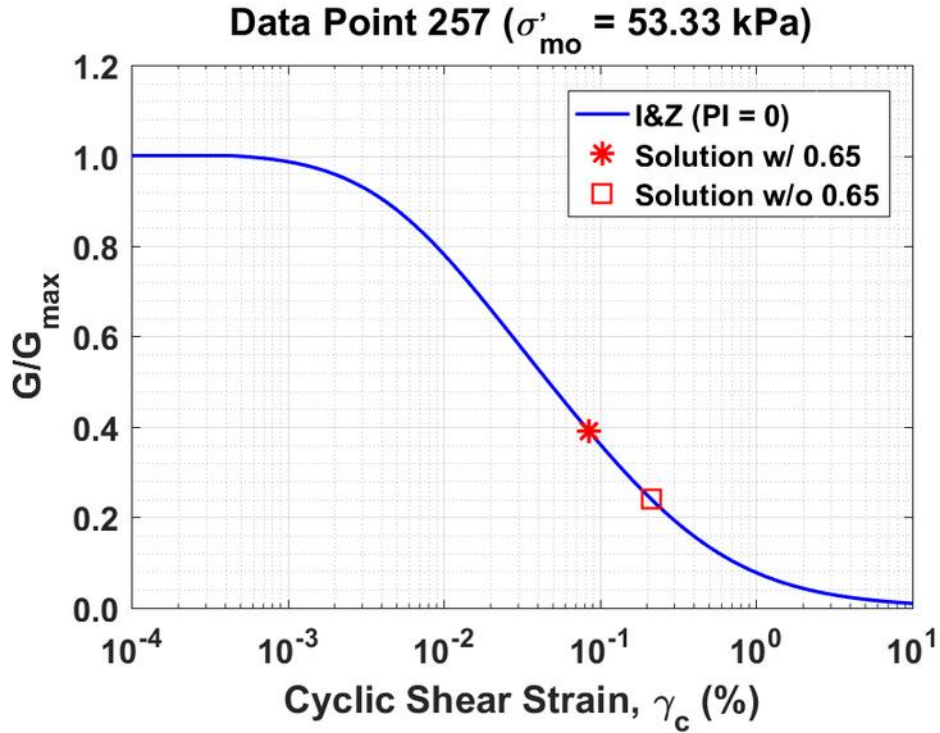


Figure B213. Normalized shear modulus reduction curves for Data Point 257 of the Kayen et al. database showing the solutions w/ and w/o the 0.65 factor

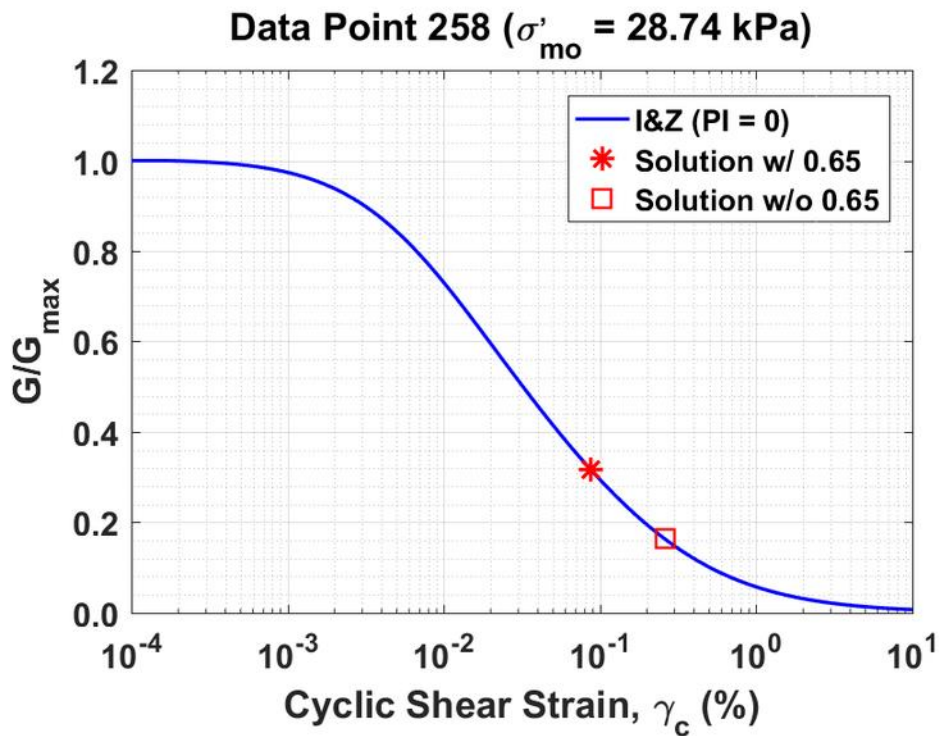


Figure B214. Normalized shear modulus reduction curves for Data Point 258 of the Kayen et al. database showing the solutions w/ and w/o the 0.65 factor

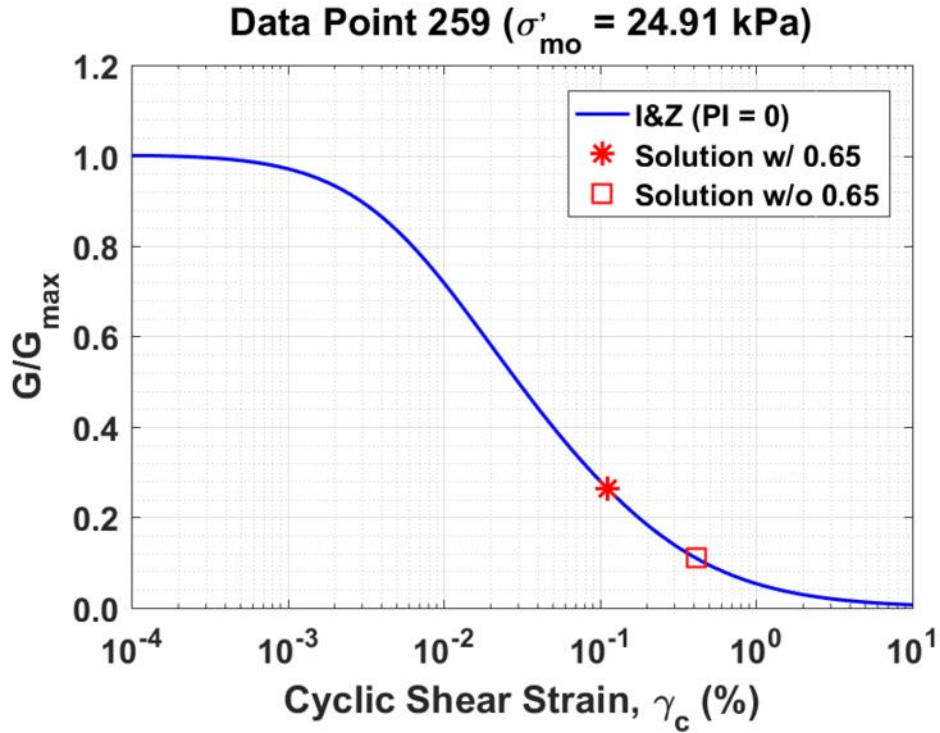


Figure B215. Normalized shear modulus reduction curves for Data Point 259 of the Kayen et al. database showing the solutions w/ and w/o the 0.65 factor

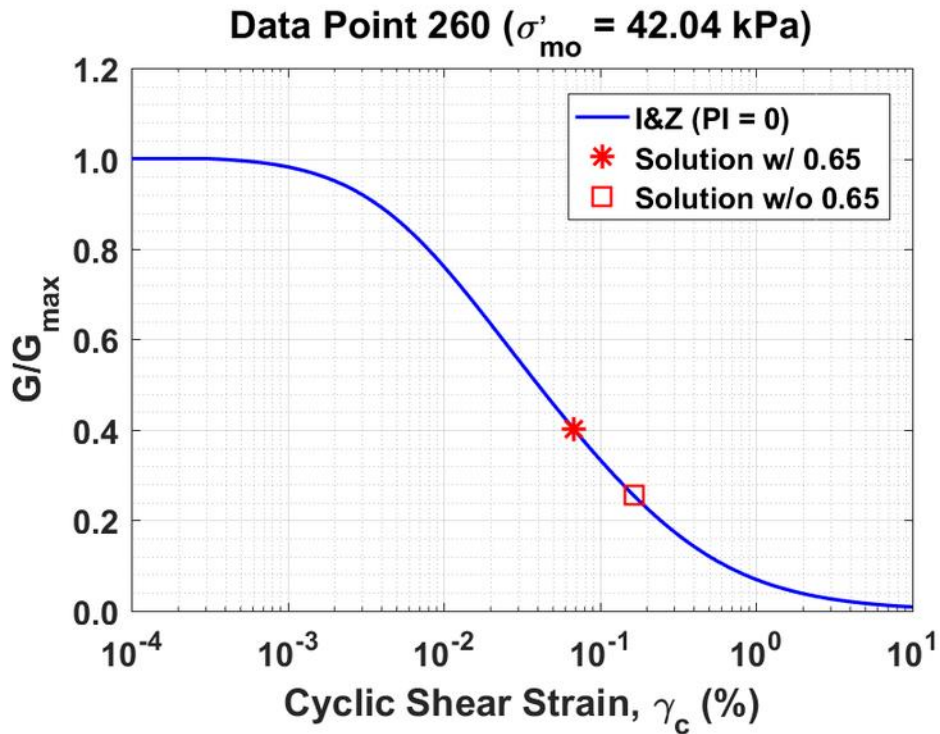


Figure B216. Normalized shear modulus reduction curves for Data Point 260 of the Kayen et al. database showing the solutions w/ and w/o the 0.65 factor

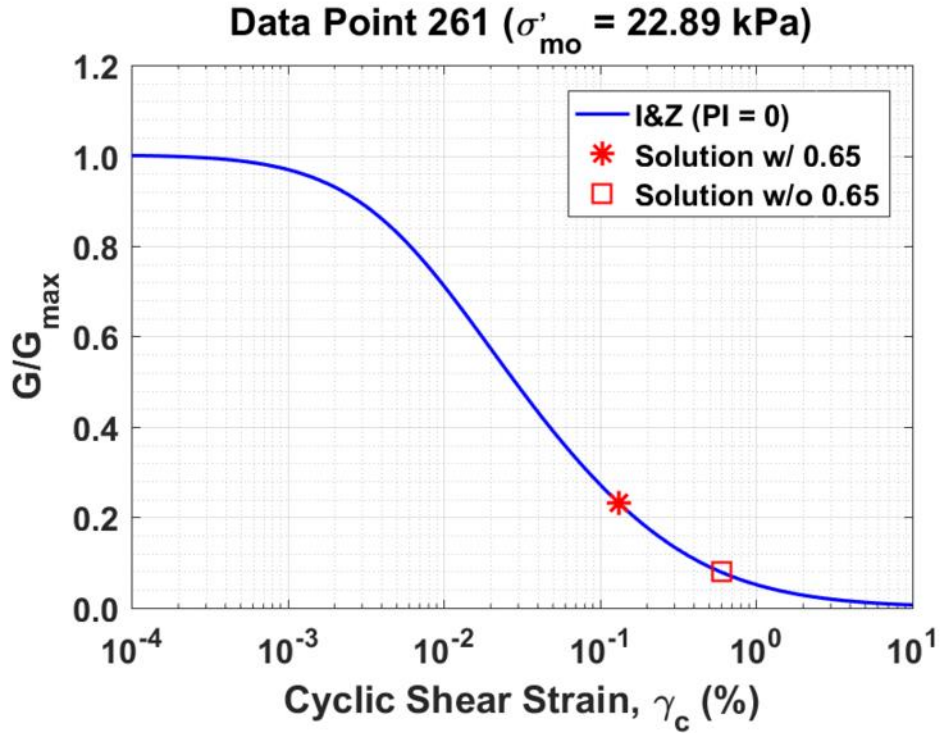


Figure B217. Normalized shear modulus reduction curves for Data Point 261 of the Kayen et al. database showing the solutions w/ and w/o the 0.65 factor

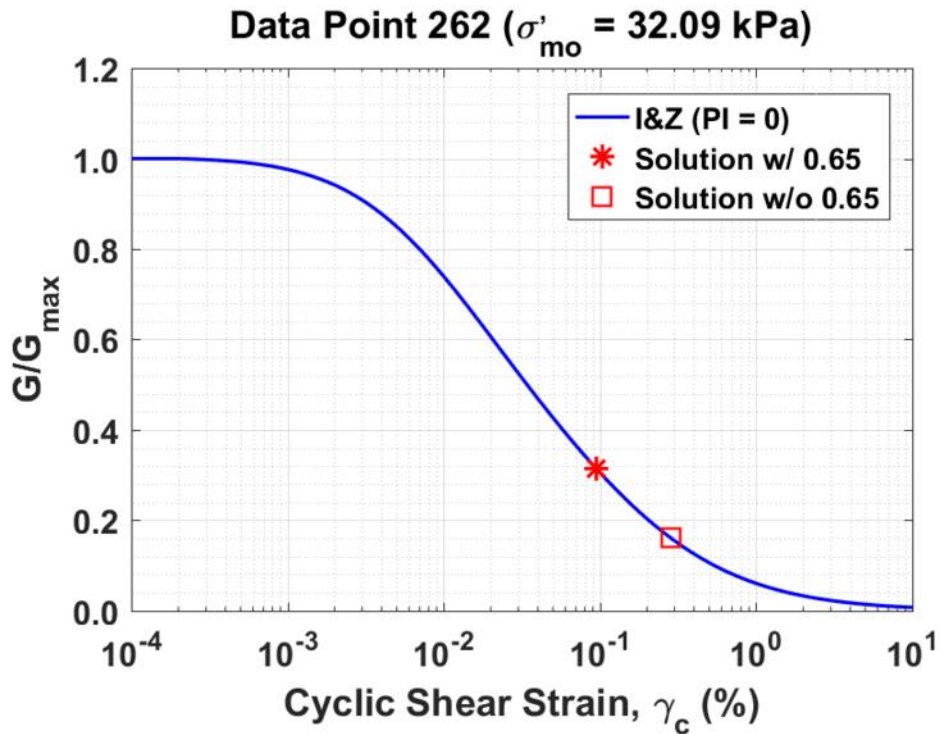


Figure B218. Normalized shear modulus reduction curves for Data Point 262 of the Kayen et al. database showing the solutions w/ and w/o the 0.65 factor

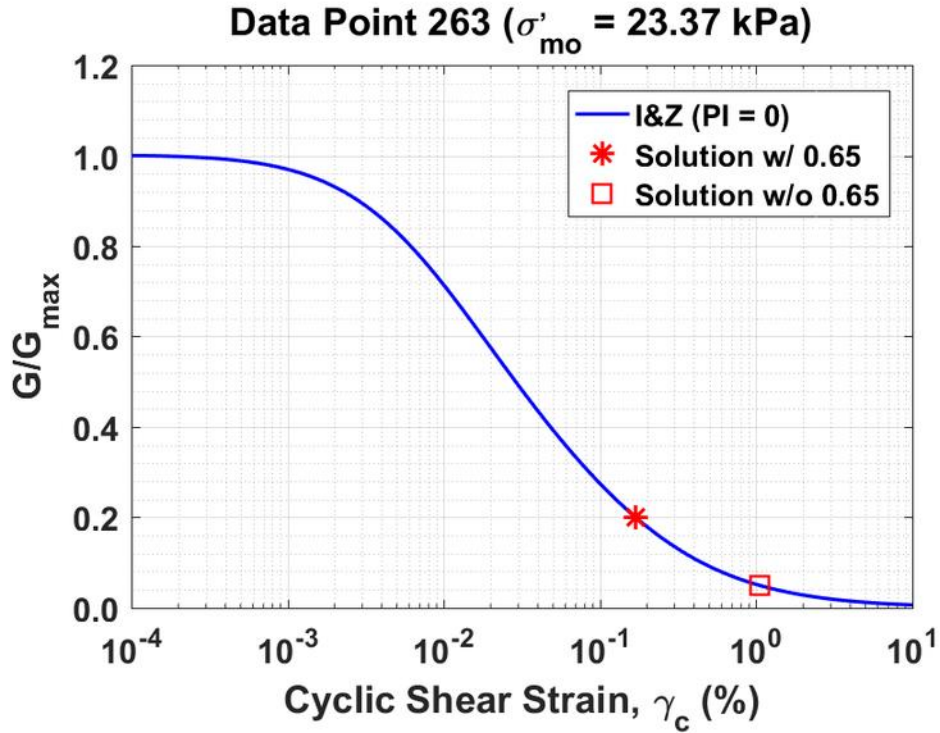


Figure B219. Normalized shear modulus reduction curves for Data Point 263 of the Kayen et al. database showing the solutions w/ and w/o the 0.65 factor

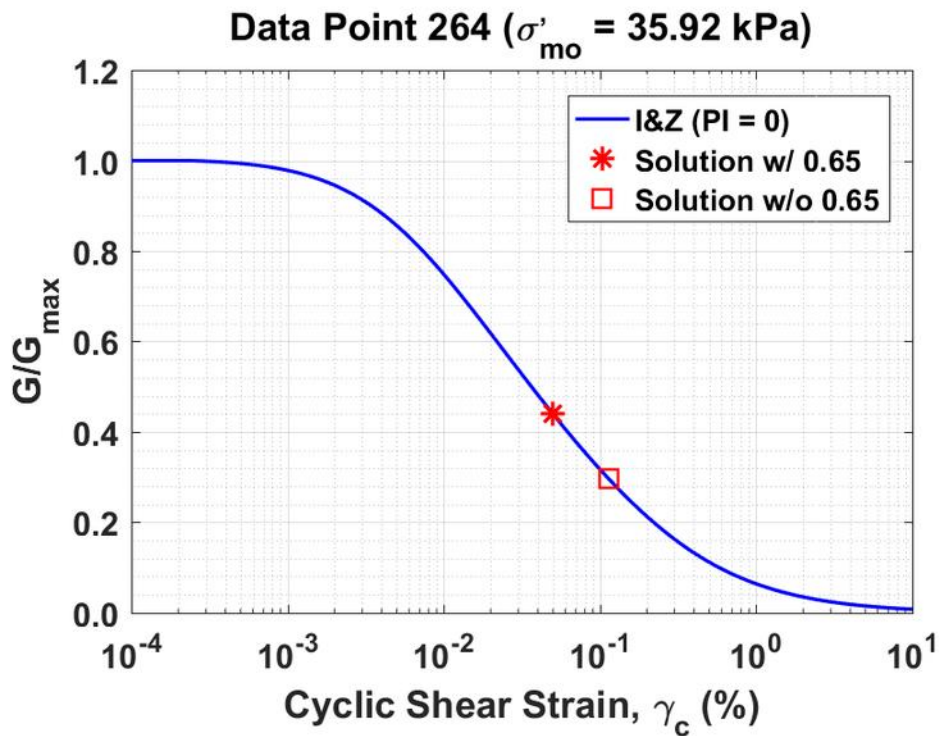


Figure B220. Normalized shear modulus reduction curves for Data Point 264 of the Kayen et al. database showing the solutions w/ and w/o the 0.65 factor

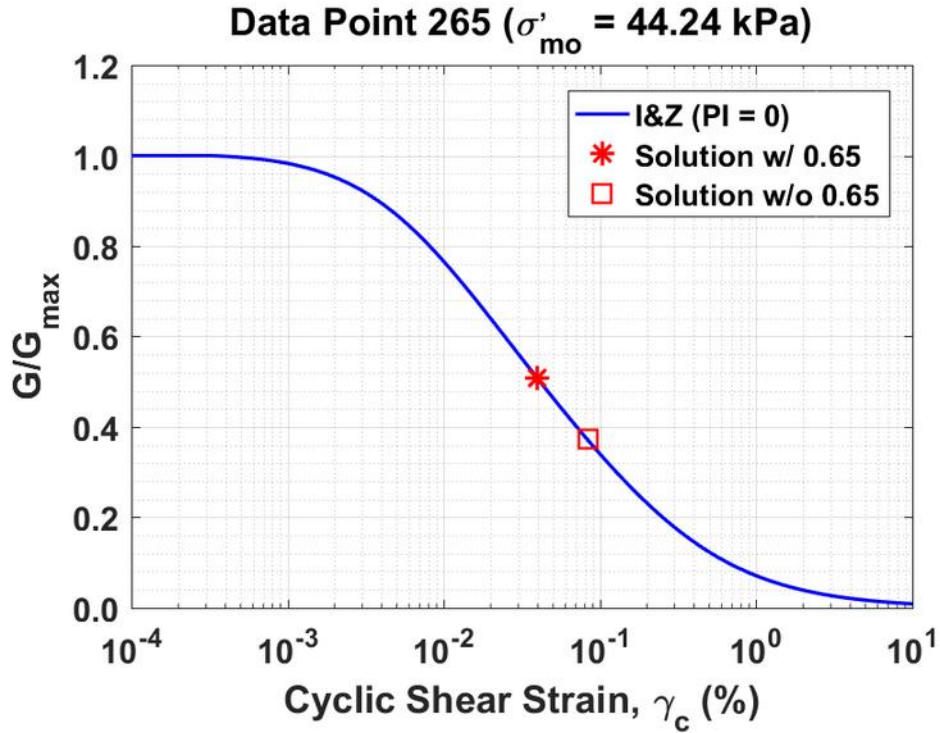


Figure B221. Normalized shear modulus reduction curves for Data Point 265 of the Kayen et al. database showing the solutions w/ and w/o the 0.65 factor

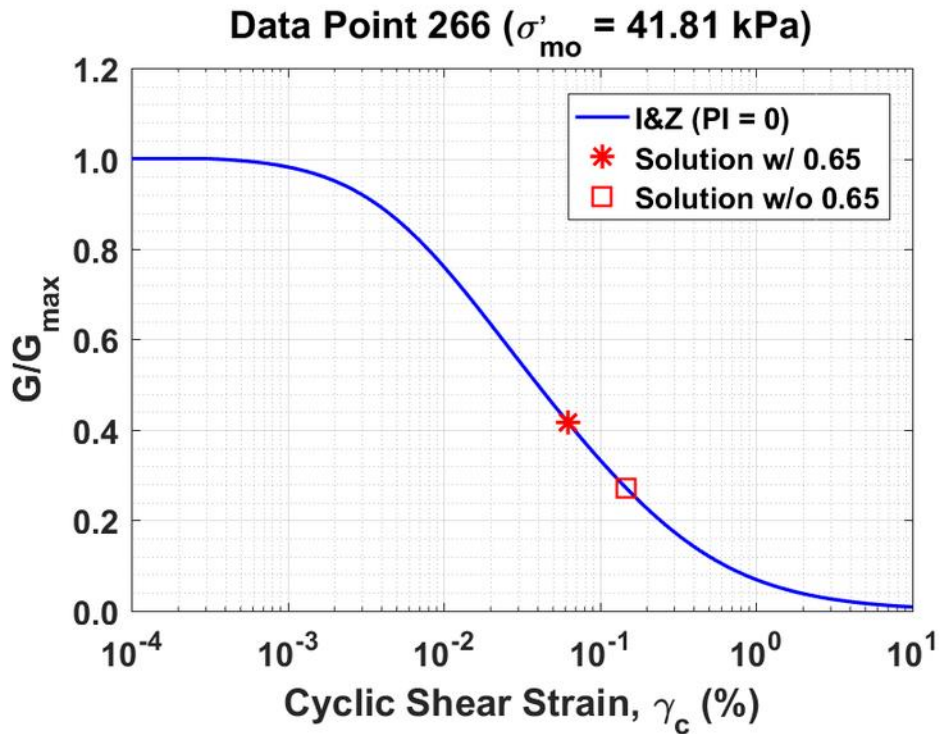


Figure B222. Normalized shear modulus reduction curves for Data Point 266 of the Kayen et al. database showing the solutions w/ and w/o the 0.65 factor

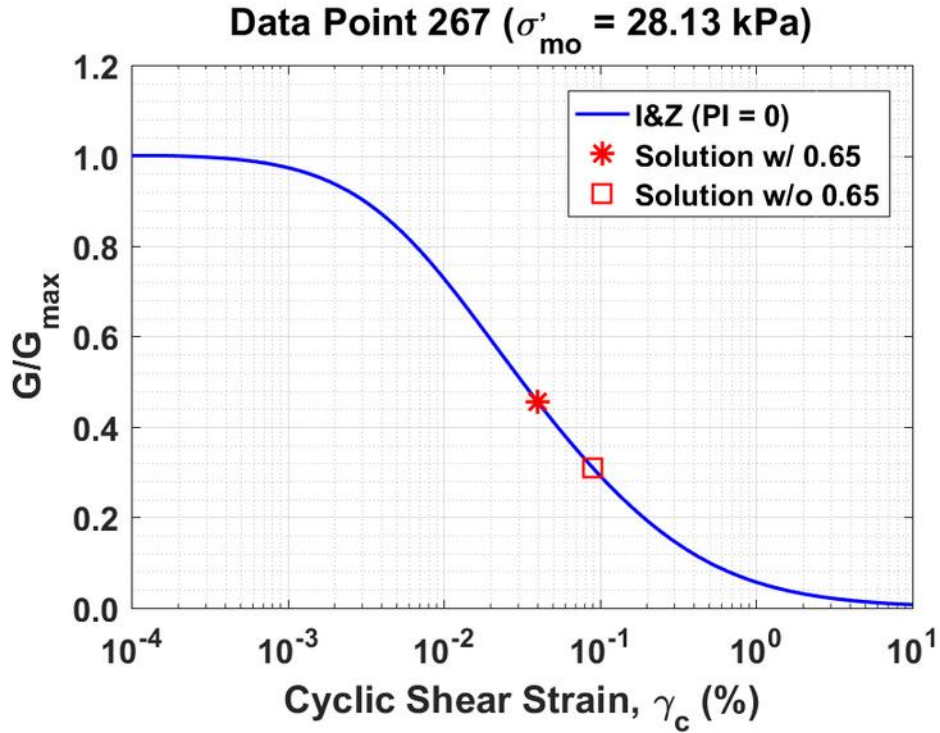


Figure B223. Normalized shear modulus reduction curves for Data Point 267 of the Kayen et al. database showing the solutions w/ and w/o the 0.65 factor

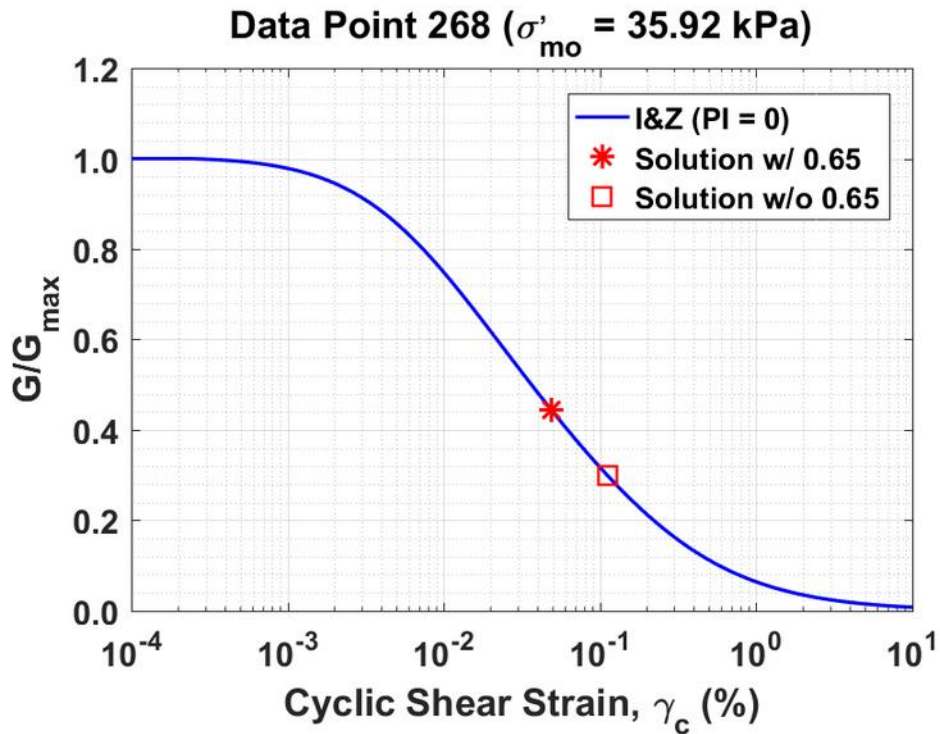


Figure B224. Normalized shear modulus reduction curves for Data Point 268 of the Kayen et al. database showing the solutions w/ and w/o the 0.65 factor

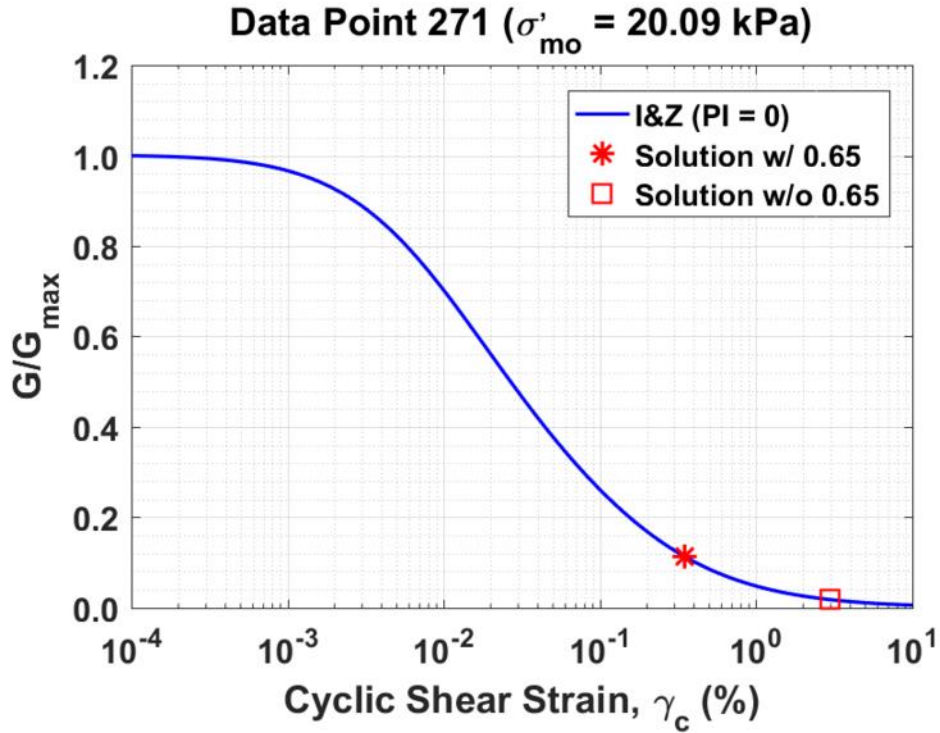


Figure B225. Normalized shear modulus reduction curves for Data Point 271 of the Kayen et al. database showing the solutions w/ and w/o the 0.65 factor

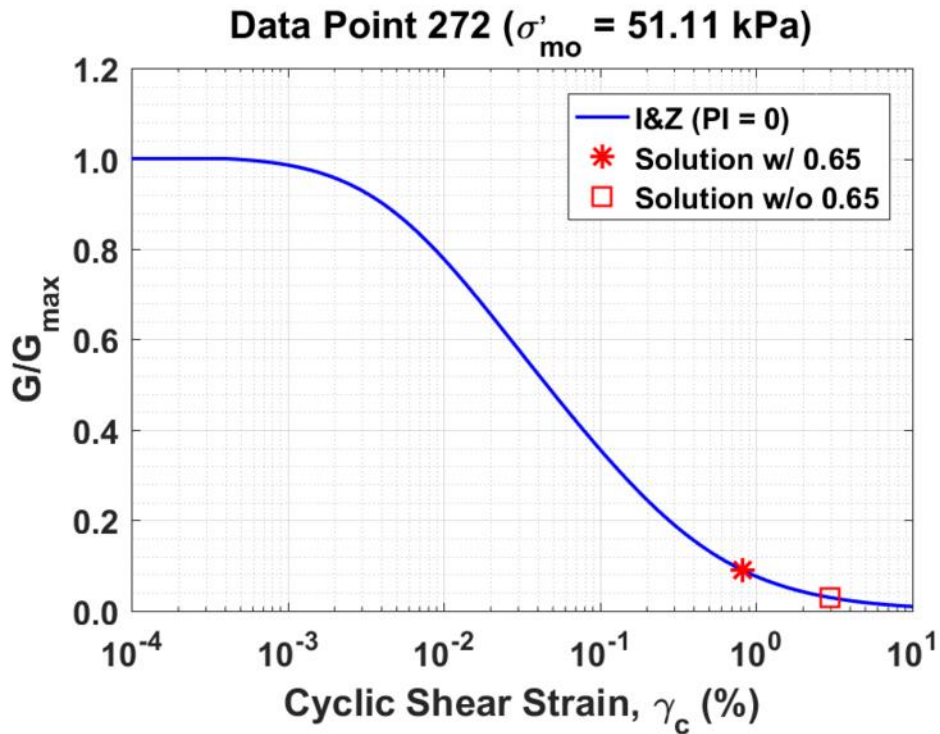


Figure B226. Normalized shear modulus reduction curves for Data Point 272 of the Kayen et al. database showing the solutions w/ and w/o the 0.65 factor

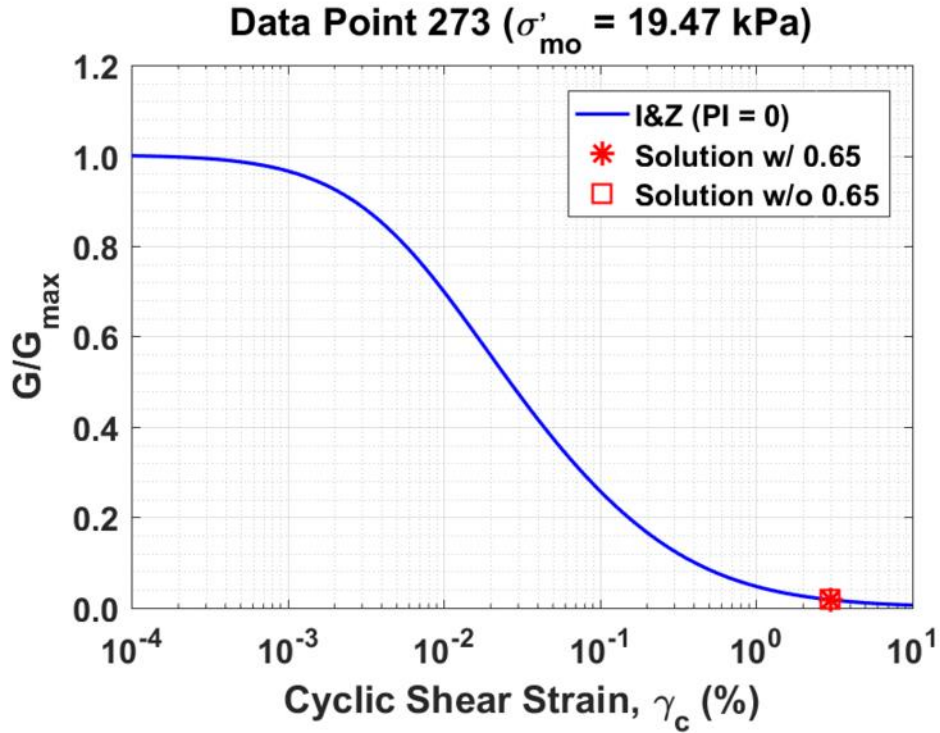


Figure B227. Normalized shear modulus reduction curves for Data Point 273 of the Kayen et al. database showing the solutions w/ and w/o the 0.65 factor

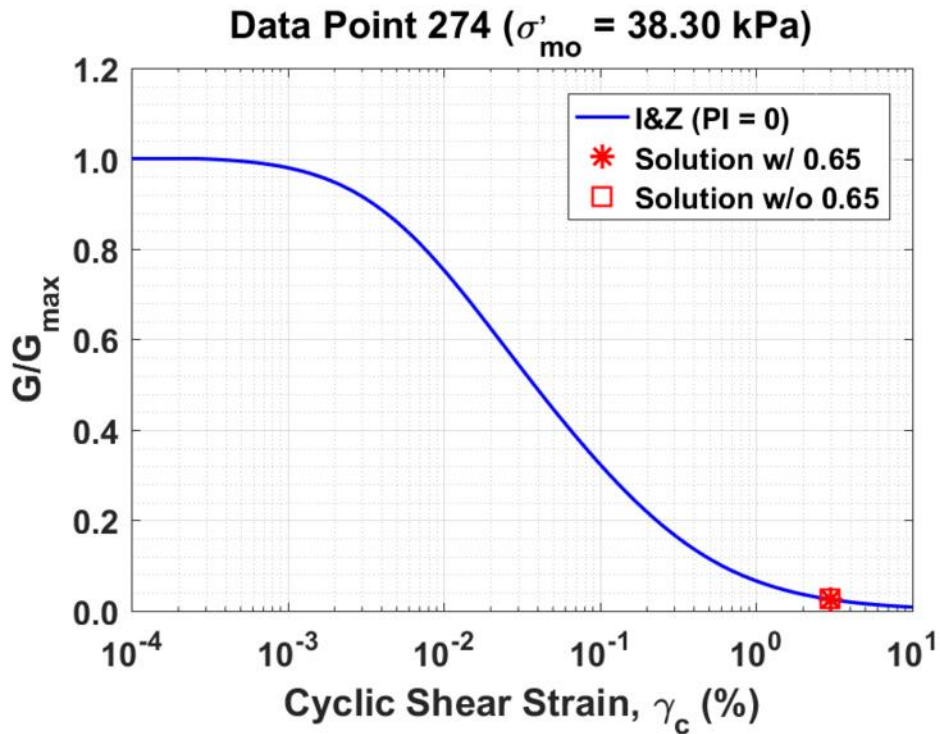


Figure B228. Normalized shear modulus reduction curves for Data Point 274 of the Kayen et al. database showing the solutions w/ and w/o the 0.65 factor

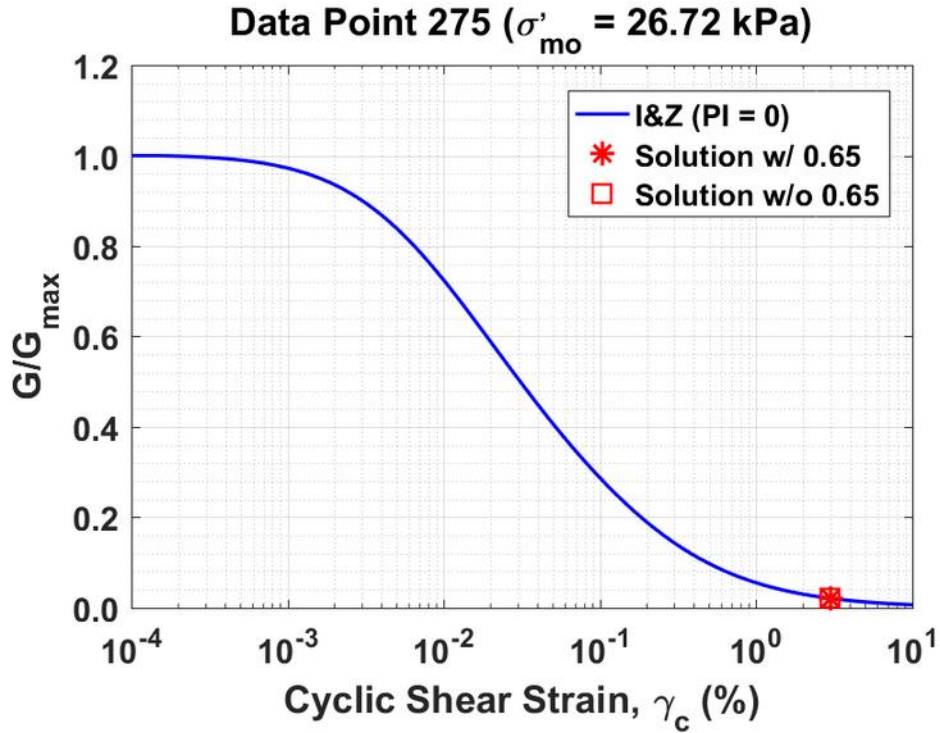


Figure B229. Normalized shear modulus reduction curves for Data Point 275 of the Kayen et al. database showing the solutions w/ and w/o the 0.65 factor

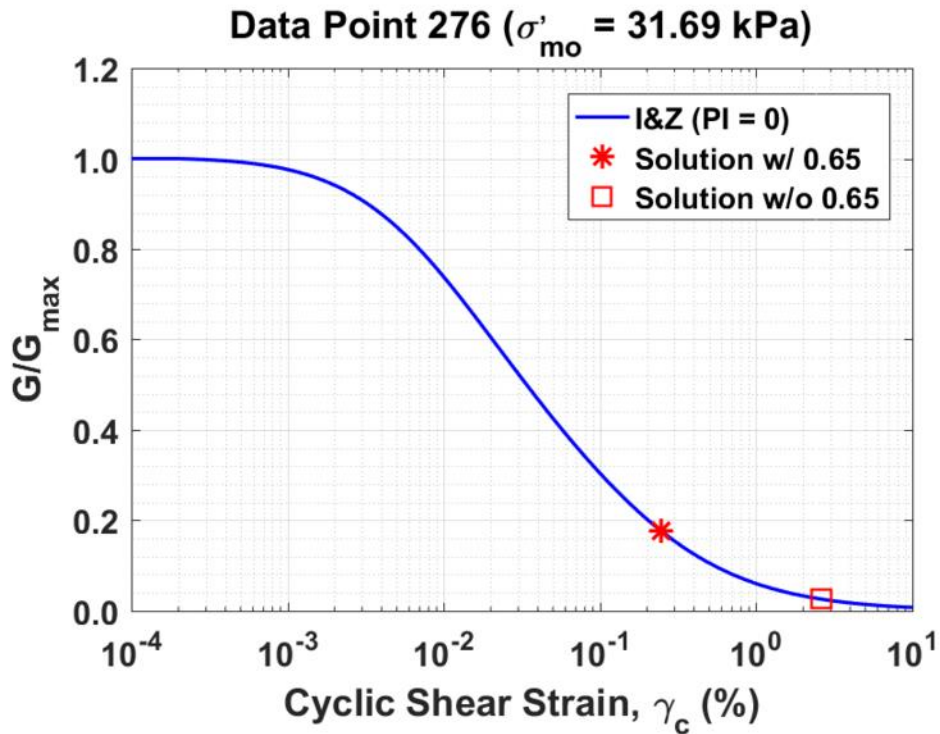


Figure B230. Normalized shear modulus reduction curves for Data Point 276 of the Kayen et al. database showing the solutions w/ and w/o the 0.65 factor

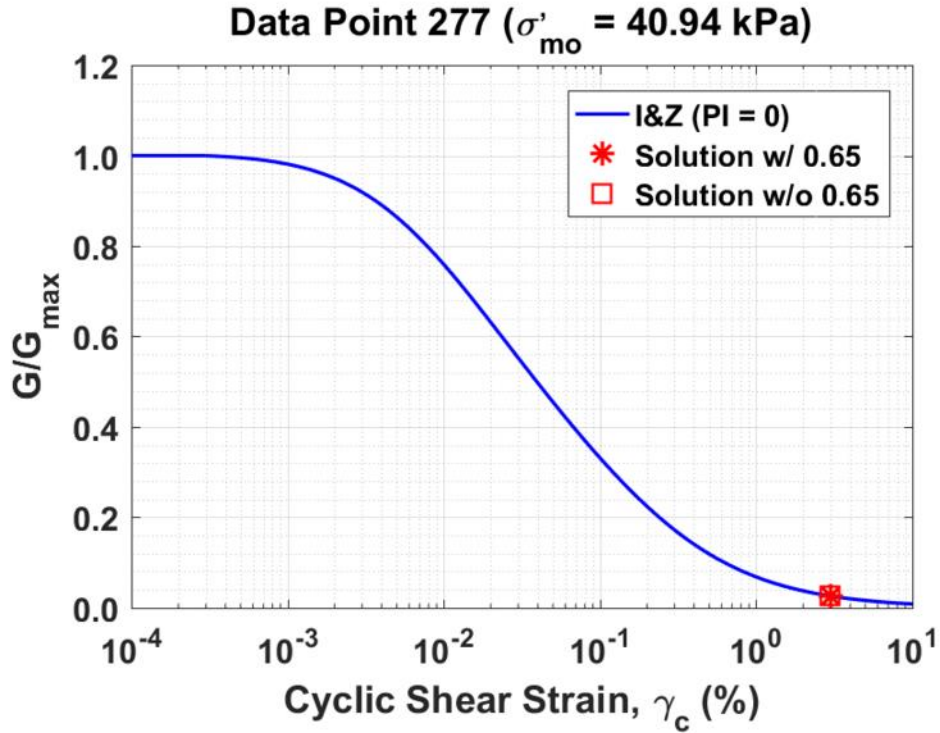


Figure B231. Normalized shear modulus reduction curves for Data Point 277 of the Kayen et al. database showing the solutions w/ and w/o the 0.65 factor

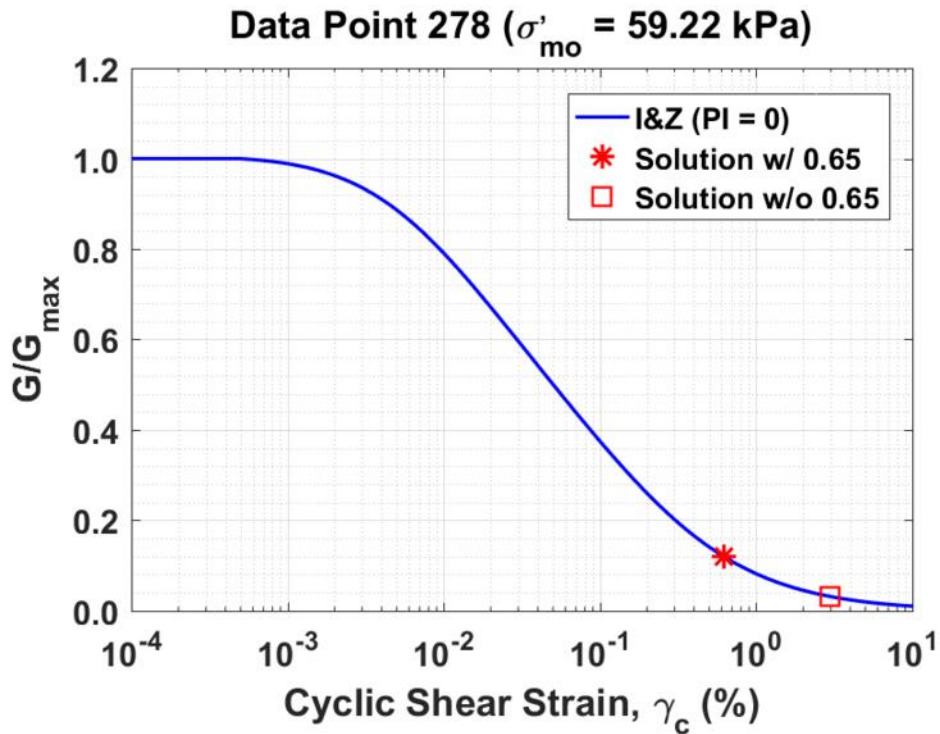


Figure B232. Normalized shear modulus reduction curves for Data Point 278 of the Kayen et al. database showing the solutions w/ and w/o the 0.65 factor

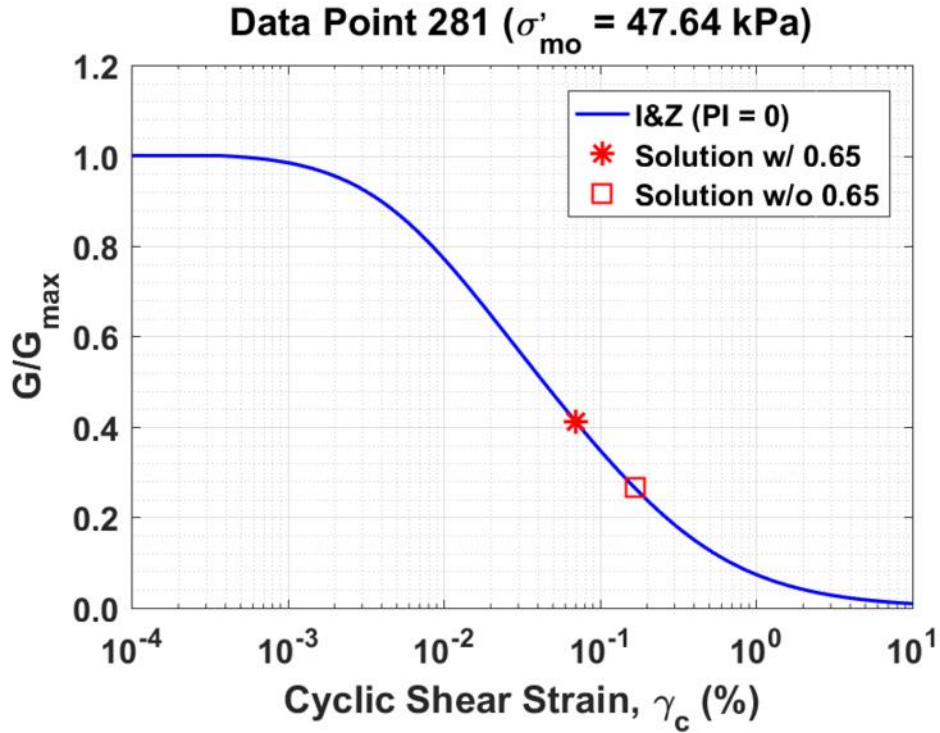


Figure B233. Normalized shear modulus reduction curves for Data Point 281 of the Kayen et al. database showing the solutions w/ and w/o the 0.65 factor

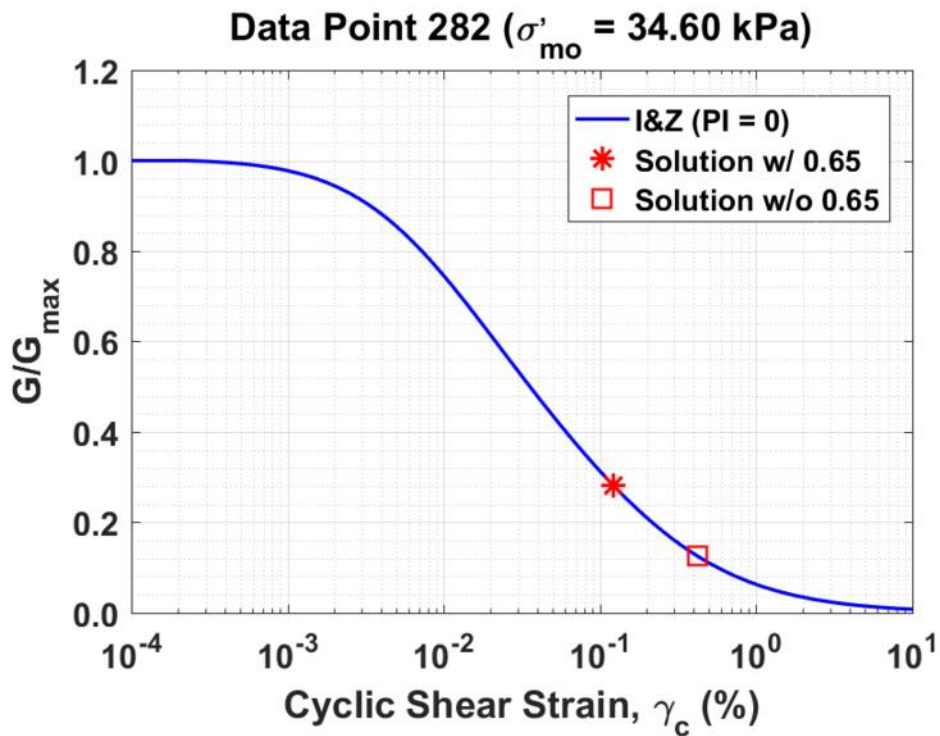


Figure B234. Normalized shear modulus reduction curves for Data Point 282 of the Kayen et al. database showing the solutions w/ and w/o the 0.65 factor

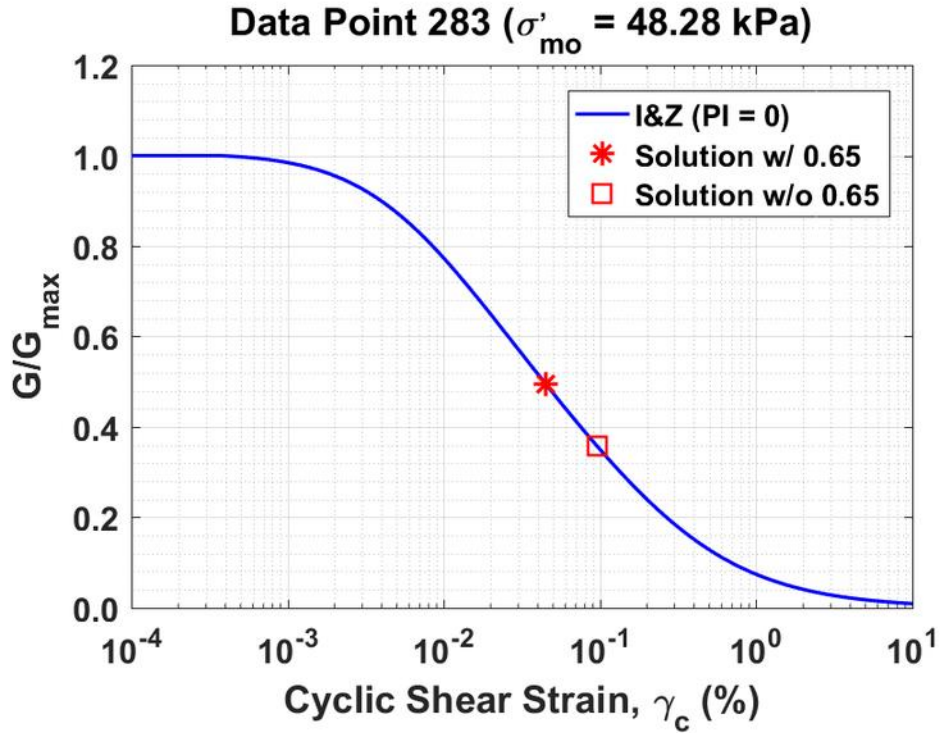


Figure B235. Normalized shear modulus reduction curves for Data Point 283 of the Kayen et al. database showing the solutions w/ and w/o the 0.65 factor

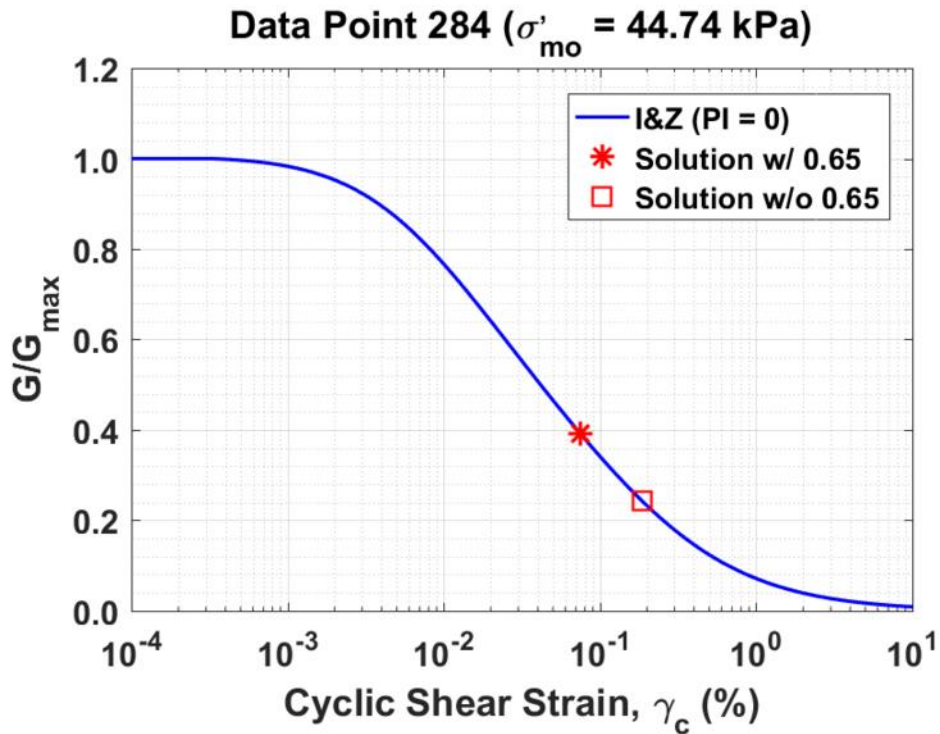


Figure B236. Normalized shear modulus reduction curves for Data Point 284 of the Kayen et al. database showing the solutions w/ and w/o the 0.65 factor

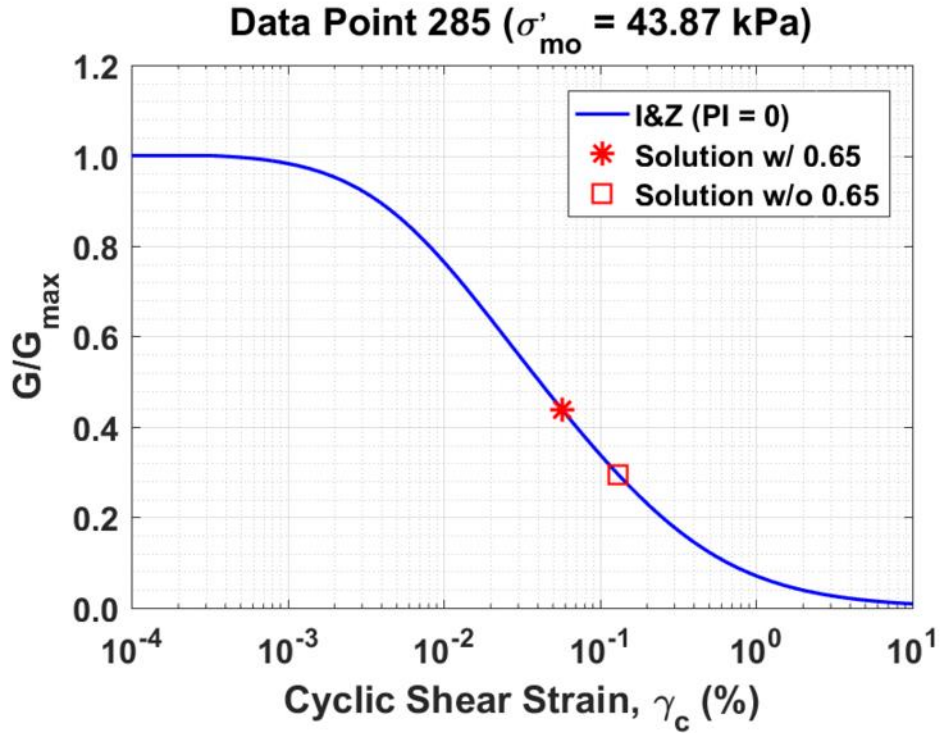


Figure B237. Normalized shear modulus reduction curves for Data Point 285 of the Kayen et al. database showing the solutions w/ and w/o the 0.65 factor

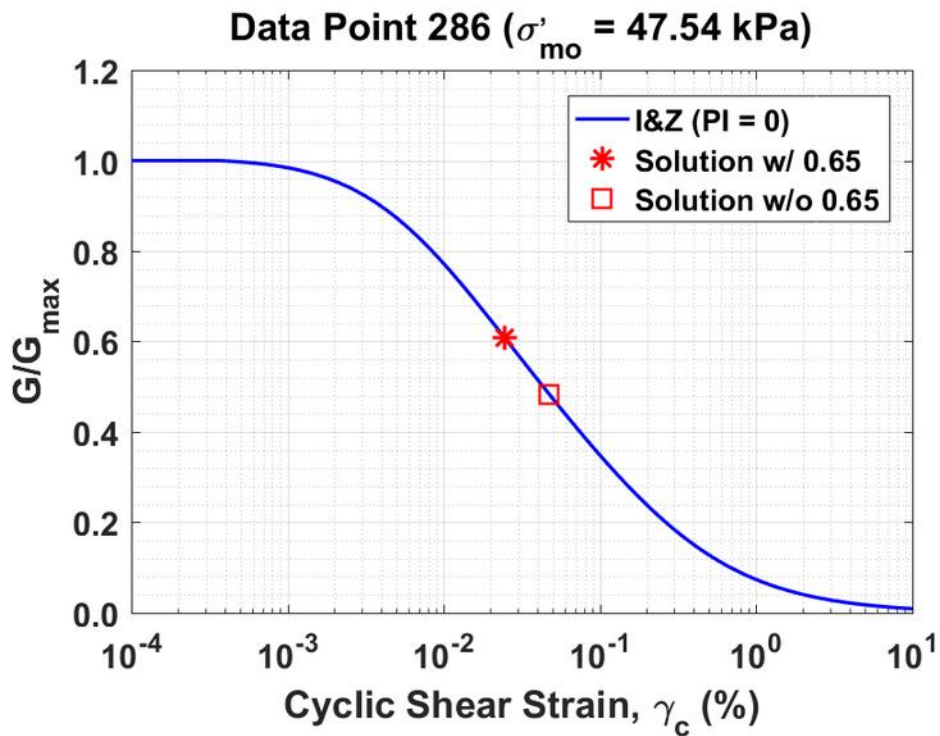


Figure B238. Normalized shear modulus reduction curves for Data Point 286 of the Kayen et al. database showing the solutions w/ and w/o the 0.65 factor

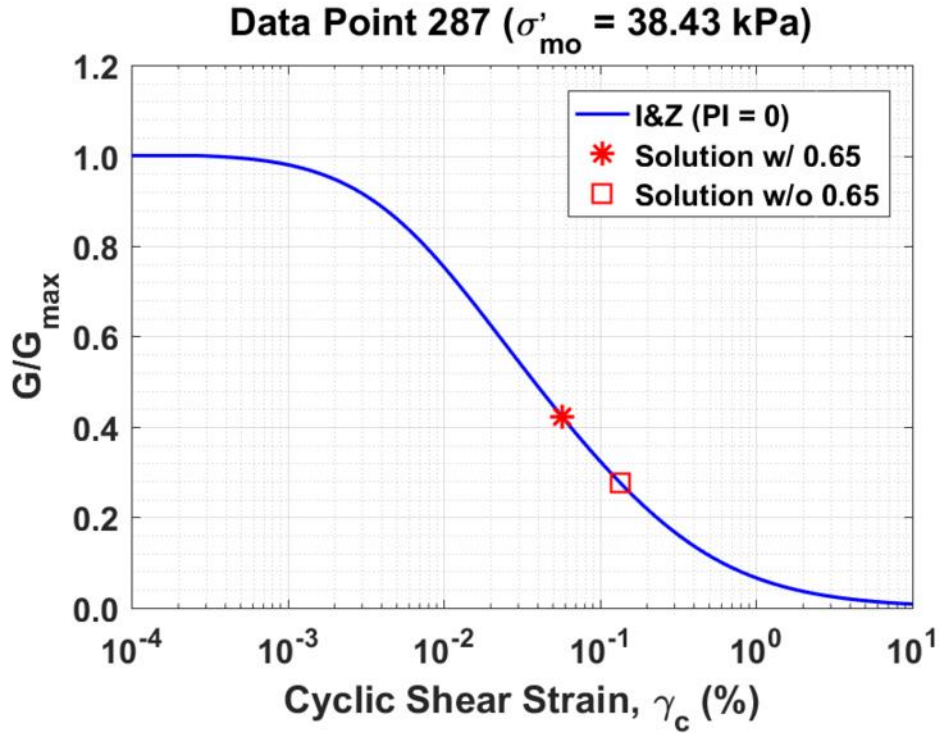


Figure B239. Normalized shear modulus reduction curves for Data Point 287 of the Kayen et al. database showing the solutions w/ and w/o the 0.65 factor

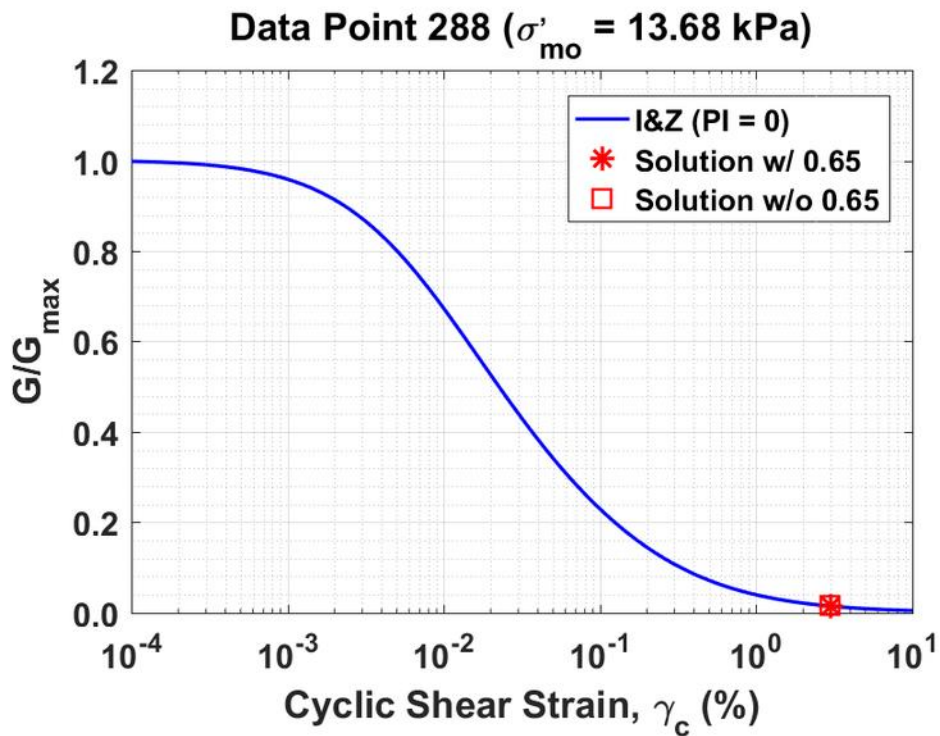


Figure B240. Normalized shear modulus reduction curves for Data Point 288 of the Kayen et al. database showing the solutions w/ and w/o the 0.65 factor

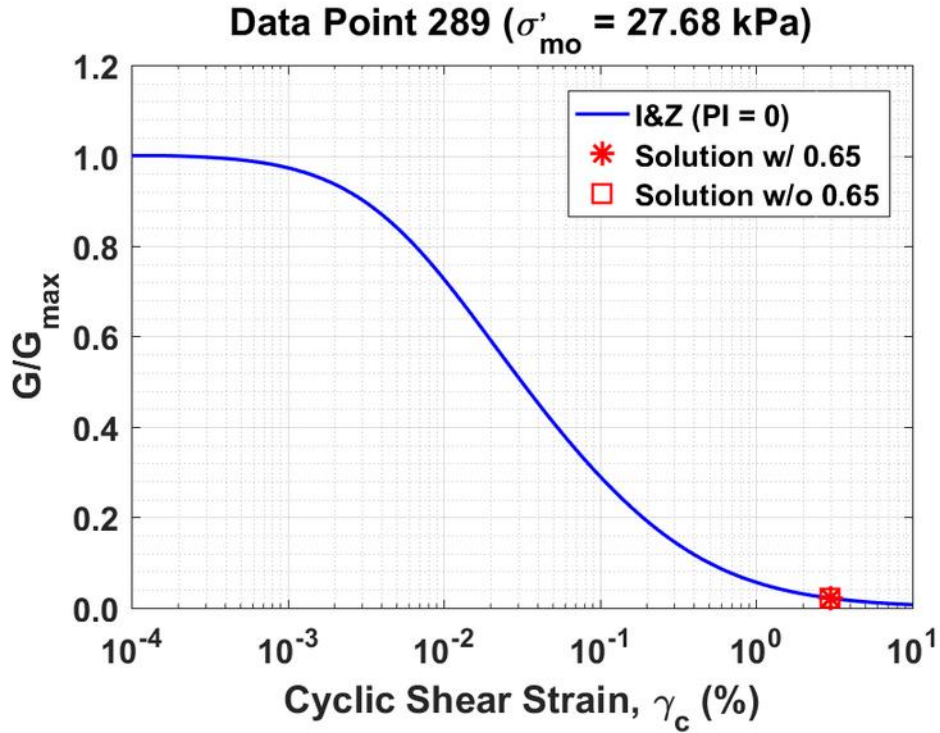


Figure B241. Normalized shear modulus reduction curves for Data Point 289 of the Kayen et al. database showing the solutions w/ and w/o the 0.65 factor

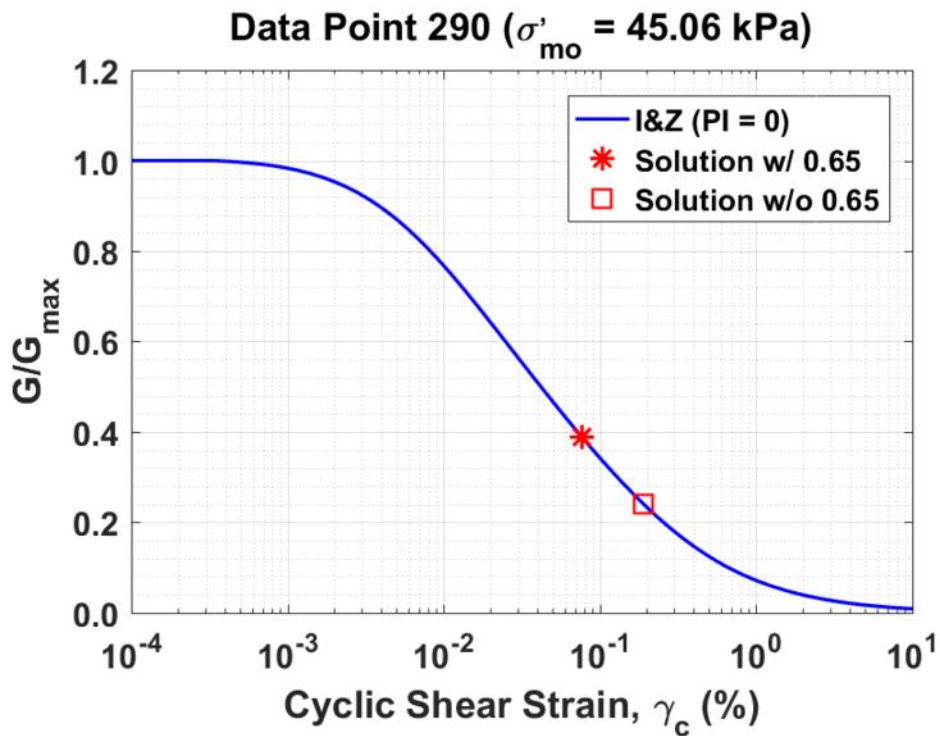


Figure B242. Normalized shear modulus reduction curves for Data Point 290 of the Kayen et al. database showing the solutions w/ and w/o the 0.65 factor

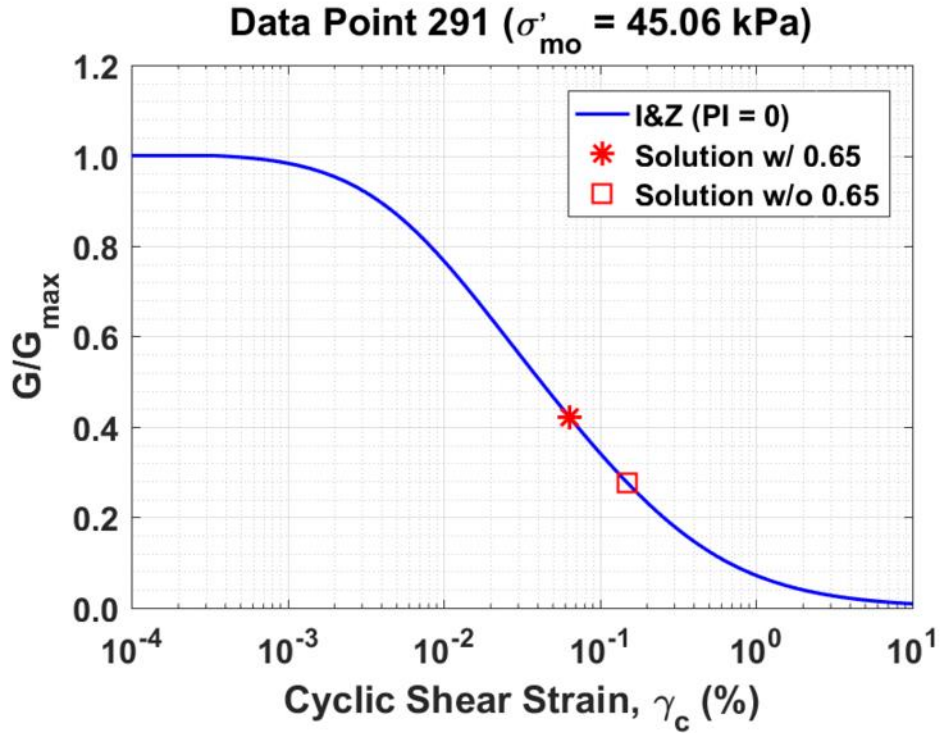


Figure B243. Normalized shear modulus reduction curves for Data Point 291 of the Kayen et al. database showing the solutions w/ and w/o the 0.65 factor

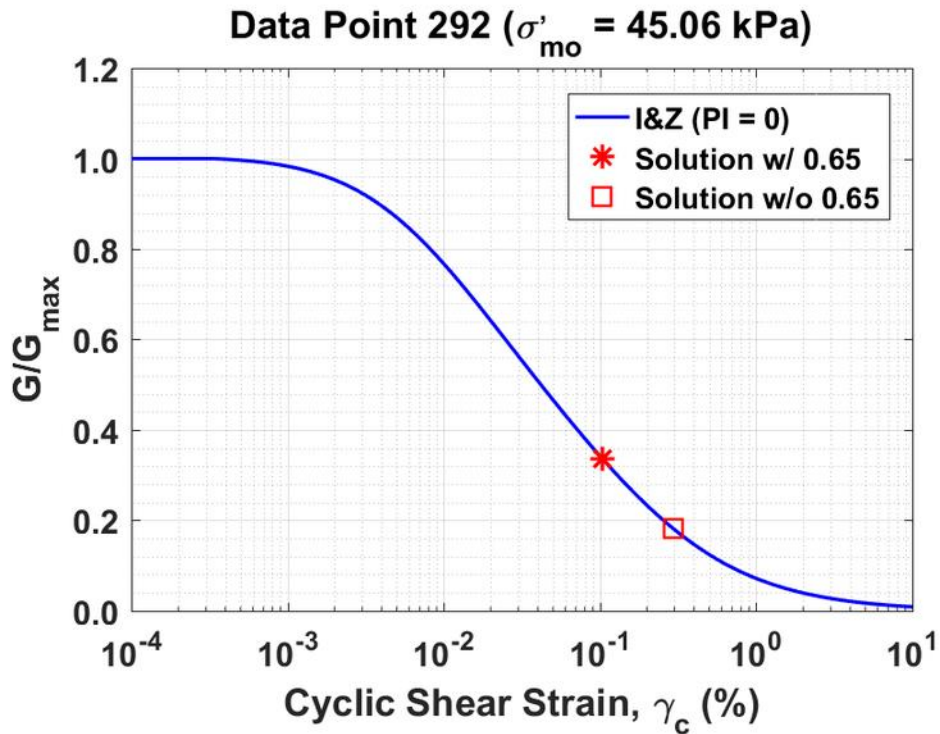


Figure B244. Normalized shear modulus reduction curves for Data Point 292 of the Kayen et al. database showing the solutions w/ and w/o the 0.65 factor

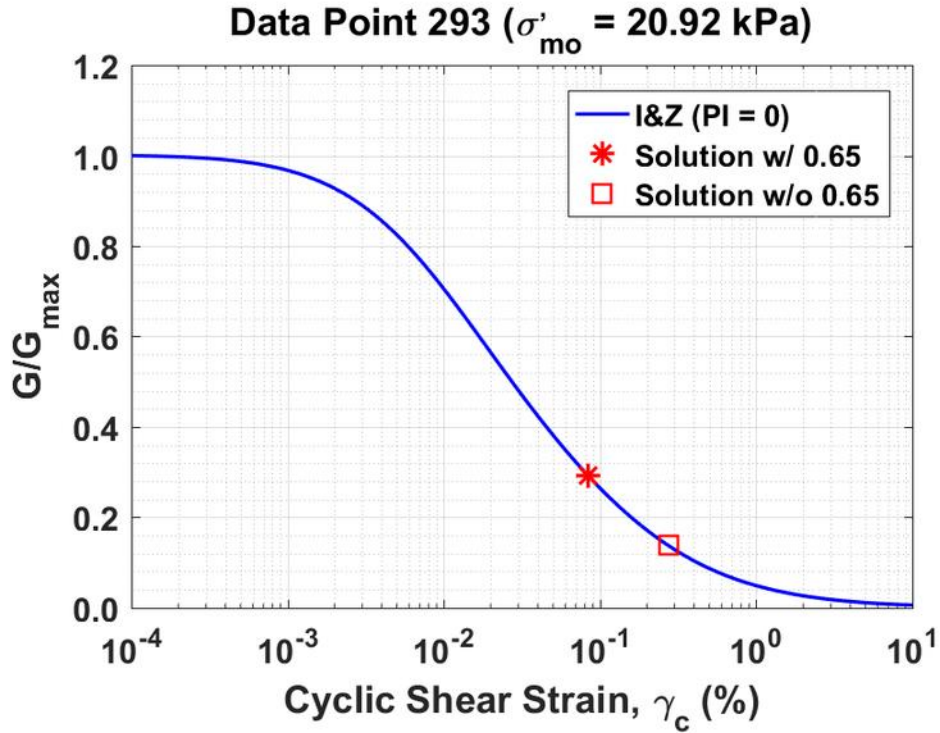


Figure B245. Normalized shear modulus reduction curves for Data Point 293 of the Kayen et al. database showing the solutions w/ and w/o the 0.65 factor

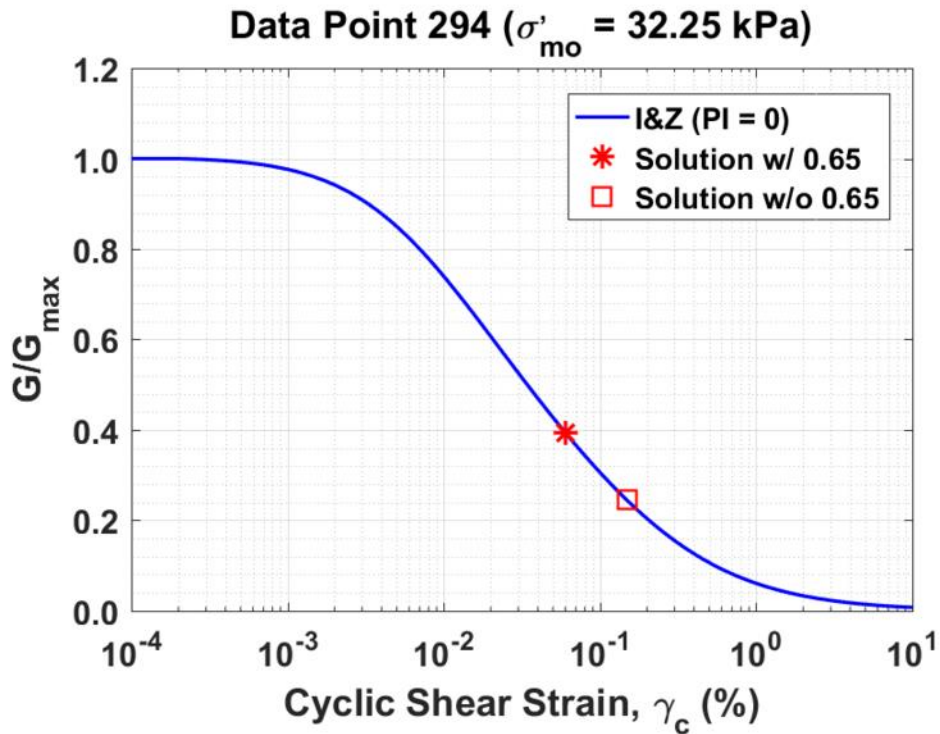


Figure B246. Normalized shear modulus reduction curves for Data Point 294 of the Kayen et al. database showing the solutions w/ and w/o the 0.65 factor

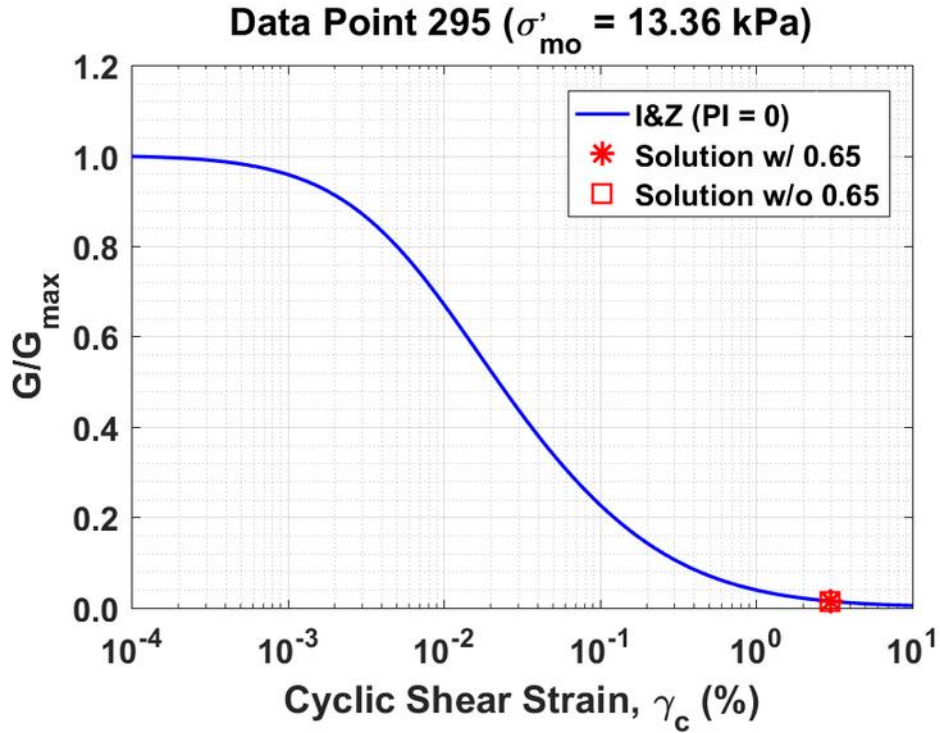


Figure B247. Normalized shear modulus reduction curves for Data Point 295 of the Kayen et al. database showing the solutions w/ and w/o the 0.65 factor

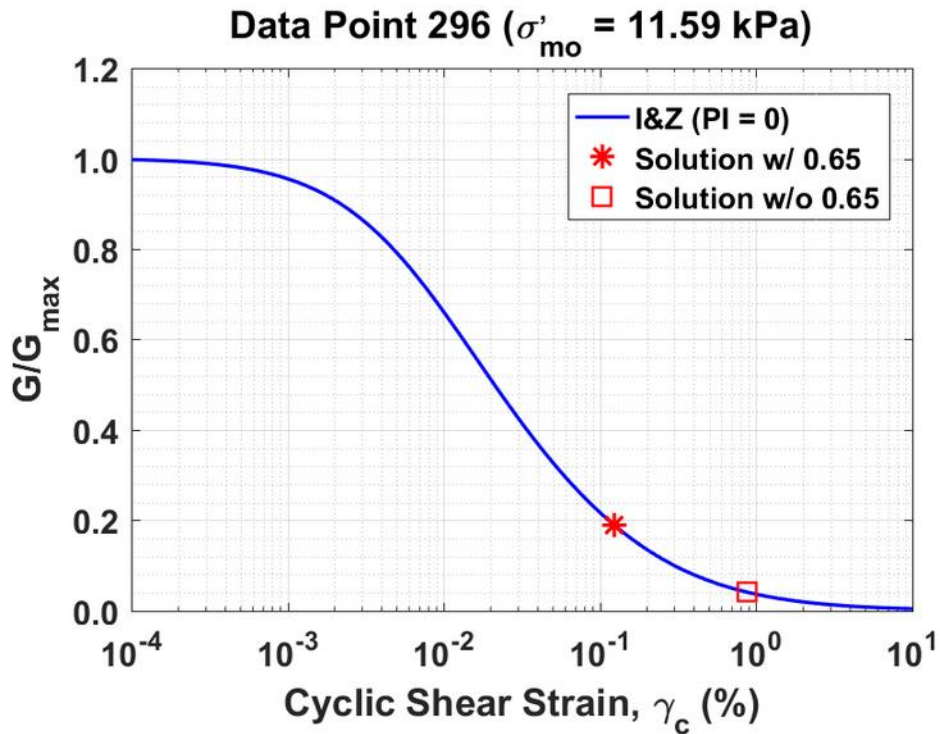


Figure B248. Normalized shear modulus reduction curves for Data Point 296 of the Kayen et al. database showing the solutions w/ and w/o the 0.65 factor

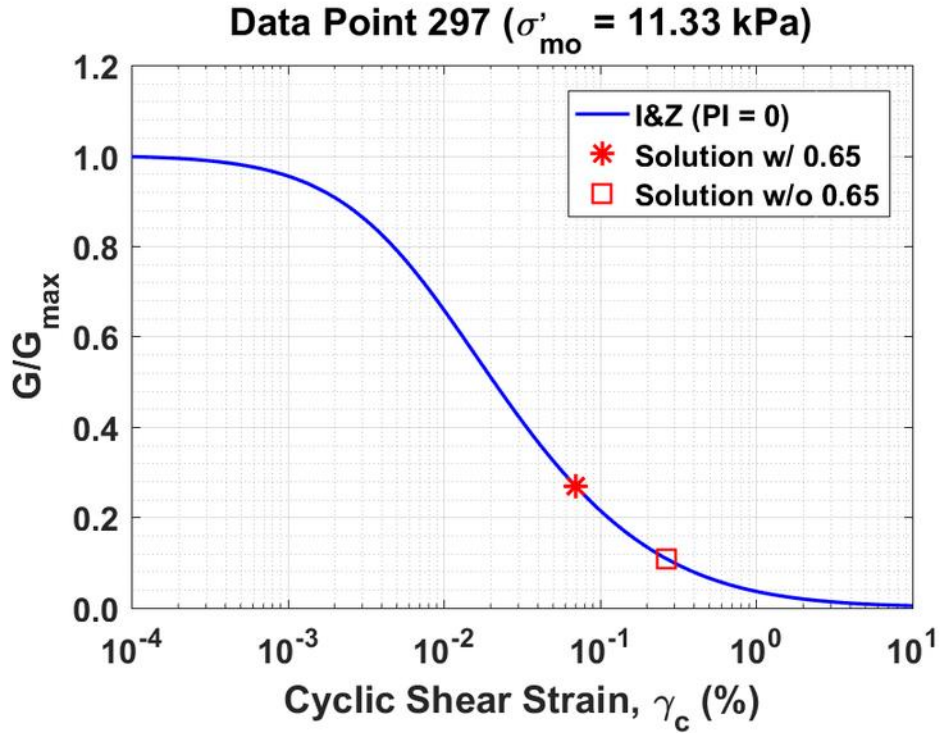


Figure B249. Normalized shear modulus reduction curves for Data Point 297 of the Kayen et al. database showing the solutions w/ and w/o the 0.65 factor

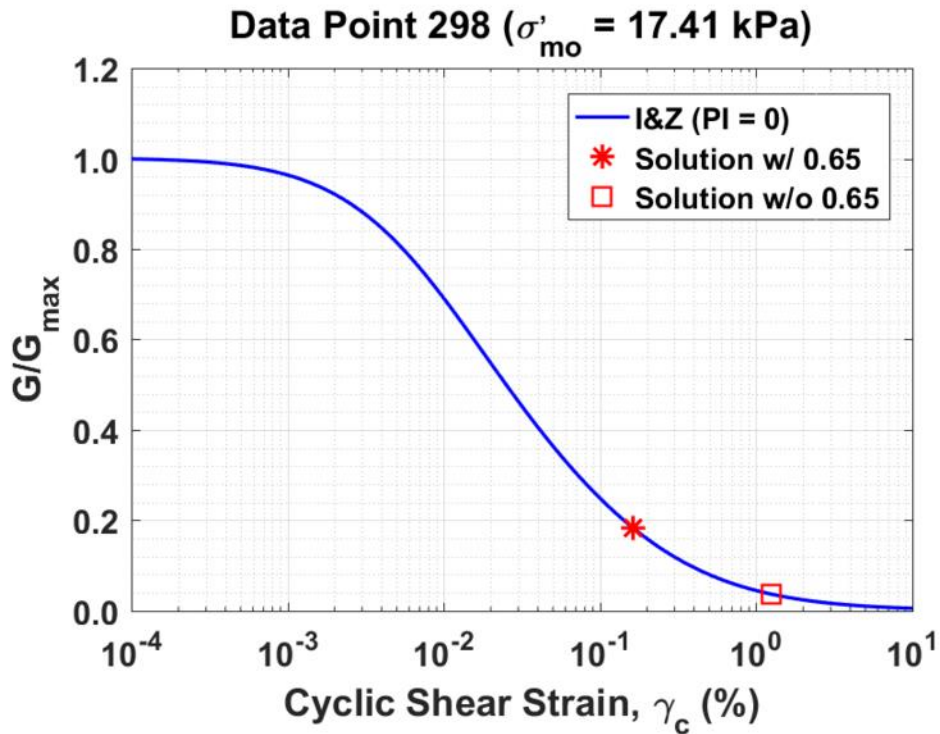


Figure B250. Normalized shear modulus reduction curves for Data Point 298 of the Kayen et al. database showing the solutions w/ and w/o the 0.65 factor

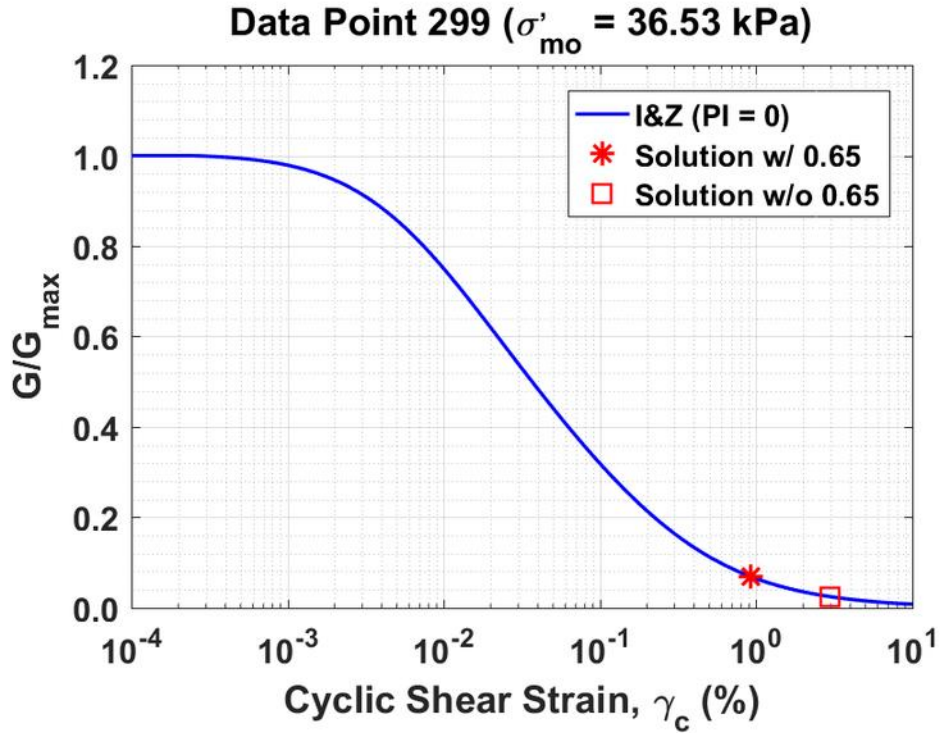


Figure B251. Normalized shear modulus reduction curves for Data Point 299 of the Kayen et al. database showing the solutions w/ and w/o the 0.65 factor

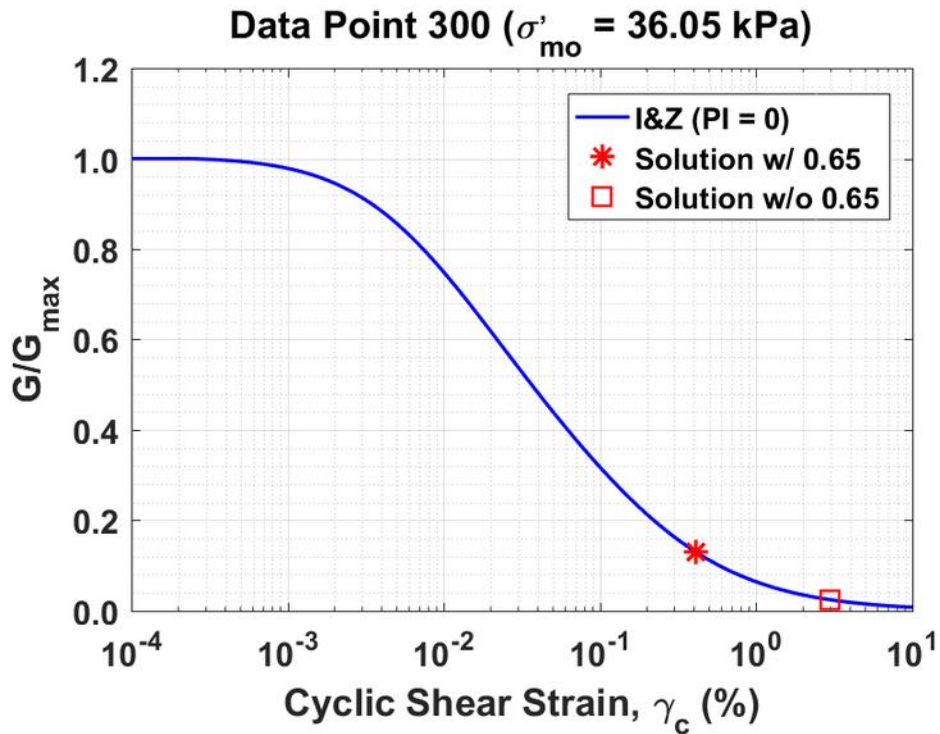


Figure B252. Normalized shear modulus reduction curves for Data Point 300 of the Kayen et al. database showing the solutions w/ and w/o the 0.65 factor

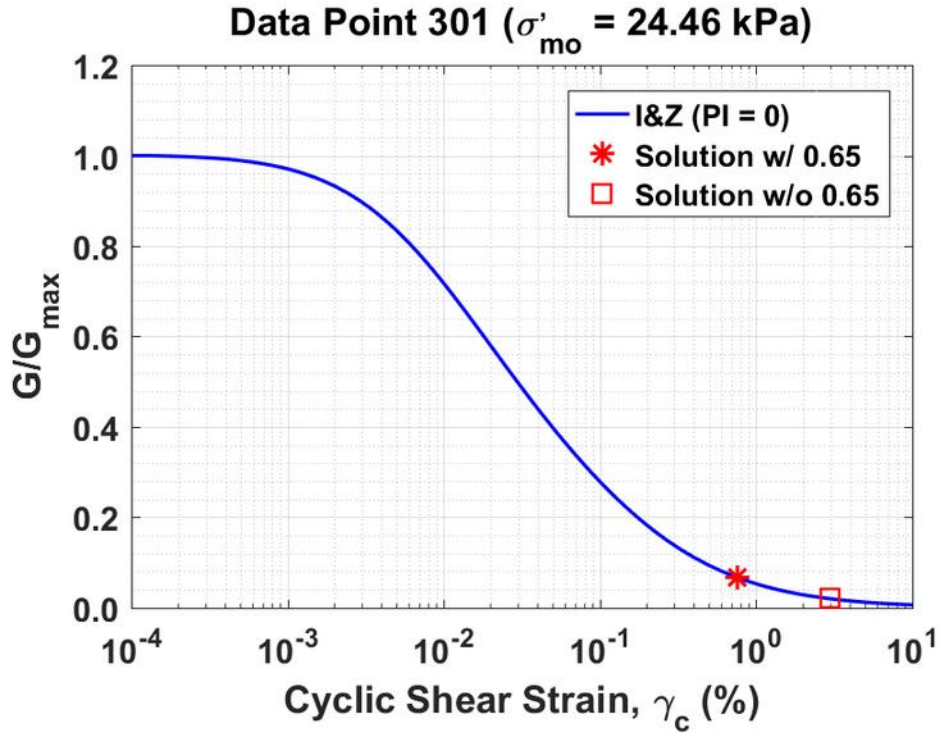


Figure B253. Normalized shear modulus reduction curves for Data Point 301 of the Kayen et al. database showing the solutions w/ and w/o the 0.65 factor

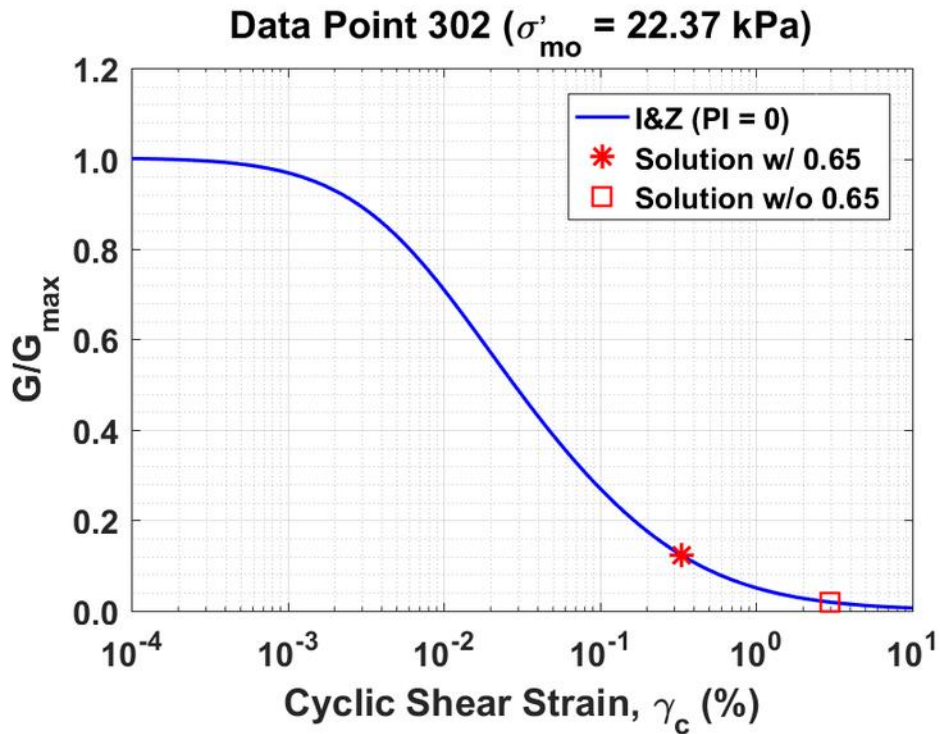


Figure B254. Normalized shear modulus reduction curves for Data Point 302 of the Kayen et al. database showing the solutions w/ and w/o the 0.65 factor

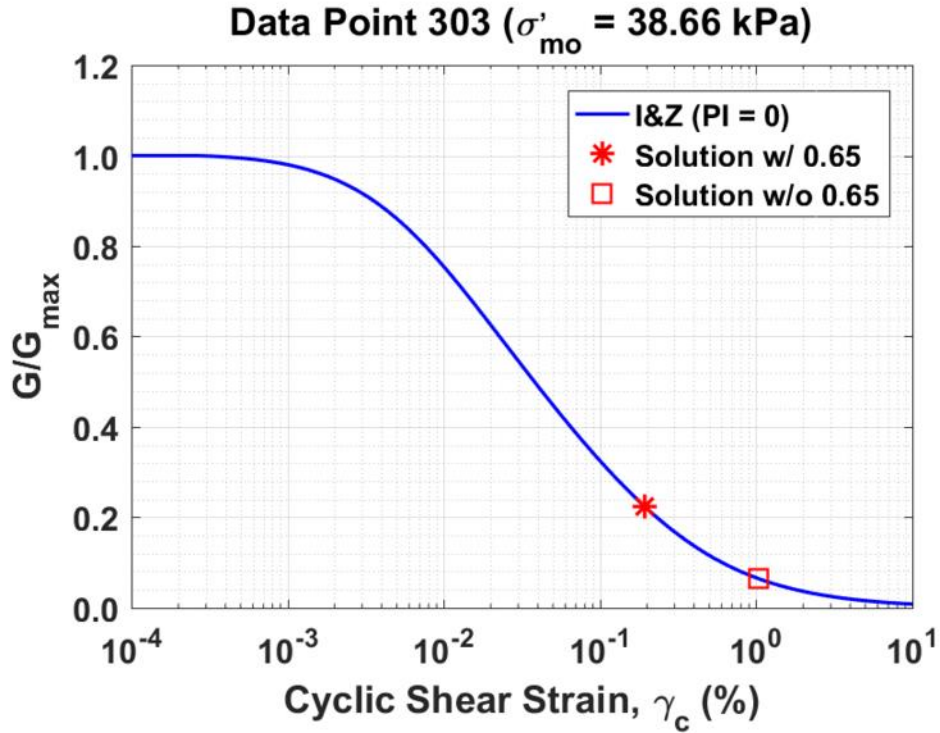


Figure B255. Normalized shear modulus reduction curves for Data Point 303 of the Kayen et al. database showing the solutions w/ and w/o the 0.65 factor

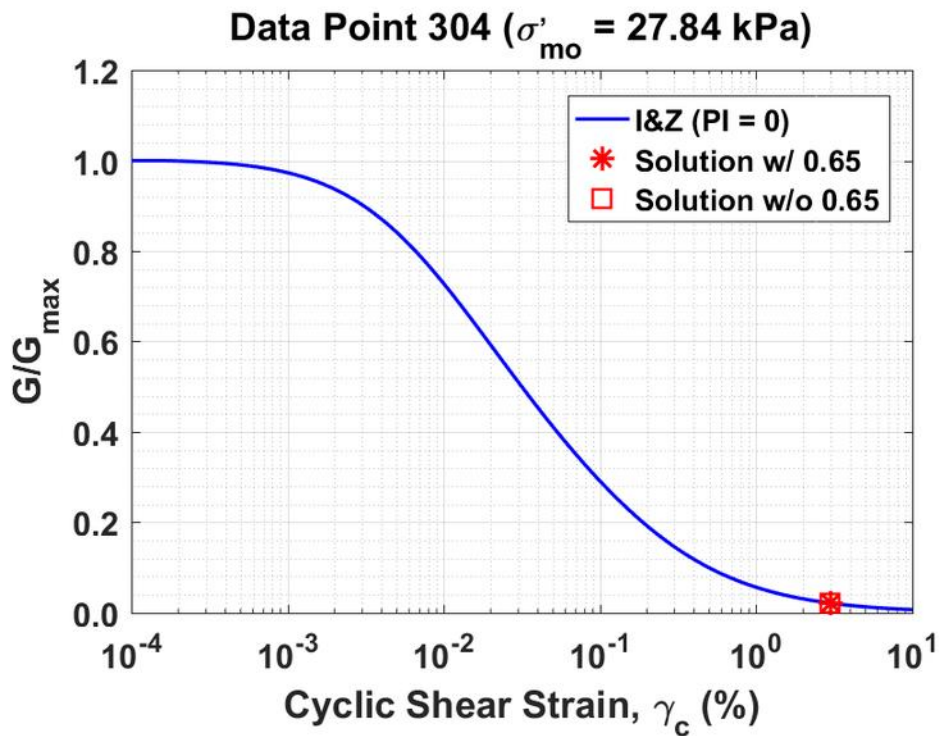


Figure B256. Normalized shear modulus reduction curves for Data Point 304 of the Kayen et al. database showing the solutions w/ and w/o the 0.65 factor

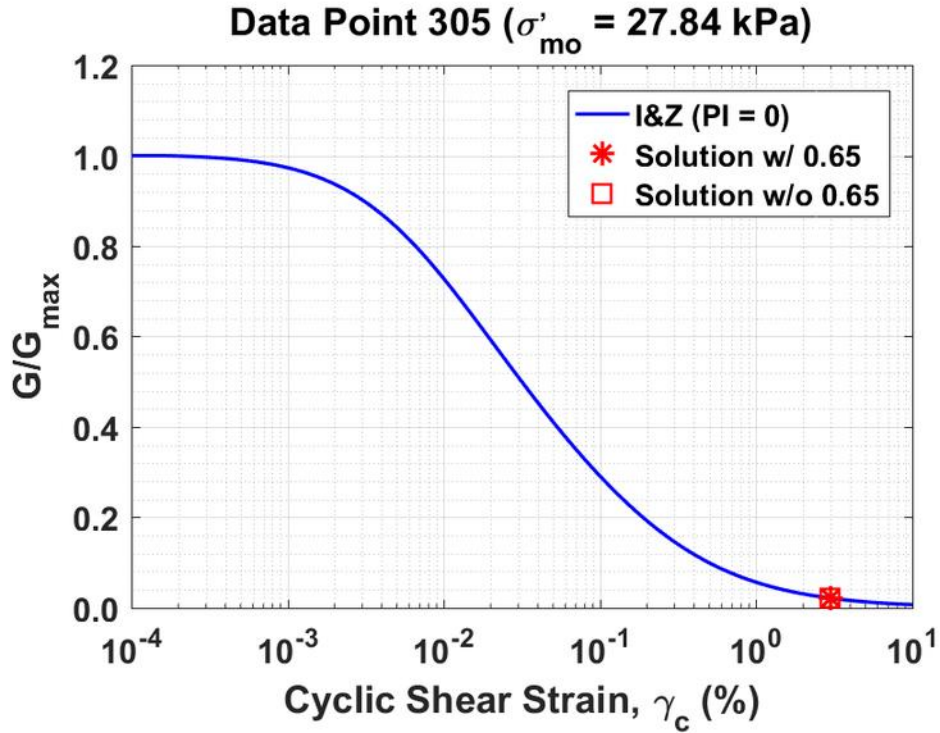


Figure B257. Normalized shear modulus reduction curves for Data Point 305 of the Kayen et al. database showing the solutions w/ and w/o the 0.65 factor

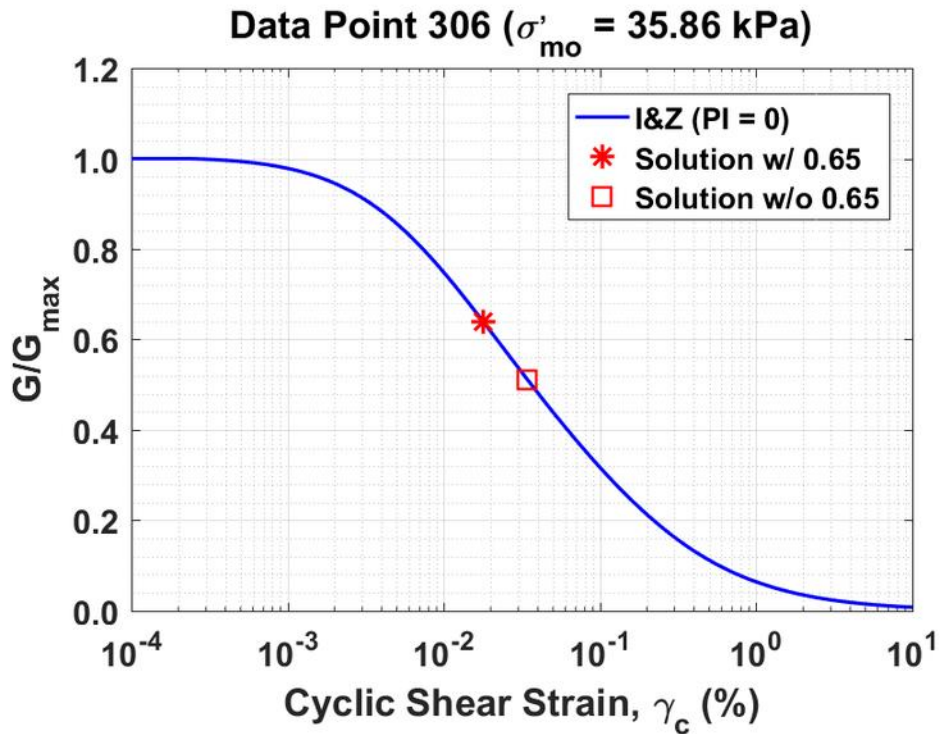


Figure B258. Normalized shear modulus reduction curves for Data Point 306 of the Kayen et al. database showing the solutions w/ and w/o the 0.65 factor

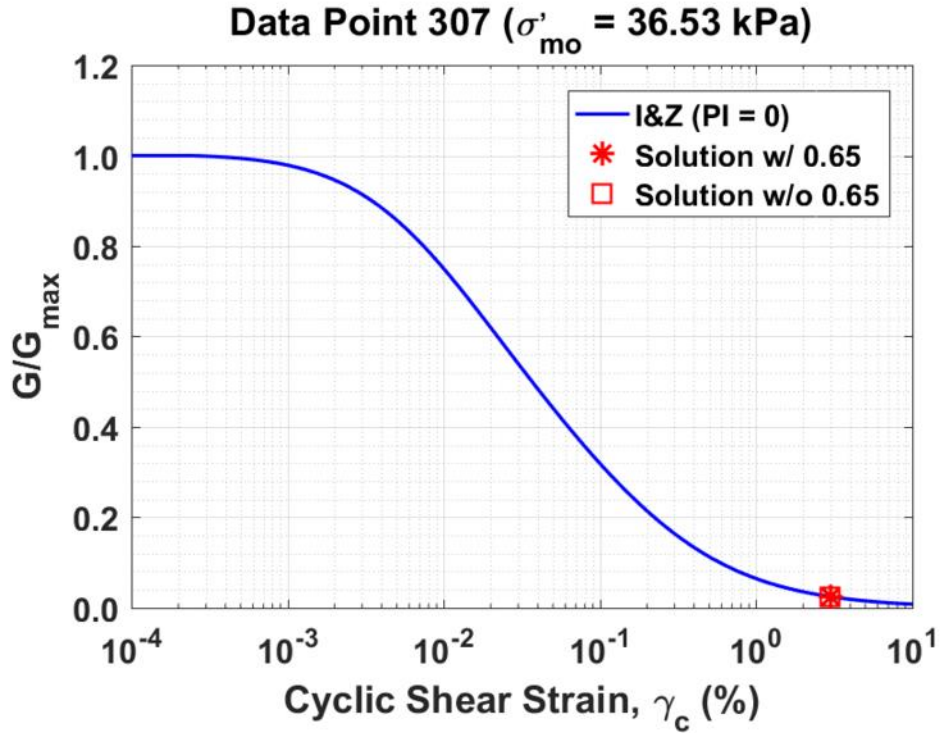


Figure B259. Normalized shear modulus reduction curves for Data Point 307 of the Kayen et al. database showing the solutions w/ and w/o the 0.65 factor

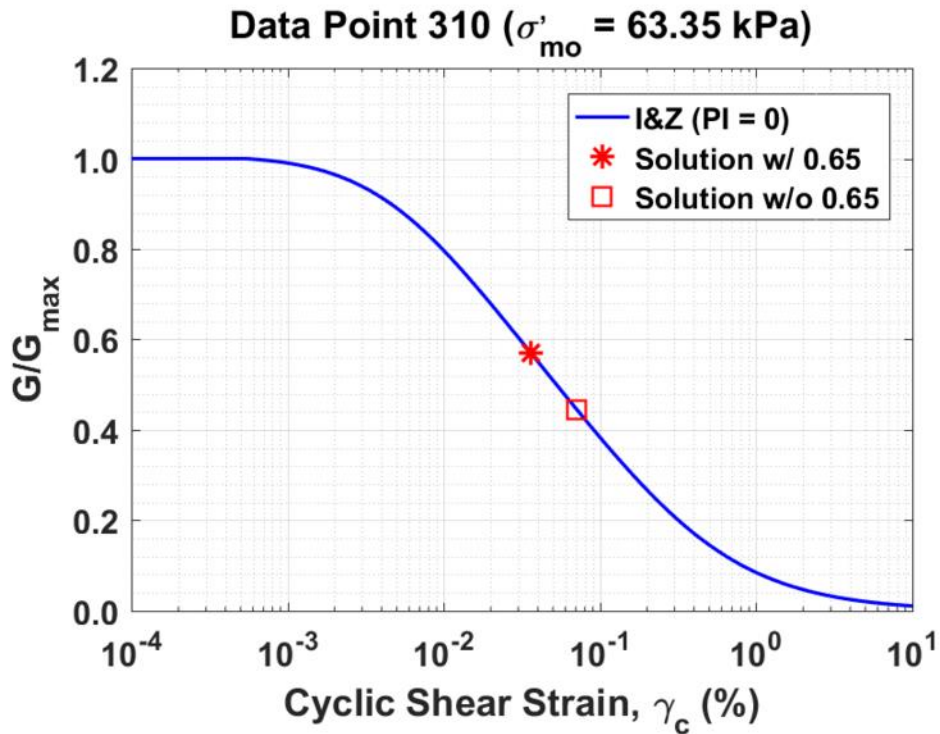


Figure B260. Normalized shear modulus reduction curves for Data Point 310 of the Kayen et al. database showing the solutions w/ and w/o the 0.65 factor

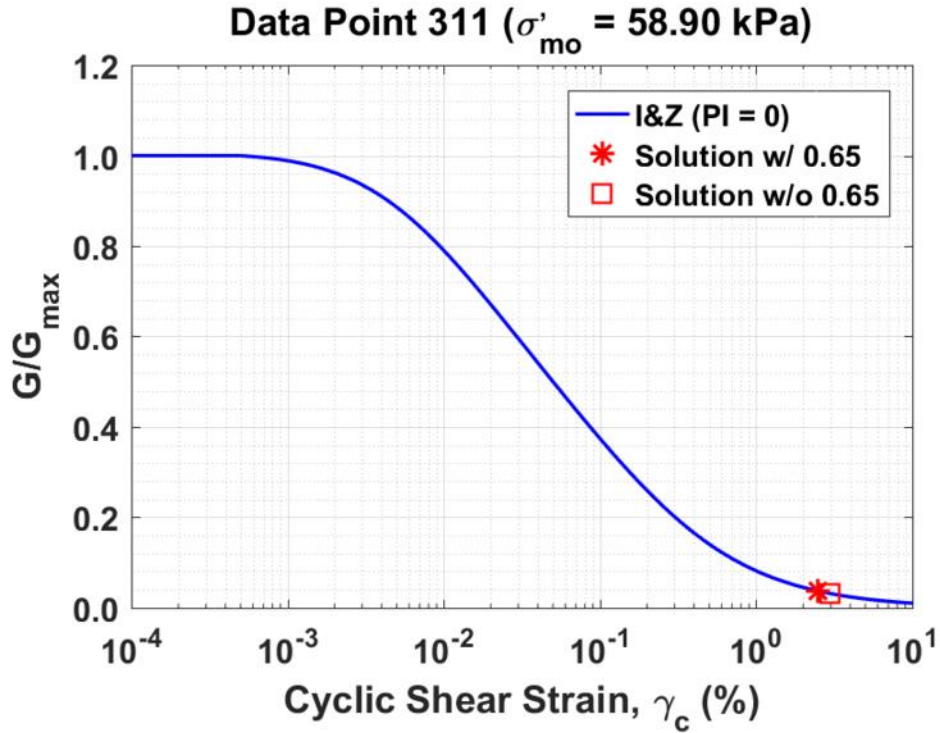


Figure B261. Normalized shear modulus reduction curves for Data Point 311 of the Kayen et al. database showing the solutions w/ and w/o the 0.65 factor

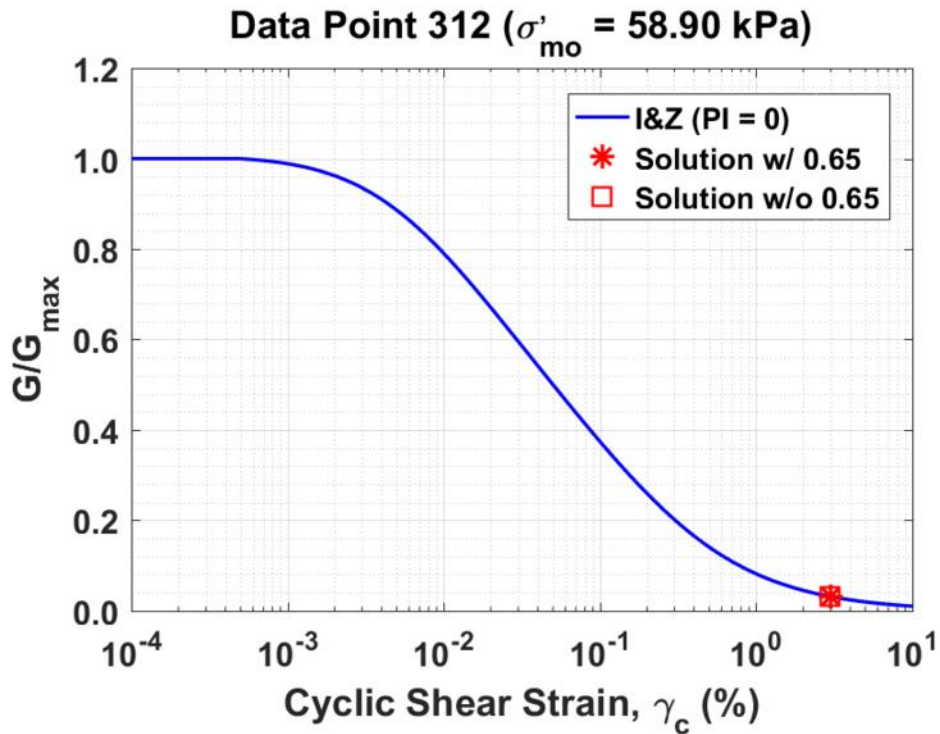


Figure B262. Normalized shear modulus reduction curves for Data Point 312 of the Kayen et al. database showing the solutions w/ and w/o the 0.65 factor

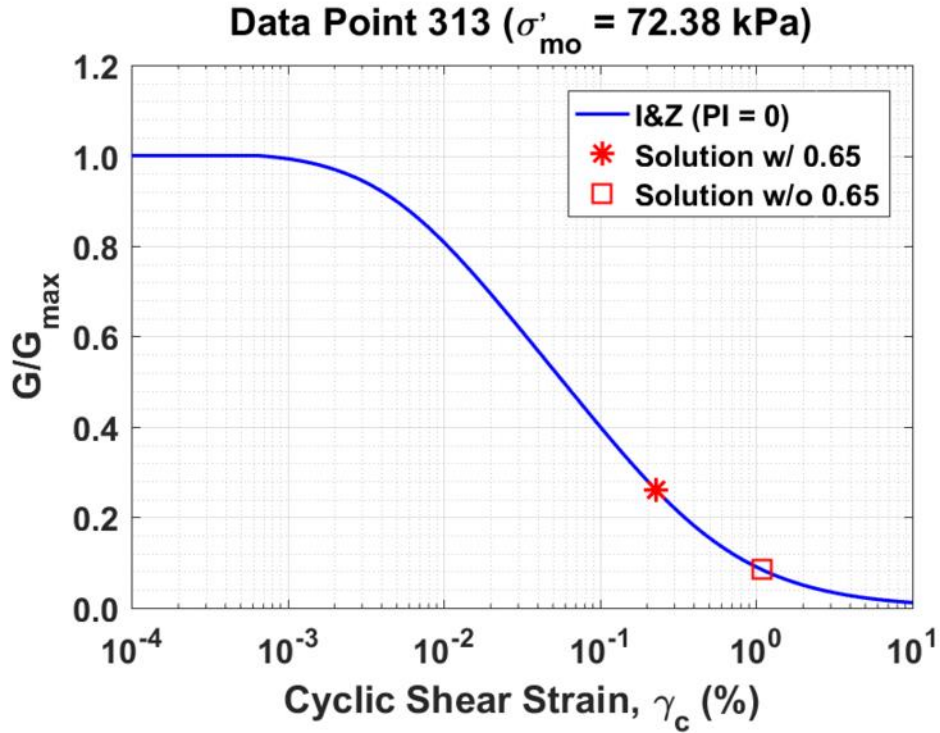


Figure B263. Normalized shear modulus reduction curves for Data Point 313 of the Kayen et al. database showing the solutions w/ and w/o the 0.65 factor

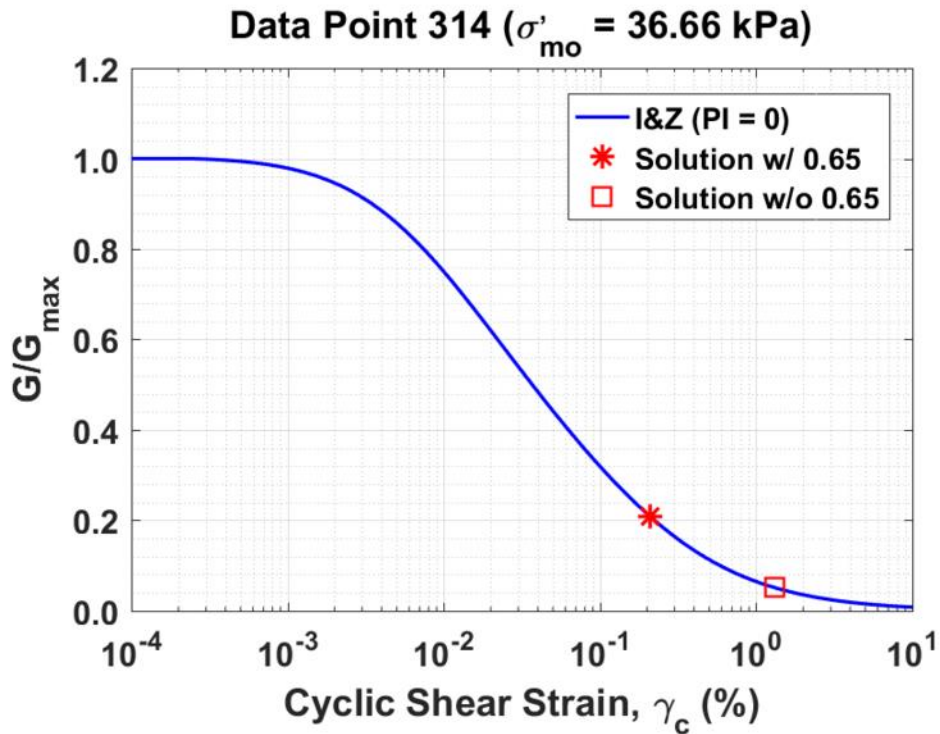


Figure B264. Normalized shear modulus reduction curves for Data Point 314 of the Kayen et al. database showing the solutions w/ and w/o the 0.65 factor

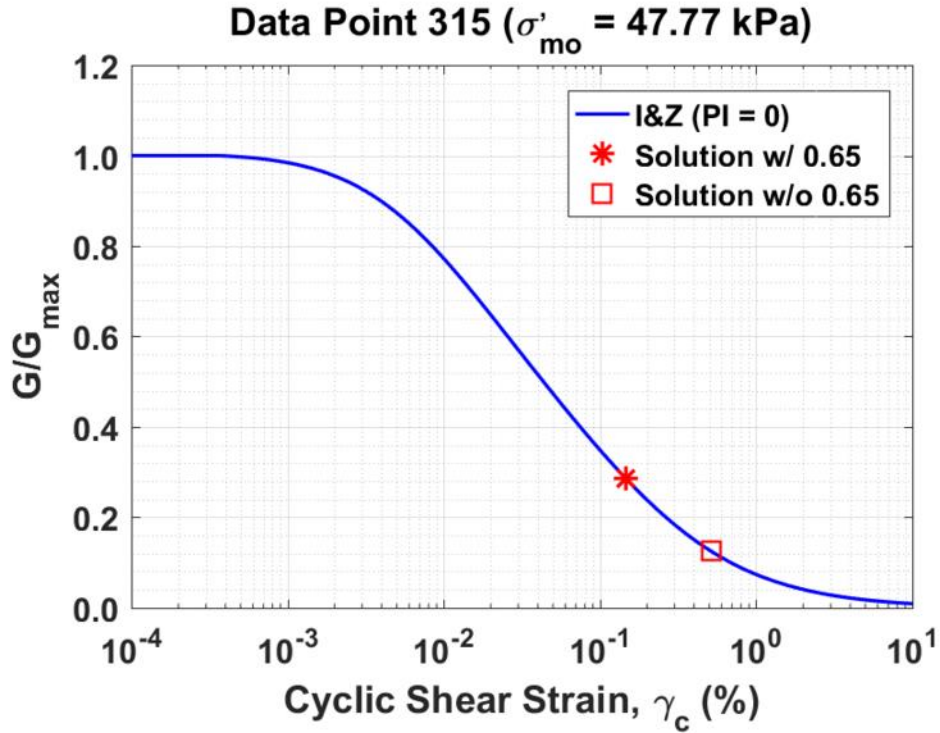


Figure B265. Normalized shear modulus reduction curves for Data Point 315 of the Kayen et al. database showing the solutions w/ and w/o the 0.65 factor

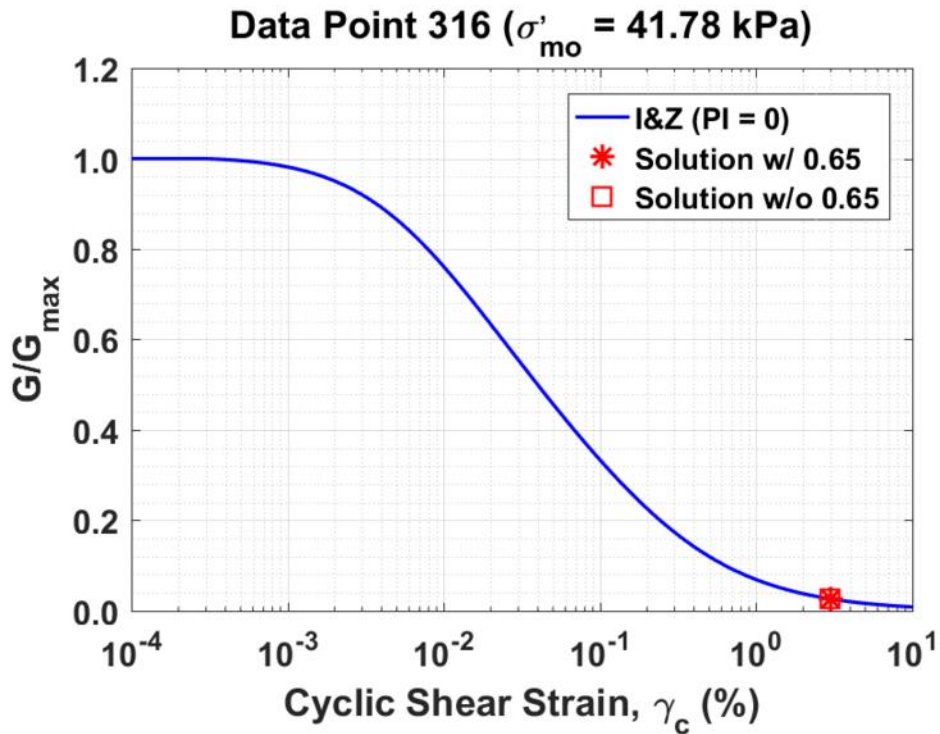


Figure B266. Normalized shear modulus reduction curves for Data Point 316 of the Kayen et al. database showing the solutions w/ and w/o the 0.65 factor

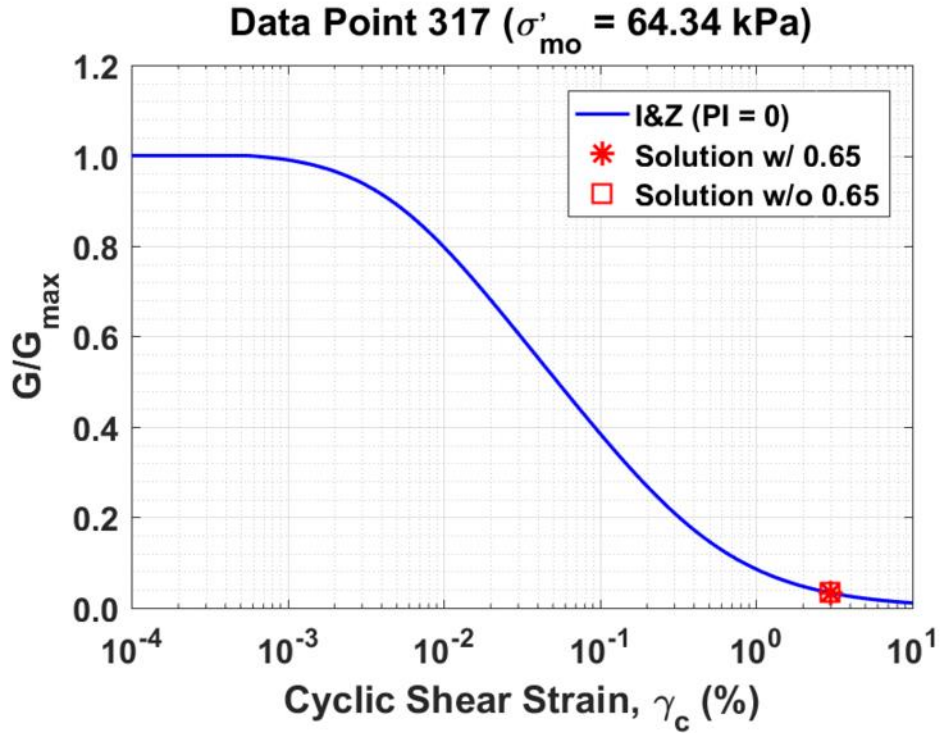


Figure B267. Normalized shear modulus reduction curves for Data Point 317 of the Kayen et al. database showing the solutions w/ and w/o the 0.65 factor

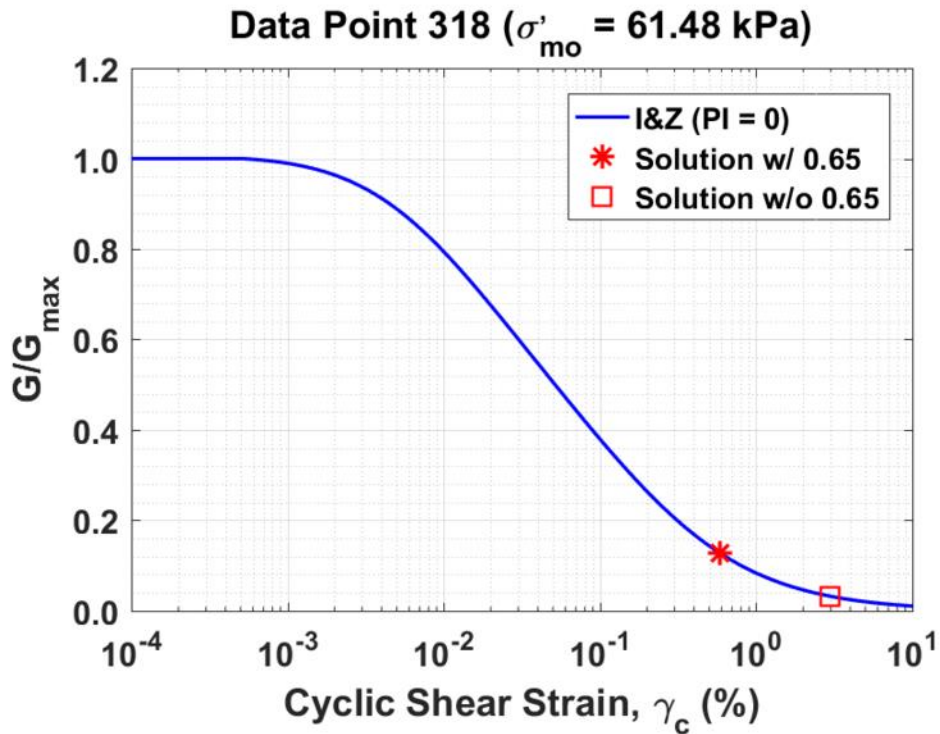


Figure B268. Normalized shear modulus reduction curves for Data Point 318 of the Kayen et al. database showing the solutions w/ and w/o the 0.65 factor

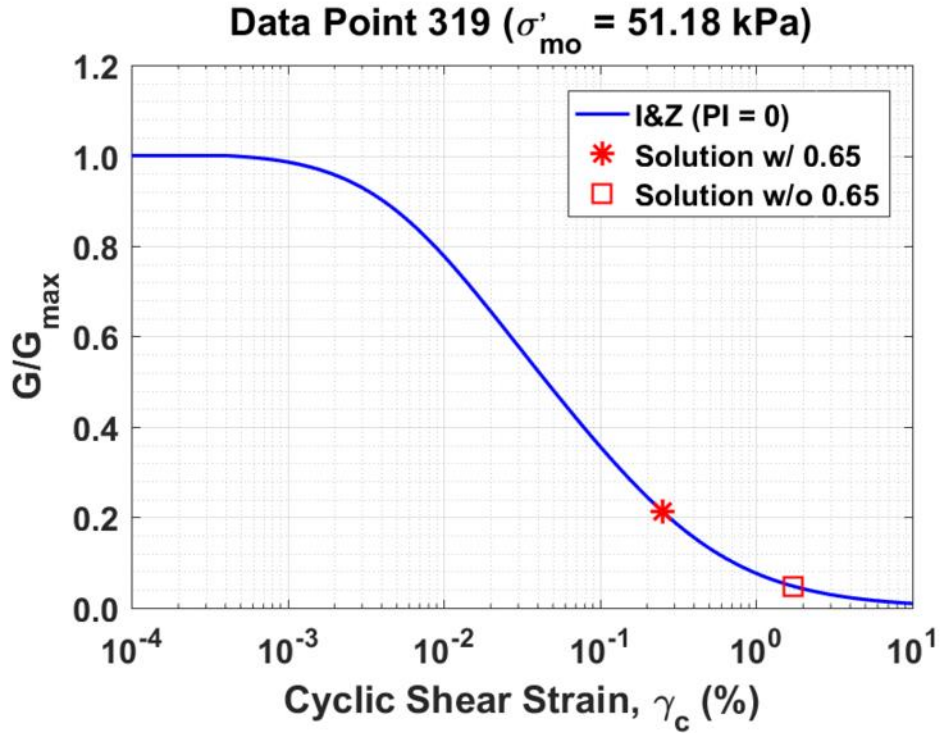


Figure B269. Normalized shear modulus reduction curves for Data Point 319 of the Kayen et al. database showing the solutions w/ and w/o the 0.65 factor

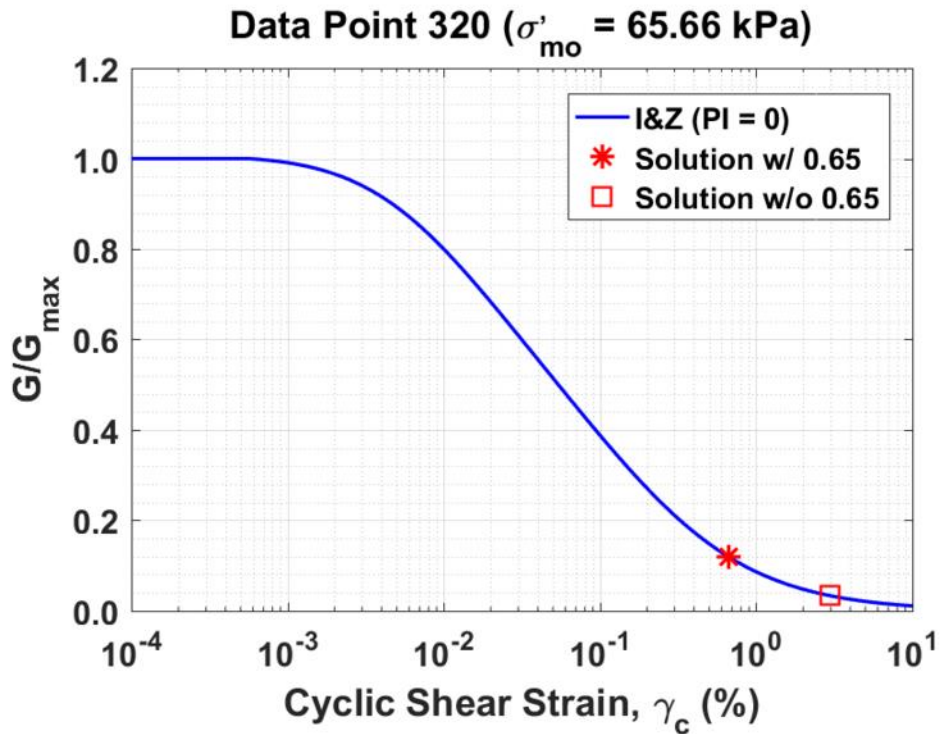


Figure B270. Normalized shear modulus reduction curves for Data Point 320 of the Kayen et al. database showing the solutions w/ and w/o the 0.65 factor

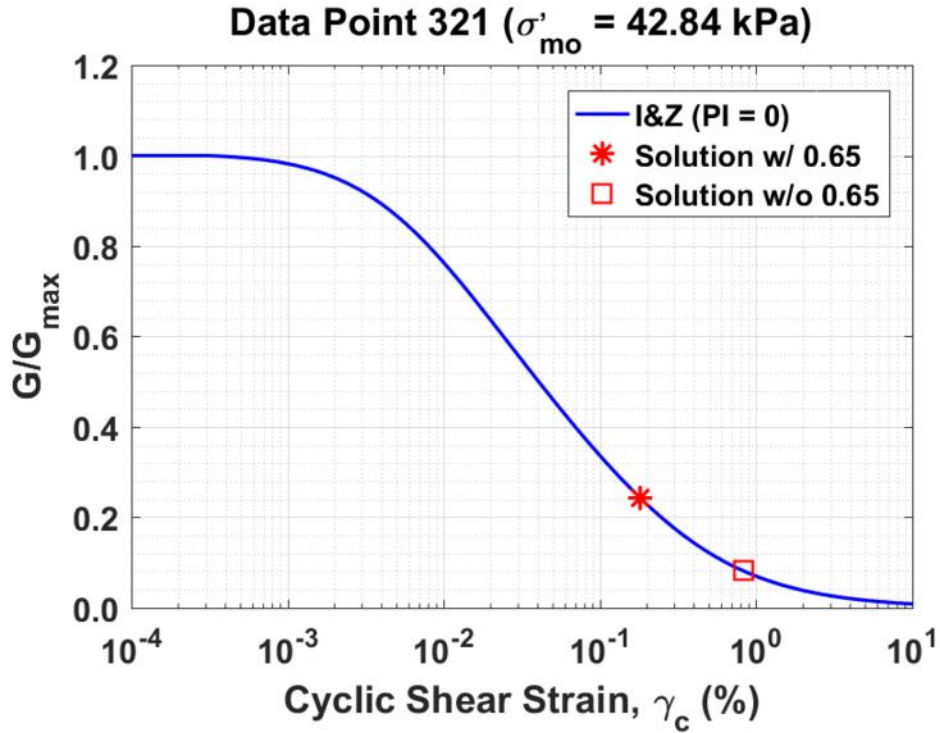


Figure B271. Normalized shear modulus reduction curves for Data Point 231 of the Kayen et al. database showing the solutions w/ and w/o the 0.65 factor

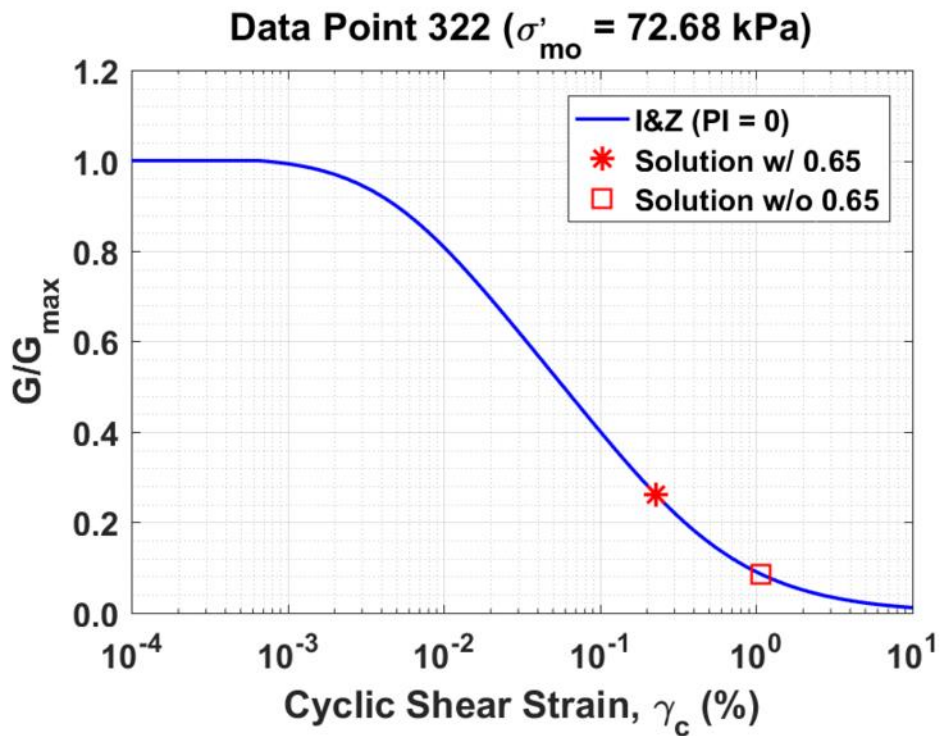


Figure B272. Normalized shear modulus reduction curves for Data Point 322 of the Kayen et al. database showing the solutions w/ and w/o the 0.65 factor

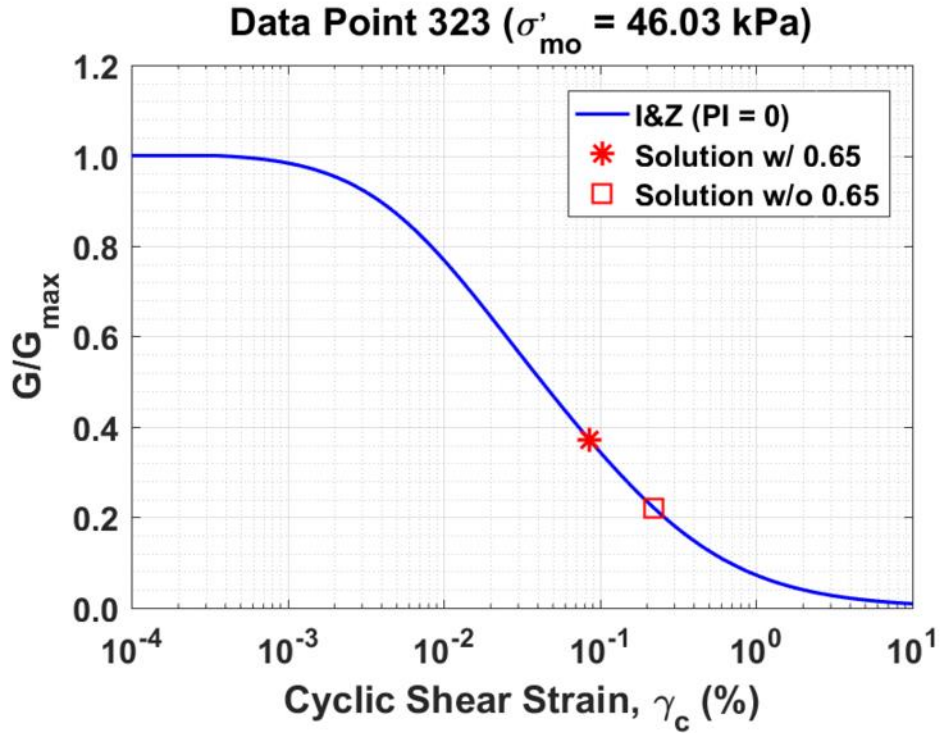


Figure B273. Normalized shear modulus reduction curves for Data Point 323 of the Kayen et al. database showing the solutions w/ and w/o the 0.65 factor

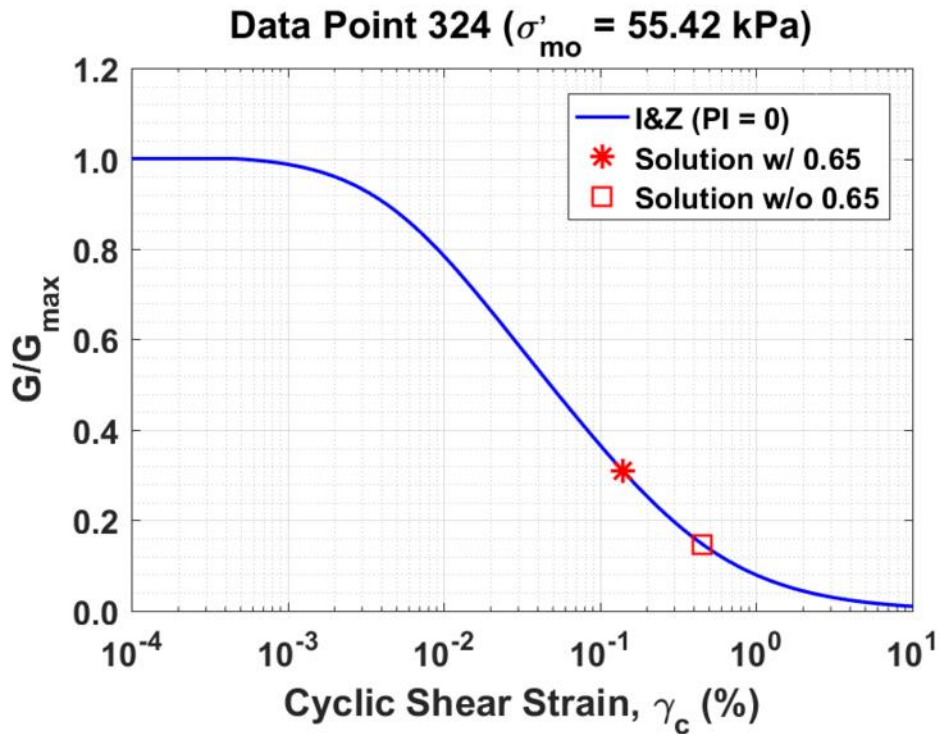


Figure B274. Normalized shear modulus reduction curves for Data Point 324 of the Kayen et al. database showing the solutions w/ and w/o the 0.65 factor

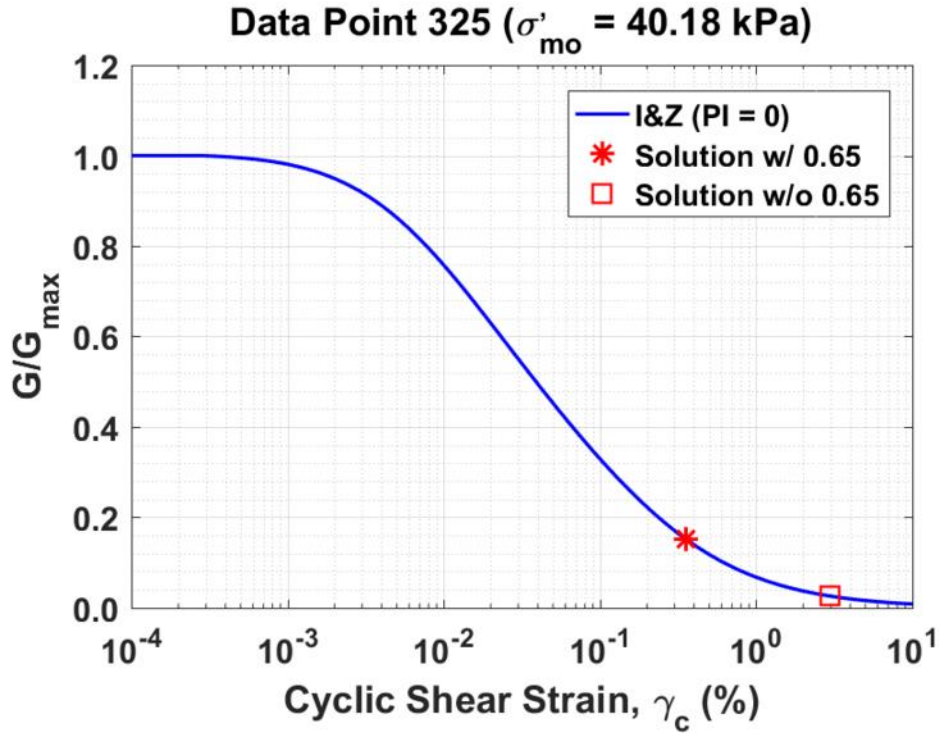


Figure B275. Normalized shear modulus reduction curves for Data Point 325 of the Kayen et al. database showing the solutions w/ and w/o the 0.65 factor

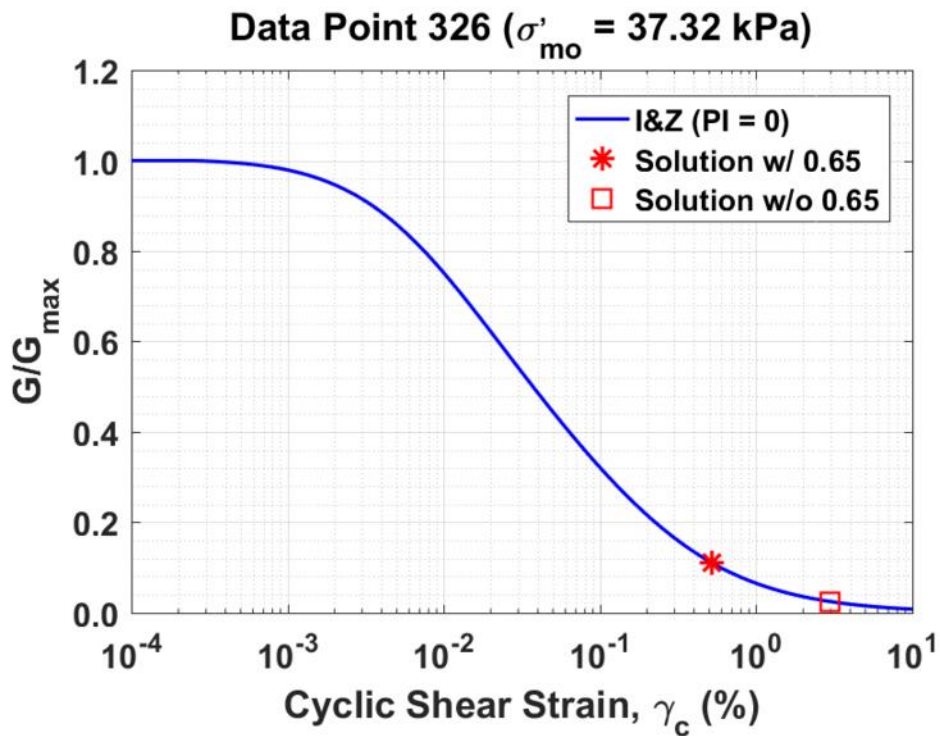


Figure B276. Normalized shear modulus reduction curves for Data Point 326 of the Kayen et al. database showing the solutions w/ and w/o the 0.65 factor

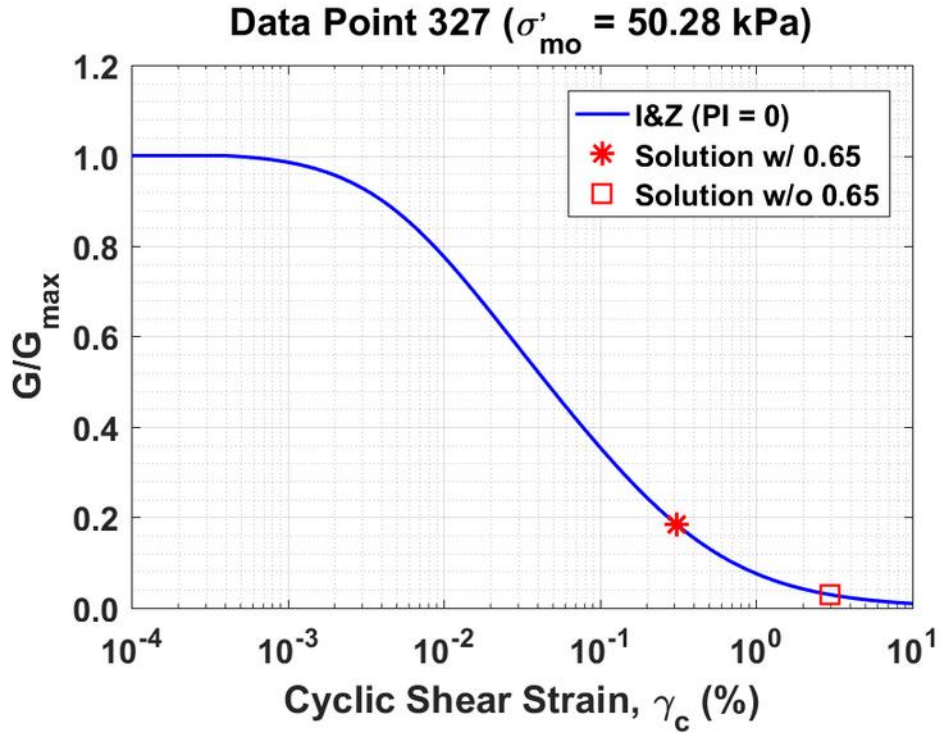


Figure B277. Normalized shear modulus reduction curves for Data Point 327 of the Kayen et al. database showing the solutions w/ and w/o the 0.65 factor

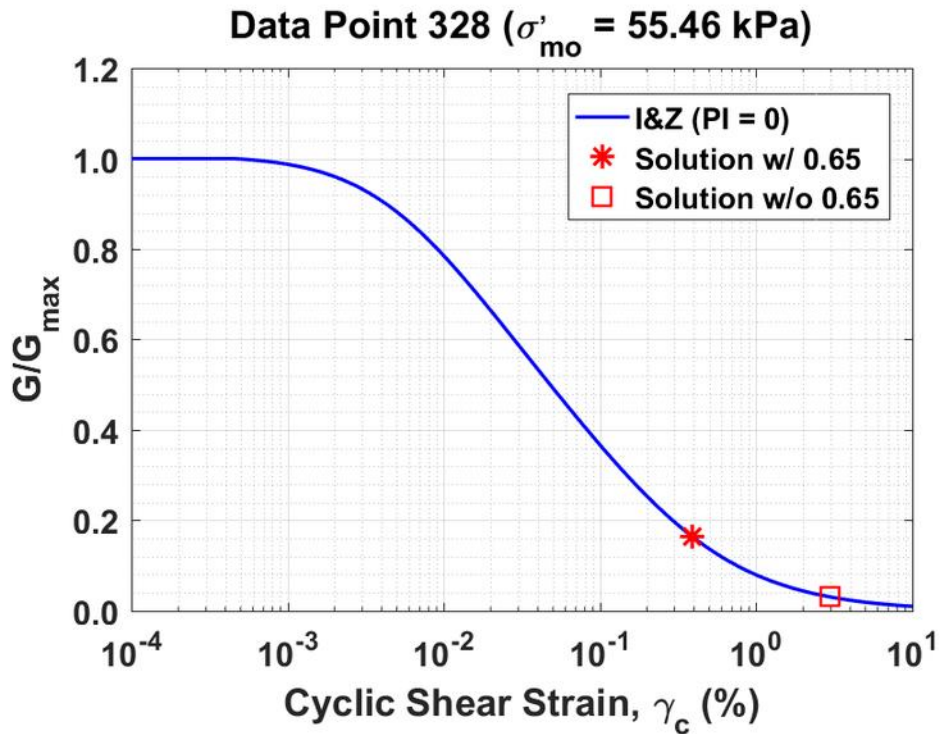


Figure B278. Normalized shear modulus reduction curves for Data Point 328 of the Kayen et al. database showing the solutions w/ and w/o the 0.65 factor

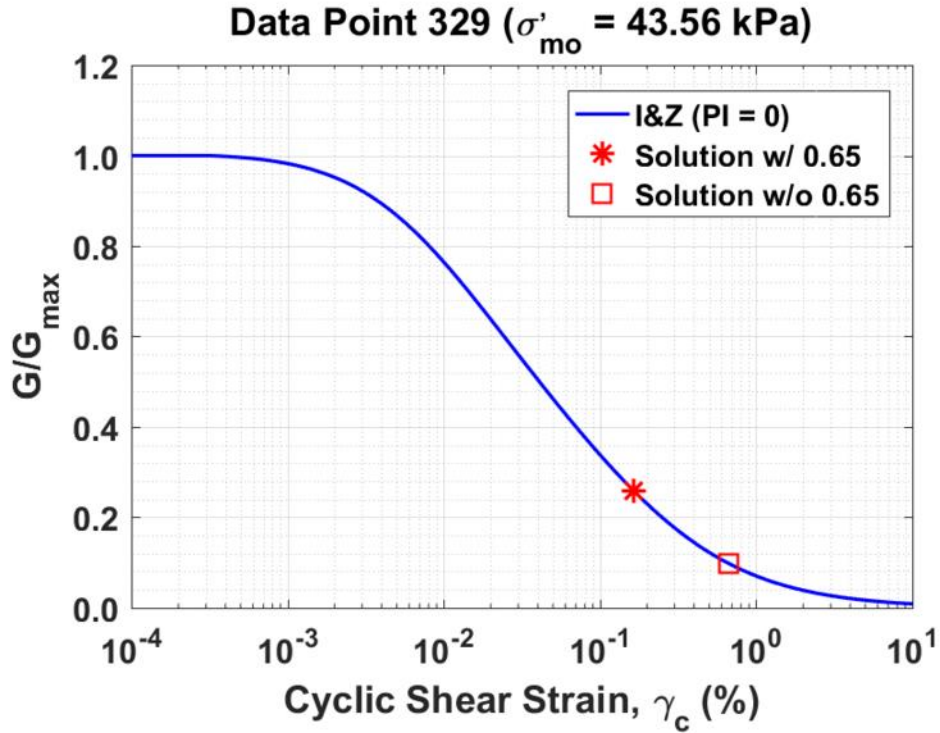


Figure B279. Normalized shear modulus reduction curves for Data Point 329 of the Kayen et al. database showing the solutions w/ and w/o the 0.65 factor

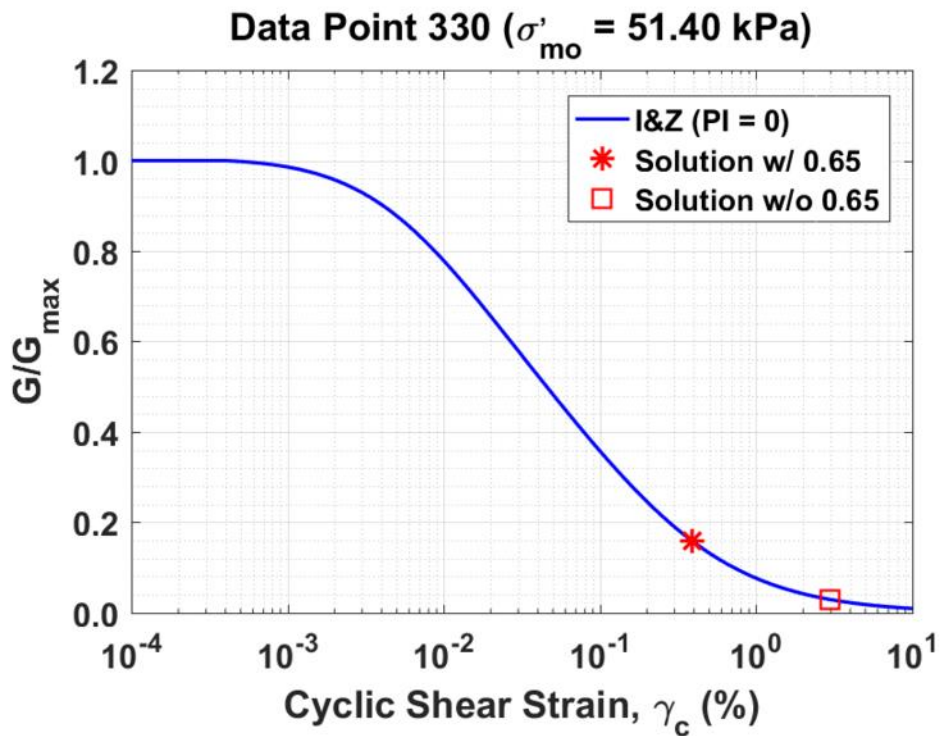


Figure B280. Normalized shear modulus reduction curves for Data Point 330 of the Kayen et al. database showing the solutions w/ and w/o the 0.65 factor

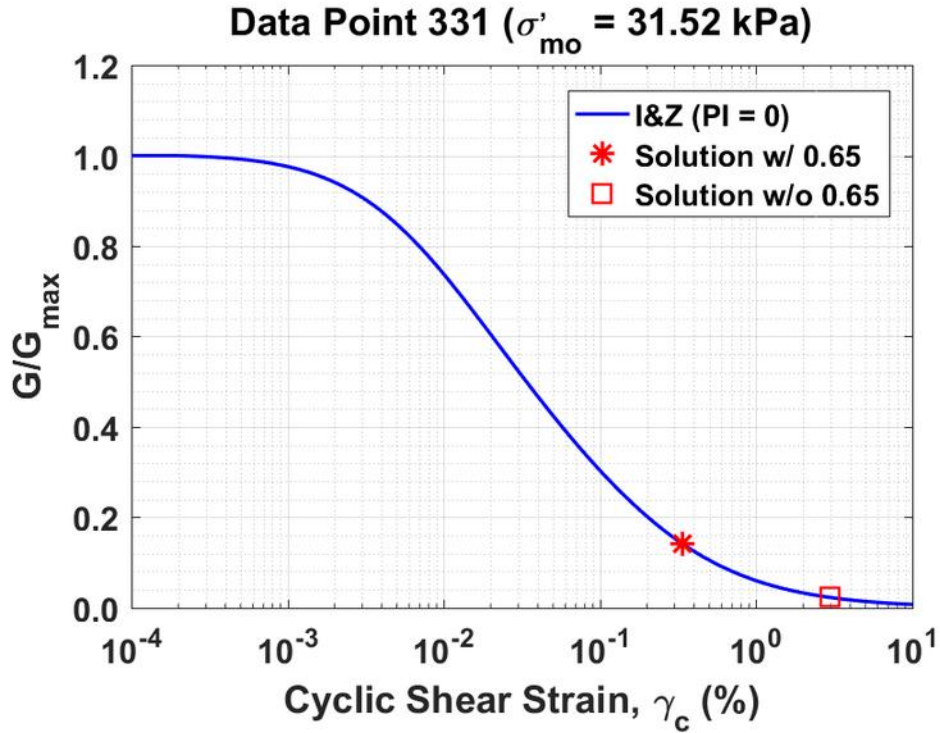


Figure B281. Normalized shear modulus reduction curves for Data Point 331 of the Kayen et al. database showing the solutions w/ and w/o the 0.65 factor

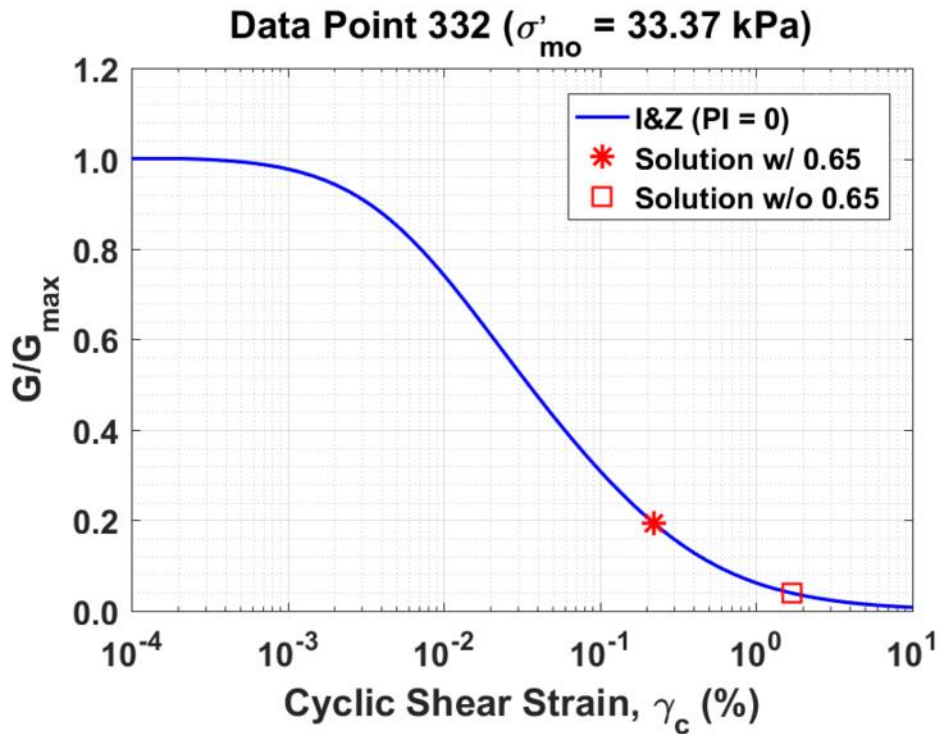


Figure B282. Normalized shear modulus reduction curves for Data Point 332 of the Kayen et al. database showing the solutions w/ and w/o the 0.65 factor

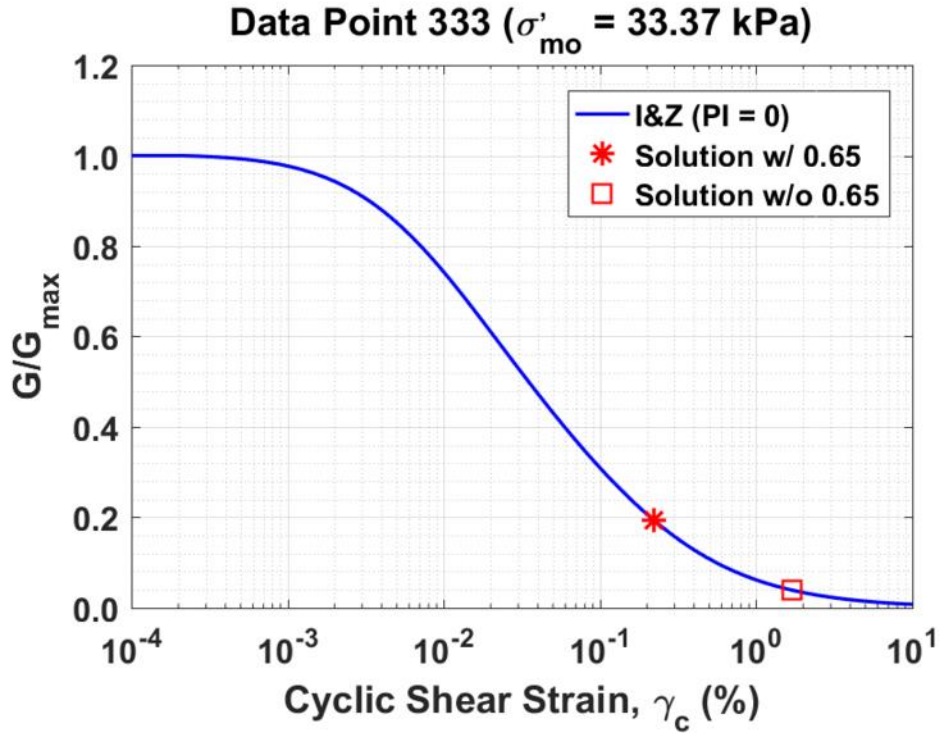


Figure B283. Normalized shear modulus reduction curves for Data Point 333 of the Kayen et al. database showing the solutions w/ and w/o the 0.65 factor

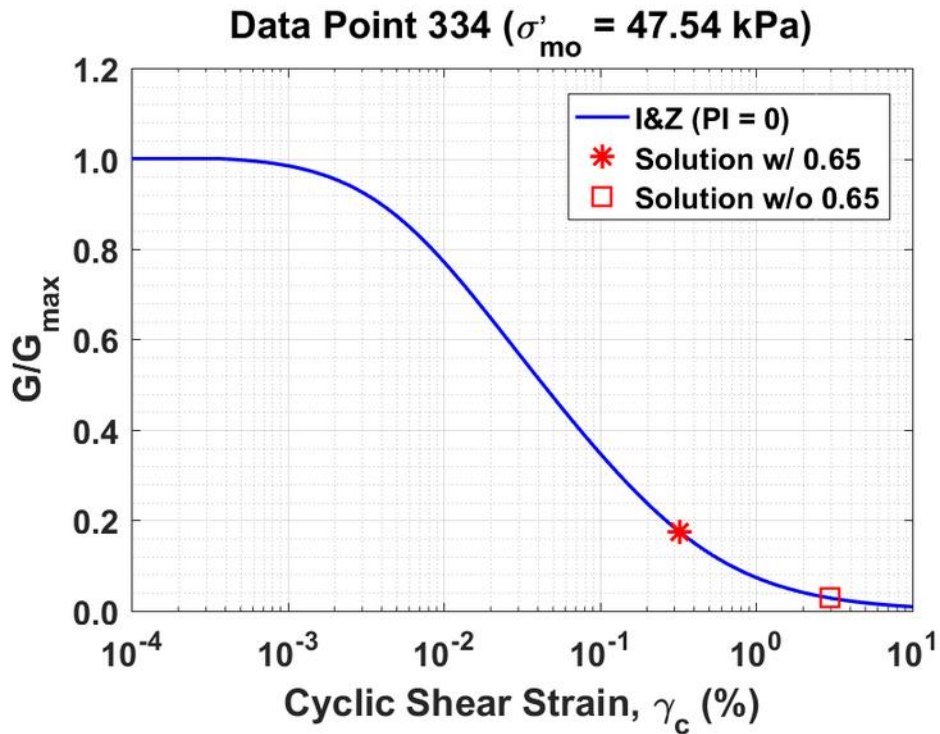


Figure B284. Normalized shear modulus reduction curves for Data Point 334 of the Kayen et al. database showing the solutions w/ and w/o the 0.65 factor

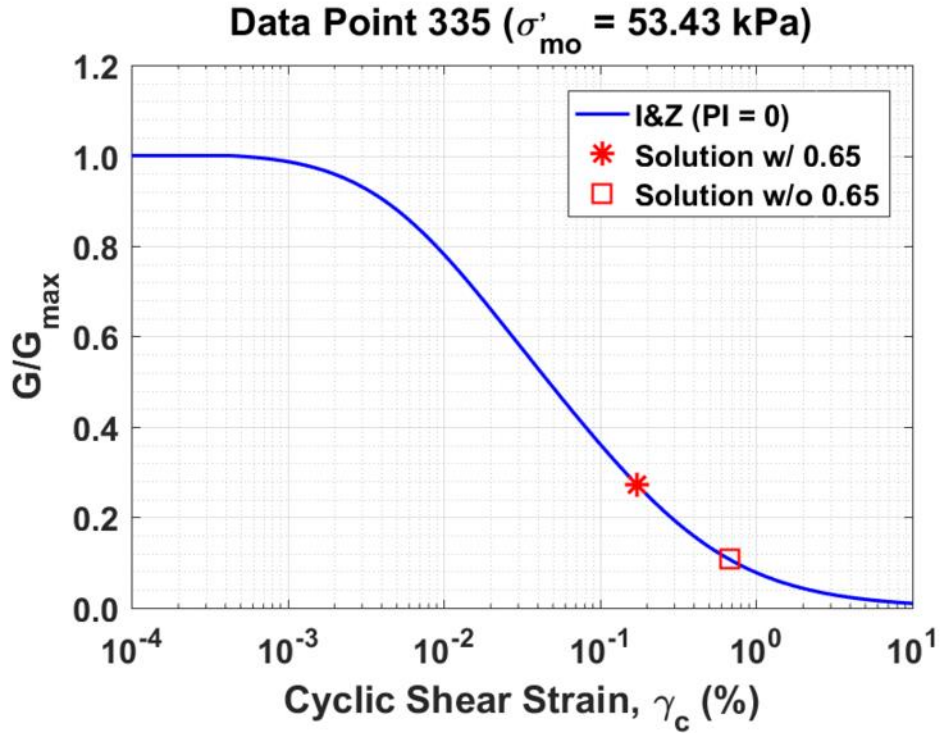


Figure B285. Normalized shear modulus reduction curves for Data Point 335 of the Kayen et al. database showing the solutions w/ and w/o the 0.65 factor

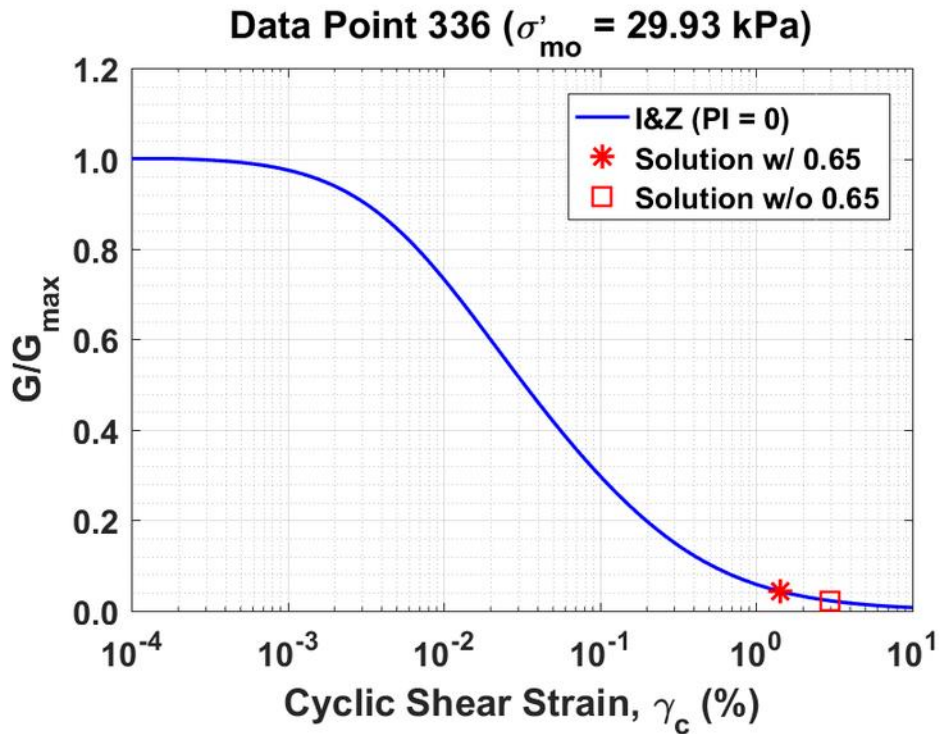


Figure B286. Normalized shear modulus reduction curves for Data Point 336 of the Kayen et al. database showing the solutions w/ and w/o the 0.65 factor

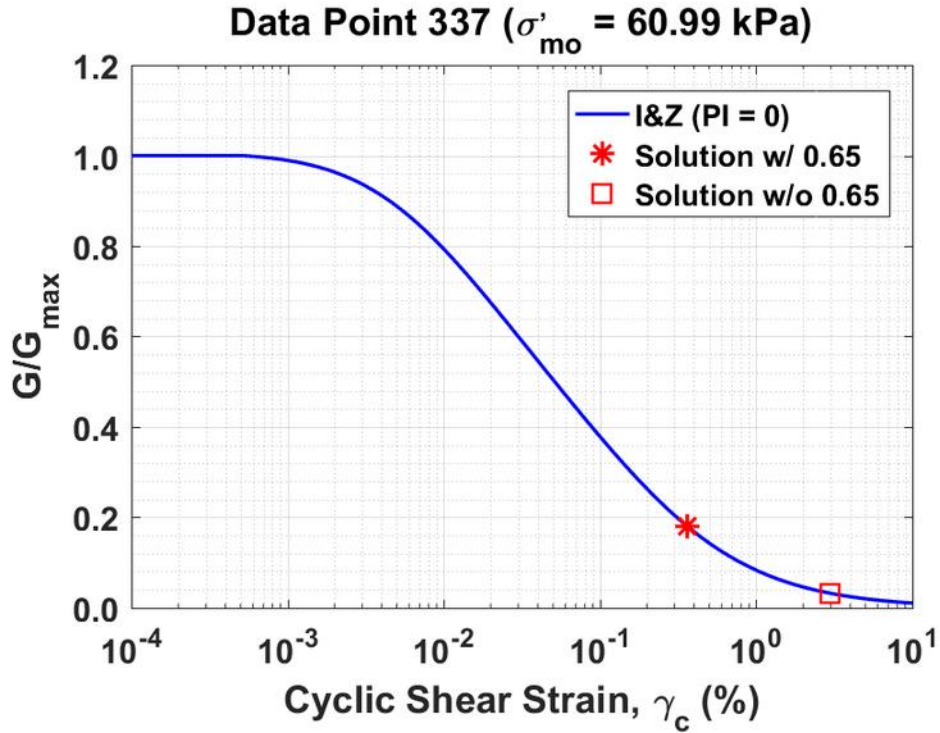


Figure B287. Normalized shear modulus reduction curves for Data Point 337 of the Kayen et al. database showing the solutions w/ and w/o the 0.65 factor

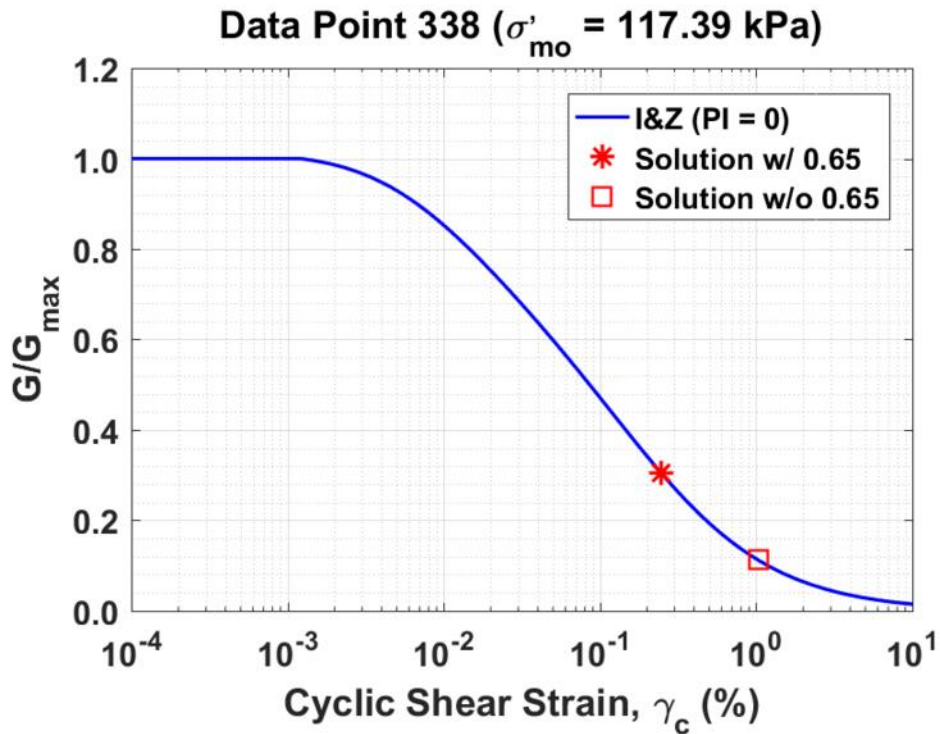


Figure B288. Normalized shear modulus reduction curves for Data Point 338 of the Kayen et al. database showing the solutions w/ and w/o the 0.65 factor

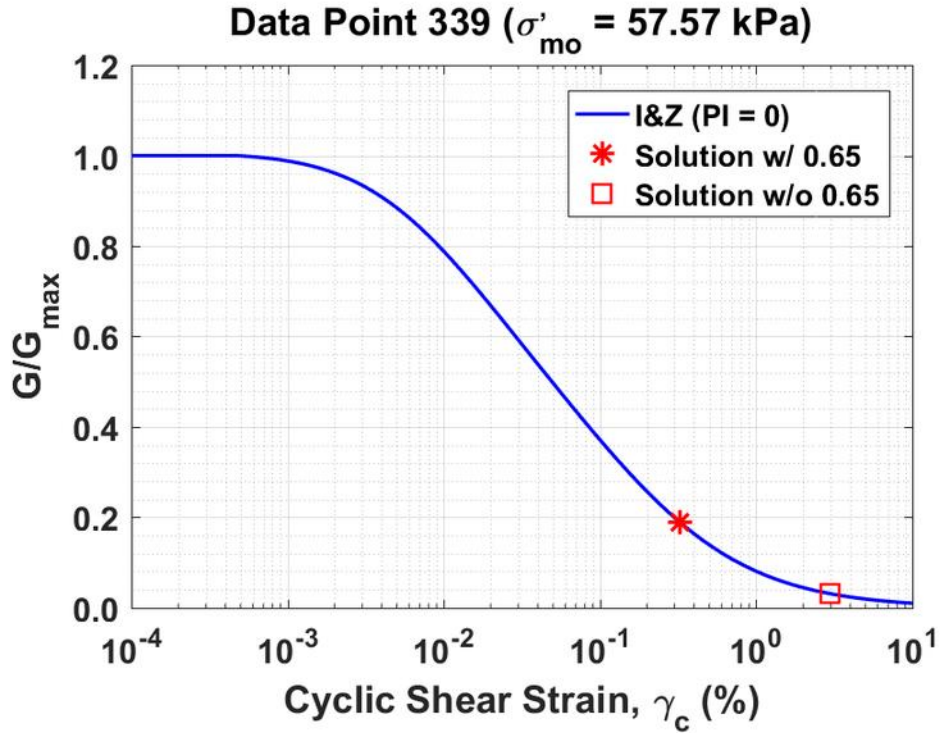


Figure B289. Normalized shear modulus reduction curves for Data Point 339 of the Kayen et al. database showing the solutions w/ and w/o the 0.65 factor

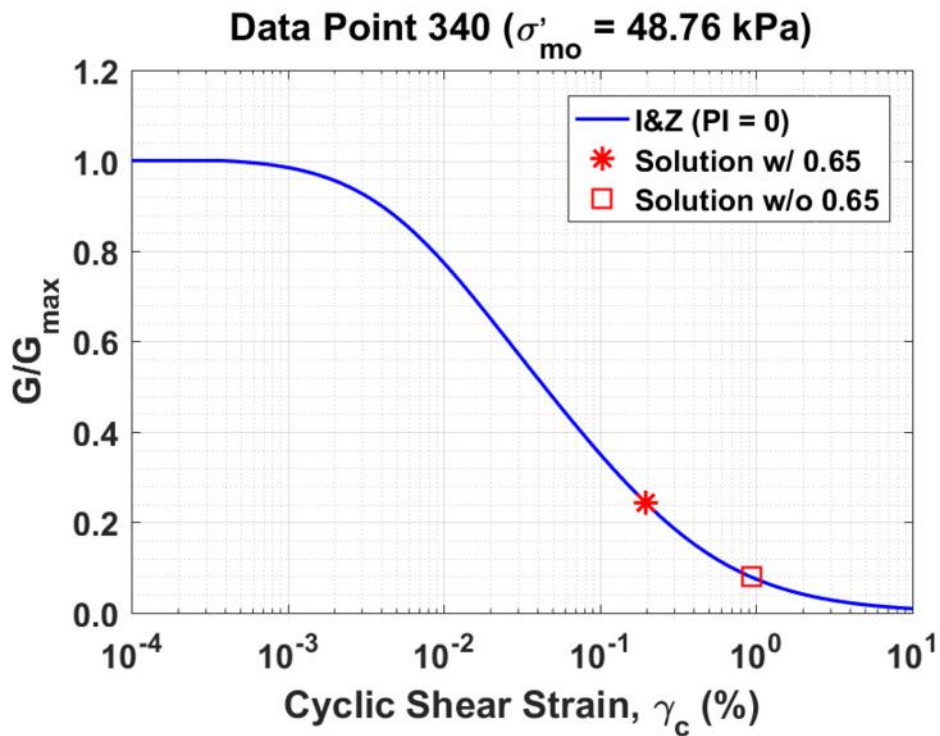


Figure B290. Normalized shear modulus reduction curves for Data Point 340 of the Kayen et al. database showing the solutions w/ and w/o the 0.65 factor

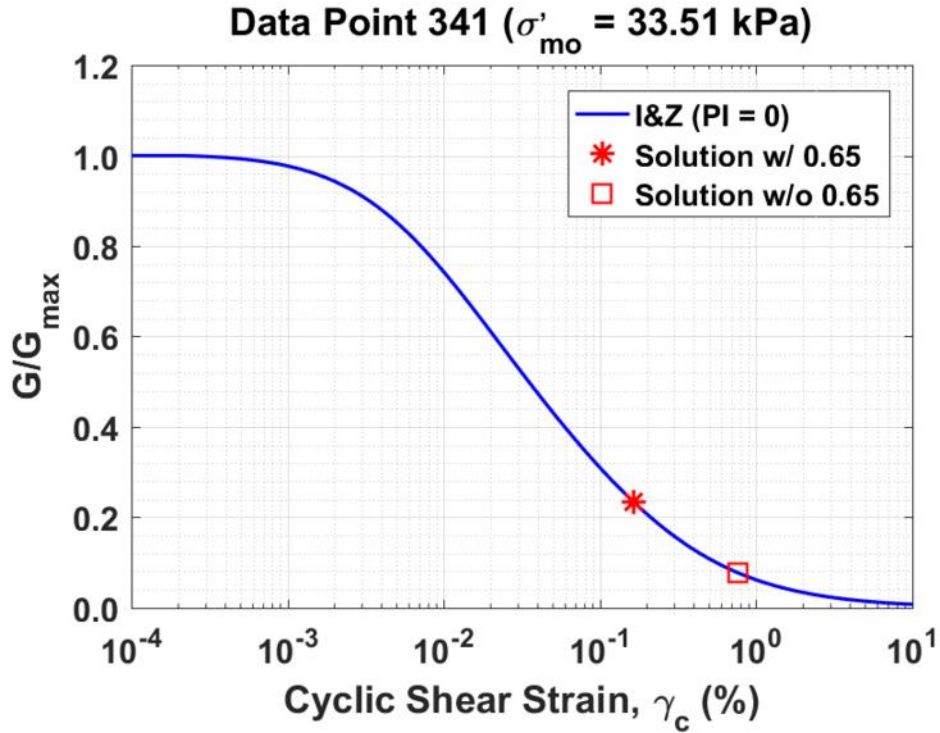


Figure B291. Normalized shear modulus reduction curves for Data Point 341 of the Kayen et al. database showing the solutions w/ and w/o the 0.65 factor

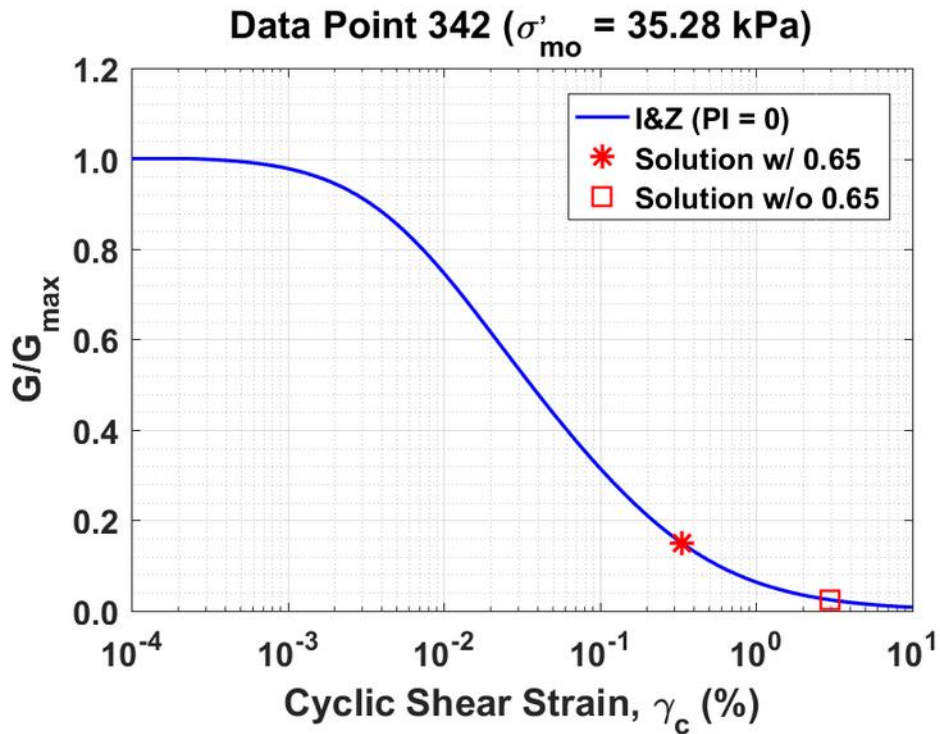


Figure B292. Normalized shear modulus reduction curves for Data Point 342 of the Kayen et al. database showing the solutions w/ and w/o the 0.65 factor

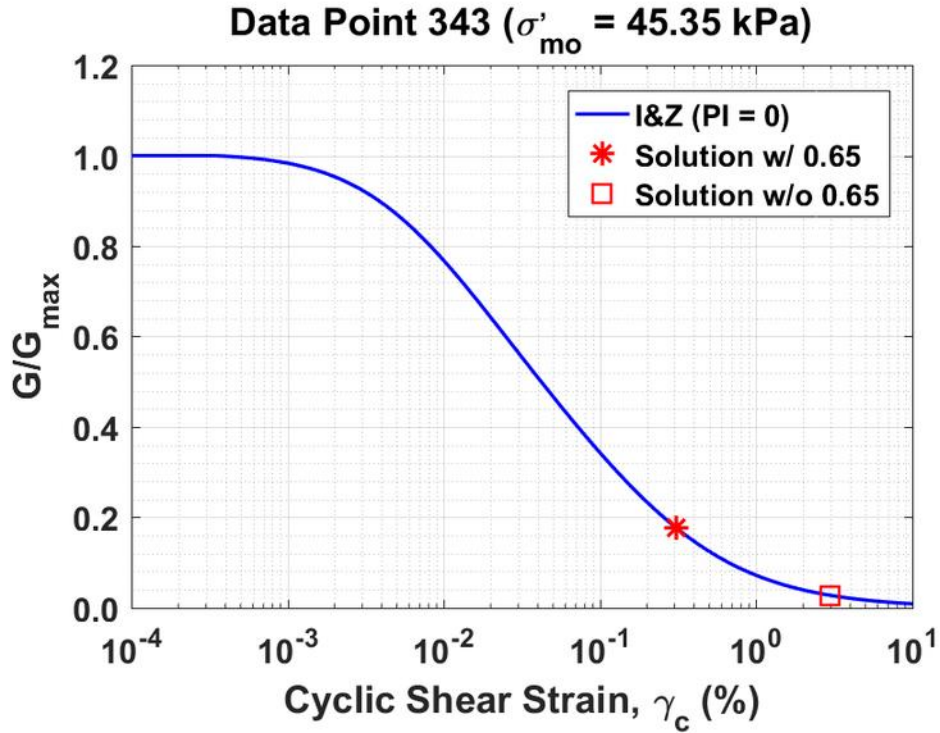


Figure B293. Normalized shear modulus reduction curves for Data Point 343 of the Kayen et al. database showing the solutions w/ and w/o the 0.65 factor

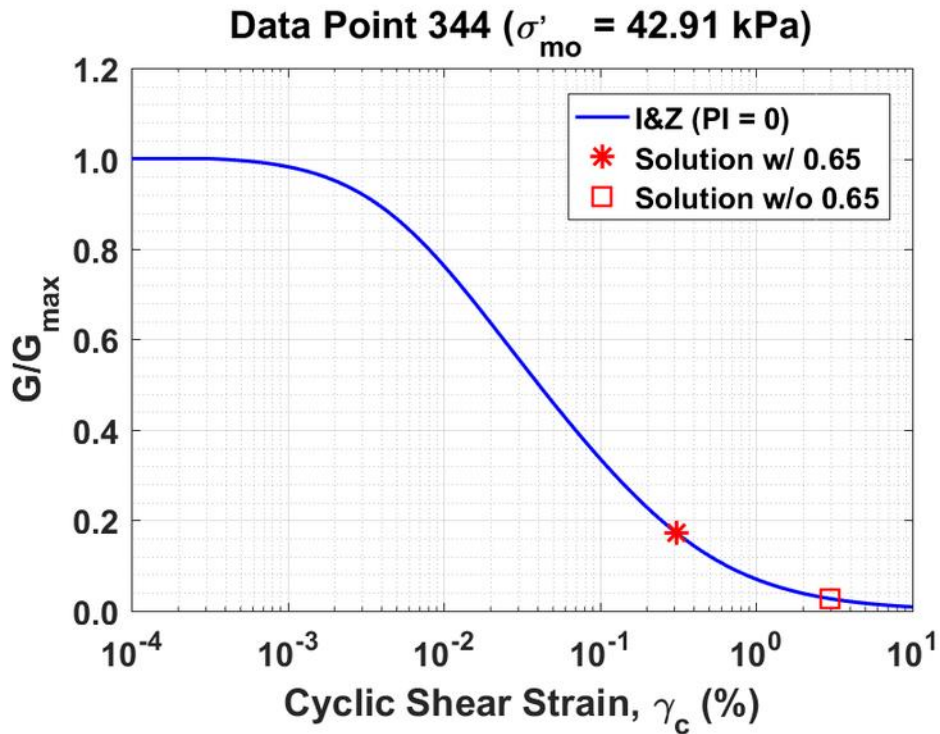


Figure B294. Normalized shear modulus reduction curves for Data Point 344 of the Kayen et al. database showing the solutions w/ and w/o the 0.65 factor

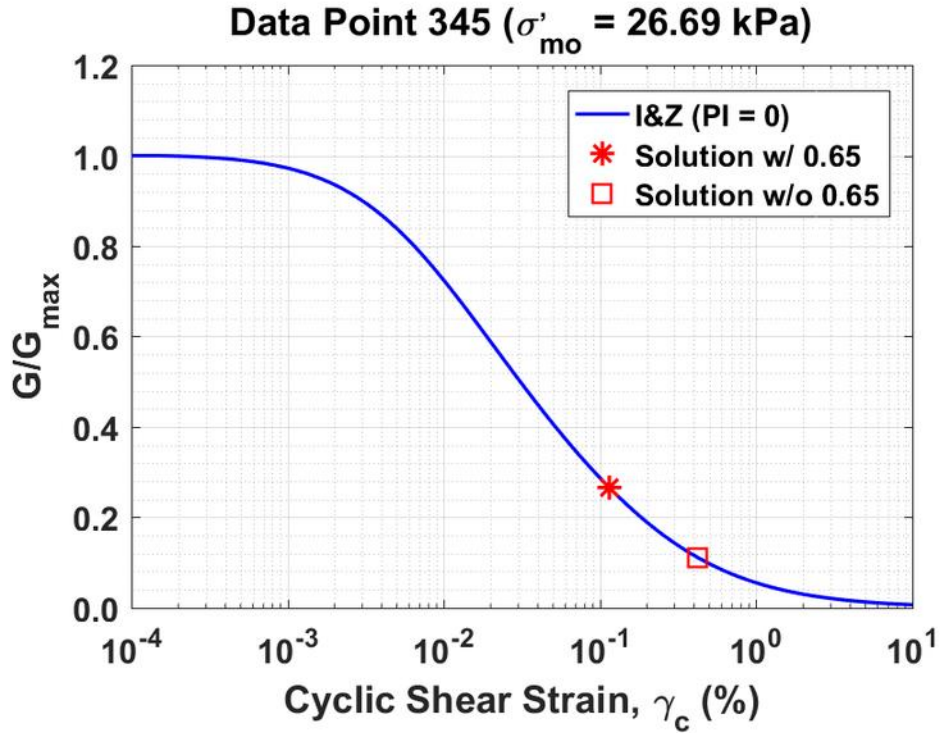


Figure B295. Normalized shear modulus reduction curves for Data Point 345 of the Kayen et al. database showing the solutions w/ and w/o the 0.65 factor

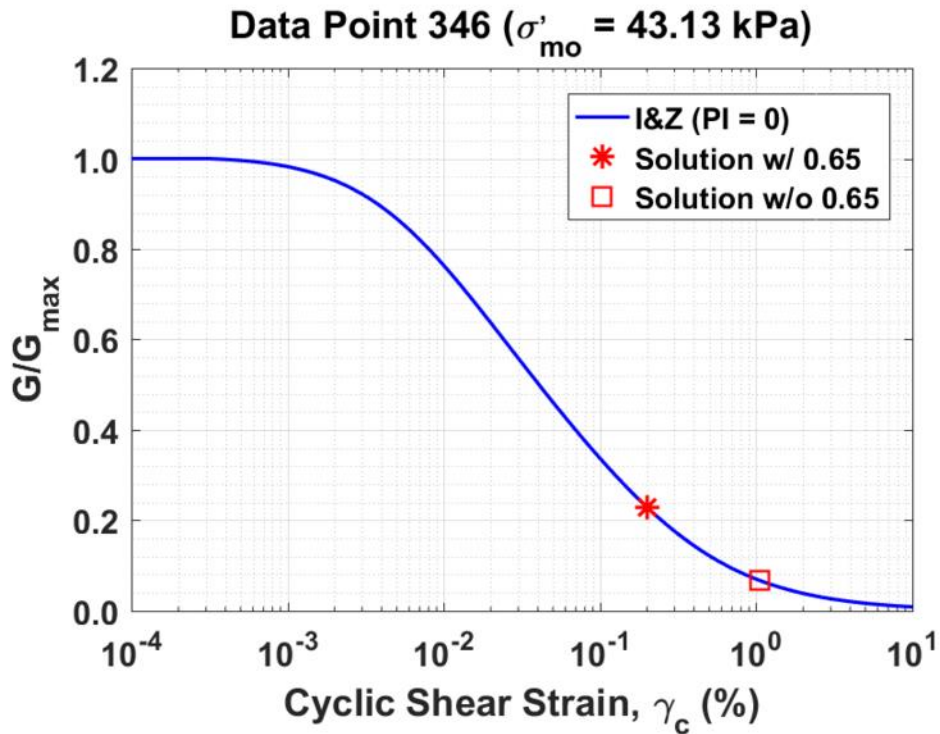


Figure B296. Normalized shear modulus reduction curves for Data Point 346 of the Kayen et al. database showing the solutions w/ and w/o the 0.65 factor

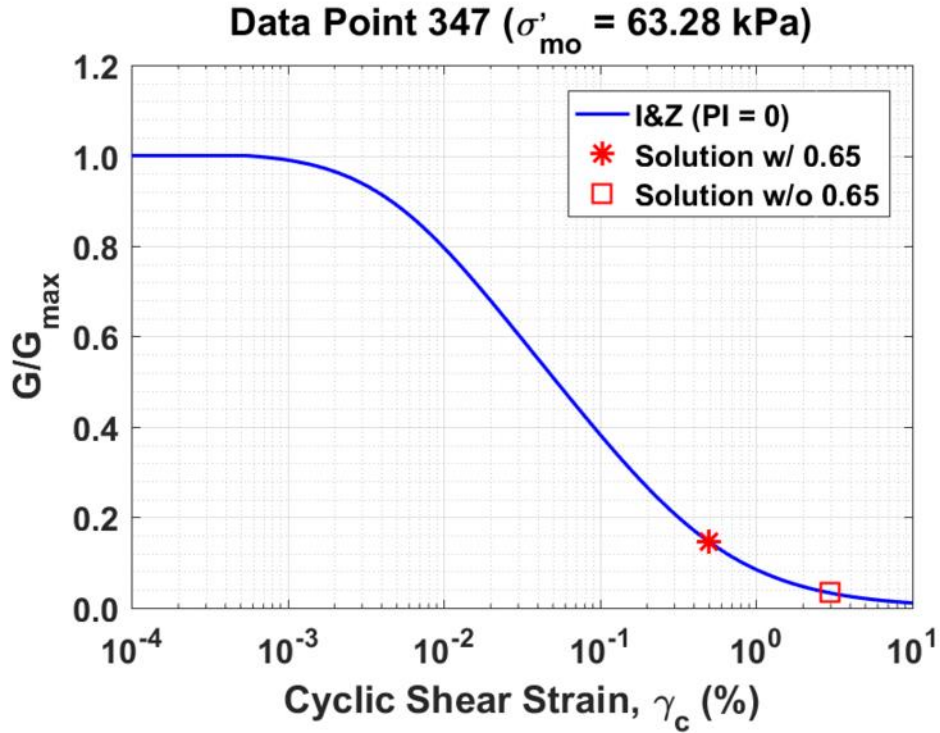


Figure B297. Normalized shear modulus reduction curves for Data Point 347 of the Kayen et al. database showing the solutions w/ and w/o the 0.65 factor

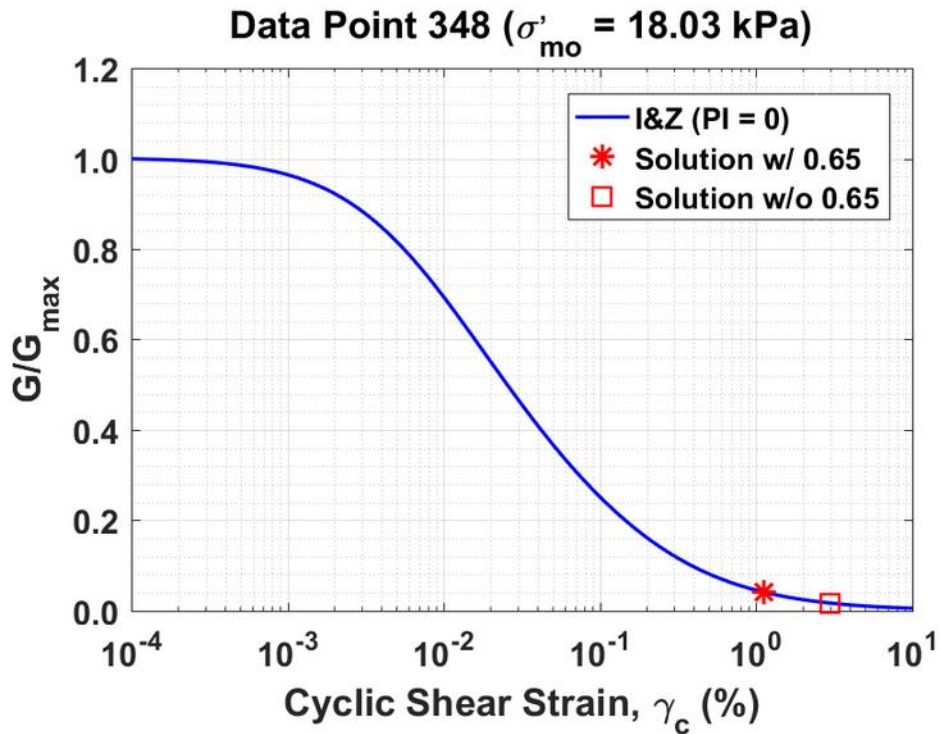


Figure B298. Normalized shear modulus reduction curves for Data Point 348 of the Kayen et al. database showing the solutions w/ and w/o the 0.65 factor

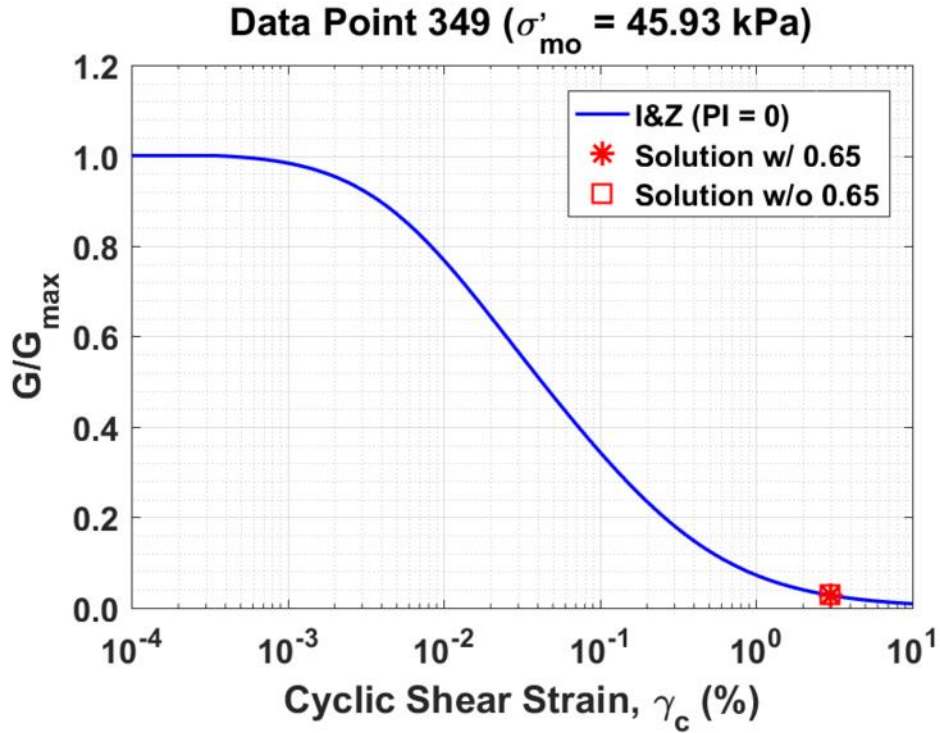


Figure B299. Normalized shear modulus reduction curves for Data Point 349 of the Kayen et al. database showing the solutions w/ and w/o the 0.65 factor

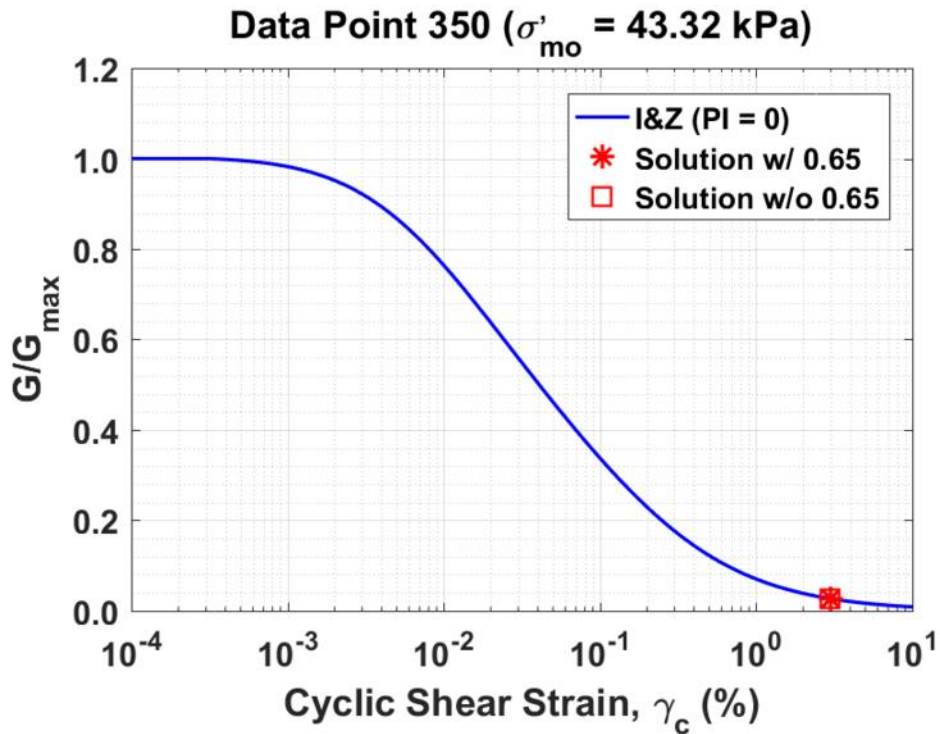


Figure B300. Normalized shear modulus reduction curves for Data Point 350 of the Kayen et al. database showing the solutions w/ and w/o the 0.65 factor

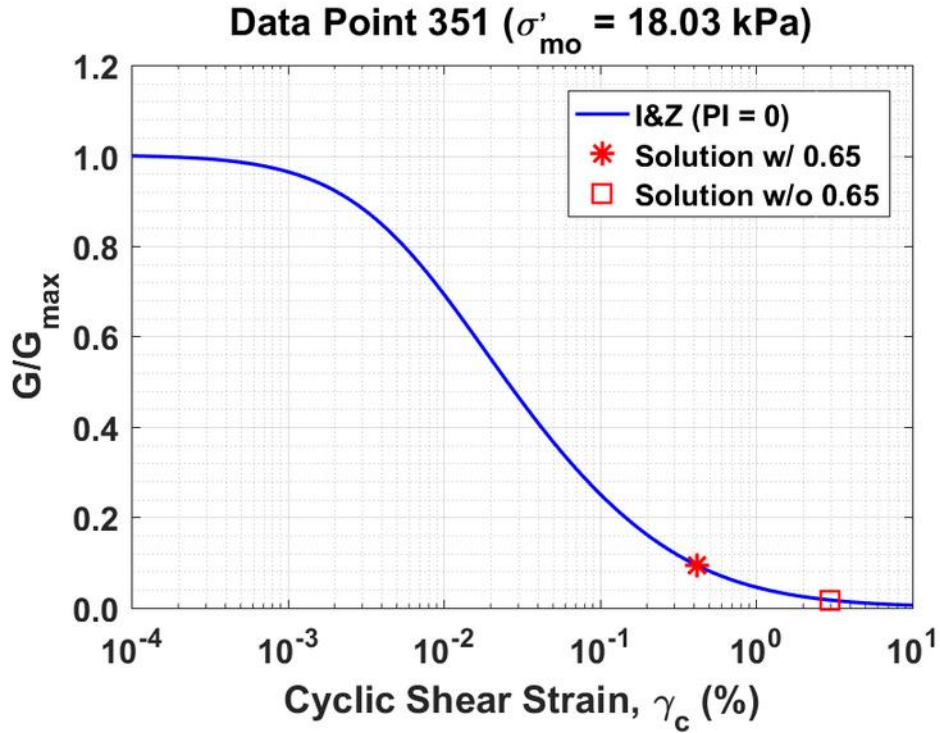


Figure B301. Normalized shear modulus reduction curves for Data Point 351 of the Kayen et al. database showing the solutions w/ and w/o the 0.65 factor

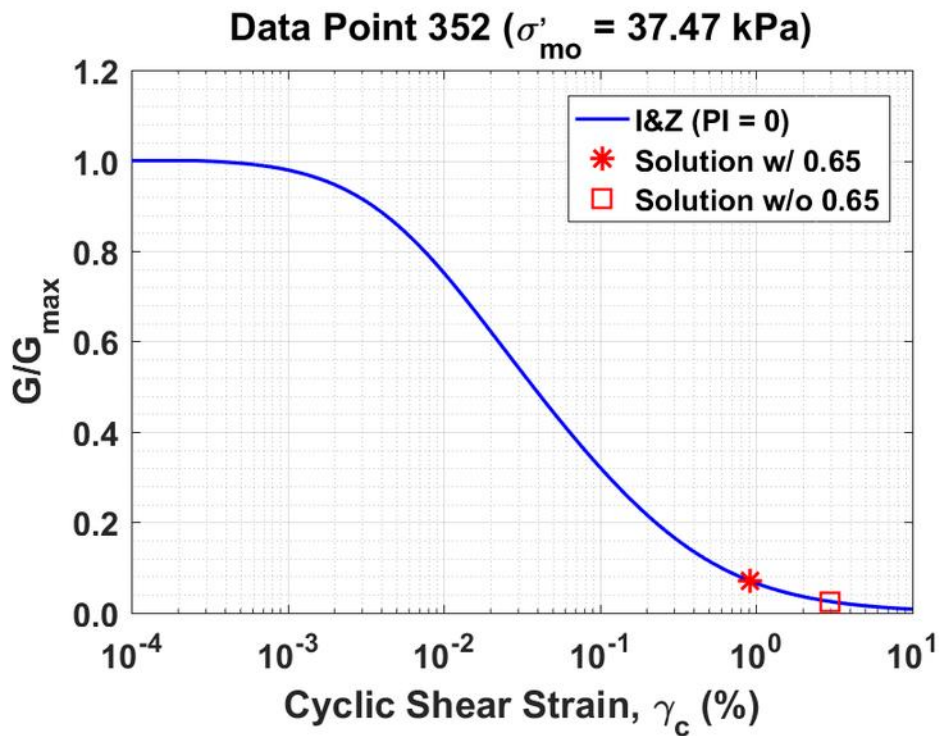


Figure B302. Normalized shear modulus reduction curves for Data Point 352 of the Kayen et al. database showing the solutions w/ and w/o the 0.65 factor

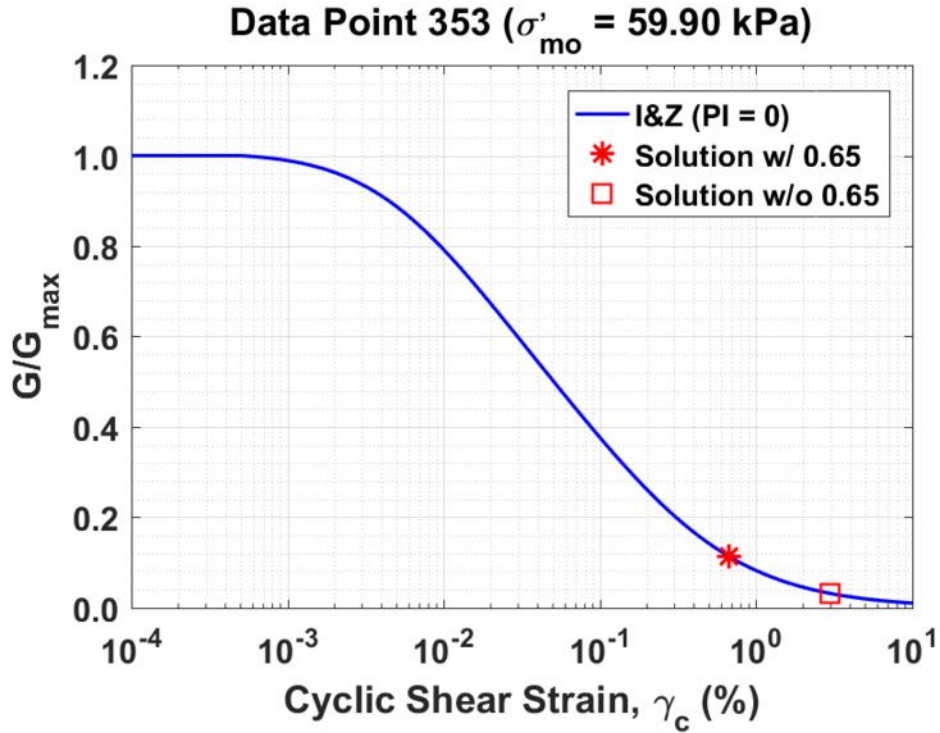


Figure B303. Normalized shear modulus reduction curves for Data Point 353 of the Kayen et al. database showing the solutions w/ and w/o the 0.65 factor

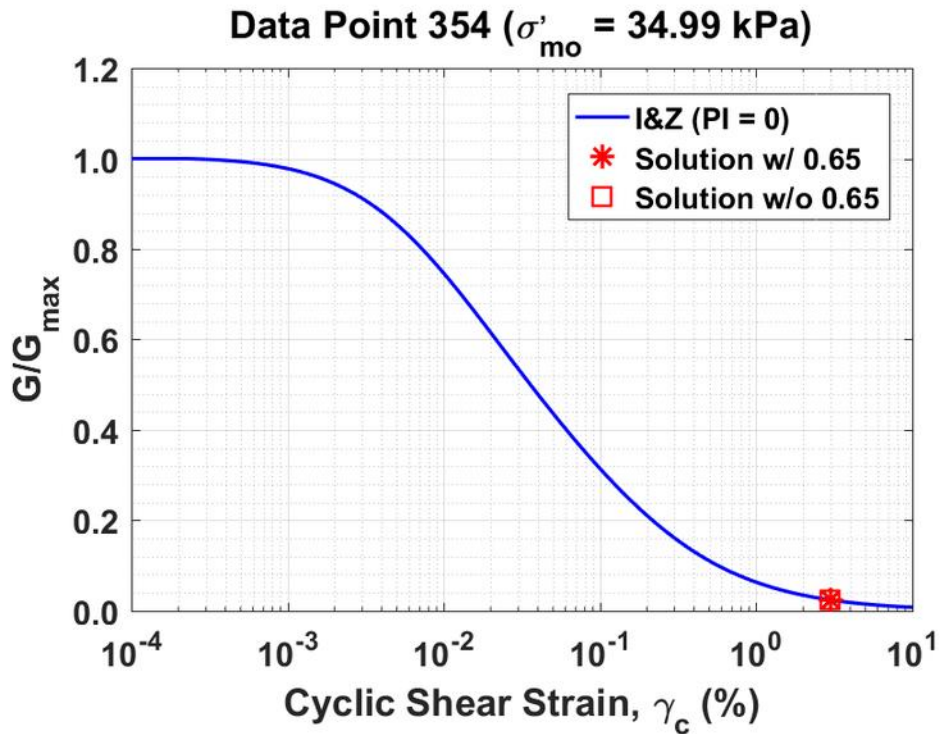


Figure B304. Normalized shear modulus reduction curves for Data Point 354 of the Kayen et al. database showing the solutions w/ and w/o the 0.65 factor

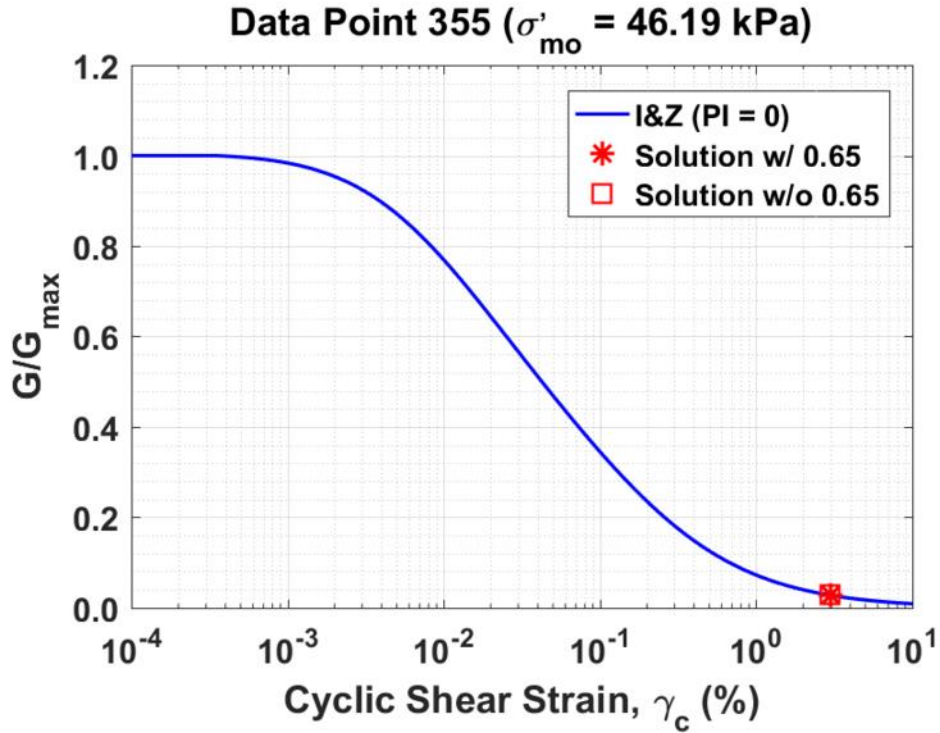


Figure B305. Normalized shear modulus reduction curves for Data Point 355 of the Kayen et al. database showing the solutions w/ and w/o the 0.65 factor

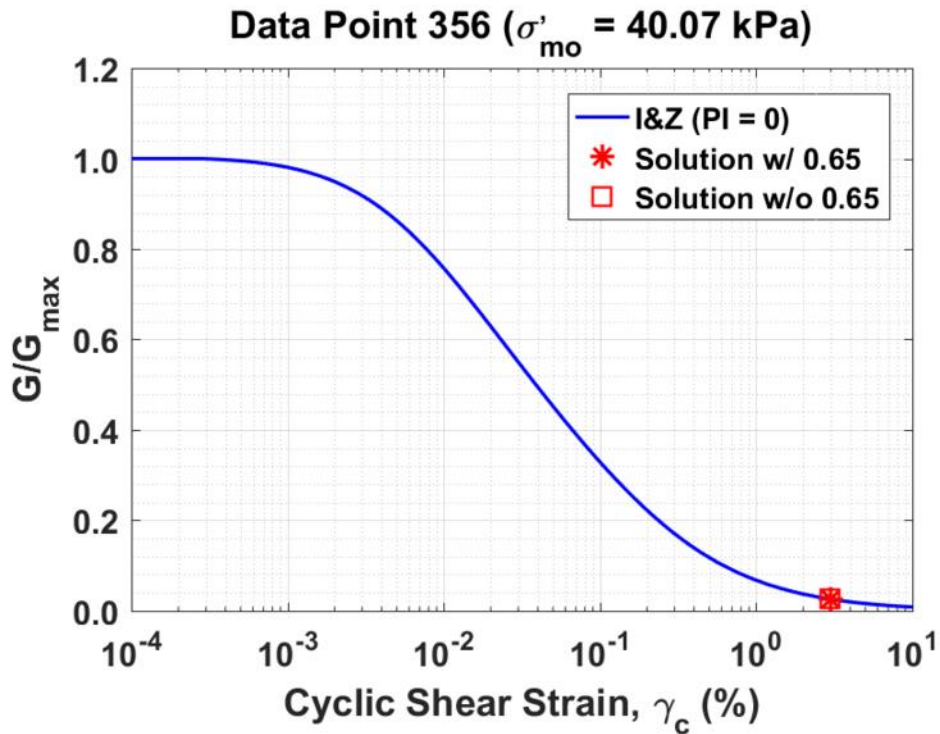


Figure B306. Normalized shear modulus reduction curves for Data Point 356 of the Kayen et al. database showing the solutions w/ and w/o the 0.65 factor

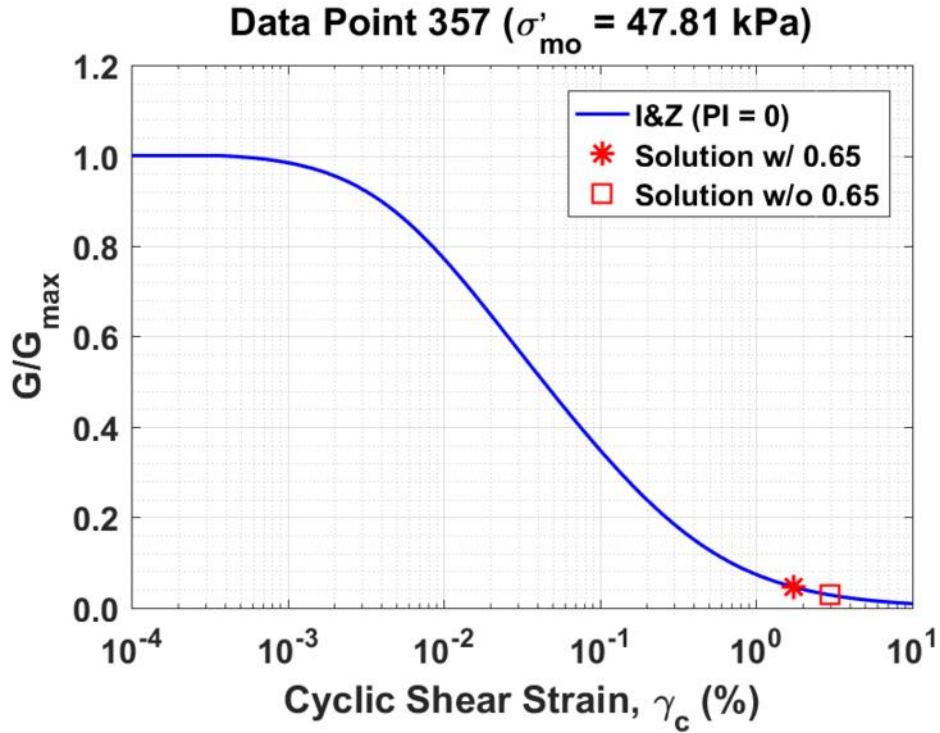


Figure B307. Normalized shear modulus reduction curves for Data Point 357 of the Kayen et al. database showing the solutions w/ and w/o the 0.65 factor

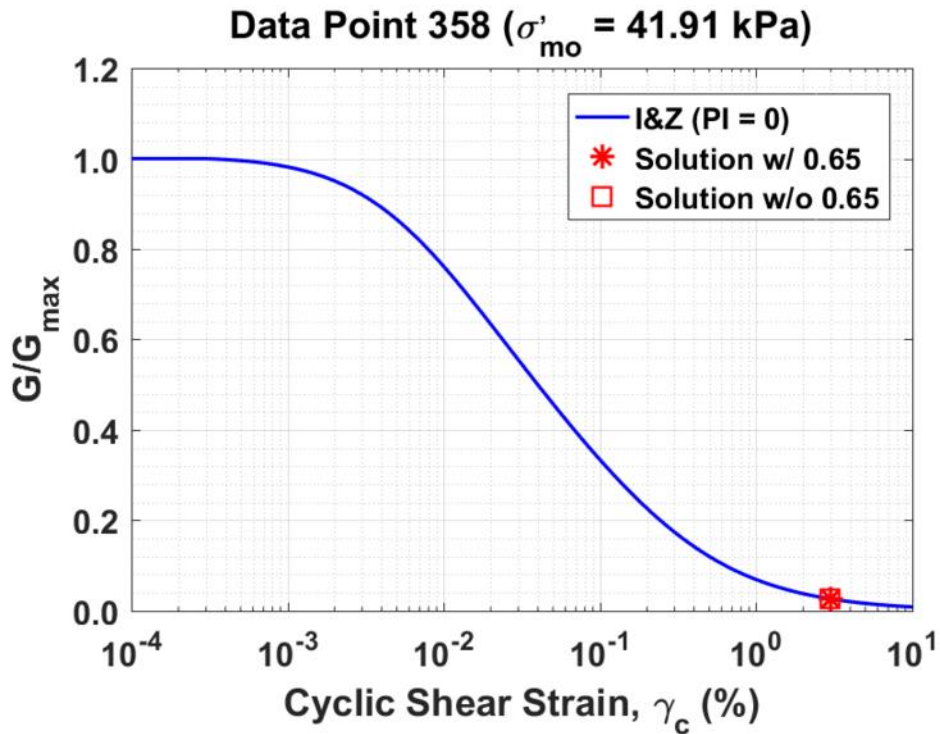


Figure B308. Normalized shear modulus reduction curves for Data Point 358 of the Kayen et al. database showing the solutions w/ and w/o the 0.65 factor

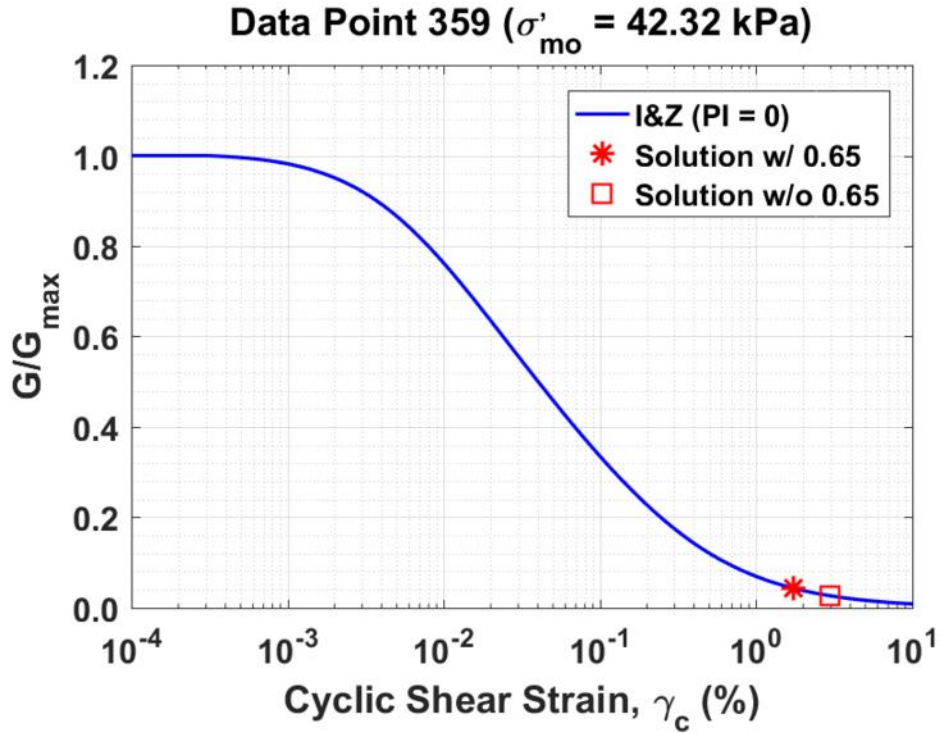


Figure B309. Normalized shear modulus reduction curves for Data Point 359 of the Kayen et al. database showing the solutions w/ and w/o the 0.65 factor

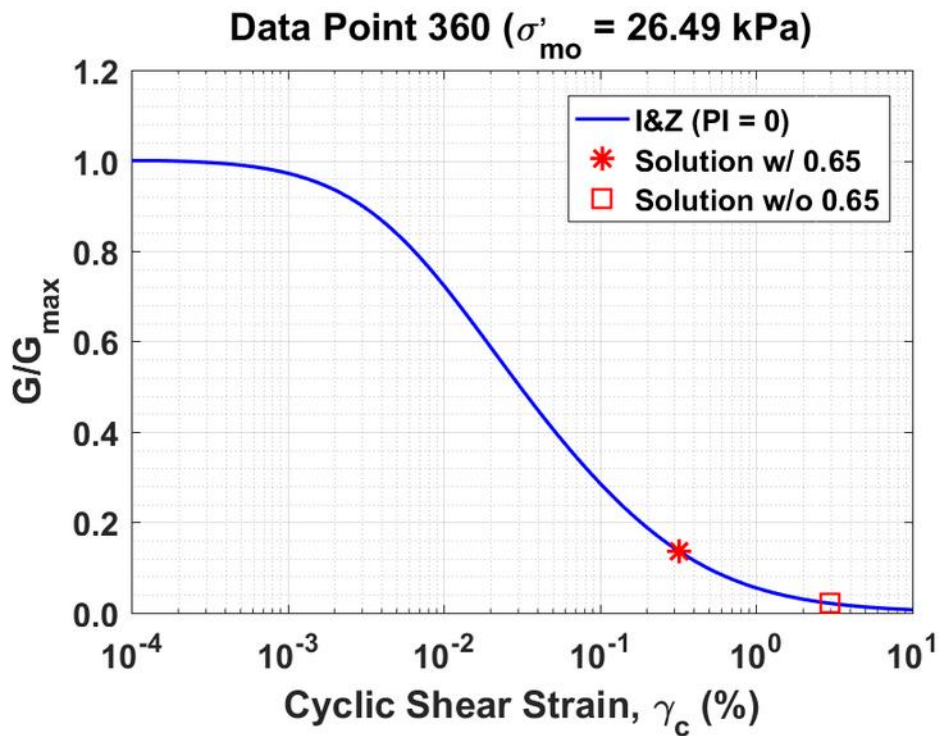


Figure B310. Normalized shear modulus reduction curves for Data Point 360 of the Kayen et al. database showing the solutions w/ and w/o the 0.65 factor

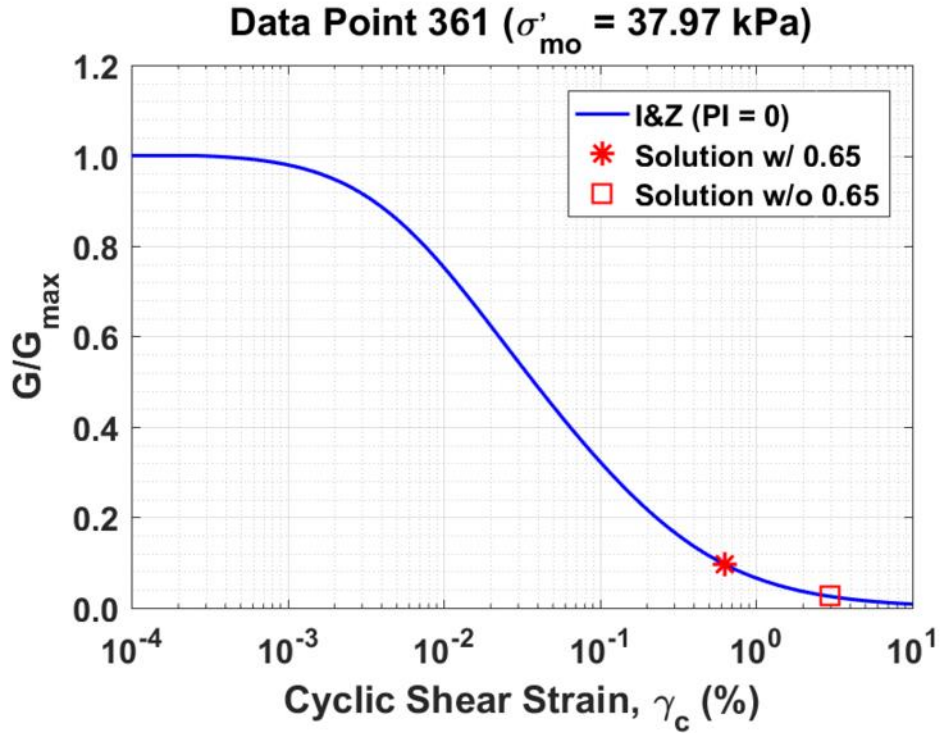


Figure B311. Normalized shear modulus reduction curves for Data Point 361 of the Kayen et al. database showing the solutions w/ and w/o the 0.65 factor

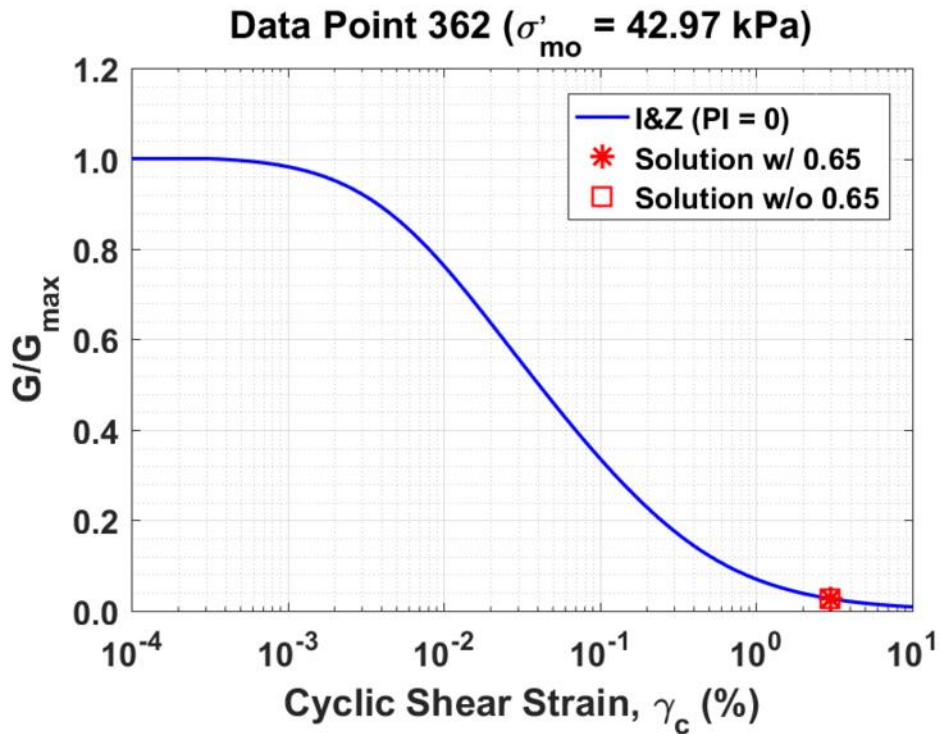


Figure B312. Normalized shear modulus reduction curves for Data Point 362 of the Kayen et al. database showing the solutions w/ and w/o the 0.65 factor

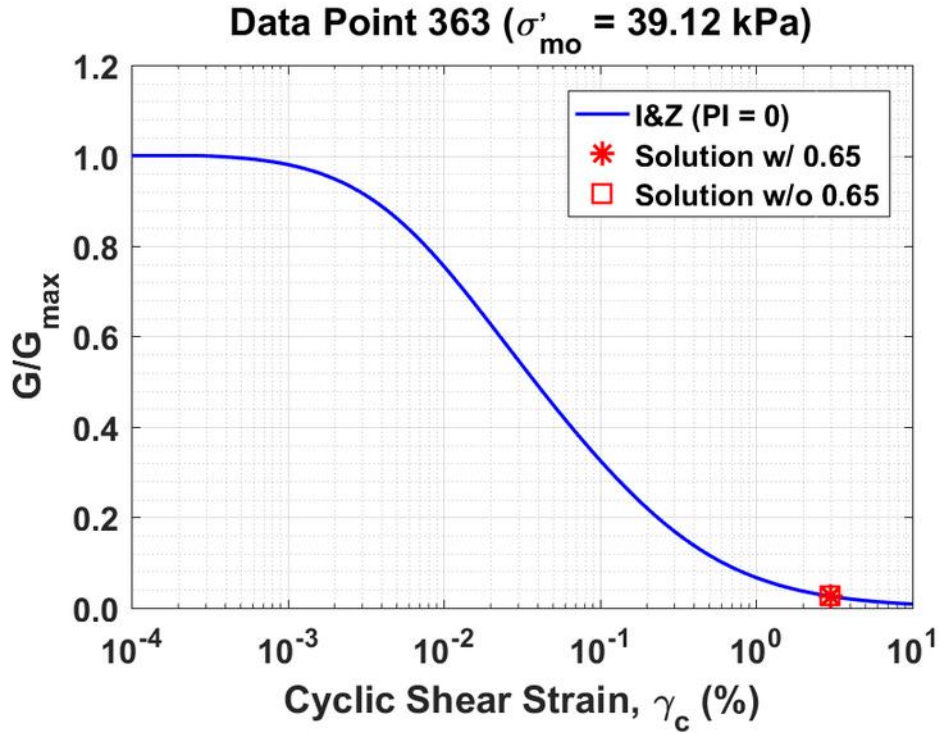


Figure B313. Normalized shear modulus reduction curves for Data Point 363 of the Kayen et al. database showing the solutions w/ and w/o the 0.65 factor

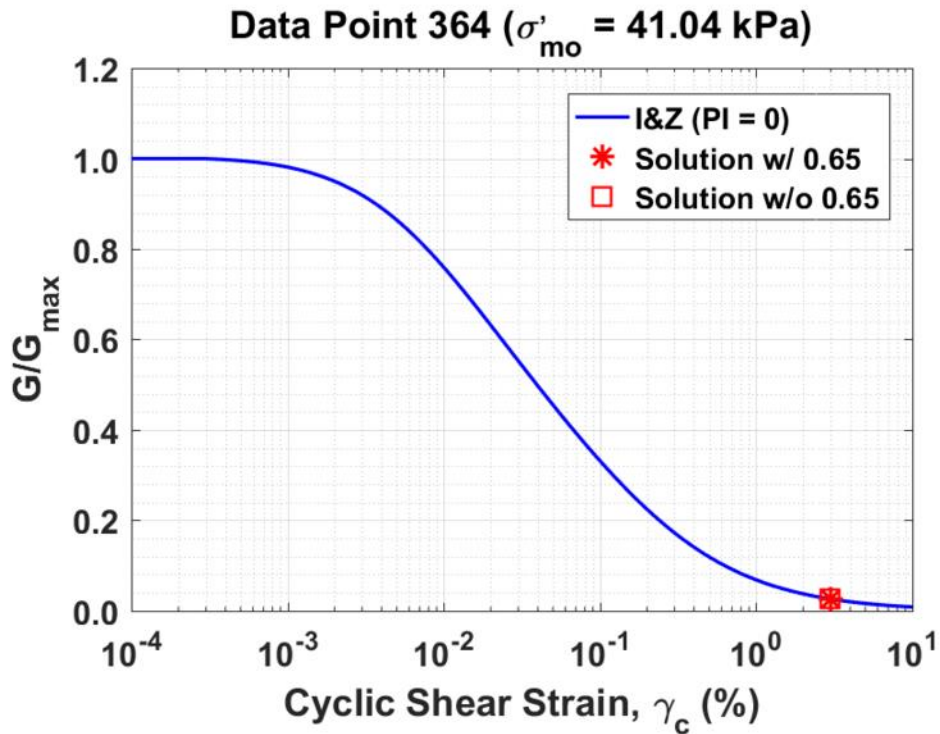


Figure B314. Normalized shear modulus reduction curves for Data Point 364 of the Kayen et al. database showing the solutions w/ and w/o the 0.65 factor

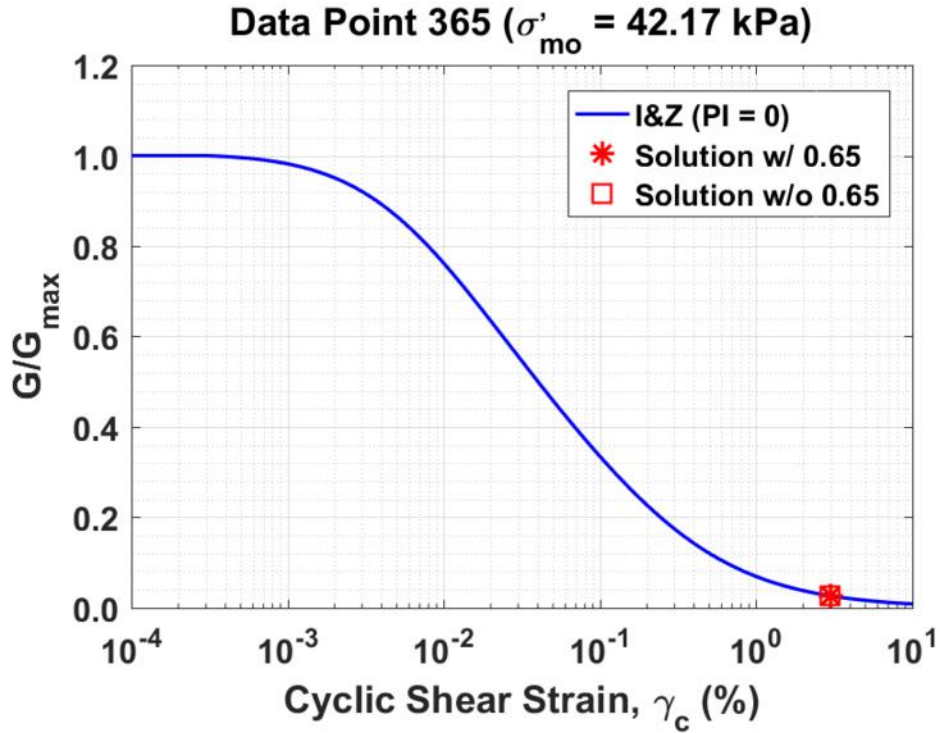


Figure B315. Normalized shear modulus reduction curves for Data Point 365 of the Kayen et al. database showing the solutions w/ and w/o the 0.65 factor

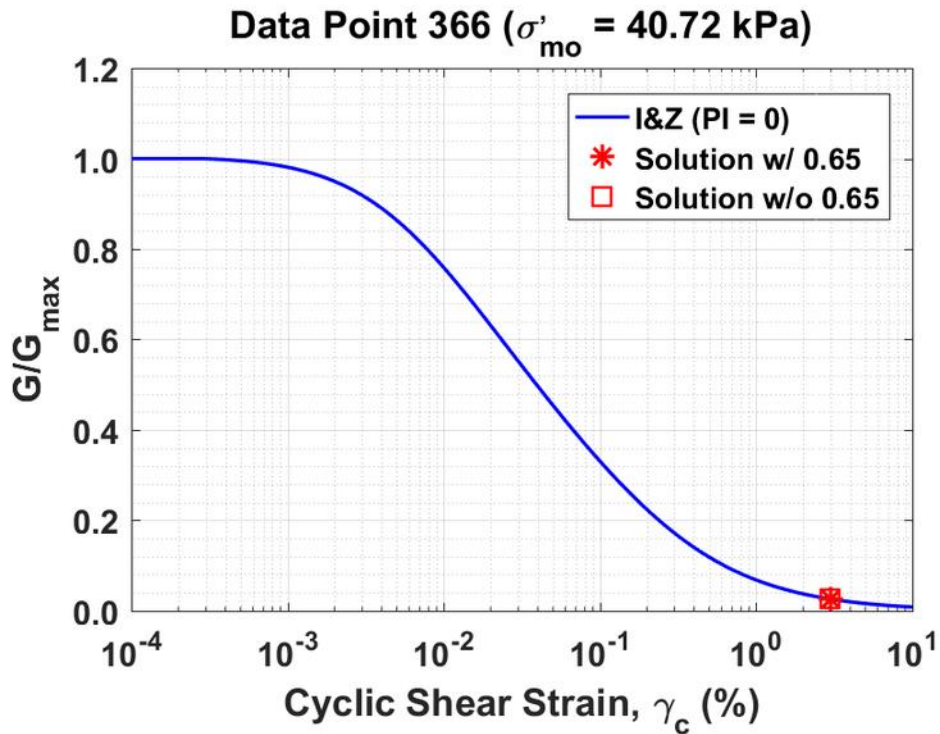


Figure B316. Normalized shear modulus reduction curves for Data Point 366 of the Kayen et al. database showing the solutions w/ and w/o the 0.65 factor

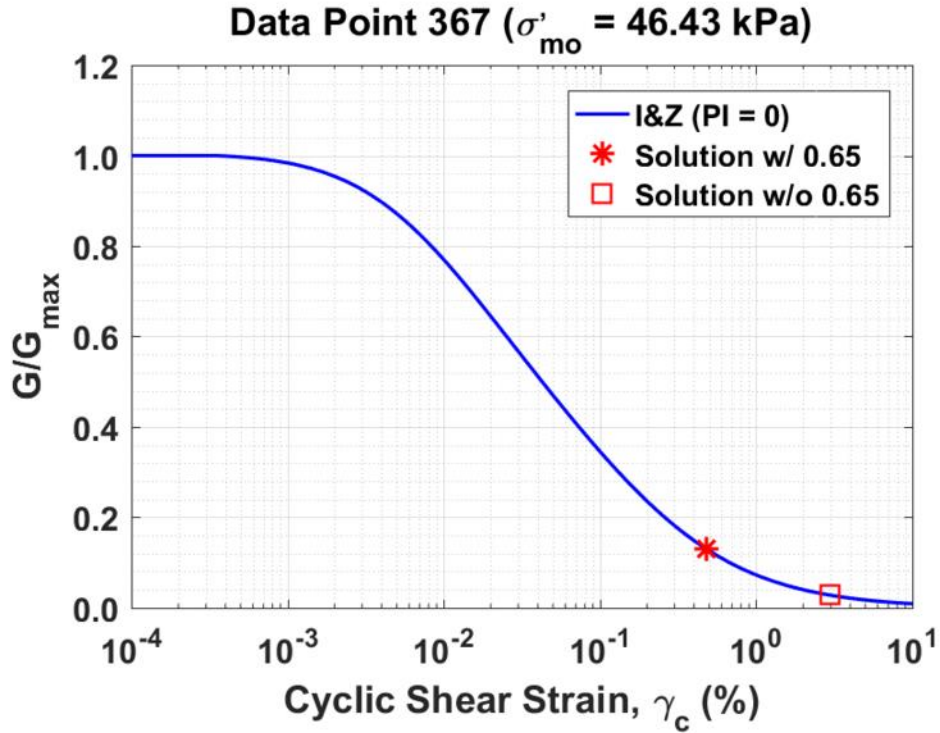


Figure B317. Normalized shear modulus reduction curves for Data Point 367 of the Kayen et al. database showing the solutions w/ and w/o the 0.65 factor

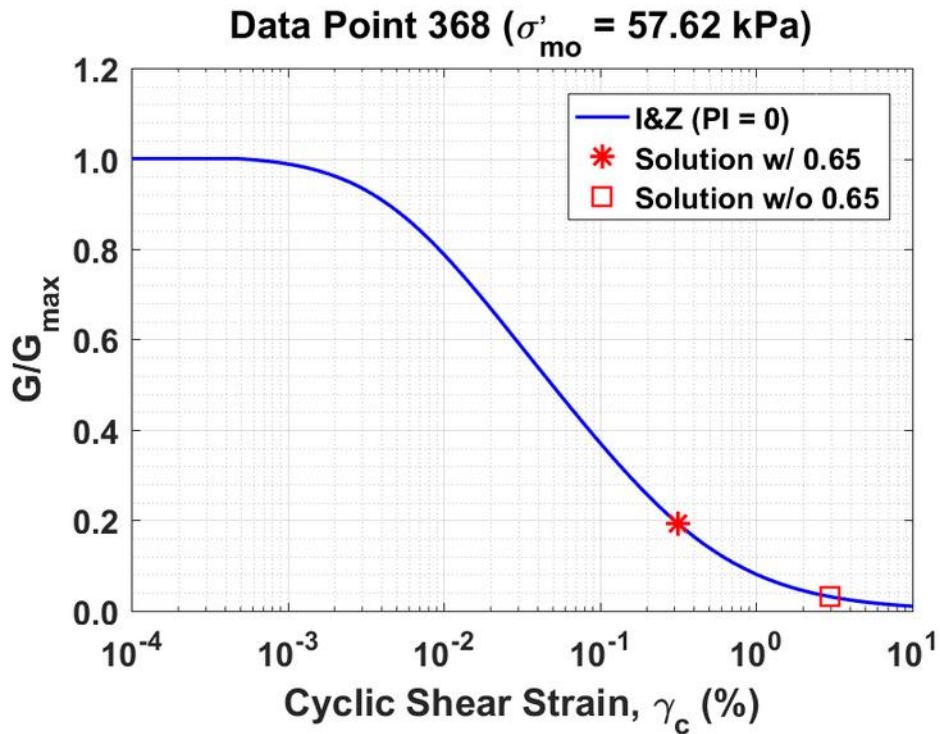


Figure B318. Normalized shear modulus reduction curves for Data Point 368 of the Kayen et al. database showing the solutions w/ and w/o the 0.65 factor

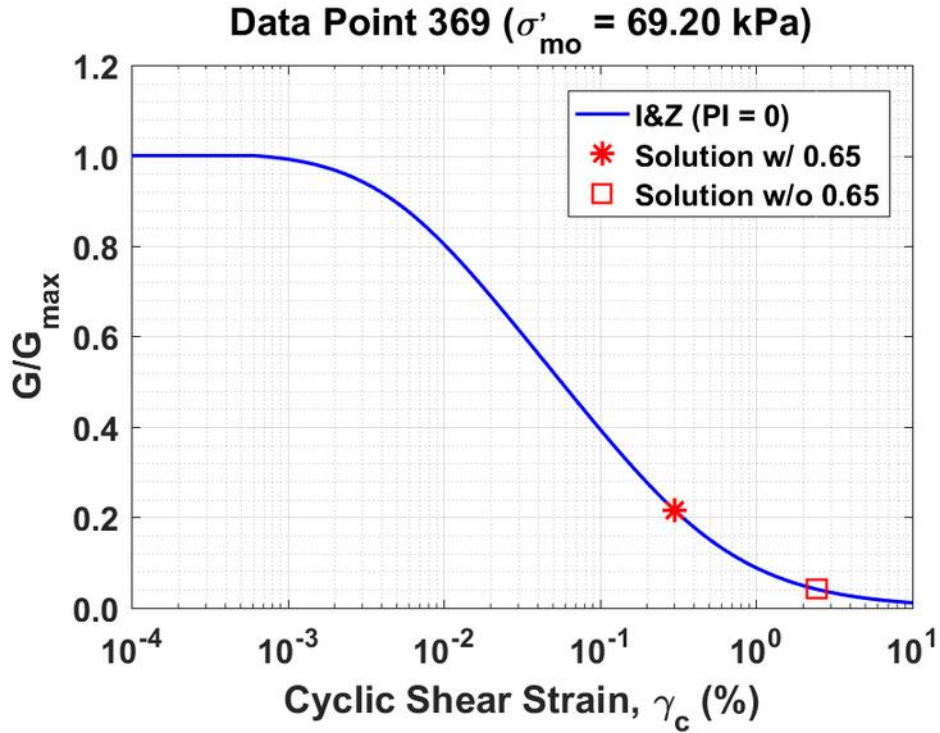


Figure B319. Normalized shear modulus reduction curves for Data Point 369 of the Kayen et al. database showing the solutions w/ and w/o the 0.65 factor

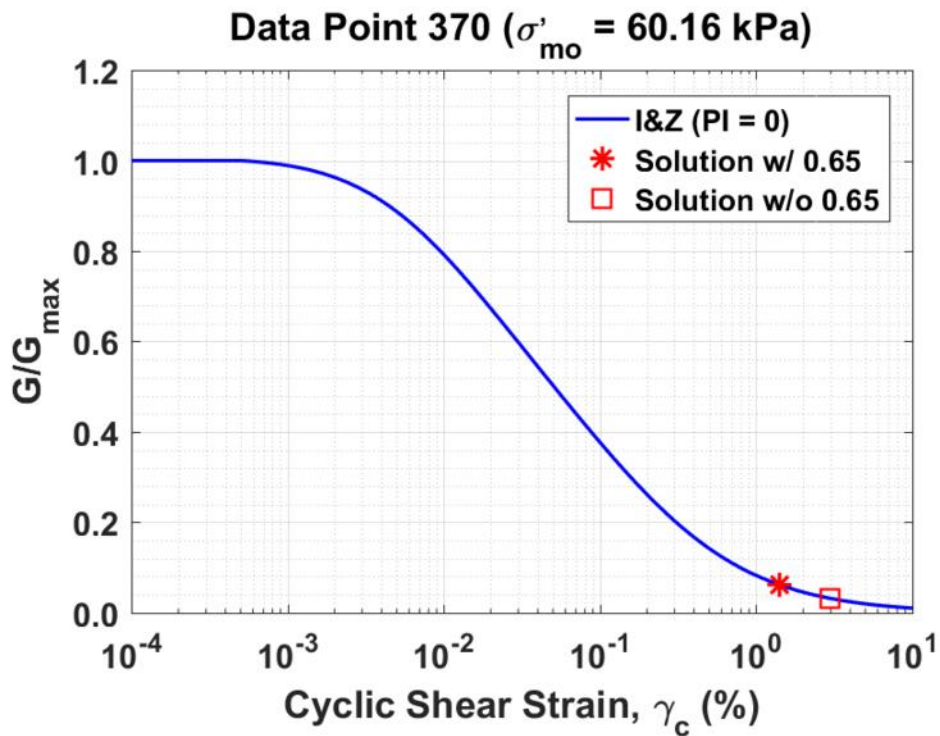


Figure B320. Normalized shear modulus reduction curves for Data Point 370 of the Kayen et al. database showing the solutions w/ and w/o the 0.65 factor

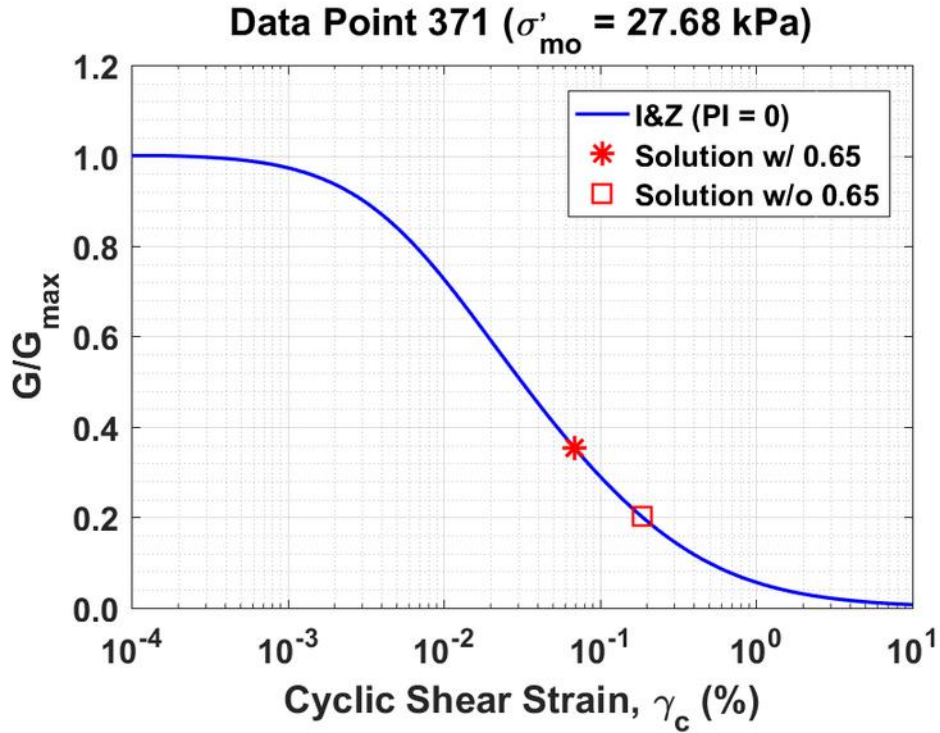


Figure B321. Normalized shear modulus reduction curves for Data Point 371 of the Kayen et al. database showing the solutions w/ and w/o the 0.65 factor

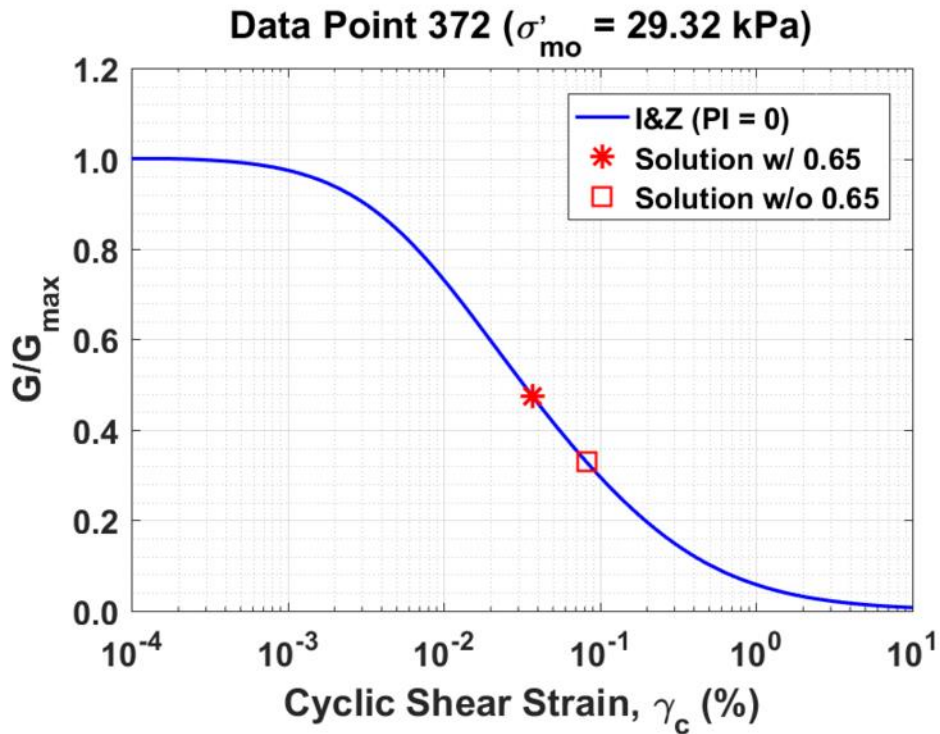


Figure B322. Normalized shear modulus reduction curves for Data Point 372 of the Kayen et al. database showing the solutions w/ and w/o the 0.65 factor

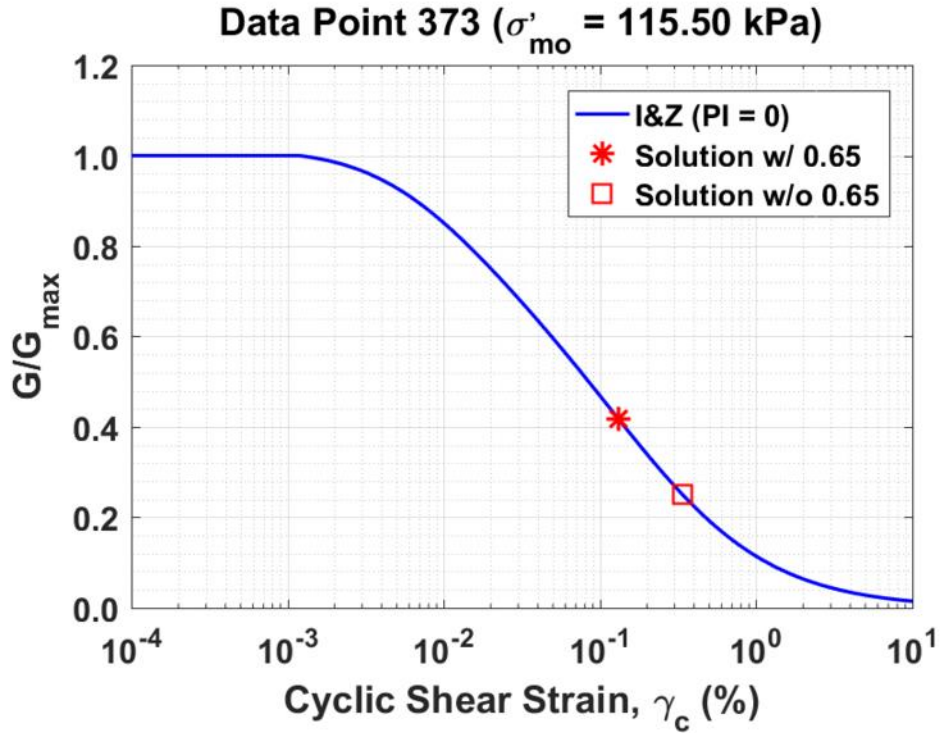


Figure B323. Normalized shear modulus reduction curves for Data Point 373 of the Kayen et al. database showing the solutions w/ and w/o the 0.65 factor

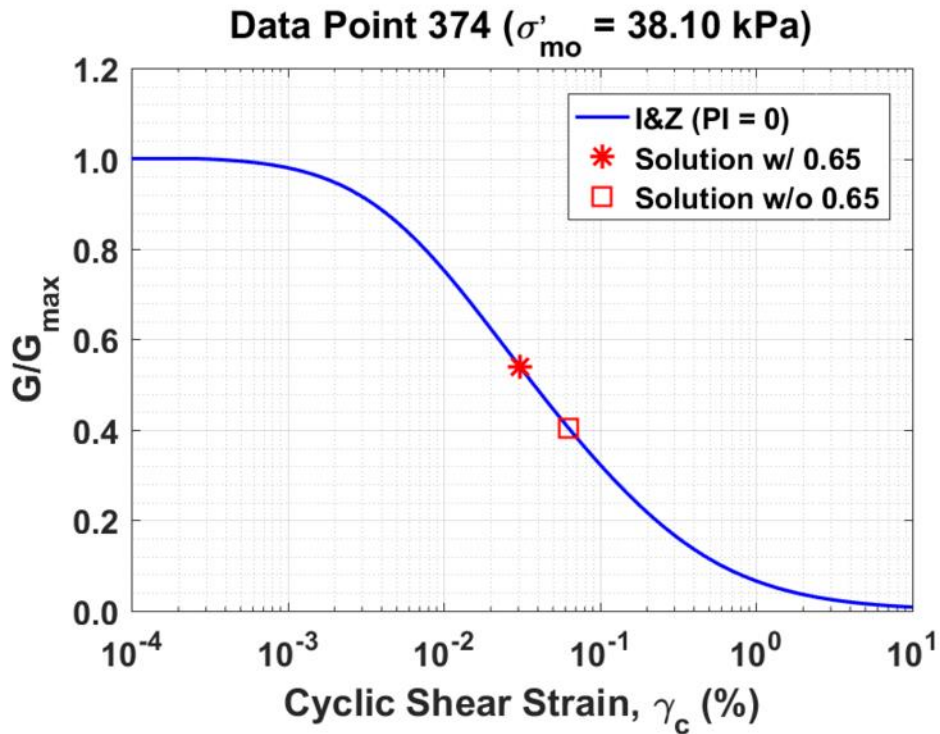


Figure B324. Normalized shear modulus reduction curves for Data Point 374 of the Kayen et al. database showing the solutions w/ and w/o the 0.65 factor

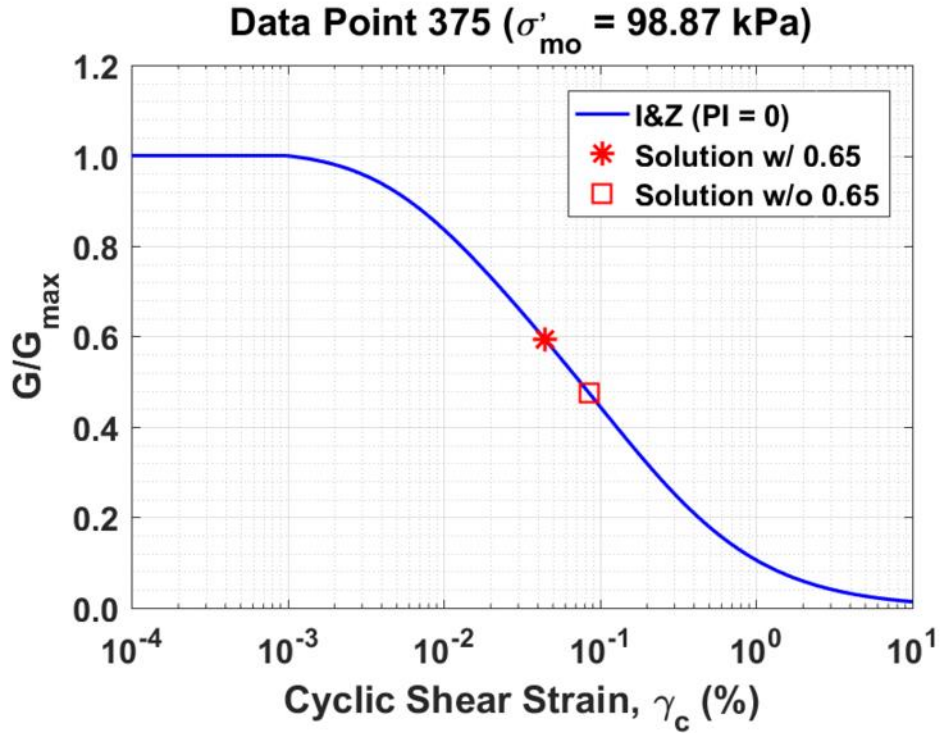


Figure B325. Normalized shear modulus reduction curves for Data Point 375 of the Kayen et al. database showing the solutions w/ and w/o the 0.65 factor

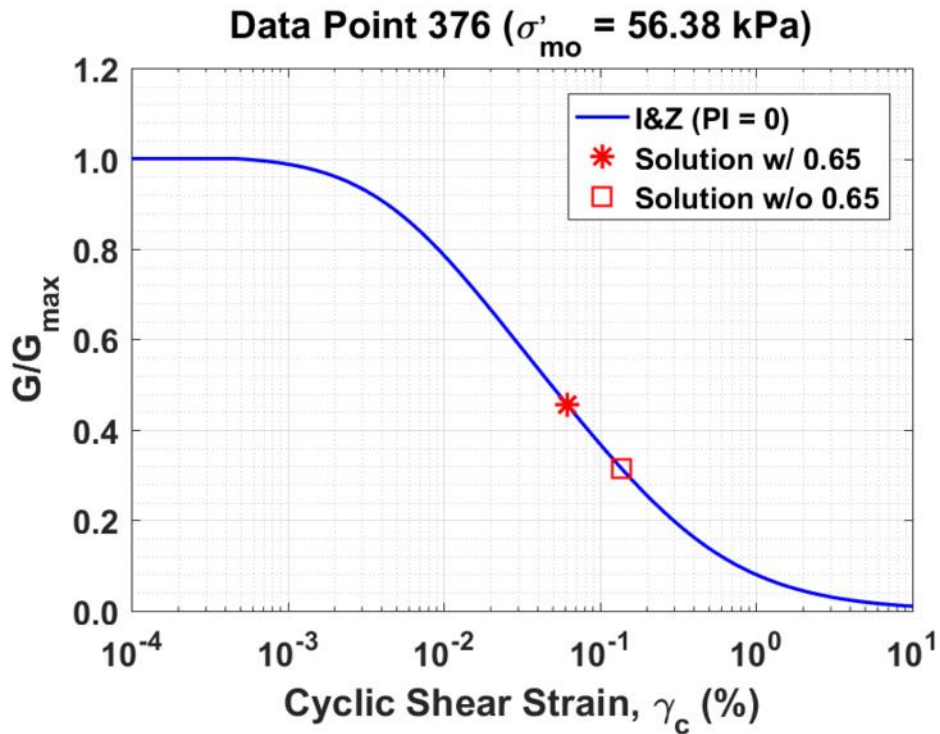


Figure B326. Normalized shear modulus reduction curves for Data Point 376 of the Kayen et al. database showing the solutions w/ and w/o the 0.65 factor

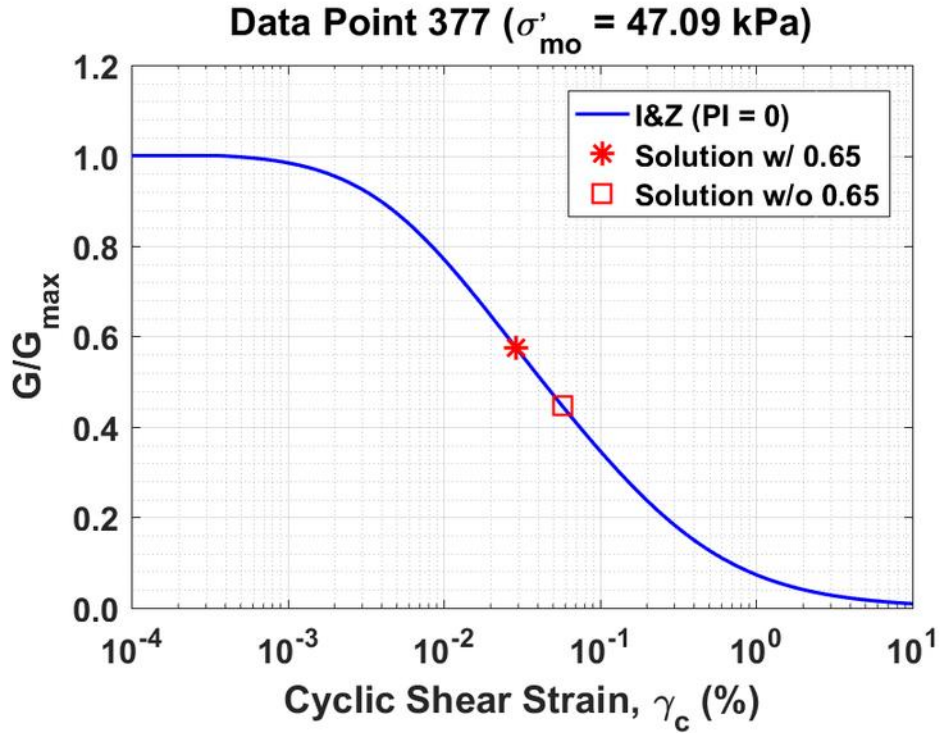


Figure B327. Normalized shear modulus reduction curves for Data Point 377 of the Kayen et al. database showing the solutions w/ and w/o the 0.65 factor

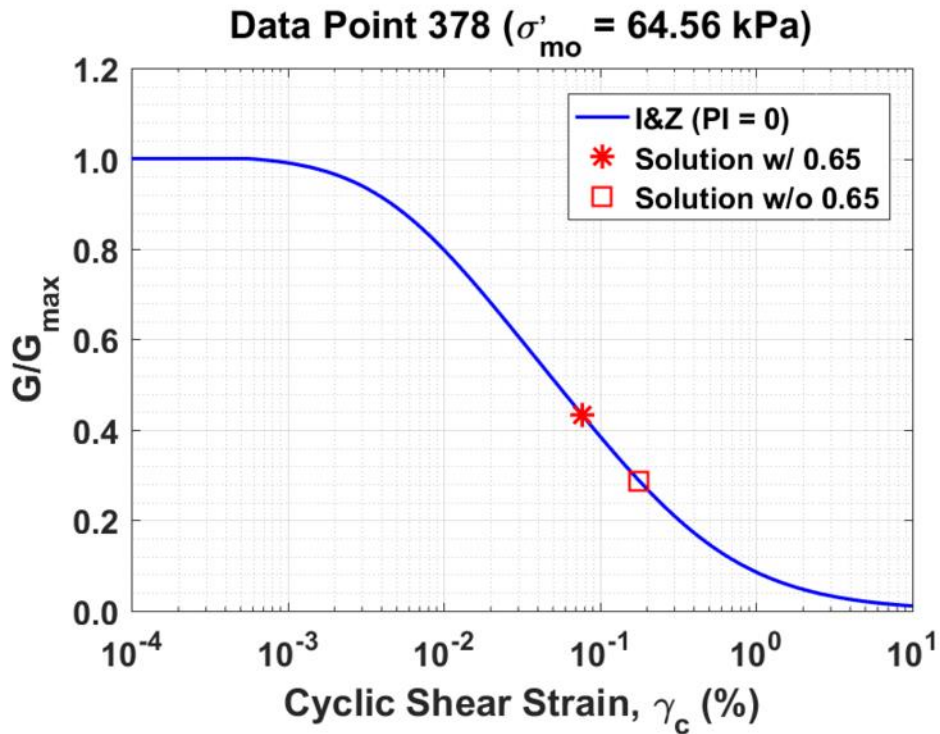


Figure B328. Normalized shear modulus reduction curves for Data Point 378 of the Kayen et al. database showing the solutions w/ and w/o the 0.65 factor

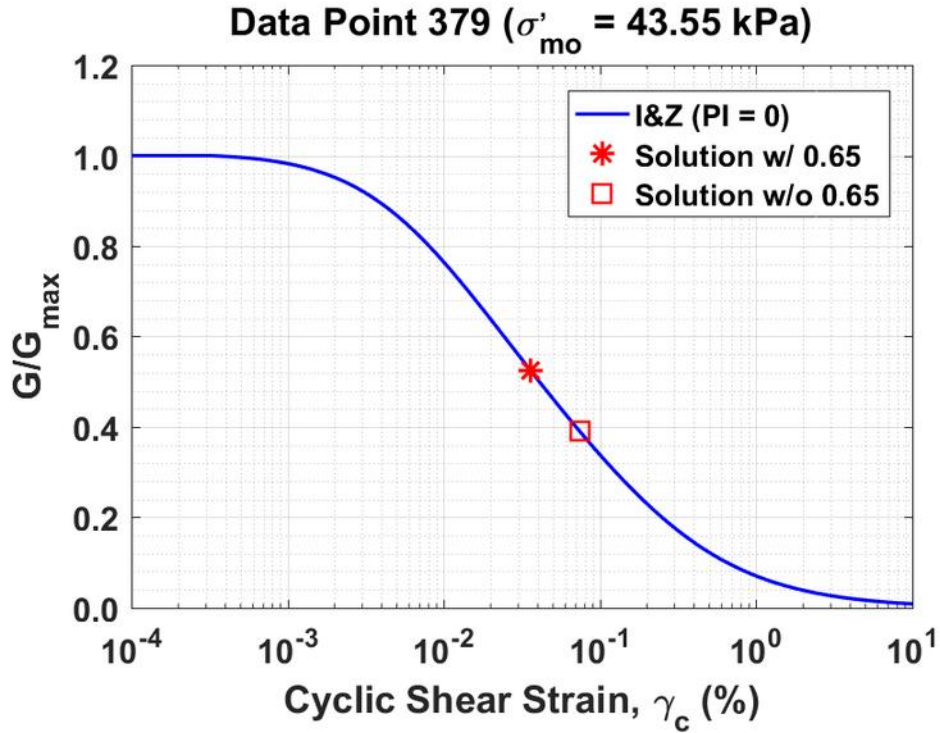


Figure B329. Normalized shear modulus reduction curves for Data Point 379 of the Kayen et al. database showing the solutions w/ and w/o the 0.65 factor

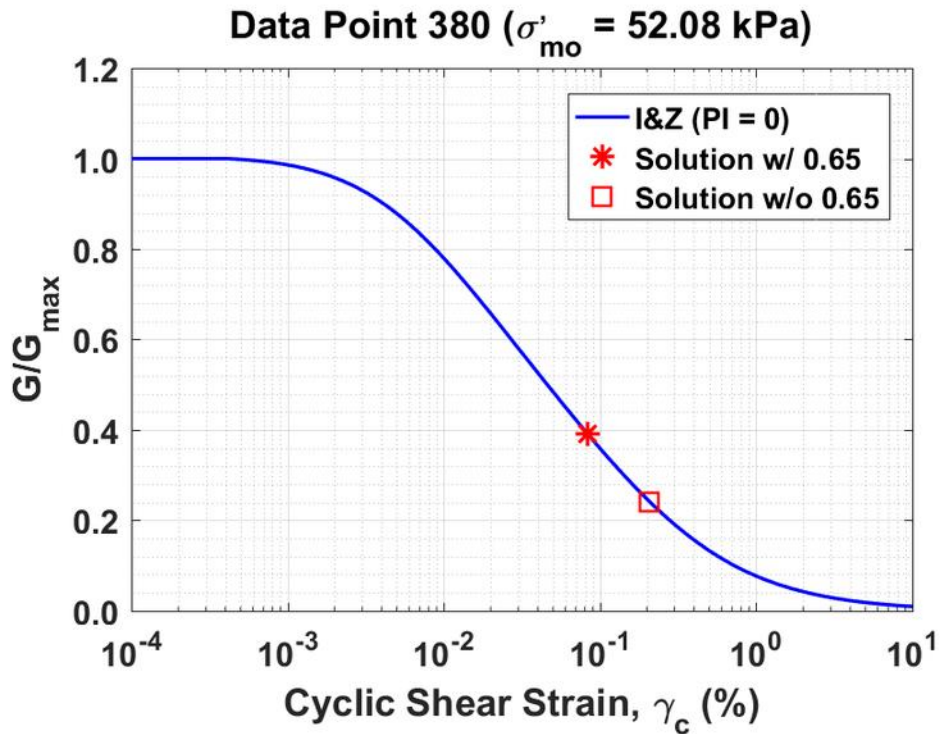


Figure B330. Normalized shear modulus reduction curves for Data Point 380 of the Kayen et al. database showing the solutions w/ and w/o the 0.65 factor

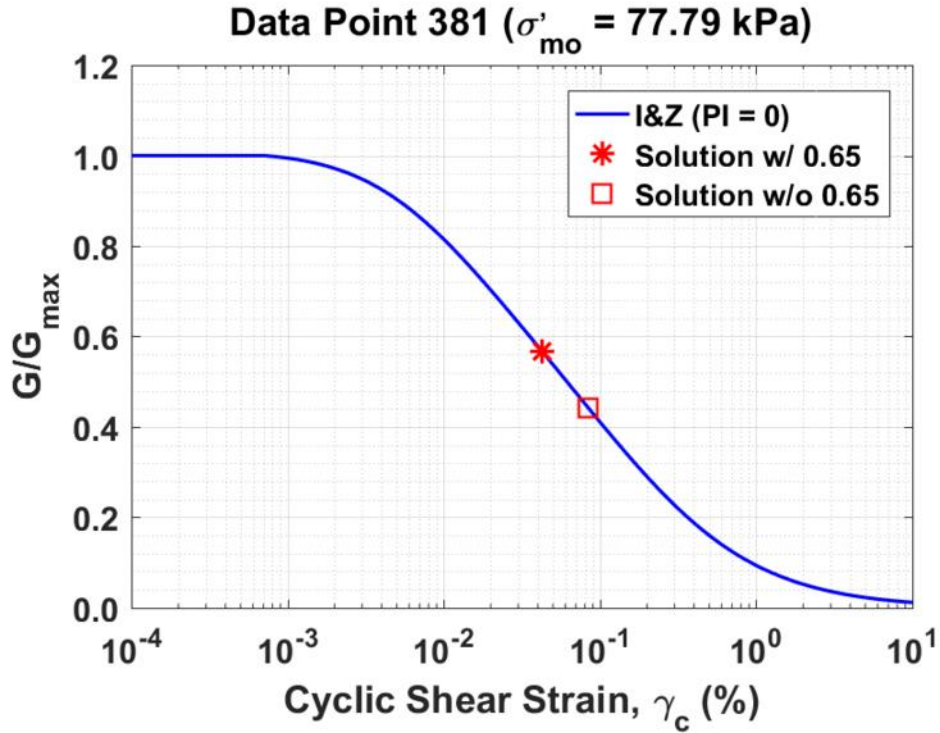


Figure B331. Normalized shear modulus reduction curves for Data Point 381 of the Kayen et al. database showing the solutions w/ and w/o the 0.65 factor

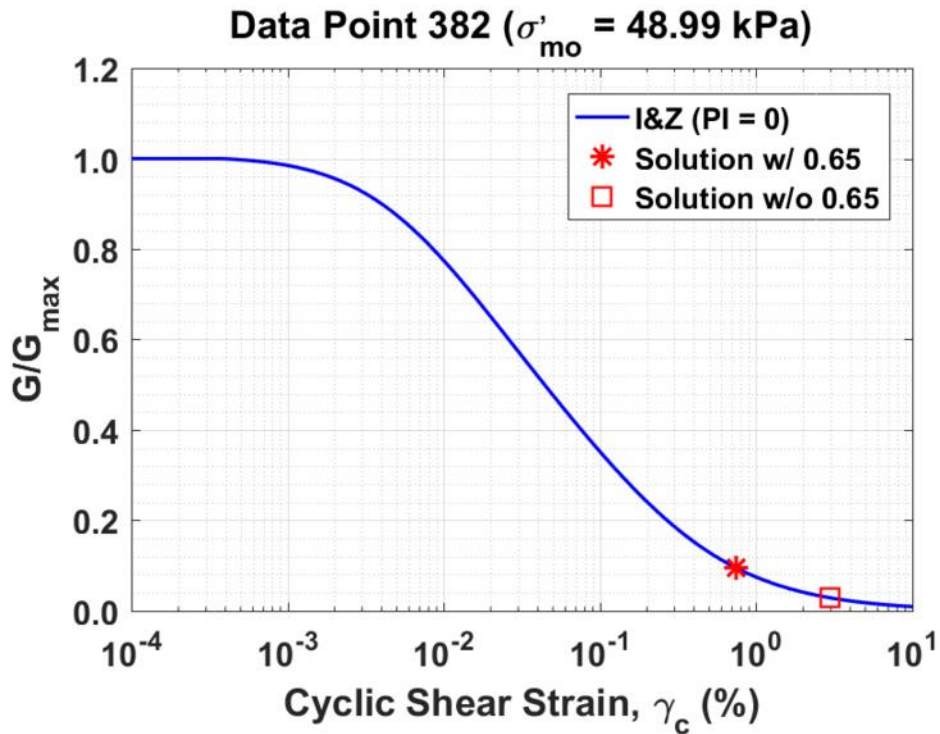


Figure B332. Normalized shear modulus reduction curves for Data Point 382 of the Kayen et al. database showing the solutions w/ and w/o the 0.65 factor

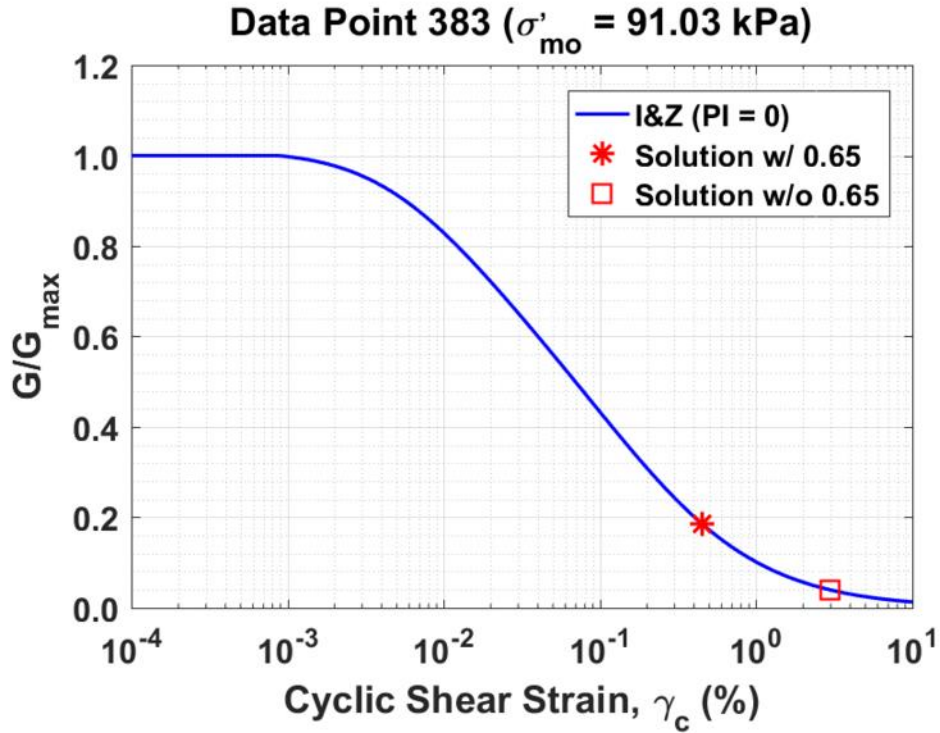


Figure B333. Normalized shear modulus reduction curves for Data Point 383 of the Kayen et al. database showing the solutions w/ and w/o the 0.65 factor

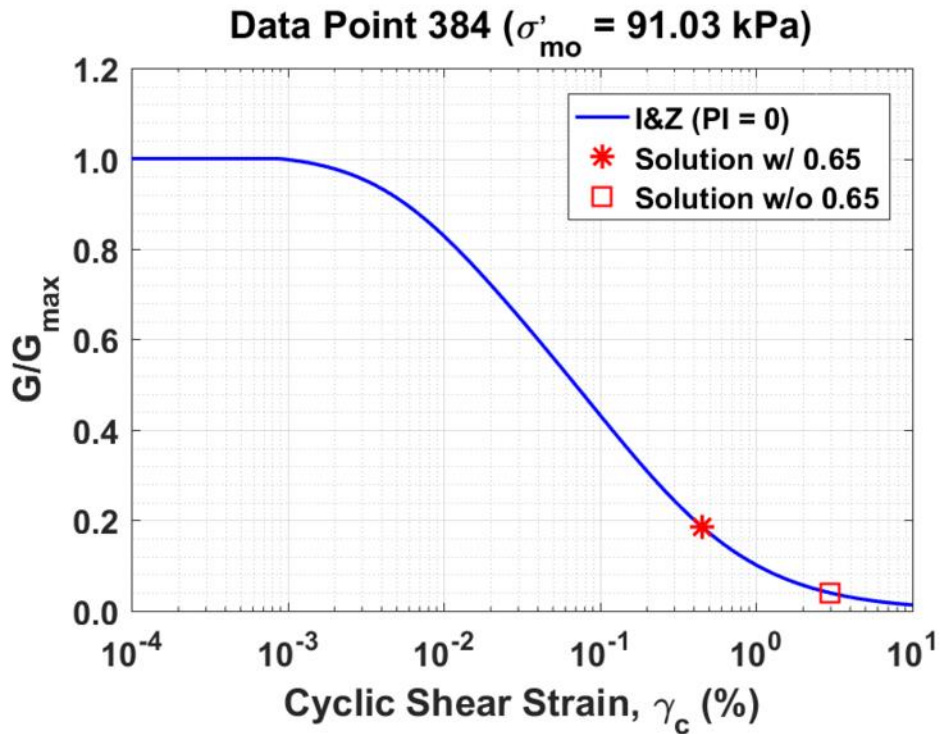


Figure B334. Normalized shear modulus reduction curves for Data Point 384 of the Kayen et al. database showing the solutions w/ and w/o the 0.65 factor

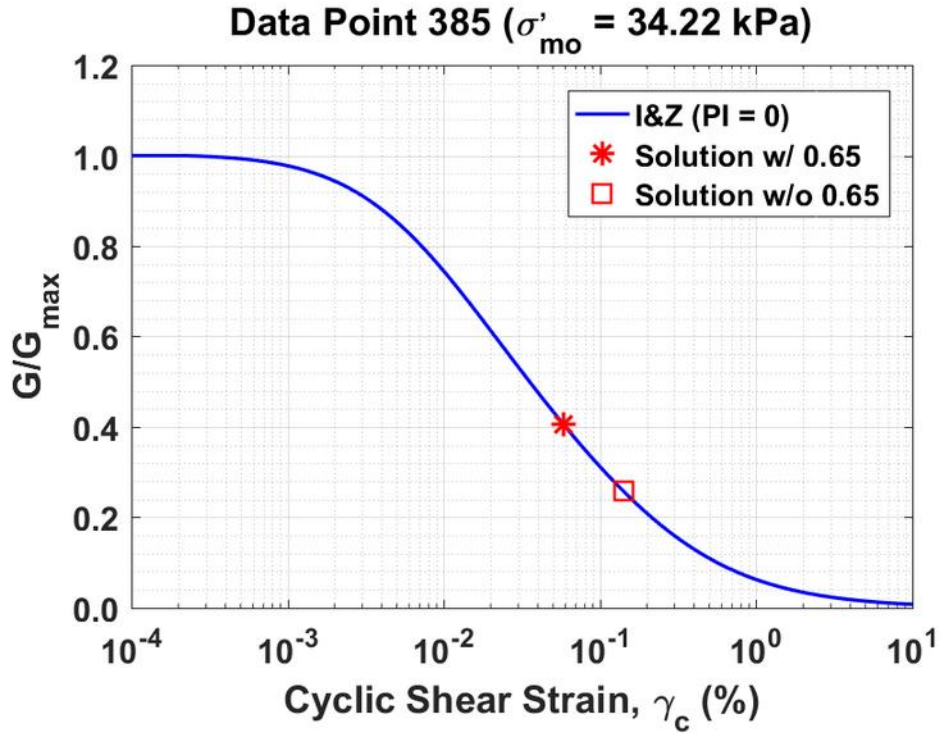


Figure B335. Normalized shear modulus reduction curves for Data Point 385 of the Kayen et al. database showing the solutions w/ and w/o the 0.65 factor

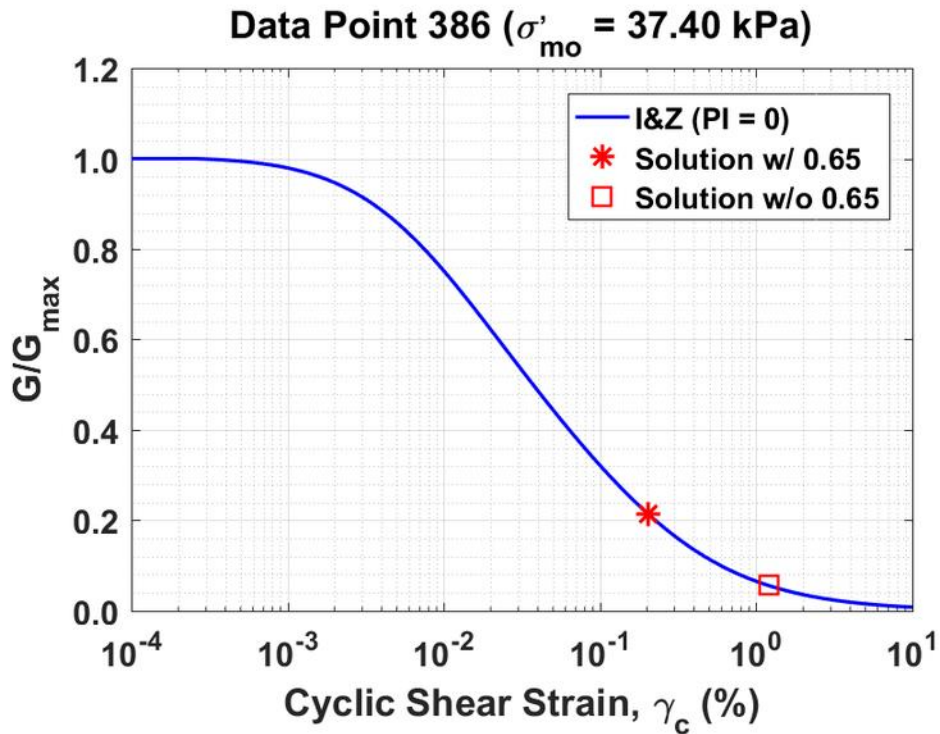


Figure B336. Normalized shear modulus reduction curves for Data Point 386 of the Kayen et al. database showing the solutions w/ and w/o the 0.65 factor

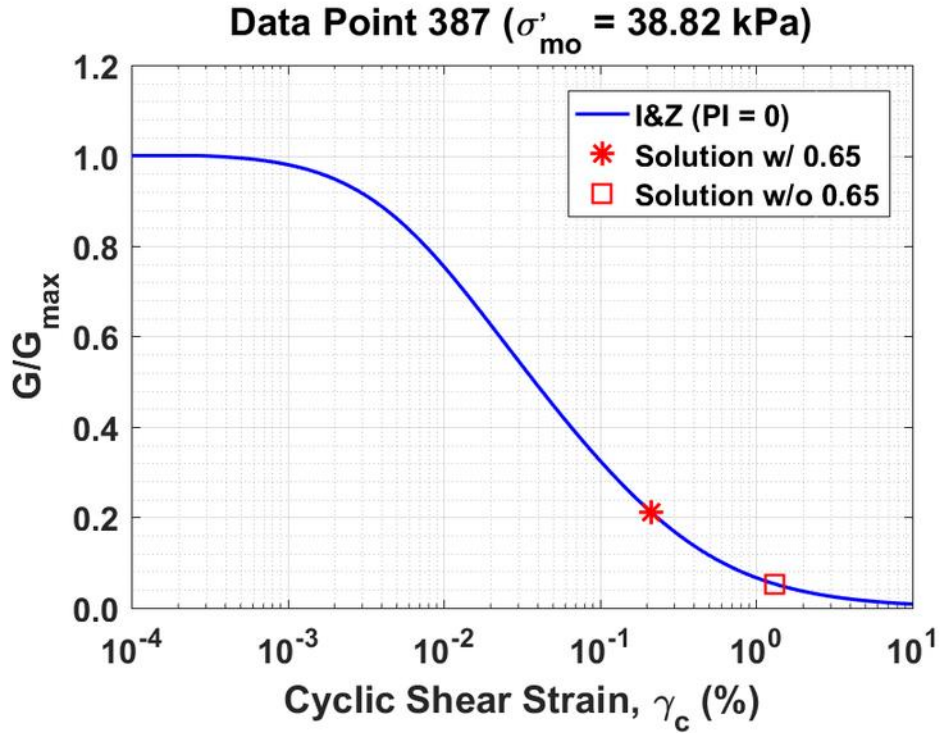


Figure B337. Normalized shear modulus reduction curves for Data Point 387 of the Kayen et al. database showing the solutions w/ and w/o the 0.65 factor

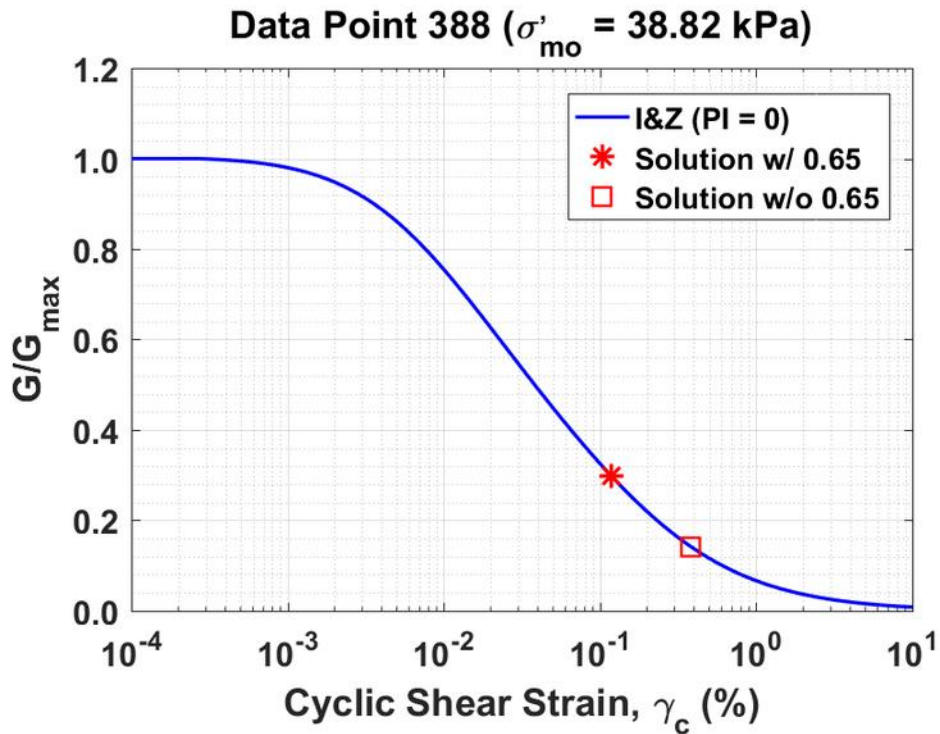


Figure B338. Normalized shear modulus reduction curves for Data Point 388 of the Kayen et al. database showing the solutions w/ and w/o the 0.65 factor

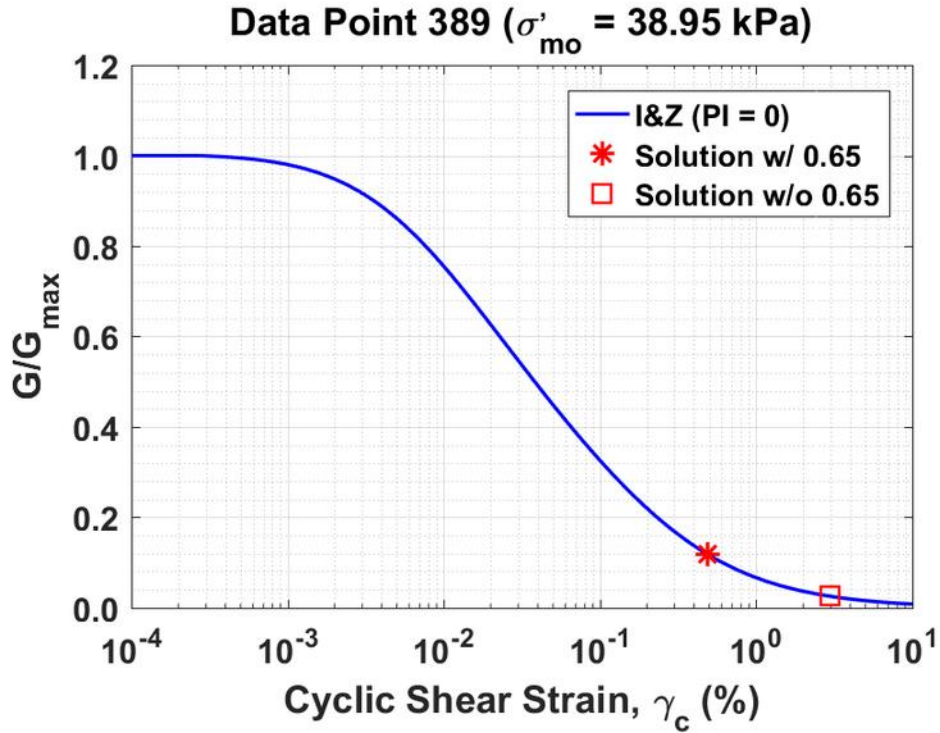


Figure B339. Normalized shear modulus reduction curves for Data Point 389 of the Kayen et al. database showing the solutions w/ and w/o the 0.65 factor

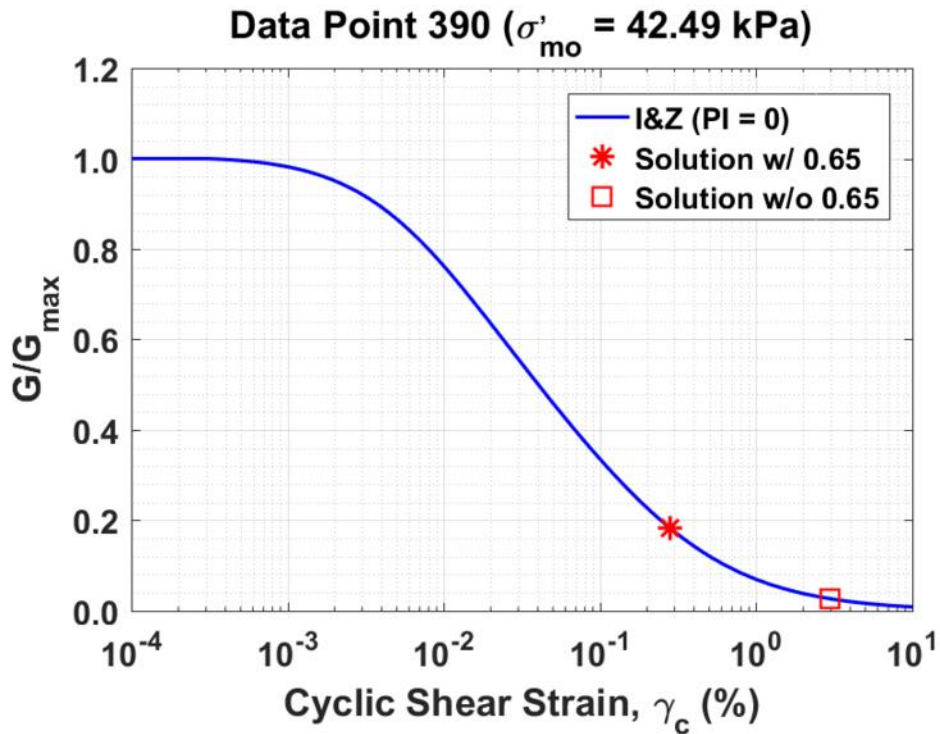


Figure B340. Normalized shear modulus reduction curves for Data Point 390 of the Kayen et al. database showing the solutions w/ and w/o the 0.65 factor

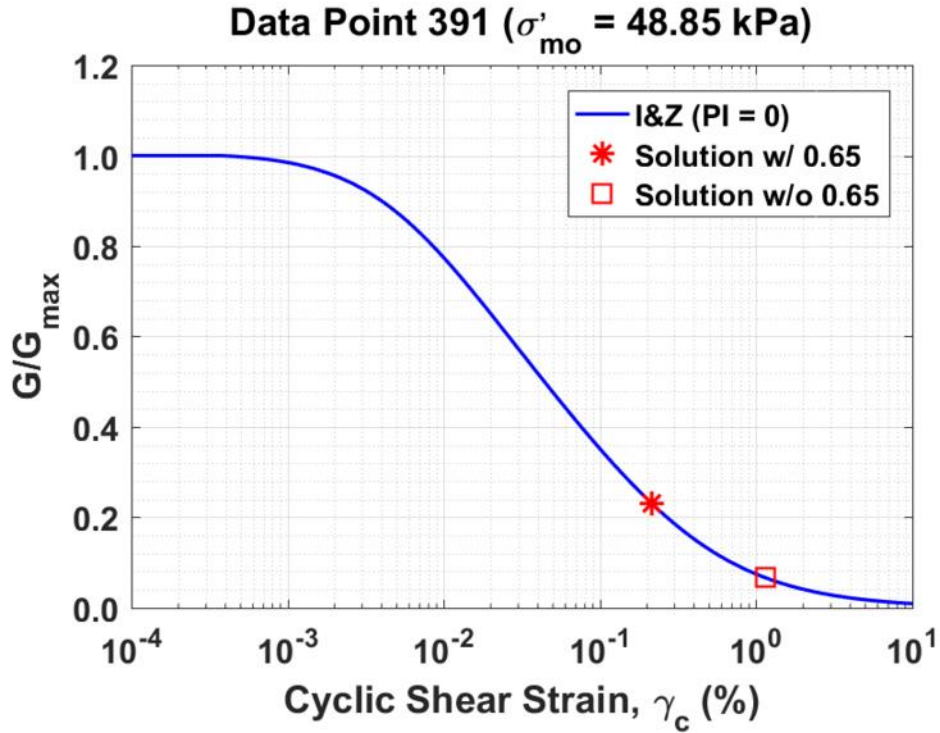


Figure B341. Normalized shear modulus reduction curves for Data Point 391 of the Kayen et al. database showing the solutions w/ and w/o the 0.65 factor

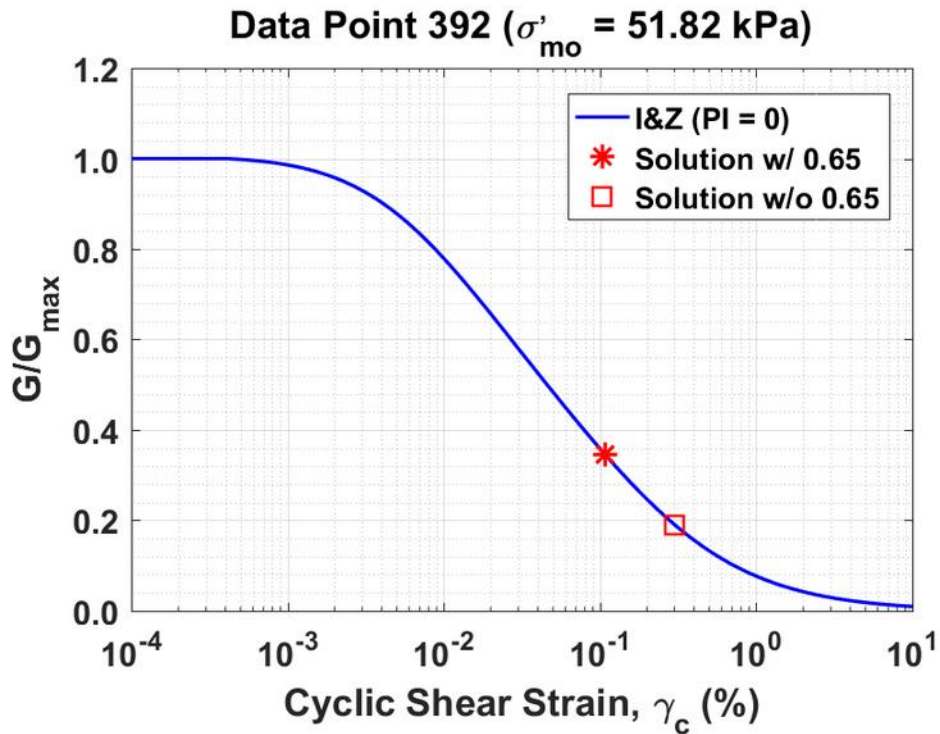


Figure B342. Normalized shear modulus reduction curves for Data Point 392 of the Kayen et al. database showing the solutions w/ and w/o the 0.65 factor

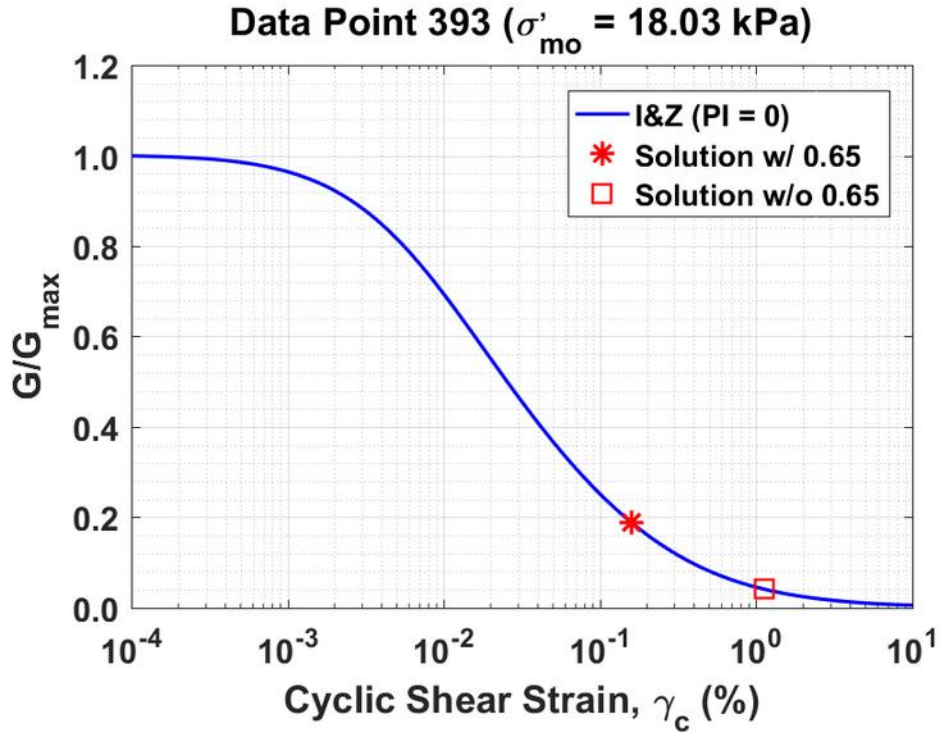


Figure B343. Normalized shear modulus reduction curves for Data Point 393 of the Kayen et al. database showing the solutions w/ and w/o the 0.65 factor

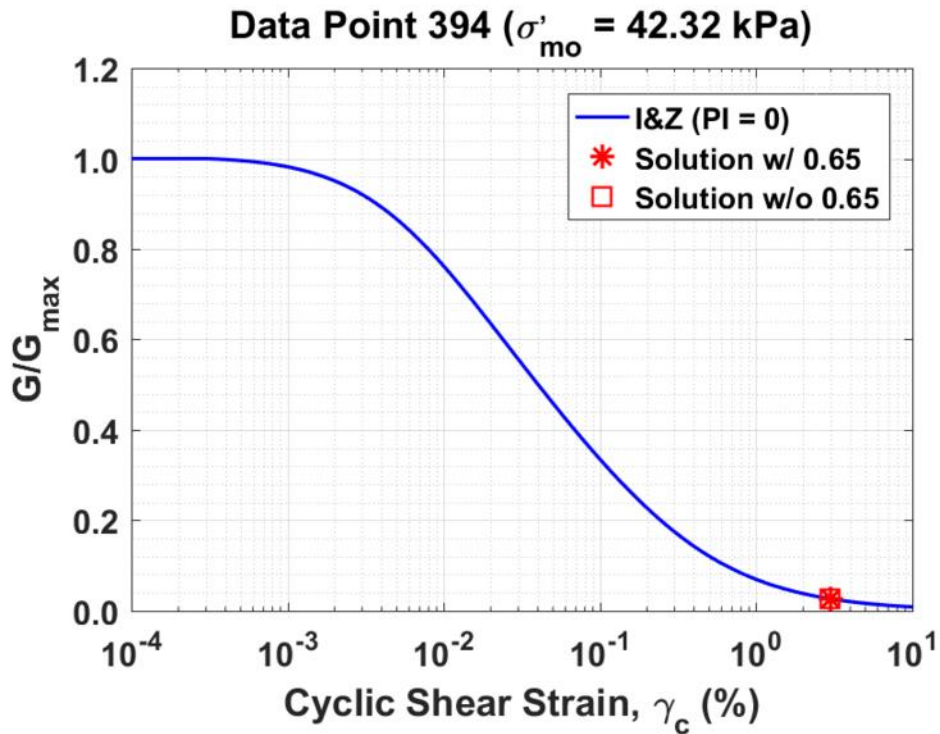


Figure B344. Normalized shear modulus reduction curves for Data Point 394 of the Kayen et al. database showing the solutions w/ and w/o the 0.65 factor

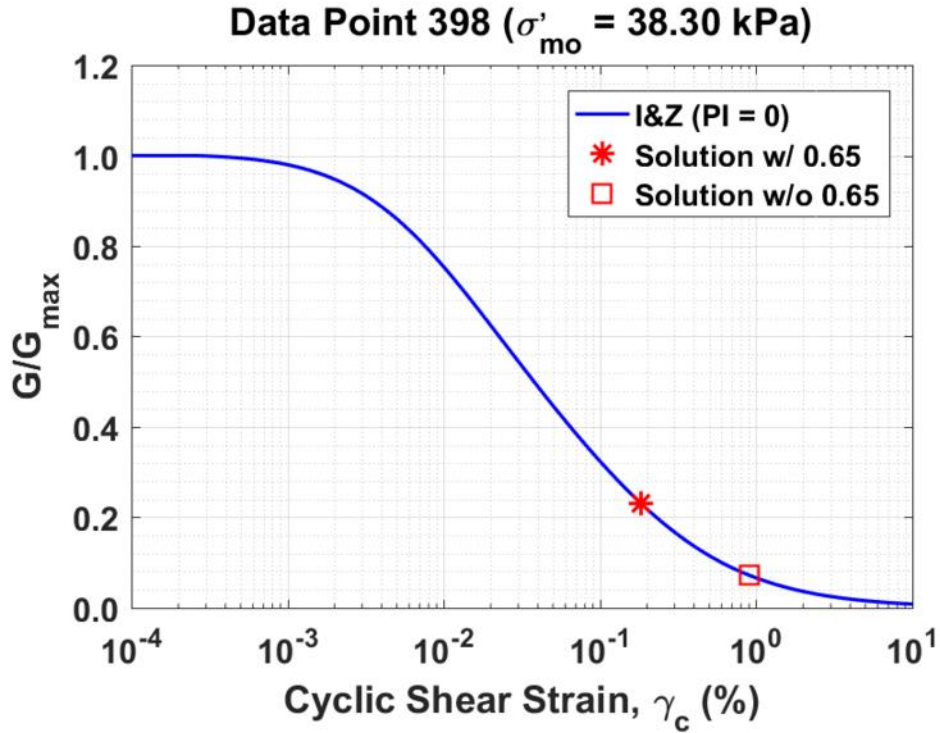


Figure B345. Normalized shear modulus reduction curves for Data Point 398 of the Kayen et al. database showing the solutions w/ and w/o the 0.65 factor

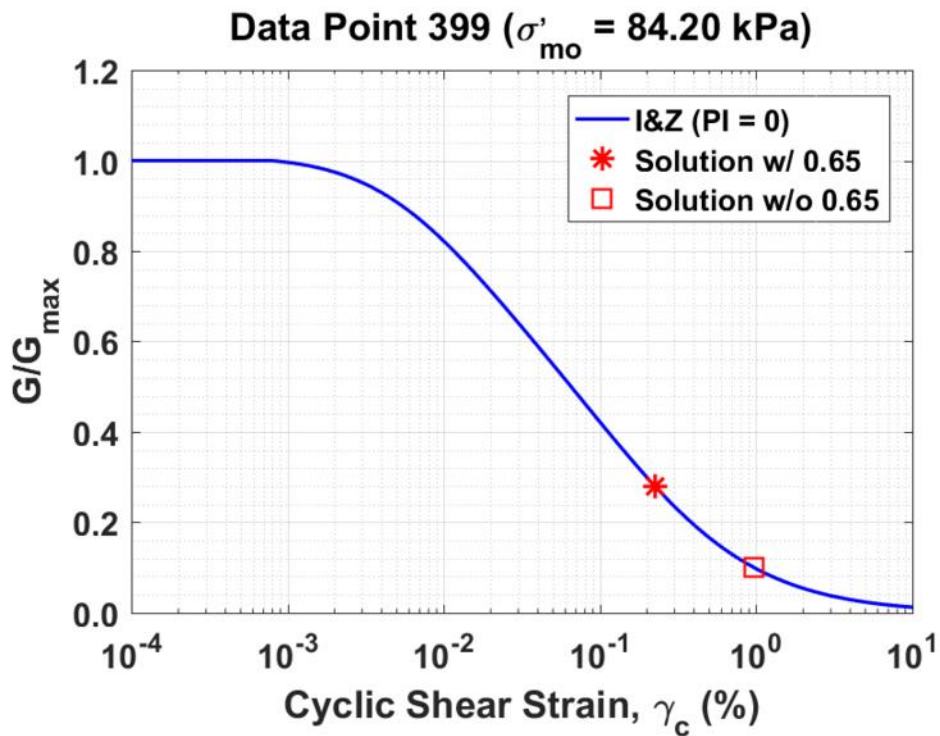


Figure B346. Normalized shear modulus reduction curves for Data Point 399 of the Kayen et al. database showing the solutions w/ and w/o the 0.65 factor

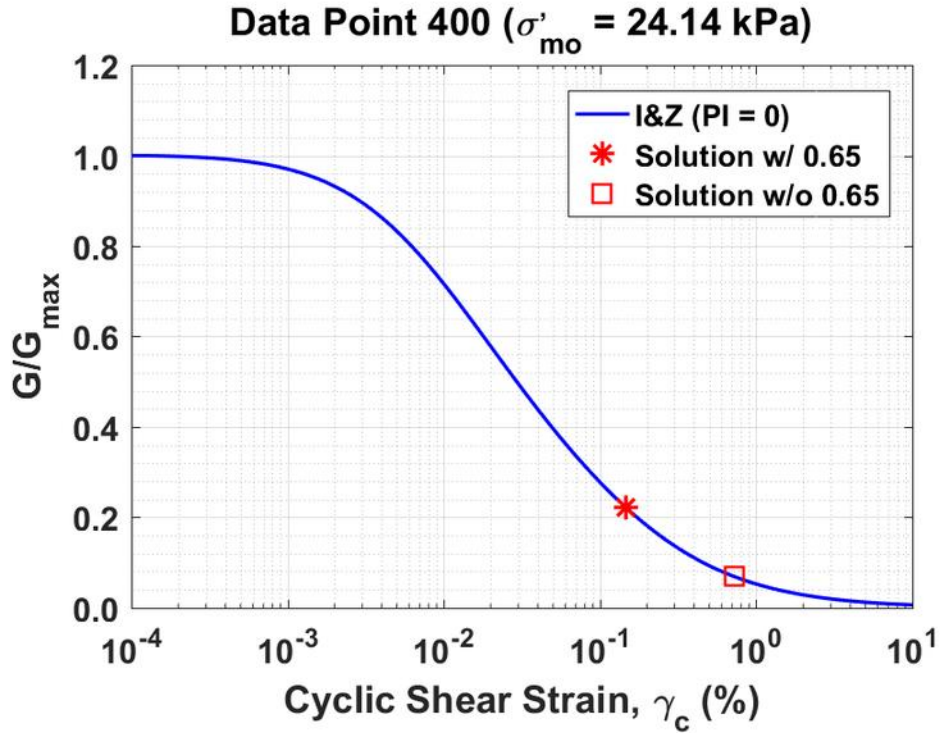


Figure B347. Normalized shear modulus reduction curves for Data Point 400 of the Kayen et al. database showing the solutions w/ and w/o the 0.65 factor

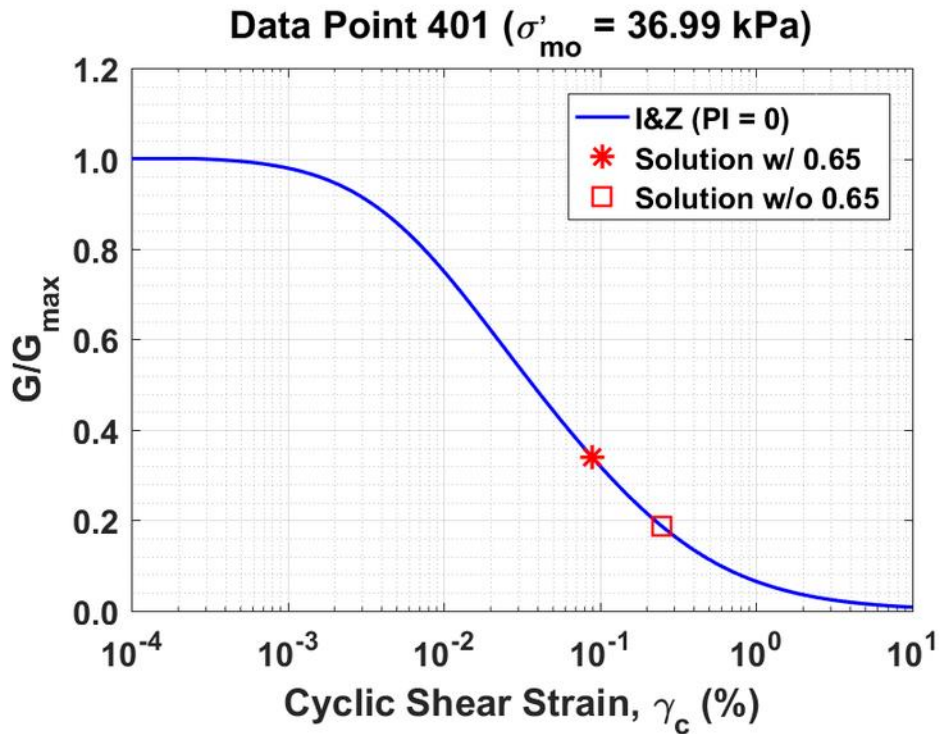


Figure B348. Normalized shear modulus reduction curves for Data Point 401 of the Kayen et al. database showing the solutions w/ and w/o the 0.65 factor

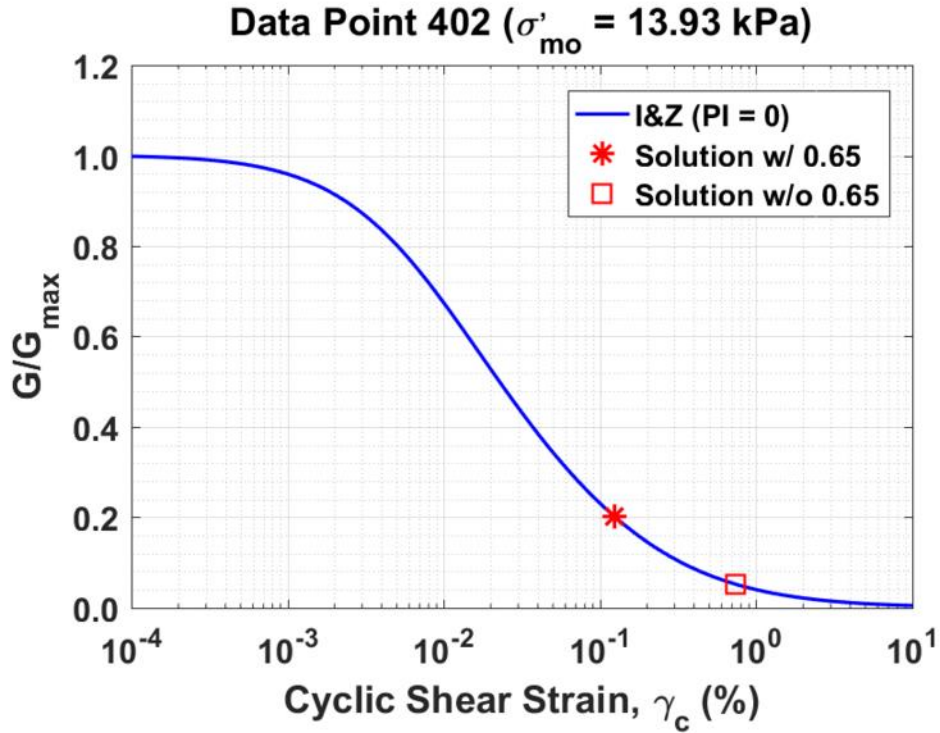


Figure B349. Normalized shear modulus reduction curves for Data Point 402 of the Kayen et al. database showing the solutions w/ and w/o the 0.65 factor

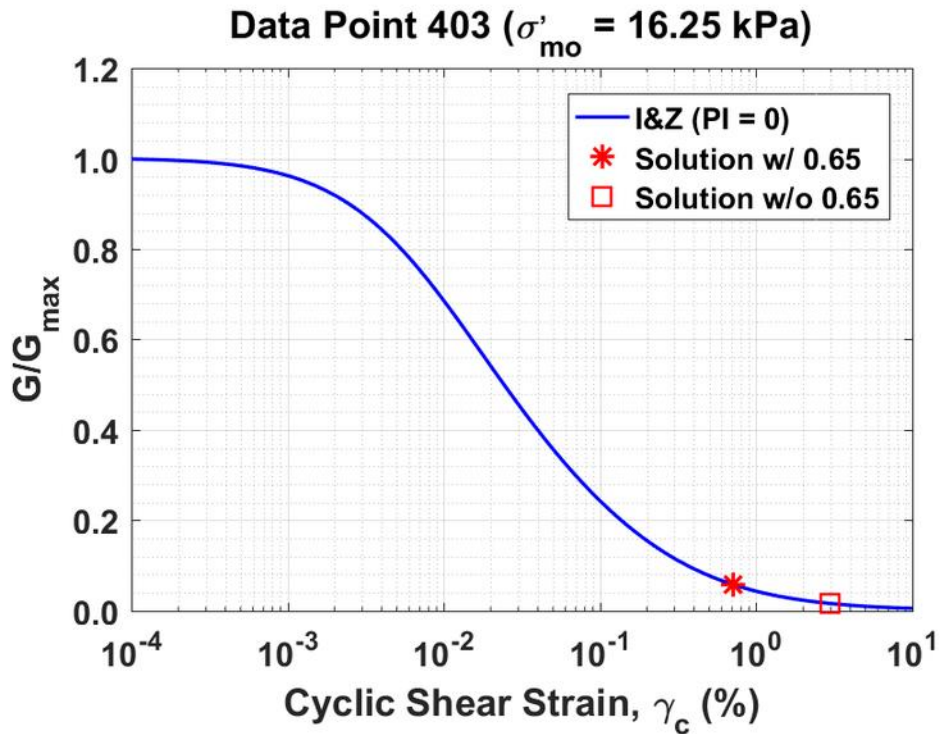


Figure B350. Normalized shear modulus reduction curves for Data Point 403 of the Kayen et al. database showing the solutions w/ and w/o the 0.65 factor

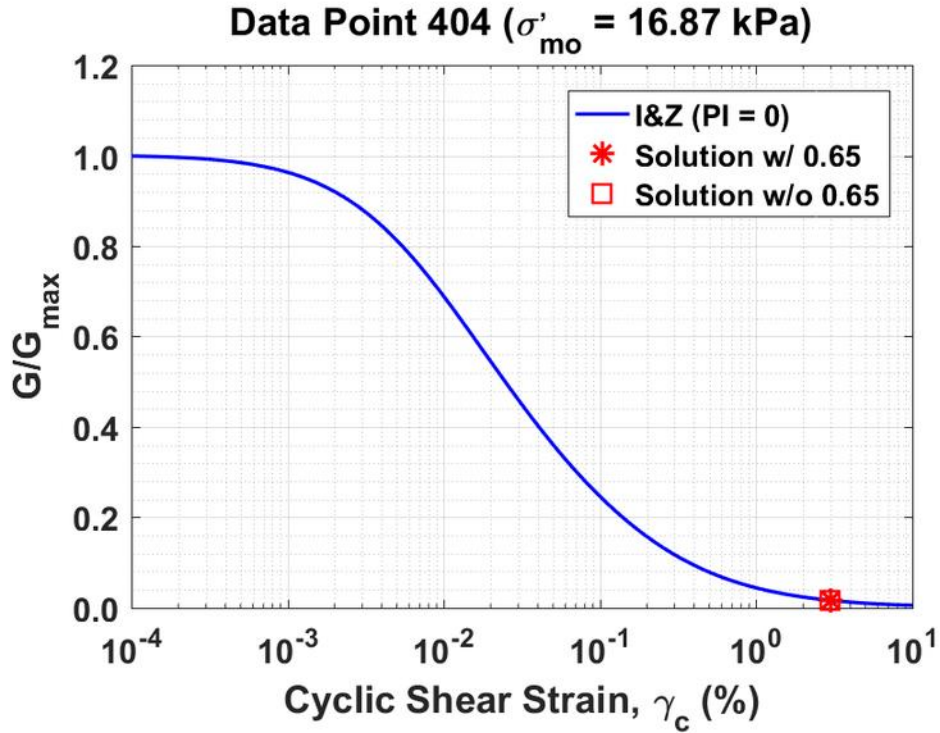


Figure B351. Normalized shear modulus reduction curves for Data Point 404 of the Kayen et al. database showing the solutions w/ and w/o the 0.65 factor

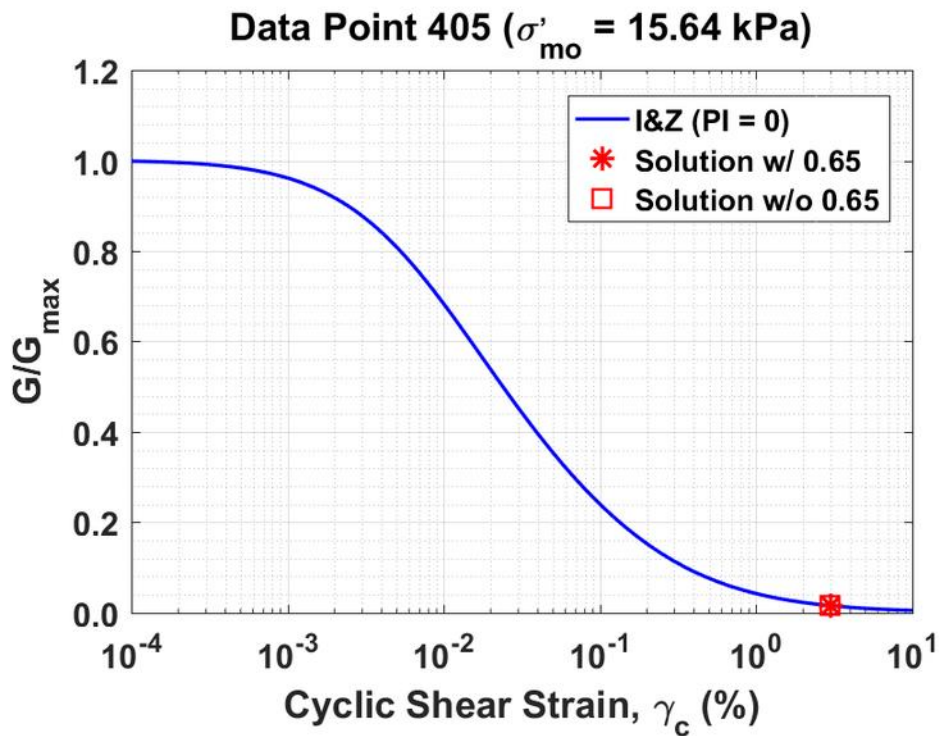


Figure B352. Normalized shear modulus reduction curves for Data Point 405 of the Kayen et al. database showing the solutions w/ and w/o the 0.65 factor

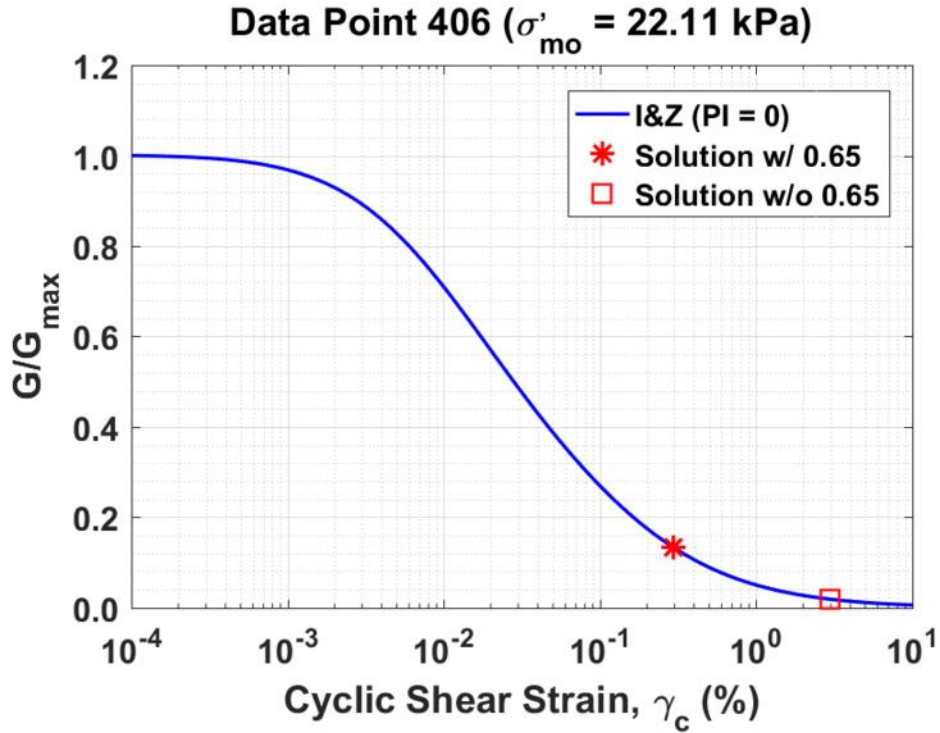


Figure B353. Normalized shear modulus reduction curves for Data Point 406 of the Kayen et al. database showing the solutions w/ and w/o the 0.65 factor

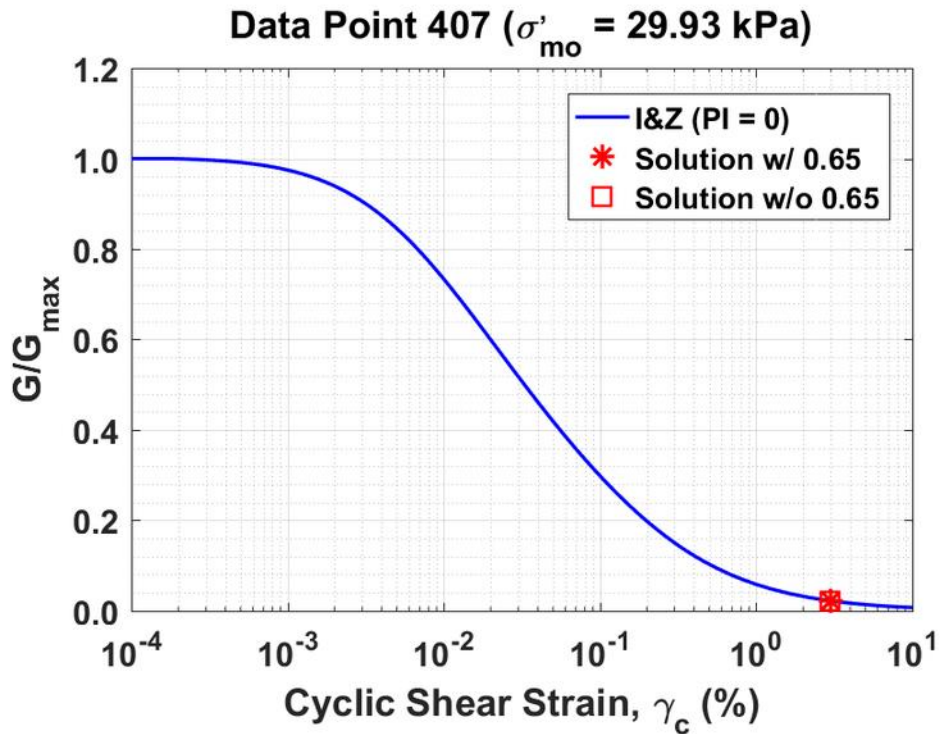


Figure B354. Normalized shear modulus reduction curves for Data Point 407 of the Kayen et al. database showing the solutions w/ and w/o the 0.65 factor

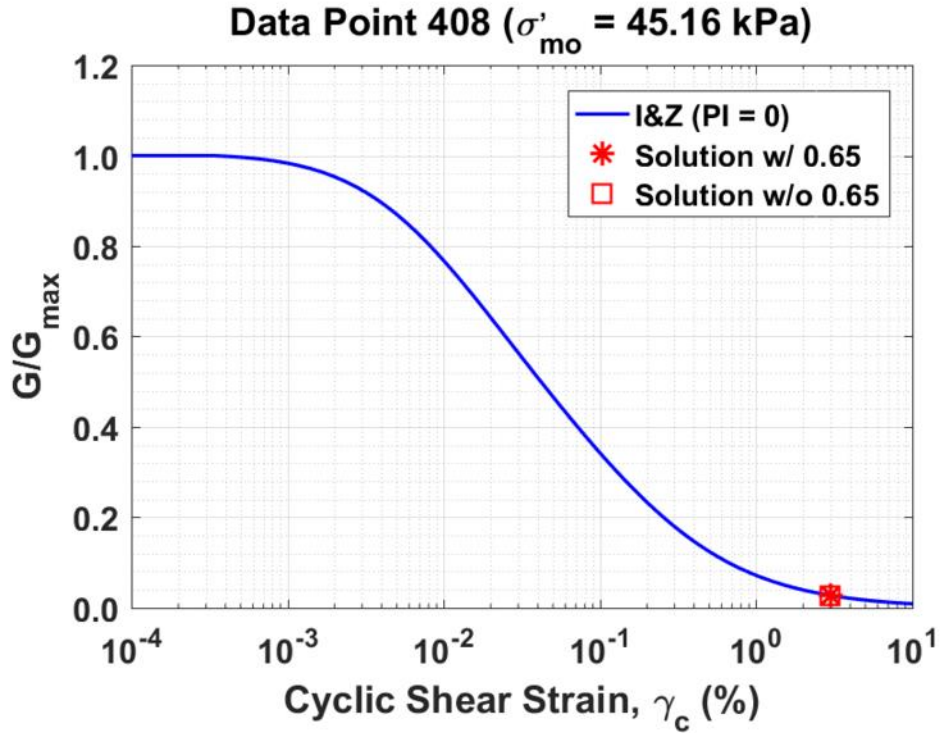


Figure B355. Normalized shear modulus reduction curves for Data Point 408 of the Kayen et al. database showing the solutions w/ and w/o the 0.65 factor

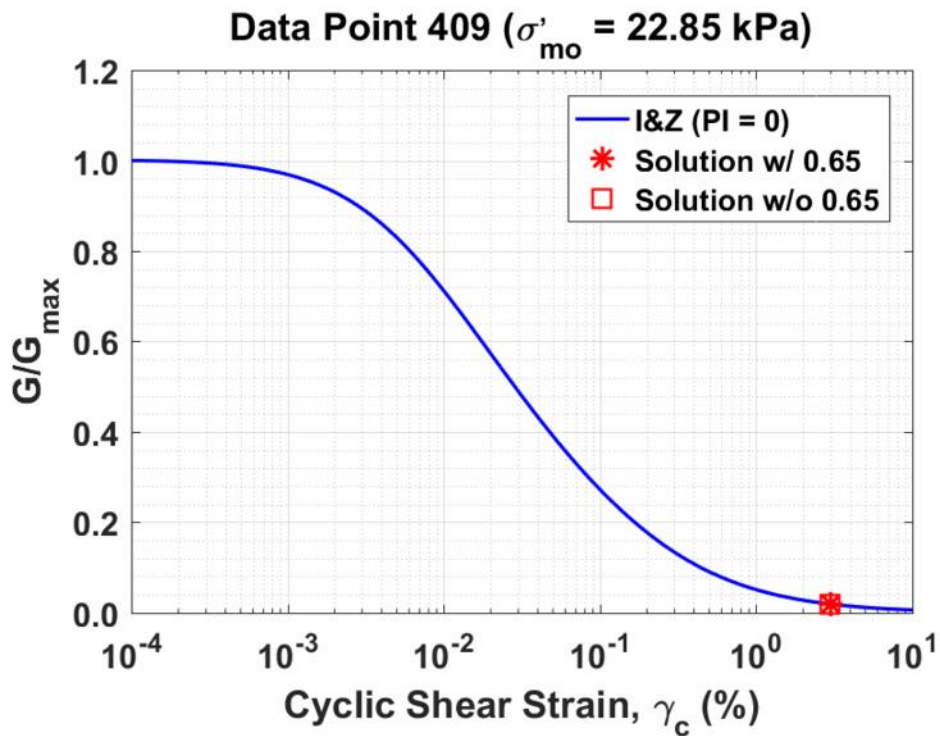


Figure B356. Normalized shear modulus reduction curves for Data Point 409 of the Kayen et al. database showing the solutions w/ and w/o the 0.65 factor

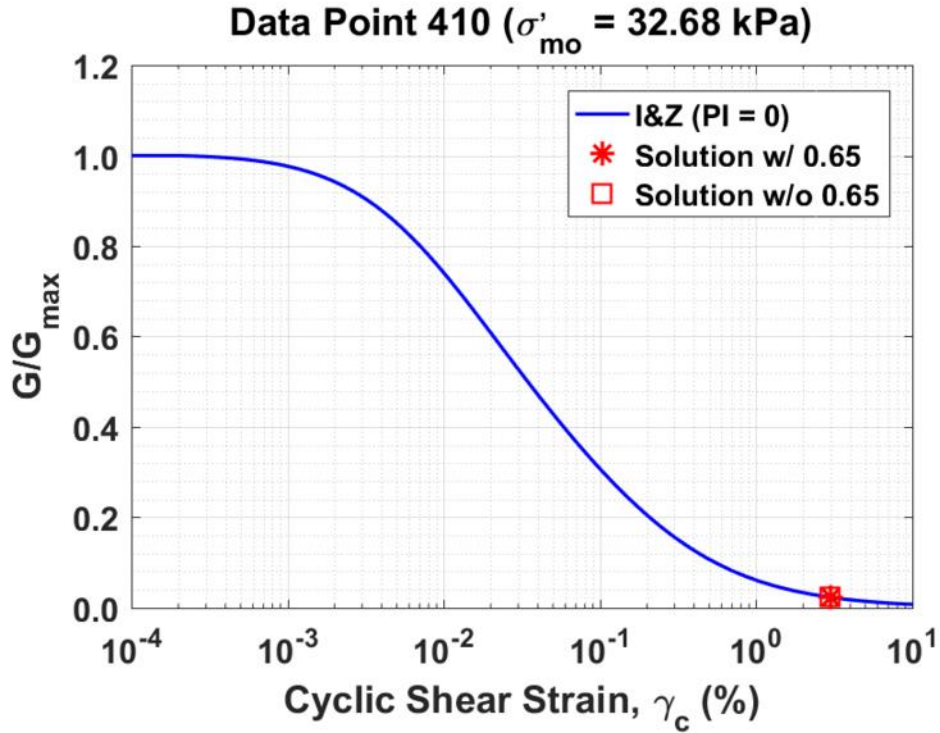


Figure B357. Normalized shear modulus reduction curves for Data Point 410 of the Kayen et al. database showing the solutions w/ and w/o the 0.65 factor

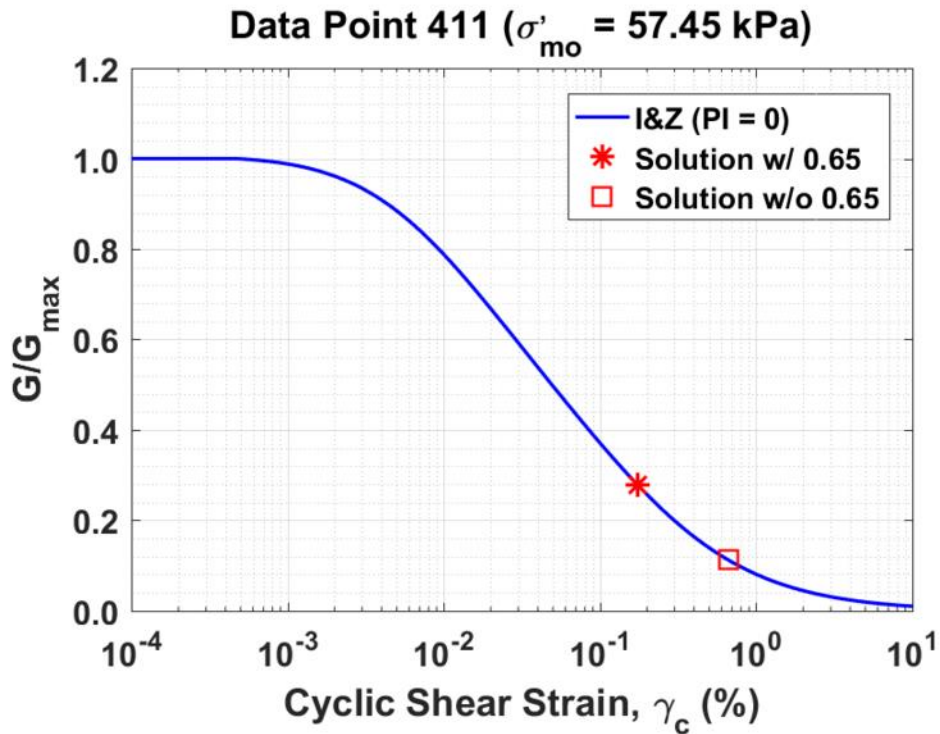


Figure B358. Normalized shear modulus reduction curves for Data Point 411 of the Kayen et al. database showing the solutions w/ and w/o the 0.65 factor

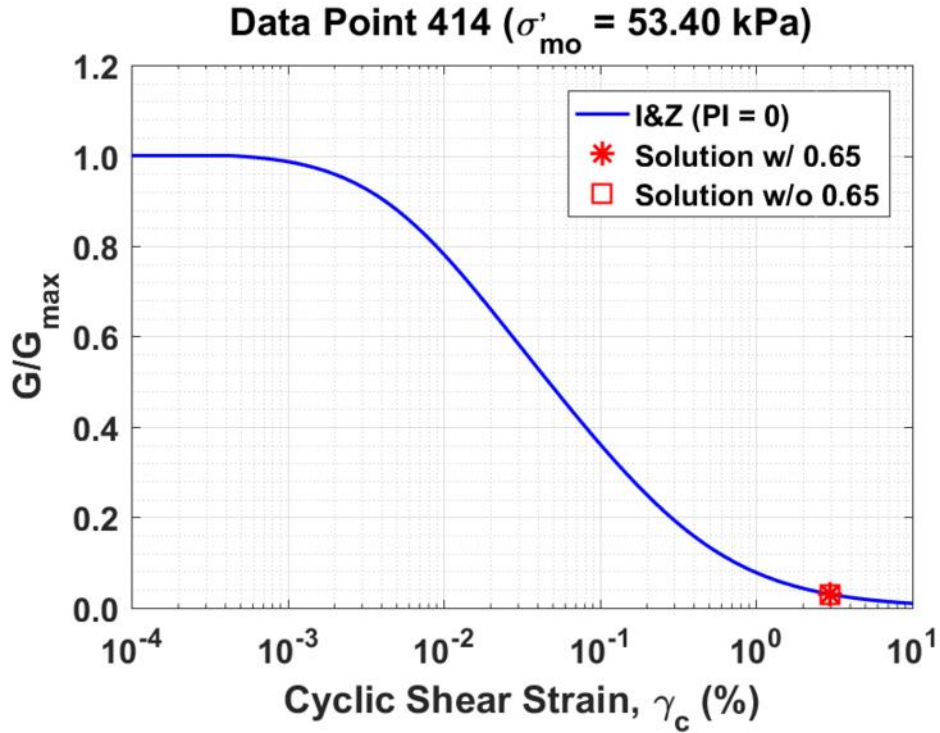


Figure B359. Normalized shear modulus reduction curves for Data Point 414 of the Kayen et al. database showing the solutions w/ and w/o the 0.65 factor

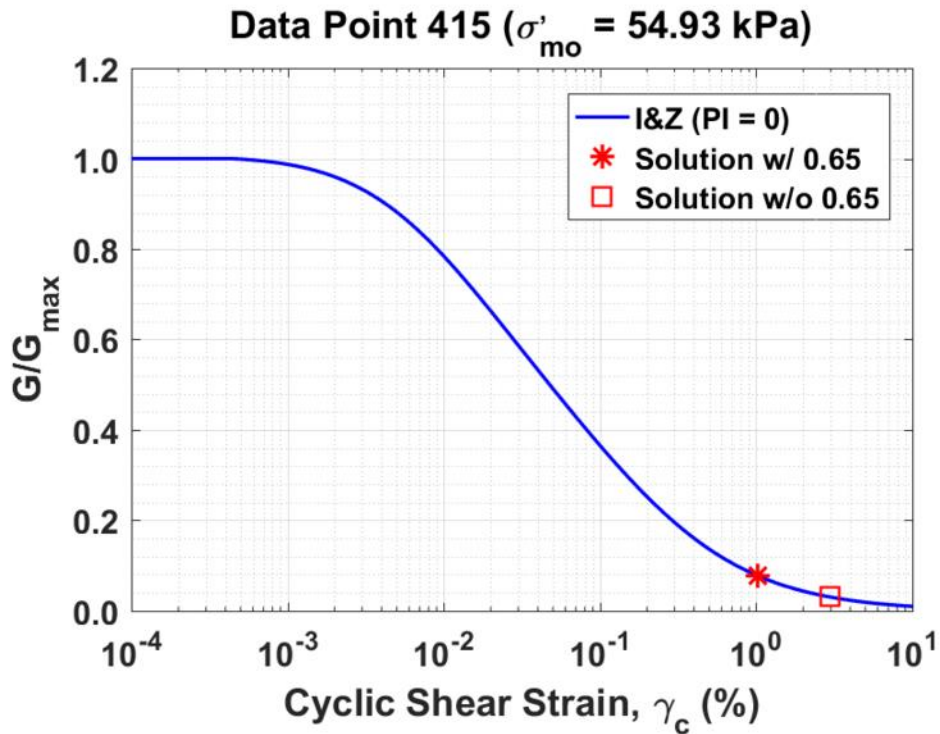


Figure B360. Normalized shear modulus reduction curves for Data Point 415 of the Kayen et al. database showing the solutions w/ and w/o the 0.65 factor

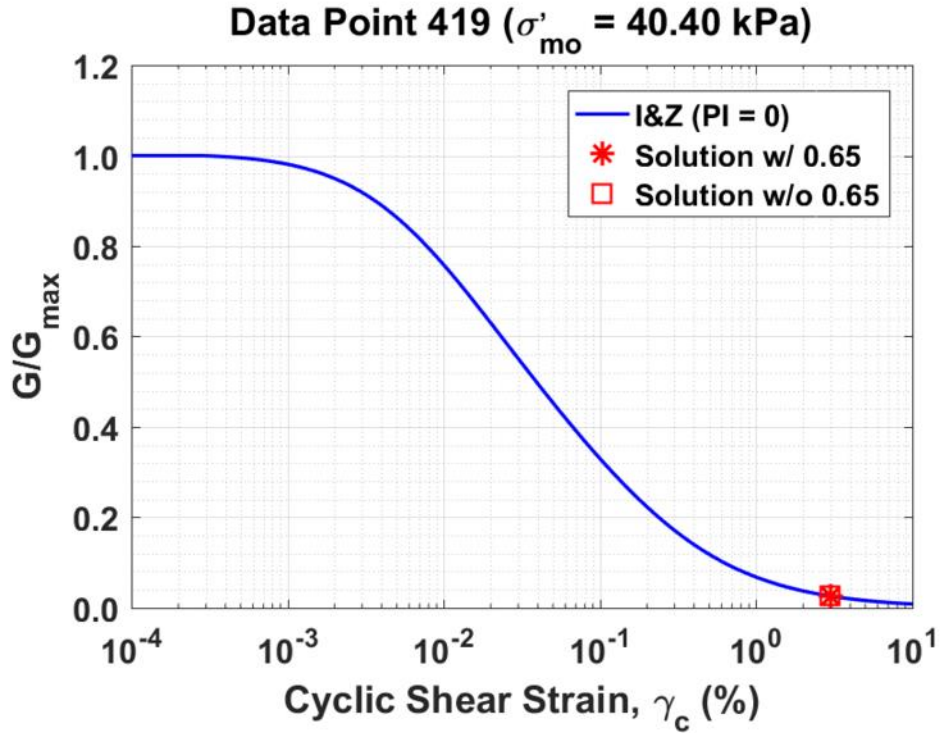


Figure B361. Normalized shear modulus reduction curves for Data Point 419 of the Kayen et al. database showing the solutions w/ and w/o the 0.65 factor

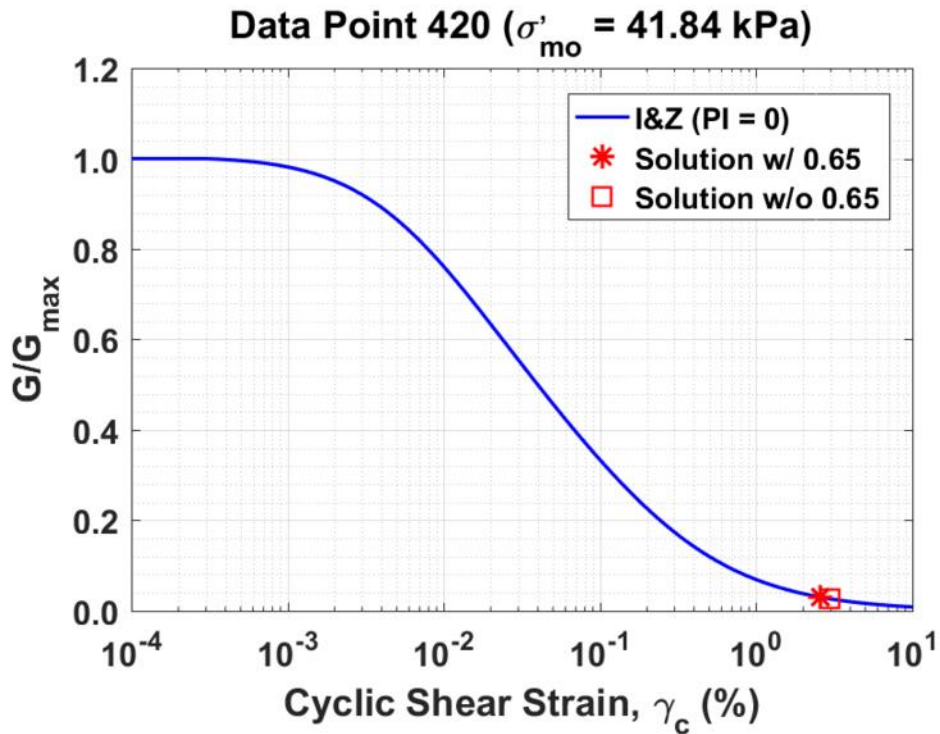


Figure B362. Normalized shear modulus reduction curves for Data Point 420 of the Kayen et al. database showing the solutions w/ and w/o the 0.65 factor

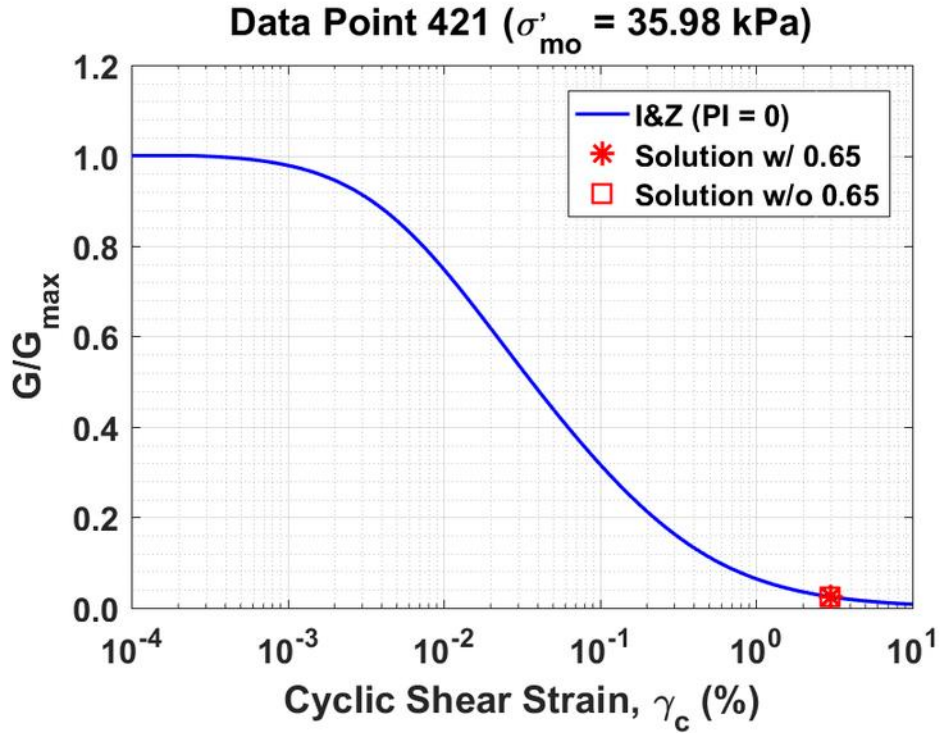


Figure B363. Normalized shear modulus reduction curves for Data Point 421 of the Kayen et al. database showing the solutions w/ and w/o the 0.65 factor

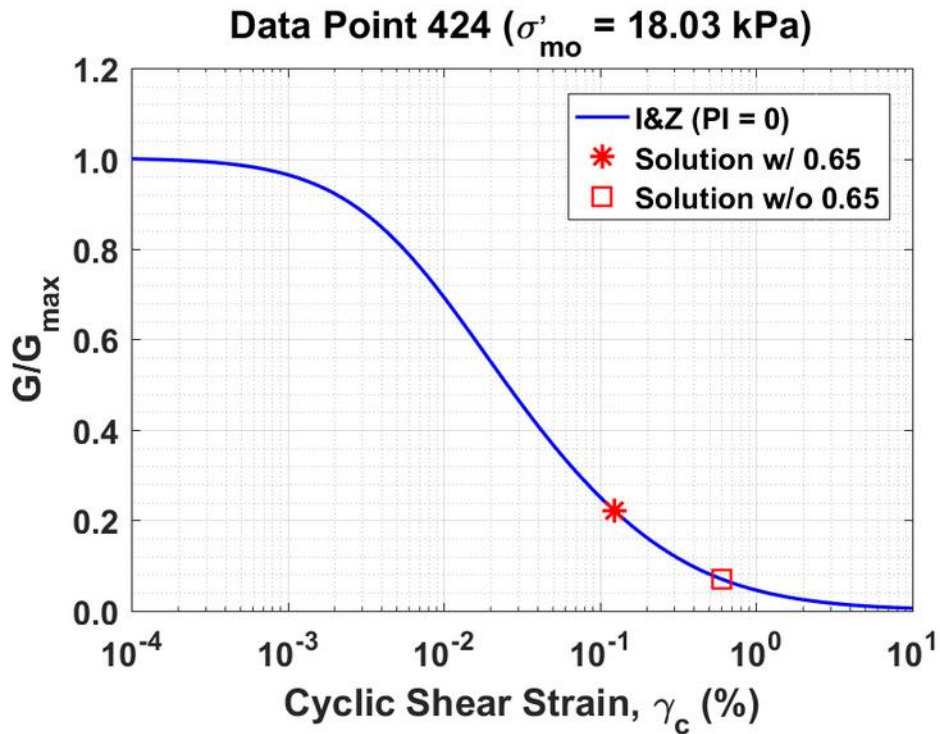


Figure B364. Normalized shear modulus reduction curves for Data Point 424 of the Kayen et al. database showing the solutions w/ and w/o the 0.65 factor

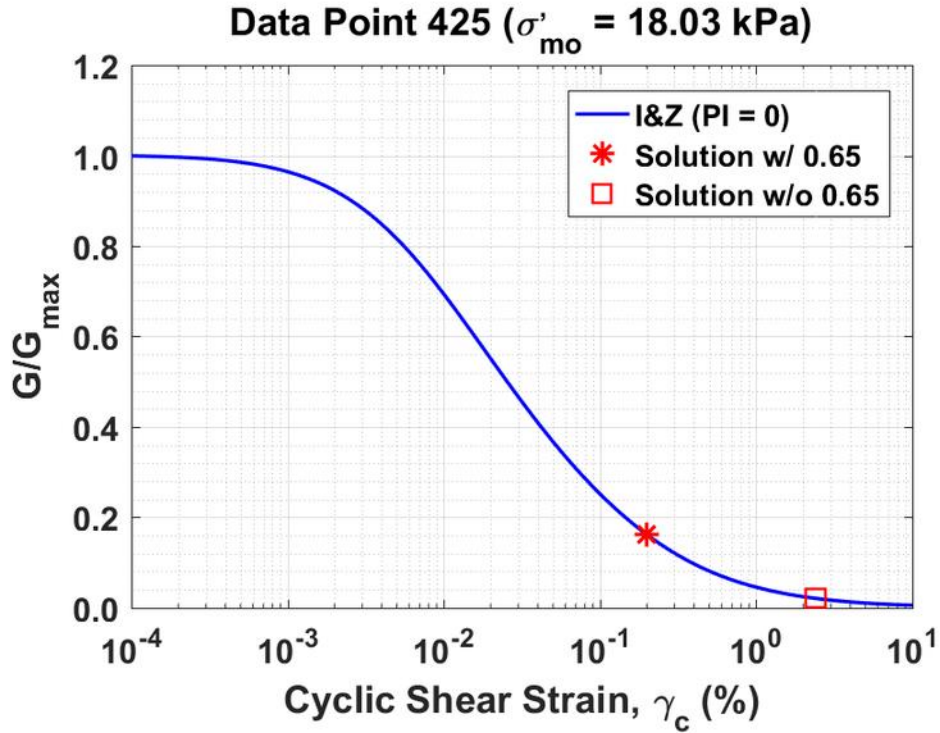


Figure B365. Normalized shear modulus reduction curves for Data Point 425 of the Kayen et al. database showing the solutions w/ and w/o the 0.65 factor

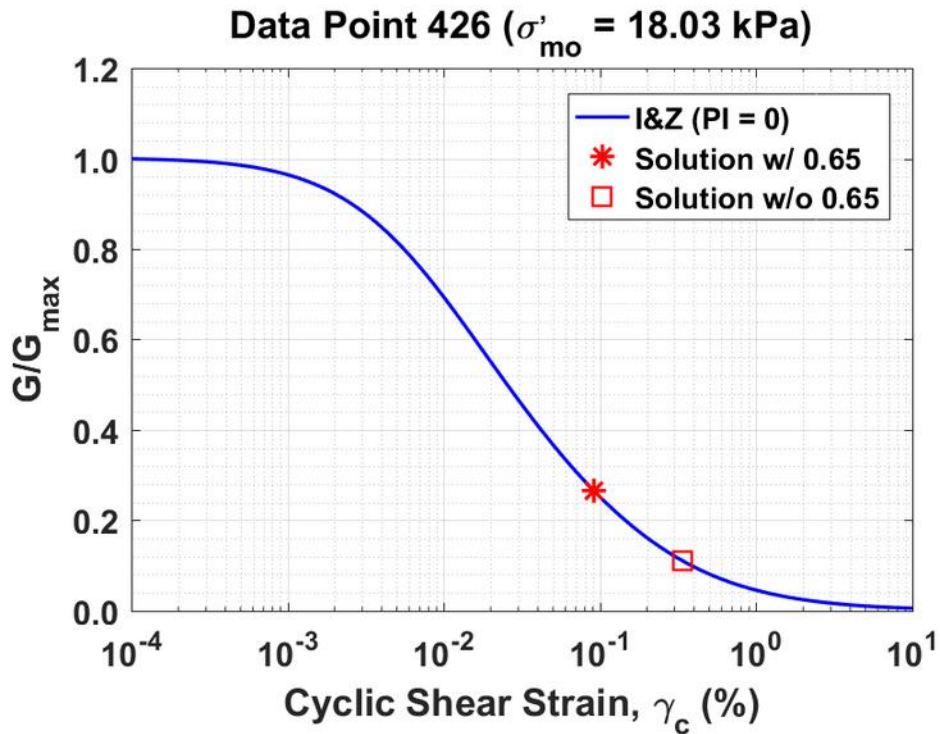


Figure B366. Normalized shear modulus reduction curves for Data Point 426 of the Kayen et al. database showing the solutions w/ and w/o the 0.65 factor

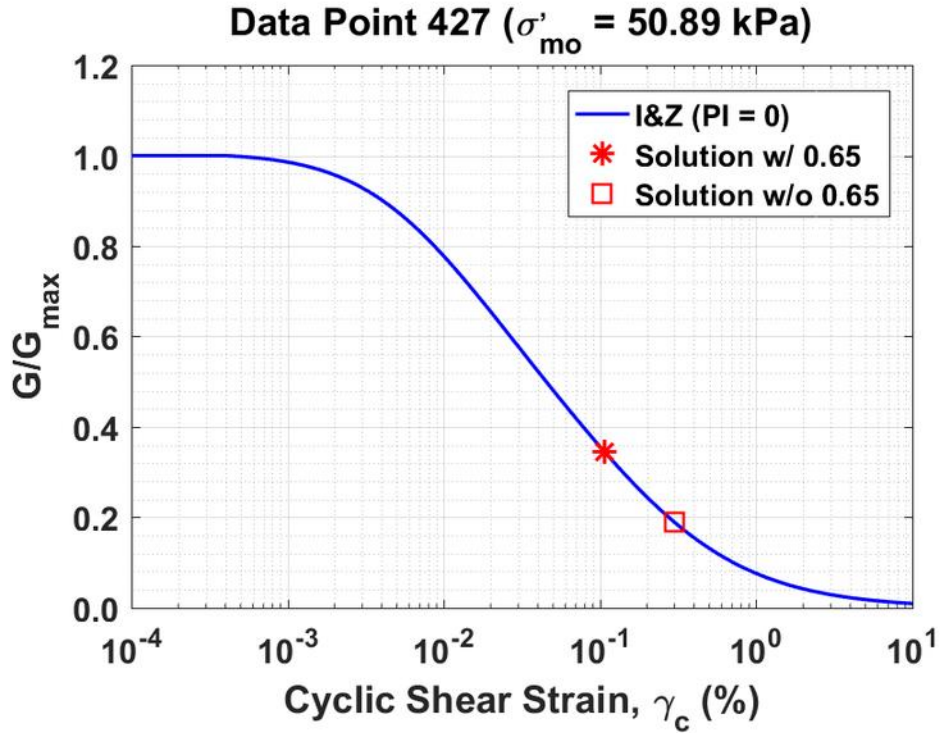


Figure B367. Normalized shear modulus reduction curves for Data Point 427 of the Kayen et al. database showing the solutions w/ and w/o the 0.65 factor

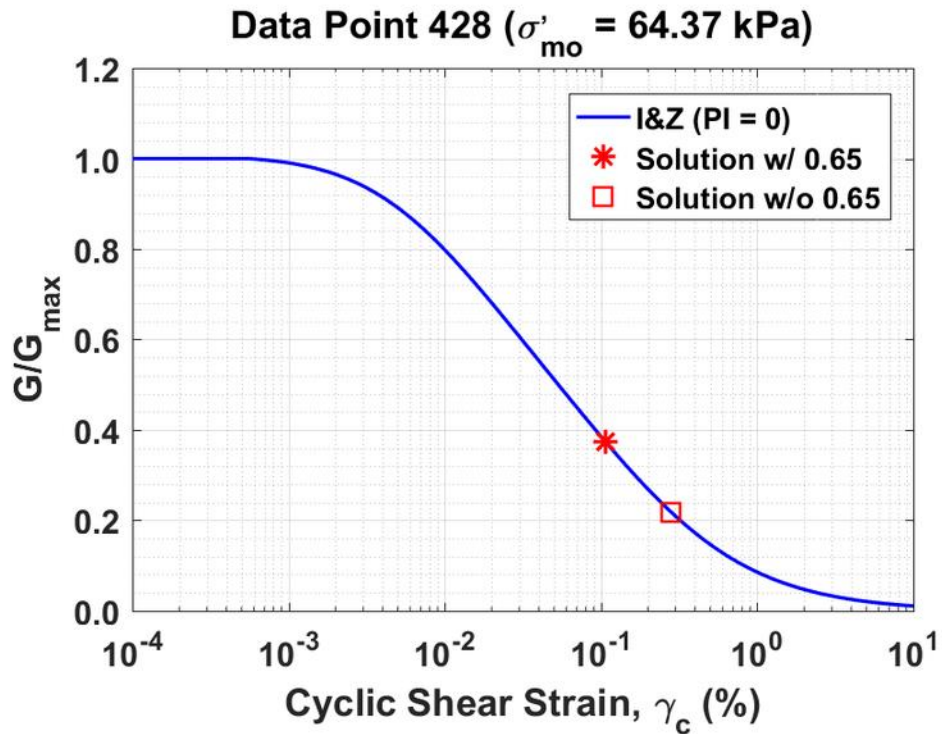


Figure B368. Normalized shear modulus reduction curves for Data Point 428 of the Kayen et al. database showing the solutions w/ and w/o the 0.65 factor

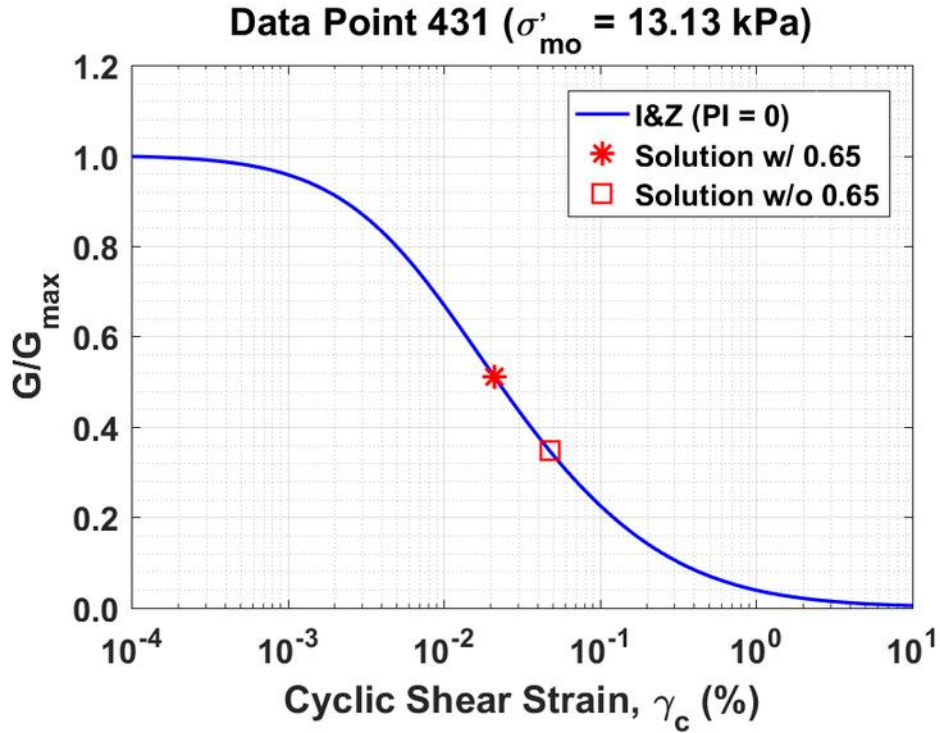


Figure B369. Normalized shear modulus reduction curves for Data Point 431 of the Kayen et al. database showing the solutions w/ and w/o the 0.65 factor

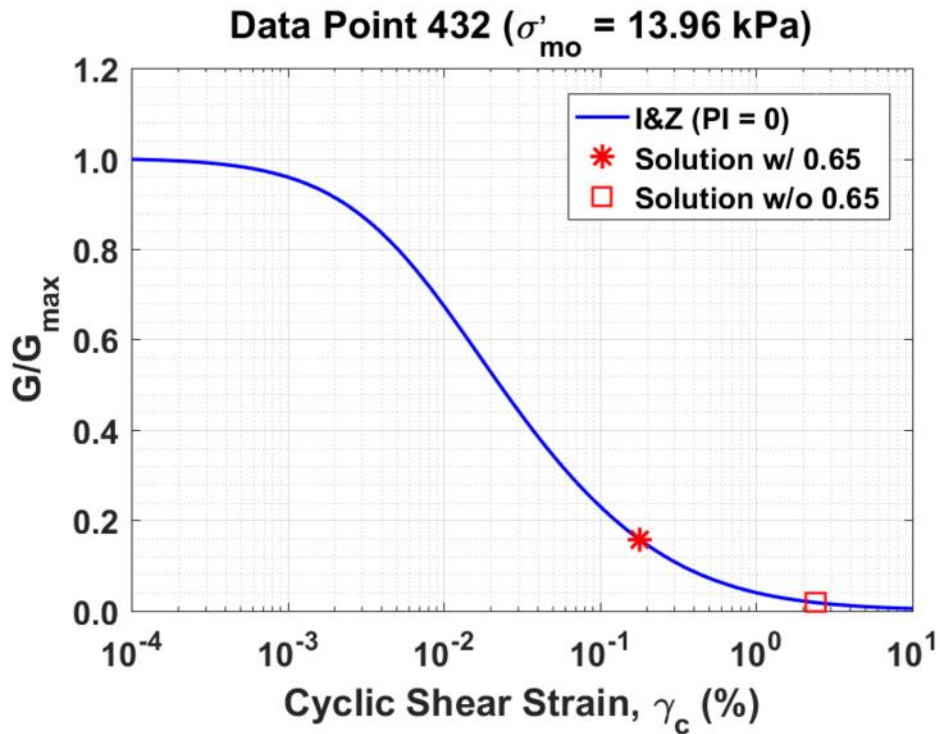


Figure B370. Normalized shear modulus reduction curves for Data Point 432 of the Kayen et al. database showing the solutions w/ and w/o the 0.65 factor

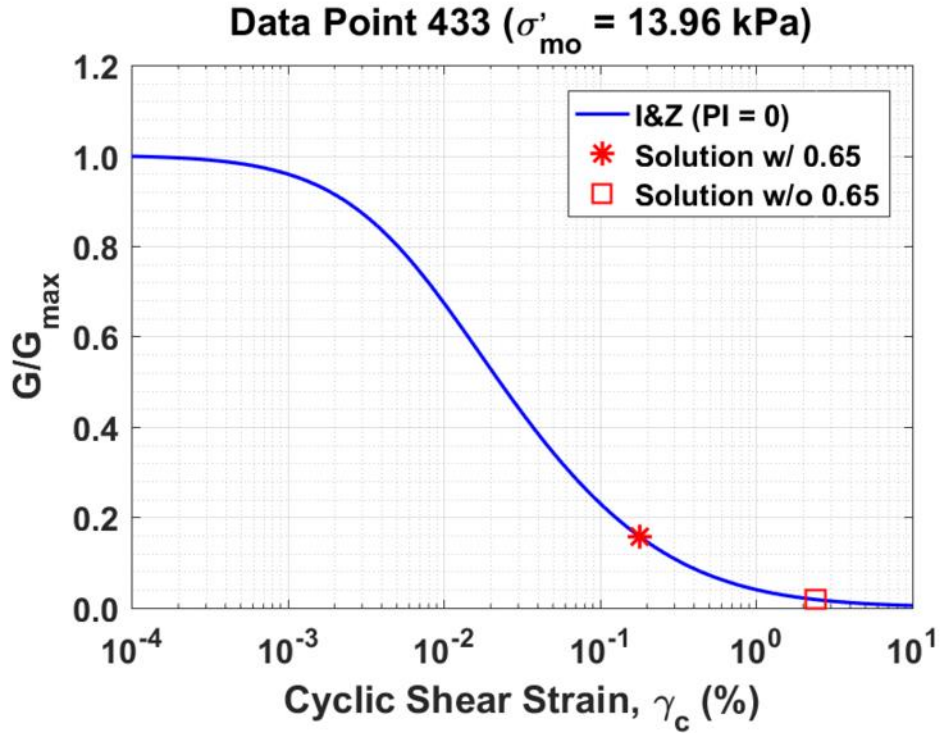


Figure B371. Normalized shear modulus reduction curves for Data Point 433 of the Kayen et al. database showing the solutions w/ and w/o the 0.65 factor

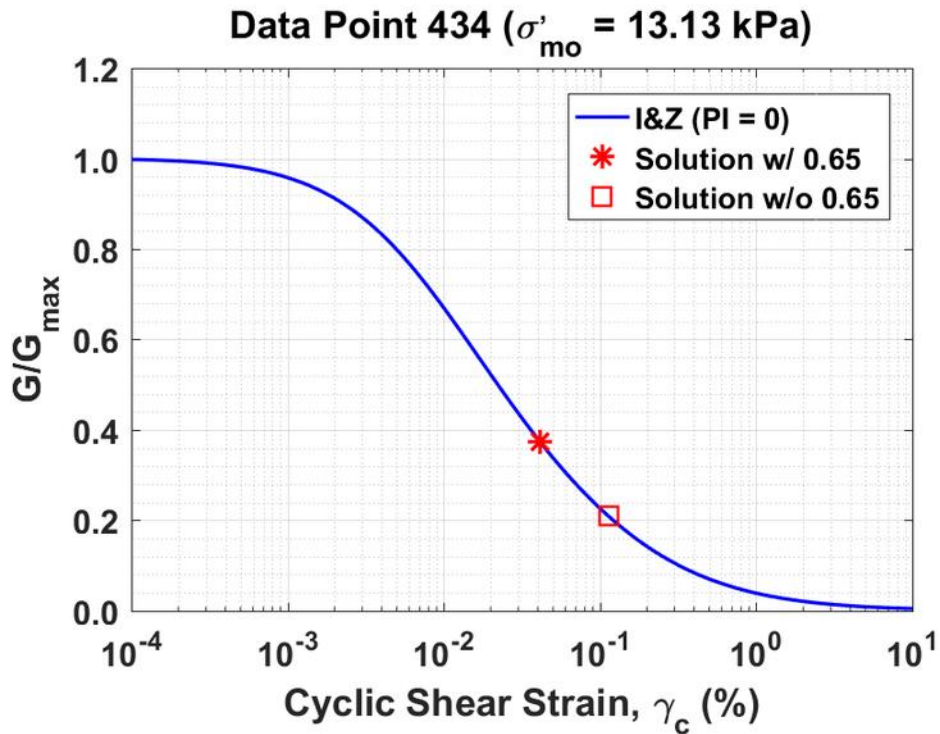


Figure B372. Normalized shear modulus reduction curves for Data Point 434 of the Kayen et al. database showing the solutions w/ and w/o the 0.65 factor

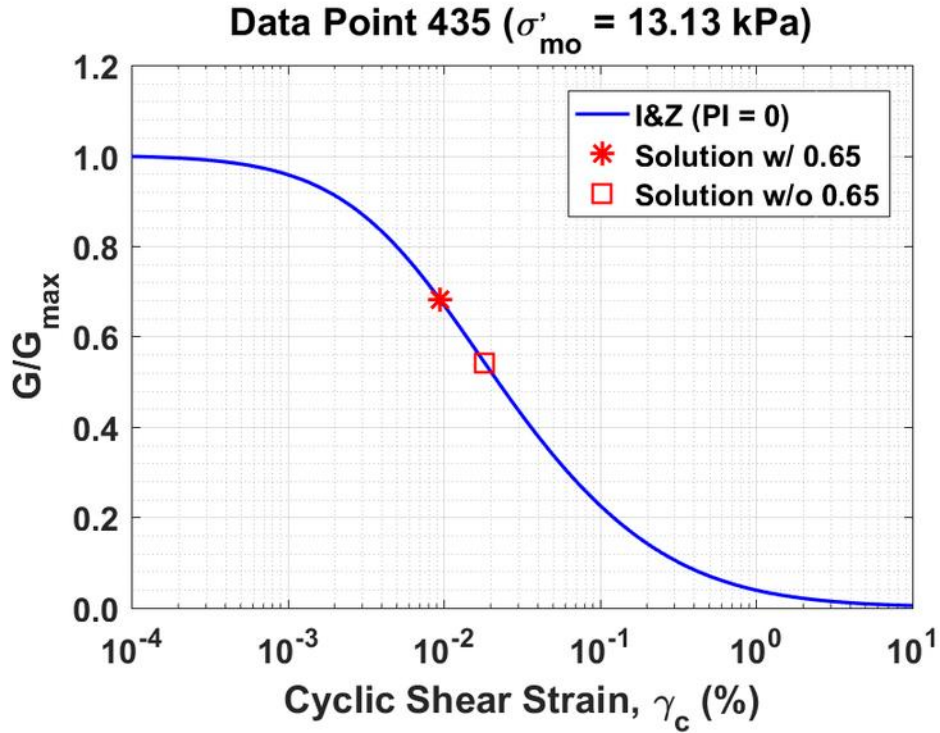


Figure B373. Normalized shear modulus reduction curves for Data Point 435 of the Kayen et al. database showing the solutions w/ and w/o the 0.65 factor

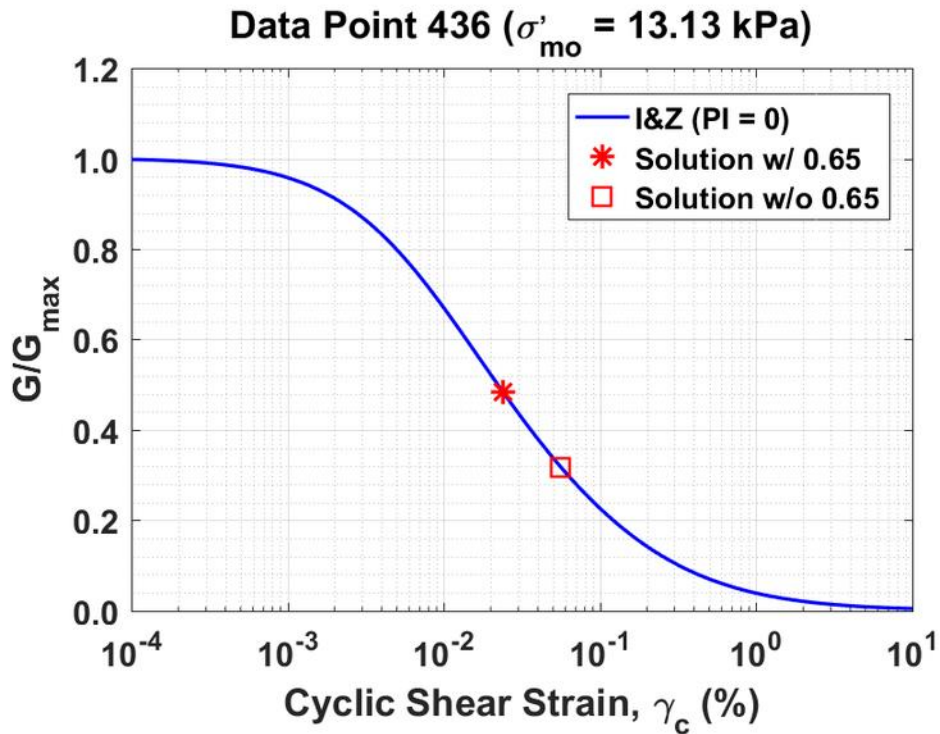


Figure B374. Normalized shear modulus reduction curves for Data Point 436 of the Kayen et al. database showing the solutions w/ and w/o the 0.65 factor

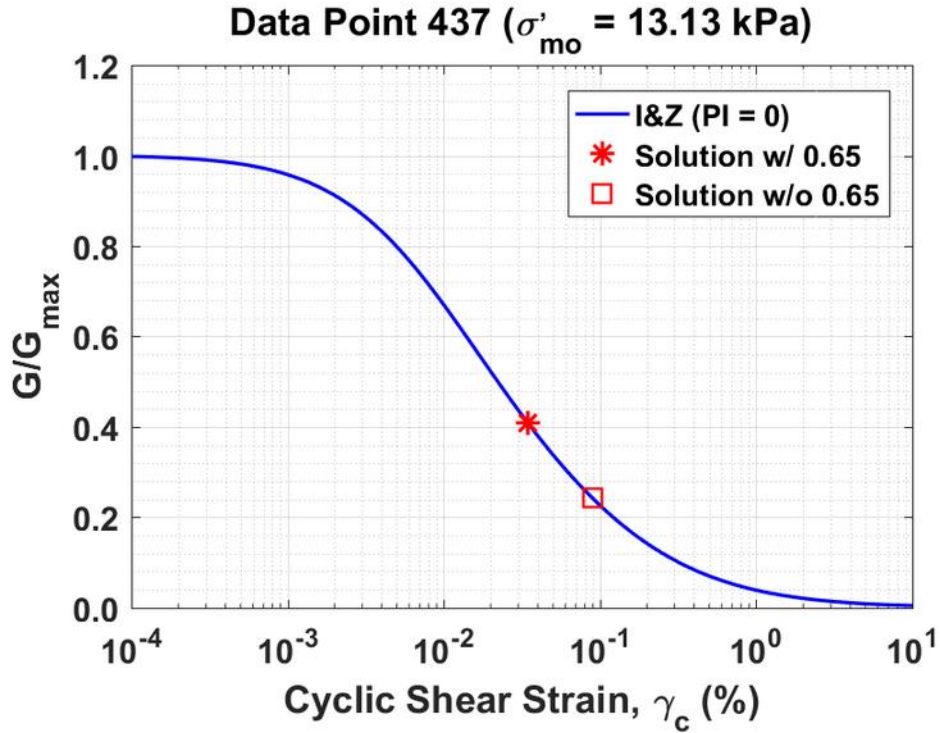


Figure B375. Normalized shear modulus reduction curves for Data Point 437 of the Kayen et al. database showing the solutions w/ and w/o the 0.65 factor

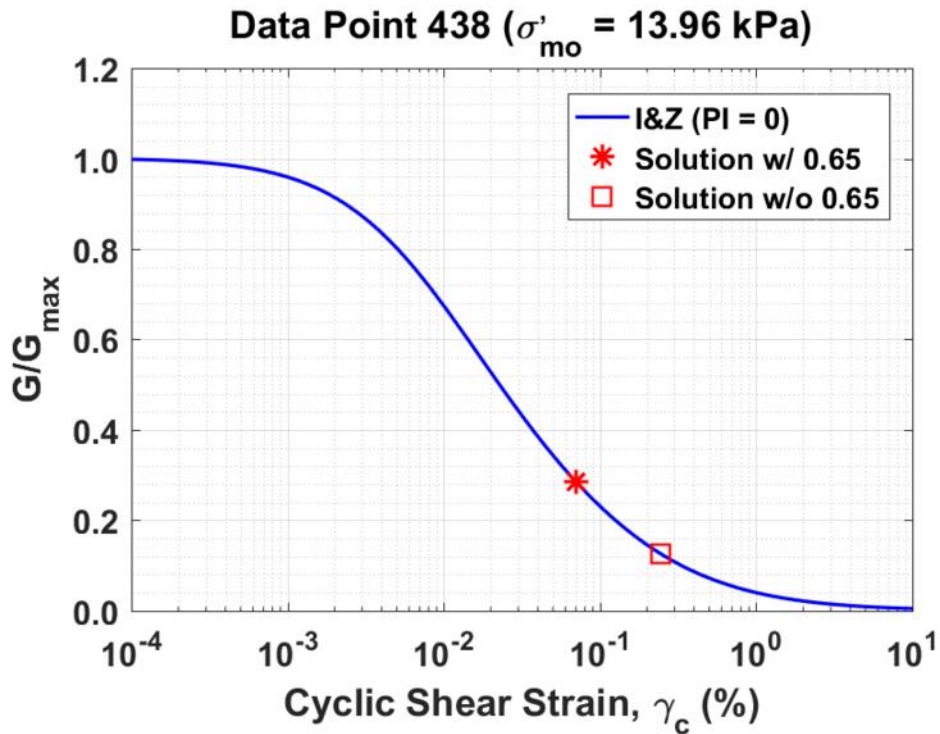


Figure B376. Normalized shear modulus reduction curves for Data Point 438 of the Kayen et al. database showing the solutions w/ and w/o the 0.65 factor

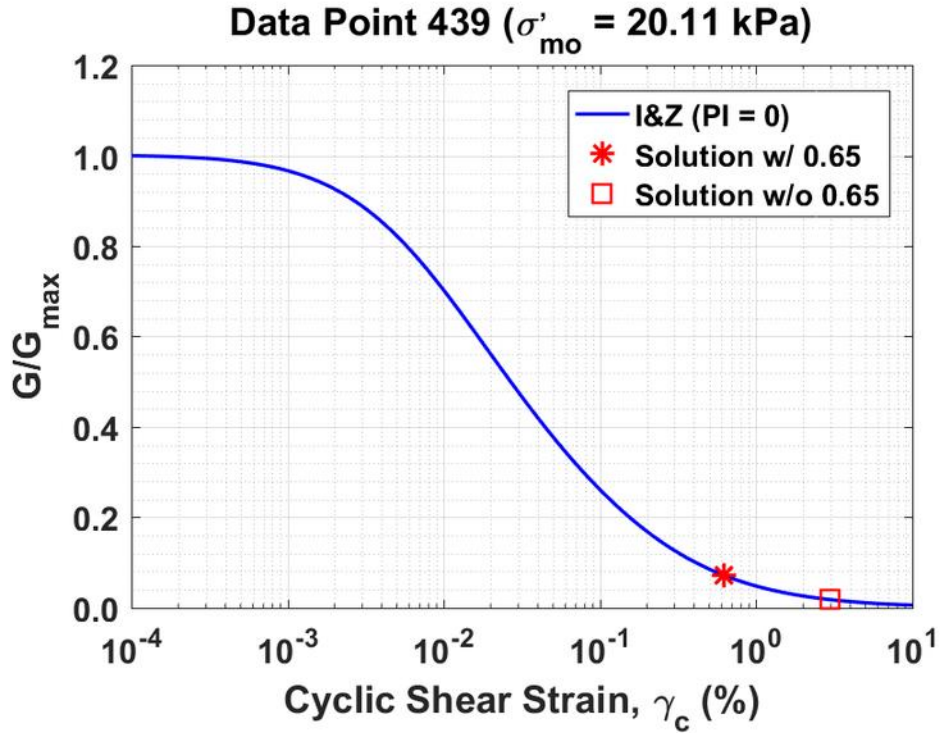


Figure B377. Normalized shear modulus reduction curves for Data Point 439 of the Kayen et al. database showing the solutions w/ and w/o the 0.65 factor

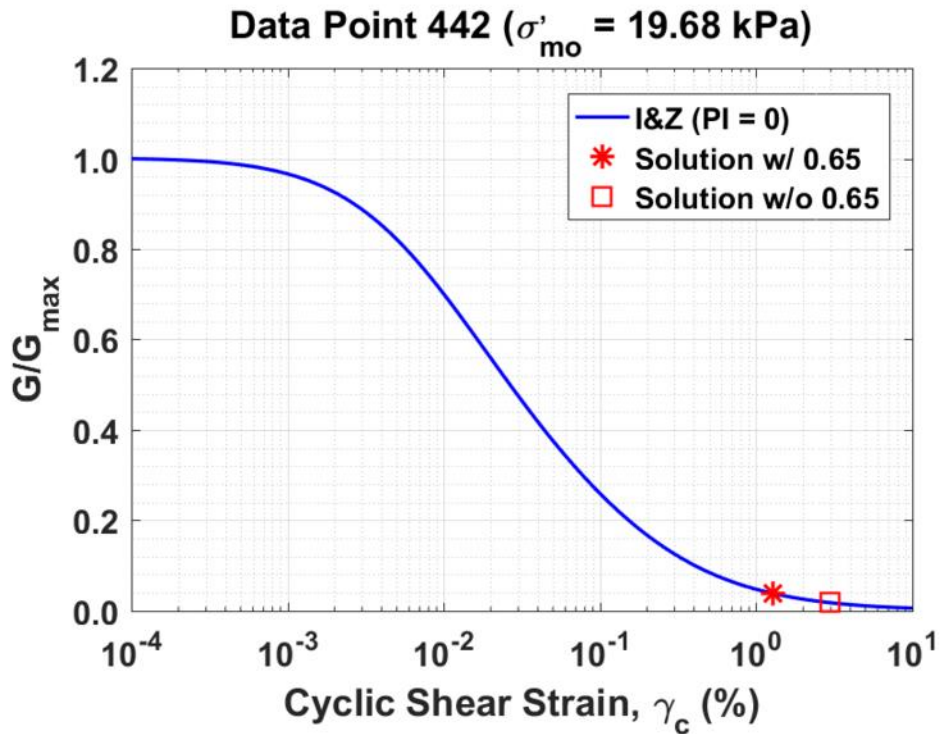


Figure B378. Normalized shear modulus reduction curves for Data Point 442 of the Kayen et al. database showing the solutions w/ and w/o the 0.65 factor

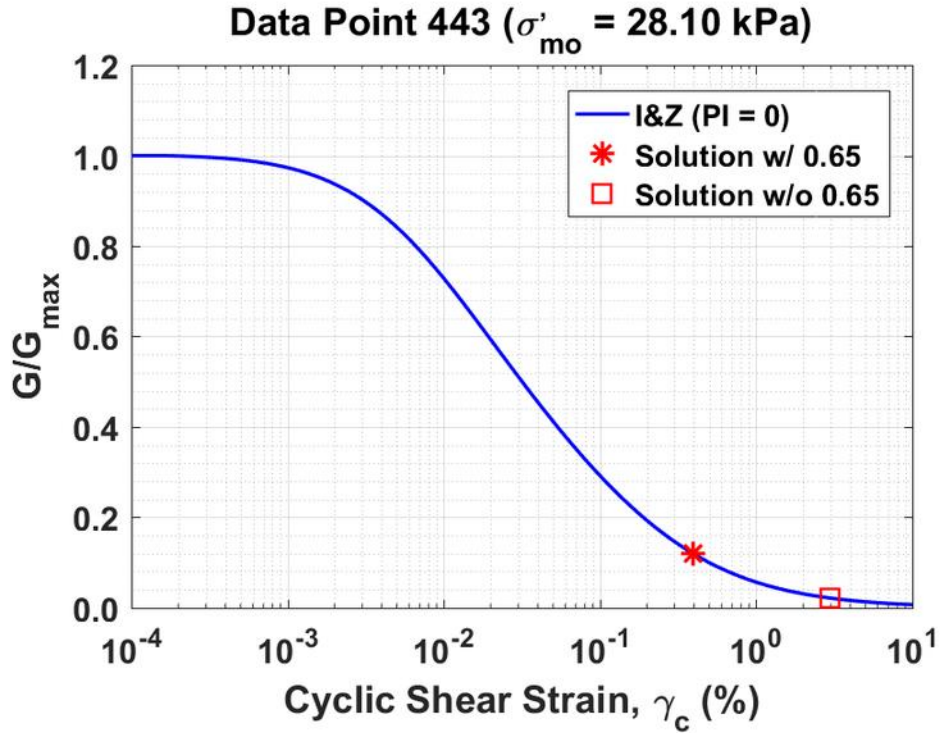


Figure B379. Normalized shear modulus reduction curves for Data Point 433 of the Kayen et al. database showing the solutions w/ and w/o the 0.65 factor

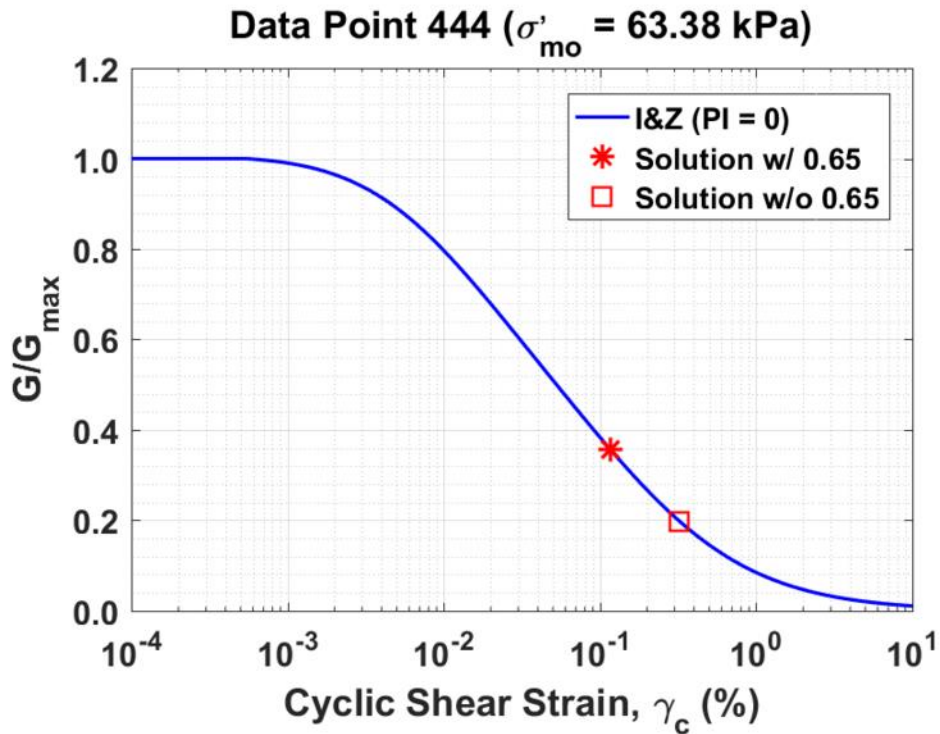


Figure B380. Normalized shear modulus reduction curves for Data Point 434 of the Kayen et al. database showing the solutions w/ and w/o the 0.65 factor

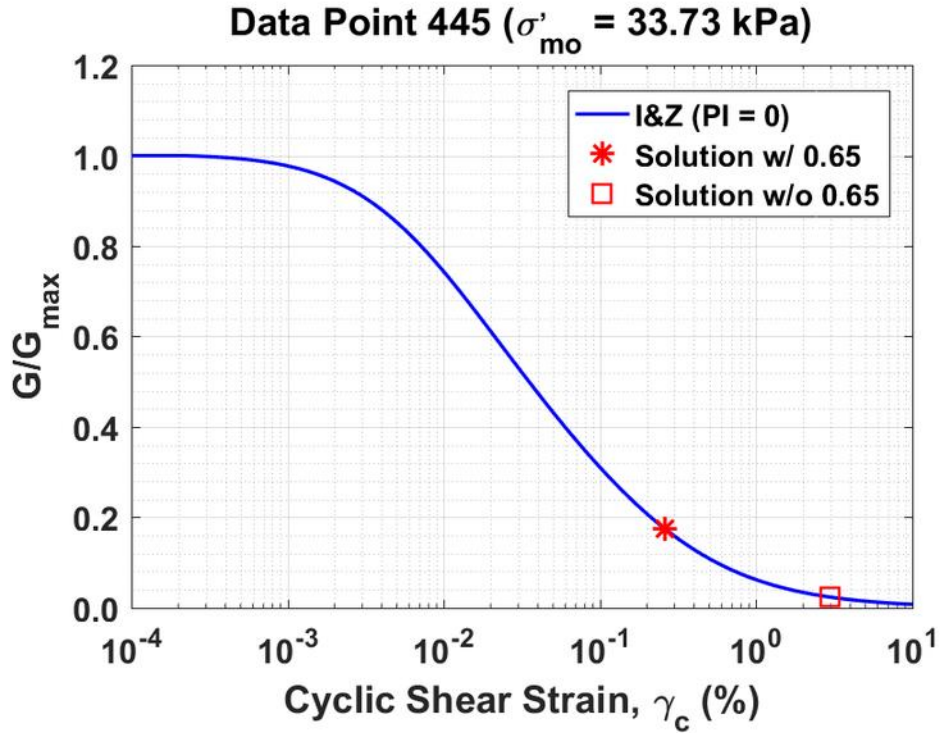


Figure B381. Normalized shear modulus reduction curves for Data Point 445 of the Kayen et al. database showing the solutions w/ and w/o the 0.65 factor

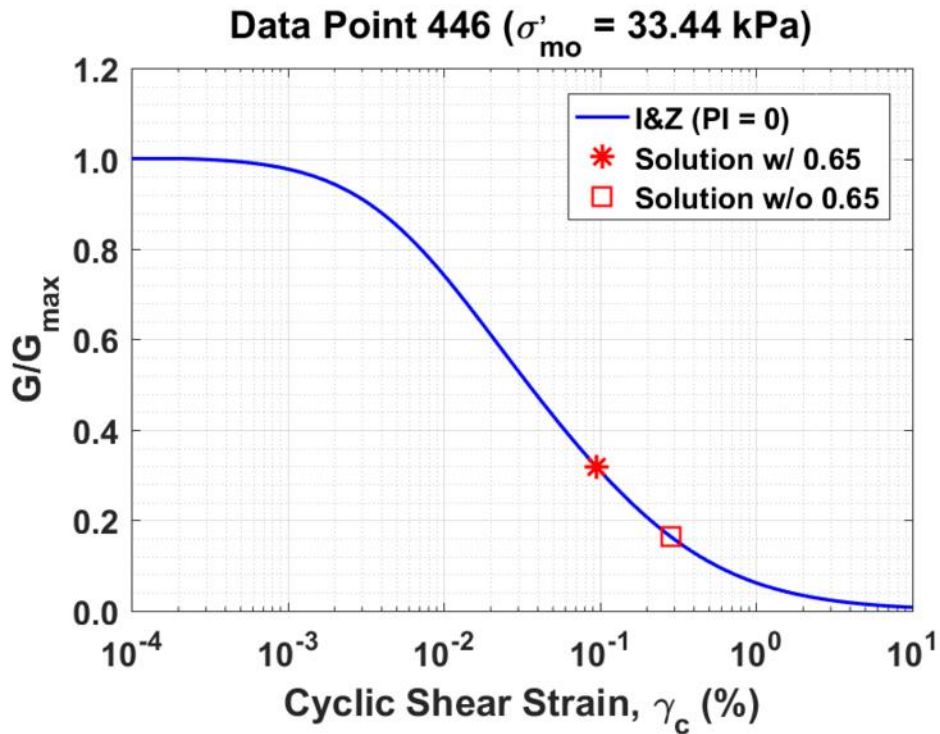


Figure B382. Normalized shear modulus reduction curves for Data Point 446 of the Kayen et al. database showing the solutions w/ and w/o the 0.65 factor

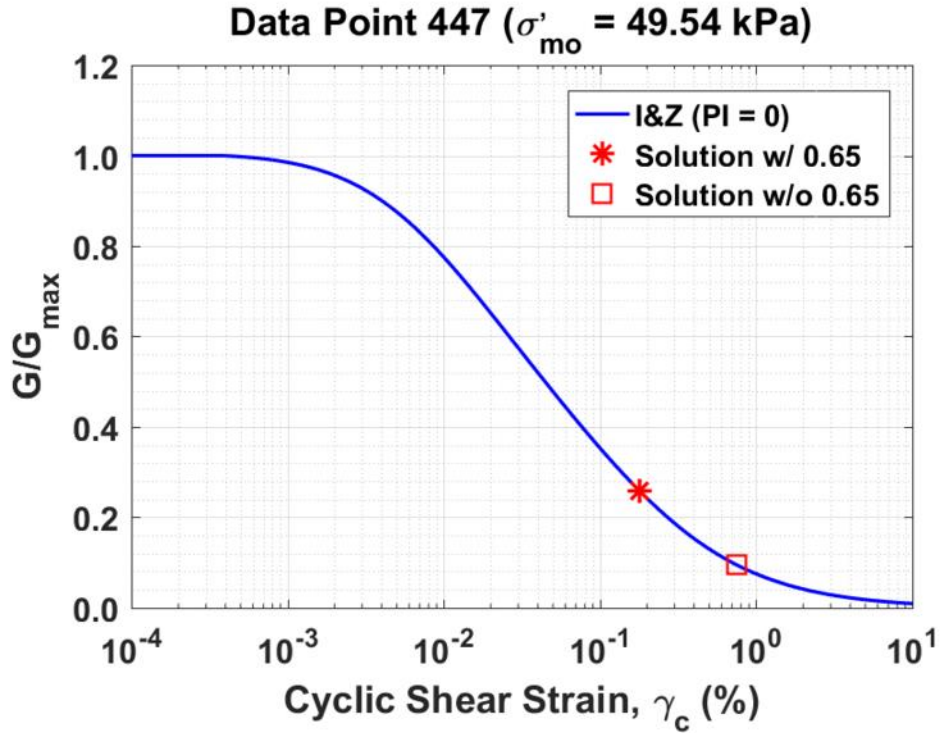


Figure B383. Normalized shear modulus reduction curves for Data Point 447 of the Kayen et al. database showing the solutions w/ and w/o the 0.65 factor

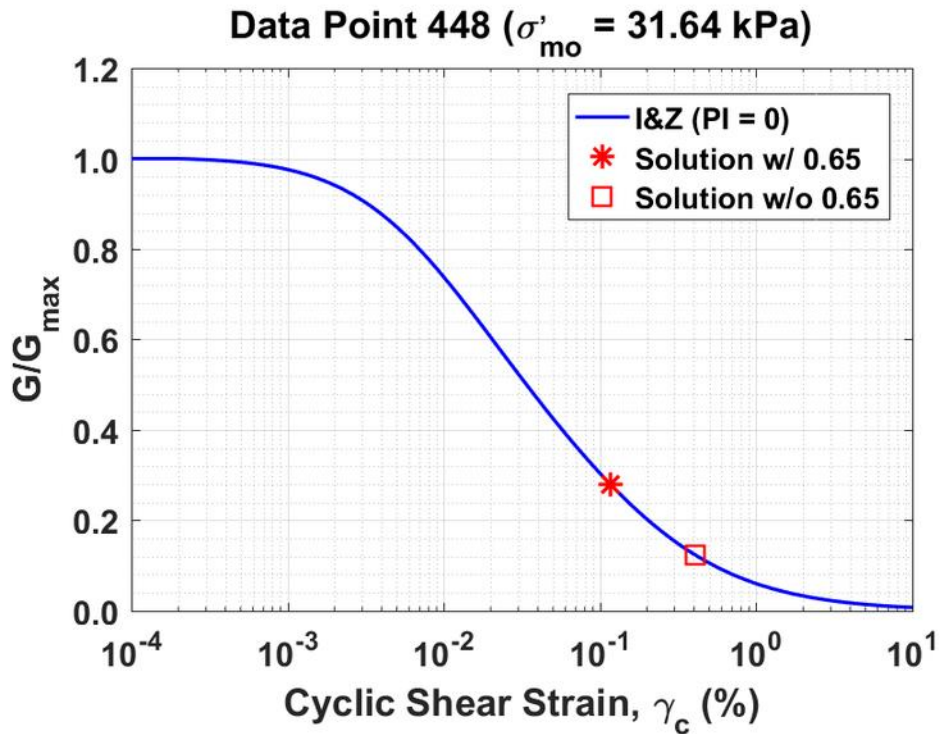


Figure B384. Normalized shear modulus reduction curves for Data Point 448 of the Kayen et al. database showing the solutions w/ and w/o the 0.65 factor

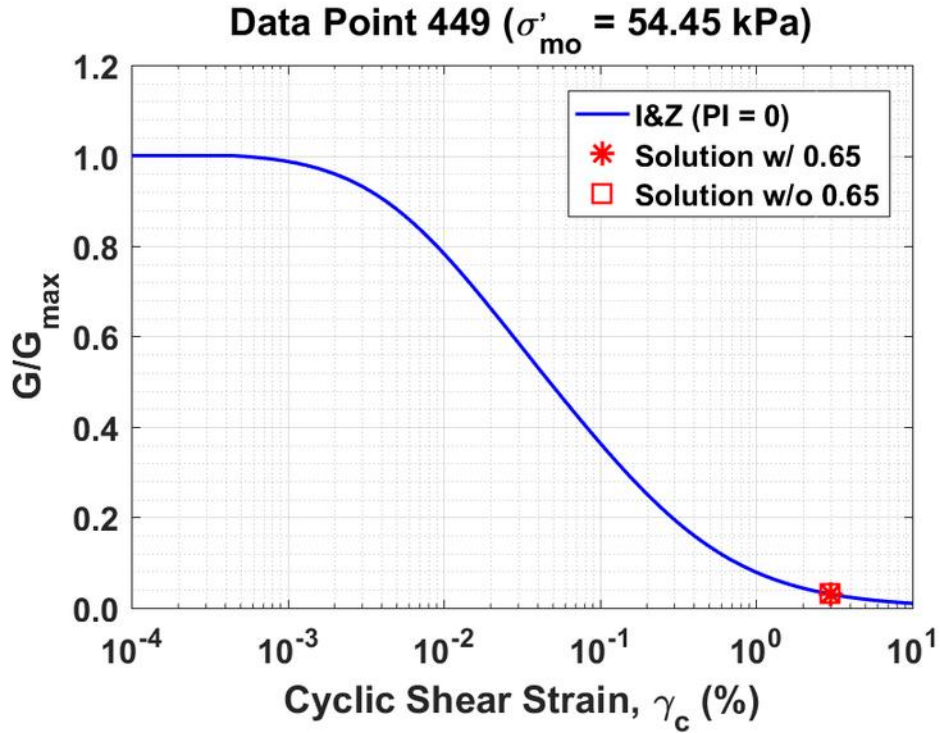


Figure B385. Normalized shear modulus reduction curves for Data Point 449 of the Kayen et al. database showing the solutions w/ and w/o the 0.65 factor

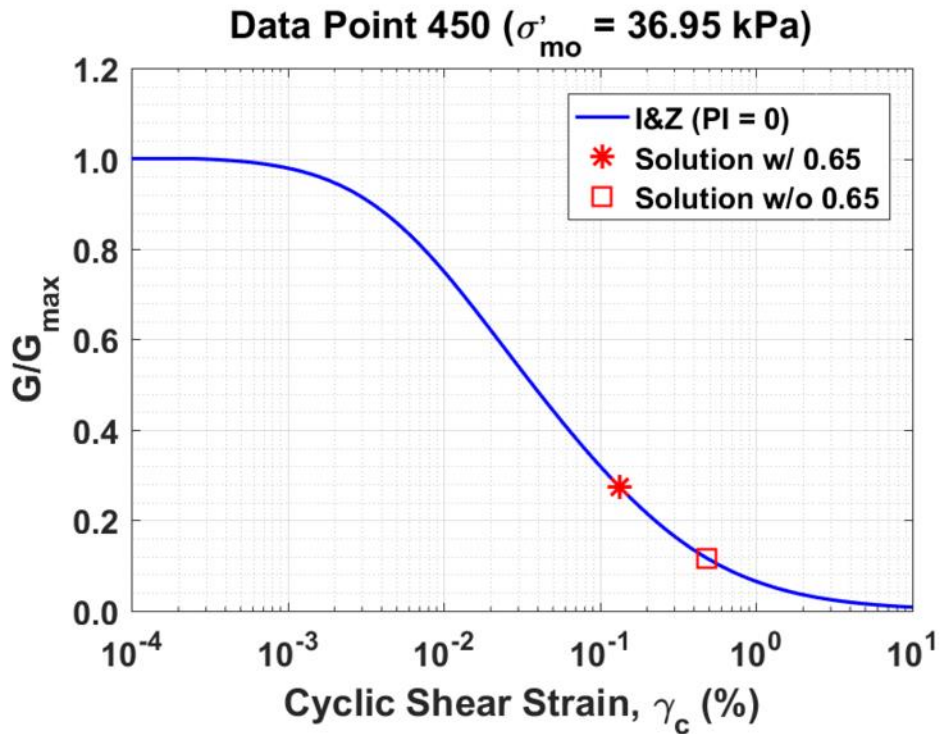


Figure B386. Normalized shear modulus reduction curves for Data Point 450 of the Kayen et al. database showing the solutions w/ and w/o the 0.65 factor

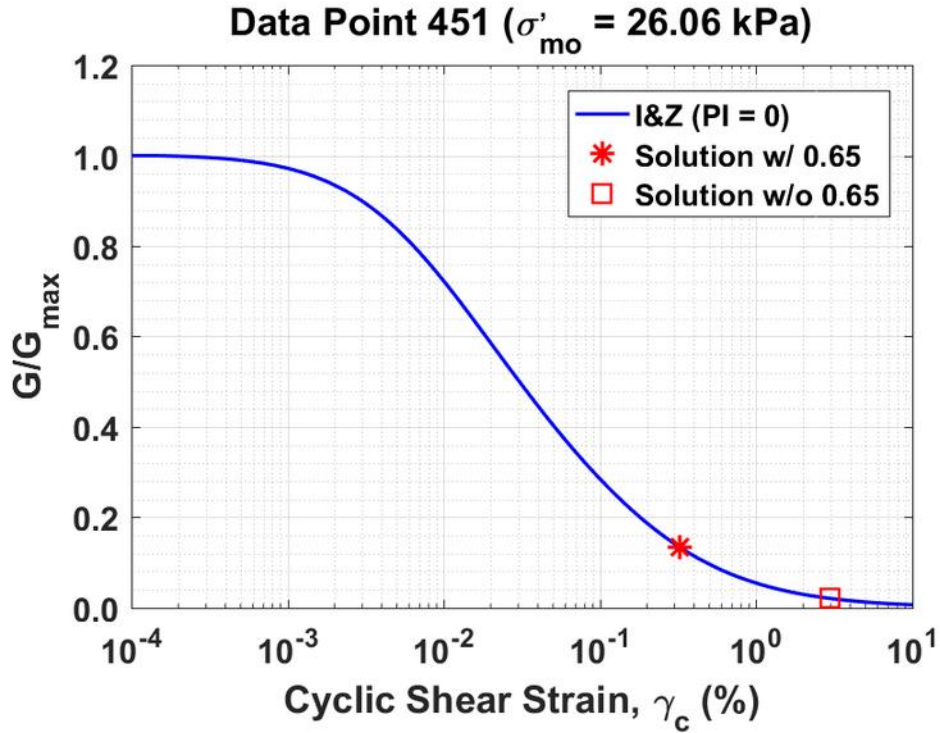


Figure B387. Normalized shear modulus reduction curves for Data Point 451 of the Kayen et al. database showing the solutions w/ and w/o the 0.65 factor

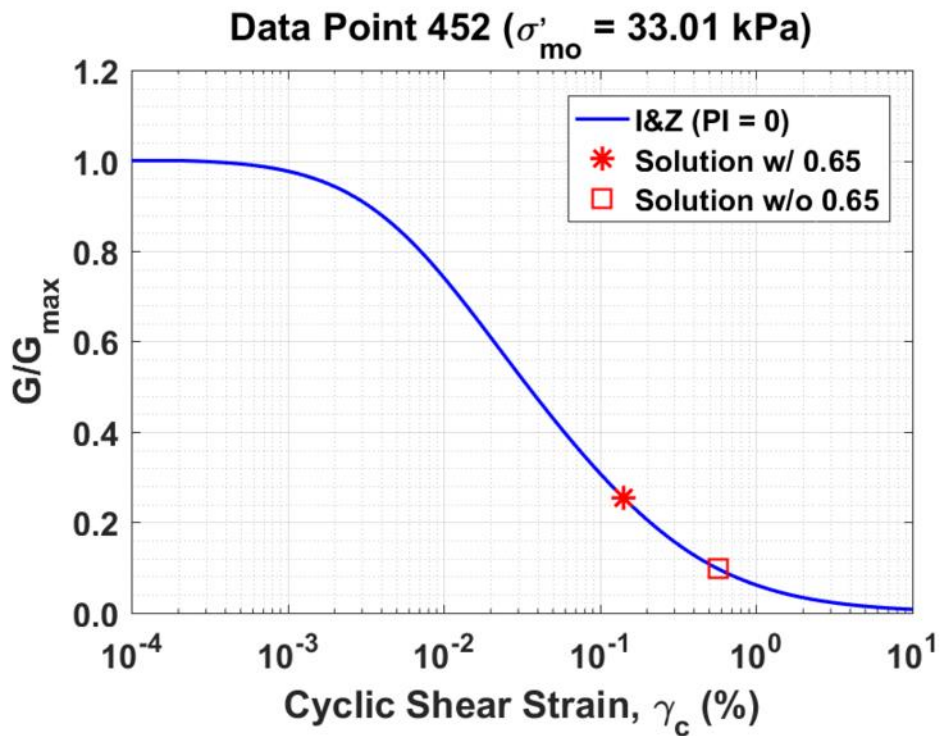


Figure B389. Normalized shear modulus reduction curves for Data Point 452 of the Kayen et al. database showing the solutions w/ and w/o the 0.65 factor

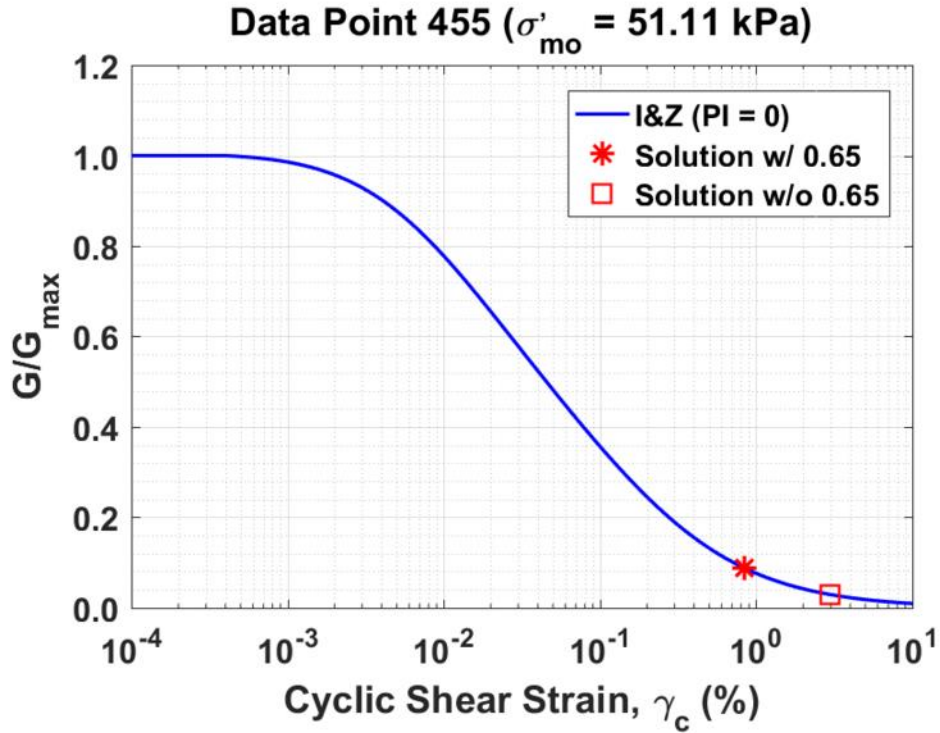


Figure B390. Normalized shear modulus reduction curves for Data Point 455 of the Kayen et al. database showing the solutions w/ and w/o the 0.65 factor

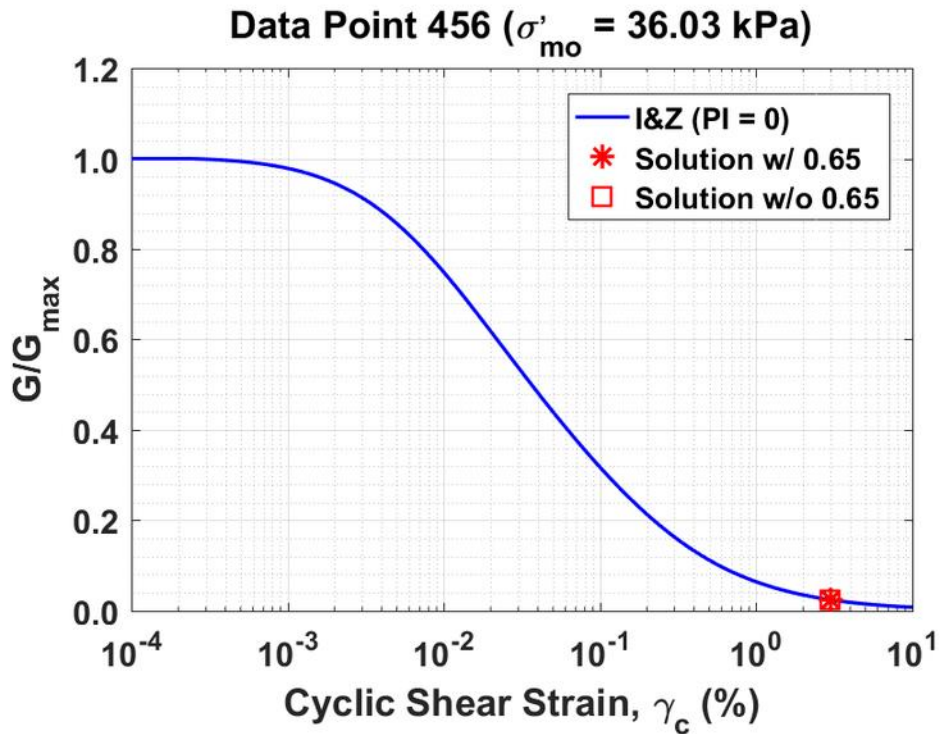


Figure B391. Normalized shear modulus reduction curves for Data Point 456 of the Kayen et al. database showing the solutions w/ and w/o the 0.65 factor

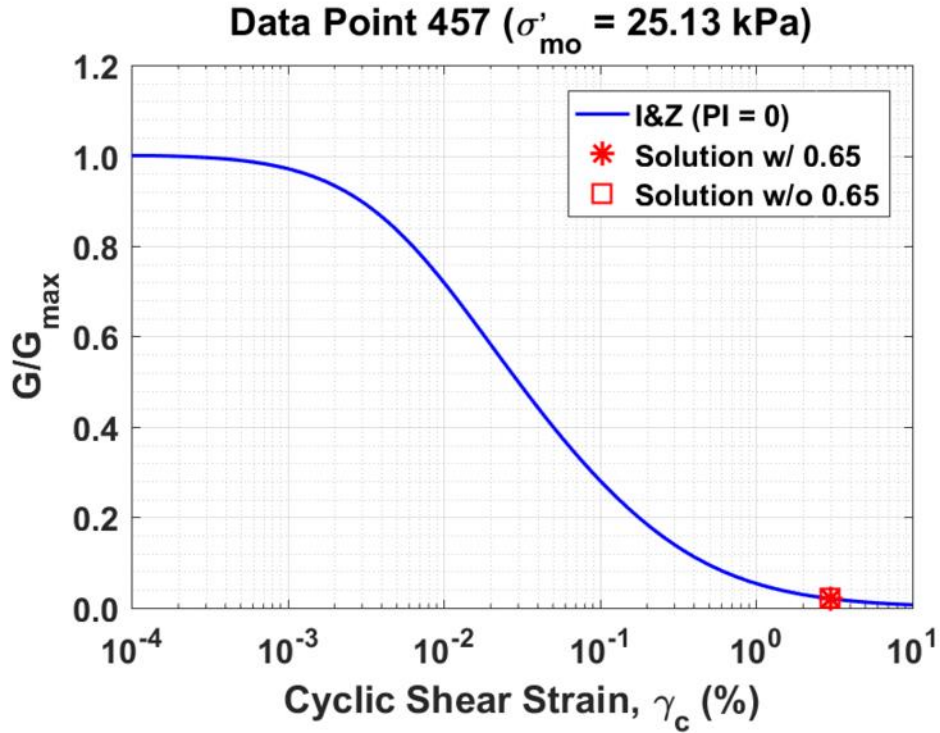


Figure B392. Normalized shear modulus reduction curves for Data Point 457 of the Kayen et al. database showing the solutions w/ and w/o the 0.65 factor

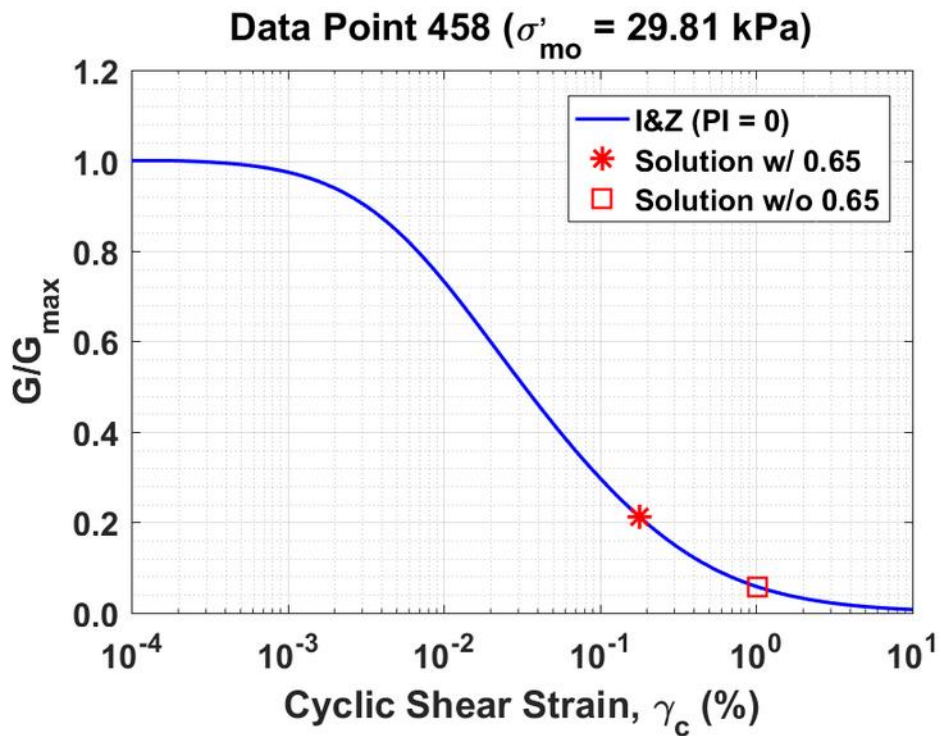


Figure B393. Normalized shear modulus reduction curves for Data Point 458 of the Kayen et al. database showing the solutions w/ and w/o the 0.65 factor

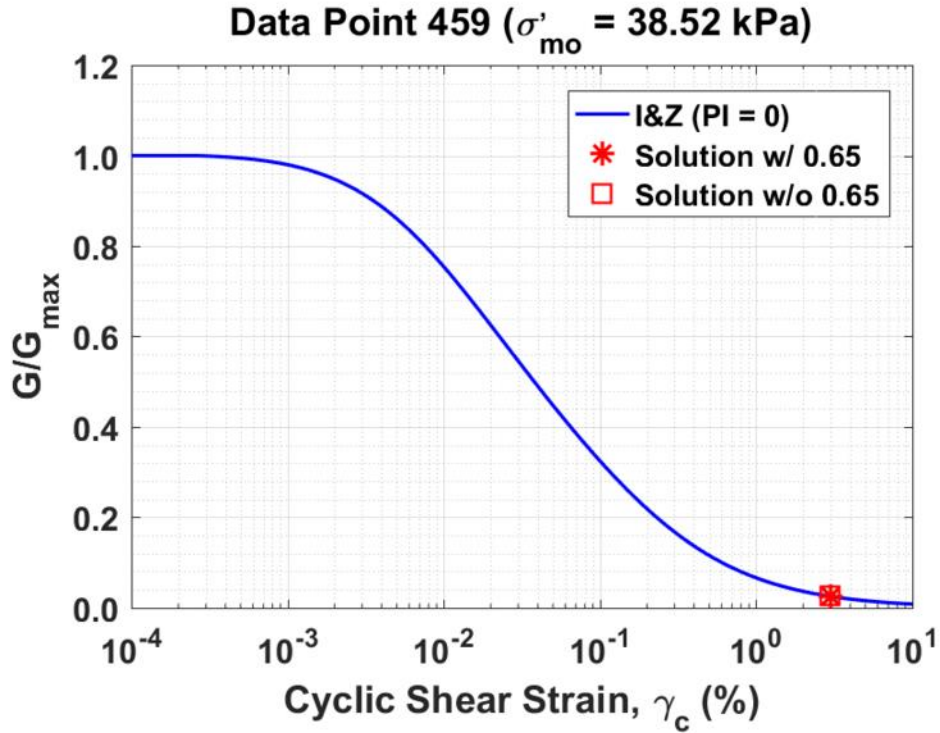


Figure B394. Normalized shear modulus reduction curves for Data Point 459 of the Kayen et al. database showing the solutions w/ and w/o the 0.65 factor

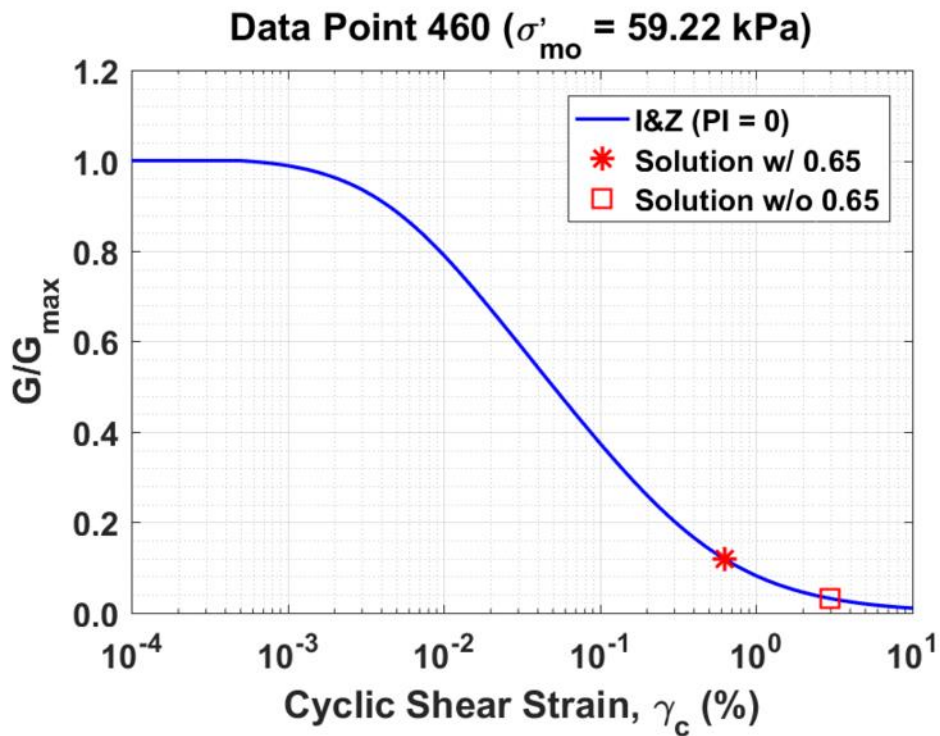


Figure B395. Normalized shear modulus reduction curves for Data Point 460 of the Kayen et al. database showing the solutions w/ and w/o the 0.65 factor

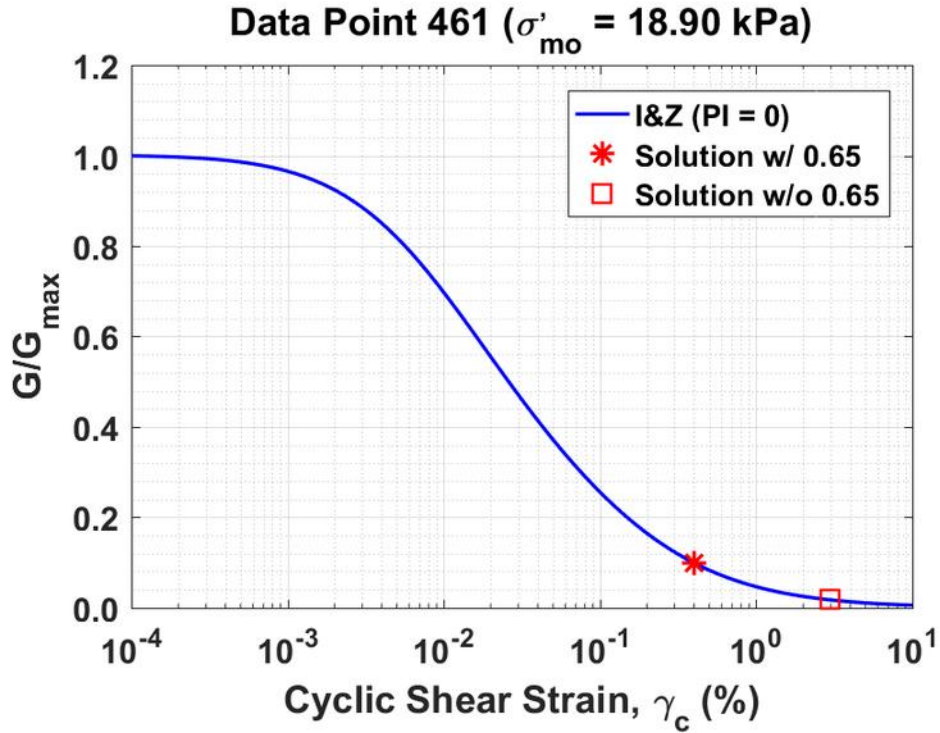


Figure B396. Normalized shear modulus reduction curves for Data Point 461 of the Kayen et al. database showing the solutions w/ and w/o the 0.65 factor

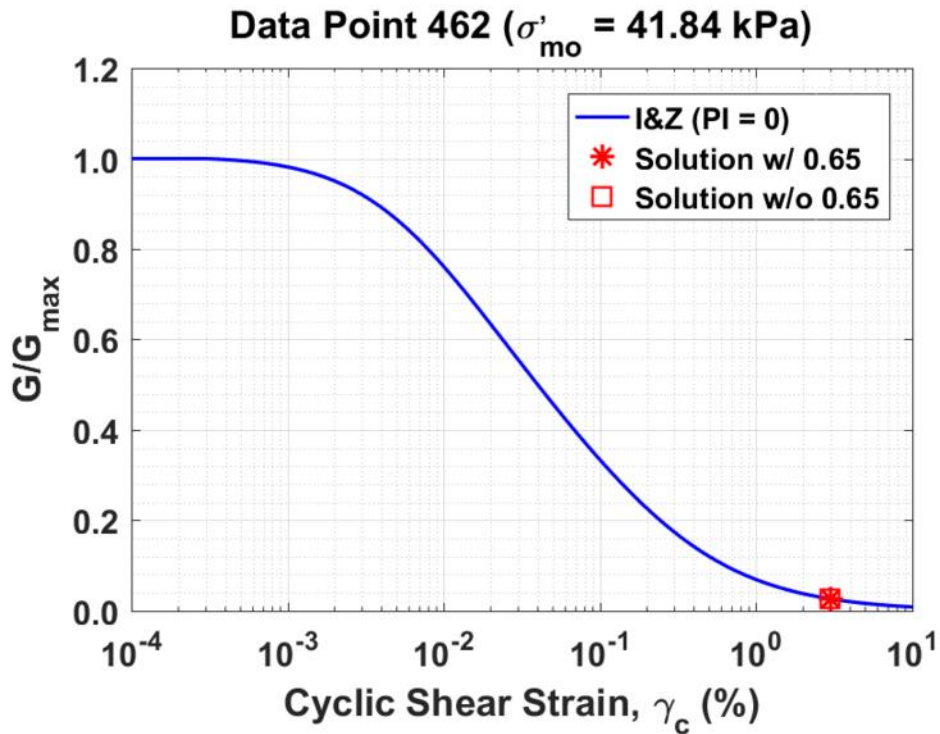


Figure B397. Normalized shear modulus reduction curves for Data Point 462 of the Kayen et al. database showing the solutions w/ and w/o the 0.65 factor

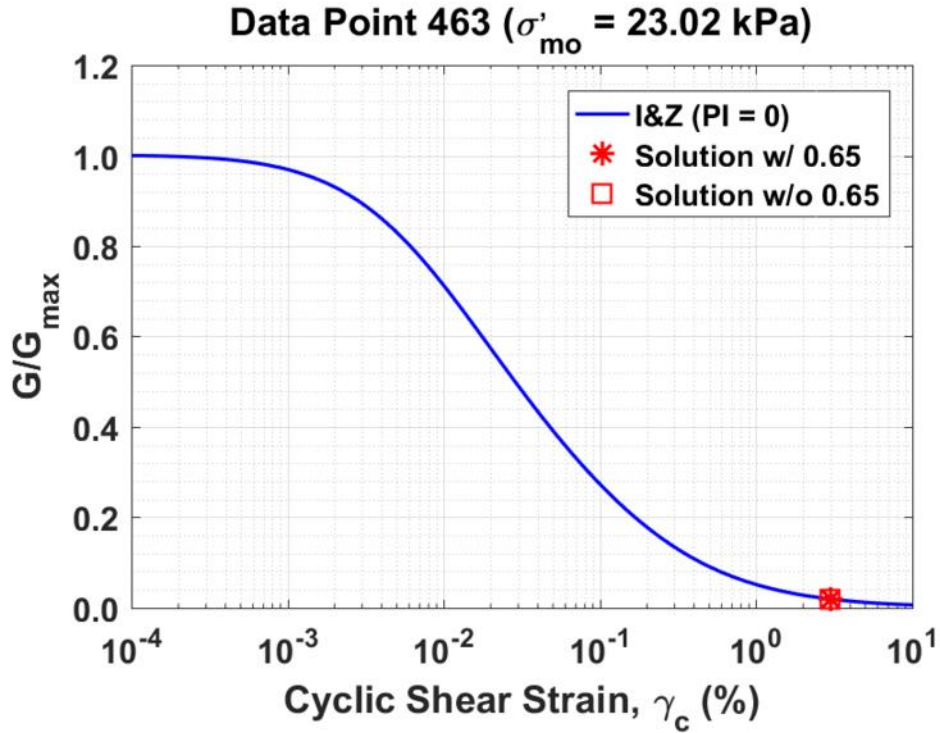


Figure B397. Normalized shear modulus reduction curves for Data Point 463 of the Kayen et al. database showing the solutions w/ and w/o the 0.65 factor

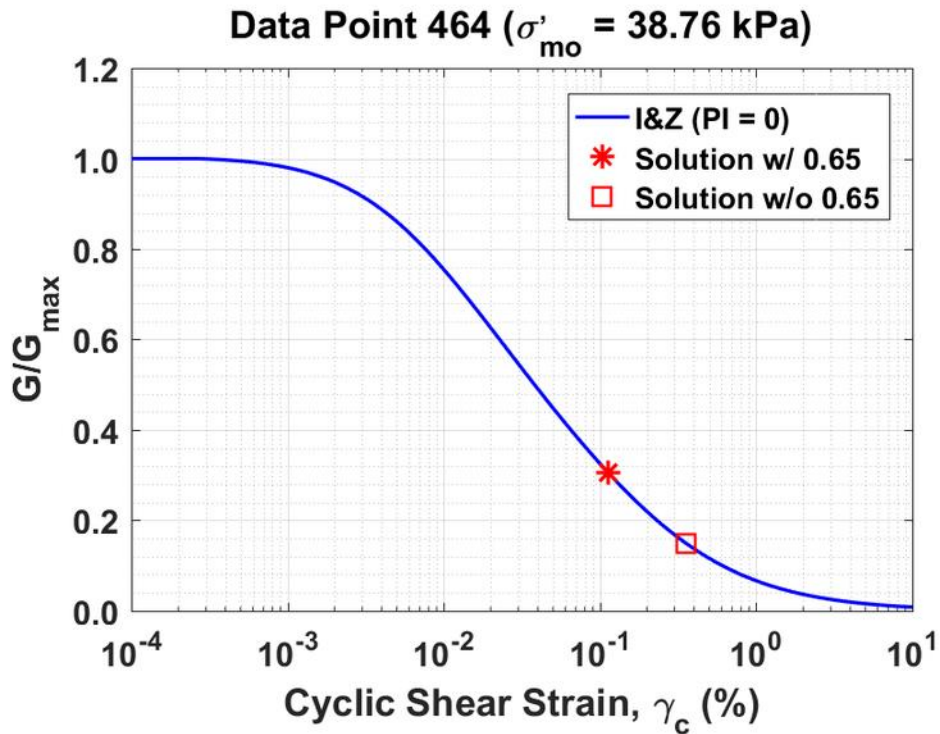


Figure B398. Normalized shear modulus reduction curves for Data Point 464 of the Kayen et al. database showing the solutions w/ and w/o the 0.65 factor

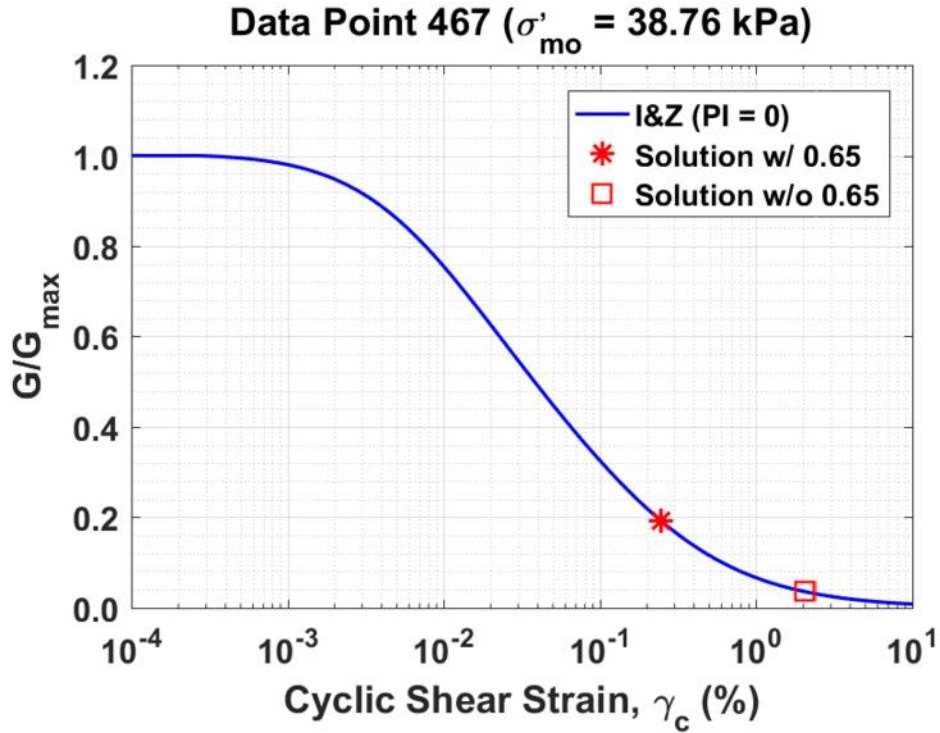


Figure B399. Normalized shear modulus reduction curves for Data Point 467 of the Kayen et al. database showing the solutions w/ and w/o the 0.65 factor

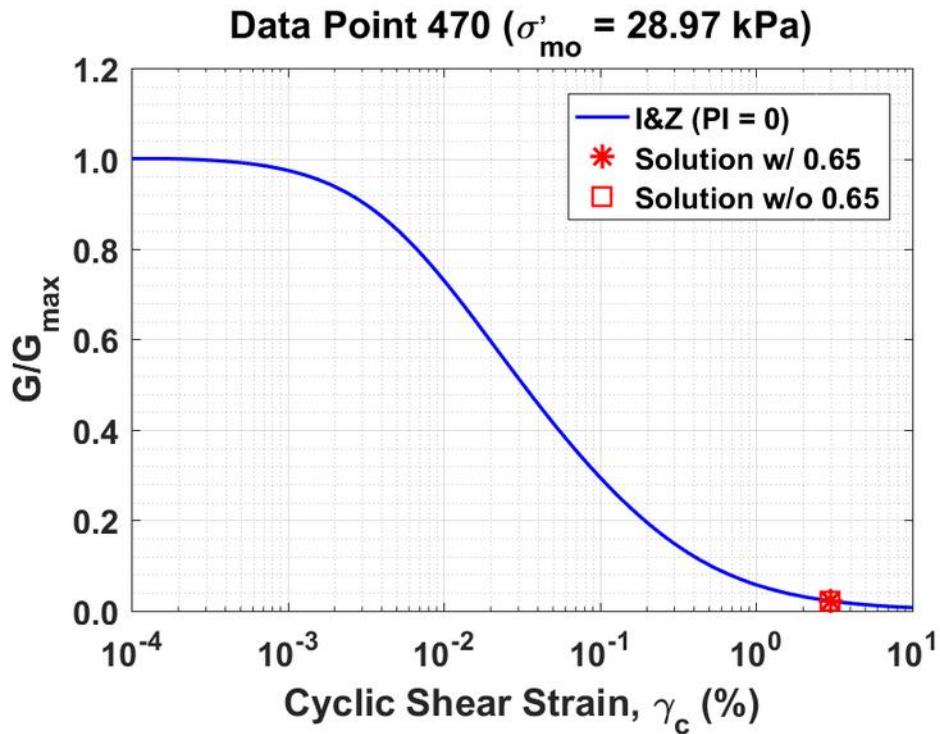


Figure B400. Normalized shear modulus reduction curves for Data Point 470 of the Kayen et al. database showing the solutions w/ and w/o the 0.65 factor

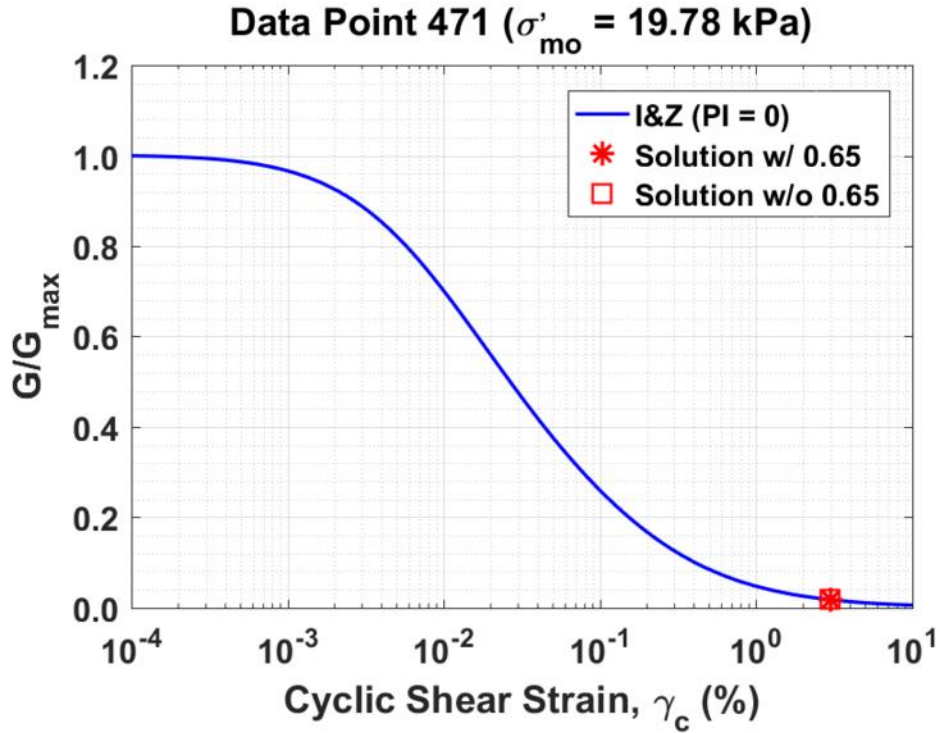


Figure B401. Normalized shear modulus reduction curves for Data Point 471 of the Kayen et al. database showing the solutions w/ and w/o the 0.65 factor

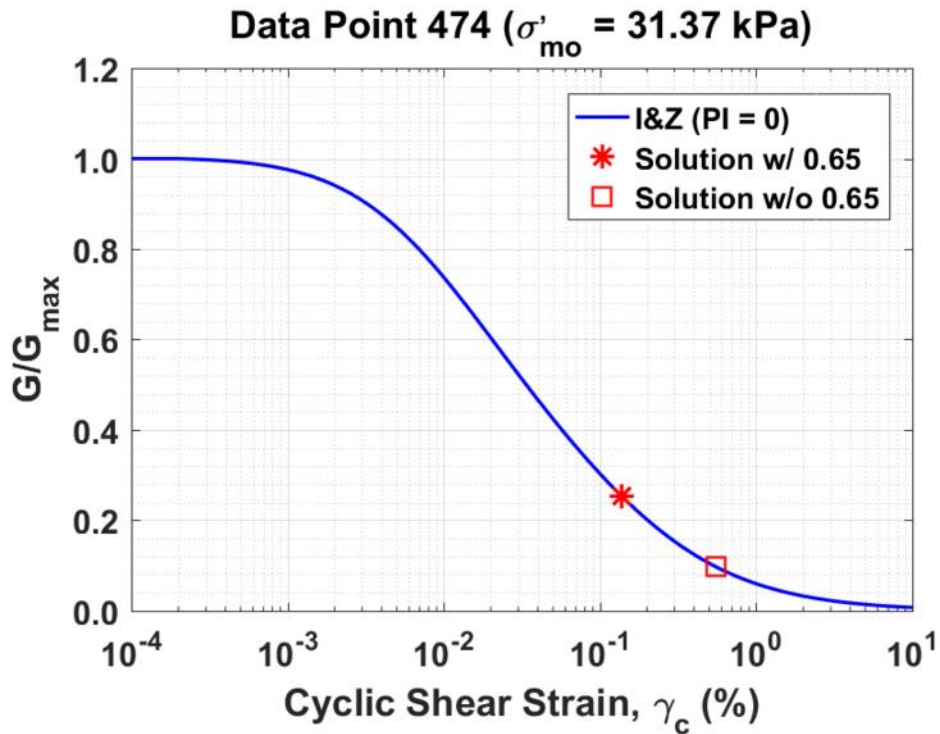


Figure B402. Normalized shear modulus reduction curves for Data Point 474 of the Kayen et al. database showing the solutions w/ and w/o the 0.65 factor

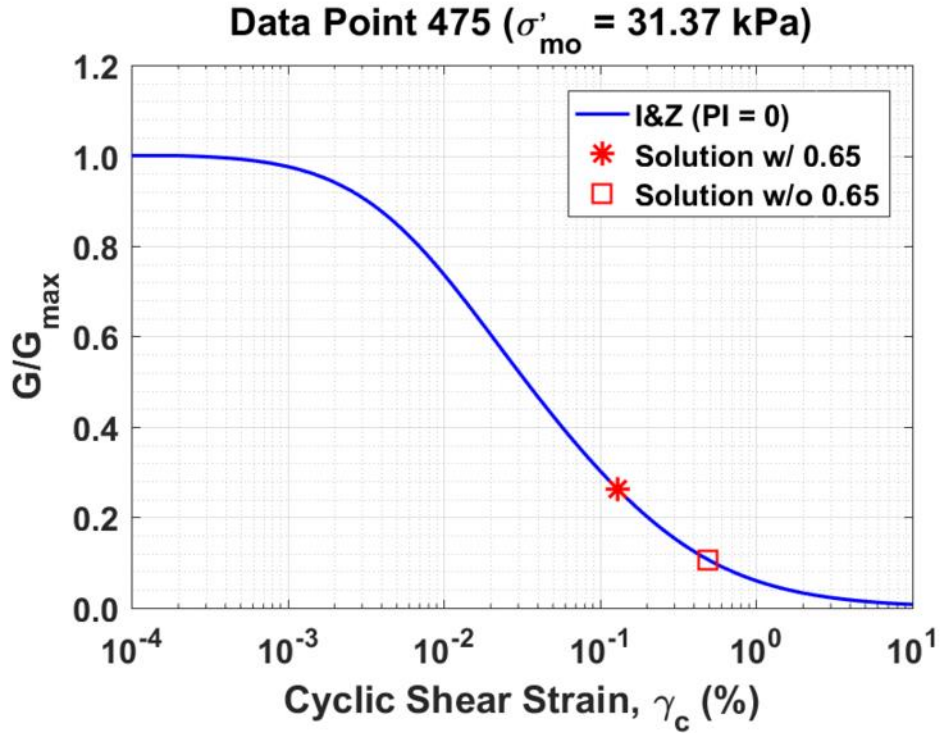


Figure B403. Normalized shear modulus reduction curves for Data Point 475 of the Kayen et al. database showing the solutions w/ and w/o the 0.65 factor

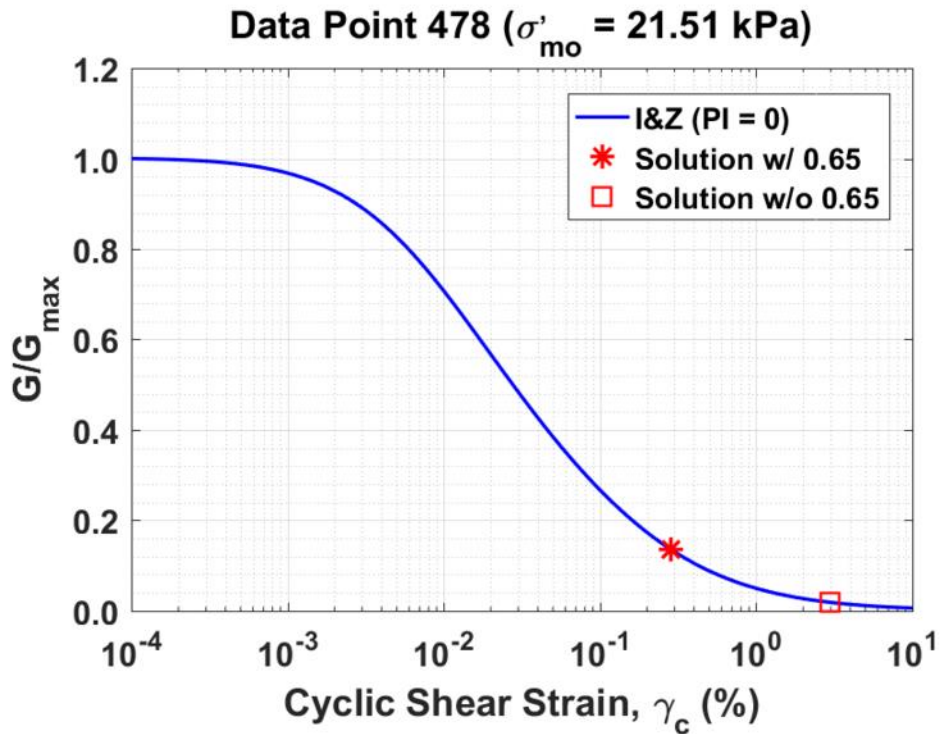


Figure B404. Normalized shear modulus reduction curves for Data Point 478 of the Kayen et al. database showing the solutions w/ and w/o the 0.65 factor

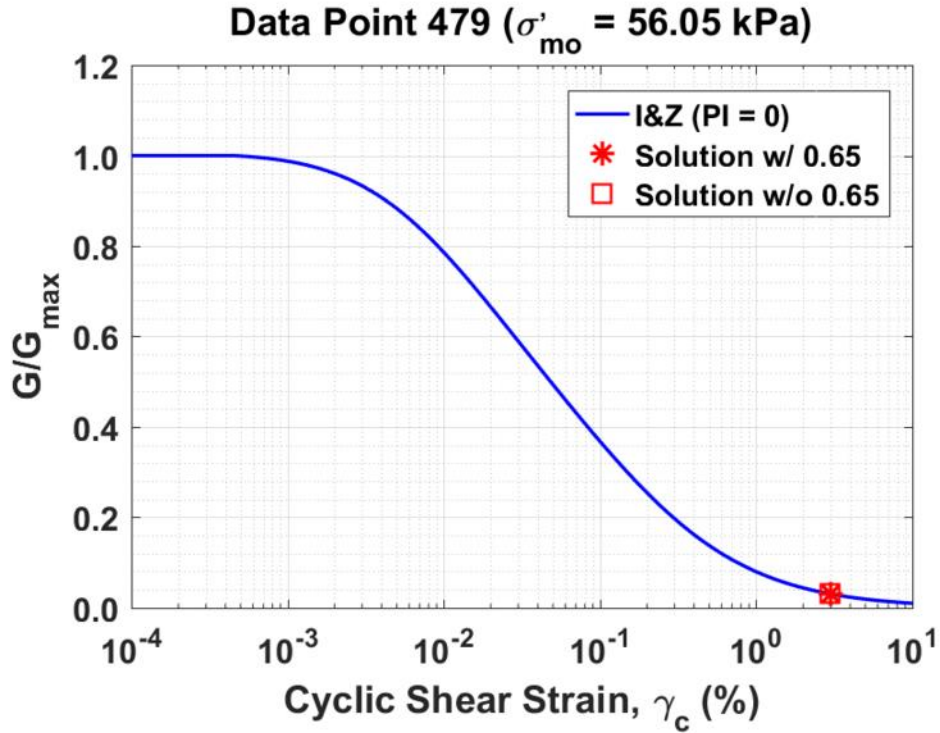


Figure B405. Normalized shear modulus reduction curves for Data Point 479 of the Kayen et al. database showing the solutions w/ and w/o the 0.65 factor

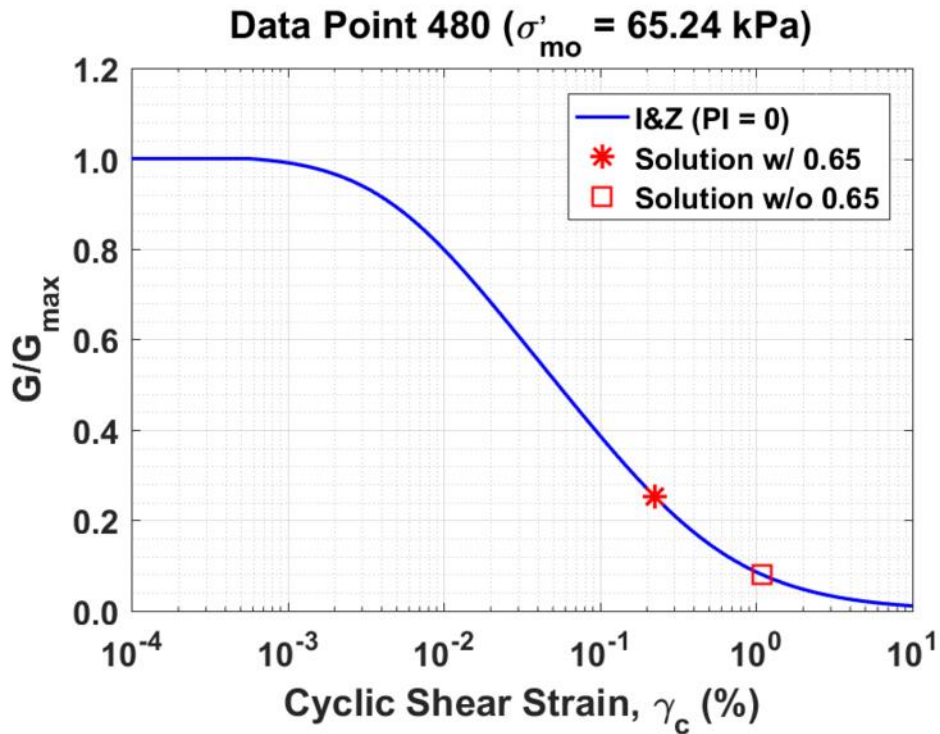


Figure B406. Normalized shear modulus reduction curves for Data Point 480 of the Kayen et al. database showing the solutions w/ and w/o the 0.65 factor

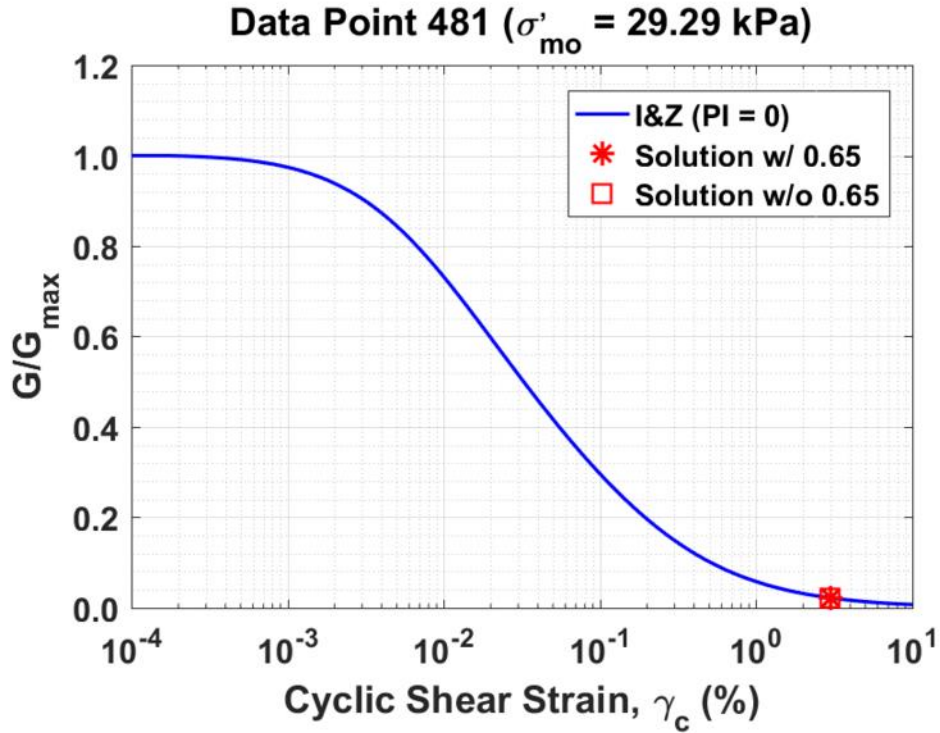


Figure B407. Normalized shear modulus reduction curves for Data Point 481 of the Kayen et al. database showing the solutions w/ and w/o the 0.65 factor

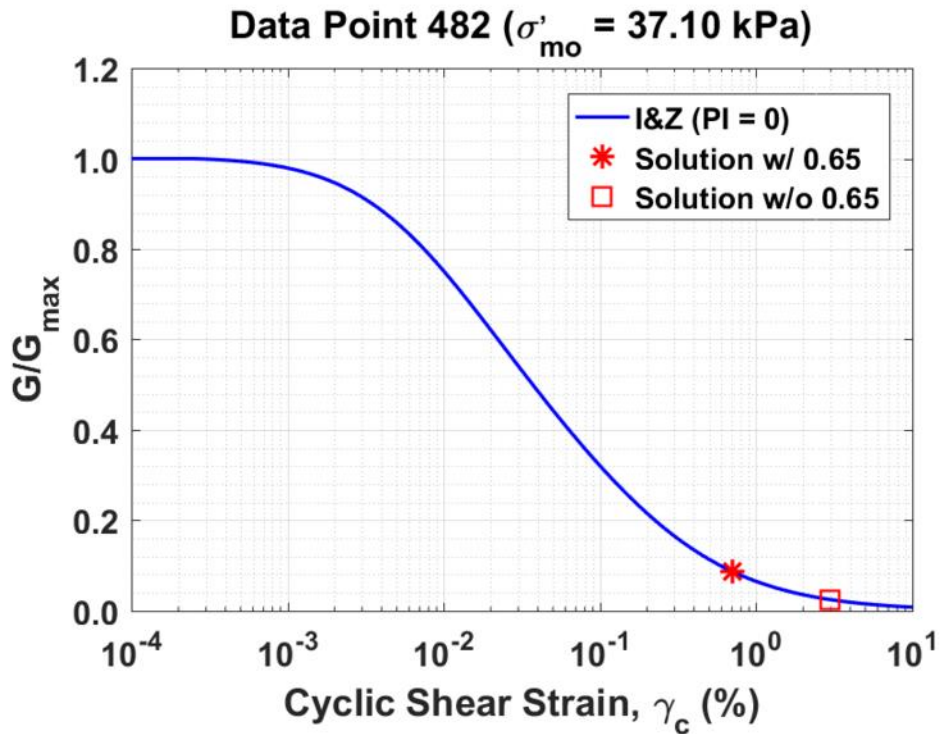


Figure B408. Normalized shear modulus reduction curves for Data Point 482 of the Kayen et al. database showing the solutions w/ and w/o the 0.65 factor

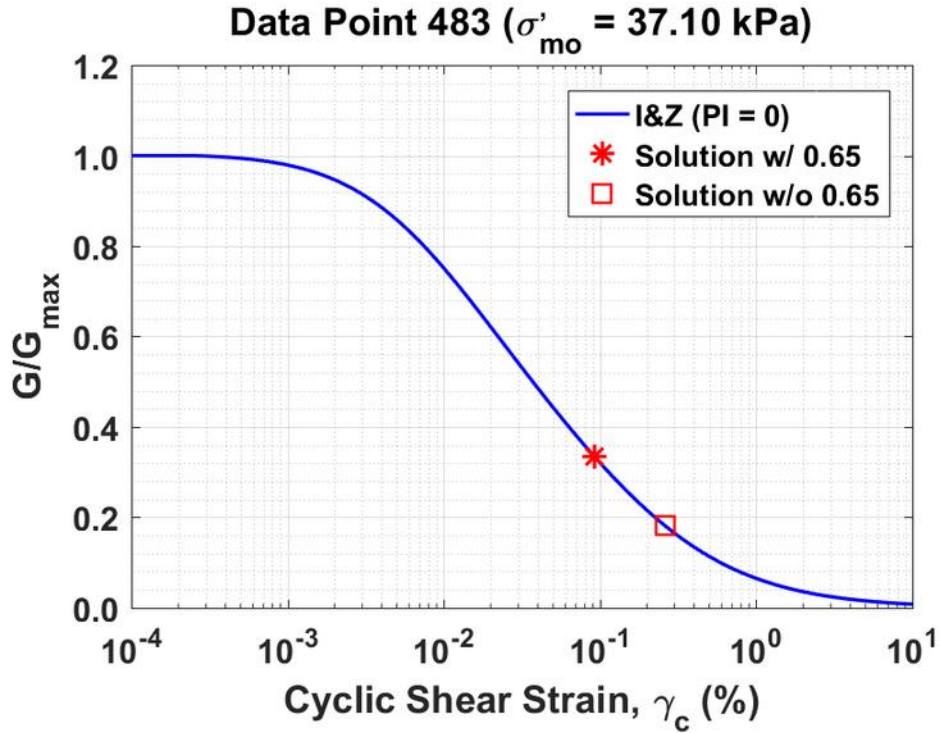


Figure B409. Normalized shear modulus reduction curves for Data Point 483 of the Kayen et al. database showing the solutions w/ and w/o the 0.65 factor

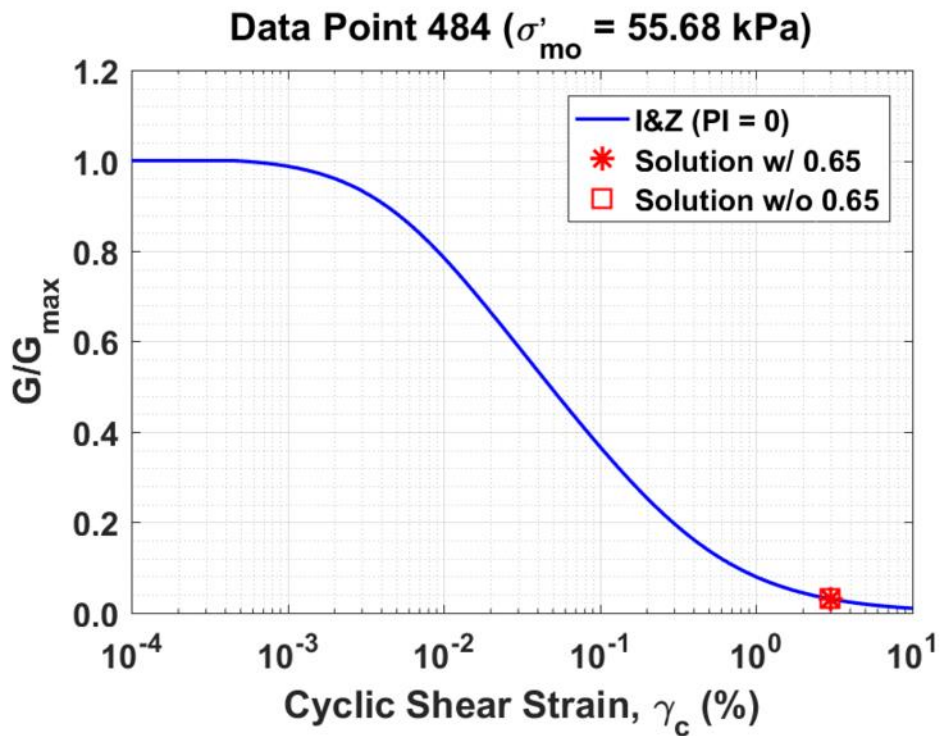


Figure B410. Normalized shear modulus reduction curves for Data Point 484 of the Kayen et al. database showing the solutions w/ and w/o the 0.65 factor

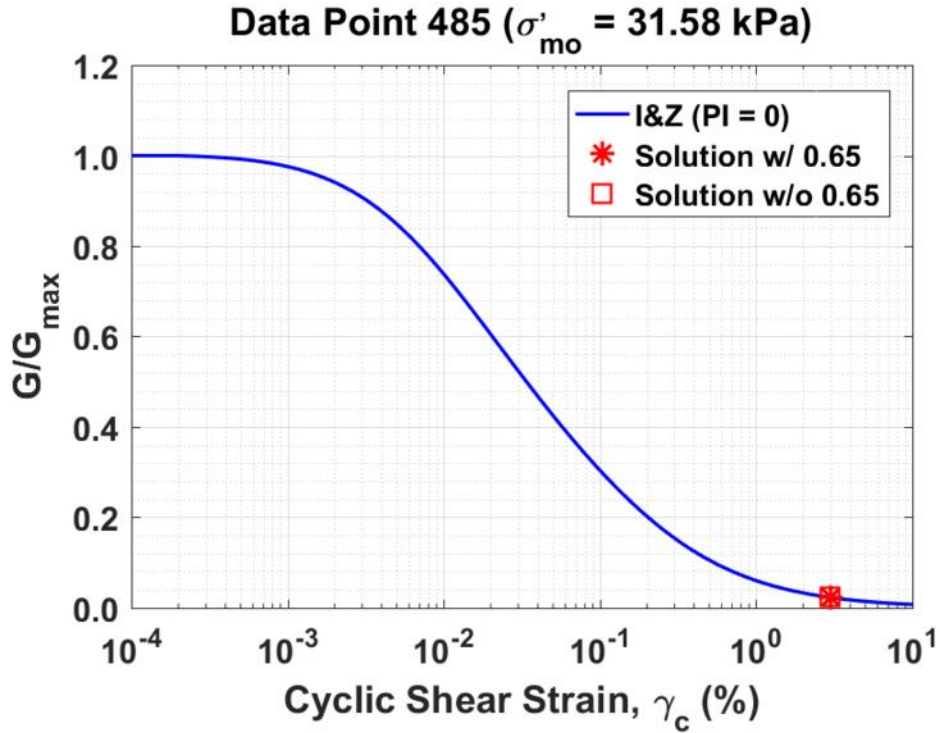


Figure B411. Normalized shear modulus reduction curves for Data Point 485 of the Kayen et al. database showing the solutions w/ and w/o the 0.65 factor

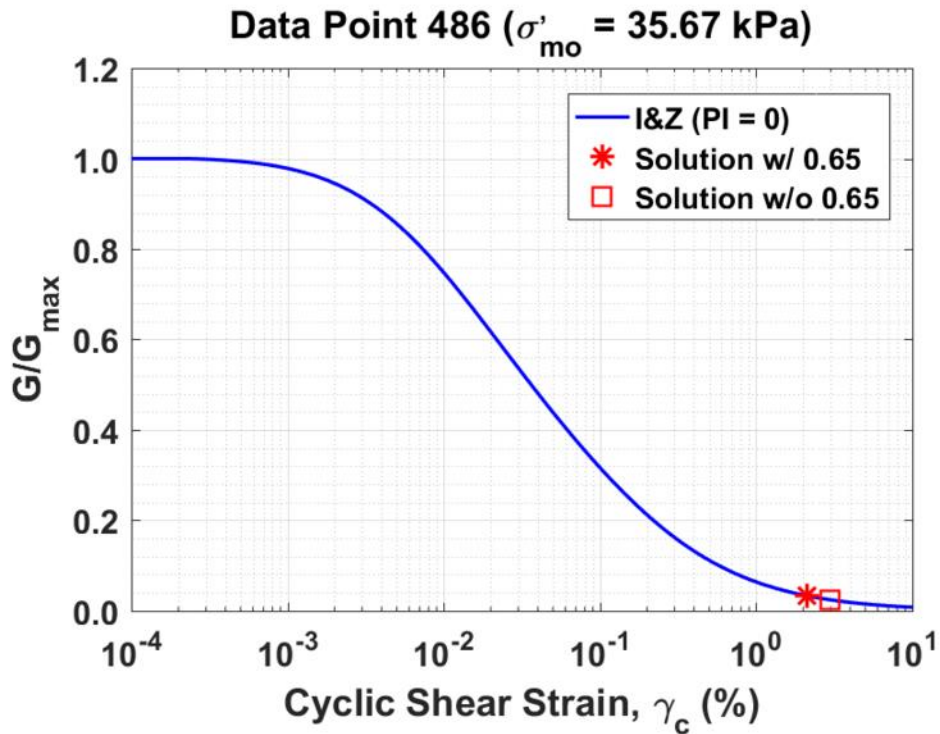


Figure B412. Normalized shear modulus reduction curves for Data Point 486 of the Kayen et al. database showing the solutions w/ and w/o the 0.65 factor

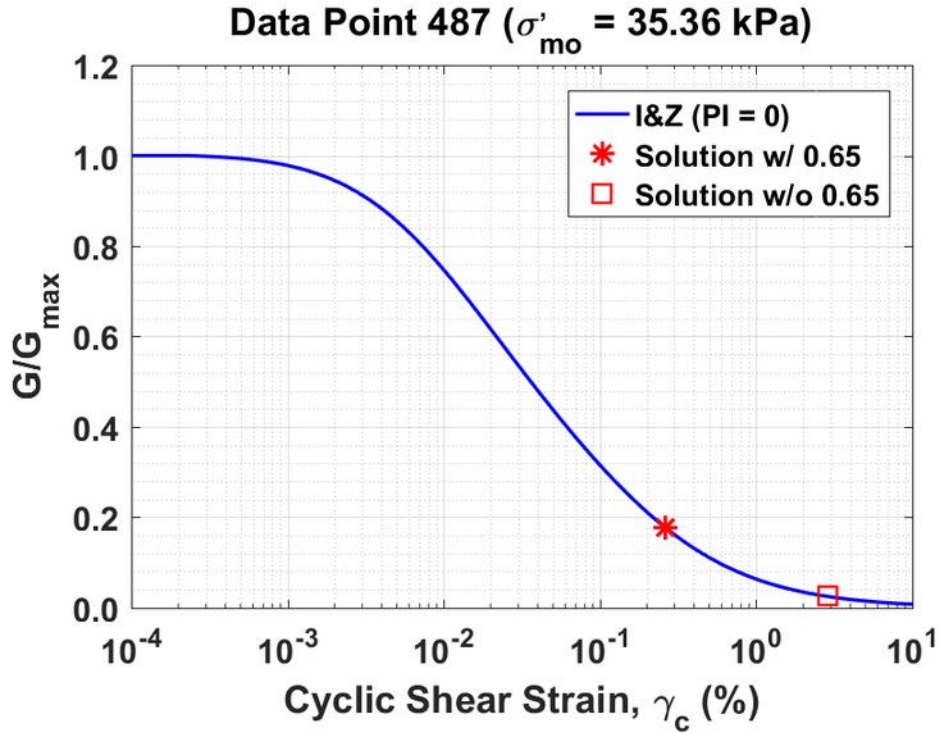


Figure B413. Normalized shear modulus reduction curves for Data Point 487 of the Kayen et al. database showing the solutions w/ and w/o the 0.65 factor

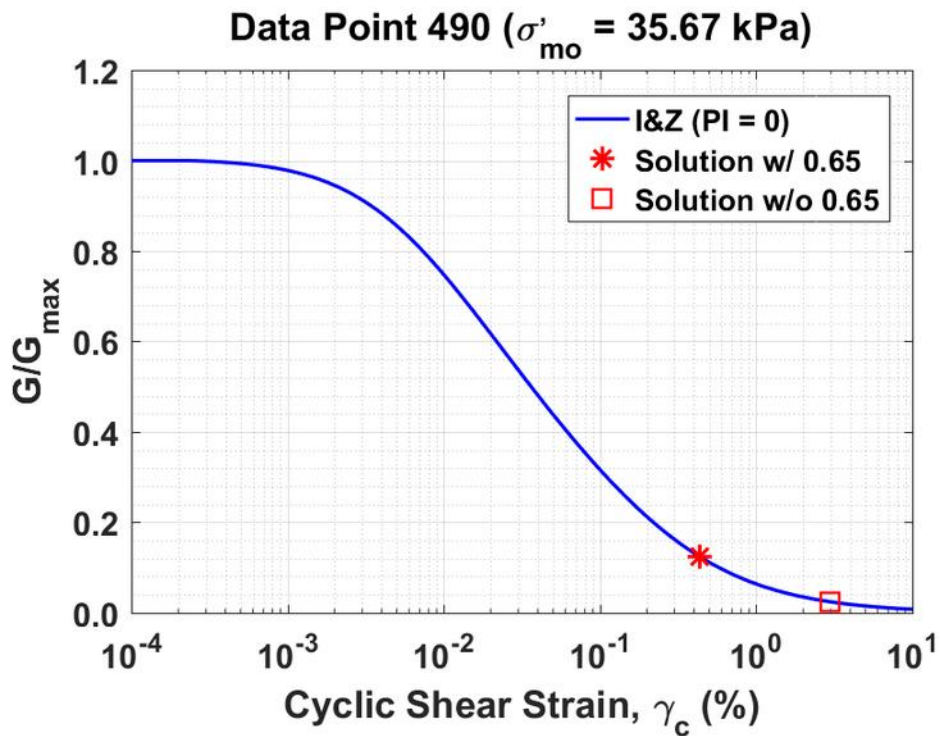


Figure B414. Normalized shear modulus reduction curves for Data Point 490 of the Kayen et al. database showing the solutions w/ and w/o the 0.65 factor

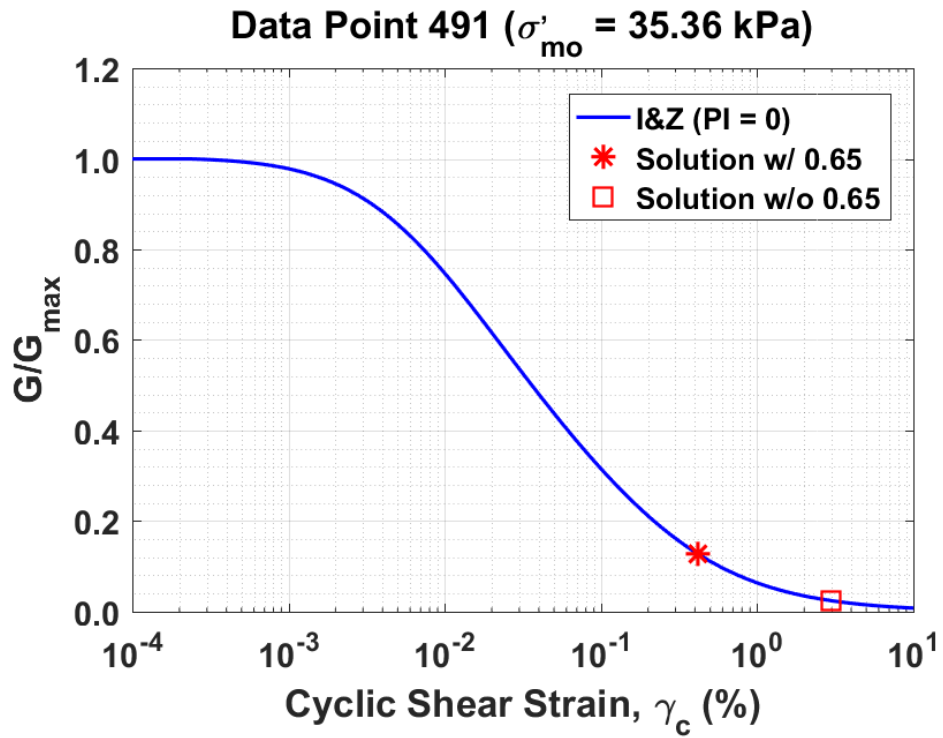


Figure B415. Normalized shear modulus reduction curves for Data Point 491 of the Kayen et al. database showing the solutions w/ and w/o the 0.65 factor

Shear Modulus Degradation Curves for the Boulanger et
al. database (230 curves)

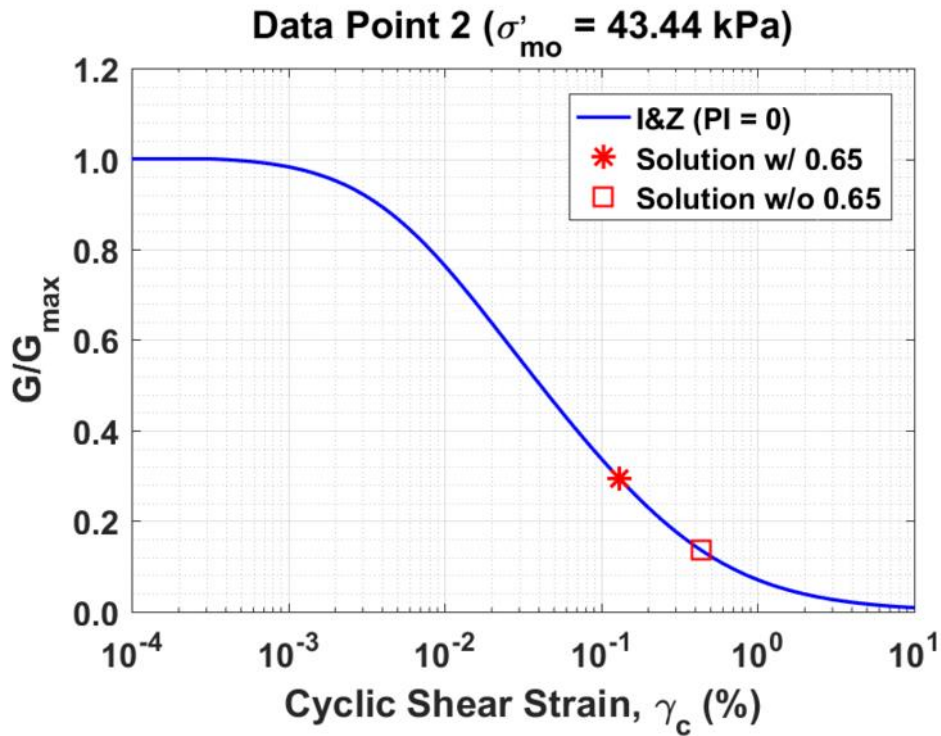


Figure B416. Normalized shear modulus reduction curves for Data Point 2 of the Boulanger et al. database showing the solutions w/ and w/o the 0.65 factor

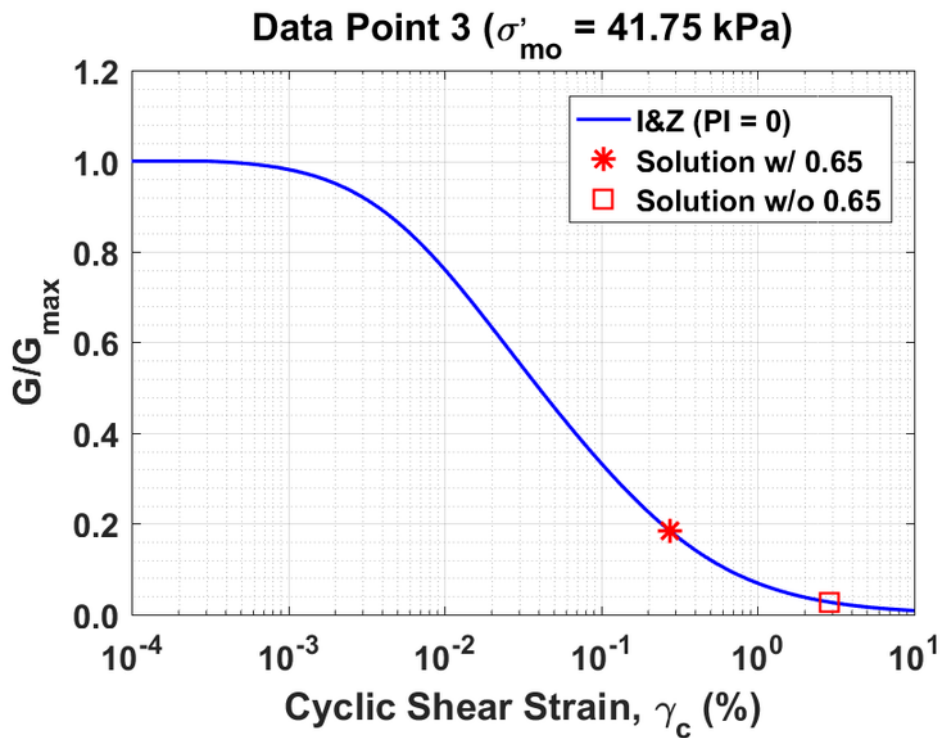


Figure B417. Normalized shear modulus reduction curves for Data Point 3 of the Boulanger et al. database showing the solutions w/ and w/o the 0.65 factor

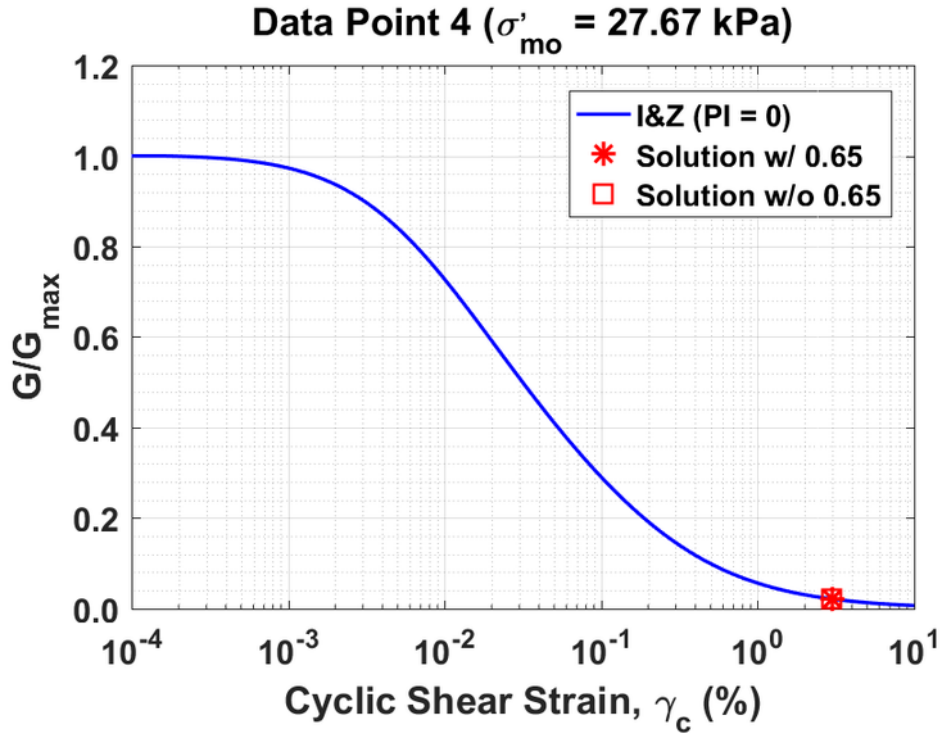


Figure B418. Normalized shear modulus reduction curves for Data Point 4 of the Boulanger et al. database showing the solutions w/ and w/o the 0.65 factor

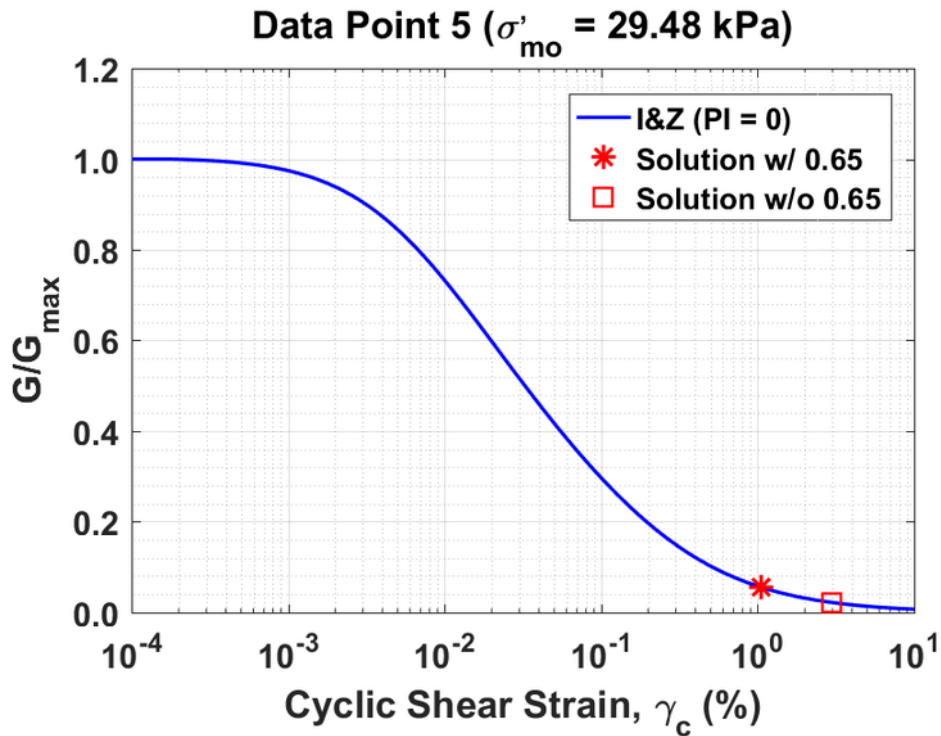


Figure B419. Normalized shear modulus reduction curves for Data Point 5 of the Boulanger et al. database showing the solutions w/ and w/o the 0.65 factor

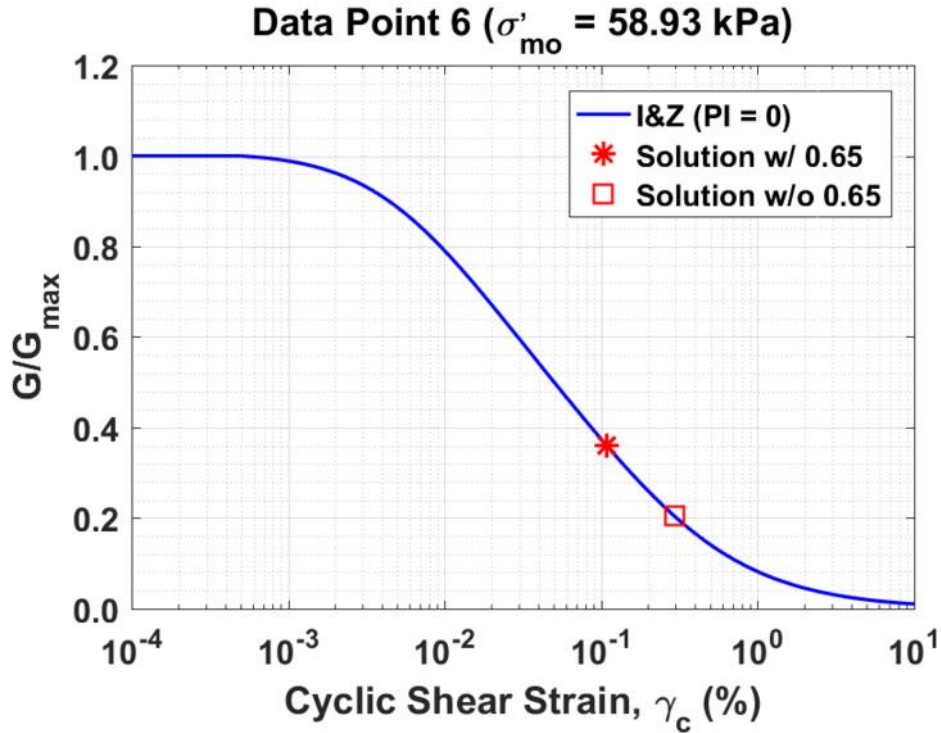


Figure B420. Normalized shear modulus reduction curves for Data Point 6 of the Boulanger et al. database showing the solutions w/ and w/o the 0.65 factor

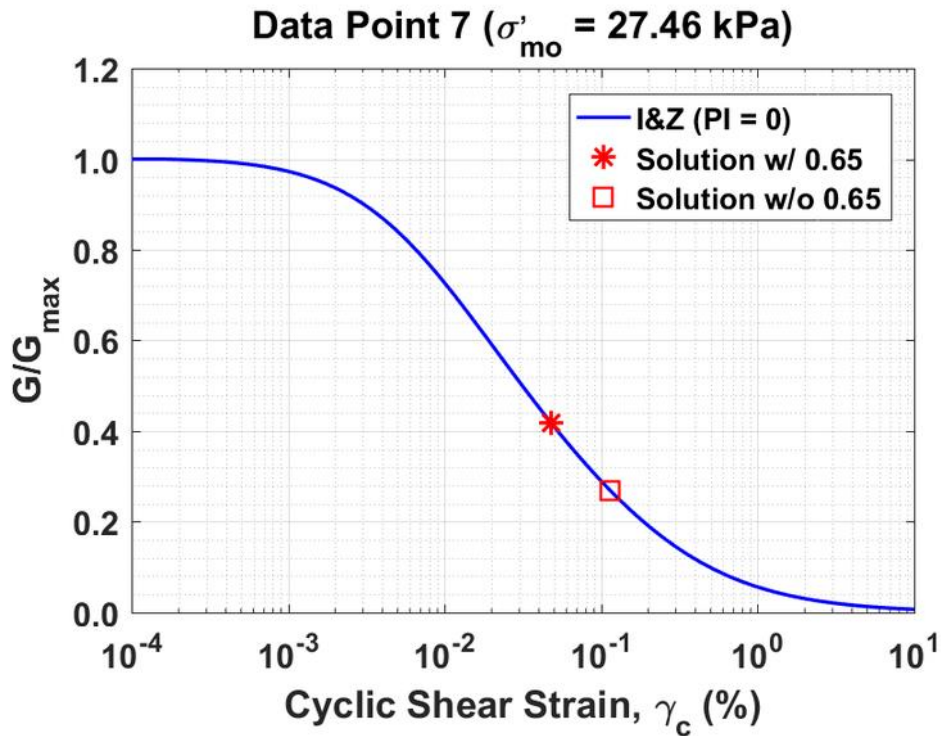


Figure B421. Normalized shear modulus reduction curves for Data Point 7 of the Boulanger et al. database showing the solutions w/ and w/o the 0.65 factor

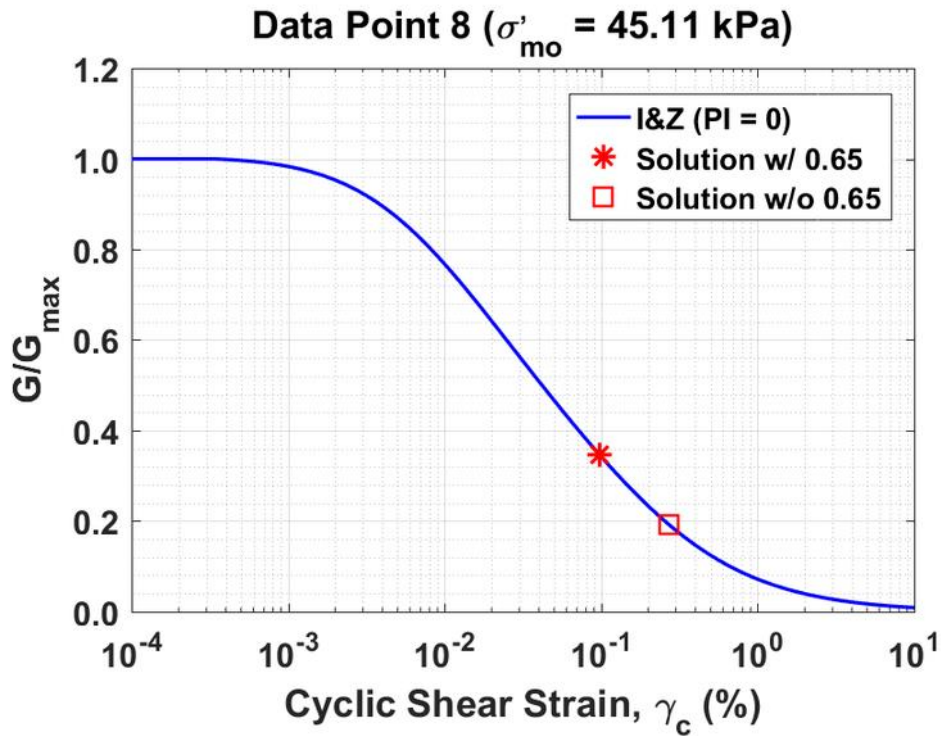


Figure B422. Normalized shear modulus reduction curves for Data Point 8 of the Boulanger et al. database showing the solutions w/ and w/o the 0.65 factor

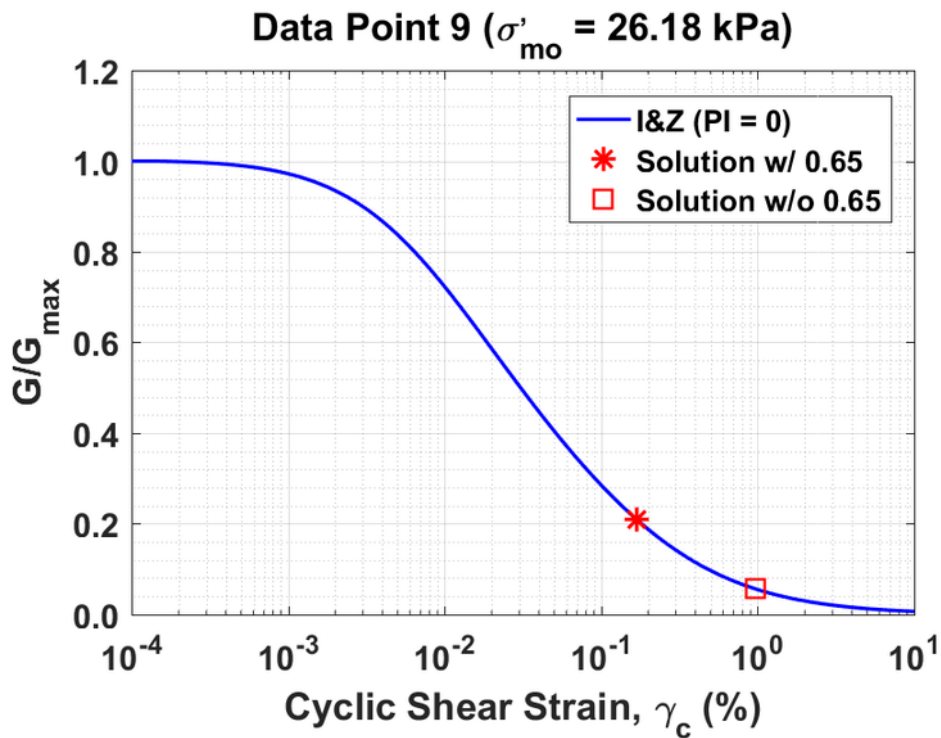


Figure B423. Normalized shear modulus reduction curves for Data Point 9 of the Boulanger et al. database showing the solutions w/ and w/o the 0.65 factor

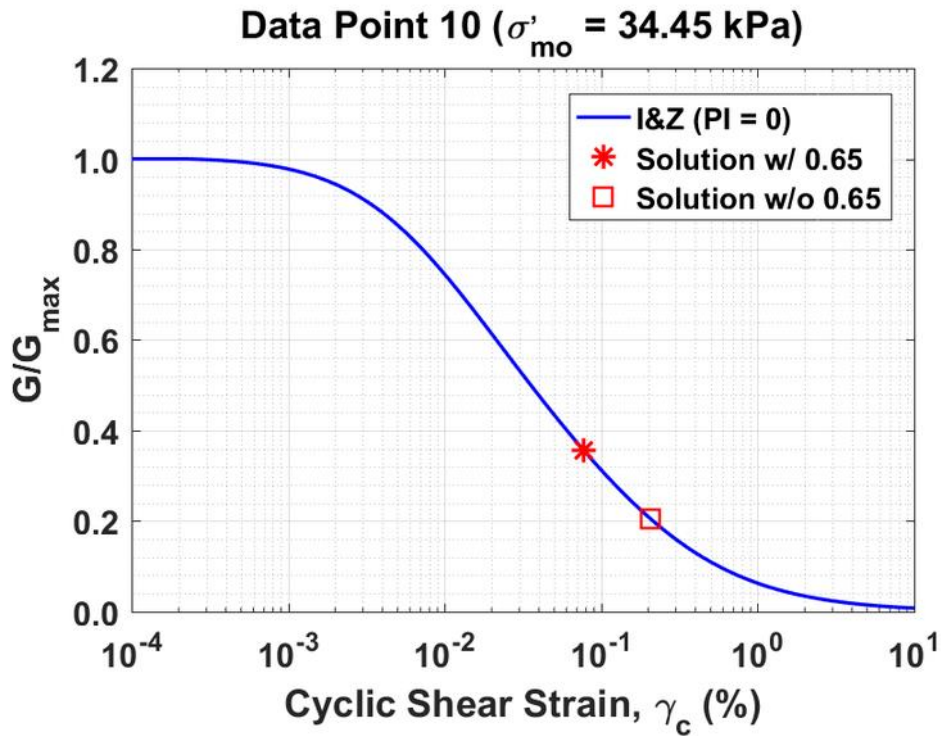


Figure B424. Normalized shear modulus reduction curves for Data Point 10 of the Boulanger et al. database showing the solutions w/ and w/o the 0.65 factor

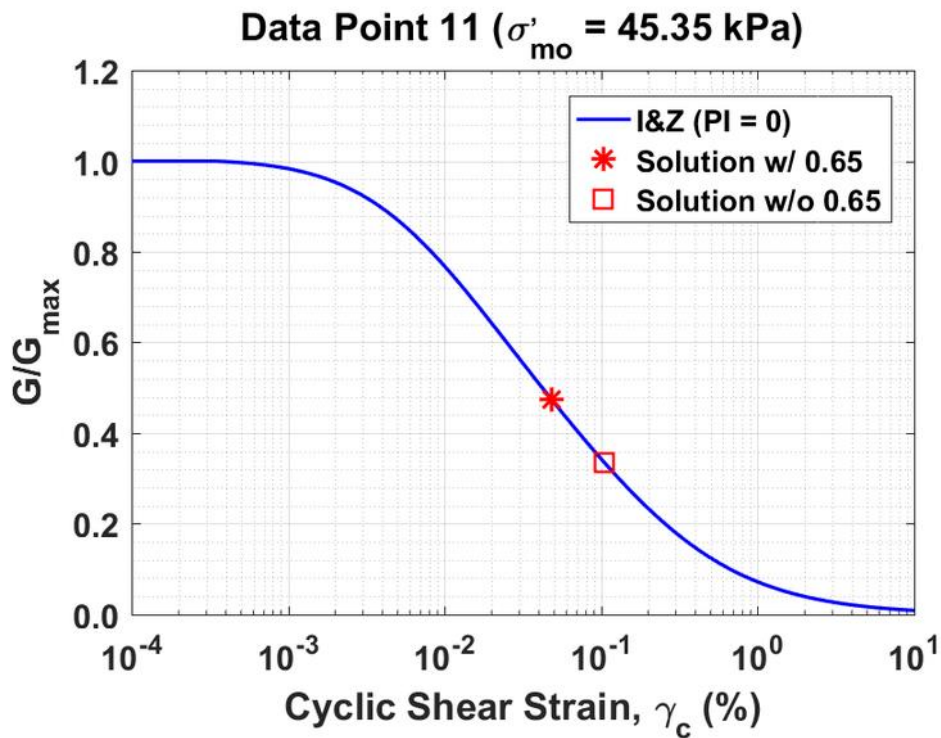


Figure B425. Normalized shear modulus reduction curves for Data Point 11 of the Boulanger et al. database showing the solutions w/ and w/o the 0.65 factor

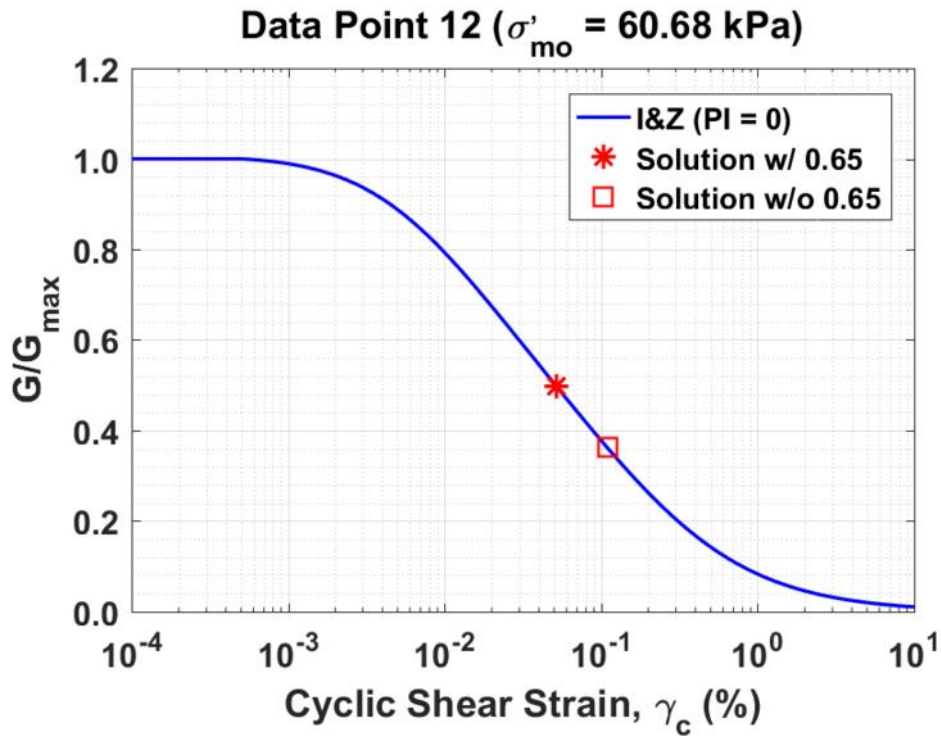


Figure B426. Normalized shear modulus reduction curves for Data Point 12 of the Boulanger et al. database showing the solutions w/ and w/o the 0.65 factor

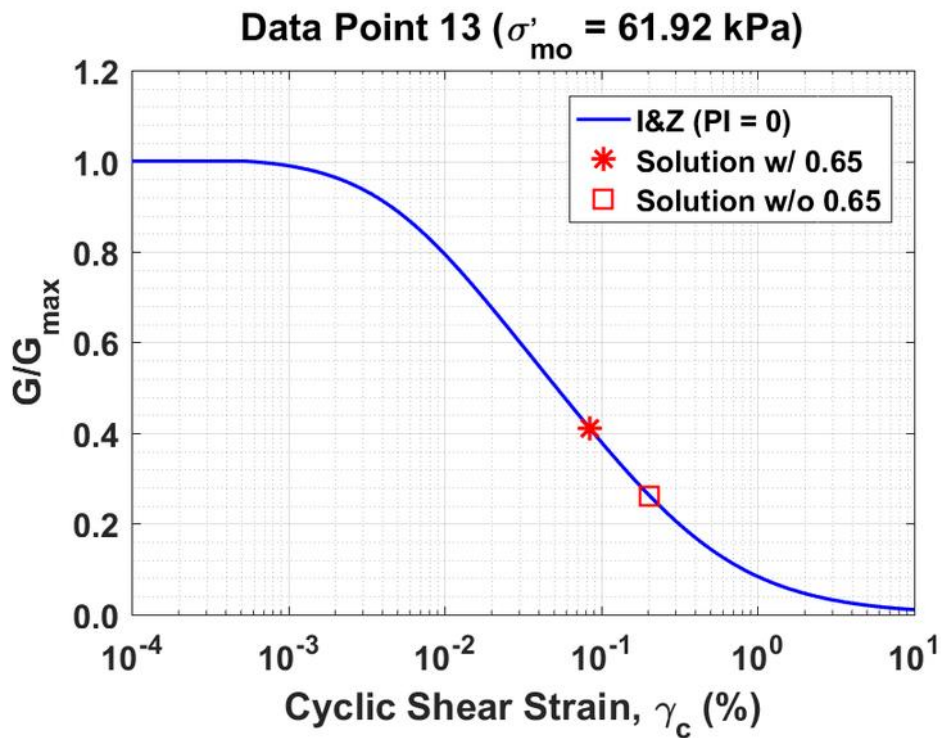


Figure B427. Normalized shear modulus reduction curves for Data Point 13 of the Boulanger et al. database showing the solutions w/ and w/o the 0.65 factor

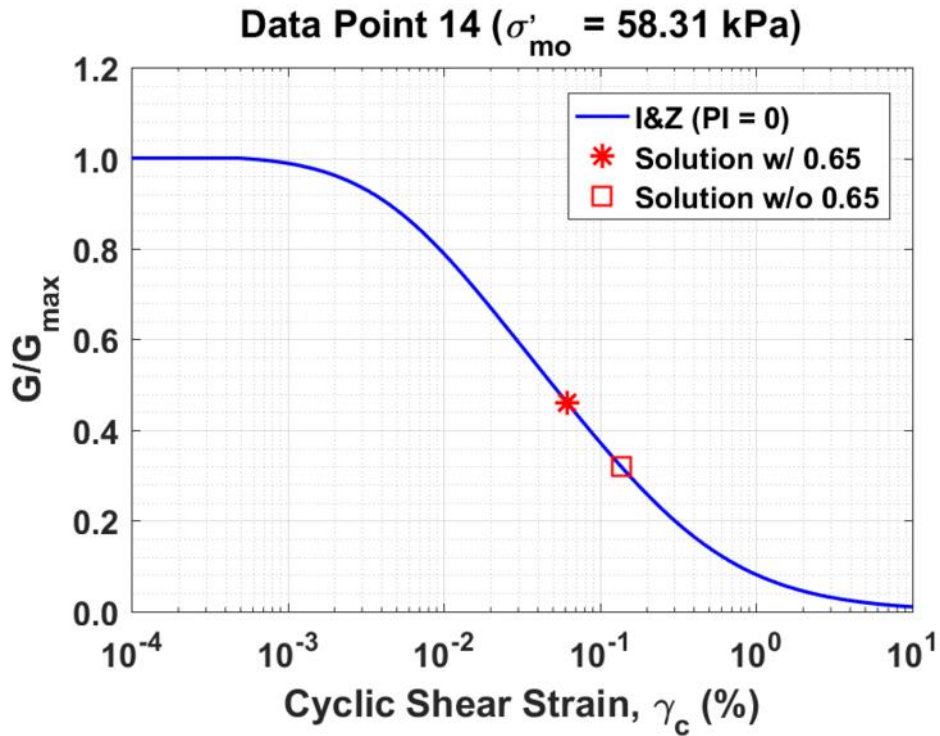


Figure B428. Normalized shear modulus reduction curves for Data Point 14 of the Boulanger et al. database showing the solutions w/ and w/o the 0.65 factor

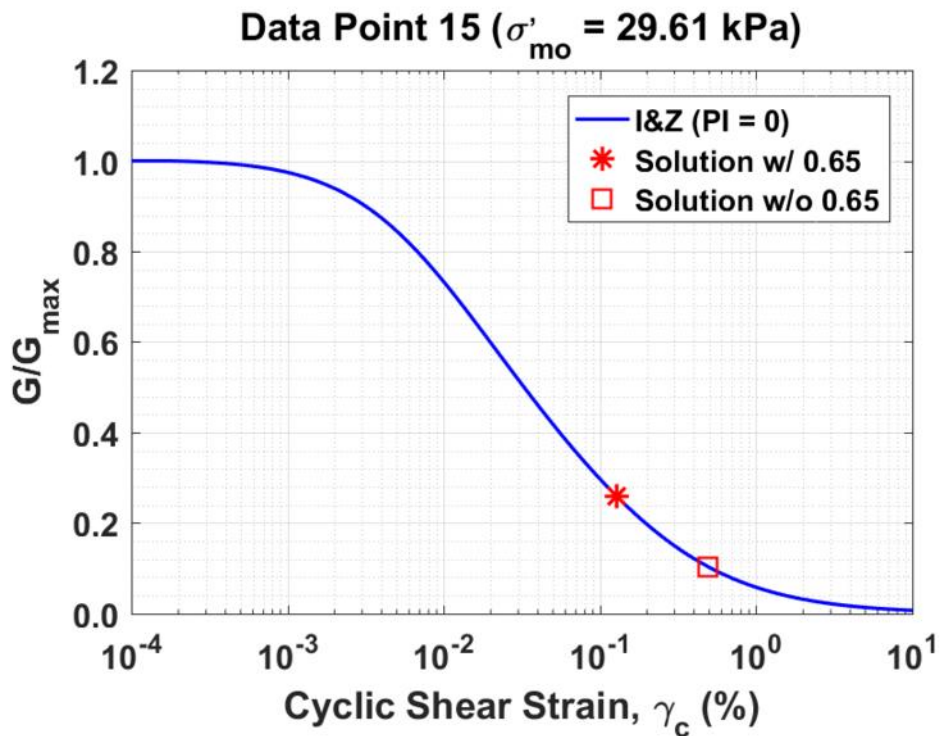


Figure B429. Normalized shear modulus reduction curves for Data Point 15 of the Boulanger et al. database showing the solutions w/ and w/o the 0.65 factor

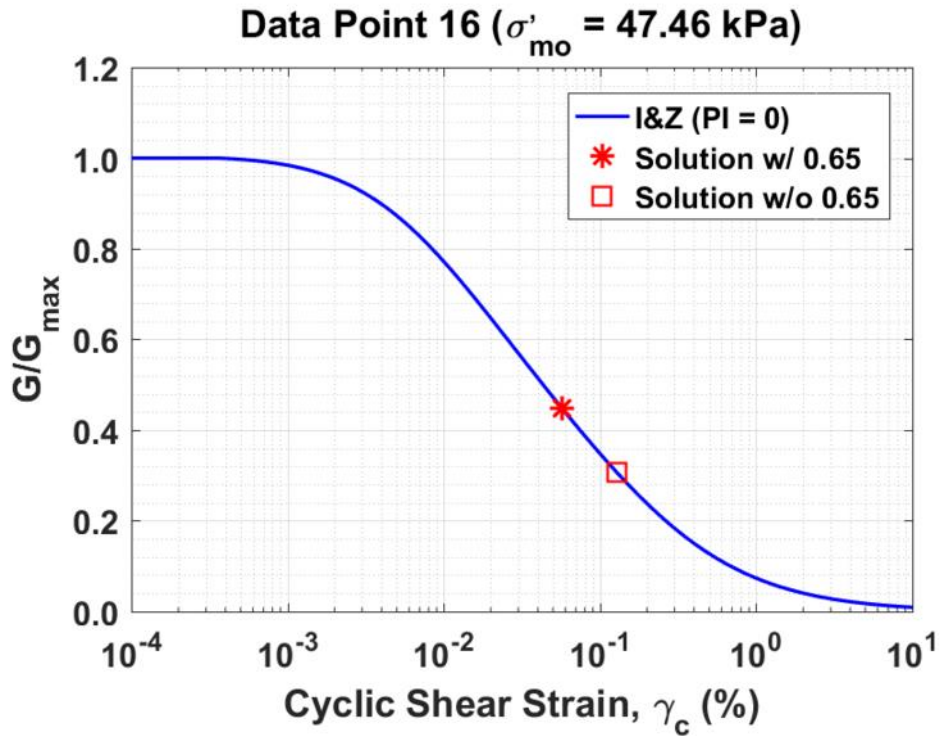


Figure B430. Normalized shear modulus reduction curves for Data Point 16 of the Boulanger et al. database showing the solutions w/ and w/o the 0.65 factor

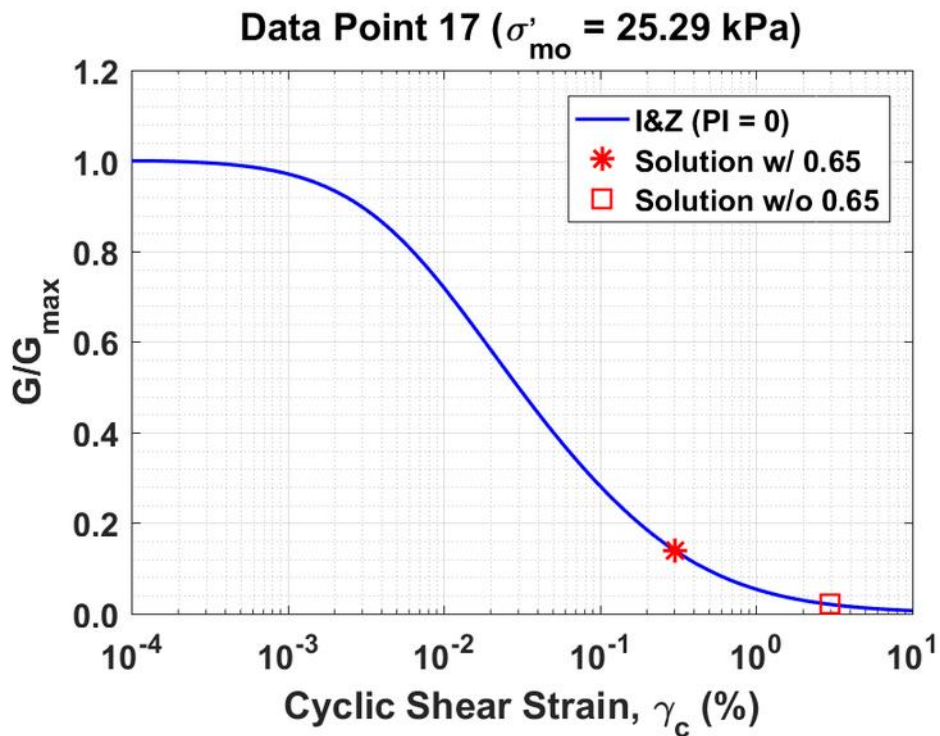


Figure B431. Normalized shear modulus reduction curves for Data Point 17 of the Boulanger et al. database showing the solutions w/ and w/o the 0.65 factor

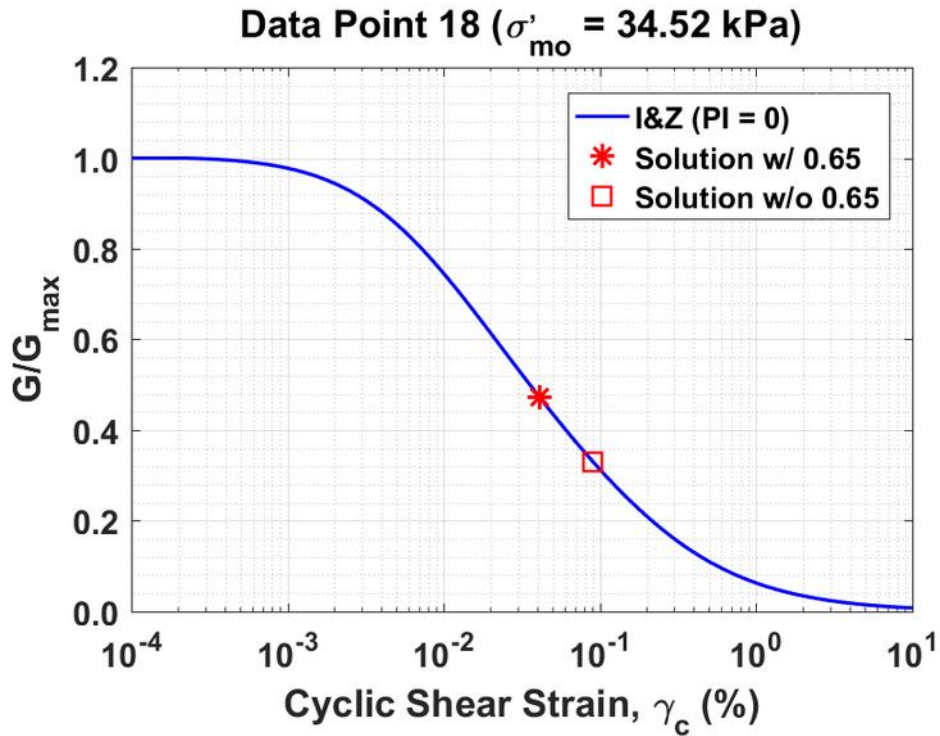


Figure B432. Normalized shear modulus reduction curves for Data Point 18 of the Boulanger et al. database showing the solutions w/ and w/o the 0.65 factor

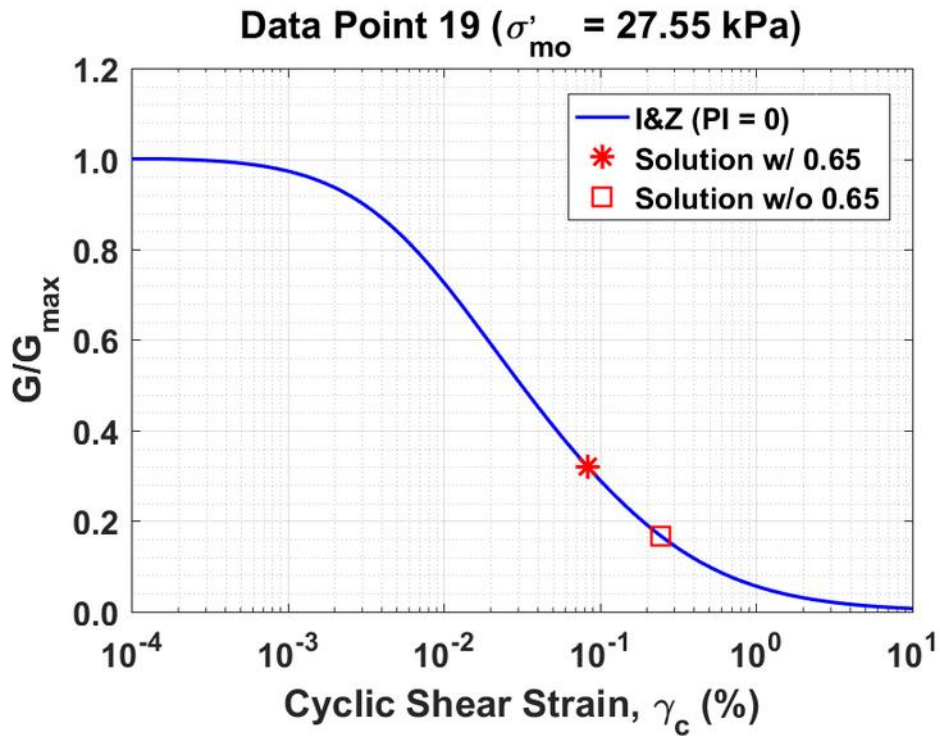


Figure B433. Normalized shear modulus reduction curves for Data Point 19 of the Boulanger et al. database showing the solutions w/ and w/o the 0.65 factor

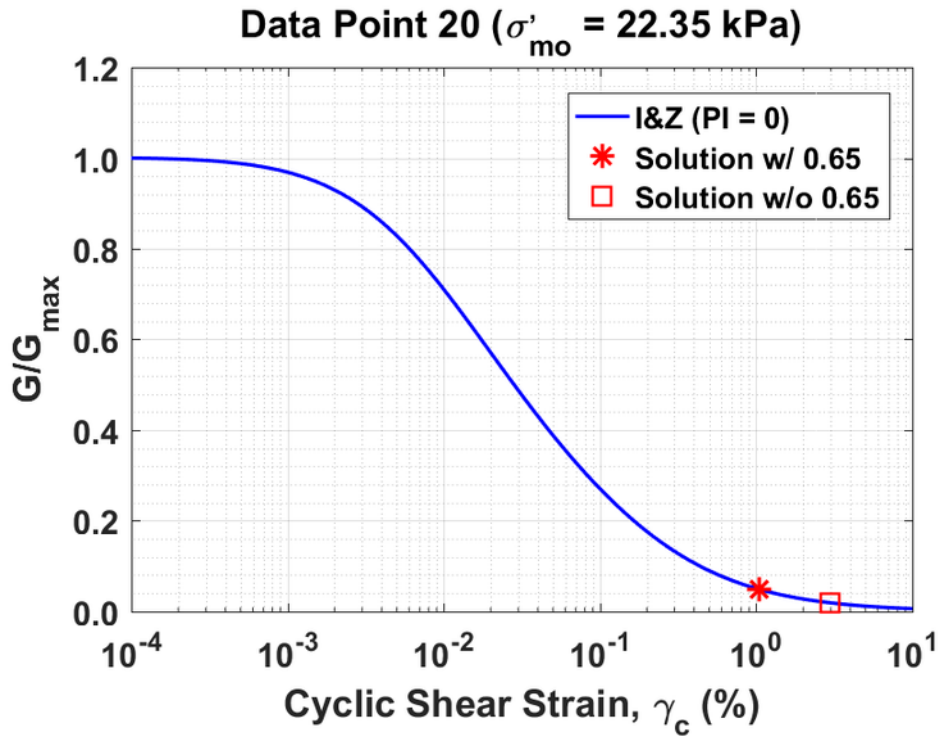


Figure B434. Normalized shear modulus reduction curves for Data Point 20 of the Boulanger et al. database showing the solutions w/ and w/o the 0.65 factor

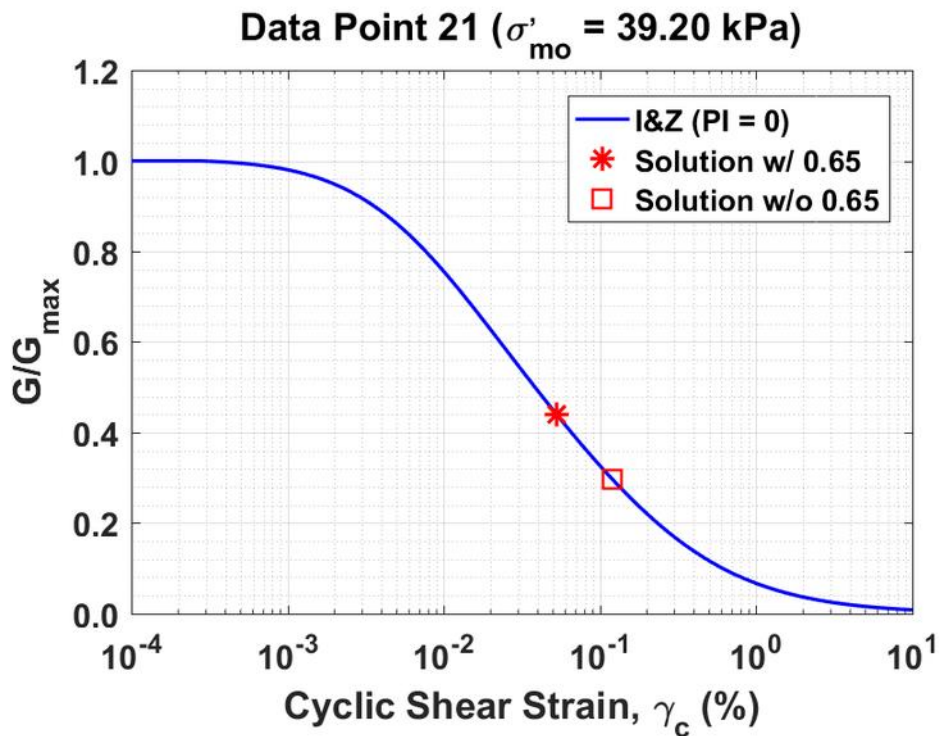


Figure B435. Normalized shear modulus reduction curves for Data Point 21 of the Boulanger et al. database showing the solutions w/ and w/o the 0.65 factor

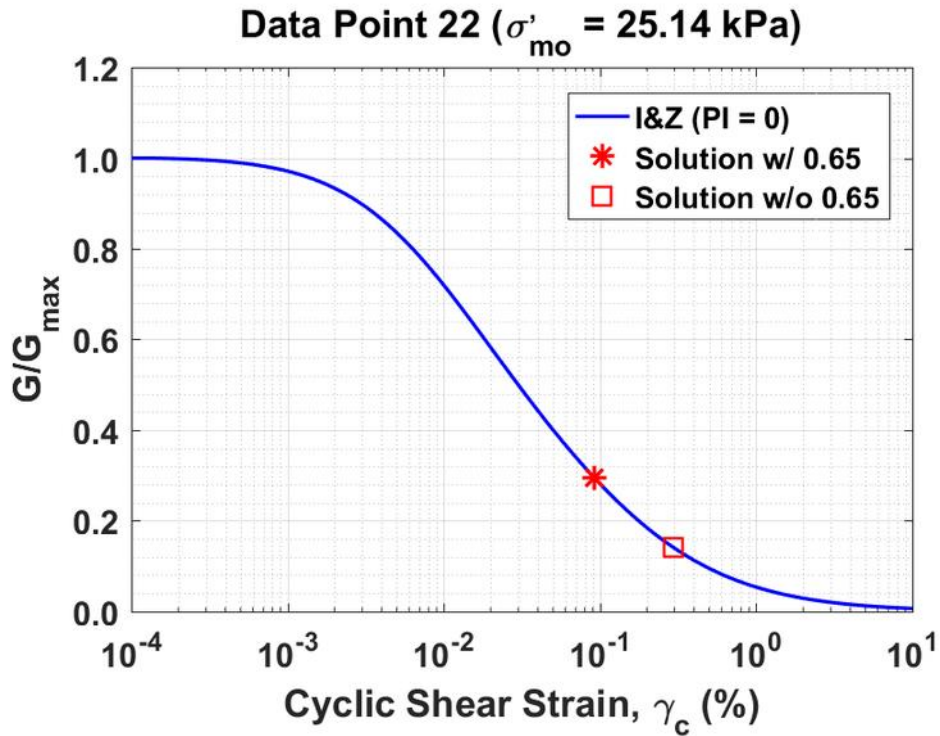


Figure B436. Normalized shear modulus reduction curves for Data Point 22 of the Boulanger et al. database showing the solutions w/ and w/o the 0.65 factor

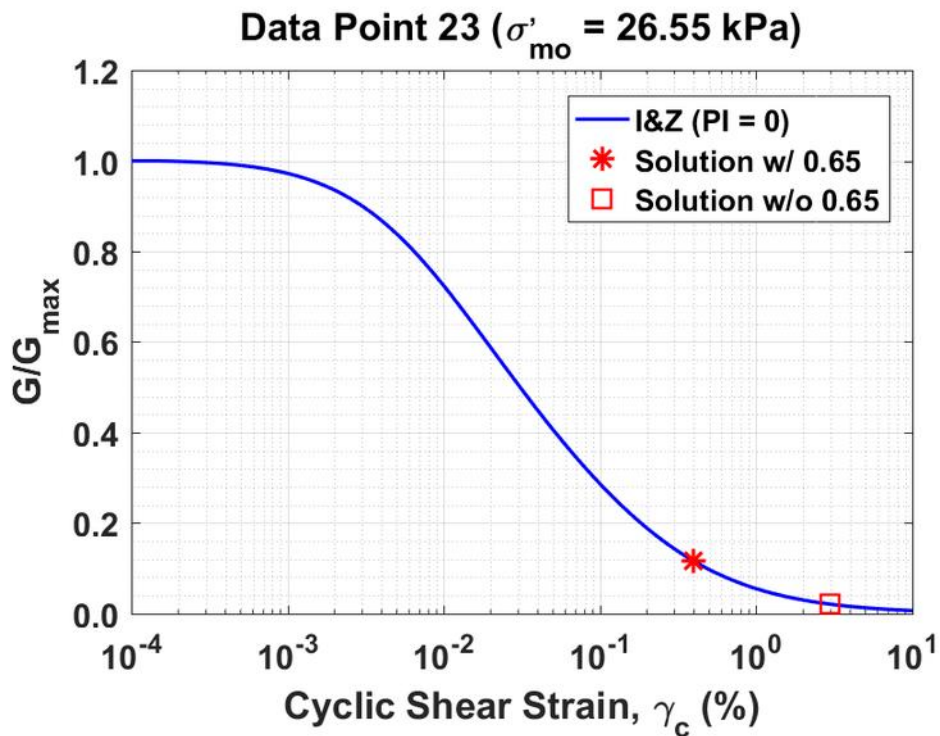


Figure B437. Normalized shear modulus reduction curves for Data Point 23 of the Boulanger et al. database showing the solutions w/ and w/o the 0.65 factor

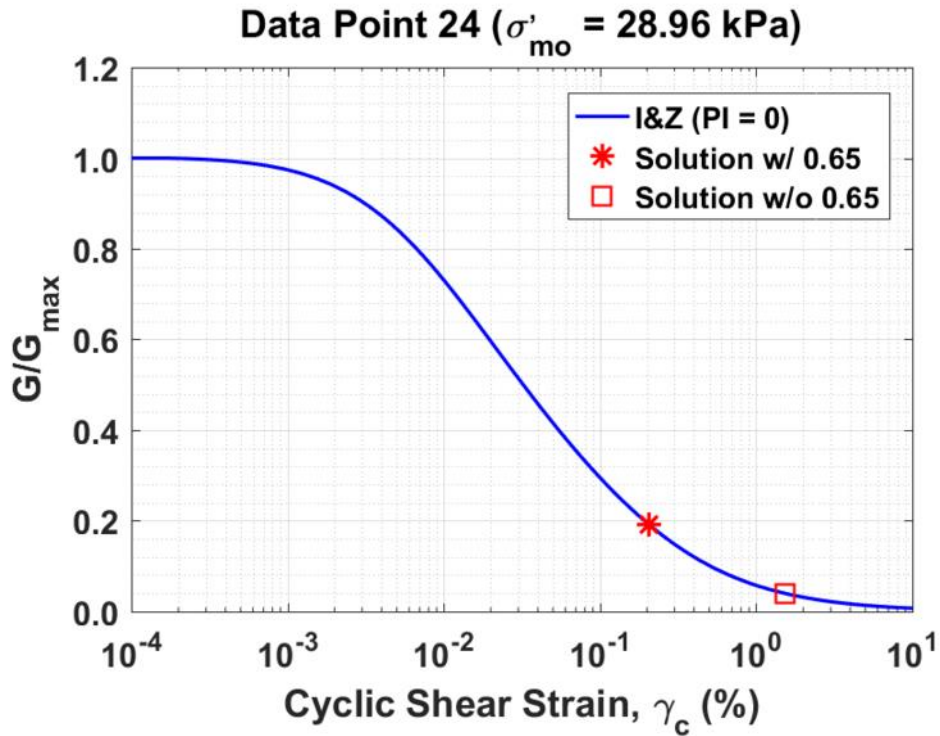


Figure B438. Normalized shear modulus reduction curves for Data Point 24 of the Boulanger et al. database showing the solutions w/ and w/o the 0.65 factor

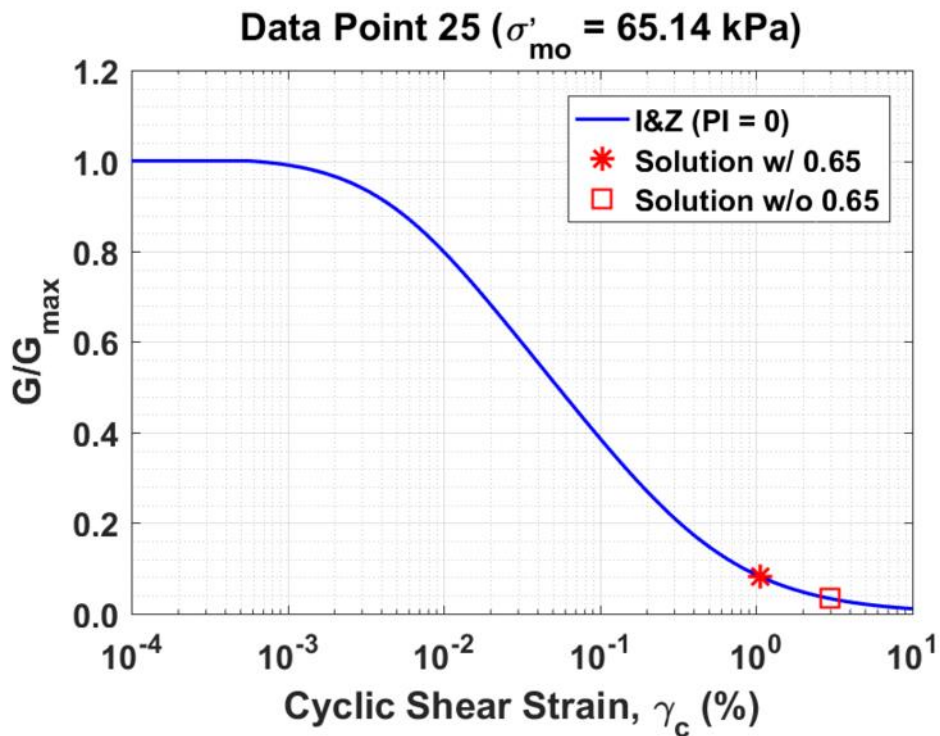


Figure B439. Normalized shear modulus reduction curves for Data Point 25 of the Boulanger et al. database showing the solutions w/ and w/o the 0.65 factor

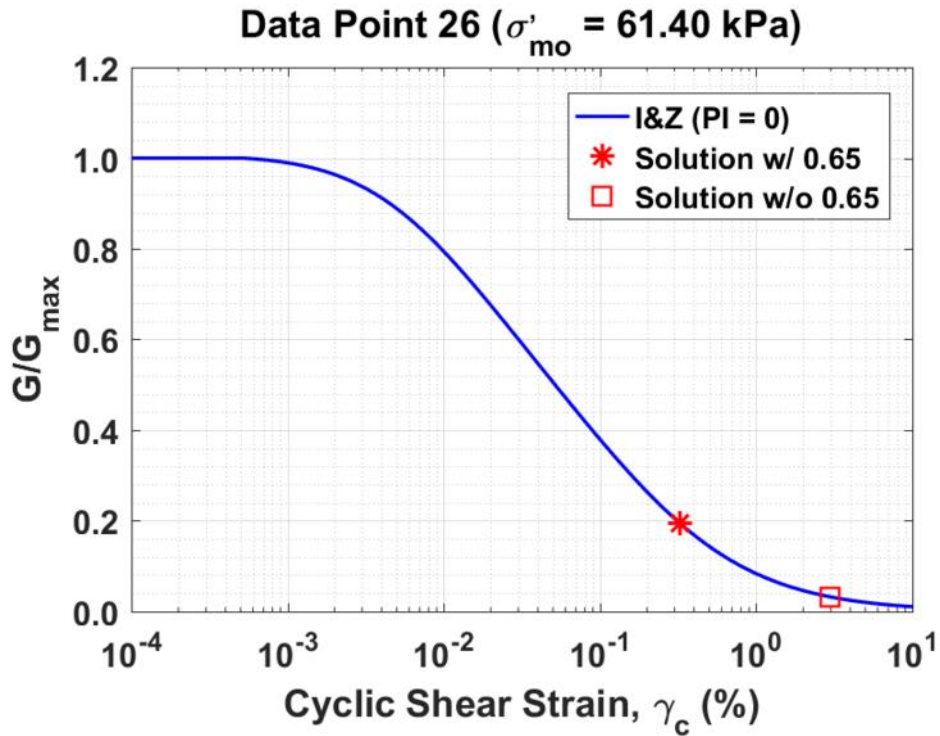


Figure B440. Normalized shear modulus reduction curves for Data Point 26 of the Boulanger et al. database showing the solutions w/ and w/o the 0.65 factor

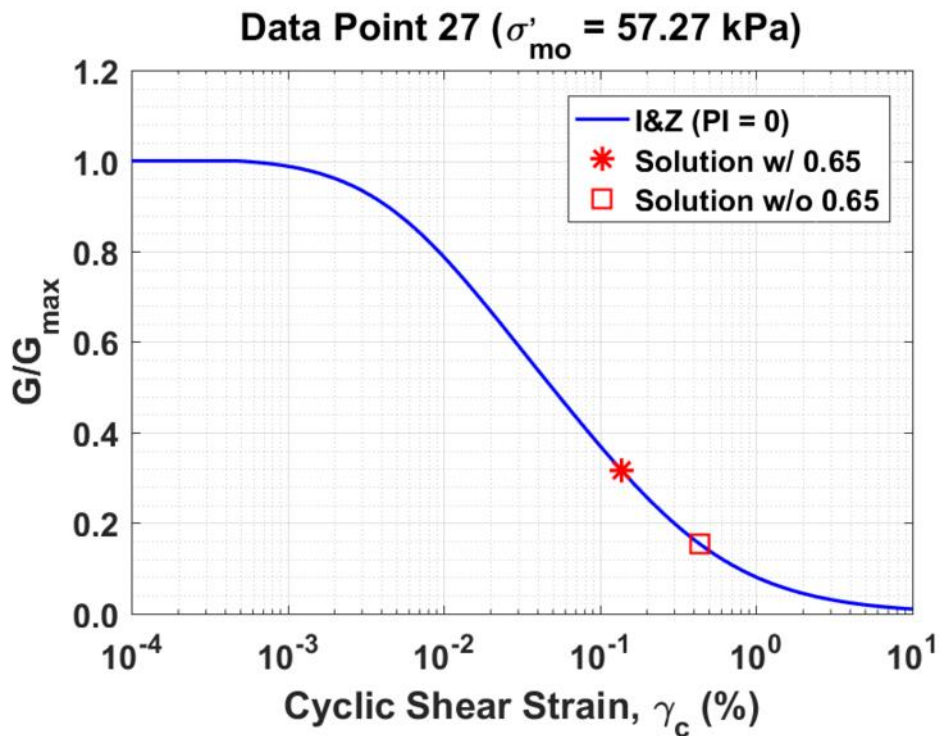


Figure B441. Normalized shear modulus reduction curves for Data Point 27 of the Boulanger et al. database showing the solutions w/ and w/o the 0.65 factor

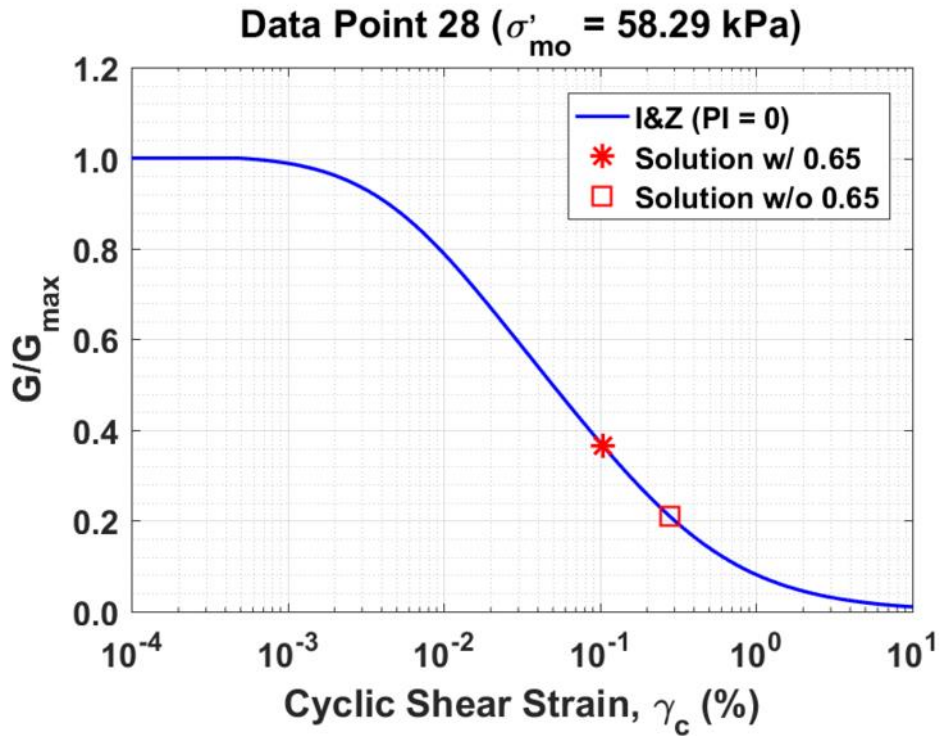


Figure B442. Normalized shear modulus reduction curves for Data Point 28 of the Boulanger et al. database showing the solutions w/ and w/o the 0.65 factor

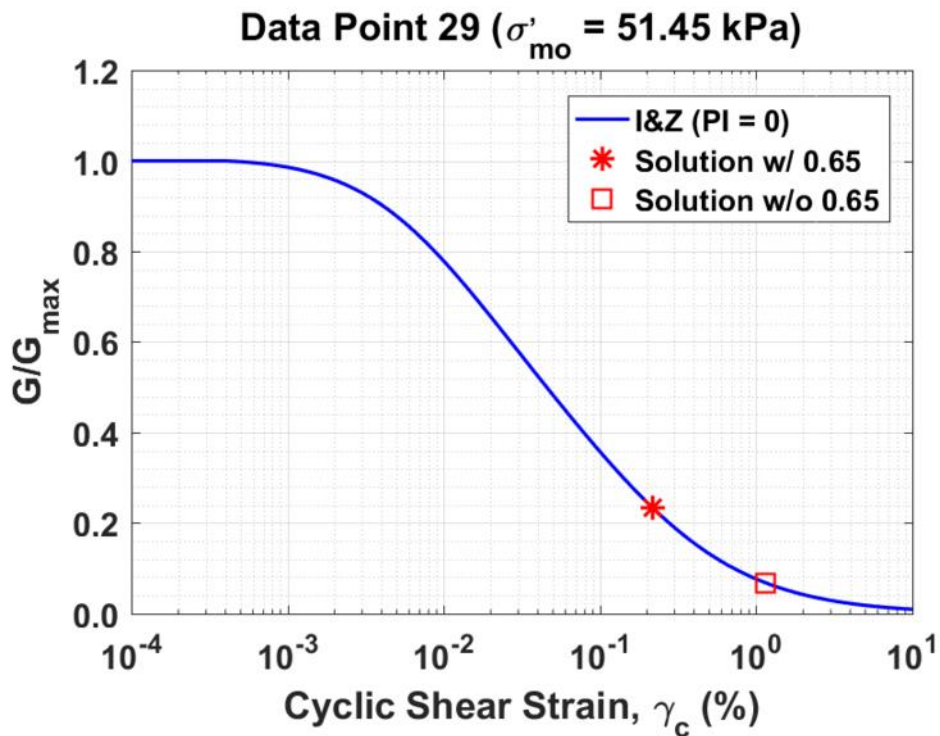


Figure B443. Normalized shear modulus reduction curves for Data Point 29 of the Boulanger et al. database showing the solutions w/ and w/o the 0.65 factor

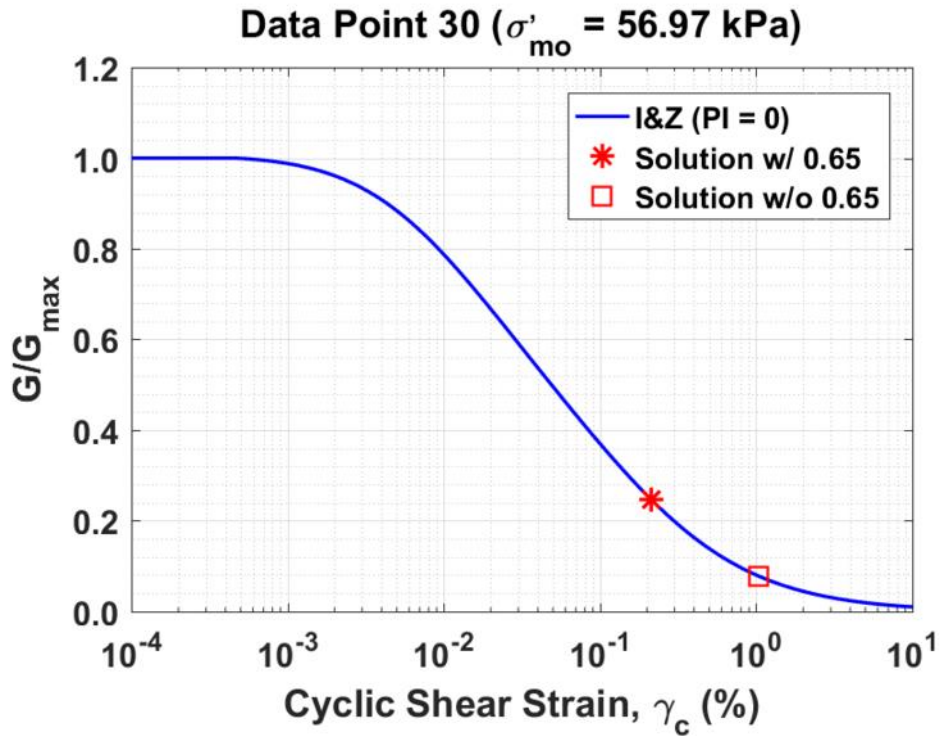


Figure B444. Normalized shear modulus reduction curves for Data Point 30 of the Boulanger et al. database showing the solutions w/ and w/o the 0.65 factor

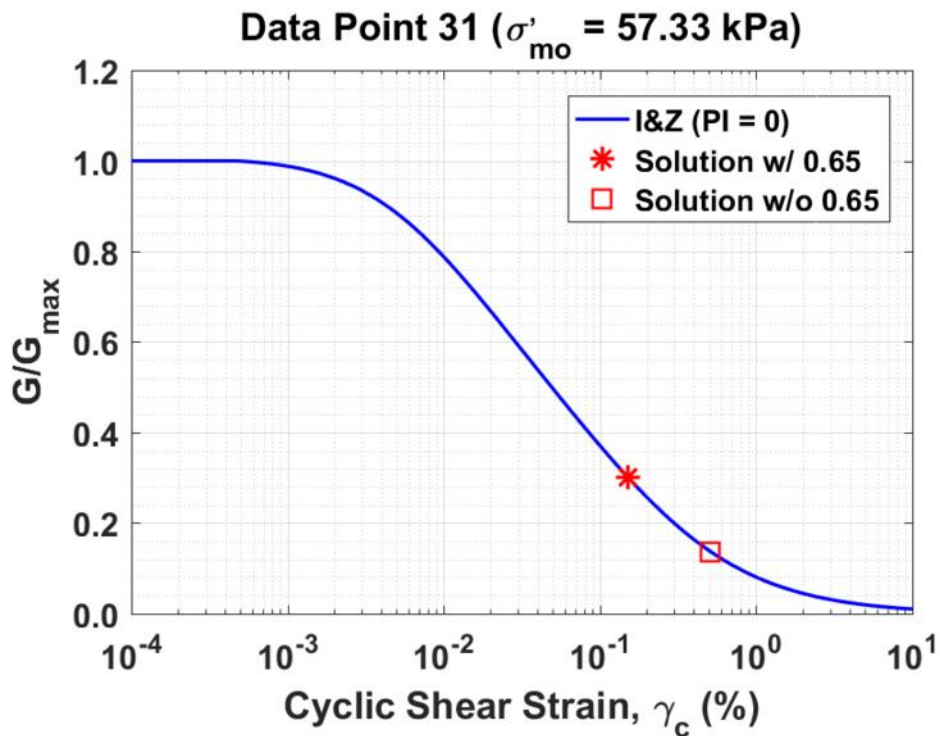


Figure B445. Normalized shear modulus reduction curves for Data Point 31 of the Boulanger et al. database showing the solutions w/ and w/o the 0.65 factor

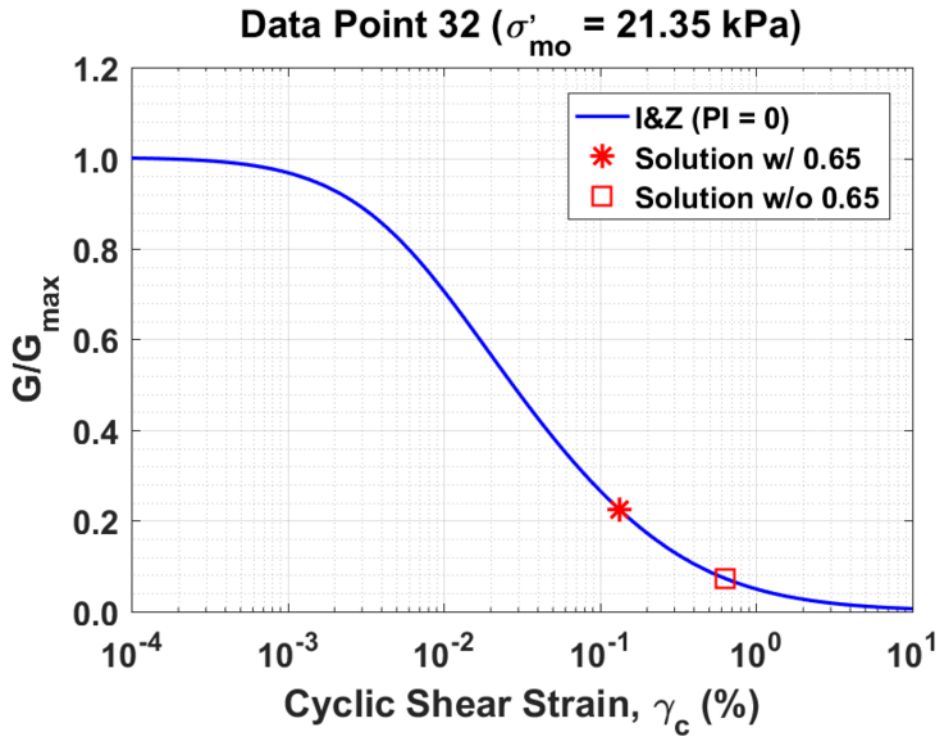


Figure B446. Normalized shear modulus reduction curves for Data Point 32 of the Boulanger et al. database showing the solutions w/ and w/o the 0.65 factor

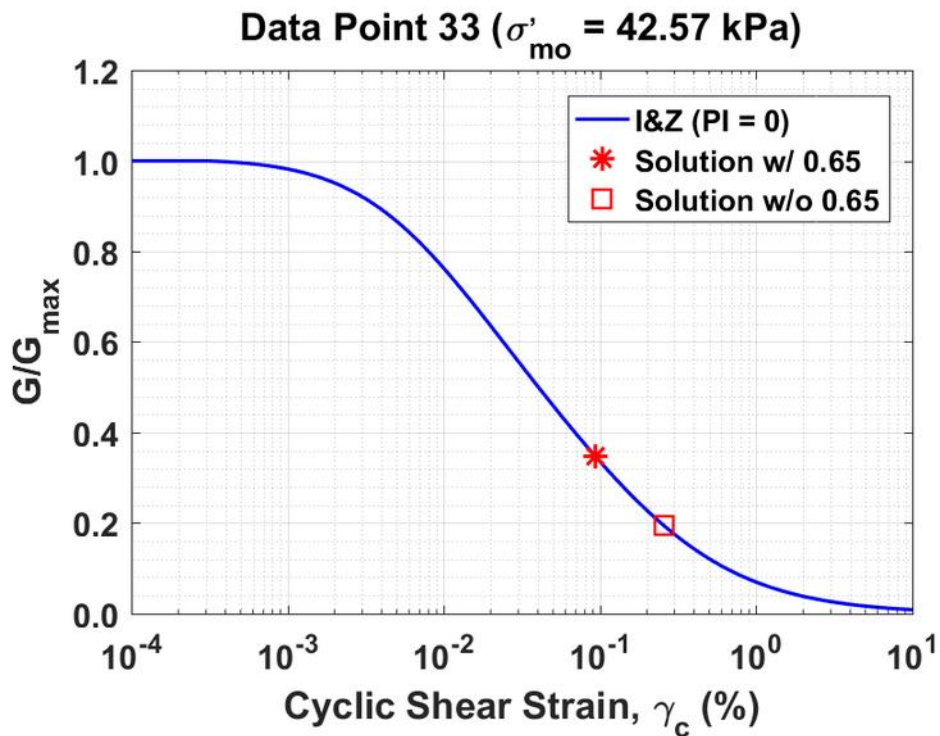


Figure B447. Normalized shear modulus reduction curves for Data Point 33 of the Boulanger et al. database showing the solutions w/ and w/o the 0.65 factor

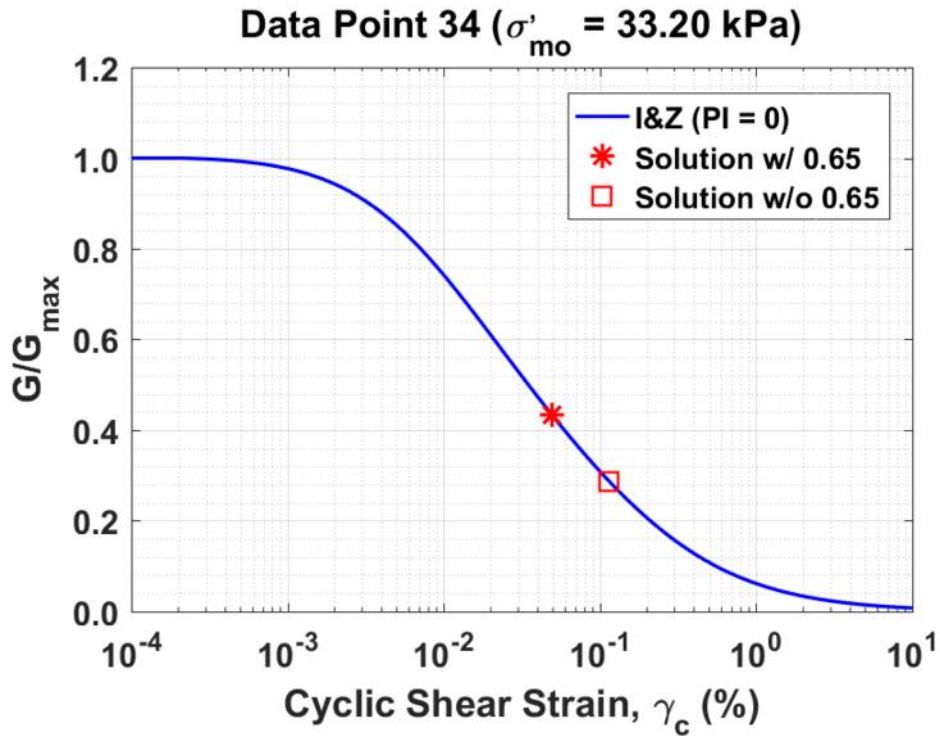


Figure B448. Normalized shear modulus reduction curves for Data Point 34 of the Boulanger et al. database showing the solutions w/ and w/o the 0.65 factor

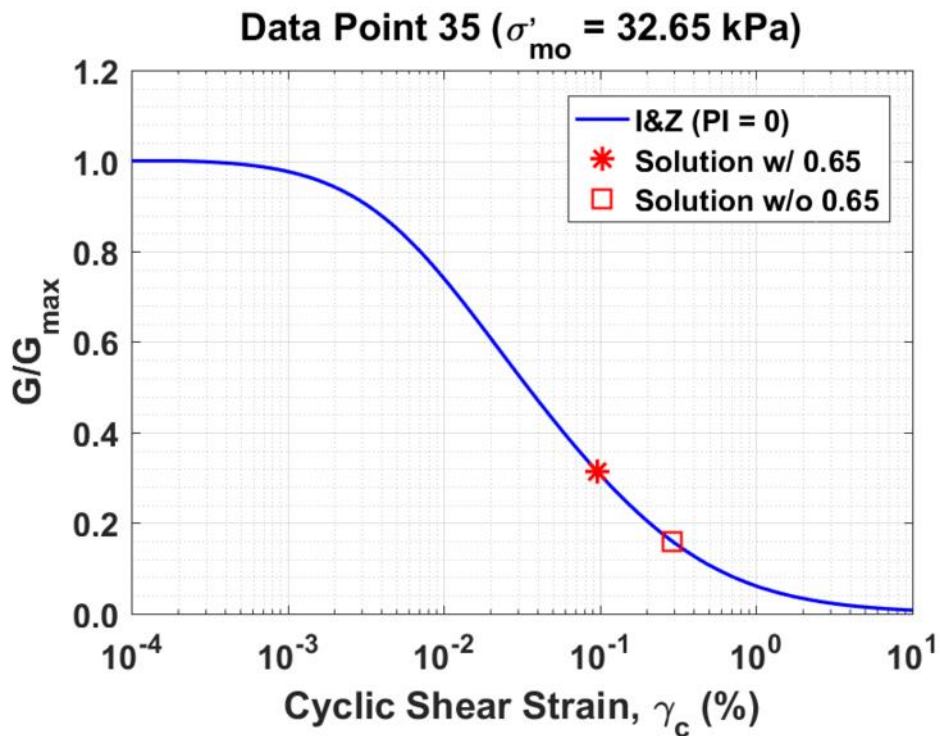


Figure B449. Normalized shear modulus reduction curves for Data Point 35 of the Boulanger et al. database showing the solutions w/ and w/o the 0.65 factor

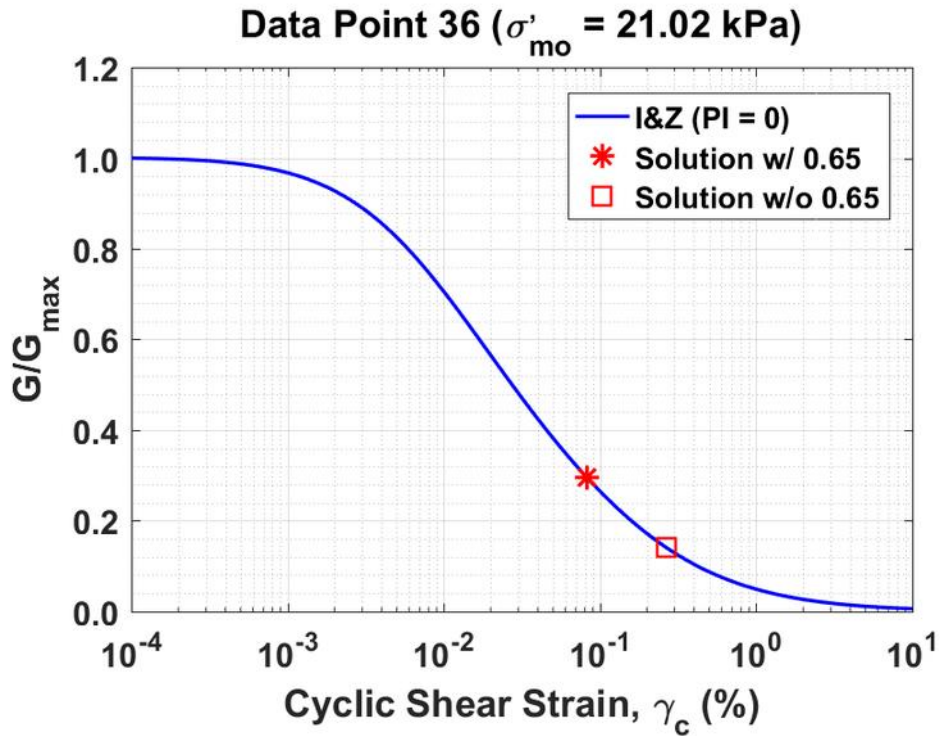


Figure B450. Normalized shear modulus reduction curves for Data Point 36 of the Boulanger et al. database showing the solutions w/ and w/o the 0.65 factor

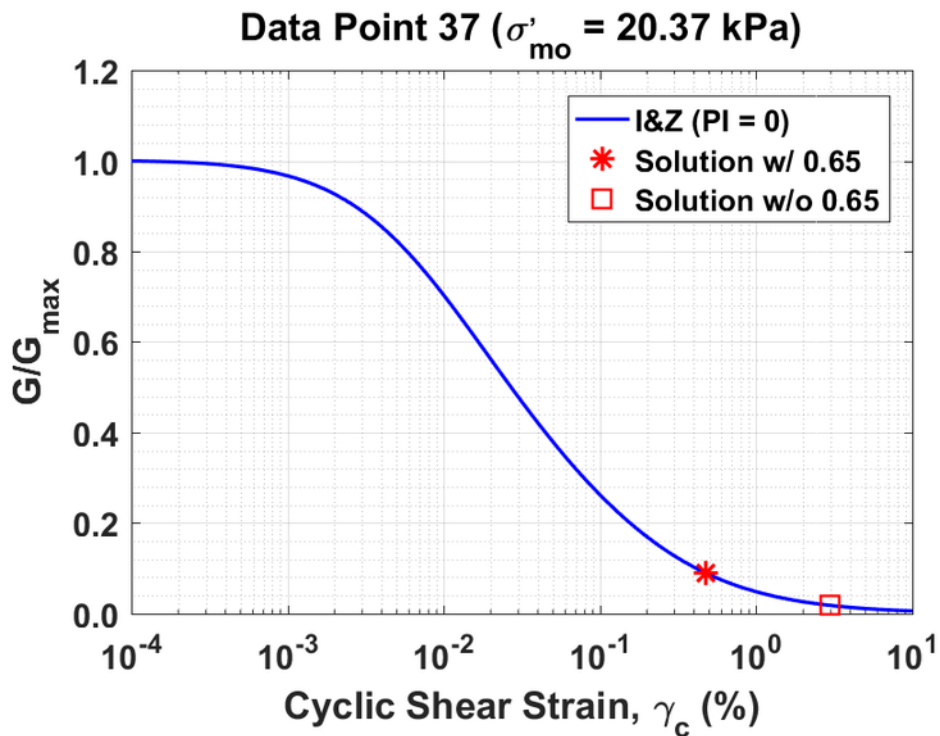


Figure B451. Normalized shear modulus reduction curves for Data Point 37 of the Boulanger et al. database showing the solutions w/ and w/o the 0.65 factor

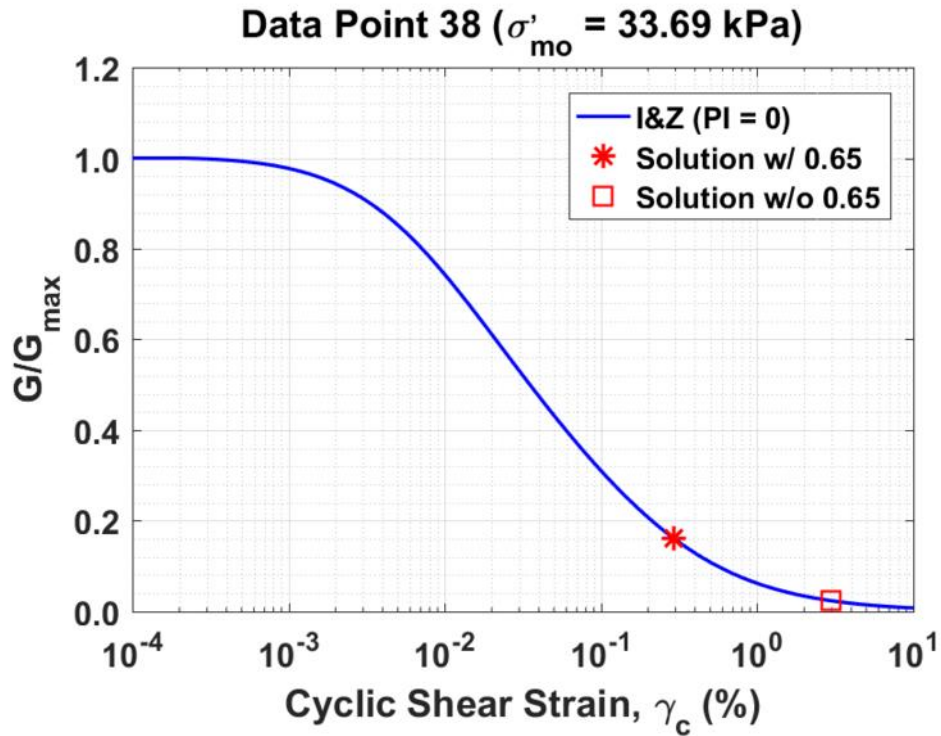


Figure B452. Normalized shear modulus reduction curves for Data Point 38 of the Boulanger et al. database showing the solutions w/ and w/o the 0.65 factor

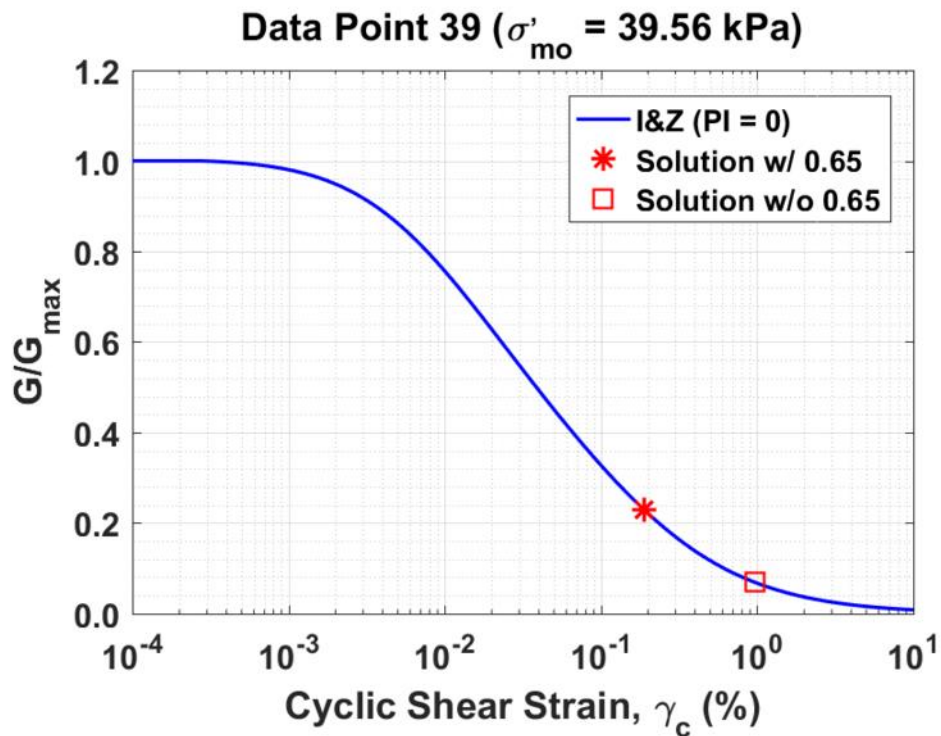


Figure B453. Normalized shear modulus reduction curves for Data Point 39 of the Boulanger et al. database showing the solutions w/ and w/o the 0.65 factor

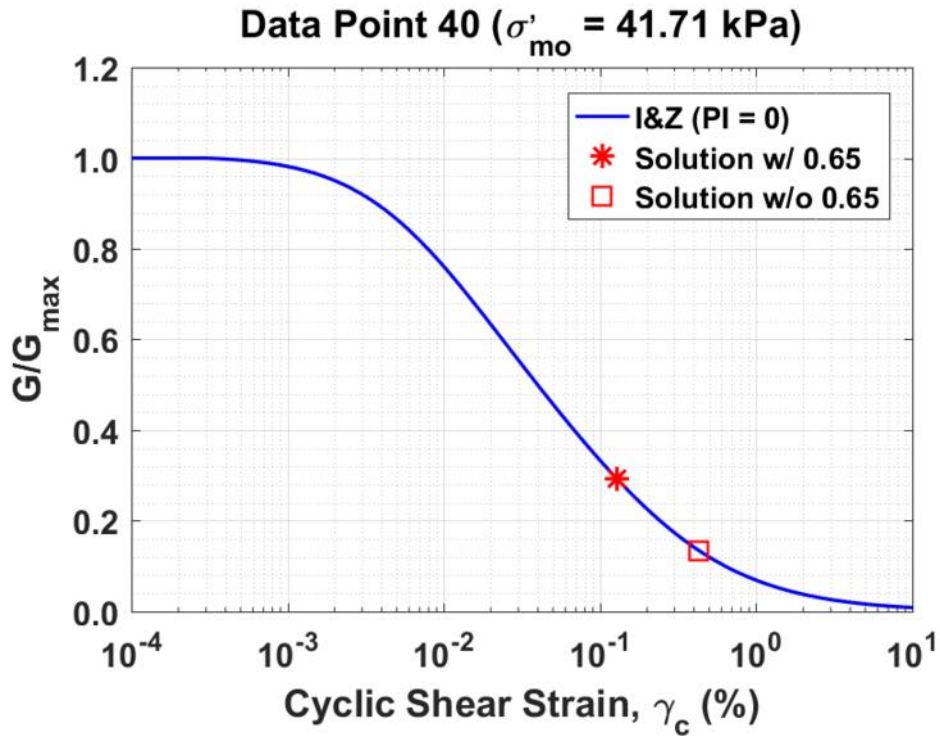


Figure B454. Normalized shear modulus reduction curves for Data Point 40 of the Boulanger et al. database showing the solutions w/ and w/o the 0.65 factor

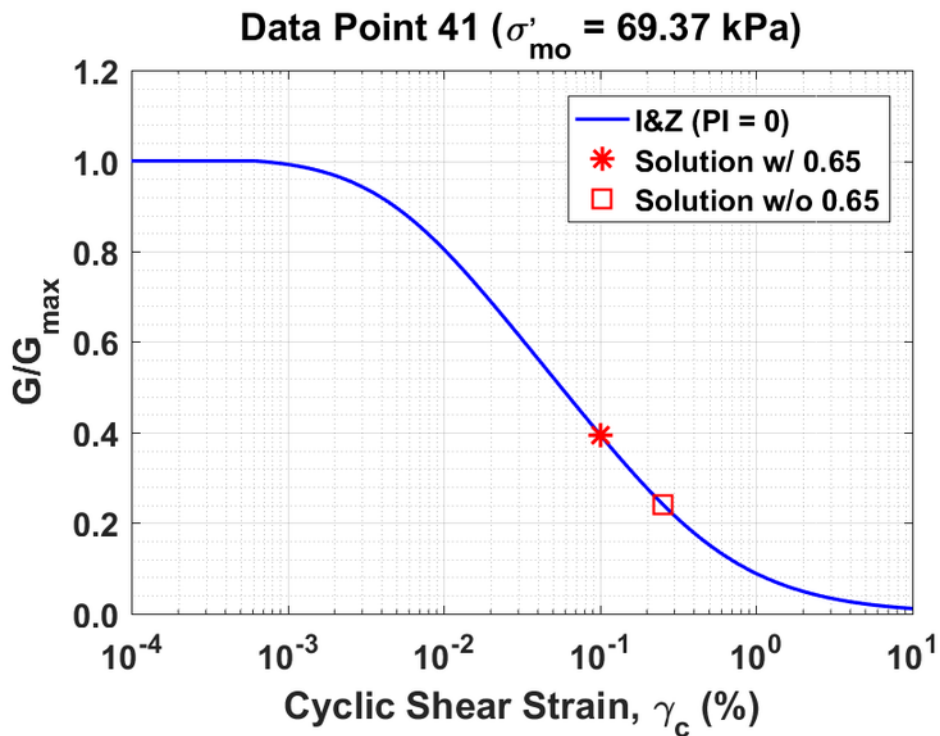


Figure B455. Normalized shear modulus reduction curves for Data Point 41 of the Boulanger et al. database showing the solutions w/ and w/o the 0.65 factor

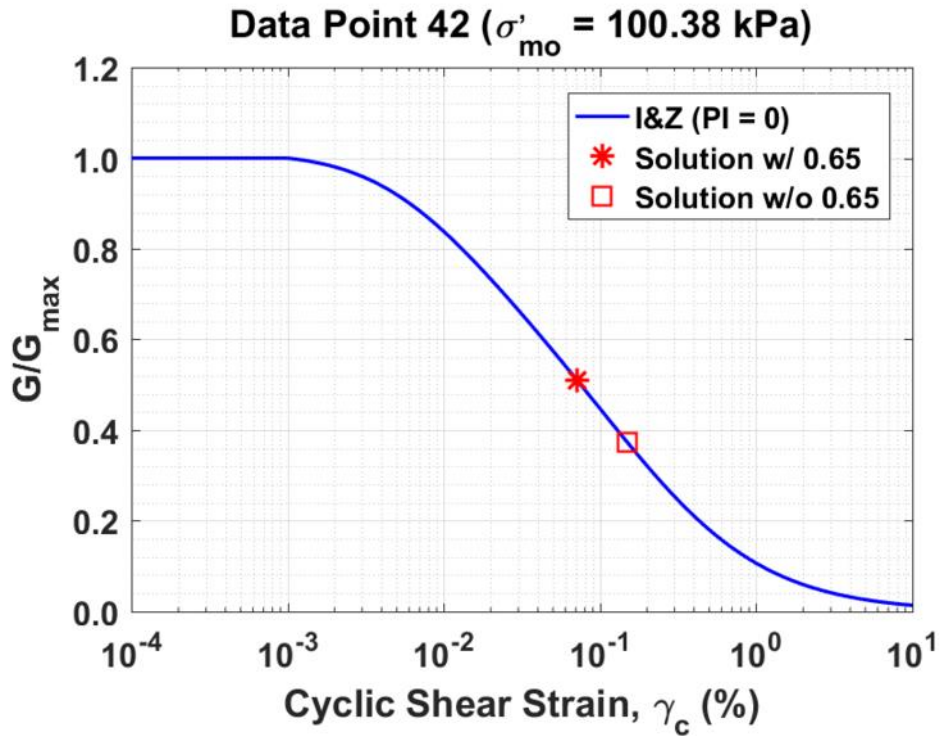


Figure B456. Normalized shear modulus reduction curves for Data Point 42 of the Boulanger et al. database showing the solutions w/ and w/o the 0.65 factor

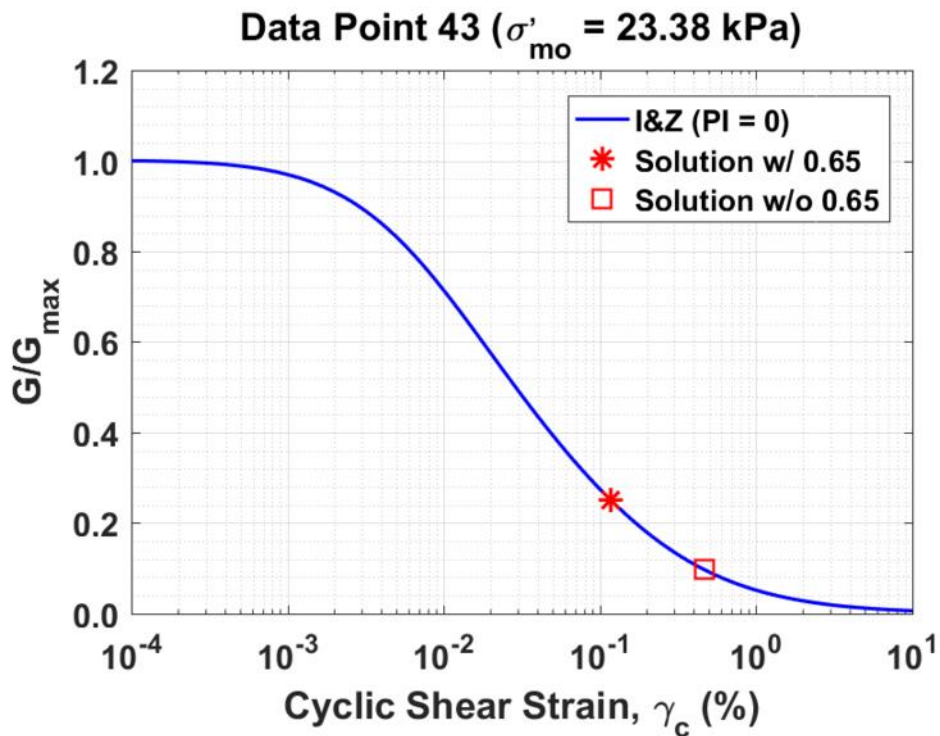


Figure B457. Normalized shear modulus reduction curves for Data Point 43 of the Boulanger et al. database showing the solutions w/ and w/o the 0.65 factor

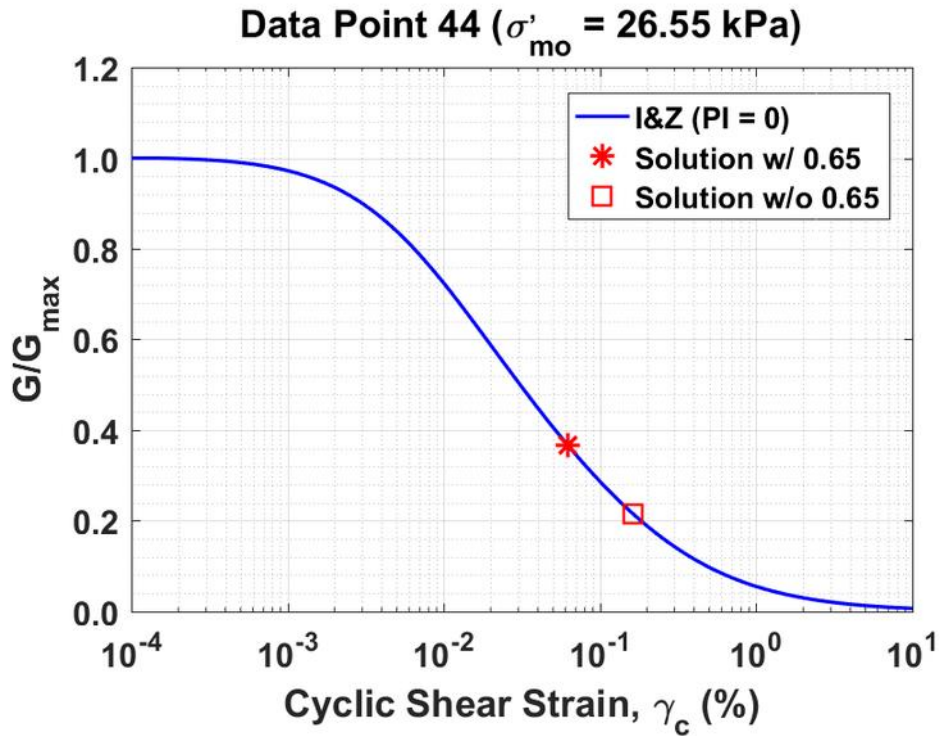


Figure B458. Normalized shear modulus reduction curves for Data Point 44 of the Boulanger et al. database showing the solutions w/ and w/o the 0.65 factor

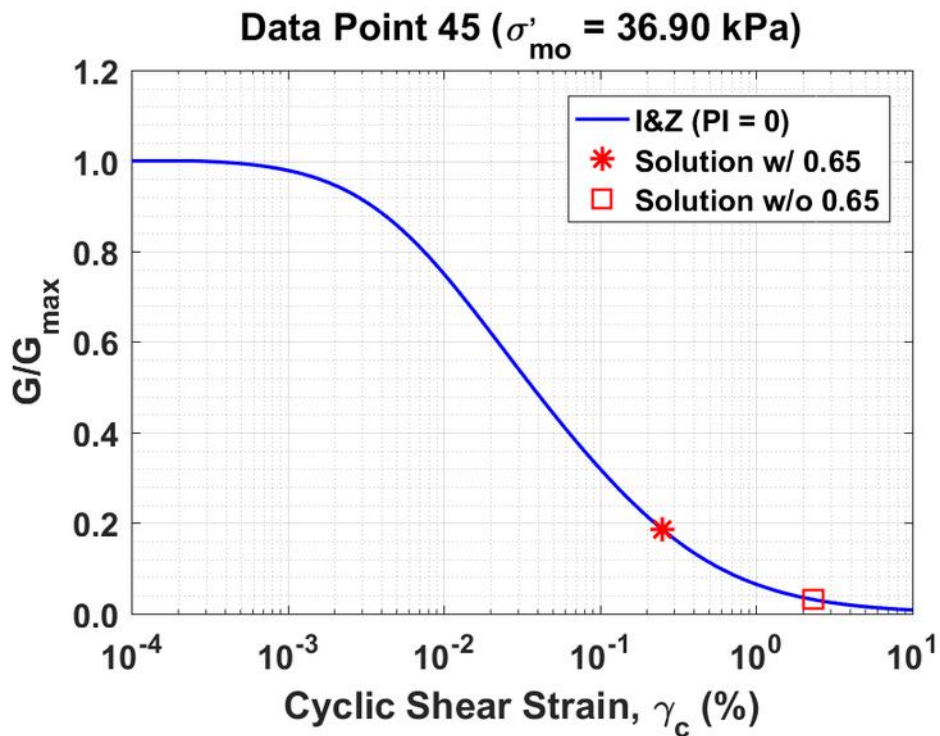


Figure B459. Normalized shear modulus reduction curves for Data Point 45 of the Boulanger et al. database showing the solutions w/ and w/o the 0.65 factor

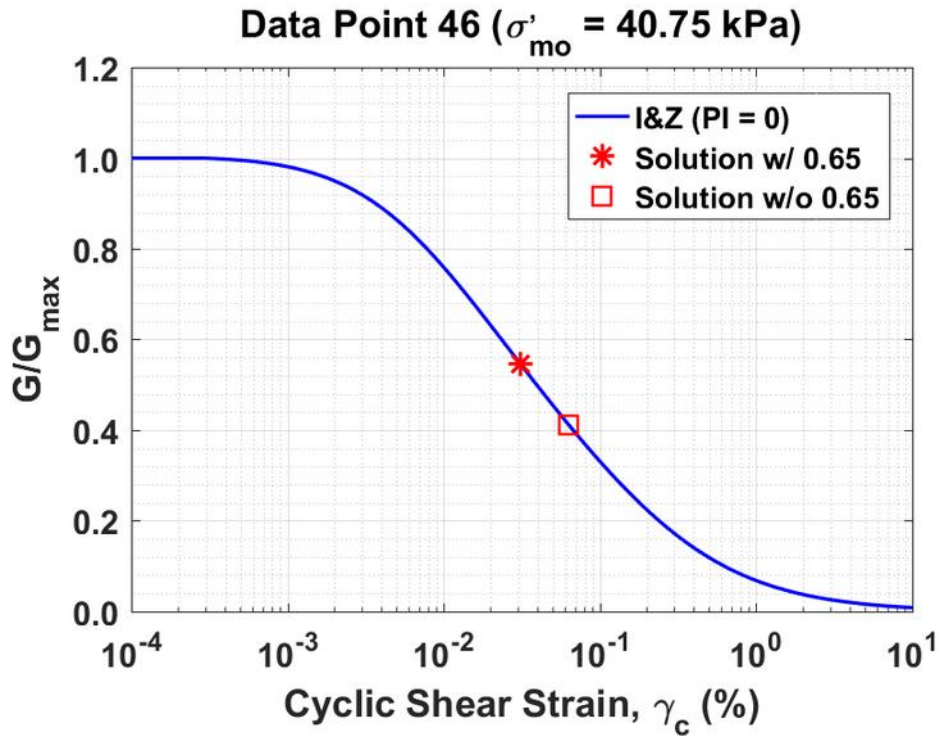


Figure B460. Normalized shear modulus reduction curves for Data Point 46 of the Boulanger et al. database showing the solutions w/ and w/o the 0.65 factor

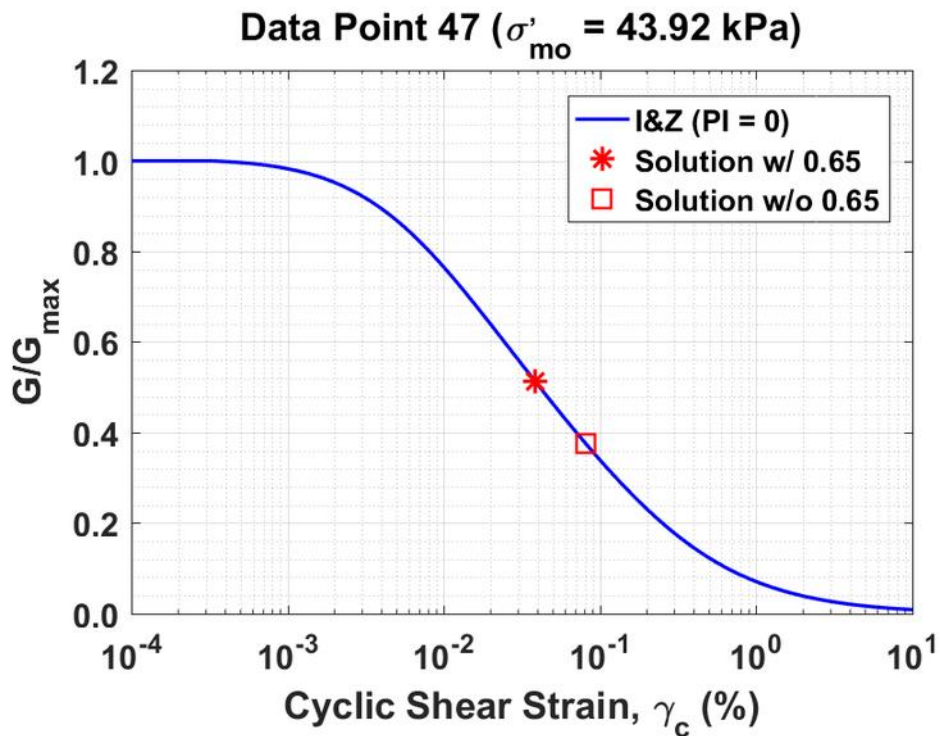


Figure B461. Normalized shear modulus reduction curves for Data Point 47 of the Boulanger et al. database showing the solutions w/ and w/o the 0.65 factor

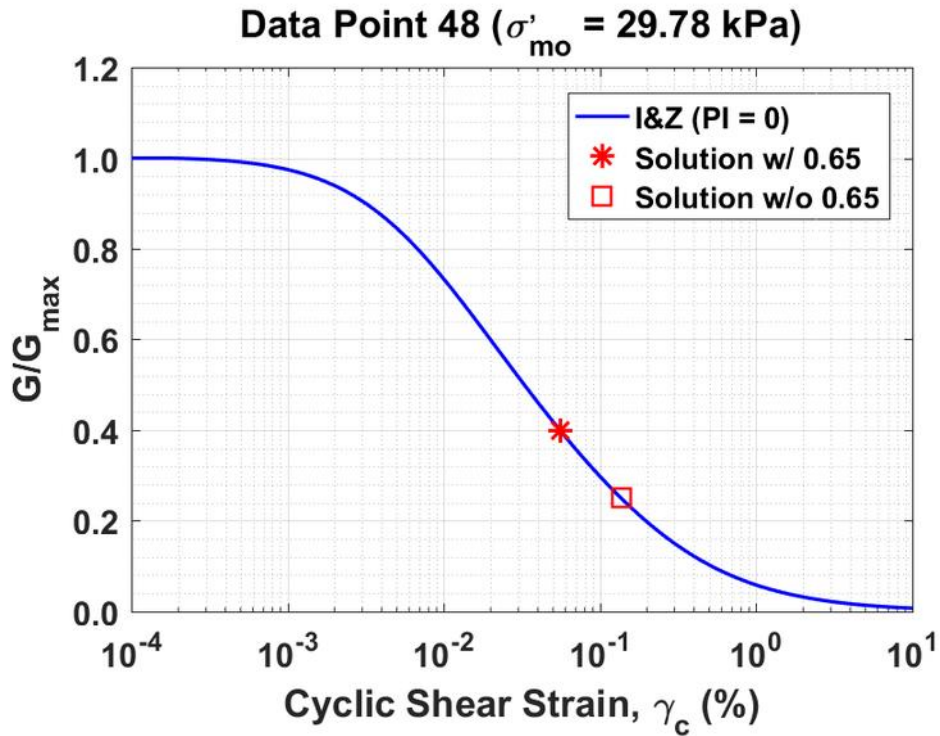


Figure B462. Normalized shear modulus reduction curves for Data Point 48 of the Boulanger et al. database showing the solutions w/ and w/o the 0.65 factor

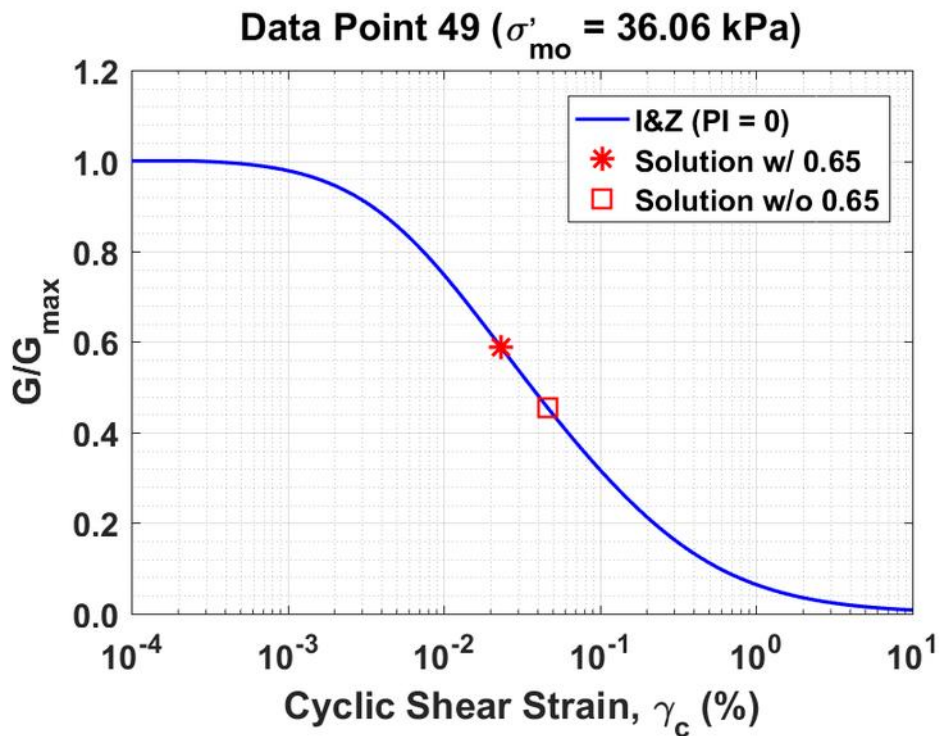


Figure B463. Normalized shear modulus reduction curves for Data Point 49 of the Boulanger et al. database showing the solutions w/ and w/o the 0.65 factor

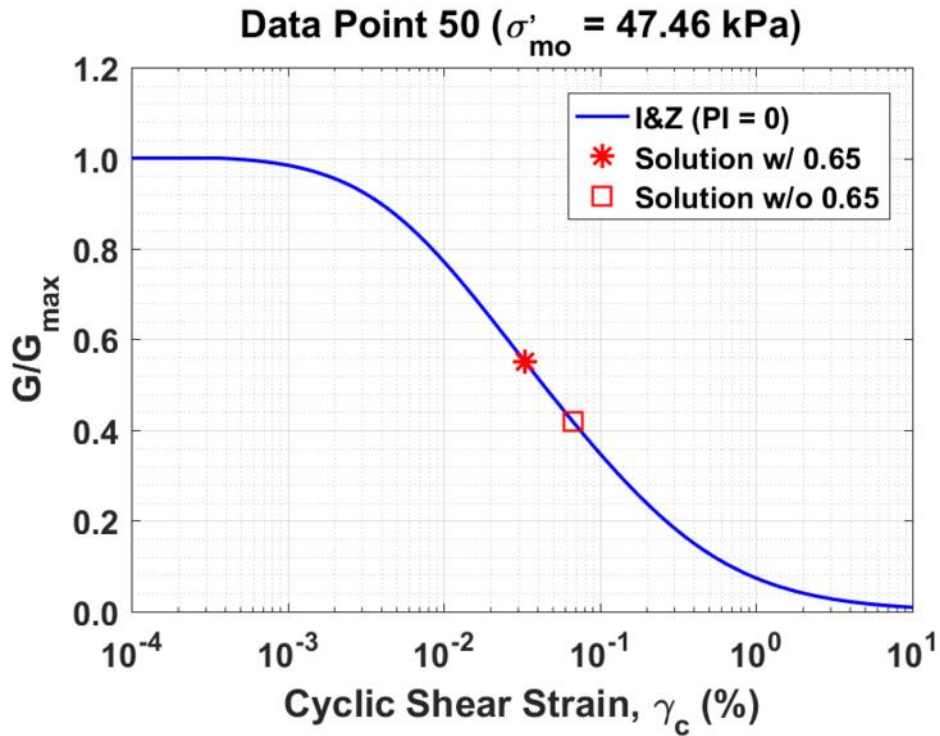


Figure B464. Normalized shear modulus reduction curves for Data Point 50 of the Boulanger et al. database showing the solutions w/ and w/o the 0.65 factor

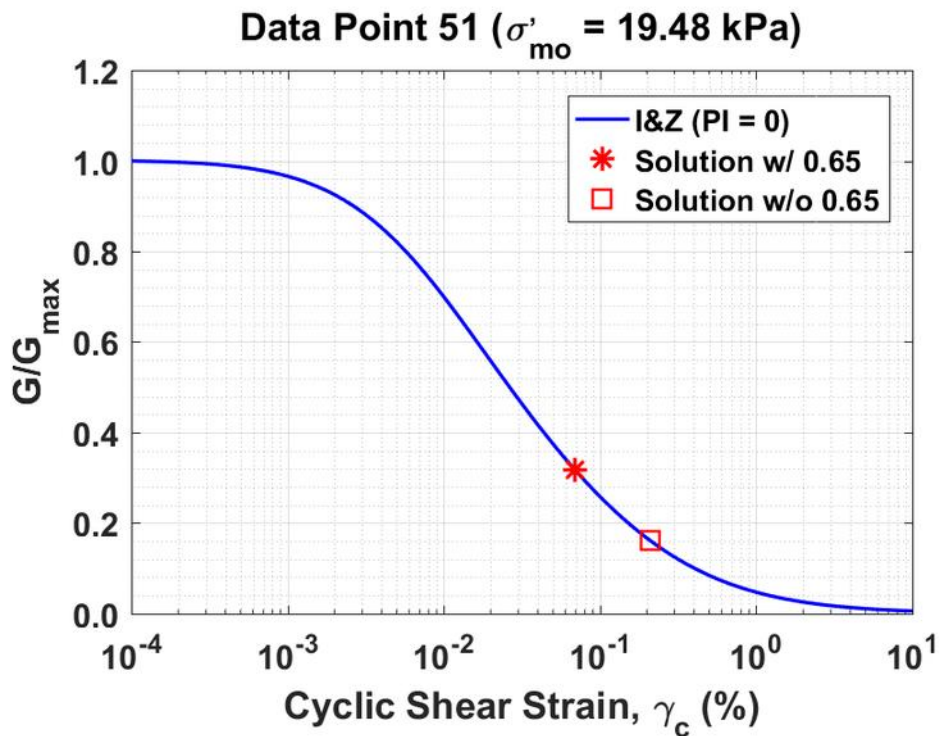


Figure B465. Normalized shear modulus reduction curves for Data Point 51 of the Boulanger et al. database showing the solutions w/ and w/o the 0.65 factor

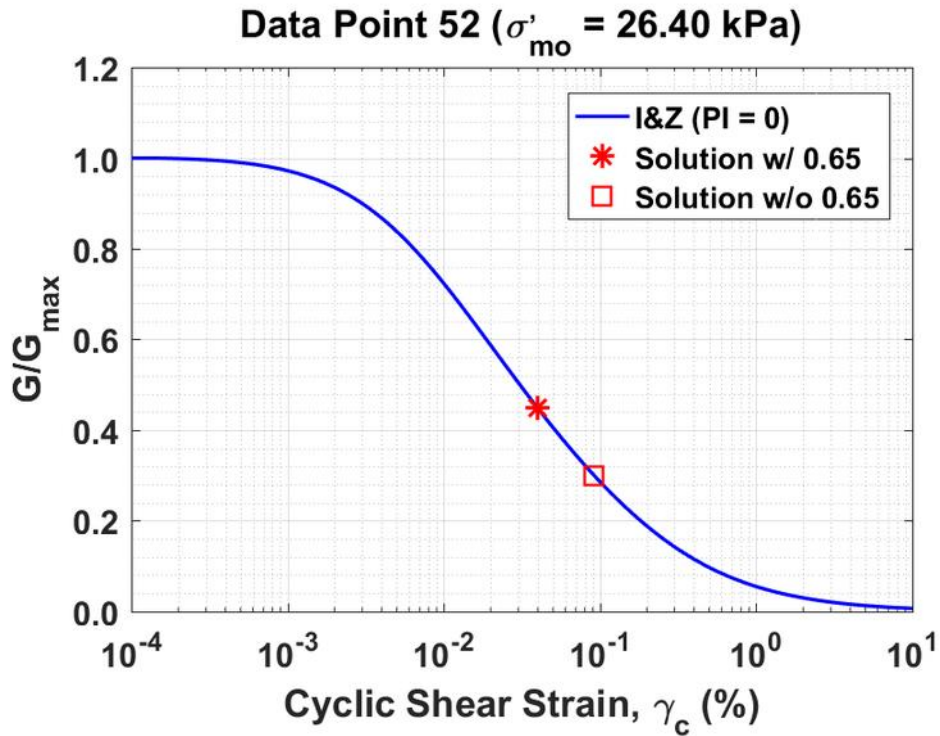


Figure B466. Normalized shear modulus reduction curves for Data Point 52 of the Boulanger et al. database showing the solutions w/ and w/o the 0.65 factor

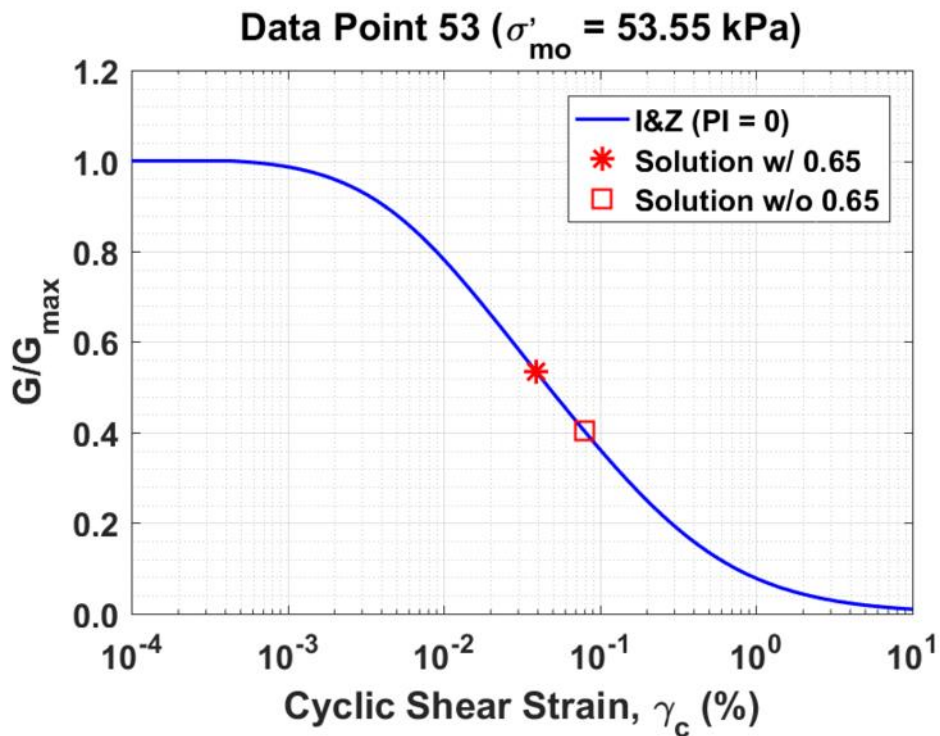


Figure B467. Normalized shear modulus reduction curves for Data Point 53 of the Boulanger et al. database showing the solutions w/ and w/o the 0.65 factor

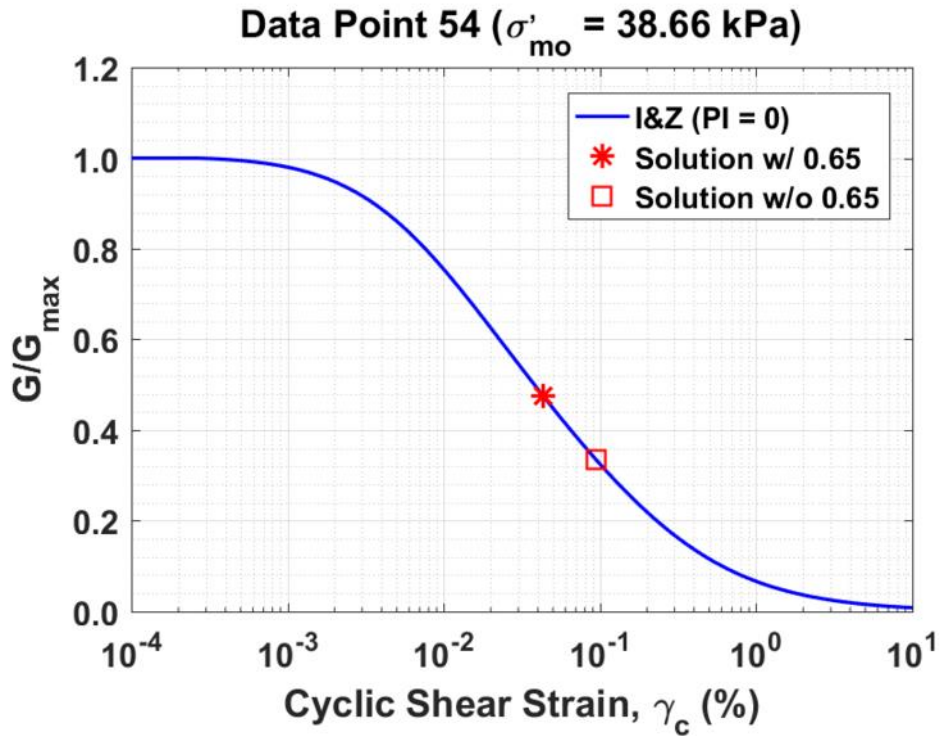


Figure B468. Normalized shear modulus reduction curves for Data Point 54 of the Boulanger et al. database showing the solutions w/ and w/o the 0.65 factor

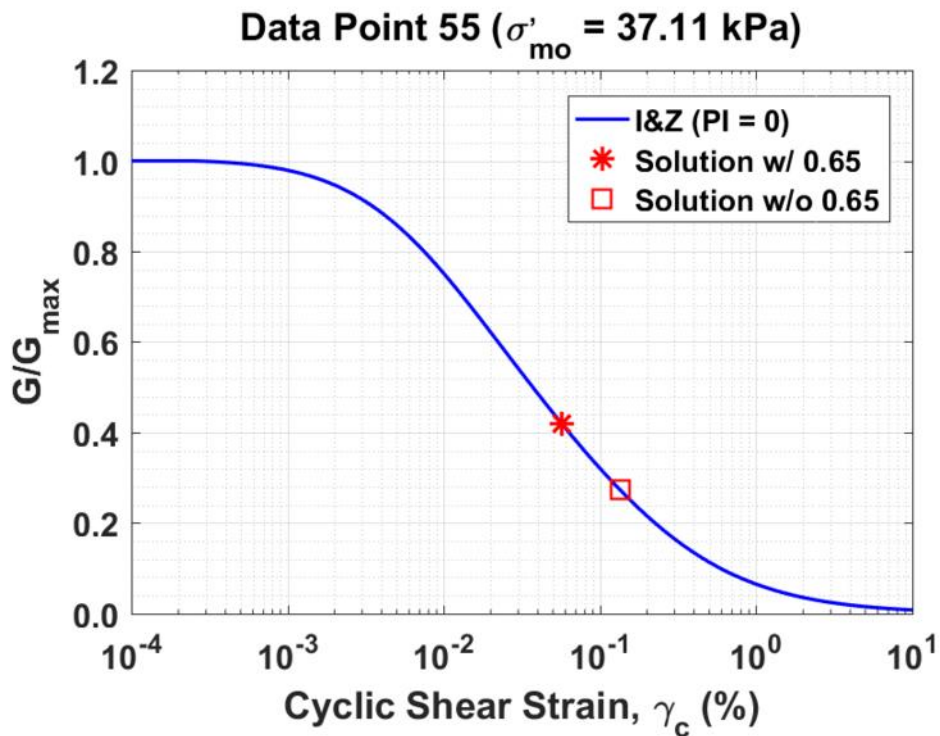


Figure B469. Normalized shear modulus reduction curves for Data Point 55 of the Boulanger et al. database showing the solutions w/ and w/o the 0.65 factor

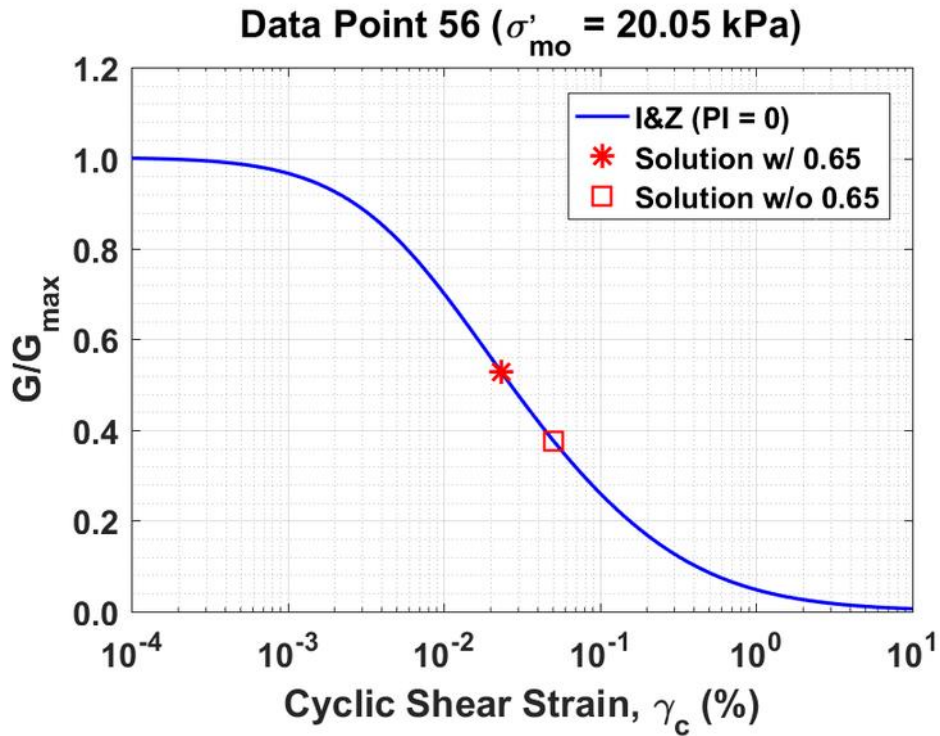


Figure B470. Normalized shear modulus reduction curves for Data Point 56 of the Boulanger et al. database showing the solutions w/ and w/o the 0.65 factor

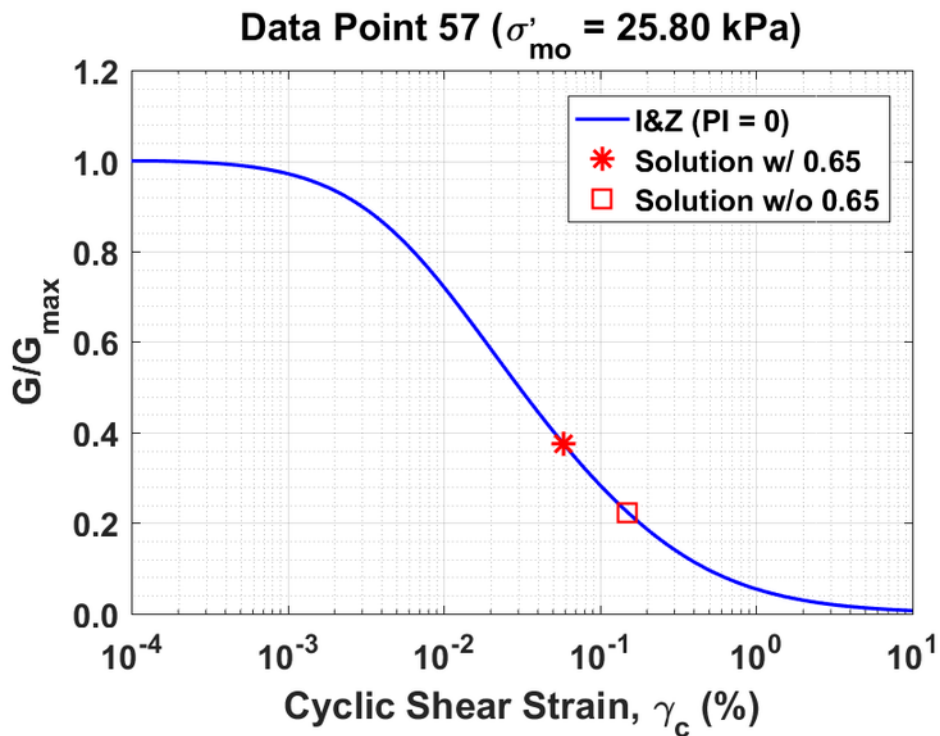


Figure B471. Normalized shear modulus reduction curves for Data Point 57 of the Boulanger et al. database showing the solutions w/ and w/o the 0.65 factor

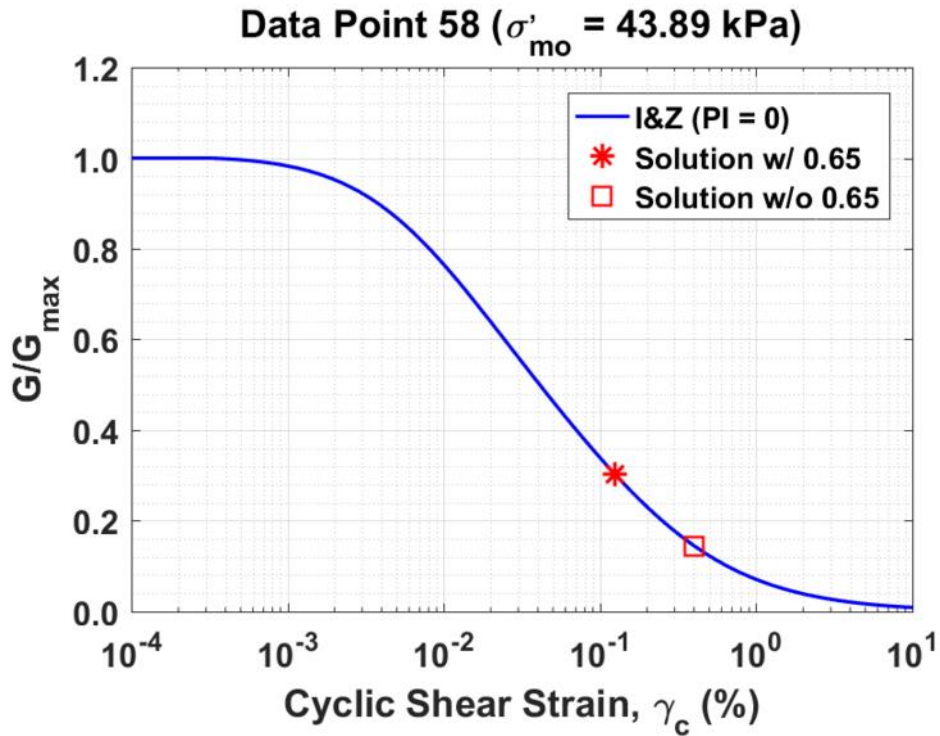


Figure B472. Normalized shear modulus reduction curves for Data Point 58 of the Boulanger et al. database showing the solutions w/ and w/o the 0.65 factor

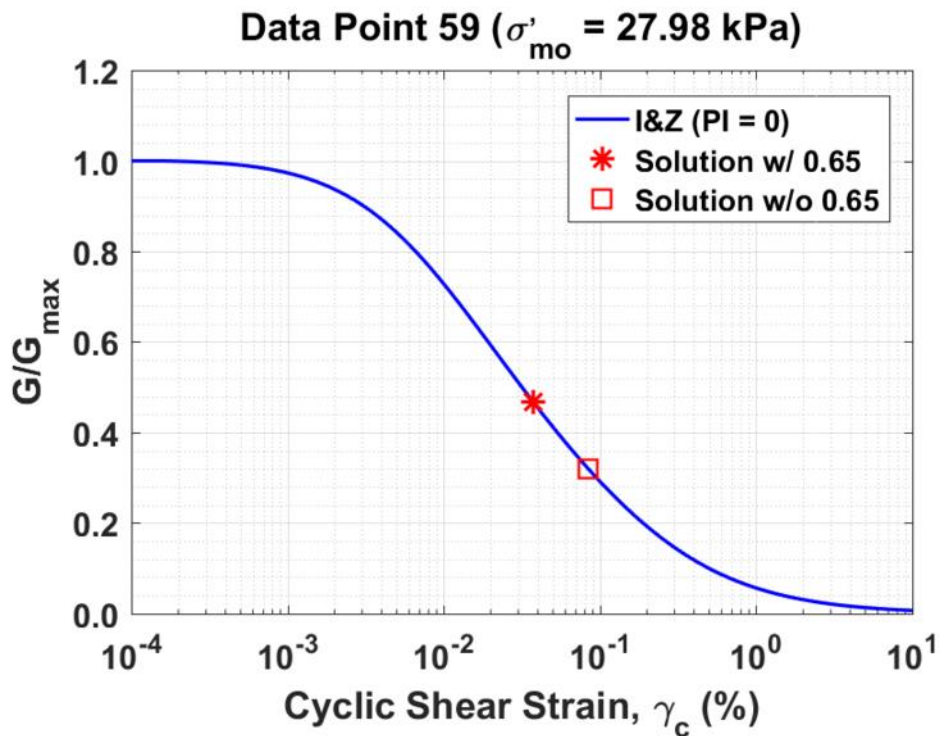


Figure B473. Normalized shear modulus reduction curves for Data Point 59 of the Boulanger et al. database showing the solutions w/ and w/o the 0.65 factor

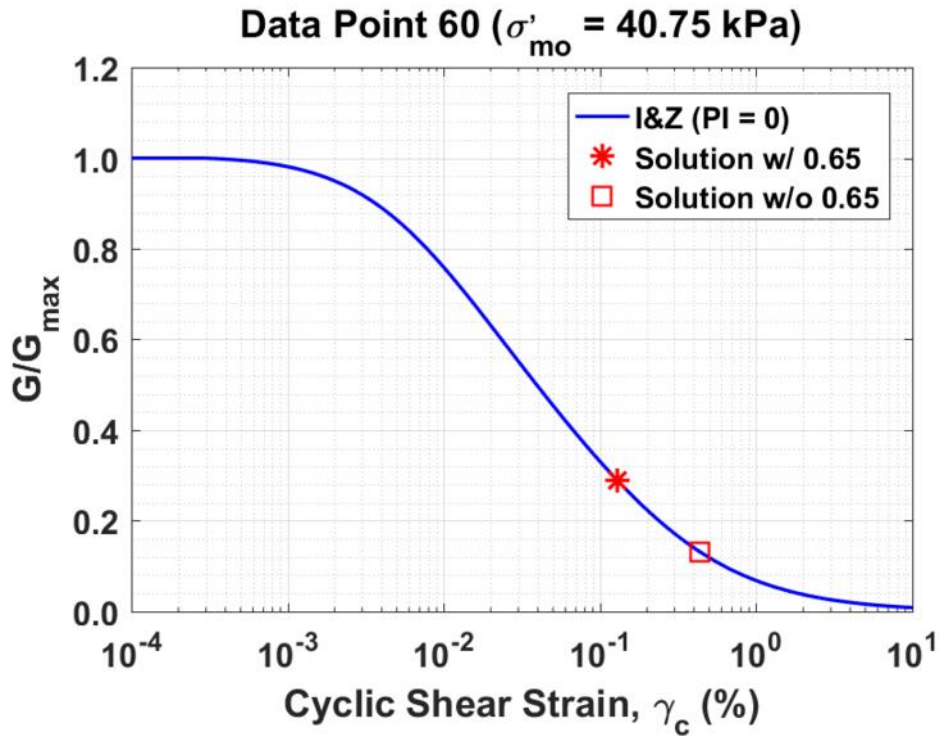


Figure B474. Normalized shear modulus reduction curves for Data Point 60 of the Boulanger et al. database showing the solutions w/ and w/o the 0.65 factor

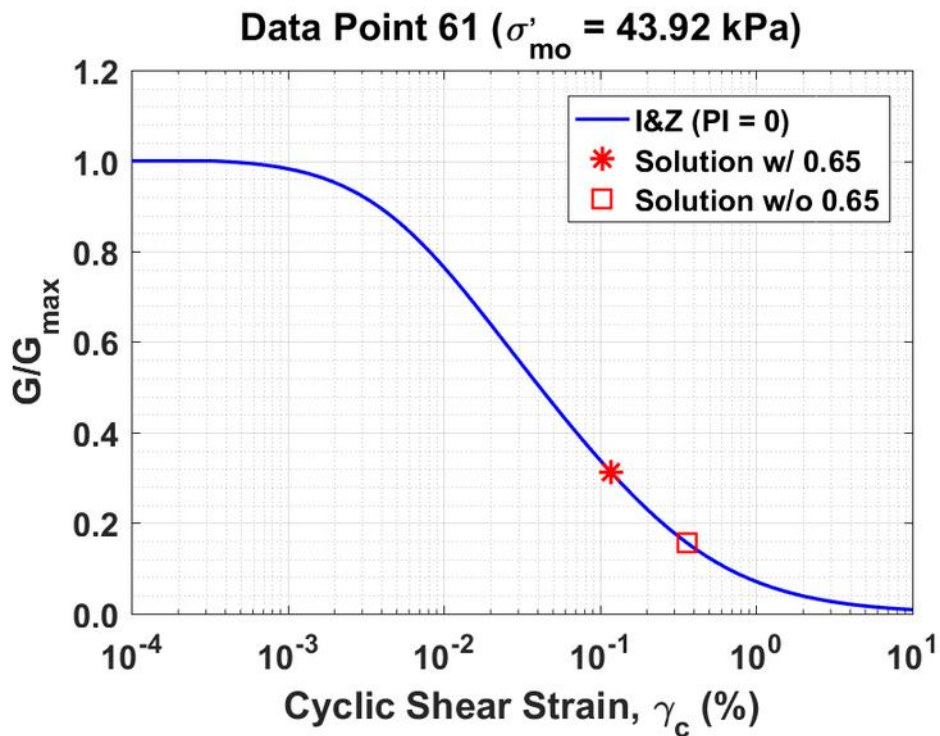


Figure B475. Normalized shear modulus reduction curves for Data Point 61 of the Boulanger et al. database showing the solutions w/ and w/o the 0.65 factor

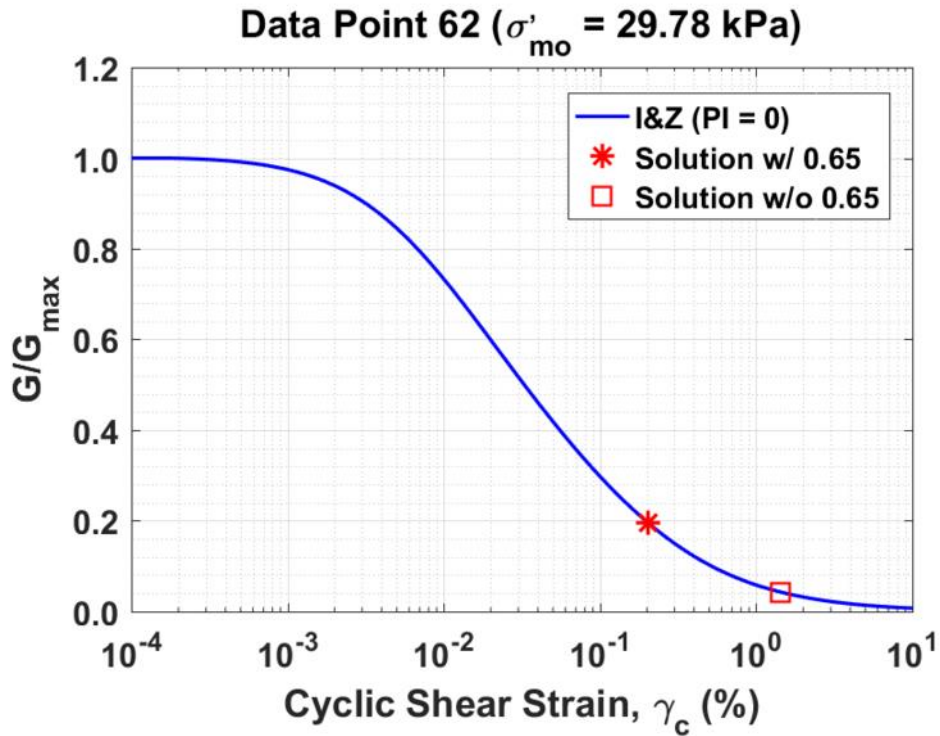


Figure B476. Normalized shear modulus reduction curves for Data Point 62 of the Boulanger et al. database showing the solutions w/ and w/o the 0.65 factor

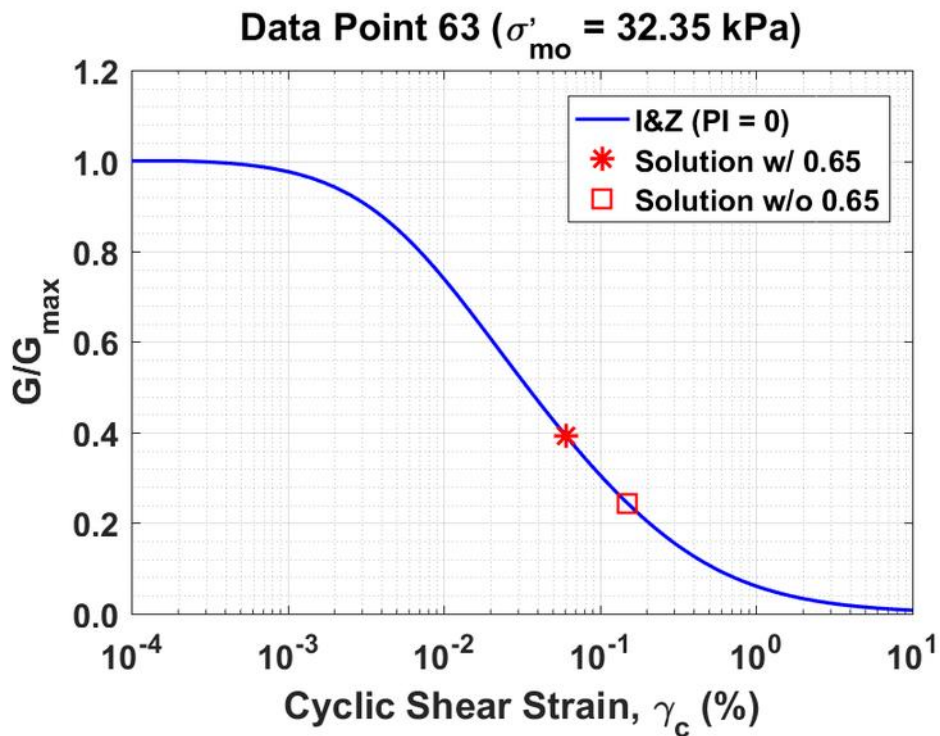


Figure B477. Normalized shear modulus reduction curves for Data Point 63 of the Boulanger et al. database showing the solutions w/ and w/o the 0.65 factor

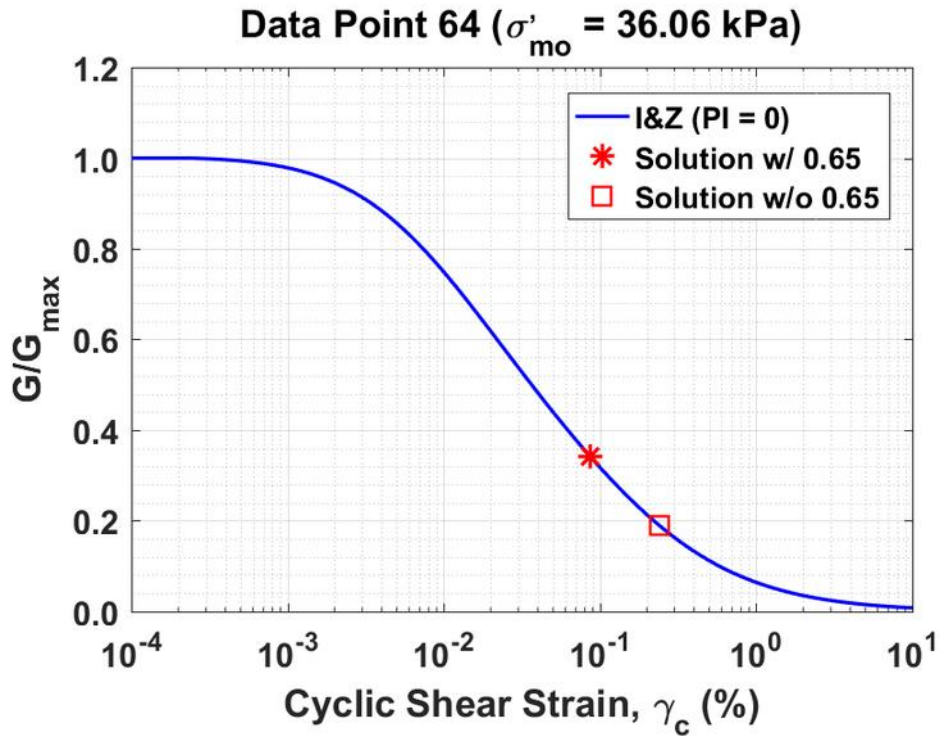


Figure B478. Normalized shear modulus reduction curves for Data Point 64 of the Boulanger et al. database showing the solutions w/ and w/o the 0.65 factor

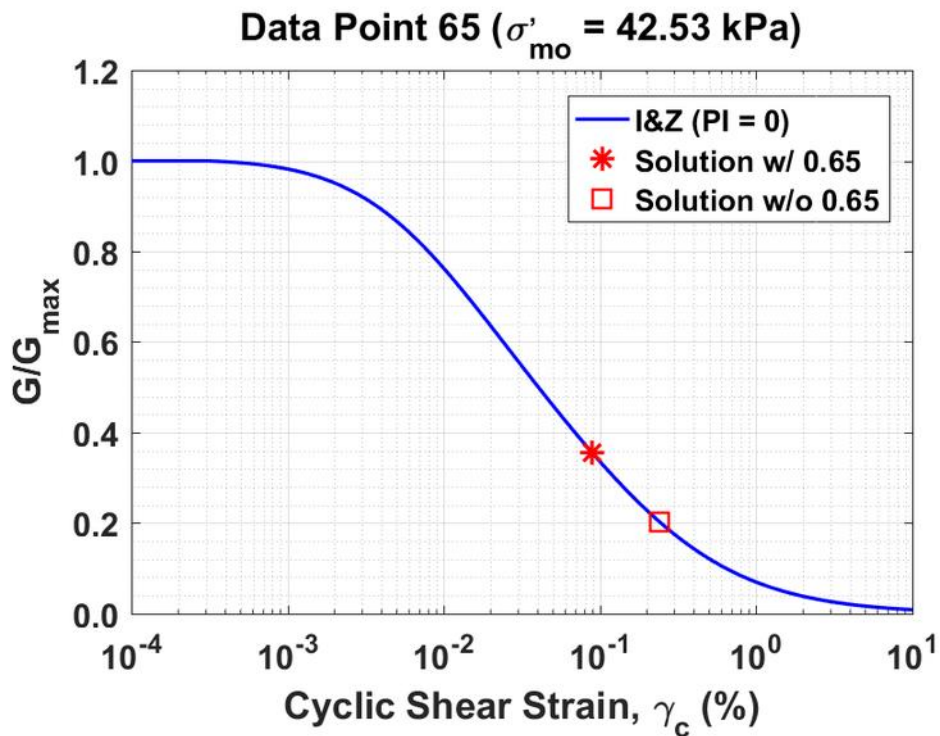


Figure B479. Normalized shear modulus reduction curves for Data Point 65 of the Boulanger et al. database showing the solutions w/ and w/o the 0.65 factor

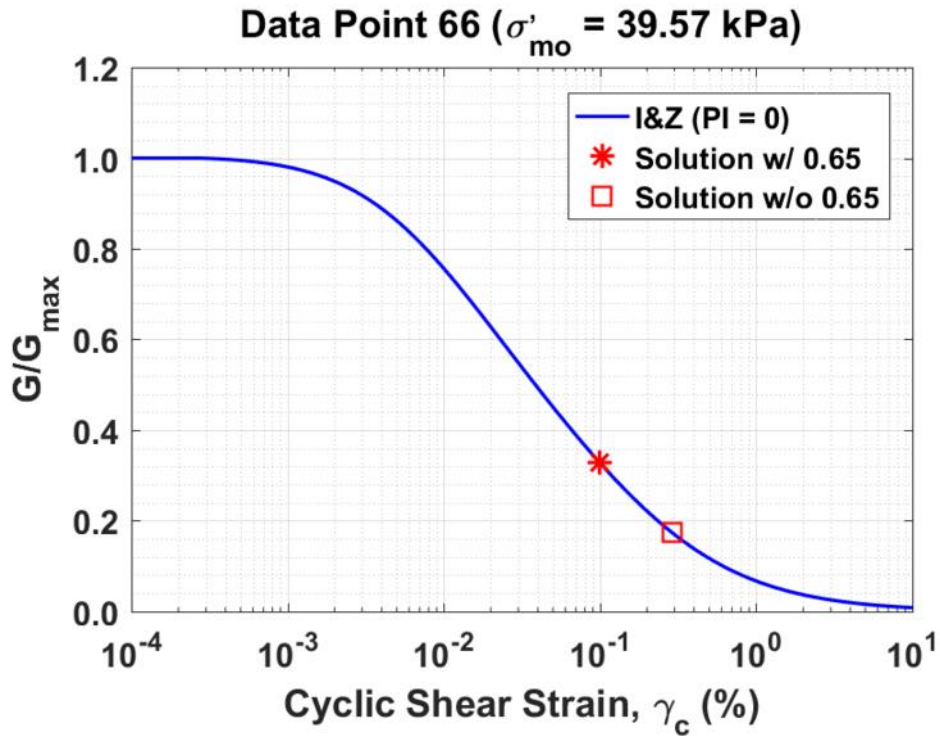


Figure B480. Normalized shear modulus reduction curves for Data Point 66 of the Boulanger et al. database showing the solutions w/ and w/o the 0.65 factor

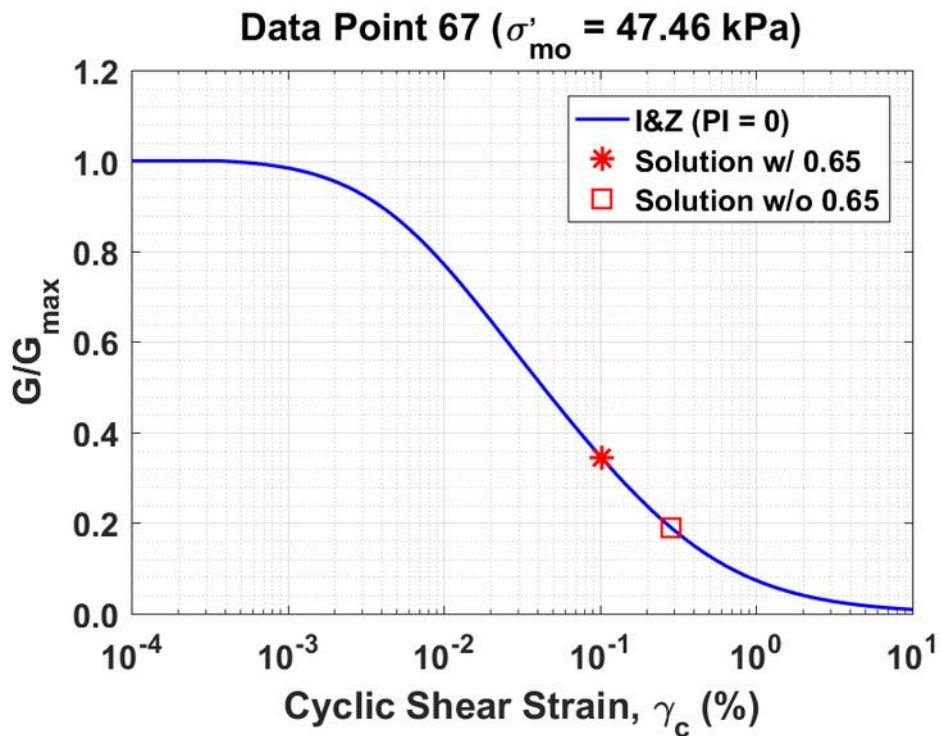


Figure B481. Normalized shear modulus reduction curves for Data Point 67 of the Boulanger et al. database showing the solutions w/ and w/o the 0.65 factor

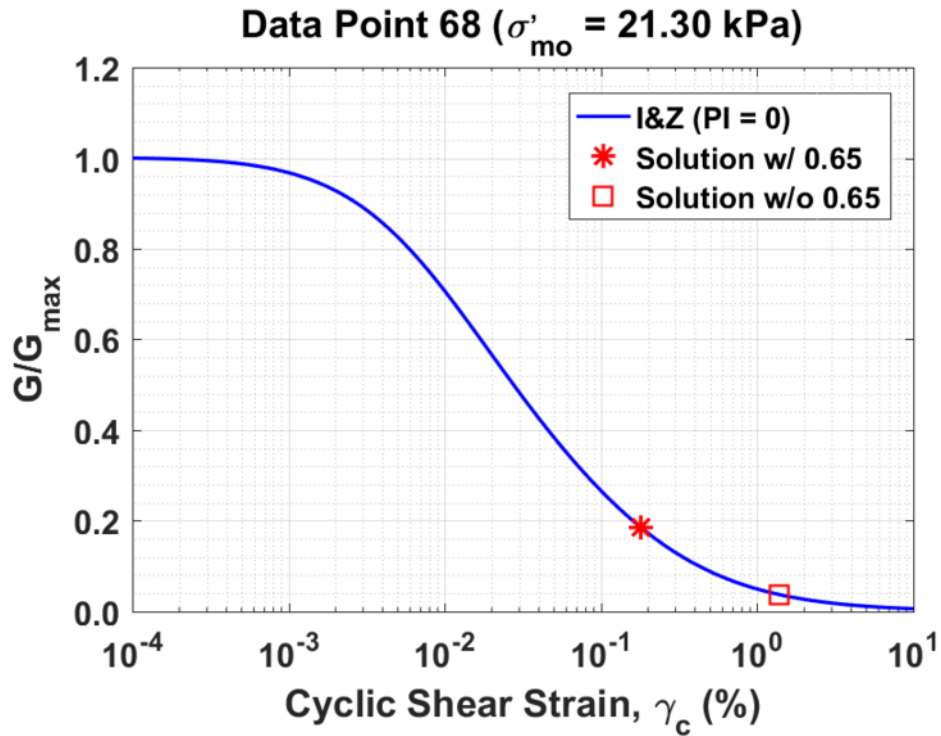


Figure B482. Normalized shear modulus reduction curves for Data Point 68 of the Boulanger et al. database showing the solutions w/ and w/o the 0.65 factor

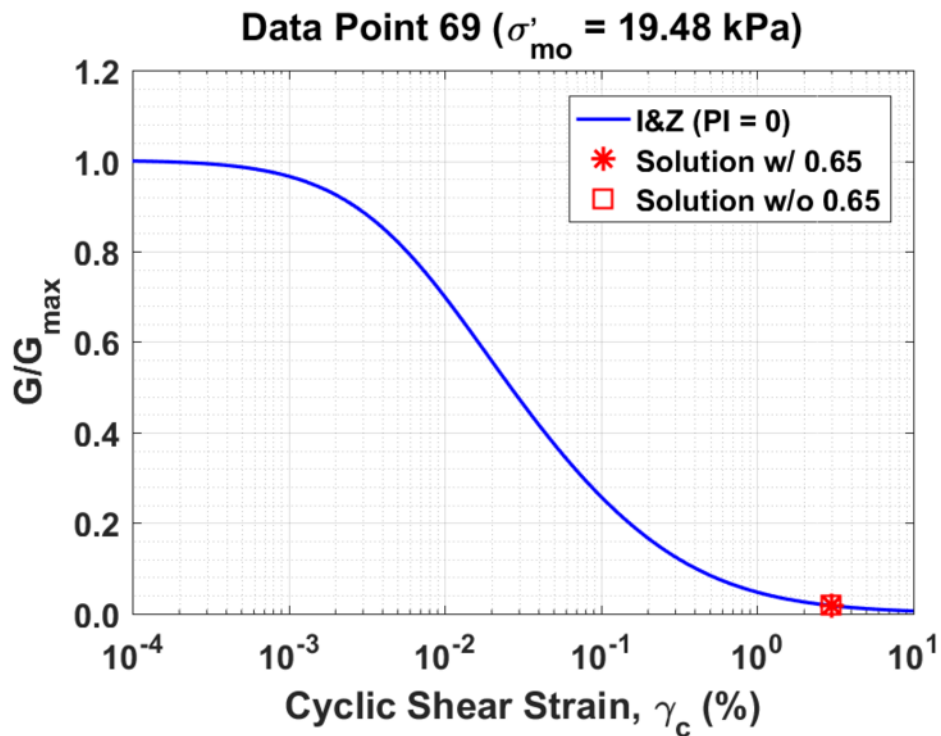


Figure B483. Normalized shear modulus reduction curves for Data Point 69 of the Boulanger et al. database showing the solutions w/ and w/o the 0.65 factor

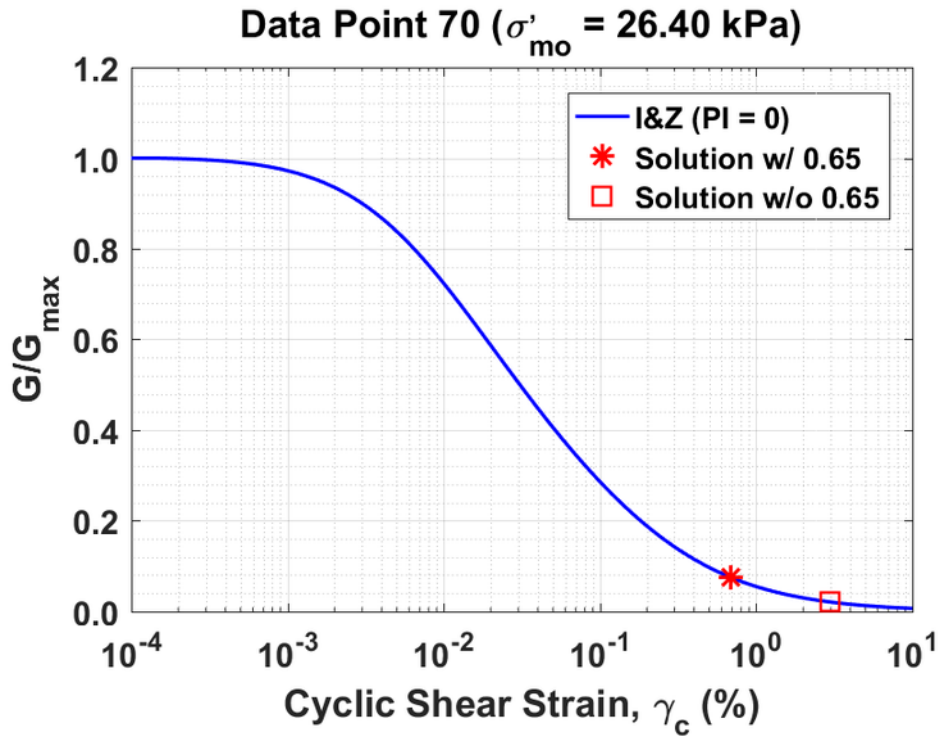


Figure B484. Normalized shear modulus reduction curves for Data Point 70 of the Boulanger et al. database showing the solutions w/ and w/o the 0.65 factor

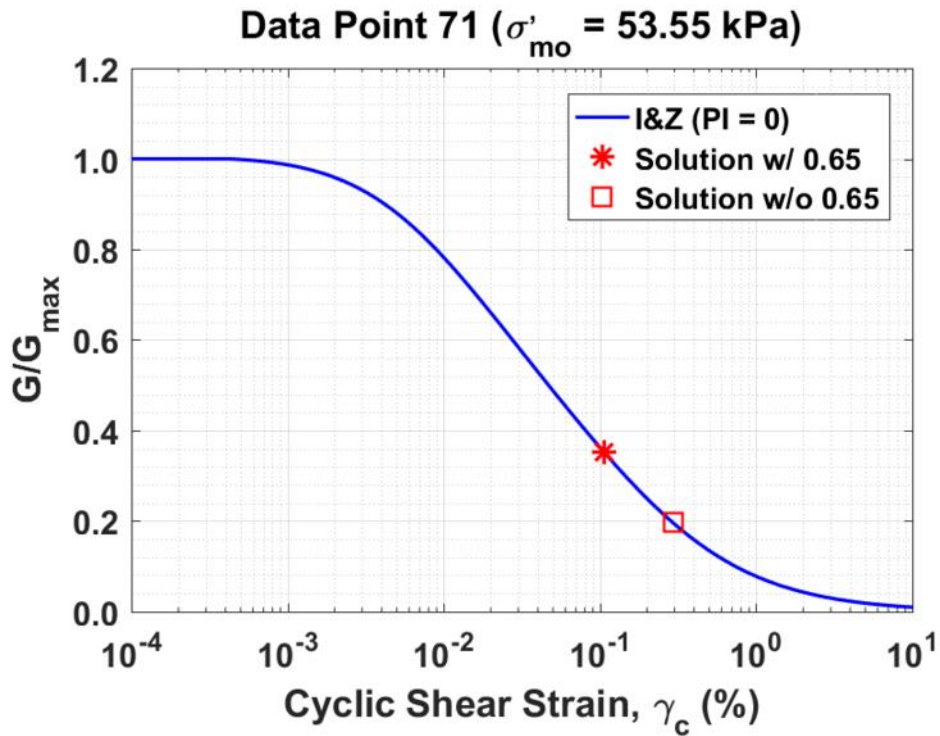


Figure B485. Normalized shear modulus reduction curves for Data Point 71 of the Boulanger et al. database showing the solutions w/ and w/o the 0.65 factor

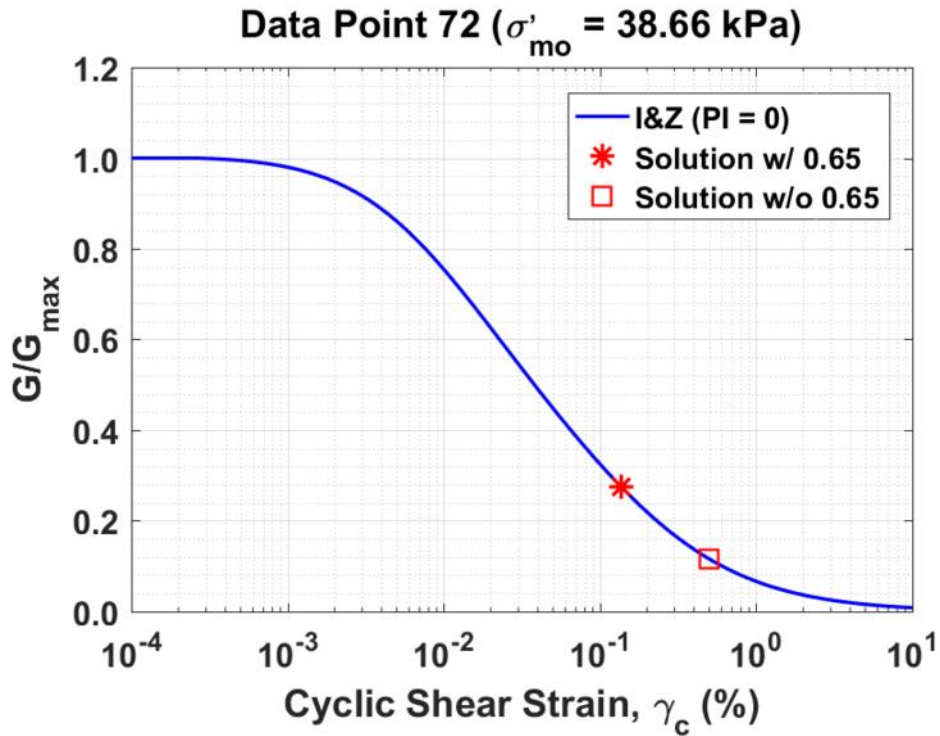


Figure B486. Normalized shear modulus reduction curves for Data Point 72 of the Boulanger et al. database showing the solutions w/ and w/o the 0.65 factor

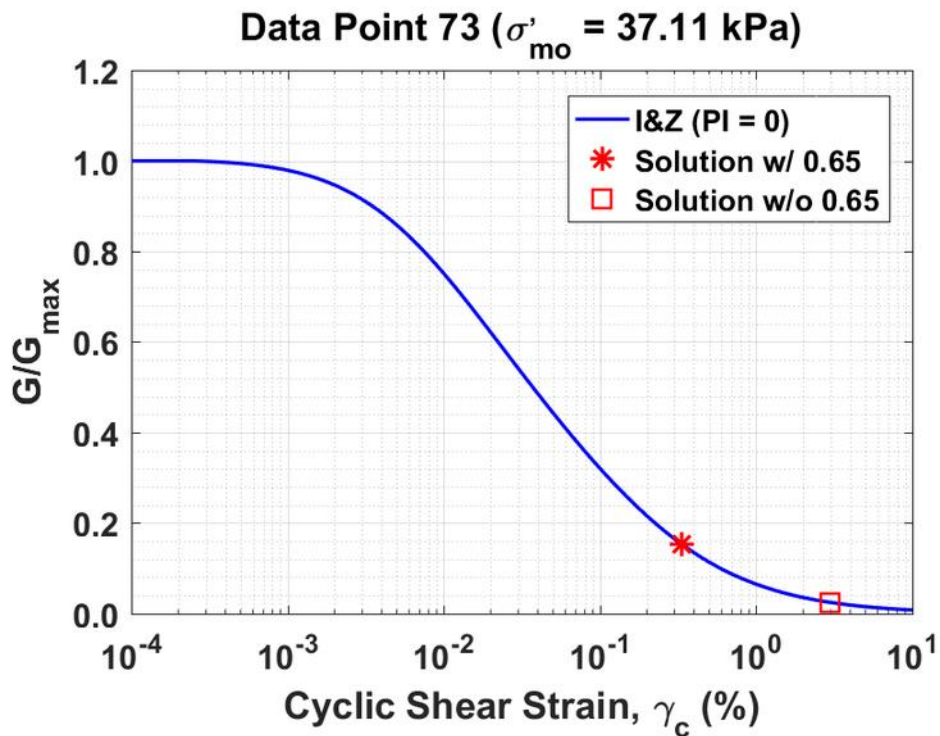


Figure B487. Normalized shear modulus reduction curves for Data Point 73 of the Boulanger et al. database showing the solutions w/ and w/o the 0.65 factor

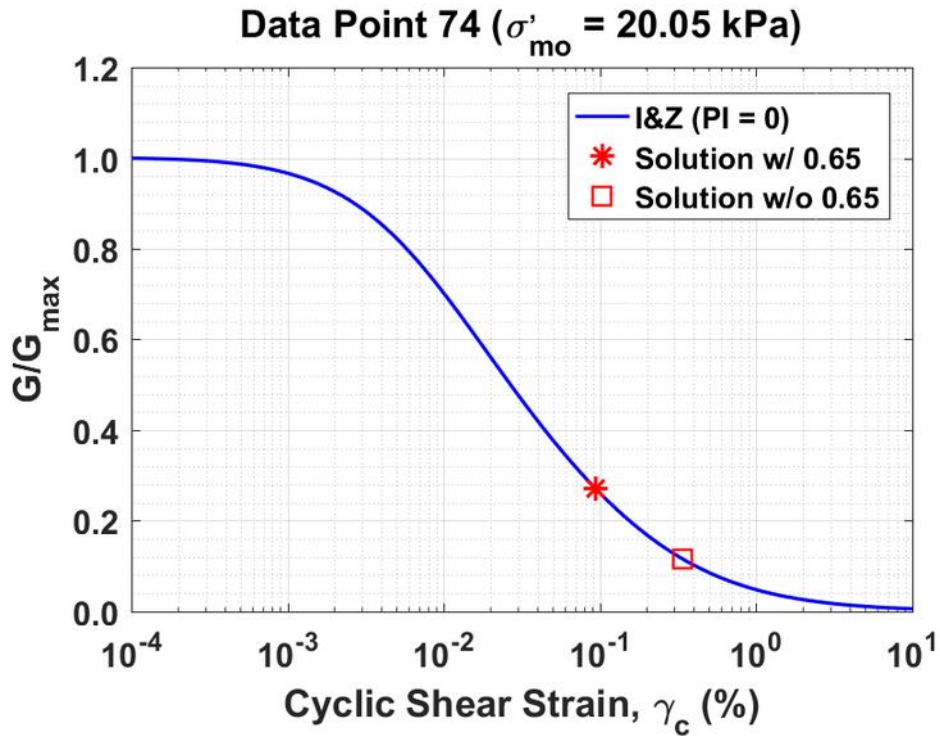


Figure B488. Normalized shear modulus reduction curves for Data Point 74 of the Boulanger et al. database showing the solutions w/ and w/o the 0.65 factor

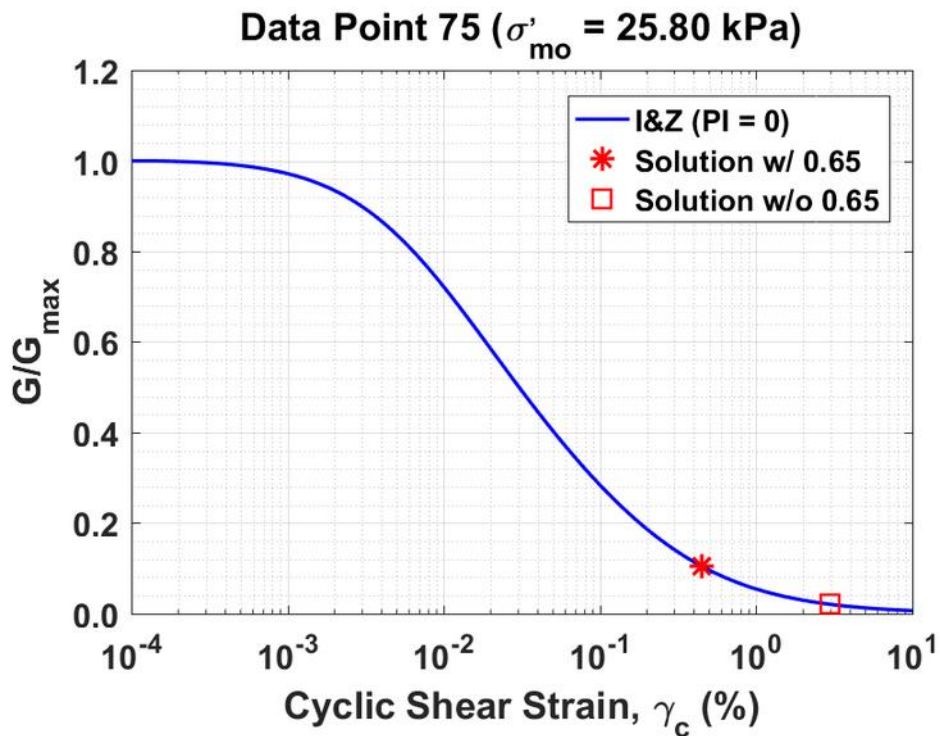


Figure B489. Normalized shear modulus reduction curves for Data Point 75 of the Boulanger et al. database showing the solutions w/ and w/o the 0.65 factor

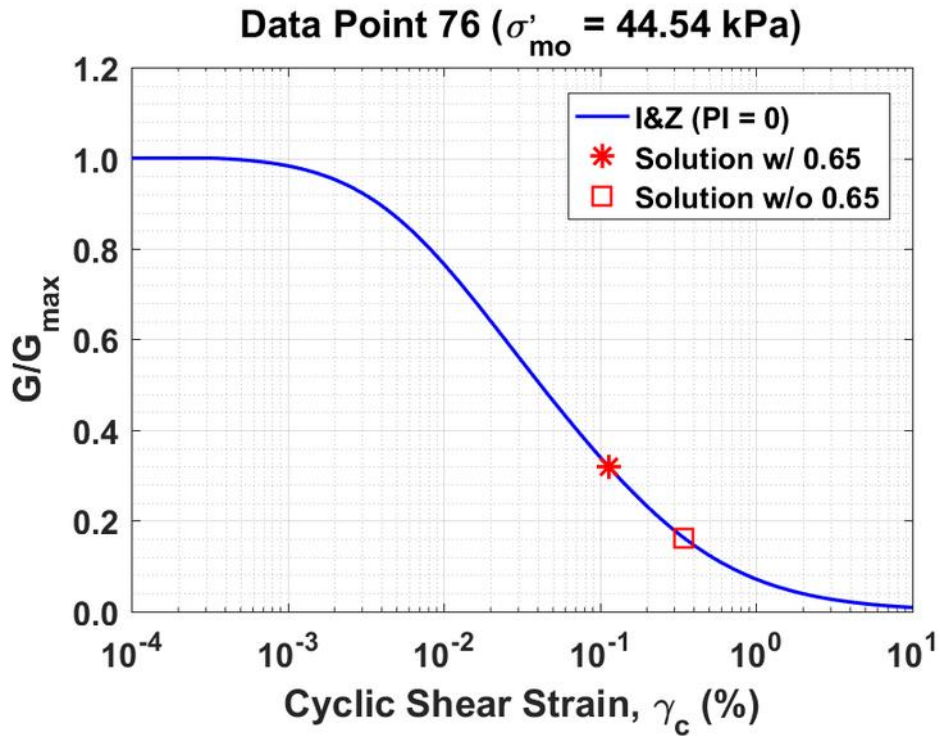


Figure B490. Normalized shear modulus reduction curves for Data Point 76 of the Boulanger et al. database showing the solutions w/ and w/o the 0.65 factor

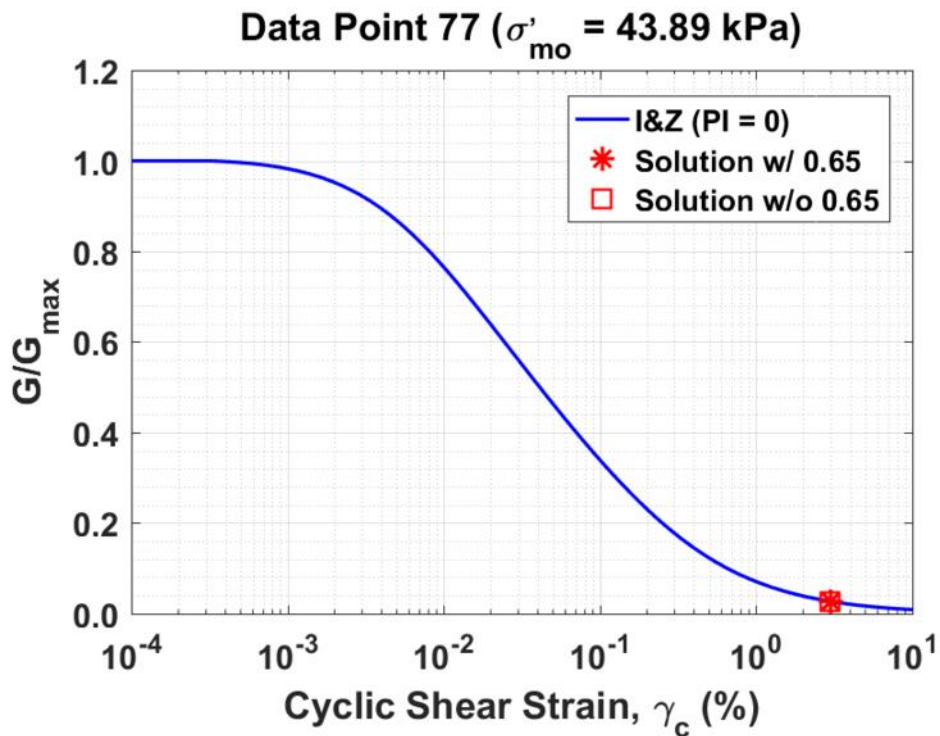


Figure B491. Normalized shear modulus reduction curves for Data Point 77 of the Boulanger et al. database showing the solutions w/ and w/o the 0.65 factor

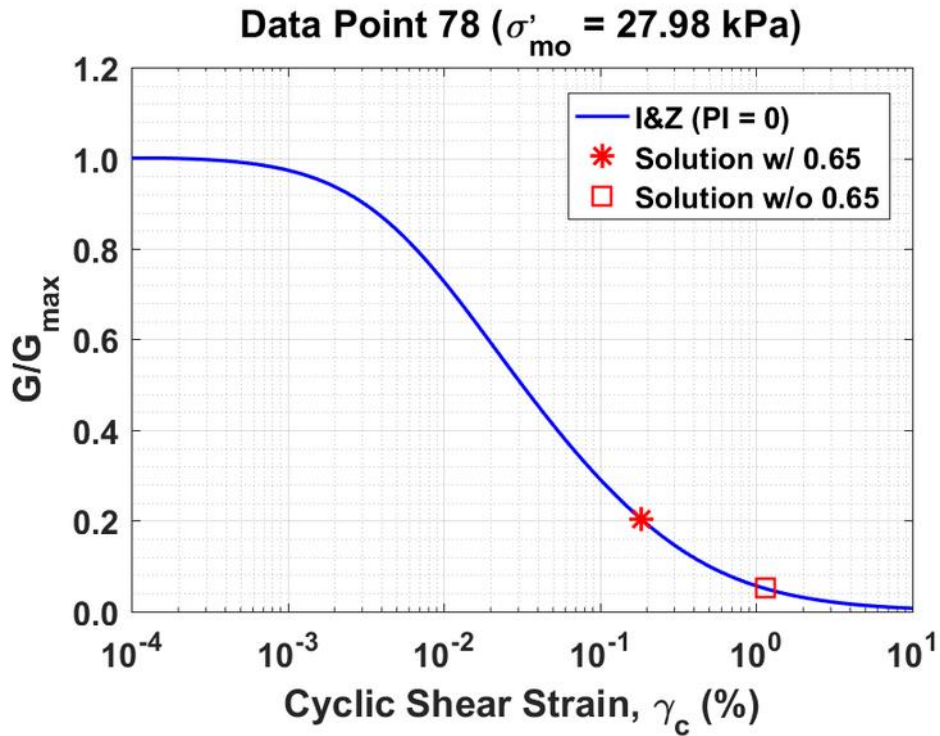


Figure B492. Normalized shear modulus reduction curves for Data Point 78 of the Boulanger et al. database showing the solutions w/ and w/o the 0.65 factor

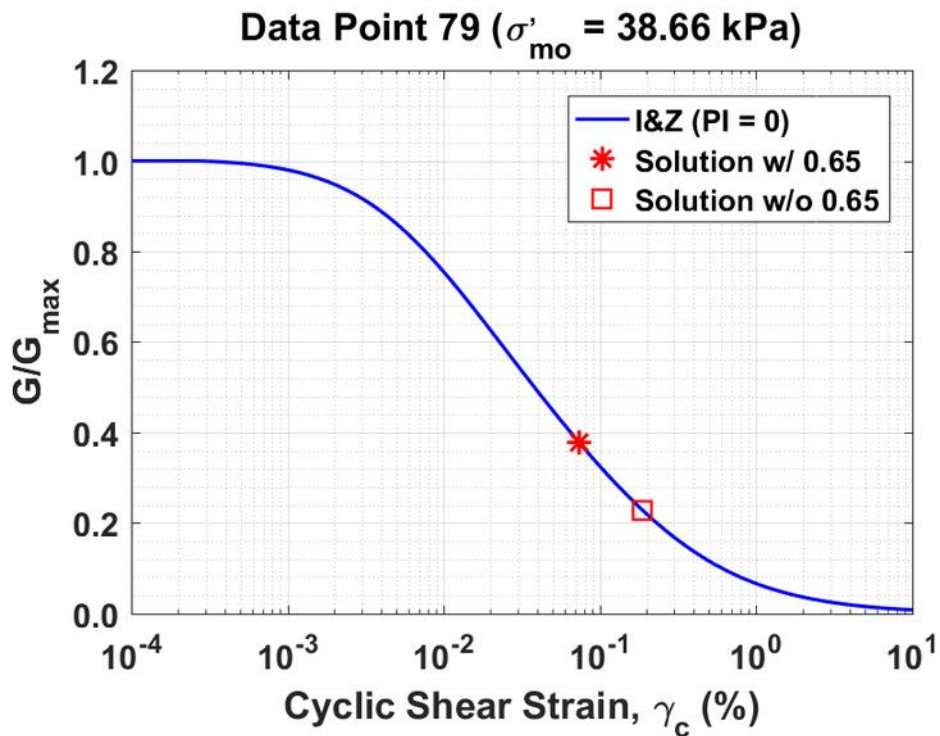


Figure B493. Normalized shear modulus reduction curves for Data Point 79 of the Boulanger et al. database showing the solutions w/ and w/o the 0.65 factor

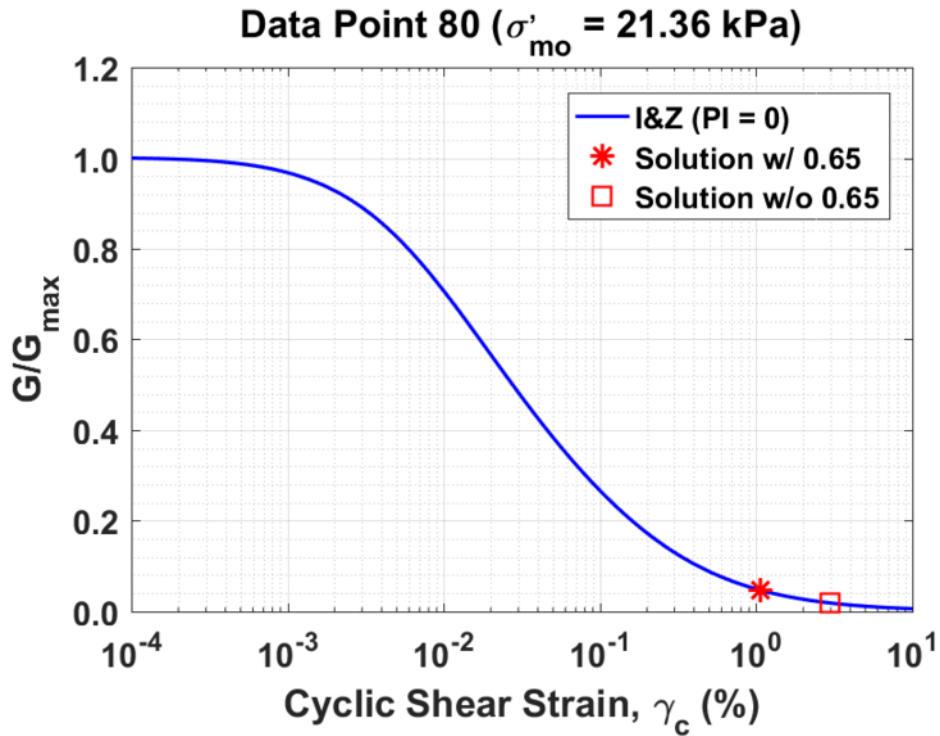


Figure B494. Normalized shear modulus reduction curves for Data Point 80 of the Boulanger et al. database showing the solutions w/ and w/o the 0.65 factor

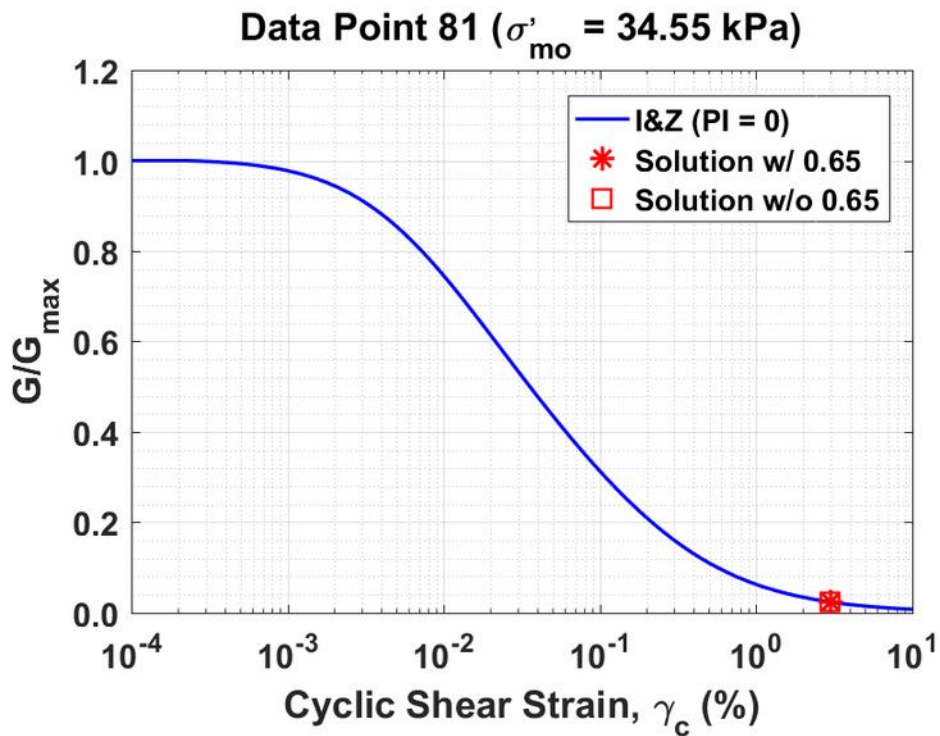


Figure B495. Normalized shear modulus reduction curves for Data Point 81 of the Boulanger et al. database showing the solutions w/ and w/o the 0.65 factor

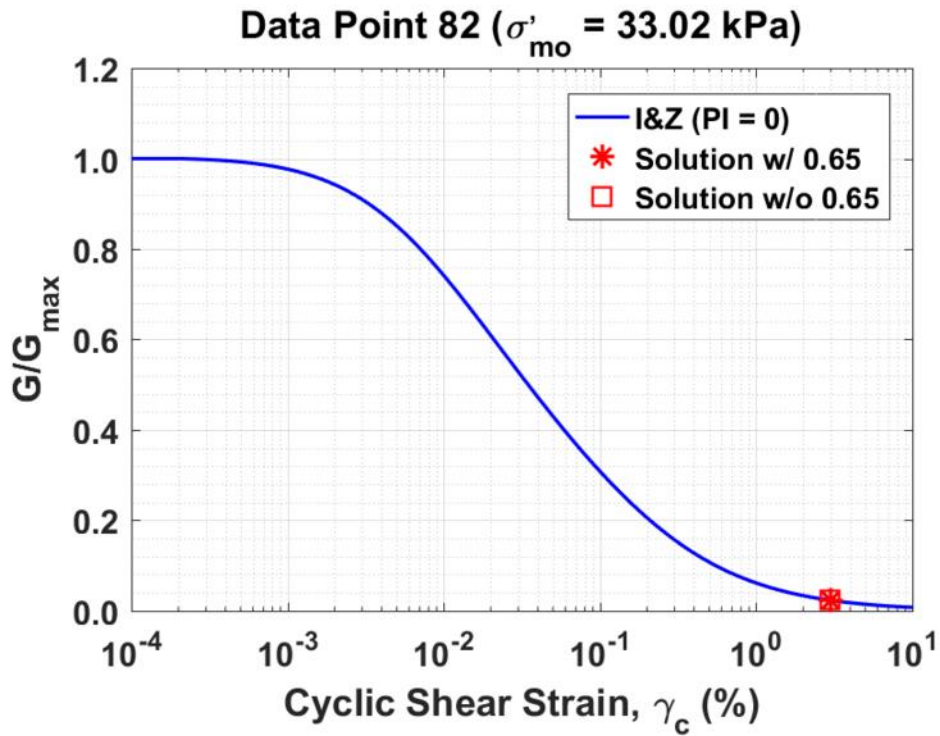


Figure B496. Normalized shear modulus reduction curves for Data Point 82 of the Boulanger et al. database showing the solutions w/ and w/o the 0.65 factor

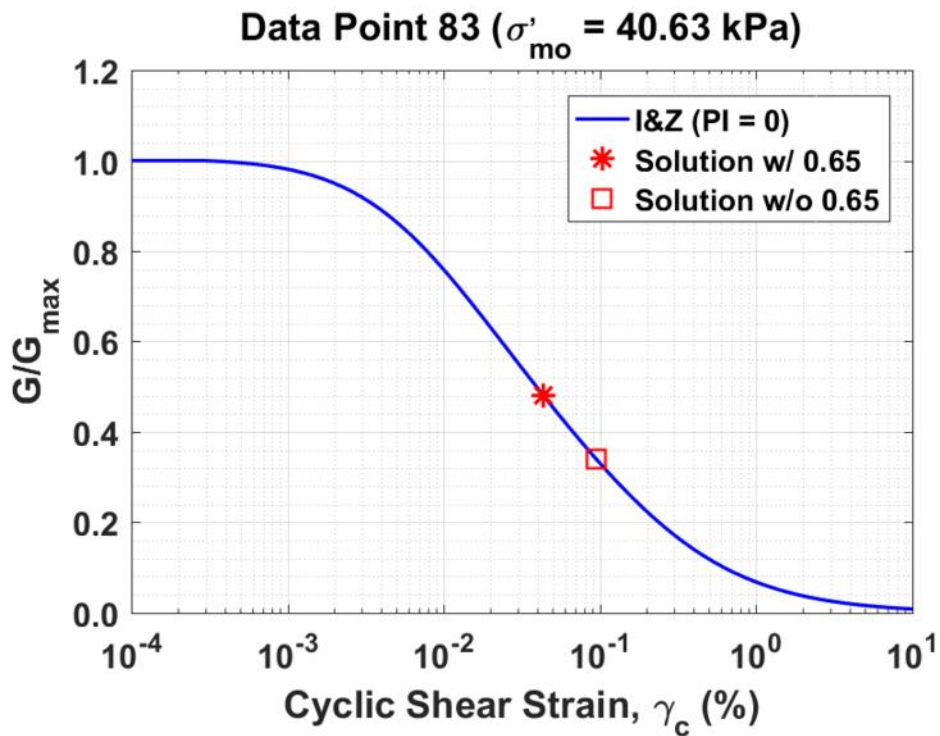


Figure B497. Normalized shear modulus reduction curves for Data Point 83 of the Boulanger et al. database showing the solutions w/ and w/o the 0.65 factor

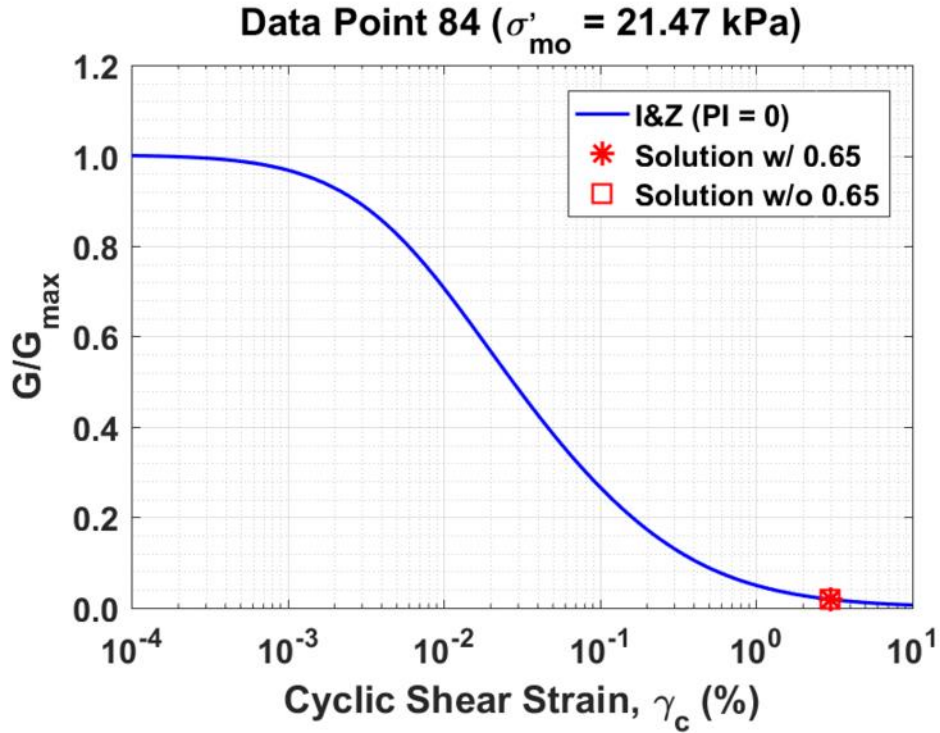


Figure B498. Normalized shear modulus reduction curves for Data Point 84 of the Boulanger et al. database showing the solutions w/ and w/o the 0.65 factor

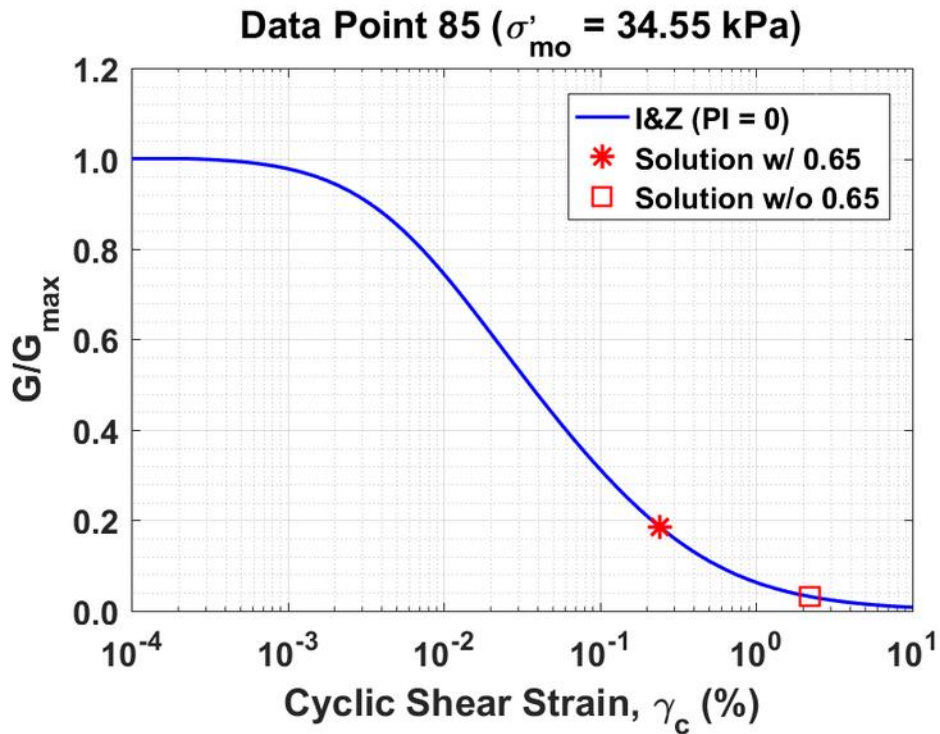


Figure B499. Normalized shear modulus reduction curves for Data Point 85 of the Boulanger et al. database showing the solutions w/ and w/o the 0.65 factor

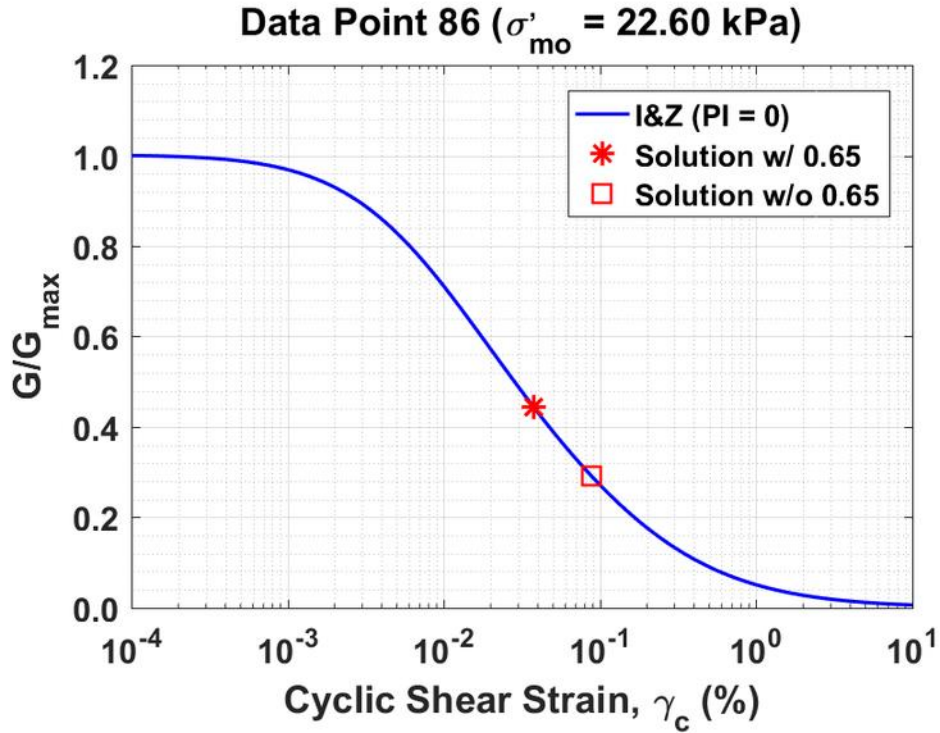


Figure B500. Normalized shear modulus reduction curves for Data Point 86 of the Boulanger et al. database showing the solutions w/ and w/o the 0.65 factor

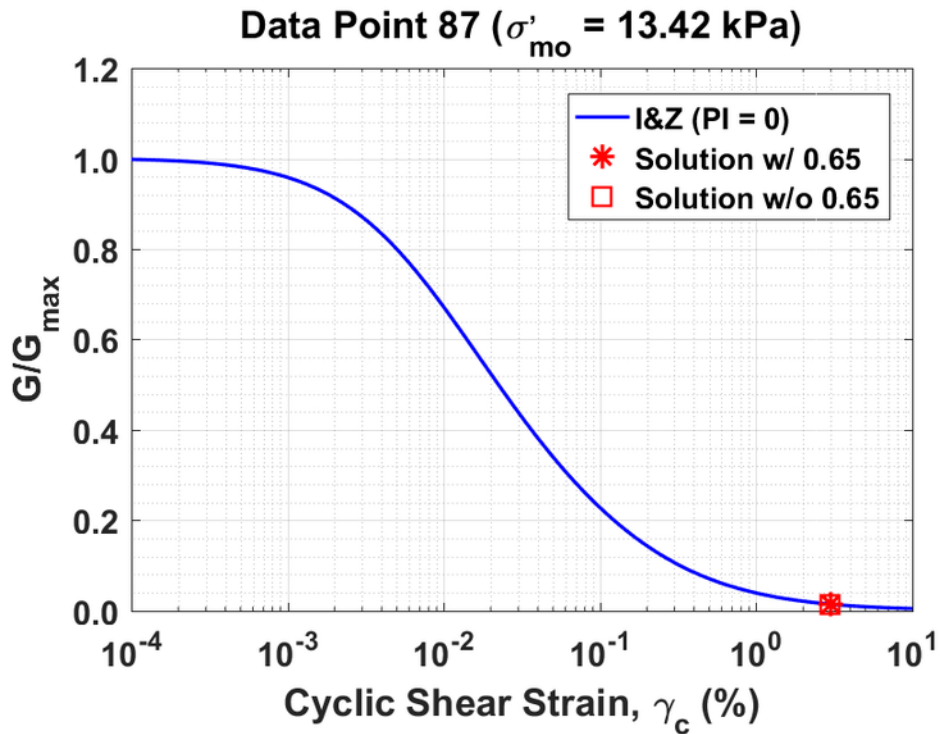


Figure B501. Normalized shear modulus reduction curves for Data Point 87 of the Boulanger et al. database showing the solutions w/ and w/o the 0.65 factor

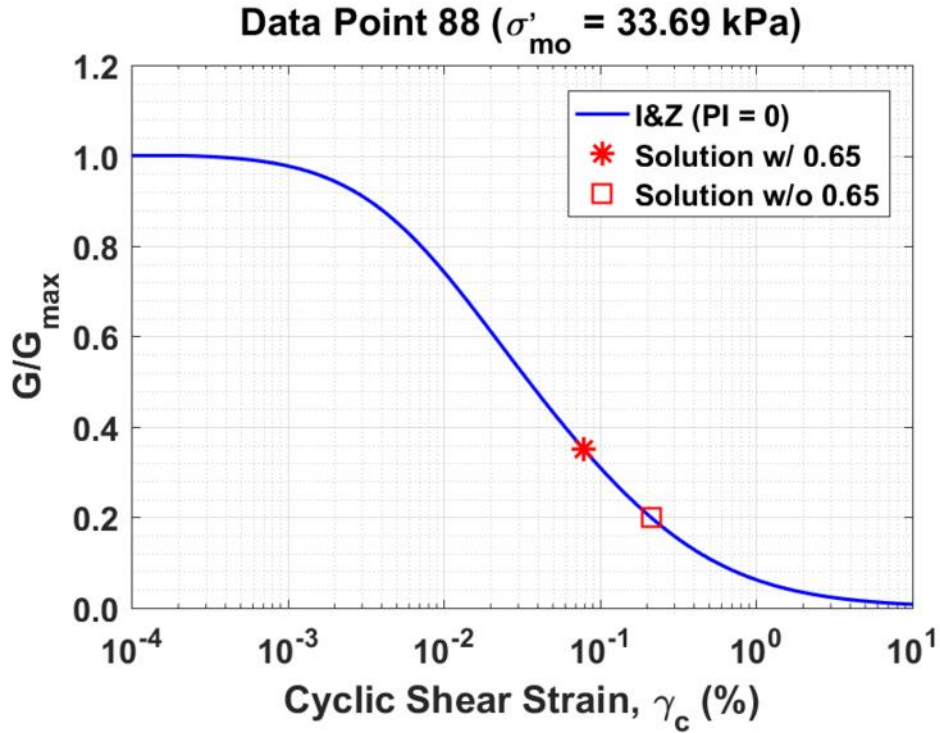


Figure B502. Normalized shear modulus reduction curves for Data Point 88 of the Boulanger et al. database showing the solutions w/ and w/o the 0.65 factor

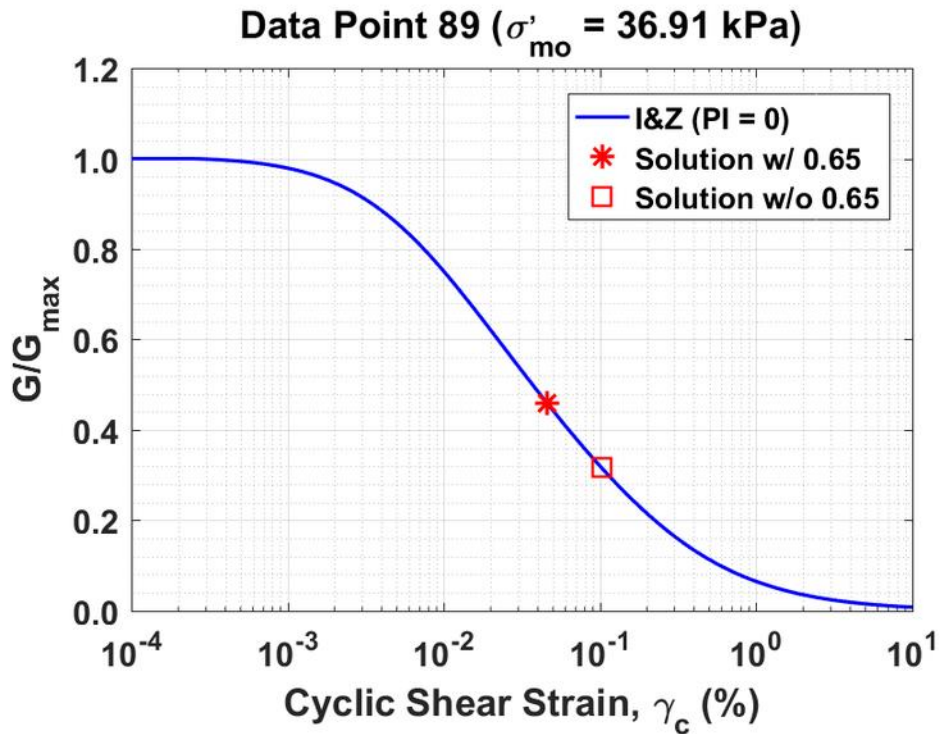


Figure B503. Normalized shear modulus reduction curves for Data Point 89 of the Boulanger et al. database showing the solutions w/ and w/o the 0.65 factor

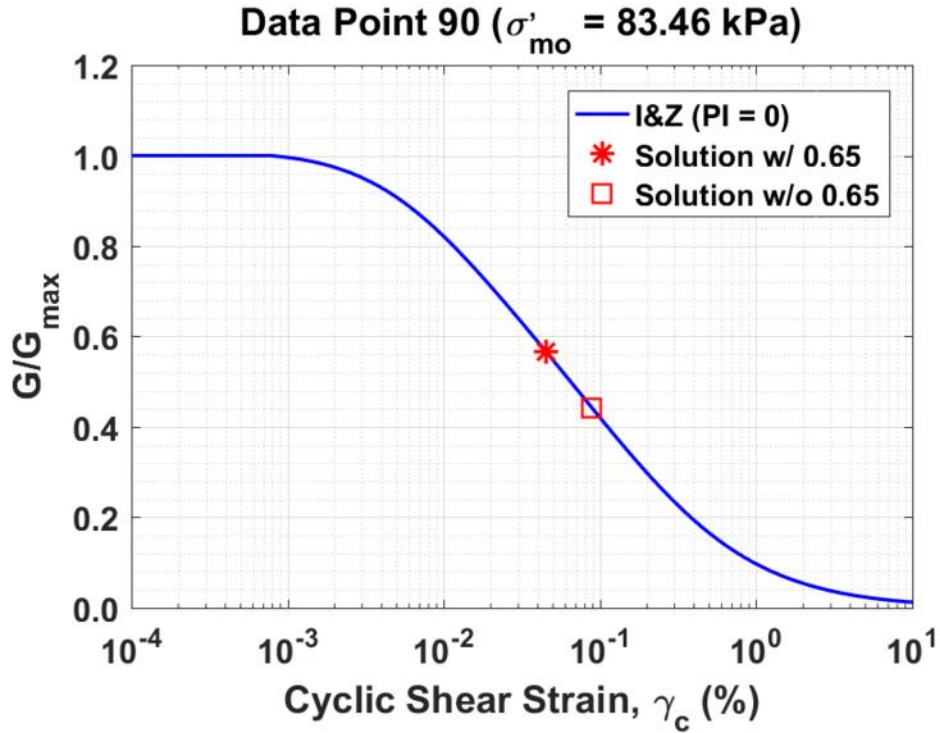


Figure B504. Normalized shear modulus reduction curves for Data Point 90 of the Boulanger et al. database showing the solutions w/ and w/o the 0.65 factor

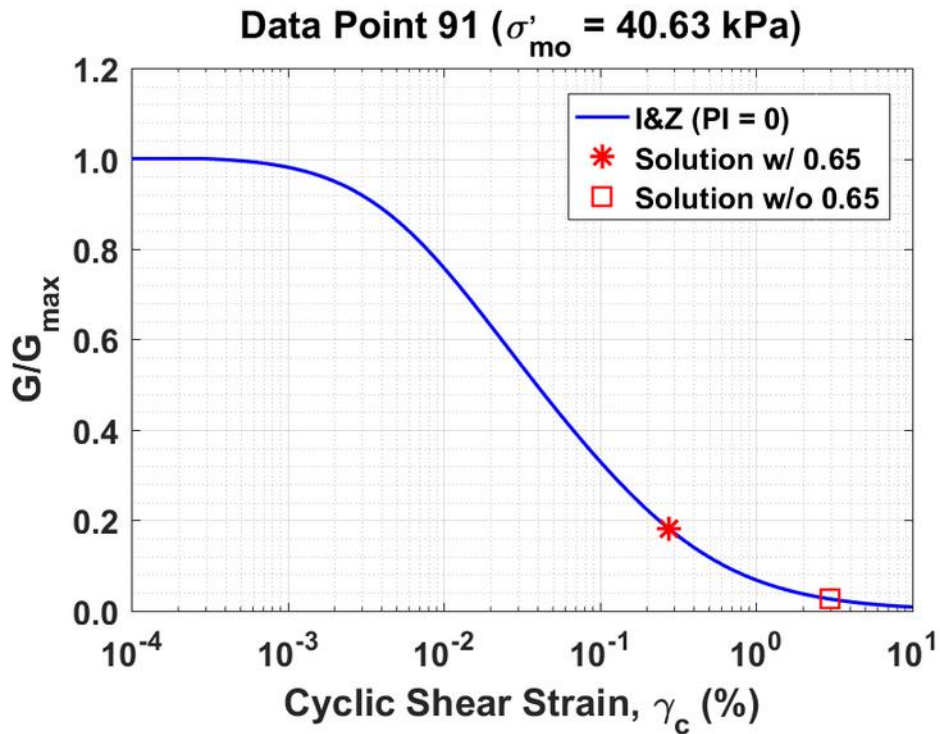


Figure B505. Normalized shear modulus reduction curves for Data Point 91 of the Boulanger et al. database showing the solutions w/ and w/o the 0.65 factor

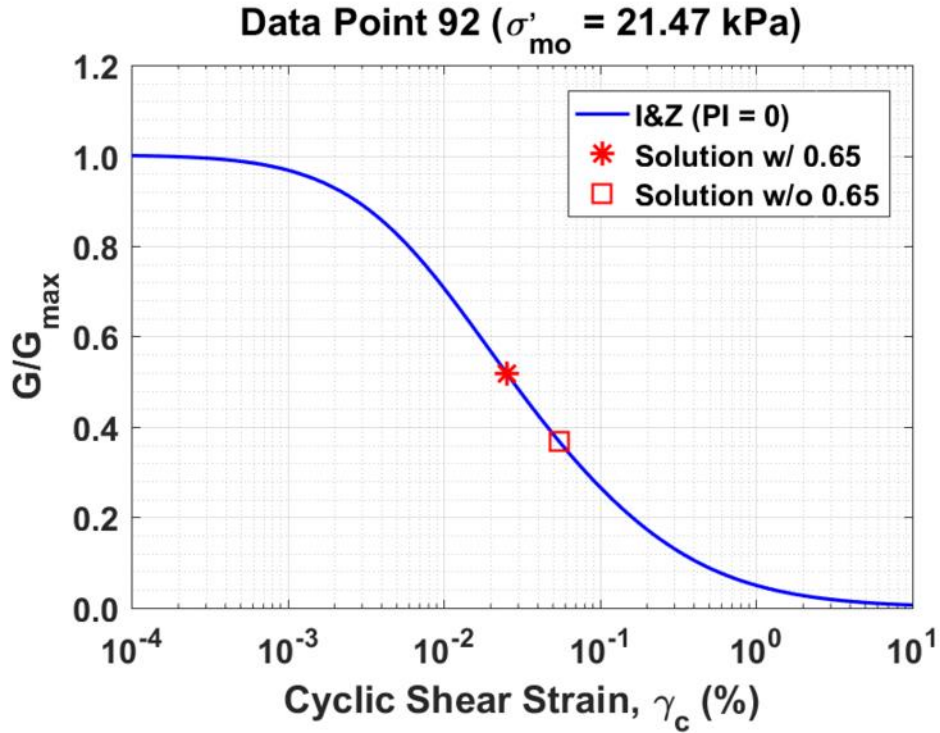


Figure B506. Normalized shear modulus reduction curves for Data Point 92 of the Boulanger et al. database showing the solutions w/ and w/o the 0.65 factor

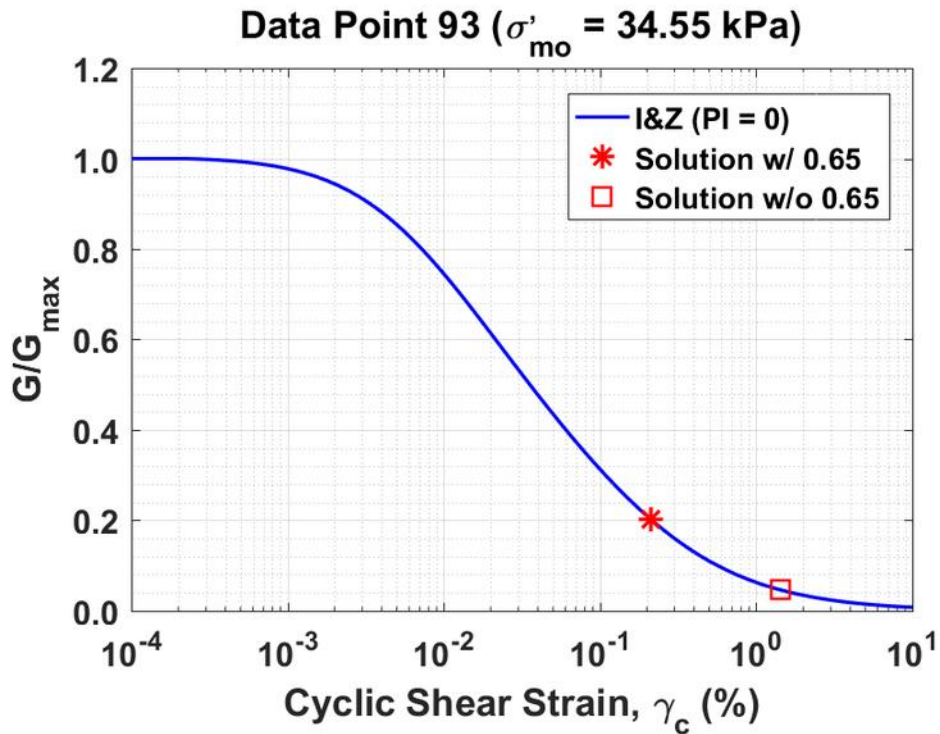


Figure B507. Normalized shear modulus reduction curves for Data Point 93 of the Boulanger et al. database showing the solutions w/ and w/o the 0.65 factor

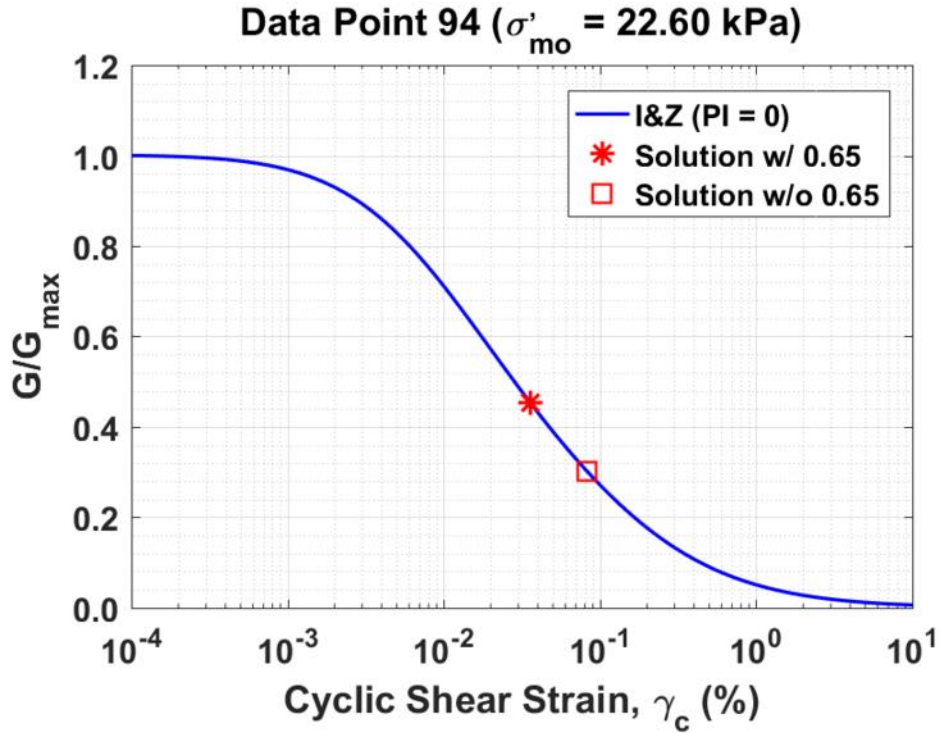


Figure B508. Normalized shear modulus reduction curves for Data Point 94 of the Boulanger et al. database showing the solutions w/ and w/o the 0.65 factor

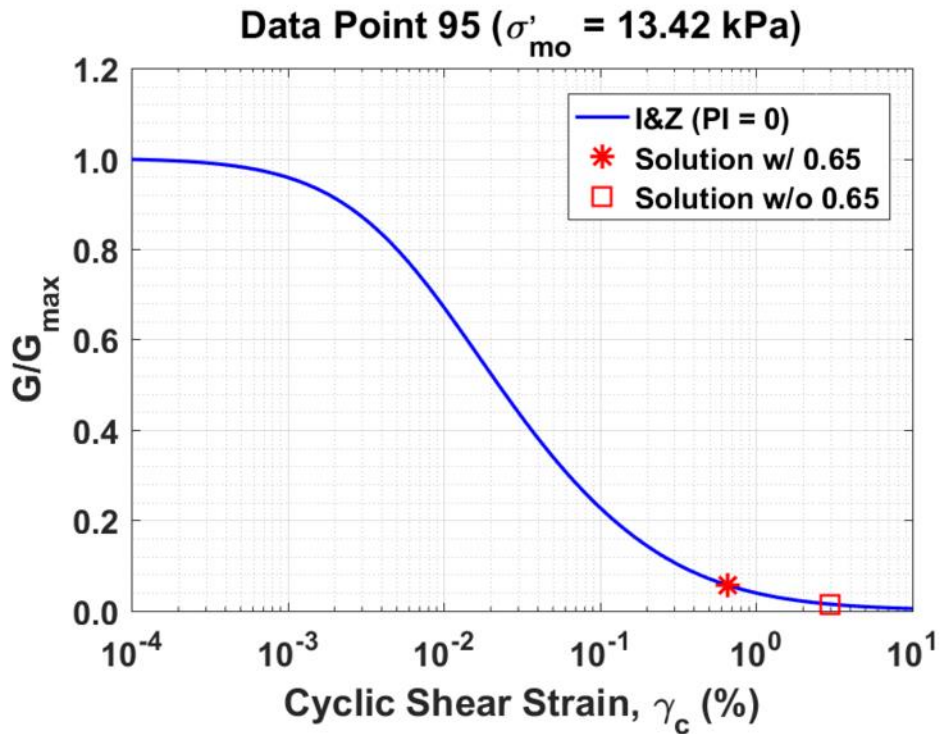


Figure B509. Normalized shear modulus reduction curves for Data Point 95 of the Boulanger et al. database showing the solutions w/ and w/o the 0.65 factor

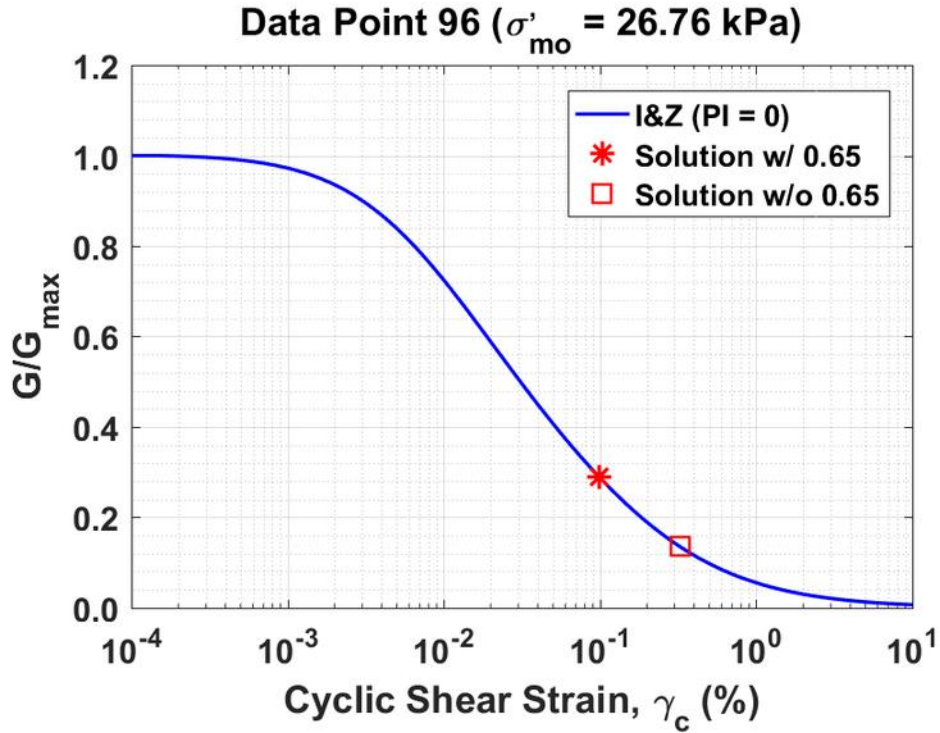


Figure B510. Normalized shear modulus reduction curves for Data Point 96 of the Boulanger et al. database showing the solutions w/ and w/o the 0.65 factor

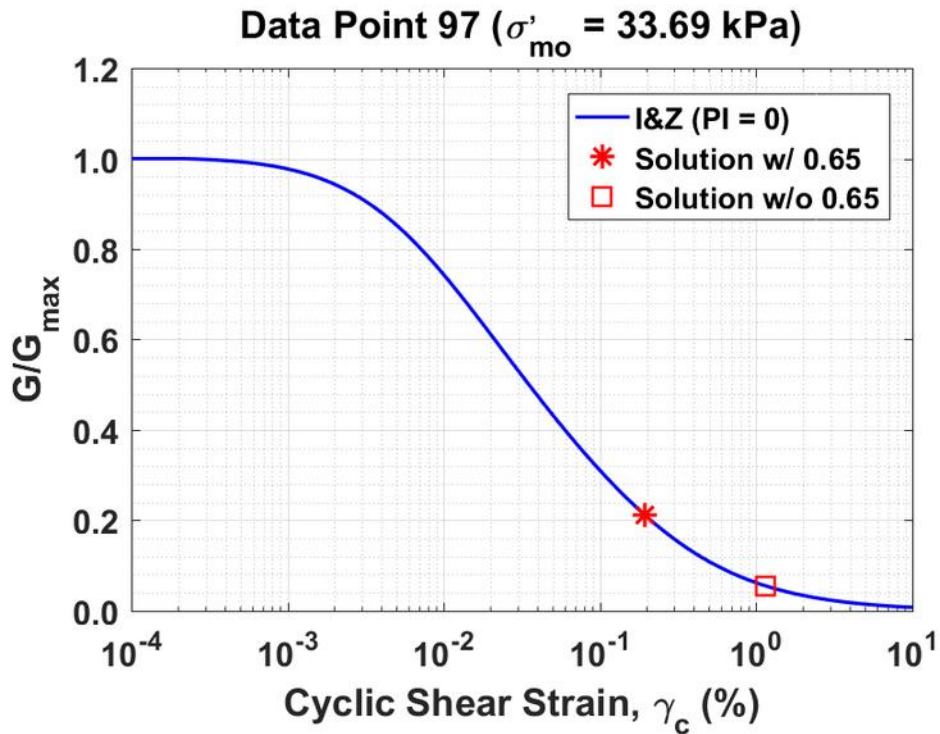


Figure B511. Normalized shear modulus reduction curves for Data Point 97 of the Boulanger et al. database showing the solutions w/ and w/o the 0.65 factor

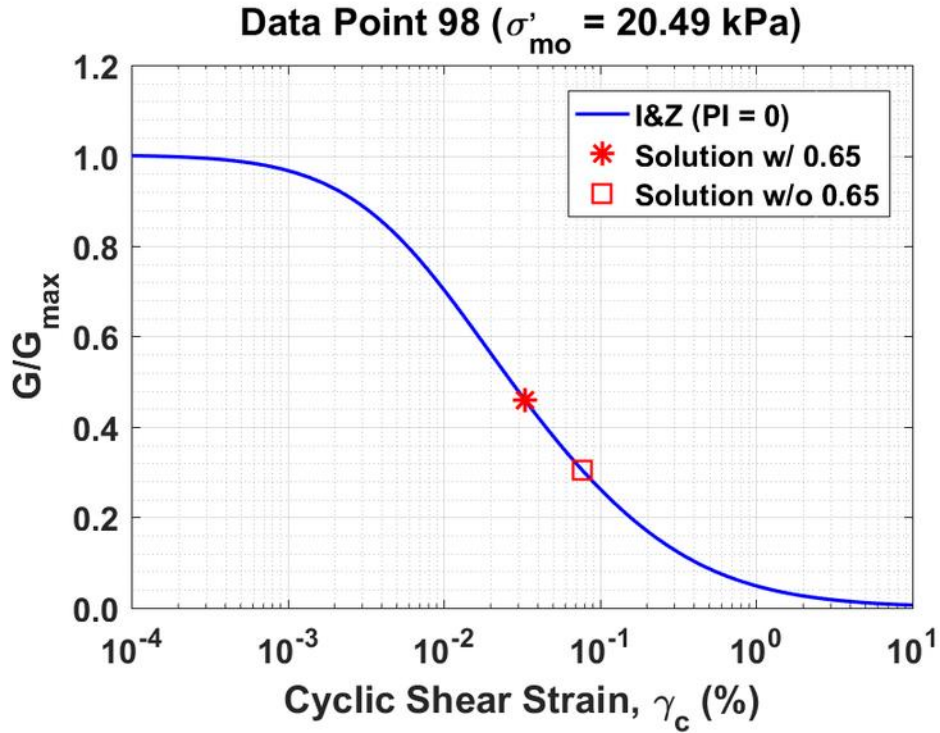


Figure B512. Normalized shear modulus reduction curves for Data Point 98 of the Boulanger et al. database showing the solutions w/ and w/o the 0.65 factor

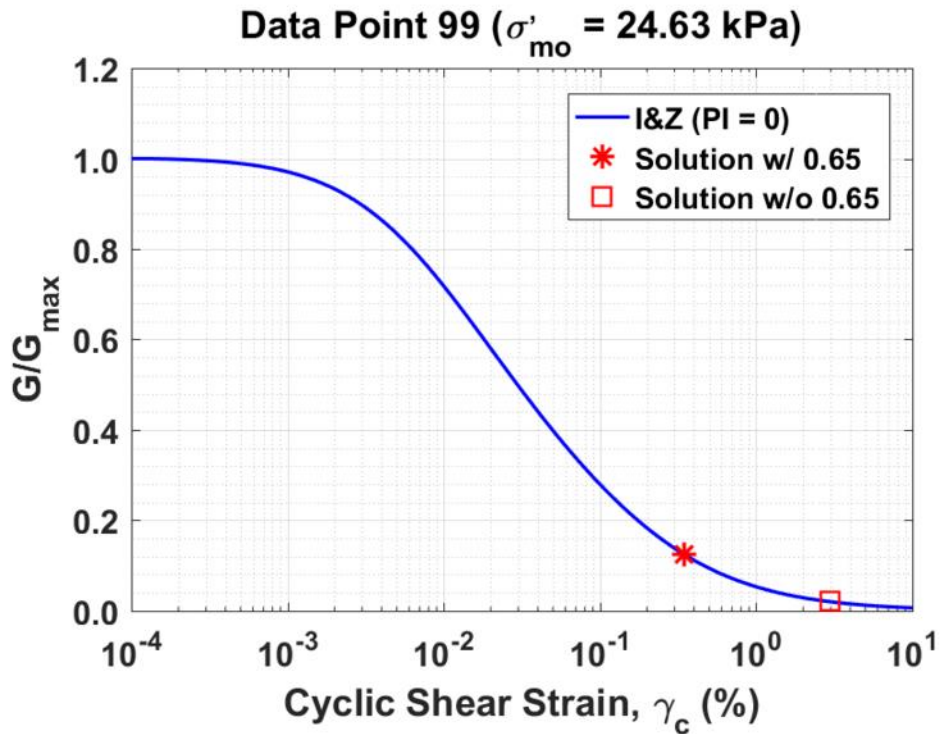


Figure B513. Normalized shear modulus reduction curves for Data Point 99 of the Boulanger et al. database showing the solutions w/ and w/o the 0.65 factor

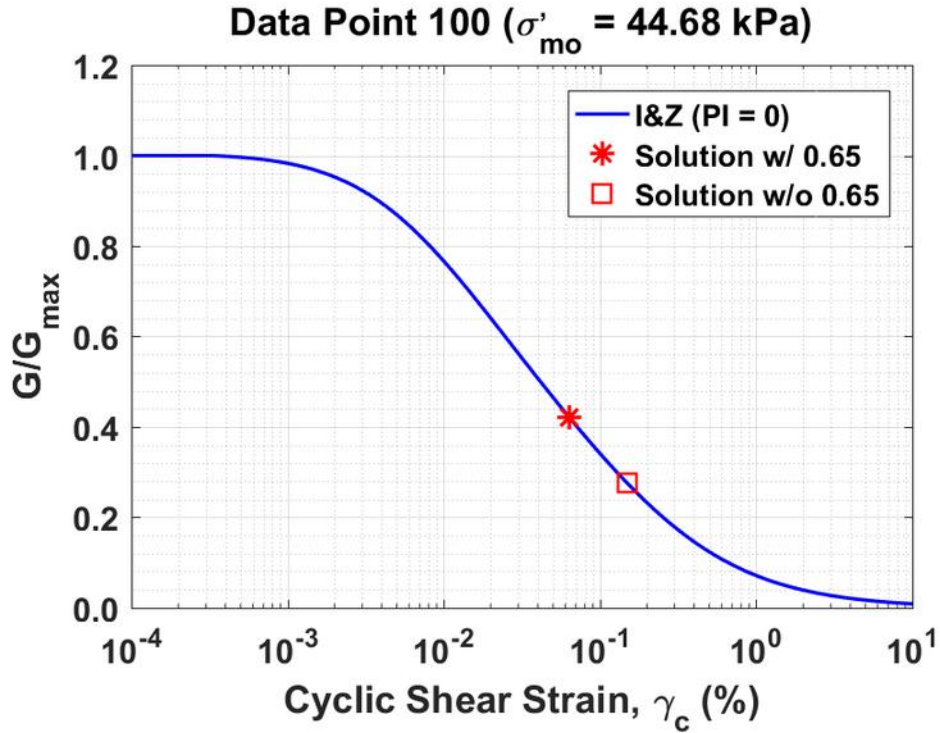


Figure B514. Normalized shear modulus reduction curves for Data Point 100 of the Boulanger et al. database showing the solutions w/ and w/o the 0.65 factor

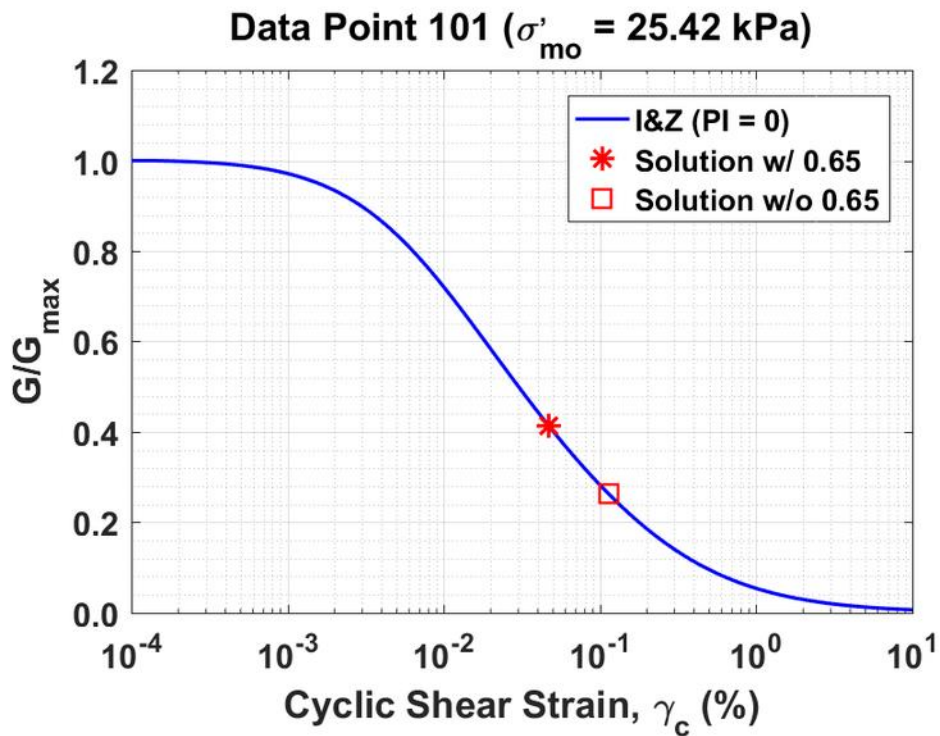


Figure B515. Normalized shear modulus reduction curves for Data Point 101 of the Boulanger et al. database showing the solutions w/ and w/o the 0.65 factor

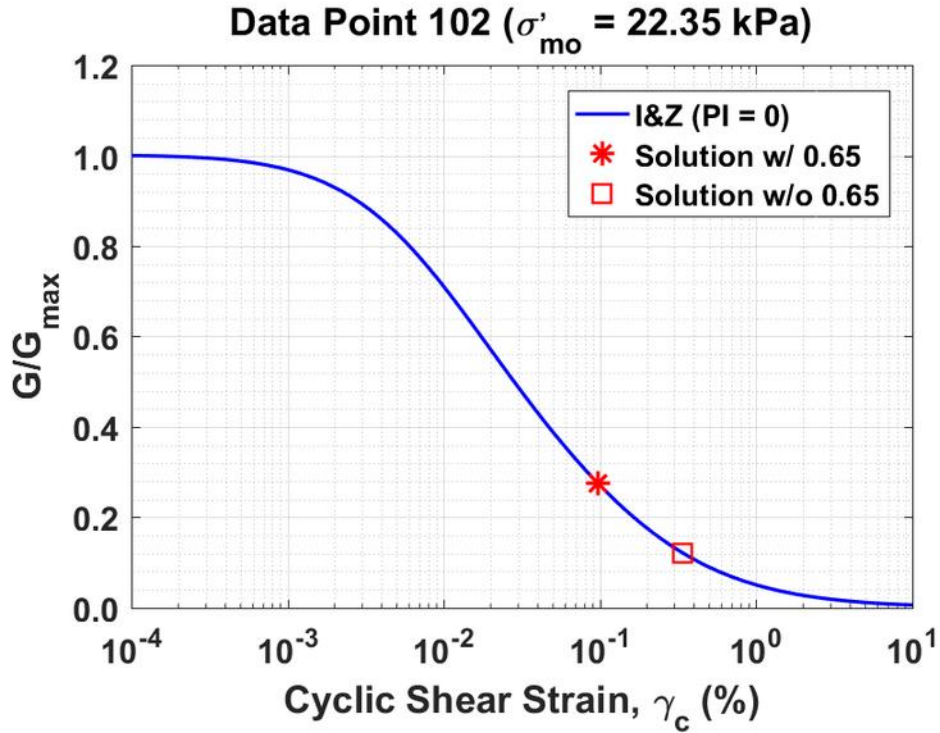


Figure B516. Normalized shear modulus reduction curves for Data Point 102 of the Boulanger et al. database showing the solutions w/ and w/o the 0.65 factor

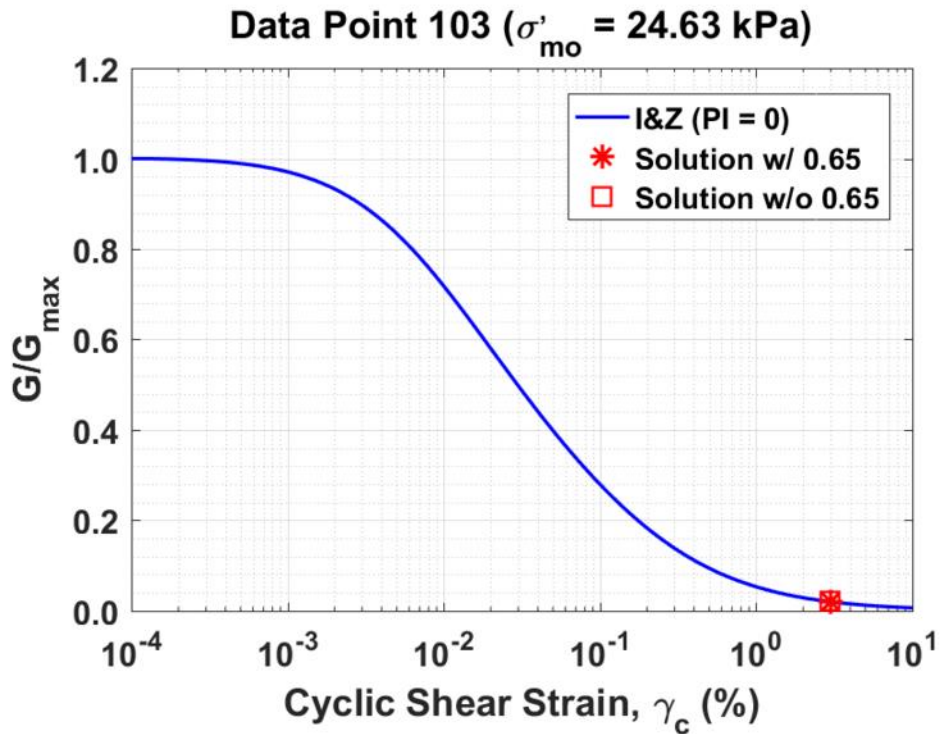


Figure B517. Normalized shear modulus reduction curves for Data Point 103 of the Boulanger et al. database showing the solutions w/ and w/o the 0.65 factor

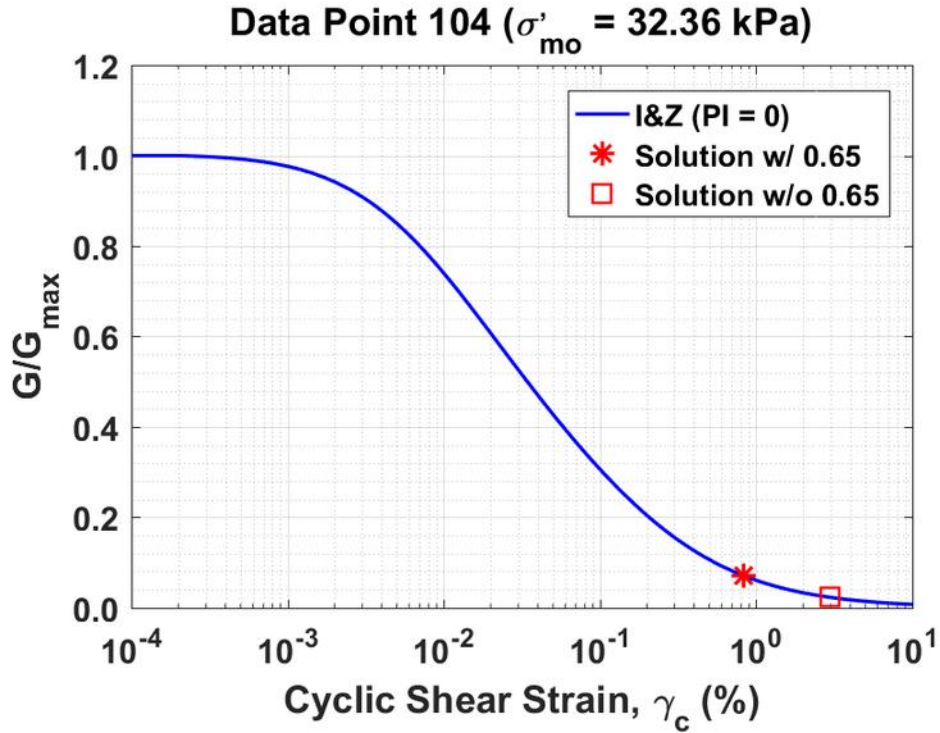


Figure B518. Normalized shear modulus reduction curves for Data Point 104 of the Boulanger et al. database showing the solutions w/ and w/o the 0.65 factor

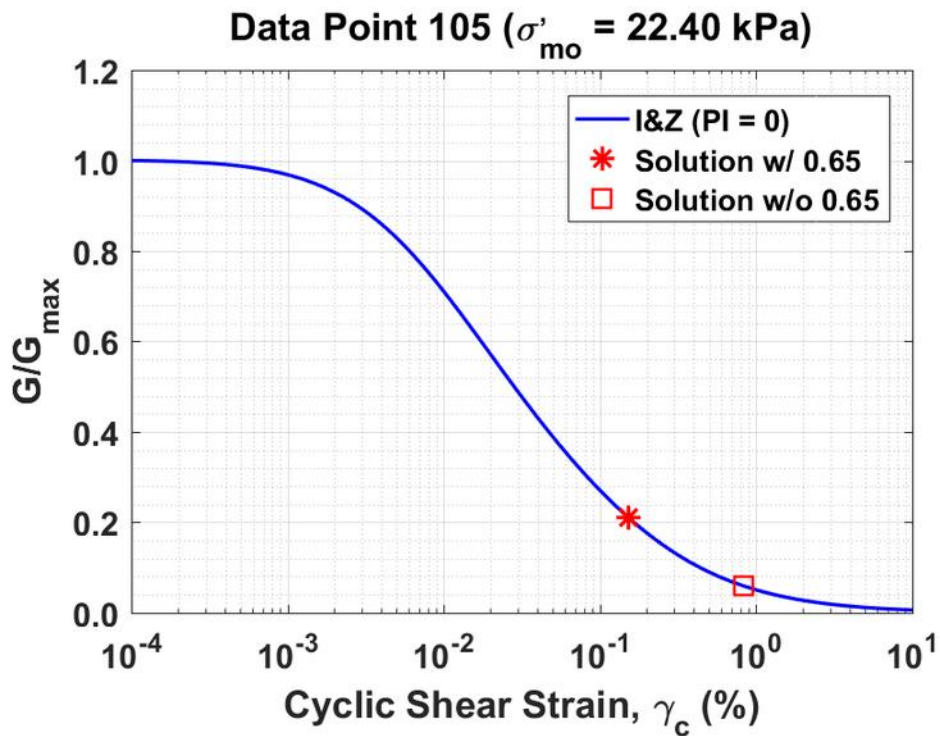


Figure B519. Normalized shear modulus reduction curves for Data Point 105 of the Boulanger et al. database showing the solutions w/ and w/o the 0.65 factor

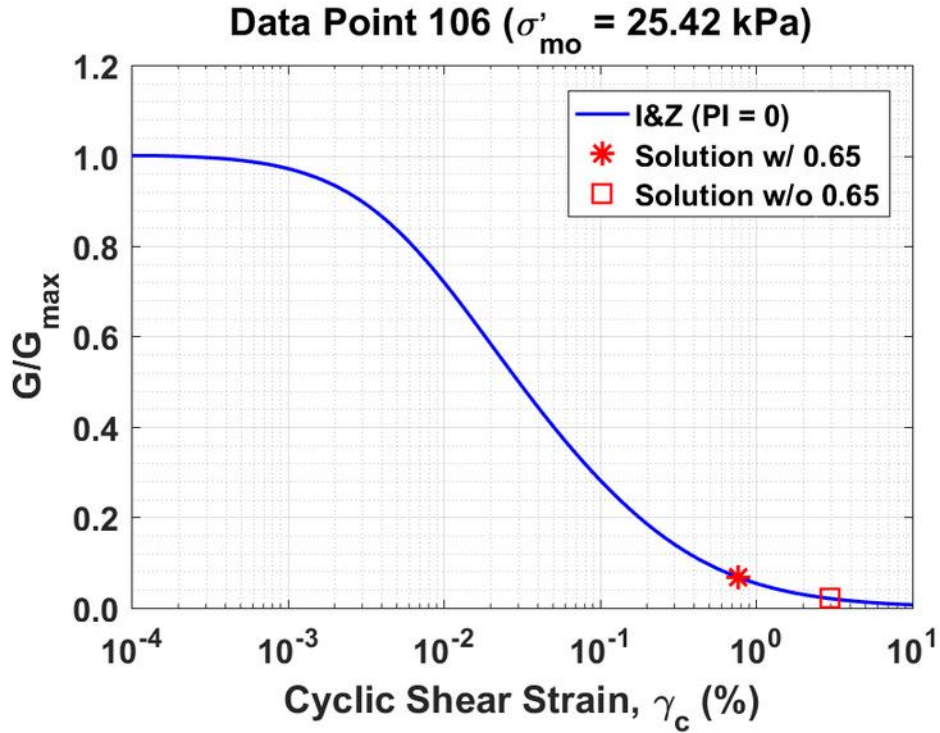


Figure B520. Normalized shear modulus reduction curves for Data Point 106 of the Boulanger et al. database showing the solutions w/ and w/o the 0.65 factor

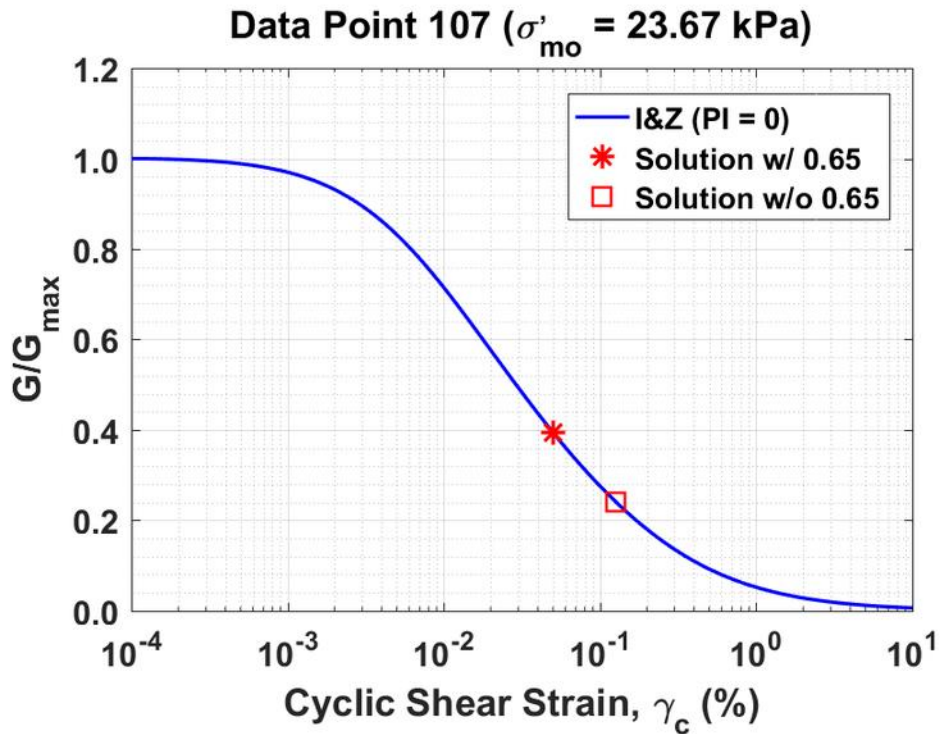


Figure B521. Normalized shear modulus reduction curves for Data Point 107 of the Boulanger et al. database showing the solutions w/ and w/o the 0.65 factor

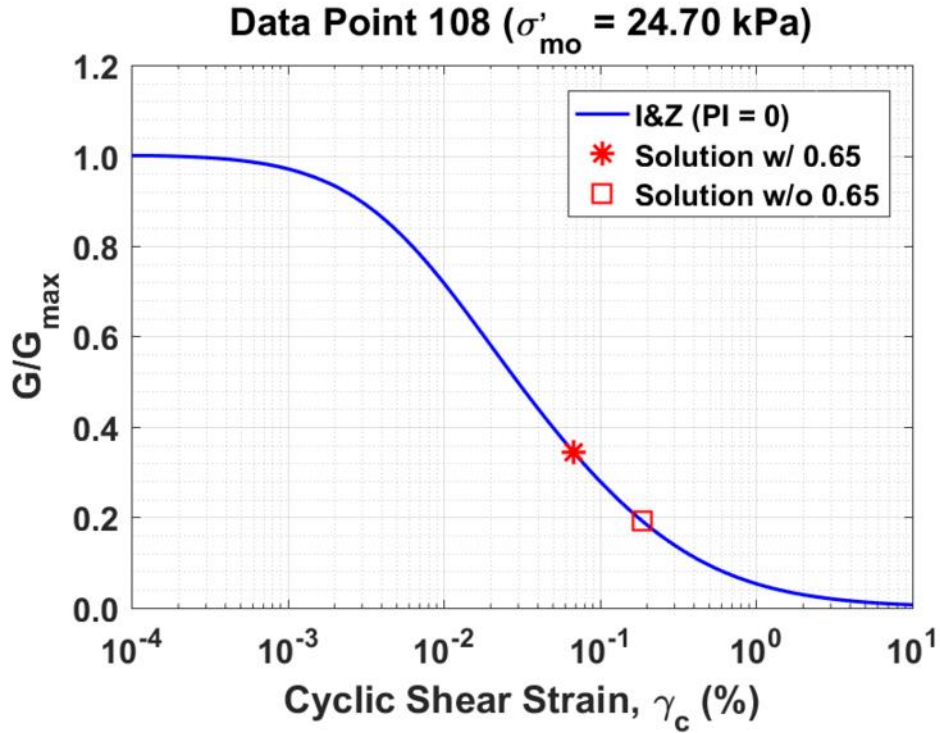


Figure B522. Normalized shear modulus reduction curves for Data Point 108 of the Boulanger et al. database showing the solutions w/ and w/o the 0.65 factor

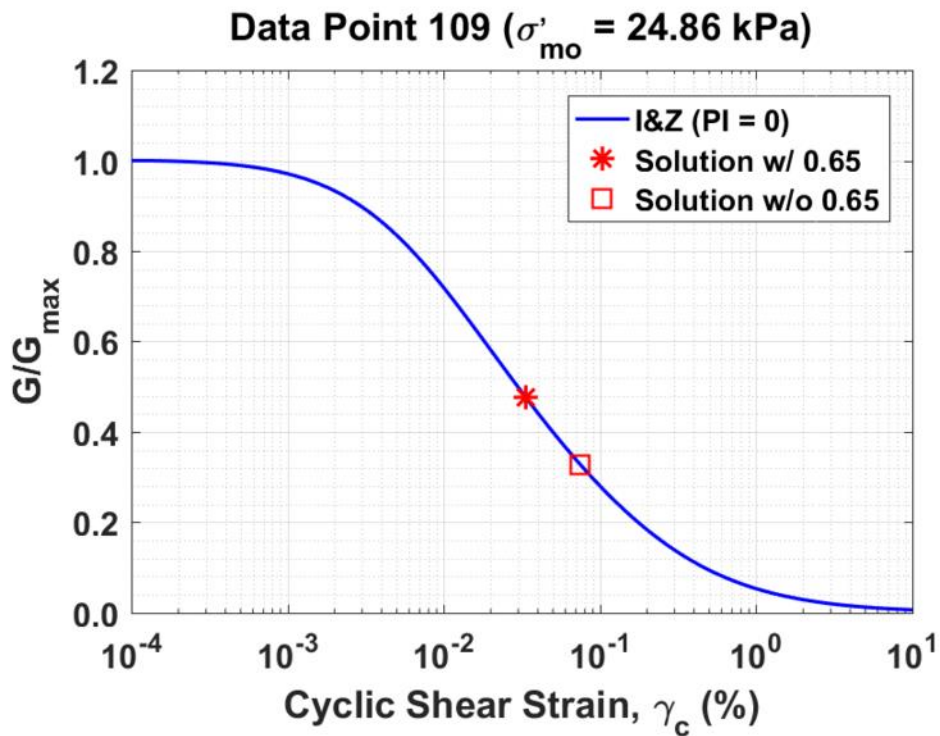


Figure B523. Normalized shear modulus reduction curves for Data Point 109 of the Boulanger et al. database showing the solutions w/ and w/o the 0.65 factor

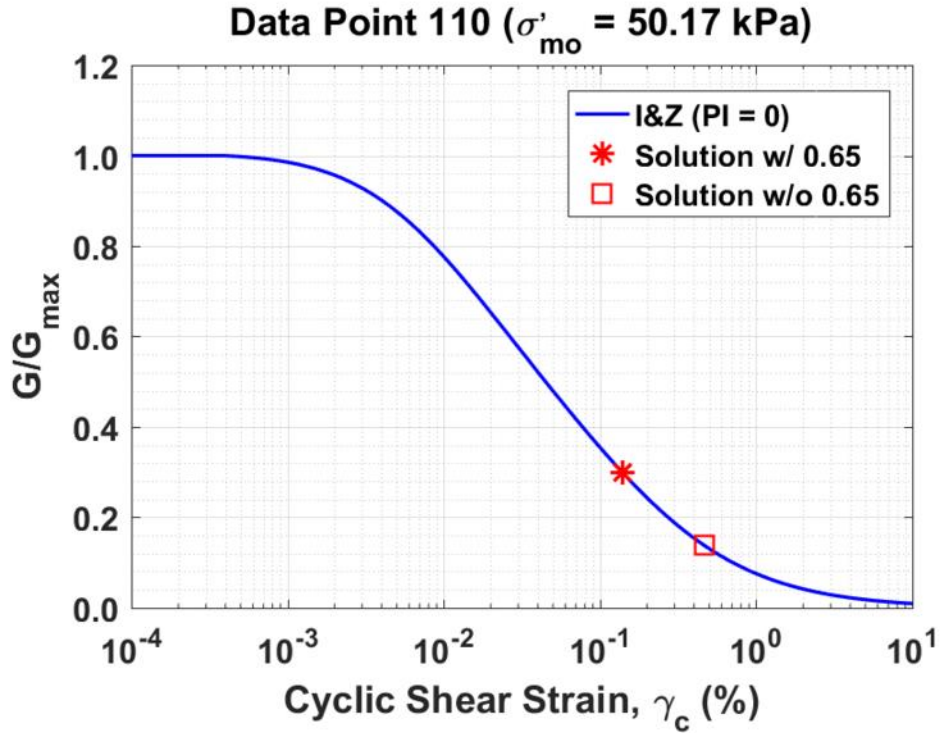


Figure B524. Normalized shear modulus reduction curves for Data Point 110 of the Boulanger et al. database showing the solutions w/ and w/o the 0.65 factor

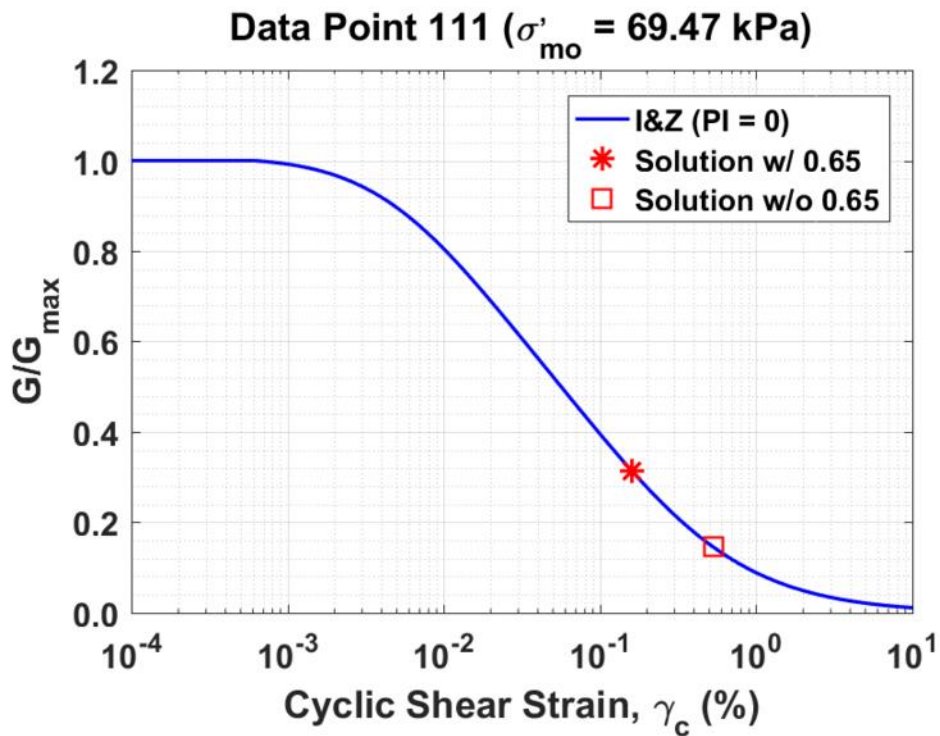


Figure B525. Normalized shear modulus reduction curves for Data Point 111 of the Boulanger et al. database showing the solutions w/ and w/o the 0.65 factor

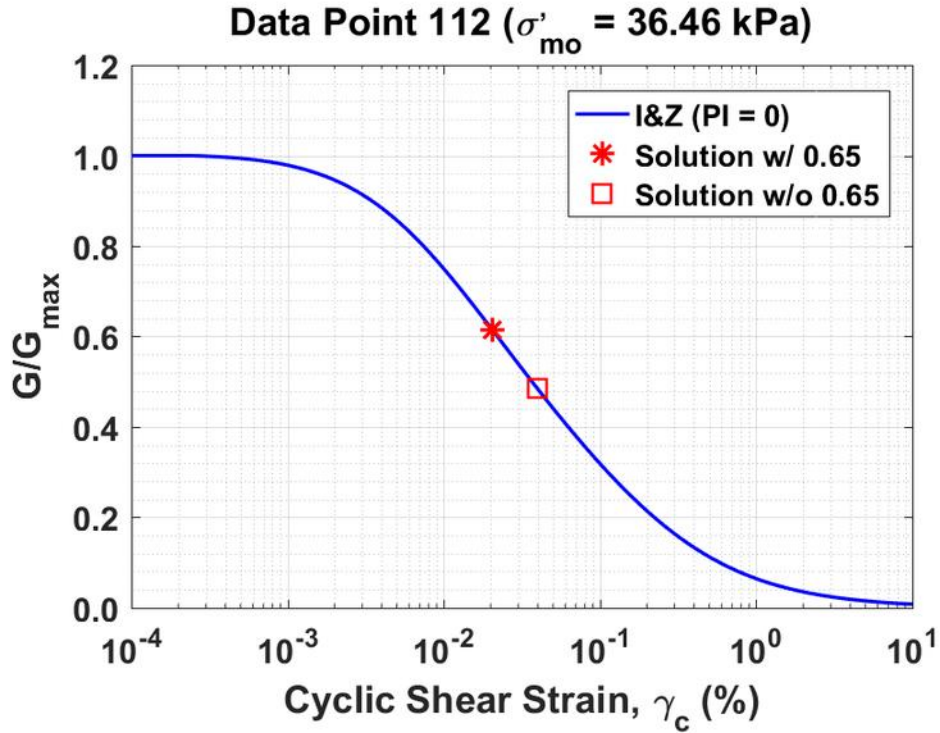


Figure B526. Normalized shear modulus reduction curves for Data Point 112 of the Boulanger et al. database showing the solutions w/ and w/o the 0.65 factor

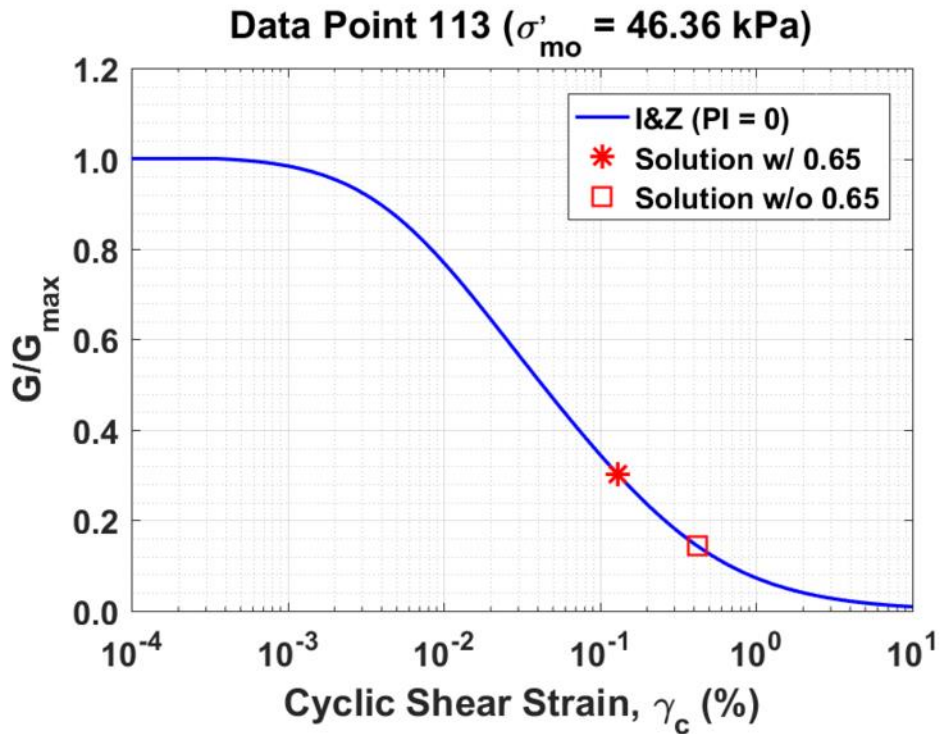


Figure B527. Normalized shear modulus reduction curves for Data Point 113 of the Boulanger et al. database showing the solutions w/ and w/o the 0.65 factor

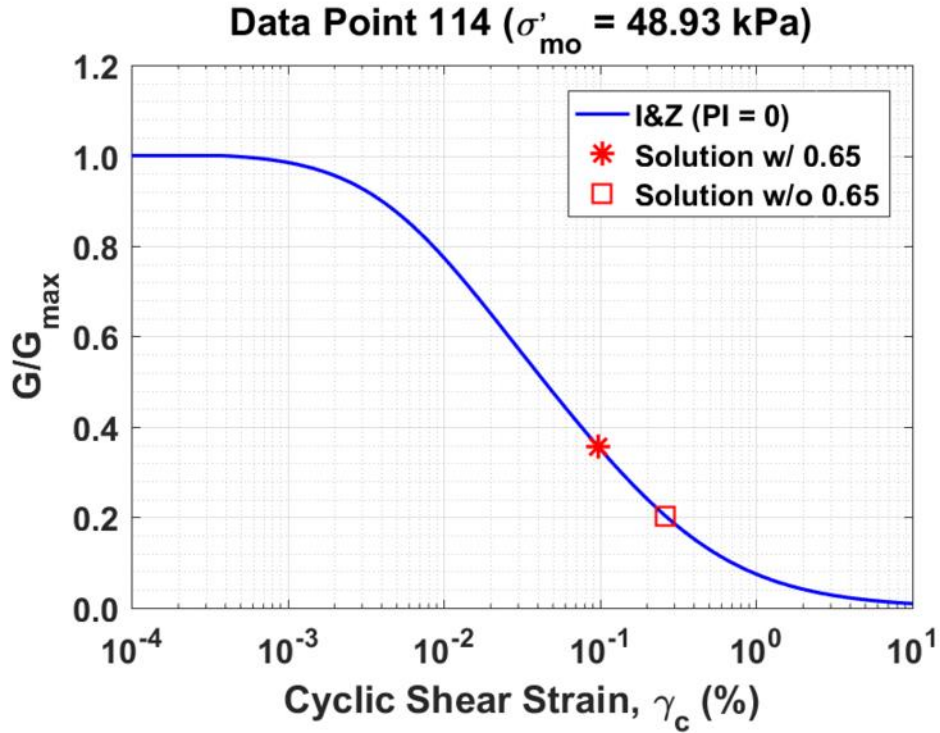


Figure B528. Normalized shear modulus reduction curves for Data Point 114 of the Boulanger et al. database showing the solutions w/ and w/o the 0.65 factor

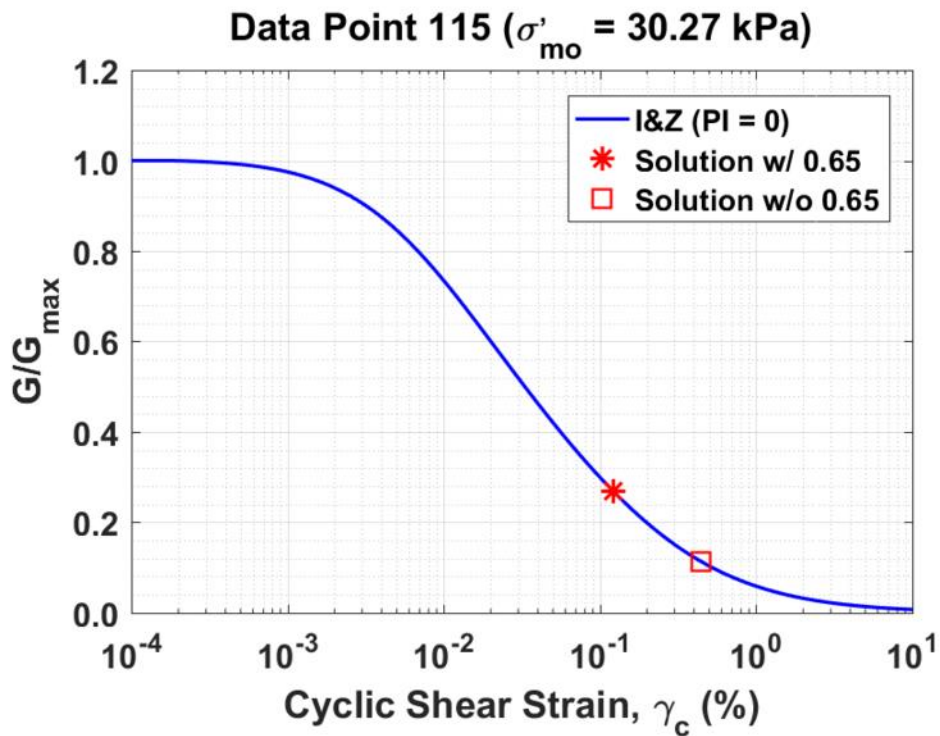


Figure B529. Normalized shear modulus reduction curves for Data Point 115 of the Boulanger et al. database showing the solutions w/ and w/o the 0.65 factor

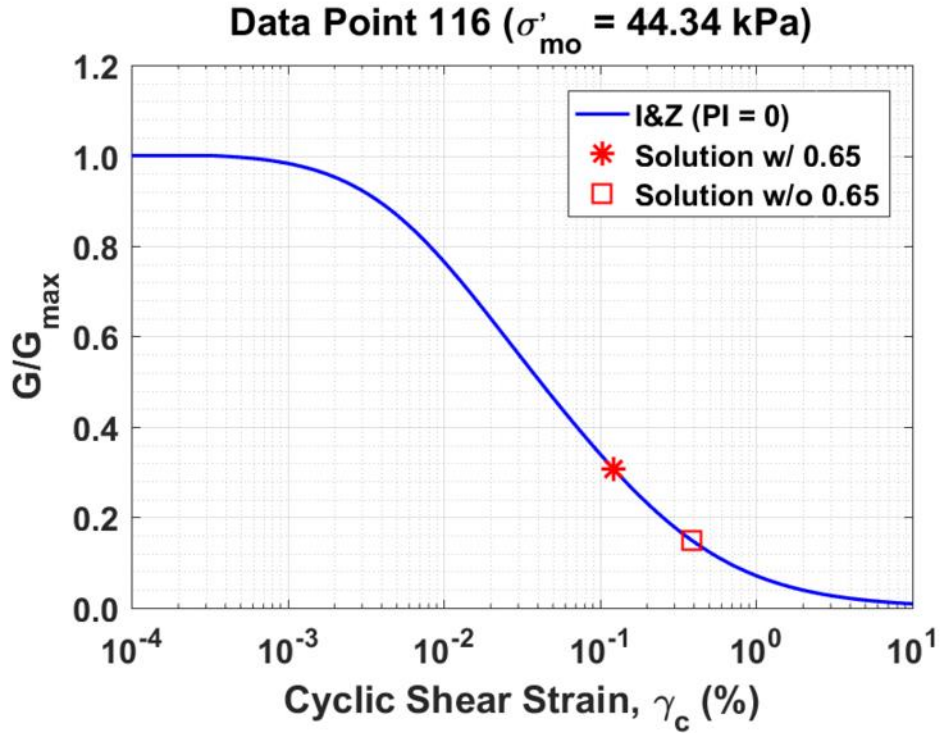


Figure B530. Normalized shear modulus reduction curves for Data Point 116 of the Boulanger et al. database showing the solutions w/ and w/o the 0.65 factor

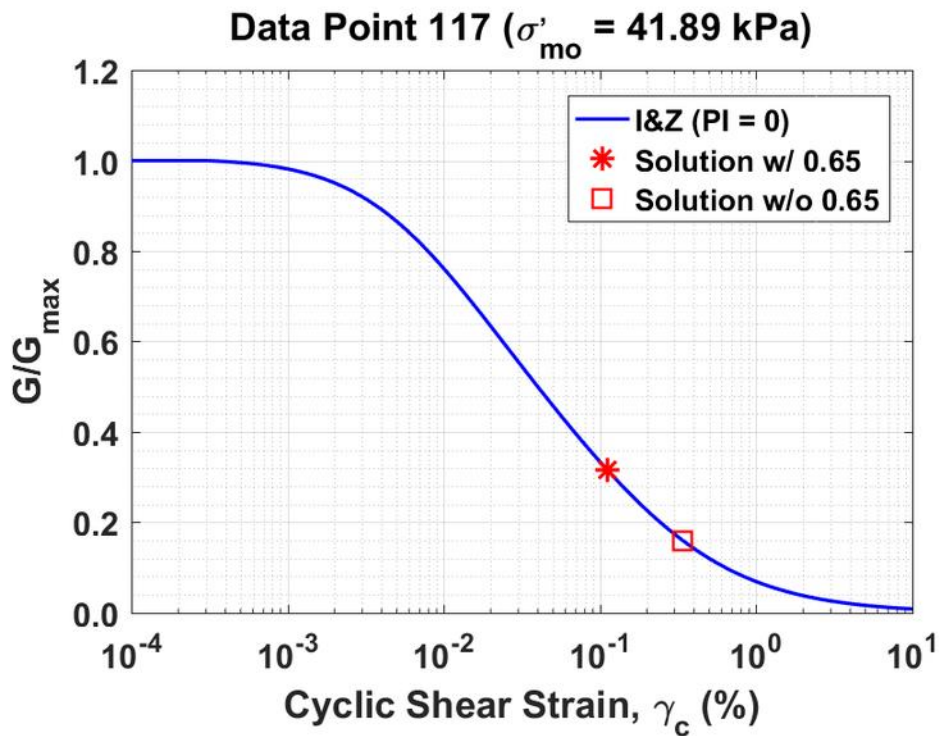


Figure B531. Normalized shear modulus reduction curves for Data Point 117 of the Boulanger et al. database showing the solutions w/ and w/o the 0.65 factor

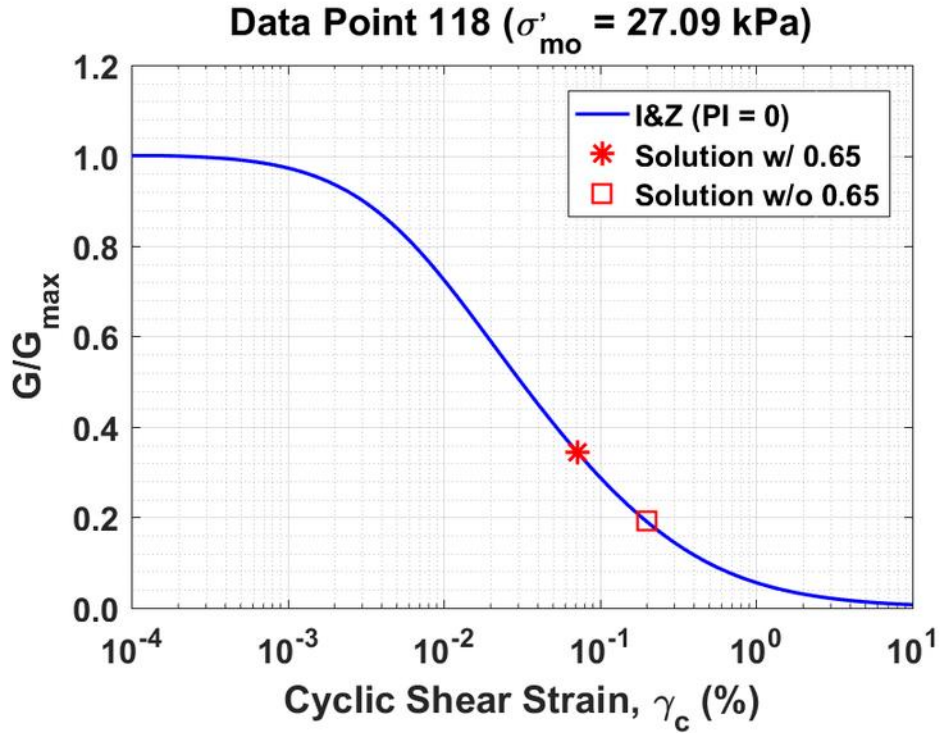


Figure B532. Normalized shear modulus reduction curves for Data Point 118 of the Boulanger et al. database showing the solutions w/ and w/o the 0.65 factor

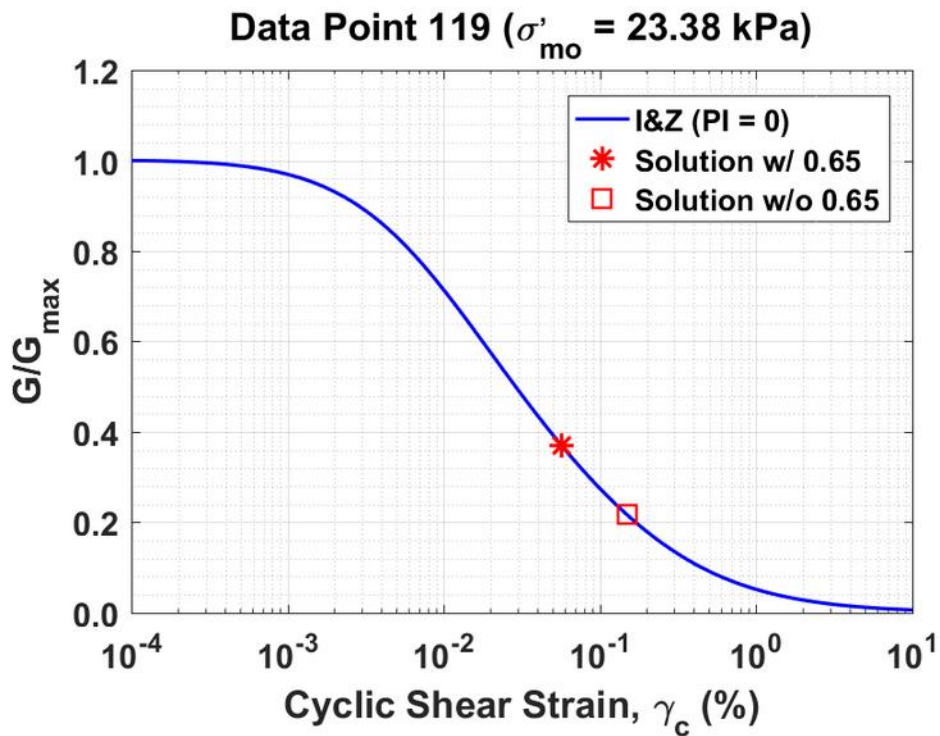


Figure B533. Normalized shear modulus reduction curves for Data Point 119 of the Boulanger et al. database showing the solutions w/ and w/o the 0.65 factor

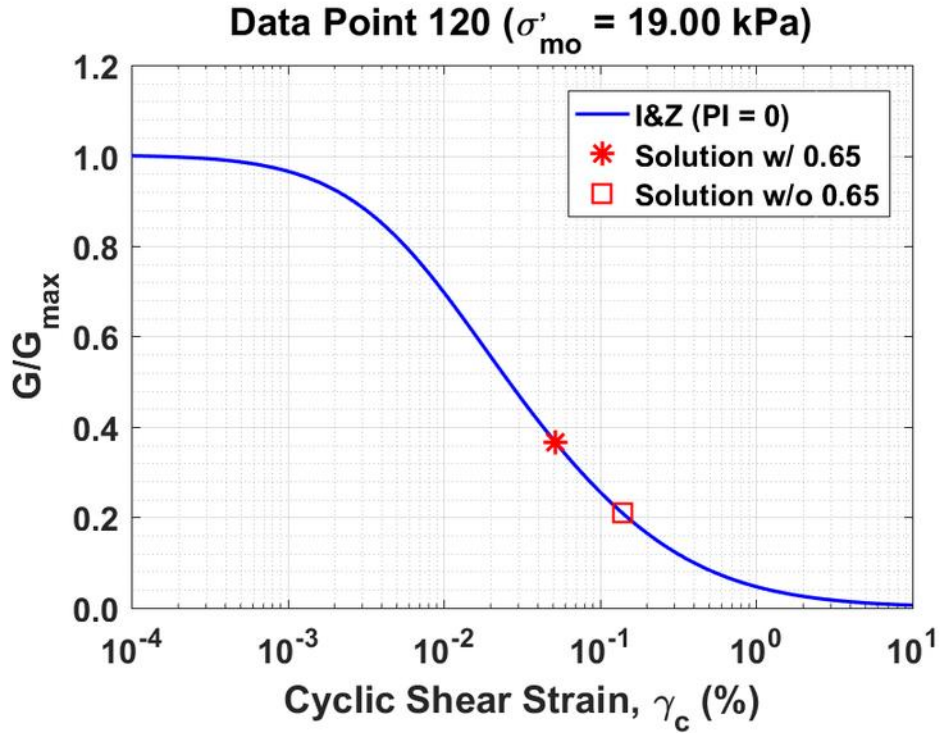


Figure B534. Normalized shear modulus reduction curves for Data Point 120 of the Boulanger et al. database showing the solutions w/ and w/o the 0.65 factor

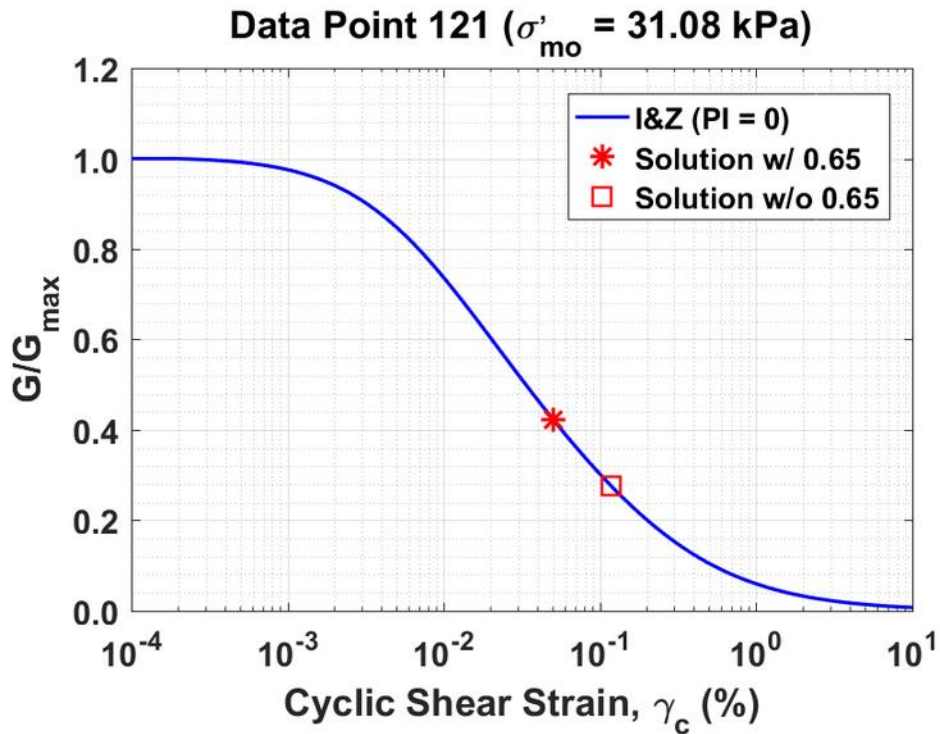


Figure B535. Normalized shear modulus reduction curves for Data Point 121 of the Boulanger et al. database showing the solutions w/ and w/o the 0.65 factor

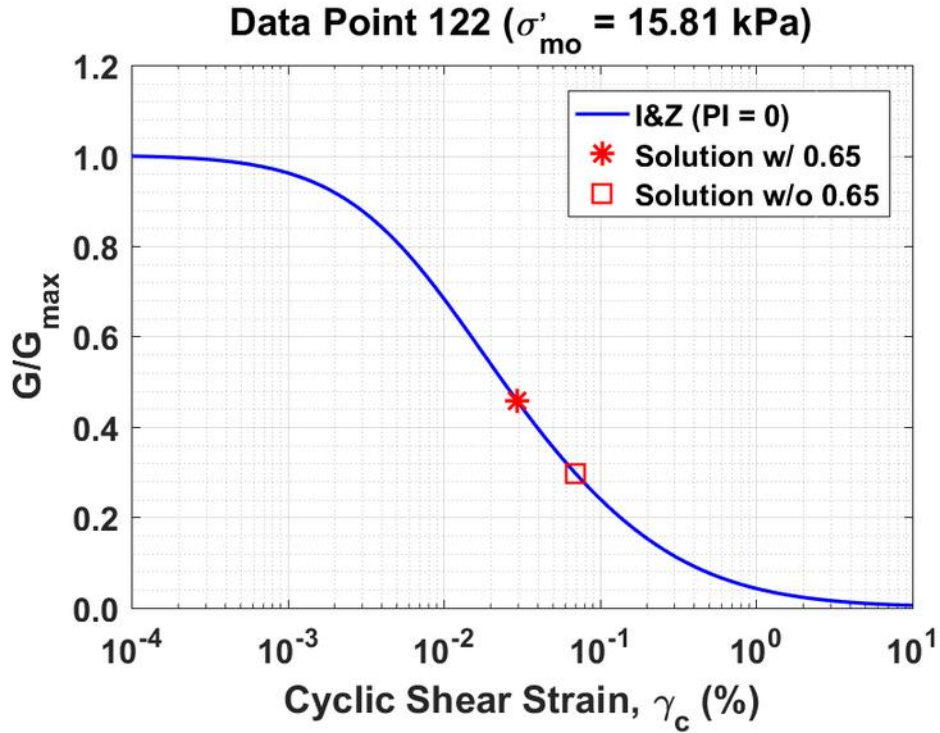


Figure B536. Normalized shear modulus reduction curves for Data Point 122 of the Boulanger et al. database showing the solutions w/ and w/o the 0.65 factor

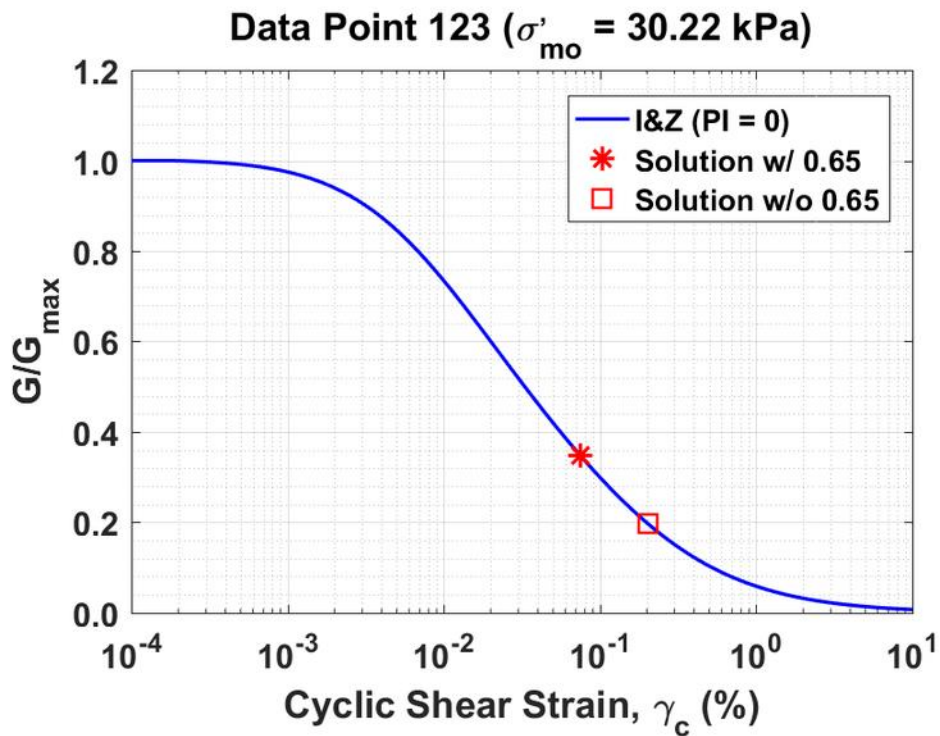


Figure B537. Normalized shear modulus reduction curves for Data Point 123 of the Boulanger et al. database showing the solutions w/ and w/o the 0.65 factor

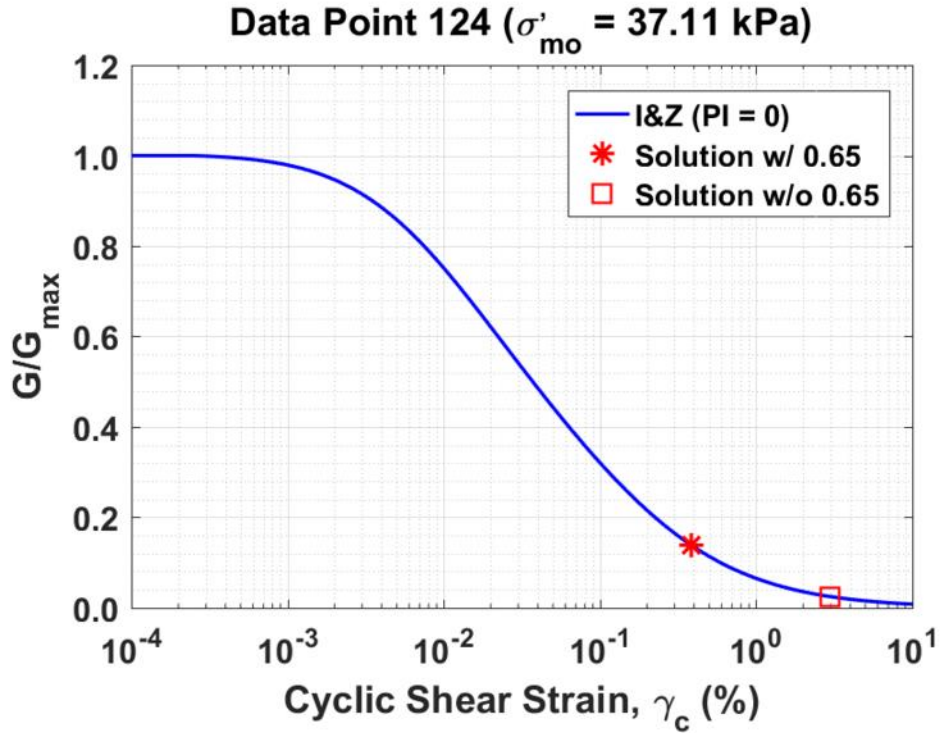


Figure B538. Normalized shear modulus reduction curves for Data Point 124 of the Boulanger et al. database showing the solutions w/ and w/o the 0.65 factor

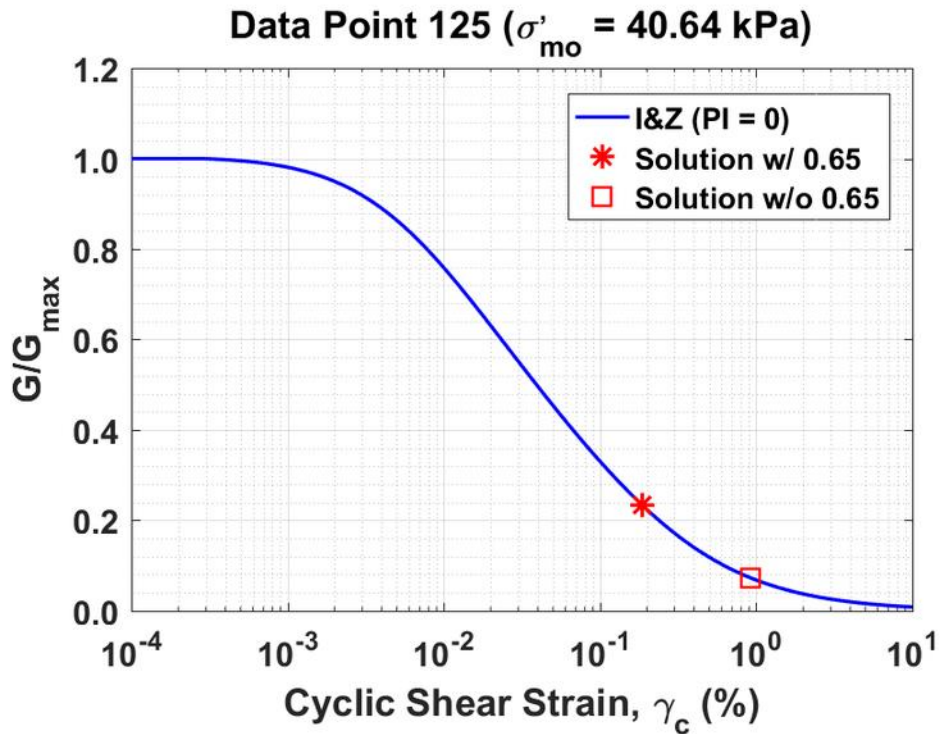


Figure B539. Normalized shear modulus reduction curves for Data Point 125 of the Boulanger et al. database showing the solutions w/ and w/o the 0.65 factor

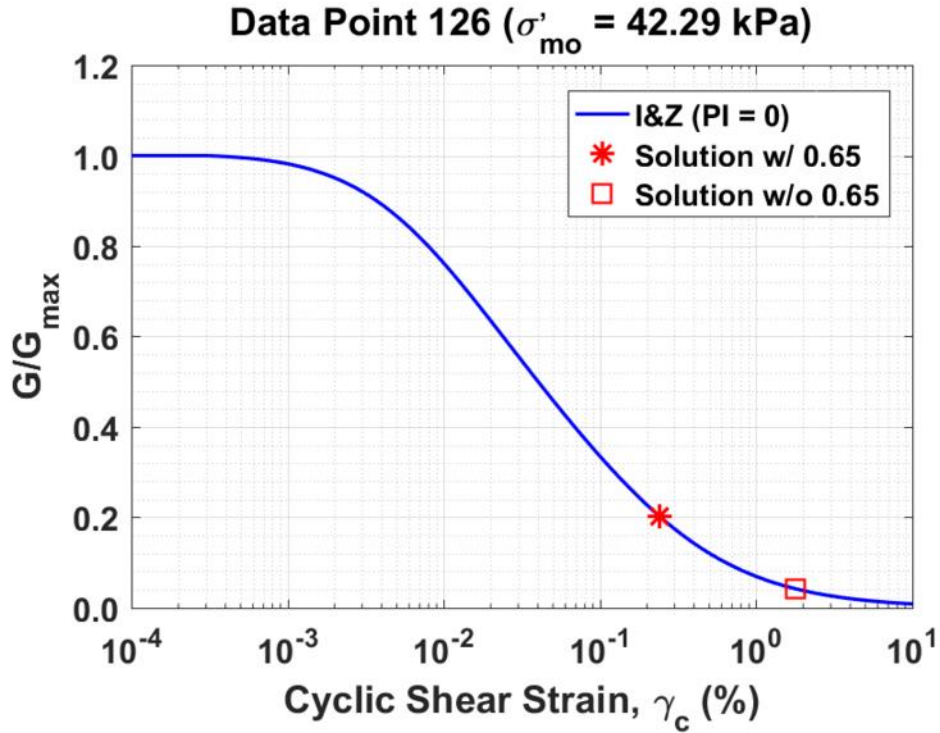


Figure B540. Normalized shear modulus reduction curves for Data Point 126 of the Boulanger et al. database showing the solutions w/ and w/o the 0.65 factor

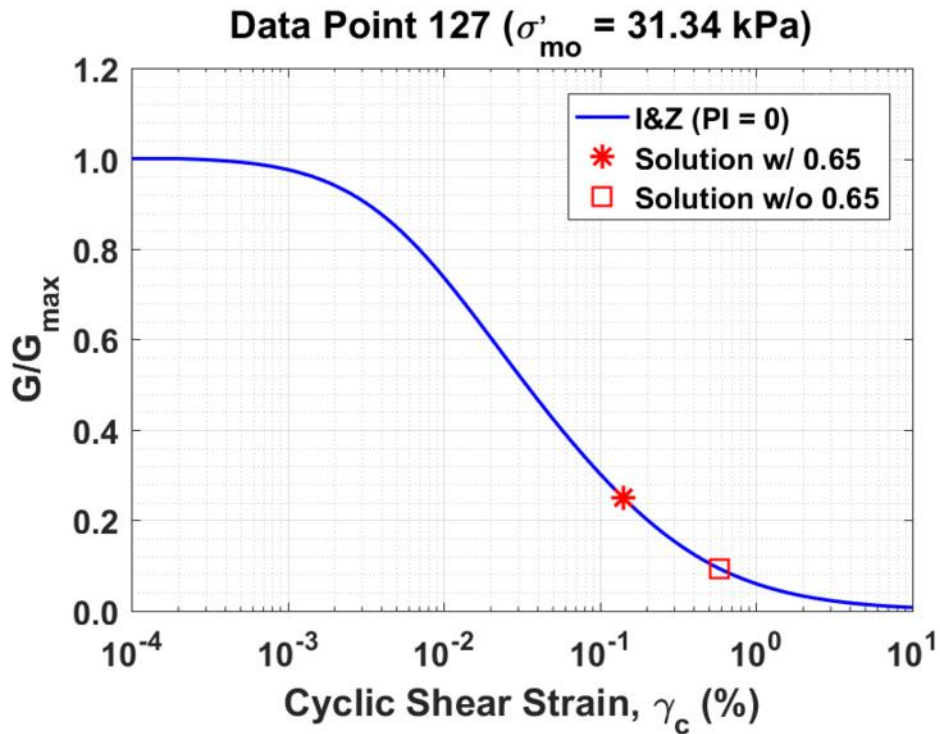


Figure B541. Normalized shear modulus reduction curves for Data Point 127 of the Boulanger et al. database showing the solutions w/ and w/o the 0.65 factor

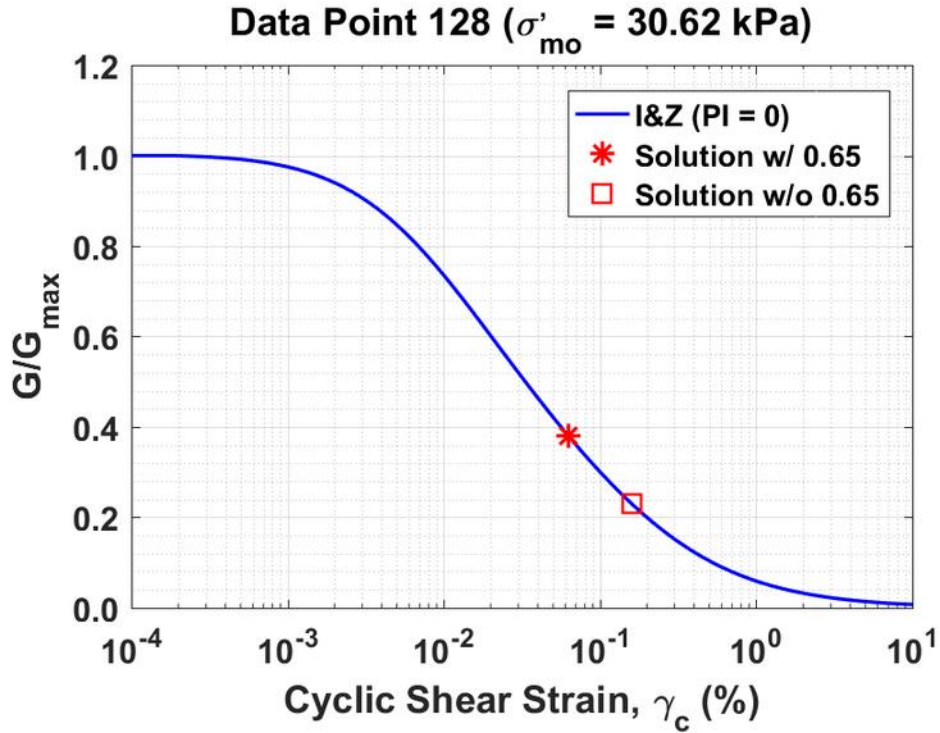


Figure B542. Normalized shear modulus reduction curves for Data Point 128 of the Boulanger et al. database showing the solutions w/ and w/o the 0.65 factor

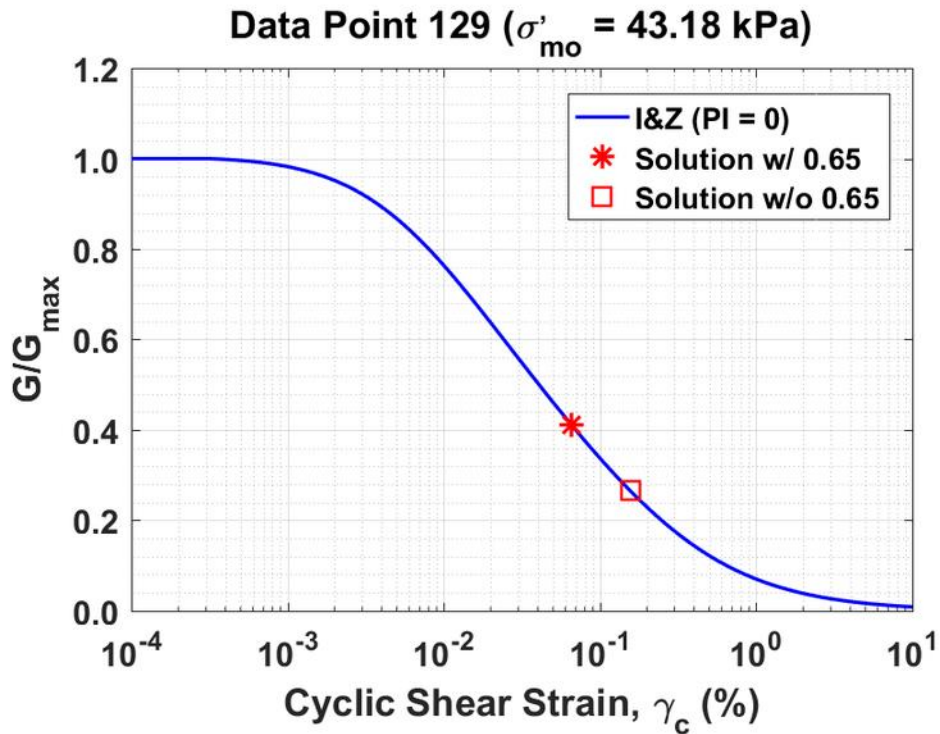


Figure B543. Normalized shear modulus reduction curves for Data Point 129 of the Boulanger et al. database showing the solutions w/ and w/o the 0.65 factor

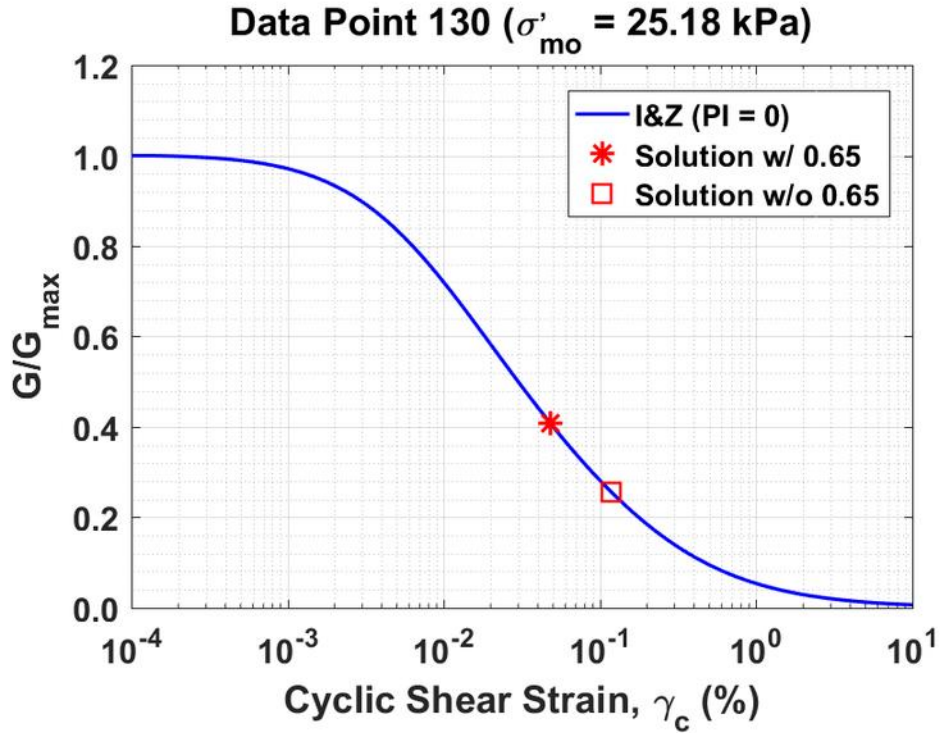


Figure B544. Normalized shear modulus reduction curves for Data Point 130 of the Boulanger et al. database showing the solutions w/ and w/o the 0.65 factor

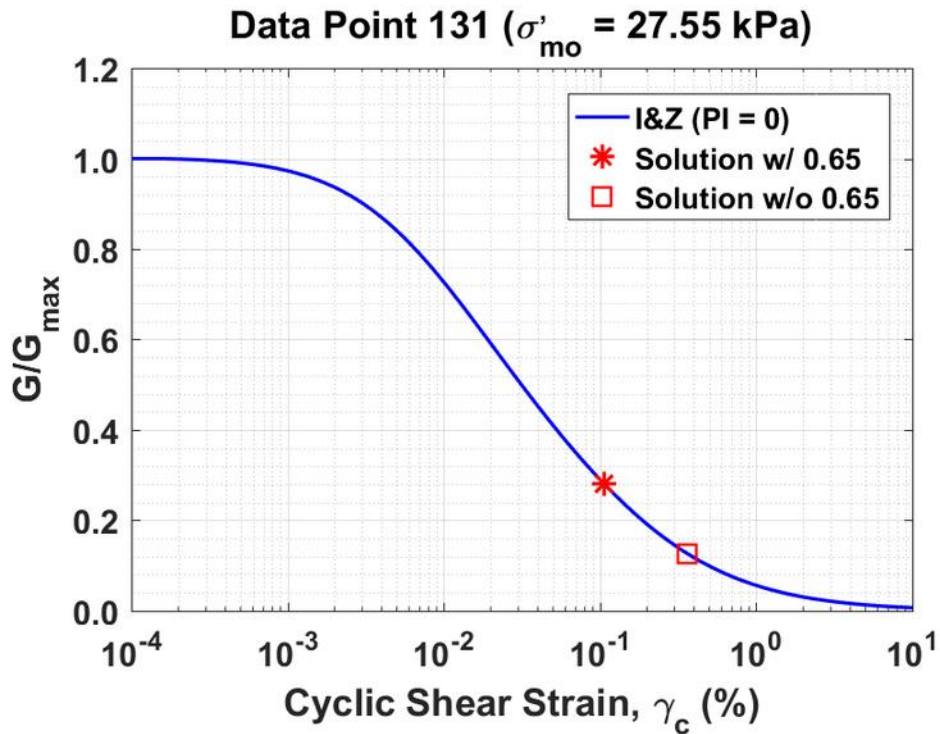


Figure B545. Normalized shear modulus reduction curves for Data Point 131 of the Boulanger et al. database showing the solutions w/ and w/o the 0.65 factor

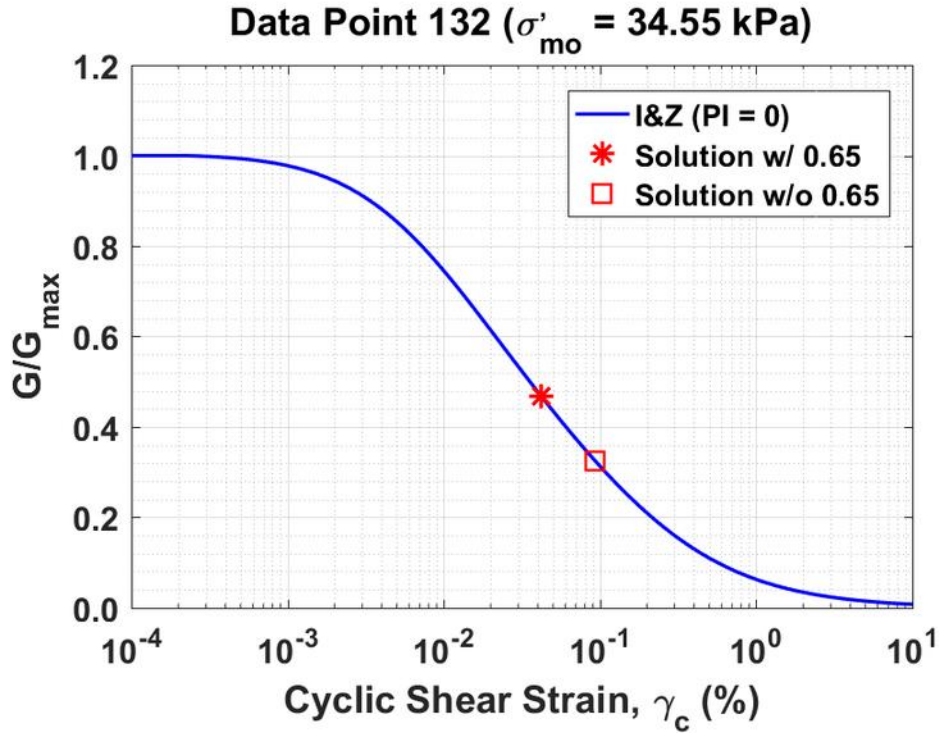


Figure B546. Normalized shear modulus reduction curves for Data Point 132 of the Boulanger et al. database showing the solutions w/ and w/o the 0.65 factor

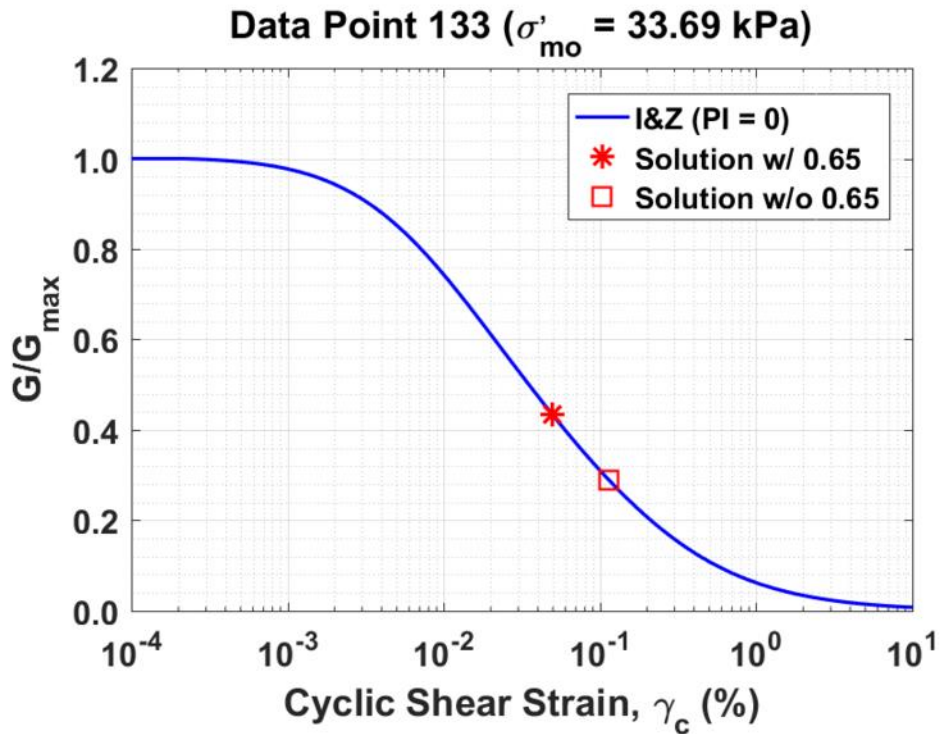


Figure B547. Normalized shear modulus reduction curves for Data Point 133 of the Boulanger et al. database showing the solutions w/ and w/o the 0.65 factor

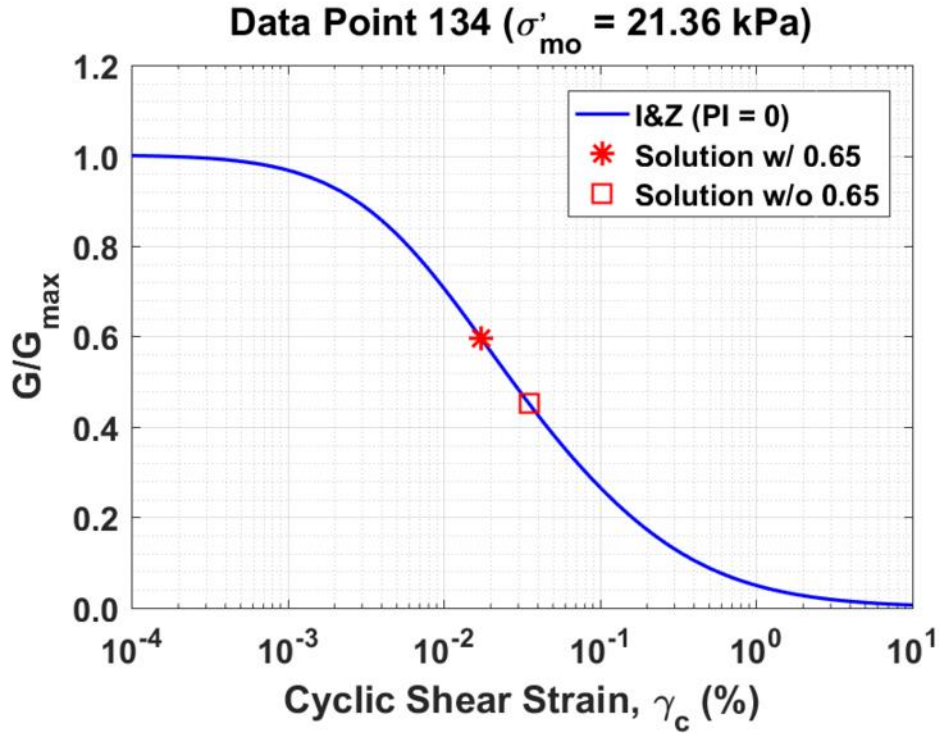


Figure B548. Normalized shear modulus reduction curves for Data Point 134 of the Boulanger et al. database showing the solutions w/ and w/o the 0.65 factor

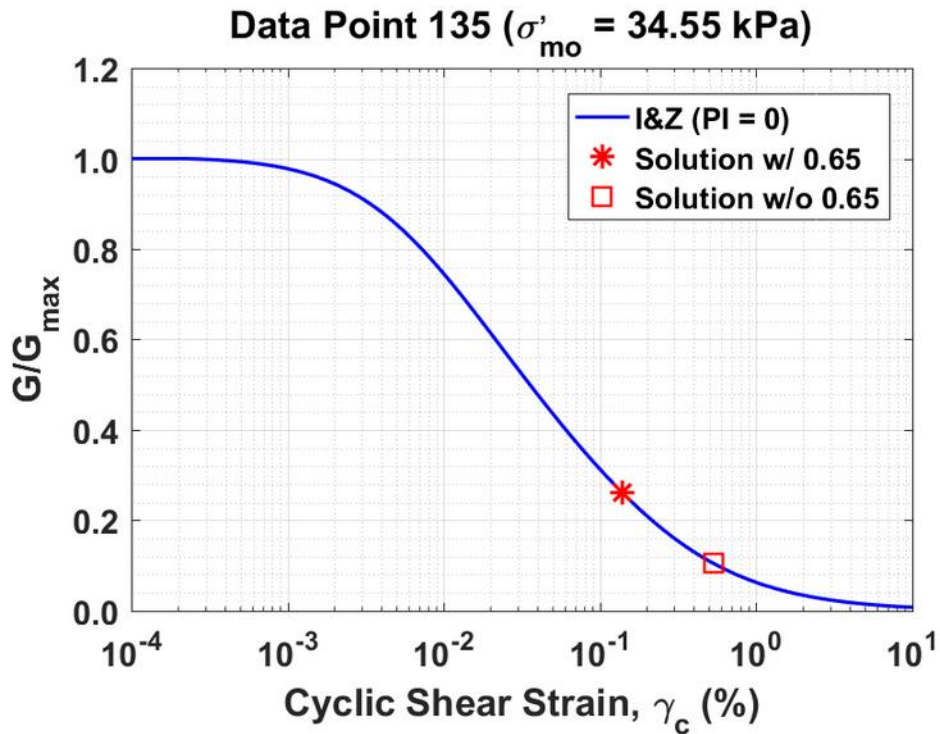


Figure B549. Normalized shear modulus reduction curves for Data Point 135 of the Boulanger et al. database showing the solutions w/ and w/o the 0.65 factor

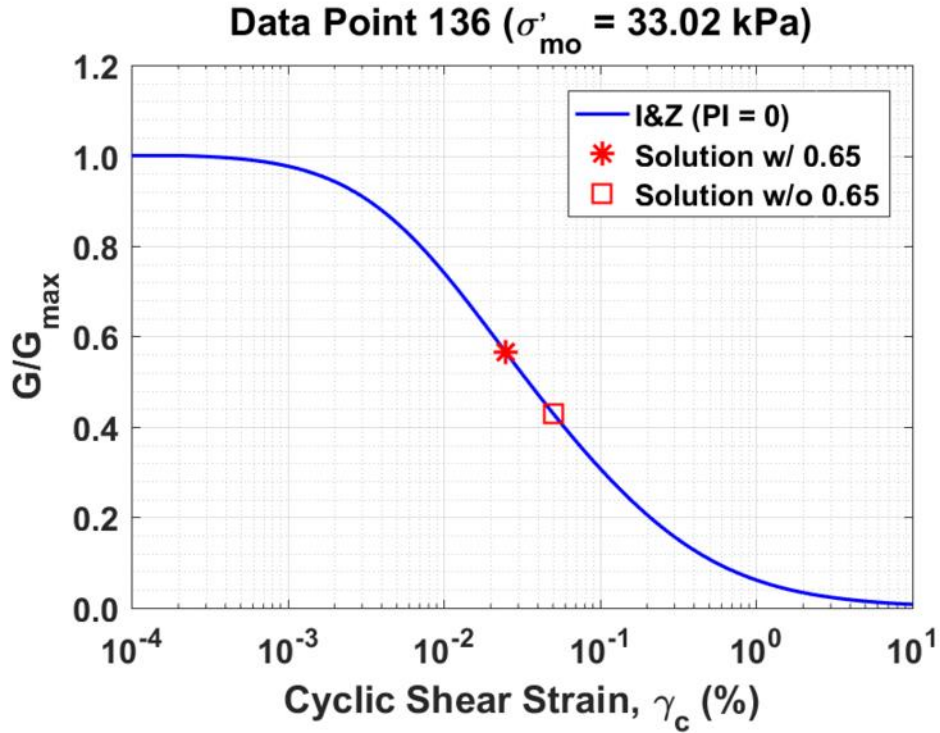


Figure B550. Normalized shear modulus reduction curves for Data Point 136 of the Boulanger et al. database showing the solutions w/ and w/o the 0.65 factor

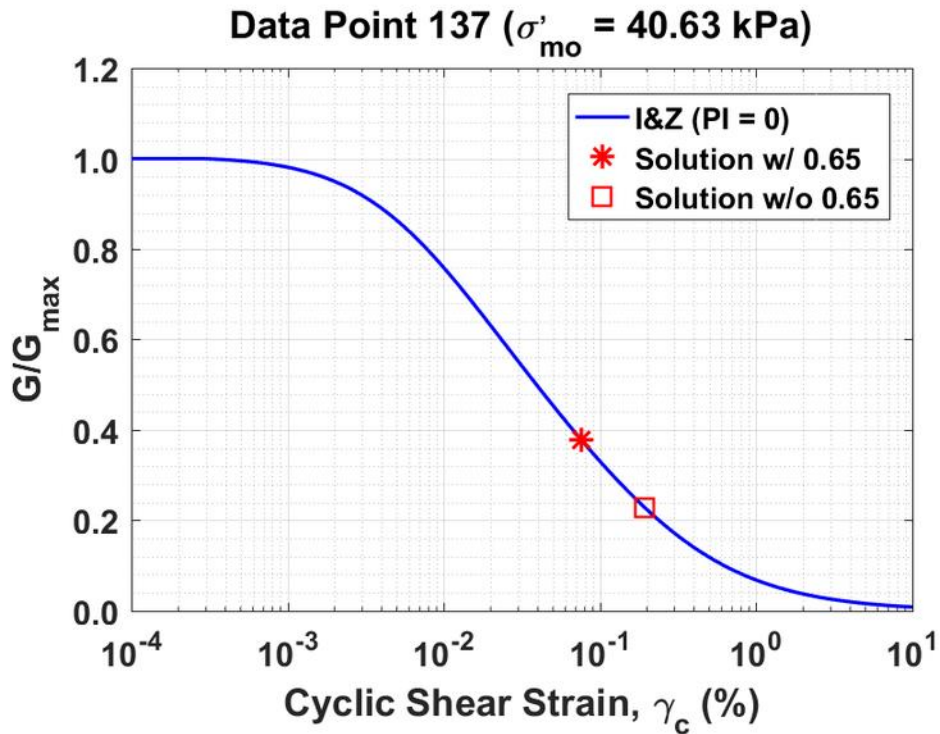


Figure B551. Normalized shear modulus reduction curves for Data Point 137 of the Boulanger et al. database showing the solutions w/ and w/o the 0.65 factor

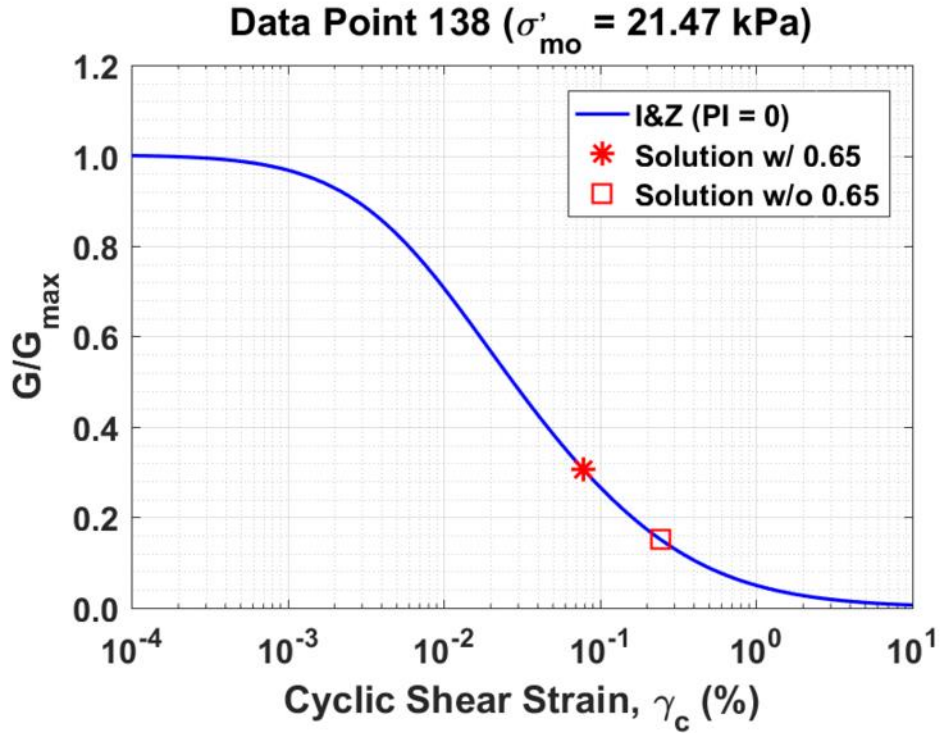


Figure B552. Normalized shear modulus reduction curves for Data Point 138 of the Boulanger et al. database showing the solutions w/ and w/o the 0.65 factor

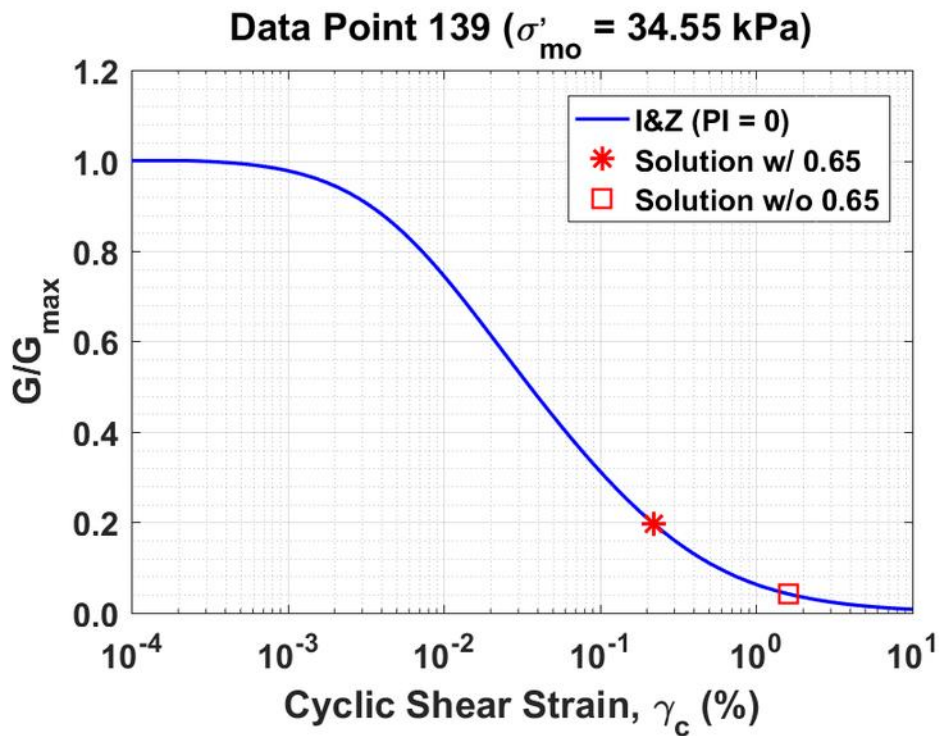


Figure B553. Normalized shear modulus reduction curves for Data Point 139 of the Boulanger et al. database showing the solutions w/ and w/o the 0.65 factor

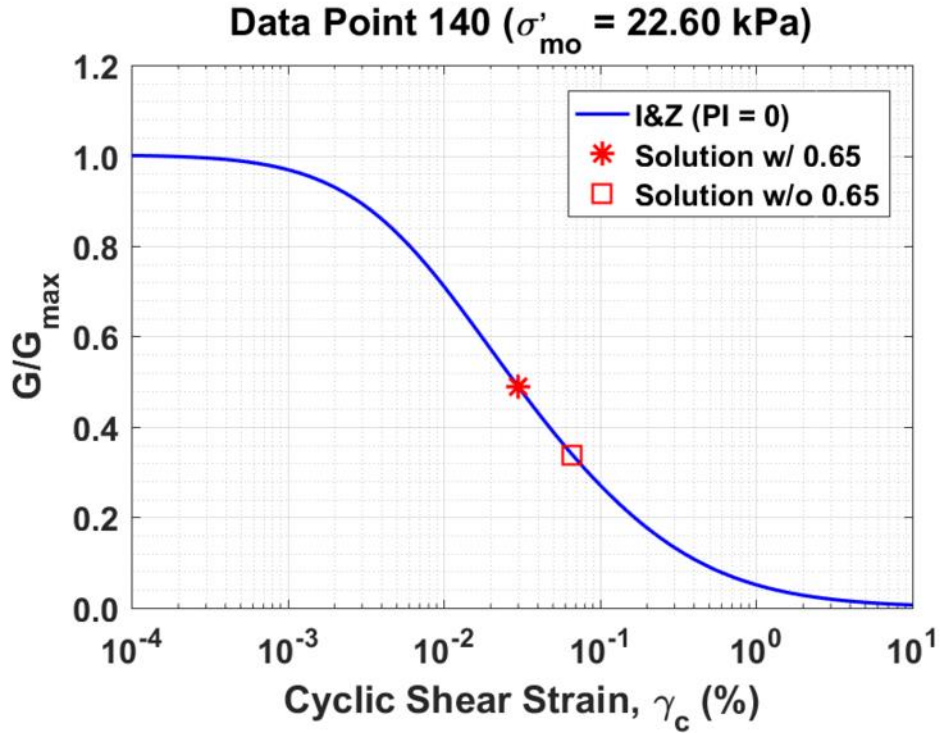


Figure B554. Normalized shear modulus reduction curves for Data Point 140 of the Boulanger et al. database showing the solutions w/ and w/o the 0.65 factor

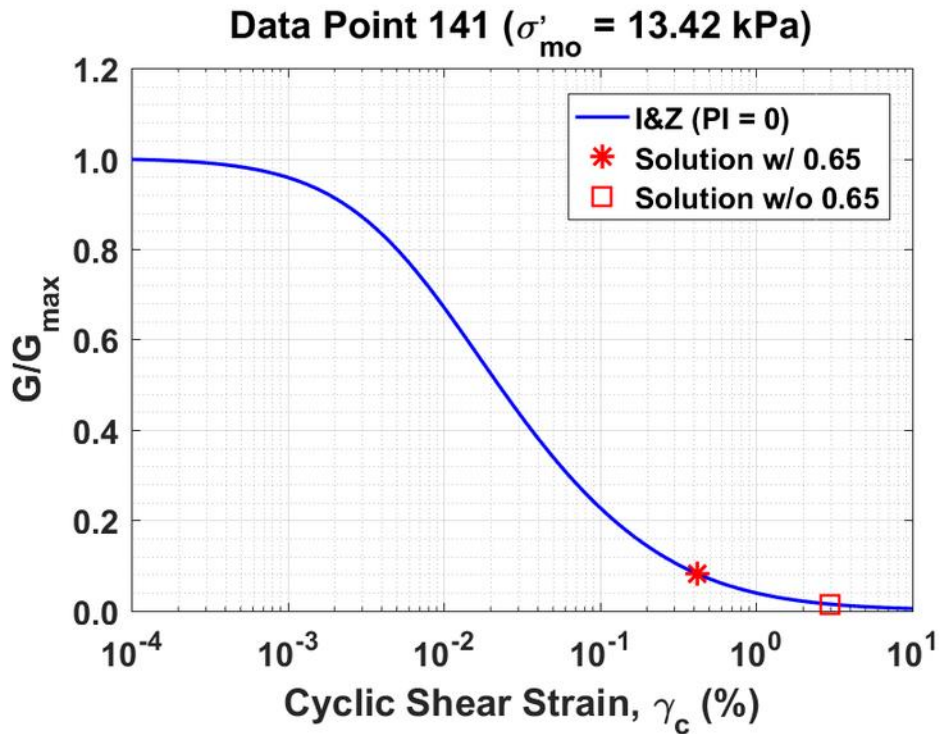


Figure B555. Normalized shear modulus reduction curves for Data Point 141 of the Boulanger et al. database showing the solutions w/ and w/o the 0.65 factor

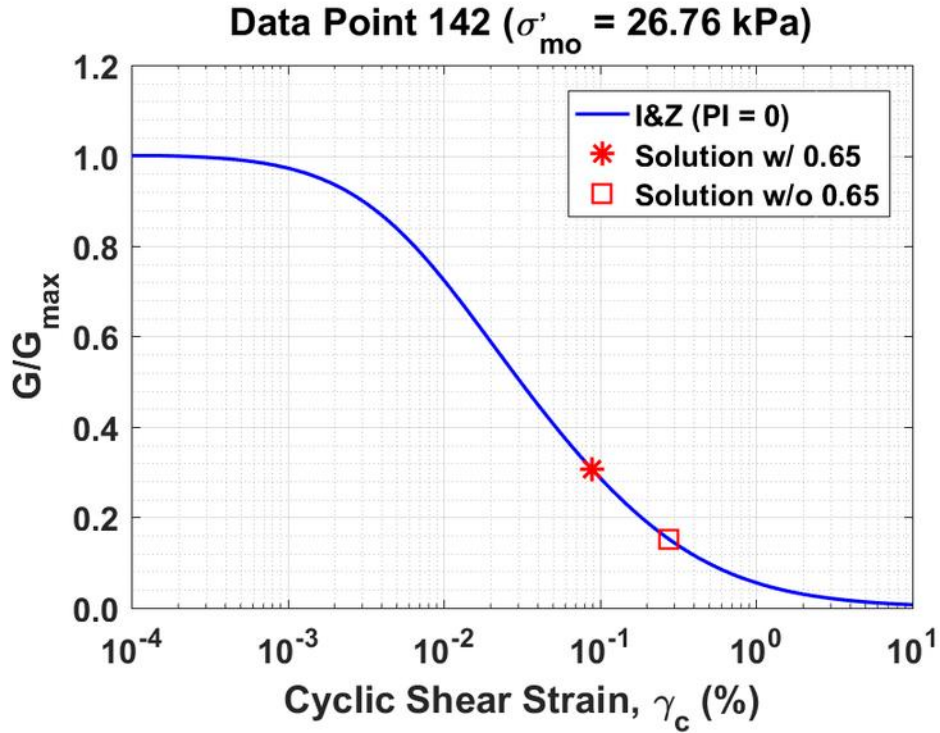


Figure B556. Normalized shear modulus reduction curves for Data Point 142 of the Boulanger et al. database showing the solutions w/ and w/o the 0.65 factor

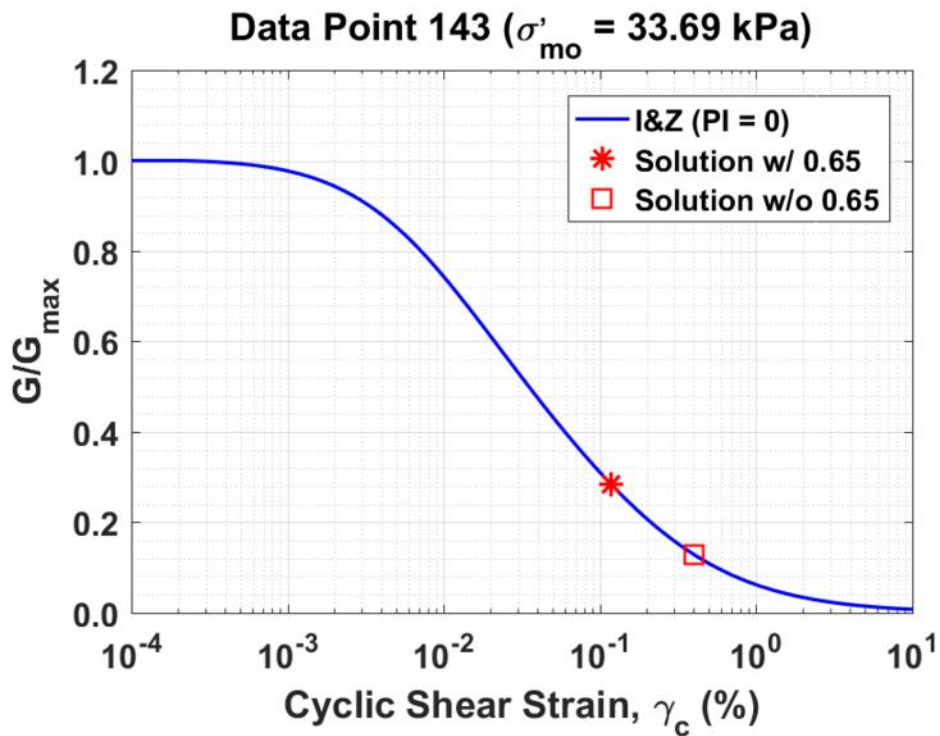


Figure B557. Normalized shear modulus reduction curves for Data Point 143 of the Boulanger et al. database showing the solutions w/ and w/o the 0.65 factor

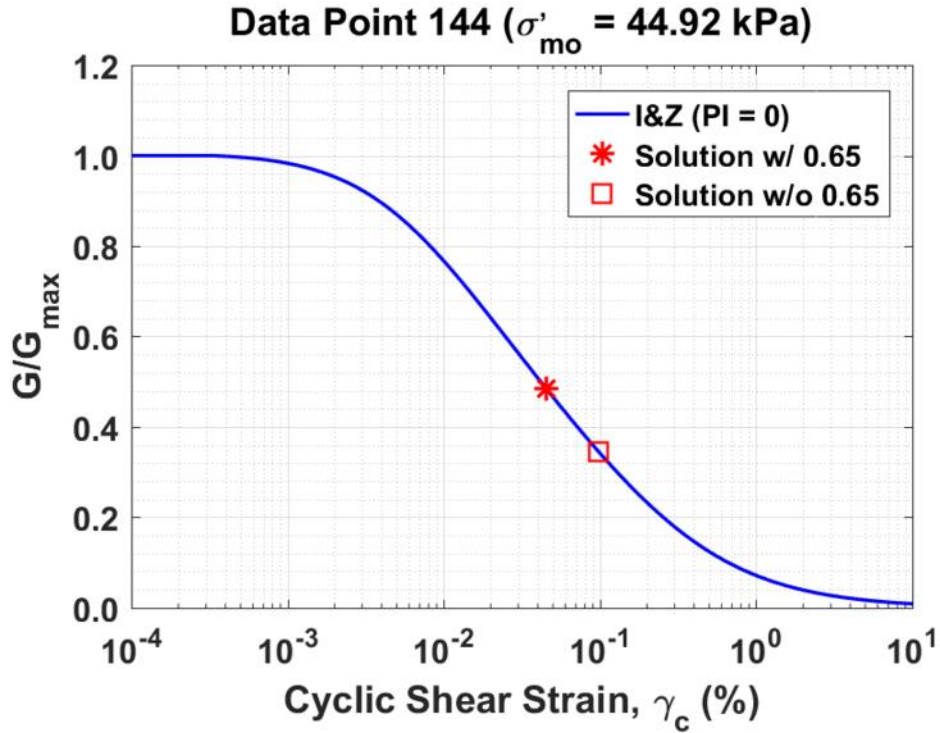


Figure B558. Normalized shear modulus reduction curves for Data Point 144 of the Boulanger et al. database showing the solutions w/ and w/o the 0.65 factor

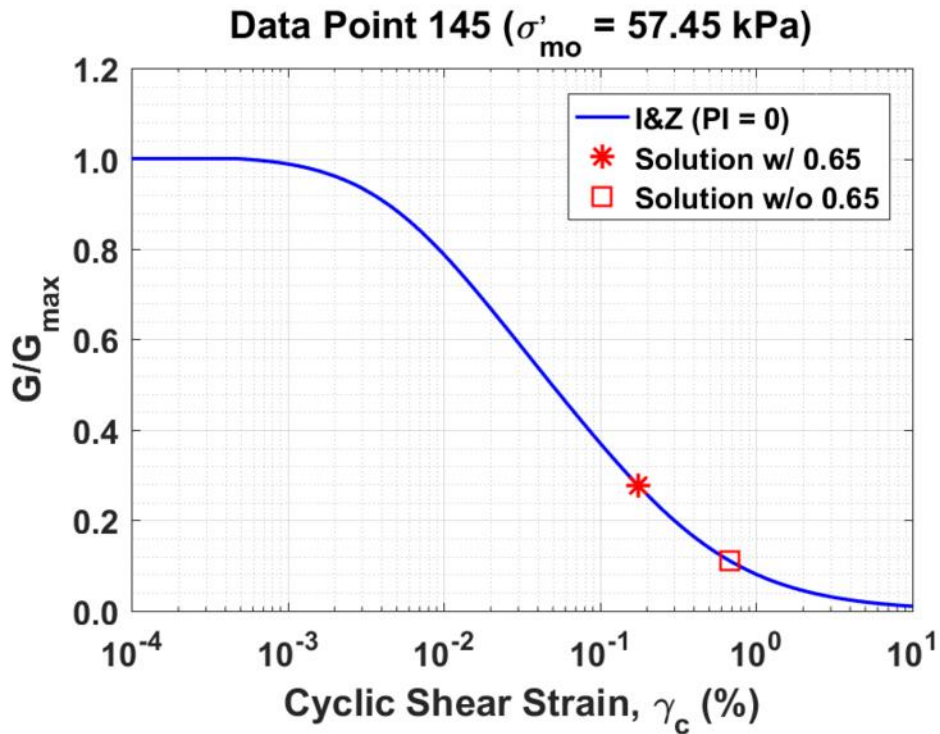


Figure B559. Normalized shear modulus reduction curves for Data Point 145 of the Boulanger et al. database showing the solutions w/ and w/o the 0.65 factor

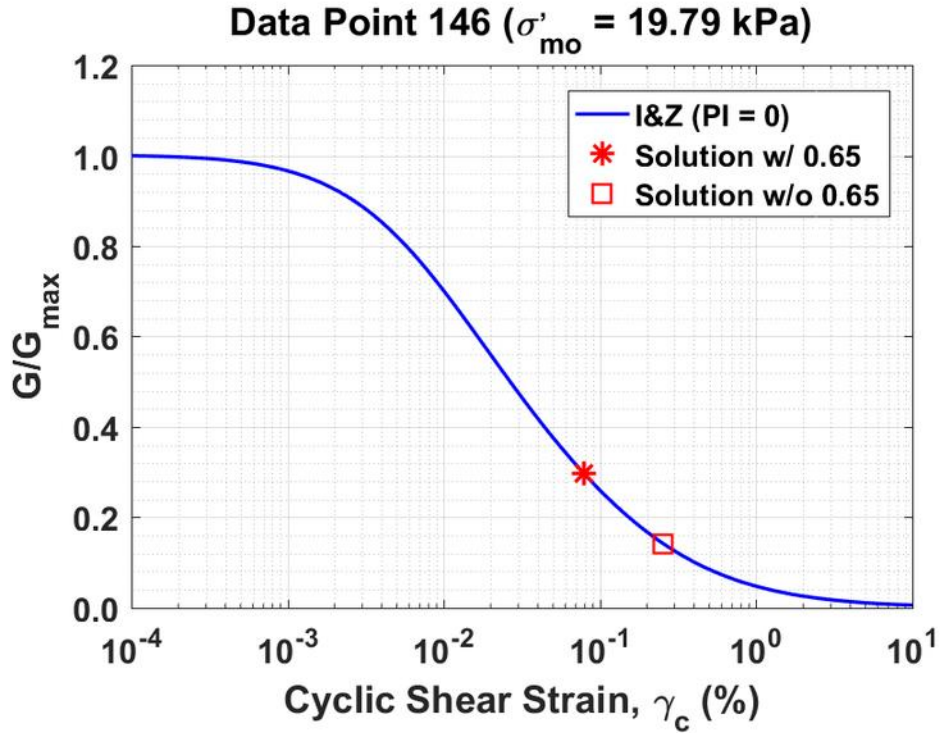


Figure B560. Normalized shear modulus reduction curves for Data Point 146 of the Boulanger et al. database showing the solutions w/ and w/o the 0.65 factor

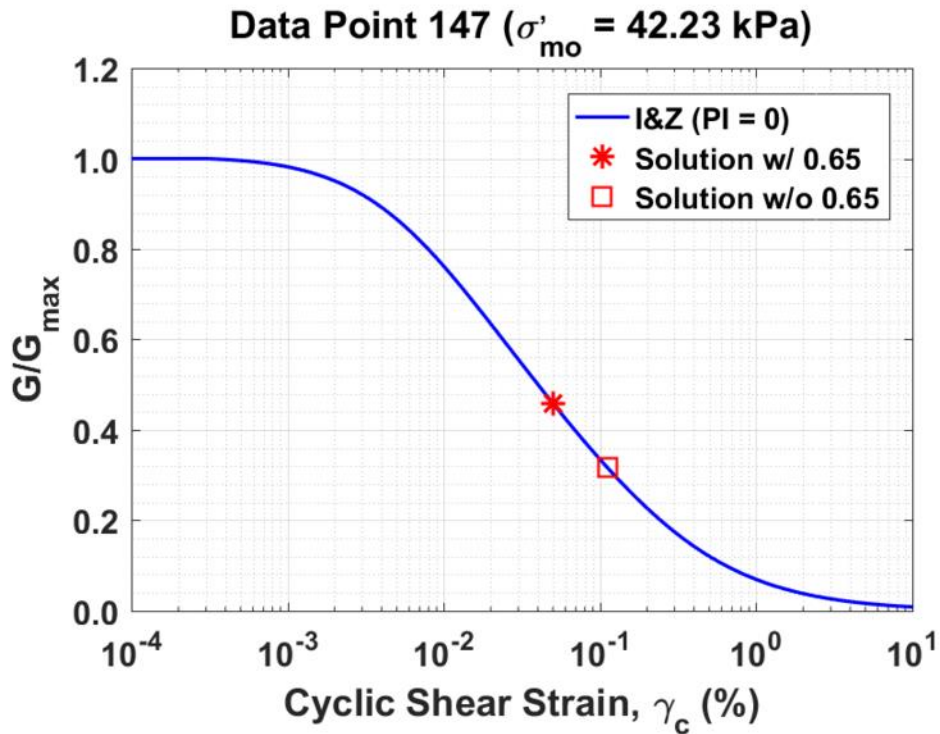


Figure B561. Normalized shear modulus reduction curves for Data Point 147 of the Boulanger et al. database showing the solutions w/ and w/o the 0.65 factor

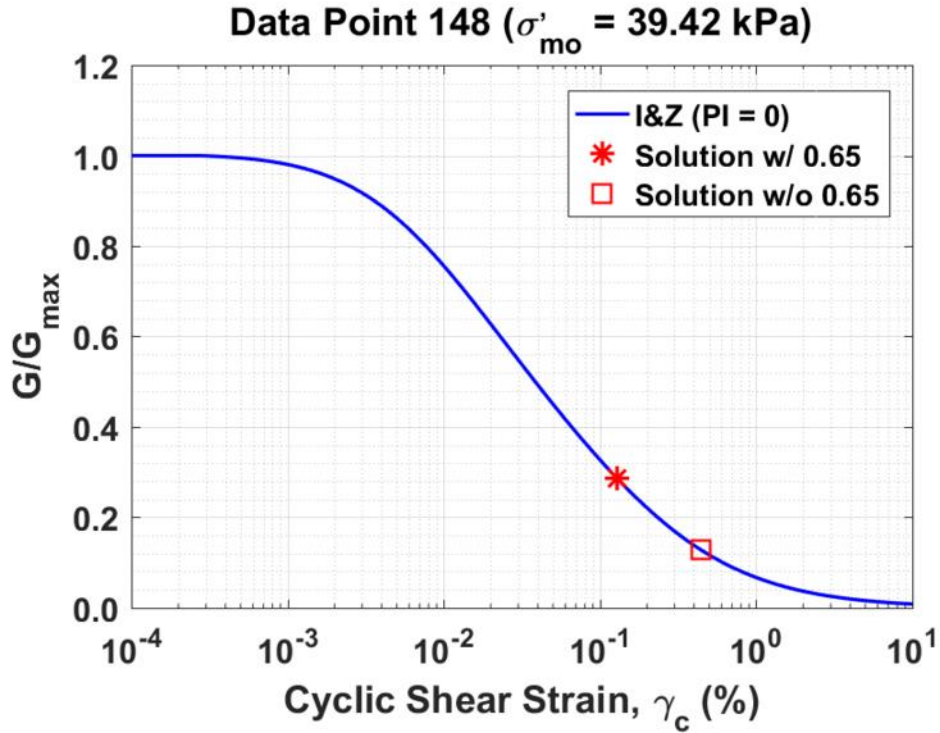


Figure B562. Normalized shear modulus reduction curves for Data Point 148 of the Boulanger et al. database showing the solutions w/ and w/o the 0.65 factor

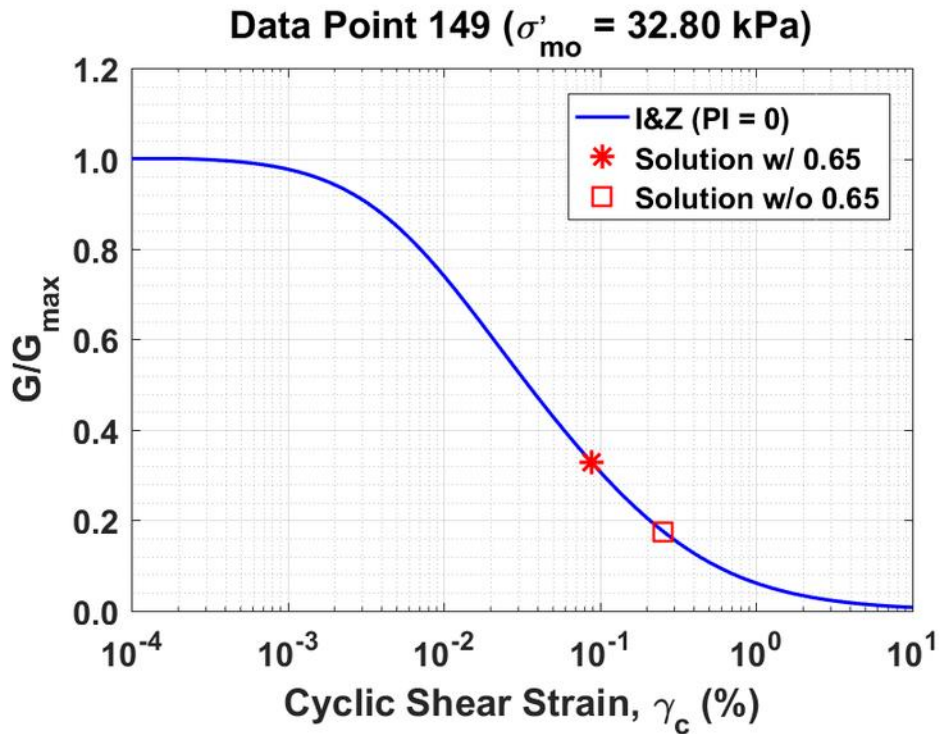


Figure B563. Normalized shear modulus reduction curves for Data Point 149 of the Boulanger et al. database showing the solutions w/ and w/o the 0.65 factor

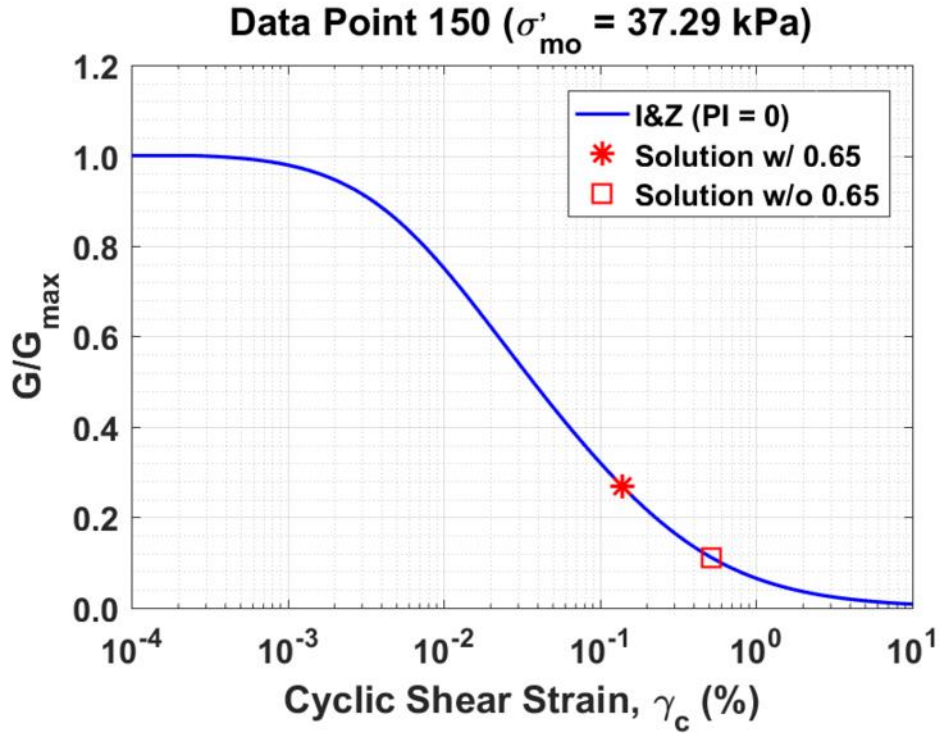


Figure B564. Normalized shear modulus reduction curves for Data Point 150 of the Boulanger et al. database showing the solutions w/ and w/o the 0.65 factor

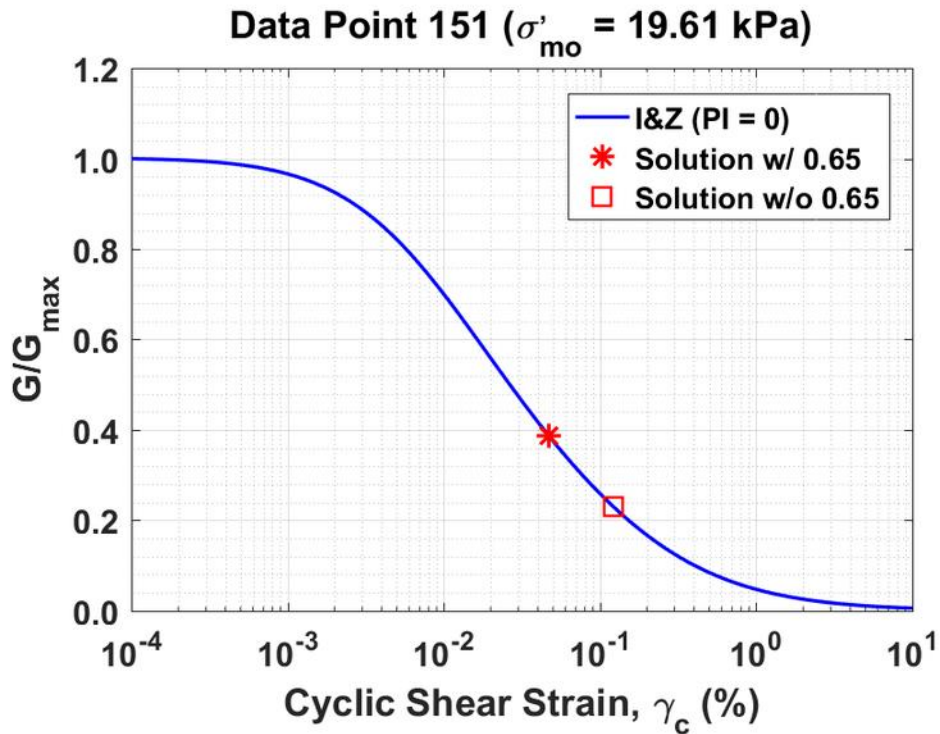


Figure B565. Normalized shear modulus reduction curves for Data Point 151 of the Boulanger et al. database showing the solutions w/ and w/o the 0.65 factor

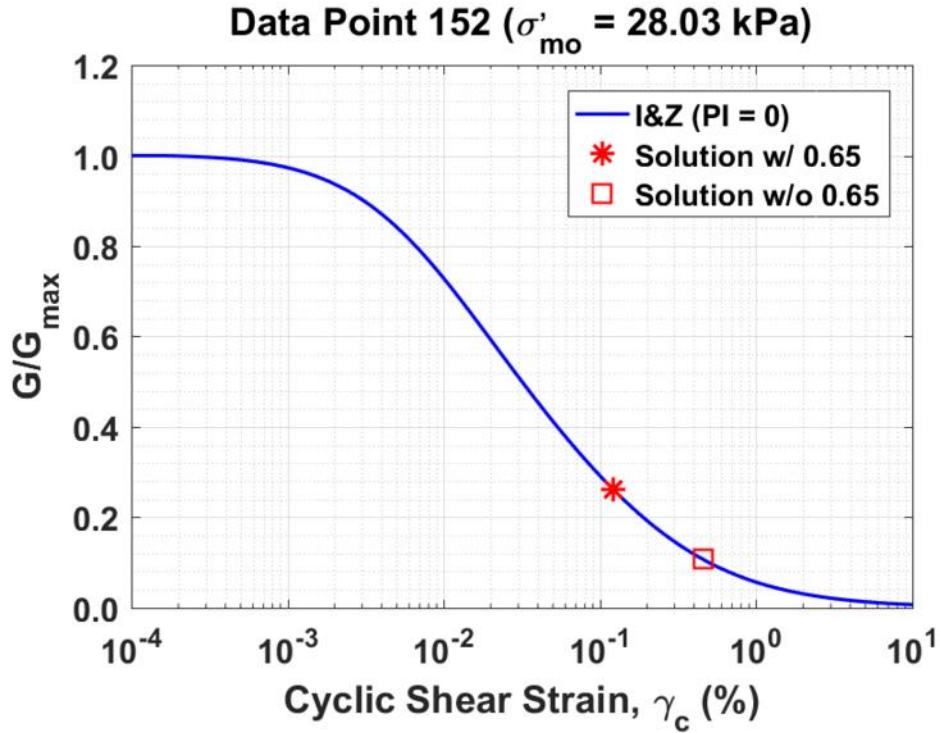


Figure B566. Normalized shear modulus reduction curves for Data Point 152 of the Boulanger et al. database showing the solutions w/ and w/o the 0.65 factor

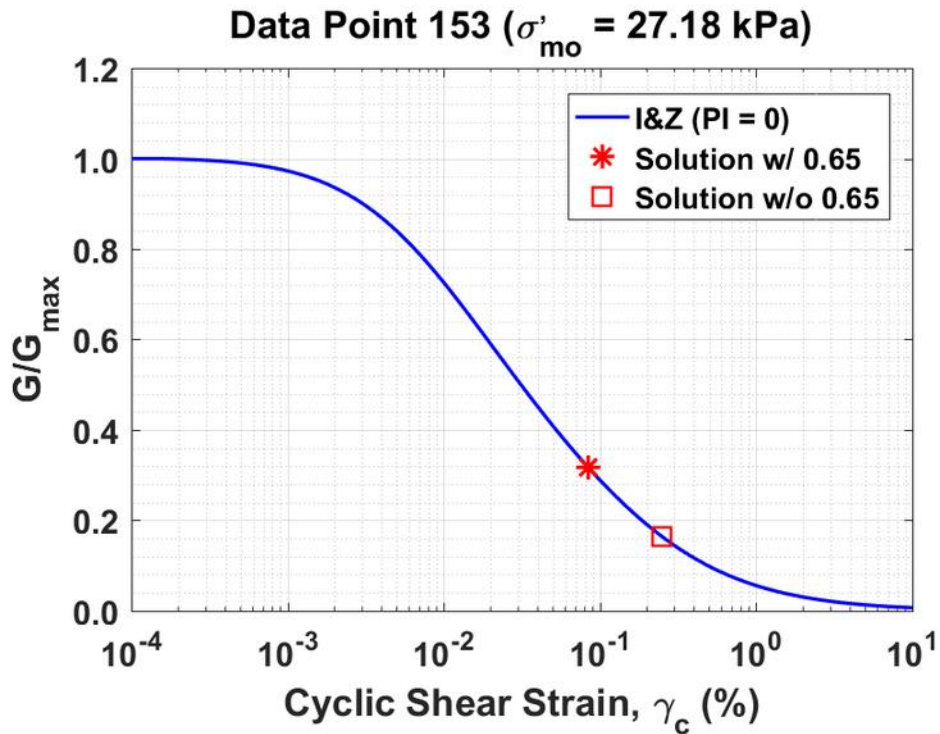


Figure B567. Normalized shear modulus reduction curves for Data Point 153 of the Boulanger et al. database showing the solutions w/ and w/o the 0.65 factor

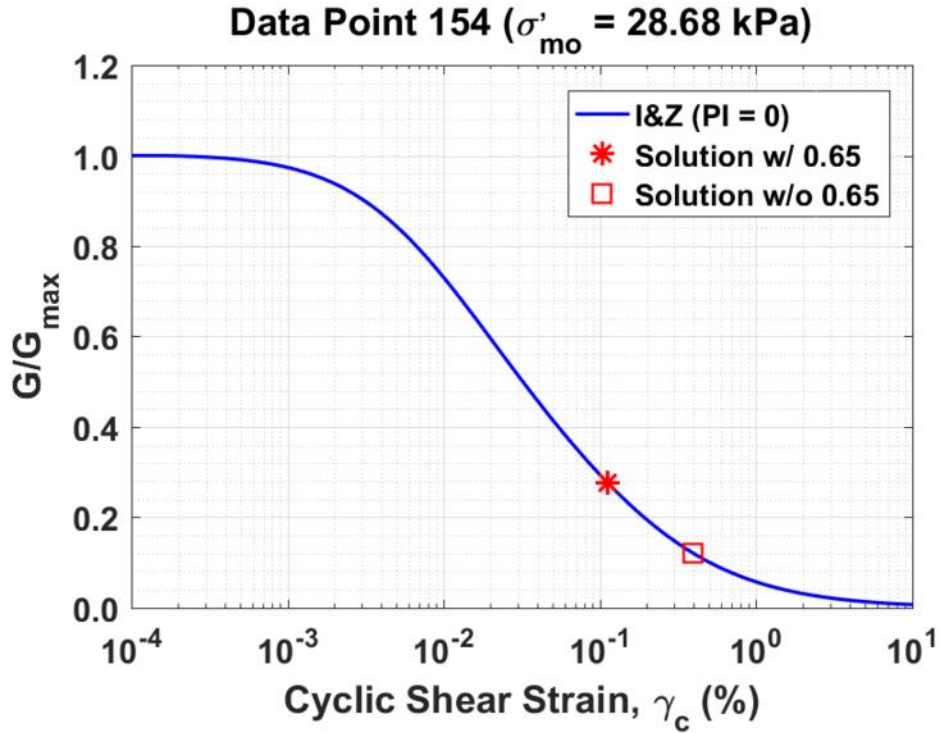


Figure B568. Normalized shear modulus reduction curves for Data Point 154 of the Boulanger et al. database showing the solutions w/ and w/o the 0.65 factor

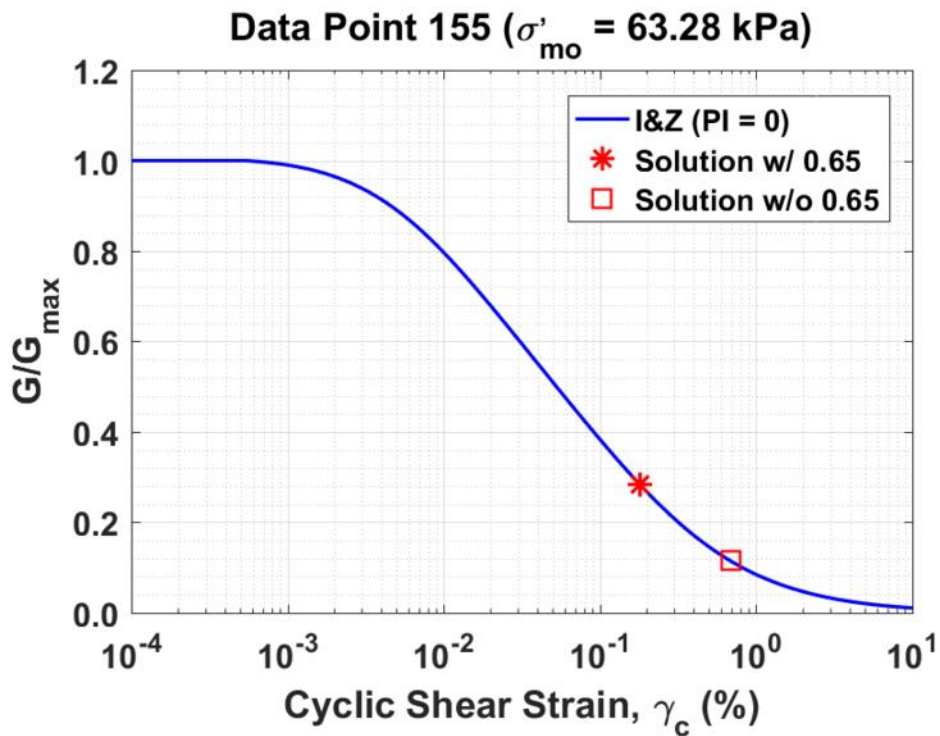


Figure B569. Normalized shear modulus reduction curves for Data Point 155 of the Boulanger et al. database showing the solutions w/ and w/o the 0.65 factor

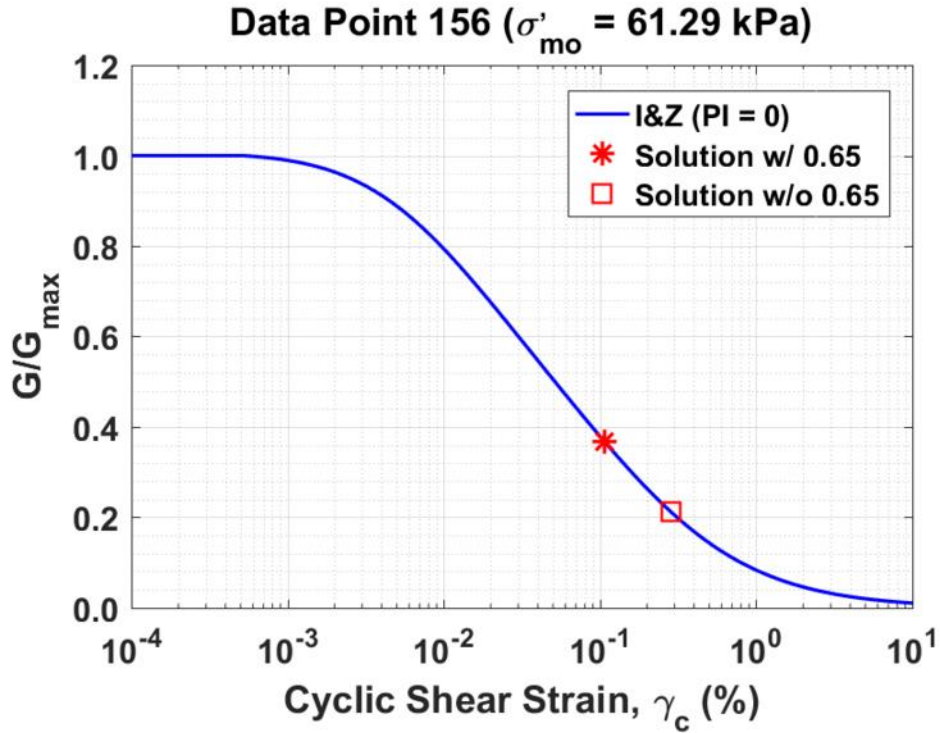


Figure B570. Normalized shear modulus reduction curves for Data Point 156 of the Boulanger et al. database showing the solutions w/ and w/o the 0.65 factor

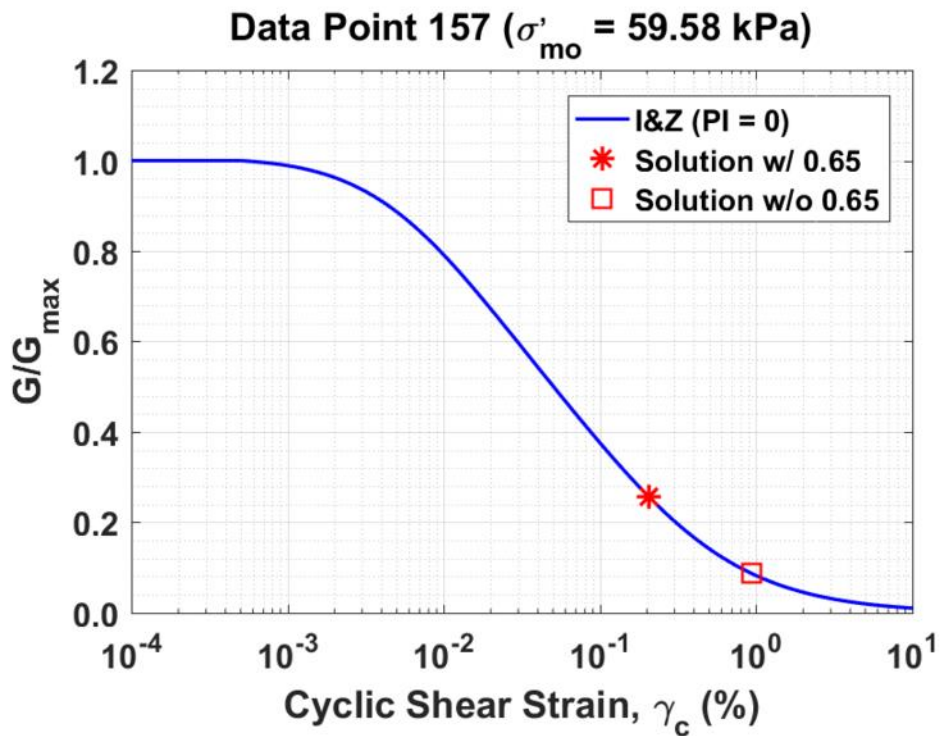


Figure B571. Normalized shear modulus reduction curves for Data Point 157 of the Boulanger et al. database showing the solutions w/ and w/o the 0.65 factor

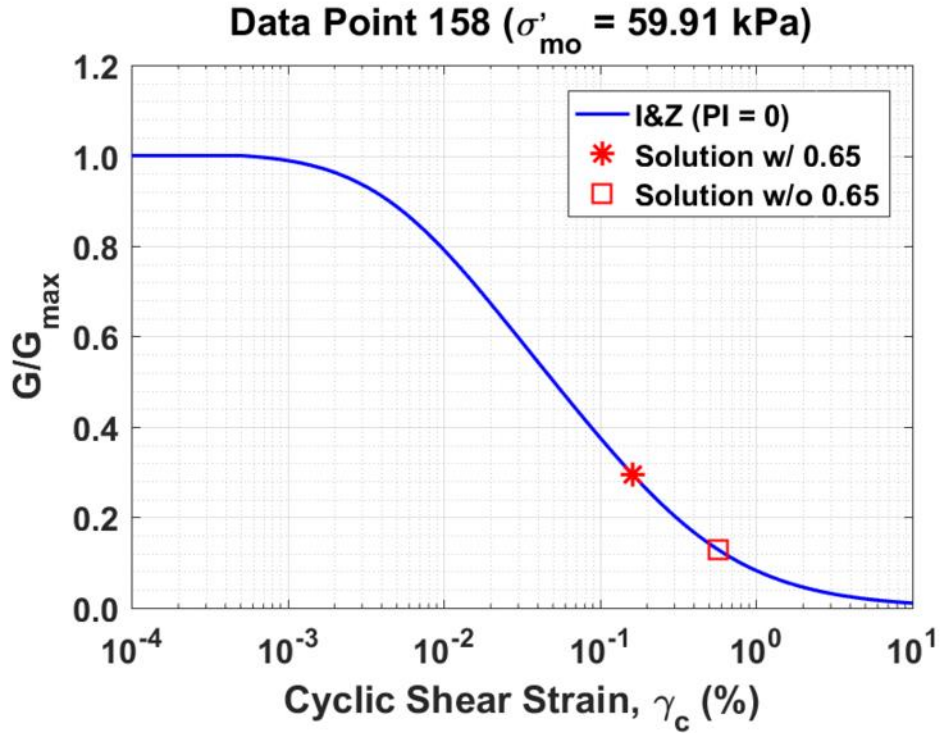


Figure B572. Normalized shear modulus reduction curves for Data Point 158 of the Boulanger et al. database showing the solutions w/ and w/o the 0.65 factor

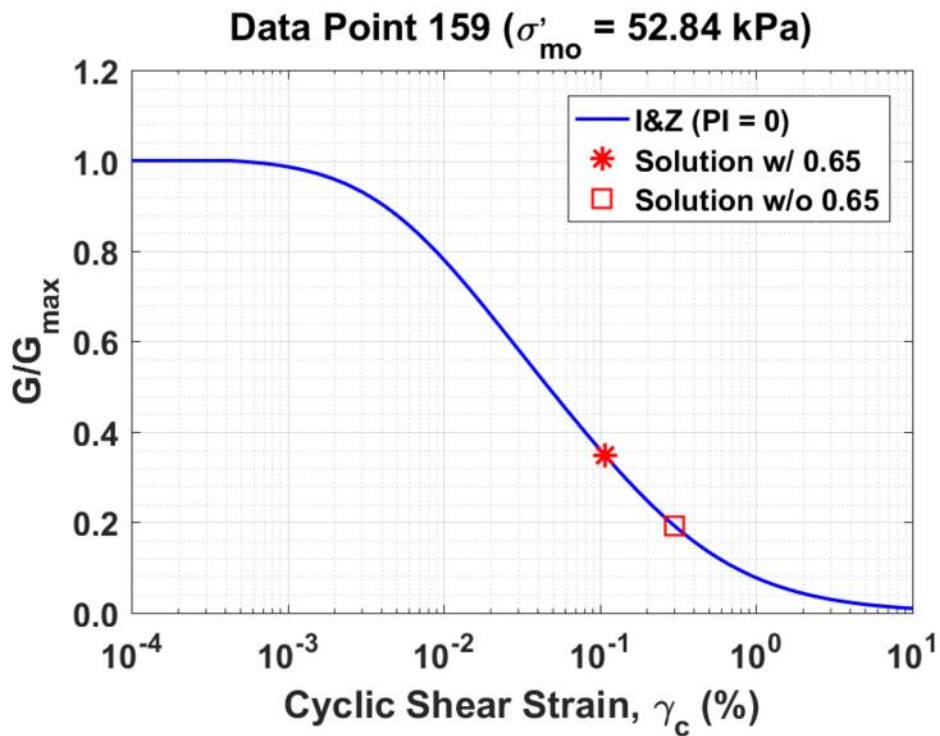


Figure B573. Normalized shear modulus reduction curves for Data Point 159 of the Boulanger et al. database showing the solutions w/ and w/o the 0.65 factor

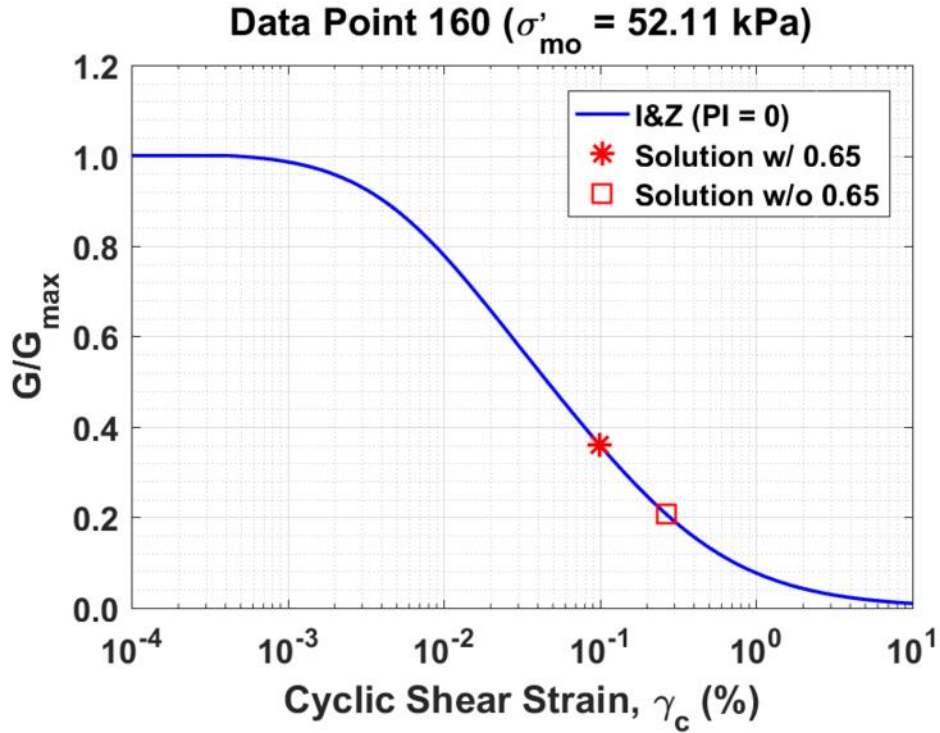


Figure B574. Normalized shear modulus reduction curves for Data Point 160 of the Boulanger et al. database showing the solutions w/ and w/o the 0.65 factor

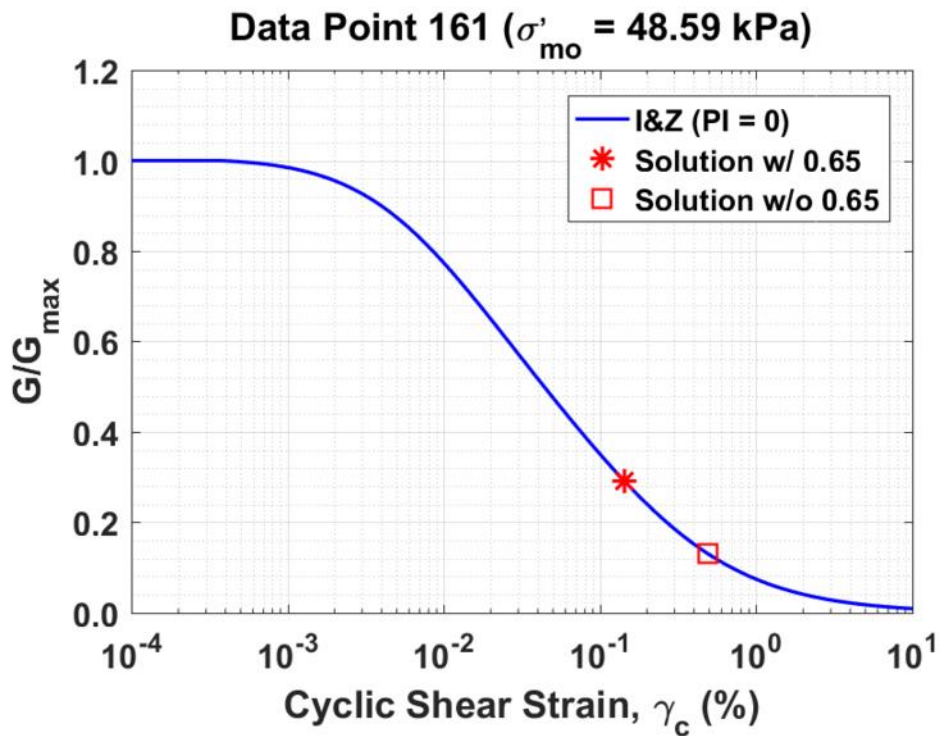


Figure B575. Normalized shear modulus reduction curves for Data Point 161 of the Boulanger et al. database showing the solutions w/ and w/o the 0.65 factor

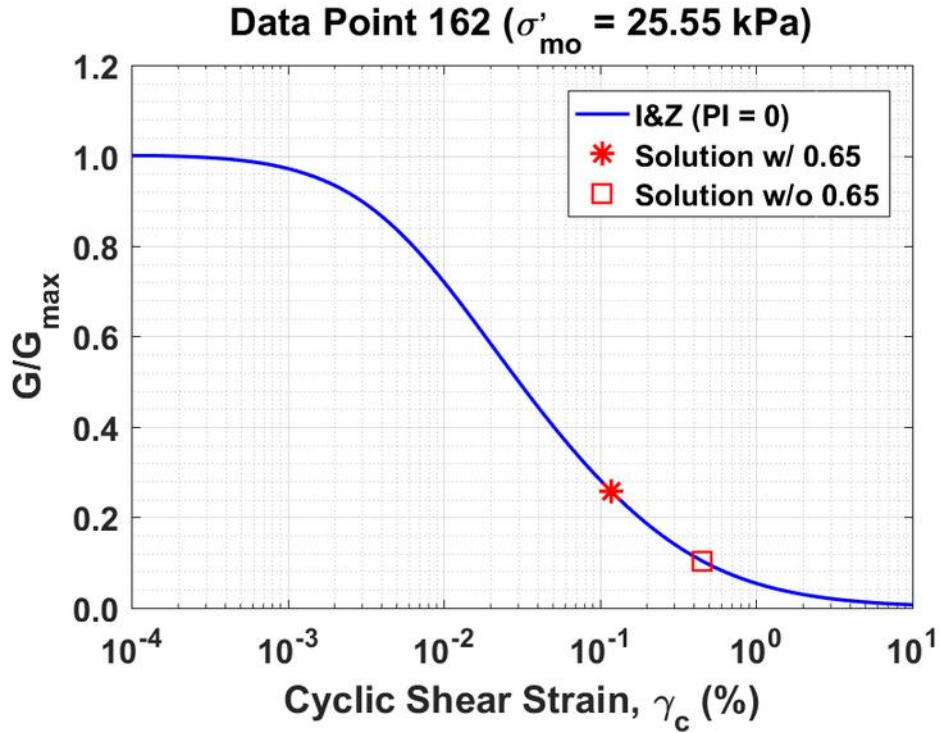


Figure B576. Normalized shear modulus reduction curves for Data Point 162 of the Boulanger et al. database showing the solutions w/ and w/o the 0.65 factor

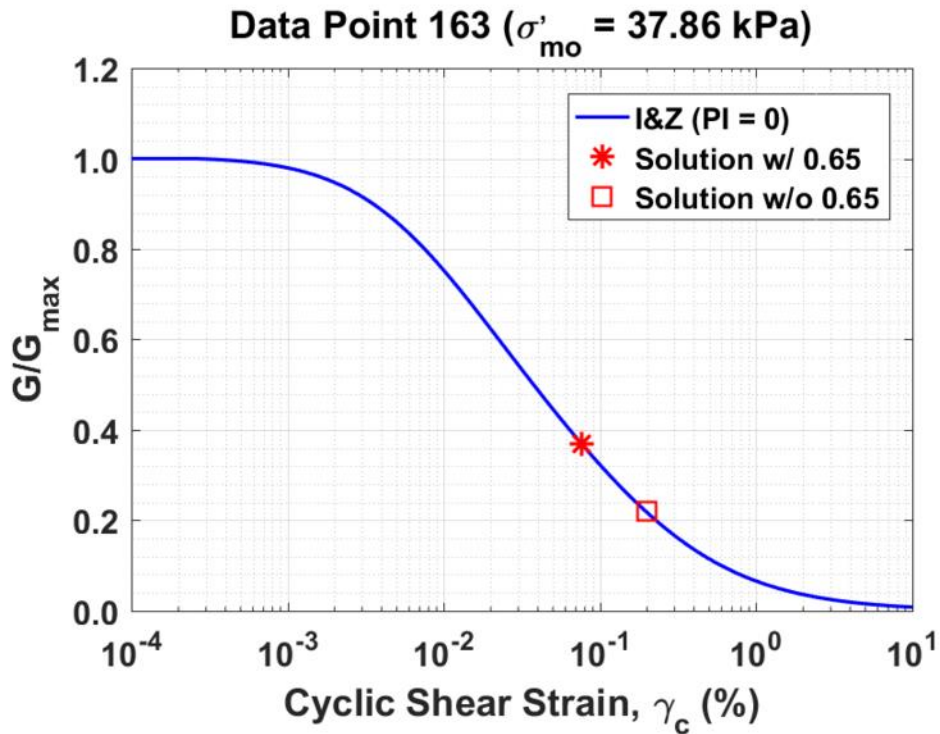


Figure B577. Normalized shear modulus reduction curves for Data Point 163 of the Boulanger et al. database showing the solutions w/ and w/o the 0.65 factor

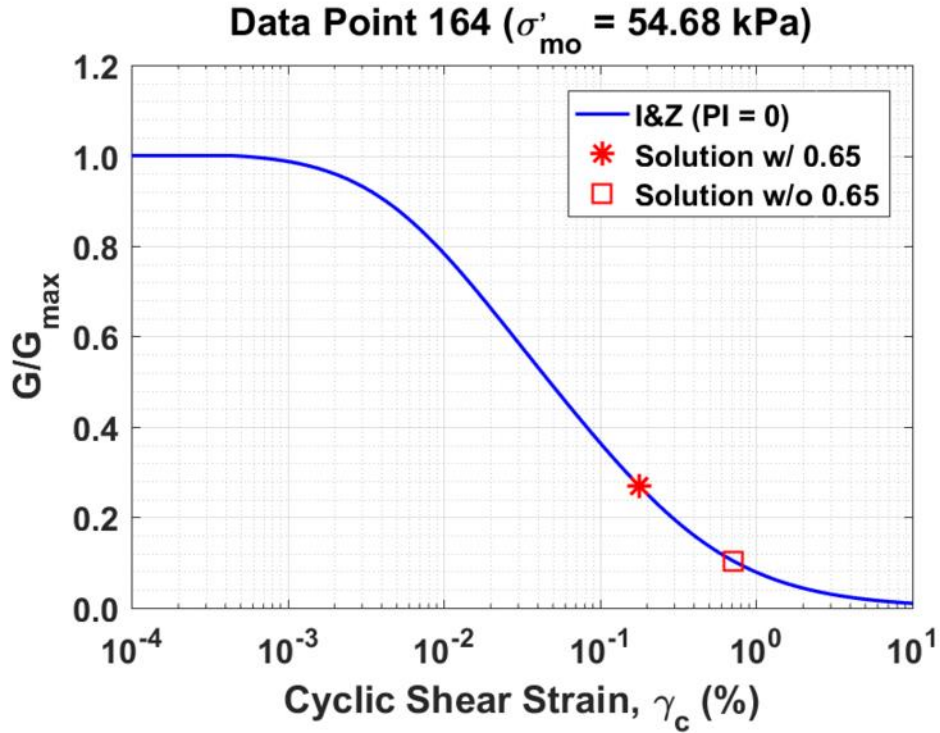


Figure B578. Normalized shear modulus reduction curves for Data Point 164 of the Boulanger et al. database showing the solutions w/ and w/o the 0.65 factor

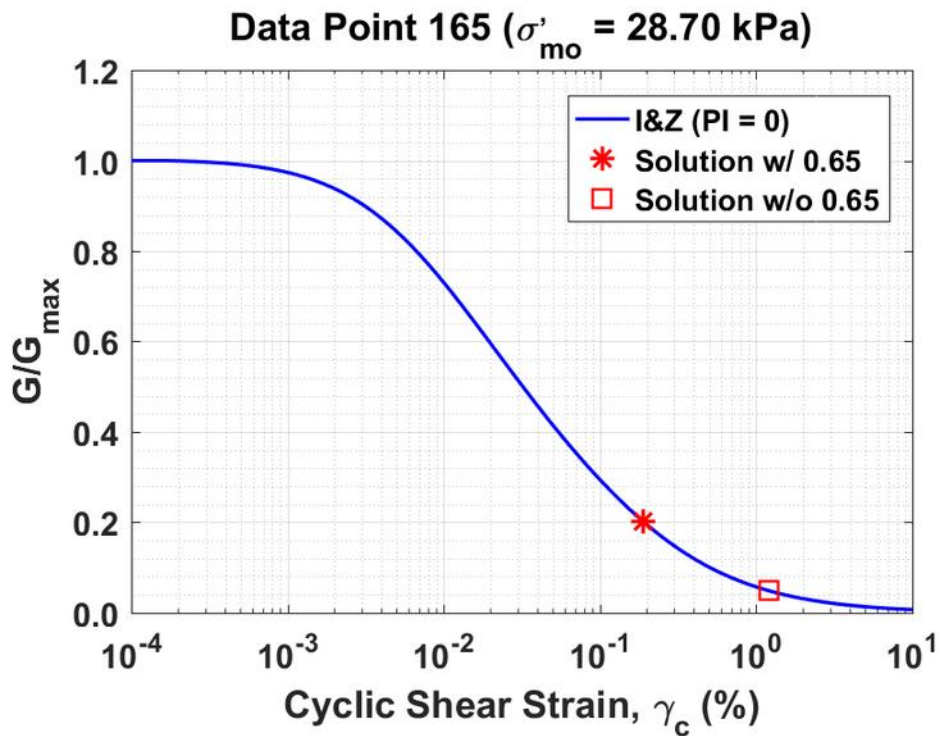


Figure B579. Normalized shear modulus reduction curves for Data Point 165 of the Boulanger et al. database showing the solutions w/ and w/o the 0.65 factor

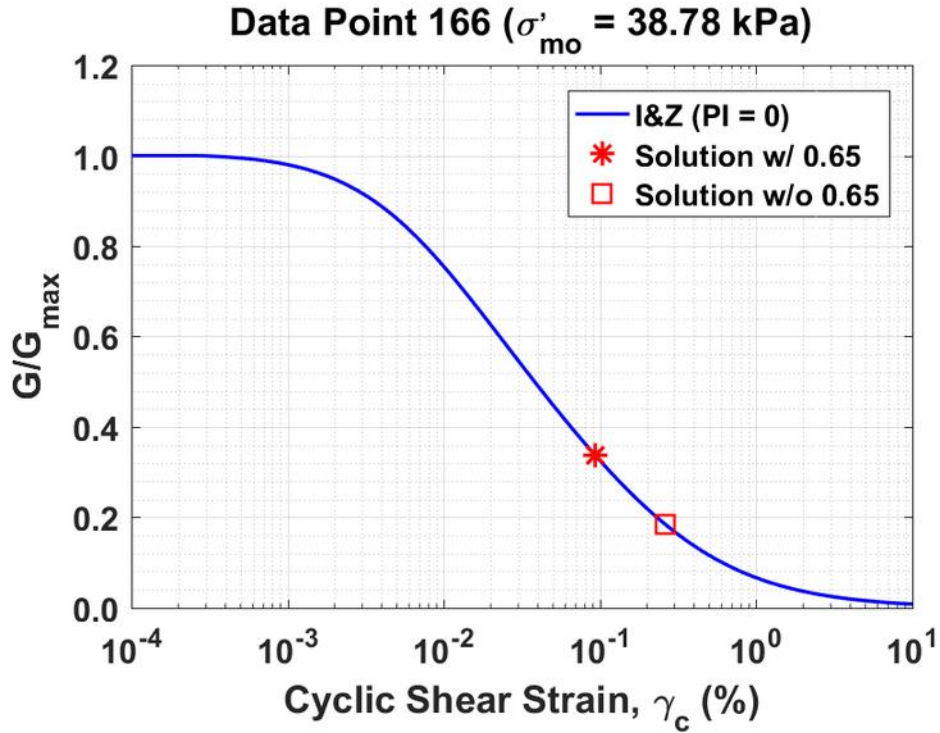


Figure B580. Normalized shear modulus reduction curves for Data Point 166 of the Boulanger et al. database showing the solutions w/ and w/o the 0.65 factor

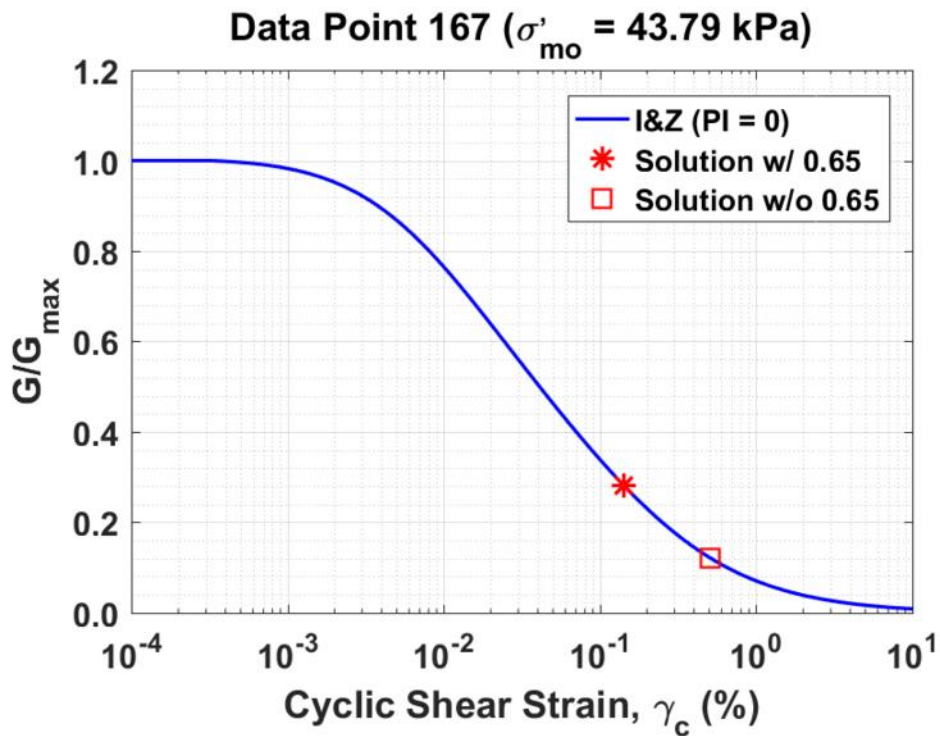


Figure B581. Normalized shear modulus reduction curves for Data Point 167 of the Boulanger et al. database showing the solutions w/ and w/o the 0.65 factor

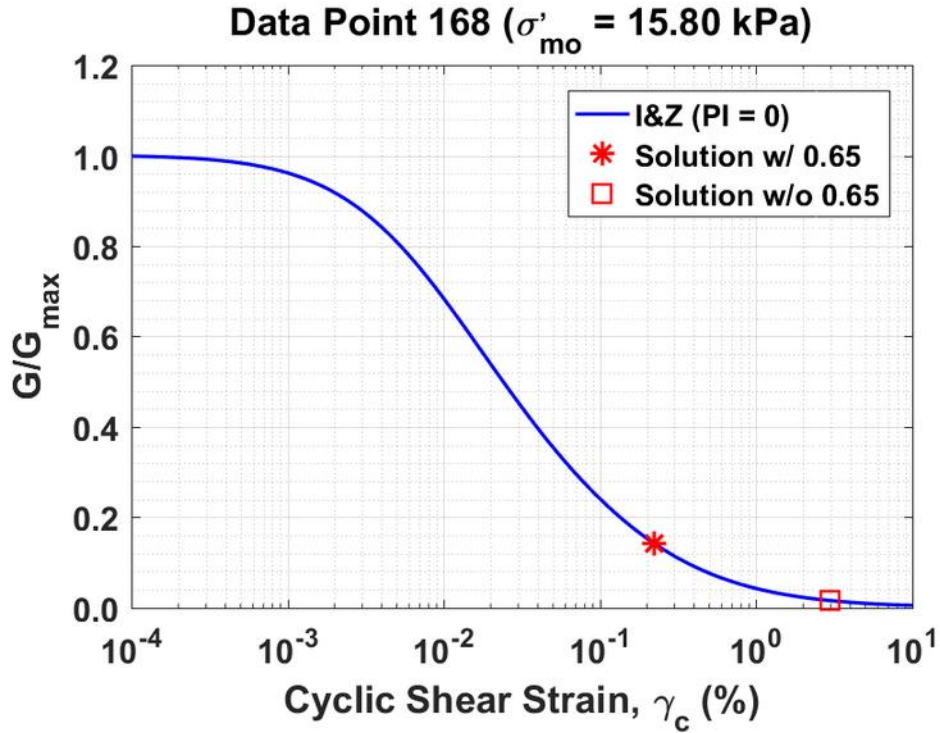


Figure B582. Normalized shear modulus reduction curves for Data Point 168 of the Boulanger et al. database showing the solutions w/ and w/o the 0.65 factor

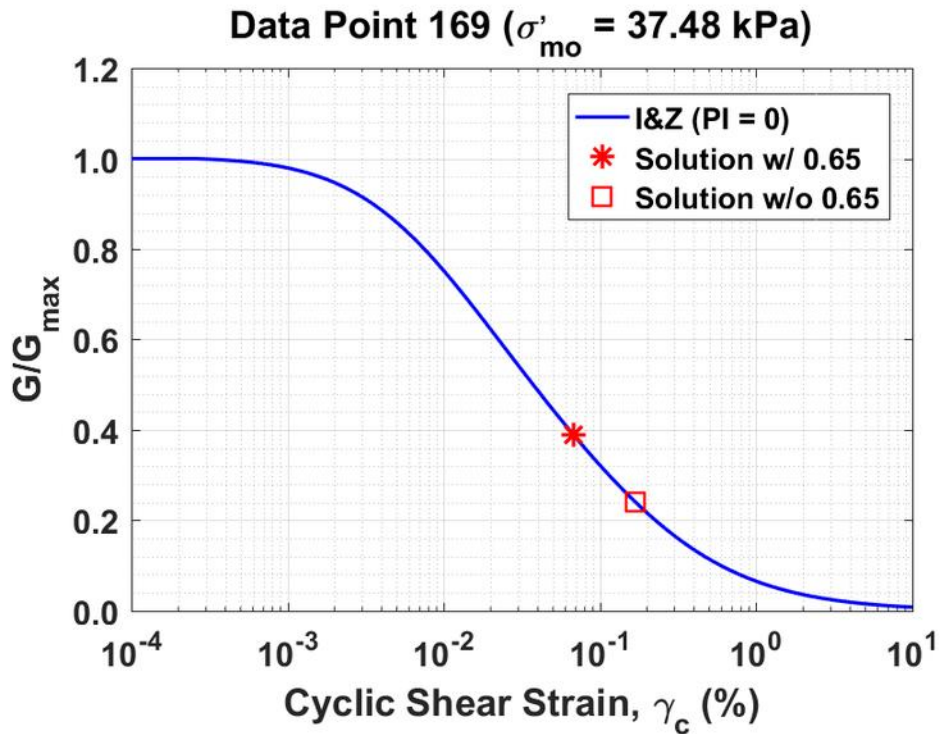


Figure B583. Normalized shear modulus reduction curves for Data Point 169 of the Boulanger et al. database showing the solutions w/ and w/o the 0.65 factor

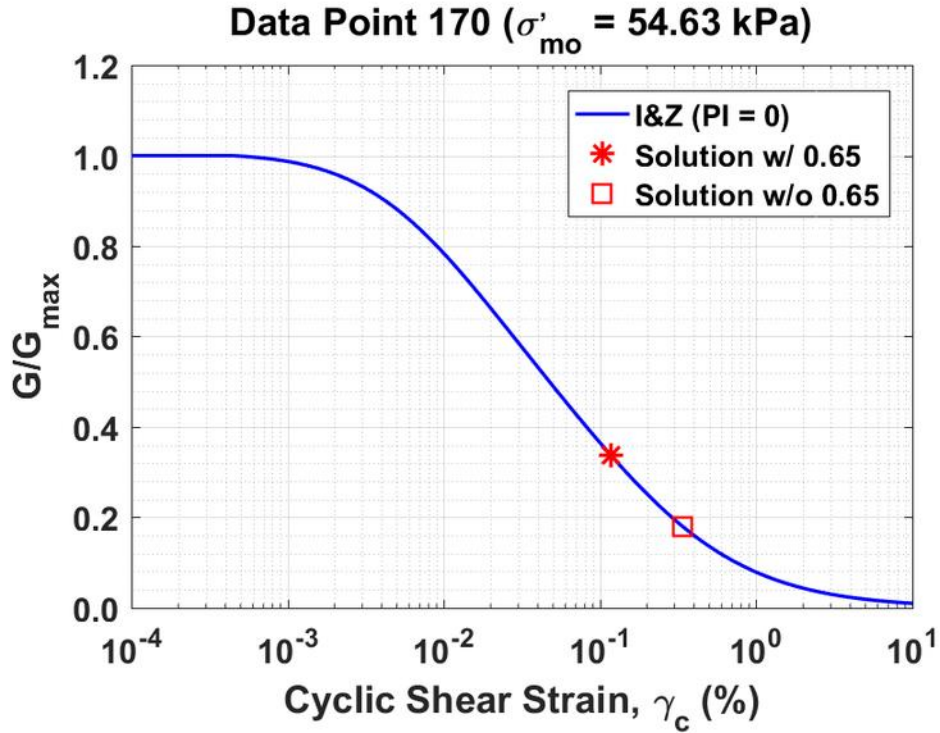


Figure B584. Normalized shear modulus reduction curves for Data Point 170 of the Boulanger et al. database showing the solutions w/ and w/o the 0.65 factor

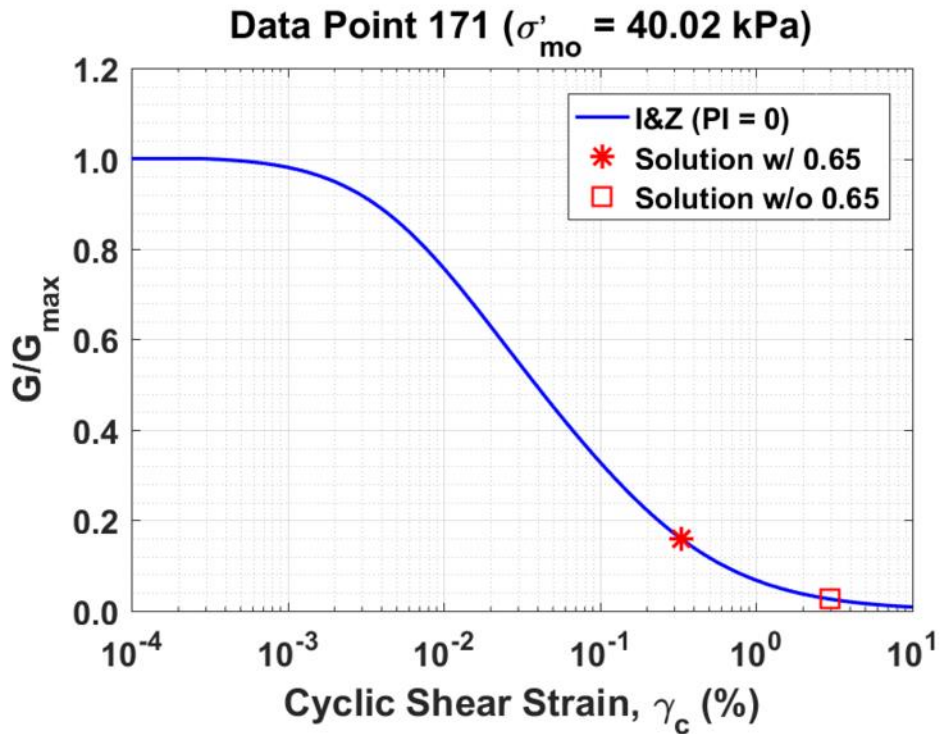


Figure B585. Normalized shear modulus reduction curves for Data Point 171 of the Boulanger et al. database showing the solutions w/ and w/o the 0.65 factor

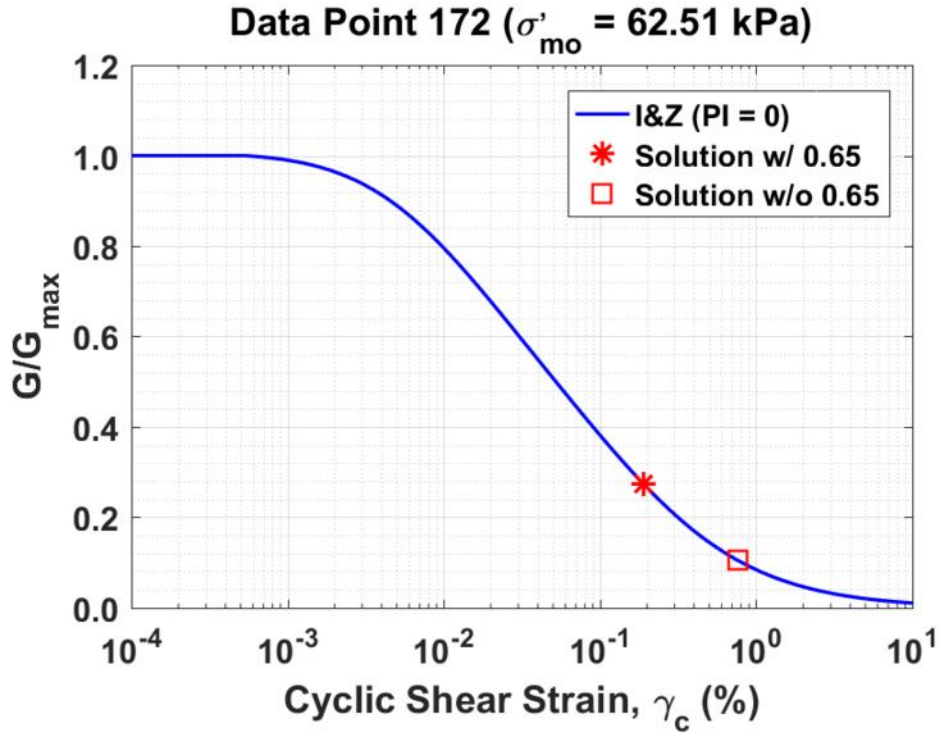


Figure B586. Normalized shear modulus reduction curves for Data Point 172 of the Boulanger et al. database showing the solutions w/ and w/o the 0.65 factor

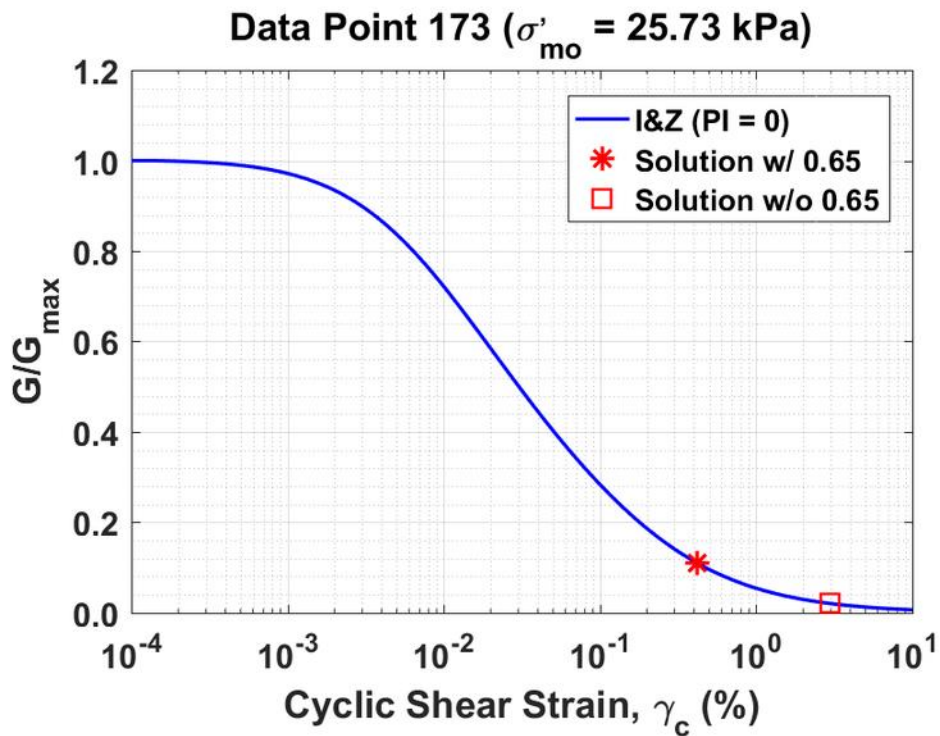


Figure B587. Normalized shear modulus reduction curves for Data Point 173 of the Boulanger et al. database showing the solutions w/ and w/o the 0.65 factor

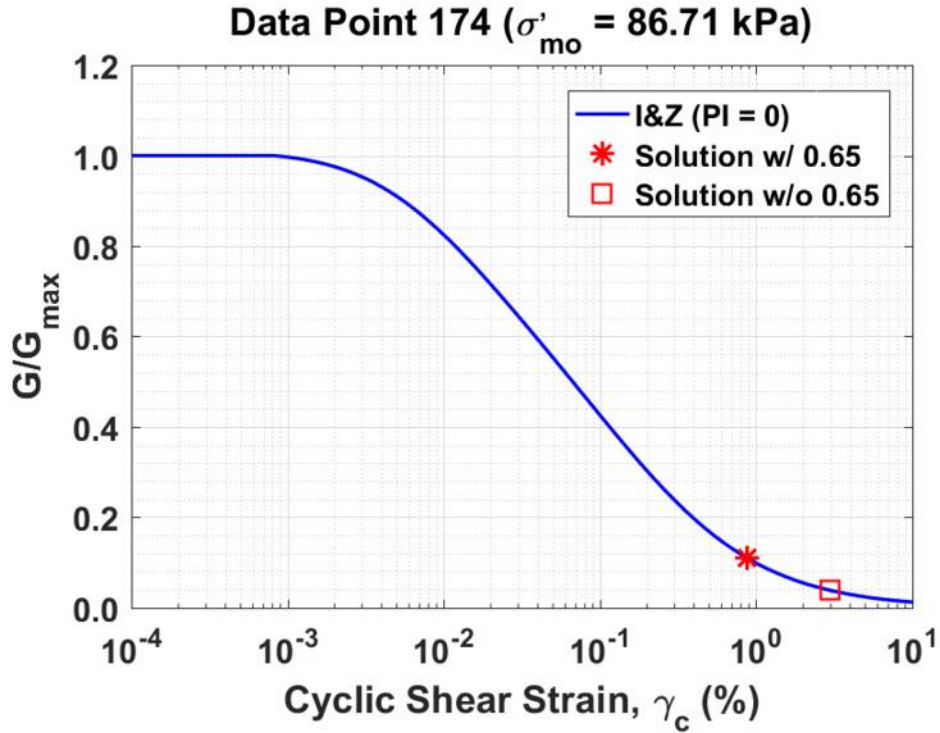


Figure B588. Normalized shear modulus reduction curves for Data Point 174 of the Boulanger et al. database showing the solutions w/ and w/o the 0.65 factor

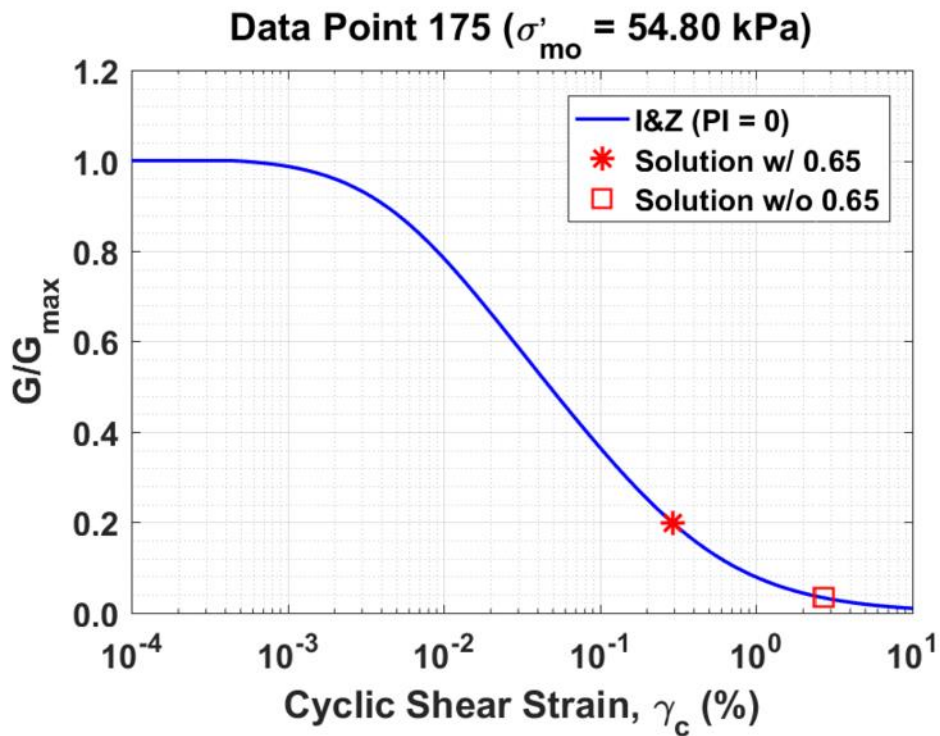


Figure B589. Normalized shear modulus reduction curves for Data Point 175 of the Boulanger et al. database showing the solutions w/ and w/o the 0.65 factor

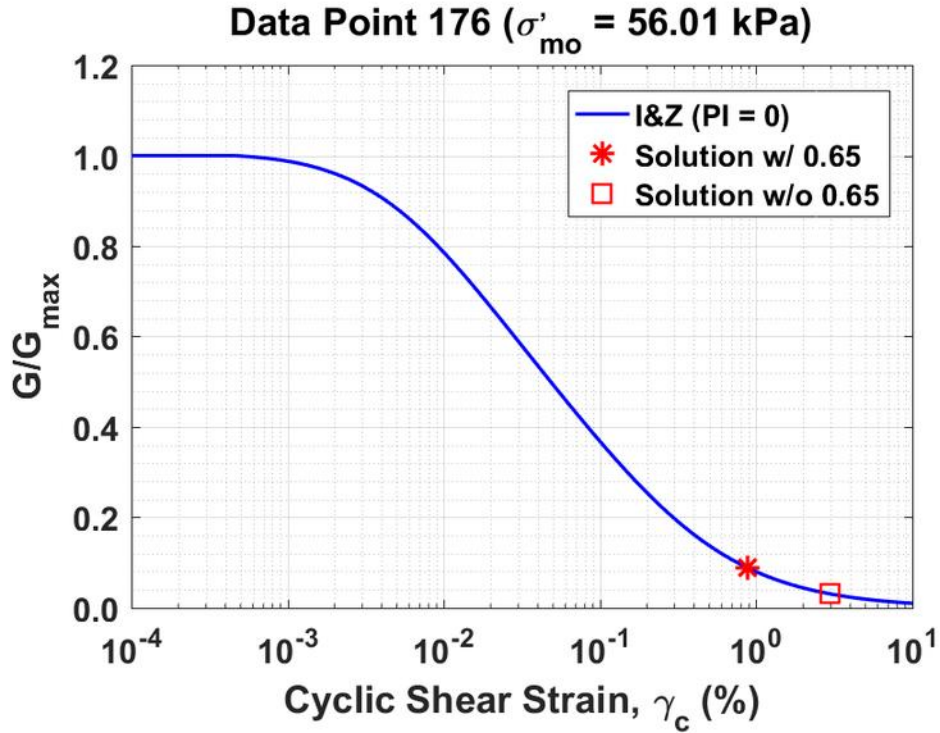


Figure B590. Normalized shear modulus reduction curves for Data Point 176 of the Boulanger et al. database showing the solutions w/ and w/o the 0.65 factor

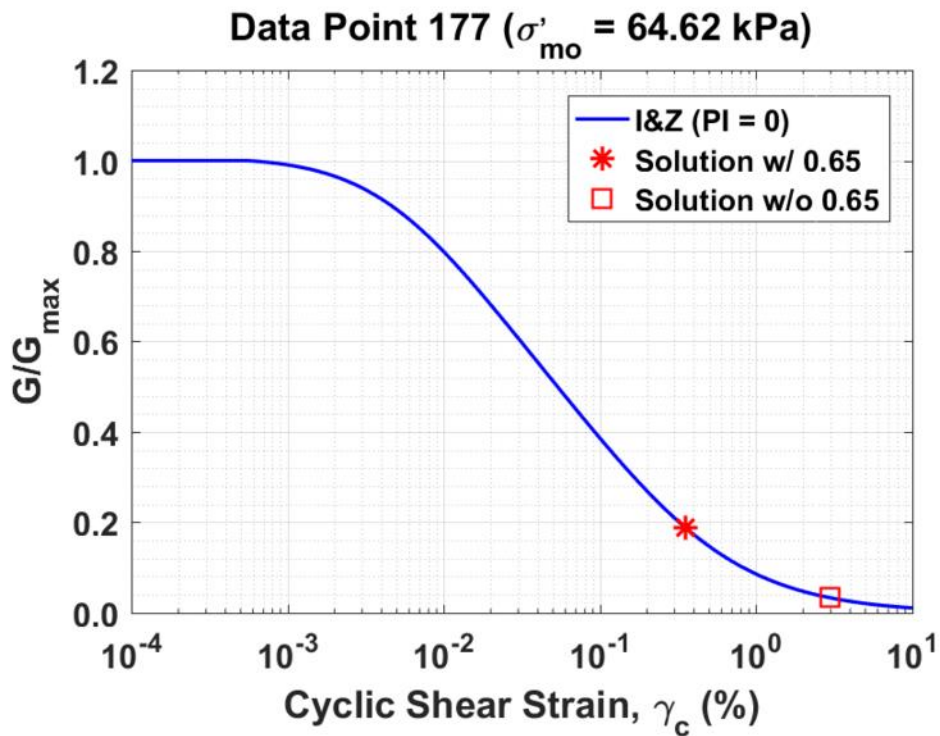


Figure B591. Normalized shear modulus reduction curves for Data Point 177 of the Boulanger et al. database showing the solutions w/ and w/o the 0.65 factor

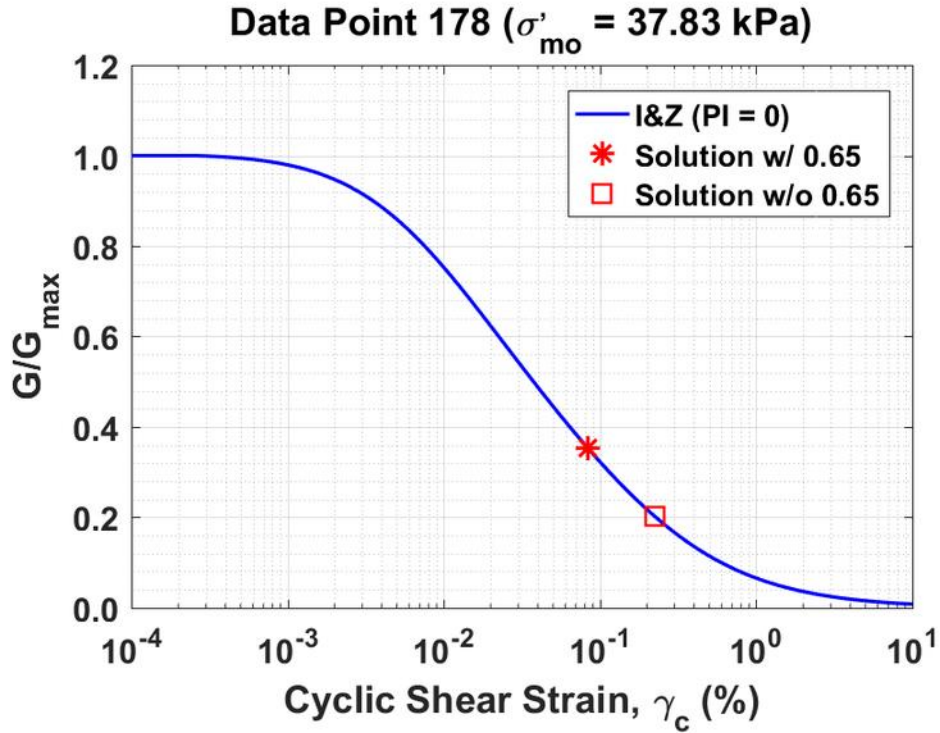


Figure B592. Normalized shear modulus reduction curves for Data Point 178 of the Boulanger et al. database showing the solutions w/ and w/o the 0.65 factor

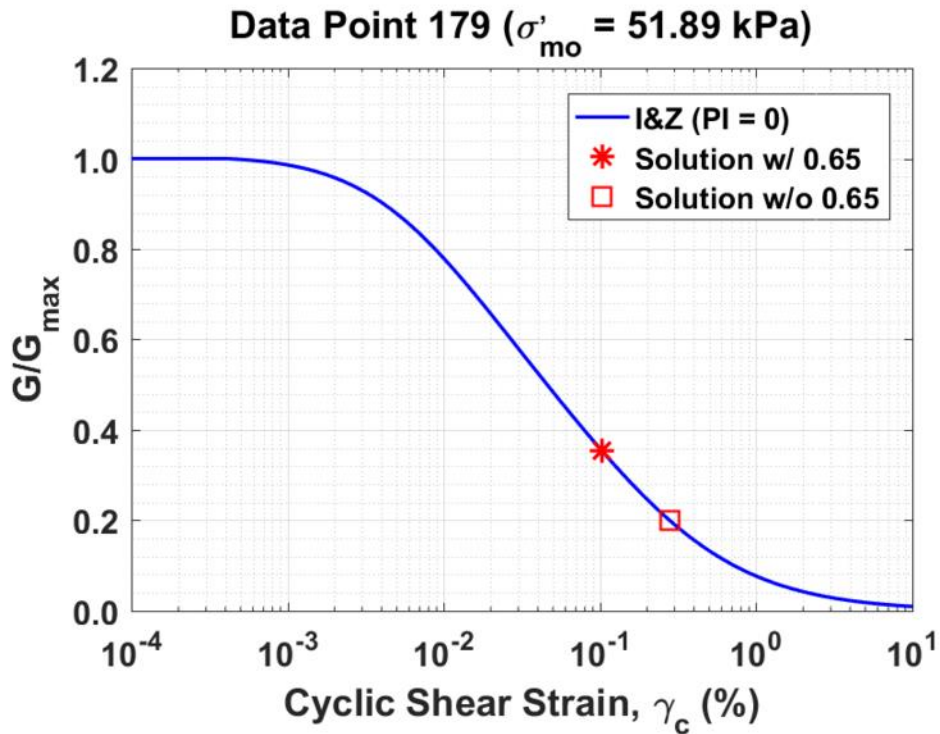


Figure B593. Normalized shear modulus reduction curves for Data Point 179 of the Boulanger et al. database showing the solutions w/ and w/o the 0.65 factor

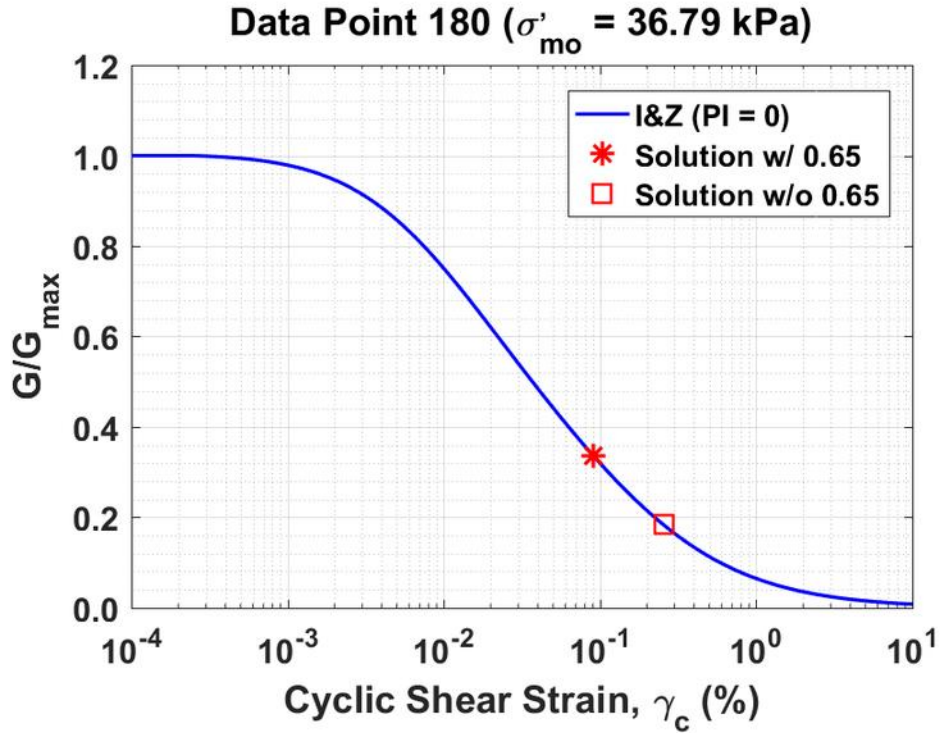


Figure B594. Normalized shear modulus reduction curves for Data Point 180 of the Boulanger et al. database showing the solutions w/ and w/o the 0.65 factor

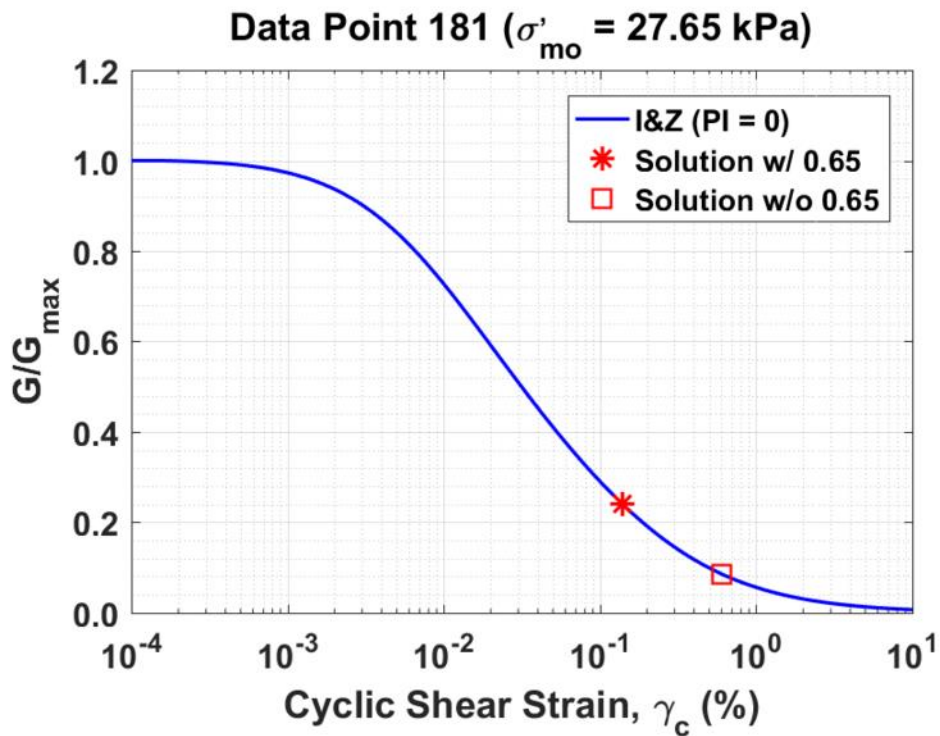


Figure B595. Normalized shear modulus reduction curves for Data Point 181 of the Boulanger et al. database showing the solutions w/ and w/o the 0.65 factor

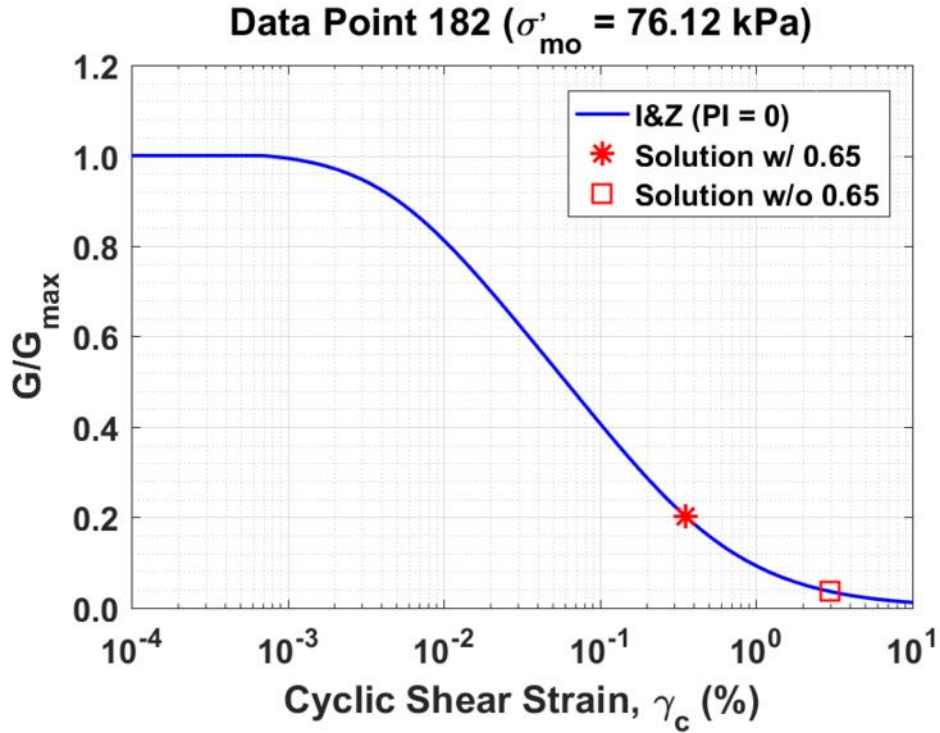


Figure B596. Normalized shear modulus reduction curves for Data Point 182 of the Boulanger et al. database showing the solutions w/ and w/o the 0.65 factor

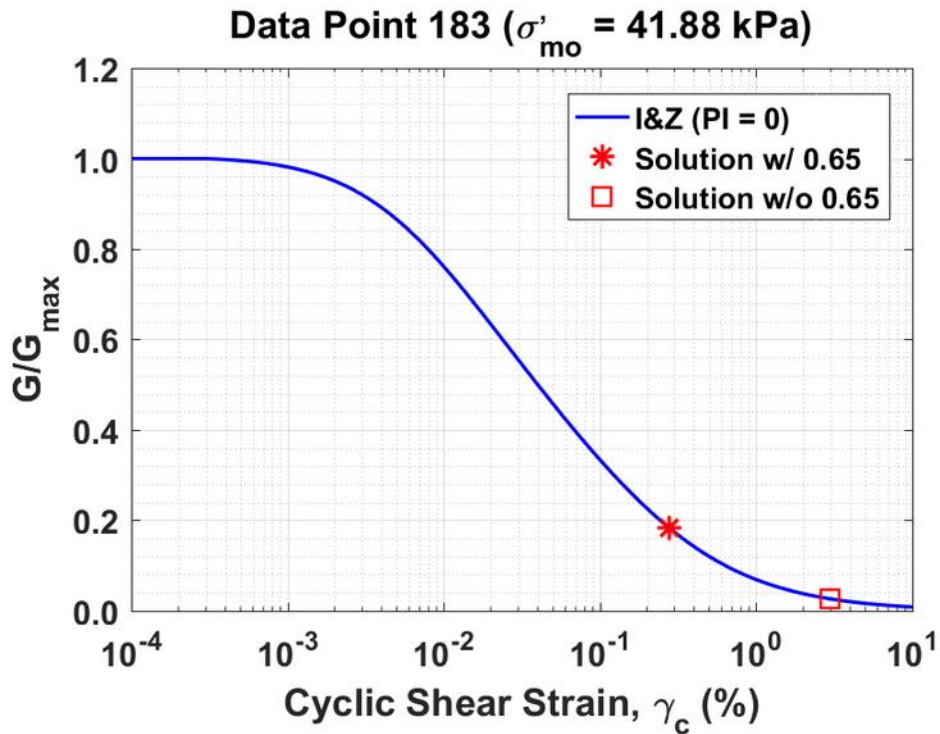


Figure B597. Normalized shear modulus reduction curves for Data Point 183 of the Boulanger et al. database showing the solutions w/ and w/o the 0.65 factor

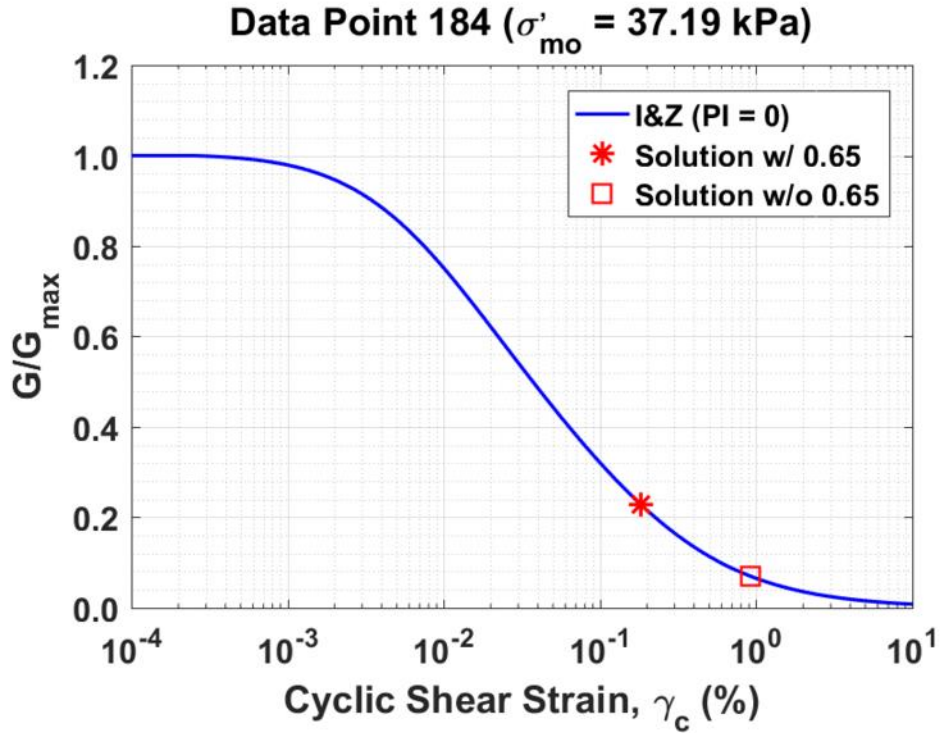


Figure B598. Normalized shear modulus reduction curves for Data Point 184 of the Boulanger et al. database showing the solutions w/ and w/o the 0.65 factor

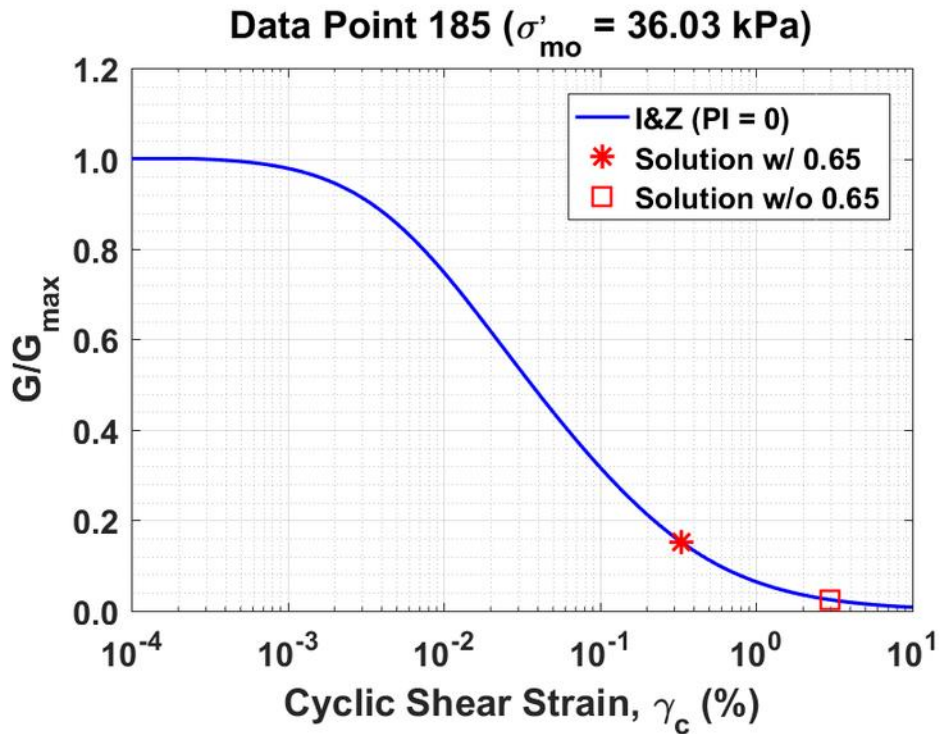


Figure B599. Normalized shear modulus reduction curves for Data Point 185 of the Boulanger et al. database showing the solutions w/ and w/o the 0.65 factor

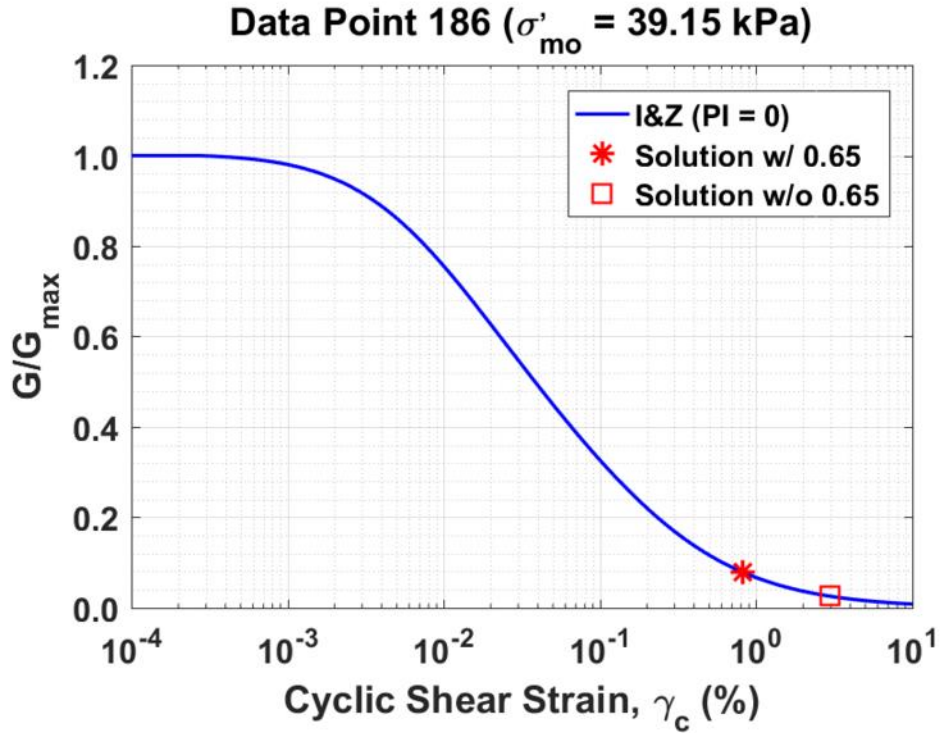


Figure B600. Normalized shear modulus reduction curves for Data Point 186 of the Boulanger et al. database showing the solutions w/ and w/o the 0.65 factor

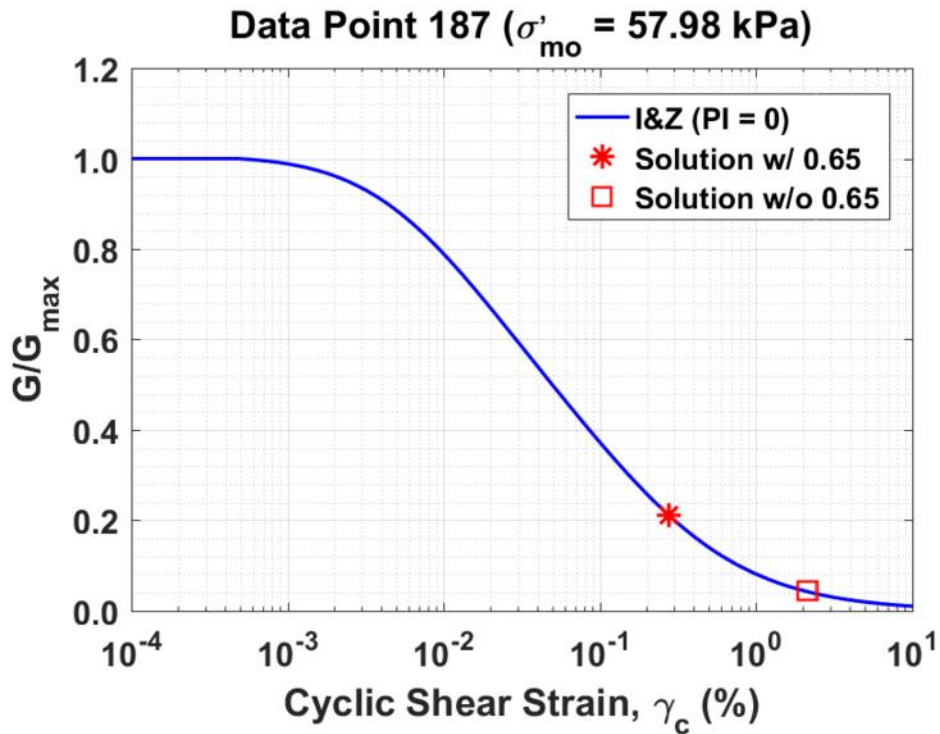


Figure B601. Normalized shear modulus reduction curves for Data Point 187 of the Boulanger et al. database showing the solutions w/ and w/o the 0.65 factor

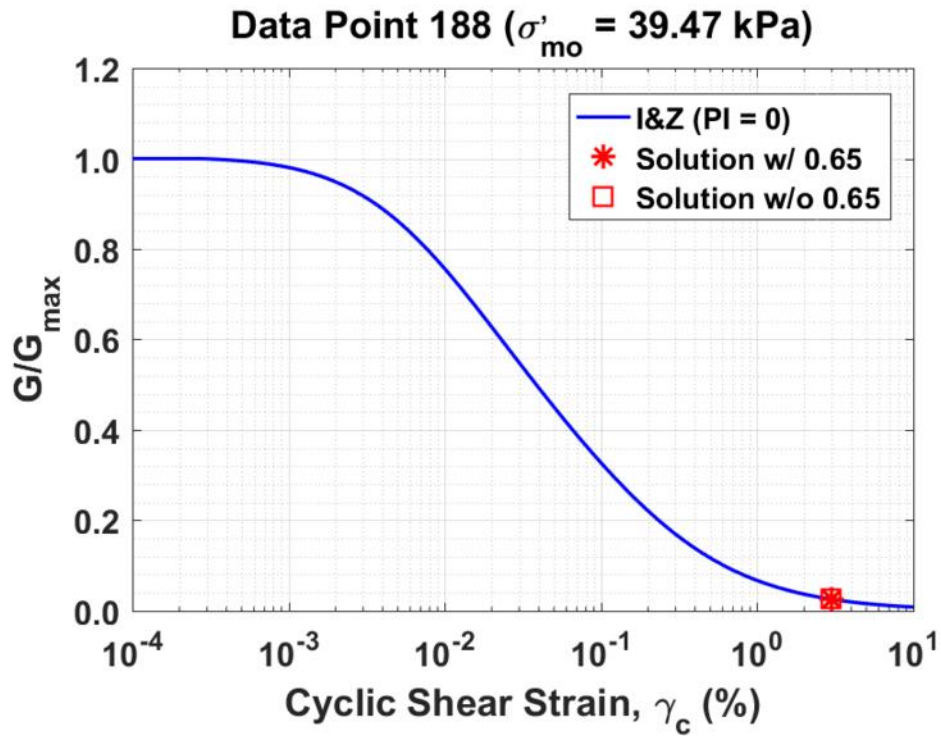


Figure B602. Normalized shear modulus reduction curves for Data Point 188 of the Boulanger et al. database showing the solutions w/ and w/o the 0.65 factor

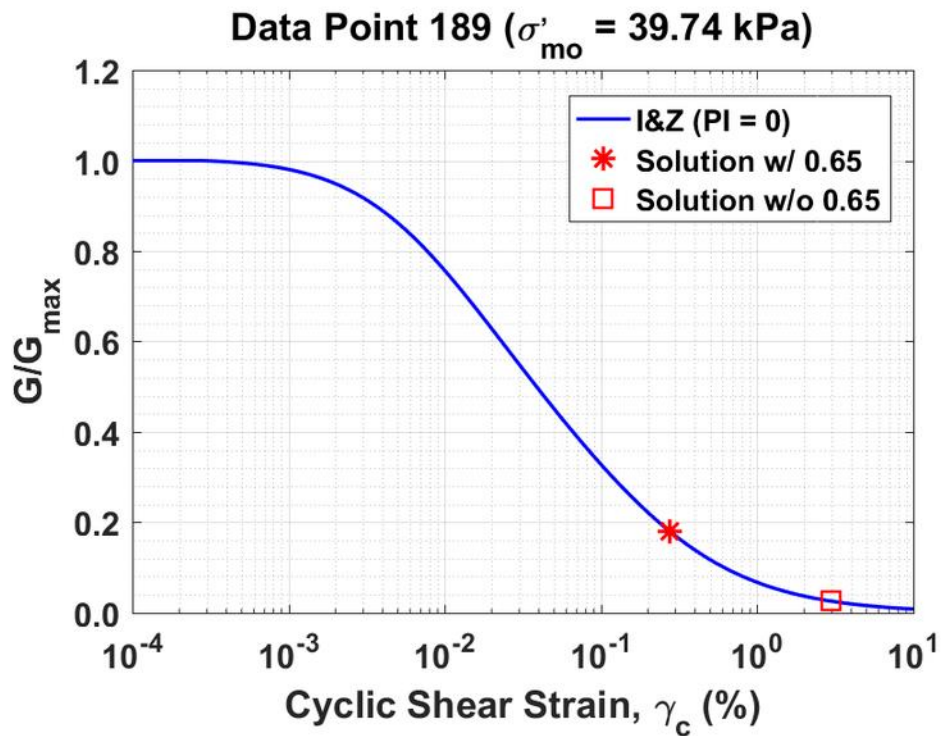


Figure B603. Normalized shear modulus reduction curves for Data Point 189 of the Boulanger et al. database showing the solutions w/ and w/o the 0.65 factor

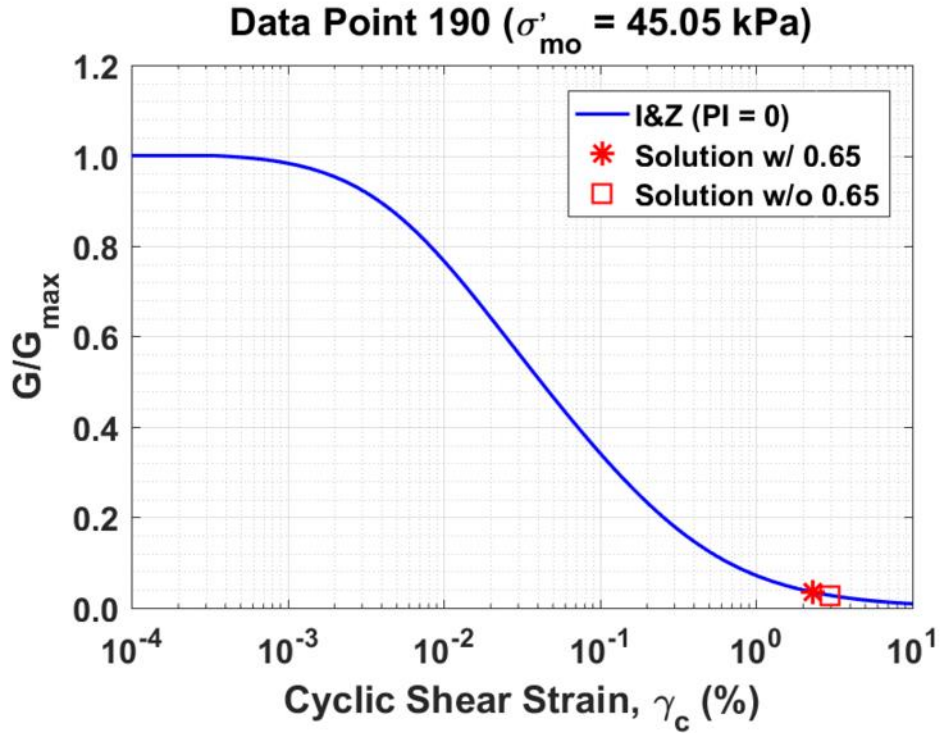


Figure B604. Normalized shear modulus reduction curves for Data Point 190 of the Boulanger et al. database showing the solutions w/ and w/o the 0.65 factor

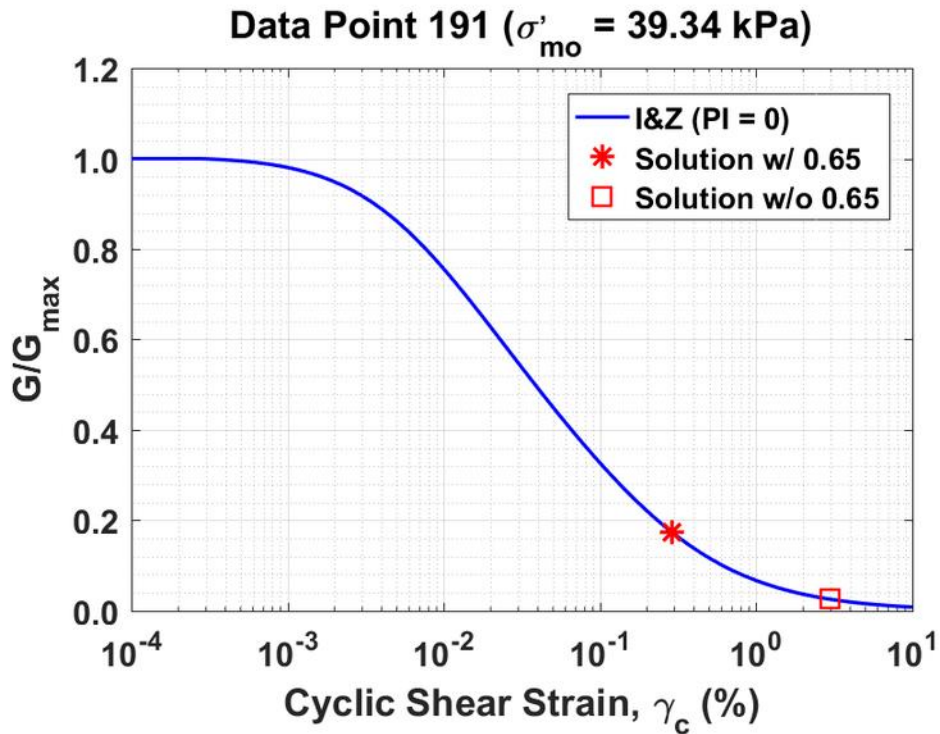


Figure B605. Normalized shear modulus reduction curves for Data Point 191 of the Boulanger et al. database showing the solutions w/ and w/o the 0.65 factor

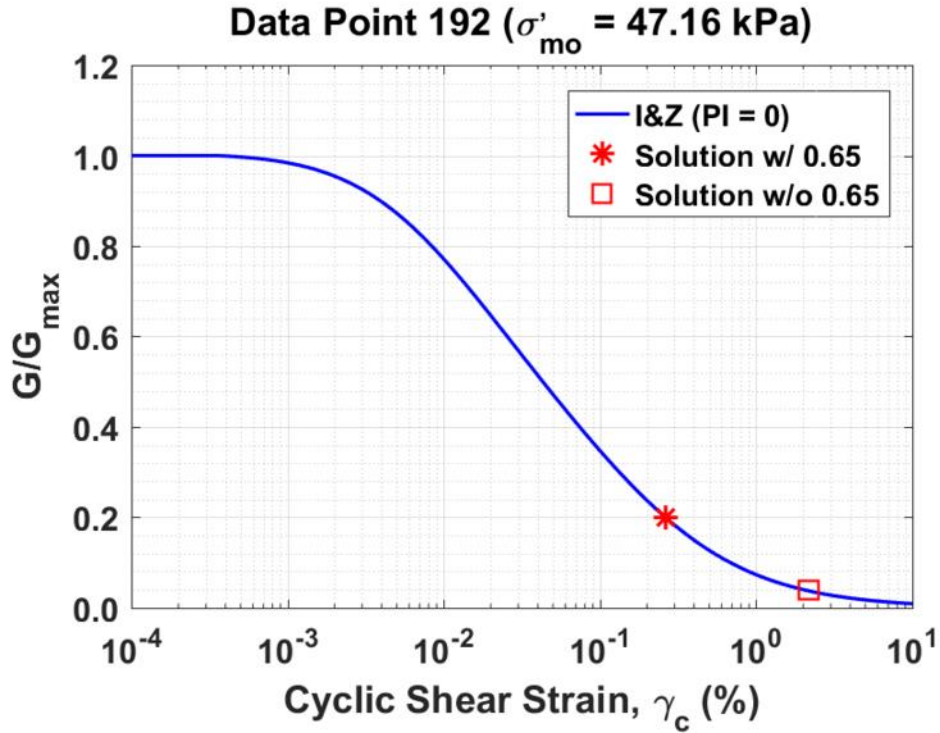


Figure B606. Normalized shear modulus reduction curves for Data Point 192 of the Boulanger et al. database showing the solutions w/ and w/o the 0.65 factor

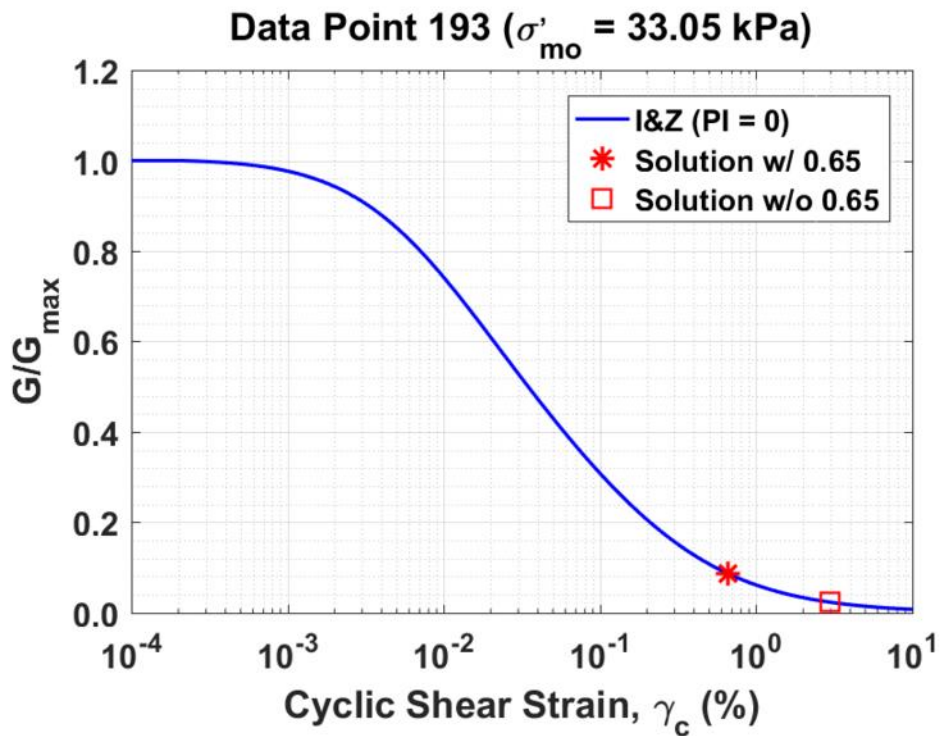


Figure B607. Normalized shear modulus reduction curves for Data Point 193 of the Boulanger et al. database showing the solutions w/ and w/o the 0.65 factor

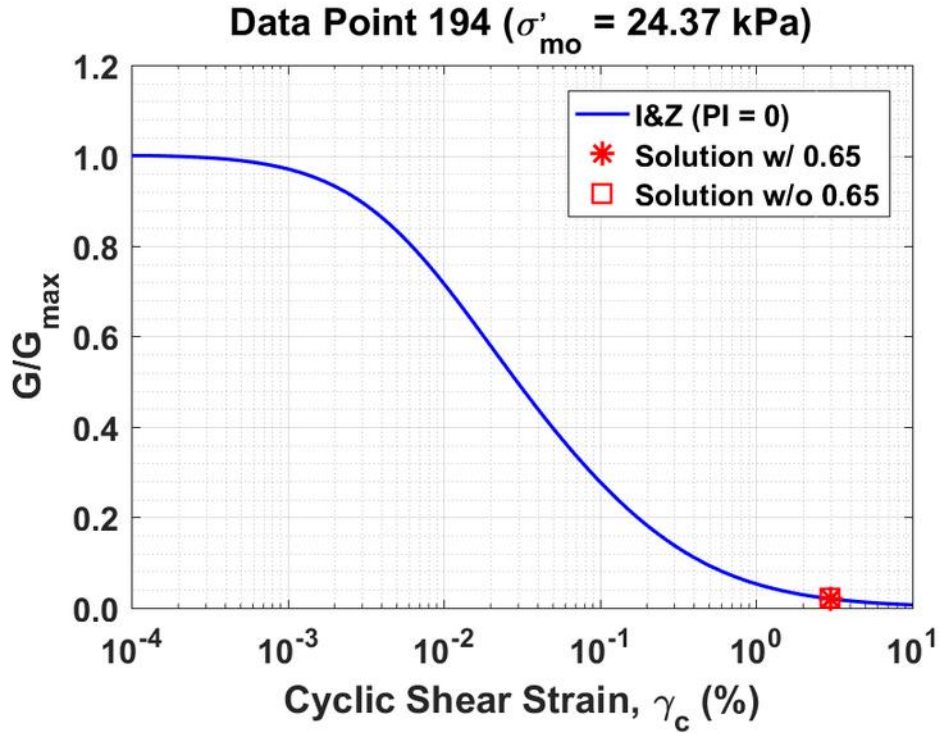


Figure B608. Normalized shear modulus reduction curves for Data Point 194 of the Boulanger et al. database showing the solutions w/ and w/o the 0.65 factor

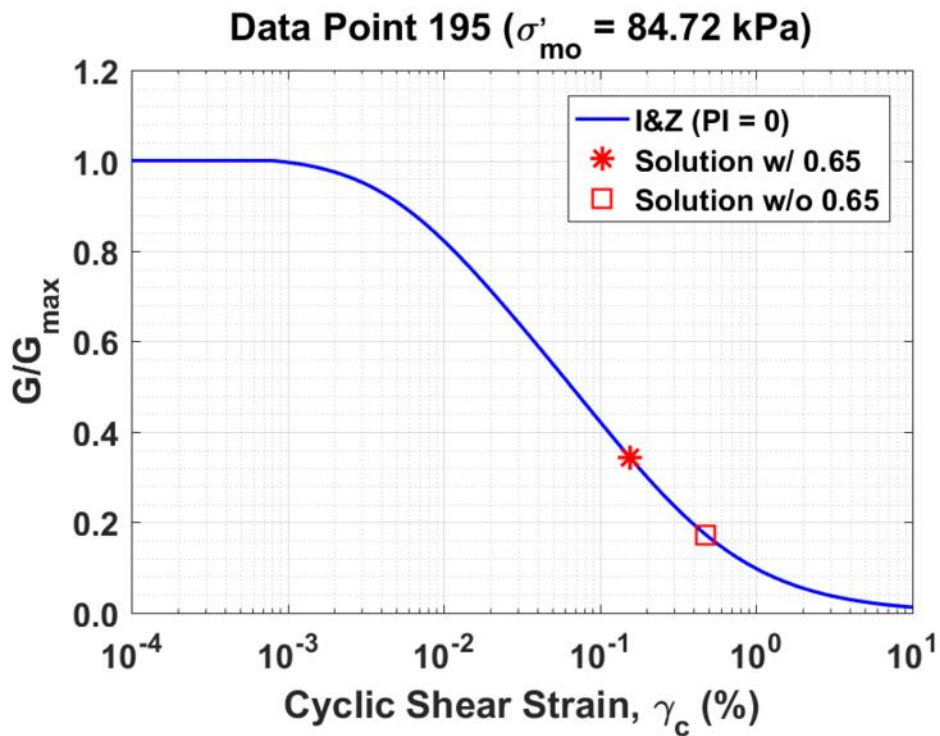


Figure B609. Normalized shear modulus reduction curves for Data Point 195 of the Boulanger et al. database showing the solutions w/ and w/o the 0.65 factor

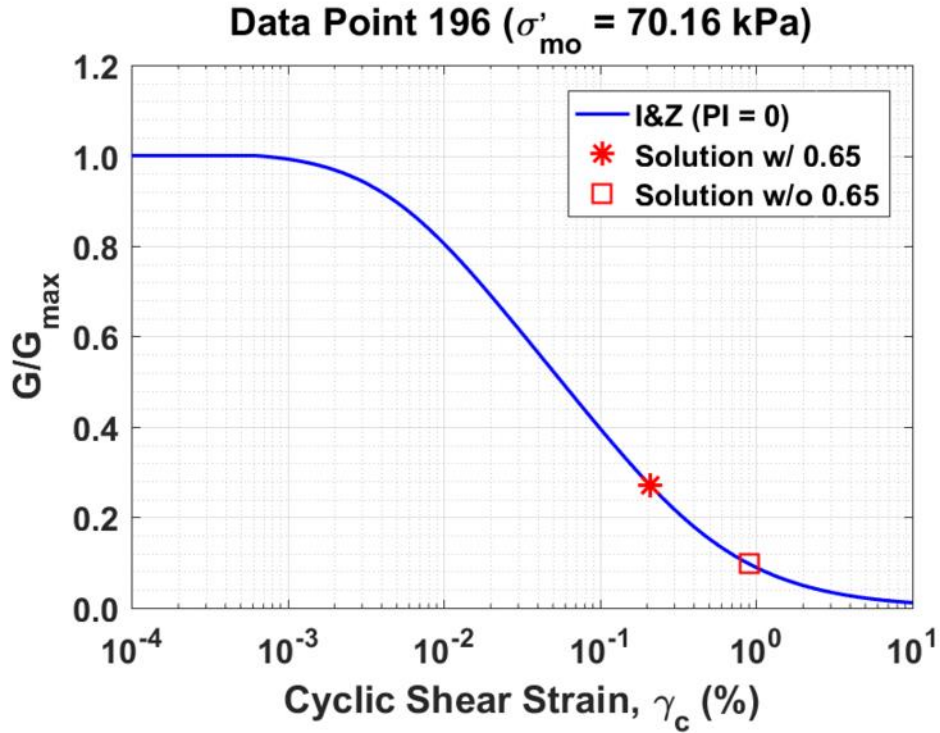


Figure B610. Normalized shear modulus reduction curves for Data Point 196 of the Boulanger et al. database showing the solutions w/ and w/o the 0.65 factor

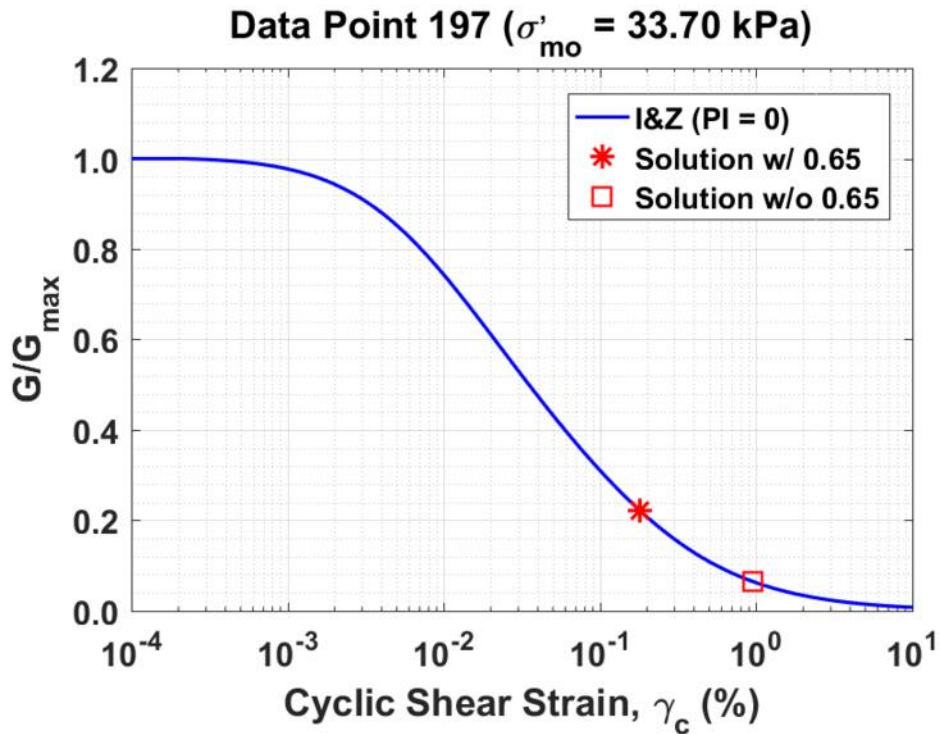


Figure B611. Normalized shear modulus reduction curves for Data Point 197 of the Boulanger et al. database showing the solutions w/ and w/o the 0.65 factor

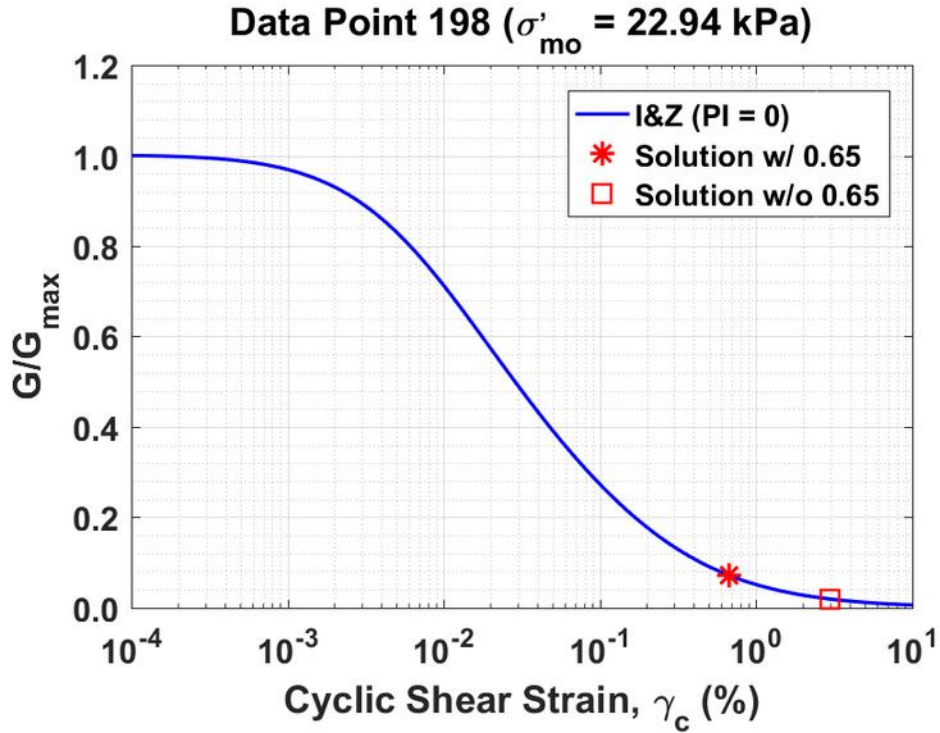


Figure B612. Normalized shear modulus reduction curves for Data Point 198 of the Boulanger et al. database showing the solutions w/ and w/o the 0.65 factor

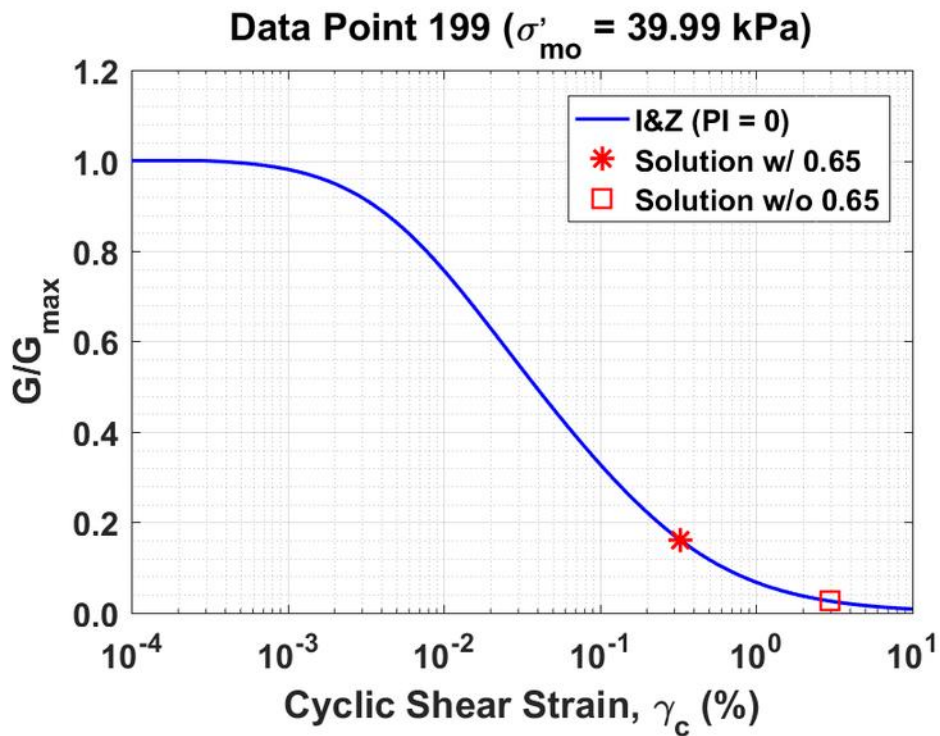


Figure B613. Normalized shear modulus reduction curves for Data Point 199 of the Boulanger et al. database showing the solutions w/ and w/o the 0.65 factor

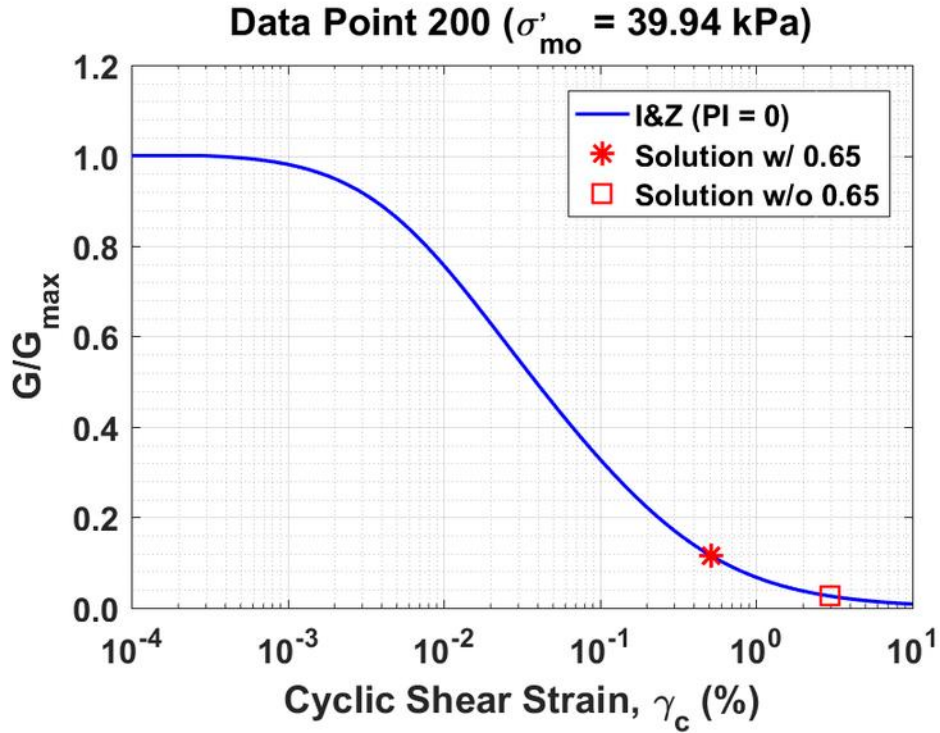


Figure B614. Normalized shear modulus reduction curves for Data Point 200 of the Boulanger et al. database showing the solutions w/ and w/o the 0.65 factor

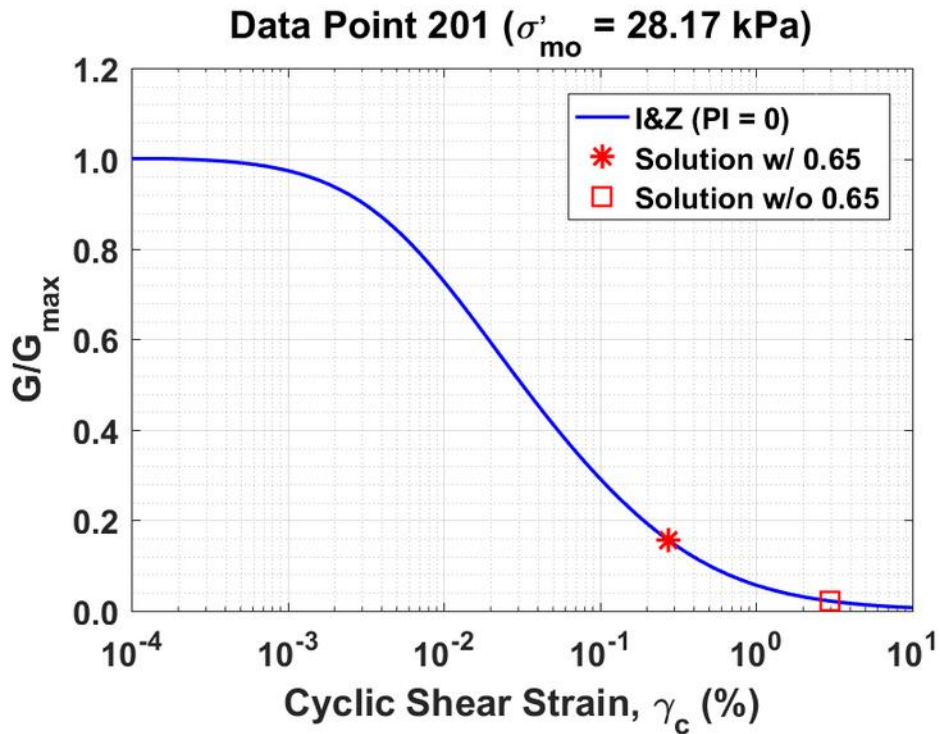


Figure B615. Normalized shear modulus reduction curves for Data Point 201 of the Boulanger et al. database showing the solutions w/ and w/o the 0.65 factor

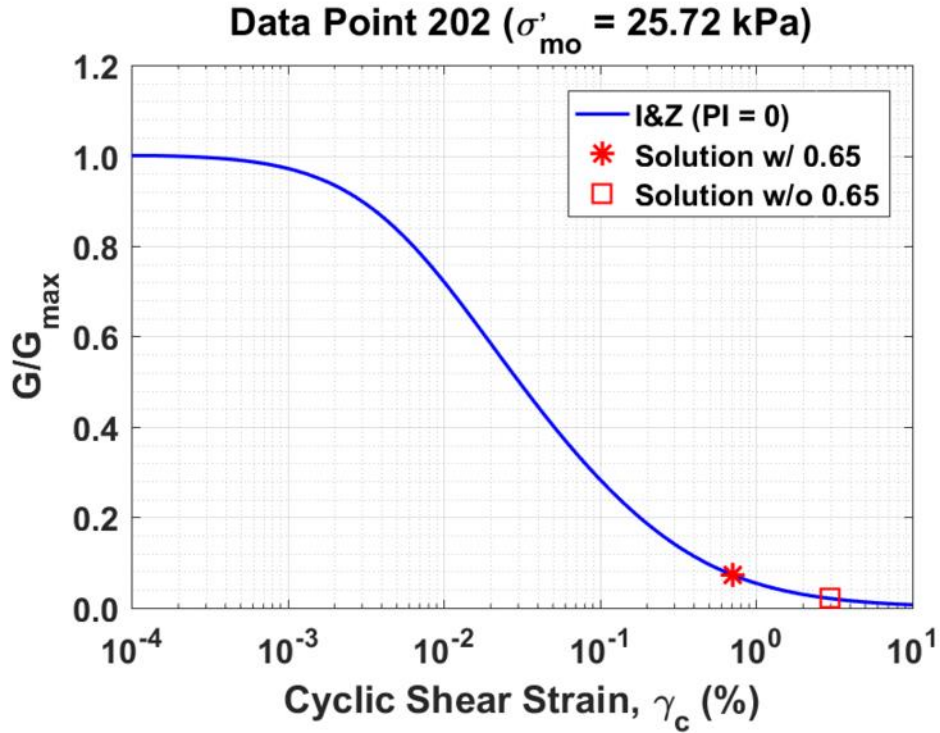


Figure B616. Normalized shear modulus reduction curves for Data Point 202 of the Boulanger et al. database showing the solutions w/ and w/o the 0.65 factor

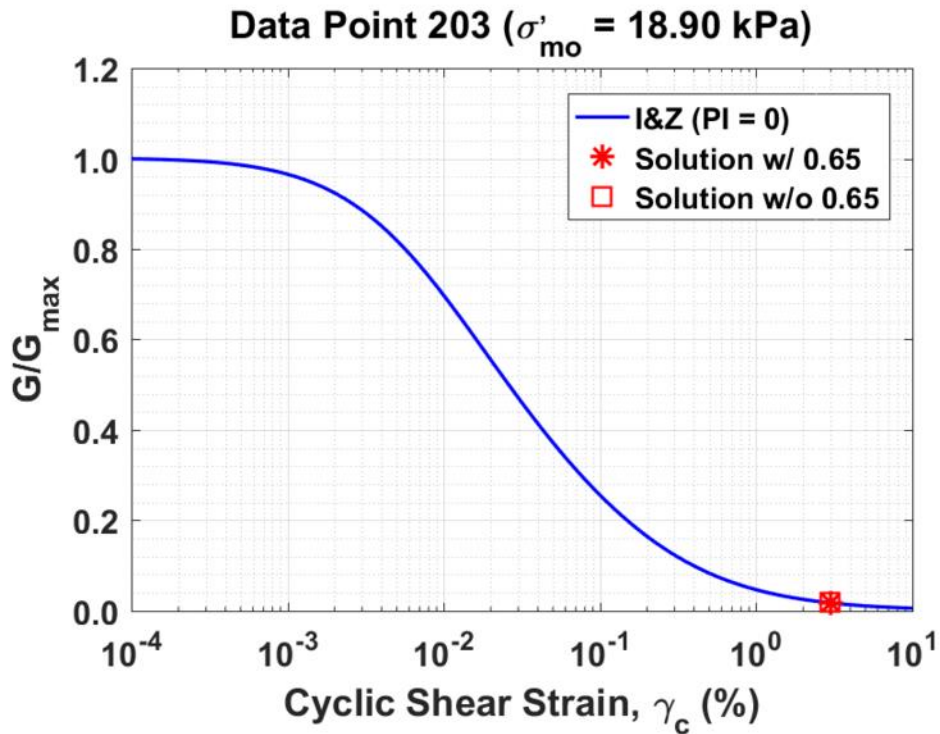


Figure B617. Normalized shear modulus reduction curves for Data Point 203 of the Boulanger et al. database showing the solutions w/ and w/o the 0.65 factor

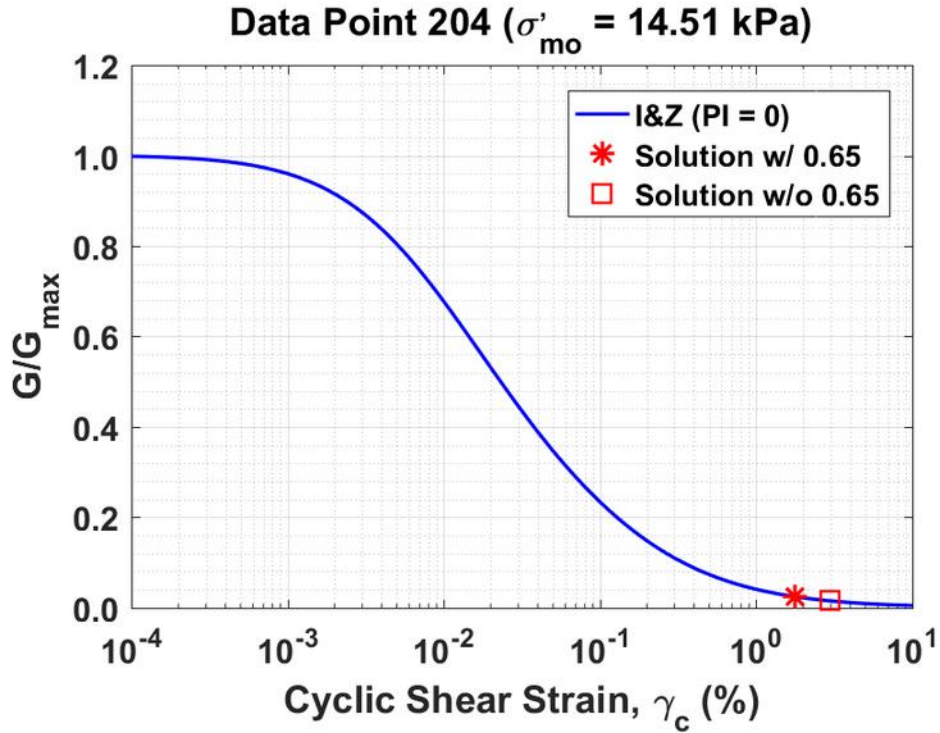


Figure B618. Normalized shear modulus reduction curves for Data Point 204 of the Boulanger et al. database showing the solutions w/ and w/o the 0.65 factor

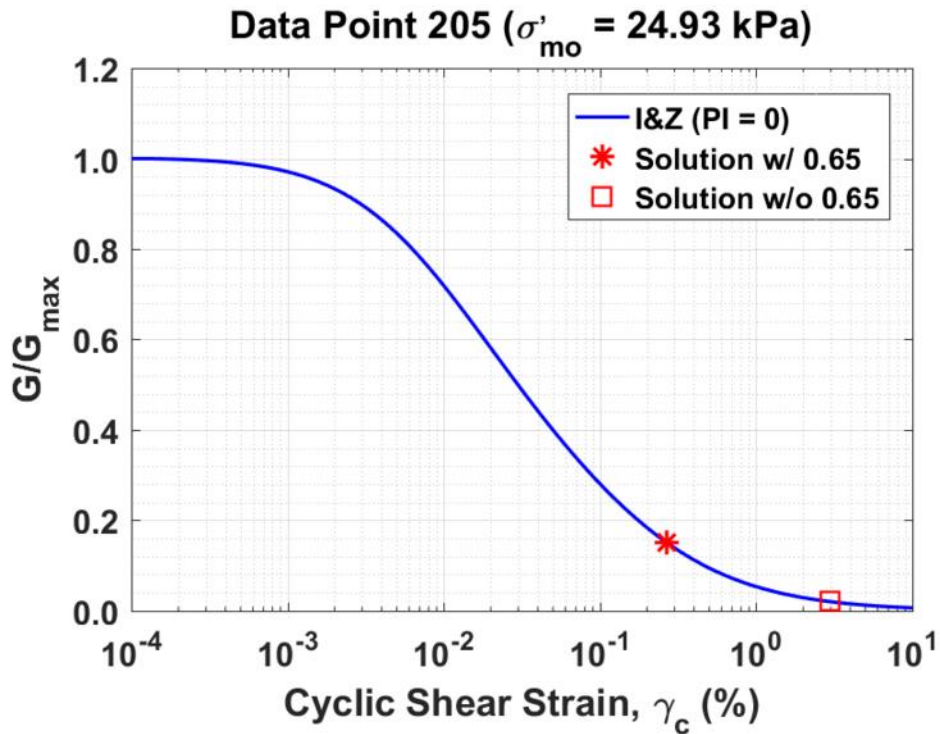


Figure B619. Normalized shear modulus reduction curves for Data Point 205 of the Boulanger et al. database showing the solutions w/ and w/o the 0.65 factor

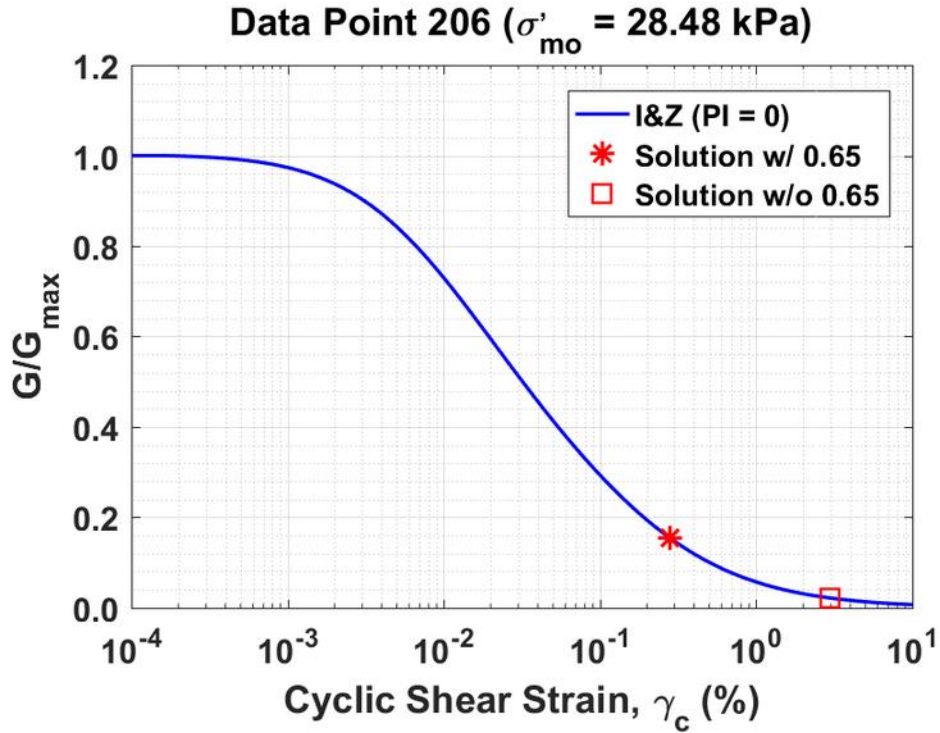


Figure B620. Normalized shear modulus reduction curves for Data Point 206 of the Boulanger et al. database showing the solutions w/ and w/o the 0.65 factor

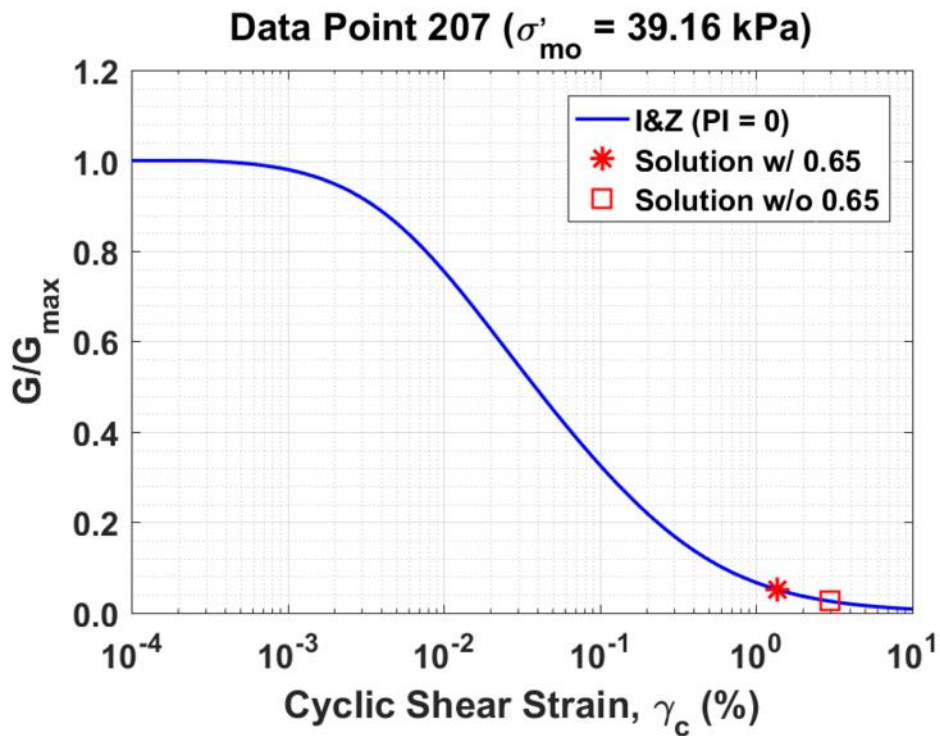


Figure B621. Normalized shear modulus reduction curves for Data Point 207 of the Boulanger et al. database showing the solutions w/ and w/o the 0.65 factor

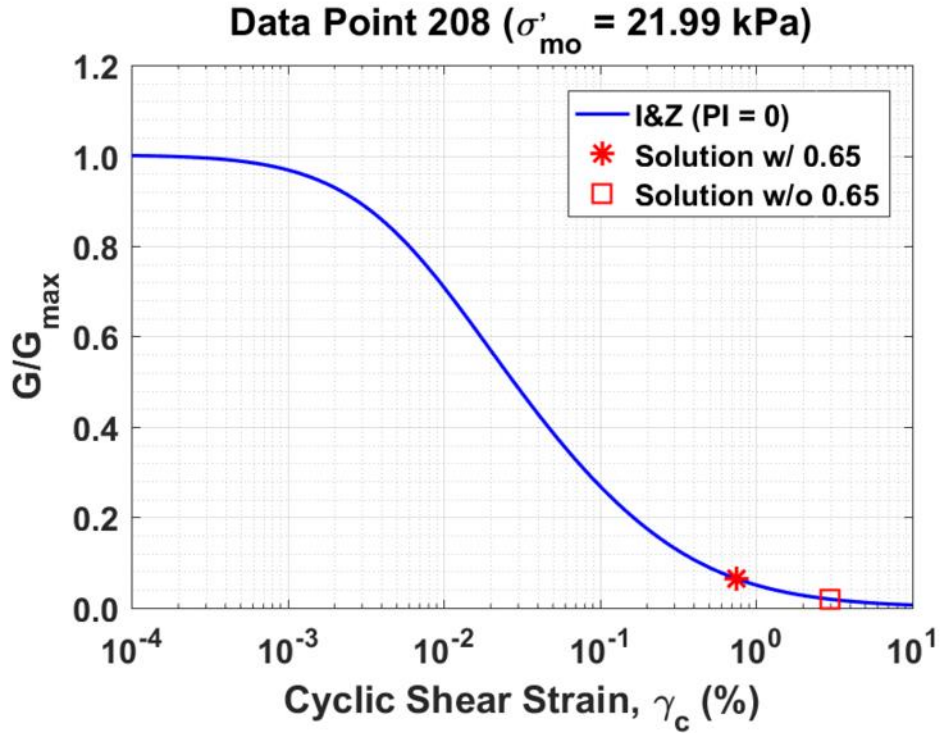


Figure B622. Normalized shear modulus reduction curves for Data Point 208 of the Boulanger et al. database showing the solutions w/ and w/o the 0.65 factor

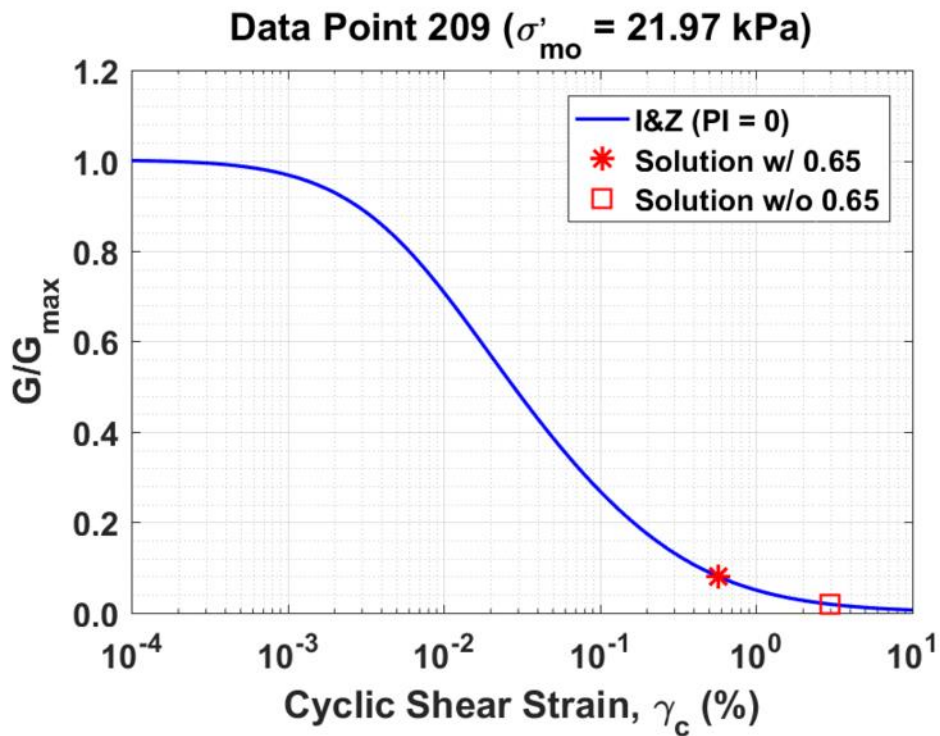


Figure B623. Normalized shear modulus reduction curves for Data Point 209 of the Boulanger et al. database showing the solutions w/ and w/o the 0.65 factor

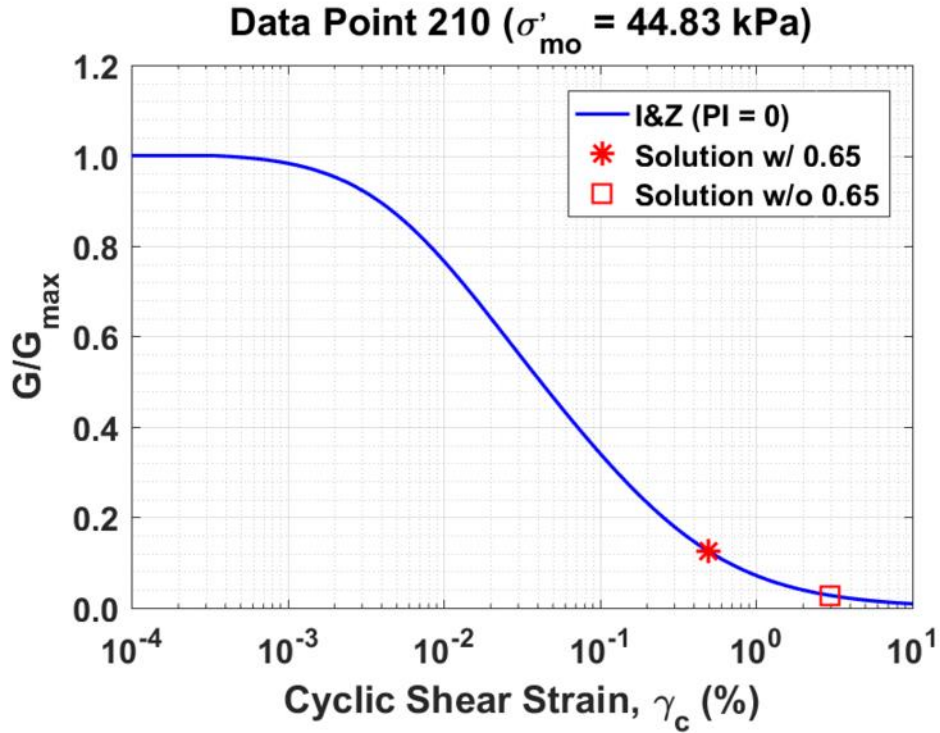


Figure B624. Normalized shear modulus reduction curves for Data Point 210 of the Boulanger et al. database showing the solutions w/ and w/o the 0.65 factor

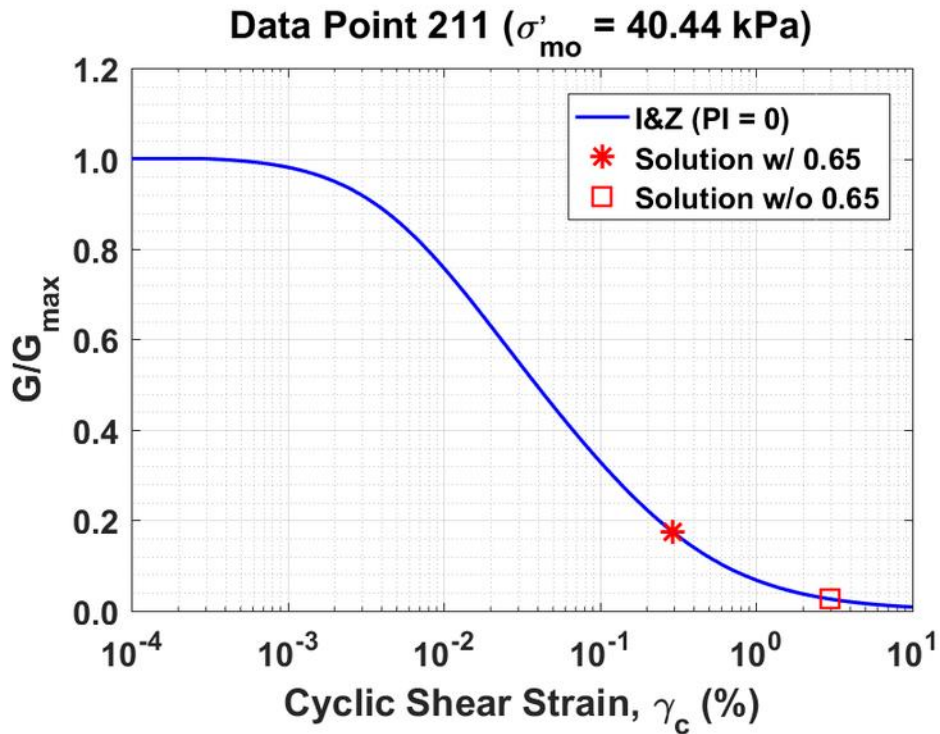


Figure B625. Normalized shear modulus reduction curves for Data Point 211 of the Boulanger et al. database showing the solutions w/ and w/o the 0.65 factor

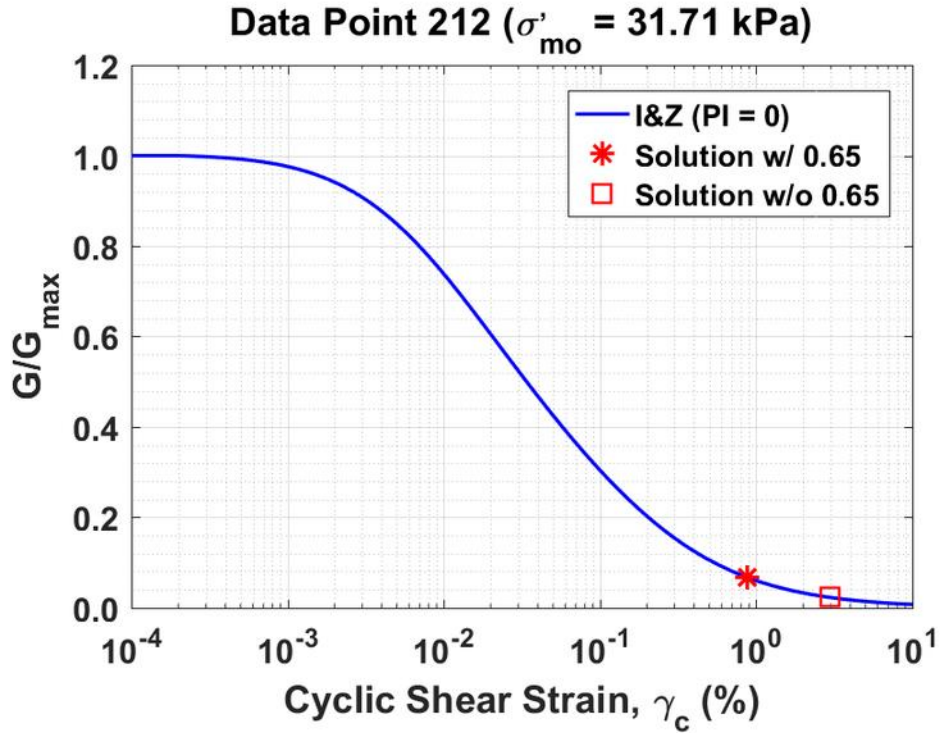


Figure B626. Normalized shear modulus reduction curves for Data Point 212 of the Boulanger et al. database showing the solutions w/ and w/o the 0.65 factor

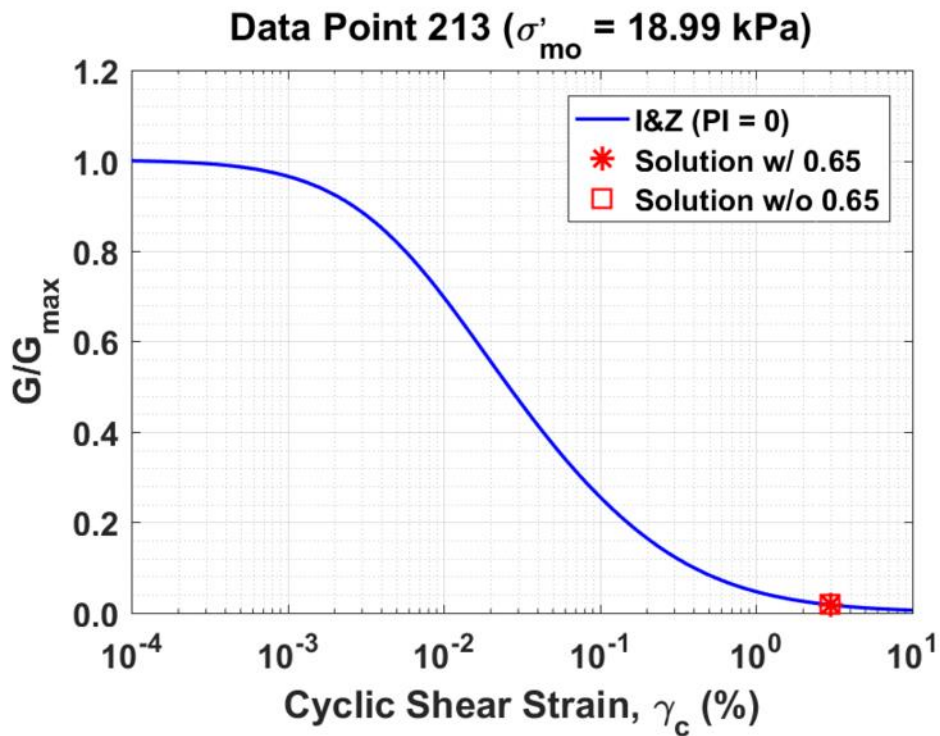


Figure B627. Normalized shear modulus reduction curves for Data Point 213 of the Boulanger et al. database showing the solutions w/ and w/o the 0.65 factor

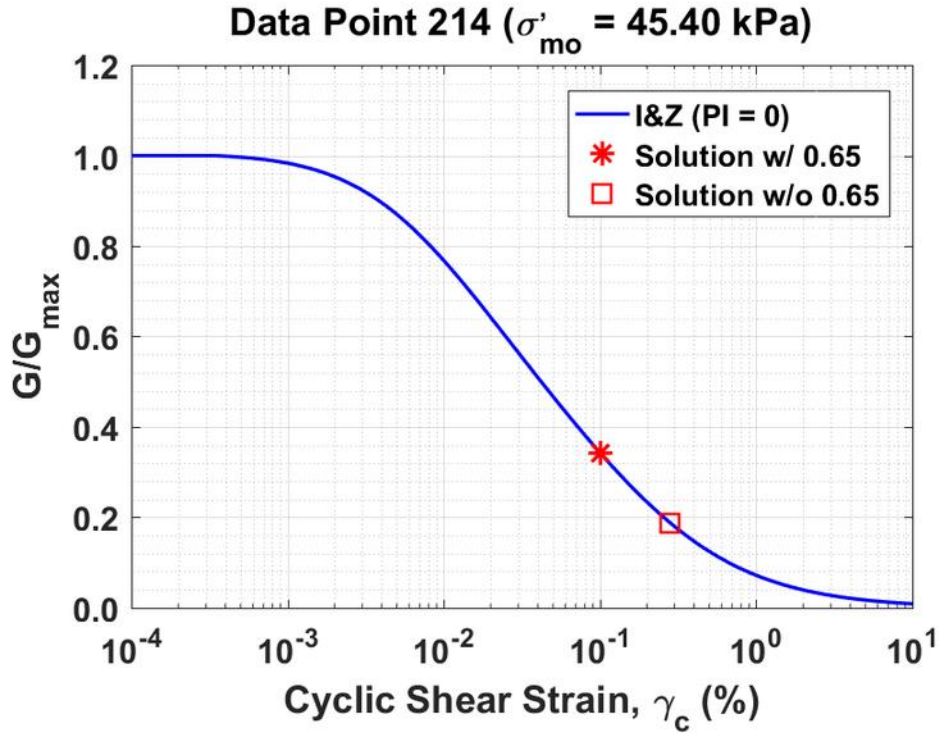


Figure B628. Normalized shear modulus reduction curves for Data Point 214 of the Boulanger et al. database showing the solutions w/ and w/o the 0.65 factor

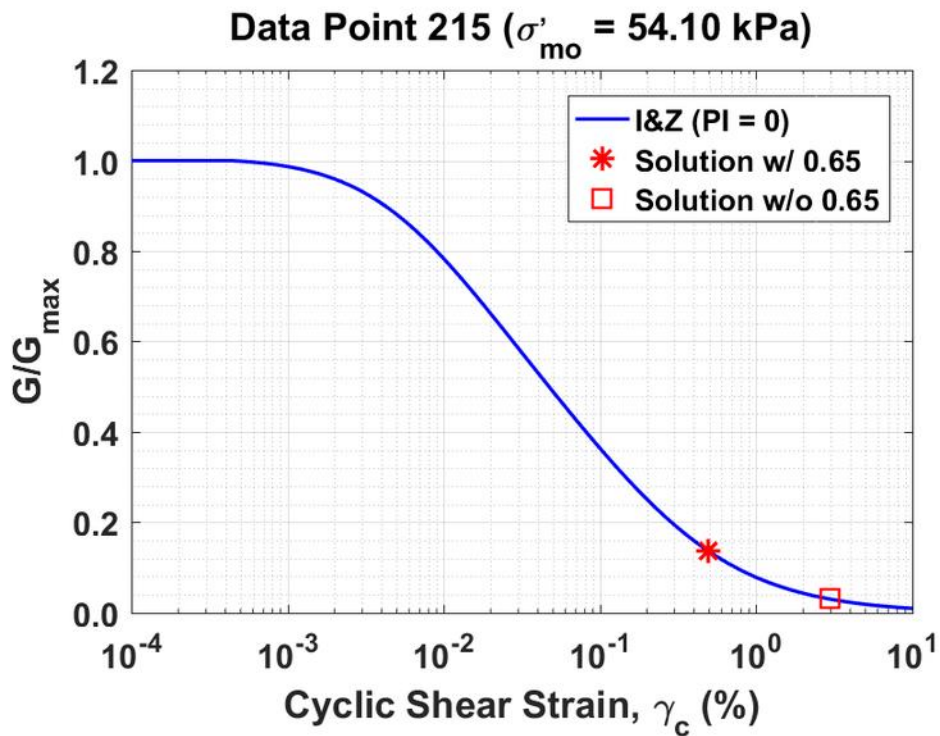


Figure B629. Normalized shear modulus reduction curves for Data Point 215 of the Boulanger et al. database showing the solutions w/ and w/o the 0.65 factor

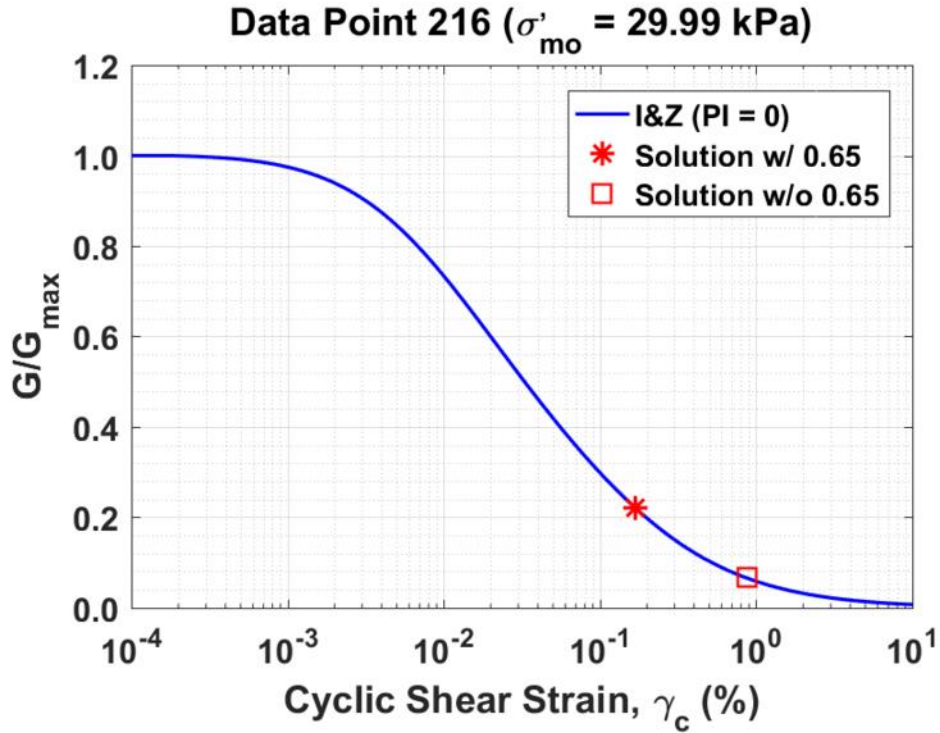


Figure B630. Normalized shear modulus reduction curves for Data Point 216 of the Boulanger et al. database showing the solutions w/ and w/o the 0.65 factor

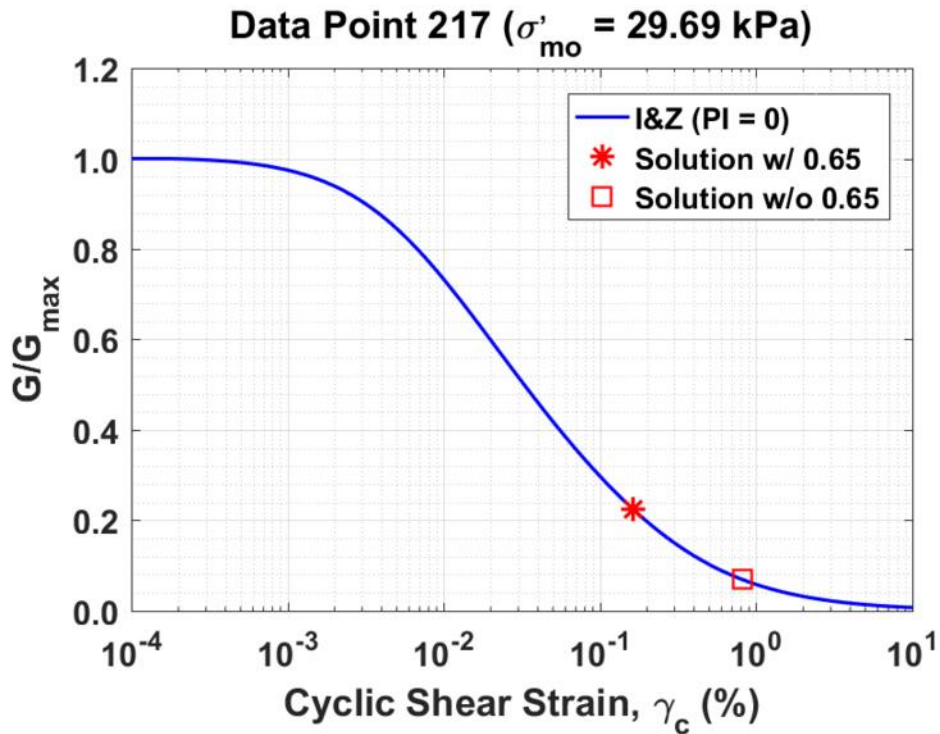


Figure B631. Normalized shear modulus reduction curves for Data Point 217 of the Boulanger et al. database showing the solutions w/ and w/o the 0.65 factor

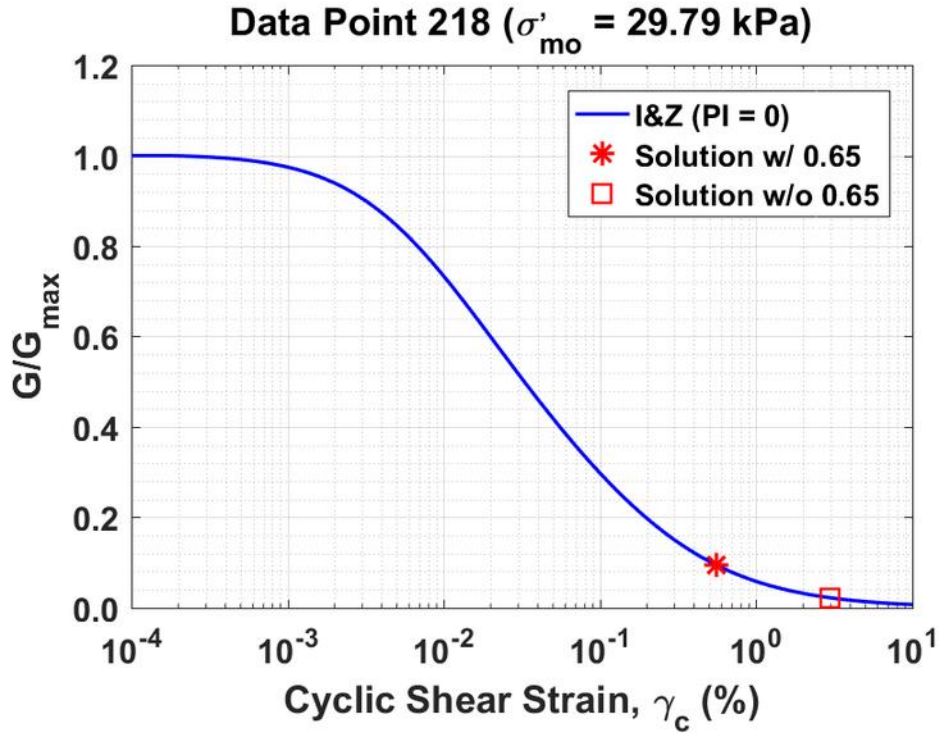


Figure B632. Normalized shear modulus reduction curves for Data Point 218 of the Boulanger et al. database showing the solutions w/ and w/o the 0.65 factor

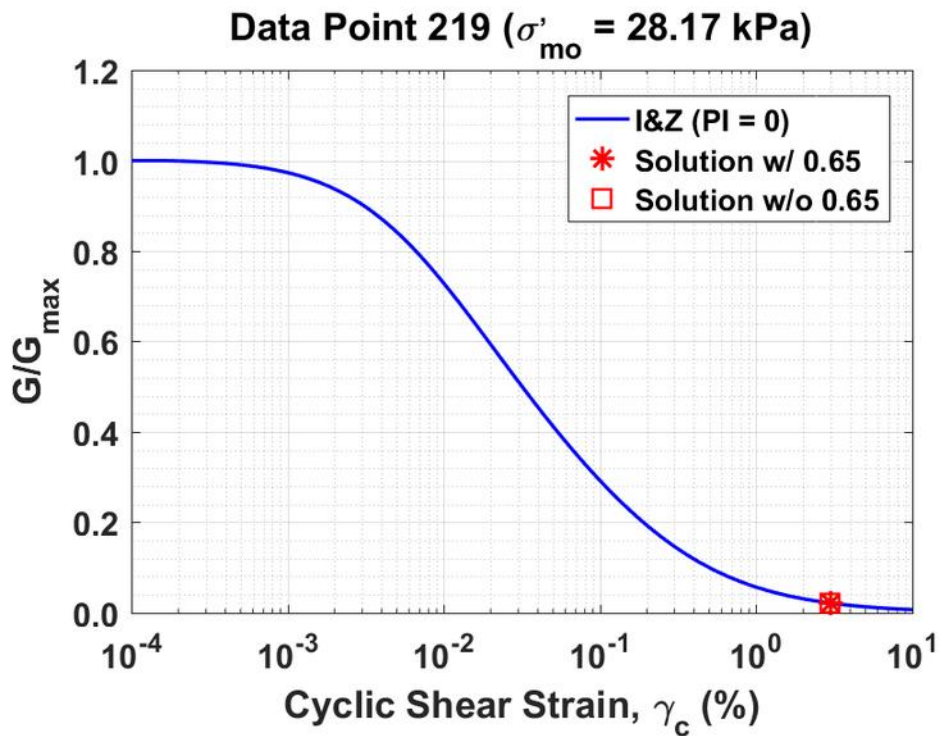


Figure B633. Normalized shear modulus reduction curves for Data Point 219 of the Boulanger et al. database showing the solutions w/ and w/o the 0.65 factor

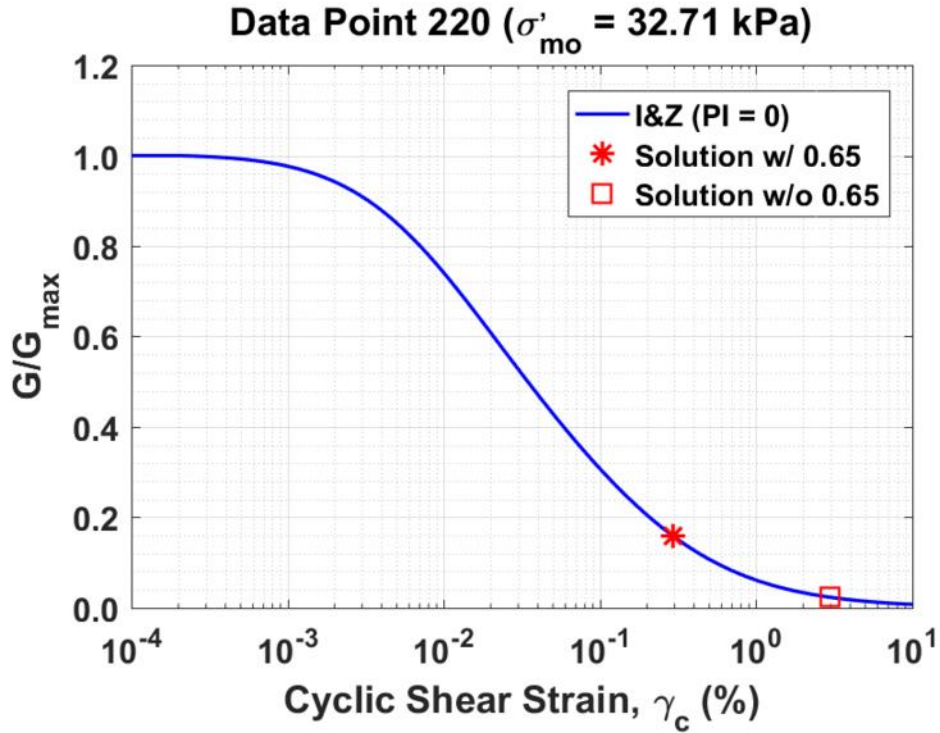


Figure B634. Normalized shear modulus reduction curves for Data Point 220 of the Boulanger et al. database showing the solutions w/ and w/o the 0.65 factor

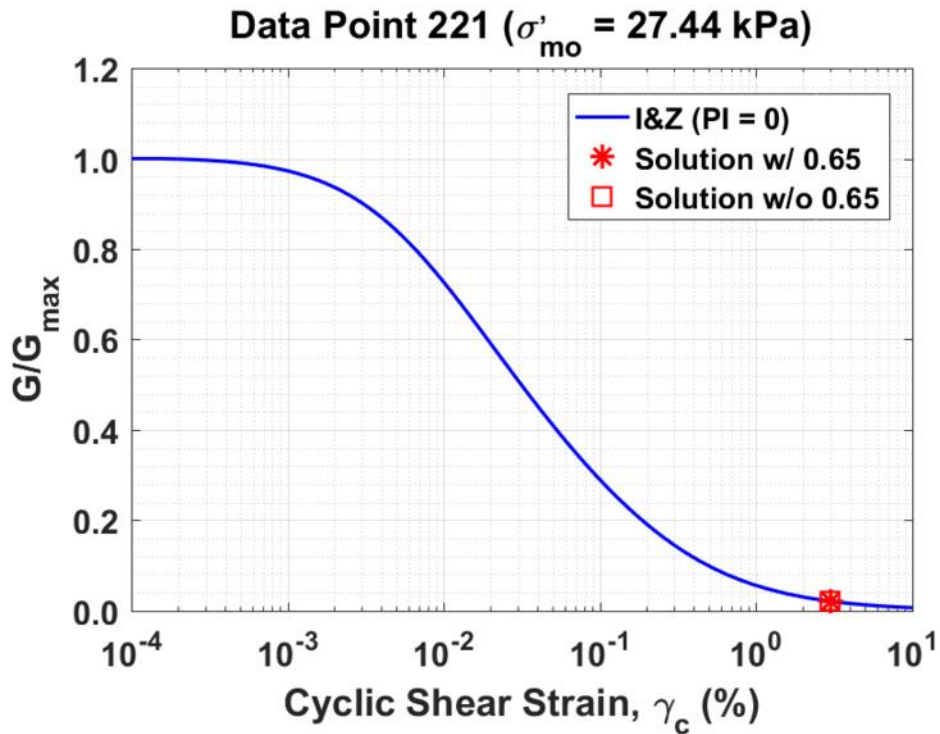


Figure B635. Normalized shear modulus reduction curves for Data Point 221 of the Boulanger et al. database showing the solutions w/ and w/o the 0.65 factor

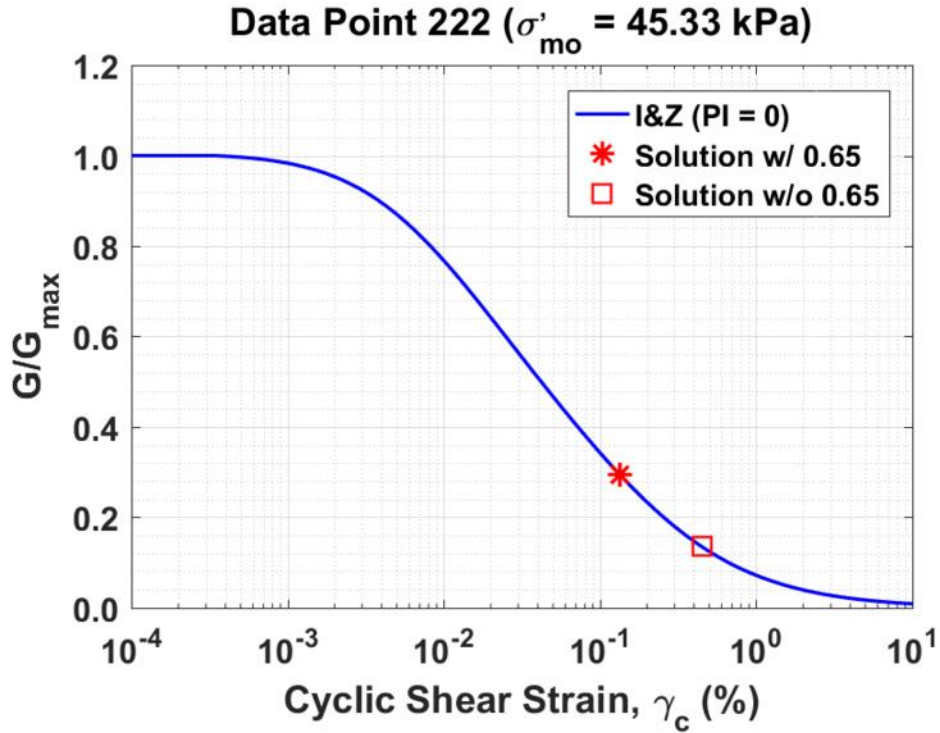


Figure B636. Normalized shear modulus reduction curves for Data Point 222 of the Boulanger et al. database showing the solutions w/ and w/o the 0.65 factor

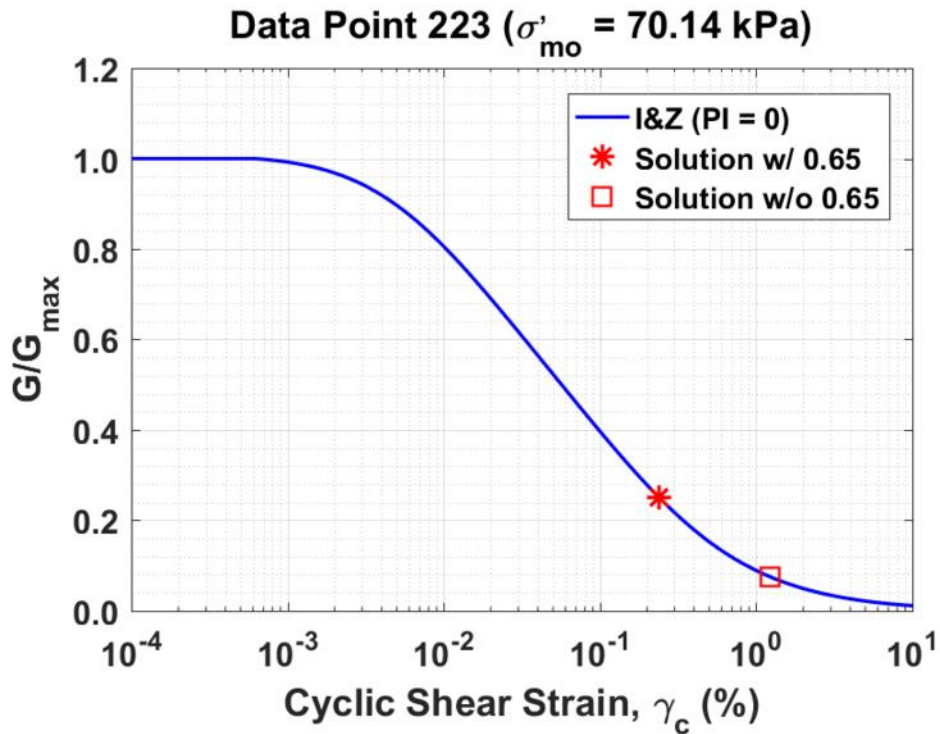


Figure B637. Normalized shear modulus reduction curves for Data Point 223 of the Boulanger et al. database showing the solutions w/ and w/o the 0.65 factor

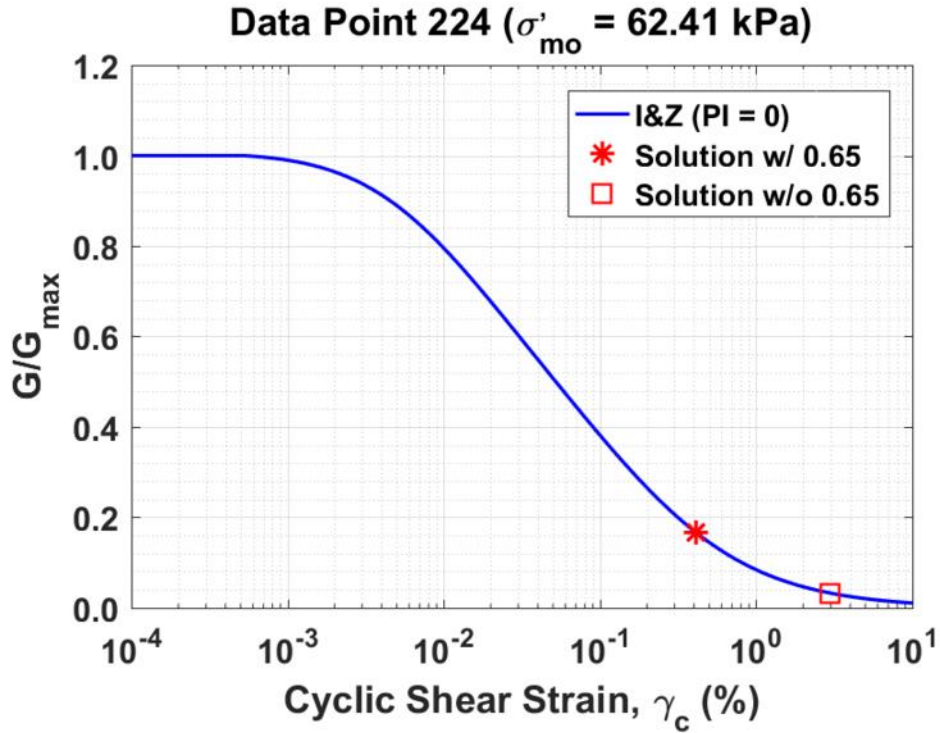


Figure B638. Normalized shear modulus reduction curves for Data Point 224 of the Boulanger et al. database showing the solutions w/ and w/o the 0.65 factor

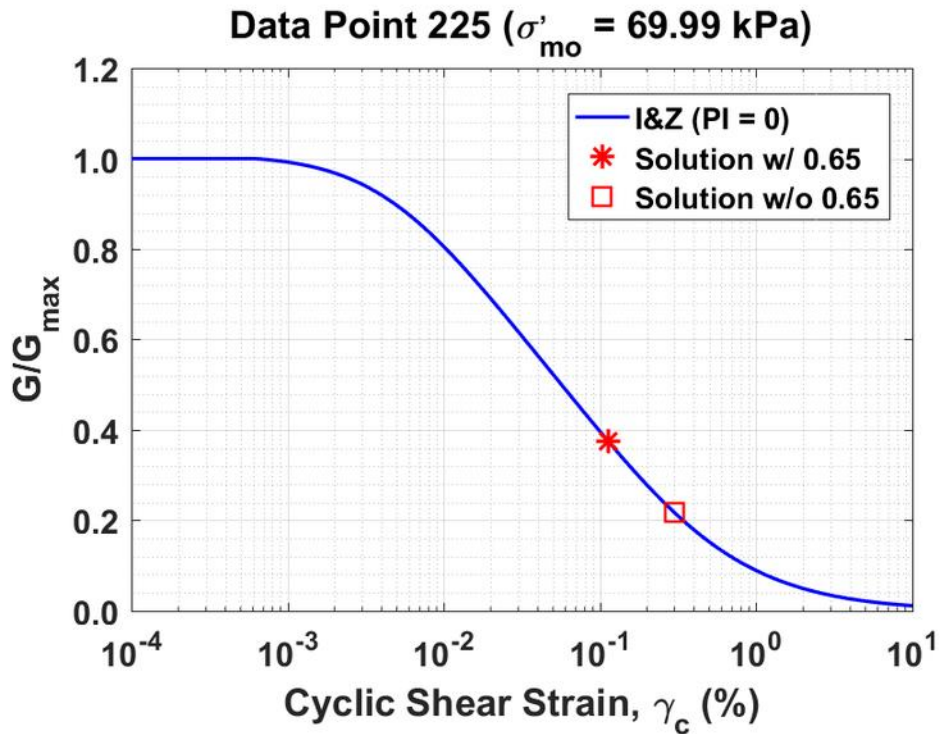


Figure B639. Normalized shear modulus reduction curves for Data Point 225 of the Boulanger et al. database showing the solutions w/ and w/o the 0.65 factor

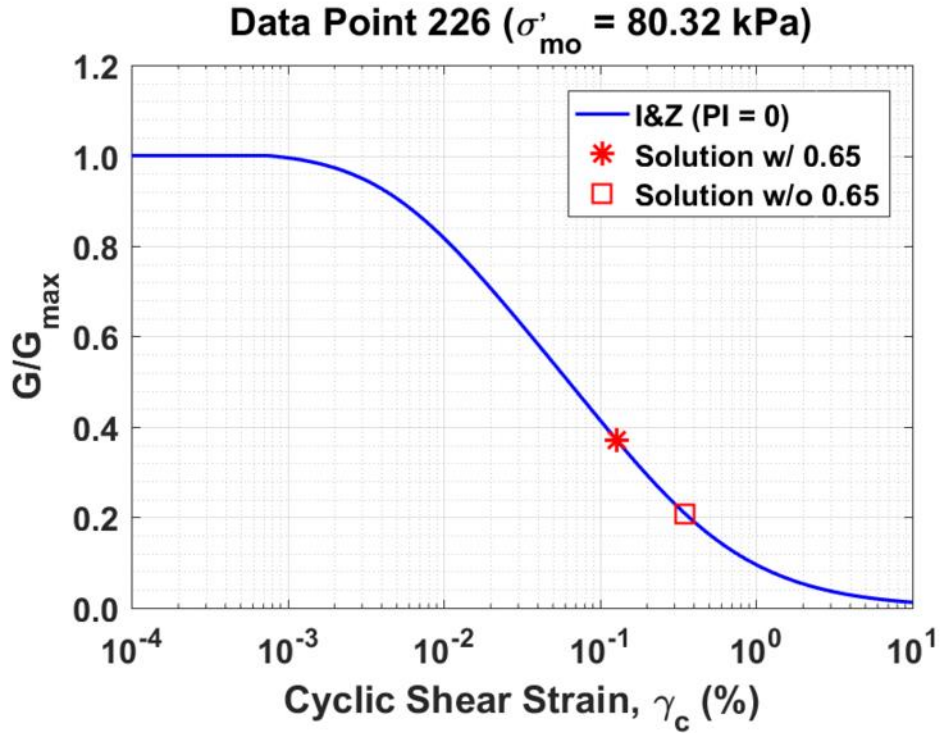


Figure B640. Normalized shear modulus reduction curves for Data Point 226 of the Boulanger et al. database showing the solutions w/ and w/o the 0.65 factor

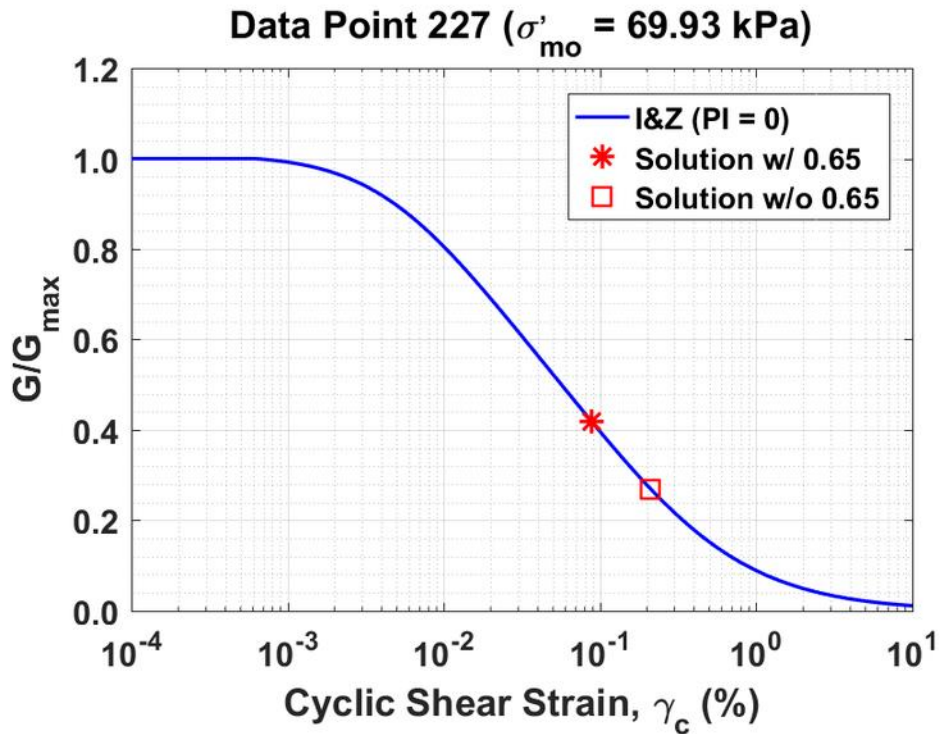


Figure B641. Normalized shear modulus reduction curves for Data Point 227 of the Boulanger et al. database showing the solutions w/ and w/o the 0.65 factor

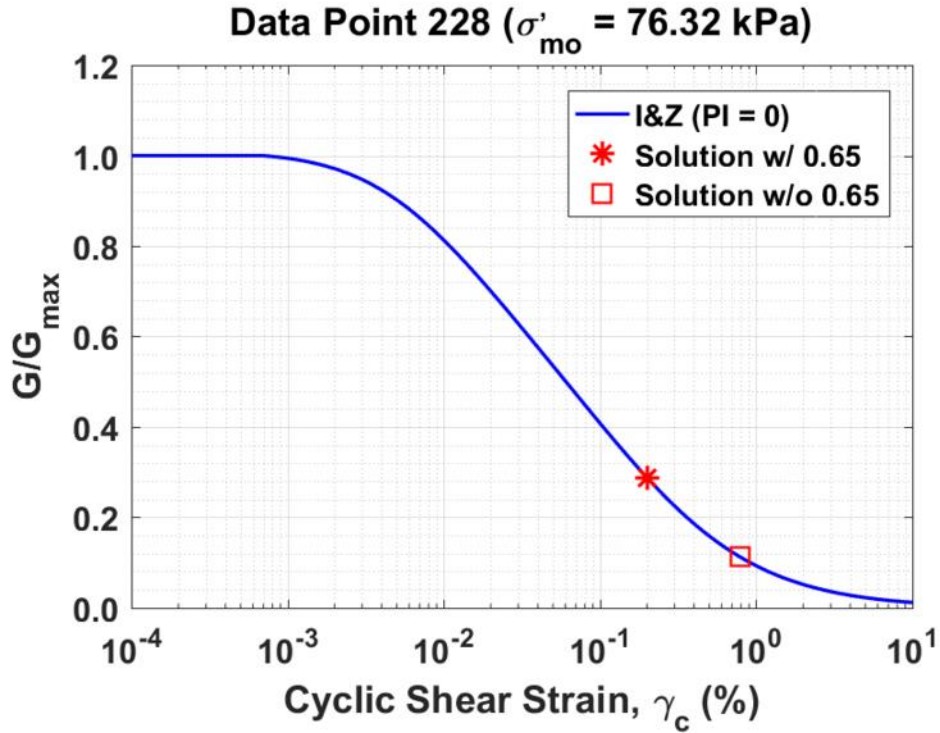


Figure B642. Normalized shear modulus reduction curves for Data Point 228 the Boulanger et al. database showing the solutions w/ and w/o the 0.65 factor

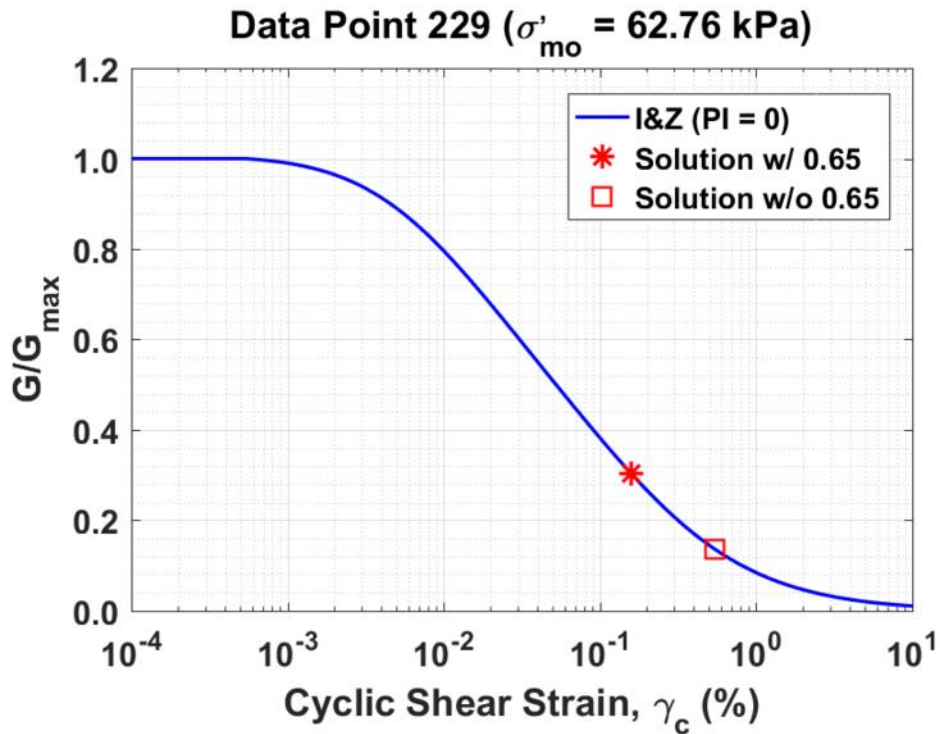


Figure B643. Normalized shear modulus reduction curves for Data Point 229 of the Boulanger et al. database showing the solutions w/ and w/o the 0.65 factor

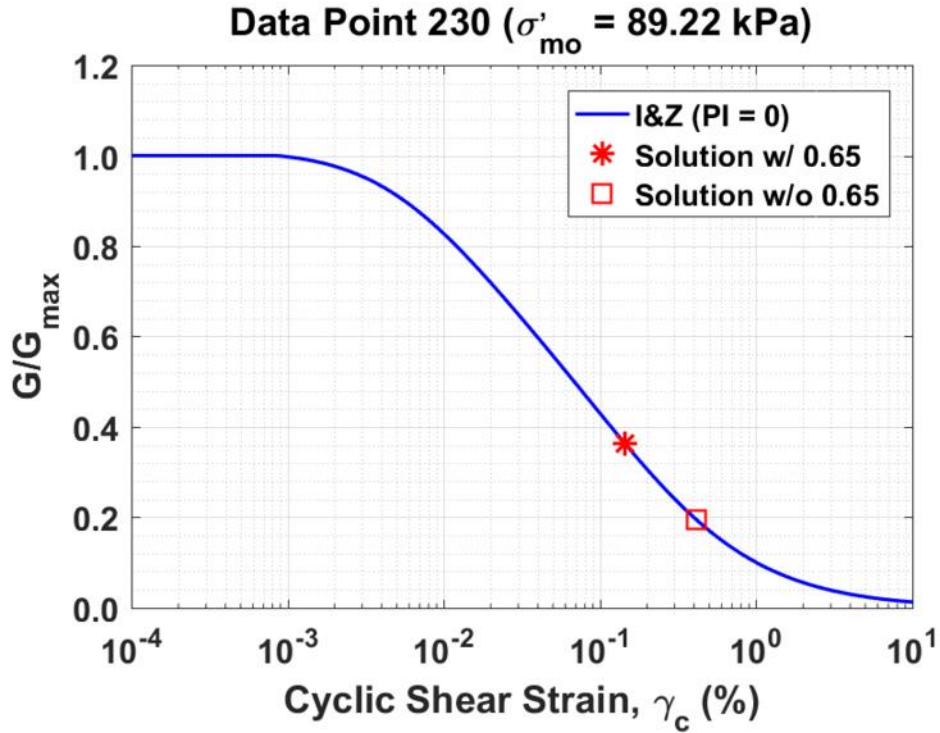


Figure B644. Normalized shear modulus reduction curves for Data Point 230 of the Boulanger et al. database showing the solutions w/ and w/o the 0.65 factor

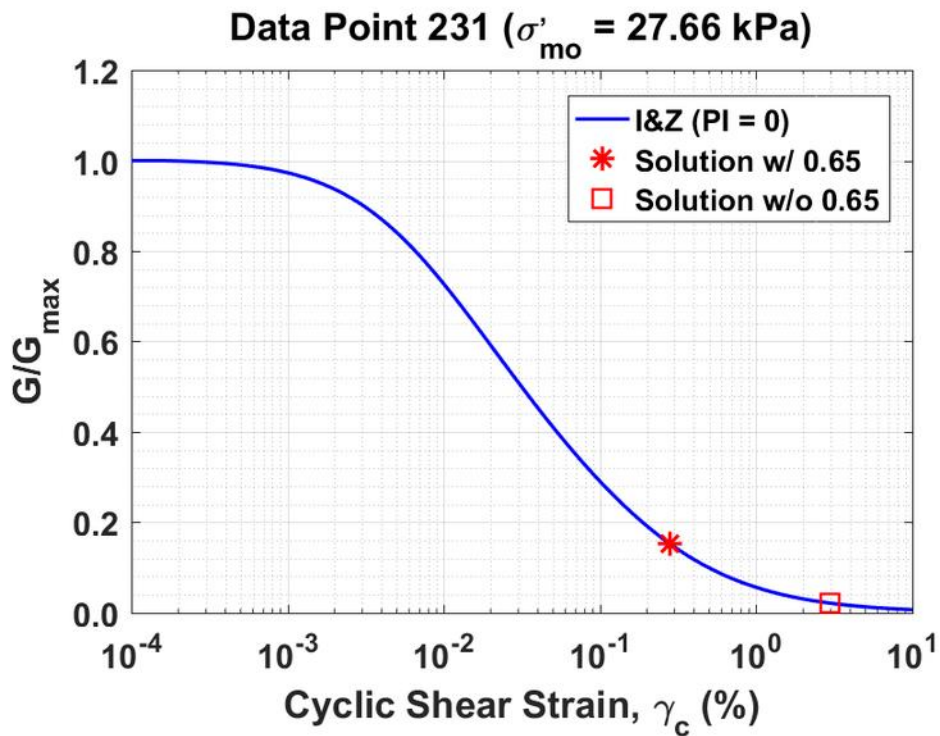


Figure B645. Normalized shear modulus reduction curves for Data Point 231 of the Boulanger et al. database showing the solutions w/ and w/o the 0.65 factor

Appendix C: Pore Pressure Ratio Versus Cyclic Shear Strain for the Kayen et al. Database using the Byrne (1991) and Vucetic and Dobry (1986) Models

Appendix C provides tables and figures showing the inputs and results of implementing both the Byrne (1991) and Vucetic and Dobry (1986) pore pressure models to the case histories in the Kayen et al. (2013) database. First the tables and figures are presented for the Byrne model, followed by the tables and figures for the Vucetic and Dobry model.

Kayen et al. database (415 cases)
Byrne model

Table C1. Parameters needed to plot figures of excess pore pressure ratio versus cyclic shear strain for the Kayen et al. (2013) database using the Byrne (1991) model

Data Point #	Year Event	Liquefied? YES/NO	M _w	V _s (m/s)	σ' _v (kPa)	Lasley n _{eq}	γ _c (%)	Byrne r _u	N _{1,60} blows
5	1906 San Francisco Earthquake, California USA	YES	7.7	146.97	54.03	14.5	0.209	1.00	26
6	1906 San Francisco Earthquake, California USA	NO	7.7	178.54	117.47	15.2	0.123	1.00	16
9	1948 Fukui Earthquake, Japan	YES	7.1	131.91	74.83	11.0	3.005	1.00	9
10	1948 Fukui Earthquake, Japan	YES	7.1	177.99	61.23	11.0	0.293	0.98	50
11	1948 Fukui Earthquake, Japan	YES	7.1	156.28	73.45	11.0	2.322	1.00	20
12	1948 Fukui Earthquake, Japan	YES	7.1	172.49	59.05	11.0	0.352	1.00	47
13	1948 Fukui Earthquake, Japan	YES	7.1	107.41	40.07	11.0	3.005	1.00	10
14	1948 Fukui Earthquake, Japan	YES	7.1	148.00	87.87	11.0	3.005	1.00	11
15	1948 Fukui Earthquake, Japan	YES	7.1	117.16	59.14	11.0	3.005	1.00	8
16	1948 Fukui Earthquake, Japan	YES	7.1	143.66	63.49	11.0	3.005	1.00	18
17	1948 Fukui Earthquake, Japan	YES	7.1	178.91	42.25	11.0	0.183	0.85	50
18	1948 Fukui Earthquake, Japan	NO	7.1	197.53	16.18	11.0	0.020	0.11	50
19	1948 Fukui Earthquake, Japan	YES	7.1	109.87	12.22	11.0	0.377	1.00	50
22	1964 Niigata Earthquake, Japan	NO	7.5	157.95	80.88	19.3	0.040	0.57	18
23	1964 Niigata Earthquake, Japan	YES	7.5	101.64	48.52	19.3	0.230	1.00	6
24	1964 Niigata Earthquake, Japan	YES	7.5	113.27	37.66	19.3	0.089	1.00	15
25	1964 Niigata Earthquake, Japan	YES	7.5	126.67	78.43	18.3	0.163	1.00	7
26	1964 Niigata Earthquake, Japan	YES	7.5	135.36	84.49	18.3	0.147	1.00	8
27	1964 Niigata Earthquake, Japan	YES	7.5	137.63	108.33	18.3	0.161	1.00	6
28	1964 Niigata Earthquake, Japan	YES	7.5	122.06	49.83	18.3	0.065	1.00	13
29	1964 Niigata Earthquake, Japan	NO	7.5	151.72	75.80	18.3	0.086	1.00	17
30	1964 Niigata Earthquake, Japan	NO	7.5	160.57	79.52	18.3	0.068	0.83	20
33	1968 Tokachi Oki Earthquake, Japan	YES	7.9	120.65	57.45	18.9	0.279	1.00	9
34	1968 Tokachi Oki Earthquake, Japan	YES	7.9	120.65	57.45	18.9	0.279	1.00	9
35	1968 Tokachi Oki Earthquake, Japan	YES	7.9	104.89	40.51	18.4	0.476	1.00	9
36	1968 Tokachi Oki Earthquake, Japan	YES	7.9	107.79	28.15	19.3	0.135	1.00	18

37	1968 Tokachi Oki Earthquake, Japan	YES	7.9	97.12	61.80	21.7	0.448	1.00	3
40	1973 Miyagi Ken Oki Earthquake, Japan	YES	7.4	87.21	31.38	17.2	0.627	1.00	6
41	1973 Miyagi Ken Oki Earthquake, Japan	YES	7.4	117.77	44.81	17.2	0.147	1.00	13
42	1973 Miyagi Ken Oki Earthquake, Japan	YES	7.4	171.19	101.05	15.9	0.096	0.98	18
43	1973 Miyagi Ken Oki Earthquake, Japan	YES	7.4	118.46	50.60	15.0	0.366	1.00	11
44	1973 Miyagi Ken Oki Earthquake, Japan	NO	7.4	144.45	50.17	15.0	0.128	1.00	28
45	1973 Miyagi Ken Oki Earthquake, Japan	YES	7.4	150.72	78.99	17.2	0.096	1.00	15
46	1973 Miyagi Ken Oki Earthquake, Japan	YES	7.4	144.36	50.45	14.2	0.294	1.00	27
47	1973 Miyagi Ken Oki Earthquake, Japan	YES	7.4	106.07	86.82	15.9	1.205	1.00	2
48	1973 Miyagi Ken Oki Earthquake, Japan	YES	7.4	144.22	58.90	17.2	0.073	0.91	21
49	1973 Miyagi Ken Oki Earthquake, Japan	YES	7.4	114.54	41.54	15.9	0.388	1.00	13
50	1973 Miyagi Ken Oki Earthquake, Japan	YES	7.4	140.14	52.62	15.9	0.166	1.00	22
53	1975 Haicheng Earthquake, China	YES	7.1	126.93	84.01	19.7	0.085	1.00	6
54	1975 Haicheng Earthquake, China	YES	7.1	92.65	70.97	19.7	0.268	1.00	2
55	1975 Haicheng Earthquake, China	YES	7.1	85.76	41.76	19.7	0.253	1.00	3
56	1975 Haicheng Earthquake, China	YES	7.1	67.23	19.17	19.7	0.264	1.00	3
57	1975 Haicheng Earthquake, China	NO	7.1	120.39	94.39	19.7	0.124	1.00	4
58	1975 Haicheng Earthquake, China	YES	7.1	120.66	40.07	19.7	0.047	0.86	18
62	1976 Tangshan Earthquake, China	NO	8	201.18	59.39	14.9	0.073	0.38	50
63	1976 Tangshan Earthquake, China	YES	8	161.56	72.64	14.2	0.411	1.00	24
64	1976 Tangshan Earthquake, China	YES	8	187.00	84.83	14.2	0.204	0.97	36
65	1976 Tangshan Earthquake, China	YES	8	137.73	40.95	14.9	3.005	1.00	32
66	1976 Tangshan Earthquake, China	YES	8	129.68	17.31	14.9	0.171	1.00	50
67	1976 Tangshan Earthquake, China	YES	8	133.17	36.69	14.2	1.921	1.00	34
68	1976 Tangshan Earthquake, China	NO	8	227.27	41.95	14.9	0.082	0.49	50
69	1976 Tangshan Earthquake, China	YES	8	130.76	29.57	15.7	0.680	1.00	41
70	1976 Tangshan Earthquake, China	NO	8	165.32	33.81	14.9	0.269	1.00	50
71	1976 Tangshan Earthquake, China	YES	8	186.66	55.98	14.9	0.283	1.00	50
72	1976 Tangshan Earthquake, China	NO	8	258.85	35.43	14.9	0.036	0.21	50
73	1976 Tangshan Earthquake, China	NO	8	172.74	22.38	14.9	0.086	0.66	50
74	1976 Tangshan Earthquake, China	YES	8	134.12	22.76	14.9	0.351	1.00	50
75	1976 Tangshan Earthquake, China	YES	8	109.41	11.03	19.7	0.033	0.37	50

76	1976 Tangshan Earthquake, China	YES	8	93.54	19.08	19.7	0.132	1.00	15
77	1976 Tangshan Earthquake, China	NO	8	188.15	36.27	19.7	0.020	0.09	50
78	1976 Tangshan Earthquake, China	YES	8	138.77	41.33	19.7	0.143	1.00	32
79	1976 Tangshan Earthquake, China	YES	8	122.80	58.42	19.7	0.174	1.00	10
80	1976 Tangshan Earthquake, China	NO	8	153.75	51.89	19.7	0.081	0.70	35
81	1976 Tangshan Earthquake, China	YES	8	146.25	39.96	14.9	0.418	1.00	44
82	1976 Tangshan Earthquake, China	NO	8	230.57	57.86	14.9	0.077	0.40	50
83	1976 Tangshan Earthquake, China	YES	8	121.01	18.88	14.2	0.415	1.00	50
84	1976 Tangshan Earthquake, China	YES	8	122.97	42.55	14.9	3.005	1.00	18
85	1976 Tangshan Earthquake, China	YES	8	136.91	26.74	16.7	0.159	0.96	50
88	1978 Miyagi Ken Oki Earthquake, Japan	NO	6.7	117.77	44.81	18.0	0.053	1.00	13
89	1978 Miyagi Ken Oki Earthquake, Japan	NO	6.7	118.46	50.60	16.9	0.067	1.00	11
90	1978 Miyagi Ken Oki Earthquake, Japan	NO	6.7	144.45	50.17	16.9	0.036	0.37	28
91	1978 Miyagi Ken Oki Earthquake, Japan	NO	6.7	150.72	78.99	18.0	0.040	0.67	15
92	1978 Miyagi Ken Oki Earthquake, Japan	YES	6.7	142.56	52.62	18.0	0.040	0.50	24
93	1978 Miyagi Ken Oki Earthquake, Japan	NO	6.7	144.22	58.90	18.0	0.032	0.43	21
94	1978 Miyagi Ken Oki Earthquake, Japan	YES	6.7	114.54	41.54	18.0	0.064	1.00	13
95	1978 Miyagi Ken Oki Earthquake, Japan	NO	6.7	140.14	52.62	18.0	0.043	0.59	22
98	1979 Imperial Valley Earthquake, California, USA	YES	6.5	117.66	41.48	9.6	3.005	1.00	15
99	1979 Imperial Valley Earthquake, California, USA	YES	6.5	122.91	39.30	9.6	1.240	1.00	21
100	1979 Imperial Valley Earthquake, California, USA	NO	6.5	159.59	38.00	9.6	0.145	0.72	50
101	1979 Imperial Valley Earthquake, California, USA	NO	6.5	157.55	42.34	9.6	0.209	0.89	50
102	1979 Imperial Valley Earthquake, California, USA	NO	6.5	98.24	50.21	17.1	0.080	1.00	5
103	1979 Imperial Valley Earthquake, California, USA	YES	6.5	121.54	33.51	9.5	2.753	1.00	25
104	1979 Imperial Valley Earthquake, California, USA	YES	6.5	81.90	48.86	13.6	3.005	1.00	2
105	1979 Imperial Valley Earthquake, California, USA	NO	6.5	96.04	49.97	17.1	0.080	1.00	4
106	1979 Imperial Valley Earthquake, California, USA	NO	6.5	102.14	48.38	16.6	0.111	1.00	6
107	1979 Imperial Valley Earthquake, California, USA	NO	6.5	113.61	48.38	16.6	0.073	1.00	10
108	1979 Imperial Valley Earthquake, California, USA	NO	6.5	111.06	48.38	16.6	0.079	1.00	9
112	1980 Mid Chiba Earthquake, Japan	NO	5.9	164.27	135.78	17.6	0.025	0.56	9
113	1980 Mid Chiba Earthquake, Japan	NO	5.9	135.24	60.62	17.6	0.026	0.45	15

116	1981 Westmorland Earthquake, California, USA	NO	5.9	125.12	39.30	31.0	0.007	0.00	23
117	1981 Westmorland Earthquake, California, USA	NO	5.9	122.91	39.30	31.0	0.007	0.00	21
118	1981 Westmorland Earthquake, California, USA	NO	5.9	159.59	38.00	31.0	0.006	0.00	50
119	1981 Westmorland Earthquake, California, USA	NO	5.9	155.49	40.17	31.0	0.006	0.00	50
120	1981 Westmorland Earthquake, California, USA	YES	5.9	98.24	50.21	9.5	3.005	1.00	5
121	1981 Westmorland Earthquake, California, USA	NO	5.9	101.73	39.59	19.8	0.024	0.85	8
122	1981 Westmorland Earthquake, California, USA	YES	5.9	81.90	48.86	12.1	1.539	1.00	2
123	1981 Westmorland Earthquake, California, USA	YES	5.9	96.04	49.97	10.3	1.141	1.00	4
124	1981 Westmorland Earthquake, California, USA	YES	5.9	102.14	48.38	10.7	1.000	1.00	6
125	1981 Westmorland Earthquake, California, USA	YES	5.9	113.61	48.38	10.7	0.361	1.00	10
126	1981 Westmorland Earthquake, California, USA	YES	5.9	111.06	48.38	10.7	0.429	1.00	9
129	1983 Nihonkai-Chubu Earthquake, Japan	YES	7.7	126.01	57.45	18.4	0.188	1.00	12
130	1983 Nihonkai-Chubu Earthquake, Japan	YES	7.7	153.41	48.76	17.5	0.085	0.66	38
131	1983 Nihonkai-Chubu Earthquake, Japan	YES	7.7	122.49	40.07	16.8	0.217	1.00	19
132	1983 Nihonkai-Chubu Earthquake, Japan	YES	7.7	149.72	68.92	16.8	0.167	1.00	19
133	1983 Nihonkai-Chubu Earthquake, Japan	YES	7.7	127.55	42.73	16.8	0.157	1.00	21
134	1983 Nihonkai-Chubu Earthquake, Japan	YES	7.7	105.12	49.20	22.0	0.129	1.00	7
135	1983 Nihonkai-Chubu Earthquake, Japan	YES	7.7	120.65	57.45	23.0	0.074	1.00	9
136	1983 Nihonkai-Chubu Earthquake, Japan	YES	7.7	98.01	40.36	16.1	3.005	1.00	7
139	1983 Nihonkai-Chubu Aftershocks, Japan	YES	7	98.01	40.36	19.5	0.112	1.00	7
140	1983 Nihonkai-Chubu Aftershocks, Japan	YES	7	120.65	57.45	19.5	0.068	1.00	9
143	1983 Bora Peak Earthquake, Idaho, USA	YES	6.9	115.02	29.02	10.5	3.005	1.00	23
144	1983 Bora Peak Earthquake, Idaho, USA	YES	6.9	96.32	21.63	13.1	0.471	1.00	15
145	1983 Bora Peak Earthquake, Idaho, USA	NO	6.9	196.19	26.17	10.9	0.046	0.29	50
146	1983 Bora Peak Earthquake, Idaho, USA	YES	6.9	93.31	33.32	12.0	3.005	1.00	7
147	1983 Bora Peak Earthquake, Idaho, USA	YES	6.9	115.02	29.02	10.5	3.005	1.00	23
148	1983 Bora Peak Earthquake, Idaho, USA	YES	6.9	158.72	29.02	10.5	0.192	0.95	50
149	1983 Bora Peak Earthquake, Idaho, USA	YES	6.9	110.63	25.49	12.9	0.172	1.00	23
150	1983 Bora Peak Earthquake, Idaho, USA	NO	6.9	266.69	43.94	14.4	0.013	0.02	50
151	1983 Bora Peak Earthquake, Idaho, USA	NO	6.9	264.39	47.66	10.9	0.024	0.09	50
152	1983 Bora Peak Earthquake, Idaho, USA	YES	6.9	86.93	33.17	12.0	3.005	1.00	5
153	1983 Bora Peak Earthquake, Idaho, USA	YES	6.9	89.80	27.43	12.0	3.005	1.00	8

154	1983 Bora Peak Earthquake, Idaho, USA	YES	6.9	96.07	25.49	12.9	0.502	1.00	12
155	1983 Bora Peak Earthquake, Idaho, USA	YES	6.9	96.14	37.37	12.0	3.005	1.00	7
156	1983 Bora Peak Earthquake, Idaho, USA	YES	6.9	115.40	37.37	12.0	0.454	1.00	17
157	1983 Bora Peak Earthquake, Idaho, USA	NO	6.9	164.09	25.11	10.5	0.123	0.76	50
158	1983 Bora Peak Earthquake, Idaho, USA	YES	6.9	129.09	35.39	12.0	0.148	1.00	31
159	1983 Bora Peak Earthquake, Idaho, USA	YES	6.9	124.38	28.39	12.0	0.146	1.00	34
160	1983 Bora Peak Earthquake, Idaho, USA	YES	6.9	103.88	29.26	12.0	0.631	1.00	14
161	1983 Bora Peak Earthquake, Idaho, USA	YES	6.9	127.72	28.39	12.0	0.128	0.93	39
162	1983 Bora Peak Earthquake, Idaho, USA	YES	6.9	113.34	28.39	12.0	0.256	1.00	22
163	1983 Bora Peak Earthquake, Idaho, USA	YES	6.9	158.60	29.45	10.5	0.200	0.96	50
164	1983 Bora Peak Earthquake, Idaho, USA	YES	6.9	96.30	21.63	13.1	0.472	1.00	15
165	1983 Bora Peak Earthquake, Idaho, USA	YES	6.9	122.26	29.02	10.5	3.005	1.00	31
166	1983 Bora Peak Earthquake, Idaho, USA	YES	6.9	145.21	31.00	12.0	0.090	0.56	50
169	1986 Lotung LSST Earthquake Events, Taiwan	NO	6.2	120.34	33.07	13.5	0.084	0.97	24
170	1986 Lotung LSST Earthquake Events, Taiwan	NO	6.2	120.34	33.07	13.5	0.084	0.97	24
171	1986 Lotung LSST Earthquake Events, Taiwan	NO	6.2	120.34	33.07	14.2	0.066	0.86	24
172	1986 Lotung LSST Earthquake Events, Taiwan	NO	6.6	120.34	33.07	14.9	0.088	0.99	24
173	1986 Lotung LSST Earthquake Events, Taiwan	NO	6.2	120.34	33.07	25.0	0.012	0.05	24
174	1986 Lotung LSST Earthquake Events, Taiwan	NO	6	120.34	33.07	20.2	0.017	0.16	24
177	1986 Chiba-Ibaragi-Kenyo, Japan	NO	6	164.27	135.78	20.2	0.020	0.39	9
178	1986 Chiba-Ibaragi-Kenyo, Japan	NO	6	135.24	60.62	20.2	0.019	0.28	15
181	1987 Chiba-Toho-Oki, Japan	NO	6.5	113.65	112.02	18.5	0.064	1.00	2
184	1987 Superstition Hills Earthquake, California, USA	NO	6.5	125.12	39.30	14.5	0.053	0.72	23
185	1987 Superstition Hills Earthquake, California, USA	NO	6.5	122.91	39.30	14.5	0.056	0.81	21
186	1987 Superstition Hills Earthquake, California, USA	NO	6.5	159.59	38.00	14.5	0.025	0.12	50
187	1987 Superstition Hills Earthquake, California, USA	NO	6.5	165.68	38.00	14.5	0.023	0.10	50
188	1987 Superstition Hills Earthquake, California, USA	NO	6.5	93.69	41.52	15.7	0.096	1.00	5
189	1987 Superstition Hills Earthquake, California, USA	NO	6.5	111.81	34.81	14.2	0.097	1.00	16
190	1987 Superstition Hills Earthquake, California, USA	NO	6.5	80.46	43.46	15.7	0.198	1.00	2
191	1987 Superstition Hills Earthquake, California, USA	NO	6.5	92.74	43.46	15.7	0.101	1.00	5
192	1987 Superstition Hills Earthquake, California, USA	YES	6.5	102.14	48.38	13.9	0.308	1.00	6

193	1987 Superstition Hills Earthquake, California, USA	YES	6.5	113.61	48.38	13.9	0.168	1.00	10
194	1987 Superstition Hills Earthquake, California, USA	YES	6.5	111.06	48.38	13.9	0.189	1.00	9
197	1987 Elmore Ranch Earthquake, California, USA	NO	5.9	125.12	39.30	26.3	0.009	0.00	23
198	1987 Elmore Ranch Earthquake, California, USA	NO	5.9	122.91	39.30	26.3	0.009	0.00	21
199	1987 Elmore Ranch Earthquake, California, USA	NO	5.9	159.59	38.00	26.3	0.007	0.00	50
200	1987 Elmore Ranch Earthquake, California, USA	NO	5.9	165.68	38.00	26.3	0.007	0.00	50
201	1987 Elmore Ranch Earthquake, California, USA	NO	5.9	98.24	50.21	13.6	0.113	1.00	5
202	1987 Elmore Ranch Earthquake, California, USA	NO	5.9	111.81	34.81	21.3	0.014	0.16	16
203	1987 Elmore Ranch Earthquake, California, USA	NO	5.9	81.90	48.86	15.4	0.151	1.00	2
204	1987 Elmore Ranch Earthquake, California, USA	NO	5.9	96.04	49.97	16.1	0.054	1.00	4
205	1987 Elmore Ranch Earthquake, California, USA	NO	5.9	102.14	48.38	14.9	0.085	1.00	6
206	1987 Elmore Ranch Earthquake, California, USA	NO	5.9	113.61	48.38	14.9	0.058	1.00	10
207	1987 Elmore Ranch Earthquake, California, USA	NO	5.9	111.06	48.38	14.9	0.063	1.00	9
210	1989 Loma Prieta Earthquake, California, USA	YES	7	171.12	78.97	12.0	0.148	0.96	27
211	1989 Loma Prieta Earthquake, California, USA	YES	7	164.19	96.07	12.6	0.141	1.00	16
212	1989 Loma Prieta Earthquake, California, USA	YES	7	134.22	99.44	11.8	0.595	1.00	6
213	1989 Loma Prieta Earthquake, California, USA	NO	7	157.57	81.86	11.8	0.135	1.00	17
214	1989 Loma Prieta Earthquake, California, USA	NO	7	165.48	62.18	12.0	0.125	0.79	36
215	1989 Loma Prieta Earthquake, California, USA	NO	7	130.23	52.98	14.1	0.208	1.00	15
216	1989 Loma Prieta Earthquake, California, USA	NO	7	127.06	41.28	14.1	0.134	1.00	22
217	1989 Loma Prieta Earthquake, California, USA	YES	7	171.25	35.30	11.0	0.106	0.61	50
218	1989 Loma Prieta Earthquake, California, USA	YES	7	175.02	85.94	15.3	0.063	0.57	26
219	1989 Loma Prieta Earthquake, California, USA	YES	7	103.64	48.57	15.3	0.264	1.00	6
220	1989 Loma Prieta Earthquake, California, USA	YES	7	125.21	74.74	15.3	0.231	1.00	7
221	1989 Loma Prieta Earthquake, California, USA	YES	7	120.61	45.77	14.5	0.161	1.00	14
222	1989 Loma Prieta Earthquake, California, USA	YES	7	139.20	72.99	14.3	0.251	1.00	12
223	1989 Loma Prieta Earthquake, California, USA	YES	7	111.03	29.40	14.3	0.170	1.00	19
224	1989 Loma Prieta Earthquake, California, USA	NO	7	165.07	41.55	14.3	0.055	0.32	50
225	1989 Loma Prieta Earthquake, California, USA	NO	7	158.97	104.97	20.0	0.030	0.59	12
226	1989 Loma Prieta Earthquake, California, USA	YES	7	135.95	80.00	18.1	0.082	1.00	9
227	1989 Loma Prieta Earthquake, California, USA	YES	7	139.24	80.00	18.1	0.076	1.00	10
228	1989 Loma Prieta Earthquake, California, USA	YES	7	125.23	80.00	18.1	0.110	1.00	6
229	1989 Loma Prieta Earthquake, California, USA	YES	7	124.83	80.00	18.1	0.112	1.00	6
230	1989 Loma Prieta Earthquake, California, USA	YES	7	141.39	90.10	11.1	0.627	1.00	9
231	1989 Loma Prieta Earthquake, California, USA	YES	7	125.76	90.71	11.7	1.579	1.00	5

232	1989 Loma Prieta Earthquake, California, USA	YES	7	145.85	96.79	11.7	0.832	1.00	9
233	1989 Loma Prieta Earthquake, California, USA	YES	7	155.29	95.57	11.1	0.399	1.00	12
234	1989 Loma Prieta Earthquake, California, USA	NO	7	146.97	54.03	16.0	0.055	0.60	26
235	1989 Loma Prieta Earthquake, California, USA	YES	7	156.88	84.69	12.3	0.182	1.00	16
236	1989 Loma Prieta Earthquake, California, USA	YES	7	160.34	95.87	12.3	0.183	1.00	14
237	1989 Loma Prieta Earthquake, California, USA	YES	7	115.70	39.15	15.0	0.118	1.00	16
238	1989 Loma Prieta Earthquake, California, USA	YES	7	106.96	51.97	12.3	3.005	1.00	6
239	1989 Loma Prieta Earthquake, California, USA	NO	7	114.72	41.24	15.0	0.111	1.00	13
240	1989 Loma Prieta Earthquake, California, USA	NO	7	101.77	45.74	15.0	0.206	1.00	6
241	1989 Loma Prieta Earthquake, California, USA	YES	7	115.61	51.97	15.0	0.184	1.00	9
242	1989 Loma Prieta Earthquake, California, USA	YES	7	106.38	54.83	14.1	0.457	1.00	6
243	1989 Loma Prieta Earthquake, California, USA	YES	7	105.14	50.69	14.1	0.404	1.00	6
244	1989 Loma Prieta Earthquake, California, USA	NO	7	175.26	41.55	14.3	0.045	0.26	50
245	1989 Loma Prieta Earthquake, California, USA	NO	7	191.76	41.55	14.3	0.035	0.18	50
246	1989 Loma Prieta Earthquake, California, USA	NO	7	178.55	117.47	17.6	0.039	0.51	16
247	1989 Loma Prieta Earthquake, California, USA	NO	7	157.40	107.92	17.6	0.048	0.92	11
248	1989 Loma Prieta Earthquake, California, USA	NO	7	166.82	44.48	11.6	0.134	0.68	50
249	1989 Loma Prieta Earthquake, California, USA	YES	7	96.31	25.60	11.6	3.005	1.00	12
250	1989 Loma Prieta Earthquake, California, USA	YES	7	100.77	25.78	11.6	3.005	1.00	15
251	1989 Loma Prieta Earthquake, California, USA	YES	7	165.59	39.40	11.6	0.087	0.49	50
252	1989 Loma Prieta Earthquake, California, USA	NO	7	127.51	28.41	11.6	0.140	0.97	38
253	1989 Loma Prieta Earthquake, California, USA	YES	7	136.12	84.59	18.1	0.080	1.00	8
254	1989 Loma Prieta Earthquake, California, USA	YES	7	132.29	46.72	15.0	0.117	1.00	21
255	1989 Loma Prieta Earthquake, California, USA	YES	7	136.22	80.78	12.7	0.190	1.00	9
256	1989 Loma Prieta Earthquake, California, USA	NO	7	137.01	64.09	18.6	0.034	0.68	14
257	1989 Loma Prieta Earthquake, California, USA	YES	7	132.51	80.00	18.1	0.090	1.00	8
258	1989 Loma Prieta Earthquake, California, USA	YES	7	135.70	43.12	14.3	0.092	0.91	27
259	1989 Loma Prieta Earthquake, California, USA	YES	7	120.60	37.37	14.3	0.117	1.00	21
260	1989 Loma Prieta Earthquake, California, USA	YES	7	166.99	63.06	14.3	0.073	0.51	36
261	1989 Loma Prieta Earthquake, California, USA	YES	7	111.14	34.33	14.3	0.137	1.00	16
262	1989 Loma Prieta Earthquake, California, USA	YES	7	142.81	48.14	14.3	0.100	0.90	28
263	1989 Loma Prieta Earthquake, California, USA	YES	7	116.58	35.05	14.3	0.174	1.00	19
264	1989 Loma Prieta Earthquake, California, USA	YES	7	126.04	53.88	17.6	0.055	1.00	13
265	1989 Loma Prieta Earthquake, California, USA	NO	7	154.27	70.54	18.6	0.045	0.59	20
266	1989 Loma Prieta Earthquake, California, USA	YES	7	131.17	62.72	17.6	0.067	1.00	12
267	1989 Loma Prieta Earthquake, California, USA	YES	7	130.77	42.20	18.1	0.045	0.63	24
	1989 Loma Prieta Earthquake, California, USA	YES	7		53.88	17.6	0.054	0.99	13

270

119.49

271	1993 Kushiro Earthquake, Japan	YES	7.6	148.59	30.13	13.6	0.353	1.00	26
272	1993 Kushiro Earthquake, Japan	YES	7.6	86.85	76.67	13.6	0.823	1.00	15
273	1993 Kushiro Earthquake, Japan	YES	7.6	110.99	29.21	13.6	3.005	1.00	6
274	1993 Kushiro Earthquake, Japan	YES	7.6	110.62	57.45	13.6	3.005	1.00	6
275	1993 Kushiro Earthquake, Japan	YES	7.6	163.52	40.07	13.6	3.005	1.00	12
276	1993 Kushiro Earthquake, Japan	YES	7.6	118.96	47.53	12.8	0.251	0.98	50
277	1993 Kushiro Earthquake, Japan	YES	7.6	158.78	61.41	13.6	3.005	1.00	8
	1993 Kushiro Earthquake, Japan	YES	7.6		88.84	13.6	0.626	1.00	16
280				136.00					
281	1993 Hokkaido Nansei Oki Earthquake, Japan	YES	7.7	103.67	71.46	21.3	0.075	1.00	11
282	1993 Hokkaido Nansei Oki Earthquake, Japan	YES	7.7	145.07	51.90	21.3	0.127	1.00	6
283	1993 Hokkaido Nansei Oki Earthquake, Japan	YES	7.7	128.59	72.42	21.6	0.050	0.89	15
284	1993 Hokkaido Nansei Oki Earthquake, Japan	YES	7.7	149.14	67.11	21.6	0.080	1.00	10
285	1993 Hokkaido Nansei Oki Earthquake, Japan	YES	7.7	195.18	65.81	20.2	0.062	0.85	20
286	1993 Hokkaido Nansei Oki Earthquake, Japan	NO	7.7	120.57	75.80	21.3	0.030	0.13	50
287	1993 Hokkaido Nansei Oki Earthquake, Japan	YES	7.7	54.80	57.65	21.3	0.062	1.00	9
288	1993 Hokkaido Nansei Oki Earthquake, Japan	YES	7.7	84.52	20.52	18.8	3.005	1.00	1
289	1993 Hokkaido Nansei Oki Earthquake, Japan	YES	7.7	158.12	41.52	18.8	3.005	1.00	3
290	1993 Hokkaido Nansei Oki Earthquake, Japan	YES	7.7	166.29	67.59	17.7	0.082	0.83	25
291	1993 Hokkaido Nansei Oki Earthquake, Japan	YES	7.7	146.16	67.59	17.7	0.069	0.59	31
292	1993 Hokkaido Nansei Oki Earthquake, Japan	YES	7.7	114.40	67.59	17.7	0.109	1.00	17
293	1993 Hokkaido Nansei Oki Earthquake, Japan	YES	7.7	147.10	31.38	19.1	0.089	1.00	20
294	1993 Hokkaido Nansei Oki Earthquake, Japan	NO	7.7	80.55	51.42	19.1	0.065	0.69	29
295	1993 Hokkaido Nansei Oki Earthquake, Japan	YES	7.7	99.96	20.04	12.7	3.005	1.00	7
296	1993 Hokkaido Nansei Oki Earthquake, Japan	YES	7.7	98.39	17.38	15.9	0.128	1.00	23
297	1993 Hokkaido Nansei Oki Earthquake, Japan	YES	7.7	99.49	16.99	19.1	0.075	1.00	22
298	1993 Hokkaido Nansei Oki Earthquake, Japan	YES	7.7	115.03	26.12	19.1	0.168	1.00	13
299	1993 Hokkaido Nansei Oki Earthquake, Japan	YES	7.7	161.14	54.80	16.8	0.929	1.00	8
300	1993 Hokkaido Nansei Oki Earthquake, Japan	YES	7.7	95.50	54.08	12.7	0.416	1.00	40
301	1993 Hokkaido Nansei Oki Earthquake, Japan	YES	7.7	114.92	36.70	15.9	0.762	1.00	7
302	1993 Hokkaido Nansei Oki Earthquake, Japan	YES	7.7	185.26	33.56	15.9	0.338	1.00	19
303	1993 Hokkaido Nansei Oki Earthquake, Japan	YES	7.7	88.98	57.99	12.7	0.198	0.85	50
304	1993 Hokkaido Nansei Oki Earthquake, Japan	YES	7.7	88.98	41.76	16.8	3.005	1.00	4
305	1993 Hokkaido Nansei Oki Earthquake, Japan	YES	7.7	180.15	41.76	16.8	3.005	1.00	4
306	1993 Hokkaido Nansei Oki Earthquake, Japan	NO	7.7	114.59	57.17	21.6	0.023	0.10	50
	1993 Hokkaido Nansei Oki Earthquake, Japan	YES	7.7		54.80	12.7	3.005	1.00	8
309				167.15					

310	1995 Hyogo Nambu Earthquake, Japan	NO	7	168.25	101.00	19.3	0.041	0.60	16
311	1995 Hyogo Nambu Earthquake, Japan	YES	7	151.59	88.35	10.8	2.490	1.00	13
312	1995 Hyogo Nambu Earthquake, Japan	YES	7	148.19	88.35	10.8	3.005	1.00	11
313	1995 Hyogo Nambu Earthquake, Japan	NO	7	160.96	115.40	11.8	0.234	1.00	10
314	1995 Hyogo Nambu Earthquake, Japan	YES	7	106.71	54.99	15.6	0.214	1.00	6
315	1995 Hyogo Nambu Earthquake, Japan	YES	7	182.32	71.65	10.8	0.151	0.70	43
316	1995 Hyogo Nambu Earthquake, Japan	YES	7	132.21	62.67	10.8	3.005	1.00	12
317	1995 Hyogo Nambu Earthquake, Japan	YES	7	156.84	96.51	10.3	3.005	1.00	13
318	1995 Hyogo Nambu Earthquake, Japan	YES	7	178.79	92.21	10.8	0.591	1.00	25
319	1995 Hyogo Nambu Earthquake, Japan	YES	7	180.81	76.77	10.8	0.257	1.00	37
320	1995 Hyogo Nambu Earthquake, Japan	YES	7	168.76	98.49	10.8	0.672	1.00	17
321	1995 Hyogo Nambu Earthquake, Japan	YES	7	188.51	64.26	10.8	0.186	0.75	50
322	1995 Hyogo Nambu Earthquake, Japan	YES	7	200.94	109.03	10.0	0.233	0.97	32
323	1995 Hyogo Nambu Earthquake, Japan	NO	7	212.82	73.39	10.8	0.091	0.38	50
324	1995 Hyogo Nambu Earthquake, Japan	NO	7	198.62	88.36	10.0	0.145	0.59	44
325	1995 Hyogo Nambu Earthquake, Japan	NO	7	188.68	64.07	10.0	0.360	1.00	50
326	1995 Hyogo Nambu Earthquake, Japan	YES	7	169.86	55.98	10.0	0.525	1.00	48
327	1995 Hyogo Nambu Earthquake, Japan	YES	7	194.45	75.42	10.0	0.315	0.95	50
328	1995 Hyogo Nambu Earthquake, Japan	YES	7	189.58	83.19	10.0	0.395	1.00	40
329	1995 Hyogo Nambu Earthquake, Japan	NO	7	220.62	69.45	10.0	0.169	0.65	50
330	1995 Hyogo Nambu Earthquake, Japan	YES	7	192.56	77.10	10.0	0.394	1.00	49
331	1995 Hyogo Nambu Earthquake, Japan	NO	7	173.22	50.26	10.0	0.342	1.00	50
332	1995 Hyogo Nambu Earthquake, Japan	NO	7	191.11	53.21	10.0	0.227	0.87	50
333	1995 Hyogo Nambu Earthquake, Japan	NO	7	191.11	53.21	10.0	0.227	0.87	50
334	1995 Hyogo Nambu Earthquake, Japan	YES	7	166.14	71.31	10.8	0.329	1.00	28
335	1995 Hyogo Nambu Earthquake, Japan	YES	7	205.52	80.15	10.8	0.178	0.67	50
336	1995 Hyogo Nambu Earthquake, Japan	YES	7	137.45	44.90	10.8	1.430	1.00	27
337	1995 Hyogo Nambu Earthquake, Japan	YES	7	185.94	91.49	10.6	0.367	1.00	31
338	1995 Hyogo Nambu Earthquake, Japan	YES	7	216.07	176.08	10.8	0.252	1.00	19
339	1995 Hyogo Nambu Earthquake, Japan	YES	7	174.19	86.35	10.8	0.330	1.00	25
340	1995 Hyogo Nambu Earthquake, Japan	YES	7	198.74	73.14	10.8	0.202	0.76	50
341	1995 Hyogo Nambu Earthquake, Japan	YES	7	133.45	50.26	12.4	0.169	1.00	19
342	1995 Hyogo Nambu Earthquake, Japan	YES	7	155.05	52.92	10.6	0.340	1.00	35
343	1995 Hyogo Nambu Earthquake, Japan	YES	7	172.44	68.03	10.8	0.313	1.00	37
344	1995 Hyogo Nambu Earthquake, Japan	YES	7	170.26	64.36	10.8	0.314	1.00	38
345	1995 Hyogo Nambu Earthquake, Japan	YES	7	163.85	40.03	10.8	0.120	0.63	50
346	1995 Hyogo Nambu Earthquake, Japan	YES	7	176.26	64.70	10.0	0.206	0.85	44
347	1995 Hyogo Nambu Earthquake, Japan	YES	7	188.90	94.92	10.0	0.503	1.00	31
348	1995 Hyogo Nambu Earthquake, Japan	YES	7	124.52	27.04	10.8	1.126	1.00	37

349	1995 Hyogo Nambu Earthquake, Japan	YES	7	129.65	68.89	10.0	3.005	1.00	10
350	1995 Hyogo Nambu Earthquake, Japan	YES	7	142.02	64.99	10.0	3.005	1.00	16
351	1995 Hyogo Nambu Earthquake, Japan	YES	7	147.93	27.04	10.0	0.423	1.00	50
352	1995 Hyogo Nambu Earthquake, Japan	YES	7	155.87	56.20	10.0	0.918	1.00	32
353	1995 Hyogo Nambu Earthquake, Japan	YES	7	161.49	89.85	10.8	0.675	1.00	16
354	1995 Hyogo Nambu Earthquake, Japan	YES	7	136.20	52.48	10.0	3.005	1.00	19
355	1995 Hyogo Nambu Earthquake, Japan	YES	7	152.96	69.28	10.0	3.005	1.00	20
356	1995 Hyogo Nambu Earthquake, Japan	YES	7	127.56	60.11	10.8	3.005	1.00	11
357	1995 Hyogo Nambu Earthquake, Japan	YES	7	149.31	71.72	10.8	1.742	1.00	17
358	1995 Hyogo Nambu Earthquake, Japan	YES	7	147.49	62.86	10.0	3.005	1.00	20
359	1995 Hyogo Nambu Earthquake, Japan	YES	7	155.84	63.49	10.8	1.738	1.00	26
360	1995 Hyogo Nambu Earthquake, Japan	YES	7	127.39	39.74	11.8	0.326	1.00	23
361	1995 Hyogo Nambu Earthquake, Japan	YES	7	152.00	56.95	10.8	0.634	1.00	28
362	1995 Hyogo Nambu Earthquake, Japan	YES	7	135.37	64.45	10.0	3.005	1.00	13
363	1995 Hyogo Nambu Earthquake, Japan	YES	7	144.03	58.69	10.0	3.005	1.00	21
364	1995 Hyogo Nambu Earthquake, Japan	YES	7	123.75	61.56	10.0	3.005	1.00	9
365	1995 Hyogo Nambu Earthquake, Japan	YES	7	136.10	63.25	10.0	3.005	1.00	14
366	1995 Hyogo Nambu Earthquake, Japan	YES	7	109.72	61.08	10.0	3.005	1.00	5
367	1995 Hyogo Nambu Earthquake, Japan	YES	7	172.31	69.65	10.0	0.485	1.00	35
368	1995 Hyogo Nambu Earthquake, Japan	YES	7	171.75	86.43	10.8	0.321	1.00	24
369	1995 Hyogo Nambu Earthquake, Japan	YES	7	185.25	103.81	10.8	0.306	1.00	24
370	1995 Hyogo Nambu Earthquake, Japan	YES	7	148.33	90.24	10.8	1.416	1.00	11
371	1995 Hyogo Nambu Earthquake, Japan	YES	7	164.14	41.52	11.8	0.074	0.41	50
372	1995 Hyogo Nambu Earthquake, Japan	NO	7	198.54	46.74	11.8	0.042	0.21	50
373	1995 Hyogo Nambu Earthquake, Japan	YES	7	228.37	173.25	11.8	0.136	0.77	26
374	1995 Hyogo Nambu Earthquake, Japan	NO	7	238.92	60.74	11.8	0.036	0.15	50
375	1995 Hyogo Nambu Earthquake, Japan	NO	7	313.20	157.64	11.8	0.049	0.14	50
376	1995 Hyogo Nambu Earthquake, Japan	NO	7	248.73	89.90	11.8	0.067	0.26	50
377	1995 Hyogo Nambu Earthquake, Japan	NO	7	276.69	75.08	11.8	0.034	0.12	50
378	1995 Hyogo Nambu Earthquake, Japan	NO	7	241.69	102.93	11.8	0.082	0.30	50
379	1995 Hyogo Nambu Earthquake, Japan	NO	7	246.98	69.43	11.8	0.041	0.16	50
380	1995 Hyogo Nambu Earthquake, Japan	YES	7	187.21	78.12	12.6	0.088	0.46	42
381	1995 Hyogo Nambu Earthquake, Japan	NO	7	260.78	124.03	13.3	0.048	0.16	50
382	1995 Hyogo Nambu Earthquake, Japan	YES	7	151.36	73.49	10.8	0.750	1.00	17
383	1995 Hyogo Nambu Earthquake, Japan	YES	7	172.13	136.54	11.4	0.456	1.00	11
384	1995 Hyogo Nambu Earthquake, Japan	YES	7	172.13	136.54	11.4	0.456	1.00	11
385	1995 Hyogo Nambu Earthquake, Japan	NO	7	203.64	54.56	12.4	0.063	0.31	50
386	1995 Hyogo Nambu Earthquake, Japan	YES	7	159.81	56.11	10.8	0.209	1.00	36
387	1995 Hyogo Nambu Earthquake, Japan	YES	7	155.30	58.23	10.8	0.218	1.00	30

388	1995 Hyogo Nambu Earthquake, Japan	YES	7	175.33	58.23	10.8	0.123	0.55	50
389	1995 Hyogo Nambu Earthquake, Japan	YES	7	141.25	58.42	11.8	0.493	1.00	19
390	1995 Hyogo Nambu Earthquake, Japan	YES	7	179.97	63.73	10.0	0.286	0.94	50
391	1995 Hyogo Nambu Earthquake, Japan	YES	7	164.73	73.27	11.8	0.220	1.00	26
392	1995 Hyogo Nambu Earthquake, Japan	YES	7	204.76	77.74	10.8	0.113	0.45	50
393	1995 Hyogo Nambu Earthquake, Japan	YES	7	154.39	27.04	10.8	0.164	0.89	50
394	1995 Hyogo Nambu Earthquake, Japan	YES	7	142.70	63.49	10.8	3.005	1.00	17
398	1999 Chi Chi Earthquake, Japan	YES	7.6	176.67	57.45	13.6	0.188	0.84	50
399	1999 Chi Chi Earthquake, Japan	YES	7.6	196.38	126.30	13.6	0.231	1.00	22
400	1999 Chi Chi Earthquake, Japan	YES	7.6	150.15	36.21	13.6	0.152	0.84	50
401	1999 Chi Chi Earthquake, Japan	YES	7.6	176.45	55.48	13.6	0.094	0.49	50
402	1999 Chi Chi Earthquake, Japan	NO	7.6	146.13	22.21	13.6	0.129	0.87	50
403	1999 Chi Chi Earthquake, Japan	YES	7.6	119.70	24.38	13.6	0.717	1.00	35
404	1999 Chi Chi Earthquake, Japan	YES	7.6	124.69	25.30	11.1	3.005	1.00	40
405	1999 Chi Chi Earthquake, Japan	YES	7.6	120.57	23.47	11.1	3.005	1.00	38
406	1999 Chi Chi Earthquake, Japan	YES	7.6	164.74	33.17	11.1	0.300	1.00	50
407	1999 Chi Chi Earthquake, Japan	YES	7.6	123.49	44.90	11.1	3.005	1.00	16
408	1999 Chi Chi Earthquake, Japan	YES	7.6	145.00	67.74	11.1	3.005	1.00	16
409	1999 Chi Chi Earthquake, Japan	YES	7.6	112.43	34.28	10.8	3.005	1.00	17
410	1999 Chi Chi Earthquake, Japan	YES	7.6	131.61	49.02	11.1	3.005	1.00	19
411	1999 Chi Chi Earthquake, Japan	YES	7.6	154.89	86.18	16.4	0.179	1.00	15
414	1999 Druce Earthquake, Turkey	YES	7.40	129.50	80.10	12.9	2.978	1.00	7
415	1999 Druce Earthquake, Turkey	YES	7.40	139.36	82.40	12.9	1.028	1.00	10
419	2000 Tottori Seibu Earthquake, Japan	YES	6.8	88.00	60.59	12.1	3.005	1.00	2
420	2000 Tottori Seibu Earthquake, Japan	YES	6.8	114.93	62.77	12.1	2.580	1.00	6
421	2000 Tottori Seibu Earthquake, Japan	YES	6.8	103.53	53.98	11.4	3.005	1.00	5
424	2001 Geiyo-Hiroshima Ken Earthquake, Japan	YES	6.8	113.83	27.04	13.6	0.129	1.00	24
425	2001 Geiyo-Hiroshima Ken Earthquake, Japan	YES	6.8	104.87	27.04	13.6	0.204	1.00	16
426	2001 Geiyo-Hiroshima Ken Earthquake, Japan	YES	6.8	120.90	27.04	13.6	0.097	0.94	32

427	2001 Geiyo-Hiroshima Ken Earthquake, Japan	YES	6.8	152.02	76.33	13.6	0.112	1.00	17
428	2001 Geiyo-Hiroshima Ken Earthquake, Japan	YES	6.8	177.11	96.56	13.4	0.112	0.92	22
431	2002 Denali Fault Earthquake, Alaska, USA	NO	7.9	189.16	20.94	15.2	0.026	0.18	50
432	2002 Denali Fault Earthquake, Alaska, USA	YES	7.9	116.86	20.94	15.2	0.185	1.00	38
433	2002 Denali Fault Earthquake, Alaska, USA	YES	7.9	116.86	20.94	15.2	0.185	1.00	38
434	2002 Denali Fault Earthquake, Alaska, USA	NO	7.9	158.03	20.94	15.2	0.046	0.37	50
435	2002 Denali Fault Earthquake, Alaska, USA	NO	7.9	244.67	20.94	15.2	0.014	0.05	50
436	2002 Denali Fault Earthquake, Alaska, USA	NO	7.9	182.41	20.94	15.2	0.029	0.20	50
437	2002 Denali Fault Earthquake, Alaska, USA	NO	7.9	165.35	20.94	15.2	0.040	0.31	50
438	2002 Denali Fault Earthquake, Alaska, USA	YES	7.9	138.75	20.94	15.2	0.075	0.61	50
439	2002 Denali Fault Earthquake, Alaska, USA	YES	7.9	110.14	30.16	14.7	0.626	1.00	18
442	2003 Sanriku-Minami Earthquake, Japan	NO	7	87.21	31.38	15.0	1.285	1.00	6
443	2003 Sanriku-Minami Earthquake, Japan	NO	7	117.77	44.81	13.6	0.400	1.00	13
444	2003 Sanriku-Minami Earthquake, Japan	NO	7	171.19	101.05	13.6	0.122	1.00	18
445	2003 Sanriku-Minami Earthquake, Japan	YES	7	118.46	50.60	14.1	0.265	1.00	11
446	2003 Sanriku-Minami Earthquake, Japan	YES	7	144.45	50.17	14.1	0.100	0.90	28
447	2003 Sanriku-Minami Earthquake, Japan	NO	7	150.72	78.99	13.6	0.184	1.00	15
448	2003 Sanriku-Minami Earthquake, Japan	NO	7	144.36	50.45	14.8	0.122	0.99	27
449	2003 Sanriku-Minami Earthquake, Japan	NO	7	106.07	86.82	13.6	3.005	1.00	2
450	2003 Sanriku-Minami Earthquake, Japan	NO	7	144.22	58.90	13.6	0.139	1.00	21
451	2003 Sanriku-Minami Earthquake, Japan	NO	7	114.54	41.54	14.8	0.329	1.00	13
452	2003 Sanriku-Minami Earthquake, Japan	NO	7	140.14	52.62	14.8	0.147	1.00	22
455	2003 Tokachi Oki Earthquake, Japan	YES	7.8	148.59	76.67	14.2	0.846	1.00	15
456	2003 Tokachi Oki Earthquake, Japan	YES	7.8	110.99	57.45	14.2	3.005	1.00	6
457	2003 Tokachi Oki Earthquake, Japan	YES	7.8	110.62	40.07	14.2	3.005	1.00	12
458	2003 Tokachi Oki Earthquake, Japan	NO	7.8	163.52	47.53	14.2	0.184	0.88	50
459	2003 Tokachi Oki Earthquake, Japan	NO	7.8	118.96	61.41	14.2	3.005	1.00	8
460	2003 Tokachi Oki Earthquake, Japan	YES	7.8	158.78	88.84	14.2	0.633	1.00	16
461	2003 Tokachi Oki Earthquake, Japan	YES	7.8	119.49	30.13	14.2	0.406	1.00	26
462	2003 Tokachi Oki Earthquake, Japan	YES	7.8	112.29	62.77	14.2	3.005	1.00	6
463	2003 Tokachi Oki Earthquake, Japan	YES	7.8	97.14	36.70	14.2	3.005	1.00	8
464	2003 Tokachi Oki Earthquake, Japan	NO	7.8	97.12	61.80	26.1	0.118	1.00	3

467	2003 Tokachi Oki Aftershock, Japan	NO	7.1	97.12	61.80	19.1	0.251	1.00	3
470	2007 Niigata Chuetsu Oki, Japan	YES	6.6	127.73	43.46	8.6	3.005	1.00	20
471	2007 Niigata Chuetsu Oki, Japan	YES	6.6	100.56	29.67	8.6	3.005	1.00	12
474	2008 Achaia-Elia Earthquake, Greece	YES	6.5	157.65	47.05	11.3	0.143	0.74	47
475	2008 Achaia-Elia Earthquake, Greece	YES	6.5	159.65	47.05	11.3	0.135	0.67	49
478	2011 Tohoku Aftershock, April 11, 2011	YES	7.40	127.39	32.26	12.9	0.289	1.00	32
479	2011 Tohoku Aftershock, April 11, 2011	YES	7.40	106.06	84.08	10.0	3.005	1.00	3
480	2011 Tohoku Aftershock, April 11, 2011	YES	7.40	171.18	97.86	13.5	0.229	1.00	19
481	2011 Tohoku Aftershock, April 11, 2011	YES	7.40	114.58	43.93	12.9	3.005	1.00	12
482	2011 Tohoku Aftershock, April 11, 2011	YES	7.40	140.17	55.65	12.9	0.709	1.00	20
483	2011 Tohoku Aftershock, April 11, 2011	YES	7.40	142.59	55.65	17.2	0.097	1.00	22
484	2011 Tohoku Aftershock, April 11, 2011	YES	7.40	150.74	83.52	10.0	3.005	1.00	14
485	2011 Tohoku Aftershock, April 11, 2011	YES	7.40	117.81	47.38	10.0	3.005	1.00	12
486	2011 Tohoku Aftershock, April 11, 2011	YES	7.40	118.49	53.50	13.2	2.120	1.00	10
487	2011 Tohoku Aftershock, April 11, 2011	YES	7.40	144.49	53.04	13.2	0.267	1.00	25
490	2011 Tohoku Earthquake Mainshock, March 11, 2011	YES	9.00	118.49	53.50	22.1	0.440	1.00	10
491	2011 Tohoku Earthquake Mainshock, March 11, 2011	YES	9.00	118.65	53.04	22.1	0.422	1.00	10

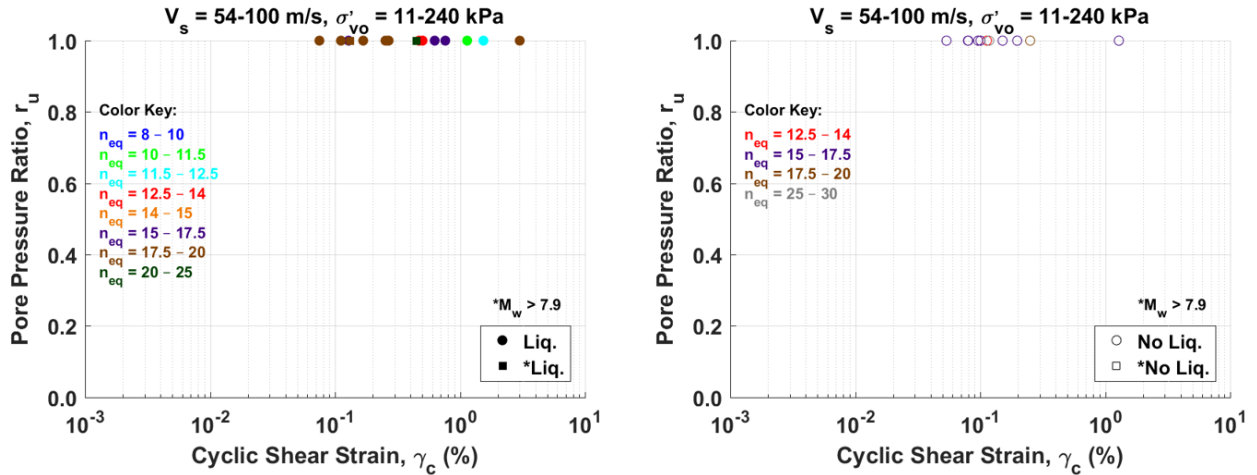


Figure C1. Excess porewater pressure buildup using the Byrne (1991) model with the Kayen et al. database

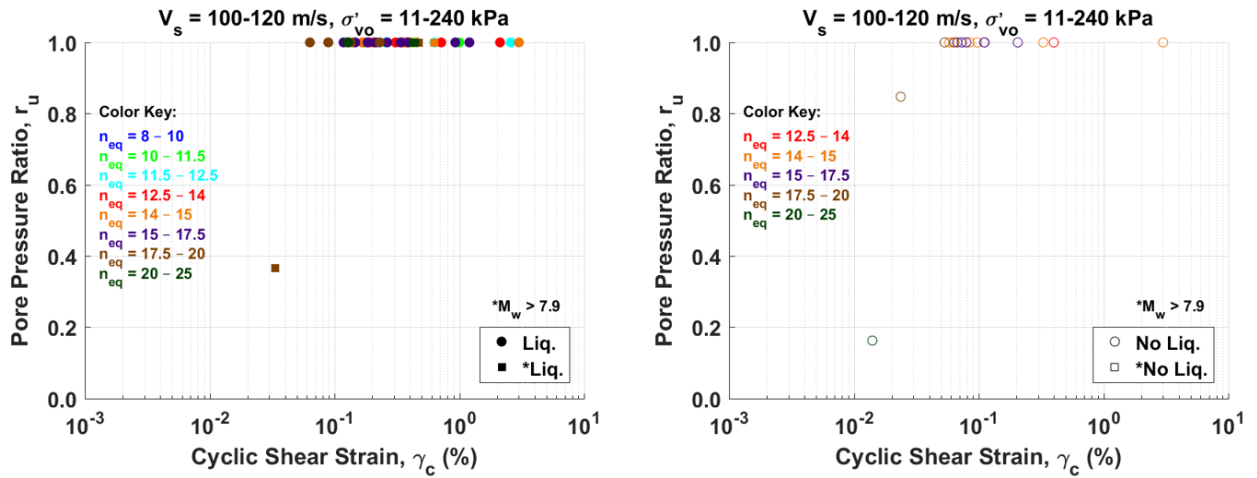


Figure C2. Excess porewater pressure buildup using the Byrne (1991) model with the Kayen et al. database

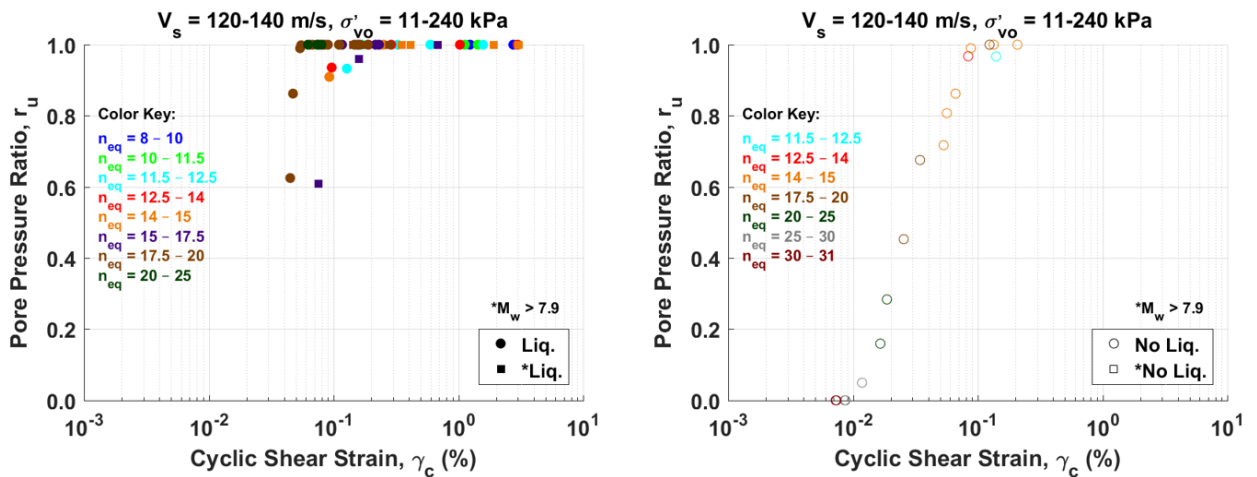


Figure C3. Excess porewater pressure buildup using the Byrne (1991) model with the Kayen et al. database

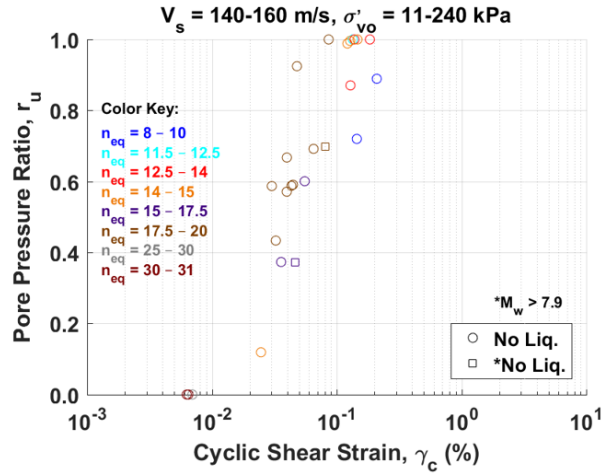
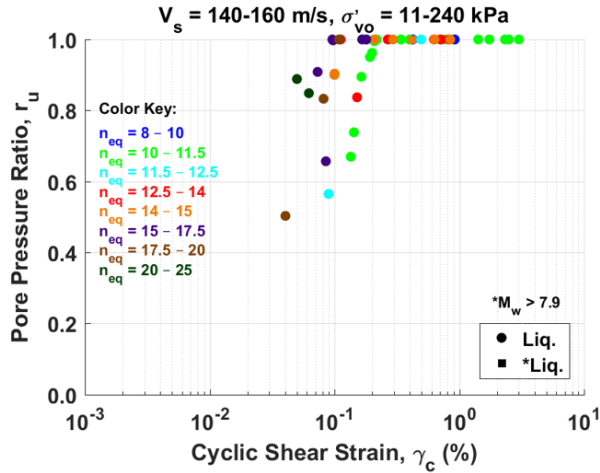


Figure C4. Excess porewater pressure buildup using the Byrne (1991) model with the Kayen et al. database

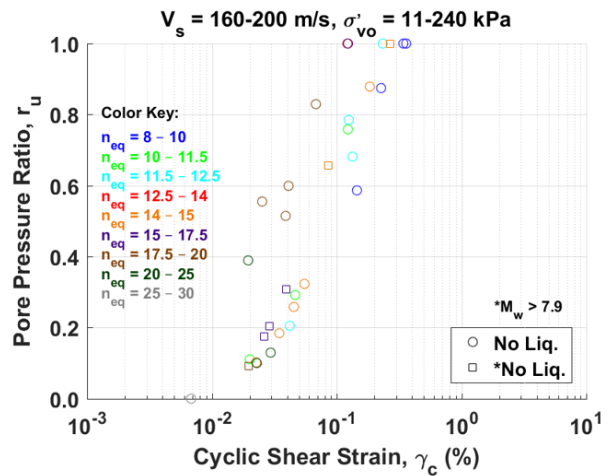
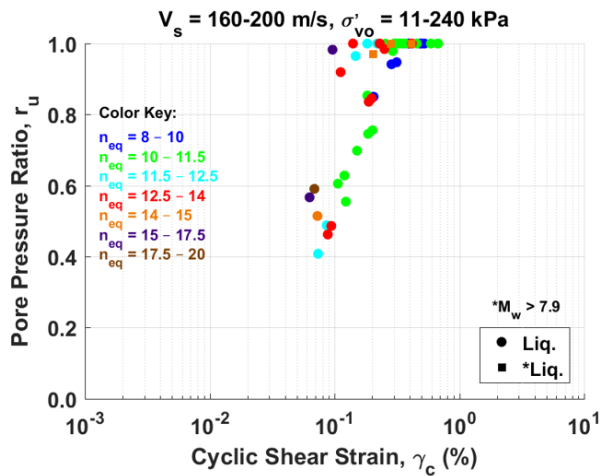


Figure C5. Excess porewater pressure buildup using the Byrne (1991) model with the Kayen et al. database

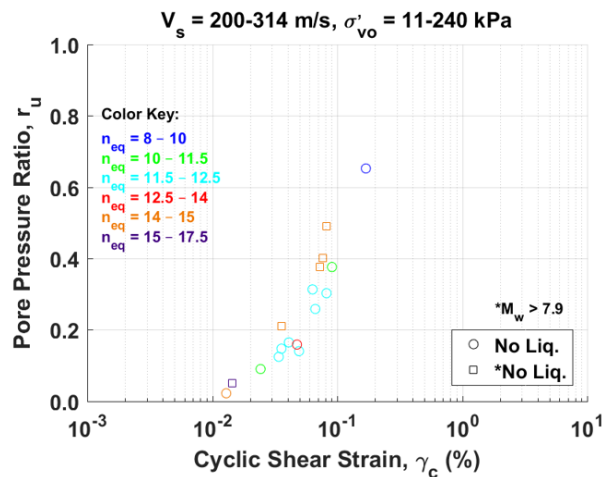
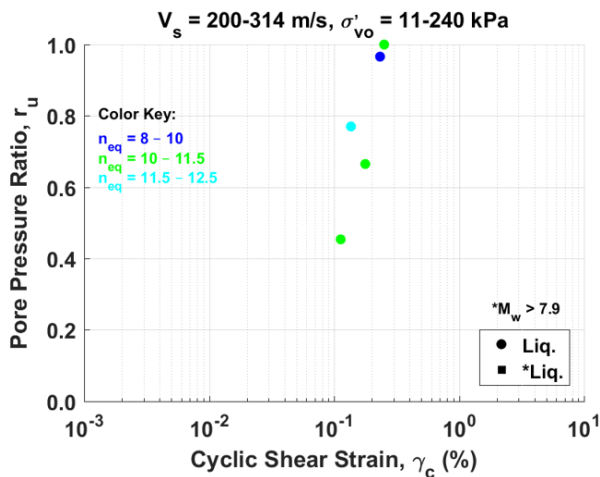


Figure C6. Excess porewater pressure buildup using the Byrne (1991) model with the Kayen et al. database

Kayen et al. database (415 cases)
Vucetic and Dobry model

Table C2. Parameters needed to plot figures of excess pore pressure ratio versus cyclic shear strain for the Kayen et al. (2013) database using the Vucetic and Dobry (1986) model

Data Point #	Year Event	Liquefied? YES/NO	M _w	V _s (m/s)	σ' _v (kPa)	Lasley n _{eq}	γ _c (%)	Vucetic and Dobry r _u	N _{1,60} blows
5	1906 San Francisco Earthquake, California USA	YES	7.7	146.97	54.03	14.5	0.204	0.82	26
6	1906 San Francisco Earthquake, California USA	NO	7.7	178.54	117.47	15.2	0.118	0.67	16
9	1948 Fukui Earthquake, Japan	YES	7.1	131.91	74.83	11.0	3.000	0.98	9
10	1948 Fukui Earthquake, Japan	YES	7.1	177.99	61.23	11.0	0.288	0.79	50
11	1948 Fukui Earthquake, Japan	YES	7.1	156.28	73.45	11.0	2.317	0.97	20
12	1948 Fukui Earthquake, Japan	YES	7.1	172.49	59.05	11.0	0.347	0.83	47
13	1948 Fukui Earthquake, Japan	YES	7.1	107.41	40.07	11.0	3.000	0.99	10
14	1948 Fukui Earthquake, Japan	YES	7.1	148.00	87.87	11.0	3.000	0.98	11
15	1948 Fukui Earthquake, Japan	YES	7.1	117.16	59.14	11.0	3.000	0.99	8
16	1948 Fukui Earthquake, Japan	YES	7.1	143.66	63.49	11.0	3.000	0.98	18
17	1948 Fukui Earthquake, Japan	YES	7.1	178.91	42.25	11.0	0.178	0.69	50
18	1948 Fukui Earthquake, Japan	NO	7.1	197.53	16.18	11.0	0.015	0.06	50
19	1948 Fukui Earthquake, Japan	YES	7.1	109.87	12.22	11.0	0.372	0.91	50
22	1964 Niigata Earthquake, Japan	NO	7.5	157.95	80.88	19.3	0.035	0.42	18
23	1964 Niigata Earthquake, Japan	YES	7.5	101.64	48.52	19.3	0.225	0.92	6
24	1964 Niigata Earthquake, Japan	YES	7.5	113.27	37.66	19.3	0.084	0.78	15
25	1964 Niigata Earthquake, Japan	YES	7.5	126.67	78.43	18.3	0.158	0.85	7
26	1964 Niigata Earthquake, Japan	YES	7.5	135.36	84.49	18.3	0.142	0.82	8
27	1964 Niigata Earthquake, Japan	YES	7.5	137.63	108.33	18.3	0.156	0.83	6
28	1964 Niigata Earthquake, Japan	YES	7.5	122.06	49.83	18.3	0.060	0.67	13
29	1964 Niigata Earthquake, Japan	NO	7.5	151.72	75.80	18.3	0.081	0.67	17
30	1964 Niigata Earthquake, Japan	NO	7.5	160.57	79.52	18.3	0.063	0.59	20
33	1968 Tokachi Oki Earthquake, Japan	YES	7.9	120.65	57.45	18.9	0.274	0.92	9
34	1968 Tokachi Oki Earthquake, Japan	YES	7.9	120.65	57.45	18.9	0.274	0.92	9
35	1968 Tokachi Oki Earthquake, Japan	YES	7.9	104.89	40.51	18.4	0.471	0.96	9
36	1968 Tokachi Oki Earthquake, Japan	YES	7.9	107.79	28.15	19.3	0.130	0.86	18

37	1968 Tokachi Oki Earthquake, Japan	YES	7.9	97.12	61.80	21.7	0.443	0.97	3
40	1973 Miyagi Ken Oki Earthquake, Japan	YES	7.4	87.21	31.38	17.2	0.622	0.98	6
41	1973 Miyagi Ken Oki Earthquake, Japan	YES	7.4	117.77	44.81	17.2	0.142	0.84	13
42	1973 Miyagi Ken Oki Earthquake, Japan	YES	7.4	171.19	101.05	15.9	0.091	0.63	18
43	1973 Miyagi Ken Oki Earthquake, Japan	YES	7.4	118.46	50.60	15.0	0.361	0.92	11
44	1973 Miyagi Ken Oki Earthquake, Japan	NO	7.4	144.45	50.17	15.0	0.123	0.74	28
45	1973 Miyagi Ken Oki Earthquake, Japan	YES	7.4	150.72	78.99	17.2	0.091	0.69	15
46	1973 Miyagi Ken Oki Earthquake, Japan	YES	7.4	144.36	50.45	14.2	0.289	0.87	27
47	1973 Miyagi Ken Oki Earthquake, Japan	YES	7.4	106.07	86.82	15.9	1.200	0.98	2
48	1973 Miyagi Ken Oki Earthquake, Japan	YES	7.4	144.22	58.90	17.2	0.068	0.63	21
49	1973 Miyagi Ken Oki Earthquake, Japan	YES	7.4	114.54	41.54	15.9	0.383	0.94	13
50	1973 Miyagi Ken Oki Earthquake, Japan	YES	7.4	140.14	52.62	15.9	0.161	0.81	22
53	1975 Haicheng Earthquake, China	YES	7.1	126.93	84.01	19.7	0.080	0.74	6
54	1975 Haicheng Earthquake, China	YES	7.1	92.65	70.97	19.7	0.263	0.94	2
55	1975 Haicheng Earthquake, China	YES	7.1	85.76	41.76	19.7	0.248	0.95	3
56	1975 Haicheng Earthquake, China	YES	7.1	67.23	19.17	19.7	0.259	0.96	3
57	1975 Haicheng Earthquake, China	NO	7.1	120.39	94.39	19.7	0.119	0.83	4
58	1975 Haicheng Earthquake, China	YES	7.1	120.66	40.07	19.7	0.042	0.59	18
62	1976 Tangshan Earthquake, China	NO	8	201.18	59.39	14.9	0.068	0.47	50
63	1976 Tangshan Earthquake, China	YES	8	161.56	72.64	14.2	0.406	0.89	24
64	1976 Tangshan Earthquake, China	YES	8	187.00	84.83	14.2	0.199	0.75	36
65	1976 Tangshan Earthquake, China	YES	8	137.73	40.95	14.9	3.000	0.99	32
66	1976 Tangshan Earthquake, China	YES	8	129.68	17.31	14.9	0.166	0.82	50
67	1976 Tangshan Earthquake, China	YES	8	133.17	36.69	14.2	1.916	0.98	34
68	1976 Tangshan Earthquake, China	NO	8	227.27	41.95	14.9	0.077	0.46	50
69	1976 Tangshan Earthquake, China	YES	8	130.76	29.57	15.7	0.675	0.95	41
70	1976 Tangshan Earthquake, China	NO	8	165.32	33.81	14.9	0.264	0.84	50
71	1976 Tangshan Earthquake, China	YES	8	186.66	55.98	14.9	0.278	0.82	50
72	1976 Tangshan Earthquake, China	NO	8	258.85	35.43	14.9	0.031	0.18	50
73	1976 Tangshan Earthquake, China	NO	8	172.74	22.38	14.9	0.081	0.58	50
74	1976 Tangshan Earthquake, China	YES	8	134.12	22.76	14.9	0.346	0.91	50
75	1976 Tangshan Earthquake, China	YES	8	109.41	11.03	19.7	0.028	0.49	50

76	1976 Tangshan Earthquake, China	YES	8	93.54	19.08	19.7	0.127	0.89	15
77	1976 Tangshan Earthquake, China	NO	8	188.15	36.27	19.7	0.015	0.10	50
78	1976 Tangshan Earthquake, China	YES	8	138.77	41.33	19.7	0.138	0.82	32
79	1976 Tangshan Earthquake, China	YES	8	122.80	58.42	19.7	0.169	0.87	10
80	1976 Tangshan Earthquake, China	NO	8	153.75	51.89	19.7	0.076	0.67	35
81	1976 Tangshan Earthquake, China	YES	8	146.25	39.96	14.9	0.413	0.91	44
82	1976 Tangshan Earthquake, China	NO	8	230.57	57.86	14.9	0.072	0.43	50
83	1976 Tangshan Earthquake, China	YES	8	121.01	18.88	14.2	0.410	0.93	50
84	1976 Tangshan Earthquake, China	YES	8	122.97	42.55	14.9	3.000	0.99	18
85	1976 Tangshan Earthquake, China	YES	8	136.91	26.74	16.7	0.154	0.82	50
88	1978 Miyagi Ken Oki Earthquake, Japan	NO	6.7	117.77	44.81	18.0	0.048	0.62	13
89	1978 Miyagi Ken Oki Earthquake, Japan	NO	6.7	118.46	50.60	16.9	0.062	0.67	11
90	1978 Miyagi Ken Oki Earthquake, Japan	NO	6.7	144.45	50.17	16.9	0.031	0.38	28
91	1978 Miyagi Ken Oki Earthquake, Japan	NO	6.7	150.72	78.99	18.0	0.035	0.42	15
92	1978 Miyagi Ken Oki Earthquake, Japan	YES	6.7	142.56	52.62	18.0	0.035	0.44	24
93	1978 Miyagi Ken Oki Earthquake, Japan	NO	6.7	144.22	58.90	18.0	0.027	0.35	21
94	1978 Miyagi Ken Oki Earthquake, Japan	YES	6.7	114.54	41.54	18.0	0.059	0.68	13
95	1978 Miyagi Ken Oki Earthquake, Japan	NO	6.7	140.14	52.62	18.0	0.038	0.48	22
98	1979 Imperial Valley Earthquake, California, USA	YES	6.5	117.66	41.48	9.6	3.000	0.99	15
99	1979 Imperial Valley Earthquake, California, USA	YES	6.5	122.91	39.30	9.6	1.235	0.96	21
100	1979 Imperial Valley Earthquake, California, USA	NO	6.5	159.59	38.00	9.6	0.140	0.65	50
101	1979 Imperial Valley Earthquake, California, USA	NO	6.5	157.55	42.34	9.6	0.204	0.74	50
102	1979 Imperial Valley Earthquake, California, USA	NO	6.5	98.24	50.21	17.1	0.075	0.78	5
103	1979 Imperial Valley Earthquake, California, USA	YES	6.5	121.54	33.51	9.5	2.748	0.98	25
104	1979 Imperial Valley Earthquake, California, USA	YES	6.5	81.90	48.86	13.6	3.000	0.99	2
105	1979 Imperial Valley Earthquake, California, USA	NO	6.5	96.04	49.97	17.1	0.075	0.78	4
106	1979 Imperial Valley Earthquake, California, USA	NO	6.5	102.14	48.38	16.6	0.106	0.82	6
107	1979 Imperial Valley Earthquake, California, USA	NO	6.5	113.61	48.38	16.6	0.068	0.71	10
108	1979 Imperial Valley Earthquake, California, USA	NO	6.5	111.06	48.38	16.6	0.074	0.73	9
112	1980 Mid Chiba Earthquake, Japan	NO	5.9	164.27	135.78	17.6	0.020	0.20	9
113	1980 Mid Chiba Earthquake, Japan	NO	5.9	135.24	60.62	17.6	0.021	0.26	15

116	1981 Westmorland Earthquake, California, USA	NO	5.9	125.12	39.30	31.0	0.002	0.00	23
117	1981 Westmorland Earthquake, California, USA	NO	5.9	122.91	39.30	31.0	0.002	0.00	21
118	1981 Westmorland Earthquake, California, USA	NO	5.9	159.59	38.00	31.0	0.001	0.00	50
119	1981 Westmorland Earthquake, California, USA	NO	5.9	155.49	40.17	31.0	0.001	0.00	50
120	1981 Westmorland Earthquake, California, USA	YES	5.9	98.24	50.21	9.5	3.000	0.99	5
121	1981 Westmorland Earthquake, California, USA	NO	5.9	101.73	39.59	19.8	0.019	0.34	8
122	1981 Westmorland Earthquake, California, USA	YES	5.9	81.90	48.86	12.1	1.534	0.99	2
123	1981 Westmorland Earthquake, California, USA	YES	5.9	96.04	49.97	10.3	1.136	0.97	4
124	1981 Westmorland Earthquake, California, USA	YES	5.9	102.14	48.38	10.7	0.995	0.97	6
125	1981 Westmorland Earthquake, California, USA	YES	5.9	113.61	48.38	10.7	0.356	0.90	10
126	1981 Westmorland Earthquake, California, USA	YES	5.9	111.06	48.38	10.7	0.424	0.92	9
129	1983 Nihonkai-Chubu Earthquake, Japan	YES	7.7	126.01	57.45	18.4	0.183	0.87	12
130	1983 Nihonkai-Chubu Earthquake, Japan	YES	7.7	153.41	48.76	17.5	0.080	0.66	38
131	1983 Nihonkai-Chubu Earthquake, Japan	YES	7.7	122.49	40.07	16.8	0.212	0.88	19
132	1983 Nihonkai-Chubu Earthquake, Japan	YES	7.7	149.72	68.92	16.8	0.162	0.81	19
133	1983 Nihonkai-Chubu Earthquake, Japan	YES	7.7	127.55	42.73	16.8	0.152	0.83	21
134	1983 Nihonkai-Chubu Earthquake, Japan	YES	7.7	105.12	49.20	22.0	0.124	0.88	7
135	1983 Nihonkai-Chubu Earthquake, Japan	YES	7.7	120.65	57.45	23.0	0.069	0.75	9
136	1983 Nihonkai-Chubu Earthquake, Japan	YES	7.7	98.01	40.36	16.1	3.000	0.99	7
139	1983 Nihonkai-Chubu Aftershocks, Japan	YES	7	98.01	40.36	19.5	0.107	0.85	7
140	1983 Nihonkai-Chubu Aftershocks, Japan	YES	7	120.65	57.45	19.5	0.063	0.70	9
143	1983 Bora Peak Earthquake, Idaho, USA	YES	6.9	115.02	29.02	10.5	3.000	0.99	23
144	1983 Bora Peak Earthquake, Idaho, USA	YES	6.9	96.32	21.63	13.1	0.466	0.95	15
145	1983 Bora Peak Earthquake, Idaho, USA	NO	6.9	196.19	26.17	10.9	0.041	0.27	50
146	1983 Bora Peak Earthquake, Idaho, USA	YES	6.9	93.31	33.32	12.0	3.000	0.99	7
147	1983 Bora Peak Earthquake, Idaho, USA	YES	6.9	115.02	29.02	10.5	3.000	0.99	23
148	1983 Bora Peak Earthquake, Idaho, USA	YES	6.9	158.72	29.02	10.5	0.187	0.73	50
149	1983 Bora Peak Earthquake, Idaho, USA	YES	6.9	110.63	25.49	12.9	0.167	0.84	23
150	1983 Bora Peak Earthquake, Idaho, USA	NO	6.9	266.69	43.94	14.4	0.008	0.00	50
151	1983 Bora Peak Earthquake, Idaho, USA	NO	6.9	264.39	47.66	10.9	0.019	0.06	50
152	1983 Bora Peak Earthquake, Idaho, USA	YES	6.9	86.93	33.17	12.0	3.000	0.99	5
153	1983 Bora Peak Earthquake, Idaho, USA	YES	6.9	89.80	27.43	12.0	3.000	0.99	8

154	1983 Bora Peak Earthquake, Idaho, USA	YES	6.9	96.07	25.49	12.9	0.497	0.95	12
155	1983 Bora Peak Earthquake, Idaho, USA	YES	6.9	96.14	37.37	12.0	3.000	0.99	7
156	1983 Bora Peak Earthquake, Idaho, USA	YES	6.9	115.40	37.37	12.0	0.449	0.93	17
157	1983 Bora Peak Earthquake, Idaho, USA	NO	6.9	164.09	25.11	10.5	0.118	0.61	50
158	1983 Bora Peak Earthquake, Idaho, USA	YES	6.9	129.09	35.39	12.0	0.143	0.76	31
159	1983 Bora Peak Earthquake, Idaho, USA	YES	6.9	124.38	28.39	12.0	0.141	0.77	34
160	1983 Bora Peak Earthquake, Idaho, USA	YES	6.9	103.88	29.26	12.0	0.626	0.95	14
161	1983 Bora Peak Earthquake, Idaho, USA	YES	6.9	127.72	28.39	12.0	0.123	0.74	39
162	1983 Bora Peak Earthquake, Idaho, USA	YES	6.9	113.34	28.39	12.0	0.251	0.88	22
163	1983 Bora Peak Earthquake, Idaho, USA	YES	6.9	158.60	29.45	10.5	0.195	0.74	50
164	1983 Bora Peak Earthquake, Idaho, USA	YES	6.9	96.30	21.63	13.1	0.467	0.95	15
165	1983 Bora Peak Earthquake, Idaho, USA	YES	6.9	122.26	29.02	10.5	3.000	0.99	31
166	1983 Bora Peak Earthquake, Idaho, USA	YES	6.9	145.21	31.00	12.0	0.085	0.60	50
169	1986 Lotung LSST Earthquake Events, Taiwan	NO	6.2	120.34	33.07	13.5	0.079	0.68	24
170	1986 Lotung LSST Earthquake Events, Taiwan	NO	6.2	120.34	33.07	13.5	0.079	0.68	24
171	1986 Lotung LSST Earthquake Events, Taiwan	NO	6.2	120.34	33.07	14.2	0.061	0.62	24
172	1986 Lotung LSST Earthquake Events, Taiwan	NO	6.6	120.34	33.07	14.9	0.083	0.71	24
173	1986 Lotung LSST Earthquake Events, Taiwan	NO	6.2	120.34	33.07	25.0	0.007	0.00	24
174	1986 Lotung LSST Earthquake Events, Taiwan	NO	6	120.34	33.07	20.2	0.012	0.07	24
177	1986 Chiba-Ibaragi-Kenyo, Japan	NO	6	164.27	135.78	20.2	0.015	0.11	9
178	1986 Chiba-Ibaragi-Kenyo, Japan	NO	6	135.24	60.62	20.2	0.014	0.12	15
181	1987 Chiba-Toho-Oki, Japan	NO	6.5	113.65	112.02	18.5	0.059	0.69	2
184	1987 Superstition Hills Earthquake, California, USA	NO	6.5	125.12	39.30	14.5	0.048	0.54	23
185	1987 Superstition Hills Earthquake, California, USA	NO	6.5	122.91	39.30	14.5	0.051	0.57	21
186	1987 Superstition Hills Earthquake, California, USA	NO	6.5	159.59	38.00	14.5	0.020	0.17	50
187	1987 Superstition Hills Earthquake, California, USA	NO	6.5	165.68	38.00	14.5	0.018	0.13	50
188	1987 Superstition Hills Earthquake, California, USA	NO	6.5	93.69	41.52	15.7	0.091	0.81	5
189	1987 Superstition Hills Earthquake, California, USA	NO	6.5	111.81	34.81	14.2	0.092	0.75	16
190	1987 Superstition Hills Earthquake, California, USA	NO	6.5	80.46	43.46	15.7	0.193	0.92	2
191	1987 Superstition Hills Earthquake, California, USA	NO	6.5	92.74	43.46	15.7	0.096	0.82	5
192	1987 Superstition Hills Earthquake, California, USA	YES	6.5	102.14	48.38	13.9	0.303	0.92	6

193	1987 Superstition Hills Earthquake, California, USA	YES	6.5	113.61	48.38	13.9	0.163	0.84	10
194	1987 Superstition Hills Earthquake, California, USA	YES	6.5	111.06	48.38	13.9	0.184	0.86	9
197	1987 Elmore Ranch Earthquake, California, USA	NO	5.9	125.12	39.30	26.3	0.004	0.00	23
198	1987 Elmore Ranch Earthquake, California, USA	NO	5.9	122.91	39.30	26.3	0.004	0.00	21
199	1987 Elmore Ranch Earthquake, California, USA	NO	5.9	159.59	38.00	26.3	0.002	0.00	50
200	1987 Elmore Ranch Earthquake, California, USA	NO	5.9	165.68	38.00	26.3	0.002	0.00	50
201	1987 Elmore Ranch Earthquake, California, USA	NO	5.9	98.24	50.21	13.6	0.108	0.81	5
202	1987 Elmore Ranch Earthquake, California, USA	NO	5.9	111.81	34.81	21.3	0.009	0.00	16
203	1987 Elmore Ranch Earthquake, California, USA	NO	5.9	81.90	48.86	15.4	0.146	0.90	2
204	1987 Elmore Ranch Earthquake, California, USA	NO	5.9	96.04	49.97	16.1	0.049	0.67	4
205	1987 Elmore Ranch Earthquake, California, USA	NO	5.9	102.14	48.38	14.9	0.080	0.75	6
206	1987 Elmore Ranch Earthquake, California, USA	NO	5.9	113.61	48.38	14.9	0.053	0.61	10
207	1987 Elmore Ranch Earthquake, California, USA	NO	5.9	111.06	48.38	14.9	0.058	0.65	9
210	1989 Loma Prieta Earthquake, California, USA	YES	7	171.12	78.97	12.0	0.143	0.68	27
211	1989 Loma Prieta Earthquake, California, USA	YES	7	164.19	96.07	12.6	0.136	0.69	16
212	1989 Loma Prieta Earthquake, California, USA	YES	7	134.22	99.44	11.8	0.590	0.93	6
213	1989 Loma Prieta Earthquake, California, USA	NO	7	157.57	81.86	11.8	0.130	0.68	17
214	1989 Loma Prieta Earthquake, California, USA	NO	7	165.48	62.18	12.0	0.120	0.65	36
215	1989 Loma Prieta Earthquake, California, USA	NO	7	130.23	52.98	14.1	0.203	0.84	15
216	1989 Loma Prieta Earthquake, California, USA	NO	7	127.06	41.28	14.1	0.129	0.78	22
217	1989 Loma Prieta Earthquake, California, USA	YES	7	171.25	35.30	11.0	0.101	0.57	50
218	1989 Loma Prieta Earthquake, California, USA	YES	7	175.02	85.94	15.3	0.058	0.48	26
219	1989 Loma Prieta Earthquake, California, USA	YES	7	103.64	48.57	15.3	0.259	0.92	6
220	1989 Loma Prieta Earthquake, California, USA	YES	7	125.21	74.74	15.3	0.226	0.88	7
221	1989 Loma Prieta Earthquake, California, USA	YES	7	120.61	45.77	14.5	0.156	0.83	14
222	1989 Loma Prieta Earthquake, California, USA	YES	7	139.20	72.99	14.3	0.246	0.86	12
223	1989 Loma Prieta Earthquake, California, USA	YES	7	111.03	29.40	14.3	0.165	0.85	19
224	1989 Loma Prieta Earthquake, California, USA	NO	7	165.07	41.55	14.3	0.050	0.44	50
225	1989 Loma Prieta Earthquake, California, USA	NO	7	158.97	104.97	20.0	0.025	0.31	12
226	1989 Loma Prieta Earthquake, California, USA	YES	7	135.95	80.00	18.1	0.077	0.70	9
227	1989 Loma Prieta Earthquake, California, USA	YES	7	139.24	80.00	18.1	0.071	0.67	10
228	1989 Loma Prieta Earthquake, California, USA	YES	7	125.23	80.00	18.1	0.105	0.79	6
229	1989 Loma Prieta Earthquake, California, USA	YES	7	124.83	80.00	18.1	0.107	0.79	6
230	1989 Loma Prieta Earthquake, California, USA	YES	7	141.39	90.10	11.1	0.622	0.92	9
231	1989 Loma Prieta Earthquake, California, USA	YES	7	125.76	90.71	11.7	1.574	0.97	5

232	1989 Loma Prieta Earthquake, California, USA	YES	7	145.85	96.79	11.7	0.827	0.94	9
233	1989 Loma Prieta Earthquake, California, USA	YES	7	155.29	95.57	11.1	0.394	0.87	12
234	1989 Loma Prieta Earthquake, California, USA	NO	7	146.97	54.03	16.0	0.050	0.52	26
235	1989 Loma Prieta Earthquake, California, USA	YES	7	156.88	84.69	12.3	0.177	0.76	16
236	1989 Loma Prieta Earthquake, California, USA	YES	7	160.34	95.87	12.3	0.178	0.75	14
237	1989 Loma Prieta Earthquake, California, USA	YES	7	115.70	39.15	15.0	0.113	0.79	16
238	1989 Loma Prieta Earthquake, California, USA	YES	7	106.96	51.97	12.3	3.000	0.99	6
239	1989 Loma Prieta Earthquake, California, USA	NO	7	114.72	41.24	15.0	0.106	0.78	13
240	1989 Loma Prieta Earthquake, California, USA	NO	7	101.77	45.74	15.0	0.201	0.89	6
241	1989 Loma Prieta Earthquake, California, USA	YES	7	115.61	51.97	15.0	0.179	0.86	9
242	1989 Loma Prieta Earthquake, California, USA	YES	7	106.38	54.83	14.1	0.452	0.94	6
243	1989 Loma Prieta Earthquake, California, USA	YES	7	105.14	50.69	14.1	0.399	0.94	6
244	1989 Loma Prieta Earthquake, California, USA	NO	7	175.26	41.55	14.3	0.040	0.35	50
245	1989 Loma Prieta Earthquake, California, USA	NO	7	191.76	41.55	14.3	0.030	0.24	50
246	1989 Loma Prieta Earthquake, California, USA	NO	7	178.55	117.47	17.6	0.034	0.34	16
247	1989 Loma Prieta Earthquake, California, USA	NO	7	157.40	107.92	17.6	0.043	0.47	11
248	1989 Loma Prieta Earthquake, California, USA	NO	7	166.82	44.48	11.6	0.129	0.65	50
249	1989 Loma Prieta Earthquake, California, USA	YES	7	96.31	25.60	11.6	3.000	0.99	12
250	1989 Loma Prieta Earthquake, California, USA	YES	7	100.77	25.78	11.6	3.000	0.99	15
251	1989 Loma Prieta Earthquake, California, USA	YES	7	165.59	39.40	11.6	0.082	0.53	50
252	1989 Loma Prieta Earthquake, California, USA	NO	7	127.51	28.41	11.6	0.135	0.75	38
253	1989 Loma Prieta Earthquake, California, USA	YES	7	136.12	84.59	18.1	0.075	0.69	8
254	1989 Loma Prieta Earthquake, California, USA	YES	7	132.29	46.72	15.0	0.112	0.75	21
255	1989 Loma Prieta Earthquake, California, USA	YES	7	136.22	80.78	12.7	0.185	0.81	9
256	1989 Loma Prieta Earthquake, California, USA	NO	7	137.01	64.09	18.6	0.029	0.40	14
257	1989 Loma Prieta Earthquake, California, USA	YES	7	132.51	80.00	18.1	0.085	0.73	8
258	1989 Loma Prieta Earthquake, California, USA	YES	7	135.70	43.12	14.3	0.087	0.68	27
259	1989 Loma Prieta Earthquake, California, USA	YES	7	120.60	37.37	14.3	0.112	0.77	21
260	1989 Loma Prieta Earthquake, California, USA	YES	7	166.99	63.06	14.3	0.068	0.53	36
261	1989 Loma Prieta Earthquake, California, USA	YES	7	111.14	34.33	14.3	0.132	0.82	16
262	1989 Loma Prieta Earthquake, California, USA	YES	7	142.81	48.14	14.3	0.095	0.68	28
263	1989 Loma Prieta Earthquake, California, USA	YES	7	116.58	35.05	14.3	0.169	0.84	19
264	1989 Loma Prieta Earthquake, California, USA	YES	7	126.04	53.88	17.6	0.050	0.60	13
265	1989 Loma Prieta Earthquake, California, USA	NO	7	154.27	70.54	18.6	0.040	0.46	20
266	1989 Loma Prieta Earthquake, California, USA	YES	7	131.17	62.72	17.6	0.062	0.65	12
267	1989 Loma Prieta Earthquake, California, USA	YES	7	130.77	42.20	18.1	0.040	0.52	24
	1989 Loma Prieta Earthquake, California, USA	YES	7		53.88	17.6	0.049	0.59	13

270

119.49

271	1993 Kushiro Earthquake, Japan	YES	7.6	148.59	30.13	13.6	0.348	0.91	26
272	1993 Kushiro Earthquake, Japan	YES	7.6	86.85	76.67	13.6	0.818	0.95	15
273	1993 Kushiro Earthquake, Japan	YES	7.6	110.99	29.21	13.6	3.000	0.99	6
274	1993 Kushiro Earthquake, Japan	YES	7.6	110.62	57.45	13.6	3.000	0.99	6
275	1993 Kushiro Earthquake, Japan	YES	7.6	163.52	40.07	13.6	3.000	0.99	12
276	1993 Kushiro Earthquake, Japan	YES	7.6	118.96	47.53	12.8	0.246	0.81	50
277	1993 Kushiro Earthquake, Japan	YES	7.6	158.78	61.41	13.6	3.000	0.99	8
	1993 Kushiro Earthquake, Japan	YES	7.6		88.84	13.6	0.621	0.92	16
280				136.00					
281	1993 Hokkaido Nansei Oki Earthquake, Japan	YES	7.7	103.67	71.46	21.3	0.070	0.71	11
282	1993 Hokkaido Nansei Oki Earthquake, Japan	YES	7.7	145.07	51.90	21.3	0.122	0.87	6
283	1993 Hokkaido Nansei Oki Earthquake, Japan	YES	7.7	128.59	72.42	21.6	0.045	0.56	15
284	1993 Hokkaido Nansei Oki Earthquake, Japan	YES	7.7	149.14	67.11	21.6	0.075	0.74	10
285	1993 Hokkaido Nansei Oki Earthquake, Japan	YES	7.7	195.18	65.81	20.2	0.057	0.61	20
286	1993 Hokkaido Nansei Oki Earthquake, Japan	NO	7.7	120.57	75.80	21.3	0.025	0.25	50
287	1993 Hokkaido Nansei Oki Earthquake, Japan	YES	7.7	54.80	57.65	21.3	0.057	0.70	9
288	1993 Hokkaido Nansei Oki Earthquake, Japan	YES	7.7	84.52	20.52	18.8	3.000	1.00	1
289	1993 Hokkaido Nansei Oki Earthquake, Japan	YES	7.7	158.12	41.52	18.8	3.000	1.00	3
290	1993 Hokkaido Nansei Oki Earthquake, Japan	YES	7.7	166.29	67.59	17.7	0.077	0.64	25
291	1993 Hokkaido Nansei Oki Earthquake, Japan	YES	7.7	146.16	67.59	17.7	0.064	0.57	31
292	1993 Hokkaido Nansei Oki Earthquake, Japan	YES	7.7	114.40	67.59	17.7	0.104	0.74	17
293	1993 Hokkaido Nansei Oki Earthquake, Japan	YES	7.7	147.10	31.38	19.1	0.084	0.78	20
294	1993 Hokkaido Nansei Oki Earthquake, Japan	NO	7.7	80.55	51.42	19.1	0.060	0.61	29
295	1993 Hokkaido Nansei Oki Earthquake, Japan	YES	7.7	99.96	20.04	12.7	3.000	0.99	7
296	1993 Hokkaido Nansei Oki Earthquake, Japan	YES	7.7	98.39	17.38	15.9	0.123	0.85	23
297	1993 Hokkaido Nansei Oki Earthquake, Japan	YES	7.7	99.49	16.99	19.1	0.070	0.78	22
298	1993 Hokkaido Nansei Oki Earthquake, Japan	YES	7.7	115.03	26.12	19.1	0.163	0.90	13
299	1993 Hokkaido Nansei Oki Earthquake, Japan	YES	7.7	161.14	54.80	16.8	0.924	0.97	8
300	1993 Hokkaido Nansei Oki Earthquake, Japan	YES	7.7	95.50	54.08	12.7	0.411	0.88	40
301	1993 Hokkaido Nansei Oki Earthquake, Japan	YES	7.7	114.92	36.70	15.9	0.757	0.97	7
302	1993 Hokkaido Nansei Oki Earthquake, Japan	YES	7.7	185.26	33.56	15.9	0.333	0.93	19
303	1993 Hokkaido Nansei Oki Earthquake, Japan	YES	7.7	88.98	57.99	12.7	0.193	0.73	50
304	1993 Hokkaido Nansei Oki Earthquake, Japan	YES	7.7	88.98	41.76	16.8	3.000	0.99	4
305	1993 Hokkaido Nansei Oki Earthquake, Japan	YES	7.7	180.15	41.76	16.8	3.000	0.99	4
306	1993 Hokkaido Nansei Oki Earthquake, Japan	NO	7.7	114.59	57.17	21.6	0.018	0.17	50
	1993 Hokkaido Nansei Oki Earthquake, Japan	YES	7.7		54.80	12.7	3.000	0.99	8
309				167.15					

310	1995 Hyogo Nambu Earthquake, Japan	NO	7	168.25	101.00	19.3	0.036	0.40	16
311	1995 Hyogo Nambu Earthquake, Japan	YES	7	151.59	88.35	10.8	2.485	0.98	13
312	1995 Hyogo Nambu Earthquake, Japan	YES	7	148.19	88.35	10.8	3.000	0.98	11
313	1995 Hyogo Nambu Earthquake, Japan	NO	7	160.96	115.40	11.8	0.229	0.79	10
314	1995 Hyogo Nambu Earthquake, Japan	YES	7	106.71	54.99	15.6	0.209	0.90	6
315	1995 Hyogo Nambu Earthquake, Japan	YES	7	182.32	71.65	10.8	0.146	0.64	43
316	1995 Hyogo Nambu Earthquake, Japan	YES	7	132.21	62.67	10.8	3.000	0.98	12
317	1995 Hyogo Nambu Earthquake, Japan	YES	7	156.84	96.51	10.3	3.000	0.98	13
318	1995 Hyogo Nambu Earthquake, Japan	YES	7	178.79	92.21	10.8	0.586	0.88	25
319	1995 Hyogo Nambu Earthquake, Japan	YES	7	180.81	76.77	10.8	0.252	0.76	37
320	1995 Hyogo Nambu Earthquake, Japan	YES	7	168.76	98.49	10.8	0.667	0.90	17
321	1995 Hyogo Nambu Earthquake, Japan	YES	7	188.51	64.26	10.8	0.181	0.68	50
322	1995 Hyogo Nambu Earthquake, Japan	YES	7	200.94	109.03	10.0	0.228	0.69	32
323	1995 Hyogo Nambu Earthquake, Japan	NO	7	212.82	73.39	10.8	0.086	0.43	50
324	1995 Hyogo Nambu Earthquake, Japan	NO	7	198.62	88.36	10.0	0.140	0.58	44
325	1995 Hyogo Nambu Earthquake, Japan	NO	7	188.68	64.07	10.0	0.355	0.80	50
326	1995 Hyogo Nambu Earthquake, Japan	YES	7	169.86	55.98	10.0	0.520	0.87	48
327	1995 Hyogo Nambu Earthquake, Japan	YES	7	194.45	75.42	10.0	0.310	0.76	50
328	1995 Hyogo Nambu Earthquake, Japan	YES	7	189.58	83.19	10.0	0.390	0.81	40
329	1995 Hyogo Nambu Earthquake, Japan	NO	7	220.62	69.45	10.0	0.164	0.58	50
330	1995 Hyogo Nambu Earthquake, Japan	YES	7	192.56	77.10	10.0	0.389	0.81	49
331	1995 Hyogo Nambu Earthquake, Japan	NO	7	173.22	50.26	10.0	0.337	0.81	50
332	1995 Hyogo Nambu Earthquake, Japan	NO	7	191.11	53.21	10.0	0.222	0.70	50
333	1995 Hyogo Nambu Earthquake, Japan	NO	7	191.11	53.21	10.0	0.222	0.70	50
334	1995 Hyogo Nambu Earthquake, Japan	YES	7	166.14	71.31	10.8	0.324	0.82	28
335	1995 Hyogo Nambu Earthquake, Japan	YES	7	205.52	80.15	10.8	0.173	0.63	50
336	1995 Hyogo Nambu Earthquake, Japan	YES	7	137.45	44.90	10.8	1.425	0.97	27
337	1995 Hyogo Nambu Earthquake, Japan	YES	7	185.94	91.49	10.6	0.362	0.81	31
338	1995 Hyogo Nambu Earthquake, Japan	YES	7	216.07	176.08	10.8	0.247	0.70	19
339	1995 Hyogo Nambu Earthquake, Japan	YES	7	174.19	86.35	10.8	0.325	0.81	25
340	1995 Hyogo Nambu Earthquake, Japan	YES	7	198.74	73.14	10.8	0.197	0.68	50
341	1995 Hyogo Nambu Earthquake, Japan	YES	7	133.45	50.26	12.4	0.164	0.79	19
342	1995 Hyogo Nambu Earthquake, Japan	YES	7	155.05	52.92	10.6	0.335	0.84	35
343	1995 Hyogo Nambu Earthquake, Japan	YES	7	172.44	68.03	10.8	0.308	0.81	37
344	1995 Hyogo Nambu Earthquake, Japan	YES	7	170.26	64.36	10.8	0.309	0.81	38
345	1995 Hyogo Nambu Earthquake, Japan	YES	7	163.85	40.03	10.8	0.115	0.61	50
346	1995 Hyogo Nambu Earthquake, Japan	YES	7	176.26	64.70	10.0	0.201	0.71	44
347	1995 Hyogo Nambu Earthquake, Japan	YES	7	188.90	94.92	10.0	0.498	0.85	31
348	1995 Hyogo Nambu Earthquake, Japan	YES	7	124.52	27.04	10.8	1.121	0.96	37

349	1995 Hyogo Nambu Earthquake, Japan	YES	7	129.65	68.89	10.0	3.000	0.98	10
350	1995 Hyogo Nambu Earthquake, Japan	YES	7	142.02	64.99	10.0	3.000	0.98	16
351	1995 Hyogo Nambu Earthquake, Japan	YES	7	147.93	27.04	10.0	0.418	0.87	50
352	1995 Hyogo Nambu Earthquake, Japan	YES	7	155.87	56.20	10.0	0.913	0.93	32
353	1995 Hyogo Nambu Earthquake, Japan	YES	7	161.49	89.85	10.8	0.670	0.91	16
354	1995 Hyogo Nambu Earthquake, Japan	YES	7	136.20	52.48	10.0	3.000	0.98	19
355	1995 Hyogo Nambu Earthquake, Japan	YES	7	152.96	69.28	10.0	3.000	0.98	20
356	1995 Hyogo Nambu Earthquake, Japan	YES	7	127.56	60.11	10.8	3.000	0.99	11
357	1995 Hyogo Nambu Earthquake, Japan	YES	7	149.31	71.72	10.8	1.737	0.97	17
358	1995 Hyogo Nambu Earthquake, Japan	YES	7	147.49	62.86	10.0	3.000	0.98	20
359	1995 Hyogo Nambu Earthquake, Japan	YES	7	155.84	63.49	10.8	1.733	0.97	26
360	1995 Hyogo Nambu Earthquake, Japan	YES	7	127.39	39.74	11.8	0.321	0.88	23
361	1995 Hyogo Nambu Earthquake, Japan	YES	7	152.00	56.95	10.8	0.629	0.91	28
362	1995 Hyogo Nambu Earthquake, Japan	YES	7	135.37	64.45	10.0	3.000	0.98	13
363	1995 Hyogo Nambu Earthquake, Japan	YES	7	144.03	58.69	10.0	3.000	0.98	21
364	1995 Hyogo Nambu Earthquake, Japan	YES	7	123.75	61.56	10.0	3.000	0.98	9
365	1995 Hyogo Nambu Earthquake, Japan	YES	7	136.10	63.25	10.0	3.000	0.98	14
366	1995 Hyogo Nambu Earthquake, Japan	YES	7	109.72	61.08	10.0	3.000	0.99	5
367	1995 Hyogo Nambu Earthquake, Japan	YES	7	172.31	69.65	10.0	0.480	0.86	35
368	1995 Hyogo Nambu Earthquake, Japan	YES	7	171.75	86.43	10.8	0.316	0.81	24
369	1995 Hyogo Nambu Earthquake, Japan	YES	7	185.25	103.81	10.8	0.301	0.78	24
370	1995 Hyogo Nambu Earthquake, Japan	YES	7	148.33	90.24	10.8	1.411	0.96	11
371	1995 Hyogo Nambu Earthquake, Japan	YES	7	164.14	41.52	11.8	0.069	0.49	50
372	1995 Hyogo Nambu Earthquake, Japan	NO	7	198.54	46.74	11.8	0.037	0.25	50
373	1995 Hyogo Nambu Earthquake, Japan	YES	7	228.37	173.25	11.8	0.131	0.55	26
374	1995 Hyogo Nambu Earthquake, Japan	NO	7	238.92	60.74	11.8	0.031	0.16	50
375	1995 Hyogo Nambu Earthquake, Japan	NO	7	313.20	157.64	11.8	0.044	0.17	50
376	1995 Hyogo Nambu Earthquake, Japan	NO	7	248.73	89.90	11.8	0.062	0.31	50
377	1995 Hyogo Nambu Earthquake, Japan	NO	7	276.69	75.08	11.8	0.029	0.12	50
378	1995 Hyogo Nambu Earthquake, Japan	NO	7	241.69	102.93	11.8	0.077	0.38	50
379	1995 Hyogo Nambu Earthquake, Japan	NO	7	246.98	69.43	11.8	0.036	0.19	50
380	1995 Hyogo Nambu Earthquake, Japan	YES	7	187.21	78.12	12.6	0.083	0.51	42
381	1995 Hyogo Nambu Earthquake, Japan	NO	7	260.78	124.03	13.3	0.043	0.23	50
382	1995 Hyogo Nambu Earthquake, Japan	YES	7	151.36	73.49	10.8	0.745	0.93	17
383	1995 Hyogo Nambu Earthquake, Japan	YES	7	172.13	136.54	11.4	0.451	0.87	11
384	1995 Hyogo Nambu Earthquake, Japan	YES	7	172.13	136.54	11.4	0.451	0.87	11
385	1995 Hyogo Nambu Earthquake, Japan	NO	7	203.64	54.56	12.4	0.058	0.38	50
386	1995 Hyogo Nambu Earthquake, Japan	YES	7	159.81	56.11	10.8	0.204	0.75	36
387	1995 Hyogo Nambu Earthquake, Japan	YES	7	155.30	58.23	10.8	0.213	0.77	30

388	1995 Hyogo Nambu Earthquake, Japan	YES	7	175.33	58.23	10.8	0.118	0.60	50
389	1995 Hyogo Nambu Earthquake, Japan	YES	7	141.25	58.42	11.8	0.488	0.91	19
390	1995 Hyogo Nambu Earthquake, Japan	YES	7	179.97	63.73	10.0	0.281	0.77	50
391	1995 Hyogo Nambu Earthquake, Japan	YES	7	164.73	73.27	11.8	0.215	0.77	26
392	1995 Hyogo Nambu Earthquake, Japan	YES	7	204.76	77.74	10.8	0.108	0.51	50
393	1995 Hyogo Nambu Earthquake, Japan	YES	7	154.39	27.04	10.8	0.159	0.71	50
394	1995 Hyogo Nambu Earthquake, Japan	YES	7	142.70	63.49	10.8	3.000	0.98	17
398	1999 Chi Chi Earthquake, Japan	YES	7.6	176.67	57.45	13.6	0.183	0.75	50
399	1999 Chi Chi Earthquake, Japan	YES	7.6	196.38	126.30	13.6	0.226	0.76	22
400	1999 Chi Chi Earthquake, Japan	YES	7.6	150.15	36.21	13.6	0.147	0.75	50
401	1999 Chi Chi Earthquake, Japan	YES	7.6	176.45	55.48	13.6	0.089	0.57	50
402	1999 Chi Chi Earthquake, Japan	NO	7.6	146.13	22.21	13.6	0.124	0.72	50
403	1999 Chi Chi Earthquake, Japan	YES	7.6	119.70	24.38	13.6	0.712	0.96	35
404	1999 Chi Chi Earthquake, Japan	YES	7.6	124.69	25.30	11.1	3.000	0.99	40
405	1999 Chi Chi Earthquake, Japan	YES	7.6	120.57	23.47	11.1	3.000	0.99	38
406	1999 Chi Chi Earthquake, Japan	YES	7.6	164.74	33.17	11.1	0.295	0.81	50
407	1999 Chi Chi Earthquake, Japan	YES	7.6	123.49	44.90	11.1	3.000	0.99	16
408	1999 Chi Chi Earthquake, Japan	YES	7.6	145.00	67.74	11.1	3.000	0.98	16
409	1999 Chi Chi Earthquake, Japan	YES	7.6	112.43	34.28	10.8	3.000	0.99	17
410	1999 Chi Chi Earthquake, Japan	YES	7.6	131.61	49.02	11.1	3.000	0.98	19
411	1999 Chi Chi Earthquake, Japan	YES	7.6	154.89	86.18	16.4	0.174	0.81	15
414	1999 Druce Earthquake, Turkey	YES	7.40	129.50	80.10	12.9	2.973	0.99	7
415	1999 Druce Earthquake, Turkey	YES	7.40	139.36	82.40	12.9	1.023	0.96	10
419	2000 Tottori Seibu Earthquake, Japan	YES	6.8	88.00	60.59	12.1	3.000	0.99	2
420	2000 Tottori Seibu Earthquake, Japan	YES	6.8	114.93	62.77	12.1	2.575	0.99	6
421	2000 Tottori Seibu Earthquake, Japan	YES	6.8	103.53	53.98	11.4	3.000	0.99	5
424	2001 Geiyo-Hiroshima Ken Earthquake, Japan	YES	6.8	113.83	27.04	13.6	0.124	0.79	24
425	2001 Geiyo-Hiroshima Ken Earthquake, Japan	YES	6.8	104.87	27.04	13.6	0.199	0.88	16
426	2001 Geiyo-Hiroshima Ken Earthquake, Japan	YES	6.8	120.90	27.04	13.6	0.092	0.71	32

427	2001 Geiyo-Hiroshima Ken Earthquake, Japan	YES	6.8	152.02	76.33	13.6	0.107	0.68	17
428	2001 Geiyo-Hiroshima Ken Earthquake, Japan	YES	6.8	177.11	96.56	13.4	0.107	0.62	22
431	2002 Denali Fault Earthquake, Alaska, USA	NO	7.9	189.16	20.94	15.2	0.021	0.16	50
432	2002 Denali Fault Earthquake, Alaska, USA	YES	7.9	116.86	20.94	15.2	0.180	0.86	38
433	2002 Denali Fault Earthquake, Alaska, USA	YES	7.9	116.86	20.94	15.2	0.180	0.86	38
434	2002 Denali Fault Earthquake, Alaska, USA	NO	7.9	158.03	20.94	15.2	0.041	0.41	50
435	2002 Denali Fault Earthquake, Alaska, USA	NO	7.9	244.67	20.94	15.2	0.009	0.00	50
436	2002 Denali Fault Earthquake, Alaska, USA	NO	7.9	182.41	20.94	15.2	0.024	0.20	50
437	2002 Denali Fault Earthquake, Alaska, USA	NO	7.9	165.35	20.94	15.2	0.035	0.34	50
438	2002 Denali Fault Earthquake, Alaska, USA	YES	7.9	138.75	20.94	15.2	0.070	0.63	50
439	2002 Denali Fault Earthquake, Alaska, USA	YES	7.9	110.14	30.16	14.7	0.621	0.96	18
442	2003 Sanriku-Minami Earthquake, Japan	NO	7	87.21	31.38	15.0	1.280	0.99	6
443	2003 Sanriku-Minami Earthquake, Japan	NO	7	117.77	44.81	13.6	0.395	0.92	13
444	2003 Sanriku-Minami Earthquake, Japan	NO	7	171.19	101.05	13.6	0.117	0.66	18
445	2003 Sanriku-Minami Earthquake, Japan	YES	7	118.46	50.60	14.1	0.260	0.89	11
446	2003 Sanriku-Minami Earthquake, Japan	YES	7	144.45	50.17	14.1	0.095	0.67	28
447	2003 Sanriku-Minami Earthquake, Japan	NO	7	150.72	78.99	13.6	0.179	0.79	15
448	2003 Sanriku-Minami Earthquake, Japan	NO	7	144.36	50.45	14.8	0.117	0.73	27
449	2003 Sanriku-Minami Earthquake, Japan	NO	7	106.07	86.82	13.6	3.000	0.99	2
450	2003 Sanriku-Minami Earthquake, Japan	NO	7	144.22	58.90	13.6	0.134	0.74	21
451	2003 Sanriku-Minami Earthquake, Japan	NO	7	114.54	41.54	14.8	0.324	0.92	13
452	2003 Sanriku-Minami Earthquake, Japan	NO	7	140.14	52.62	14.8	0.142	0.78	22
455	2003 Tokachi Oki Earthquake, Japan	YES	7.8	148.59	76.67	14.2	0.841	0.95	15
456	2003 Tokachi Oki Earthquake, Japan	YES	7.8	110.99	57.45	14.2	3.000	0.99	6
457	2003 Tokachi Oki Earthquake, Japan	YES	7.8	110.62	40.07	14.2	3.000	0.99	12
458	2003 Tokachi Oki Earthquake, Japan	NO	7.8	163.52	47.53	14.2	0.179	0.77	50
459	2003 Tokachi Oki Earthquake, Japan	NO	7.8	118.96	61.41	14.2	3.000	0.99	8
460	2003 Tokachi Oki Earthquake, Japan	YES	7.8	158.78	88.84	14.2	0.628	0.93	16
461	2003 Tokachi Oki Earthquake, Japan	YES	7.8	119.49	30.13	14.2	0.401	0.93	26
462	2003 Tokachi Oki Earthquake, Japan	YES	7.8	112.29	62.77	14.2	3.000	0.99	6
463	2003 Tokachi Oki Earthquake, Japan	YES	7.8	97.14	36.70	14.2	3.000	0.99	8
464	2003 Tokachi Oki Earthquake, Japan	NO	7.8	97.12	61.80	26.1	0.113	0.89	3

467	2003 Tokachi Oki Aftershock, Japan	NO	7.1	97.12	61.80	19.1	0.246	0.93	3
470	2007 Niigata Chuetsu Oki, Japan	YES	6.6	127.73	43.46	8.6	3.000	0.98	20
471	2007 Niigata Chuetsu Oki, Japan	YES	6.6	100.56	29.67	8.6	3.000	0.99	12
474	2008 Achaia-Elia Earthquake, Greece	YES	6.5	157.65	47.05	11.3	0.138	0.68	47
475	2008 Achaia-Elia Earthquake, Greece	YES	6.5	159.65	47.05	11.3	0.130	0.67	49
478	2011 Tohoku Aftershock, April 11, 2011	YES	7.40	127.39	32.26	12.9	0.284	0.88	32
479	2011 Tohoku Aftershock, April 11, 2011	YES	7.40	106.06	84.08	10.0	3.000	0.99	3
480	2011 Tohoku Aftershock, April 11, 2011	YES	7.40	171.18	97.86	13.5	0.224	0.79	19
481	2011 Tohoku Aftershock, April 11, 2011	YES	7.40	114.58	43.93	12.9	3.000	0.99	12
482	2011 Tohoku Aftershock, April 11, 2011	YES	7.40	140.17	55.65	12.9	0.704	0.94	20
483	2011 Tohoku Aftershock, April 11, 2011	YES	7.40	142.59	55.65	17.2	0.092	0.71	22
484	2011 Tohoku Aftershock, April 11, 2011	YES	7.40	150.74	83.52	10.0	3.000	0.98	14
485	2011 Tohoku Aftershock, April 11, 2011	YES	7.40	117.81	47.38	10.0	3.000	0.99	12
486	2011 Tohoku Aftershock, April 11, 2011	YES	7.40	118.49	53.50	13.2	2.115	0.98	10
487	2011 Tohoku Aftershock, April 11, 2011	YES	7.40	144.49	53.04	13.2	0.262	0.85	25
490	2011 Tohoku Earthquake Mainshock, March 11, 2011	YES	9.00	118.49	53.50	22.1	0.435	0.96	10
491	2011 Tohoku Earthquake Mainshock, March 11, 2011	YES	9.00	118.65	53.04	22.1	0.417	0.95	10

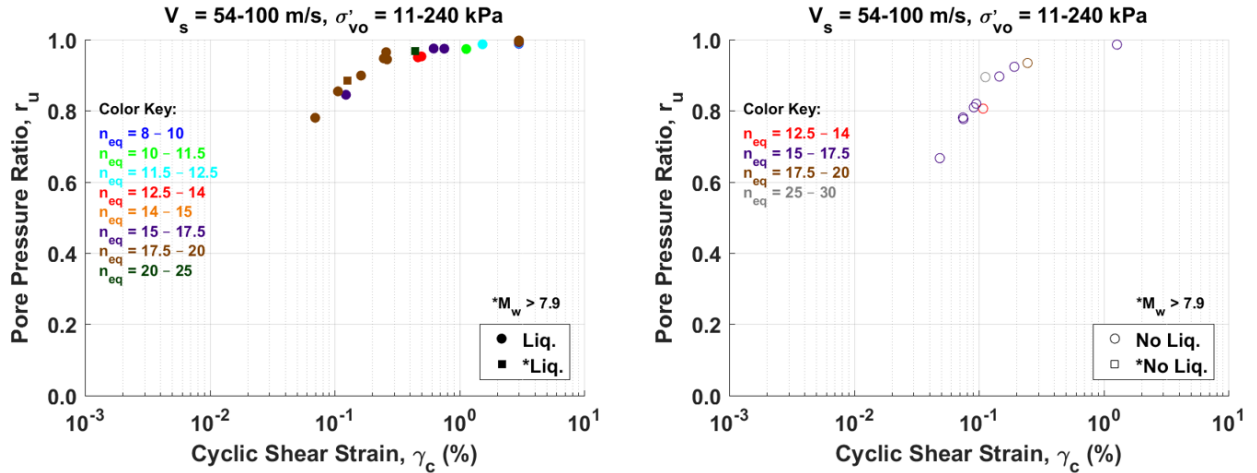


Figure C7. Excess porewater pressure buildup using the Vucetic and Dobry (1986) model with the Kayen et al. database

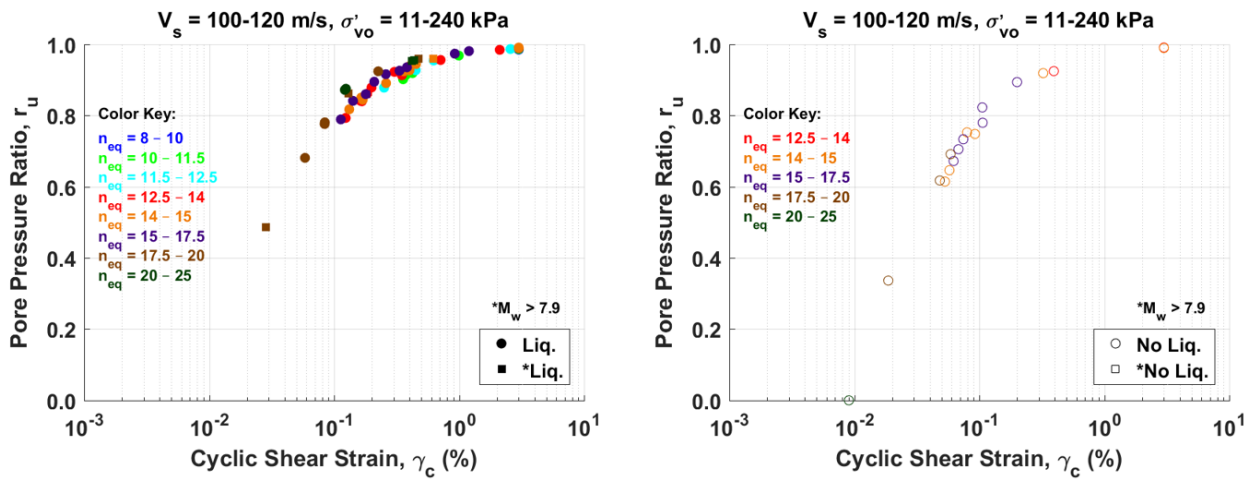


Figure C8. Excess porewater pressure buildup using the Vucetic and Dobry (1986) model with the Kayen et al. database

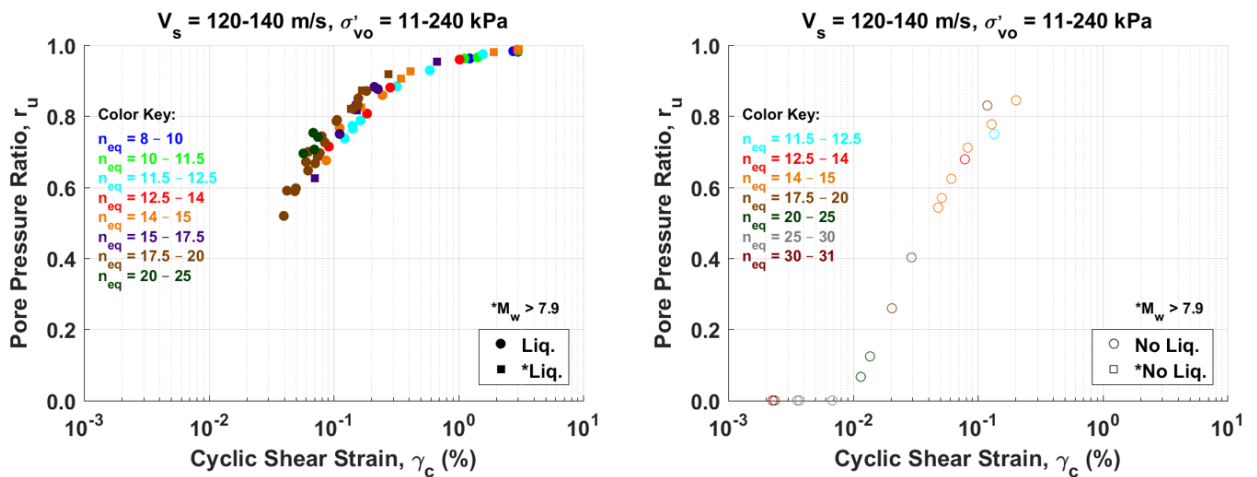


Figure C9. Excess porewater pressure buildup using the Vucetic and Dobry (1986) model with the Kayen et al. database

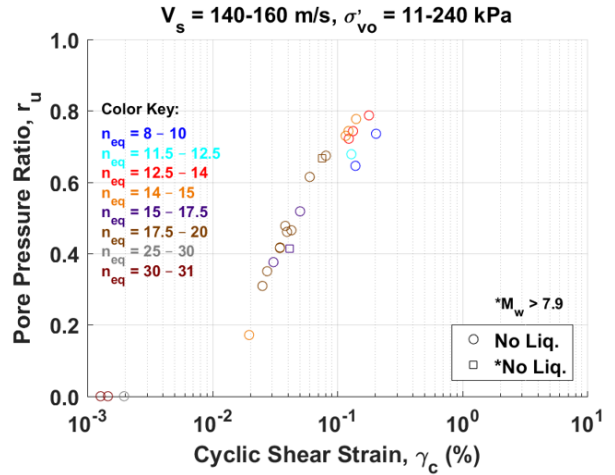
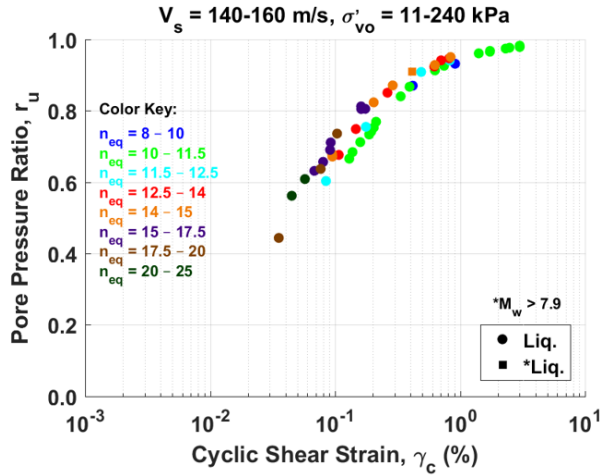


Figure C10. Excess porewater pressure buildup using the Vucetic and Dobry (1986) model with the Kayen et al. database

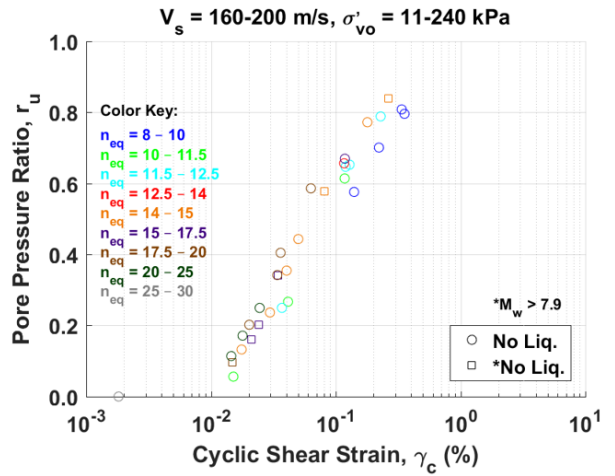
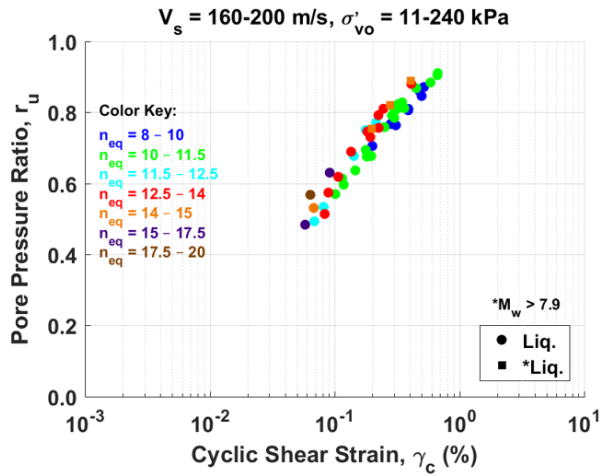


Figure C11. Excess porewater pressure buildup using the Vucetic and Dobry (1986) model with the Kayen et al. database

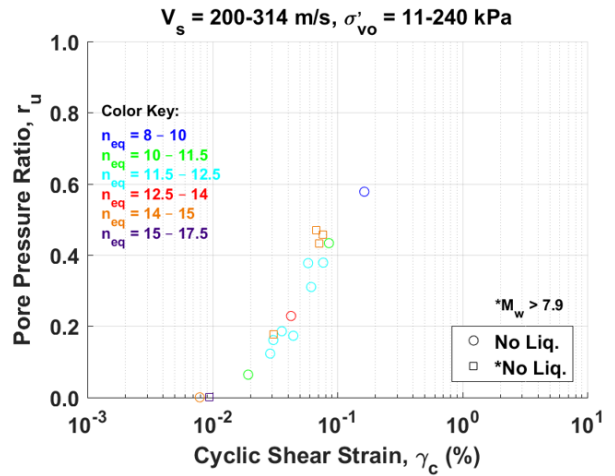
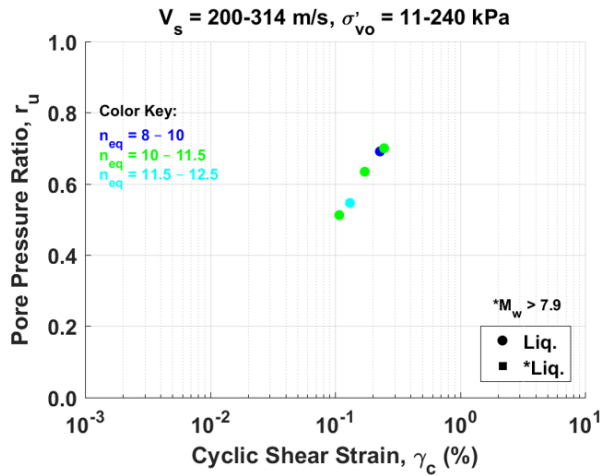


Figure C12. Excess porewater pressure buildup using the Vucetic and Dobry (1986) model with the Kayen et al. database

Appendix D: Pore Pressure Ratio Versus Cyclic Shear Strain for the Boulanger et al. Database using the Byrne (1991) and Vucetic and Dobry (1986) Models

Appendix D provides tables and figures showing the inputs and results of implementing both the Byrne (1991) and Vucetic and Dobry (1986) pore pressure models to the case histories in the Boulanger et al. (2013) database. First the tables and figures are presented for the Byrne model, followed by the tables and figures for the Vucetic and Dobry model. In addition, the first set of tables and figures correspond to all cases in the Boulanger et al. database, followed by the cases with $FC \leq 5\%$, and finally the cases having the additional V_s measurements.

All cases in the Boulanger et al. database (230 cases)

Byrne model

Table D1. Parameters needed to plot figures of excess pore pressure ratio versus cyclic shear strain for the Boulanger et al. (2012) database (all cases) using the Byrne (1991) model

Data Point #	Year Event	Liquefied? YES/NO	M _w	N _{1,60cs} blows	σ' _v (kPa)	Lasley n _{eq}	γ _c (%)	Byrne r _u	D _r (%)	FC (%)
2	1944 Tohankai earthquake M=8.1 - Dec 7	YES	8.1	9.3	68	20.2	0.136	1.00	45.0	10
3	1944 Tohankai earthquake M=8.1 - Dec 7	YES	8.1	8.7	61	20.2	0.280	1.00	43.5	30
4	1944 Tohankai earthquake M=8.1 - Dec 7	YES	8.1	6.9	39	20.2	3.005	1.00	38.7	27
5	1948 Fukui earthquake M=7.3 - June 28	YES	7	11.8	48	11.8	1.057	1.00	50.6	0
6	1948 Fukui earthquake M=7.3 - June 28	YES	7	21.1	104	12.4	0.114	0.92	67.7	4
7	1964 Niigata earthquake M=7.6 - June 16	YES	7.6	4.7	41	24.9	0.053	1.00	32.0	5
8	1964 Niigata earthquake M=7.6 - June 16	YES	7.6	9.9	72	19.7	0.103	1.00	46.4	2
9	1964 Niigata earthquake M=7.6 - June 16	YES	7.6	13	43	19.7	0.174	1.00	53.2	8
10	1964 Niigata earthquake M=7.6 - June 16	YES	7.6	6.8	53	19.6	0.082	1.00	38.4	5
11	1964 Niigata earthquake M=7.6 - June 16	NO	7.6	22.7	81	18.8	0.053	0.60	70.2	2
12	1964 Niigata earthquake M=7.6 - June 16	NO	7.6	23.5	109	18.8	0.057	0.55	71.5	2
13	1964 Niigata earthquake M=7.6 - June 16	YES	7.6	11	100	19.7	0.090	1.00	48.9	2
14	1964 Niigata earthquake M=7.6 - June 16	YES	7.6	17.5	100	19.7	0.067	0.86	61.7	2
15	1964 Niigata earthquake M=7.6 - June 16	YES	7.6	9.4	47	19.7	0.133	1.00	45.2	0
16	1964 Niigata earthquake M=7.6 - June 16	NO	7.6	14.1	79	18.8	0.062	0.97	55.4	0
17	1964 Niigata earthquake M=7.6 - June 16	YES	7.6	8.2	39	19.7	0.308	1.00	42.2	10
18	1964 Niigata earthquake M=7.6 - June 16	NO	7.6	35.5	67	18.8	0.046	0.35	87.8	0
19	1968 earthquake M=7.5 - April 1	NO	7.5	17.6	45	16.3	0.089	1.00	61.9	36
20	1968 Tokachi-Oki earthquake M=8.3 - May 16	YES	8.3	16.5	38	20.6	1.051	1.00	59.9	3
21	1968 Tokachi-Oki earthquake M=8.3 - May 16	NO	8.3	35.3	76	20.0	0.058	0.44	87.6	5
22	1968 Tokachi-Oki earthquake M=8.3 - May 16	NO	8.3	23	45	20.0	0.097	1.00	70.7	5
23	1968 Tokachi-Oki earthquake M=8.3 - May 16	YES	8.3	9.1	42	20.0	0.402	1.00	44.5	5
24	1968 Tokachi-Oki earthquake M=8.3 - May 16	YES	8.3	12	45	21.2	0.211	1.00	51.1	20
25	1971 San Fernando earthquake M=6.6 - Feb 9	YES	6.61	9.5	96	10.3	1.067	1.00	45.4	55
26	1971 San Fernando earthquake M=6.6 - Feb 9	YES	6.61	13.7	96	10.3	0.330	1.00	54.6	50
27	1975 Haicheng earthquake M=7.0 - Feb 4	YES	7	13.2	89	15.6	0.143	1.00	53.6	67
28	1975 Haicheng earthquake M=7.0 - Feb 4	NO	7	14.6	92	15.6	0.110	1.00	56.3	50
29	1975 Haicheng earthquake M=7.0 - Feb 4	YES	7	19	85	13.3	0.223	1.00	64.3	48
30	1975 Haicheng earthquake M=7.0 - Feb 4	YES	7	11	92	13.3	0.218	1.00	48.9	5
31	1976 Guatemala earthquake M=7.5 - Feb 4	YES	7.5	5	86	20.6	0.156	1.00	33.0	3
32	1976 Guatemala earthquake M=7.5 - Feb 4	YES	7.5	9.7	34	20.6	0.138	1.00	45.9	3
33	1976 Guatemala earthquake M=7.5 - Feb 4	NO	7.5	14.3	71	20.6	0.098	1.00	55.8	3
34	1976 Tangshan earthquake M=7.6 - July 27	YES	7.6	13.8	54	21.4	0.054	0.99	54.8	12

35	1976 Tangshan earthquake M=7.6 - July 27	YES	7.6	13.5	53	18.0	0.101	1.00	54.2	12
36	1976 Tangshan earthquake M=7.6 - July 27	NO	7.6	24.4	38	17.3	0.088	0.98	72.8	5
37	1976 Tangshan earthquake M=7.6 - July 27	YES	7.6	8.5	32	17.3	0.481	1.00	43.0	3
38	1976 Tangshan earthquake M=7.6 - July 27	YES	7.6	24.6	59	14.3	0.298	1.00	73.1	20
39	1976 Tangshan earthquake M=7.6 - July 27	NO	7.6	32.7	75	12.4	0.194	0.99	84.3	10
40	1976 Tangshan earthquake M=7.6 - July 27	YES	7.6	15	67	18.0	0.133	1.00	57.1	20
41	1977 Argentina earthquake M=7.4 - Nov 23	YES	7.5	10.7	106	17.6	0.106	1.00	48.2	20
42	1977 Argentina earthquake M=7.4 - Nov 23	YES	7.5	7.6	156	17.6	0.076	1.00	40.6	5
43	1977 Argentina earthquake M=7.4 - Nov 23	NO	7.5	14.3	39	17.6	0.122	1.00	55.8	4
44	1977 Argentina earthquake M=7.4 - Nov 23	NO	7.5	13.6	44	17.6	0.067	1.00	54.4	3
45	1977 Argentina earthquake M=7.4 - Nov 23	YES	7.5	11.4	56	17.6	0.256	1.00	49.8	50
46	1978 Miyagiken-Oki earthquake M=6.5 - Feb 20	NO	6.5	12.8	67	18.5	0.036	0.75	52.8	0
47	1978 Miyagiken-Oki earthquake M=6.5 - Feb 20	NO	6.5	15.5	71	16.1	0.044	0.71	58.0	20
48	1978 Miyagiken-Oki earthquake M=6.5 - Feb 20	NO	6.5	6.7	45	17.1	0.061	1.00	38.2	10
49	1978 Miyagiken-Oki earthquake M=6.5 - Feb 20	NO	6.5	12.3	59	16.1	0.028	0.60	51.7	5
50	1978 Miyagiken-Oki earthquake M=6.5 - Feb 20	NO	6.5	14.1	79	16.1	0.038	0.66	55.4	3
51	1978 Miyagiken-Oki earthquake M=6.5 - Feb 20	YES	6.5	6.9	30	17.1	0.074	1.00	38.7	5
52	1978 Miyagiken-Oki earthquake M=6.5 - Feb 20	NO	6.5	9.6	42	17.1	0.045	1.00	45.7	4
53	1978 Miyagiken-Oki earthquake M=6.5 - Feb 20	NO	6.5	9.4	85	16.1	0.044	0.97	45.2	5
54	1978 Miyagiken-Oki earthquake M=6.5 - Feb 20	NO	6.5	8.6	60	16.1	0.048	1.00	43.2	10
55	1978 Miyagiken-Oki earthquake M=6.5 - Feb 20	NO	6.5	6.5	56	17.1	0.062	1.00	37.6	10
56	1978 Miyagiken-Oki earthquake M=6.5 - Feb 20	NO	6.5	16.3	34	17.1	0.028	0.58	59.5	7
57	1978 Miyagiken-Oki earthquake M=6.5 - Feb 20	NO	6.5	13.9	42	17.1	0.063	1.00	55.0	12
58	1978 Miyagiken-Oki earthquake M=6.5 - Feb 20	NO	6.5	8.1	63	17.1	0.130	1.00	42.0	60
59	1978 Miyagiken-Oki earthquake M=6.5 - Feb 20	NO	6.5	15.1	47	17.1	0.042	0.83	57.3	0
60	1978 Miyagiken-Oki earthquake M=7.7 - June 12	YES	7.7	12.8	67	18.4	0.134	1.00	52.8	0
61	1978 Miyagiken-Oki earthquake M=7.7 - June 12	YES	7.7	15.5	71	17.1	0.123	1.00	58.0	20
62	1978 Miyagiken-Oki earthquake M=7.7 - June 12	YES	7.7	6.7	45	18.4	0.208	1.00	38.2	10
63	1978 Miyagiken-Oki earthquake M=7.7 - June 12	NO	7.7	22	57	18.4	0.066	0.83	69.2	10
64	1978 Miyagiken-Oki earthquake M=7.7 - June 12	YES	7.7	12.3	59	16.1	0.092	1.00	51.7	5
65	1978 Miyagiken-Oki earthquake M=7.7 - June 12	NO	7.7	17.6	73	16.1	0.094	1.00	61.9	0
66	1978 Miyagiken-Oki earthquake M=7.7 - June 12	NO	7.7	17.8	65	17.1	0.105	1.00	62.2	26
67	1978 Miyagiken-Oki earthquake M=7.7 - June 12	YES	7.7	14.1	79	17.1	0.108	1.00	55.4	3
68	1978 Miyagiken-Oki earthquake M=7.7 - June 12	NO	7.7	26.2	39	15.2	0.185	1.00	75.5	4
69	1978 Miyagiken-Oki earthquake M=7.7 - June 12	YES	7.7	6.9	30	15.2	3.005	1.00	38.7	5
70	1978 Miyagiken-Oki earthquake M=7.7 - June 12	YES	7.7	9.6	42	15.2	0.693	1.00	45.7	4
71	1978 Miyagiken-Oki earthquake M=7.7 - June 12	YES	7.7	9.4	85	17.1	0.111	1.00	45.2	5
72	1978 Miyagiken-Oki earthquake M=7.7 - June 12	YES	7.7	8.6	60	17.1	0.142	1.00	43.2	10
73	1978 Miyagiken-Oki earthquake M=7.7 - June 12	YES	7.7	6.5	56	17.1	0.339	1.00	37.6	10

74	1978 Miyagiken-Oki earthquake M=7.7 - June 12	YES	7.7	16.3	34	17.1	0.099	1.00	59.5	7
75	1978 Miyagiken-Oki earthquake M=7.7 - June 12	YES	7.7	13.9	42	17.1	0.453	1.00	55.0	12
76	1978 Miyagiken-Oki earthquake M=7.7 - June 12	NO	7.7	24	78	17.1	0.119	0.98	72.2	17
77	1978 Miyagiken-Oki earthquake M=7.7 - June 12	YES	7.7	8.1	63	17.1	3.005	1.00	42.0	60
78	1978 Miyagiken-Oki earthquake M=7.7 - June 12	YES	7.7	15.1	47	17.1	0.189	1.00	57.3	0
79	1978 Miyagiken-Oki earthquake M=7.7 - June 12	NO	7.7	24.6	70	17.1	0.079	0.80	73.1	0
80	1979 Imperial Valley earthquake ML=6.5 - Oct 15	NO	6.53	40	42	8.0	1.070	1.00	90.0	12
81	1979 Imperial Valley earthquake ML=6.5 - Oct 15	YES	6.53	7	50	8.0	3.005	1.00	39.0	18
82	1979 Imperial Valley earthquake ML=6.5 - Oct 15	NO	6.53	21.2	56	8.0	3.005	1.00	67.9	25
83	1979 Imperial Valley earthquake ML=6.5 - Oct 15	NO	6.53	11.7	62	16.7	0.048	0.97	50.4	92
84	1979 Imperial Valley earthquake ML=6.5 - Oct 15	YES	6.53	10	32	9.6	3.005	1.00	46.6	31
85	1979 Imperial Valley earthquake ML=6.5 - Oct 15	YES	6.53	8.5	50	14.0	0.247	1.00	43.0	64
86	1979 Imperial Valley earthquake ML=6.5 - Oct 15	NO	6.53	20.6	38	14.0	0.043	0.65	66.9	30
87	1979 Imperial Valley earthquake ML=6.5 - Oct 15	YES	6.53	10.2	20	13.0	3.005	1.00	47.1	80
88	1979 Imperial Valley earthquake ML=6.5 - Oct 15	NO	6.53	15.7	54	15.0	0.084	1.00	58.4	30
89	1980 Mid-Chiba earthquake M=6.0 - Sept 24 (UTC)	NO	6	9.6	57	16.8	0.051	1.00	45.7	13
90	1980 Mid-Chiba earthquake M=6.0 - Sept 24 (UTC)	NO	6	9.1	123	16.8	0.050	0.98	44.5	27
91	1981 WestMorland earthquake M=5.9 - April 26	YES	5.9	11.7	62	10.0	0.282	1.00	50.4	92
92	1981 WestMorland earthquake M=5.9 - April 26	NO	5.9	10	32	16.8	0.030	0.94	46.6	31
93	1981 WestMorland earthquake M=5.9 - April 26	YES	5.9	8.5	50	12.1	0.217	1.00	43.0	64
94	1981 WestMorland earthquake M=5.9 - April 26	NO	5.9	20.6	38	12.1	0.041	0.59	66.9	30
95	1981 WestMorland earthquake M=5.9 - April 26	NO	5.9	10.2	20	11.9	0.663	1.00	47.1	80
96	1981 WestMorland earthquake M=5.9 - April 26	NO	5.9	19.3	45	11.9	0.104	1.00	64.8	18
97	1981 WestMorland earthquake M=5.9 - April 26	YES	5.9	15.7	54	10.9	0.199	1.00	58.4	30
98	1982 Urakawa-Oki earthquake M=6.9 - Mar 21	NO	6.9	17	35	16.4	0.038	0.75	60.8	5
99	1983 Nihonkai-Chubu earthquake M=6.8 - June 21	NO	6.8	5.1	37	16.8	0.351	1.00	33.3	5
100	1983 Nihonkai-Chubu earthquake M=6.8 - June 21	NO	6.8	18.1	77	16.8	0.069	0.88	62.7	0
101	1983 Nihonkai-Chubu earthquake M=6.8 - June 21	YES	6.8	13.3	42	19.0	0.052	1.00	53.8	0
102	1983 Nihonkai-Chubu earthquake M=7.7 - May 26	YES	7.7	16.5	38	23.0	0.102	1.00	59.9	3
103	1983 Nihonkai-Chubu earthquake M=7.7 - May 26	YES	7.7	5.1	37	18.4	3.005	1.00	33.3	5
104	1983 Nihonkai-Chubu earthquake M=7.7 - May 26	YES	7.7	12.4	53	17.5	0.837	1.00	51.9	1
105	1983 Nihonkai-Chubu earthquake M=7.7 - May 26	YES	7.7	16.2	38	16.8	0.157	1.00	59.3	1
106	1983 Nihonkai-Chubu earthquake M=7.7 - May 26	YES	7.7	13.3	42	16.0	0.773	1.00	53.8	0
107	1983 Nihonkai-Chubu earthquake M=7.7 - May 26	NO	7.7	18.7	41	18.2	0.055	0.90	63.8	3
108	1983 Nihonkai-Chubu earthquake M=7.7 - May 26	NO	7.7	13.8	41	18.2	0.073	1.00	54.8	3
109	1983 Nihonkai-Chubu earthquake M=7.7 - May 26	NO	7.7	13.1	41	23.0	0.039	0.93	53.4	5
110	1983 Nihonkai-Chubu earthquake M=7.7 - May 26	YES	7.7	8.7	79	18.2	0.145	1.00	43.5	3
111	1983 Nihonkai-Chubu earthquake M=7.7 - May 26	YES	7.7	6.9	107	18.2	0.165	1.00	38.7	4
112	1983 Nihonkai-Chubu earthquake M=7.7 - May 26	NO	7.7	9.8	54	31.9	0.025	0.81	46.2	66

113	1983 Nihonkai-Chubu earthquake M=7.7 - May 26	YES	7.7	10.4	74	18.2	0.135	1.00	47.5	8
114	1983 Nihonkai-Chubu earthquake M=7.7 - May 26	YES	7.7	13.5	81	18.2	0.102	1.00	54.2	3
115	1983 Nihonkai-Chubu earthquake M=7.7 - May 26	YES	7.7	9.4	48	18.2	0.127	1.00	45.2	7
116	1983 Nihonkai-Chubu earthquake M=7.7 - May 26	YES	7.7	10.2	71	18.2	0.127	1.00	47.1	2
117	1983 Nihonkai-Chubu earthquake M=7.7 - May 26	YES	7.7	11.5	68	18.2	0.117	1.00	50.0	2
118	1983 Nihonkai-Chubu earthquake M=7.7 - May 26	NO	7.7	18.9	47	18.2	0.077	1.00	64.1	3
119	1983 Nihonkai-Chubu earthquake M=7.7 - May 26	NO	7.7	23.5	42	18.2	0.062	0.83	71.5	2
120	1983 Nihonkai-Chubu earthquake M=7.7 - May 26	NO	7.7	23	34	18.2	0.057	0.84	70.7	1
121	1983 Nihonkai-Chubu earthquake M=7.7 - May 26	NO	7.7	34.6	60	18.2	0.055	0.45	86.7	3
122	1983 Nihonkai-Chubu earthquake M=7.7 - May 26	NO	7.7	37.3	31	18.2	0.035	0.33	90.0	1
123	1983 Nihonkai-Chubu earthquake M=7.7 - May 26	NO	7.7	20.3	53	18.2	0.080	0.98	66.4	2
124	1983 Nihonkai-Chubu earthquake M=7.7 - May 26	YES	7.7	5.4	56	18.2	0.390	1.00	34.3	2
125	1983 Nihonkai-Chubu earthquake M=7.7 - May 26	YES	7.7	7.4	63	18.2	0.191	1.00	40.1	2
126	1983 Nihonkai-Chubu earthquake M=7.7 - May 26	YES	7.7	5.6	64	18.2	0.246	1.00	34.9	2
127	1983 Nihonkai-Chubu earthquake M=7.7 - May 26	YES	7.7	8.1	49	18.2	0.146	1.00	42.0	2
128	1983 Nihonkai-Chubu earthquake M=7.7 - May 26	NO	7.7	23.5	55	18.2	0.068	0.82	71.5	2
129	1983 Nihonkai-Chubu earthquake M=7.7 - May 26	NO	7.7	22.5	77	18.2	0.071	0.78	69.9	4
130	1983 Nihonkai-Chubu earthquake M=7.7 - May 26	NO	7.7	25.9	46	18.2	0.053	0.65	75.0	0
131	1984 earthquake M=6.9 - Aug 7	NO	6.9	17.6	45	13.6	0.111	1.00	61.9	36
132	1987 Superstition Hills earthquakes M=6.2 and M=6.5 - 01 & 02 - Nov 24	NO	6.22	8.5	50	18.1	0.047	1.00	43.0	64
133	1987 Superstition Hills earthquakes M=6.2 and M=6.5 - 01 & 02 - Nov 24	NO	6.22	15.7	54	15.4	0.055	0.90	58.4	30
134	1987 Superstition Hills earthquakes M=6.2 and M=6.5 - 01 & 02 - Nov 24	NO	6.54	40	42	15.5	0.022	0.13	90.0	12
135	1987 Superstition Hills earthquakes M=6.2 and M=6.5 - 01 & 02 - Nov 24	NO	6.54	7	50	15.8	0.144	1.00	39.0	18
136	1987 Superstition Hills earthquakes M=6.2 and M=6.5 - 01 & 02 - Nov 24	NO	6.54	21.2	56	16.8	0.030	0.38	67.9	25
137	1987 Superstition Hills earthquakes M=6.2 and M=6.5 - 01 & 02 - Nov 24	NO	6.54	11.7	62	14.9	0.081	1.00	50.4	92
138	1987 Superstition Hills earthquakes M=6.2 and M=6.5 - 01 & 02 - Nov 24	NO	6.54	10	32	15.4	0.083	1.00	46.6	31
139	1987 Superstition Hills earthquakes M=6.2 and M=6.5 - 01 & 02 - Nov 24	NO	6.54	8.5	50	14.0	0.226	1.00	43.0	64
140	1987 Superstition Hills earthquakes M=6.2 and M=6.5 - 01 & 02 - Nov 24	NO	6.54	20.6	38	14.7	0.035	0.53	66.9	30
141	1987 Superstition Hills earthquakes M=6.2 and M=6.5 - 01 & 02 - Nov 24	NO	6.54	10.2	20	14.3	0.425	1.00	47.1	80
142	1987 Superstition Hills earthquakes M=6.2 and M=6.5 - 01 & 02 - Nov 24	NO	6.54	19.3	45	14.3	0.094	1.00	64.8	18
143	1987 Superstition Hills earthquakes M=6.2 and M=6.5 - 01 & 02 - Nov 24	YES	6.54	15.7	54	13.9	0.123	1.00	58.4	30
144	1989 Loma Prieta earthquake M=6.9 - Oct 18	NO	6.93	43.4	91	14.3	0.050	0.24	90.0	7
145	1989 Loma Prieta earthquake M=6.9 - Oct 18	YES	6.93	10.6	92	12.0	0.181	1.00	48.0	8
146	1989 Loma Prieta earthquake M=6.9 - Oct 18	NO	6.93	21.4	35	13.4	0.084	0.99	68.2	5
147	1989 Loma Prieta earthquake M=6.9 - Oct 18	NO	6.93	11	64	17.8	0.055	1.00	48.9	30
148	1989 Loma Prieta earthquake M=6.9 - Oct 18	YES	6.93	13.1	65	13.4	0.134	1.00	53.4	3
149	1989 Loma Prieta earthquake M=6.9 - Oct 18	YES	6.93	14.9	55	13.4	0.093	1.00	56.9	3
150	1989 Loma Prieta earthquake M=6.9 - Oct 18	YES	6.93	17.6	64	13.4	0.144	1.00	61.9	3
151	1989 Loma Prieta earthquake M=6.9 - Oct 18	NO	6.93	22.6	35	13.4	0.052	0.73	70.1	1

152	1989 Loma Prieta earthquake M=6.9 - Oct 18	NO	6.93	14.9	47	13.4	0.127	1.00	56.9	1
153	1989 Loma Prieta earthquake M=6.9 - Oct 18	NO	6.93	21.2	48	13.4	0.089	0.98	67.9	5
154	1989 Loma Prieta earthquake M=6.9 - Oct 18	NO	6.93	14.7	48	13.4	0.117	1.00	56.5	4
155	1989 Loma Prieta earthquake M=6.9 - Oct 18	YES	6.93	15.3	101	11.7	0.185	1.00	57.7	32
156	1989 Loma Prieta earthquake M=6.9 - Oct 18	YES	6.93	23.4	108	11.7	0.112	0.84	71.3	13
157	1989 Loma Prieta earthquake M=6.9 - Oct 18	YES	6.93	14.9	95	11.7	0.211	1.00	56.9	25
158	1989 Loma Prieta earthquake M=6.9 - Oct 18	NO	6.93	24.6	105	11.7	0.167	0.99	73.1	20
159	1989 Loma Prieta earthquake M=6.9 - Oct 18	YES	6.93	15.4	89	13.4	0.113	1.00	57.9	3
160	1989 Loma Prieta earthquake M=6.9 - Oct 18	YES	6.93	17	89	13.4	0.105	1.00	60.8	3
161	1989 Loma Prieta earthquake M=6.9 - Oct 18	YES	6.93	10.7	73	16.1	0.148	1.00	48.2	50
162	1989 Loma Prieta earthquake M=6.9 - Oct 18	YES	6.93	15.3	43	13.4	0.123	1.00	57.7	2
163	1989 Loma Prieta earthquake M=6.9 - Oct 18	NO	6.93	34.4	73	13.4	0.081	0.55	86.5	5
164	1989 Loma Prieta earthquake M=6.9 - Oct 18	YES	6.93	9	86	13.6	0.184	1.00	44.2	8
165	1989 Loma Prieta earthquake M=6.9 - Oct 18	YES	6.93	10.3	46	13.4	0.194	1.00	47.3	1
166	1989 Loma Prieta earthquake M=6.9 - Oct 18	YES	6.93	18.4	67	13.4	0.098	1.00	63.2	1
167	1989 Loma Prieta earthquake M=6.9 - Oct 18	YES	6.93	10.8	67	16.9	0.147	1.00	48.5	20
168	1989 Loma Prieta earthquake M=6.9 - Oct 18	YES	6.93	14.6	25	13.4	0.228	1.00	56.3	35
169	1990 Luzon earthquake M=7.7 - July 16	NO	7.7	29.2	68	16.8	0.073	0.65	79.7	19
170	1990 Luzon earthquake M=7.7 - July 16	YES	7.7	17.3	90	16.8	0.123	1.00	61.3	19
171	1993 Koshiro-Oki earthquake M=7.6 - Jan 15	YES	7.6	16.4	68	13.6	0.337	1.00	59.7	2
172	1993 Koshiro-Oki earthquake M=7.6 - Jan 15	NO	7.6	30.9	118	13.6	0.195	0.96	82.0	0
173	1993 Koshiro-Oki earthquake M=7.6 - Jan 15	YES	7.6	25.9	47	12.7	0.425	1.00	75.0	5
174	1994 Northridge earthquake M=6.7 - Jan 17	YES	6.69	18.7	143	8.1	0.880	1.00	63.8	50
175	1994 Northridge earthquake M=6.7 - Jan 17	NO	6.69	32.3	101	9.9	0.298	1.00	83.8	25
176	1994 Northridge earthquake M=6.7 - Jan 17	YES	6.69	14.1	88	10.6	0.886	1.00	55.4	64
177	1994 Northridge earthquake M=6.7 - Jan 17	YES	6.69	17	105	9.9	0.358	1.00	60.8	33
178	1995 Hyogoken-Nambu (Kobe) earthquake M=6.9 - Jan 16	NO	6.9	50	80	11.5	0.089	0.37	90.0	3
179	1995 Hyogoken-Nambu (Kobe) earthquake M=6.9 - Jan 16	NO	6.9	42.7	103	11.5	0.108	0.47	90.0	15
180	1995 Hyogoken-Nambu (Kobe) earthquake M=6.9 - Jan 16	NO	6.9	49.8	77	11.5	0.096	0.41	90.0	3
181	1995 Hyogoken-Nambu (Kobe) earthquake M=6.9 - Jan 16	NO	6.9	36.6	54	11.5	0.144	0.87	89.2	1
182	1995 Hyogoken-Nambu (Kobe) earthquake M=6.9 - Jan 16	YES	6.9	6.1	116	12.2	0.359	1.00	36.4	1
183	1995 Hyogoken-Nambu (Kobe) earthquake M=6.9 - Jan 16	NO	6.9	22.5	72	11.5	0.283	1.00	69.9	21
184	1995 Hyogoken-Nambu (Kobe) earthquake M=6.9 - Jan 16	YES	6.9	10.9	60	11.5	0.188	1.00	48.7	0
185	1995 Hyogoken-Nambu (Kobe) earthquake M=6.9 - Jan 16	YES	6.9	24.1	65	10.5	0.337	1.00	72.4	0
186	1995 Hyogoken-Nambu (Kobe) earthquake M=6.9 - Jan 16	YES	6.9	12.2	64	10.5	0.825	1.00	51.5	2
187	1995 Hyogoken-Nambu (Kobe) earthquake M=6.9 - Jan 16	NO	6.9	28	107	9.8	0.281	1.00	78.0	9
188	1995 Hyogoken-Nambu (Kobe) earthquake M=6.9 - Jan 16	YES	6.9	8.5	62	10.5	3.005	1.00	43.0	5
189	1995 Hyogoken-Nambu (Kobe) earthquake M=6.9 - Jan 16	NO	6.9	27.6	72	10.5	0.281	1.00	77.5	14
190	1995 Hyogoken-Nambu (Kobe) earthquake M=6.9 - Jan 16	YES	6.9	16	74	10.5	2.310	1.00	59.0	15

191	1995 Hyogoken-Nambu (Kobe) earthquake M=6.9 - Jan 16	NO	6.9	24.5	69	10.5	0.294	1.00	73.0	19
192	1995 Hyogoken-Nambu (Kobe) earthquake M=6.9 - Jan 16	YES	6.9	19.2	82	10.5	0.268	1.00	64.6	5
193	1995 Hyogoken-Nambu (Kobe) earthquake M=6.9 - Jan 16	NO	6.9	25	60	9.8	0.665	1.00	73.7	5
194	1995 Hyogoken-Nambu (Kobe) earthquake M=6.9 - Jan 16	YES	6.9	21.1	43	10.5	3.005	1.00	67.7	5
195	1995 Hyogoken-Nambu (Kobe) earthquake M=6.9 - Jan 16	NO	6.9	42.6	171	9.2	0.161	0.50	90.0	0
196	1995 Hyogoken-Nambu (Kobe) earthquake M=6.9 - Jan 16	NO	6.9	22.5	124	9.8	0.215	1.00	69.9	10
197	1995 Hyogoken-Nambu (Kobe) earthquake M=6.9 - Jan 16	NO	6.9	50	75	10.1	0.185	0.69	90.0	0
198	1995 Hyogoken-Nambu (Kobe) earthquake M=6.9 - Jan 16	NO	6.9	33.5	44	9.8	0.676	1.00	85.3	0
199	1995 Hyogoken-Nambu (Kobe) earthquake M=6.9 - Jan 16	NO	6.9	38.6	79	9.8	0.332	1.00	90.0	6
200	1995 Hyogoken-Nambu (Kobe) earthquake M=6.9 - Jan 16	NO	6.9	25.1	72	9.8	0.520	1.00	73.9	10
201	1995 Hyogoken-Nambu (Kobe) earthquake M=6.9 - Jan 16	YES	6.9	24.6	51	10.5	0.279	1.00	73.1	0
202	1995 Hyogoken-Nambu (Kobe) earthquake M=6.9 - Jan 16	NO	6.9	35.8	50	9.2	0.713	1.00	88.2	3
203	1995 Hyogoken-Nambu (Kobe) earthquake M=6.9 - Jan 16	NO	6.9	37	37	9.8	3.005	1.00	89.7	0
204	1995 Hyogoken-Nambu (Kobe) earthquake M=6.9 - Jan 16	NO	6.9	42	29	9.8	1.774	1.00	90.0	10
205	1995 Hyogoken-Nambu (Kobe) earthquake M=6.9 - Jan 16	YES	6.9	21.4	44	11.5	0.273	1.00	68.2	8
206	1995 Hyogoken-Nambu (Kobe) earthquake M=6.9 - Jan 16	YES	6.9	17.9	49	11.5	0.286	1.00	62.4	0
207	1995 Hyogoken-Nambu (Kobe) earthquake M=6.9 - Jan 16	NO	6.9	41.3	78	9.8	1.372	1.00	90.0	10
208	1995 Hyogoken-Nambu (Kobe) earthquake M=6.9 - Jan 16	NO	6.9	49.7	46	9.8	0.753	1.00	90.0	0
209	1995 Hyogoken-Nambu (Kobe) earthquake M=6.9 - Jan 16	NO	6.9	29.2	41	10.5	0.577	1.00	79.7	6
210	1995 Hyogoken-Nambu (Kobe) earthquake M=6.9 - Jan 16	NO	6.9	33.5	83	10.5	0.500	1.00	85.3	50
211	1995 Hyogoken-Nambu (Kobe) earthquake M=6.9 - Jan 16	YES	6.9	25	73	11.5	0.297	1.00	73.7	9
212	1995 Hyogoken-Nambu (Kobe) earthquake M=6.9 - Jan 16	YES	6.9	18.9	55	10.5	0.882	1.00	64.1	6
213	1995 Hyogoken-Nambu (Kobe) earthquake M=6.9 - Jan 16	NO	6.9	31.6	36	9.8	3.005	1.00	82.9	3
214	1995 Hyogoken-Nambu (Kobe) earthquake M=6.9 - Jan 16	YES	6.9	19.3	79	12.2	0.106	0.98	64.8	0
215	1995 Hyogoken-Nambu (Kobe) earthquake M=6.9 - Jan 16	YES	6.9	19.1	94	10.5	0.499	1.00	64.4	5
216	1995 Hyogoken-Nambu (Kobe) earthquake M=6.9 - Jan 16	NO	6.9	50	66	9.8	0.174	0.68	90.0	0
217	1995 Hyogoken-Nambu (Kobe) earthquake M=6.9 - Jan 16	NO	6.9	39.7	59	9.8	0.168	0.84	90.0	0
218	1995 Hyogoken-Nambu (Kobe) earthquake M=6.9 - Jan 16	YES	6.9	15	50	11.5	0.562	1.00	57.1	0
219	1995 Hyogoken-Nambu (Kobe) earthquake M=6.9 - Jan 16	YES	6.9	13.2	46	11.5	3.005	1.00	53.6	10
220	1995 Hyogoken-Nambu (Kobe) earthquake M=6.9 - Jan 16	YES	6.9	19.6	55	12.2	0.299	1.00	65.3	20
221	1995 Hyogoken-Nambu (Kobe) earthquake M=6.9 - Jan 16	YES	6.9	8.3	43	11.5	3.005	1.00	42.5	5
222	1995 Hyogoken-Nambu (Kobe) earthquake M=6.9 - Jan 16	NO	6.9	25.2	80	11.5	0.139	0.97	74.0	18
223	1995 Hyogoken-Nambu (Kobe) earthquake M=6.9 - Jan 16	YES	6.9	12.5	115	11.5	0.244	1.00	52.1	2
224	1995 Hyogoken-Nambu (Kobe) earthquake M=6.9 - Jan 16	YES	6.9	11.3	96	12.3	0.417	1.00	49.6	20
225	1995 Hyogoken-Nambu (Kobe) earthquake M=6.9 - Jan 16	NO	6.9	27.2	125	11.5	0.118	0.74	76.9	20
226	1995 Hyogoken-Nambu (Kobe) earthquake M=6.9 - Jan 16	NO	6.9	24	140	11.5	0.133	0.85	72.2	20
227	1995 Hyogoken-Nambu (Kobe) earthquake M=6.9 - Jan 16	NO	6.9	39.1	135	11.5	0.093	0.40	90.0	20
228	1995 Hyogoken-Nambu (Kobe) earthquake M=6.9 - Jan 16	YES	6.9	15.3	123	12.3	0.206	1.00	57.7	20
229	1995 Hyogoken-Nambu (Kobe) earthquake M=6.9 - Jan 16	YES	6.9	21.9	107	11.5	0.164	1.00	69.0	25

230	1995 Hyogoken-Nambu (Kobe) earthquake M=6.9 - Jan 16	YES	6.9	16.8	146	12.3	0.150	1.00	60.4	20
231	1995 Hyogoken-Nambu (Kobe) earthquake M=6.9 - Jan 16	YES	6.9	18.5	46	13.9	0.285	1.00	63.4	20

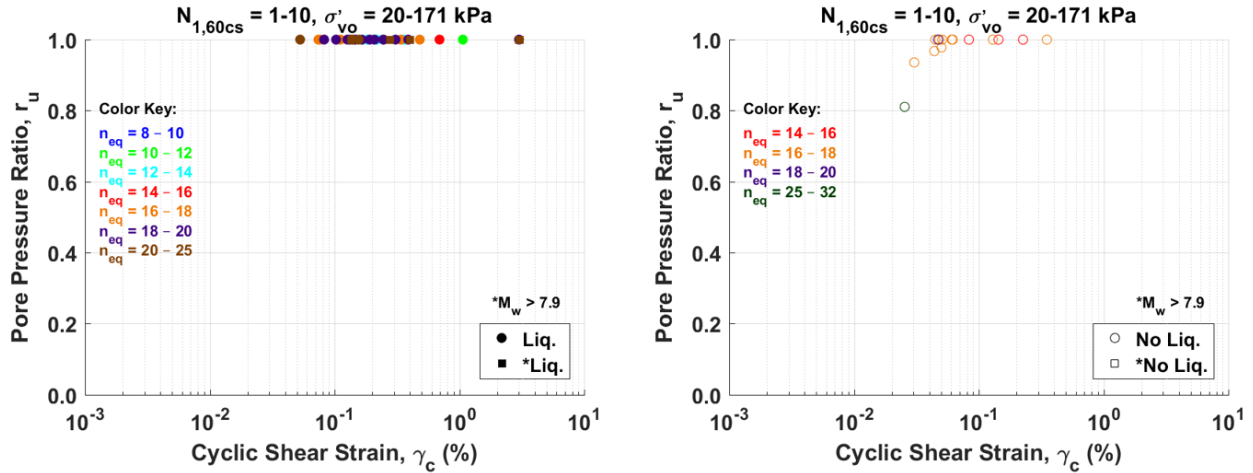


Figure D1. Excess porewater pressure buildup using the Byrne (1991) model with the Boulanger et al. database all cases

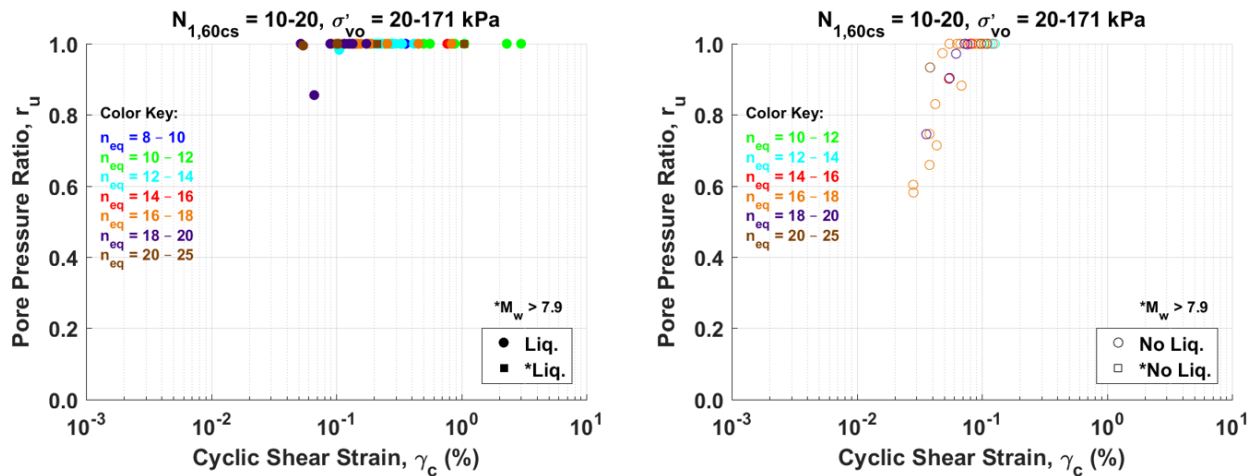


Figure D2. Excess porewater pressure buildup using the Byrne (1991) model with the Boulanger et al. database all cases

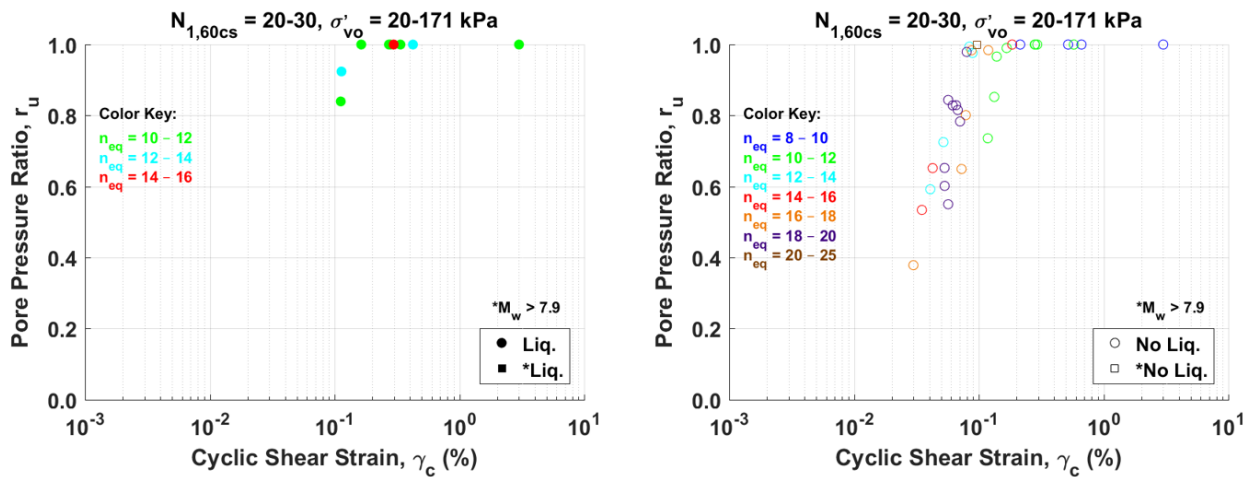


Figure D3. Excess porewater pressure buildup using the Byrne (1991) model with the Boulanger et al. database all cases

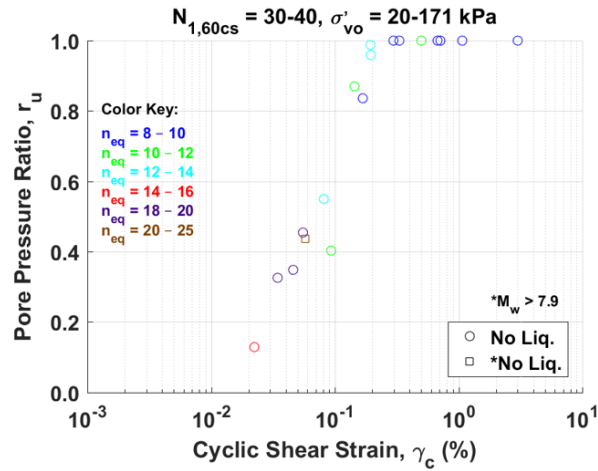


Figure D4. Excess porewater pressure buildup using the Byrne (1991) model with the Boulanger et al. database all cases

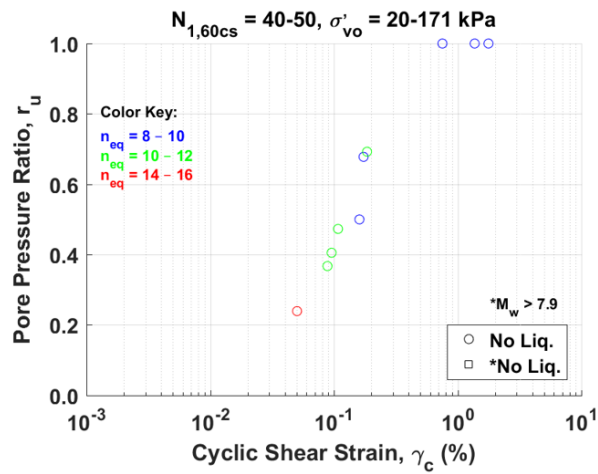


Figure D5. Excess porewater pressure buildup using the Byrne (1991) model with the Boulanger et al. database all cases

All cases in the Boulanger et al. database (230 cases)

Vucetic and Dobry model

Table D2. Parameters needed to plot figures of excess pore pressure ratio versus cyclic shear strain for the Boulanger et al. (2012) database (all cases) using the Vucetic and Dobry (1986) model

Data Point #	Year Event	Liquefied? YES/NO	M _w	N _{1,60cs} blows	σ' _v (kPa)	Lasley n _{eq}	γ _c (%)	Vucetic and Dobry r _u	D _r (%)	FC (%)
2	1944 Tohankai earthquake M=8.1 - Dec 7	YES	8.1	9.3	68	20.2	0.131	0.79	45.0	10
3	1944 Tohankai earthquake M=8.1 - Dec 7	YES	8.1	8.7	61	20.2	0.275	0.89	43.5	30
4	1944 Tohankai earthquake M=8.1 - Dec 7	YES	8.1	6.9	39	20.2	3.000	0.99	38.7	27
5	1948 Fukui earthquake M=7.3 - June 28	YES	7	11.8	48	11.8	1.052	0.94	50.6	0
6	1948 Fukui earthquake M=7.3 - June 28	YES	7	21.1	104	12.4	0.109	0.56	67.7	4
7	1964 Niigata earthquake M=7.6 - June 16	YES	7.6	4.7	41	24.9	0.048	0.62	32.0	5
8	1964 Niigata earthquake M=7.6 - June 16	YES	7.6	9.9	72	19.7	0.098	0.72	46.4	2
9	1964 Niigata earthquake M=7.6 - June 16	YES	7.6	13	43	19.7	0.169	0.81	53.2	8
10	1964 Niigata earthquake M=7.6 - June 16	YES	7.6	6.8	53	19.6	0.077	0.68	38.4	5
11	1964 Niigata earthquake M=7.6 - June 16	NO	7.6	22.7	81	18.8	0.048	0.42	70.2	2
12	1964 Niigata earthquake M=7.6 - June 16	NO	7.6	23.5	109	18.8	0.052	0.44	71.5	2
13	1964 Niigata earthquake M=7.6 - June 16	YES	7.6	11	100	19.7	0.085	0.68	48.9	2
14	1964 Niigata earthquake M=7.6 - June 16	YES	7.6	17.5	100	19.7	0.062	0.54	61.7	2
15	1964 Niigata earthquake M=7.6 - June 16	YES	7.6	9.4	47	19.7	0.128	0.78	45.2	0
16	1964 Niigata earthquake M=7.6 - June 16	NO	7.6	14.1	79	18.8	0.057	0.53	55.4	0
17	1964 Niigata earthquake M=7.6 - June 16	YES	7.6	8.2	39	19.7	0.303	0.90	42.2	10
18	1964 Niigata earthquake M=7.6 - June 16	NO	7.6	35.5	67	18.8	0.041	0.37	87.8	0
19	1968 earthquake M=7.5 - April 1	NO	7.5	17.6	45	16.3	0.084	0.58	61.9	36
20	1968 Tokachi-Oki earthquake M=8.3 - May 16	YES	8.3	16.5	38	20.6	1.046	0.96	59.9	3
21	1968 Tokachi-Oki earthquake M=8.3 - May 16	NO	8.3	35.3	76	20.0	0.053	0.46	87.6	5
22	1968 Tokachi-Oki earthquake M=8.3 - May 16	NO	8.3	23	45	20.0	0.092	0.62	70.7	5
23	1968 Tokachi-Oki earthquake M=8.3 - May 16	YES	8.3	9.1	42	20.0	0.397	0.92	44.5	5
24	1968 Tokachi-Oki earthquake M=8.3 - May 16	YES	8.3	12	45	21.2	0.206	0.85	51.1	20
25	1971 San Fernando earthquake M=6.6 - Feb 9	YES	6.61	9.5	96	10.3	1.062	0.94	45.4	55
26	1971 San Fernando earthquake M=6.6 - Feb 9	YES	6.61	13.7	96	10.3	0.325	0.81	54.6	50
27	1975 Haicheng earthquake M=7.0 - Feb 4	YES	7	13.2	89	15.6	0.138	0.73	53.6	67
28	1975 Haicheng earthquake M=7.0 - Feb 4	NO	7	14.6	92	15.6	0.105	0.65	56.3	50
29	1975 Haicheng earthquake M=7.0 - Feb 4	YES	7	19	85	13.3	0.218	0.75	64.3	48
30	1975 Haicheng earthquake M=7.0 - Feb 4	YES	7	11	92	13.3	0.213	0.79	48.9	5
31	1976 Guatemala earthquake M=7.5 - Feb 4	YES	7.5	5	86	20.6	0.151	0.84	33.0	3
32	1976 Guatemala earthquake M=7.5 - Feb 4	YES	7.5	9.7	34	20.6	0.133	0.79	45.9	3
33	1976 Guatemala earthquake M=7.5 - Feb 4	NO	7.5	14.3	71	20.6	0.093	0.69	55.8	3

34	1976 Tangshan earthquake M=7.6 - July 27	YES	7.6	13.8	54	21.4	0.049	0.52	54.8	12
35	1976 Tangshan earthquake M=7.6 - July 27	YES	7.6	13.5	53	18.0	0.096	0.67	54.2	12
36	1976 Tangshan earthquake M=7.6 - July 27	NO	7.6	24.4	38	17.3	0.083	0.56	72.8	5
37	1976 Tangshan earthquake M=7.6 - July 27	YES	7.6	8.5	32	17.3	0.476	0.93	43.0	3
38	1976 Tangshan earthquake M=7.6 - July 27	YES	7.6	24.6	59	14.3	0.293	0.80	73.1	20
39	1976 Tangshan earthquake M=7.6 - July 27	NO	7.6	32.7	75	12.4	0.189	0.69	84.3	10
40	1976 Tangshan earthquake M=7.6 - July 27	YES	7.6	15	67	18.0	0.128	0.73	57.1	20
41	1977 Argentina earthquake M=7.4 - Nov 23	YES	7.5	10.7	106	17.6	0.101	0.70	48.2	20
42	1977 Argentina earthquake M=7.4 - Nov 23	YES	7.5	7.6	156	17.6	0.071	0.63	40.6	5
43	1977 Argentina earthquake M=7.4 - Nov 23	NO	7.5	14.3	39	17.6	0.117	0.71	55.8	4
44	1977 Argentina earthquake M=7.4 - Nov 23	NO	7.5	13.6	44	17.6	0.062	0.55	54.4	3
45	1977 Argentina earthquake M=7.4 - Nov 23	YES	7.5	11.4	56	17.6	0.251	0.86	49.8	50
46	1978 Miyagiken-Oki earthquake M=6.5 - Feb 20	NO	6.5	12.8	67	18.5	0.031	0.34	52.8	0
47	1978 Miyagiken-Oki earthquake M=6.5 - Feb 20	NO	6.5	15.5	71	16.1	0.039	0.36	58.0	20
48	1978 Miyagiken-Oki earthquake M=6.5 - Feb 20	NO	6.5	6.7	45	17.1	0.056	0.56	38.2	10
49	1978 Miyagiken-Oki earthquake M=6.5 - Feb 20	NO	6.5	12.3	59	16.1	0.023	0.23	51.7	5
50	1978 Miyagiken-Oki earthquake M=6.5 - Feb 20	NO	6.5	14.1	79	16.1	0.033	0.32	55.4	3
51	1978 Miyagiken-Oki earthquake M=6.5 - Feb 20	YES	6.5	6.9	30	17.1	0.069	0.62	38.7	5
52	1978 Miyagiken-Oki earthquake M=6.5 - Feb 20	NO	6.5	9.6	42	17.1	0.040	0.43	45.7	4
53	1978 Miyagiken-Oki earthquake M=6.5 - Feb 20	NO	6.5	9.4	85	16.1	0.039	0.41	45.2	5
54	1978 Miyagiken-Oki earthquake M=6.5 - Feb 20	NO	6.5	8.6	60	16.1	0.043	0.45	43.2	10
55	1978 Miyagiken-Oki earthquake M=6.5 - Feb 20	NO	6.5	6.5	56	17.1	0.057	0.57	37.6	10
56	1978 Miyagiken-Oki earthquake M=6.5 - Feb 20	NO	6.5	16.3	34	17.1	0.023	0.22	59.5	7
57	1978 Miyagiken-Oki earthquake M=6.5 - Feb 20	NO	6.5	13.9	42	17.1	0.058	0.52	55.0	12
58	1978 Miyagiken-Oki earthquake M=6.5 - Feb 20	NO	6.5	8.1	63	17.1	0.125	0.75	42.0	60
59	1978 Miyagiken-Oki earthquake M=6.5 - Feb 20	NO	6.5	15.1	47	17.1	0.037	0.37	57.3	0
60	1978 Miyagiken-Oki earthquake M=7.7 - June 12	YES	7.7	12.8	67	18.4	0.129	0.75	52.8	0
61	1978 Miyagiken-Oki earthquake M=7.7 - June 12	YES	7.7	15.5	71	17.1	0.118	0.69	58.0	20
62	1978 Miyagiken-Oki earthquake M=7.7 - June 12	YES	7.7	6.7	45	18.4	0.203	0.85	38.2	10
63	1978 Miyagiken-Oki earthquake M=7.7 - June 12	NO	7.7	22	57	18.4	0.061	0.49	69.2	10
64	1978 Miyagiken-Oki earthquake M=7.7 - June 12	YES	7.7	12.3	59	16.1	0.087	0.63	51.7	5
65	1978 Miyagiken-Oki earthquake M=7.7 - June 12	NO	7.7	17.6	73	16.1	0.089	0.60	61.9	0
66	1978 Miyagiken-Oki earthquake M=7.7 - June 12	NO	7.7	17.8	65	17.1	0.100	0.64	62.2	26
67	1978 Miyagiken-Oki earthquake M=7.7 - June 12	YES	7.7	14.1	79	17.1	0.103	0.67	55.4	3
68	1978 Miyagiken-Oki earthquake M=7.7 - June 12	NO	7.7	26.2	39	15.2	0.180	0.72	75.5	4
69	1978 Miyagiken-Oki earthquake M=7.7 - June 12	YES	7.7	6.9	30	15.2	3.000	0.99	38.7	5
70	1978 Miyagiken-Oki earthquake M=7.7 - June 12	YES	7.7	9.6	42	15.2	0.688	0.94	45.7	4
71	1978 Miyagiken-Oki earthquake M=7.7 - June 12	YES	7.7	9.4	85	17.1	0.106	0.71	45.2	5
72	1978 Miyagiken-Oki earthquake M=7.7 - June 12	YES	7.7	8.6	60	17.1	0.137	0.77	43.2	10

73	1978 Miyagiken-Oki earthquake M=7.7 - June 12	YES	7.7	6.5	56	17.1	0.334	0.90	37.6	10
74	1978 Miyagiken-Oki earthquake M=7.7 - June 12	YES	7.7	16.3	34	17.1	0.094	0.63	59.5	7
75	1978 Miyagiken-Oki earthquake M=7.7 - June 12	YES	7.7	13.9	42	17.1	0.448	0.91	55.0	12
76	1978 Miyagiken-Oki earthquake M=7.7 - June 12	NO	7.7	24	78	17.1	0.114	0.64	72.2	17
77	1978 Miyagiken-Oki earthquake M=7.7 - June 12	YES	7.7	8.1	63	17.1	3.000	0.99	42.0	60
78	1978 Miyagiken-Oki earthquake M=7.7 - June 12	YES	7.7	15.1	47	17.1	0.184	0.79	57.3	0
79	1978 Miyagiken-Oki earthquake M=7.7 - June 12	NO	7.7	24.6	70	17.1	0.074	0.52	73.1	0
80	1979 Imperial Valley earthquake ML=6.5 - Oct 15	NO	6.53	40	42	8.0	1.065	0.89	90.0	12
81	1979 Imperial Valley earthquake ML=6.5 - Oct 15	YES	6.53	7	50	8.0	3.000	0.97	39.0	18
82	1979 Imperial Valley earthquake ML=6.5 - Oct 15	NO	6.53	21.2	56	8.0	3.000	0.96	67.9	25
83	1979 Imperial Valley earthquake ML=6.5 - Oct 15	NO	6.53	11.7	62	16.7	0.043	0.44	50.4	92
84	1979 Imperial Valley earthquake ML=6.5 - Oct 15	YES	6.53	10	32	9.6	3.000	0.98	46.6	31
85	1979 Imperial Valley earthquake ML=6.5 - Oct 15	YES	6.53	8.5	50	14.0	0.242	0.83	43.0	64
86	1979 Imperial Valley earthquake ML=6.5 - Oct 15	NO	6.53	20.6	38	14.0	0.038	0.29	66.9	30
87	1979 Imperial Valley earthquake ML=6.5 - Oct 15	YES	6.53	10.2	20	13.0	3.000	0.98	47.1	80
88	1979 Imperial Valley earthquake ML=6.5 - Oct 15	NO	6.53	15.7	54	15.0	0.079	0.56	58.4	30
89	1980 Mid-Chiba earthquake M=6.0 - Sept 24 (UTC)	NO	6	9.6	57	16.8	0.046	0.47	45.7	13
90	1980 Mid-Chiba earthquake M=6.0 - Sept 24 (UTC)	NO	6	9.1	123	16.8	0.045	0.47	44.5	27
91	1981 WestMorland earthquake M=5.9 - April 26	YES	5.9	11.7	62	10.0	0.277	0.79	50.4	92
92	1981 WestMorland earthquake M=5.9 - April 26	NO	5.9	10	32	16.8	0.025	0.27	46.6	31
93	1981 WestMorland earthquake M=5.9 - April 26	YES	5.9	8.5	50	12.1	0.212	0.79	43.0	64
94	1981 WestMorland earthquake M=5.9 - April 26	NO	5.9	20.6	38	12.1	0.036	0.25	66.9	30
95	1981 WestMorland earthquake M=5.9 - April 26	NO	5.9	10.2	20	11.9	0.658	0.92	47.1	80
96	1981 WestMorland earthquake M=5.9 - April 26	NO	5.9	19.3	45	11.9	0.099	0.54	64.8	18
97	1981 WestMorland earthquake M=5.9 - April 26	YES	5.9	15.7	54	10.9	0.194	0.71	58.4	30
98	1982 Urakawa-Oki earthquake M=6.9 - Mar 21	NO	6.9	17	35	16.4	0.033	0.31	60.8	5
99	1983 Nihonkai-Chubu earthquake M=6.8 - June 21	NO	6.8	5.1	37	16.8	0.346	0.91	33.3	5
100	1983 Nihonkai-Chubu earthquake M=6.8 - June 21	NO	6.8	18.1	77	16.8	0.064	0.51	62.7	0
101	1983 Nihonkai-Chubu earthquake M=6.8 - June 21	YES	6.8	13.3	42	19.0	0.047	0.48	53.8	0
102	1983 Nihonkai-Chubu earthquake M=7.7 - May 26	YES	7.7	16.5	38	23.0	0.097	0.71	59.9	3
103	1983 Nihonkai-Chubu earthquake M=7.7 - May 26	YES	7.7	5.1	37	18.4	3.000	0.99	33.3	5
104	1983 Nihonkai-Chubu earthquake M=7.7 - May 26	YES	7.7	12.4	53	17.5	0.832	0.95	51.9	1
105	1983 Nihonkai-Chubu earthquake M=7.7 - May 26	YES	7.7	16.2	38	16.8	0.152	0.74	59.3	1
106	1983 Nihonkai-Chubu earthquake M=7.7 - May 26	YES	7.7	13.3	42	16.0	0.768	0.94	53.8	0
107	1983 Nihonkai-Chubu earthquake M=7.7 - May 26	NO	7.7	18.7	41	18.2	0.050	0.45	63.8	3
108	1983 Nihonkai-Chubu earthquake M=7.7 - May 26	NO	7.7	13.8	41	18.2	0.068	0.58	54.8	3
109	1983 Nihonkai-Chubu earthquake M=7.7 - May 26	NO	7.7	13.1	41	23.0	0.034	0.42	53.4	5
110	1983 Nihonkai-Chubu earthquake M=7.7 - May 26	YES	7.7	8.7	79	18.2	0.140	0.78	43.5	3
111	1983 Nihonkai-Chubu earthquake M=7.7 - May 26	YES	7.7	6.9	107	18.2	0.160	0.82	38.7	4

112	1983 Nihonkai-Chubu earthquake M=7.7 - May 26	NO	7.7	9.8	54	31.9	0.020	0.33	46.2	66
113	1983 Nihonkai-Chubu earthquake M=7.7 - May 26	YES	7.7	10.4	74	18.2	0.130	0.76	47.5	8
114	1983 Nihonkai-Chubu earthquake M=7.7 - May 26	YES	7.7	13.5	81	18.2	0.097	0.68	54.2	3
115	1983 Nihonkai-Chubu earthquake M=7.7 - May 26	YES	7.7	9.4	48	18.2	0.122	0.75	45.2	7
116	1983 Nihonkai-Chubu earthquake M=7.7 - May 26	YES	7.7	10.2	71	18.2	0.122	0.75	47.1	2
117	1983 Nihonkai-Chubu earthquake M=7.7 - May 26	YES	7.7	11.5	68	18.2	0.112	0.72	50.0	2
118	1983 Nihonkai-Chubu earthquake M=7.7 - May 26	NO	7.7	18.9	47	18.2	0.072	0.56	64.1	3
119	1983 Nihonkai-Chubu earthquake M=7.7 - May 26	NO	7.7	23.5	42	18.2	0.057	0.46	71.5	2
120	1983 Nihonkai-Chubu earthquake M=7.7 - May 26	NO	7.7	23	34	18.2	0.052	0.43	70.7	1
121	1983 Nihonkai-Chubu earthquake M=7.7 - May 26	NO	7.7	34.6	60	18.2	0.050	0.42	86.7	3
122	1983 Nihonkai-Chubu earthquake M=7.7 - May 26	NO	7.7	37.3	31	18.2	0.030	0.26	90.0	1
123	1983 Nihonkai-Chubu earthquake M=7.7 - May 26	NO	7.7	20.3	53	18.2	0.075	0.56	66.4	2
124	1983 Nihonkai-Chubu earthquake M=7.7 - May 26	YES	7.7	5.4	56	18.2	0.385	0.92	34.3	2
125	1983 Nihonkai-Chubu earthquake M=7.7 - May 26	YES	7.7	7.4	63	18.2	0.186	0.84	40.1	2
126	1983 Nihonkai-Chubu earthquake M=7.7 - May 26	YES	7.7	5.6	64	18.2	0.241	0.88	34.9	2
127	1983 Nihonkai-Chubu earthquake M=7.7 - May 26	YES	7.7	8.1	49	18.2	0.141	0.79	42.0	2
128	1983 Nihonkai-Chubu earthquake M=7.7 - May 26	NO	7.7	23.5	55	18.2	0.063	0.49	71.5	2
129	1983 Nihonkai-Chubu earthquake M=7.7 - May 26	NO	7.7	22.5	77	18.2	0.066	0.50	69.9	4
130	1983 Nihonkai-Chubu earthquake M=7.7 - May 26	NO	7.7	25.9	46	18.2	0.048	0.41	75.0	0
131	1984 earthquake M=6.9 - Aug 7	NO	6.9	17.6	45	13.6	0.106	0.60	61.9	36
132	1987 Superstition Hills earthquakes M=6.2 and M=6.5 - 01 & 02 - Nov 24	NO	6.22	8.5	50	18.1	0.042	0.47	43.0	64
133	1987 Superstition Hills earthquakes M=6.2 and M=6.5 - 01 & 02 - Nov 24	NO	6.22	15.7	54	15.4	0.050	0.43	58.4	30
134	1987 Superstition Hills earthquakes M=6.2 and M=6.5 - 01 & 02 - Nov 24	NO	6.54	40	42	15.5	0.017	0.10	90.0	12
135	1987 Superstition Hills earthquakes M=6.2 and M=6.5 - 01 & 02 - Nov 24	NO	6.54	7	50	15.8	0.139	0.77	39.0	18
136	1987 Superstition Hills earthquakes M=6.2 and M=6.5 - 01 & 02 - Nov 24	NO	6.54	21.2	56	16.8	0.025	0.21	67.9	25
137	1987 Superstition Hills earthquakes M=6.2 and M=6.5 - 01 & 02 - Nov 24	NO	6.54	11.7	62	14.9	0.076	0.58	50.4	92
138	1987 Superstition Hills earthquakes M=6.2 and M=6.5 - 01 & 02 - Nov 24	NO	6.54	10	32	15.4	0.078	0.61	46.6	31
139	1987 Superstition Hills earthquakes M=6.2 and M=6.5 - 01 & 02 - Nov 24	NO	6.54	8.5	50	14.0	0.221	0.82	43.0	64
140	1987 Superstition Hills earthquakes M=6.2 and M=6.5 - 01 & 02 - Nov 24	NO	6.54	20.6	38	14.7	0.030	0.24	66.9	30
141	1987 Superstition Hills earthquakes M=6.2 and M=6.5 - 01 & 02 - Nov 24	NO	6.54	10.2	20	14.3	0.420	0.90	47.1	80
142	1987 Superstition Hills earthquakes M=6.2 and M=6.5 - 01 & 02 - Nov 24	NO	6.54	19.3	45	14.3	0.089	0.56	64.8	18
143	1987 Superstition Hills earthquakes M=6.2 and M=6.5 - 01 & 02 - Nov 24	YES	6.54	15.7	54	13.9	0.118	0.65	58.4	30
144	1989 Loma Prieta earthquake M=6.9 - Oct 18	NO	6.93	43.4	91	14.3	0.045	0.34	90.0	7
145	1989 Loma Prieta earthquake M=6.9 - Oct 18	YES	6.93	10.6	92	12.0	0.176	0.74	48.0	8
146	1989 Loma Prieta earthquake M=6.9 - Oct 18	NO	6.93	21.4	35	13.4	0.079	0.49	68.2	5
147	1989 Loma Prieta earthquake M=6.9 - Oct 18	NO	6.93	11	64	17.8	0.050	0.50	48.9	30
148	1989 Loma Prieta earthquake M=6.9 - Oct 18	YES	6.93	13.1	65	13.4	0.129	0.68	53.4	3
149	1989 Loma Prieta earthquake M=6.9 - Oct 18	YES	6.93	14.9	55	13.4	0.088	0.57	56.9	3
150	1989 Loma Prieta earthquake M=6.9 - Oct 18	YES	6.93	17.6	64	13.4	0.139	0.67	61.9	3

151	1989 Loma Prieta earthquake M=6.9 - Oct 18	NO	6.93	22.6	35	13.4	0.047	0.33	70.1	1
152	1989 Loma Prieta earthquake M=6.9 - Oct 18	NO	6.93	14.9	47	13.4	0.122	0.65	56.9	1
153	1989 Loma Prieta earthquake M=6.9 - Oct 18	NO	6.93	21.2	48	13.4	0.084	0.51	67.9	5
154	1989 Loma Prieta earthquake M=6.9 - Oct 18	NO	6.93	14.7	48	13.4	0.112	0.63	56.5	4
155	1989 Loma Prieta earthquake M=6.9 - Oct 18	YES	6.93	15.3	101	11.7	0.180	0.71	57.7	32
156	1989 Loma Prieta earthquake M=6.9 - Oct 18	YES	6.93	23.4	108	11.7	0.107	0.53	71.3	13
157	1989 Loma Prieta earthquake M=6.9 - Oct 18	YES	6.93	14.9	95	11.7	0.206	0.74	56.9	25
158	1989 Loma Prieta earthquake M=6.9 - Oct 18	NO	6.93	24.6	105	11.7	0.162	0.64	73.1	20
159	1989 Loma Prieta earthquake M=6.9 - Oct 18	YES	6.93	15.4	89	13.4	0.108	0.62	57.9	3
160	1989 Loma Prieta earthquake M=6.9 - Oct 18	YES	6.93	17	89	13.4	0.100	0.59	60.8	3
161	1989 Loma Prieta earthquake M=6.9 - Oct 18	YES	6.93	10.7	73	16.1	0.143	0.75	48.2	50
162	1989 Loma Prieta earthquake M=6.9 - Oct 18	YES	6.93	15.3	43	13.4	0.118	0.64	57.7	2
163	1989 Loma Prieta earthquake M=6.9 - Oct 18	NO	6.93	34.4	73	13.4	0.076	0.47	86.5	5
164	1989 Loma Prieta earthquake M=6.9 - Oct 18	YES	6.93	9	86	13.6	0.179	0.78	44.2	8
165	1989 Loma Prieta earthquake M=6.9 - Oct 18	YES	6.93	10.3	46	13.4	0.189	0.78	47.3	1
166	1989 Loma Prieta earthquake M=6.9 - Oct 18	YES	6.93	18.4	67	13.4	0.093	0.56	63.2	1
167	1989 Loma Prieta earthquake M=6.9 - Oct 18	YES	6.93	10.8	67	16.9	0.142	0.76	48.5	20
168	1989 Loma Prieta earthquake M=6.9 - Oct 18	YES	6.93	14.6	25	13.4	0.223	0.78	56.3	35
169	1990 Luzon earthquake M=7.7 - July 16	NO	7.7	29.2	68	16.8	0.068	0.49	79.7	19
170	1990 Luzon earthquake M=7.7 - July 16	YES	7.7	17.3	90	16.8	0.118	0.68	61.3	19
171	1993 Kushiro-Oki earthquake M=7.6 - Jan 15	YES	7.6	16.4	68	13.6	0.332	0.84	59.7	2
172	1993 Kushiro-Oki earthquake M=7.6 - Jan 15	NO	7.6	30.9	118	13.6	0.190	0.71	82.0	0
173	1993 Kushiro-Oki earthquake M=7.6 - Jan 15	YES	7.6	25.9	47	12.7	0.420	0.84	75.0	5
174	1994 Northridge earthquake M=6.7 - Jan 17	YES	6.69	18.7	143	8.1	0.875	0.89	63.8	50
175	1994 Northridge earthquake M=6.7 - Jan 17	NO	6.69	32.3	101	9.9	0.293	0.74	83.8	25
176	1994 Northridge earthquake M=6.7 - Jan 17	YES	6.69	14.1	88	10.6	0.881	0.92	55.4	64
177	1994 Northridge earthquake M=6.7 - Jan 17	YES	6.69	17	105	9.9	0.353	0.80	60.8	33
178	1995 Hyogoken-Nambu (Kobe) earthquake M=6.9 - Jan 16	NO	6.9	50	80	11.5	0.084	0.46	90.0	3
179	1995 Hyogoken-Nambu (Kobe) earthquake M=6.9 - Jan 16	NO	6.9	42.7	103	11.5	0.103	0.52	90.0	15
180	1995 Hyogoken-Nambu (Kobe) earthquake M=6.9 - Jan 16	NO	6.9	49.8	77	11.5	0.091	0.48	90.0	3
181	1995 Hyogoken-Nambu (Kobe) earthquake M=6.9 - Jan 16	NO	6.9	36.6	54	11.5	0.139	0.60	89.2	1
182	1995 Hyogoken-Nambu (Kobe) earthquake M=6.9 - Jan 16	YES	6.9	6.1	116	12.2	0.354	0.87	36.4	1
183	1995 Hyogoken-Nambu (Kobe) earthquake M=6.9 - Jan 16	NO	6.9	22.5	72	11.5	0.278	0.76	69.9	21
184	1995 Hyogoken-Nambu (Kobe) earthquake M=6.9 - Jan 16	YES	6.9	10.9	60	11.5	0.183	0.74	48.7	0
185	1995 Hyogoken-Nambu (Kobe) earthquake M=6.9 - Jan 16	YES	6.9	24.1	65	10.5	0.332	0.77	72.4	0
186	1995 Hyogoken-Nambu (Kobe) earthquake M=6.9 - Jan 16	YES	6.9	12.2	64	10.5	0.820	0.92	51.5	2
187	1995 Hyogoken-Nambu (Kobe) earthquake M=6.9 - Jan 16	NO	6.9	28	107	9.8	0.276	0.72	78.0	9
188	1995 Hyogoken-Nambu (Kobe) earthquake M=6.9 - Jan 16	YES	6.9	8.5	62	10.5	3.000	0.98	43.0	5
189	1995 Hyogoken-Nambu (Kobe) earthquake M=6.9 - Jan 16	NO	6.9	27.6	72	10.5	0.276	0.74	77.5	14

190	1995 Hyogoken-Nambu (Kobe) earthquake M=6.9 - Jan 16	YES	6.9	16	74	10.5	2.305	0.97	59.0	15
191	1995 Hyogoken-Nambu (Kobe) earthquake M=6.9 - Jan 16	NO	6.9	24.5	69	10.5	0.289	0.75	73.0	19
192	1995 Hyogoken-Nambu (Kobe) earthquake M=6.9 - Jan 16	YES	6.9	19.2	82	10.5	0.263	0.75	64.6	5
193	1995 Hyogoken-Nambu (Kobe) earthquake M=6.9 - Jan 16	NO	6.9	25	60	9.8	0.660	0.86	73.7	5
194	1995 Hyogoken-Nambu (Kobe) earthquake M=6.9 - Jan 16	YES	6.9	21.1	43	10.5	3.000	0.97	67.7	5
195	1995 Hyogoken-Nambu (Kobe) earthquake M=6.9 - Jan 16	NO	6.9	42.6	171	9.2	0.156	0.57	90.0	0
196	1995 Hyogoken-Nambu (Kobe) earthquake M=6.9 - Jan 16	NO	6.9	22.5	124	9.8	0.210	0.66	69.9	10
197	1995 Hyogoken-Nambu (Kobe) earthquake M=6.9 - Jan 16	NO	6.9	50	75	10.1	0.180	0.63	90.0	0
198	1995 Hyogoken-Nambu (Kobe) earthquake M=6.9 - Jan 16	NO	6.9	33.5	44	9.8	0.671	0.87	85.3	0
199	1995 Hyogoken-Nambu (Kobe) earthquake M=6.9 - Jan 16	NO	6.9	38.6	79	9.8	0.327	0.76	90.0	6
200	1995 Hyogoken-Nambu (Kobe) earthquake M=6.9 - Jan 16	NO	6.9	25.1	72	9.8	0.515	0.83	73.9	10
201	1995 Hyogoken-Nambu (Kobe) earthquake M=6.9 - Jan 16	YES	6.9	24.6	51	10.5	0.274	0.74	73.1	0
202	1995 Hyogoken-Nambu (Kobe) earthquake M=6.9 - Jan 16	NO	6.9	35.8	50	9.2	0.708	0.86	88.2	3
203	1995 Hyogoken-Nambu (Kobe) earthquake M=6.9 - Jan 16	NO	6.9	37	37	9.8	3.000	0.97	89.7	0
204	1995 Hyogoken-Nambu (Kobe) earthquake M=6.9 - Jan 16	NO	6.9	42	29	9.8	1.769	0.94	90.0	10
205	1995 Hyogoken-Nambu (Kobe) earthquake M=6.9 - Jan 16	YES	6.9	21.4	44	11.5	0.268	0.75	68.2	8
206	1995 Hyogoken-Nambu (Kobe) earthquake M=6.9 - Jan 16	YES	6.9	17.9	49	11.5	0.281	0.78	62.4	0
207	1995 Hyogoken-Nambu (Kobe) earthquake M=6.9 - Jan 16	NO	6.9	41.3	78	9.8	1.367	0.93	90.0	10
208	1995 Hyogoken-Nambu (Kobe) earthquake M=6.9 - Jan 16	NO	6.9	49.7	46	9.8	0.748	0.88	90.0	0
209	1995 Hyogoken-Nambu (Kobe) earthquake M=6.9 - Jan 16	NO	6.9	29.2	41	10.5	0.572	0.86	79.7	6
210	1995 Hyogoken-Nambu (Kobe) earthquake M=6.9 - Jan 16	NO	6.9	33.5	83	10.5	0.495	0.84	85.3	50
211	1995 Hyogoken-Nambu (Kobe) earthquake M=6.9 - Jan 16	YES	6.9	25	73	11.5	0.292	0.76	73.7	9
212	1995 Hyogoken-Nambu (Kobe) earthquake M=6.9 - Jan 16	YES	6.9	18.9	55	10.5	0.877	0.91	64.1	6
213	1995 Hyogoken-Nambu (Kobe) earthquake M=6.9 - Jan 16	NO	6.9	31.6	36	9.8	3.000	0.97	82.9	3
214	1995 Hyogoken-Nambu (Kobe) earthquake M=6.9 - Jan 16	YES	6.9	19.3	79	12.2	0.101	0.55	64.8	0
215	1995 Hyogoken-Nambu (Kobe) earthquake M=6.9 - Jan 16	YES	6.9	19.1	94	10.5	0.494	0.85	64.4	5
216	1995 Hyogoken-Nambu (Kobe) earthquake M=6.9 - Jan 16	NO	6.9	50	66	9.8	0.169	0.61	90.0	0
217	1995 Hyogoken-Nambu (Kobe) earthquake M=6.9 - Jan 16	NO	6.9	39.7	59	9.8	0.163	0.60	90.0	0
218	1995 Hyogoken-Nambu (Kobe) earthquake M=6.9 - Jan 16	YES	6.9	15	50	11.5	0.557	0.89	57.1	0
219	1995 Hyogoken-Nambu (Kobe) earthquake M=6.9 - Jan 16	YES	6.9	13.2	46	11.5	3.000	0.98	53.6	10
220	1995 Hyogoken-Nambu (Kobe) earthquake M=6.9 - Jan 16	YES	6.9	19.6	55	12.2	0.294	0.79	65.3	20
221	1995 Hyogoken-Nambu (Kobe) earthquake M=6.9 - Jan 16	YES	6.9	8.3	43	11.5	3.000	0.98	42.5	5
222	1995 Hyogoken-Nambu (Kobe) earthquake M=6.9 - Jan 16	NO	6.9	25.2	80	11.5	0.134	0.59	74.0	18
223	1995 Hyogoken-Nambu (Kobe) earthquake M=6.9 - Jan 16	YES	6.9	12.5	115	11.5	0.239	0.78	52.1	2
224	1995 Hyogoken-Nambu (Kobe) earthquake M=6.9 - Jan 16	YES	6.9	11.3	96	12.3	0.412	0.87	49.6	20
225	1995 Hyogoken-Nambu (Kobe) earthquake M=6.9 - Jan 16	NO	6.9	27.2	125	11.5	0.113	0.54	76.9	20
226	1995 Hyogoken-Nambu (Kobe) earthquake M=6.9 - Jan 16	NO	6.9	24	140	11.5	0.128	0.58	72.2	20
227	1995 Hyogoken-Nambu (Kobe) earthquake M=6.9 - Jan 16	NO	6.9	39.1	135	11.5	0.088	0.47	90.0	20
228	1995 Hyogoken-Nambu (Kobe) earthquake M=6.9 - Jan 16	YES	6.9	15.3	123	12.3	0.201	0.75	57.7	20

229	1995 Hyogoken-Nambu (Kobe) earthquake M=6.9 - Jan 16	YES	6.9	21.9	107	11.5	0.159	0.64	69.0	25
230	1995 Hyogoken-Nambu (Kobe) earthquake M=6.9 - Jan 16	YES	6.9	16.8	146	12.3	0.145	0.66	60.4	20
231	1995 Hyogoken-Nambu (Kobe) earthquake M=6.9 - Jan 16	YES	6.9	18.5	46	13.9	0.280	0.81	63.4	20

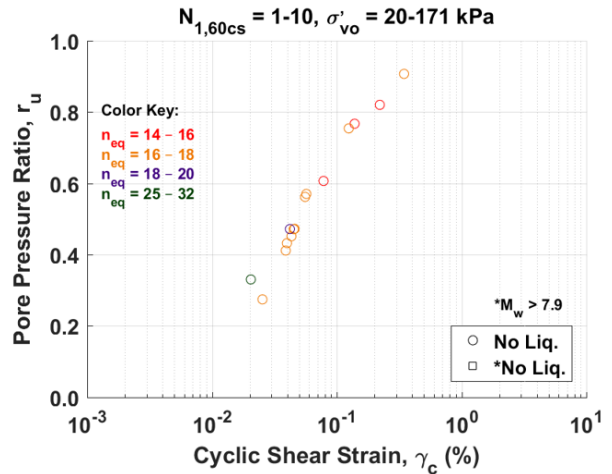
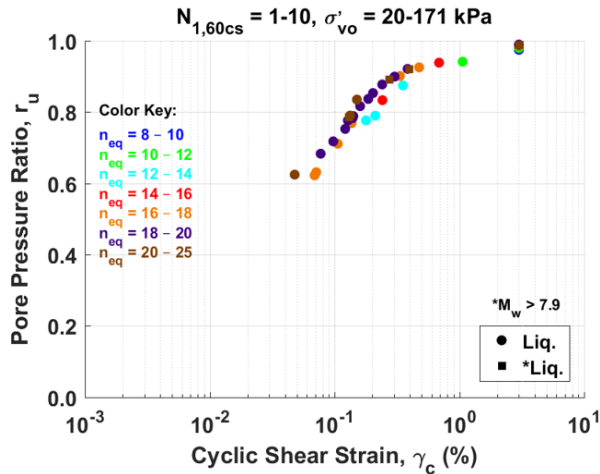


Figure D6. Excess porewater pressure buildup using the Vucetic and Dobry (1986) model with the Boulanger et al. database all cases

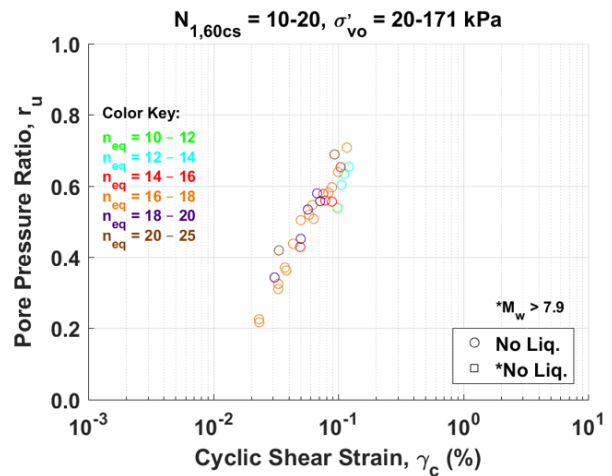
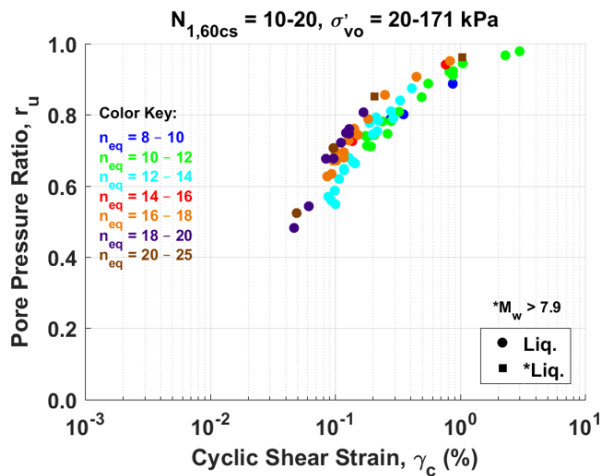


Figure D7. Excess porewater pressure buildup using the Vucetic and Dobry (1986) model with the Boulanger et al. database all cases

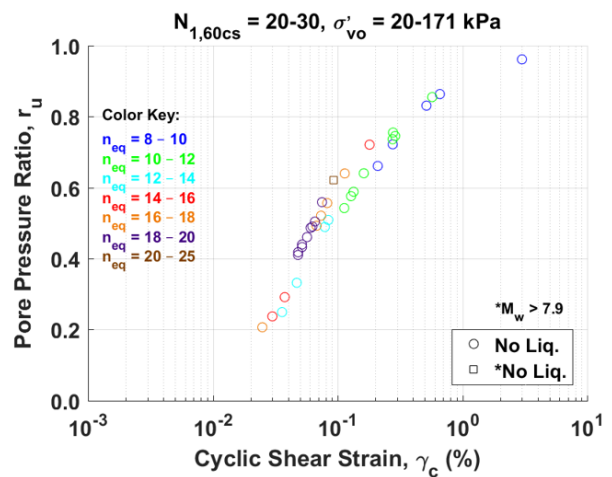
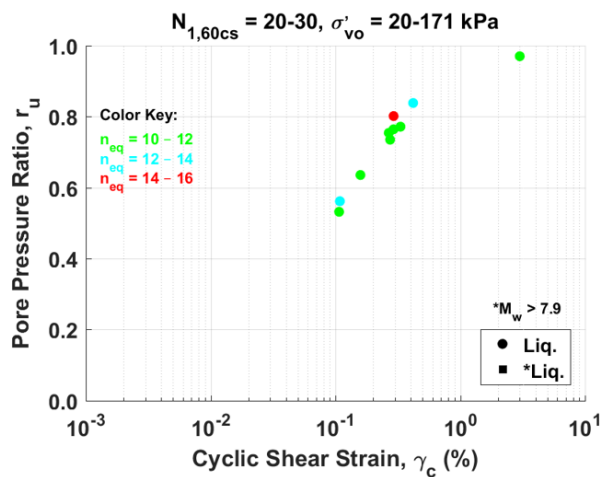


Figure D8. Excess porewater pressure buildup using the Vucetic and Dobry (1986) model with the Boulanger et al. database all cases

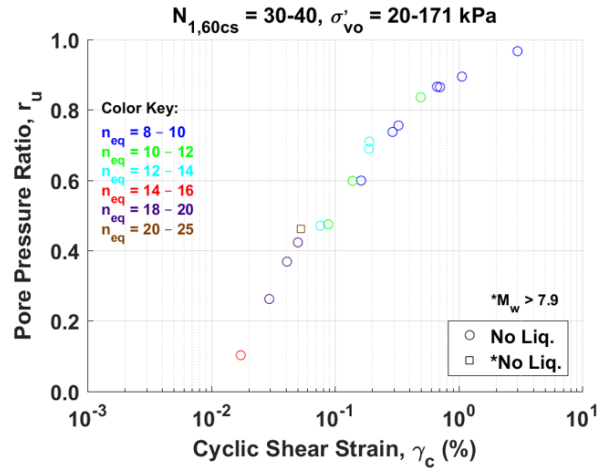


Figure D9. Excess porewater pressure buildup using the Vucetic and Dobry (1986) model with the Boulanger et al. database all cases

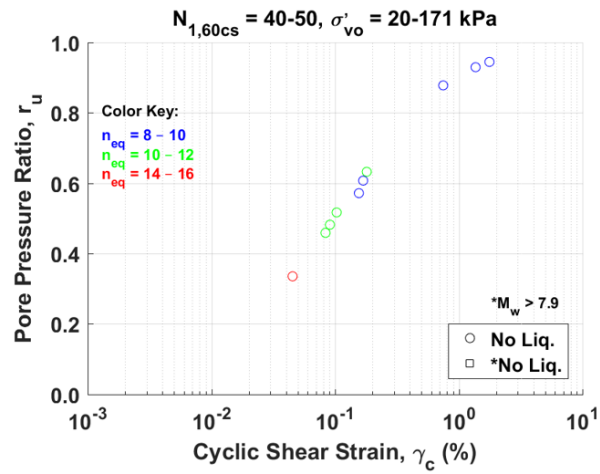


Figure D10. Excess porewater pressure buildup using the Vucetic and Dobry (1986) model with the Boulanger et al. database all cases

Cases in the Boulanger et al. database with $FC \leq 5\%$ (116 cases)

Byrne model

Table D3. Parameters needed to plot figures of excess pore pressure ratio versus cyclic shear strain for the Boulanger et al. (2012) database (cases with FC ≤ 5%) using the Byrne (1991) model

Data Point #	Year Event	Liquefied? YES/NO	M _w	N _{1,60cs} blows	σ' _v (kPa)	Lasley n _{eq}	γ _c (%)	Byrne r _u	D _r (%)	FC
5	1948 Fukui earthquake M=7.3 - June 28	YES	7	11.8	48	11.8	1.057	1.00	50.6	0
6	1948 Fukui earthquake M=7.3 - June 28	YES	7	21.1	104	12.4	0.114	0.92	67.7	4
7	1964 Niigata earthquake M=7.6 - June 16	YES	7.6	4.7	41	24.9	0.053	1.00	32.0	5
8	1964 Niigata earthquake M=7.6 - June 16	YES	7.6	9.9	72	19.7	0.103	1.00	46.4	2
10	1964 Niigata earthquake M=7.6 - June 16	YES	7.6	6.8	53	19.6	0.082	1.00	38.4	5
11	1964 Niigata earthquake M=7.6 - June 16	NO	7.6	22.7	81	18.8	0.053	0.60	70.2	2
12	1964 Niigata earthquake M=7.6 - June 16	NO	7.6	23.5	109	18.8	0.057	0.55	71.5	2
13	1964 Niigata earthquake M=7.6 - June 16	YES	7.6	11	100	19.7	0.090	1.00	48.9	2
14	1964 Niigata earthquake M=7.6 - June 16	YES	7.6	17.5	100	19.7	0.067	0.86	61.7	2
15	1964 Niigata earthquake M=7.6 - June 16	YES	7.6	9.4	47	19.7	0.133	1.00	45.2	0
16	1964 Niigata earthquake M=7.6 - June 16	NO	7.6	14.1	79	18.8	0.062	0.97	55.4	0
18	1964 Niigata earthquake M=7.6 - June 16	NO	7.6	35.5	67	18.8	0.046	0.35	87.8	0
20	1968 Tokachi-Oki earthquake M=8.3 - May 16	YES	8.3	16.5	38	20.6	1.051	1.00	59.9	3
21	1968 Tokachi-Oki earthquake M=8.3 - May 16	NO	8.3	35.3	76	20.0	0.058	0.44	87.6	5
22	1968 Tokachi-Oki earthquake M=8.3 - May 16	NO	8.3	23	45	20.0	0.097	1.00	70.7	5
23	1968 Tokachi-Oki earthquake M=8.3 - May 16	YES	8.3	9.1	42	20.0	0.402	1.00	44.5	5
30	1975 Haicheng earthquake M=7.0 - Feb 4	YES	7	11	92	13.3	0.218	1.00	48.9	5
31	1976 Guatemala earthquake M=7.5 - Feb 4	YES	7.5	5	86	20.6	0.156	1.00	33.0	3
32	1976 Guatemala earthquake M=7.5 - Feb 4	YES	7.5	9.7	34	20.6	0.138	1.00	45.9	3
33	1976 Guatemala earthquake M=7.5 - Feb 4	NO	7.5	14.3	71	20.6	0.098	1.00	55.8	3
36	1976 Tangshan earthquake M=7.6 - July 27	NO	7.6	24.4	38	17.3	0.088	0.98	72.8	5
37	1976 Tangshan earthquake M=7.6 - July 27	YES	7.6	8.5	32	17.3	0.481	1.00	43.0	3
42	1977 Argentina earthquake M=7.4 - Nov 23	YES	7.5	7.6	156	17.6	0.076	1.00	40.6	5
43	1977 Argentina earthquake M=7.4 - Nov 23	NO	7.5	14.3	39	17.6	0.122	1.00	55.8	4
44	1977 Argentina earthquake M=7.4 - Nov 23	NO	7.5	13.6	44	17.6	0.067	1.00	54.4	3
46	1978 Miyagiken-Oki earthquake M=6.5 - Feb 20	NO	6.5	12.8	67	18.5	0.036	0.75	52.8	0
49	1978 Miyagiken-Oki earthquake M=6.5 - Feb 20	NO	6.5	12.3	59	16.1	0.028	0.60	51.7	5
50	1978 Miyagiken-Oki earthquake M=6.5 - Feb 20	NO	6.5	14.1	79	16.1	0.038	0.66	55.4	3
51	1978 Miyagiken-Oki earthquake M=6.5 - Feb 20	YES	6.5	6.9	30	17.1	0.074	1.00	38.7	5
52	1978 Miyagiken-Oki earthquake M=6.5 - Feb 20	NO	6.5	9.6	42	17.1	0.045	1.00	45.7	4
53	1978 Miyagiken-Oki earthquake M=6.5 - Feb 20	NO	6.5	9.4	85	16.1	0.044	0.97	45.2	5
59	1978 Miyagiken-Oki earthquake M=6.5 - Feb 20	NO	6.5	15.1	47	17.1	0.042	0.83	57.3	0

60	1978 Miyagiken-Oki earthquake M=7.7 - June 12	YES	7.7	12.8	67	18.4	0.134	1.00	52.8	0
64	1978 Miyagiken-Oki earthquake M=7.7 - June 12	YES	7.7	12.3	59	16.1	0.092	1.00	51.7	5
65	1978 Miyagiken-Oki earthquake M=7.7 - June 12	NO	7.7	17.6	73	16.1	0.094	1.00	61.9	0
67	1978 Miyagiken-Oki earthquake M=7.7 - June 12	YES	7.7	14.1	79	17.1	0.108	1.00	55.4	3
68	1978 Miyagiken-Oki earthquake M=7.7 - June 12	NO	7.7	26.2	39	15.2	0.185	1.00	75.5	4
69	1978 Miyagiken-Oki earthquake M=7.7 - June 12	YES	7.7	6.9	30	15.2	3.005	1.00	38.7	5
70	1978 Miyagiken-Oki earthquake M=7.7 - June 12	YES	7.7	9.6	42	15.2	0.693	1.00	45.7	4
71	1978 Miyagiken-Oki earthquake M=7.7 - June 12	YES	7.7	9.4	85	17.1	0.111	1.00	45.2	5
78	1978 Miyagiken-Oki earthquake M=7.7 - June 12	YES	7.7	15.1	47	17.1	0.189	1.00	57.3	0
79	1978 Miyagiken-Oki earthquake M=7.7 - June 12	NO	7.7	24.6	70	17.1	0.079	0.80	73.1	0
98	1982 Urakawa-Oki earthquake M=6.9 - Mar 21	NO	6.9	17	35	16.4	0.038	0.75	60.8	5
99	1983 Nihonkai-Chubu earthquake M=6.8 - June 21	NO	6.8	5.1	37	16.8	0.351	1.00	33.3	5
100	1983 Nihonkai-Chubu earthquake M=6.8 - June 21	NO	6.8	18.1	77	16.8	0.069	0.88	62.7	0
101	1983 Nihonkai-Chubu earthquake M=6.8 - June 21	YES	6.8	13.3	42	19.0	0.052	1.00	53.8	0
102	1983 Nihonkai-Chubu earthquake M=7.7 - May 26	YES	7.7	16.5	38	23.0	0.102	1.00	59.9	3
103	1983 Nihonkai-Chubu earthquake M=7.7 - May 26	YES	7.7	5.1	37	18.4	3.005	1.00	33.3	5
104	1983 Nihonkai-Chubu earthquake M=7.7 - May 26	YES	7.7	12.4	53	17.5	0.837	1.00	51.9	1
105	1983 Nihonkai-Chubu earthquake M=7.7 - May 26	YES	7.7	16.2	38	16.8	0.157	1.00	59.3	1
106	1983 Nihonkai-Chubu earthquake M=7.7 - May 26	YES	7.7	13.3	42	16.0	0.773	1.00	53.8	0
107	1983 Nihonkai-Chubu earthquake M=7.7 - May 26	NO	7.7	18.7	41	18.2	0.055	0.90	63.8	3
108	1983 Nihonkai-Chubu earthquake M=7.7 - May 26	NO	7.7	13.8	41	18.2	0.073	1.00	54.8	3
109	1983 Nihonkai-Chubu earthquake M=7.7 - May 26	NO	7.7	13.1	41	23.0	0.039	0.93	53.4	5
110	1983 Nihonkai-Chubu earthquake M=7.7 - May 26	YES	7.7	8.7	79	18.2	0.145	1.00	43.5	3
111	1983 Nihonkai-Chubu earthquake M=7.7 - May 26	YES	7.7	6.9	107	18.2	0.165	1.00	38.7	4
114	1983 Nihonkai-Chubu earthquake M=7.7 - May 26	YES	7.7	13.5	81	18.2	0.102	1.00	54.2	3
116	1983 Nihonkai-Chubu earthquake M=7.7 - May 26	YES	7.7	10.2	71	18.2	0.127	1.00	47.1	2
117	1983 Nihonkai-Chubu earthquake M=7.7 - May 26	YES	7.7	11.5	68	18.2	0.117	1.00	50.0	2
118	1983 Nihonkai-Chubu earthquake M=7.7 - May 26	NO	7.7	18.9	47	18.2	0.077	1.00	64.1	3
119	1983 Nihonkai-Chubu earthquake M=7.7 - May 26	NO	7.7	23.5	42	18.2	0.062	0.83	71.5	2
120	1983 Nihonkai-Chubu earthquake M=7.7 - May 26	NO	7.7	23	34	18.2	0.057	0.84	70.7	1
121	1983 Nihonkai-Chubu earthquake M=7.7 - May 26	NO	7.7	34.6	60	18.2	0.055	0.45	86.7	3
122	1983 Nihonkai-Chubu earthquake M=7.7 - May 26	NO	7.7	37.3	31	18.2	0.035	0.33	90.0	1
123	1983 Nihonkai-Chubu earthquake M=7.7 - May 26	NO	7.7	20.3	53	18.2	0.080	0.98	66.4	2
124	1983 Nihonkai-Chubu earthquake M=7.7 - May 26	YES	7.7	5.4	56	18.2	0.390	1.00	34.3	2
125	1983 Nihonkai-Chubu earthquake M=7.7 - May 26	YES	7.7	7.4	63	18.2	0.191	1.00	40.1	2
126	1983 Nihonkai-Chubu earthquake M=7.7 - May 26	YES	7.7	5.6	64	18.2	0.246	1.00	34.9	2
127	1983 Nihonkai-Chubu earthquake M=7.7 - May 26	YES	7.7	8.1	49	18.2	0.146	1.00	42.0	2
128	1983 Nihonkai-Chubu earthquake M=7.7 - May 26	NO	7.7	23.5	55	18.2	0.068	0.82	71.5	2
129	1983 Nihonkai-Chubu earthquake M=7.7 - May 26	NO	7.7	22.5	77	18.2	0.071	0.78	69.9	4

130	1983 Nihonkai-Chubu earthquake M=7.7 - May 26	NO	7.7	25.9	46	18.2	0.053	0.65	75.0	0
146	1989 Loma Prieta earthquake M=6.9 - Oct 18	NO	6.93	21.4	35	13.4	0.084	0.99	68.2	5
148	1989 Loma Prieta earthquake M=6.9 - Oct 18	YES	6.93	13.1	65	13.4	0.134	1.00	53.4	3
149	1989 Loma Prieta earthquake M=6.9 - Oct 18	YES	6.93	14.9	55	13.4	0.093	1.00	56.9	3
150	1989 Loma Prieta earthquake M=6.9 - Oct 18	YES	6.93	17.6	64	13.4	0.144	1.00	61.9	3
151	1989 Loma Prieta earthquake M=6.9 - Oct 18	NO	6.93	22.6	35	13.4	0.052	0.73	70.1	1
152	1989 Loma Prieta earthquake M=6.9 - Oct 18	NO	6.93	14.9	47	13.4	0.127	1.00	56.9	1
153	1989 Loma Prieta earthquake M=6.9 - Oct 18	NO	6.93	21.2	48	13.4	0.089	0.98	67.9	5
154	1989 Loma Prieta earthquake M=6.9 - Oct 18	NO	6.93	14.7	48	13.4	0.117	1.00	56.5	4
159	1989 Loma Prieta earthquake M=6.9 - Oct 18	YES	6.93	15.4	89	13.4	0.113	1.00	57.9	3
160	1989 Loma Prieta earthquake M=6.9 - Oct 18	YES	6.93	17	89	13.4	0.105	1.00	60.8	3
162	1989 Loma Prieta earthquake M=6.9 - Oct 18	YES	6.93	15.3	43	13.4	0.123	1.00	57.7	2
163	1989 Loma Prieta earthquake M=6.9 - Oct 18	NO	6.93	34.4	73	13.4	0.081	0.55	86.5	5
165	1989 Loma Prieta earthquake M=6.9 - Oct 18	YES	6.93	10.3	46	13.4	0.194	1.00	47.3	1
166	1989 Loma Prieta earthquake M=6.9 - Oct 18	YES	6.93	18.4	67	13.4	0.098	1.00	63.2	1
171	1993 Kushiro-Oki earthquake M=7.6 - Jan 15	YES	7.6	16.4	68	13.6	0.337	1.00	59.7	2
172	1993 Kushiro-Oki earthquake M=7.6 - Jan 15	NO	7.6	30.9	118	13.6	0.195	0.96	82.0	0
173	1993 Kushiro-Oki earthquake M=7.6 - Jan 15	YES	7.6	25.9	47	12.7	0.425	1.00	75.0	5
178	1995 Hyogoken-Nambu (Kobe) earthquake M=6.9 - Jan 16	NO	6.9	50	80	11.5	0.089	0.37	90.0	3
180	1995 Hyogoken-Nambu (Kobe) earthquake M=6.9 - Jan 16	NO	6.9	49.8	77	11.5	0.096	0.41	90.0	3
181	1995 Hyogoken-Nambu (Kobe) earthquake M=6.9 - Jan 16	NO	6.9	36.6	54	11.5	0.144	0.87	89.2	1
182	1995 Hyogoken-Nambu (Kobe) earthquake M=6.9 - Jan 16	YES	6.9	6.1	116	12.2	0.359	1.00	36.4	1
184	1995 Hyogoken-Nambu (Kobe) earthquake M=6.9 - Jan 16	YES	6.9	10.9	60	11.5	0.188	1.00	48.7	0
185	1995 Hyogoken-Nambu (Kobe) earthquake M=6.9 - Jan 16	YES	6.9	24.1	65	10.5	0.337	1.00	72.4	0
186	1995 Hyogoken-Nambu (Kobe) earthquake M=6.9 - Jan 16	YES	6.9	12.2	64	10.5	0.825	1.00	51.5	2
188	1995 Hyogoken-Nambu (Kobe) earthquake M=6.9 - Jan 16	YES	6.9	8.5	62	10.5	3.005	1.00	43.0	5
192	1995 Hyogoken-Nambu (Kobe) earthquake M=6.9 - Jan 16	YES	6.9	19.2	82	10.5	0.268	1.00	64.6	5
193	1995 Hyogoken-Nambu (Kobe) earthquake M=6.9 - Jan 16	NO	6.9	25	60	9.8	0.665	1.00	73.7	5
194	1995 Hyogoken-Nambu (Kobe) earthquake M=6.9 - Jan 16	YES	6.9	21.1	43	10.5	3.005	1.00	67.7	5
195	1995 Hyogoken-Nambu (Kobe) earthquake M=6.9 - Jan 16	NO	6.9	42.6	171	9.2	0.161	0.50	90.0	0
197	1995 Hyogoken-Nambu (Kobe) earthquake M=6.9 - Jan 16	NO	6.9	50	75	10.1	0.185	0.69	90.0	0
198	1995 Hyogoken-Nambu (Kobe) earthquake M=6.9 - Jan 16	NO	6.9	33.5	44	9.8	0.676	1.00	85.3	0
201	1995 Hyogoken-Nambu (Kobe) earthquake M=6.9 - Jan 16	YES	6.9	24.6	51	10.5	0.279	1.00	73.1	0
202	1995 Hyogoken-Nambu (Kobe) earthquake M=6.9 - Jan 16	NO	6.9	35.8	50	9.2	0.713	1.00	88.2	3
203	1995 Hyogoken-Nambu (Kobe) earthquake M=6.9 - Jan 16	NO	6.9	37	37	9.8	3.005	1.00	89.7	0
206	1995 Hyogoken-Nambu (Kobe) earthquake M=6.9 - Jan 16	YES	6.9	17.9	49	11.5	0.286	1.00	62.4	0
208	1995 Hyogoken-Nambu (Kobe) earthquake M=6.9 - Jan 16	NO	6.9	49.7	46	9.8	0.753	1.00	90.0	0
213	1995 Hyogoken-Nambu (Kobe) earthquake M=6.9 - Jan 16	NO	6.9	31.6	36	9.8	3.005	1.00	82.9	3
214	1995 Hyogoken-Nambu (Kobe) earthquake M=6.9 - Jan 16	YES	6.9	19.3	79	12.2	0.106	0.98	64.8	0

215	1995 Hyogoken-Nambu (Kobe) earthquake M=6.9 - Jan 16	YES	6.9	19.1	94	10.5	0.499	1.00	64.4	5
216	1995 Hyogoken-Nambu (Kobe) earthquake M=6.9 - Jan 16	NO	6.9	50	66	9.8	0.174	0.68	90.0	0
217	1995 Hyogoken-Nambu (Kobe) earthquake M=6.9 - Jan 16	NO	6.9	39.7	59	9.8	0.168	0.84	90.0	0
218	1995 Hyogoken-Nambu (Kobe) earthquake M=6.9 - Jan 16	YES	6.9	15	50	11.5	0.562	1.00	57.1	0
221	1995 Hyogoken-Nambu (Kobe) earthquake M=6.9 - Jan 16	YES	6.9	8.3	43	11.5	3.005	1.00	42.5	5
223	1995 Hyogoken-Nambu (Kobe) earthquake M=6.9 - Jan 16	YES	6.9	12.5	115	11.5	0.244	1.00	52.1	2

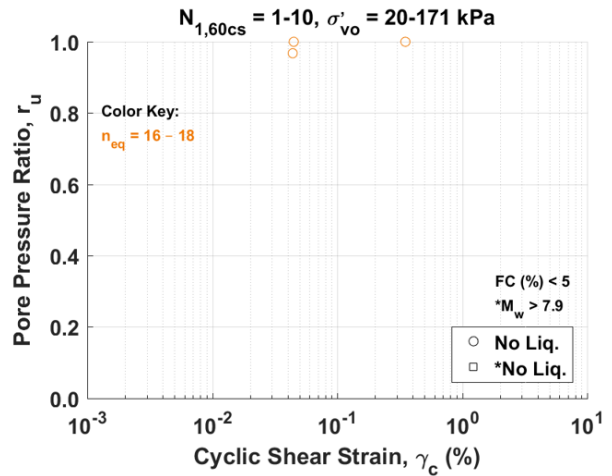
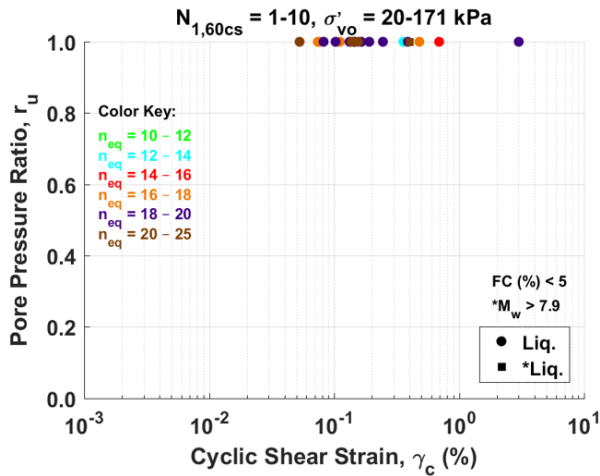


Figure D11. Excess porewater pressure buildup using the Byrne (1991) model with the Boulanger et al. database cases having $FC \leq 5\%$

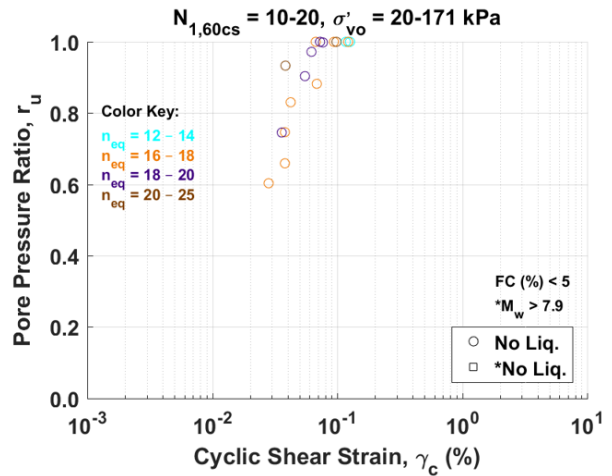
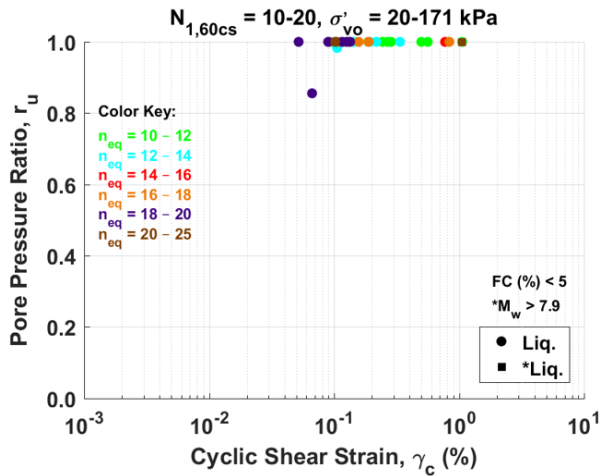


Figure D12. Excess porewater pressure buildup using the Byrne (1991) model with the Boulanger et al. database cases having $FC \leq 5\%$

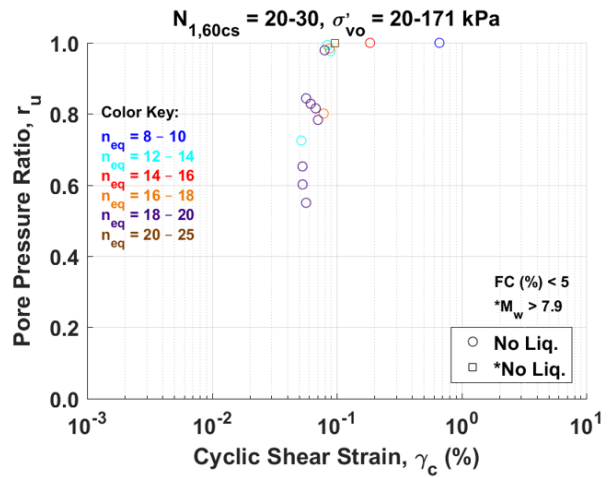
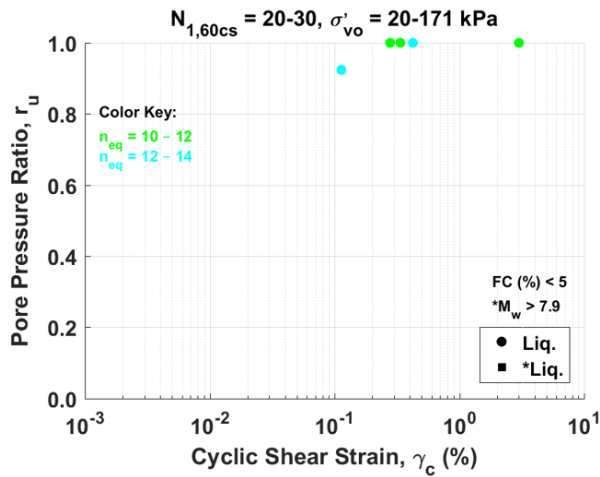


Figure D13. Excess porewater pressure buildup using the Byrne (1991) model with the Boulanger et al. database cases having $FC \leq 5\%$

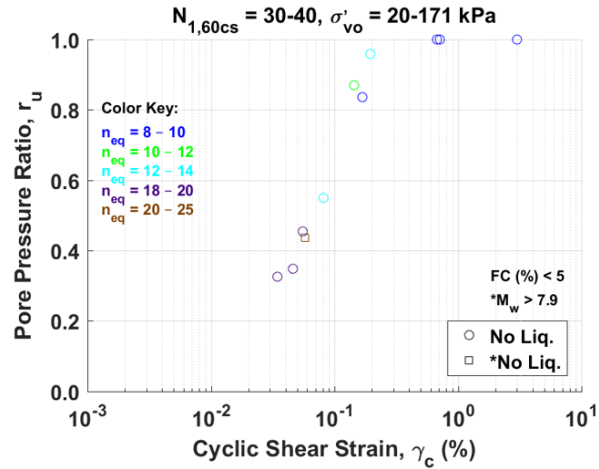


Figure D14. Excess porewater pressure buildup using the Byrne (1991) model with the Boulanger et al. database cases having $FC \leq 5\%$

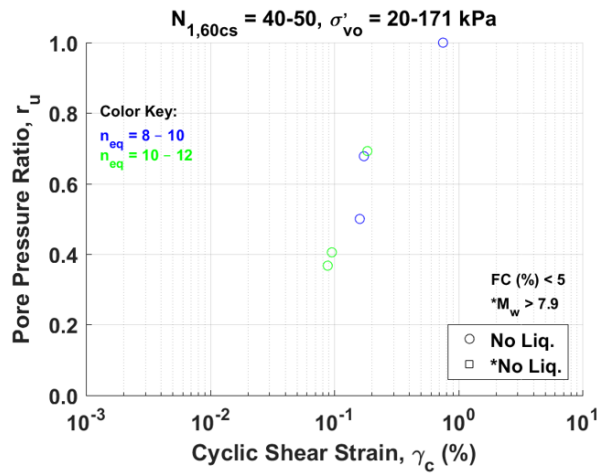


Figure D15. Excess porewater pressure buildup using the Byrne (1991) model with the Boulanger et al. database cases having $FC \leq 5\%$

Cases in the Boulanger et al. database with $FC \leq 5\%$ (116 cases)

Vucetic and Dobry model

Table D4. Parameters needed to plot figures of excess pore pressure ratio versus cyclic shear strain for the Boulanger et al. (2012) database (cases with FC ≤ 5%) using the Vucetic and Dobry (1986) model

Data Point #	Year Event	Liquefied? YES/NO	M _w	N _{1,60cs} blows	σ' _v (kPa)	Lasley n _{eq}	γ _c (%)	Vucetic and Dobry r _u	D _r (%)	FC
5	1948 Fukui earthquake M=7.3 - June 28	YES	7	11.8	48	11.8	1.052	0.94	50.6	0
6	1948 Fukui earthquake M=7.3 - June 28	YES	7	21.1	104	12.4	0.109	0.56	67.7	4
7	1964 Niigata earthquake M=7.6 - June 16	YES	7.6	4.7	41	24.9	0.048	0.62	32.0	5
8	1964 Niigata earthquake M=7.6 - June 16	YES	7.6	9.9	72	19.7	0.098	0.72	46.4	2
10	1964 Niigata earthquake M=7.6 - June 16	YES	7.6	6.8	53	19.6	0.077	0.68	38.4	5
11	1964 Niigata earthquake M=7.6 - June 16	NO	7.6	22.7	81	18.8	0.048	0.42	70.2	2
12	1964 Niigata earthquake M=7.6 - June 16	NO	7.6	23.5	109	18.8	0.052	0.44	71.5	2
13	1964 Niigata earthquake M=7.6 - June 16	YES	7.6	11	100	19.7	0.085	0.68	48.9	2
14	1964 Niigata earthquake M=7.6 - June 16	YES	7.6	17.5	100	19.7	0.062	0.54	61.7	2
15	1964 Niigata earthquake M=7.6 - June 16	YES	7.6	9.4	47	19.7	0.128	0.78	45.2	0
16	1964 Niigata earthquake M=7.6 - June 16	NO	7.6	14.1	79	18.8	0.057	0.53	55.4	0
18	1964 Niigata earthquake M=7.6 - June 16	NO	7.6	35.5	67	18.8	0.041	0.37	87.8	0
20	1968 Tokachi-Oki earthquake M=8.3 - May 16	YES	8.3	16.5	38	20.6	1.046	0.96	59.9	3
21	1968 Tokachi-Oki earthquake M=8.3 - May 16	NO	8.3	35.3	76	20.0	0.053	0.46	87.6	5
22	1968 Tokachi-Oki earthquake M=8.3 - May 16	NO	8.3	23	45	20.0	0.092	0.62	70.7	5
23	1968 Tokachi-Oki earthquake M=8.3 - May 16	YES	8.3	9.1	42	20.0	0.397	0.92	44.5	5
30	1975 Haicheng earthquake M=7.0 - Feb 4	YES	7	11	92	13.3	0.213	0.79	48.9	5
31	1976 Guatemala earthquake M=7.5 - Feb 4	YES	7.5	5	86	20.6	0.151	0.84	33.0	3
32	1976 Guatemala earthquake M=7.5 - Feb 4	YES	7.5	9.7	34	20.6	0.133	0.79	45.9	3
33	1976 Guatemala earthquake M=7.5 - Feb 4	NO	7.5	14.3	71	20.6	0.093	0.69	55.8	3
36	1976 Tangshan earthquake M=7.6 - July 27	NO	7.6	24.4	38	17.3	0.083	0.56	72.8	5
37	1976 Tangshan earthquake M=7.6 - July 27	YES	7.6	8.5	32	17.3	0.476	0.93	43.0	3
42	1977 Argentina earthquake M=7.4 - Nov 23	YES	7.5	7.6	156	17.6	0.071	0.63	40.6	5
43	1977 Argentina earthquake M=7.4 - Nov 23	NO	7.5	14.3	39	17.6	0.117	0.71	55.8	4
44	1977 Argentina earthquake M=7.4 - Nov 23	NO	7.5	13.6	44	17.6	0.062	0.55	54.4	3
46	1978 Miyagiken-Oki earthquake M=6.5 - Feb 20	NO	6.5	12.8	67	18.5	0.031	0.34	52.8	0
49	1978 Miyagiken-Oki earthquake M=6.5 - Feb 20	NO	6.5	12.3	59	16.1	0.023	0.23	51.7	5
50	1978 Miyagiken-Oki earthquake M=6.5 - Feb 20	NO	6.5	14.1	79	16.1	0.033	0.32	55.4	3
51	1978 Miyagiken-Oki earthquake M=6.5 - Feb 20	YES	6.5	6.9	30	17.1	0.069	0.62	38.7	5
52	1978 Miyagiken-Oki earthquake M=6.5 - Feb 20	NO	6.5	9.6	42	17.1	0.040	0.43	45.7	4
53	1978 Miyagiken-Oki earthquake M=6.5 - Feb 20	NO	6.5	9.4	85	16.1	0.039	0.41	45.2	5
59	1978 Miyagiken-Oki earthquake M=6.5 - Feb 20	NO	6.5	15.1	47	17.1	0.037	0.37	57.3	0

60	1978 Miyagiken-Oki earthquake M=7.7 - June 12	YES	7.7	12.8	67	18.4	0.129	0.75	52.8	0
64	1978 Miyagiken-Oki earthquake M=7.7 - June 12	YES	7.7	12.3	59	16.1	0.087	0.63	51.7	5
65	1978 Miyagiken-Oki earthquake M=7.7 - June 12	NO	7.7	17.6	73	16.1	0.089	0.60	61.9	0
67	1978 Miyagiken-Oki earthquake M=7.7 - June 12	YES	7.7	14.1	79	17.1	0.103	0.67	55.4	3
68	1978 Miyagiken-Oki earthquake M=7.7 - June 12	NO	7.7	26.2	39	15.2	0.180	0.72	75.5	4
69	1978 Miyagiken-Oki earthquake M=7.7 - June 12	YES	7.7	6.9	30	15.2	3.000	0.99	38.7	5
70	1978 Miyagiken-Oki earthquake M=7.7 - June 12	YES	7.7	9.6	42	15.2	0.688	0.94	45.7	4
71	1978 Miyagiken-Oki earthquake M=7.7 - June 12	YES	7.7	9.4	85	17.1	0.106	0.71	45.2	5
78	1978 Miyagiken-Oki earthquake M=7.7 - June 12	YES	7.7	15.1	47	17.1	0.184	0.79	57.3	0
79	1978 Miyagiken-Oki earthquake M=7.7 - June 12	NO	7.7	24.6	70	17.1	0.074	0.52	73.1	0
98	1982 Urakawa-Oki earthquake M=6.9 - Mar 21	NO	6.9	17	35	16.4	0.033	0.31	60.8	5
99	1983 Nihonkai-Chubu earthquake M=6.8 - June 21	NO	6.8	5.1	37	16.8	0.346	0.91	33.3	5
100	1983 Nihonkai-Chubu earthquake M=6.8 - June 21	NO	6.8	18.1	77	16.8	0.064	0.51	62.7	0
101	1983 Nihonkai-Chubu earthquake M=6.8 - June 21	YES	6.8	13.3	42	19.0	0.047	0.48	53.8	0
102	1983 Nihonkai-Chubu earthquake M=7.7 - May 26	YES	7.7	16.5	38	23.0	0.097	0.71	59.9	3
103	1983 Nihonkai-Chubu earthquake M=7.7 - May 26	YES	7.7	5.1	37	18.4	3.000	0.99	33.3	5
104	1983 Nihonkai-Chubu earthquake M=7.7 - May 26	YES	7.7	12.4	53	17.5	0.832	0.95	51.9	1
105	1983 Nihonkai-Chubu earthquake M=7.7 - May 26	YES	7.7	16.2	38	16.8	0.152	0.74	59.3	1
106	1983 Nihonkai-Chubu earthquake M=7.7 - May 26	YES	7.7	13.3	42	16.0	0.768	0.94	53.8	0
107	1983 Nihonkai-Chubu earthquake M=7.7 - May 26	NO	7.7	18.7	41	18.2	0.050	0.45	63.8	3
108	1983 Nihonkai-Chubu earthquake M=7.7 - May 26	NO	7.7	13.8	41	18.2	0.068	0.58	54.8	3
109	1983 Nihonkai-Chubu earthquake M=7.7 - May 26	NO	7.7	13.1	41	23.0	0.034	0.42	53.4	5
110	1983 Nihonkai-Chubu earthquake M=7.7 - May 26	YES	7.7	8.7	79	18.2	0.140	0.78	43.5	3
111	1983 Nihonkai-Chubu earthquake M=7.7 - May 26	YES	7.7	6.9	107	18.2	0.160	0.82	38.7	4
114	1983 Nihonkai-Chubu earthquake M=7.7 - May 26	YES	7.7	13.5	81	18.2	0.097	0.68	54.2	3
116	1983 Nihonkai-Chubu earthquake M=7.7 - May 26	YES	7.7	10.2	71	18.2	0.122	0.75	47.1	2
117	1983 Nihonkai-Chubu earthquake M=7.7 - May 26	YES	7.7	11.5	68	18.2	0.112	0.72	50.0	2
118	1983 Nihonkai-Chubu earthquake M=7.7 - May 26	NO	7.7	18.9	47	18.2	0.072	0.56	64.1	3
119	1983 Nihonkai-Chubu earthquake M=7.7 - May 26	NO	7.7	23.5	42	18.2	0.057	0.46	71.5	2
120	1983 Nihonkai-Chubu earthquake M=7.7 - May 26	NO	7.7	23	34	18.2	0.052	0.43	70.7	1
121	1983 Nihonkai-Chubu earthquake M=7.7 - May 26	NO	7.7	34.6	60	18.2	0.050	0.42	86.7	3
122	1983 Nihonkai-Chubu earthquake M=7.7 - May 26	NO	7.7	37.3	31	18.2	0.030	0.26	90.0	1
123	1983 Nihonkai-Chubu earthquake M=7.7 - May 26	NO	7.7	20.3	53	18.2	0.075	0.56	66.4	2
124	1983 Nihonkai-Chubu earthquake M=7.7 - May 26	YES	7.7	5.4	56	18.2	0.385	0.92	34.3	2
125	1983 Nihonkai-Chubu earthquake M=7.7 - May 26	YES	7.7	7.4	63	18.2	0.186	0.84	40.1	2
126	1983 Nihonkai-Chubu earthquake M=7.7 - May 26	YES	7.7	5.6	64	18.2	0.241	0.88	34.9	2
127	1983 Nihonkai-Chubu earthquake M=7.7 - May 26	YES	7.7	8.1	49	18.2	0.141	0.79	42.0	2
128	1983 Nihonkai-Chubu earthquake M=7.7 - May 26	NO	7.7	23.5	55	18.2	0.063	0.49	71.5	2
129	1983 Nihonkai-Chubu earthquake M=7.7 - May 26	NO	7.7	22.5	77	18.2	0.066	0.50	69.9	4

130	1983 Nihonkai-Chubu earthquake M=7.7 - May 26	NO	7.7	25.9	46	18.2	0.048	0.41	75.0	0
146	1989 Loma Prieta earthquake M=6.9 - Oct 18	NO	6.93	21.4	35	13.4	0.079	0.49	68.2	5
148	1989 Loma Prieta earthquake M=6.9 - Oct 18	YES	6.93	13.1	65	13.4	0.129	0.68	53.4	3
149	1989 Loma Prieta earthquake M=6.9 - Oct 18	YES	6.93	14.9	55	13.4	0.088	0.57	56.9	3
150	1989 Loma Prieta earthquake M=6.9 - Oct 18	YES	6.93	17.6	64	13.4	0.139	0.67	61.9	3
151	1989 Loma Prieta earthquake M=6.9 - Oct 18	NO	6.93	22.6	35	13.4	0.047	0.33	70.1	1
152	1989 Loma Prieta earthquake M=6.9 - Oct 18	NO	6.93	14.9	47	13.4	0.122	0.65	56.9	1
153	1989 Loma Prieta earthquake M=6.9 - Oct 18	NO	6.93	21.2	48	13.4	0.084	0.51	67.9	5
154	1989 Loma Prieta earthquake M=6.9 - Oct 18	NO	6.93	14.7	48	13.4	0.112	0.63	56.5	4
159	1989 Loma Prieta earthquake M=6.9 - Oct 18	YES	6.93	15.4	89	13.4	0.108	0.62	57.9	3
160	1989 Loma Prieta earthquake M=6.9 - Oct 18	YES	6.93	17	89	13.4	0.100	0.59	60.8	3
162	1989 Loma Prieta earthquake M=6.9 - Oct 18	YES	6.93	15.3	43	13.4	0.118	0.64	57.7	2
163	1989 Loma Prieta earthquake M=6.9 - Oct 18	NO	6.93	34.4	73	13.4	0.076	0.47	86.5	5
165	1989 Loma Prieta earthquake M=6.9 - Oct 18	YES	6.93	10.3	46	13.4	0.189	0.78	47.3	1
166	1989 Loma Prieta earthquake M=6.9 - Oct 18	YES	6.93	18.4	67	13.4	0.093	0.56	63.2	1
171	1993 Kushiro-Oki earthquake M=7.6 - Jan 15	YES	7.6	16.4	68	13.6	0.332	0.84	59.7	2
172	1993 Kushiro-Oki earthquake M=7.6 - Jan 15	NO	7.6	30.9	118	13.6	0.190	0.71	82.0	0
173	1993 Kushiro-Oki earthquake M=7.6 - Jan 15	YES	7.6	25.9	47	12.7	0.420	0.84	75.0	5
178	1995 Hyogoken-Nambu (Kobe) earthquake M=6.9 - Jan 16	NO	6.9	50	80	11.5	0.084	0.46	90.0	3
180	1995 Hyogoken-Nambu (Kobe) earthquake M=6.9 - Jan 16	NO	6.9	49.8	77	11.5	0.091	0.48	90.0	3
181	1995 Hyogoken-Nambu (Kobe) earthquake M=6.9 - Jan 16	NO	6.9	36.6	54	11.5	0.139	0.60	89.2	1
182	1995 Hyogoken-Nambu (Kobe) earthquake M=6.9 - Jan 16	YES	6.9	6.1	116	12.2	0.354	0.87	36.4	1
184	1995 Hyogoken-Nambu (Kobe) earthquake M=6.9 - Jan 16	YES	6.9	10.9	60	11.5	0.183	0.74	48.7	0
185	1995 Hyogoken-Nambu (Kobe) earthquake M=6.9 - Jan 16	YES	6.9	24.1	65	10.5	0.332	0.77	72.4	0
186	1995 Hyogoken-Nambu (Kobe) earthquake M=6.9 - Jan 16	YES	6.9	12.2	64	10.5	0.820	0.92	51.5	2
188	1995 Hyogoken-Nambu (Kobe) earthquake M=6.9 - Jan 16	YES	6.9	8.5	62	10.5	3.000	0.98	43.0	5
192	1995 Hyogoken-Nambu (Kobe) earthquake M=6.9 - Jan 16	YES	6.9	19.2	82	10.5	0.263	0.75	64.6	5
193	1995 Hyogoken-Nambu (Kobe) earthquake M=6.9 - Jan 16	NO	6.9	25	60	9.8	0.660	0.86	73.7	5
194	1995 Hyogoken-Nambu (Kobe) earthquake M=6.9 - Jan 16	YES	6.9	21.1	43	10.5	3.000	0.97	67.7	5
195	1995 Hyogoken-Nambu (Kobe) earthquake M=6.9 - Jan 16	NO	6.9	42.6	171	9.2	0.156	0.57	90.0	0
197	1995 Hyogoken-Nambu (Kobe) earthquake M=6.9 - Jan 16	NO	6.9	50	75	10.1	0.180	0.63	90.0	0
198	1995 Hyogoken-Nambu (Kobe) earthquake M=6.9 - Jan 16	NO	6.9	33.5	44	9.8	0.671	0.87	85.3	0
201	1995 Hyogoken-Nambu (Kobe) earthquake M=6.9 - Jan 16	YES	6.9	24.6	51	10.5	0.274	0.74	73.1	0
202	1995 Hyogoken-Nambu (Kobe) earthquake M=6.9 - Jan 16	NO	6.9	35.8	50	9.2	0.708	0.86	88.2	3
203	1995 Hyogoken-Nambu (Kobe) earthquake M=6.9 - Jan 16	NO	6.9	37	37	9.8	3.000	0.97	89.7	0
206	1995 Hyogoken-Nambu (Kobe) earthquake M=6.9 - Jan 16	YES	6.9	17.9	49	11.5	0.281	0.78	62.4	0
208	1995 Hyogoken-Nambu (Kobe) earthquake M=6.9 - Jan 16	NO	6.9	49.7	46	9.8	0.748	0.88	90.0	0
213	1995 Hyogoken-Nambu (Kobe) earthquake M=6.9 - Jan 16	NO	6.9	31.6	36	9.8	3.000	0.97	82.9	3
214	1995 Hyogoken-Nambu (Kobe) earthquake M=6.9 - Jan 16	YES	6.9	19.3	79	12.2	0.101	0.55	64.8	0

215	1995 Hyogoken-Nambu (Kobe) earthquake M=6.9 - Jan 16	YES	6.9	19.1	94	10.5	0.494	0.85	64.4	5
216	1995 Hyogoken-Nambu (Kobe) earthquake M=6.9 - Jan 16	NO	6.9	50	66	9.8	0.169	0.61	90.0	0
217	1995 Hyogoken-Nambu (Kobe) earthquake M=6.9 - Jan 16	NO	6.9	39.7	59	9.8	0.163	0.60	90.0	0
218	1995 Hyogoken-Nambu (Kobe) earthquake M=6.9 - Jan 16	YES	6.9	15	50	11.5	0.557	0.89	57.1	0
221	1995 Hyogoken-Nambu (Kobe) earthquake M=6.9 - Jan 16	YES	6.9	8.3	43	11.5	3.000	0.98	42.5	5
223	1995 Hyogoken-Nambu (Kobe) earthquake M=6.9 - Jan 16	YES	6.9	12.5	115	11.5	0.239	0.78	52.1	2

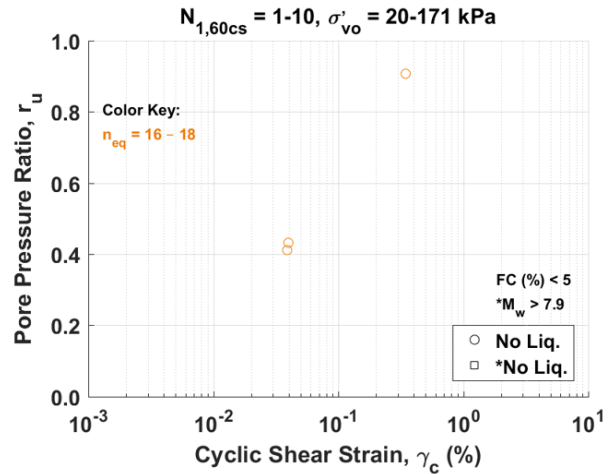
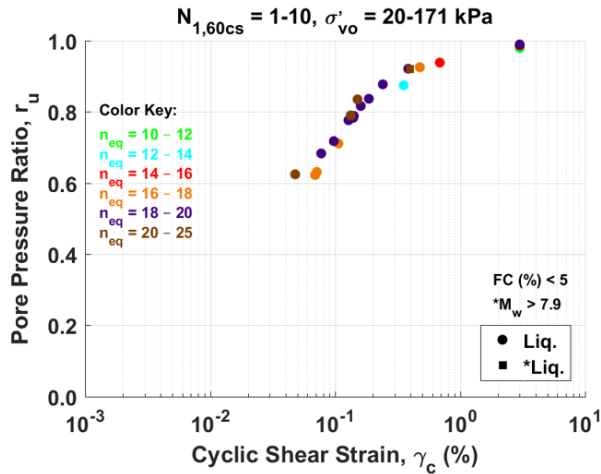


Figure D16. Excess porewater pressure buildup using the Vucetic and Dobry (1986) model with the Boulanger et al. database cases having $FC \leq 5\%$

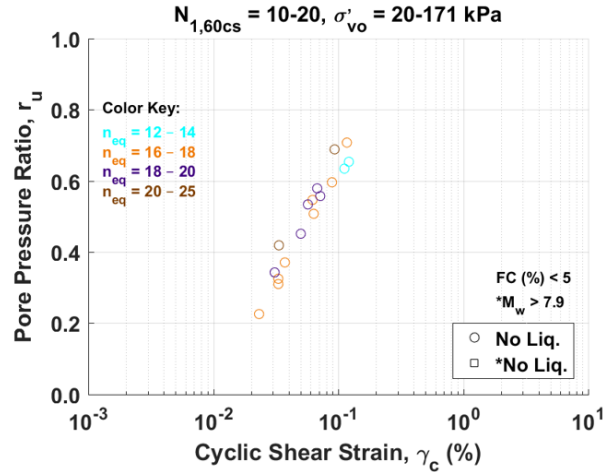
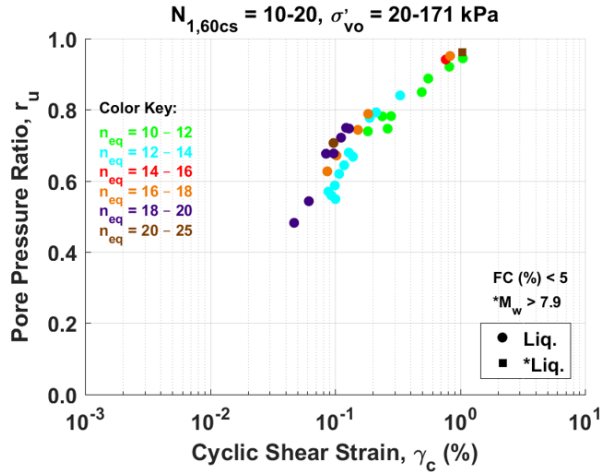


Figure D17. Excess porewater pressure buildup using the Vucetic and Dobry (1986) model with the Boulanger et al. database cases having $FC \leq 5\%$

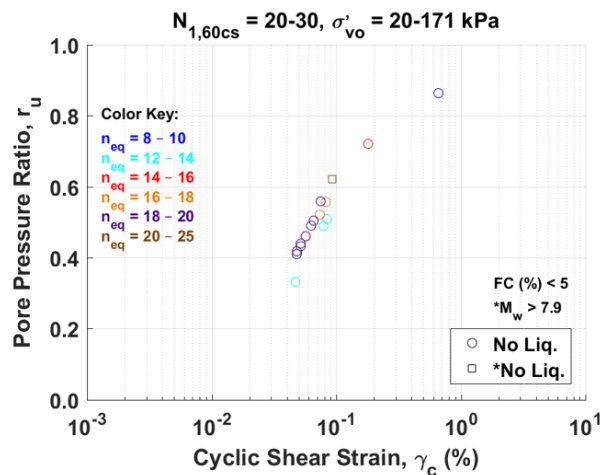
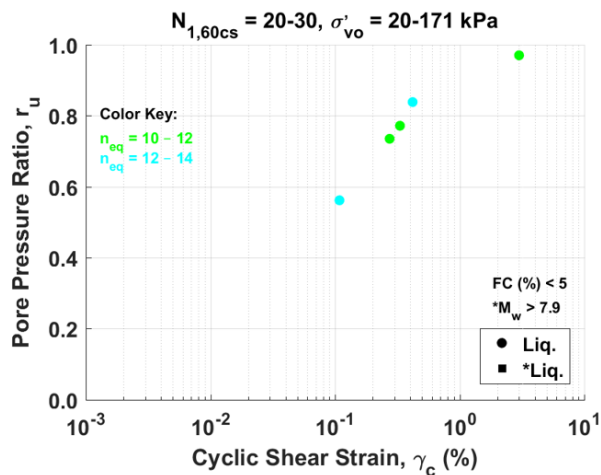


Figure D18. Excess porewater pressure buildup using the Vucetic and Dobry (1986) model with the Boulanger et al. database cases having $FC \leq 5\%$

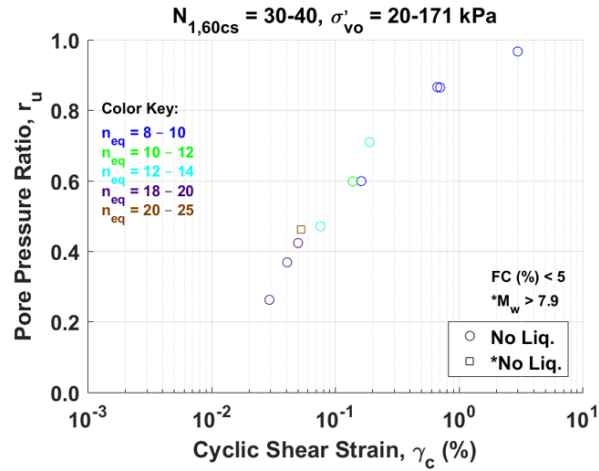


Figure D19. Excess porewater pressure buildup using the Vucetic and Dobry (1986) model with the Boulanger et al. database cases having FC \leq 5%

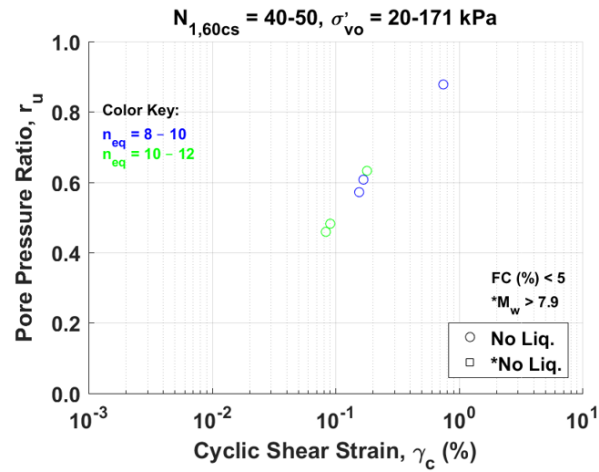


Figure D20. Excess porewater pressure buildup using the Vucetic and Dobry (1986) model with the Boulanger et al. database cases having FC \leq 5%